ІНСТИТУТ БІОЛОГІЇ КЛІТИНИ
НАЦІОНАЛЬНА АКАДЕМІЯ НАУК УКРАЇНИ
ІНСТИТУТ БІОЛОГІЇ КЛІТИНИ
НАЦІОНАЛЬНА АКАДЕМІЯ НАУК УКРАЇНИ

Кваліфікаційна наукова праця на правах наукової доповіді за сукупністю статей

Стасюк Наталія Євгенівна

УДК 579.2+577+543.6+543.9+544.6+544.7

ДИСЕРТАЦІЯ

Мікробні ензими у поєднанні з нанозимами для створення біо(хемо)сенсорів та тест-наборів для визначення вмісту практично важливих аналітів

03.00.07 – мікробіологія

Подається на здобуття наукового ступеня доктора біологічних наук

Дисертація містить результати власних досліджень. Використання ідей, результатів і текстів інших авторів мають посилання на відповідне джерело

_____Н.Є. Стасюк

Львів – 2023

Присвячується моїм батькам
та сестрі

Висловлюю щиру подяку завідувачу відділу аналітичної біотехнології Інституту біології клітини НАН України проф., д.б.н. Гончару М.В. за наукове консультування при виконанні досліджень, а також за незліченні години консультацій, виправлень перших версій цієї роботи і приємний час спілкування.

Сердечно вдячна усім співробітникам відділу за їхню допомогу та співавторство при виконанні спільних експериментів:

– с.н.с., к.х.н. Гайді Г.З. – за підтримку, розуміння, цінні поради та оптимізм на всіх етапах виконання роботи;

– к.б.н. Закальському А.Є. – за надання ензимів, а також консультування на всіх етапах досліджень;

– д.б.н. Смутку О.В. – за консультування та допомогу на етапі конструювання біосенсорів;

– к.б.н. Прокопів Т.М. та к.б.н. Демків О.М. – за цінні пропозиції при мікробіологічних дослідженнях;

– пров. інж. Закальській О.М., інж. Горечій М.В. та інж. Іваш М.Ф. – за технічну допомогу та приємну емоційну робочу атмосферу;

– інж. Серкісу Р.Я. – за проведення мікроскопічних досліджень.

Глибоко вдячна директору Інституту біології клітини НАН України, акад. НАН України, проф., д.б.н. Сибірному А.А. – за можливість виконання наукової роботи в Інституті, всебічну підтримку та плідне співробітництво (разом з к.б.н. Фаюрою Л.Р.).

Із приємністю хочу подякувати керівнику наукової групи наноелектрохімії Інституту фізичної хімії Польської академії наук, к.х.н. Войцеху Ногалі (Dr. Wojciech Nogala) за цінні поради на етапі електрохімічних досліджень властивостей біосенсорів.

Щиро вдячна Національній академії наук України та Національному фонду досліджень України за фінансову підтримку досліджень у рамках наукових проєктів.

АНОТАЦІЯ

Стасюк Н.Є. Мікробні ензими у поєднанні з нанозимами для створення біо(хемо)сенсорів та тест-наборів для визначення вмісту практично важливих аналітів. – **Кваліфікаційна наукова праця на правах наукової доповіді за сукупністю статей.**

Дисертація на здобуття наукового ступеня доктора біологічних наук за спеціальністю 03.00.07 «Мікробіологія» – Інститут біології клітини Національної академії наук України, Львів, 2023.

Представлена робота присвячена комплексному дослідженню структурних, фізико-хімічних та каталітичних властивостей нанозимів у поєднанні їх з мікробними ензимами, а також вивченню біологічної та токсичної дії (*in vivo*) нанозимних композитів на клітини дріжджів *Ogataea (Hansenula) polymorpha*. Основну увагу в роботі зосереджено на кон'югації наноматеріалів з мікробними ензимами та створенню на їх основі нових біо(хемо)сенсорів та тест-наборів для визначення вмісту практично важливих аналітів, зокрема, креатиніну, L-аргініну, L-лактату, глюкози, етанолу та метиламіну.

Постійно зростаюча необхідність ранньої діагностики багатьох захворювань, поліпшення охорони навколишнього середовища, контролю біотехнологічних процесів, якості харчових продуктів і питної води потребують дедалі ширшого використання у практиці високочутливих, селективних, швидких та економічних методів аналізу. Серед різних аналітичних підходів особлива роль відводиться аналітичній біотехнології – науці, яка використовує принципи біомолекулярного розпізнавання для детекції практично важливих аналітів. Біосенсори є найновішим досягненням аналітичної біотехнології, вони складаються з двох функціональних частин: біоселективного елемента — іммобілізованого біологічно активного матеріалу та фізичного перетворювача, який відповідає за трансляцію біохімічного сигналу в електричний. Головними перевагами біосенсорних підходів є висока чутливість, селективність та відтворюваність сигналу, задовільні діапазони та

низькі границі визначення метаболітів, швидкість аналізу, простота у використанні, портативність, економічність, придатність до масового виробництва.

На сьогодні, у розпізнавальних елементах біосенсорів найчастіше використовують ензими завдяки їхній унікальній каталітичній дії. Проте природні ензими, як правило, мають обмежену хімічну та біологічну стабільність, високу вартість, що пов'язано зі складними технологіями їх виділення та очищення з біологічних джерел. Розглядаючи ензими в ролі біоспецифічних перетворювачів, що перетворюють аналіт у форму, яка детектується різними фізичними або хімічними методами, в останні роки особливий інтерес викликає використання нанорозмірних матеріалів, особливо у поєднанні з ензимами, у тому числі, для розробки технологій одержання біонаноматеріалів із каталітичними властивостями. Розробка нових нанокаталізаторів – нанозимів з високою каталітичною активністю розширює їх застосування в біоаналітиці.

Нанозими – це найновіший клас функціональних наноматеріалів, які мають ензимоподібну активність. Порівняно з природними ензимами, нанозими володіють підвищеною стабільністю та більшою доступністю завдяки відносно простим технологіям синтезу. Важлива перевага нанозимів – залежність їхньої активності від розміру/складу наночастинок (НЧ). Це дозволяє створювати нові матеріали з широким діапазоном каталітичної активності, просто змінюючи форму, структуру та склад НЧ. Нанозими (НЗ) також мають унікальні властивості, порівнюючи з іншими штучними ензимами, зокрема велику питому площу поверхні, що значно полегшує їхню подальшу модифікацію та біокон'югацію. Здатність наноматеріалів до спонтанної структурної самоорганізації також є дуже важливою характеристикою для біології та медицини завдяки легшому включенню біологічних компонентів у структуру наноматеріалу. Завдяки своїй каталітичній активності НЗ можуть застосовуватися в наукових дослідженнях, біотехнології та харчовій промисловості, сільському господарстві, для деградації забруднювачів навколишнього середовища (очищення стічних вод, деградація хімічних бойових речовин), а також у клінічній діагностиці та фармакології. Крім їхнього використання як діагностичних засобів, нанозими є перспективними

каталітичними компонентами терапевтичних препаратів. Завдяки біосумісності та магнітним властивостям деяких нанозимів, їх можна використовувати для локального цілеспрямованого лікування злоякісних утворень. Нанозими можуть слугувати антиоксидантами при лікуванні аутоімунних захворювань, хвороб Альцгеймера та Паркінсона, а також застосовуватись як антибактерійні засоби. Із відкриттям НЗ як штучних ензимів стало можливим використання явища прямого електронного перенесення при створенні нанозимних біосенсорів «третього покоління», а також для забезпечення вимог щодо їхньої високої каталітичної активності, хімічної та біологічної стабільності, розміру.

Таким чином, прості методики синтезу нанозимів, їхні унікальні каталітичні властивості, а також здатність до специфічного зв'язування ензимів робить їх привабливими кандидатами для досліджень у біосенсорних технологіях. Саме тому, створення нових біонанокомпозитів (іммобілізованих мікробних ензимів на поверхні наноматеріалів) із подальшим використанням їх у біосенсориці, а також в ензиматичному аналізі є актуальним завданням.

Метою роботи було дослідження структурних, фізико-хімічних і каталітичних властивостей штучних ензимів – нанозимів у поєднанні з мікробними ензимами для створення на їхній основі нових діагностичних методів, придатних для використання у клінічній діагностиці, фармацевтиці та харчових технологіях, а також вивчення біологічної дії нанозимних композитів на еукаріотичні клітини (зокрема, на моделі дріжджів).

У роботі використано комплекс різноманітних методів, зокрема, мікробіологічні, генно-інженерні, біохімічні, фізико-хімічні, електрохімічні, аналітичні та біосенсорні методи дослідження. При аналізі активності ензимів та чистоти ензимних препаратів використано методи спектрофотометричного аналізу, електрофорезу білків за нативних та денатуруючих умов, іонообмінна та афінна хроматографія. Для фізико-хімічного та структурного аналізу нанономатеріалів використано методи сканувальної електронної мікроскопії, рентгеноспектрального аналізу, атомно-силової мікроскопії, трансмісійної електронної мікроскопії, Раман-спектроскопії та спектроскопії ядерного магнітного резонансу. Як референтні

методи для аналізу іонів металів (Mn^{2+} та Co^{2+}) використано атомно-абсорбційну спектроскопію. При конструюванні амперометричних біосенсорів застосовано циклічну вольтамперометрію та хроноамперометрію, статистичний і кореляційний аналіз.

Отримано експериментальні дані, які вперше в науковій практиці доводять можливість заміни природного ензиму – каталази штучними «катазимами», які повністю відновлюють здатність мутантних безкаталазних клітин метилотрофних дріжджів рости на метанолі. Молекулярно-генетичний аналіз та секвенування локусу геному штаму дріжджів *Ogataea polymorpha* С-105 виявив дві мутації у гені каталази: заміна азотистої основи цитозину (С) у 895 положенні кодуючої послідовності на азотисту основу тимін (Т) та делеція С у положенні 896. Така комбінація веде до зсуву рамки зчитування і утворення стоп-кодону TGA, що спричинює у клітинах штаму С-105 продукцію нефункціонального, неповного протеїну. Уперше показано різну цитотоксичну дію синтезованих нанозимів на клітини дріжджів *O. polymorpha.* На моделі високоочищеної Манган-залежної рекомбінантної людської аргінази I вперше отримано препарати апоензиму, позбавленого металу, та здійснено реконструкцію холоензиму. Уперше розроблено новий ензиматичний метод на основі апоензиму аргінази I та 2,3-бутандіонмонооксиму для селективного та ультрачутливого визначення вмісту йонів Mn^{2+} та Co^{2+} (на рівні 1пМ для йонів Mn^{2+} та 2,5 пМ для йонів Co^{2+}). Уперше опрацьовано чутливі та селективні ензиматичні методи кількісного аналізу L-аргініну із флуоресцентним та спектрофотометричним способом детектування кольорового продукту реакції за допомогою *о*-фталевого альдегіду та високоочищених препаратів аргінази I і уреази або аргініндеімінази. Уперше використано поєднання каталітичних наноматеріалів та високоочищених препаратів ензимів класу гідролаз: аргінази I, креатиніндеімінази, аргініндеімінази при формуванні біоселективних елементів амперометричних біосенсорів на L-аргінін та креатинін. Уперше за використання наноміметиків пероксидази і природної алкогольоксидази створено нові ензимо-нанозимні методи аналізу етанолу.

Ключові слова: мікробні клітини, ензими, аргініноксидаза, метиламінооксидаза, алкогольоксидаза, глюкозооксидаза, пероксидаза, креатиніндеіміназа, аргіназа, аргініндеіміназа, L-лактат:цитохром *c*-оксидоредуктаза (флавоцитохром b_2), нанозими.

SUMMARY

Stasyuk N.Ye. "Microbial enzymes combined with nanozymes for creation of bio(chemo)sensors and test kits for determining the content of practically important analytes" – Qualifying scientific work in the form of a scientific report based on research articles.

Thesis for Doctor of Sciences degree in Biology (specialty 03.00.07 – Microbiology). Institute of Cell Biology, National Academy of Sciences of Ukraine, Lviv, 2023.

The presented work is devoted to a comprehensive study of the structural, physicochemical, and catalytic properties of nanozymes in combination with microbial enzymes, as well as to the study of the biological and toxic effects (*in vivo*) of nanozyme composites on *Ogataea (Hansenula) polymorpha* yeast cells. The main focus of the work is directed on the conjugation of nanomaterials with microbial enzymes and on their basis the creation of new bio(chemo)sensors and test kits for determining the content of practically important analytes, in particular, creatinine, L-arginine, glucose L-lactate, ethanol and methylamine.

The ever-increasing need for early diagnosis of many diseases, improvement of environmental protection, control of biotechnological processes, quality of food products and drinking water require the wider use in practice of highly sensitive, selective, fast and economical methods of analysis. Among various analytical approaches, a special role is assigned to analytical biotechnology – a science that uses the principles of biomolecular recognition for the detection of practically important analytes. Biosensors are the newest achievement of analytical biotechnology, they consist of two functional parts: a bioselective element — an immobilized biologically active material and a

physical transduser responsible for translating a biochemical signal into an electrical one. The main advantages of biosensor approaches are high sensitivity, selectivity and reproducibility of the signal, satisfactory ranges and low limits of determination of metabolites, speed of analysis, ease of use, portability, economy, suitability for mass production.

Nowadays, enzymes are most often used in the recognition elements of biosensors due to their unique catalytic action. However, natural enzymes, as a rule, have limited chemical and biological stability, high cost, which is associated with complex technologies for their isolation and purification from biological sources.

To consider enzymes as biospecific transducers that convert the analyte into a form that can be detected by various physical or chemical methods, the use of nanoscale materials, especially in combination with enzymes, including for the development of technologies for obtaining bionanomaterials with catalytic properties, has attracted special interest in recent years. The development of new nanocatalysts – nanozymes with high catalytic activity expands their use in bioanalysis. Thus, the simple methods of synthesis of nanozymes, their unique catalytic properties, as well as the ability to specifically bind enzymes make them attractive candidates for research in biosensor technologies. Nanozymes are the newest class of functional nanomaterials that have enzyme-like activity. Compared to natural enzymes, nanozymes have increased stability and greater availability due to relatively simple synthesis technologies. An important advantage of nanozymes is the dependence of their activity on the size/composition of nanoparticles (NPs). This makes it possible to create new materials with a wide range of catalytic activity by simply changing the shape, structure and composition of NPs. Nanozymes also have unique properties compared to other artificial enzymes, in particular, a large specific surface area, which greatly facilitates their further modification and bioconjugation. The ability of nanomaterials for spontaneous structural self-organization is also a very important characteristic for biology and medicine due to the easier incorporation of biological components into the nanomaterial structure. Due to their catalytic activity, NPs can be used in scientific research, biotechnology and the food industry, agriculture, for the degradation of environmental pollutants (wastewater

treatment, degradation of chemical warfare agents), as well as in clinical diagnostics and pharmacology. In addition to their use as diagnostic tools, nanozymes are promising catalytic components of therapeutic drugs. Due to the biocompatibility and magnetic properties of some nanozymes, they can be used for local targeted treatment of malignant formations. Nanozymes can serve as antioxidants in the treatment of autoimmune diseases, Alzheimer's and Parkinson's diseases, and can also be used as antibacterial agents. With the discovery of NPs as artificial enzymes, it became possible to use the phenomenon of direct electron transfer in the creation of "third generation" nanoscale biosensors, as well as to meet the requirements for their high catalytic activity, chemical and biological stability, and size. So, the creation of new bionanocomposites (immobilized microbial enzymes on the surface of nanomaterials) and their further application in biosensors, as well as in enzymatic analysis, is an urgent task.

The main aim of the work was to study the structural, physicochemical and catalytic properties of artificial enzymes – nanozymes in combination with microbial enzymes to create new diagnostic methods on their basis, suitable for use in clinical diagnostics, pharmaceuticals and food technologies, as well as to study the biological effect of nanozyme composites on eukaryotic cells (on the yeast model).

A complex of various methods was used in the work, in particular, microbiological, genetic engineering, biochemical, physicochemical, electrochemical, analytical and biosensor research methods. The methods of spectrophotometric analysis, protein electrophoresis under native and denaturing conditions, ion exchange and affinity chromatography were used to analyze the activity of enzymes and the purity of enzyme preparations. The methods of scanning electron microscopy, X-ray spectral analysis, atomic force microscopy, transmission electron microscopy, Raman spectroscopy and nuclear magnetic resonance spectroscopy were used for the physicochemical and structural analysis of nanomaterials. Atomic absorption spectrophotometry was used as a reference method for the analysis of metal ions (Mn^{2+} and Co^{2+}). During the construction of amperometric biosensors, cyclic voltammetry, chronoamperometry, statistical and correlation analysis were used.

Experimental data were obtained which, for the first time in the world, prove the

possibility of replacing the natural enzyme catalase with artificial "catazyme", which restores the ability of mutant non-catalase yeast cells to grow on methanol. Molecular-genetic analysis and sequencing of the genome locus of the yeast strain *Ogataea polymorpha* C-105 revealed two mutations in the catalase gene: replacement of nitrogenous base of cytosine (C) at the 895 position of the coding sequence by thymine (T) and deletion of C at the 896 position; this combination leads to a shift in the reading frame and the formation of the stop codon TGA, which causes the production of non-functional, incomplete catalase protein in the strain C-105. For the first time, different cytotoxic effect of synthesized nanozymes on the yeast *O. polymorpha* cells was shown. Highly purified manganese-dependent recombinant human arginase I preparations of the metal-free apoenzyme were obtained for the first time, and the reconstruction of the holo-enzyme was carried out. For the first time, a new enzymatic method based on apoenzyme arginase I and 2,3-butanedione monooxime was developed for the selective and ultrasensitive determination of the content of Mn^{2+} and Co^{2+} ions (on the level 1 pM for the Mn^{2+} ions and 2,5 pM for – Co^{2+} ions). For the first time, sensitive and selective enzymatic methods for the quantitative detection of L-arginine with fluorescent and spectrophotometric detection of the colored reaction product using *o*-phthalaldehyde and highly purified preparations of arginase I and urease or arginine deiminase were developed. For the first time, a combination of catalytic nanomaterials and highly purified preparations of enzymes of hydrolases, in particular, arginase I, creatinine deaminase, arginine deaminase was used in the formation of bioselective elements of amperometric biosensors selective for L-arginine and creatinine. For the first time, a new enzyme-nanozyme methods for ethanol analysis were created using nanomimetics of peroxidase and natural alcohol oxidase.

Key words: microbial cells, enzymes, arginine oxidase, methylamine oxidase, alcohol oxidase, glucose oxidase, peroxidase, creatinine deiminase, arginase, arginine deiminase, L-lactate: cytochrome c oxidoreductase (flavocytochrome b_2), nanozymes.

СПИСОК ПУБЛІКАЦІЙ ЗДОБУВАЧА

Наукові праці, що розкривають основні наукові результати дисертації:

1) **Stasyuk N**, Zakalskiy A, Nogala W, Gawinkowski S, Ratajczyk T, Bonarowska M, Demkiv O Zakalska O, Gonchar M (2023) A reagentless amperometric biosensor for creatinine assay based on recombinant creatinine deiminase and N-methylhydantoin-sensitive CoCu nanocomposite. Sensors and Actuators B: Chemical 393: 34276. https://doi.org/10.1016/j.snb.2023.134276. **[IF 8,4; SCOPUS, WoS; SCImago – Q1]** (*Особистий внесок здобувача: концептуалізація, планування і виконання експериментів, написання рукопису та підготовка статті до друку*)

2) Prokopiv T, **Stasyuk N,** Gonchar M (2023) Nanozyme can substitute a natural *Ogataea polymorpha* catalase enzyme *in vivo*. Microchimica Acta 190(5): 174. doi: 10.1007/s00604-023-05753-8 **[IF 5,7; SCOPUS, WoS; SCImago – Q1]** (*Особистий внесок здобувача: концептуалізація, планування і виконання експериментів, написання рукопису та підготовка статті до друку*)

3) **Stasyuk N,** Demkiv O, Gayda G, Zakalska O, Nogala W, Gonchar M (2022) Amperometric biosensors based on alcohol oxidase and peroxidase-like nanozymes for ethanol assay. Microchimica Acta 189: 474. **[IF 5,7; SCOPUS, WoS; SCImago –Q1]** https://doi.org/10.1007/s00604-022-05568-z (*Особистий внесок здобувача: концептуалізація, синтез та скринінг нанозимів на псевдопероксидазну активність і конструювання біосенсорів, написання рукопису та підготовка статті до друку*)

4) **Stasyuk N**, Gayda G, Kavetskyy T, Gonchar M (2022) Nanozymes with reductase-like activities: electrochemical and antioxidant properties. RSC Advances 12**:** 2026 – 2035. doi: 10.1039/d1ra08127f **[IF 4,04; SCOPUS, WoS; SCImago –Q2]** (*Особистий внесок здобувача: концептуалізація, планування і виконання експериментів, написання рукопису та підготовка статті до друку*)

5) **Stasyuk N**, Demkiv O, Gayda G, Zakalska O, Zakalskiy A, Serkiz R, Kavetskyy T, Gonchar M (2022) Reusable alcohol oxidase-nPtCu/alginate beads for highly sensitive

ethanol assay in beverages. RSC Advances 12: 21309 – 21317. doi: 10.1039/d2ra02106d **[IF 4,04; SCOPUS, WoS; SCImago – Q2]** (*Особистий внесок здобувача: концептуалізація, планування і виконання експериментів, написання рукопису та підготовка статті до друку*).

6) **Stasyuk N**, Demkiv O, Gayda G, Zakalskiy A, Klepach H, Bisko N, Gonchar M, Nisnevitch M (2022) Highly Porous 3D Gold Enhances Sensitivity of Amperometric Biosensors Based on Oxidases and CuCe Nanoparticles. Biosensors 12: 472. doi: 10.3390/bios12070472 **[IF 5,4; SCOPUS, WoS; SCImago – Q2]** (*Особистий внесок здобувача: концептуалізація, планування і виконання експериментів, написання рукопису та підготовка статті до друку*).

7) **Stasyuk NYe**, Gayda GZ, Zakalskiy AE, Fayura LR, Zakalska OM, Sibirny AA, Nisnevitch M, Gonchar MV (2022) Amperometric biosensors for L-arginine and creatinine assay based on recombinant deiminases and ammonium-sensitive Cu/Zn(Hg)S nanoparticles. Talanta 238 (1): 122996, https://doi.org/10.1016/j.talanta.2021.122996 **[IF 6,1; SCOPUS, WoS; SCImago– Q1]** (*Особистий внесок здобувача: концептуалізація, планування і виконання експериментів, написання рукопису та підготовка статті до друку*).

8) **Stasyuk N**, Gayda G, Demkiv O, Darmohray L, Gonchar M, Nisnevitch M (2021) Amperometric biosensors for L-arginine determination based on L-arginine oxidase and peroxidase-like nanozymes. Applied Sciences 11(15): 7024. https://doi.org/10.3390/app11157024 **[IF 2,7; SCOPUS, WoS; SCImago – Q2]** (*Дисертантка спільно зі співавторами провела дослідження, взяла участь в аналізі отриманих даних, написанні та оформленні публікації*).

9) Demkiv O, **Stasyuk N**, Serkiz R, Gayda G, Nisnevitch, M, Gonchar M (2021) Peroxidase-Like Metal-Based Nanozymes: Synthesis, Catalytic Properties, and Analytical Application. Applied Science 11: 777. https://doi.org/10.3390/app11020777 **[IF 2,7; SCOPUS, WoS; SCImago – Q2]** (*Дисертантка спільно зі співавторами провела дослідження, взяла участь в аналізі отриманих даних, написанні та оформленні публікації*).

10) Zakalskiy A, **Stasyuk N**, Zakalska O, Boretsky Y, Gonchar M (2020) Overexpression and one-step renaturation-purification of the tagged creatinine deiminase of *Corynebacterium glutamicum* in *Escherichia coli* cells. Cell Biology International 44 (5), 1204–1211 **[IF 3,612; SCOPUS, WoS; SCImago – Q3]** https://pubmed.ncbi.nlm.nih.gov/32039507/ (*Дисертантка спільно із співавторами провела ензимологічні дослідження ензиму та статистичну обробку результатів, взяла участь у написанні та оформленні публікації*).

11) **Stasyuk N**, Gayda G, Zakalskiy A, Zakalska O, Serkiz R, Gonchar M (2019) Amperometric biosensors based on oxidases and PtRu nanoparticles as artificial peroxidase. Food Chemistry 285: 213-220. https://doi.org/10.1016/j.foodchem.2019.01.117 **[IF 6,306; SCOPUS, WoS; SCImago – Q1]** (*Особистий внесок здобувача: концептуалізація, планування і виконання експериментів, написання рукопису та підготовка статті до друку*)

12) **Stasyuk N,** Gayda G, Zakalskiy A, Zakalska O, Errachid A, Gonchar M (2018) Highly selective apo-arginase based method for sensitive enzymatic assay of manganese (II) and cobalt (II) ions. Spectrochimica Acta, Part A: Molecular and Biomolecular Spectroscopy 193, 349 – 356. doi: 10.1016/j.saa.2017.12.031. **[IF 2,931; SCOPUS, WoS; SCImago – Q2]** (*Особисто дисертанткою підготовлено дизайн дослідження, проведено аналіз і обговорення отриманих результатів та написано статтю*).

13) **Stasyuk N**, Gayda G, Yepremyan H, Stepien A, Gonchar M (2017) Fluorometric enzymatic assay of L-arginine. Spectrochimica Acta, Part A: Molecular and Biomolecular Spectroscopy 193 170: 184-190. https://doi.org/10.1016/j.saa.2016.07.019 **[IF 2,931; SCOPUS, WoS; SCImago – Q2]** (*Особисто дисертантом запропоновано ідею дослідження, проведено аналіз і обговорення отриманих результатів, формулювання висновків та написання статті*).

14) **Stasyuk N**, Gayda G, Zakalskiy A, Zakalska O, Fayura L, Vovk O, Stasyk O, Sibirny A, Gonchar M (2017) Recombinant Forms of Arginase and Arginine Deiminase as Catalytic Components of Argitest Enzymatic Kit. Science and Innovation 13(4): 56—63. [**фахове видання України**] http://scinn-eng.org.ua/archive/13(4)/13(4)06

(*Особисто дисертанткою проведено аналізування і обговорення отриманих результатів, формулювання висновків та написання статті*).

15) **Stasyuk N**, Gayda G, Fayura L, Boretskyy Y, Gonchar M, Sibirny A (2016) Novel arginine deiminase-based method to assay L-Arginine in beverages. Food Chemistry 201: 320-326. https://doi.org/10.1016/j.foodchem.2016.01.093 **[IF 4,529; SCOPUS, WoS; SCImago – Q1]** (*Особисто дисертантом запропоновано ідею дослідження, проведено аналіз і обговорення отриманих результатів, формулювання висновків та написання статті*).

16) **Stasyuk N**, Gayda G, Serkiz RJa, Gonchar M (2016) The "green" synthesis of gold nanoparticles by the yeast *Hansenula polymorpha*. Вісник Львівського університету. Серія біологічна. 73: 96 – 102. [**фахове видання України**] http://nbuv.gov.ua/UJRN/VLNU_biol_2016_73_18 (*Особисто дисертанткою проведено аналізування і обговорення отриманих результатів, формулювання висновків та написання статті*).

17) Karkovska M, Smutok O, **Stasyuk N**, Gonchar M (2015) L-Lactate-selective microbial sensor based on flavocytochrome b_2-enriched yeast cells using recombinant and nanotechnology approaches, Talanta 144, 1195–1200. **[IF 4,035; SCOPUS, WoS; SCImago – Q1]** (*Особисто дисертанткою проведено синтез наночастинок та проведено іммобілізацію ФЦ b_2 на поверхні наноматеріалів, обговорення отриманих результатів та формулювання висновків, написання статті*).

18) **Stasyuk NYe**, Bass S. R., Gayda G. Z., Yepremyan H. S., Gonchar MV (2015) New enzymatic method for L-arginine assay based on human arginase I and urease. ScienceRise 6 (1), 43-48. [**фахове видання України**] https://journals.uran.ua/sciencerise/article/view/45126 (*Особисто дисертанткою проведено аналізування і обговорення отриманих результатів, формулювання висновків та написання статті*).

19) **Stasyuk N**, Gayda G, Gonchar M (2014) L-arginine-selective microbial amperometric sensor based on recombinant yeast cell over-producing human liver arginase I. Sensors and Actuators B: Chemical 204: 515-521. https://doi.org/10.1016/j.snb.2014.06.112 **[IF 4,589; SCOPUS, WoS; SCImago –**

Q1] (*Особисто дисертантом запропоновано ідею дослідження, проведено аналіз і обговорення отриманих результатів, формулювання висновків та написання статті*)

20) **Stasyuk NYe,** Smutok OV, Zakalskiy AE, Zakalska OM, Gonchar MV (2014) Methylamine-sensitive amperometric biosensor based on $(His)_6$-tagged *Hansenula polymorpha* methylamine oxidase immobilized on the gold nanoparticles. BioMed Research International 2014: 1-8. doi: 10.1155/2014/480498 **[IF 2,239; SCOPUS, WoS; SCImago – Q2]** (*Особисто дисертанткою проведено конструювання амперометричних біосенсорів на основі метиламінооксидази та апробація отриманих сенсорів на реальних зразках, обговорення отриманих результатів та формулювання висновків, написання статті*).

21) Synenka MM, **Stasyuk NYe**, Semashko TV, Gayda GZ, Mikhailova RV, Gonchar MV (2014) Immobilization of oxidoreductases at/on gold and silver nanoparticles. Studia Biologica 8 (3-4): 5–12. [**фахове видання України**] http://publications.lnu.edu.ua/journals/index.php/biology/article/view/192 (*Особисто дисертанткою проведено аналізування і обговорення отриманих результатів, формулювання висновків та написання статті*).

Статті, що додатково відображають зміст дисертації:

1) **Stasyuk N**, Gayda G, Klepach H, Semashko T, Gonchar M (2017) Nanoparticles of Noble Metals for Enzymatic Sensors: An Amperometric Glucose Biosensor for Wine Analysis. Sensors Letters 15(8), 647 – 654. https://doi.org/10.1166/sl.2017.3862 (*Особисто дисертанткою проведено аналізування і обговорення отриманих результатів, формулювання висновків та написання статті*).

2) **Stasyuk N**, Gayda G, Klepach H, Gonchar M (2016) Nanoparticles of noble metals as effective platforms for the fabrication of amperometric biosensor on hydrogen peroxide. Sensors Letters 14: 1169 – 1179 https://doi.org/10.1166/sl.2016.3748. (*Особисто дисертанткою проведено аналізування і обговорення отриманих результатів, формулювання висновків та написання статті*).

3) **Stasyuk NYe**, Gayda GZ, Serkiz RJa, Gonchar MV (2015) Cell Imaging with Fluorescent Bi-Metallic Nanoparticles. Journal of Advances in Chemistry 11 (4): 3499 – 3511. https://rajpub.com/index.php/jac/article/view/6694 (*Особисто дисертанткою проведено аналізування і обговорення отриманих результатів, формулювання висновків та написання статті*).

Патенти:

1. Патент України на корисну модель №142490 Україна, МПК G01N21/64 Моноензиматичний спосіб визначення вмісту креатиніну та амонію в біологічних рідинах людини / Гончар М.В., Закальський А.Є., Закальська О.М., **Стасюк Н.Є.**, Прокопів Т.М., Борецький Ю.Р., Демків О.М.; заявник і власник Інститут біології клітини НАН України, Львівський державний університет фізичної культури імені Івана Боберського – № u201911544, заявл. 29.11.2019, опубл. 10.06.2020, Бюл. №11. – 8 с. [**патент України на корисну модель**] (*Особистий внесок здобувача: виконання експериментів, написання і підготовка тексту патенту*).

2. Патент України на корисну модель №107543 Україна, МПК G01N 21/64 Ензиматичний метод визначення L-аргініну в крові людини / **Стасюк Н.Є.,** Гайда Г.З., Закальський А.Є., Закальська О.М., Гончар М.В.; заявник і власник Інститут біології клітини НАН України – № u201512716, заявл. 22.12.2015, опубл. 10.06.2016, Бюл. №11. – 5 с. [**патент України на корисну модель**] (*Особистий внесок здобувача: виконання експериментів, написання і підготовка тексту патенту*).

3. Патент на корисну модель №108773 Україна, МПК G01N 33/52, G01N 21/64 Ензиматично-хімічний метод визначення вмісту L-аргініну в харчових продуктах та алкогольних напоях / **Стасюк Н.Є.**, Гайда Г.З., Фаюра Л.Р., Борецький Ю.Р., Сибірний А.А., Гончар М.В.; заявник і власник Інститут біології клітини НАН України – № u201601804, заявл. 25.02.2016, опубл. 25.07.2016, Бюл. №14. – 7 с. [**патент України на корисну модель**] (*Особистий внесок здобувача: виконання експериментів, написання і підготовка тексту патенту*).

Розділи монографій:

1. Gayda G, **Stasyuk N**, Zakalskiy A, Gonchar M, Katz E (2022) Arginine-hydrolyzing enzymes for electrochemical biosensors. Current Opin Electrochem. 33: 100941 **[IF 8,5; SCOPUS, WoS; SCImago – Q1]** https://www.sciencedirect.com/science/article/abs/pii/S2451910322000060 (*Особисто дисертанткою проведено аналізування даних літературних джерел та написано частину розділу «Електрохімічні біосенсори для аналізу L-аргініну*).

2. **Stasyuk N**, Smutok O, Demkiv O, Prokopiv T, Gayda G, Nisnevitch M, Gonchar M. (2020) Synthesis, Catalytic Properties and Application in Biosensorics of Nanozymes and Electronanocatalysts: A Review. Sensors, 20 (16): 4509 **[IF 3,847; SCOPUS, WoS; SCImago – Q1]** https://www.mdpi.com/1424-8220/20/16/4509 (*Особисто дисертанткою проведено аналізування даних літературних джерел та написано розділ 2 «Методи синтезу каталітичних наноматеріалів» і розділ 3 «Каталітичні властивості нанозимів»*).

3. Zakalskiy A., **Stasyuk N.**, Gonchar M. (2019) Creatinine Deiminase: Characterization, Using in Enzymatic Creatinine Assay, and Production of the Enzyme. Curr Protein Pept Sci. 20: 465-470 https://pubmed.ncbi.nlm.nih.gov/30426898/ **[IF 2,52; SCOPUS, WoS; SCImago – Q2]** (*Особисто дисертанткою проведено аналізування даних літературних джерел та написано розділ 3 «Хімічні та фізико-хімічні методи для аналізу креатиніну»*).

4. Gayda G, **Stasyuk N**, Serkiz R, Gonchar M. Fluorescent nanoparticles of noble metals for cell imaging (ред. Н.А.Серебрякова). Київ: НВП «Видавництво «Проект наукова книга»; 2017. С. 156 – 165. http://ir.librarynmu.com/handle/123456789/7658 (*Особисто дисертанткою проведено аналізування даних літературних джерел та написано частину розділу 4.3 «Дослідження цитотоксичності наноматеріалів на клітини дріжджів»*).

5. Карковська М, **Стасюк Н.**, Гайда Г., Смуток О., Гончар М. Наноматеріали у конструюванні біосенсорів медичного призначення (ред. Н.А.Серебрякова). Київ: НВП «Видавництво «Проект наукова книга»; 2017. С. 165 – 177.

http://ir.librarynmu.com/handle/123456789/7658 (*Особисто дисертанткою проведено аналізування даних літературних джерел та написано розділ 4.4 «Наноматеріали у конструюванні біосенсорів біомедичного призначення»*).

6. Gonchar M, Smutok O, Karkovska M, **Stasyuk N**, Gayda G. Yeast-based biosensors for clinical diagnostics and food control (Ed. A.A. Sibirny). Springer International Publishing AG "Biotechnology of Yeasts and Filamentous Fungi"; 2017. P. 392 – 400. https://dokumen.pub/non-conventional-yeasts-from-basic-research-to-application-1st-ed-2019-978-3-030-21109-7-978-3-030-21110-3.html (*Особисто дисертанткою проведено аналізування даних літературних джерел та написано розділ 14.3.2 «Аналіз амінокислот»*).

Список тез доповідей на конференціях, з'їздах та симпозіумах, на яких апробовано результати дисертації

1. Gayda G., Klepach H., **Stasyuk N.**, Ivash N., Bilek M., Broda D., Gonchar M. Application of recombinant glycerol dehydrogenase for glycerol assay in wines. 5 th Polish-Ukrainian Weigl Conference on Microbiology: abstracts, Chernivtsi, 23-25 May, 2013. Chernivtsi, Ukraine, 2013. P. 72.

2. Gonchar M., **Stasyuk N.**, Zakalskiy A., Smutok O., Zakalska A., Gaida G. Assay of arginine and manganese by amperometric biosensors based on the recombinant human arginase and its apo-enzyme. IX Jakub K. Parnas Conference "Proteins from Birth to Death": abstracts, Jerusalem, Israel, 29 September – 2 October, 2013. Jerusalem, Israel, 2013. P. 97.

3. Zakalskiy A., Gayda G., **Stasyuk N.**, Zakalska O., Smutok O., Gonchar M. Biosensor for assay of manganese ions using apoenzyme of Mn^{2+}-dependent recombinant arginase I. International Workshop "Recent advances in Micro/Nano Sensors for Mono- and Multi-Target assays": abstracts, Kyiv, Ukraine, 19-23 May, 2013. Kyiv, Ukraine, 2013. P. 71-72.

4. **Stasyuk N.**, Gayda G., Gonchar M. L-arginine-selective microbial amperometric sensor based on recombinant yeast cell over-producing human liver arginase I. International Symposium on Cell Biology jointly with 4rd Ukrainian

Congress for Cell Biology: abstracts, Uzhhorod, Ukraine, 17 – 20 September, 2014. Uzhhorod, Ukraine, 2014. P. 19.

5. **Stasyuk N.**, Gayda G., Gonchar M. New bioanalytical methods based on arginase I for L-arginine assay. 5th International Young Scientists Conference "Human-Nutrition-Environment" "Biotechnology for sustainable development": abstracts, Rzeszow, Poland. 24 – 25 April, 2014. Rzeszow, Poland. P. 78.

6. **Stasyuk N.**, Gayda G., Gonchar M. Arginase-based bioanalytical approaches to L-arginine assay for prediction of urethane formation in fermented foods. International Scientific Conference "Microorganisms in detoxification of heavy metals and xenobiotics": abstracts, Krasiczyn, Poland. 28 September – 1 October 2014. Krasiczyn, Poland. P. 15.

7. Gonchar M., Karkovska M., **Stasyuk N.**, Smutok O. Gene and Protein Engineering in Production of the Enzymes of Analytical Importance. 27th International conference on yeast genetics and molecular biology: abstacts, Levico Terme, Italy, 6–12 September 2015. Levico Terme, Italy. P. 153.

8. Karkovska M., Smutok O., **Stasyuk N.**, Gonchar M. L-lactate-selective microbial sensor based on flavocytochrome b_2-enriched yeast cells using recombinant and nanotechnology approaches. International conference "Advances in Cell Biology and Biotechnology": abstracts, Lviv, Ukraine, 11–13 October, 2015. Lviv, Ukraine. P. 69.

9. **Stasyuk N.**, Gayda G., Klepach H., Gonchar M. Nanoparticles of Noble metals as effective platforms for the fabrication of amperometric biosensors on hydrogen peroxide. International Symposium on Cell Biology jointly with 5th Ukrainian Congress for Cell Biology: abstracts, Odesa, Ukraine, 2–6 October, 2016. Odesa, Ukraine. P. 19.

10. Gayda G., **Stasyuk N.**, Fayura L., Gonchar M., Sibirny A. Application of arginine-hydrolizing enzymes in bioanalytics. XV З'їзд товариства мікробіологів України ім. С.М. Виноградського: тези доповідей, Одеса, Україна, 11-15 вересня 2017, Одеса, Україна, P. 239.

11. Gayda G., **Stasyuk N.**, Klepach H., Zakalskiy A., Zakalska O., Semashko T., Gonchar M. Peroxidase-like nanozymes as efficient platforms for oxidase-based

amperometric biosensors. 7th International Weigl Conference: abstarcts, Lviv, Ukraine, 26-29 September 2017. Lviv, Ukraine. P. 100.

12. **Stasyuk N.**, Zakalskyi A., Zakalska O., Gonchar M. $(His)_6$-tagged *Corynebacterium glutamicum* creatinine deiminase as a biosensing element for creatinine assay. 7th International Weigl Conference: abstarcts, Lviv, Ukraine, 26-29 September 2017. Lviv, Ukraine. P. 34.

13. Гончар М.В., **Стасюк Н.Є.**, Закальський А.Є., Закальська О.М. Рекомбінантна $(His)_6$-тагована креатиніндеіміназа *Corynebacterium clutamicum* як біосенсорний елемент для аналізу креатиніну. XV З'їзд товариства мікробіологів України ім. С.М. Виноградського: тези доповідей, Одеса, Україна, 11-15 вересня 2017. Одеса, Україна. С.256.

14. Gayda G., Smutok O., Klepach H., **Stasyuk N.**, Gonchar M. Microbial enzymes as the effective analytical tools for wine analysis. III International Scientific Conference "Microbiology and Immunology – the Development Outlook in the 21st century: abstracts, Kyiv, Ukraine, 19-20 April, 2018. Kyiv, Ukraine. P.42.

15. Gayda G., Demkiv O., Klepach H., **Stasyuk N.**, Ivash M., Zakalska O., Gonchar M. The development of cost-effective technology for purification of some enzymes from the yeast *Ogataea polymorpha* and their bioanalytical application. International Conference "Non-conventional Yeasts: from Basic Research to Application": abstracts, Rzeszow, Poland, 15-18 May, 2018. Rzeszow, Poland. P. 92.

16. Gayda G., **Stasyuk N.**, Demkiv O., Klepach H., Koretskiy S., Ivash M., Lootsik M., Stolyarchuk I., Gonchar M. Synthesis and characterization of nanomaterials promising for medicine and bioanalytics. International Conference "Advances in Microbiology and Biotechnology": abstracts, Lviv, Ukraine, 29-31 October, 2018. Lviv, Ukraine. P.71.

17. Gayda G., **Stasyuk N.**, Fayura L., Zakalskiy A., Zakalska O., Vovk O., Stasyk O., Gonchar M., Sibirny A. Enzymatic methods based on recombinant forms of arginase and arginine deiminase for arginine analysis. International Conference "Advances in Microbiology and Biotechnology": abstracts, Lviv, Ukraine, 29-31 October, 2018. Lviv, Ukraine. P.97.

18. Gayda G., Demkiv O., **Stasyuk N.**, Klepach H., Lootsik M., Ivash M., Gonchar M. Amperometric biosensors based on glycerol oxidase and nanoparticles of noble metals as artificial peroxidase. International Conference "Advances in Microbiology and Biotechnology": abstracts, Lviv, Ukraine, 29-31 October, 2018. Lviv, Ukraine. P.114.

19. Gonchar M., **Stasyuk N.**, Gayda. G., Zakalskiy A., Zakalska O. Alcohol oxidase from the yeast *Ogataea polymorpha* coupled with an artificial peroxidase, Pt/Ru nanoparticles, as a biosensing element. International Conference "Non-conventional Yeasts: from Basic Research to Application": abstracts, Rzeszow, Poland, 15-18 May, 2018. Rzeszow, Poland. P. 151.

20. Gonchar M., Zakalskiy A., Smutok O., **Stasyuk N.**, Demkiv O., Prokopiv T., Zakalska O. Engineered microorganisms for analytical purposes. International Conference "Advances in Microbiology and Biotechnology": abstracts, Lviv, Ukraine, 29-31 October, 2018. Lviv, Ukraine. P.55.

21. Smutok O., Karkovska M., **Stasyuk N.**, Gonchar M. Isolation, purification, stabilization and characterisation of flavocytochrome b_2 from overproducing cells of *Ogataea polymorpha* "tr1" (*gcr1 catx cyb2*). International Conference "Advances in Microbiology and Biotechnology": abstracts, Lviv, Ukraine, 29-31 October, 2018. Lviv, Ukraine. P.122.

22. **Stasyuk N.**, Gayda G., Myronovskij S., Lukavetskyy O., Kit Y., Gonchar M. Simultaneous enzymatic assay of l-arginine and l-citrulline in serum of patients with dysfunction of thyroid gland. International Conference "Advances in Microbiology and Biotechnology": abstracts, Lviv, Ukraine, 29-31 October, 2018. Lviv, Ukraine. P.123.

23. **Stasyuk N.**, Kukhazh Y., Hoivanovych N., Smutok O., Demkiv O., Kavetskyy T., Gonchar M. Improvement of amperometric laccase biosensor using gold nanoparticles coupling with ureasil polymer as a host matrix. International Conference "Advances in Microbiology and Biotechnology": Lviv, Ukraine, 29-31 October, 2018. Lviv, Ukraine. P.113.

24. Zakalskiy A., **Stasyuk N.**, Zakalska O., Gonchar M. Recombinant $(His)_6$-tagged creatininedeiminase of *Corynebacterium glutamicum*: purification and enzymological characterization. International Conference "Advances in Microbiology

and Biotechnology": abstracts, Lviv, Ukraine, 29-31 October 2018. Lviv, Ukraine. P.100.

25. Демків О., **Стасюк Н.**, Клепач Г., Гайда Г., Гончар М. Скринінг різних синтетичних нанокомпозитних матеріалів із потенційною пероксидазною активністю. Збірник матеріалів IV Міжнародної науково-практичної конференції, присвяченої 80-річчю Дрогобицького державного педагогічного університету імені Івана Франка «Стан природних ресурсів: перспективи їх збереження та відновлення у контексті сталого розвитку»: тези доповідей, м. Дрогобич, 27-28 жовтня 2020 р. Дрогобич, Україна. С. 129-133.

26. **Стасюк Н.**, Фаюра Л., Демків О., Клепач Г., Гайда Г. Флуорометричний ензиматично-хімічний метод одночасного визначення вмісту L-аргініну та L-цитруліну в крові. IV Міжнародна науково-практична конференція, присвячена 80-річчю Дрогобицького державного педагогічного університету імені Івана Франка «Стан природних ресурсів: перспективи їх збереження та відновлення у контексті сталого розвитку»: тези доповідей, 27-28 жовтня 2020 р. Дрогобич, Україна. С. 140-143.

ЗМІСТ

Перелік умовних скорочень……..... 27
Вступ…… 30
РОЗДІЛ 1. Огляд літератури…..……..... 39
РОЗДІЛ 2. Матеріали досліджень……..……. 123
2.1 Матеріали досліджень……..... 123
2.1.1 Організми…… 123
2.1.2 Характеристика використаних реактивів та препаратів …….. 123
2.2 Методи досліджень……. 124
2.2.1 Склад середовищ, культивування клітин і отримання безклітинних екстрактів…… 124
2.2.2 Пермеабілізація клітин дріжджів……..... 125
2.2.3 Визначення життєздатності клітин у присутності наноматеріалів флуоресцентним методом……..... 125
2.2.4 Визначення вмісту Гідроген пероксиду в культуральній рідині дріжджів..... 126
2.2.5 Виділення і очистка ензимів…….. 126
2.3. SDS-ПААГ електрофорез……. 127
2.4 Визначення активності ензимів…… 127
2.4.1 Визначення активності флавоцитохрому b_2……..... 127
2.4.2. Визначення активності аргінази……..…… 128
2.4.3 Визначення активності алкогольоксидази …….. 128
2.4.4 Визначення активності метиламінооксидази …….. 129
2.4.5 Визначення активності аргініноксидази ……..... 129
2.4.6 Визначення активності креатиніндеімінази …… 129
2.4.7 Визначення активності аргініндеімінази……..... 130
2.4.8 Визначення активності пероксидази……..... 130
2.4.9 Визначення активності глюкозооксидази……..……..... 130
2.5 Збагачення клітин ензимами, кон'югованими з золотими наночастинками …… 130

2.5.1 Збагачення клітин дріжджів *O. polymorpha* NCYC 495 аргіназою I… 130
2.5.2 Збагачення клітин дріжджів *O. polymorpha C-105* алкогольоксидазою…….. 131
2.6 Методи синтезу НЧ…….…….... 132
2.6.1 Синтез металевих НЧ методом відновлення…… 132
2.6.2 Синтез наночастинок методом осадження на пластині…….. 132
2.7 Методи «зеленого» синтезу НЧ……..……..... 132
2.7.1 Біосинтез Au-НЧ позаклітинними метаболітами дріжджів *“in .vitro”*……... 132
2.7.2 Біосинтез біметалевих НЧ позаклітинними метаболітами дріжджів *“in vitro”*…… 133
2.8 Методики досліджень розміру та структури НЧ……..……. 133
2.8.1 Фізико-хімічна характеристика розміру НЧ…… 133
2.8.2 УФ-видима спектроскопія……. 134
2.8.3 Атомно-силова мікроскопія……... 134
2.8.4 Флуоресцентна мікроскопія……... 134
2.8.5. Трансмісійна електронна мікроскопія …….……... 134
2.8.6 Спектроскопія ядерного магнітного резонансу……... 135
2.8.7 Спектроскопія комбінаційного розсіювання світла (Раман-спектроскопія)…….. 135
2.8.8 Квантово-хімічне моделювання…… 136
2.8.9 Дослідження площі та пористості НЧ методом БЕТ…….. 136
2.8.10 Дослідження НЧ за допомогою динамічного світлорозсіювання…… 136
2.8.11 Рентгеноструктурний аналіз НЧ……..... 137
2.9 Методи аналізу псевдоензиматичної активності НЧ…… 137
2.9.1 Визначення пероксидазо-подібної активності НЧ в розчині за використання *о*-діанізидину……... 137
2.9.2 Визначення пероксидазо-подібної активності НЧ в розчині за використання ТМБ……... 137

2.9.3 Визначення пероксидазо-подібної активності НЧ в розчині за використання АБТС……..... 138
2.9.4 Визначення редуктазної активності НЧ в розчині за використання катіон-радикалу $АБТС^{+}$……... 138
2.9.5 Визначення глутатіонредуктазної активності НЧ в розчині…….. 138
2.9.6 Визначення глутатіонпероксидазної активності НЧ в розчині……. 139
2.9.7 Визначення каталазо-подібної активності НЧ в розчині…… 139
2.9.8 Визначення антиоксидантної активності за використання радикалу 2,2-дифеніл-1-пікрилгідразилу (ДППГ)…… 139
2.9.9 Визначення константи Міхаеліса-Ментен ($К_м$) НЗ та константи швидкості реакції k_{cat} стостовно H_2O_2…….. 140
2.9.10 Визначення субстратної специфічності……. 140
2.10 Конструювання та дослідження функціональних властивостей біосенсорів…….…… 141
2.11. Підготовка реальних зразків до аналізу……... 143
2.12 Статистичний аналіз експериментальних даних……..... 143
РОЗДІЛ 3. СКРИНІНГ НОВИХ НАНОМАТЕРІАЛІВ НА ПСЕВДОЕНЗИМАТИЧНУ АКТИВНІСТЬ ТА ДОСЛІДЖЕННЯ СТРУКТУРНИХ І КАТАЛІТИЧНИХ ВЛАСТИВОСТЕЙ ОТРИМАНИХ НАНОЗИМІВ……... 145
3.1 Синтез та структурно-морфологічна характеристика металевих наночастинок із оксидоредуктазною активністю…….. 147
3.2 Синтез, скринінг, антиоксидантні властивості та електрохімічна поведінка нанозимів із потенційною редуктазною активністю…… 162
3.3 Біосинтез металевих наночастинок клітинами дріжджів *O. polymorpha* та застосування їх в флуоресцентному аналізі…… 173
РОЗДІЛ 4. ВИВЧЕННЯ БІОЛОГІЧНОЇ ТА МОЖЛИВОЇ ТОКСИЧНОЇ ДІЇ НАНОЗИМНИХ КОМПОЗИТІВ НА ДРІЖДЖОВІ КЛІТИНИ *OGATAEA POLYMORPHA*…… 181

4.1 Вивчення біологічної та можливої токсичної дії катазимів на еукаріотичні клітини безкаталазного штаму дріжджів *O. polymorpha* C-105 *(gcr1catX)*…… 183

4.2 Візуалізація та дослідження клітин за використання флуоресцентних наноматеріалів…… 193

РОЗДІЛ 5. СТВОРЕННЯ АМПЕРОМЕТРИЧНИХ БІОСЕНСОРІВ НА ОСНОВІ НАНОКОМПОЗИТІВ – ХЕМОМІМЕТИКІВ ПЕРОКСИДАЗИ І МІКРОБНИХ ЕНЗИМІВ, ПРИДАТНИХ ДЛЯ АНАЛІЗУ ЕТАНОЛУ, МЕТИЛАМІНУ ТА L-АРГІНІНУ…… 232

5.1 Дослідження методів іммобілізації оксидаз на поверхні наноносіїв…….. 234

5.2 Конструювання амперометричних біонаносенсорів за використання електродів, модифікованих пористим золотом, пероксидазними нанозимами та мікробними оксидазами…… 247

5.3 Розробка нового фотометричного методу аналізу етанолу на основі АО та нанозимів PtCu, інкапсульованих в альгінатні кульки…….. 267

5.4 Створення амперометричних біонаносенсорів на основі мікробних оксидаз (АО, МАО, АргО) та НЗ – міметиків ПО……..... 277

РОЗДІЛ 6. СТВОРЕННЯ МІКРОБНИХ АМПЕРОМЕТРИЧНИХ БІОСЕНСОРІВ НА ОСНОВІ КЛІТИН, ДОДАТКОВО ЗБАГАЧЕНИХ ЦІЛЬОВИМ ЕНЗИМОМ *IN VITRO*…….. 342

6.1 Конструювання біоелектродів на основі пермеабілізованих клітин дріжджів *O. polymorpha,* збагачених ензимо-нанокомпозитними матеріалами…… 344

6.2 Оцінювання можливості посилення сенсорного сигналу клітин веденням у клітини цільових ензимів за допомогою нанорозмірних носіїв……. 351

РОЗДІЛ 7. СТВОРЕННЯ АМПЕРОМЕТРИЧНИХ БІО(ХЕМО)СЕНСОРІВ ТА ТЕСТ-НАБОРІВ НА ОСНОВІ МІКРОБНИХ ГІДРОЛАЗ: АРГІНІНДЕІМІНАЗИ ТА АРГІНАЗИ І ДЛЯ КІЛЬКІСНОГО АНАЛІЗУ L-

АРГІНІНУ…….. 380

7.1 Створення амперометричних біосенсорів для аналізу L-аргініну за використання амоній-селективних наночастинок Cu/Zn(Hg)S та рекомбінантних деіміназ…….. 383

7.2 Розробка ензиматичних методів аналізу L-аргініну……... 394

7.3 Ензиматичний та біосенсорний аналіз йонів Mn^{2+} і Co^{2+} за використання апоензиму Mn^{2+}-залежної рекомбінантної аргінази……... 435

РОЗДІЛ 8. СТВОРЕННЯ АМПЕРОМЕТРИЧНИХ БІО(ХЕМО)СЕНСОРІВ ТА ТЕСТ-НАБОРІВ ЗА ВИКОРИСТАННЯ РЕКОМБІНАНТНОЇ КРЕАТИНІНДЕІМІНАЗИ ДЛЯ КІЛЬКІСНОГО АНАЛІЗУ КРЕАТИНІНУ…… 444

8.1 Клонування гена мікробної креатиніндеімінази, конструювання ефективного надпродуцента ензиму та опрацювання технології отримання очищеного рекомбінантного ензиму…… 446

8.2 Розробка біосенсорного методу визначення вмісту креатиніну в біологічних рідинах на основі рекомбінантної креатиніндеімінази та наночастинок CoCu…… 455

8.3 Розробка ензиматичного методу визначення вмісту креатиніну за використання рекомбінантної креатиніндеімінази……..……..... 466

РОЗДІЛ 9. УЗАГАЛЬНЕННЯ РЕЗУЛЬТАТІВ ДОСЛІДЖЕНЬ……. 476

ВИСНОВКИ…… 494

СПИСОК ВИКОРИСТАНОЇ ЛІТЕРАТУРИ……... 498

ДОДАТОК. СПИСОК ОПУБЛІКОВАНИХ ПРАЦЬ ЗА ТЕМОЮ ДИСЕРТАЦІЇ……..... 505

ПЕРЕЛІК УМОВНИХ ПОЗНАЧЕНЬ

АБТС	–	2,2-азино-біс(3-етилбензтіазолін-6-сульфонова) кислота, діамонієва сіль
АДІ	–	аргініндеіміназа
Арг	–	аргіназа І печінки людини
АСМ	–	атомно-силова мікроскопія
АргС	–	аргініносукцинат синтаза
АО	–	алкогольоксидаза
ААП	–	4-аміноантипірин
АргО	–	аргініноксидаза
БЕ	–	безклітинний екстракт
Біо-СМ	–	біокарбонові матеріали
БНР	–	безбілкова надосадова рідина
ГО	–	глюкозооксидаза
ГЕ	–	графітовий електрод
ГДГ	–	глутаматдегідрогеназа
ГСІ	–	N-гідроксисукцинімід
ДМО	–	2,3-бутандіон моноксим
ДППГ	–	2,2-дифеніл-1-пікрилгідразил
ЕДК	–	1-етил-3-(3-диметиламінопропіл)карбодімід
Е-СФ	–	ензиматично-спектрофотометричний метод
ЕФ	–	електрофорез
Е-ФЛ	–	ензиматично-флуоресцентний метод
ЕДТА	–	етилендіамінтетраоцтова кислота
ЕТД	–	електрод із трафаретним друком
І	–	сила струму, А
КВ	–	коефіцієнт варіації, %
$К_М$	–	константа Міхаеліса-Ментен, мМ

КФ	–	Комісія по ензимах (використовується перед класифікаційним кодом ензима)
МАО	–	метиламінооксидаза
МЗ	–	мікрозими
МС	–	метиленовий синій
НМВ	–	нижня межа визначення
НЧ	–	наночастинки
НЗ	–	нанозими
ОФА	–	*о*-фталевий альдегід
ПДК	–	піруватфосфат дикіназа
ПО	–	пероксидаза хрону
РСМ	–	рентгеноспектральний мікроаналіз
СБ	–	середовище Беркгольдера
СЕМ	–	сканувальна електронна мікроскопія
СОД	–	супероксидоксидаза
ТЕМ	–	трансмісійна (просвітлювальна) електронна мікроскопія
ТМВ	–	3,3',5,5'-тетраметилбензидину
ФБ	–	фосфатний буфер
ФЦ b_2	–	L-лактат: цитохром *c*-оксидоредуктаза (флавоцитохром b_2)
ЦТАБ	–	цетилтриметиламоній бромід
R	–	коефіцієнт кореляції
L-Arg	–	L-аргінін
n	–	число електронів
N	–	фактор розведення досліджуваного зразка
NAD^+	–	нікотинамідаденіндинуклеотид, окиснений
NADH	–	нікотинамідаденіндинуклеотид, відновлений
N-МГ	–	N-метилгідантоїн

$pH_{опт}$	–	оптимальне значення pH розчину
Pt	–	платиновий електрод
R	–	коефіцієнт кореляції
[S]	–	рівноважна концентрація субстрату, мМ
S	–	площа поверхні електрода, $мм^2$ або $м^2$
S_E	–	швидкість розгортки потенціалу, $мВ \cdot с^{-1}$
t	–	час, с
V*s*	–	об’єм субстратної суміші ензиму, мл
V*e*	–	об’єм аліквоти розчину ензиму, мл
$\xi_{мМ}$	–	мілімолярний коефіцієнт екстинкції, $мМ^{-1} \cdot см^{-1}$

ВСТУП

Сучасна медична діагностика, дослідження в галузі екологічної безпеки навколишнього середовища та безпеки харчових продуктів значною мірою базуються на використанні компонентів та властивостей молекулярного рівня організації живого. Такі актуальні проблеми, як контроль якості питної води та харчових ресурсів, створення надійних та експресних методів діагностики і лікування, часто не можуть бути вирішені традиційними підходами. Існує гостра необхідність у розробці й впровадженні принципово нових методів та технологій, які ґрунтуються на високоспецифічних ензимах, отриманих із традиційних мікробних джерел або рекомбінантних мікроорганізмів.

На сьогодні, одним із досягнень прикладної мікробіології є покращення як існуючих продуцентів біологічно активних сполук, так і конструювання нових генетично модифікованих штамів, здатних до надсинтезу цільових продуктів. Поєднання досягнень у сфері мікробіології, біохімії, генетики, ензимології, біотехнології та мікроелектроніки привело до створення нового класу аналітичних систем — біологічних сенсорів, в яких у ролі біоселективного елемента використовують ензими або генетично-модифіковані організми [1–5]. Головними перевагами біосенсорних підходів є їхня висока чутливість та можливість проведення масштабних досліджень навіть у польових умовах, та порівняно невисока вартість аналізу загалом [6].

Сучасна аналітична біотехнологія використовує різноманітні системи біорозпізнавання, створені природою: ензим - субстрат (кофактор, ефектор - активатор або інгібітор), гормон - рецептор, антиген - антитіло, комплементарні взаємодії нуклеїнових кислот, комплекси, що беруть участь у регуляції експресії генів, сигнальні каскадні комплекси [7]. В останні роки штучні біоміметики – аптамери, абзими, нанозими – також використовуються в ролі біоаналітичних інструментів [8].

До складу біоселективного шару біосенсорів найчастіше входять ензими. Вони каталізують біохімічі реакції і специфічно зв'язуються зі своїми субстратами. Ензими давно стали незамінним інструментом у багатьох хімічних та

біотехнологічних процесах, які широко використовуються у харчовій промисловості, сільському господарстві та медицині [9–10]. Вони характеризуються високою селективністю та надзвичайно високою каталітичною активністю. Однак природні ензими здебільшого мають обмежену хімічну та біологічну стабільність, а також високу вартість через складні технології, що застосовуються для їхнього виділення та очищення з біологічних джерел. Хоча сучасна прикладна мікробіологія та генетична інженерія значно полегшують ці процедури, отримання високоочищених ензимів у комерційних кількостях все ще залишається ключовим викликом для практичної ензимології.

На сьогодні, перспективним підходом щодо розробки електрохімічних біосенсорів є встановлення прямої електронної комунікації між біомолекулами та поверхнею електрода. Це дозволяє створити біосенсори «третього покоління» на основі оксидоредуктаз або їх штучних аналогів – нанозимів.

Нанозими – це найновіший клас функціональних наноматеріалів [11–12], які мають ензимоподібну активність. Порівняно з природними ензимами, нанозими володіють підвищеною стабільністю та більшою доступністю завдяки відносно простим технологіям синтезу. Важлива перевага нанозимів – залежність їхньої активності від розміру/складу наночастинок (НЧ). Це дозволяє створювати нові матеріали з широким діапазоном каталітичної активності, просто змінюючи форму, структуру та склад НЧ. Нанозими (НЗ) також мають унікальні властивості, порівнюючи з іншими штучними ензимами, зокрема велику питому площу поверхні, що значно полегшує їхню подальшу модифікацію та біокон'югацію [13]. Здатність наноматеріалів до спонтанної структурної самоорганізації також є дуже важливою характеристикою для біології та медицини завдяки легшому включенню біологічних компонентів у структуру наноматеріалу.

Завдяки своїй каталітичній активності НЗ можуть застосовуватися в наукових дослідженнях, біотехнології та харчовій промисловості, сільському господарстві, для деградації забруднювачів навколишнього середовища (очищення стічних вод, деградація хімічних бойових речовин), а також у клінічній діагностиці та фармакології [14]. Крім їхнього використання як

діагностичних засобів, нанозими є перспективними каталітичними компонентами терапевтичних препаратів [15]. Завдяки біосумісності та магнітним властивостям деяких нанозимів, їх можна використовувати для локального цілеспрямованого лікування злоякісних утворень. Нанозими можуть слугувати антиоксидантами при лікуванні аутоімунних захворювань, хвороб Альцгеймера та Паркінсона, а також застосовуватись як антибактерійні засоби. Із відкриттям НЗ як штучних ензимів [16–17], стало можливим використання явища прямого електронного перенесення при створенні нанозимних біосенсорів «третього покоління», а також для забезпечення вимог щодо їхньої високої каталітичної активності, хімічної та біологічної стабільності, розміру.

Отже, прості методи синтезу НЗ, їхні унікальні каталітичні властивості, а також здатність до специфічного зв'язування з багатьма біологічними молекулами робить їх привабливими об'єктами для досліджень у біосенсорних технологіях. Зважаючи на актуальність вищезгаданих проблем, основну увагу в дисертаційній роботі приділено синтезу нових наноматеріалів із каталітичною активністю, а саме, штучних ензимів – нанозимів; дослідженню структурних, фізико-хімічних та каталітичних властивостей НЗ у поєднанні їх з мікробними ензимами; вивченню біологічної та можливої токсичної дії (*in vivo*) нанозимних композитів на клітини дріжджів *Ogataea (Hansenula) polymorpha*; кон'югації наноматеріалів з мікробними ензимами та створення на їній основі нових біоаналітичних методів – біонаносенсорних та нанозимно-ензиматичних.

Дисертаційна робота є результатом досліджень, які проведено автором на базі відділу аналітичної біотехнології Інституту біології клітини НАН України, в якому одним із напрямків досліджень є розробка ензиматичних та біосенсорних методів аналізу практично важливих сполук у біологічних рідинах, харчових продуктах та об'єктах навколишнього середовища. Дисертаційна робота відповідає основному плану науково-дослідних робіт відділу і виконувалася в рамках бюджетних тем: "Розробка нових біоаналітичних методів визначення вмісту L- і D-лактату та L-аргініну для діагностики деяких захворювань, контролю їх перебігу" (№ держреєстрації 0113U000142, 2013-2015 рр.), "Створення нових біосенсорних

та ензиматичних методів визначення вмісту креатиніну як біомаркера функціонального стану нирок та контролю процесу гемодіалізу” (№ держреєстрації 0116U002208, 2016-2018 рр.), «Нанозими і наномедіатори: пошук, синтез, характеристика та використання для біосенсорного та ензиматичного аналізу на основі мікробних оксидоредуктаз» (№ держреєстрації 0119U001418, 2019-2021 рр.), комплексної науково-технічної програми фундаментальних досліджень НАН України у 2015 р. «Розробка, тестування та випуск пробної серії ензиматичного набору “Аргітест” для аналізу аргініну в клінічних зразках. Розділ 1. Оптимізація складу набору, умов проведення аналізу та розробка науково-технічної документації» (проєкт 29-2015), цільової програми наукових досліджень НАН України у 2013-2017 рр. “Сенсорні прилади для медико-екологічних та промислово-технологічних потреб: метрологічне забезпечення та дослідна експлуатація” (№ держреєстрації 0112U002963, 2013-2016 рр.), науково-технічної програми «Розумні» сенсорні прилади нового покоління на основі сучасних матеріалів та технологій» в межах наукового проєкту «Створення смарт-сенсорних приладів для аналізу креатиніну та йонів амонію на основі нових нанокомпозитних плівок. Розділ 1. Розробка амперометричного портативного аналізатора, сумісного із сучасними ґаджетами, для визначення креатиніну та йонів амонію» (№ держреєстрації 0118U006259, 2018-2022 рр.) та в рамках конкурсів НФД України "Підтримка досліджень провідних та молодих вчених" (грант 2020.02/0100 «Створення нових нанозимів як каталітичних елементів для ензиматичних наборів та хемо/біосенсорів», № держреєстрації 0120U104115, 2020-2022 рр.) та «Наука для безпеки і сталого розвитку України» (грант 2021.01/0010 «Створення ензиматичного набору та портативних біосенсорів для експрес-аналізу креатиніну – маркера гострих функціональних порушень нирок», № держреєстрації 0123U102859, 2023-2025 рр.). Автор дисертаційної роботи є одним із виконавців вищезгаданих досліджень. Робота виконувалась також у рамках міжнародного наукового гранту НАТО «Наука заради миру»: «Сучасні електрохімічні наносенсори для виявлення токсичних йонів» (SPS(NUKR)SFPP 984173, 2012 – 2016 рр.) та міжнародних індивідуальних проєктів: FEMS-2013 (UA-SMU2013-

1Stasyuk) «The development of the new bioanalytical approaches for L-arginine assay by the use recombinant human liver arginase I and the yeast cells, over-producers of the target enzyme»; FEBS-2022 “Enzymatic biofuel cells and bionanosensors for monitoring of creatinine, a marker of acute functional disorders of the kidneys”, гранту для підтримки молодих вчених провідних вищих навчальних закладів та наукових установ від компанії «ОПТЕК» для проведення наукового дослідження: «The development of the new bioanalytical approaches for L-arginine assay by the use of recombinant human liver arginase I conjugated with nanocarriers» (2014 р.) та стипендії президента України для молодих вчених у 2016-2017 р.

Метою дослідження було вивчення структурних, фізико-хімічних і каталітичних властивостей штучних ензимів – нанозимів у поєднанні з мікробними ензимами для створення на їхній основі нових діагностичних методів, придатних для використання у клінічній діагностиці, фармацевтиці та харчових технологіях, а також вивчення біологічної дії нанозимних композитів на еукаріотичні, зокрема дріжджові клітини.

Для досягнення поставленої мети до завдань роботи входило:

1. Провести синтез і скринінг нових наноматеріалів на псевдоензиматичну активність. Дослідити каталітичні властивості та субстратну специфічність отриманих нанозимів (НЗ).

2. Отримати НЗ із каталазною активністю та дослідити біологічну та можливу цитотоксичну дію «катазимів» на еукаріотичні клітини метилотрофних дріжджів *Hansenula (Ogataea) polymorpha C-105 (gcr1 catX).*

3. Отримати НЗ із редуктазною активністю та протестувати їх на антиоксидантну активність відносно вільних радикалів АБТС$^{\bullet+}$ та DPPH$^{\bullet}$. На основі найактивніших редуктазних НЗ сконструювати амперометричний біосенсор для аналізу вмісту селеніту та протестувати його на реальних зразках.

4. Отримати НЗ із пероксидазною активністю та сконструювати амперометричні біосенсори на основі різних мікробних оксидаз та НЗ як міметиків пероксидази. Створені біоелектроди протестувати для аналізу вмісту етанолу, метиламіну та L-аргініну.

5. Синтезувати нові метал-гібридні наноматеріали та електропровідні полімери селективні до іонів амонію, та сконструювати на їхній основі біосенсори з використанням мікробних деаміназ (аргініндеімінази та креатиніндеімінази) для кількісного аналізу вмісту L-аргініну та креатиніну.

6. Розробити ензиматичні методи кількісного аналізу вмісту L-аргініну із флуоресцентним і спектрофотометричним способом детектування кольорового продукту реакції на основі аргінін-гідролізуючих ензимів: аргінази I та аргініндеімінази.

7. На моделі високоочищеної Манган-залежної рекомбінантної людської аргінази I провести дослідження з отримання препаратів апоензиму, позбавленого металу, та реконструкції холоензиму. Дослідити можливість використання препаратів апоензиму аргінази I для ензиматичного моніторингу вмісту іонів Mn^{2+} та Co^{2+} у зразках стічних вод.

8. Сконструювати амперометричний біосенсор для аналізу вмісту креатиніну за використання рекомбінантної КДІ та НЧ CoCu, чутливих до N-метилгідантоїну, та дослідити можливу структуру утвореного комплексу.

9. Провести апробацію розроблених біоаналітичних підходів на реальних зразках рідин людини, харчових продуктів, стічних вод та фармацевтичних препаратів.

Об’єкт дослідження – очищені препарати мікробних оксидоредуктаз та деаміназ, нанорозмірні матеріали з ензимоподібною активністю; комбінації природних ензимів із нанозимами.

Предмет дослідження – структурно-функціональні та каталітичні властивості наноматеріалів, кон’югованих з ензимами; дія нанозимів на клітини дріжджів; використання синтетичних нанокомпозитів для створення нових біосенсорних та ензиматичних методів аналізу.

Методи дослідження. У роботі використано різноманітні мікробіологічні, генно-інженерні, біохімічні, фізико-хімічні, електрохімічні, аналітичні та біосенсорні методи дослідження. При аналізі активності ензимів та чистоти ензимних препаратів використано методи спектрофотометричного аналізу, електрофорезу білків за нативних та денатуруючих умов, іонообмінна та афінна

хроматографія. Для фізико-хімічного та структурного аналізу наноматеріалів використано методи сканувальної електронної мікроскопії, флуоресцентної мікроскопії, рентгеноспектрального та рентгеноструктурного аналізу, атомно-силової мікроскопії, трансмісійної електронної мікроскопії, динамічного світлорозсіювання, Раман-спектроскопії, спектроскопії ядерного магнітного резонансу, а також метод математичного моделювання фізичної сорбції. При конструюванні амперометричних біосенсорів використано циклічну вольтамперометрію, хроноамперометрію та статистичний аналіз.

Наукова новизна отриманих результатів. Уперше в науковій практиці показано можливість заміни природного ензиму – каталази штучними «катазимами», які повністю відновлюють здатність мутантних безкаталазних клітин метилотрофних дріжджів рости на метанолі. Молекулярно-генетичний аналіз та секвенування локусу геному безкаталазного штаму дріжджів *Ogataea polymorpha* С-105 виявив дві мутації у гені каталази: заміна азотистої основи цитозину (С) у 895 положенні кодуючої послідовності на іншу азотисту основу тимін (Т) та делеція С у положенні 896. Така комбінація веде до зсуву рамки зчитування і утворення стоп-кодону TGA, що спричинює у клітинах штаму С-105 продукцію нефункціонального, неповного протеїну. Уперше показано цитотоксичну дію синтезованих нанозимів (НЗ) на клітини дріжджів *O.polymorpha*. На моделі високоочищеної Манган-залежної рекомбінантної людської аргінази I отримано препарати апоензиму, позбавленого металу, та здійснено реконструкцію холоензиму. Вперше розроблено новий ензиматичний метод на основі апоензиму аргінази I та 2,3-бутандіонмонооксиму для селективного та ультрачутливого визначення вмісту іонів Mn^{2+} та Co^{2+} (на рівні 1 пМ та 2,5 пМ для йонів Mn^{2+} та Co^{2+}, відповідно). Вперше опрацьовано чутливі та селективні ензиматичні методи кількісного аналізу вмісту L-аргініну із флуоресцентним та спектрофотометричним способом детектування кольорового продукту реакції за допомогою *о*-фталевого альдегіду та високоочищених препаратів аргінази I і уреази або аргініндеімінази. Уперше використано поєднання каталітичних наноматеріалів і високоочищених препаратів ензимів класу гідролаз: аргінази I, креатиніндеімінази, аргініндеімінази

при формуванні біоселективних елементів амперометричних біосенсорів на L-аргінін та креатинін. Уперше за використання наноміметиків пероксидази і алкогольоксидази створено нові ензимо-нанозимні методи аналізу вмісту етанолу.

Практичне значення отриманих результатів. Отримано нові нанозимні композити, придатні для біоаналітичного використання. Опрацьовано нові ензиматичні методи та відповідні біоаналітичні набори для визначення вмісту L-аргініну та креатиніну, а також створено прототипи ензимних та мікробних біосенсорів на основі очищених препаратів ензимів класу гідролаз, клітин надпродуцентих штамів дріжджів та метал-гібридних наночастинок.

Опрацьовано нові методи ензиматичного та біосенсорного моніторингу етанолу, L-аргініну, глюкози та метиламіну на основі L-селективних оксидоредуктаз та наноміметиків пероксидази.

За результатами виконання дисертаційної роботи одержано три патенти України на корисну модель (№142490 від 10.06.2020 р.; №107543 від 10.06.2016 р.; №108773 від 25.07.2016 р.), що стосуються розробки ензиматичних методів для кількісного визначення L-аргініну, креатиніну та амонію в біологічних рідинах людини, у харчових продуктах та алкогольних напоях за використання високоочищених препаратів аргінази I, кратиніндеімінази та аргініндеімінази, відповідно.

Особистий внесок здобувача. Роботи здобувачки, представлені в цій дисертації, основані на результатах отриманих нею особисто, або за її безпосередньої участі чи під її керівництвом. Автором проведено науковий пошук і критичний аналіз наявних даних літератури щодо обґрунтування вибору оптимального нанозиму та його поєднання із ензимом для створення біоаналітичних систем, придатних для аналізу вмісту практично важливих сполук. Мету і завдання дослідження, а також планування експериментів, аналіз та обговорення отриманих результатів проведено спільно із д.б.н., проф. М.В. Гончаром. Експериментальні дослідження, результати яких викладені в дисертації, проведено спільно зі співавторами відповідних публікацій.

Апробація результатів дисертації. Основні положення роботи опубліковано у вигляді наукових статей у профільних журналах та представлено у формі тез усних або стендових доповідей на міжнародних наукових конференціях. Результати роботи доповідалися на V Польсько-Українській Вайглівській мікробіологічній конференції **(**Чернівці, Україна, 2013), IV з'їзді Українського товариства клітинної біології (Ужгород, Україна, 2014), V міжнародній науковій конференції молодих учених „Human - Nutrition - Environment" "Biotechnology for sustainable development" (Rzeszow, Poland 2014), XXVII Міжнародній конференції з генетики та молекулярної біології дріжджів (Levico Terme, Italy, 2015), Міжнародній конференції "Актуальні проблеми клітинної біології та біотехнології" (Львів, Україна, 2015), V з'їзді Українського товариства клітинної біології з міжнародним представництвом (Одеса, Україна, 2016), VII Польсько-Українській Вайглівській мікробіологічній конференції (Львів, Україна, 2017), III Міжнародній науковій конференції "Microbiology and Immunology – the Development Outlook in the 21st Century" (Київ, Україна, 2018), Міжнародній конференції "Non-conventional Yeasts: from Basic Research to Application" (Rzeszow, Poland, 2018) та Міжнародній конференції "Advances in Microbiology and Biotechnology" (Львів, Україна, 2018).

Публікації. За темою дисертації опубліковано 59 наукових праць, включаючи 24 статті у фахових виданнях (20 – у закордонних та 4 – у вітчизняних виданнях), з них 16 статей у виданнях, віднесених до першого і другого квартилів (*Q1 і Q2*) відповідно до класифікації SCImago Journal and Country Rank, 6 розділів монографій (4 – у закордонних, із них – 2 огляди належать до *Q1* SCImago та 2 – у вітчизняному виданні), 3 патенти України на корисну модель, 26 тез доповідей на міжнародних наукових конференціях. Сумарний імпакт фактор публікацій за темою дисертації – 90,82.

Структура та обсяг дисертації. Дисертаційна робота є кваліфікаційною науковою працею на правах наукової доповіді за сукупністю статей, викладена на 516 друкованих сторінках. Дисертація складається зі вступу, огляду літератури, розділу матеріалів та методів досліджень, результатів досліджень, узагальнення результатів досліджень, висновків, переліку використаних джерел і додатка.

РОЗДІЛ 1 Огляд літератури

Аналітична біотехнологія – важлива складова сучасної біотехнології, яка пов'язана з використанням біологічних об’єктів (ензимів, тканин, клітин, органел), субмолекулярних комплексів, біомолекул або навіть принципів функціонування живих систем для аналітичних цілей [18]. Значний прогрес аналітичної біотехнології у великій мірі визначається бурхливим розвитком генетичної та клітинної інженерії, ензимології, нанотехнологій та біоелектроніки. Здобутки аналітичної біотехнології використовуються як у фундаментальних дослідженнях, так і в практичних галузях діяльності людини – медицині (діагностика і контроль ефективності лікування та профілактики захворювань), фармацевтичній і харчовій промисловості (контроль якості лікувальних препаратів та харчових продуктів), а також для моніторингу стану довкілля (аналіз токсичних речовин).

Пошук біомаркерів найпоширеніших захворювань та індикаторів для оцінки перебігу і лікування хвороб – пріоритетні напрямки світової науки в галузі аналітичної біотехнології. Серед таких біомаркерів важлива роль належить, зокрема, креатиніну, L-аргініну, L-лактату, глюкозі, етанолу та метиламіну [19]. Більшість із вказаних речовин є природними метаболітами людини, а також складниками багатьох косметичних, фармацевтичних препаратів, миючих та дезінфікуючих засобів. Вміст креатиніну у сироватці крові та сечі є важливим діагностичним біомаркером для виявлення захворювань нирок різного генезу, зокрема гострого хронічного інтерстиціального нефриту, нефрозу, ниркової недостатності, а також інфаркту міокарда [20–21]. Вміст цього метаболіту в діалізаті або ультрафільтраті може слугувати інформативною кількісною оцінкою ефективності гемодіалізу [22]. Аналіз L-лактату широко використовують у молочній галузі харчової промисловості, а також для контролю якості продуктів, які містять солі лактату або саму молочну кислоту як pH-стабілізувальну та консервувальну добавку [23]. У клінічній діагностиці L-лактат є біомаркером при діагностиці гіпоксії, молочнокислого ацидозу, деяких гострих серцевих захворювань, а також ефекту Варбурга для виявлення злоякісних пухлин [24]. Рівень L-аргініну в сироватці крові є важливим клініко-діагностичним індикатором

таких складних захворювань, як астма та туберкульоз легень, гепатокарцинома, меланома, колоректальний рак, ішемічна хвороба серця, серцева недостатність та гіпертензія [25–30]. Вміст етанолу необхідно контролювати у біологічних зразках, оскільки він є важливим маркером для контролю при лікуванні алкоголізму [31–33], тоді як метиламін є прекурсором у виробництві метамфетаміну та діагностичним маркером триметиламінурії [34–35].

Отже, з кожним роком моніторинг довкілля, харчових продуктів, питної води та потреби медицини вимагають більш високочутливих, селективних, швидких та економічних методів аналізу. Саме тому, у опублікованих оглядах нами розглянуто сучасні біоаналітичні підходи щодо кількісного визначення L-аргініну, L-лактату, глюкози, етанолу та метиламіну за використання специфічних до вказаних речовин ензимів, зокрема, аргінази I, флавоцитохрому b_2, глюкозоксидази, алкогольоксидази та метиламіноксидази, відповідно [36–38]. Нами також розглянуто основні принципи, щодо конструювання сенсорних систем для кількісного визначення вмісту креатиніну, у тому числі ензиматичні, на основі використання креатиніндеімінази [39]. В опублікованих оглядах показано роль як ензимів мікробного походження, так і рекомбінантних клітин мікроорганізмів здатних до надсинтезу ензимів біоаналітичного значення.

На сьогодні, основною перевагою біоаналітичних систем є їх виняткова специфічність, що пояснюється надзвичайною селективністю біорозпізнавання на молекулярному рівні. Завдяки цим властивостям, природні ензими найчастіше застосовують при створенні біоаналітичних систем. Протягом останніх років інтенсивні дослідження сфокусовано на створенні штучних ензимів на основі каталітично активних наноматеріалів – нанозимів [40–42] та їх використанні в біосенсориці. Нанозими (НЗ) – це наноматеріали, які виявляють ензимоподібну активність і здатні підсилювати сигнали у біоаналітичних системах [43–44]. Як правило, активність штучних ензимів є нижчою, ніж активність природних ензимів, і їх каталітичні показники в значній мірі залежать від різних чинників: методу синтезу (pH, час реакції та температура) [45]; складу наноматеріалу [46]; форми, розміру, кристалічності та кінцевої морфології [47]; масового

співвідношення компонентів у нанокомпозиті та поверхневої функціоналізації [48]. НЗ виявляють унікальні властивості порівняно з природними ензимами, включаючи велику питому площу поверхні, що значно полегшує їхню подальшу модифікацію та біокон'югацію. Нещодавно встановлено, що вони можуть бути чудовою альтернативою природним ензимам при виготовленні сучасних біосенсорів, а використання НЗ у поєданні з ензимами як компонентів у біоселективному шарі сенсорних систем приводить до покращення аналітичних параметрів та мініатюризації біоаналітичних систем. Синтез НЗ, дослідження їхніх унікальних каталітичних властивостей, а також здатність до зв’язування з багатьма ензимами робить їх привабливими кандидатами для досліджень у біосенсорних технологіях. Усі вивчені, на сьогодні, аспекти синтезу НЗ, їхні властивості та кон’югація з ензимами повно описано в огляді автора [49].

Таким чином, усі оглядові публікації автора охоплюють результати досліджень аналітичних характеристик моноензимних біосенсорів, хемосенсорів, біосенсорних систем та ензиматичних методів аналізу практично важливих речовин. Представлені напрацювання можуть бути основою при розробці та налагодженні промислового випуску конкурентоспроможних вимірювальних портативних приладів чи ензиматичних наборів для експресного та селективного аналізу низки аналітів, що мають діагностичне значення в сучасній клінічній діагностиці та необхідні для контролю якості продуктів харчової та інших галузей промисловості.

Анотація: *Опублікований автором огляд присвячено нанозимам, зокрема, наноструктурованим штучним каталізаторам, які імітують каталітичні властивості природних ензимів. Використання терміну «нанозим» до усіх наночастинок не завжди виправдано. Наприклад, в літературі часто використовують термін «нанозим» для наноматеріалів, які іммобілізовані на електродах і володіють каталітичною активністю лише при подачі електричного потенціалу. Якщо ензимоподібна активність такого матеріалу не доведена в розчині (без застосування потенціалу), такий каталізатор слід називати «електронокаталізатором», а не нанозимом. У цьому розділі нами наведено огляд класифікації нанозимів, їхні переваги порівняно з природними ензимами та їхнє практичне застосування. Особливу увагу приділено методам синтезу нанозимів (гідротермальний та сольвотермічний, хімічне відновлення, золь-гель метод, співосадження, полімеризація/поліконденсація, електрохімічне осадження). Нами також проведено детальний аналіз оцінки каталітичної ефективності нанозимів та дослідження їхніх каталітичних параметрів. Центральна частина огляду присвячена характеристикам нанозимів, які імітують природні ензими аналітичного значення («нанопероксидази», «нанооксидази», «нанолаккази»), та їхньому використанню при конструюванні електрохімічних (біо)сенсорів («нанобіосенсорів»).*

sensors

MDPI

Review

Synthesis, Catalytic Properties and Application in Biosensorics of Nanozymes and Electronanocatalysts: A Review

Nataliya Stasyuk [1], Oleh Smutok [1,2], Olha Demkiv [1,3], Tetiana Prokopiv [1], Galina Gayda [1], Marina Nisnevitch [4] and Mykhailo Gonchar [1,2,*]

1 Institute of Cell Biology, National Academy of Sciences of Ukraine, 79005 Lviv, Ukraine; stasukne@nas.gov.ua (N.S.); smutok@cellbiol.lviv.ua (O.S.); demkivo@nas.gov.ua (O.D.); t.prokopiv@nas.gov.ua (T.P.); galina.gayda@nas.gov.ua (G.G.)

2 Department of Biology and Chemistry, Drohobych Ivan Franko State Pedagogical University, 82100 Drohobych, Ukraine

3 Faculty of Veterinary Hygiene, Ecology and Law, Stepan Gzhytskyi National University of Veterinary Medicine and Biotechnologies, 79000 Lviv, Ukraine

4 Department of Chemical Engineering, Ariel University, Kyriat-ha-Mada, Ariel 4070000, Israel; marinan@ariel.ac.il

* Correspondence: gonchar@cellbiol.lviv.ua; Tel.: +380-32-2612144; Fax: +380-32-2612148

Received: 16 July 2020; Accepted: 7 August 2020; Published: 12 August 2020

Abstract: The current review is devoted to nanozymes, i.e., nanostructured artificial enzymes which mimic the catalytic properties of natural enzymes. Use of the term "nanozyme" in the literature as indicating an enzyme is not always justified. For example, it is used inappropriately for nanomaterials bound with electrodes that possess catalytic activity only when applying an electric potential. If the enzyme-like activity of such a material is not proven in solution (without applying the potential), such a catalyst should be named an "electronanocatalyst", not a nanozyme. This paper presents a review of the classification of the nanozymes, their advantages vs. natural enzymes, and potential practical applications. Special attention is paid to nanozyme synthesis methods (hydrothermal and solvothermal, chemical reduction, sol-gel method, co-precipitation, polymerization/polycondensation, electrochemical deposition). The catalytic performance of nanozymes is characterized, a critical point of view on catalytic parameters of nanozymes described in scientific papers is presented and typical mistakes are analyzed. The central part of the review relates to characterization of nanozymes which mimic natural enzymes with analytical importance ("nanoperoxidase", "nanooxidases", "nanolaccase") and their use in the construction of electro-chemical (bio)sensors ("nanosensors").

Keywords: nanoparticle; nanocomposite; nanozyme; synthesis; catalytic properties; nano-peroxidase; nanooxidase; nanolaccase; electronanocatalyst; amperometric (bio)sensors

1. Introduction: Definition of Nanozymes, Classification, Advantages vs. Natural Enzymes, and Potential Practical Applications

Enzymes are biological catalysts that play a key role in biological processes. They have long been an indispensable tool in many chemical and biotechnological processes that are widely used in food processing, industry, agriculture and medicine. Natural enzymes (except for ribozymes) are proteins and are responsible for almost all biochemical reactions in living organisms. They are characterized by high selectivity and extremely high catalytic activity (Table 1). However, natural enzymes tend to have limited chemical and biological stability as well as a high cost due to complicated technologies employed for their isolation and purification from biological sources. Although modern

molecular technologies (gene cloning, genetic and protein engineering, etc.) significantly facilitate these procedures, obtaining highly purified enzymes in commercial quantities is still a key challenge for practical enzymology.

Table 1. Natural enzymes—biocatalysts of protein origin (except for ribozymes).

Advantages	Drawbacks
An extremely high rate of enzymatic reactions: spontaneous reactions can run for millions of years, while enzymatic ones run for milliseconds. Examples of particularly active enzymes: -Catalase ($2H_2O_2 \rightarrow 2H_2O + O_2$) 1 molecule of the enzyme catalyzes the decay of 5 mln S per 1 min; -Carbanhydrase ($CO_2 + H_2O \Leftrightarrow H_2CO_3 \Leftrightarrow H^+ + HCO_3^-$): 36 mln turnovers per 1 min.	Physicochemical instability to action of environmental (chemical and physical) factors. Biological instability (susceptibility to degradation by proteases).
High selectivity	High costs of isolation and purification.

Artificial substitutes for enzymes were invented toward the end of the twentieth century [1,2]. Artificial enzymes include cyclodextrins with catalytic activity, abzymes (antibodies with catalytic activity), synzymes (synthetic enzymes) and aptamers (DNAzymes and RNAzymes). They are usually more stable than natural enzymes but are inferior in their catalytic activity and preparation costs due to complicated synthesis technologies. As a rule, artificial enzymes are unfortunately not as substrate specific as natural enzymes.

Nanozymes (NZs) are the newest class of functional nanomaterials [3–6] that have enzyme-like activity. They possess increased stability and greater availability due to their simpler preparation technologies. Described nanoscale materials include catalysts with different reaction specificities. They are mainly oxidoreductases: peroxidase [7], haloperoxidase, catalase, glucose oxidase, sulfite oxidase, superoxide dismutase (SOD), laccase, monoxygenase, CO oxidase, ferritin ferrooxidase [8], different hydrolases (phosphatase, phosphotriesterase, chymotrypsin, carbonic anhydrase), as well as proteases, endonucleases, DNA-ases, NO synthases, etc. [9–11].

The term "nanozyme" was defined by Wei and Wang in 2013 [3], although the first exciting discovery of Fe_3O_4-based ferromagnetic nanoparticles (NPs) with peroxidase(PO)-like catalytic activity was made in 2007 by Gao [12], as cited by Huang [6]. In our opinion, Prussian Blue is another nanomaterial candidate for which catalytic activity toward hydrogen peroxide was proven for the first time (see, for example, a review by Karyakin in 2001 [13]).

The most important advantage of nanozymes is their size/composition-dependent activity. This allows the design of materials with a broad range of catalytic activity simply by varying shape, structure, and composition. NZs also have unique properties compared to other artificial enzymes, including large surface areas which significantly facilitate their further modification and bioconjugation. The ability of nanomaterials to self-assemble is also a very important characteristic for biology and medicine, due to easier incorporation of biological components into the nanomaterial's structure (Table 2).

Table 2. Advantages of nanozymes.

(1)	Availability and low preparation costs.
(2)	Physicochemical and biological stability.
(3)	High surface area.
(4)	Self-assembling activity.
(5)	Size/composition-dependent activity. Broad possibility for modification and regulation of activity.
(6)	Compatibility with biological elements.

There is no official classification of NZs. Huang et al. (2019) [6] proposed dividing NZs into two categories: (1) oxidoreductases (oxidases, peroxidase, catalase, superoxide dismutase, and nitrate

reductase); (2) hydrolases (nucleases, esterases, phosphatases, proteases, and silicatein). Such a classification could easily be expanded upon the discovery of novel NZs with other catalytic activities, similarly to other natural enzymes allocated to Enzyme Committee (EC) classes.

Additional problems arise when attempting to classify NZs according to the chemical structure of the catalytic nanocomposite (see Table 1 from [6]). Such classification will be rather cumbersome, due to the broad chemical diversity of NZs. For example, the list of known NZs includes: NPs of noble and transient metals, their hybrid forms, carbon NPs (graphene, carbon nanotubes, fullerene), metal oxides, metal sulfides and tellurides, carbon nitride, quantum dots, 2D-nanomaterials with confined single metal and nonmetal atoms [14], Prussian Blue NPs, polypirrole, hemin micelles and many nanomaterials that have been functionalized or modified by organic ligands [3,5].

In many cases, the term "NZ" or "enzyme-mimicking activity" is used without a sufficiently strong reason. On our opinion, these terms can be used properly only for materials whose enzyme-mimicking activity has been proven in solution. In most papers, the catalytic activity was revealed only after applying a potential to an electrode modified by the tested nanocomposite. In this case, the catalytic nanomaterial should be named an "electrocatalyst" ("electronanocatalyst"), but not, strictly speaking, a "nanozyme" or "enzyme mimic" (Figure 1). We therefore propose naming a catalytic nanomaterial as a "NZ" (nanooxidase, nanoperoxidase, nanocatalase, nanolaccase, and so on) only when the nanomaterial exhibits the enzyme-like catalytic activity in solution/suspension, without applying an electrochemical potential.

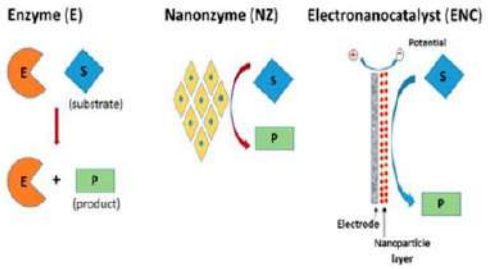

Figure 1. Principal scheme of catalytic action of enzyme, nanozyme and electronanocatalyst.

Although in most cases the catalytic efficiency of NZs is lower compared to natural analogues, it was reported that some NZs can compete with the enzymes. For example, the highest values for any NZ reported to date belong to $MnFe_2O_4$ with a nanooctahedron morphology, whose turnover number (k_{cat}) and catalytic efficiency (k_{cat}/K_M) in the oxidation of 3,3′,5,5′-tetramethylbenzidine (TMB) are 8.34×10^4 s^{-1} and 2.21×10^9 $M^{-1} \cdot s^{-1}$, respectively [15,16].

It is worth noting that in many (or even most) publications, the catalytic activity is presented only by a V_{max} value, without indicating the catalyst concentration. This is problematic, since the V_{max} depends on the catalyst (enzyme) concentration ($V_{max} = [E] \cdot k_{cat}$). In order to compare the intrinsic kinetic parameters of different nanocatalysts with each other or with natural enzymes, a catalytic constant (a turnover number, k_{cat}) must be used, or at least the V_{max} value, but in conjunction with the concentration at which the maximal reaction rate of the nanocatalyst was determined. Valuable recommendations on this problem and standardization of experimental protocols for measurement of enzyme-mimicking activity are presented by Jiang et al. [17].

As a consequence of their catalytic activity, NZs can be applied for practical use in scientific research, biotechnology and food industries, agriculture, degradation of environmental pollutants (wastewater treatment, degradation of chemical warfare agents), clinical diagnostics and pharmacology [6,17–19]. In addition to their use as diagnostic tools, nanozymes are promising catalytic components of therapeutic drugs [6,8–11,20,21]. Due to the biocompatibility and magnetic properties of some NZs, they can be used for targeted treatment of malignancies. NZs have the potential for serving as antioxidants in the

treatment of autoimmune, Alzheimer's and Parkinson's diseases, and for application as antibacterial agents. Using NZs in the construction of biosensors [18,19,22–24] and biofuel cells is very promising, where high catalytic activity, chemical and biological stability, nanoscale size of catalytic elements, and more cost-effective preparation are the most important challenges.

In the future, we can expect a sophisticated design of NZs in silico which will allow them to compete with natural enzymes in catalytic efficiency and selectivity. NZs sensitive to regulation by low-molecular effectors (activators and inhibitors) and able to catalyze cascade reactions will be created, and their catalytic behavior will be adapted to different environmental conditions. Large scale production will also be developed, based on cost-effective physicochemical methods and "green synthesis" approaches.

To date, over 300 types of nanomaterials were found to possess intrinsic enzyme-like activity. A large variety of NZs (or ENCs) simultaneously exhibit dual- or multienzyme mimetic activity [10]. Several reviews that summarize the new data concerning synthesis, characterization, bioanalytical and medical application of NZs are published every year, and the number of these reports is rising in a geometrical progression [10,23,24]. Thus, "nanozymology", as a new field of science connecting nanotechnology and enzymology, has great potential for further development and for many practical future applications [10,17].

The current paper is devoted to reviewing the recent advantages and current challenges of using NZs (or electronanocatalysts) as catalytic and recognition elements in biosensors. The catalytic performance of NZs is characterized, a critical point of view on catalytic parameters of NZs described in scientific papers is presented, and typical mistakes are analyzed. The central part of the review relates to characterization of NZs which mimic natural enzymes with analytical importance ("nanoperoxidase", "nanooxidases", "nanolaccase") and their use in the construction of electro-chemical (bio)sensors ("nanosensors").

2. Methods for the Synthesis of Catalytic Nanomaterials

Catalytic nanomaterials are known to possess unique properties compared with natural enzymes [25]. It was shown that activities of NZs are greatly dependent on the chemical structure, particle size, shape and surface morphology, which could be affected by charges, coatings, dopings, loadings and external fields. The morphology of synthesized NZs can be controlled due to rapid development of nanotechnology techniques [16,26].

This section summarizes different methods for preparation of nanomaterials possessing catalytic, mainly electrocatalytic, properties, in particular hydrothermal and solvothermal methods, co-precipitation and sol-gel methods, etc. Their applications for construction of biosensors are also described. Figure 2 presents the principal scheme illustrating methods of nanocatalyst synthesis. The kinetic parameters for different types of nanocatalysts are summarized in Tables 3–11. Table 3 relates to the effect of synthetic methods on the structural and functional properties of ENCs.

Figure 2. Principal scheme of the methods for nanocatalyst synthesis.

2.1. Hydrothermal and Solvothermal Methods

The main characteristics of the obtained NZs can be changed in accordance with the method chosen for NZ synthesis. The most promising techniques for synthesizing nanomaterials are the hydrothermal and solvothermal methods. Low-cost nanocrystals with well-controlled dimensions can be obtained using the proposed approaches [26].

A series of spinel-type Co_xNi_1-xFe_2O_4 (x = 0, 0.2, 0.4, 0.5, 0.6, 0.8, 1.0) nanocatalysts were synthesized using the solvothermal method, where ethylene glycol served as the solvent. The obtained NZs were employed as enzyme mimics for the detection of H_2O_2. The $Co_{0.5}Ni_{0.5}Fe_2O_4$/CPE exhibited a wider linear range and a higher sensitivity compared with H_2O_2-selective enzymatic biosensors based on spinel-type ferrites, indicating a promising future for Co_xNi_1-xFe_2O_4 as enzyme mimics for the construction of chemosensors [27]. The surface morphology of the synthesized Co_xNi_1-xFe_2O_4 ENCs was studied and a diameter of 70 to 130 nm was observed. The small size of the nanocatalysts greatly increases the effective surface area for electrocatalytically active sites, and thus improves the physicochemical properties of the amperometric biosensor [27] (Table 3).

Solid spherical crystals of CuO (CuO-ENCs) having an average size of 45 nm were prepared by thermal decomposition of a precursor-Cu-based metal-organic gel (Cu-MOG). It was shown that the obtained CuO-ENCs possessed high electrocatalytic activity in glucose oxidation and exhibited PO-like catalytic ability. The CuO-ENC can also be used as a biomimetic for detection of cholesterol [28]. CuO-ENCs have high Brunauer-Emmett-Teller (BET) surface area of 20.16 $m^2 \cdot g^{-1}$, high pore volume of 0.11 $cm^3 \cdot g^{-1}$ and the average pore diameter of ~2.5 nm [29]. In another example, two kinds of carbon-based nanocatalysts with a size of 100–150 nm were synthesized using a combination of two methods, a thermal method and a solid-state reaction, from the zeolitic imidazolate framework-8 (ZIF-8) [30,31]. The carbon cubic nanomaterial (labelled HCC) with the hollow structure was obtained by chemically etching ZIF-8 with tannic acid, followed by a calcination process. The carbon cubic nanomaterial with the porous surface (labelled PCC) was obtained by direct pyrolysis. The two types of synthesized NZs, HCC and PCC, possess a BET specific surface area of 356 and 756 $m^2 \cdot g^{-1}$, respectively [30].

Electrochemical detection of glucose and fructose based on gold nanoparticles (AuNPs) deposited onto graphene paper has recently been proposed. These nanostructures were synthesized via two approaches: thermal and laser dewetting processes [32]. Gold nanostructures obtained by both methods exhibited major differences in their particle morphology. Both types of AuNPs were examined by their ability to oxidize glucose and fructose. The corresponding analytical characteristics of the constructed chemosensors are presented in Table 3.

It was shown that the BET of PCC was higher than that of HCC, indicating that PCC had more specific area for analyte adhesion (Table 3) [30].

The gold/cobalt (Au/Co) bimetallic nanocomposite-decorated hollow nanoporous carbon framework (Au/Co@HNCF) was synthesized as an ENC by thermal pyrolysis at 900 °C of the Au (III)-etching zeolitic imidazolate framework-67 (ZIF-67) [33]. An ultrasensitive electrochemical biosensor was developed to identify low levels of uric acid in human serum. Scanning electron microscopy images showed that the Au (III)-etching ZIF-67 has a dodecahedron shape (Table 3). The Au/Co@HNCF biosensor (7.88 cm^2) exhibited a significantly higher electrochemical active surface area than the bare glassy carbon electrode (GCE, 0.0155 cm^2), indicating the existence of abundant active sites on the Au/Co@HNCF modified layers.

2.2. Chemical Reduction

Chemical reduction is the most frequently used method, due to its rapidity and simplicity. This technique enables producing NPs in which the morphology and particle size distribution are controlled by changing the molar concentration of the reactants, the reductant type and the reaction temperature [34]. The critical factor in achieving high chemical reduction is choosing the appropriate reductants. Reduction of metal salts requires reactivity of the reduction agent to the redox potential

of the metal. The obtained particles are small if the reaction rate during the synthesis process is too fast [35]. However, if the reaction rate is too slow, particle aggregation may occur [36]. The synthesis of hollow copper sulfide nanocubes (h-CuS NCs) was conducted via the chemical reduction method [37]. The average particle size was 50 nm and the specific surface area was 57.84 $m^2 \cdot g^{-1}$, which is larger than that of general solid CuS (34.76 $m^2 \cdot g^{-1}$). h-CuS NCs exhibited promising signs for high enzyme-mimicking catalytic activity (Table 3).

The chemical reduction method has been used for the synthesis of a peroxidase (PO)-like NZ based AuNPs in combination with *Pseudomonas aeruginosa*–specific aptamer [38]. The average particle size was ~20 ± 3 nm. The proposed bioelectrode structure can be used for detection of other bacterial pathogens in water or biological fluids.

ENC-carbon supported Pt-NiNPs stabilized with oleylamine (Pt-Ni) were synthesized by chemical reduction of metal salts [39]. The synthesized ENCs were near-spherical in shape, with a mean diameter of 8.4 nm. The ENCs exhibited an active electrochemical surface area of 2.3 $m^2 \cdot g^{-1}$, which is lower than that of the etched particles without surfactant (Table 3).

Metal-organic frameworks (MOFs) are composed of metal ions as nodes and organic ligands as linkers and have diversified and tailorable structures. MOFs have high surface area and porosity, exposed active sites and good biocompatibility, and for these reasons they attact wide attention as a blooming alternative material. A multifunctional artificial enzyme was synthesized through a combination of the chemical reduction method and electrodeposition technique by modifying PtNPs on the metalloporphyrin MOF [40]. In the Pt@PMOF(Fe) complex, PMOF(Fe) could prevent the aggregation of PtNPs, leading to high stability of the Pt NPs. Furthermore, PtNPs exhibited catalase-and PO-like activities. In another example, oxidase-like nanosheets were prepared [41] using the chemical reduction method modified by Hummers et al. [42], in which histidine enantiomers served as both a reducing agent and a protecting ligand. Compared to the previously developed strategies, this synthesis method is very rapid and mild and does not require heating, pressuring, and special media. It is a mild synthesis strategy, where only two reactants of $HAuCl_4$ and the His enantiomers are involved, without additional catalysts or templates. The oxidase-like and electrocatalytic activity of His@AuNCs/RGO was evaluated for the determination of nitrite (Table 3). The developed method was used for the detection of nitrites in real samples [41].

The green synthesis procedure was recently proposed as an important method for producing inorganic NZs. It is well known that living organisms can produce substances that act as reducing agents [6,11,16]. For example, Han et al. proposed a new environmentally friendly technology for synthesis of MoO_3 NZs in which green algae (*Enteromorpha prolifera*, EP) were used as the reducing agent [43]. The obtained MoO_3 NZs revealed excellent PO-like activity and were used, together with GOx, for colorimetric detection of glucose in human serum. In another work, Han and co-authors [44] used bovine serum albumin (BSA) as a biotemplate for Co_3O_4 NZs synthesis. The obtained NZs had a spherical morphology with an average diameter of 60 nm and exhibited catalase-like activities.

2.3. Sol-gel Method

In this method, a gel-like network containing both a liquid phase and a solid phase is formed. The crystallinity, morphology and magnetic properties of the NZs can be controlled by choosing an appropriate complexing agent, concentration and type of chemical additives, and temperature conditions [28].

The synthesis of PtNPs polyaniline (PAni) hydrogel heterostructures was performed via the sol-gel method [45]. Phytic acid was used as a complexing agent. The PtNPs loaded into the hydrogel matrix were found to act as active catalysts for the oxidation of H_2O_2. The obtained PtNP/PAni hydrogel had a 3D hierarchical structure consisting of connected PAni nanofibers with diameters of approximately 100 nm (Table 3). The porous structure of the PAni hydrogel allows immobilization of concentrated enzyme solutions. Since water-soluble molecules can penetrate through the hydrogel, the PtNPs preserve their ability to catalyze glucose oxidation.

2.4. Co-Precipitation

Co-precipitation is a fast method for the synthesis of different types of nanocatalysts. Co-precipitation is an excellent choice when higher purity and better stoichiometric control are required [46]. Xuan Cai et al. [47] prepared two kinds of nanomaterials by applying the co-precipitation synthesis method: carbon spheres (Mn-MPSA-HCS) and hollow carbon cubic materials (Mn-MPSA-HCC) with a size of 100 to 200 nm, respectively, for $O_2^{\bullet-}$ sensing (Table 3). Physicochemical characterization of the obtained nanocatalyst demonstrates that the $Mn_x(PO_4)_y$ monolayer was homogeneously dispersed on the surface of the carbon structures without visible size or morphologies, thus providing numerous active sites for reaction of analytes. The proposed method can be adapted as a universal strategy for fabricating transition metal phosphates with all kinds of shapes and sizes for different applications and is particularly promising for biosensing. In another example, Dashtestani et al. [48] used a combination of two methods for nanocomposite synthesis: chemical reduction of $HAuCl_4$ and co-precipitation of the obtained gold nanoparticles (GNPs) with the copper(II) complex of cysteine (GNP/Cu-Cys). The combination of GNPs and Cu-Cys complex increased the electrochemical signal toward $O_2^{\bullet}$ (Table 3).

The sensitive electrochemical biosensor based on dual aptamers was proposed for detection of cardiac troponin I (cTnI). The biosensor included DNA nanotetrahedron (NTH) capture probes and multifunctional hybrid nanoprobes. First, the NTH-based Tro4 aptamer probes were immobilized on a screen-printed gold electrode (SPGE) surface through the Au–S bond. Then, the hybrid nanoprobes were prepared using magnetic Fe_3O_4 NPs as nanocarriers for immobilization of a cTnI-specific Tro6 aptamer, horseradish peroxidase (PO), PO-mimicking Au@Pt nanozymes and G-quadruplex/hemin DNAzyme [49]. The constructed sensor exhibited a wide linear concentration range (10 pg·mL^{-1} to 100 ng·mL^{-1}) and a low LOD (7.5 pg·mL^{-1}) for cTnI (Table 3).

2.5. Polymerization and Polycondensation

NZs can be obtained either by using insoluble polymers or by cross-linking of a soluble polymer [50]. Mesoporous SiO_2–L-lysine hybrid nanodisks were synthesized by Han et al. [51] via hydrolyte polycondensation of tetraethylorthosilicate in the presence of CTMB and L-lysine. The prepared hybrid nanodisks have a high surface area (570 $m^2 \cdot g^{-1}$) and ordered mesopores with a size of about 2.9 nm. The obtained hybrid nanodisks possessed excellent biocompatibility to L-lysine. An electrochemical biosensor for superoxide anions ($O_2^{\bullet-}$) was constructed based on this result.

In another example, Santhosh et al. [52] synthesized composite core-shell nanofibers consisting of gold NPs on poly(methylmethacrylate) (PMMA) by the combination of an electrospinning technique and in situ polymerization of aniline. The average diameter of the PMMA fibers was 400–500 nm. The surface of the fibers was fairly smooth and randomly oriented. The proposed core-shell fibers were used for electrochemical detection of the superoxide anion ($O_2^{\bullet-}$).

2.6. Electrochemical Deposition

Electrochemical deposition is a low-cost method for obtaining metal nanocatalysts. However, it is usually used less often than chemical reduction methods [53]. The process is simple and includes an immersion of a conductive surface into a solution containing ions of the material to be deposited and application of a voltage across the solid/electrolyte interface. In the course of this procedure a charge transfer reaction causes the film deposition [54]. The disadvantage of this method is in impossibility of controlling the morphology. However, it has certain advantages: (1) short synthesis time; (2) absence of chemical reductants or oxidants; (3) absence of undesired byproducts [55]. Electrodeposition is applied using different electrochemical techniques: cyclic voltammetry, potential step deposition method and double-pulse deposition [56]. The particle size can be controlled by adjusting the current density or applied potential and the electrolysis time [57]. Electrodeposition is used for synthesis of nanostructural materials with and without templates. Templates utilized for electrodeposition include porous membranes with a 1D-channel, liquid crystal materials and surfactants [58].

Table 3. Preparation and properties of nanocatalysts and corresponding electrochemical biosensors.

Mimetic Enzyme	Enzyme-Like Activity	Preparation Method	Pore Diameter, nm	Shape	Particle Size, nm	BET, $m^2\ g^{-1}$	Potential, V	Detection	Linear Range, μM	LOD, μM	References
Au/Co@HNCF	Urease	Thermal	1.2	Dodeca hedron	300–400	7.88	+0.3	Uric acid	0.1–2500	0.023	[10]
$Co_{0.5}Ni_{0.5}Fe_2O_4$	PO	Solvothermal		Sphere	70–130		+0.5	H_2O_2	0.01–1000	0.001	[25]
SOD/mesoporous SiO_2-(L)-lysine	SOD	Hydrolyte polycondensation	3	disk	40–70	570	0.05		3.11–177	800	[27]
SOD/PMMA/PANI-Au	SOD	Electrospinning/polymerization		fiber	400–500		0.3		0.5–2.4	300	[28]
CuO-NZs	GOx	Thermal	2.5	Sphere	~45	20.16	+0.55	Glucose	5–600	0.59	[29]
	PO							Cholesterol	1–15	0.43	
GOx/PtNP/PAni/Pt		Sol-gel method		Sphere/fiber	2/100		+0.56	Glucose	10–8000	0.7	[43]
HCC/SPCE	SOD	Solid statereaction		Hollow cubic	100–150	356	−0.5	Superoxide-anion O_2^-	0–192	0.207	[30]
PCC/SPCE		Thermal		hexahedral		756			192–912	0.140	
									0–112		
									112–1152		
							+0.17	Glucose	20–8000	2.5	
Graphene paper/AuNPs	GOx	Laser		Sphere	10–150		+0.5	Fructose	40–4000	≥20	[32]
		Thermal		Plate	200–400		+0.19	Glucose	15–6000	2.5	
							+0.4	Fructose	5–4000		
								Glucose	$10–1·10^4$		[37]
PCC/SPCE	Ox	Thermal		Sphere	20 ± 3		+0.4	*P. aeruginosa*	60.0–6.0 × 10^7 CFU/mL	60.0 CFU/mL	[38]
AgNP/NCF/GCE	SOD CAT, PO Ox	Thermal/Electrodeposition		sphere/fiber	15–20/5–8 μm		−0.5		$6.96·10^{-11}$–72	$1.66·10^{-4}$	[38]
			~2	Sphere	8.4	2.3	0.04–1.0	Oxygen reduction			[39]
Pt@PMOF(Fe)		Chemical reduction/Electrodeposition		Ellipsoid	300		−0.45	Glucose	100–10,000	6	[40]
His@AuNCs/RGO-GCE		Chemical reduction		Sheet	1.72		+0.8	Nitrite	1.0–7000	0.5	[41]
GOx/PtNP/PAni/Pt		Sol-gel method		Sphere/fiber	2/100		+0.56	Glucose	10–8000	0.7	[43]
Mn-MPSA-HCC	GOx	Co-precipitation		Hollow cubic	100–200		+0.75				[47]
Mn-MPSA-HCS				Hollow sphere					0–1260	0.001	
AuNPs/Cu-Cys		Chemical reduction/Co-precipitation		sphere	77		0.25		3.1–326	2.8	[48]
Fe_3O_4/Au@Pt-HRP-DNAzyme@Co6	PO	Co-precipitation		Sphere	158		−0.25		$4.2·10^{-15}$–$4.2·10^{-9}$	$3.1·10^{-15}$	[49]
GCE/MWCNTs–Au/RuNPs/bsaGOx		Drop-coating/Electrodeposition		Tubes/sphere	1000		−0.05	Glucose	20–1230	3.3	[59]
nPtRu/AO		Electrodeposition		Sphere	5–150		−0.1	Ethanol	25–200	2.5	[60]
nPtRu/AMO								Methylamine	20–600	3	

Gallay et al. [59] prepared a hybrid nanocomposite using the electrochemical electrodeposition of RuNPs on the surface of avidin-functionalized multiwalled carbon nanotubes by applying a potential of −0.600 V for 15 s in a 50 ppm ruthenium solution under stirring. The nanohybrid-electrochemical interfaces had excellent PO-like properties toward H_2O_2 (Table 3).

A simple method for the electrochemical detection of methylamine and ethanol in real samples of food and alcoholic beverages using PtRu NZ as artificial PO was reported recently [60]. PtRuNPs were synthesized on the surface of a graphite electrode (nPtRu/GE) by electrodeposition of 1 mM $RuCl_3$ and a H_2PtCl_6-containing solution using the method of cyclic voltammetry in the range of −1000 to +1000 mV with a scan rate of 50 mV·min^{-1} during 10 cycles. The resultant nPtRu/GE turned dark brown-golden due to the formation of nPtRu. Morphological properties of the PtRu-film were studied. It was shown that the average thickness of the deposited layer was 60 nm and it was proven that the obtained layer was nanosized.

Electrosynthesis of AgNP/NCF/GCE was performed by a combination of thermal reduction and electrodeposition methods through thermal synthesis of an electroconductive nitrogen-doped cotton carbon fiber composite (NCF) followed by electrodeposition of AgNPs onto NCF [61]. The developed AgNP/NCF/GCE electrode exhibited outstanding performance toward $O_2^{\bullet-}$, with a wide linear range and a super-low detection limit.

As mentioned, the applied nanocatalyst synthesis methods can influence their structural and physical properties [25,62–64]. The effect of different synthesis methods on structural properties of ENCs with electrocatalytic interfaces are presented in Table 3.

3. Catalytic Performance of Nanozymes

Development of new nanocatalysts, including NZs, with higher catalytic activity expands their applications in bioanalytics. As a rule, the activity of NZs is lower than that of enzymes and their catalytic performance strongly depends on: (1) the method of synthesis (pH, reaction time and temperature) [25]; the composition of the nanomaterial [16,65]; the shape, size, dispersity and final morphology [66]; the mass ratio of the components in the nanocomposite [67]; and surface functionalization [40,68–70].

The catalytic performance of NZs, as well as their efficiency, is quantitatively estimated by kinetic properties: K_M, V_{max} (at a defined nanocatalyst concentration), k_{cat}, k_{cat}/K_M ratio, IC_{50} and morphological characteristics: specific BET surface areas, pore volume, pore diameter, crystallite size.

The enzyme mimics follow Michaelis–Menten kinetics, which is similar to natural enzymes. It has been found that the activity of NZs is strongly dependent on the pH, temperature and substrate concentration. The rate of the reaction is generally determined by the reaction extent as a function of time. It is known that K_M and k_{cat} are two key parameters for quantifying the catalytic ability of an enzyme, where K_M characterizes the affinity of the enzyme to its substrate. The main manifestation is that low K_M values reflect high affinity of the enzyme for the substrate. V_{max} describes the reactivity of the enzyme (at a fixed concentration) when saturated with the substrate. K_M and k_{cat} are therefore among the important reference standards for judging the superiority of an enzyme vs. a NZ [27]. Different substrates (chromogenic, fluorogenic or chemiluminescent) are used for experimental detection of the enzyme-like activity of NZs. It was shown that His@AuNCs/reduced graphene oxide (His@AuNCs/RGO) exhibits phenol oxidase mimic activity and possesses a low K_M value (0.031 mM) with a V_{max} value of 6.55×10^{-8} M·s^{-1} at a nanocatalyst concentration of 8.28 mg·L^{-1}. Of the other four synthesized types of AuNCs, the best catalytic performance for oxidizing TMB was shown for the His@AuNCs/RGO variant. It was assumed that His@AuNCs react via enzyme-like catalytic centers, when substrates and active sites of His@AuNCs are located on the RGO sheets. The "co-interaction" between the His@AuNCs and RGO increases the speed of electron transfer from TMB to oxygen, leading to enhanced catalytic activity [41].

In another example, the catalytic steady-state kinetics for $CoFe_2O_4$ CF300 was estimated using TMB and H_2O_2 as substrates [71]. It was shown that the PO-like reaction followed a Michaelis-Menten

kinetics toward both substrates. The K_M^{aPP} for TMB of the CF300 is 0.387 mM, which is practically the same as reported for PO (0.434 mM). The K_M for H_2O_2 of the CF300 is 8.89 mM, which is two-fold higher than for PO (3.7 mM), showing that CF300 has a lower affinity for H_2O_2.

Although in most cases the catalytic efficiency of NZs is lower compared to natural analogues, it was reported that some NZs can compete with the enzymes. For example, the highest values for any NZ reported to date belong to $MnFe_2O_4$ with a nanooctahedron morphology (see Introduction) [14,15].

Three-dimensional nanomaterials, containing confined single atoms, possess increased catalytic activity due to mutual effects of unique geometric and electronic structures of the matrix and intrinsic catalytic activity of confined atoms [65]. Shackery and coworkers [72] recently prepared a glucose oxidase-like catalyst based on cobalt hydroxide [$Co(OH)_2$] nanorods on a 3D-graphene network using the chemical deposition method. The obtained nanocomposite was used for glucose detection. It was demonstrated earlier that the redox reaction of $Co(OH)_2$ at the graphene surface is a diffusion-controlled electrochemical process [73]. Oxidation of $Co(OH)_2$ to CoOOH is reflected by the peak at ~0.445 V (vs. Ag/AgCl), and the reverse process corresponds to the cathodic peak at around ~−0.08 V (vs. Ag/AgCl). A possible electrochemical reaction is as follows:

$$Co(OH)_2 + OH^- \xleftarrow{\text{Oxidoreduction}} CoOOH + H_2O + e^-$$

The constructed amperometric sensor demonstrated a high sensitivity for glucose (36,900 $A \cdot M^{-1} \cdot M^{-2}$) and a very low LOD (16 nM).

In another example, it was shown that octahedral cuprous oxide (Cu_2O) in combination with carbon quantum dots (CQDs) could be an efficient electrocatalyst for the detection of glucose [74], The CQDs/octahedral Cu_2O showed higher electrocatalysis for glucose oxidation and H_2O_2 reduction than the octahedral Cu_2O. The cyclic voltammograms showed an oxidation peak at +0.6 V reflecting the conversion of Cu(II) to Cu(III) and showing high electrocatalytic ability for oxidation of glucose by the CQDs/octahedral Cu_2O [75]. Equations (1)–(5) of the electrocatalytic oxidation reaction are presented in Figure 3.

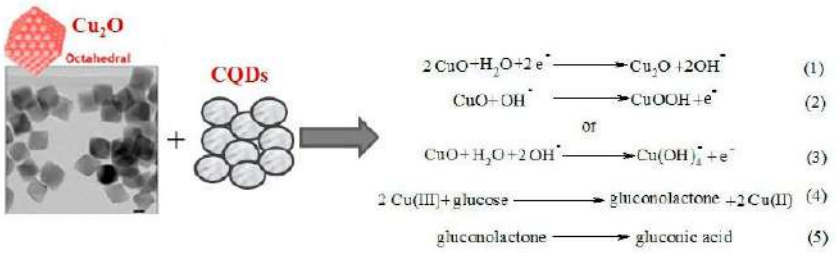

Figure 3. Carbon quantum dots/octahedral Cu_2O nanocomposites for non-enzymatic glucose assay.

Pirmohamed et al. [76] showed that nanoceria (CeNPs) is a redox active catalyst which possesses two oxidation states (Ce^{+3}/Ce^{+4}) and contains transportable lattice oxygen located on its surface which facilitates the interchangeable conversion of Ce^{+4} and Ce^{+3}. Hayat et al. [77] found that the dual oxidation state and high mobility of surface oxygen are responsible for the oxidase-like activity of CeNPs toward phenolic compounds. It was shown that CeNPs exhibits the lowest K_M^{aPP} value: 0.25 μM for dopamine and 180 μM for catechol, among the other nanomaterials (Table 10). For comparison, the K_M^{aPP} values of the optimized enzymatic reaction using tyrosinase under the same reaction conditions were 0.3 μM and 200 μM for dopamine and catechol, respectively.

Another quantitative characteristic that evaluates the effectiveness of NZs is the half maximal inhibitory concentration (IC_{50}), reflecting the ability of a substance to inhibit certain biological or biochemical functions. A nanocomposite based on gold NPs and the copper(II) complex of cysteine

(GNPs/Cu-Cys) was synthesized by Dashtestani and colleagues [48]. The SOD mimetic activity of a Cu-Cys and GNPs/Cu-Cys nanocomposite was determined using the pyrogallol autoxidation inhibition assay. The half-maximal inhibitory concentration of the nanocomposite was 0.3 $\mu g \cdot mL^{-1}$, which is 3-fold higher than that of the native enzyme. However, the authors did not indicate how the concentrations of both catalysts were normalized. The IC_{50} values of the compounds indicate that all individual components related to the GNPs/Cu-Cys nanocomposite exhibited SOD mimic activity.

The enzyme-like activity can be controlled by the shape, size, crystallinity and final morphology of the NZs [78–80]. Liu et al. [79] showed that different nanocrystalline shapes had different PO-like activities. The activities of the NZs in descending order according to shape, can be presented in the following order: cluster spheres > triangular plates > octahedral. The activity depends on the exposure of catalytically active iron atoms or crystal planes. Two kinds of nanomaterials for $O_2^{\bullet -}$ sensing were prepared: hollow carbon spheres and hollow carbon cubic nanomaterials with a size of 100 to 200 nm, respectively [47]. The electrochemical sensor prepared using the hollow carbon sphere NZ exhibited an extremely low detection limit of 1.25 nM and was successfully employed in the dynamic monitoring of $O_2^{\bullet -}$ released from HeLa cells (Table 3). In another example, a detailed study for investigating the effects of particle size and morphology on the PO-like catalytic activity of magnetic cobalt ferrite ($CoFe_2O_4$) was performed [81]. $CoFe_2O_4$ NZs having different shapes (near corner-grown cubic, near cubic, polyhedron and star-like) were synthesized when varying the amounts of iron and cobalt acetylacetonates precursors and changing the reaction temperature. To increase the suspensibility of NPs in water solution, the obtained $CoFe_2O_4$ were modified with PEG-3,4-dihydroxybenzylamine. The catalytic activity was structure dependent (in descending order according to a shape): spherical > near corner-grown cubic) > star like > near cubic (> nanopolyhedrons. The kinetic studies of the obtained $CoFe_2O_4$ showed that star-like shaped $CoFe_2O_4$NPs with 4 nm-sized had the highest affinity for TMB and H_2O_2 compared to the other NPs obtained in the study [81].

The affinity of the NZs to substrates can be changed by a procedure of surface functionalization [82]. Ling et al. recently synthesized a new artificial nanocatalyst based on metalloporphyrinic metal organic frameworks (PMOF(Fe)) and PtNPs [83]. It was shown that Pt@PMOF(Fe)NPs showed high activity toward the oxidation of o-phenylenediamine (OPD) as a chromogenic substrate and H_2O_2 as the oxidant. This mechanism can be summarized in the following reaction:

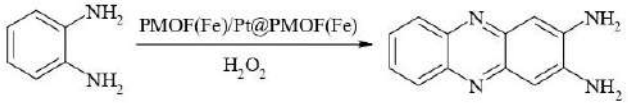

It was found that when Pt@PMOF(Fe) was mixed with H_2O_2 and OPD, the Fe center provided an electron to PtNPs forming high-valence Fe, due to the synergistic effects between PMOF and PtNPs, and the compound, which included Fe(IV) = O and a porphyrin π cation radical, generated via the reaction between Fe(III) and H_2O_2. OPD then was easily oxidized. Thus, PtNPs enhanced the PO-like activity of Pt@PMOF(Fe) [40].

The mass ratio (Ni-MOFs to Fe-MOFs) is one of the crucial factors influencing the catalytic activity of nanocatalysts. The catalytic performance of Fe-Ni-*n* (where *n* is the mass ratios) was explored by optimizing the mass ratios (Ni-MOFs@Fe-MOFs). Due to differences in the morphology and specific surface area of Ni-MOFs and Fe-MOFs, the optimal load of Ni-MOF nanosheets on octahedral Fe-MOFs was realized with the increase in *n*. When $n = 2$, the nanosheets and octahedron achieve relatively sufficient mixing. However, the *n* value is too small for the nanosheets to adequately cover every surface of the octahedrons. On the other hand, if the n is too large, there would be extra nanosheets that are not coated on the octahedrons [67].

It was shown that the activity of nanocatalysts is strongly dependent on their composition. PtRuNP alloy with a suitable degree of alloying (e.g., $Pt_{90}Ru_{10}$) can mimic oxidase (ferroxidase), PO,

SOD and catalase. These enzyme-like activities correspond to the redox enzymes: oxidase and PO which catalyze oxygen and H_2O_2 reduction, respectively, and SOD and catalase which are responsible for disproportionation of superoxide and H_2O_2 decomposition, respectively. It was found that varying the composition of PtRu alloys affects their ability to facilitate electron transfer, since these reactions involve a transfer of electrons. Such dependence on the alloy composition was observed for all four enzyme-like reactions [66].

A fast, effective and low-cost method for production of $ZnFe_2O_4$ nanoparticle-decorated ZnO nanofibers using co-electrospinning and the sequence annealing process has recently been proposed [83]. It was shown that the presence of $ZnFe_2O_4$ NPs on the surface of ZnO nanofibers and formation of heterostructures significantly improved the PO-like activity compared with $ZnFe_2O_4$ NPs. Furthermore, the smaller-sized NPs had a higher activity. The obtained results suggest that the surface-to-volume ratio, the composition and the size of the NZs play a critical role in their catalytic activities [84].

4. Nanozymes as Peroxidase Mimetics

Peroxidases (PO, E.C. 1.11.1.7) are oxidoreductases from a variety of sources, including plants, animals and microbes, that contain an iron-porphyrin derivative (heme) in their active site and catalyze the oxidation of diverse organic compounds using H_2O_2 as the electron acceptor. Some of the most popular PO substrates with the highest chromogenic ability are 3,3′,5,5′-tetramethylbenzidine (TMB), 2,2′-azinobis[3-ethylbenzothiazoline-6-sulfonic acid] (ABTS) and *o*-phenylenediamine (OPD).

In the catalytic process, the Fe of the heme of natural PO provides H_2O_2 dissociation by changing the Fe(III) to the Fe(IV) valence state in an intermediate with high oxidative activity. The enzyme's oxidative activity enables realization of the catalytic cycle. Therefore, if a nanomaterial is able to cause a similar electron transfer, it can be called a NZ with PO-like activity ("nanoperoxidase"). Due to the high reduction potential of POs, they are very promising for use as bioelectrocatalysts in biosensorics, fuel cell technology as well as environmental biotechnology. Despite the benefits of POs, their wide usage is still restricted, due to their fast inactivation in the presence of H_2O_2 under native physiological conditions. Their low thermal and environmental stability reduces the possibilities for their practical application. Screening the highly stable synthetic nanomaterials with PO-like activity for practical application in the different fields of modern technologies thus seems very promising.

In 2007, ferromagnetic NPs became the first reported nanomaterials with PO-like enzymatic activity [12]. Since then, the number of such materials has been growing constantly. These include different material types, such as Nafion-cytochrome *c* [85], supramolecular complexes of hydrogel [86], nanocomplexes of lanthanides [87–92], Co_3O_4@CeO_2 hybrid microspheres [93], transition metal oxides and their composites [71,94–99], as well as noble metals: Au [100], Fe/Au [101], Au/Pt [102], Pt [103,104], Ru [105], Pt/Ru [60], Pd, Pd@Pt [106], Pd/Pt [107], Pd@γ-Fe_2O_3 [108], etc. In the last decade, special interest in bionanotechnology has focused on the use of NZs based on carbon materials such as fullerenes [109], Prussian blue [110], TiO_2 [111] or Fe_2O_3/Pt-modified [112] multi-walled carbon nanotubes, hemin-graphene hybrid nanosheets [113], Pt/Ru/3D graphene foam [114], graphene oxide [115], Au/Pt/Au-graphene oxide nanosheets [116], Pd-magnetic graphene nanosheets [117], hemin-graphene-Au hybrid [118], IrO_2 [119], Cu-Ag [120] or Fe_2O_3-modified graphene oxide [121] (Figure 4), Co-modified magnetic carbon [122], Co_3O_4 graphene composite [123], carbon nanofibers [124], graphene quantum dots [125–127], graphene nanotubes nickel-/nitrogen-doped and functionalyzed by PtNPs [128], carbon fiber-supported ultrathin CuAl layered double hydroxide nanosheets [129], Fe^{3+}-doped mesoporous carbon nanospheres [130] (Figure 5), and many others.

The kinetic parameters of different artificial POs toward H_2O_2 are presented in Table 4.

Table 4. Comparison of the kinetic parameters of different types of artificial peroxidases and natural enzyme toward H_2O_2 in solution.

Catalyst	Concentration	K_M^{app}, mM	V_{max}, $\mu M \cdot s^{-1}$	k_{cat}, s^{-1}	Reference
Fe_3O_4 NPs	11.4×10^{-13} M	154.0	0.098	8.58×10^4	[12]
HRP	2.5×10^{-11} M	3.7	0.087	3.48×10^3	[12]
$CoFe_2O_4$	20 $\mu g \cdot mL^{-1}$	8.89	0.019		[71]
CeO_2-MMT	300 $\mu g \cdot mL^{-1}$	3.4	0.010		[88]
CeO_2 NPs	300 $\mu g \cdot mL^{-1}$	3.18	0.009		[88]
H/WS2-NSs	3.2 $\mu g \cdot mL^{-1}$	0.926	0.028		[89]
CeO_2 NPs	40 $\mu g \cdot mL^{-1}$	0.28	0.009		[90]
BNNS@CuS	30 $\mu g \cdot mL^{-1}$	25	0.125		[92]
Co_3O_4@CeO_2	50 $\mu g \cdot mL^{-1}$	7.09	0.430		[93]
Fe_3O_4@Cu@Cu_2O	50 $\mu g \cdot mL^{-1}$	2.3	0.119		[95]
H_2TCPP-γ-Fe_2O_3	18.5 $\mu g \cdot mL^{-1}$	21.1	1.3×10^{-3}		[96]
γ-Fe_2O_3 NPs	100 $\mu g \cdot mL^{-1}$	157.2	0.013		[97]
Fe_3O_4@C YSNs	20 $\mu g \cdot mL^{-1}$	0.035	0.033		[99]
CuO	100 $\mu g \cdot mL^{-1}$	440	0.161		[98]
Zn-CuO	100 $\mu g \cdot mL^{-1}$	71	0.003		[98]
H_2TCPP-CeO_2	40 $\mu g \cdot mL^{-1}$	0.25	0.013		[90]
Pt/CeO_2 NPs	10 $\mu g \cdot mL^{-1}$	0.21	0.085		[91]
Pt NCs	1×10^{-4} M	3.07	0.182	1.8×10^{-5}	[104]
Ru NPs	10 $\mu g \cdot mL^{-1}$	2.2	0.580		[105]
Pd NPs	5.06×10^{-12} M	4.4	0.065	1.3×10^4	[106]
Pd@Pt NPs	1.9×10^{-12} M	2.23	0.050	2.5×10^4	[106]
Pd@γ-Fe_2O_3	1.35×10^{-6} M	0.25	0.128	9.4×10^{-2}	[108]
$C_{60}[C(COOH)_2]_2$	2×10^{-5} M	~50	0.003	1.6×10^{-4}	[109]
Fe_2O_3/Pt/CNTs	10 $\mu g \cdot mL^{-1}$	~0.1	6×10^{-5}		[112]
GO-COOH	40 $\mu g \cdot mL^{-1}$	3.99	0.039		[115]
H-rGO-Au	0.5 $\mu g \cdot mL^{-1}$	3.1	0.121		[118]
IrO_2/GO	2.4 $\mu g \cdot mL^{-1}$	5.19	~0.300		[119]
Cu-Ag/rGO	5 $\mu g \cdot mL^{-1}$	8.63	0.070		[120]
GO-Fe_2O_3	~1.25×10^{-1} M	305.0	0.101	8.1×10^{-7}	[121]
MC	10 $\mu g \cdot mL^{-1}$	0.74	0.028		[122]
CNFs	5 $\mu g \cdot mL^{-1}$	3.0	0.390	7.8×10^{-2} mmole$\cdot g^{-1} \cdot s^{-1}$	[124]
CQDs	15 $\mu g \cdot mL^{-1}$	26.77	0.306		[125]
CQDs		0.49	0.026		[126]
GQDs/CuO	70 $\mu g \cdot mL^{-1}$	0.098	0.032		[127]
CF@CuAl-LDH	50 $\mu g \cdot mL^{-1}$	0.59	0.003		[129]
Fe^{3+}-MCNs	25 $\mu g \cdot mL^{-1}$	161.0	0.007		[130]

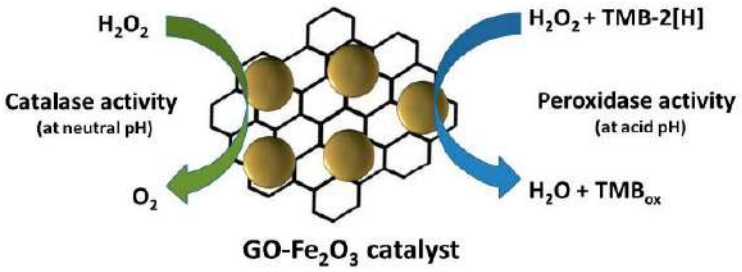

Figure 4. Scheme of catalytic action of graphene oxide-based Fe_2O_3 enzyme-like mimetic of peroxidase and catalase [121] (modified).

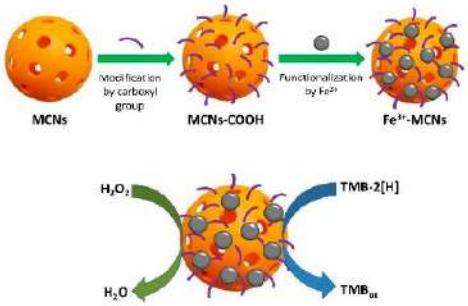

Figure 5. Schematic representation of the synthesis of Fe^{3+}-decorated mesoporous carbon nanospheres (Fe^{3+}-MCNs) and their peroxidase-mimicking catalytic activity [130] (modified).

H_2O_2 molecules are known to participate in numerous biological processes. Its analysis is routine for all newly synthesized PO mimics. Moreover, many natural enzymes (oxidases) produce H_2O_2 as a byproduct of their enzymatic reaction, so that detection of the target substrate can be performed bymeasuring generation of H_2O_2. PO-like NZs can be combined with oxidases of protein nature expanding the detection range of analytes using electrochemical biosensing. In the last decade, numerous hybrid amperometric biosensors based on PO mimetics coupled with natural enzymes, mostly oxidases (e.g., glucose oxidase, alcohol oxidase, and lactate oxidase), have been described. Because of the high pull of researches in this field, we singled out only recently described NZ-based sensors for H_2O_2 detection, without describing the hybrid biosensors. All analyzed PO-sensitive sensors belong to electrochemical ones with voltammetric or amperometric detection. Their main operational characteristics are presented in Table 5.

Table 5. The main operational characteristics of the recently described electrochemical sensors based on H_2O_2-sensitive nanozymes.

Catalyst/Electrode Type	Working Potential, V	Linearity, mM	LOD, μM	Sensitivity, $A \cdot M^{-1} \cdot m^{-2}$	Reference
Fe_3O_4/3D GNCs//GCE	−0.2	0.0008–0.33	0.08	2742	[131]
α-MnO2//GCE	−0.4	0.0002–0.1	0.08	5.5	[132]
AuNBP/MWCNTs//GCE	−0.5	0.005–47.3	1.50	1706	[133]
Fer/rGO-Pt//GCE	+0.1	0.0075–4.27	~0.38	3400	[134]
rGO/Pt-Ag//GCE	−0.05	0.005–1.5	0.04	6996	[135]
GBR//GCE	+0.9	0.1–10.0	48.0		[136]
CMC@Pd/Al-LDH//GCE	−0.38	0.001–0.12	0.30	163	[137]
Pt/PANI/MXene//SPCE	+0.3	0.001–7.0	1.00		[138]
CuOx/NiOy//GCE	−0.35	0.0003–9.0	0.09	2711	[139]
GDCh-NiO//RDE	+0.13	0.00001–0.0039	0.0015	1072	[140]
Pt-Pd/MoS_2//GCE	−0.35	0.01–0.08	3.4	764	[141]
N-CNFht//GCE	−0.4	0.01–0.71	0.62	3570	[142]
Cu_2O/PANI/rGOn//GCE	−0.2	0.0008–12.78	0.3	394	[143]
WCC//GCE	−0.4	0.05–1.0	0.006	67	[144]

Prussian blue (PB) is one of the most effective PO mimetics. PB or iron(III) hexacyanoferrate(II) is a member of a well-documented family of synthetic coordination compounds with an extensive 300-year history. It was produced commercially in the past and used as a pigment for paints, lacquers, printing inks and laundry dyes [145,146].

PB and its analogues (PBAs) are cheap, easy to synthesize, environmentally friendly and are prospect for wide applications in different fields, including basic research and industrial purposes [10,147–151] as well as in medicine [24,152–158].

Despite their multifunctionality, the composition of PBAs is quite complicated and tightly depends on a method of synthesis and storage conditions. [146,149–151,159,160]. Insoluble PB can be described by the formula $Fe_4[Fe(CN)_6]_3$. $KFe[Fe(CN)_6]$ corresponds to a colloidal solution of PB [149,151]. The general formula of hexacyanoferrate (HCF) is $M_k[Fe(CN)_6]{\cdot}xH_2O$, where M is a transition metal (Figure 6). PBAs are usually obtained via various techniques, including chemical [146,149,159–162] and alternative biological methods [163].

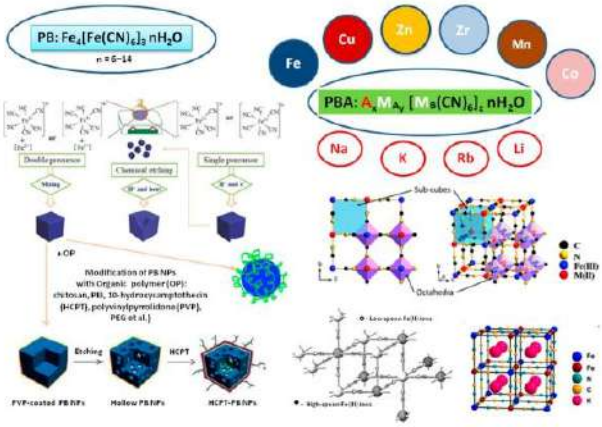

Figure 6. Hexacyanoferrates of transition metals: composition, structure and modification.

PBAs have gained extensive worldwide attention in the last two decades. The charge transfer through two transition metal ions in the complex-compound salt, as well as the nanosize of HCF particles, are the reasons for PBAs' redox activity and super-magnetic properties. Due to these remarkable properties, PBAs are widely applied as NZs in biosensors [146,147,150,164–168] and alternative energy sources [149,160,165,168].

The enzyme-like properties of PBA in solution are difficult to analyze because of the ability of PB and PBAs to simultaneously mimic the activities of several ROS-enzymes (PO, SOD and catalase). Numerous papers (see Table 6) described the ability of PBA-NZ to react with typical ROS-enzyme substrates, such as TMB, ABTS and NADH [169].

Table 6. The main kinetic characteristics of the PBA-based PO-like nanozymes in solution.

PBA	Concentration	Chromo-Gene	K_M^{app}, mM	V_{max}, μM·min^{-1}	k_{cat}, nmol·μg^{-1}·min^{-1}	LR, μM	Reference
PB/γ-Fe_2O_3	20 μg·mL^{-1}	TMB	323.6	1.17	0.059		[12]
VOxBG hydrogel	5 μg·mL^{-1}	TMB	20	0.045	0.009		[161]
PO		TMB	3.7	0.009			[161]
PB-MIL-101 (Fe)	200 μg·mL^{-1}	TMB	0.058	1.32	0.0066	2.4–100	[166]
MoS xNi-Fe		TMB					[169]
PB, soluble form	6 μg·mL^{-1}	TMB	14.7	0.012	0.002		[170]
PS@Au@PB	300 μg·mL^{-1}	TMB	0.17	0.38	0.001		[171]
Au@HMPB (40 °C)	40 μg·mL^{-1}	TMB	88.72	2.50	0.063		[172]
PB	0.2 μM	ABTS	0.028				[173]
PB-Ferritin	0.74 nM	TMB	11.984	43.2	58.38×10^3 min^{-1}		[174]
	0.74 nM	ABTS	0.537	0.36	0.49×10^3 min^{-1}		
PB/Fe_2O_3	0.31 nM	TMB	323.6	70.2	226.5×10^3 min^{-1}		
MWCNTs-PB			1.33	6.6	0	1–1500	[175]

PB and PBAs are used successfully in optical biosensors as a result of their PO-like properties [12,16,169–175]. The first communications concerning electrochemical reduction of H_2O_2 on PB-modified glassy carbon electrode were done by Itaya and colleagues [164,165]. Karyakin and

colleagues published many reports over the last 25 years on the use of PB as an artificial PO in amperometric biosensors [13,150,162,176–181]. In 2000, this group named PB an "artificial PO" [177]. At the same time, a large number of other scientific groups, especially from China, worked hard on this problem [148,154,156–159,166,168–174].

PBAs demonstrated intrinsic PO-like activity when coupled with carbon, graphene, natural polysaccharides or synthetic polymers. This property was successfully used in electrochemical (bio)sensors (Figure 7).

Table 7 presents selected examples of PBA application as amperometric chemo-sensors on H_2O_2 and the analytical characteristics of the developed sensors. The main peculiarities of these catalysts are high stability, sensitivity and selectivity to H_2O_2 in extra-wide linear ranges. PBAs are more stable in neutral and alkaline solutions compared to PB [181], and may be used in a physiologically compatible medium containing biorecognition elements. Some PBAs show good selectivity against easily oxidizable interfering species, for example organic acids, although the electrocatalytic activity in H_2O_2 reduction is similar to that of PB [146,147,149].

Table 7. Amperometric H_2O_2-sensitive sensors based on PBA as a PO-like nanozyme.

Electrode	Working Potential, V	Nanozyme	Sensitivity, $A \cdot M^{-1} \cdot m^{-2}$	LOD, μM	Linear Range, μM	Reference
GCE	−0.05	PB/BG	2850		4–83,000	[167]
		AuNPs-PB/BG	11243		9.2–8100	
GCE	0.65	MnPBA	1472	3	3–8610	[168]
GCE	−0.3	MoS xNi-Fe PBA			0.1–2500	[169]
GCE	0.18	PB	10,000/20,000	1	1–5000	[176]
GCE	0.05	PB	6000	0.1	0.1–100	[177]
GCE/	0.0	Ni-FePBA	18,000		up to 100	[178]
DBD	−0.05	PB	2100			
DBD	−0.05	Ni-FePBA	1500	0.5	0.5–1000	[179]
GE	−0.05	PB/NZ	4500			
Planar screen-printed		Ni-PB	3500		0.1–1000	[180]
Carbon planar screen-printed	0.0	PB/film PB/NZ	6500 8500		up to 500 up to 500	[181]
GCE	0.0	PNAANI–PB	5073	0.07	1–1000	[182]
Graphene		CoPBA		0.007	5–1200	[183]
Graphene nanocomposite		CoPBA		0.1	0.6–380	[184]
Graphite-string	0.05		6413		30–1000	[185]
Graphite paste		Cu-FePBA	2030	0.2	0.5–1000	[186]
		Ni-FePBA	1130	2	2–1000	
Nanoporous gold film		PB	7080	0.22	1–17,000	[187]
GCE		Ni-FePBA	0.192 A/M	1		[188]
GCE	0.33	Ni–Fe PBA-HNCs	361.3	0.291	0.1–20,000	[189]
GE		Thionine-NiPBA		0.557	1.67–1110	[190]
CNE		PB	500,000		10–3000	[191]

Electrochemical biosensors have long been used as an efficient way for quantitative detection of different analytes (biomarkers) of interest. PBA-based NZs, being PO-mimetics, may comprise a promising platform for the construction of biosensors that can be applied in clinical diagnostics, theranostics, for control of therapy, cell/tissue growth and proliferation [5–11,146–148,152,170,192].

The main drawback of the many H_2O_2-sensitive NZ-based electrochemical sensors is the application of rather high or low working potentials. As a result, they suffer from non-selectivity. It is known that H_2O_2 is prone to direct auto-oxidation on electroactive surfaces (e.g., Pt) at an operational potential above +0.4 V or auto-reduction at −0.4 V or less vs. Ag/AgCl. Moreover, the real samples consisted mostly of organic compounds which are easily co-oxidized/co-reduced at the above-mentioned potentials (e.g., ascorbic or uric acids, neurotransmitters, pigments, drugs, and even glucose), consequently resulting in overestimation of the target analytes. There are only a few possibilities for decreasing this interfering impact, for example by restricting the access of the

potentially interfering compounds by perm-selective membranes. The weak point of this approach is the additional diffusion limitations, resulting in deterioration of the sensor's operational parameters. A much more successful strategy is the screening of new NZ types that work at operating potentials close to zero (0) V vs. Ag/AgCl [193].

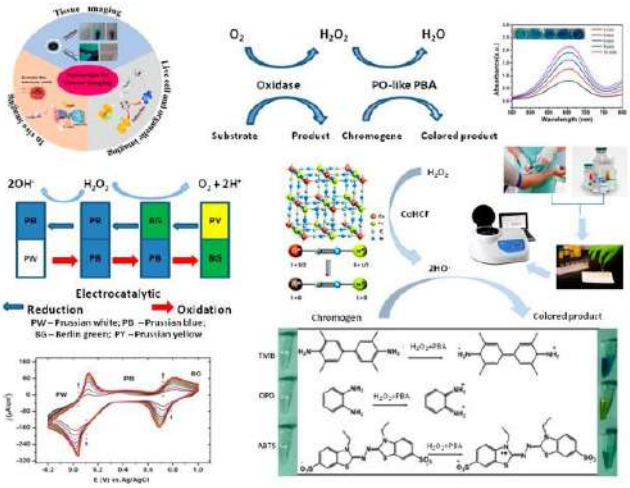

Figure 7. Peroxidase-like catalytic activity of Prussian blue analogues (PBAs) as a platform for the development of amperometric and colorimetric (bio)sensors.

5. Nanooxidases

Natural oxidases, which belong to the EC class 1.1.3, catalyze the oxidation of many substrates that contain the CH-OH group (electron donors). They use molecular oxygen as the electron acceptor, and form hydrogen peroxide as a byproduct [194]. Generally, a specific oxidase name is given according to the target oxidized substrate.

For example, glucose oxidase (GOx), alcohol oxidase (AOx), lactate oxidase (LOx), cholesterol oxidase (COx), etc. are the specific oxidases that catalyze the oxidation of glucose, ethanol, lactate, and cholesterol, respectively:

$$\text{Glucose} + O_2 \rightarrow \text{Gluconic acid} + H_2O_2 \text{ (GOx)}$$

$$\text{Alcohol} + O_2 \rightarrow \text{Aldehyde} + H_2O_2 \text{ (AOx)}$$

$$\text{Lactate} + O_2 \rightarrow \text{Pyruvate} + H_2O_2 \text{ (LOx)}$$

$$\text{Cholesterol} + O_2 \rightarrow \text{Cholestenone} + H_2O_2 \text{ (COx)}$$

Due to the generation of H_2O_2, natural oxidases and oxidase-like NZs can efficiently oxidize the colorless substrates (in the presence of PO) into corresponding colored products, which make them promising tools for analysis of a number of biological molecules. Many forms of nanomaterials that exhibit nonenzymatic oxidase-like catalytic activities have been reported in recent decades: ferrous metals, their oxides or bimetallic/alloys [195–198], nanocomplexes of lanthanides [199–201], transition metals [105,202,203], as well as noble metals and their combinations: (IrPd)/Au [204], PtNPs [205,206], Au@Pt [207], Au/Pt/Ag [208], Au-Pd NPs [209], Au/TiO_2 [210] and many others [211]. Although the metallic GOx-like NPs yielded >99% gluconic acid, these materials suffered from high adsorption of reaction products resulting in their oxidation and inactivation [212]. The most extensively studied nanooxidases used for selective oxidation of glucose to gluconic acid are AuNPs [4,210,213–222] (see

Table 8). Gold NPs are much more resistant to O_2 compared with Pt and PdNPs and their reaction products have a lower affinity to adsorption onto the Au surface, in addition to being more active and selective under mild conditions [212]. Their main drawbacks are strong dependence of catalytic activity on a type of Au surface and nanoparticle size affected by of sintering [223]. Carbon-based materials and metal/carbon composites have also demonstrated catalytic oxidation of glucose in the presence of O_2 [224–227] as an alternative to metallic NPs.

Table 8. Comparison of the kinetic parameters of different types of artificial GOx and natural enzyme toward glucose in solution.

Catalyst	Concentration	K_M^{app}, mM	V_{max}, $\mu M \cdot s^{-1}$	k_{cat}, s^{-1}	Reference
Au/MCM-41	0.025 $mg \cdot mL^{-1}$	55.2	18.0	14.2	[212]
AuNPs	34×10^{-9} M	6.97	0.63	18.52	[213]
GOx	34×10^{-9} M	5.0	0.69	9.7	[213]
AuNPs	0.05 $mg \cdot mL^{-1}$	0.41	0.10		[221]
AuNPs-MIP	0.05 $mg \cdot mL^{-1}$	0.18	0.42	3.76×10^{-7} $mmole \cdot g^{-1} \cdot s^{-1}$	[221]
AuNPs-PFOP	0.05 $mg \cdot mL^{-1}$	0.09	0.58	5.21×10^{-7} $mmole \cdot g^{-1} \cdot s^{-1}$	[221]
AuNP	2×10^{-9} M			4.5×10^{7}	[222]
β-CD@AuNPs		9.60	1.80×10^{-2}		[228]
EMSN-AuNPs	562.0 $mg \cdot mL^{-1}$	26.2	0.53		[229]
MnO_2NFs	0.02 $mg \cdot mL^{-1}$	21	0.43		[230]

Unfortunately, the catalytic parameters were not determined for many of the above-mentioned nanooxidases. It is therefore not possible to compare the efficiency of GOx-mimicking nanocomposites.

Ortega-Liebana and coauthors [212] (Figure 8) described an Au-silica nanohybrid Au-MCM-41 with a determined K_M^{app} of ~55 mM, which is significantly higher compared with the values reported for free AuNZ (K_M^{app} ~7 mM) [213], polymer-coated gold-based mimics (K_M ~0.4 mM) [221], gold-supported mimicking systems (K_M^{app} ~27 mM) [229], as well as the natural GOx (K_M^{app} ~5 mM) [213]. Au-MCM-41 NZ showed a slightly lower affinity towards glucose as a substrate. Nevertheless, the corresponding catalytic constant k_{cat}, a true catalytic parameter for comparison determined as the V_{max}/concentration of catalyst ratio, is close to the value reported for natural GOx (k_{cat} ~14.2 s^{-1} vs. k_{cat} ~9.7 s^{-1}, respectively) and similar to freestanding Au NPs (k_{cat} ~18.5 s^{-1}) as reported by Luo and coauthors [213]. The Au-MCM-41 NZ showed a good response, possibly due to a good homogeneous distribution of active sites of Au in the mesoporous carrier, which improved their availability [212].

Some of the described NZs are characterized by double enzyme-like properties. They are named "tandem NZs" (nanomaterials with tandem enzyme-like characteristics). Ma and coauthors [222] investigated catalytic properties of single AuNPs and Ag-Au hybrid NPs as possible GOx and PO mimetics. The electrochemical experiments demonstrated that a high turnover of NZs was obtained from individual catalytic elements compared to results from ensemble-averaged measurements as a classic approach. The authors concluded that the unique increasing catalytic activity of single NZ supports is due to the high accessible surface area of monodispersed NPs and high activities of carbon-supported NP during single particle collisions on a carbon ultra-microelectrode. It was proposed as a new method for accurate characterization of NZs' catalytic activities that opens further prospects for the design of highly efficient catalytic nanomaterials. Kou and coauthors [228] described the synthesis of β-CD@AuNPs that are characterized by simultaneous GOx-like and PO-like activities (Table 8). Han and coauthors [230] desribed the synthesis of 2D MnO_2-based NPs with dual enzyme activities in a similar pH range. Moreover, a one-pot nonenzymatic approach was proposed for the colorimetric analysis of glucose, where the oxidation of glucose and the colorimetric detection of H_2O_2 are conducted simultaneously as a result of the single NZ (MnO_2 NPs) catalysis. This method is

characterised by a high sensitivity, low LOD and a short time of analysis, because of the proximity effect and in situ reaction [230]. However, the weak point of the most widely described oxidase mimics is their nonselective oxidation of a number of substrates, contrary to natural enzymes. Improving the selectivity of oxidase-like NZs is therefore a great challenge that needs to be solved before their successful application in analytical technologies.

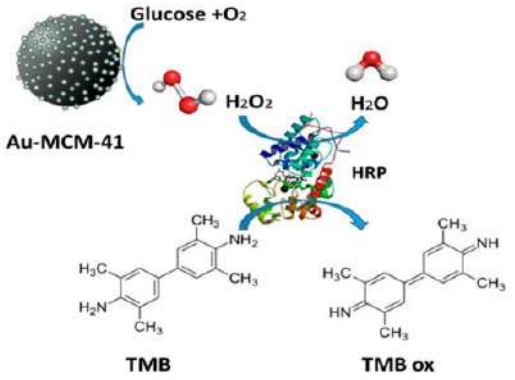

Figure 8. Determination of H_2O_2 as a product generated in the reaction of glucose oxidation [212] (modified).

Summarizing the above-mentioned data on nanocomposites with GOx-like activity, it is worth emphasizing that many of them (see Table 8) have a very low activity that does not enable defining them as NZs. There is an enormous difference in catalytic efficiency of the described GOx-mimetics: k_{cat} values differ more than 107-fold. Although according to BRENDA data this parameter is also very variable for natural GOs-from 0.005 to 2300 s^{-1} [231], it is obvious that improving the catalytic efficiency of synthetic NZs is a very important challenge. Nevertheless, the most effective nanooxidases (including those presented in Table 9) can be a good basis for the creation of non-enzymatic sensors for glucose analysis [72,222–227].

Table 9. Comparison of the main operational properties of glucose-sensitive amperometric sensors based on GOx-like nanozymes.

Electrode Material	Potential, V	Linearity, mM	LOD, µM	Sensitivity, $A \cdot M^{-1} \cdot m^{-2}$	Selectivity	Reference
3DG/$Co(OH)_2$	+0.6	0.1–10	0.016	36900	AA, UA, fructose, lactose, urea	[72]
Au/MWCNTs	+0.15	0.01–36.0	3.0	1012	DA, UA, AA, fructose, saccharose, maltose, Ca^{2+}, Cl^-	[133]
PtNi-ERGO	−0.35	0.01–35	10	204.2	AA, UA, urea, fructose	[224]
CuO NW/CF	+0.35	0.001–18.8	0.3	22174	AA, UA, DA, lactose, sucrose, maltose	[225]
Octahedral Cu_2O	+0.6	0.3–4.1	128	2410	AA, UA, DA, NaCl	[225]
CQDs/octahedral Cu_2O	+0.6	0.02–4.3	8.4	2980	AA, UA, DA, NaCl	[225]
CuNWs/rGO	+0.58	0.01–11	0.2	16250	AA, UA, DA, AP, fructose, sucrose	[226]
AKCN	+0.7		0.8		fructose, lactose, maltose	[227]
β-CD@AuNPs	−0.05				Cu^{2+}, Al^{3+}, UA, AA, guanine, guanosine	[228]
Ni–Pd/Si-MCP	−0.1			0.081 $A \cdot M^{-1}$	AA	[232]
Pd-Pt core-shell NCs	−0.05	0.3–6.8	41.1	1700		[233]
Pt NPs	−0.05	0.3–5.2	91.8	457		[233]
Cu_2O/GNs	+0.1	0.3–3.3	3.3	2850		[234]
Cu_2O nanocubes	+0.1		5.9	2000		[234]
ITO/PbS/SiO_2/AuNPs	−0.2	0.001–1	0.46		AA, UA, L-Cys, lactose, maltose, sucrose	[235]

Many sensors for glucose detection are based on its electrochemical oxidation directly on a nanocatalyst-covered electrode have been reported (Table 9). A silicon-based amperometric

non-enzymatic sensor for the glucose determination (nEGS) was described by Miao and coauthors [232]. Ni–Pd NPs adhered onto a supporter comprising the 3D ordered silicon microchannel plate (MCP) were proposed as sensing materials and were used as an electrode. The 3D structure provided ample space allowed a fast mass transport of ions/gas through the electrolyte/electrode interface, thus causing fast electrochemical reactions. The Ni–Pd/Si-MCP nanocomposite electrode showed strong electrocatalysis of glucose under alkaline conditions. The nanocomposite was characterized by a good selectivity even in the presence of high concentrations of interfering agents, excellent storage stability and reproducibility. Ye and coauthors [233] synthesized and employed heterostructured Pd-Pt core-shell nanocubic materials (NCs) as nEGSs, due to their electrocatalytic activity in glucose oxidation. These core-shell NCs with a large surface area show remarkable GOx catalytic activity and can potentially be applicable as nEGSs. Gao and coauthors [224] developed a PtNi alloy NP-graphene composite and found that the PtNi-ERGO nanocomposite-based nEGS possessed many merits in terms of high selectivity, superior resistance to poisoning, low LOD, rapid response, excellent reproducibility and stability, which outmatches the performance of any other reported Pt-based nEGSs. The nEGS retained 93.2 and 90.5% of its initial sensitivity at 10 and 50 days postpreparation, respectively. The combination of these unique characteristics has enabled the application of this new type of nanoelectrocatalyst-loaded electrodes for analysis of real human samples. Li and coauthors [225] proposed utilizing 3D porous copper foam (CF) as an electroconductive base and a precursor for a growth of CuO nanowires (NWs) in situ used for the construction of electrochemical nEGSs. CF has a high surface area due to its unique 3D porous structure, resulting in good sensitivity for glucose detection. The CuO NWs/CF-based nEGSs are characterized by good selectivity, reproducibility, repeatability and stability (Table 9).

The CuO NWs/CF based nEGSs have also been employed for glucose assay in human serum and saliva (which indicated that CuO NWs/CF are promising for noninvasive glucose detection). Li and coauthors [225] designed an electrochemical nEGS based on a novel nanostructured electrocatalyst of carbon quantum dots (CQDs)/octahedral cuprous oxide (Cu_2O) nanocomposites [74]. Compared to octahedral Cu_2O, the CQDs/octahedral Cu_2O exhibited preference for electrocatalysis over glucose oxidation and H_2O_2 reduction. The experimental results demonstrated that nEGSs have a good potential for practical determination of glucose in real samples of biological liquids [75,236]. Ju and coauthors [226] synthesized a nanocomposite consisting of 1D CuNWs and 2D reduced graphene oxide nanosheets (CuNWs/rGO) and constructed amperometric nEGSs. Contrary to the CuNWs, the CuNWs/rGO hybrids exhibit a higher current response relative to their auto background current, indicating a stronger electrocatalytic capacity toward the oxidation of glucose. The sensor is characterized by very high sensitivity (16,250 $A{\cdot}M^{-1}{\cdot}m^{-2}$) and low LOD (0.2 μM). Shackery and coauthors [72] described the porous, conducting, chemically stable structure of $Co(OH)_2$/3DG. The unique $Co(OH)_2$ NRs electrode morphology displays a unique high sensitivity—36,900 $A{\cdot}M^{-1}{\cdot}m^{-2}$ with sufficient selectivity (Table 9).

The bifunctional cascade catalysis was successfully tested for the real-time colorimetric glucose detection with 0.8 μM LOD for 30 s. Alkalized graphitic carbon nitride (AKCN) exhibited perfect photoactivity for H_2O_2 generation at neutral pH-conditions, which are typical for natural GOx. The photocatalytic GOx-like activity of AKCN was successfully demonstrated by an in situ photoproduction of H_2O_2 which was proportional to the rate of glucose. The production of H_2O_2 exhibited a wide linear range proportional to glucose concentration (up to 0.1 M). The production of CO_2 from the photocatalytic oxidation of glucose was negligible (2 μM), compared with that of H_2O_2. This indicates that the photocatalytic mineralization of glucose is inhibited at the applied conditions, and glucose is selectively phototransformed into gluconic acid on AKCN.

In addition to amperometric sensors, recent publications described several promising photoelectrochemical nEGSs using oxidase-like NZs. Zhang and coauthors [237] reported a synthesis of metal-free oxidase mimicking NZ based on modified graphitic carbon nitride (Figure 9). The H_2O_2 is generated as a result of coupled photocatalytic oxidation of glucose and O_2 reduction under visible

light irradiation with about 100% apparent quantum efficiency. The generated in situ H_2O_2 serves for oxidation of a chromogenic substrate on the same catalyst in a dark to complete the nonenzymatic glucose detection.

Figure 9. Comparison of two glucose detection systems: based on the glucose oxidase (GOx) combined with horseradish peroxidase (HRP) (above); based on synthetic NZ aerobic photocatalytic oxidation of glucose combined with in situ H_2O_2-production on AKCN (alkalized GCN—graphitic carbon nitride) (below) [237] (modified).

Cao and coauthors [235] recently reported the development of a photoelectrochemical glucose sensor using complicated ternary layered NPs of ITO/PbS/SiO_2/AuNPs (ITO-indium tin oxide). Thioglycolic acid-capped PbS quantum dots that are highly sensitive to oxygen were employed as a photoelectrochemical active probe. The AuNPs were used as the GOx-like NZ for aerobic catalytic glucose oxidation. The catalysis promoted oxygen consuming, resulting in a decrease in the cathodic photocurrent. The insertion layer of SiO_2 NPs between PbS and AuNPs could efficiently reduce the base current due to its low electroconductivity, which improved the LOD. The described sensor showed high sensitivity and good selectivity. The LR toward glucose was in the frames from 1.0 μM to 1.0 mM with 0.46 μM LOD.

Thus, glucose sensors are practically the only oxidase-like NZ-based electrochemical sensors that are currently being developed and characterized. GOx-like NZs incorporated on the electrode covered layer enhanced their catalytic power due to intrinsic catalytic activity and a synergetic effect of applied potential. In our opinion, due to additional electrocatalytic activity, such NZs can be a promising alternative for natural enzymes in the construction of electrochemical sensors. They are cost-effective, possess high sensitivity, favorable stability, reproducibility, simplicity in development and avoid complex enzymatic immobilization techniques. Unfortunately, performing a multielectron oxidation reaction in the presence of easily oxidized interfering agents has some severe constraints. For example, platinum electrodes lose their activity quickly in glucose solutions through accumulation of chemisorbed intermediates which block the electrocatalyst's surface [238].

6. Laccase-Mimicking Nanozymes

Natural laccases [239–242] are members of the multi-copper oxidases which catalyze the single-electron oxidation of a wide range of organic substrates, such as polyamines, aryl diamines, ortho- and para-diphenols as well as polyphenols, with the subsequent four-electron reduction of molecular oxygen to water (Figure 10). Due to their activities, laccases can be used as "green" catalysts in water treatment and soil bioremediation [243,244]. However, the poor stability of natural laccases in complex environments, the difficulty of their recycling, and the high cost of the purified enzyme preparations severely hamper practical applications of this enzyme [12,245–248].

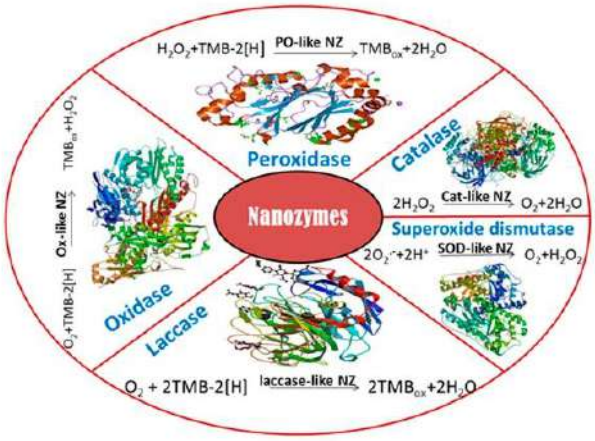

Figure 10. Scheme of reactions catalyzed by oxido-reductases-mimicking nanozymes (NZs).

Many synthetic methods for obtaining various types of laccase-like nanomaterials have been described, when most of them are based on the use of copper ions as a catalyst, because the active centers of natural laccases also contain these ions. A large number of copper-based complexes with different types of organic ligands are reported as laccase mimetics [249–253]. Ren and other authors [254–257] reported one-pot synthesis of copper-containing carbon dots as laccase mimics. Shams and coauthors [258] described the synthesis of Cu/H_3BTC MOF (copper ions with 1,3,5-benzene tricarboxylic acid, H_3BTC and metal–organic framework, MOF) possessing laccase-like activity with regard to oxidation of phenolic compounds. Cu/H_3BTC MOF was used for quantitative detection of epinephrine. This NZ showed excellent stability under different conditions compared with natural laccase [258] (Figure 11).

Water-soluble nucleotides have a significant potential for use as ligands for different nanostructures. Nucleotide coordinated Cu^{2+} complexes were demonstrated as having laccase-like activity [259,260]. Such coordination complexes were immobilized onto magnetic NPs forming Fe_3O_4@Cu/nucleotide NPs [260,261]. The guanosine monophosphate (GMP) based laccase mimicking Cu/GMP NZ [262] and Fe_3O_4@Cu/GMP NZ [263] demonstrated excellent laccase-like catalytic activity toward high spectra of phenolic substrates, e.g., hydroquinone, naphthol, catechol, epinephrine and o-phenylenediamine. The K_M^{app} of Cu/GMP toward 2,4-dichlorophenol was quite similar to that of natural laccase (0.59 mM vs. 0.65 mM, respectively). Although it was reported that the V_{max} of Cu/GMP was 5.4-fold higher compared with the natural enzyme, the value of the intrinsic catalytic parameter (k_{cat}) was not indicated. Cu/GMP also showed better stability over pH 3–9, temperatures of 30–90 °C, and a high ionic strength of 500 mM NaCl, as well as long-term storage for 9 days. Analysis of epinephrine with Cu/GMP was nearly 16-fold more sensitive and 2400-fold more cost-effective than using natural laccase [262]. The magnetic Fe_3O_4@Cu/GMP NZ is able to oxidize toxic o-phenylenediamine and showed higher activity and stability compared with natural laccase [263]. However, the K_M^{app} of laccase was 18-fold lower than that of the Fe_3O_4@Cu/GMP NZ, which means that laccase had a better affinity toward the substrate. On the other hand, the Vmax of Fe_3O_4@Cu/GMP was almost 4.2-fold higher than that of laccase (see our remark on the irrelevance of such a comparison). Fe_3O_4@Cu/GMP retained about 90% of its residual activity at 90 °C, with little change at pH 3–9, and showed excellent storage stability.

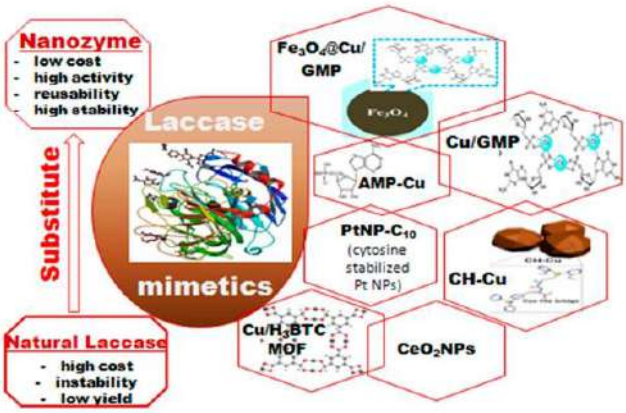

Figure 11. Laccase-mimicking nanozyme for oxidizing phenolic compounds [263–265].

Huang and coauthors [264] described a laccase-mimic NZ based on copper ions and adenosine monophosphate (AMP-CuNZ) with a 15-fold higher catalytic activity than that of natural laccase (at the same mass concentration; normalization to the molar concentration of both catalysts for calculating k_{cat} was not reported). It also has a higher V_{max} and a lower K_M^{app}. The V_{max} of AMP-Cu was 4.5-fold higher than that of natural laccase (1.30 $\mu M \cdot min^{-1}$ vs. 0.28 $\mu M \cdot min^{-1}$ at the same mass concentration of both catalysts, 0.1 $mg \cdot mL^{-1}$), with a 4-fold lower K_M^{app} (0.09 mM vs. 0.36 mM). The lower K_M^{app} of AMP-Cu indicates that the simulated enzyme had a stronger affinity toward the substrate. The concentration linear range (LR) of phenolic compounds detected by AMP-CuNZ was 0.1–100 µM, and the LOD was 0.033 µM (lower than that of laccase). The AMP-Cu had good stability (over 9 days of storage) under conditions of 30–90 °C and pH > 6. AMP-Cu NZ can be used to detect a variety of phenolic compounds: phenol, hydroquinone, p-chlorophenol, resorcinol, phloroglucinol and catechol [264]. It could be predicted that due to its favorable properties, AMP-Cu NZ has a great potential for applications and can replace native laccase in biosensors.

Wang and coauthors [265] presented a new class of laccase-like NZs (denoted as CH-Cu). The electron transfer in this system was providedvia the coordination of Cu^{+}/Cu^{2+} with a cysteine (Cys)-histidine (His) dipeptide. The CH-Cu has similar K_M^{app} values to the natural enzyme (K_M^{app} 0.42 mM and 0.41 mM, respectively) and increased V_{max} values compared to the natural enzyme (7.32 $\mu M \cdot min^{-1}$ and 6.41 $\mu M \cdot min^{-1}$, respectively, at a catalyst concentration of 0.1 $mg \cdot mL^{-1}$ for CH-Cu or laccase). The k_{cat} value of CH-Cu is much higher than that of laccase (1.91×10^4 min^{-1} and 4.13 min^{-1}, respectively), indicating a higher turnover number and catalytic efficiency of a single CH-Cu NZ particle, which has a larger number of active sites than the natural protein molecule. A similar result was found for Fe_3O_4 NPs with PO-mimicking activity ($k_{cat} = 3.1 \times 10^5$ s^{-1}) [17].

The catalytic activity of NPs is dependent on the copper ions content. The authors therefore measured the catalytic activity of laccase and CH-Cu NZ with the same amount of Cu atoms. The amount of copper in laccase is 0.32 wt. % and in CH-Cu it is 38.3 wt. %. As a result, the weight ratio of laccase to NZ was 120:1 for the activity test. Due to increasing the number of active sites in a single particle, CH-Cu shows good laccase-like catalytic activity. The higher efficiency of CH-Cu compared with laccase in the degradation of chlorophenols and bisphenols was also demonstrated in a batch mode. Moreover, using CH-Cu a new method for the quantitative detection of epinephrine was developed [265].

Nanomaterials that do not contain copper could also possess laccase mimicking activity. Many metal-based catalysts have been described recently, including noble metal NPs: gold [266], platinum [267], or oxides such as iron oxide [12,17], cerium(IV) oxide [268,269], manganese oxide [270], etc.

NZs placed on Pt in combination with oligonucleotides as stabilizing agents (adenine-A10, thymine-T10, cytosine-C_{10}, and guanine-G_{10}) display excellent catalytic performance in oxidation of multiple substrates, including 2,4-dichlorophenol (2,4-DCP), dopamine, p-phenylenediamine, catechol and hydroquinone [267]. This kind of Pt NZs has high stability in the range of 20–90 °C and pH 3–9, which exceeds the range of native laccase. It was shown that the laccase-like activities of PtNPs are strongly associated with particle size (2.5–5 nm). PtNPs modified with the oligonucleotides cytosine (C_{10}), with a particle size of 4.6 nm, showed the highest activity in the oxidation of 2,4-DCP. These NPs exhibit an apparent K_M^{app} value of 0.12 mM toward 2,4-DCP, whereas laccase exhibits a K_M^{app} of 0.40 mM. Enzyme-like kinetics was observed in the oxidation of 2,4-DCP catalyzed by DNA-stabilized PtNPs which have a three-fold better substrate affinity compared to natural laccase [267]. Nanozymes PtNP-C_{10} and AMP-Cu possess lower K_M values (0.12 mM and 0.09 mM, respectively), that indicate their better affinity toward 2,4-DCP compared to natural laccases: from *Pycnoporus sanguineus* sp. CS43 (0.224 mM) and *Trametes versicolor* (0.40 mM).

The main catalytic characteristics of the synthetic laccase mimetics and natural enzyme toward different substrates are presented in Table 10.

Table 10. The main catalytic characteristics of the synthetic laccase mimetics and natural enzyme toward typical substrates.

Chemo/Biocatalyst	Substrate	K_M^{app}, mM	V_{max}, mM·min^{-1}	NP Concentration, mg·mL^{-1}	Reference
CeO_2 NPs	Dopamine	0.25×10^{-3}			[77]
	Catechol	0.180			
Cu/H_3BTC MOF	Epinephrine	0.068	94×10^{-3}	0.1	[258,262]
Laccase		0.062	5.81×10^{-3}	0.1	
Cu/GMP	Epinephrine	0.59	0.83	0.1	
Laccase	2,4-Dichlorophenol	0.65	0.15	0.1	
AMP-Cu	2,4-Dichlorophenol	0.09	1.3×10^{-3}	0.1	[264]
Laccase	2,4-Dichlorophenol	0.36	0.29×10^{-3}	0.1	
CH-Cu Cys-His dipeptide	Epinephrine/2,4-dichlorophenol	0.58	2.74×10^{-2}	0.1	[265]
		0.42	7.32×10^{-3}		
Laccase	Epinephrine/2,4-Dichlorophenol	0.16	3.10×10^{-3}	0.1	
		0.41	6.41×10^{-3}		
PtNP-C_{10} (cytosine stabilized Pt NPs)	2,4-Dichlorophenol	0.12	8.49×10^{-3}	0.01	[267]
Laccase from *Trametes versicolor*	2,4-Dichlorophenol	0.40	3.51×10^{-3}	0.16	
Laccase from *Pycnoporus sanguineus* sp. CS43	2,4-Dichlorophenol	0.224	2.21×10^{-3}		[271]

Since the synthetic laccase mimetics have preferential properties compared with natural enzymes, they appear to be very promising for the development of new non-enzymatic amperometric sensors for assaying phenolic compounds (Figure 12).

Garcia and coauthors [272] reported the construction of a CPS2 (copper oxide-based carbon paste) biomimetic sensor for phenol, rutin and catechol determination in natural samples, such as dried extracts of red fruits and coffee. The enhanced sensitivity towards catechol as a model substrate correlated to the amount of incorporated copper oxide, resulting in improvement of electroactive surface area and electrocatalytic ability os the sensor. The sensor can be characterized by high sensitivity and selectivity for rutin (LR of 1 to 120 μM and LOD of 0.4 μM) and catechol (LR of 10 to 600 μM) (Table 11) that is better compared to laccase-based biosensors.

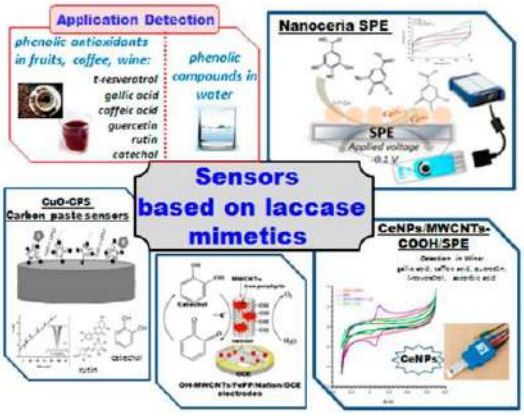

Figure 12. Sensors based on laccase-mimicking nanozymes of different chemical nature in detection of phenolic compounds [268,269,272,273].

Table 11. Analytical characteristics of the amperometric sensors based on synthetic laccase mimetics and natural enzyme toward typical substrates.

Sensor	Analyte	Linear Range, μM	LOD, μM	Reference
CeNPs	Gallic acid	2–20	1.5	[268]
	Caffeic acid	50–200	15.3	
	Quercetine	20–200	8.6	
	Ascorbic acid	0.5–20	0.4	
CeNPs/MWCNTs-COOH/SPE	Gallic acid	25–50	7	[269]
	Caffeic acid	33–100	10	
	Quercetin	25–100	8	
	t-Resveratrol	25–50	8	
	Ascorbic acid	25–100	7	
Laccase/Fc/SPE	Caffeic acid	2.0–30.0	1.6	[269]
Laccase/PAP/SWCNTs/SPE	Gallic acid	0.53–96		[269]
Laccase immobilized in polyzetidine prepolymer and SWCNTs	Gallic acid	0.53–96		[269]
CuO-C-CPS2	Rutin	1 to 120	0.4	[272]
	Catechol	10 to 600	2.0	
Laccase on CP	Catechol	20 to 700	4.5	[272]
FePP modified multi-walled carbon nanotubes (OH-MWCNTs/FePP/Nafion/GCE)	Catechol	65 to 1600	3.75	[273]

Andrei and coauthors [268] reported the construction and characterization of a disposable single-use electrochemical sensor (SPE) based on CeNPs for the detection of phenolic antioxidants. The nanoceria supported oxidation of phenolic compounds to their corresponding quinones that can be detected at the SPE surface. For analysis of reactivity of gallic acid, ascorbic acid, quercetin, caffeic acid and epicatechin the amperometric detection was performed at the working potential −0.1 V vs. Ag/AgCl. The LR for gallic acid was between 50–200 μM, with a LOD of 15.3 μM (Table 11). The electrode did not respond to glucose, tartaric acid, ethanol, citric acid and sulfur dioxide at the applied conditions. The developed CeNPs SPE electrodes are low-cost, stable and disposable, making them promising for rapid field detection of antioxidant-rich samples and for screening purposes.

Another sensor has been developed for the analysis of antioxidants in wines based on CeNPs as a biomimetic [269]. The proposed single-use electrochemical screen-printed electrode, modified by CeNPs, was applied for detection of a number of antioxidant compounds which are present in wines (Table 11). The LR of the sensor is similar, and in some cases better, than for other analogs. The sensor does not require any specific storage conditions (e.g., buffer and low temperature) as opposed to enzymatic biosensors. Furthermore, the CeNP-modified electrode has a broader LR for gallic acid and ascorbic acid [269].

Wang and coworkers [270] proposed different crystalline nanostructured manganese oxide (MnO_2) and Mn_3O_4 on an electrode surface, which showed laccase-like catalytic activity toward ABTS and 17β-estradiol (E2). The best catalytic performance of the six different crystal structures for oxidizing ABTS and E2 was shown for the γ-MnO_2 variant. ABTS oxidation by γ-MnO_2 NPs under different pH values proved high oxidation activity of γ-MnO_2 at pH values of 3–4. The findings add to the understanding of the laccase-like catalysts based on MnOx [270].

Bin and coauthors [273] developed a novel highly stable sensor for cost-effective and efficient catechol detection based on the functionalized surface of multi-walled carbon nanotubes (MWCNTs) and iron porphyrins (FePP). Under optimal condition, the LOD for this NZ is slightly higher than that of the laccase sensor with the broader LR (Table 11). The reproducibility test showed that OH-MWCNTs/FePP/Nafion/GCE has better reproducibility than other laccase sensors. Storage analysis demonstrated that the oxidation current maintained 98.3% of its initial output after storage at −4 °C for 35 days.

7. Conclusions and Potential Applications

Only a small part of the known NZs and electronanocatalysts used in the construction of electrochemical sensors is presented in this review. At present, nanozymology is progressing faster than could be described directly as a real-time review. However, we believe that the presented data will be valuable for demonstrating the preferability of a combination of novel progressive nanotechnologies with electroanalytical approaches compared to classic enzymological methods.

Enzyme-based sensors are already successful commercial products in different application fields. Using cost-effective synthetic enzyme-like nanomaterials seems to be a very promising way for sensor development. It should be noted that NZs have several limitations for their application that need to be solved. The main disadvantage of most known NZs is the lack of substrate specificity. This drawback raises concerns regarding "nanozyme" term since in some cases these nanomaterials operate like chemical or electrochemical catalysts. The second drawback is the fouling of the NZ surface due to aggressive impact or adsorption of some compounds of the real environmental or biological samples. The third is a rather low reaction rate as a result of pH-sensitivity. Many common NZs work best in an acidic pH, while the pH of biological samples is often neutral. The fourth is a limited reaction type of the current NZs that are mainly capable of mimicking oxidoreductases (oxidases, peroxidase, catalase, SOD). Known NZs are thus currently able to mimic only a small fraction of enzymes. These critical problems must be solved in order to create highly selective, stable, reliable NZs that are suitable for practical use. However, considering the high scientific interest, progress in this field will focus on the creation of novel materials with new improved catalytic as well as physic-chemical properties, maximally fitted for (bio)chemosensing devices.

Funding: This work was funded in part by the Ministry of Education and Science of Ukraine (projects Nos. 0118U000297 and 0119U100671; Ukrainian- Lithuanian R&D Project in 2020–2021: "Development of biosensors and biofuel cells based on redox enzymes"), National Academy of Sciences of Ukraine in the frame of the Scientific-Technical Program "Smart sensor devices of a new generation based on modern materials and technologies" (projects No. 13 and No. 10/3).

Acknowledgments: The authors are thankfull to A. Zakalskiy for his help in literature analysis. The work was supported by the Research Authority of the Ariel University, Israel.

Conflicts of Interest: The authors declare no conflicts of interest.

Abbreviations

AA	Ascorbic acid
ABTS	2,2′-Azinobis-(3-ethylbenzthiazoline-6-sulphonate)
AKCN	Alkalized graphitic carbon nitride
AMP	Adenosine monophosphate
AOx	Alcohol oxidase
AP	Acetamidophenol

AuNPs	Gold nanoparticles
Au/Co@HNCF	Gold/cobalt nanoporous carbon framework
AuNBP/MWCNTs	Gold nanobipyramids supported by multi-walled carbon nanotubes
Fer/rGO	ferumoxytol and reduced graphene oxide
BET	Brunauer-Emmett-Teller
BG	Bucky gel consisting of carbon nanotubes and ionic liquid
biot-GOx	Biotinylated glucose oxidase
BNNS@CuS	Boron nitride nanosheet and copper sulfide nanohybrids
BSA	Bovine serum albumin
$C_{60}[C(COOH)_2]_2$	C_{60}-carboxyfullerene
CeNPs	Nanoceria particles
CF@CuAl-LDH	Carbon fiber-supported ultrathin cual layered double hydroxides (LDH) nanosheets
CF-H-Au	Carbon microfibers-hemin-gold nanoparticles
CMC@Pd/Al-LDH	Pd/Al layered double hydroxide/carboxymethyl cellulose nanocomposite;
CNE	Carbon nanoelectrodes fabricated within a quartz nanopipette and electrochemically etched
CNFs	Carbon nanofibers
CNTs	Multi-walled carbon nanotubes
COx	Cholesterol oxidase
CP	Carbon paste
CPS	Carbon paste sensors
CQDs	Carbon quantum dots
cTnI	Cardiac troponin I
CTMB	Cetyltrimethylammonium bromide
Cu-Cys	Copper(II) complex of cysteine
Cu-MOG	Cu-based metal-organic gel
CuNWs/rGO	One-dimensional copper nanowires and two-dimensional reduced graphene oxide nanosheets
DA	Dopamine
2,4-DCP	2,4-Dichlorophenol
3D GNCs	3D graphene-supported quantum dots
3DG	Three-dimensional graphene
DBD	Diamond Boron-doped
EMSN-AuNPs	Expanded mesoporous silica-encapsulated gold nanoparticles
ENC	Electronanocatalyst
ERGO	Electrochemically reduced graphene oxide
FePP	Iron porphyrins
GBR	Metal-free brominated graphene
GCE	Glassy carbon electrode
GCE/MWCNTs-Av/RuNPs/biot-GOx	Glassy carbon electrode/avidin-functionalized multi-walled carbon/nanotubes/Ru nanoparticles/biotinylated glucose oxidase
GDCh	Glucose derived sheet-like carbons
GE	Graphite electrode
GNP/Cu-Cys	Gold nanoparticles with the copper(II) complex of cysteine
GNPs	Gold nanoparticles
GNs	Graphene nanosheets
GO	Graphene oxide
GOx	Glucose oxidase
GOx/PtNP/PAni/Pt	Glucose Sensor Based on Pt Nanoparticle/Polyaniline Hydrogel
H_2TCPP	*meso*-Tetrakis(4-carboxyphenyl)-porphyrin
HCC	Carbon cubic nanomaterial
HCF	Hexacyanoferrate
h-CuS NCs	Hollow copper sulfide nanocubes
H-GNs	Hemin-graphene hybrid nanosheets
His@AuNCs	Histidine-capped gold nanoclusters

HNCs	Hollow nanocubes
H-rGO-Au	Hemin-graphene-gold nanoparticles
HRP	Horseradish peroxidase
H/WS2-NSs	Hemin-functionalized/Tungsten disulfide nanosheets
ITO	Indium tin oxide
L-Cys	L-Cysteine
LOD	Limit of detection
LOx	Lactate oxidase
LR	Linear range
MCM-41	Mobil composition of matter No. 41
MCNs	Mesoporous carbon nanospheres
MCP	Microchannel plate
MIP	Molecularly imprinted polymer
MMT	Montmorillonite
MC	Magnetic carbon
Mn-MPSA-HCC	Mn nanomaterials: hollow carbon cubic
Mn-MPSA-HCS	Mn nanomaterials: hollow carbon sphere
MOFs	Metal-Organic Frameworks
MWCNTs	Multi-walled carbon nanotubes
MWCNTs-Av	Avidin-functionalized multi-walled carbon nanotubes
NCs	Nanoclusters
NCF	Nitrogen doped cotton carbon fiber composite
N-CNFht	Nitrogen-doped carbon nanofibers
NFs	Nanoflakes
NPs	Nanoparticles
NTH	Nanotetrahedron
NW/CF	Nanowires/copper foam
NZ	Nanozyme
OPD	*o*-Phenylenediamine
PAni	Polyaniline
PANI/MXene	Polyaniline and $Ti_3C_2T_x$
PB	Prussian Blue
PEG-HCCs	Poly(ethylene glycolated) hydrophilic carbon clusters
PFOP	Heptadecafluoro-*n*-octyl bromide
PMMA	Poly(methylmethacrylate)
PNAANI	Poly(N-acetylaniline)
PO	Natural horseradish peroxidase
RDE	Rotating disk electrode
RGO	Reduced graphene oxide
rGO	Reduced graphene oxide
SOD	Superoxide dismutase
SPCE	Screen-printed carbon electrode
TMB	3,5,3′,5′-Tetramethylbenzidine
UA	Uric acid
WCC	Tungsten carbide decorated by cobalt nanoparticles
YSNs	Yolk-shell nanostructures
ZIF	Zeolitic imidazolate framework
β-CD	β-Cyclodextrin

References

1. Breslow, R.; Overman, L.E. An "Artificial Enzyme" combining a metal catalytic group and a hydrophobic binding cavity. *J. Am. Chem. Soc.* **1970**, *92*, 1075–1077. [CrossRef] [PubMed]
2. Cheng, H.; Wang, X.; Wei, H. Artificial enzymes: The next wave. In *Encyclopedia of Physical Organic Chemistry*, 1st ed.; Wang, Z., Ed.; John Wiley & Sons: Hoboken, NJ, USA, 2017; p. 64. ISBN 978-1-118-46858-6.

3. Wei, H.; Wang, E. Nanomaterials with enzyme-like characteristics (nanozymes): Next-generation artificial enzymes. *Chem. Soc. Rev.* **2013**, *42*, 6060–6093. [CrossRef] [PubMed]
4. Lin, Y.; Ren, J.; Qu, X. Nano-Gold as Artificial Enzymes: Hidden Talents. *Adv. Mater.* **2014**, *26*, 4200–4217. [CrossRef] [PubMed]
5. Wu, J.; Wang, X.; Wang, Q.; Lou, Z.; Li, S.; Zhu, Y.; Qin, L.; Wei, H. Nanomaterials with enzyme-like characteristics (nanozymes): Next-generation artificial enzymes (II). *Chem. Soc. Rev.* **2019**, *48*, 1004–1076. [CrossRef] [PubMed]
6. Huang, Y.; Ren, J.; Qu, X. Nanozymes: Classification, Catalytic Mechanisms, Activity Regulation, and Applications. *Chem. Rev.* **2019**, *119*, 4357–4412. [CrossRef]
7. Carmona-Ribeiro, A.; Prieto, T.; Nantes, I.L. Peroxidases in nanostructures. *Front. Mol. Biosci.* **2015**, *2*, 50. [CrossRef]
8. Jiang, B.; Fang, L.; Wu, K.; Yan, X.; Fan, K. Ferritins as natural and artificial nanozymes for theranostics. *Theranostics* **2020**, *10*, 687–706. [CrossRef]
9. Wang, P.; Wang, T.; Hong, J.; Yan, X.; Liang, M. Nanozymes: A New Disease Imaging Strategy. *Front. Bioeng. Biotech.* **2020**, *8*, 1–10. [CrossRef]
10. Liang, M.; Yan, X. Nanozymes: From New Concepts, Mechanisms, and Standards to Applications. *Acc. Chem. Res.* **2019**, *5*, 2190–2200. [CrossRef]
11. Jiang, D.; Ni, D.; Rosenkrans, Z.T.; Huang, P.; Yan, X.; Cai, W. Nanozyme: New horizons for responsive biomedical applications. *Chem. Soc. Rev.* **2019**, *48*, 3683–3704. [CrossRef]
12. Gao, L.Z.; Zhuang, J.; Nie, L.; Zhang, J.B.; Zhang, Y.; Gu, N.; Wang, T.H.; Feng, J.; Yang, D.L.; Perrett, S.; et al. Intrinsic peroxidase-like activity of ferromagnetic nanoparticles. *Nat. Nanotechnol.* **2007**, *2*, 577–583. [CrossRef] [PubMed]
13. Karyakin, A.A. Prussian Blue and Its Analogues: Electrochemistry and Analytical Applications. *Electroanalysis* **2001**, *13*, 813–819. [CrossRef]
14. Wang, Y.; Mao, J.; Meng, X.; Yu, L.; Deng, D.; Bao, X. Catalysis with Two-Dimensional Materials Confining Single Atoms: Concept, Design, and Applications. *Chem. Rev.* **2019**, *119*, 1806–1854. [CrossRef] [PubMed]
15. Vernekar, A.A.; Das, T.; Ghosh, S.; Mugesh, G. A Remarkably Efficient $MnFe_2O_4$-based Oxidase Nanozyme. *Chem. Asian, J.* **2016**, *11*, 72–76. [CrossRef] [PubMed]
16. Wang, H.; Wan, K.; Xinghua, S. Recent Advances in Nanozyme Research. *Adv. Mater.* **2019**, *31*, 1805368. [CrossRef] [PubMed]
17. Jiang, B.; Duan, D.; Gao, L.; Zhou, M.; Fan, K.; Tang, Y.; Xi, J.; Bi, Y.; Tong, Z.; Gao, G.F.; et al. Standardized assays for determining the catalytic activity and kinetics of peroxidase-like nanozymes. *Nat. Protoc.* **2018**, *13*, 1506–1520. [CrossRef]
18. Liu, J. Special Topic: Nanozyme-Based Analysis and Testing. *J. Anal. Test.* **2019**, *3*, 189–190. [CrossRef]
19. Golchin, J.; Golchin, K.; Alidadian, N.; Ghaderi, S.; Eslamkhah, S.; Eslamkhah, M.; Akbarzadeh, A. Nanozyme applications in biology and medicine: An overview. *Artif. Cells Nanomed. Biotechnol.* **2017**, *45*, 1–8. [CrossRef]
20. Liu, X.; Gao, Y.; Chandrawati, R.; Hosta-Rigau, L. Therapeutic applications of multifunctional nanozymes. *Nanoscale* **2019**, *11*, 21046–21060. [CrossRef]
21. Gu, Y.; Huang, Y.; Qiu, Z.; Xu, Z.; Li, D.; Chen, L.; Jiang, J.; Gao, L. Vitamin B_2 functionalized iron oxide nanozymes for mouth ulcer healing. *Sci. China Life Sci.* **2019**, *62*, 12. [CrossRef]
22. Wang, Q.; Wei, H.; Zhang, Z.; Wang, E.; Dong, S. Nanozyme: An emerging alternative to natural enzyme for biosensing and immunoassay. *Trends Anal. Chem.* **2018**, *105*, 218–224. [CrossRef]
23. Nayl, A.A.; Abd-Elhamid, A.I.; El-Moghazy, A.Y.; Hussin, M.; Abu-Saied, M.A.; El-Shanshory, A.A.; Soliman, H.M.A. The nanomaterials and recent progress in biosensing systems: A review. *Trends Environ. Anal. Chem.* **2020**, e00087. [CrossRef]
24. Mahmudunnabi, R.G.; Farhana, N.F.; Kashaninejad, Z.; Firoz, S.H.; Shim, Y.; Shiddiky, M.J.A. Nanozymes-based electrochemical biosensors for disease biomarker detection. *Analyst* **2020**, *145*, 4398–4420. [CrossRef] [PubMed]
25. Qin, L.; Hu, Y.; Wei, H. Nanozymes: Preparation and Characterization. In *Nanostructure Science and Technology*; Yan, X., Ed.; Springer: Singapore, 2020.
26. Li, J.; Wu, Q.; Wu, J. Synthesis of Nanoparticles via Solvothermal and Hydrothermal Methods. In *Handbook of Nanoparticles*; Aliofkhazraei, M., Ed.; Springer International Publishing: Cham, Switzerland, 2016; pp. 295–328.

27. Luo, L.; Zhang, Y.; Li, F.; Si, X.; Ding, Y.; Wang, T. Enzyme mimics of spinel-type $Co_xNi_1-xFe_2O_4$ magnetic nanomaterial for eletroctrocatalytic oxidation of hydrogen peroxide. *Anal. Chim. Acta* **2013**, *788*, 46–51. [CrossRef]
28. Wu, Q.; He, L.; Jiang, Z.W.; Li, Y.; Zheng, M.C.; Cheng, Z.H.; Li, Y.F. CuO Nanoparticles Derived from Metal-Organic Gel with Excellent Electrocatalytic and Peroxidase-Mimicking Activities for Glucose and Cholesterol Detection. *Biosens. Bioelectron.* **2019**, *145*, 111704. [CrossRef]
29. Zheng, S.; Li, B.; Tang, Y.; Li, Q.; Xue, H.; Pang, H. Ultrathin Nanosheet-Assembled $[Ni_3(OH)_2(PTA)_2(H_2O)_4]\cdot 2H_2O$ Hierarchical Flowers for High-Performance Electrocatalysis of Glucose Oxidation Reactions. *Nanoscale* **2018**, *10*, 13270–13276. [CrossRef]
30. Li, Y.; Zhang, H.; Cai, X.; Zhao, H.; Magdassi, S.; Lan, M. Electrochemical detection of superoxide anions in HeLa cells by using two enzyme-free sensors prepared from ZIF-8-derived carbon nanomaterials. *Mikrochim. Acta* **2019**, *186*, 370. [CrossRef]
31. Wang, C.; Liu, C.; Li, J.; Sun, X.; Shen, J.; Han, W.; Wang, L. Electrospun metal–organic framework derived hierarchical carbon nanofibers with high performance for supercapacitors. *Chem. Commun.* **2017**, *53*, 1751–1754. [CrossRef]
32. Scandurra, A.; Ruffino, F.; Sanzaro, S.; Grimaldi, M.G. Laser and Thermal Dewetting of Gold Layer onto Graphene Paper for non-Enzymatic Electrochemical Detection of Glucose and Fructose. *Sens. Actuators B Chem.* **2019**, *301*, 127113. [CrossRef]
33. Wang, K.; Wu, C.; Wang, F.; Liao, M.; Jiang, G. Bimetallic nanoparticles decorated hollow nanoporous carbon framework as nanozyme biosensor for highly sensitive electrochemical sensing of uric acid. *Biosens. Bioelectron.* **2020**, *150*, 111869. [CrossRef]
34. Chou, K.S.; Ren, C.Y. Synthesis of nanosized silver particles by chemical reduction method. *Mater. Chem. Phys.* **2000**, *64*, 241–246. [CrossRef]
35. Rane, A.V.; Kanny, K.; Abitha, V.K.; Sabu, T. Chapter 5. Methods for Synthesis of Nanoparticles and Fabrication of Nanocomposites. In *Synthesis of Inorganic Nanomaterials Advances and Key Technologies Micro and Nano Technologies*, 1st ed.; Bhagyaraj, S.M., Oluwafemi, O.S., Kalarikkal, N., Sabu, T., Eds.; Woodhead Publishing Company: Sawston, UK, 2018; pp. 121–139.
36. Suriati, G.M.; Mariatti, M.; Azizan, A. Synthesis of silver nanoparticles bu chemical reduction method: Effect of reducing agent and surfactant concentration. *Int. J. Automot. Mech. Eng.* **2014**, *10*, 1920–1927. [CrossRef]
37. Zhu, J.; Peng, X.; Nie, W.; Wang, Y.; Gao, J.; Wen, W.; Wang, S. Hollow copper sulfide nanocubes as multifunctional nanozymes for colorimetric detection of dopamine and electrochemical detection of glucose. *Biosens. Bioelectron.* **2019**, *141*, 111450. [CrossRef] [PubMed]
38. Das, R.; Dhiman, A.; Kapil, A.; Bansal, V.; Sharma, T.K. Aptamer-mediated colorimetric and electrochemical detection of *Pseudomonas aeruginosa* utilizing peroxidase-mimic activity of gold NanoZyme. *Anal. Bioanal. Chem.* **2019**, *411*, 1229–1238. [CrossRef] [PubMed]
39. Benedetti, T.M.; Andronescu, C.; Cheong, S.; Wilde, P.; Wordsworth, J.; Kientz, M.; Tilley, R.D.; Schuhmann, W.; Gooding, J.J. Electrocatalytic Nanoparticles That Mimic the Three-Dimensional Geometric Architecture of Enzymes: Nanozymes. *J. Am. Chem. Soc.* **2018**, *140*, 13449–13455. [CrossRef] [PubMed]
40. Ling, P.; Cheng, S.; Chen, N.; Qian, C.; Gao, F. Nanozyme-Modified Metal–Organic Frameworks with Multienzymes Activity as Biomimetic Catalysts and Electrocatalytic Interfaces. *ACS Appl. Mater. Interfaces* **2020**, *12*, 17185–17192. [CrossRef]
41. Liu, L.; Du, J.; Liu, W.E.; Guo, Y.; Wu, G.; Qi, W.; Lu, X. Enhanced His@AuNCs Oxidase-Like Activity by Reduced Graphene Oxide and Its Application for Colorimetric and Electrochemical Detection of Nitrite. *Anal. Bioanal. Chem.* **2019**, *411*, 2189–2200. [CrossRef]
42. Hummers, W.S.; Offeman, R.E. Preparation of graphitic oxide. *J. Am. Chem. Soc.* **1958**, *80*, 1339. [CrossRef]
43. Han, R.; Lu, Y.; Mingjun, L.; Yanbo, W.; Xuan, L.; Chongyang, L.; Kun, L.; Lingxing, Z.; Aihua, L. Green tide biomass templated synthesis of molybdenum oxide nanorods supported on carbon as efficient nanozyme for sensitive glucose colorimetric assay. *Sens. Actuators B Chem.* **2019**, *296*, 126517. [CrossRef]
44. Han, L.; Zhang, H.; Li, F. Bioinspired Nanozymes with pH-Independent and Metal Ions-Controllable Activity: Field-Programmable Logic Conversion of Sole Logic Gate System. *Part. Part. Syst. Char.* **2018**, 1800207. [CrossRef]
45. Zhai, D.; Liu, B.; Shi, Y.; Pan, L.; Wang, Y.; Li, W.; Zhang, R.; Yu, G. Highly Sensitive Glucose Sensor Based on Pt Nanoparticle/Polyaniline Hydrogel Heterostructures. *ACS Nano* **2013**, *7*, 3540–3546. [CrossRef] [PubMed]

46. Chen, H.I.; Chang, H.Y. Synthesis of nanocrystalline cerium oxide particles by the precipitation method. *Ceram. Int.* **2005**, *31*, 795–802. [CrossRef]
47. Cai, X.; Wang, Z.; Zhang, H.; Li, Y.; Chen, K.; Zhao, H.; Lan, M. Carbon-mediated synthesis of shape-controllable manganese phosphate as nanozymes for modulation of superoxide anions in HeLa cells. *J. Mater. Chem. B* **2019**, *7*, 401–407. [CrossRef] [PubMed]
48. Dashtestani, F.; Ghourchian, H.; Eskandari, K.; Rafiee-Pour, H.A. A superoxide dismutase mimic nanocomposite for amperometric sensing of superoxide anions. *Microchim. Acta* **2015**, *82*, 1045–1053. [CrossRef]
49. Sun, D.; Lin, X.; Lu, J.; Wei, P.; Luo, Z.; Lu, X.; Chen, Z.; Zhang, L. DNA Nanotetrahedron-Assisted Electrochemical Aptasensor for Cardiac Troponin I Detection Based on the Co-Catalysis of Hybrid Nanozyme, Natural Enzyme and Artificial DNAzyme. *Biosens. Bioelectron.* **2019**, *42*, 111578. [CrossRef] [PubMed]
50. Wurm, F.R.; Weiss, C.K. Nanoparticles from renewable polymers. *Front. Chem.* **2014**, *2*, 49. [CrossRef]
51. Han, M.; Guo, P.; Wang, X.; Tu, W.; Bao, J.; Dai, Z. Mesoporous SiO_2–(L)-lysine hybrid nanodisks: Direct electron transfer of superoxide dismutase, sensitive detection of superoxide anions and its application in living cell monitoring. *RSC Adv.* **2013**, *3*, 20456–20463. [CrossRef]
52. Manesh, K.M.; Lee, S.H.; Uthayakumar, S.; Gopalan, A.I.; Lee, K.P. Sensitive electrochemical detection of superoxide anion using gold nanoparticles distributed poly(methyl methacrylate)–polyaniline core–shell electrospun composite electrode. *Analyst* **2011**, *136*, 1557–1561.
53. Tonelli, D.; Scavetta, E.; Gualandi, I. Electrochemical Deposition of Nanomaterials for Electrochemical Sensing. *Sensors* **2019**, *19*, 1186. [CrossRef]
54. Al-Bat'hi, S.A.M. Electrodeposition of nanostructure materials. In *Electroplating of Nanostructures*; Aliofkhazraei, M., Ed.; InTech: Rijeka, Croatia, 2015; pp. 3–25.
55. Cioffi, N.; Colaianni, L.; Ieva, E.; Pilolli, R.; Ditaranto, N.; Daniela, M.; Cotrone, S.; Buchholt, K.; Lloyd, A.; Sabbatini, L.; et al. Electrosynthesis and characterization of gold nanoparticles for electronic capacitance sensing of pollutants. *Electrochim. Acta* **2011**, *56*, 3713–3720. [CrossRef]
56. Dominguez-Dominguez, S.; Arias-Pardilla, J.; Berenguer-Murcia, A.; Morallon, E.; Cazorla-Amoros, D. Electrochemical deposition of platinum nanoparticles on different carbon supports and conducting polymers. *J. Appl. Electrochem.* **2008**, *38*, 259–268. [CrossRef]
57. Rodriguez-Sanchez, L.; Blanco, M.C.; Lopez-Quintela, M.A. Electrochemical Synthesis of Silver Nanoparticles. *J. Phys. Chem. B* **2000**, *104*, 9683–9688. [CrossRef]
58. Guangwei, S.; Lixuan, M.; Wensheng, S. Electroplating of nanostructures. *Recent Pat. Nanotech.* **2009**, *3*, 182–191.
59. Gallay, P.; Eguílaz, M.; Rivas, G. Designing Electrochemical Interfaces Based on Nanohybrids of Avidin Functionalized-Carbon Nanotubes and Ruthenium Nanoparticles as Peroxidase-Like Nanozyme With Supramolecular Recognition Properties for Site-Specific Anchoring of Biotinylated Residues. *Biosens. Bioelectron.* **2020**, *148*, 111764. [CrossRef]
60. Stasyuk, N.; Gayda, G.; Zakalskiy, A.; Zakalska, O.; Serkiz, R.; Gonchar, M. Amperometric biosensors based on oxidases and PtRu nanoparticles as artificial peroxidase. *Food Chem.* **2019**, *285*, 213–220. [CrossRef]
61. Wu, T.; Li, L.; Song, G.; Ran, M.; Lu, X.; Liu, X. An ultrasensitive electrochemical sensor based on cotton carbon fiber composites for the determination of superoxide anion release from cells. *Microchim. Acta* **2019**, *186*, 198. [CrossRef]
62. Lu, Z.; Wu, L.; Zhang, J.; Dai, W.; Mo, G.; Ye, J. Bifunctional and highly sensitive electrochemical non-enzymatic glucose and hydrogen peroxide biosensor based on $NiCo_2O_4$ nanoflowers decorated 3D nitrogen doped holey graphene hydrogel. *Mater. Sci. Eng. C Mater. Biol. Appl.* **2019**, *102*, 708–717. [CrossRef]
63. Lin, S.; Zhang, Y.; Cao, W.; Wang, X.; Qin, L.; Zhou, M.; Wei, H. Nucleobase-mediated synthesis of nitrogen-doped carbon nanozymes as efficient peroxidase mimics. *Dalton Trans.* **2019**, *48*, 1993–1999. [CrossRef]
64. Jiang, B.; Yan, L.; Zhang, J.; Zhou, M.; Shi, G.; Tian, X.; Fan, K.; Hao, C.; Yan, X. Biomineralization Synthesis of the Cobalt Nanozyme in SP94-Ferritin Nanocages for Prognostic Diagnosis of Hepatocellular Carcinoma. *ACS Appl. Mater. Interfaces* **2019**, *11*, 9747–9755. [CrossRef]
65. Zhang, D.; Shen, N.; Zhang, J.; Zhu, J.; Guo, Y.; Xu, L. A novel nanozyme based on selenopeptide-modified gold nanoparticles with a tunable glutathione peroxidase activity. *RSC Adv.* **2020**, *10*, 8685–8691. [CrossRef]

66. Liu, L.; Yan, Y.; Zhang, X.; Mao, Y.; Ren, X.; Hu, C.; He, W.; Yin, J. Regulating the Pro- and Anti-Oxidant Capability of Bimetallic Nanozymes for Detection of Fe^{2+} and Protection of *Monascus* pigments. *Nanoscale* **2020**, *12*, 3068–3075. [CrossRef] [PubMed]
67. Liu, M.; Kong, L.; Wang, X.; He, J.; Bu, X.H. Engineering Bimetal Synergistic Electrocatalysts Based on Metal–Organic Frameworks for Efficient Oxygen Evolution. *Nano Micro. Small* **2019**, *15*, 1903410. [CrossRef] [PubMed]
68. Cao-Milán, R.; He, L.D.; Shorkey, S.; Tonga, G.Y.; Wang, L.S.; Zhang, X.; Uddin, I.; Das, R.; Sulak, M.; Rotello, V.M. Modulating the Catalytic Activity of Enzyme-like Nanoparticles Through their Surface Functionalization. *Mol. Syst. Des. Eng.* **2017**, *2*, 624–628. [CrossRef] [PubMed]
69. Wang, X.; Sun, H.; Wang, C. Functionalization of GroEL nanocages with hemin for label-free colorimetric assays. *Anal. Bioanal. Chem.* **2019**, *411*, 3819–3827. [CrossRef]
70. Gao, M.; Lu, X.; Nie, G.; Chi, M.; Wang, C. Hierarchical CNFs/$MnCo_2O_{4.5}$ nanofibers as a highly active oxidase mimetic and its application in biosensing. *Nanotechnology* **2017**, *28*, 485708. [CrossRef]
71. Wu, L.; Wan, G.; Hu, N.; He, Z.; Shi, S.; Suo, Y.; Wang, K.; Xu, X.; Tang, Y.; Wang, G. Synthesis of Porous $CoFe_2O_4$ and Its Application as a Peroxidase Mimetic for Colorimetric Detection of H_2O_2 and Organic Pollutant Degradation. *Nanomaterials* **2018**, *8*, 451. [CrossRef]
72. Shackery, I.; Patil, U.; Pezeshki, A.; Shinde, N.M.; Im, S.; Jun, S.C. Enhanced Non-enzymatic amperometric sensing of glucose using $Co(OH)_2$ nanorods deposited on a three dimensional graphene network as an electrode material. *Microchim. Acta* **2016**, *183*, 2473–2479. [CrossRef]
73. Tyagi, M.; Tomar, M.; Gupta, V. Glad assisted synthesis of NiO nanorods for realization of enzymatic reagentless urea biosensor. *Biosens. Bioelectron.* **2014**, *52*, 196–201. [CrossRef]
74. Li, Y.; Zhong, Y.; Zhang, Y.; Weng, W.; Li, S. Carbon quantum dots/octahedral Cu_2O nanocomposites for non-enzymatic glucose and hydrogen peroxide amperometric sensor. *Sens. Actuators B Chem.* **2015**, *206*, 735–743. [CrossRef]
75. Wu, H.X.; Cao, W.M.; Li, Y.; Liu, G.; Wen, Y.; Yang, H.F.; Yang, S.P. In situ growth of copper nanoparticles on multiwalled carbon nanotubes and their application as non-enzymatic glucose sensor materials. *Electrochim. Acta* **2010**, *55*, 3734–3740. [CrossRef]
76. Pirmohamed, T.; Dowding, J.M.; Singh, S.; Wasserman, B.; Heckert, E.; Karakoti, A.S.; King, J.E.S.; Seal, S.; Self, W.T. Nanoceria exhibit redox state-dependent catalase mimetic activity. *Chem. Commun.* **2010**, *46*, 2736–2738. [CrossRef] [PubMed]
77. Hayat, A.; Cunningham, J.; Bulbula, G.; Andreescu, S. Evaluation of the oxidase like activity of nanoceria and its application in colorimetric assays. *Anal. Chim. Acta* **2015**, *885*, 140–147. [CrossRef] [PubMed]
78. Mumtaz, S.; Wang, L.-S.; Abdullah, M.; Hussain, S.Z.; Iqbal, Z.; Rotello, V.M.; Hussain, I. Facile method to synthesize dopamine-capped mixed ferrite nanoparticles and their peroxidase-like activity. *J. Phys. D Appl. Phys.* **2017**, *50*, 11LT02. [CrossRef]
79. Liu, S.; Lu, F.; Xing, R.; Zhu, J.J. Structural effects of Fe_3O_4 nanocrystals on peroxidase-like activity. *Chem. Eur. J.* **2011**, *17*, 620–625. [CrossRef]
80. Rauf, S.; Ali, N.; Tayyab, Z.; Shah, M.Y.; Yang, C.P.; Hu, J.F.; Kong, W.; Huang, Q.A.; Hayat, A.; Muhammad, M. Ionic liquid coated zerovalent manganese nanoparticles with stabilized and enhanced peroxidase-like catalytic activity for colorimetric detection of hydrogen peroxide. *Mater. Res. Express* **2020**, *7*, 035018. [CrossRef]
81. Zhang, K.; Zuo, W.; Wang, Z.; Liu, J.; Li, T.; Wang, B.; Yang, Z. A simple route to $CoFe_2O_4$ nanoparticles with shape and size control and their tunable peroxidase-like activity. *RSC Adv.* **2015**, *5*, 10632–10640. [CrossRef]
82. Liu, B.; Liu, J. Surface modification of nanozymes. *Nano Res.* **2017**, *10*, 1125–1148. [CrossRef]
83. Zhao, M.; Huang, J.; Zhou, Y.; Pan, X.; He, H.; Ye, Z.; Pan, X. Controlled synthesis of spinel $ZnFe_2O_4$ decorated ZnO heterostructures as peroxidase mimetics for enhanced colorimetric biosensing. *Chem. Commun.* **2013**, *49*, 7656–7658. [CrossRef]
84. Cheng, X.; Huang, L.; Yang, X.; Elzatahry, A.A.; Alghamdi, A.; Deng, Y. Rational design of a stable peroxidase mimic for colorimetric detection of H_2O_2 and glucose: A synergistic CeO_2/Zeolite Y nanocomposite. *J. Colloid Interface Sci.* **2019**, *535*, 425–435. [CrossRef]
85. Hong, J.; Wang, W.; Huang, K.; Yang, W.; Zhao, Y.; Xiao, B.; Gao, Y.; Moosavi-Movahedi, Z.; Ahmadian, S.; Bohlooli, M.; et al. A self-assembled nano-cluster complex based on cytochrome c and nafion: An efficient nanostructured peroxidise. *Biochem. Eng. J.* **2012**, *65*, 16–22. [CrossRef]

86. Rui, Q.; Liangliang, S.; Aoting, Q.; Ruolin, W.; Yingli, A.; Linqi, S. Artificial Peroxidase/Oxidase Multiple Enzyme System Based on Supramolecular Hydrogel and Its Application as a Biocatalyst for Cascade Reactions. *ACS Appl. Mater. Interfaces* **2015**, *7*, 16694–16705. [CrossRef]
87. Zeng, H.H.; Qiu, W.B.; Zhang, L.; Liang, R.P.; Qiu, J.D. Lanthanide Coordination Polymer Nanoparticles as an Excellent Artificial Peroxidase for Hydrogen Peroxide Detection. *Anal. Chem.* **2016**, *88*, 6342–6348. [CrossRef] [PubMed]
88. Sun, L.; Ding, Y.; Jiang, Y.; Liu, Q. Montmorillonite-loaded ceria nanocomposites with superior peroxidase-like activity for rapid colorimetric detection of H_2O_2. *Sens. Actuators B Chem.* **2017**, *239*, 848–856. [CrossRef]
89. Chen, Q.; Chen, J.; Gao, C.; Zhang, M.; Chen, J.; Qiu, H. Hemin-functionalized WS2 nanosheets as highly active peroxidase mimetics for label-free colorimetric detection of H_2O_2 and glucose. *Analyst* **2015**, *140*, 2857–2863. [CrossRef]
90. Liu, Q.; Yang, Y.; Lv, X.; Ding, Y.; Zhang, Y.; Jing, J.; Xu, C. Onestep synthesis of uniform nanoparticles of porphyrin functionalized ceria with promising peroxidase mimetics for H_2O_2 and glucose colorimetric detection. *Sens. Actuators B Chem.* **2017**, *240*, 726–734. [CrossRef]
91. Li, Z.; Yang, X.; Yang, Y.; Tan, Y.; He, Y.; Liu, M.; Liu, X.; Yuan, Q. Peroxidase-mimicking nanozyme with enhanced activity and high stability based on metal-support interaction. *Chem. Eur. J.* **2018**, *24*, 409–415. [CrossRef]
92. Zhang, Y.; Wang, Y.N.; Sun, X.T.; Chen, L.; Xu, Z.R. Boron nitride nanosheet/CuS nanocomposites as mimetic peroxidase for sensitive colorimetric detection of cholesterol. *Sens. Actuators B Chem.* **2017**, *246*, 118–126. [CrossRef]
93. Jampaiah, D.; Reddy, T.S.; Coyle, V.E.; Nafady, A.; Bhargava, S.K. Co_3O_4@CeO_2 hybrid flower-like microspheres: A strong synergistic peroxidase-mimicking artificial enzyme with high sensitivity for glucose detection. *J. Mater. Chem. B.* **2017**, *5*, 720–773. [CrossRef]
94. Vallabani, N.V.; Karakoti, A.S.; Singh, S. ATP-mediated intrinsic peroxidase-like activity of Fe_3O_4-based nanozyme: One step detection of blood glucose at physiological pH. *Colloids Surf. B Biointerfaces* **2017**, *153*, 52–60. [CrossRef]
95. Wang, Z.H.; Chen, M.; Shu, J.X.; Li, Y. One-step solvothermal synthesis of Fe_3O_4@Cu@Cu_2O nanocomposite as magnetically recyclable mimetic peroxidase. *J. Alloys Compd.* **2016**, *682*, 432–440. [CrossRef]
96. Liu, Q.Y.; Zhang, L.Y.; Li, H.; Jia, Q.; Jiang, Y.; Yang, Y.; Zhu, R. One-pot synthesis of porphyrin functionalized gamma-Fe_2O_3 nanocomposites as peroxidase mimics for H_2O_2 and glucose detection. *Mat. Sci. Eng. C Mater.* **2015**, *55*, 193–200. [CrossRef] [PubMed]
97. Roy, A.; Sahoo, R.; Ray, C.; Dutta, S.; Pa, T. Soft template induced phase selective synthesis of Fe_2O_3 nanomagnets: One step towards peroxidase-mimic activity allowing colorimetric sensing of thioglycolic acid. *RSC Adv.* **2016**, *6*, 32308–32318. [CrossRef]
98. Nagvenkar, A.P.; Gedanken, A. Cu0.89Zn0.11O, A New Peroxidase-Mimicking Nanozyme with High Sensitivity for Glucose and Antioxidant Detection. *ACS Appl. Mater. Interfaces* **2016**, *8*, 22301–22308. [CrossRef] [PubMed]
99. Lu, N.; Zhang, M.; Ding, L.; Zheng, J.; Zeng, C.; Wen, Y.; Liu, G.; Aldalbahi, A.; Shi, J.; Song, S.; et al. Yolk-shell nanostructured Fe_3O_4@C magnetic nanoparticles with enhanced peroxidase-like activity for label-free colorimetric detection of H_2O_2 and glucose. *Nanoscale* **2017**, *9*, 4508–4515. [CrossRef]
100. He, W.W.; Zhou, Y.T.; Wamer, W.G.; Hu, X.; Wu, X.; Zheng, Z.; Boudreau, M.D.; Yin, J.J. Intrinsic catalytic activity of Au nanoparticles with respect to hydrogen peroxide decomposition and superoxide scavenging. *Biomaterials* **2013**, *34*, 765–773. [CrossRef]
101. Bustami, Y.; Murray, M.Y.; William, A.A. Manipulation of Fe/Au Peroxidase-Like Activity for Development of a Nanocatalytic-Based Assay. *J. Eng. Sci.* **2017**, *13*, 29–52. [CrossRef]
102. He, W.; Han, X.; Jia, H.; Cai, J.; Zhou, Y.; Zheng, Z. AuPt Alloy Nanostructures with Tunable Composition and Enzyme-like Activities for Colorimetric Detection of Bisulfide. *Sci. Rep.* **2017**, *7*, e40103. [CrossRef]
103. He, S.B.; Chen, R.T.; Wu, Y.Y.; Wu, G.W.; Peng, H.P.; Liu, A.L.; Deng, H.H.; Xia, X.H.; Chen, W. Improved enzymatic assay for hydrogen peroxide and glucose by exploiting the enzyme-mimicking properties of BSA-coated platinum nanoparticles. *Mikrochim. Acta* **2019**, *186*, e778. [CrossRef]
104. Jin, L.; Meng, Z.; Zhang, Y.; Cai, S.; Zhang, Z.; Li, C.; Shang, L.; Shen, Y. Ultrasmall Pt Nanoclusters as Robust Peroxidase Mimics for Colorimetric Detection of Glucose in Human Serum. *ACS Appl. Mater. Interfaces* **2017**, *9*, 10027–10033. [CrossRef]

105. Cao, G.; Jiang, X.; Zhang, H.; Croleyb, T.R.; Yin, J. Mimicking horseradish peroxidase and oxidase using ruthenium nanomaterials. *RSC Adv.* **2017**, *7*, 52210–52217. [CrossRef]
106. Wei, J.; Chen, X.; Shi, S.; Moa, S.; Zheng, N. An investigation of the mimetic enzyme activity of two-dimensional Pd-based nanostructures. *Nanoscale* **2015**, *7*, 19018–19026. [CrossRef] [PubMed]
107. Shkotova, L.; Bohush, A.; Voloshina, I.; Smutok, O.; Dzyadevych, S. Amperometric biosensor modified with platinum and palladium nanoparticles for detection of lactate concentrations in wine. *SN Appl. Sci.* **2019**, *1*, 306. [CrossRef]
108. Kluenker, M.; Tahir, M.N.; Ragg, R.; Korschelt, K.; Simon, P.; Gorelik, T.E.; Barton, B.; Shylin, S.I.; Panthöfer, M.; Herzberger, J.; et al. Pd@Fe_2O_3 Superparticles with Enhanced Peroxidase Activity by Solution Phase Epitaxial Growth. *Chem. Mater.* **2017**, *29*, 1134–1146. [CrossRef]
109. Li, R.; Zhen, M.; Guan, M.; Chen, D.; Zhang, G.; Ge, J.; Gong, P.; Wang, C.; Shu, C. A novel glucose colorimetric sensor based on intrinsic peroxidase-like activity of C_{60}-carboxyfullerenes. *Biosens. Bioelectron.* **2013**, *47*, 502–507. [CrossRef]
110. Sajjadi, S.; Keihan, A.H.; Norouzi, P.; Habibi, M.M.; Eskandari, K.; Shirazi, N.H. Fabrication of an Amperometric Glucose Biosensor Based on a Prussian Blue/Carbon Nanotube/Ionic Liquid Modified Glassy Carbon Electrode. *J. Appl. Biotechnol. Rep.* **2017**, *4*, 603–608.
111. Guerrero, L.A.; Fernández, L.; González, G.; Montero-Jiménez, M.; Uribe, R.; Díaz Barrios, A.; Espinoza-Montero, P.J. Peroxide Electrochemical Sensor and Biosensor Based on Nanocomposite of TiO_2 Nanoparticle/Multi-Walled Carbon Nanotube Modified Glassy Carbon Electrode. *Nanomaterials* **2020**, *10*, 64. [CrossRef]
112. Chen, Y.; Yuchi, Q.; Li, T.; Yang, G.; Miao, J.; Huang, C.; Liu, J.; Li, A.; Qin, Y.; Zhang, L. Precise engineering of ultra-thin Fe_2O_3 decorated Pt-based nanozymes via atomic layer deposition to switch off undesired activity for enhanced sensing performance. *Sens. Actuators B Chem.* **2020**, *305*, 127436. [CrossRef]
113. Guo, Y.; Deng, L.; Li, J.; Guo, S.; Wang, E.; Dong, S. Hemin-graphene hybrid nanosheets with intrinsic peroxidase-like activity for label-free colorimetric detection of single-nucleotide polymorphism. *ACS Nano* **2011**, *5*, 1282–1290. [CrossRef]
114. Kung, C.C.; Lin, P.Y.; Buse, F.J.; Xue, Y.; Yu, X.; Dai, L.; Liu, C.C. Preparation and characterization of three-dimensional graphene foam supported platinum-ruthenium bimetallic nanocatalysts for hydrogen peroxide based electrochemical biosensors. *Biosens. Bioelectron.* **2014**, *52*, 1–7. [CrossRef]
115. Song, Y.; Qu, K.; Zhao, C.; Ren, J.; Qu, X. Graphene oxide: Intrinsic peroxidase catalytic activity and its application to glucose detection. *Adv. Mater.* **2010**, *22*, 2206–2210. [CrossRef]
116. Li, X.-R.; Xu, M.; Chen, H.; Xu, J. Bimetallic Au@Pt@Au core–shell nanoparticles on graphene oxide nanosheets for high-performance H_2O_2 bi-directional sensing. *J. Mater. Chem. B* **2015**, *3*, 4355–4362. [CrossRef] [PubMed]
117. Li, S.; Li, H.; Chen, F.; Liu, J.; Zhang, H.; Yang, Z.; Wang, B. Strong coupled palladium nanoparticles decorated on magnetic graphene nanosheets as enhanced peroxidase mimetics for colorimetric detection of H_2O_2. *Dye. Pigment.* **2016**, *125*, 64–71. [CrossRef]
118. Lv, X.; Weng, J. Ternary composite of hemin, gold nanoparticles and graphene for highly efficient decomposition of hydrogen peroxide. *Sci. Rep.* **2013**, *3*, e3285. [CrossRef] [PubMed]
119. Sun, H.; Liu, X.; Wang, X.; Han, Q.; Qi, C.; Li, Y.; Wang, C.; Chen, Y.; Yang, R. Colorimetric determination of ascorbic acid using a polyallylamine-stabilized IrO_2/graphene oxide nanozyme as a peroxidase mimic. *Microchim. Acta* **2020**, *187*, 110. [CrossRef]
120. Darabdhara, G.; Sharma, B.; Das, M.R.; Boukherroub, R.; Szunerits, S. Cu-Ag bimetallic nanoparticles on reduced graphene oxidenanosheets as peroxidase mimic for glucose and ascorbic acid detection. *Sens. Actuators B Chem.* **2017**, *238*, 842–851. [CrossRef]
121. Song, L.N.; Huang, C.; Zhang, W.; Ma, M.; Chen, Z.; Gu, N.; Zhang, Y. Graphene oxide-based Fe_2O_3 hybrid enzyme mimetic with enhanced peroxidase and catalase-like activities. *Colloid Surf. A* **2016**, *506*, 747–755. [CrossRef]
122. Dong, W.; Zhuang, Y.; Li, S.; Zhang, X.; Chai, H.; Huang, Y. High peroxidase-like activity of metallic cobalt nanoparticles encapsulated in metal–organic frameworks derived carbon for biosensing. *Sens. Actuators B Chem.* **2018**, *255*, 2050–2057. [CrossRef]
123. Karuppiah, C.; Palanisamy, S.; Chen, S.; Veeramani, V.; Periakaruppan, P. A novel enzymatic glucose biosensor and sensitive non-enzymatic hydrogen peroxide sensor based on graphene and cobalt oxide nanoparticles composite modified glassy carbon electrode. *Sens. Actuators B Chem.* **2014**, *196*, 450–456. [CrossRef]

124. Bahreini, M.; Movahedi, M.; Peyvandi, M.; Nematollahi, F.; Tehrani, H.S. Thermodynamics and kinetic analysis of carbon nanofibers as nanozymes. *Nanotechmol. Sci. Appl.* **2019**, *12*, 3–10. [CrossRef]
125. Shi, W.; Wang, Q.; Long, Y.; Cheng, Z.; Chen, S.; Zheng, H.; Huang, Y. Carbon nanodots as peroxidase mimetics and their applications to glucose detection. *Chem. Commun.* **2011**, *47*, 6695–6697. [CrossRef]
126. Zhang, Y.; Wu, C.; Zhou, X.; Wu, X.; Yang, Y.; Wu, H.; Guo, S.; Zhang, J. Graphene quantum dots/gold electrode and its application in living cell H_2O_2 detection. *Nanoscale* **2013**, *5*, 1816–1819. [CrossRef]
127. Zhang, L.; Hai, X.; Xia, C.; Chen, X.W.; Wang, J.H. Growth of CuO nanoneedles on graphene quantum dots as peroxidase mimics for sensitive colorimetric detection of hydrogen peroxide and glucose. *Sens. Actuators B Chem.* **2017**, *248*, 374–384. [CrossRef]
128. Fakhri, N.; Salehnia, F.; Beigi, S.M.; Aghabalazadeh, S.; Hosseini, M.; Ganjali, M.R. Enhanced peroxidase-like activity of platinum nanoparticles decorated on nickel- and nitrogen-doped graphene nanotubes: Colorimetric detection of glucose. *Microchim. Acta* **2019**, *186*, e385. [CrossRef] [PubMed]
129. Wu, L.; Wan, G.; Shi, S.; He, Z.; Xu, X.; Tang, Y.; Hao, C.; Wang, G. Atomic layer deposition-assisted growth of CuAl LDH on carbon fiber as a peroxidase mimic for colorimetric determination of H_2O_2 and glucose. *New J. Chem.* **2019**, *15*, 5826–5832. [CrossRef]
130. Sang, Y.; Huang, Y.; Li, W.; Ren, J.; Qu, X. Bioinspired Design of Fe^{3+}-doped mesoporous carbon nanospheres for enhanced nanozyme activity. *Chemistry* **2018**, *24*, 7259–7263. [CrossRef] [PubMed]
131. Zhao, Y.; Huo, D.; Bao, J.; Yang, M.; Chen, M.; Hou, J.; Fa, H.; Hou, C. Biosensor based on 3D graphene-supported Fe_3O_4 quantum dots as biomimetic enzyme for in situ detection of H_2O_2 released from living cells. *Sens. Actuators B Chem.* **2017**, *244*, 1037–1044. [CrossRef]
132. Song, H.; Zhao, H.; Zhang, X.; Xu, Y.; Cheng, X.; Gao, S.; Huo, L. Ahollow urchin-like α-mno2 as an electrochemical sensor for hydrogen peroxide and dopamine with high selectivity and sensitivity. *Microchim. Acta* **2019**, *186*, 210–221. [CrossRef]
133. Mei, H.; Wang, X.; Zeng, T.; Huang, L.; Wang, Q.; Ru, D.; Huang, T.; Tian, F.; Wu, H.; Gao, J. A nanocomposite consisting of gold nanobipyramids and multiwalled carbon nanotubes for amperometric nonenzymatic sensing of glucose and hydrogen peroxide. *Microchim. Acta* **2019**, *186*, 235–242. [CrossRef]
134. Zhang, Y.; Duan, Y.; Shao, Z.; Chen, C.; Yang, M.; Lu, G.; Xu, W.; Liao, X. Amperometric hydrogen peroxide sensor using a glassy carbon electrode modified with a nanocomposite prepared from ferumoxytol and reduced graphene oxide decorated with platinum nanoparticles. *Microchim. Acta* **2019**, *186*, 386. [CrossRef]
135. Zhang, C.; Zhang, Y.; Du, X.; Chen, Y.; Dong, W.; Han, B.; Chen, Q. Facile fabrication of Pt-Ag bimetallic nanoparticles decorated reduced graphene oxide for highly sensitive non-enzymatic hydrogen peroxide sensing. *Talanta* **2016**, *159*, 280–286. [CrossRef]
136. Singh, S.; Singh, M.; Mitra, K.; Singh, R.; Kumar, S.; Gupta, S.; Tiwari, I.; Ray, B. Electrochemical sensing of hydrogen peroxide using brominated graphene as mimetic catalase. *Electrochim. Acta* **2017**, *258*, 1435–1444. [CrossRef]
137. Fazli, G.; Bahabadi, S.E.; Adlnasab, L.; Ahmar, H. A glassy carbon electrode modified with a nanocomposite prepared from Pd/Al layered double hydroxide and carboxymethyl cellulose for voltammetric sensing of hydrogen peroxide. *Mikrochim. Acta* **2019**, *186*, 821. [CrossRef] [PubMed]
138. Neampet, S.; Ruecha, N.; Qin, J.; Wonsawat, W.; Chailapakul, O.; Rodthongkum, N. A nanocomposite prepared from platinum particles, polyaniline and a Ti_3C_2 MXene for amperometric sensing of hydrogen peroxide and lactate. *Mikrochim. Acta* **2019**, *186*, 752. [CrossRef] [PubMed]
139. Long, L.; Liu, X.; Chen, L.; Li, D.; Jia, J. A hollow CuO_x/NiO_y nanocomposite for amperometric and non-enzymatic sensing of glucose and hydrogen peroxide. *Microchim. Acta* **2019**, *186*, 74–84. [CrossRef] [PubMed]
140. Sivakumar, M.; Veeramani, V.; Chen, S.M.; Madhu, R.; Liu, S.B. Porous carbon-NiO nanocomposites for amperometric detection of hydrazine and hydrogen peroxide. *Microchim. Acta* **2019**, *186*, 59–66. [CrossRef]
141. Sha, R.; Vishnu, N.; Badhulika, S. Bimetallic Pt-Pd nanostructures supported on MoS_2 as an ultra-high performance electrocatalyst for methanol oxidation and nonenzymatic determination of hydrogen peroxide. *Microchim. Acta* **2018**, *185*, 399–409. [CrossRef]
142. Lyu, Y.P.; Wu, Y.S.; Wang, T.P.; Lee, C.L.; Chung, M.Y.; Lo, C.T. Hydrothermal and plasma nitrided electrospun carbon nanofibers for amperometric sensing of hydrogen peroxide. *Microchim. Acta* **2018**, *185*, 371–377. [CrossRef]

143. Liu, J.; Yang, C.; Shang, Y.; Zhang, P.; Liu, J.; Zheng, J. Preparation of a nanocomposite material consisting of cuprous oxide, polyaniline and reduced graphene oxide, and its application to the electrochemical determination of hydrogen peroxide. *Microchim. Acta* **2018**, *185*, 172–179. [CrossRef]
144. Annalakshmi, M.; Balasubramanian, P.; Chen, S.M.; Chen, T.W. Enzyme-free electrocatalytic sensing of hydrogen peroxide using a glassy carbon electrode modified with cobalt nanoparticle-decorated tungsten carbide. *Mikrochimica. Acta* **2019**, *186*, 265. [CrossRef]
145. Davidson, D. The Prussian blue paradox. *J. Chem. Educ.* **1937**, *14*, 238–241. [CrossRef]
146. Guari, Y.; Larionova, J. (Eds.) *Prussian Blue-Type Nanoparticles and Nanocomposites: Synthesis, Devices and Applications*; Jenny Stanford Publishing: Singapore, 2019; p. 314. ISBN 97898148000510.
147. Matos-Peralta, Y.; Antuch, M. Review—Prussian Blue and Its Analogs as Appealing Materials for Electrochemical Sensing and Biosensing. *J. Electrochem. Soc.* **2020**, *167*, 037510. [CrossRef]
148. Cinti, S.; Basso, M.; Moscone, D.; Arduini, F. A paper-based nanomodified electrochemical biosensor for ethanol detection in beers. *Anal. Chim. Acta* **2017**, *960*, 123–130. [CrossRef] [PubMed]
149. Ojwang, D.O. Prussian Blue Analogue Copper Hexacyanoferrate: Synthesis, Structure Characterization and Its Applications as Battery Electrode and CO_2 Adsorbent. Ph.D. Thesis, Stockholm University, Stockholm, Sweden, 13 October 2017. Available online: http://www.diva-portal.org/smash/record.jsf?pid=diva2%3A1136799&dswid=8693 (accessed on 7 May 2020).
150. Komkova, M.A.; Andreev, E.A.; Ibragimova, O.A.; Karyakin, A.A. Prussian Blue based flow-through (bio)sensors in power generation mode: New horizons for electrochemical analyzers. *Sens. Actuators B Chem.* **2019**, *292*, 284–288. [CrossRef]
151. Ivanov, V.D. Four decades of electrochemical investigation of Prussian blue. *Ionics* **2020**, *26*, 531–547. [CrossRef]
152. Chen, W.; Gao, G.; Jin, Y.; Deng, C. A facile biosensor for $A\beta_{40}O$ based on fluorescence quenching of prussian blue nanoparticles. *Talanta* **2020**, *216*, 120390. [CrossRef]
153. Meng, X.; Gao, L.; Fan, K.; Yan, X. Nanozyme-Based Tumor Theranostics. In *Nanostructure Science and Technology*; Yan, X., Ed.; Springer: Singapore, 2020; pp. 425–457. ISBN 978-981-15-1489-0.
154. He, L.; Li, Z.; Guo, C.; Hu, B.; Wang, M.; Zhang, Z.; Du, M. Bifunctional bioplatform based on NiCo Prussian blue analogue: Label-free impedimetric aptasensor for the early detection of carcino-embryonic antigen and living cancer cells. *Sens. Actuators B Chem.* **2019**, *298*. [CrossRef]
155. Tabrizi, M.A.; Shamsipur, M.; Saber, R.; Sarkar, S.; Zolfaghari, N. An ultrasensitive sandwich-type electrochemical immunosensor for the determination of SKBR-3 breast cancer cell using rGOTPA/FeHCF-labeld Anti-HCT as a signal tag. *Sens. Actuators B Chem.* **2017**, *243*, 823–830. [CrossRef]
156. Wang, M.; Hu, B.; Ji, H.; Song, Y.; Liu, J.; Peng, D.; He, L.; Zhang, Z. Aptasensor based on hierarchical core-shell nanocomposites of zirconium hexacyanoferrate nanoparticles and mesoporous mFe_3O_4@mC: Electrochemical quantitation of epithelial tumor marker mucin-1. *ACS Omega* **2017**, *2*, 6809–6818. [CrossRef]
157. Gao, Z.; Li, Y.; Zhang, C.; Zhang, S.; Jia, Y.; Dong, Y. An enzyme-free immunosensor for sensitive determination of procalcitonin using NiFe PBA nanocubes@TB as the sensing matrix. *Anal. Chim. Acta* **2020**, *1097*, 169–175. [CrossRef]
158. Jia, Q.; Li, Z.; Guo, C.; Huang, X.; Kang, M.; Song, Y.; He, L.; Zhou, N.; Wang, M.; Zhang, Z.; et al. PEGMA-modified bimetallic NiCo Prussian blue analogue doped with Tb (III) ions: Efficiently pH-responsive and controlled release system for anticancer drug. *Chem. Eng.* **2020**, *389*. [CrossRef]
159. Qin, Z.; Chen, B.; Huang, X.; Mao, Y.; Li, Y.; Yang, F.; Gu, N. Magnetic internal heating-induced high performance Prussian blue nanoparticle preparation and excellent catalytic activity. *Dalton. Trans.* **2019**, *48*, 17169–17173. [CrossRef] [PubMed]
160. Nwamba, O.C.; Echeverria, E.; McIlroy, D.N.; Shreeve, J.M.; Aston, D.R. Electrochemical stability and capacitance of in-situ synthesized Prussian blue on thermally-activated graphite. *SN. Appl. Sci.* **2019**, *1*, 731–746. [CrossRef]
161. Sahar, S.; Zeb, A.; Ling, C.; Raja, A.; Wang, G.; Ullah, N.; Lin, X.M.; Xu, A.-W. A Hybrid VOx Incorporated Hexacyanoferrate Nanostructured Hydrogel as a Multienzyme Mimetic via Cascade Reactions. *ACS Nano* **2020**, *14*, 3017–3031. [CrossRef] [PubMed]
162. Komkova, M.A.; Karyakina, E.E.; Karyakin, A.A. Catalytically Synthesized Prussian Blue Nanoparticles Defeating Natural Enzyme Peroxidase. *J. Am. Chem. Soc.* **2018**, *140*, 11302–11307. [CrossRef] [PubMed]

163. Koshiyama, T.; Tanaka, M.; Honjo, M.; Fukunaga, Y.; Okamura, T.; Ohba, M. Direct Synthesis of Prussian Blue Nanoparticles in Liposomes Incorporating Natural Ion Channels for Cs+ Adsorption and Particle Size Control. *Langmuir* **2018**, *34*, 1666–1672. [CrossRef]
164. Itaya, K.; Shoji, N.; Uchida, I. Catalysis of the reduction of molecular oxygen to water at Prussian blue modified electrodes. *J. Am. Chem. Soc.* **1984**, *106*, 3423–3429. [CrossRef]
165. Itaya, K.; Uchida, I.; Neff, V.D. Electrochemistry of polynuclear transition metal cyanides: Prussian blue and its analogues. *Acc. Chem. Res.* **1986**, *19*, 162–168. [CrossRef]
166. Cui, F.; Deng, Q.; Sun, L. Prussian blue modified metal–organic framework MIL-101(Fe) with intrinsic peroxidase-like catalytic activity as a colorimetric biosensing platform. *RSC Adv.* **2015**, *5*, 98215–98221. [CrossRef]
167. Keihan, A.H.; Karimi, R.R.; Sajjadi, S. Wide dynamic range and ultrasensitive detection of hydrogen peroxide based on beneficial role of gold nanoparticles on the electrochemical properties of prussian blue. *J. Electroanal. Chem.* **2020**, *862*, 114001. [CrossRef]
168. Pang, H.; Zhang, Y.; Cheng, T.; Lai, W.Y.; Huang, W. Uniform manganese hexacyanoferrate hydrate nanocubes featuring superior performance for low-cost supercapacitors and nonenzymatic electrochemical sensors. *Nanoscale* **2015**, *7*, 16012–16019. [CrossRef]
169. Wang, C.; Ren, G.; Yuan, B.; Zhang, W.; Lu, M.; Liu, J.; Li, K.; Lin, Y. Enhancing Enzyme-like Activities of Prussian Blue Analog Nanocages by Molybdenum Doping: Toward Cytoprotecting and Online Optical Hydrogen Sulfide Monitoring. *Anal. Chem.* **2020**, *92*, 7822–7830. [CrossRef] [PubMed]
170. Zhang, W.; Hu, S.; Yin, J.J.; He, W.; Ma, M.; Gu, N.; Zhang, Y. Prussian Blue Nanoparticles as Multienzyme Mimetics and Reactive Oxygen Species Scavengers. *J. Am. Chem. Soc.* **2016**, *138*, 5860–5865. [CrossRef] [PubMed]
171. Zhang, X.Z.; Zhou, Y.; Zhang, W.; Zhang, Y.; Gu, N. Polystyrene@Au@Prussian Blue Nanocomposites with Enzyme-Like Activity and Their Application in Glucose Detection. *Colloids Surf. A* **2016**, *490*, 291–299. [CrossRef]
172. Zhou, D.; Zeng, K.; Yang, M. Gold Nanoparticle-Loaded Hollow Prussian Blue Nanoparticles with Peroxidase-Like Activity for Colorimetric Determination of L-Lactic Acid. *Microchim. Acta* **2019**, *186*, 121. [CrossRef] [PubMed]
173. Zhang, W.; Ma, D.; Du, J. Prussian blue nanoparticles as peroxidase mimetics for sensitive colorimetric detection of hydrogen peroxide and glucose. *Talanta* **2014**, *120*, 362–367. [CrossRef]
174. Zhang, W.; Zhang, Y.; Chen, Y.; Li, S.; Gu, N.; Hu, S.; Sun, Y.; Chen, X.; Li, Q. Prussian Blue Modified Ferritin as Peroxidase Mimetics and Its Applications in Biological Detection. *J. Nanosci. Nanotechnol.* **2013**, *13*, 60–67. [CrossRef]
175. Wang, T.; Fu, Y.; Chai, L.; Chao, L.; Bu, L.; Meng, Y.; Chen, C.; Ma, M.; Xie, Q.; Yao, S. Filling Carbon Nanotubes with Prussian Blue Nanoparticles of High Peroxidase-Like Catalytic Activity for Colorimetric Chemo- And Biosensing. *Chem. Eur. J.* **2014**, *20*, 2623–2630. [CrossRef]
176. Karyakin, A.A.; Gitelmacher, O.V.; Karyakina, E.E. Prussian Blue-Based First-Generation Biosensor. A Sensitive Amperometric Electrode for Glucose. *Anal. Chem.* **1995**, *67*, 2419–2423. [CrossRef]
177. Karyakin, A.A.; Karyakina, E.E.; Gorton, L. Amperometric Biosensor for Glutamate Using Prussian Blue-Based "Artificial Peroxidase" as a Transducer for Hydrogen Peroxide. *Anal. Chem.* **2000**, *72*, 1720–1723. [CrossRef]
178. Karpova, E.V.; Karyakina, E.E.; Karyakin, A.A. Communication—Accessing Stability of Oxidase-Based Biosensors via Stabilizing the Advanced H_2O_2 Transducer. *J. Electrochem. Soc.* **2017**, *164*, B3056–B3058. [CrossRef]
179. Komkova, M.A.; Pasquarelli, A.; Andreev, E.A.; Galushin, A.A.; Karyakin, A.A. Prussian Blue modified boron-doped diamond interfaces for advanced H_2O_2 electrochemical sensors. *Electrochim. Acta.* **2020**, *339*. [CrossRef]
180. Vokhmyanina, D.V.; Andreeva, K.D.; Komkova, M.A.; Karyakina, E.E.; Karyakin, A.A. Artificial peroxidase" nanozyme—Enzyme based lactate biosensor. *Talanta* **2020**, *208*, 120393. [CrossRef] [PubMed]
181. Sitnikova, N.A.; Borisova, A.V.; Komkova, M.A.; Karyakin, A.A. Superstable advanced hydrogen peroxide transducer based on transition metal hexacyanoferrates. *Anal. Chem.* **2011**, *83*, 2359–2363. [CrossRef]
182. Zhou, L.; Wu, S.; Xu, H.; Zhao, Q.; Zhang, Z.; Yao, Y. Preparation of poly (N-acetylaniline)–Prussian blue hybrid composite film and its application to hydrogen peroxide sensing. *Anal. Methods* **2014**, *6*, 8003–8010. [CrossRef]

183. Zhao, H.-C.; Zhang, P.; Li, S.-H.; Luo, H.-X. Cobalt hexacyanoferrate-modified graphene platform electrode and its electrochemical sensing toward hydrogen peroxide. *Chin. J. Anal. Chem.* **2017**, *45*, 830–836. [CrossRef]
184. Yang, S.; Li, G.A.; Wang, G.; Zhao, J.; Hu, M.; Qu, L. A novel nonenzymatic H_2O_2 sensor based on cobalt hexacyanoferrate nanoparticles and graphene composite modified electrode. *Sens. Actuators B Chem.* **2015**, *208*, 593. [CrossRef]
185. Lee, S.H.; Chung, J.-H.; Park, H.-K.; Lee, G.-J. A Simple and Facile Glucose Biosensor Based on Prussian Blue Modified Graphite String. *J. Sens.* **2016**, *2016*, 1859292. [CrossRef]
186. Pandey, P.C.; Panday, D.; Pandey, A.K. Polyethylenimine mediated synthesis of copper-iron and nickel-iron hexacyanoferrate nanoparticles and their electroanalytical applications. *J. Electroanal. Chem.* **2016**, *780*, 90–102. [CrossRef]
187. Huang, J.; Fang, X.; Liu, X.; Lu, S.; Li, S.; Yang, Z.; Feng, X. High-Linearity Hydrogen Peroxide Sensor Based on Nanoporous Gold Electrode. *J. Electrochem. Soc.* **2019**, *166*, B814. [CrossRef]
188. Kumar, A.V.; Harish, S.; Joseph, J.; Phani, K.L. Nix–Fe(1−x)Fe(CN)6 hybrid thin films electrodeposited on glassy carbon: Effect of tuning of redox potentials on the electrocatalysis of hydrogen peroxide. *J. Electroanal. Chem.* **2011**, *659*, 128–133. [CrossRef]
189. Niu, Q.; Bao, C.; Cao, X.; Liu, C.; Wang, H.; Lu, W. Ni–Fe PBA hollow nanocubes as efficient electrode materials for highly sensitive detection of guanine and hydrogen peroxide in human whole saliva. *Biosens. Bioelectron.* **2019**, *141*, 111445. [CrossRef] [PubMed]
190. Sangeetha, N.S.; Narayanan, S.S. A novel bimediator amperometric sensor for electrocatalytic oxidation of gallic acid and reduction of hydrogen peroxide. *Anal. Chim. Acta* **2014**, *828*, 34–45. [CrossRef] [PubMed]
191. Clausmeyer, J.; Actis, P.; Córdoba, A.L.; Korchev, Y.; Schuhmann, W. Nanosensors for the detection of hydrogen peroxide. *Electrochem. Commun.* **2014**, *40*, 28–30. [CrossRef]
192. Ju, H.; Zhang, X.; Wang, J. *NanoBiosensing: Principles, Development and Application, Biological and Medical Physics, Biomedical Engineering Series*; Springer: New York, NY, USA, 2016; p. 586. ISBN 978-1441996213.
193. Dimcheva, N. Nanostructures of noble metals as functional materials in biosensors. *Curr. Opin. Electrochem.* **2020**, *19*, 35–41. [CrossRef]
194. Singh, S. Nanomaterials Exhibiting Enzyme-Like Properties (Nanozymes): Current Advances and Future Perspectives. *Front. Chem.* **2019**, *7*, 46. [CrossRef]
195. Fan, J.; Yin, J.J.; Ning, B.; Wu, X.; Hu, Y.; Ferrari, M.; Anderson, G.J.; Wei, J.; Zhao, Y.; Nie, G. Direct evidence for catalase and peroxidase activities of ferritin-platinum nanoparticles. *Biomater* **2011**, *32*, 1611–1618. [CrossRef]
196. Shah, K.; Bhagat, S.; Varade, D.; Singh, S. Novel synthesis of polyoxyethylene cholesteryl ether coated Fe-Pt nanoalloys: A multifunctional and cytocompatible bimetallic alloy exhibiting intrinsic chemical catalysis and biological enzyme-like activities. *Colloids Surf. A Physicochem. Eng. Asp.* **2018**, *553*, 50–57. [CrossRef]
197. Su, L.; Feng, J.; Zhou, X.; Ren, C.; Li, H.; Chen, X. Colorimetric detection of urine glucose based $ZnFe_2O_4$ magnetic nanoparticles. *Anal. Chem.* **2012**, *84*, 5753–5758. [CrossRef]
198. Zhang, X.; He, S.; Chen, Z.; Huang, Y. $CoFe_2O_4$ Nanoparticles as Oxidase Mimic-Mediated Chemiluminescence of Aqueous Luminol for Sulfite in White Wines. *J. Agric. Food Chem.* **2013**, *61*, 840–847. [CrossRef]
199. Dalapati, R.; Sakthivel, B.; Ghosalya, M.K.; Dhakshinamoorthy, A.; Biswas, S. A cerium-based metal–organic framework having inherent oxidase-like activity applicable for colorimetric sensing of biothiols and aerobic oxidation of thiols. *Cryst. Eng. Comm.* **2017**, *19*, 5915–5925. [CrossRef]
200. Estevez, A.Y.; Stadler, B.; Erlichman, J.S. In vitro analysis of catalase-, oxidase- and SOD-mimetic activity of commercially available and custom synthesized cerium oxide nanoparticles and assessment of neuroprotective effects in a hippocampal brain slice model of ischemia. *FASEB J.* **2017**, *31*, 693–695. [CrossRef]
201. Song, Y.; Zhao, M.; Li, H.; Wang, X.; Cheng, Y.; Ding, L.; Chen, S. Facile preparation of urchin-like $NiCo_2O_4$ microspheres as oxidase mimetic for colormetric assay of hydroquinone. *Sens. Actuators B Chem.* **2018**, *255*, 1927–1936. [CrossRef]
202. Yan, X.; Song, Y.; Wu, X.; Zhu, C.; Su, X.; Du, D.; Lin, Y. Oxidase-mimicking activity of ultrathin MnO_2 nanosheets in colorimetric assay of acetylcholinesterase activity. *Nanoscale* **2017**, *9*, 2317–2323. [CrossRef] [PubMed]
203. Cui, M.; Zhao, Y.; Wang, C.; Song, Q. The oxidase-like activity of iridium nanoparticles, and their application to colorimetric determination of dissolved oxygen. *Microchim. Acta* **2017**, *184*, 3113–3119. [CrossRef]
204. Zhang, H.; Lu, L.; Kawashima, K.; Okumura, M.; Haruta, M.; Toshima, N. Synthesis and Catalytic Activity of Crown Jewel-Structured (IrPd)/Au Trimetallic Nanoclusters. *Adv. Mater.* **2015**, *27*, 1383–1388. [CrossRef]

205. Deng, H.-H.; Lin, X.-L.; Liu, Y.-H.; Li, K.-L.; Zhuang, Q.-Q.; Peng, H.-P.; Chen, W. Chitosan-stabilized platinum nanoparticles as effective oxidase mimics for colorimetric detection of acid phosphatase. *Nanoscale* **2017**, *9*, 10292–10300. [CrossRef]
206. Jin, X.; Zhao, M.; Shen, J.; Yan, W.; He, L.; Thapa, P.S.; Ren, S.; Subramaniam, B.; Chaudhari, R.V. Exceptional performance of bimetallic Pt_1Cu_3/TiO_2 nanocatalysts for oxidation of gluconic acid and glucose with O_2 to glucaric acid. *J. Catal.* **2015**, *330*, 323–329. [CrossRef]
207. He, W.; Liu, Y.; Yuan, J.; Yin, J.J.; Wu, X.; Hu, X.; Zhang, K.; Liu, J.; Chen, C.; Ji, Y.; et al. Au@Pt nanostructures as oxidase and peroxidase mimetics for use in immunoassays. *Biomater* **2011**, *32*, 1139–1147. [CrossRef]
208. Zhang, H.; Toshima, N. Preparation of novel Au/Pt/Ag trimetallic nanoparticles and their high catalytic activity for aerobic glucose oxidation. *Appl. Catal. A Gen.* **2011**, *400*, 9–13. [CrossRef]
209. Khawaji, M.; Zhang, Y.; Loh, M.; Graça, L.; Ware, E.; Chadwick, D. Composition dependent selectivity of bimetallic Au-Pd NPs immobilised on titanate nanotubes in catalytic oxidation of glucose. *Appl. Catal. B Environ.* **2019**, *256*, 117799. [CrossRef]
210. Guo, S.; Fang, Q.; Li, Z.; Zhang, J.; Zhang, J.; Li, G. Efficient base-free direct oxidation of glucose to gluconic acid over TiO_2-supported gold clusters. *Nanoscale* **2019**, *11*, 1326–1334. [CrossRef] [PubMed]
211. Xie, J.; Zhang, X.; Wang, H.; Zheng, H.; Huang, Y. Analytical and environmental applications of nanoparticles as enzyme mimetics. *TrAC Trends Anal. Chem.* **2012**, *39*, 114–129. [CrossRef]
212. Ortega-Liebana, M.C.; Bonet-Aleta, J.; Hueso, J.L.; Santamaria, J. Gold-Based Nanoparticles on Amino-Functionalized Mesoporous Silica Supports as Nanozymes for Glucose Oxidation. *Catalysts* **2020**, *10*, 333. [CrossRef]
213. Luo, W.J.; Zhu, C.F.; Su, S.; Li, D.; He, Y.; Huang, Q.; Fan, C.H. Self-Catalyzed, Self-Limiting Growth of Glucose Oxidase-Mimicking Gold Nanoparticles. *ACS Nano* **2010**, *4*, 7451–74584. [CrossRef] [PubMed]
214. Kusema, B.T.; Murzin, D.Y. Catalytic oxidation of rare sugars over gold catalysts. *Catal. Sci. Technol.* **2013**, *3*, 297–307. [CrossRef]
215. Benkó, T.; Beck, A.; Geszti, O.; Katona, R.; Tungler, A.; Frey, K.; Guczi, L.; Schay, Z. Selective oxidation of glucose versus CO oxidation over supported gold catalysts. *Appl. Catal. A Gen.* **2010**, *388*, 31–36. [CrossRef]
216. Cao, X.; Wang, N. A novel non-enzymatic glucose sensor modified with Fe_2O_3 nanowire arrays. *Analyst* **2011**, *136*, 4241–4246. [CrossRef]
217. Megías-Sayago, C.; Ivanova, S.; López-Cartes, C.; Centeno, M.A.; Odriozola, J.A. Gold catalysts screening in base-free aerobic oxidation of glucose to gluconic acid. *Catal. Today* **2017**, *279*, 148–154. [CrossRef]
218. Megías-Sayago, C.; Bobadilla, L.F.; Ivanova, S.; Penkova, A.; Centeno, M.A.; Odriozola, J.A. Gold catalyst recycling study in base-free glucose oxidation reaction. *Catal. Today* **2018**, *301*, 72–77. [CrossRef]
219. Okatsu, H.; Kinoshita, N.; Akita, T.; Ishida, T.; Haruta, M. Deposition of gold nanoparticles on carbons for aerobic glucose oxidation. *Appl. Catal. A Gen.* **2009**, *369*, 8–14. [CrossRef]
220. Lang, N.J.; Liu, B.; Liu, J. Characterization of glucose oxidation by gold nanoparticles using nanoceria. *J. Colloid Interface Sci.* **2014**, *428*, 78–83. [CrossRef] [PubMed]
221. Fan, L.; Lou, D.D.; Wu, H.A.; Zhang, X.Z.; Zhu, Y.F.; Gu, N.; Zhang, Y. A Novel AuNP-Based Glucose Oxidase Mimic with Enhanced Activity and Selectivity Constructed by Molecular Imprinting and O_2-Containing Nanoemulsion Embedding. *Adv. Mater. Interfaces* **2018**, *5*, 1801070. [CrossRef]
222. Ma, W.; Hafez, M.E.; Ma, H.; Long, Y.-T. Unveiling the Intrinsic Catalytic Activities of Single Gold Nanoparticle-based Enzyme Mimetics. *Angew. Chem.* **2019**, *58*, 6327–6332. [CrossRef]
223. Cao, Y.; Liu, X.; Iqbal, S.; Miedziak, P.J.; Edwards, J.K.; Armstrong, R.D.; Morgan, D.J.; Wang, J.; Hutchings, G.J. Base-free oxidation of glucose to gluconic acid using supported gold catalysts. *Catal. Sci. Technol.* **2016**, *6*, 107–117. [CrossRef]
224. Gao, H.; Xiao, F.; Ching, C.B.; Duan, H. One-Step Electrochemical Synthesis of PtNi Nanoparticle-Graphene Nanocomposites for Nonenzymatic Amperometric Glucose Detection. *ACS Appl. Mater. Interfaces* **2011**, *3*, 3049–3057. [CrossRef]
225. Li, Z.; Chen, Y.; Xin, Y.; Zhang, Z. Sensitive electrochemical nonenzymatic glucose sensing based on anodized CuO nanowires on three-dimensional porous copper foam. *Sci. Rep.* **2015**, *5*, 16115. [CrossRef]
226. Ju, L.; Wu, G.; Lu, B.; Li, X.; Wu, H.; Liu, A. Non-enzymatic Amperometric Glucose Sensor Based on Copper Nanowires Decorated Reduced Graphene Oxide. *Electroanalysis* **2016**, *28*, 2543–2551. [CrossRef]
227. Zhang, X.; Shi, H.; Chi, Q.; Liu, X.; Chen, L. Cellulose-supported Pd nanoparticles: Effective for the selective oxidation of glucose into gluconic acid. *Polym. Bull.* **2019**, *77*, 1003–1014. [CrossRef]

228. Kou, B.; Yuan, Y.; Yuan, R.; Chai, Y. Electrochemical biomolecule detection based on the regeneration of high-efficiency cascade catalysis for bifunctional nanozymes. *Chem. Commun.* **2020**, *56*, 2276–2279. [CrossRef]
229. Lin, Y.; Li, Z.; Chen, Z.; Ren, J.; Qu, X. Mesoporous silica-encapsulated gold nanoparticles as artificial enzymes for self-activated cascade catalysis. *Biomater* **2013**, *34*, 2600–2610. [CrossRef]
230. Han, L.; Zhang, H.; Chen, D.; Li, F. Protein-Directed Metal Oxide Nanoflakes with Tandem Enzyme-Like Characteristics: Colorimetric Glucose Sensing Based on One-Pot Enzyme-Free Cascade Catalysis. *Adv. Funct. Mater.* **2018**, *28*, e1800018. [CrossRef]
231. Glucose Oxidase BRENDA. Available online: https://www.brenda-enzymes.org/all_enzymes.php?ecno=1.1.3.4&table=Turnover_%20Number#TABSingh (accessed on 5 May 2020).
232. Miao, F.; Tao, B.; Sun, L.; Liu, T.; You, J.; Wang, L.; Chu, P.K. Amperometric glucose sensor based on 3D ordered nickel–palladium nanomaterial supported by silicon MCP array. *Sens. Actuators Chem.* **2009**, *141*, 338–342. [CrossRef]
233. Ye, J.-S.; Hong, B.-D.; Wu, Y.-S.; Chen, H.-R.; Lee, C.-L. Heterostructured palladium-platinum core-shell nanocubes for use in a nonenzymatic amperometric glucose sensor. *Microchim. Acta* **2016**, *183*, 3311–3320. [CrossRef]
234. Liu, M.; Liu, R.; Chen, W. Graphene wrapped Cu_2O nanocubes: Non-enzymatic electrochemical sensors for the detection of glucose and hydrogen peroxide with enhanced stability. *Biosens. Bioelectron.* **2013**, *45*, 206–212. [CrossRef] [PubMed]
235. Cao, L.; Wang, P.; Chen, L.; Wu, Y.; Di, J. A photoelectrochemical glucose sensor based on gold nanoparticles as a mimic enzyme of glucose oxidase. *RSC Adv.* **2019**, *9*, 15307–15313. [CrossRef]
236. Espro, C.; Marini, S.; Giusi, D.; Ampelli, C.; Neri, G. Non-enzymatic screen printed sensor based on Cu_2O nanocubes for glucose determination in bio-fermentation processes. *J. Electroanal. Chem.* **2020**, *873*, 114354. [CrossRef]
237. Zhang, P.; Sun, D.; Cho, A.; Weon, S.; Lee, S.; Lee, J.; Choi, W. Modified carbon nitride nanozyme as bifunctional glucose oxidase-peroxidase for metal-free bioinspired cascade photocatalysis. *Nat. Commun.* **2019**, *10*, 940. [CrossRef]
238. Beden, B.; Largeaud, F.; Kokoh, K.B.; Lamy, C. Fourier transform infrared reflectance spectroscopic investigation of the electrocatalytic oxidation of d-glucose: Identification of reactive intermediates and reaction products. *Electrochim. Acta* **1996**, *41*, 701–709. [CrossRef]
239. Chandra, R.; Chowdhary, P. Properties of bacterial laccases and their application in bioremediation of industrial wastes. *Environ. Sci. Process. Impacts* **2015**, *17*, 326–342. [CrossRef]
240. Fathali, Z.; Rezaei, S.; Faramarzi, M.A.; Habibi-Rezaei, M. Catalytic phenol removal using entrapped cross-linked laccase aggregates. *Int. J. Biol. Macromol.* **2019**, *122*, 359–366. [CrossRef]
241. Galli, C.; Madzak, C.; Vadalà, R.; Jolivalt, C.; Gentili, P. Concerted electron/proton transfer mechanism in the oxidation of phenols by laccase. *Chembiochem* **2013**, *14*, 2500–2505. [CrossRef] [PubMed]
242. Jones, S.M.; Solomon, E.I. Electron transfer and reaction mechanism of laccases. *Cell. Mol. Life Sci.* **2015**, *72*, 869–883. [CrossRef] [PubMed]
243. Vernekar, M.; Lele, S.S. Laccase: Properties and Applications. *BioResources* **2009**, *4*, 1694–1717.
244. Yesilada, O.; Birhanli, E.; Geckil, H. Bioremediation and Decolorization of Textile Dyes by White Rot Fungi and Laccase Enzymes. In *Mycoremediation and Environmental Sustainability. Fungal Biology*; Prasad, R., Ed.; Springer: Berlin, Germany, 2018; pp. 121–153.
245. Shekher, R.; Sehgal, S.; Kamthania, M.; Kumar, A. Laccase: Microbial sources, production, purification, and potential biotechnological applications. *Enzym. Res.* **2011**, *2011*, 217861. [CrossRef]
246. Gao, L.; Yan, X. Nanozymes: An emerging field bridging nanotechnology and biology. *Sci. China Life Sci.* **2016**, *59*, 400–402. [CrossRef]
247. He, X.; Tan, L.; Chen, D.; Wu, X.; Ren, X.; Zhang, Y.; Meng, X.; Tang, F. Fe_3O_4-Au@mesoporous SiO_2 microspheres: An ideal artificial enzymatic cascade system. *Chem. Commun.* **2013**, *49*, 4643–4645. [CrossRef]
248. Zhou, Y.B.; Liu, B.W.; Yang, R.H.; Liu, J.W. Filling in the gaps between nanozymes and enzymes: Challenges and opportunities. *Bioconjug. Chem.* **2017**, *28*, 2903–2909. [CrossRef]
249. Tanaka, Y.; Hoshino, W.; Shimizu, S.; Youfu, K.; Aratani, N.; Maruyama, N.; Fujita, S.; Osuka, A. Thermal splitting of bis-Cu(II) octaphyrin (1.1.1.1.1.1.1.1) into two Cu(II) porphyrins. *J. Am. Chem. Soc.* **2004**, *126*, 3046–3047. [CrossRef]

250. Zhou, L.; Powell, D.; Nicholas, K.M. Tripodal bis(imidazole) thioether copper(I) complexes: Mimics of the Cu(b) site of hydroxylase enzymes. *Inorg. Chem.* **2006**, *45*, 3840–3842. [CrossRef]
251. Rivas, M.V.; De Leo, L.P.; Hamer, M.; Carballo, R.; Williams, F.J. Self-assembled monolayers of disulfide Cu porphyrins on Au surfaces: Adsorption induced reduction and demetalation. *Langmuir* **2011**, *27*, 10714–10721. [CrossRef]
252. Uhlmann, C.; Swart, I.; Repp, J. Controlling the orbital sequence in individual Cu-phthalocyanine molecules. *Nano Lett.* **2013**, *13*, 777–780. [CrossRef] [PubMed]
253. Ge, S.; Li, D.; Huang, S.; Chen, W.; Tu, G.; Yu, S.; He, Q.; Gong, J.; Li, Y.; Hong, C.; et al. A magnetically recyclable Fe_3O_4@C@TNCuPc composite catalyst for chromogenic identification of phenolic pollutants. *J. Mol. Catal. A Chem.* **2015**, *410*, 193–201. [CrossRef]
254. Ren, X.; Liu, J.; Ren, J.; Tang, F.; Meng, X. One-pot synthesis of active copper-containing carbon dots with laccase-like activities. *Nanoscale* **2015**, *7*, 19641–19646. [CrossRef] [PubMed]
255. Meng, X.Q.; Fan, K.L. Application of nanozymes in disease diagnosis. *Prog. Biochem. Biophys.* **2018**, *45*, 218–236. [CrossRef]
256. Tang, Y.; Qiu, Z.Y.; Xu, Z.B.; Gao, L.Z. Antibacterial mechanism and applications of nanozymes. *Prog. Biochem. Biophys.* **2018**, *45*, 118–128. [CrossRef]
257. Lv, Y.; Ma, M.; Huang, Y.; Xia, Y. Carbon Dot Nanozymes: How to Be Close to Natural Enzymes. *Chem. Eur. J.* **2019**, *25*, 954. [CrossRef]
258. Shams, S.; Ahmad, W.; Memon, A.H.; Wei, Y.; Yuan, Q.; Liang, H. Facile synthesis of laccase mimic Cu/H 3 BTC MOF for efficient dye degradation and detection of phenolic pollutants. *RSC Adv.* **2019**, *9*, 40845–40854. [CrossRef]
259. Zhou, P.; Shi, R.; Yao, J.-F.; Sheng, C.-F.; Li, H. Supramolecular self-assembly of nucleotide–metal coordination complexes: From simple molecules to nanomaterials. *Coordin. Chem. Rev.* **2015**, *292*, 107–143. [CrossRef]
260. Liang, H.; Zhang, Z.; Yuan, Q.; Liu, J. Self-healing metal-coordinated hydrogels using nucleotide ligands. *Chem. Commun.* **2015**, *51*, 15196–15199. [CrossRef]
261. Frey, N.A.; Peng, S.; Cheng, K.; Sun, S. Magnetic nanoparticles: Synthesis, functionalization, and applications in bioimaging and magnetic energy storage. *Chem. Soc. Rev.* **2009**, *38*, 2532–2542. [CrossRef]
262. Liang, H.; Lin, F.; Zhang, Z.; Liu, B.; Jiang, S.; Yuan, Q.; Liu, J. Multicopper laccase mimicking nanozymes with nucleotides as ligands. *ACS Appl. Mater. Inter.* **2017**, *9*, 1352–1360. [CrossRef] [PubMed]
263. Zhang, S.; Lin, F.; Yuan, Q.; Liu, J.; Li, Y.; Liang, H. Robust magnetic laccase-mimicking nanozyme for oxidizing o-phenylenediamine and removing phenolic pollutants. *J. Environ. Sci. (China)* **2020**, *88*, 103–111. [CrossRef] [PubMed]
264. Huang, H.; Lei, L.; Bai, J.; Zhang, L.; Song, D.; Zhao, J.; Li, J.; Li, Y. Efficient elimination and detection of phenolic compounds in juice using laccase mimicking nanozymes. *Chin. J. Chem. Eng.* **2020**. [CrossRef]
265. Wang, J.; Huang, R.; Qi, W.; Su, R.; Binks, B.P.; He, Z. Construction of a bioinspired laccase-mimicking nanozyme for the degradation and detection of phenolic pollutants. *Appl. Catal. B Environ.* **2019**, *254*, 452–462. [CrossRef]
266. Manea, F.; Houillon, F.B.; Pasquato, L.; Scrimin, P. Nanozymes: Gold-nanoparticle-based transphosphorylation catalysts. *Angew. Chem. Int. Ed. Engl.* **2004**, *43*, 6165–6169. [CrossRef] [PubMed]
267. Wang, Y.; He, C.; Li, W.; Zhang, J.; Fu, Y. Catalytic Performance of Oligonucleotide-Templated Pt Nanozyme Evaluated by Laccase Substrates. *Catal. Lett.* **2017**, *147*, 2144–2152. [CrossRef]
268. Andrei, V.; Sharpe, E.; Vasilescu, A.; Andreescu, S. A single use electrochemical sensor based on biomimetic nanoceria for the detection of wine antioxidants. *Talanta* **2016**, *156*, 112–118. [CrossRef] [PubMed]
269. Tortolini, C.; Bollella, P.; Zumpano, R.; Favero, G.; Mazzei, F.; Antiochia, R. Metal Oxide Nanoparticle Based Electrochemical Sensor for Total Antioxidant Capacity (TAC) Detection in Wine Samples. *Biosensors* **2018**, *8*, 108. [CrossRef]
270. Wang, X.; Liu, J.; Qu, R.; Wang, Z.; Huang, Q. The laccase-like reactivity of manganese oxide nanomaterials for pollutant conversion: Rate analysis and cyclic voltammetry. *Sci. Rep.* **2017**, *7*, 7756. [CrossRef] [PubMed]
271. Rodríguez-Delgado, M.; Orona-Navar, C.; García-Morales, R.; Hernandez-Luna, C.; Parra, R.; Mahlknecht, J.; Ornelas-Soto, N. Biotransformation kinetics of pharmaceutical and micropollutants in groundwaters by a laccase cocktail from *Pycnoporus sanguineus* CS43 fungi. *Int. Biodeterior. Biodegrad.* **2016**, *108*, 34–41.

272. Garcia, L.F.; Souza, A.R.; Lobón, G.S.; dos Santos, W.T.P.; Alecrim, M.F.; Santiago, M.F.; de Sotomayor, R.L.Á.; Gil, E.S. Efficient Enzyme-Free Biomimetic Sensors for Natural Phenol Detection. *Molecules* **2016**, *21*, 1060. [CrossRef] [PubMed]
273. Bin, Z.; Yanhong, C.; Jiaojiao, X. Biomimetic oxidase sensor based on functionalized surface of carbon nanotubes and iron prophyrins for catechol detection. *Bioprocess Biosyst. Eng.* **2018**, 42. [CrossRef] [PubMed]

© 2020 by the authors. Licensee MDPI, Basel, Switzerland. This article is an open access article distributed under the terms and conditions of the Creative Commons Attribution (CC BY) license (http://creativecommons.org/licenses/by/4.0/).

Оригінал доступний за посиланням: https://www.mdpi.com/1424-8220/20/16/4509

Анотація: *Наука, медицина, клінічна діагностика, біотехнології, в тому числі, харчові технології і виробництво напоїв, а також екологічні технології потребують селективних, чутливих, швидких та надійних методів визначення вмісту ключових інгредієнтів або метаболітів, які визначають якість продукту або виступають маркерами деяких захворювань, фізіологічного стану організму людини або екологічної безпеки. Біосенсори є найбільш перспективним інструментом для цих цілей. Хоча більшість створених біосенсорів ґрунтуються на використанні ензимів у ролі біокаталізаторів, в останні роки активно розробляються клітинні сенсори, особливо, мікробні. Мікробний біосенсор складається з фізичного перетворювача в поєднанні з іммобілізованими мікробними клітинами. Цільовий аналіт зазвичай є або субстратом, або інгібітором клітинного метаболізму. У цьому огляді нами розглянуто основні досягнення в галузі створення мікробних сенсорів на основі дріжджових клітин та перспективи їх використання в клінічній діагностиці та контролю якості харчових продуктів.*

Yeast-Based Biosensors for Clinical Diagnostics and Food Control

14

Mykhailo Gonchar, Oleh Smutok, Maria Karkovska, Nataliya Stasyuk, and Galina Gayda

Abstract

Science; medicine; clinical diagnostics; biotechnologies, including those in food and beverage industries; as well as environmental technologies need highly selective, sensitive, rapid, and reliable methods of identifying the key ingredients or metabolites which determine the quality of the product or serve as markers for diseases, the physiological state of human organism, or environmental safety. Biosensors are the most promising tool for these aims. Although the most of created biosensors are based on using enzymes as biocatalytic elements, cell sensors, especially microbial ones, have been actively developed only in recent years. A microbial biosensor consists of a transducer in conjunction with immobilized viable or nonviable microbial cells, an economical substitute for enzymes. The target analyte is usually either a substrate or an inhibitor of cell metabolism. In this review, the main achievements in the elaboration of microbial sensors, based on yeast cells, are described, and perspectives of their usage in clinical diagnostics and food control are discussed.

Contents

14.1 Introduction 392
14.2 Microbial Sensors for Clinical Diagnostics 396
14.2.1 Glucose 396
14.2.2 Lactate 397
14.2.3 Hormones 398
14.2.4 Vitamin B_1 399
14.2.5 L-Lysine 399
14.2.6 Urate 400
14.2.7 Intracellular Metabolites 400

M. Gonchar (✉) • O. Smutok • M. Karkovska • N. Stasyuk • G. Gayda
Department of Analytical Biotechnology, Institute of Cell Biology, NAS of Ukraine, 14/16, Drahomanov Street, Lviv 79005, Ukraine
e-mail: mykhailo1952@gmail.com

© Springer International Publishing AG 2017

A.A. Sibirny (ed.), *Biotechnology of Yeasts and Filamentous Fungi*,
DOI 10.1007/978-3-319-58829-2_14

14.2.8 Toxic Compounds 401
14.3 Microbial Sensors Based on Yeast Cells for Food Analysis 403
14.3.1 Ethanol Assay 403
14.3.2 Amino Acid Assay 406
14.3.3 L-Lactate Assay 407
14.3.4 Assay of Contaminants 407
References 408

14.1 Introduction

Modern science; medicine; clinical diagnostics; biotechnologies, including those in food and beverage industries; as well as environmental technologies need highly selective, sensitive, rapid, and reliable methods of identifying the key ingredients or metabolites which determine the quality of the product or serve as markers for diseases, the physiological state of human organism, or environmental safety (Turner et al. 1990).

Among different analytical approaches, a special role is attributed to *analytical biotechnology* which exploits the principles of biomolecular recognition, highly developed during the evolution. Biomolecular recognition is responsible for storing (on molecular level) and reading (on supramolecular level) of information and is the fundamental characteristic of the life. Such property of biomolecules and their complexes is used in analytical biotechnology. It can be defined as a branch of biotechnology related with the use of tissues, cells, organelles, biomolecules, their complexes, and even principles of their functioning for analytical purposes (Gonchar et al. 2002).

Biosensors are the most novel achievement of analytical biotechnology. Although up to now IUPAC has not accepted an official definition of the term biosensor, its electrochemical representative is defined as "a self-contained integrated device, which is capable of providing specific quantitative or semi-quantitative analytical information using a biological recognition element (biochemical receptor) which is retained in direct spatial contact with an electrochemical transduction element" (Thevenot et al. 2001). Generally, a biosensor is a hybrid device containing two functional parts: a bioelement (*biorecognition unit*)—an immobilized biologically active material—and a physical transducer (*signal converting unit*). Figuratively speaking, biosensors may be called "chemical canaries" based on historical fact about miners using such birds to detect toxic methane.

Basically, biosensors can be regarded as information transducers in which the energy of biospecific interactions is transformed into the information about the nature and concentration of an analyte in the sample. Pieces of tissue, microbial cells, organelles, natural biomembranes or liposomes, receptors, enzymes, antibodies and antigens, nucleic acids and other biomolecules, and even biomimetics which imitate structural and functional features of the natural analogue can be used as biorecognition elements. The bioelement is a recognition unit providing selective binding or biochemical/metabolic conversion of the analyte that results in

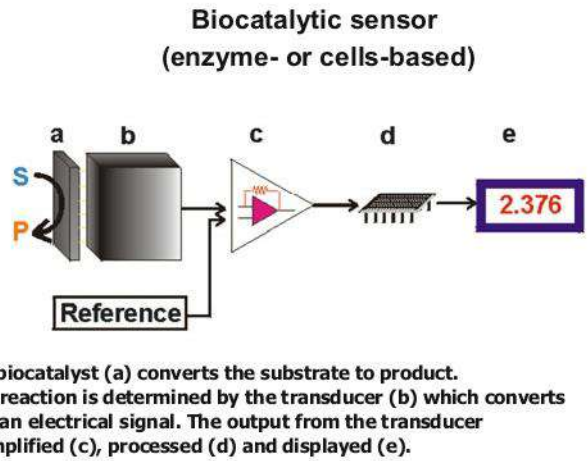

Fig. 14.1 Functional units of biosensor (Atta et al. 2011)

changes of physical or physicochemical characteristics of the transducer (Schmidt and Karube 1998). The output from the transducer is amplified, processed, and displayed (Fig. 14.1).

The biosensor bioelement is usually prepared in the immobilized form and often covered with an outer membrane (or placed between two membranes in a sandwich manner), which either prevents the penetration of interfering substances into a sensitive bioselective layer and transducer surface or creates a diffusion barrier for the analyte. Such membrane structures increase the stability of the biorecognizing element, enhance its selectivity, and provide the diffusion limitations for biochemical reactions. Electrochemical, optical, piezoelectric, thermoelectric, transistor, acoustic, and other elements are used as transducers in biosensor systems.

The most essential advantages of biosensors are their excellent chemical selectivity and high sensitivity, possibility of miniaturization, and compatibility with computers. Their drawbacks are limited stability and rather a complicated procedure of preparing the biologically active material.

The enzyme biosensors are the most widespread devices; some of them are produced commercially. The world market of biosensors was estimated at approx. $11.39 billion in 2013 and is expected to reach $22.68 billion by 2020 with an annual growth of 10.00% from 2014 to 2020 (http://www.marketsandmarkets.com/PressReleases/biosensors.asp).

The commercially produced biosensors are used mostly in clinical medicine (as points of care), in home diagnostics, in research labs, in biodefense, in environmental monitoring, for online control of biotechnological processes, in food industry, and for military or law enforcement (Fig. 14.2). The use of biosensors for fundamental research, e.g., in metabolomics, is also very promising (Kraly et al. 2009).

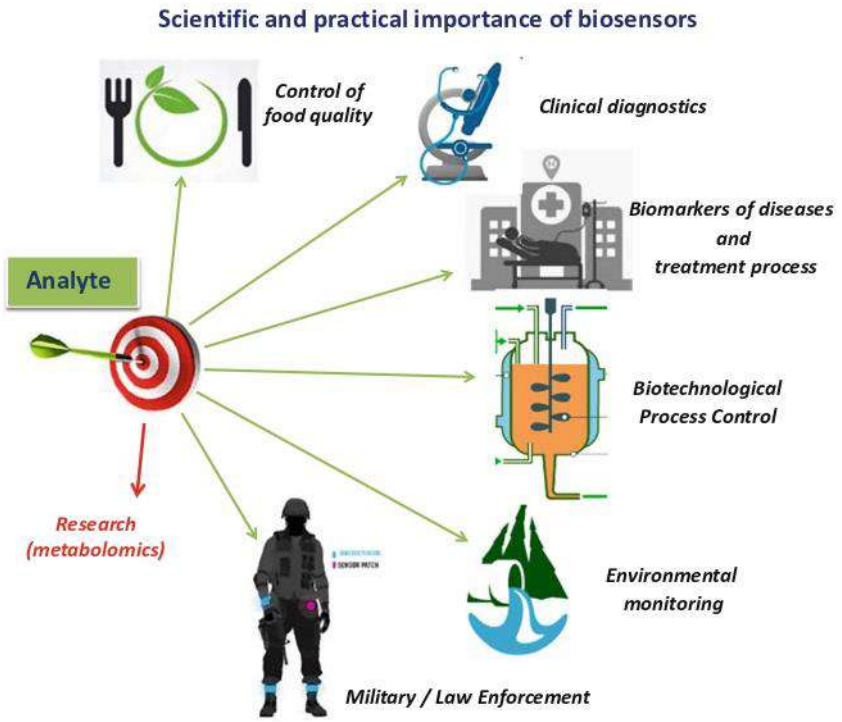

Fig. 14.2 Application of biosensors in practice and research

Biosensors are characterized by their high selectivity. They also provide fast output due to high activity and/or high local concentration of catalytic or binding element in a biosensitive layer. The drawbacks of biosensors are their insufficient stability and the high price of some purified biomolecules.

Cell sensors, especially microbial ones, have been actively developed only in recent years. A microbial biosensor consists of a transducer in conjunction with immobilized viable or nonviable microbial cells, an economical substitute for enzymes (D'Souza 2001; Lei et al. 2006). The target analyte is usually either a substrate or an inhibitor of cell metabolism.

Cell biosensors have a range of considerable advantages when compared to their enzyme analogues: availability of cells, low price and simple procedure of cell isolation, possibility to use long metabolic chains, avoiding purification of enzymes and coenzymes, advanced opportunity for genetic manipulations of metabolic pathways, integrity of the cell response (important in assaying total toxicity and mutagenic action of environmental pollutants), possibility to retain viability of sensing cells and even to provide their propagation, and, in some cases, higher stability of cell elements compared to enzyme ones (Gonchar et al. 2002; Nakamura et al. 2008; Shimomura-Shimizu and Karube 2010a, b). The main drawbacks of microbial biosensors are a long response time due to a lower concentration of

enzymes involved in cellular response, as well as low selectivity of cell output (e.g., in case of microbial O_2 electrode sensors due to the broad substrate specificity of cellular respiration).

These drawbacks are not absolute, taking into account recent progress in metabolic and genetic engineering and the possibility to overexpress the key analytical enzyme in the cell. The most known microbial sensors which exploit genetically constructed cells and are used for toxicity and bioavailability testing are bioluminescence-based biosensors created by fusing the *lux* gene with an inducible gene promoter(Nunes-Halldorson and Duran 2003; Yagi 2006; Narsaiah et al. 2012).

In recent years, nanotechnology approaches have been successfully used for improvement of functional properties of microbial sensors (Lim et al. 2015; Adeniran et al. 2015). The integration of micro- and nanotechnologies seems to be very promising in further development and production of such biosensors.

Many types of yeast-based biosensors (YBB) have been developed as analytical tools since the first microbial sensors (MS) were proposed by Karube et al. in 1977. The characteristics of MS are in absolute contrast to those of enzyme sensors or immunosensors, which are highly specific for the substrates of interest, although the specificity of MS has been improved by genetic modification of the microbe used as the sensing element. MS have the advantages of tolerance to measuring conditions, a long lifetime, and cost performance, but also the disadvantage of a long response time (Nakamura et al. 2008; Shimomura-Shimizu and Karube 2010a).

Integrated approaches, including the best advantages of nanotechnology and synthetic biology, provided a better perspective for developing specific and sensitive biosensors with high regenerative potentials for diverse usage (Bereza-Malcolm et al. 2015; Adeniran et al. 2015; He et al. 2016; Vigneshvar et al. 2016; Ponamoreva et al. 2011; Yudina et al. 2015; Jarque et al. 2016). MS appear to be quite promising for online wastewater control; their advantages lie in the fact that organic compounds in samples can be directly measured without any pretreatment such as filtration and dialysis (Dragone et al. 2014; Shimomura-Shimizu and Karube 2010a).

YBB, based on electrochemical devices, usually contain one of three types of electrodes: (1) oxygen electrodes (BOD) used for respiration testing (Chan et al. 1999; Shimomura-Shimizu and Karube 2010a); (2) fuel cell electrodes (MFC), self-powered portable devices of the next-generation biosensing innovative technology (Sun et al. 2015); and (3) membrane electrodes.

The YBB, based on genetically engineered cells, use a reporter gene under the control of an inducible promoter. The promoters are activated in the presence of a ligand of interest, either directly by the ligand/receptor dimer or via a signaling cascade. Both the receptor and the promoter may be native to yeast or adapted from other organisms. The most common reporting systems for YBB are based on optical methods for detection, namely, fluorescence (GFP, RFP, YFP), luminescence (Lux bacterial and Luc firefly), colorimetry (beta-galactosidase), as well as electrical methods (amperometry, potentiometry, conductometry, voltammetry) and growth activity (*HIS3*, *TRP1*, *LEU2*). The advantages of optical methods are their high

sensitivity and simplicity; the colorimetric variant is promising due to the visibility of its results to the naked eye. Fluorescence and luminescence detection does not need any substrate addition. The main advantages of electric methods are their high sensitivity and fastness of procedure (Eldridge et al. 2011; Adeniran et al. 2015).

Many YBB are dependent upon the signaling capabilities of G-protein-coupled receptors (GPCRs)—the largest family of human membrane proteins that mediate cellular signaling and represent primary targets of about one third of currently marketed drugs. Molecular dynamic simulations have been utilized to investigate GPCR signaling mechanisms, to design novel small-molecule drug candidates and to develop the methods of its analysis. The incorporation of GPCRs from higher organisms with functionalities, not naturally available to yeast, greatly expands the capability of YBB (Jacobson 2015; Miao and McCammon 2016).

In this review, the main achievements in the elaboration of microbial sensors, based on yeast cells, are described, and perspectives of their usage in clinical diagnostics and food control are discussed.

14.2 Microbial Sensors for Clinical Diagnostics

Widely used in vitro diagnostic approaches have a number of shortcomings; e.g., chemical methods suffer from low selectivity and sensitivity; ELISA is labor-intensive and challenging to implement multiplex detection; PCR requires a complicated sample preparation and has potential for false positives. When compared to the described above approaches in clinical diagnostics, biosensors have a number of advantages which include small sample volume, required for analysis, short assay time, low energy consumption, low prices, high portability, high throughput, and multiplexing ability.

Most of the described yeast-/fungi-based biosensors for clinical diagnostics are of amperometric mode. The measurements are carried out at a fixed potential regarding a reference electrode and involve the detection of the current generated by the oxidation or reduction of the substrate, mediators, or products of enzymatic reaction at the surface of the electrode. Glucose, lactate, and ethanol are the most frequently detected metabolic substrates in clinical diagnostics.

14.2.1 Glucose

The most well-known example in use today is the glucose sensor, which has a great effect on the management of diabetes. About 3% of the population worldwide suffers from diabetes, a leading cause of death, and its incidence is growing fast. Diabetic individuals are at the greater risk of heart disease, stroke, high blood pressure, blindness, kidney failure, neurological disorders, and other health-related complications without diligent monitoring of blood glucose concentrations. Although glucose oxidase-based sensors are widely used for glucose assay, specially treated *Saccharomyces cerevisiae cells were* used in combination with an

oxygen electrode, to be applied in aerobic conditions, or with a carbon dioxide sensor, to be used in anaerobic conditions (Mascini and Memoli 1986). To reduce the interference due to the changes in oxygen and CO_2 pressure, a potentiometric sensor was proposed based on the use of *Hansenula anomala for monitoring of* pH change correlating with glucose concentration (Racek 1991). To reduce the interference due to the changes in oxygen and CO_2 pressure, a potentiometric sensor was proposed based on the use of *Hansenula anomala for monitoring of* pH change correlating with glucose concentration (Wang et al. 2013). Microbial sensors for glucose determination based on co-immobilized *Gluconobacter oxydans* and *Saccharomyces cerevisiae* and co-immobilized *G. oxydans* and *Kluyveromyces marxianus* cells were also developed (Svitel et al. 1998).

To address the challenges of biosensors with low selectivity and inability to distinguish between substrates, *Ogataea methanolica* was combined with *Gluconobacter oxydans* to make a biosensor able to determine ethanol and glucose concentrations in various ethanol–glucose mixtures. The use of an artificial neural network to analyze the data provided accurate estimation of ethanol and glucose concentrations from 1 to 10 mM (Lobanov et al. 2001).

14.2.2 Lactate

Lactate measurement is helpful in respiratory insufficiencies, diabetes, shocks, heart failure, metabolic disorders, intoxification, and monitoring the physical condition of athletes.

The earliest analysis of L-lactate in blood plasma and whole blood was carried out by the sensor based on *H. anomala* cells. The sensor was based on yeast cells, suspended in a semipermeable membrane attached to an amperometric electrode (Racek and Musil 1987a). *H. anomala* cells have also been used in conjunction with a carbon paste electrode for lactate determination in serum (Kulys et al. 1992).

The analysis of lactate in blood plasma and whole blood was carried out by another sensor based on *H. anomala* cells. The sensor has high reproducibility, stability, and rate of assay. The analysis results were in agreement with the data obtained using conventional spectrophotometric technique and lactate dehydrogenase-based enzyme sensor (Racek and Musil 1987b). There are a few described microbial amperometric biosensors for L-lactate analysis based on baker's yeast *S. cerevisiae* (Garjonyte et al. 2006, 2008). Drying temperature was found to have an effect on lactic acid sensor performance. The K2 killer-type strain of *S. cerevisiae* was dried at temperatures as high as 90 °C for the use in a sensor that showed higher sensitivity, lower noise, and quicker response time than previous *S. cerevisiae* lactate sensors (Garjonyte et al. 2009).

In recent years, a number of L-lactate-selective amperometric biosensors based on genetically modified *H. (Ogataea) polymorpha* (*gcr1 catX/prAOX_CYB2*) overproducing L-lactate: cytochrome *c*-oxidoreductase (EC 1.1.2.3, flavocytochrome b_2, FC b_2) have been reported (Smutok et al. 2007; Shkil et al. 2009). The usage of permeabilized cells of *H. polymorpha* containing FC b_2 at a

high level in combination with free-defuse electron transfer mediator demonstrated better sensor characteristics: fast response, prolonged linearity, and operation at low working potential (Smutok et al. 2007). Another amperometric microbial sensor is based on the phenomenon of bioelectrochemical monitoring of L-lactate respiration. It was shown that in the case of *H. polymorpha* cells, overproducing FC b_2, the O_2 reduction current is decreased upon the addition of L-lactate to the electrolyte solution in contrast to the cells from the parental strain (Shkil et al. 2009). Recently, a new approach based on the additional enrichment of the recombinant yeast cell *H. polymorpha* by the FC b_2 bound with nanoparticles to improve the analytical parameters of microbial amperometric sensor has been reported (Karkovska et al.2015). Moreover, D-lactate-selective amperometric biosensor based on the cell debris of recombinant yeast *H. polymorpha* overproducing D-lactate: cytochrome *c*-oxidoreductase (EC 1.1.2.4, DLDH) in combination with cytochrome *c* and OS-contained dye was constructed. The sensor was characterized by high selectivity to D-lactate due to the deletion of *CYB2* gene responsible for the synthesis of L-lactate: cytochrome *c*-oxidoreductase (Smutok et al. 2014).

14.2.3 Hormones

It is known that the decreased levels of neurotensin and estrogen are associated with the occurrence of Parkinson's disease, as well as with many other disorders. On the other hand, a deficiency in serotonin causes the serotonin syndrome.

The modulation in optical properties such as fluorescence caused by the interaction of the biocatalyst with the target analyte is the basis for optical microbial biosensors. There are a number of described fluorescent microbial sensors for the analysis of human hormones based on recombinant yeast cells with incorporated fluorescent reporters.

Neurotensin receptor type-1 (NTSR1) is a member of the G-protein-coupled receptor (GPCR) family. The natural ligand of NTSR1 is neurotensin (NT), a neuromodulator of the central nervous system. Because NT is also involved in many oncogenic events, the signaling mediator NTSR1 is a significant molecular target in medicinal and therapeutic fields. It was used to construct a fluorescence-based microbial *S. cerevisiae*-based biosensor that can monitor the activation of human NTSR1 signaling responding to its agonist (Ishii et al. 2014).

The monoamine neurotransmitter serotonin (5-HT) regulates a wide spectrum of human physiology through the 5-HT receptor family. Yeast-based fluorescent reporter systems have proven to be especially useful for GPCR assays, since the detection using a fluorescent reporter considerably simplifies measurement procedures. A refined yeast-based GPCR biosensor employing *S. cerevisiae* cells with both incorporated Gα-engineered receptor and a fluorescent reporter (*ZsGreen*) was elaborated (Nakamura et al. 2015).

In addition to fluorescence, there are reports on the construction of amperometric microbial sensor for estrogen analysis. A phytase under the control of the estrogen-induced promoter in the yeast *Arxula adeninivorans* was used as a biorecognition

element. When the appropriate substrate was added, the induced phytase catalyzed the formation of *p*-aminophenol, which can be oxidized at an electrode and thus monitored amperometrically (Pham et al. 2012).

14.2.4 Vitamin B_1

Vitamin B_1 (thiamine) is one of the most important members of the B group of vitamins. Vitamin B_1 deficiency can be caused by a number of factors and diseases such as alcoholism, HIV, vomiting, and some gastrointestinal illnesses.

An amperometric whole-cell biosensor based on *S. cerevisiae* cells immobilized in gelatin was developed for selective determination of vitamin B_1. The biosensor was constructed using gelatin and cross-linking agent glutaraldehyde to immobilize *S. cerevisiae* cells on the Teflon membrane of dissolved oxygen (DO) probe used as the basic electrode system combined with a digital oxygen meter. The cells were induced by vitamin B_1 in the culture medium and used as a carbon source in the absence of glucose. So, when the vitamin B_1 solution was injected into the whole-cell biosensor system, an increase in the respiration activity of the cells resulting from the metabolic activity and causing a decrease in the DO concentration related to vitamin B_1 content was observed. Certainly, such a biosensor is unselective and can be used only for the assay of the target analyte in vitamin B_1 pills (Akyilmaz et al. 2006).

14.2.5 L-Lysine

A naturally occurring amino acid, L-lysine is one of the only 20 amino acids that serve as building blocks for proteins. The analysis of L-lysine is helpful in the diagnostics of a variety of health conditions in medicine. As a drug, Lys can be used to control cholesterol levels, prevent osteoporosis and other age-related bone density conditions, support growth, and reduce anxiety and stress. The nutrient is also effective in preventing herpes, treating shingles, relieving pain due to inflammation, and maintaining heart health.

An amperometric microbial biosensor for sensitive determination of L-lysine based on the cells of *S. cerevisiae* NRRL-12632, producing L-lysine oxidase (EC 1.4.3.14), was developed. The cells were immobilized on a pretreated oxygen-sensitive Teflon membrane using gelatin and glutaraldehyde. The assay procedure for the microbial biosensor was based on the determination of the differences in the respiration activity of the cells using oxygen meter in the absence and presence of L-lysine (Akyilmaz et al. 2007).

14.2.6 Urate

Uric acid is a final purine intermediate of purine nucleotide catabolism in mammals. Normally, uric acid is not accumulated in human fluids, and its availability in amounts exceeding the threshold levels in body fluids (e.g., serum and urine) is a clinically valuable diagnostic indicator. The presence of elevated uric acid levels is a sign of gout, hyperuricemia, or Lesch–Nyhan syndrome. An elevated uric acid concentration is related also to increased alcohol and cholesterol consumption, obesity, diabetes, and kidney and heart diseases. A urate-selective microbial biosensor was developed using cellular debris of recombinant methylotrophic yeast *H. polymorpha* overproducing urate-oxygen oxidoreductase (urate oxidase, uricase, 1.7.3.3) as a bioselective element. The cellular debris coupled with peroxidase were either immobilized onto the graphite electrode by physical entrapment of the suspension by means of a dialysis membrane or by integration in the electrochemically generated layer using a cathodic electrodeposition paint as well as an Os-complex modified cathodic electrodeposition paint or their combinations. The uric acid content in urine samples was determined by this sensor, and the values obtained exhibited a good correlation with the reference method (Dmytruk et al. 2011).

14.2.7 Intracellular Metabolites

Mitochondria play a pivotal role in energy metabolism, programmed cell death, and oxidative stress. Mutated mitochondrial DNA in diseased cells compromises the structure of key enzyme complexes and, therefore, mitochondrial function, which leads to a myriad of health-related conditions such as cancer, neurodegenerative diseases, diabetes, and aging. Early detection of mitochondrial and metabolic anomalies is an essential step toward effective diagnosis and therapeutic intervention. Reduced nicotinamide adenine dinucleotide (NADH) and flavin adenine dinucleotide (FAD) play important roles in a wide range of cellular oxidation–reduction reactions (Heikal 2010).

Cellular energy and redox carriers can also be directly monitored by yeast-based sensors. FRET-based sensors have been employed to monitor cytosolic ATP, using a subunit from bacterial ATP synthase as the recognition element (Bermejo et al. 2010). The protein can also be targeted specifically to the mitochondria by adding a mitochondrial targeting sequence from cytochrome *c* to the N-terminal, allowing in vivo monitoring of mitochondrial function (Vevea et al. 2013). Bulk NADH and NADPH redox states can be monitored electrically with the use of mediator compounds that shuttle electrons from the cell to an electrode (Baronian et al. 2002; Heiskanen et al. 2004). This technique also allows for nearly real-time monitoring—for example, monitoring NAD(P)H levels upon substrate addition to the yeast with an overexpressed reductase enzyme (Kostesha et al. 2009). The system has even been implemented onto a microfluidic platform (Heiskanen et al. 2013). NAD(P)H can also be assayed by autofluorescence, although this method

has been criticized for a low sensitivity and specificity (Hung et al. 2011). Recently, genetically encoded fluorescent NADH sensors with subcellular resolution have been developed using mammalian cells (Hung et al. 2011; Bilan et al. 2014); however, to our knowledge they have not, as yet, been implemented in yeast. Finally, yeast cells have been engineered to report their own pH. This is commonly achieved through pH-sensitive GFP variants (Miesenböck et al. 1998; Ullah et al. 2012), although a new bioluminescence resonance energy transfer (BRET)-based system can report pH without excitation from an external light source (Zhang et al. 2012).

14.2.8 Toxic Compounds

14.2.8.1 Alcohols

Ethanol determination is of great relevance in clinical toxicological tests. Although alcohol is used very often in human nutrition, alcoholism is considered an ailment. Ethanol ingestion could affect nervous, circulatory, or digestive system. On the other hand, methanol intoxication is an uncommon but serious poisoning. The consumption of methanol could cause coma or even death.

Besides chemosensors and enzyme-based biosensors, the microbial sensors have been proposed for alcohol determination. The methylotrophic yeasts of genera *Hansenula*, *Pichia*, and *Candida* are generally characterized by a high intracellular content of alcohol oxidase (alcohol:O_2 oxidoreductase, AOX, EC 1.1.3.13) which has rather broad specificity to primary alcohols. The improvement of AOX selectivity by biochemical or genetic manipulations is very important (Voronova et al. 2008; Akyilmaz and Dinçkaya 2005; Korpan et al. 1993). In the papers (Gonchar et al. 1998, 2002), two microbial alcohol sensors based on recombinant *H. polymorpha* (*gcr1 catX*) cells have been described. The first sensor utilized the cells with highly active alcohol oxidase immobilized on an oxygen electrode, while the second one was based on catalase-deficient cells and involved a peroxide electrode as a transducer. A conductometric microbial sensor for ethanol based on alginate-immobilized yeast cells attached to gold planar electrodes was also described (Korpan et al. 1994).

The co-immobilization *of O. methanolica* and *Gluconobacter oxydans* on chromatographic paper and fixation on the Clark-type oxygen electrode was used for the construction of another alcohol biosensor. Among the tested substrates (ethanol, methanol, isopropanol, glucose, xylose, xylitol, arabinose, arabitol, glycerol, pyruvate, citrate, acetate), the *O. methanolica*-based sensor demonstrated higher selectivity and was sensitive only to ethanol and methanol and insignificantly sensitive to isopropanol (Reshetilov et al. 2001).

An amperometric biosensor based on *C. tropicalis* cells which contain alcohol oxidase, immobilized in gelatin by glutaraldehyde, was described for sensitive determination of ethanol. This microorganism detects alcohol oxidase which is specific to several short-chain primary alcohols; therefore, the sensor was characterized by low selectivity to ethanol (Akyilmaz and Dinçkaya 2005).

A microbial biosensor for ethanol determination was prepared by the immobilization of yeast *S. ellipsoideus* cells on the surface of the oxygen electrode with the electrolyte in nonaqueous medium. The analytical determination was based on the respiratory activity of the microorganism in the presence of the analyte (Rotariu and Bala 2003).

14.2.8.2 Hormone-Active Chemicals (Xenoestrogens)

Endocrine disruptors that act like hormones in the endocrine system might have toxic effects. The yeast cells were used as biosensors since they were genetically engineered to respond to the presence of hormone-active chemicals by synthesizing beta-galactosidase as a reporter. To achieve higher sensitivity, the interdigitated array (IDA) electrodes were incorporated into the analytical chamber of the microfluidic device. The yeast cells, precultured with a hormone-active chemical, 17-beta-estradiol (E2), were trapped from the main channel of the device to the analytical chamber by electrophoresis. After trapping in the analytical chamber, electrochemical detection of beta-galactosidase induced in the yeast cells with the IDA electrodes was performed. Actually, electrochemical detection was also performed on *p*-aminophenol, formed from *p*-aminophenyl-beta-D-galactopyranoside, with beta-galactosidase. The electrochemical signals from the yeast cells precultured with 17-beta-estradiol were successfully determined with the device. Furthermore, the inhibitory effects of antagonists such as tamoxifen were also detected electrochemically using the device (Ino et al. 2009).

14.2.8.3 Poisons

The microbial sensor for cyanide detection, based on *S. cerevisiae* cells and the oxygen electrode, was described. The principle of detection is based on the inhibition of cell respiration and hence the decrease of oxygen consumption rate in the presence of cyanide, which is the approach typical for most toxicity sensors (Nakanishi et al. 1996; Ikebukuro et al. 1996).

14.2.8.4 Toxins

Toxins are classified according to their mode of action as follows: (1) membrane pore-forming toxins (hemolysin), diarrheagenic toxins (activating secondary messenger pathways—cholera toxin), superantigens (activating immune responses—staphylococcal enterotoxin B), neurotoxins (botulinum toxin), and protein synthesis inhibitory toxins (*Shiga* toxin). Both prokaryotic (bacteria) and eukaryotic (yeast, invertebrate, and vertebrate) cells have been used in developing of biosensors. The biotoxins are usually detected using higher eukaryotic cells (such as insect, fish, mammalian, or other vertebrate origins) or bacterial cells (Woutersen et al. 2011). But in scientific literature, there is also a description of the biosensor based on yeast cells. Such biosensor was developed for detection of mycotoxins. Mycotoxins are compounds produced by mold fungi in moist conditions. Approximately 25% of the world's crops are contaminated with mold or fungal growth, and mycotoxins may be produced both before and after harvest (Bryden 2007). In both humans and animals ingestion of food or feed contaminated by mycotoxins can lead to

mycotoxicoses, the possible symptoms of which are acute intoxication, losses in productivity, reduced weight gain, immunosuppression, and increased risk of cancer (Bryden 2007; Fink-Gremmels 2008). The mycotoxin zearalenone produced by *Fusarium* species as well as its metabolites zearalanone, α-zearalanol, and ß-zearalanol are harmful for health mainly due to their estrogenic activity. The estrogenic response was detected by a whole-cell biosensor based on a genetically modified *Saccharomyces cerevisiae* strain that in the presence of an estrogenic compound produces firefly luciferase enzyme and further light emission within a system provided with D-luciferin substrate. The results show that the yeast sensor reacts to mycotoxins with typical sigmoidal response at nanomolar concentrations. The response differs in different milk products with regards to the fat content of milk (Valima et al. 2010).

14.3 Microbial Sensors Based on Yeast Cells for Food Analysis

The development of biosensors for food safety applications has been an area of tremendous activity in recent years. Food safety is of great concern for many countries; e.g., the European Commission has identified it as a priority area of attention. The Commission has formulated a new food policy to ensure human health and protect consumer health. Testing and identifying foods that are unsafe is the first step for ensuring food safety (Sankarankutty 2014; Mello and Kubota 2002).

The food quality depends essentially on its biochemical composition (Mello and Kubota 2002). Quick and specific analytical tools are needed for monitoring of nutritional parameters and food contaminants (D'Souza 2001). Microbial biosensors are a rapid and affordable instrument to ensure the quality of products. There are a lot of described biosensors for the assay of various components in food samples and during fermentation processes in winemaking and other biotechnological processes (Karube and Suzuki 1983; Karube and Tamiya 1987; Karube and Sode 1989; Lim et al. 2015; Dai and Choi 2013).

14.3.1 Ethanol Assay

Ethanol assays are necessary in many industries and biotechnologies (Otles and Yalcin 2012; Shimomura-Shimizu and Karube 2010a). The content of ethanol should be monitored in its production in fermentation processes as well as when it is utilized as a substrate in different biotechnologies, for instance, in production of liquors, alcoholic beverages, and some foodstuffs (Rotariu and Bala 2003). The development of simple and sensitive biosensors for estimating the content of ethanol is an urgent problem. There are a lot of known biosensors for ethanol detection, and almost all of them are based on the usage of enzymes in the bioselective layer, but the construction of biosensors based on yeast cells is also described (Tkac et al. 2003; Rotariu et al. 2003; Rotariu and Bala 2003; Rotariu

et al. 2004; Korpan et al. 1994). Most of these biosensors exhibit good stability and a sensitive response to the target analyte. The main analytical characteristics of the proposed sensors for ethanol and other analytes are presented in Table 14.1.

One of the described biosensors is based on the cells of the yeast *Saccharomyces ellipsoideus* immobilized on the surface of an oxygen electrode with electrolyte in nonaqueous medium. The analytical signal is based on the respiratory activity of the microorganism in the presence of ethanol. The response time of approximately 5 min for steady-state method and 2 min for kinetic method was registered. The detection limit of 6 μM of the proposed biosensor was achieved (Rotariu and Bala 2003) (see Table 14.1). The similar mechanism of biosensor functioning was proposed by Rotariu and coauthors (Rotariu et al. 2004). The biosensor was used for selective determination of ethanol in the presence of glucose using a Teflon membrane. The biosensor is practically specific to ethanol, while the interference of glucose in determination of ethanol for a biosensor with dialysis membrane is about 30%. This biosensor was used to determine ethanol concentration in alcoholic beverages. Good correlation of the results obtained using the biosensor and by the spectrometric method with alcohol dehydrogenase was observed (Table 14.1).

Amperometric biosensors for simultaneous determination of glucose, sucrose, and lactose based on the cells of *S. cerevisiae* and *Kluyveromyces marxianus* immobilized on the surface of an oxygen electrode were proposed too (Svitel et al. 1998). Selective potentiometric microbial sensors using *Pichia methanolica* (Reshetilov et al. 1998) and *S. cerevisiae* (Rotariu et al. 2002, 2004) cells were described for the analysis of sucrose in soft drinks (Lobanov et al. 2001) as well as glucose and ethanol in alcoholic beverages.

To analyze the ethanol level in some alcoholic beverages, a conductometric biosensor based on immobilized *S. cerevisiae* cells was constructed (Korpan et al. 1994). To develop the conductometric biosensor, a membrane with yeast cells, immobilized in 2% Ca-alginate gel, was attached to gold planar electrodes. The changes in conductivity due to the specific consumption of ethanol by the yeast cells were registered by the computer-controlled sensor system. The response time of the constructed microbial sensor was less than 5 min; the linearity was observed in the range of 5–100 mM alcohol concentration (see Table 14.1). The minimal detectable level of ethanol was 1 mM, and the relative standard deviation was found to be 10–12% for 15 repeated assays. When the system was operated and stored at 20–25 °C, the biosensor response was stable for only 3 days. Good correlation between the results obtained by a conductometric cell biosensor and gas chromatography was observed.

Table 14.1 Comparison of different types of microbial biosensors based on yeast cells for food analysis

Sample of food	Analyte	Microorganism	Mode of signal registration	Detection limit, μM	Linearity range, mM	Reference
Alcoholic beverages	Ethanol	*S. ellipsoideus*	Amperometric	6	–	Rotariu and Bala (2003)
		S. ellipsoideus	Potentiometric	–	0.02–50	Rotariu et al. (2004)
		S. cerevisiae	Conductometric	1000	5–100	Korpan et al. (1994)
	L-Lysine	*S. cerevisiae*	Amperometric	–	1×10^{-3}–0.01	Akyilmaz et al. (2007)
Wines and juices	L-Arginine	*H. polymorpha*	Amperometric	85	Till 0.6	Stasyuk et al. (2014)
Milk, sour milk, and yogurts	L-Lactic acid	*S. cerevisiae*	Amperometric	–	Up to 1 mM	Garjonyte et al. (2006)
Fruit brandies	Cyanide	*S. cerevisiae*	Amperometric	8	–	Filipović-Kovačević et al. (2002)
Milk	Estrogenic mycotoxin	*S. cerevisiae*	Luminescence	–	1×10^{-6}–2.6×10^{-4}	Valima et al. (2010)

14.3.2 Amino Acid Assay

Amino acids serve as the nitrogen source for yeast during the fermentation of wine. Hernández-Orte et al. (2002) reported that amino acids are also a mark of the quality of wine because they contribute to wine taste, aroma, and color. Amino acids serve as the nitrogen source for yeast during the fermentation of wine. The industry of fermented foods and beverages, especially winemaking, is an important area of L-arginine (Arg) assay. Urea, a final product of L-Arg metabolism in the urea cycle during juice fermentation and wine maturation, is partly assimilated by the cells of microorganisms. In case of elevated Arg level in grape juice, urea remains in the fermentation medium and spontaneously reacts with ethanol to produce ethyl carbamate (EC) or urethane (Huang and Ough 1989). Citrulline, formed from Arg metabolism *via* the arginine deiminase pathway by wine malolactic bacteria, is the second significant precursor of EC in wine (Uthurry et al. 2006; Spayd et al. 1994).

Both urea and citrulline accumulation in the fermentation medium mainly depend on the Arg level and the type of microorganism. If L-Arg concentration in juice is higher than 1000 mg L^{-1} (5.0 mM), the potential EC concentration in wine will be above 15 μg L^{-1}, the current voluntary limit in the United States. To ensure high quality of the final product and avoid potential health hazard of urethane, the determination of Arg content in fruit juices and wine is necessary. The biosensor approach for Arg determination seems to be perspective. The construction of Arg biosensor with *Hansenula (Ogataea) polymorpha* cells in biorecognition layer has already been reported (Stasyuk et al. 2014). Both urea and citrulline accumulation in the fermentation medium mainly depend on the Arg level and the type of microorganism. If L-Arg concentration in juice is higher than 1000 mg L^{-1} (5.0 mM), the potential EC concentration in wine will be above 15 μg L^{-1}, the current voluntary limit in the United States. To ensure high quality of the final product and avoid potential health hazard of urethane, the determination of Arg content in fruit juices and wine is necessary. The biosensor approach for Arg determination seems to be perspective. The construction of Arg biosensor with *Hansenula (Ogataea) polymorpha* cells in biorecognition layer has already been reported.

L-Lysine (Lys) is the most easily damaged essential amino acid, and therefore, Lys is a vital marker for the nutritional value of food. It is abundant in animal proteins, unlike plant proteins, which are often low in lysine content, making it the limiting amino acid in most cereal proteins (Kelly et al. 2000). However, lysine is an indicator of the effect on foods by various industrial processes or during cooking treatment (Karalemas et al. 2000).

In addition, Lys is an essential constituent of the diet and of great interest in the nutrition and pharmaceutical fields. Lys is often added as a dietary supplement to food and drugs in order to correct possible deficiencies of this amino acid in humans (Saurina et al. 1999). To provide high quality of a food product, it is necessary to determine Lys content. Recently, a new amperometric microbial biosensor based on *S. cerevisiae* cells for Lys determination in alcoholic beverages has been developed

(Akyilmaz et al. 2007). The proposed amperometric sensor is suitable for the determination of Lys content in food products in the absence and presence of other amino acids (see Table 14.1).

14.3.3 L-Lactate Assay

Reliable determination of L-lactate is important in food technology, fermentation, and wine industries (Garjonyte et al. 2006, 2008). The use of cell-based amperometric biosensors seems to be very promising due to the favorable coupling of the selectivity of the biological recognition element and the sensitivity of electrochemical transducer (Smutok et al. 2007; Shkil et al. 2009). Most of the proposed amperometric biosensors for the detection of L-lactate are based on baker's yeast *S. cerevisiae* and *H. polymorpha* cells (sources of flavocytochrome b_2) and different types of mediators (potassium ferricyanide, phenazine methosulphate, 1,2-naphthoquinone-4-sulfonic acid sodium salt, and *p*-benzoquinone) (Akyilmaz et al. 2007; Shkil et al. 2009). The suitability of the developed bioelectrodes for the determination of L-lactic acid in milk and dairy products such as sour milk and yogurt was also suggested (Garjonyte et al. 2009).

Recently, the microbial L-lactate-selective sensor based on the recombinant *H. polymorpha* cells overproducing flavocytochrome b_2 (FC b_2), as well as additionally fortified by the immobilized FC b_2 with gold nanoparticles (nAu), has been proposed (Karkovska et al. 2015). The FC b_2-nAu-enriched living and permeabilized yeast cells were used for construction of a bioselective membrane of microbial L-lactate-selective amperometric biosensor. The main analytical characteristics of the proposed sensor are presented in Table 14.1. The obtained results confirm that the additional enrichment of the recombinant yeast cell by the enzyme bound with nanoparticles improves the analytical parameters of the microbial sensor.

14.3.4 Assay of Contaminants

Contaminants should be carefully detected in order to ensure the quality of the food products. Mycotoxins of zearalenone family are common contaminants in milk which can cause mycotoxicoses (Bryden 2007). In order to ensure the quality of milk, genetically modified *S. cerevisiae* cells were used as the bioelement of the microbial biosensor for the detection of zearalenone mycotoxins in milk (Valima et al. 2010).

S. cerevisiae cells, immobilized on an oxygen electrode, were used for cyanide detection in fruit brandies (Filipović-Kovačević et al. 2002). For quality control of meat freshness, a yeast-based sensor using *Trichosporon cutaneum* was developed. The detection of polyamines and amino acids from the meat in washwater was estimated by this sensor system (Yano et al. 2001).

References

Adeniran A, Sherer M, Tyo K (2015) Yeast-based biosensors: design and applications. FEMS Yeast Res 15(1):1–15

Akyilmaz E, Dinçkaya E (2005) An amperometric microbial biosensor development based on *Candida tropicalis* yeast cells for sensitive determination of ethanol. Biosens Bioelectron 20:1263–1269

Akyilmaz E, Yaşa I, Dinçkaya E (2006) Whole cell immobilized amperometric biosensor based on *Saccharomyces cerevisiae* for selective determination of vitamin B1 (thiamine). Anal Biochem 354(1):78–84

Akyilmaz E, Erdogan A, Ozturk R et al (2007) Sensitive determination of L-lysine with a new amperometric microbial biosensor based on *Saccharomyces cerevisiae* yeast cells. Biosens Bioelectron 22(6):1055–1060

Atta NF, Galal A, Ali S (2011) Nanobiosensors for health care, Chapter 4. In: Serra PA (ed) Biosensors for health, environment and biosecurity. doi:10.5772/17996

Baronian KH, Downard AJ, Lowen RK et al (2002) Detection of two distinct substrate-dependent catabolic responses in yeast cells using a mediated electrochemical method. Appl Microbiol Biotechnol 60(1–2):108–113

Bereza-Malcolm LT, Mann G, Franks AE (2015) Environmental sensing of heavy metals through whole cell microbial biosensors: a synthetic biology approach review. ACS Synth Biol 4 (5):535–546

Bermejo C, García R, Straede A et al (2010) Characterization of sensor-specific stress response by transcriptional profiling of *wsc1* and *mid2* deletion strains and chimeric sensors in *Saccharomyces cerevisiae*. OMICS 14(6):679–688

Bilan DS, Matlashov ME, Gorokhovatsky AY et al (2014) Genetically encoded fluorescent indicator for imaging NAD_+/NADH ratio changes in different cellular compartments. Biochim Biophys Acta 1840:951–957

Bryden WL (2007) Mycotoxins in the food chain: human health implications. Asia Pac J Clin Nutr 16(1):95–101

Chan C, Lehmann M, Tag K, Lung M, Kunze G, Riedel K, Gruendig B, Renneberg R (1999) Measurement of biodegradable substances using the salt-tolerant yeast *Arxula adeninivorans* for a microbial sensor immobilized with poly(carbamoyl) sulfonate (PCS) part I: construction and characterization of the microbial sensor. Biosens Bioelectron 14(2):131–138

D'Souza SF (2001) Microbial biosensors. Biosens Bioelectron 16(6):337–353

Dai C, Choi S (2013) Technology and applications of microbial biosensor. OJAB 2:83–93

Dmytruk K, Smutok O, Dmytruk O et al (2011) Construction of uricase-overproducing strain of *Hansenula polymorpha* and its application as biological recognition element in microbial urate biosensor. BMC Biotechnol 11:58–66

Dragone R, Frazzoli C, Grasso G, Rossi G (2014) Sensor with intact or modified yeast cells as rapid device for toxicological test of chemicals. J Agric Chem Environ 3:35–40

Eldridge M, Sanseverino J, Umbuzeiro GA, Sayler GS (2011) Analysis of environmental samples with yeast-based bioluminescent bioreporters, environmental monitoring. In: Ekundayo E (ed) InTech. doi:10.5772/27139. http://www.intechopen.com/books/environmental-monitoring/analysis-of-environmental-samples-with-yeast-based-bioluminescent-bioreporters

Filipović-Kovačević Ž, Mikšaj M, Šalamon D (2002) Cyanide determination in fruit brandies by an amperometric biosensor with immobilised *Saccharomyces cerevisiae*. Eur Food Res Technol 215(4):347–352

Fink-Gremmels J (2008) Mycotoxins in cattle feeds and carry-over to dairy milk: a review. Food Addit Contam 25:172–180

Garjonyte R, Melvydas V, Malinauskas A (2006) Mediated amperometric biosensors for lactic acid based on carbon paste electrodes modified with baker's yeast *Saccharomyces cerevisiae*. Bioelectrochemisty 68(2):191–196

Garjonyte R, Melvydas V, Malinauskas A (2008) Effect of yeast pretreatment on the characteristics of yeast-modified electrodes as mediated amperometric biosensors for lactic acid. Bioelectrochemistry 74:188–194

Garjonyte R, Melvydas V, Malinauskas A (2009) Amperometric biosensors for lactic acid based on baker's and wine yeast. Microchim Acta 164:177–183

Gonchar MV, Maidan MM, Moroz OM et al (1998) Microbial O_2- and H_2O_2- electrode sensors for alcohol assays based on the use of permeabilized mutant yeast cells as the sensitive bioelements. Biosens Bioelectron 139:945–952

Gonchar M, Maidan M, Korpan Y et al (2002) Metabolically engineered methylotrophic yeast cells and enzymes as sensor biorecognition elements. FEMS Yeast Res 2:307–314

He W, Yuan S, Zhong WH et al (2016) Application of genetically engineered microbial whole-cell biosensors for combined chemosensing. Appl Microbiol Biotechnol 100(3):1109–1119

Heikal AA (2010) Intracellular coenzymes as natural biomarkers for metabolic activities and mitochondrial anomalies. Biomark Med 4(2):241–263

Heiskanen A, Yakovleva J, Spegel C et al (2004) Amperometric monitoring of redox activity in living yeast cells: comparison of menadione and menadione sodium bisulfite as electron transfer mediators. Electrochem Commun 6:219–224

Heiskanen J, Saksa T, Luoranen J (2013) Soil preparation method affects outplanting success of Norway spruce container seedlings on till soils susceptible to frost heave. Silva Fennica 47(1). http://www.silvafennica.fi/article/893

Hernández-Orte P, Cacho JF, Ferreira V (2002) Relationship between varietal amino acid profile of grapes and wine aromatic composition. Experiments with model solutions and chemometric study. J Agric Food Chem 50(10):2891–2899

Huang Z, Ough CS (1989) Effect of vineyard locations, varieties and rootstocks on the juice amino acid composition of several cultivars. Am J Enol Vitic 40:135–139

Hung KW, Suen MF, Chen YF et al (2011) Detection of water toxicity using cytochrome P450 transgenic zebrafish as live biosensor: for polychlorinated biphenyls toxicity. Biosens Bioelectron 31(1):548–553

Ikebukuro K, Honda M, Nakanishi K et al (1996) Flow-type cyanide sensor using an immobilized microorganism. Electroanalysis 8(10):876–879

Ino K, Kitagawa Y, Watanabe T et al (2009) Detection of hormone active chemicals using genetically engineered yeast cells and microfluidic devices with interdigitated array electrodes. Electrophoresis 19:3406–3412

Ishii J, Oda A, Togawa S et al (2014) Microbial fluorescence sensing for human neurotensin receptor type 1 using Gα-engineered yeast cells. Anal Biochem 1(446):37–43

Jacobson KA (2015) New paradigms in GPCR drug discovery. Biochem Pharmacol 98 (4):541–555

Jarque S, Bittner M, Blaha L, Hilscherova K (2016) Yeast biosensors for detection of environmental pollutants: current state and limitations review article. Trends Biotechnol 34 (5):408–419

Karalemas ID, Georgiou CA, Papastathopoulos DS (2000) Construction of a L-lysine biosensor by immobilizing lysine oxidase on a gold-poly(o-phenylenediamine) electrode. Talanta 53:391–402

Karkovska M, Smutok O, Stasyuk N et al (2015) L-lactate-selective microbial sensor based on flavocytochrome b_2-enriched yeast cells using recombinant and nanotechnology approaches. Talanta 144:1195–1200

Karube I, Sode K (1989) Biosensors for fermentation process control. In: Ghose TK (ed) Bioprocess engineering: the first generation. Chapman Hall, London

Karube I, Suzuki S (1983) Application of biosensor in fermentation processes, Chapter 8. In: Tsao GT (ed) Annual reports on fermentation processes, vol 6. Academic, New York

Karube I, Tamiya E (1987) Biosensors for the food industry. Food Biotechnol 1:147–165

Kelly SC, O'Connell PJ, O'Sullivan CK et al (2000) Development of an interferent free amperometric biosensor for determination of L-lysine in food. Anal Chim Acta 412:111–119

Korpan YI, Gonchar MV, Starodub NF et al (1993) A Cell biosensor specific for formaldehyde based on pH-sensitive transistors coupled to methylotrophic yeast cells with genetically adjusted metabolism. Anal Biochem 215(2):216–222

Korpan YI, Dzyadevich SV, Zharova VP et al (1994) Conductometric biosensor for ethanol detection based on whole yeast cells. Ukr Biokhim Zh 66(1):78–82

Kostesha NV, Almeida JR, Heiskanen AR et al (2009) Electrochemical probing of *in vivo* 5-hydroxymethyl furfural reduction in *Saccharomyces cerevisiae*. Anal Chem 81 (24):9896–8901

Kraly JR, Holcomb RE, Guan Q et al (2009) Review: microfluidic applications in metabolomics and metabolic profiling. Anal Chim Acta 653(1):23–35

Kulys J, Wang L, Razumas V (1992) Sensitive yeast bioelectrode to L-lactate. *Electroanalysis* 4:527–532

Lei Y, Chen W, Mulchandani A (2006) Microbial biosensors. Anal Chim Acta 568:200–210

Lim JW, Ha D, Lee J et al (2015) Review of micro/nanotechnologies for microbial biosensors. Front Bioeng Biotechnol 3(61):1–13

Lobanov AV, Borisov IA, Gordon SH et al (2001) Analysis of ethanol-glucose mixtures by two microbial sensors: application of chemometrics and artificial neural networks for data processing. Biosens Bioelectron 16:1001–1007

Mascini M, Memoli A (1986) Comparison of microbial sensors based on amperometric and potentiometric electrodes. Anal Chim Acta 182:113–122

Mello LD, Kubota LT (2002) Review of the use of bio-sensors as analytical tools in the food and drink industries. Food Chem 77(2):237–256

Miao Y, McCammon JA (2016) G-protein coupled receptors: advances in simulation and drug discovery. Curr Opin Struct Biol 41:83–89

Miesenböck G, De Angelis DA, Rothman JE (1998) Visualizing secretion and synaptic transmission with pH-sensitive green fluorescent proteins. Nature 394(6689):192–195

Nakamura H, Shimomura-Shimizu M, Karube I (2008) Development of microbial sensors and their application. Adv Biochem Eng Biotechnol 109:351–394

Nakamura Y, Ishii J, Kondo A (2015) Applications of yeast-based signaling sensor for characterization of antagonist and analysis of site-directed mutants of the human serotonin 1A receptor. Biotechnol Bioeng 112(9):1906–1915

Nakanishi K, Ikebukuro K, Karube I (1996) Determination of cyanide using a microbial sensor. Appl Biochem Biotechnol 60(2):97–106

Narsaiah K, Jha SN, Bhardwaj R et al (2012) Optical biosensors for food quality and safety assurance – a review. J Food Sci Technol 49(4):383–406

Nunes-Halldorson VS, Duran NL (2003) Bioluminescent bacteria: *lux* genes as environmental biosensors. Braz J Microbiol 34(2):91–96

Otles S, Yalcin B (2012) Review on the application of nanobiosensors in food analysis. Acta Sci Pol Technol Aliment 11(1):7–18

Pham H, Giersberga M, Uhligb S et al (2012) Estra monitor – a monitor for amperometric detection of estrogenic activity with *Arxula adeninivorans* yeast cells as the biocomponent. Sens Actuators Chem 161:137–145

Ponamoreva ON, Arliapov VA, Alferov VA, Reshetilov AN (2011) Microbial biosensors for detection of biological oxygen demand (a review). Prikl Biokhim Mikrobiol 47(1):5–15

Racek J (1991) A yeast biosensor for glucose determination. Appl Microbiol Biotechnol 34:473–477

Racek J, Musil J (1987a) Biosensor for lactate determination in biological fluids. I. Construction and properties of the biosensor. Clin Chim Acta 162:129–139

Racek J, Musil J (1987b) Biosensor for lactate determination in biological fluids. 2. Interference studies. Clin Chim Acta 167:59–65

Reshetilov AN, Lobanov AV, Morozova NO et al (1998) Detection of ethanol in a two-component glucose/ethanol mixture using a nonselective microbial sensor and a glucose enzyme electrode. Biosens Bioelectron 13:787–793

Reshetilov AN, Trotsenko JA, Morozova NO et al (2001) Characteristics of *Gluconobacter oxydans* B-1280 and *Pichia methanolica* MN4 cell based biosensors for detection of ethanol. Process Chem 36(10):1015–1020

Rotariu L, Bala C (2003) New type of ethanol microbial biosensor based on a highly sensitive amperometric oxygen electrode and yeast cells. Anal Lett 36(11):2459–2471

Rotariu L, Bala C, Magearu V (2002) Yeast cells sucrose biosensor based on a potentiometric oxygen electrode. Anal Chim Acta 458(1):215–222

Rotariu L, Bala C, Magearu V (2003) Microbial biosensors for ethanol determination in alcoholic beverages. Ann Univ Buchar XII(I–II):69–76

Rotariu L, Bala C, Magearu V (2004) New potentiometric microbial biosensor for ethanol determination in alcoholic beverages. Anal Chim Acta 513:119–123

Sankarankutty KM (2014) Biosensors and their applications for ensuring food safety. Global J Pathol Microbiol 2:15–21

Saurina J, Hernández-Cassou S, Alegret S, Fàbregas E (1999) Amperometric determination of lysine using a lysine oxidase biosensor based on rigid-conducting composites. Biosens Bioelectron 14:211–220

Schmidt RD, Karube I (1998) Biotechnology. In: Rehm HJ, Reed G (eds) Biosensors and bioelectronics, vol 6b. VCH Verlagsgesellschaft, Weinheim, pp 317–365

Shimomura-Shimizu M, Karube I (2010a) Applications of microbial cell sensors. Biochem Biotechnol 118:1–30

Shimomura-Shimizu M, Karube I (2010b) Yeast based sensors. Adv Biochem Eng Biotechnol 117:1–19

Shkil H, Stoica L, Dmytruk K et al (2009) Bioelectrochemical detection of L-lactate respiration using genetically modified *Hansenula polymorpha* yeast cells overexpressing flavocytochrome b_2. Bioelectrochemistry 76:175–179

Smutok O, Dmytruk K, Gonchar M et al (2007) Permeabilized cells of flavocytochrome b_2 over-producing recombinant yeast *Hansenula polymorpha* as biological recognition element in amperometric lactate biosensors. Biosens Bioelectron 23:599–605

Smutok O, Dmytruk K, Karkovska M et al (2014) D-lactate-selective amperometric biosensor based on the cell debris of the recombinant yeast *Hansenula polymorpha*. Talanta 125:227–232

Spayd SE, Wample RL, Evans RG et al (1994) Nitrogen fertilization of white Riesling grapes in Washington. Must and wine composition. Am J Enol Vitic 45:34–42

Stasyuk NY, Gayda GZ, Gonchar MV (2014) L-arginine-selective microbial amperometric sensor based on recombinant yeast cells over-producing human liver arginase I. Sens Actuat B Chem 204:515–521

Sun JZ, Peter Kingori G, Si RW et al (2015) Microbial fuel cell-based biosensors for environmental monitoring: a review. Water Sci Technol 71(6):801–809

Svitel J, Curilla O, Tkac J (1998) Microbial cell-based biosensor for sensing glucose, sucrose or lactose. Biotechnol Appl Biochem 27(2):153–158

Thevenot D, Toth K, Durst R et al (2001) Electrochemical biosensors: recommended definitions and classification. Biosens Bioelectron 16:121–131

Tkac J, Vostiar I, Gorton L et al (2003) Improved selectivity of microbial biosensor using membrane coating. Application to the analysis of ethanol during fermentation. Biosens Bioelectron 18:1125–1134

Turner AP, Karube I, Wilson GS (eds) (1990) Biosensors: fundamentals and applications. Oxford University Press, London

Ullah A, Orij R, Brul S et al (2012) Quantitative analysis of the modes of growth inhibition by weak organic acids in Saccharomyces cerevisiae. Appl Environ Microbiol 78(23):8377–8387

Uthurry CA, Lepe JA, Lombardero J et al (2006) Ethyl carbamate production by selected yeasts and lactic acid bacteria in red wine. Food Chem 94:262–270

Valima A, Kivisto AT, Leskinen PI et al (2010) A novel biosensor for the detection of zearalenone family mycotoxins in milk. J Microb Met 80(1):44–48

Vevea JD, Wolken DM, Swayne TC et al (2013) Ratiometric biosensors that measure mitochondrial redox state and ATP in living yeast cells. J Vis Exp 77:e50633

Vigneshvar S, Sudhakumari CC, Senthilkumaran B, Prakash H (2016) Recent advances in biosensor technology for potential applications an overview. Front Bioeng Biotechnol 4 (11):1–9

Voronova E, Iliasov P, Reshetilov A (2008) Development, investigation of parameters and estimation of possibility of adaptation of *Pichia angusta* based microbial sensor for ethanol detection. Anal Lett 41(3):377–391

Wang S, Horn PJ, Liou LC et al (2013) A peroxisome biogenesis deficiency prevents the binding of alpha-synuclein to lipid droplets in lipid-loaded yeast. Biochem Biophys Res Commun 438 (2):452–456

Woutersen M, Belkin S, Brouwer B et al (2011) Are luminescent bacteria suitable for online detection and monitoring of toxic compounds in drinking water and its sources? Anal Bioanal Chem 400:915–929

Yagi K (2006) Applications of whole-cell bacterial sensors in biotechnology and environmental science. Appl Microbiol Biotechnol 3(6):1251–1258

Yano Y, Numata M, Hachiya H et al (2001) Application of a microbial sensor to the quality control of meat freshness. Talanta 54:255–262

Yudina NY, Arlyapov VA, Chepurnova MA, Alferov SV, Reshetilov AN (2015) A yeast co-culture-based biosensor for determination of waste water contamination levels. Enzyme Microb Technol 78:46–53

Zhang J, Liu M, Su Y et al (2012) A targeted in vivo RNAi screen reveals deubiquitinases as new regulators of notch signaling. G3 (Bethesda) 2(12):1563–1575

View publication stats

Оригінал доступний за посиланням: https://link.springer.com/chapter/10.1007/978-3-319-58829-2_14

Анотація: *Для людини L-аргінін є напівнезамінною амінокислотою, його достатню кількість необхідно споживати в раціоні, щоб запобігти негативним наслідкам, пов'язаним з недостатнім синтезом цієї амінокислоти за певних фізіологічних умов. Метаболізм L-аргініну важливий для синтезу біохімічно різноманітних продуктів, зокрема, сечовини, деяких амінокислот, креатину, поліамінів, оксиду Нітрогену та ін. L-аргінін є важливим біомаркером у клінічній діагностиці, зокрема, він використовується для профілактики/лікування деяких захворювань, у тому числі онкологічних та COVID-19. Крім того, рівень L-аргініну служить індикатором якості харчових продуктів та напоїв. На сьогодні, запропоновано різноманітні оптичні та електрохімічні методи визначення вмісту L-аргініну. Досліджено, що біосенсорні системи на основі ензимів метаболізму L-аргініну можуть бути найбільш перспективним інструментом для аналізу L-аргініну. Цей огляд зосереджено на висвітленні особливостей функціонування електрохімічних біосенсорів для аналізу L-аргініну, зокрема, на використанні ензимів, що розщеплюють L-аргінін, а також на аналізі їхніх переваг порівняно з іншими підходами.*

Available online at www.sciencedirect.com

ScienceDirect

Current Opinion in Electrochemistry

ELSEVIER

Review Article

Arginine-hydrolyzing enzymes for electrochemical biosensors

Galina Gayda[1], Nataliya Stasyuk[1,2], Andriy Zakalskiy[1], Mykhailo Gonchar[1,2] and Evgeny Katz[3]

Abstract

Since L-Arginine (Arg) is a semi-essential amino acid for humans, its adequate amount must be consumed in the diet to prevent certain negative consequences related to insufficient synthesis of this amino acid under specific physiological conditions. Arg metabolism results in the production of a biochemically diverse range of such products as urea, some amino acids, creatine, polyamines, nitric oxide, etc. Arg, an important biomarker in clinical diagnostics, is also used for prevention/treatment of different diseases, including cancer and COVID-19. Furthermore, it serves as an indicator of food and beverages quality.

A variety of optic and electrochemical methods for Arg determination have already been suggested. The biosensor systems based on the enzymes of Arg metabolism were shown to be the most promising tools for Arg assay. This review focuses on the peculiarities of electrochemical biosensors for Arg assay based on the use of Arg-degrading enzymes and on the analysis of their advantages as compared to other approaches.

Addresses

[1] Institute of Cell Biology, NAS of Ukraine, Lviv, 79005, Ukraine

[2] Drohobych Ivan Franko State Pedagogical University, Drohobych, 82100, Ukraine

[3] Department of Chemistry and Biomolecular Science, Clarkson University, 8 Clarkson Avenue, Potsdam, NY, 13699, New York, USA

Corresponding author: Gonchar, Mykhailo (mykhailo1952@gmail.com), (gonchar@cellbiol.lviv.ua)

Current Opinion in Electrochemistry 2022, **33**:100941

This review comes from a themed issue on **Bioelectrochemistry**

Edited by **Sabine Kuss**

For a complete overview see the Issue and the Editorial

Available online 24 January 2022

https://doi.org/10.1016/j.coelec.2022.100941

2451-9103/© 2022 Elsevier B.V. All rights reserved.

Keywords

Bioelectrochemistry, L-arginine, Arginase, Arginine deiminase, Arginine oxidase, Electrochemical biosensors.

Introduction

Since L-Arginine (Arg) is a semi-essential amino acid for humans, its adequate amount must be consumed in the diet to prevent certain negative consequences related to insufficient synthesis of this amino acid under specific physiological conditions. For higher organisms, including humans, arginine metabolism results in the production of a biochemically diverse range of products: urea, ornithine, citrulline, creatine, proline, glutamate, agmatine, homoarginine, polyamines, nitric oxide, methylated derivatives of Arg, and post-translationally modified (arginylated) proteins [1].

Arg is involved in numerous human metabolic pathways, including ammonia detoxification, hormone secretion, and immune modulation. This amino acid is a precursor of nitric oxide, a key component of endothelial-derived relaxing factor, and an endogenous messenger molecule engaged into in a variety of endothelium-dependent physiological effects in the cardiovascular system. Due to its great physiological importance, Arg can be used as a drug/supplement for treatment of angina pectoris, congestive heart failure, hypertension, coronary heart disease, preeclampsia, intermittent claudication, erectile dysfunction, diabetes mellitus, and other diseases [1,2].

Arg is an important player in cellular growth which becomes a limiting stage of rapid turnover (*e.g.*, malignancy). Thus, Arg deprivation therapy is treated as an adjuvant cancer therapy [3–5], although Arg is also necessary for immune destruction of malignant cells [6].

It is obvious that Arg is an importing biomarker in clinical diagnostics [7,8] as well as an indicator of food and food supplement quality [9–11] due to its significant role in many physiological processes. Arg is an important analyte used for the identification of the dangerous genetic disorder in newborns – hyperargininemia (Figure 1a) – and for its immediate correction and therapy [12]. It is also utilized to control the normal course of pregnancy [2] and to estimate the treatment efficiency of certain cancers [3–5,13–15], COVID-19 [16–18] and other disorders [19,20]. Additionally, Arg is a helpful indicator of the nutritional status assessment [9–11]. Although Arg is an important diet component, particularly of some fermented food products and beverages where its content is limited, it should be noted that an increased level of Arg in grape

juice or wine results in the formation of ethyl carbamate, a dangerous carcinogen (Figure 1b) [21,22].

A variety of optic and electrochemical approaches to Arg determination in biological liquids has been developed to date. The optical analytical methods (colorimetric, fluorescent and other ones) [22,24], being simple and quick, suffer, however, from serious interference from some organic compounds present in the samples. Other traditional methods used for Arg analysis are based on capillary electrophoresis, gas chromatography, mass-spectrophotometry, high-performance liquid chromatography (HPLC), electrochemistry, luminescence, and Raman spectroscopy [20,22–24]. These techniques, being promising for application in clinical and industrial laboratories, possess, however, insufficient selectivity and require expensive equipment. To overcome these drawbacks, the enzymatic approaches, including biosensors, have been developed [25–39].

The highly selective enzymes involved in Arg metabolism, especially recombinant ones, are promising tools for biosensors' construction [2,23,40]. For Arg analysis, arginine deiminase (ADI) [22,24,26–32], arginase (ARG) in combination with urease [22,23,33–35], arginine oxidase (ArgO) and natural or artificial peroxidase (PO) [36–40] as well as arginine decarboxylase (ADC) can be applied (Figure 1c). This review focuses on the peculiarities of electrochemical enzyme-based biosensors for Arg analysis and their advantages over other approaches. The review is primarily based on the analysis of papers published within the last two years.

Electrochemical biosensors on Arg

Arginine-degrading enzymes as biorecognition elements

Arginase

ARG (L-arginine amidinohydrolase, EC 3.5.3.1) catalyzes conversion of Arg to L-ornithine and urea. This enzyme exists in two forms (I and II) and is found in variety of organisms, from bacteria to mammals. ARG I is abundantly expressed in liver and is a key enzyme of the urea cycle.

Recombinant human ARG I has been successfully cloned and heterologously expressed in *Bacillus subtilis* and *Escherichia coli* [3]. The recombinant strain of the yeast *Saccharomyces cerevisiae*, overproducing $(His)_6$-tagged ARG I, was constructed by us, and the highly purified enzyme was isolated with a high specific activity (up to 1600 μmol min^{-1}·mg^{-1} protein) using one-step metal affinity purification [41]. In addition, the methylotrophic yeast *Ogataea polymorpha*, one of the best eukaryotic expression platforms, was used for secretory over-expression of human ARG I [3].

Figure 1

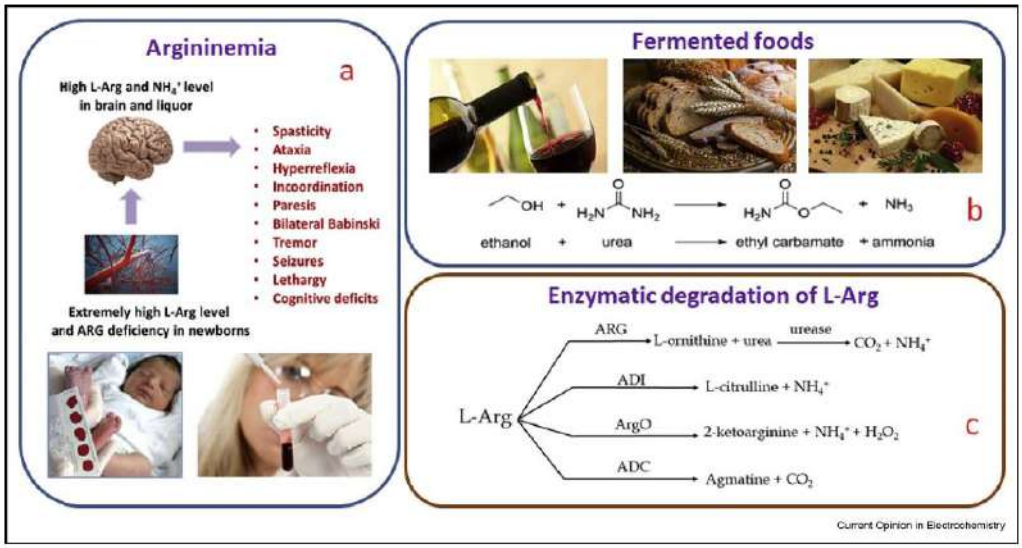

Importance of Arg analysis in medicine (a) and food control (b); arginine-hydrolyzing reactions (c) catalyzed by ARG/urease, ADI, ArgO and ADC. Modified Fig. 1c is reproduced with permission from ref. 23.

Arginine deiminase

ADI (L-arginine iminohydrolase, EC 3.5.3.6) catalyzes the reaction of Arg hydrolysis to L-citrulline and ammonia. The ADI gene from different species of *Mycoplasma* and *Pseudomonas* was heterologously expressed in *E. coli* and *B. subtilis*. An advanced protocol for the ADI expression in *E. coli*, its extraction and renaturation, has been developed. The main improvements were as follows: (*i*) utilization of the dense suspensions of *E. coli* in the cheap synthetic medium, (*ii*) use of inexpensive lactose as an inducer instead of isopropyl β-D-1-thiogalactopyranoside, and (*iii*) a cheaper, although not inefficient buffer for solubilization of ADI inclusion bodies [42].

Arginine oxidase

ArgO (L-arginine oxygen oxidoreductase, EC 1.4.3.25) is a FAD-containing enzyme which catalyzes the conversion of Arg to 5-guanidino-2-oxopentoneate, ammonia, and hydrogen peroxide. ArgO is a poorly studied enzyme to date. A detailed description concerning the properties of ArgO in different organisms and the procedure of enzyme isolation from a wild forest mushroom *Amanita phalloides* was published by Stasyuk [36].

Arginine decarboxylase

ADC (EC 4.1.1.19) catalyzes the conversion of arginine to toxic agmatine and carbon dioxide [23,40]. Unfortunately, this enzyme is not commercially available and its analytical application is problematic.

Principles of Arg analysis with enzyme-based biosensors

Enzyme-based biosensors, in general, rely on the measurements of reactants consumed or products generated from enzymatic cascade reactions [25]. In the case of Arg analysis, ammonia, H_2O_2 and CO_2 can be potentially monitored as the final products of Arg-specific reactions (Figure 2).

The necessity of using several enzymes in the bioselective layer complicates the process of biosensor fabrication, increases the cost of analysis, and causes losses in bioelectrode stability and sensitivity. Therefore, using only one enzyme, co-immobilized with electroactive functional nanomaterials, may be a more effective way for the fabrication of highly sensitive and stable biosensors.

As an alternative, extra-sensitive non-enzymatic sensors based on functional materials, including metal–organic polymers and nanoparticles of different compositions, have been suggested [43–45]. The main drawback of the reported methods is insufficient selectivity towards the goal analyte. In our opinion, the best way to fabricate the improved highly sensitive, selective, and stable sensor devices is to combine natural enzymes with appropriate nanomaterials [29,36,46–49].

Detection of ammonia as a by-product of Arg degradation

In ADI-catalyzed and ARG/Urease-catalyzed reactions, Arg produces ammonia/ammonium (NH_3/NH_4^+) which can be monitored using electrochemical biosensors. There are several reports concerning conductometric and potentiometric sensors based on ion-selective electrodes (ISE) for the detection of NH_3/NH_4^+ [50] and enzymes-coupled NH_4^+-ISE for the detection of Arg [33]. Although being extremely popular, the potentiometric technique suffers from several weaknesses, namely, the dependence of a membrane potential on the ionic strength of the solution, instability of the potential during a series of assays, the complexity of a multi-enzyme system's construction, and some other deficiencies [51].

Amperometric sensors are more promising for NH_4^+ analysis due to their higher sensitivity and selectivity as well as the quickness of the analytic procedure [26,27,50–53]. The most studied electrodes are based on NH_4^+-sensitive polymers, such as polyaniline (PANi) and polypyrrole [51–53], oxides of transition metals [52], and sulfur-containing metal-based nanoparticles [29,32,54]. Advanced processable, catalyst-free NH_4^+ sensors were proposed based on PANi coupled with Nafion, copper oxide, and other composites [31,51–53]. An effective sensor with an extremely high sensitivity was fabricated using PANi-coupled polystyrene-sulphonate [53]. Sulfides of transitional metals were reported to be promising materials for biosensor fabrication due to their excellent properties, such as large active surface areas, high catalytic activity and conductivity as well as the suitable bandgaps [30,32,54].

There are limited data on amperometric biosensors (ABSs) based on deiminases producing ammonium as a byproduct of the enzymatic reaction [26–32]. The most frequently proposed biosensors utilizing such a detection mode are based on the potentiometric transducers which contain at least two enzymes in the bioselective layer. This complicates the procedure and increases the cost of the analysis. Thus, the construction of a one-enzyme ABS is a practical problem solution.

Analytical characteristics of several amperometric highly selective sensors on ammonium/ammonia, reported till now, are presented in Table 1. The most effective ones were used for the fabrication of ADI- and ARG/Urease-based amperometric biosensors (ABSs) for Arg analysis (Table 2). The fabricated ABSs contain highly purified recombinant enzymes co-immobilized with ammonium-sensitive films on the surfaces of graphite electrodes. The released ammonium ions react

Figure 2

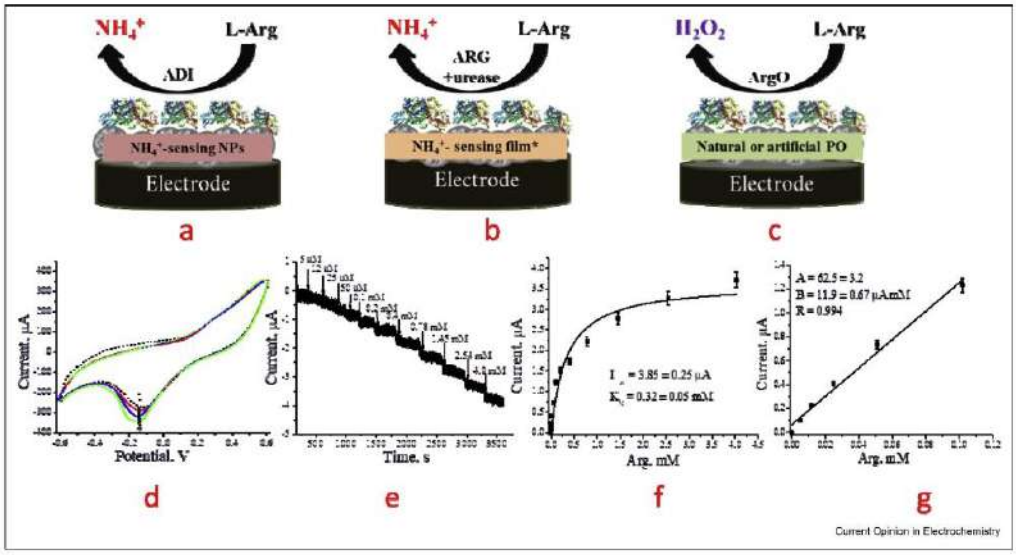

Architectures and the monitored products for Arg-sensitive ABSs (a–c). Amperometric characteristics of ArgO-ABS (d–g), reproduced with permission from ref. 36; (d) – cyclic voltammogram at scan rate 50 mV s^{-1}; (e) – chronoamperometric response upon subsequent additions of Arg; (f) – dependence of amperometric signal on Arg concentration; (g) – calibration graph for Arg in linear range. Conditions: Ag/AgCl as a reference electrode in 50 mM phosphate buffer, pH 7.0, working potential −150 mV (e–g).

Table 1

Analytical characteristics of the most effective chemo-sensors as platforms for construction of Arg-sensitive ABSs.

No	Electrode composition	Target analyte	Working potential, mV	Sensitivity, $A \cdot M^{-1} \cdot m^{-2}$	Linear range, up to μM	LOD, μM	Optimal pH	Reference
1	PANi/Nafion/Pt-SPE	NH_3/NH_4^+	−200	4000	10	10	6.8	[51]
			+300	400	1000	5	10.5	
2	PANi/Nafion/Cu_2O/Pt-SPE		−450	2500	1000	0.5	7.4	[52]
3	Cu/Zn(Hg)S/Nafion/GE		+170	5660	50	0.02	7.0	[29]
			−300	1870	200	1.5		
4	PANI: PSS/GCE		−200	1060	100–11700	0.5	7.0	[53]
5	nNiPtPd/Nafion/GE	H_2O_2	−200	13,250	1000	5	7.0	[36]
6	nCeCu/Nafion/GE		−50	2164	1.5	0.5		
7	nCuHCF/Nafion/GE		−150	1620	0.8	10		

with NH_4-sensitive films/compounds according to a doping/de-doping mechanism and produce an amperometric signal (Figure 2a and b).

To date, there are limited data on the mono-enzyme ABSs which are designed for monitoring ammonium ions. A simple construction of a stable ABS based on ADI co-immobilized with NH_4-sensitive nanoparticles in the bioselective layer remains an evident problem.

Detection of hydrogen peroxide as a by-product of Arg degradation

The majority of traditionally constructed ABSs with oxidases are based on the detection of hydrogen peroxide generated as a byproduct of the oxidase-catalyzed reaction with its own substrate. To achieve the detection of H_2O_2 under a low reducing potential, peroxidase (PO) is usually considered when designing the ABS. The most frequently cited Arg-sensitive oxidase-based ABSs contain at least

Table 2

Analytical characteristics of the most effective ABSs on Arg.

Enzyme	Source of enzyme	Biosensing film	Sensitivity, $A \cdot M^{-1} \cdot m^{-2}$	Linear range, μM	K_M^{app}, mM	Reference
rhARG	r*O. polymorpha*	ARG/urease/PANi	110	70–600	1.27	22
rADI	r*E. coli*	ADI/PANi	684	3–200	0.31	27
rADI	r*E. coli*	ADI/Cu/Zn(Hg)S	1570	13–800	1.75	29
ArgO	mushroom *Amanita phalloides*	ArgO/nCeCu	1630	5–100	0.32	36
		ArgO/nNiPtPd	578	10–250	0.35	36

two enzymes in the bioselective layer, thus making the procedure more cumbersome and increasing the cost of the analysis. Although PO has a high specificity and sensitivity, the application of natural enzyme is limited by its high cost. To date, there are limited data concerning ABSs for Arg determination based on artificial PO for the decomposition of H_2O_2 [36].

As artificial POs, nano-sized mimetics of the enzyme or nanozymes (NZs) have been used [36,46–49]. Table 1 demonstrates analytical characteristics of the most effective PO-like NZs for the H_2O_2 detection. Novel artificial PO-mimetics demonstrate a great promise for the successful assay of various real samples including food and biological liquids. They have been used as platforms for the construction of Arg-selective ArgO-based ABSs.

Table 2 demonstrates the ABSs with the highest sensitivities to Arg which are based on the enzymes of Arg catabolism.

It was mentioning, that the ArgO-based ABSs are not sufficiently stable, they remain approx. 50% of their activity during 5 days of storage [36]. The half-life of the ADI/Cu/Zn(Hg)S-based ABS is 8 days, that is rather low too [29]. On the contrary, the ADI/PANi/Nafion/Pt-SPE-based ABS was very stable, remaining 93% of its activity after 35 days' storage and following 100 assays [26]. This result can be explained by several reasons: 1) highly purified recombinant enzyme ADI was used, 2) ADI was stabilized with BSA and 3) it was covalently immobilized on PANi/Nafion by cross-linking using glutaraldehyde. The laboratory prototypes of the proposed ABSs have been successfully applied to Arg determination in the real samples of juices, wine, and commercial pharmaceuticals [24,29,36].

Thus, these ABSs may be potentially suitable for Arg analysis in industrial and medical laboratories.

Conclusion

Arg is an important biomarker in clinical diagnostics and useful drug/supplement for the treatment of different diseases, including cancer and COVID-19. Arg is also a valuable indicator of food and beverages quality. Arg monitoring in fermented food products is necessary to predict generation in the foods of carcinogenic ethyl carbamate. In the current review, we summarized a variety of optical and electrochemical methods for Arg detection which were proposed to date. Electrochemical biosensors based on the enzymes of Arg metabolism are the most promising analytical tools for Arg assay due to their rapid response, high sensitivity and specificity. Ammonium and H_2O_2 are the main by-products generated during enzymatic hydrolysis of Arg, so they are chosen for monitoring by the corresponding chemosensing elements.

Analysis of recent scientific sources demonstrated that combining nanomaterials with electrochemical biosensors has become a novel strategy for the development of simple and reliable systems for Arg monitoring in industry and medicine. Catalytically active nanomaterials or nanozymes, having a higher stability and a lower cost in comparison with natural enzymes, are promising catalysts for biosensing applications. The usage of electroactive nanozymes makes the detection more sensible, accurate, selective, with lower limits of detection, wider ranges of linear response, and shorter response times. Future outlook and possible areas of investigation in biosensorics may be formulated as the search of new electroactive and catalytically active nanomaterials with advanced characteristics as chemosensing platforms for biosensors construction, obtaining novel enzymes from the over-producing cells, fabrication of highly sensitive and selective biosensors on the base of enzymes and nanomaterials.

Declaration of competing interest

The authors declare that they have no known competing financial interests or personal relationships that could have appeared to influence the work reported in this paper.

Acknowledgements

This work was funded by the National Academy of Sciences of Ukraine (the program "Smart sensor devices of a new generation based on modern materials and technologies", project 0118U006260), by the Ministry of

Education and Science of Ukraine (Ukrainian-Lithuanian R&D, project 0120U103398), and by the National Research Foundation of Ukraine (projects 2020.02/0100 and 2021.01/0010).

List of abbreviations

AA	amino acid
ABS	amperometric biosensor
ADC	arginine decarboxylase
ADI	arginine deiminase
Arg	L-arginine
ArgO	arginine oxidase
ARG	arginase
BSA	bovine serum albumin
GCE	glassy-carbon electrode
GE	graphite electrode
HCF	hexacyanoferrate
ISE	ion-selective electrodes
n, NPs	nanoparticles
NZ	nanozyme
PANi	polyaniline
PO	peroxidase
PSS	anofibrous polyaniline:polystyrene-sulphonate
Pt-SPE	platinum screen-printed electrode
rADI	recombinant bacterial arginine deiminase
rE. coli	recombinant cells *E. coli*
rhARG	recombinant human arginase
rO. polymorpha	recombinant cells *O. polymorpha*

References

Papers of particular interest, published within the period of review, have been highlighted as:

* of special interest
** of outstanding interest

1. Morris Jr SM: **Arginine metabolism revisited**. *J Nutr* 2016, **146**: 2579S–2586S.

2. Terstappen F, Tol AJC, Gremmels H, Wever KE, Paauw ND, Joles JA, Beek EMV, Lely AT: **Prenatal amino acid supplementation to improve fetal growth: a systematic review and meta-analysis.** *Nutrients* 2020, **12**:2535.

3. Stasyk O, Boretsky Y, Gonchar M, Sibirny A: **Recombinant arginine-degrading enzymes in metabolic anticancer therapy and biosensorics**. *Cell Biol Int* 2015, 39:246.

4. Butler M, van der Meer LT, van Leeuwen FN: **Amino acid depletion therapies: starving cancer cells to death**. *Trends Endocrinol Metabol* 2021, **32**.

5. Zhang Y, Chung S-F, Tam S-Y, Leung Y-C, Guan X: **Arginine deprivation as a strategy for cancer therapy: an insight into drug design and drug combination**. *Review. Cancer Lett* 2021, **502**:58–70.

6. Albaugh VL, Pinzon-Guzman C, Barbul A: **Arginine - dual roles as an onconutrient and immunonutrient**. *J Surg Oncol* 2017, **115**:273–280.

7. * Tomé D: **Amino acid metabolism and signalling pathways: potential targets in the control of infection and immunity**. *Nutr Diabetes* 2021, 11:20.

This review demonstrates the significance of Arg monitoring in mammals under therapy of viral infection, such as SarCoV2. Defenses to pathogens involves interactions between immune functions and metabolic pathways to eradicate infection while preventing hyperinflammation. Pharmacological antiviral strategy was proposed: usage of Arg-metabolising enzymes results in Arg depletion, that limits the hyperinflammation and decreases availability of Arg for viral replication.

8. Cao B, Deng R, Wang D, Li L, Ren Z, Xu L, Gao X: **Association between arginine catabolism and major depressive disorder: a protocol for the systematic review and meta-analysis of metabolic pathway**. *Medicine (Baltim)* 2020, **99**:e21068.

9. Huang J, Ladeiras D, Yu Y, Ming XF, Yang Z: **Detrimental effects of chronic L-arginine rich food on aging kidney**. *Front Pharmacol* 2021, 11:582155.

10. Mirmiran P, Bahadoran Z, Gaeini Z, Azizi F: **Habitual intake of dietary L-arginine in relation to risk of type 2 diabetes: a prospective study**. *BMC Endocr Disord* 2021, **21**:113.

11. Li P, He W, Wu G: **Composition of amino acids in foodstuffs for humans and animals.** *Adv Exp Med Biol* 2021, **1332**: 189–210.

12. Kido J, Matsumoto S, Takeshita E, Hayasaka C, Yamada K, Kagawa J, Nakajima Y, Ito T, Iijima H, Endo F, Nakamura K: **Current status of surviving patients with arginase 1 deficiency in Japan**. *Mol Genet Metab Rep* 2021, **29**:100805.

13. Bednarz-Misa I, Fleszar MG, Zawadzki M, Kapturkiewicz B, Kubiak A, Neubauer K, Witkiewicz W, Krzystek-Korpacka M: **L-Arginine/NO pathway metabolites in colorectal cancer: relevance as disease biomarkers and predictors of adverse clinical outcomes following surgery**. *J Clin Med* 2020, 9:1782.

14. Karatsai O, Shliaha P, Jensen ON, Stasyk O, Rędowicz MJ: **Combinatory treatment of canavanine and arginine deprivation efficiently targets human glioblastoma cells via pleiotropic mechanisms**. *Cells* 2020, **9**:2217.

15. Chen C-L, Hsu S-C, Ann DK, Yen Y, Kung H-J: **Arginine signaling and cancer metabolism**. *Cancers* 2021, **13**:3541.

16. Adebayo A, Varzideh F, Wilson S, Gambardella J, Eacobacci M, Jankauskas SS, Donkor K, Kansakar U, Trimarco V, Mone P, Lombardi A, Santulli G: **L-arginine and COVID-19: an update**. *Nutrients* 2021, **13**:3951.

17. Fiorentino G, Coppola A, Izzo R, Annunziata A, Bernardo M, Lombardi A, Trimarco V, Santulli G, Trimarco B: **Effects of adding L-arginine orally to standard therapy in patients with COVID-19: a randomized, double-blind, placebo-controlled, parallel-group trial. Results of the first interim analysis**. *EClinicalMedicine* 2021, **40**:101125.

18. * Grimes JM, Khan S, Badeaux M, Rao RM, Rowlinson SW, Carvajal RD: **Arginine depletion as a therapeutic approach for patients with COVID-19**. *Int J Infect Dis* 2021, **102**:566–570.

This review demonstrates the perspectives of using arginine-degrading therapeutics, namely, PEGilated ADI, as a strategy to treat hepatocellular carcinoma, COVID-19 and other viral diseases.

19. * Marsden AJ, Riley DRJ, Birkett S, Rodriguez-Barucg Q, Guinn B-A, Carroll S, Ingle L, Sathyapalan T, Beltran-Alvarez P: **Love is in the hair: arginine methylation of human hair proteins as novel cardiovascular biomarkers**. *Amino Acids* 2021, https://doi.org/10.1007/s00726-021-03024-5.

This study reports for the first time that human hair proteins, which were post-translationally modifed by arginine methylation, may be in future clinically useful cardiovascular biomarkers for prevention and diagnosis of cardiovascular disease.

20. Post A, Bollenbach A, Bakker SJL, Tsikas D: **Whole-body arginine dimethylation is associated with all-cause mortality in adult renal transplant recipients**. *Amino Acids* 2021, **53**:541–554.

21. Gowd V, Su H, Karlovsky P, Chen W: **Ethyl carbamate: an emerging food and environmental toxicant**. *Food Chem* 2018, **248**:312–321.

22. Gayda G, Stasyuk N, Klepach H, Gonchar M, Nisnevitch M: **Promising bioanalytical approaches to wine analysis**. In Grumezescu A, Holban AM. *Quality control in the beverage industry, ch. 12*, vol. 17. Amsterdam: Elsevier; 2019:419. The science of beverages.

23. Schriek S, Rückert C, Staiger D, Pistorius EK, Michel K-P: **Bioinformatic evaluation of L-arginine catabolic pathways in 24 cyanobacteria and transcriptional analysis of genes encoding enzymes of L-arginine catabolism in the cyanobacterium *Synechocystis* sp. PCC 6803**. *BMC Genom* 2007, **8**:437.

24. Stasyuk N, Gayda G, Fayura L, Boretskyy Y, Gonchar M, Sibirny A: **Novel arginine deiminase-based method to assay L-arginine in beverages**. *Food Chem* 2016, **201**:320–326.

25. Bollella P, Katz E: **Biosensors – recent advances and future challenges**. *Sensors* 2020, **20**:6645.

26. Verma N, Singh A, Singh M: **L-arginine biosensors: a comprehensive review**. *Biochem Biophys Rep* 2017, **12**:228.

27. Zhybak M, Fayura L, Boretsky Y, Gonchar M, Sibirny, Dempsey E, Turner A, Korpan Y: **Amperometric L-arginine biosensor based on a novel recombinant arginine deiminase**. *Microchim Acta* 2017, **184**:2679.

28. Tam S-Y, Chung S-F, Chen YW, So Y-H, So P-K, Cheong W-L, Wong K-Y, Leung Y-C: **Design of a structure-based fluorescent biosensor from bioengineered arginine deiminase for rapid determination of L-arginine**. *Int J Biol Macromol* 2020, **165**:472.

29. ** Stasyuk N, Gayda G, Zakalskiy A, Fayura L, Zakalska O, Sibirny A, Nisnevitch M, Gonchar M: **Amperometric biosensors for L-arginine and creatinine assay based on recombinant deiminases and ammonium-sensitive Cu/Zn(Hg)S nanoparticles**. *Talanta* 2022, **238**:122996.

For the first time, novel metal sulfide nanoparicles were used for amperometric ammonium determination, as well as ammonium-sensitive platform for ADI-based biosensor. Highly sensitive and selective biosensor for arginine determination, based on co-immobilized with Cu/Zn(Hg)S nanoparticles recombinant ADI, was fabricated and characterized. Detection of arginine in real samples was demonstrated.

30. Singh A, Sharma R, Singh M, Verma N: **Electrochemical determination of L-arginine in leukemic blood samples based on a polyaniline-multiwalled carbon nanotube—magnetite nanocomposite film modified glassy carbon electrode**. *Instrum Sci Technol* 2020, **48**:400–416.

31. Zarei M, Rahbar M, Morowvat M, Nezafat N, Negahdaripour M, Berenjian A, Ghasemi Y: **Arginine deiminase: current understanding and applications**. *Recent Pat Biotechnol* 2019, **13**:124.

32. Verma N, Singh AK, Saini N: **Synthesis and characterization of ZnS quantum dots and application for development of arginine biosensor**. *Sens Bio-Sens Res* 2017, **15**:41.

33. Berninger T, Bliem C, Piccinini E, Azzaroni O, Knoll W: **Cascading reaction of arginase and urease on a graphene-based FET for ultrasensitive, real-time detection of arginine**. *Biosens Bioelectron* 2018, **115**:104.

34. Siddappa S, Marathe GK: **What we know about plant arginases? Review**. *Plant Physiol Biochem* 2020, **156**:600–610.

35. Kucherenko IS, Soldatkin OO, Dzyadevych SV, Soldatkin AP: **Electrochemical biosensors based on multienzyme systems: main groups, advantages and limitations – a review**. *Anal Chim Acta* 2020, **1111**:114–131.

36. Stasyuk N, Gayda G, Demkiv O, Darmohray L, Gonchar M, Nisnevitch M: **Amperometric biosensors for L-arginine determination based on L-arginine oxidase and peroxidase-like nanozymes**. *Appl Sci* 2021, **11**:7024.

37. Sarkar P, Tothill IE, Setford SJ, Turner AP: **Screen-printed amperometric biosensors for the rapid measurement of L- and D-amino acids**. *Analyst* 1999, **124**:865–870.

38. Kacaniklic V, Johansson K, Marko-Varga G, Gorton L, Jönsson-Pettersson G, Csöregi E: **Amperometric biosensors for detection of L- and D-amino acids based on co-immobilized peroxidase and L- and D-amino acid oxidases in carbon paste electrodes**. *Electroanalysis* 1994, **6**:381–390.

39. Nakano S, Niwa M, Asano Y: **Following the evolutionary track of a highly specific L-Arginine oxidase by reconstruction and biochemical analysis of ancestral and native enzymes**. *Appl Environ Microbiol* 2019, **30**:567–570.

40. Riess C, Shokraie F, Classen CF, Kreikemeyer B, Fiedler T, Junghanss C, Maletzki C: **Arginine-depleting enzymes – an increasingly recognized treatment strategy for therapy-refractory malignancies**. *Cell Physiol Biochem* 2018, **51**:854–870.

41. Zakalskiy AE, Zakalska OM, Rzhepetskyy YA, Potocka N, Stasyk OV, Horak D, Gonchar MV: **Overexpression of $(His)_6$-tagged human arginase I in *Saccharomyces cerevisiae* and enzyme purification using metal affinity chromatography**. *Protein Expr Purif* 2012, **81**:63–68.

42. Fayura L, Boretsky Y, Pynyaha Y, Wheatley D, Sibirny A: **Improved method for expression and isolation of the Mycoplasma hominis arginine deiminase from the recombinant strain of Escherichia coli**. *J Biotechnol* 2013, **167**:420.

43. He Y, Zhou L, Deng L, Feng Z, Cao Z, Yin Y: **An electrochemical impedimetric sensing platform based on a peptide aptamer identified by high-throughput molecular docking for sensitive L-arginine detection**. *Bioelectrochemistry* 2021, **137**:107634.

44. Zhu K-J, Zhou L, Wu L, Feng S-F, Hu H-Y, He J-L, He Y-M, Feng Z-Mg, Yin Y-L, Yu D, Cao Z: **An enzyme-free amperometric sensor based on self-assembling ferrocene-conjugated oligopeptide for specific determination of L-arginine**. *Chin J Chem* 2021, **39**:2755–2762.

45. Soldatkin OO, Marchenko SV, Soldatkina OV, Cherenok S, Kalchenko O, Prynova O, Sylenko O, Kalchenko V, Dzyadevych S: **Conductometric sensor with calixarene-based chemosensitive element for the arginine detection**. *Chem Pap* 2018, **72**:2687–2697.

46. Neumann B, Wollenberger U: **Electrochemical biosensors employing natural and artificial heme peroxidases on semiconductors**. *Sensors* 2020, **20**:369.

47. Komkova MA, Pasquarelli A, Andreev EA, Galushin AA, Karyakin AA: **Prussian Blue modified boron-doped diamond interfaces for advanced H_2O_2 electrochemical sensors**. *Electrochim Acta* 2020, **339**:135924.

48. Keihan AH, Karimi RR, Sajjadi S: **Wide dynamic range and ultrasensitive detection of hydrogen peroxide based on beneficial role of gold nanoparticles on the electrochemical properties of Prussian blue**. *J Electroanal Chem* 2020, **862**:114001.

49. Nayl AA, Abd-Elhamid AI, El-Moghazy AY, Hussin M, Abu-Saied MA, El-Shanshory AA, Soliman HMA: **The nanomaterials and recent progress in biosensing systems: a review**. *Trends Environ. Anal Chem* 2020, **26**:e00087.

50. Cuartero M, Colozza N, Fernández-Pérez BM, Crespo GA: **Why ammonium detection is particularly challenging but insightful with ionophore-based potentiometric sensors – an overview of the progress in the last 20 years**. *Analyst* 2020, **145**:3188.

51. Strehlitz B, Gründig B, Kopinke H: **Sensor for amperometric determination of ammonia and ammonia-forming enzyme reactions**. *Anal Chim Acta* 2000, **403**:11.

52. Zhybak MT, Vagin MY, Beni V, Liu X, Dempsey E, Turner APF, Korpan YI: **Direct detection of ammonium ion by means of oxygen electrocatalysis at a copper- polyaniline composite on a screen-printed electrode**. *Microchim Acta* 2016, **183**:1981.

53. ** Uzunçar S, Meng L, Turner APF, Mak WC: **Processable and nanofibrous polyaniline: polystyrene-sulphonate (nano-PANI: PSS) for the fabrication of catalyst-free ammonium sensors and enzyme-coupled urea biosensors**. *Biosens Bioelectron* 2021, **171**:112725.

Authors report an advanced composite nano-PANI:PSS as a functional ink for the fabrication of catalyst-free NH_4^+ sensors and enzyme-coupled urea biosensors. The PSS provides both a soft-template for nanofibre formation and a poly-anionic charge compensator, enabling the detection of NH_4^+ with a wide linear range (up to 11.5 mM), high sensitivity (1060 A $M^{-1}m^{-2}$) and good selectivity. It was demonstrated that nano-PANI:PSS as the advanced conducting polymer may be promising transducer material for development of printed organic sensors and biosensors.

54. * Li C, Wang Y, Jiang H, Wang X: **Biosensors based on advanced sulfur-containing nanomaterials**. *Sensors* 2020, **20**:3488.

This review describes the peculiarities of sulfur-containing nanomaterials, their applications in biosensors, as well as future perspective and challenges of biosensors based on sulfur-containing nanomaterials.

Оригінал доступний за посиланням: https://www.sciencedirect.com/science/article/abs/pii/S2451910322000060

Анотація: *Цей огляд зосереджено на висвітленні основних характеристик креатиніндеімінази (КДІ), важливого біоаналітичного інструменту для аналізу креатиніну (Крн). Крн є незамінним метаболітом для діагностики дисфункції нирок та деяких інших захворювань, біомаркером для контролю процедури гемодіалізу, а також важливим аналітом для спортивної медицини (оцінка загального фізіологічного стану спортсменів). Нами проаналізовано важливі джерела для виділення КДІ, клонування відповідного гена, конструювання мікробних рекомбінантних штамів та подано характеристики ензиму з різних мікроорганізмів. Також розглядаються нові біоаналітичні методи кількісного визначення Крн, у тому числі, ензиматичні на основі використання КДІ.*

FINAL

Send Orders for Reprints to reprints@benthamscience.ae

Current Protein and Peptide Science, 2019, *20*, 1-6

REVIEW ARTICLE

Creatinine Deiminase: Characterization, Using in Enzymatic Creatinine Assay, and Production of the Enzyme

Andriy Zakalskiy[a,b,*], Nataliya Stasyuk[a] and Mykhailo Gonchar[a,b]

[a]*Institute of Cell Biology, National Academy of Sciences of Ukraine, 14/16 Drahomanov Str., 79005, Lviv, Ukraine;*
[b]*Lviv State University of Physical Culture, 11 Kostiushko Str., 79000, Lviv, Ukraine*

ARTICLE HISTORY

Received: February 12, 2018
Revised: October 19, 2018
Accepted: November 08, 2018

DOI:
10.2174/1389203720666181114111731

Abstract: The goal of the review is description of the main characteristics of creatinine deiminase (CDI), an important bioanalytical tool for creatinine (Crn) assay. Crn is an essential metabolite for diagnostics of kidney disfunction and some other diseases, a biomarker to control the hemodialysis procedure, as well as an important analyte for sport medicine (estimation of general physiological status of athletes). We have described the important sources for CDI isolation, cloning of the corresponding gene, the construction of microbial recombinant strains, overproducing CDI, and characteristics of the enzyme from different microorganisms. There are reviewing also the new bioanalytical methods for quantitative determination of Crn, including enzymatic ones based on using CDI.

Keywords: Creatinine deiminase, protein characterization, gene cloning, enzyme isolation, creatinine, creatinine enzymatic assay.

1. INTRODUCTION

Analytical biotechnology, an important part of modern biotechnology, involves the use of biological objects (tissues, cells and organelles), multimolecular complexes, biomolecules or even principles of living systems for analytical purposes. Relevance of the analytical biotechnology for clinical medicine is associated with the development of selective, sensitive and inexpensive methods for assay of practically important analytes - biomarkers of the most common diseases. The main advantage of bioanalytical systems is an exceptional specificity due to their extraordinary ability for biorecognition at the molecular level. Significant progress of analytical biotechnology is largely determined by the rapid development of gene, protein and cell engineering, enzymology, bioelectronics and nanotechnology. Achievements of analytical biotechnology are used both in basic research and in practical areas of human activity - medicine (diagnostics and monitoring the treatment effectiveness), pharmaceutical and food industry (quality control of drugs and foods), and detection of toxic substances in environment.

The goal of this paper is a review of new bioanalytical methods for quantitative determination of creatinine (Crn), a protein metabolite, an important biomarker of kidney functioning. We have described also the main characteristics of creatinine deiminase (CDI) as the most promising bioanalytical tool for Crn assay, the important sources of the enzyme, cloning of the corresponding gene and construction of microbial recombinant strains overproducing CDI. Crn determination methods are very important for clinical diagnostics of renal dysfunction: to assess the severity of the disease, monitor its course and treatment process (including dialysis method), as well as for sport medicine (estimation of general physiological status of athletes, especially at risk of disturbing hydroelectrolytic balance of the body).

*Address correspondence to this author at the Department of Analytical Biotechnology, Institute of Cell Biology, National Academy of Sciences of Ukraine, 14/16 Drahomanov Str., P.O. Box: 79005, Lviv, Ukraine;
Tel./Fax: +38-032-261-21-44, +38-032-261-21-48;
E-mail: andriy.zakalskiy@yahoo.com

2. CRN AS A BIOMARKER OF RENAL FUNCTION

Crn is the final protein breakdown product in the body of animals and humans. It is formed in the muscles and excreted in the blood. Serum Crn is an important indicator of renal function, because it is an easily measured byproduct of muscle metabolism that is excreted unchanged by the kidney, mainly, by glomerular filtration [1]. When the filtration in the kidney is damaged, Crn levels in blood rise. Therefore, assay of Crn in biological fluids (serum and urine) may be used to calculate the Crn clearance, which correlates with the glomerular filtration rate.

Crn in serum and urine is an important diagnostic biomarker for monitoring kidney diseases, such as acute chronic interstitial nephritis, urethrophraxis, mercurialism, nephrosis, renal insufficiency, as well as myocardial infarction [2]. The content of this metabolite in the effluent dialysate or ultrafiltrate is also informative quantitative estimation of hemodialysis efficiency.

A comrehensive review on Crn and creatine metabolism has been published recently by Wyss and Kaddurah-Daouk [3]. Limited arguments suggest a link between disturbances in creatine metabolism and muscle diseases as well as neuro-

1389-2037/19 $58.00+.00

© 2019 Bentham Science Publishers

logical disorders, and healing effects of oral creatine supplementation in such diseases have in fact been notified. It has been shown that oral creatine consumption results in improving athletic execution, so it is widely used by many athletes as a performance-boosting supplement. Unfortunately, it was shown that creatine and Crn may act as precursors of food mutagens and uremic toxins [3].

A normal level of Crn for a man is 62-115 μM and for a woman 44-97 μM. In the case where only one kidney is functioning, this Crn level rises to 159-168 μM [4]. Increased Crn concentration in serum (for children – more than 177 μM, for adults - more than 885 μM) indicates a serious renal failure. Hypercreatininemia may be associated with chronic or acute renal diseases and renal toxic factors, including medications (compounds for X-ray radiography, aminoglycoside antibiotics, cephalosporin antibiotics, statins, *etc.*). Increasing the level of Crn in serum is also observed after consumption of large amounts of meat (if, in addition, there is a high content of Crn in urine). The Crn level increases at dehydration and muscle lesions. Reducing the concentration of Crn is observed at low consumption of meat, vegetarian diet, fasting, and in I and II trimesters of pregnancy. Levels less than 40 μM indicate decreased muscle mass [5].

It should be noted that recently there was proposed an alternative biomarker for the assessment of kidney function, cystatin C [6, 7]. This protein belongs to a group 2 of cystatin genetic family, found in human blood plasma and excreted from the body by the kidneys. Cystatin C is regarded as the "gold standard" for characterization of glomerular filtration rate as an integral indicator of renal function (inulin test, albeit ideal in terms of precision, is a very difficult in performance and could not be regarded for a routine investigation in medical practice). Unlike Crn, the rate of cystatin C synthesis is not influenced by different factors, such as age, sex, muscle mass, nutrition, the presence of inflammation in the body [8]. Increased cystatin C level in serum correlates with impaired renal function, but it occurs also at serious cardiovascular diseases, in the elderly, and some forms of brain amyloidosis.

The main obstacle for using cystatin C as a biomarker in clinical practice is the high cost and complexity of analysis. For example, commercial immuno-enzymatic kits for 96 tests based on ELISA method cost 495-636 Euro [9, 10]. Biosensors described in the literature, based on monitoring of interaction of cystatin C with monoclonal antibodies using reflectometric interference spectrometry [11] or analysis of specific inhibitory action of cystatin C on proteases (bromelain, ficin or chymopapain) using surface plasmon resonance [12], are rather unsuitable for practical implementation.

3. CHEMICAL AND PHYSICO-CHEMICAL METHODS FOR THE DETERMINATION OF CRN CONTENT

Since the Crn assay is widely used for assessment of the patient's condition, the accuracy of such detection in case of renal dysfunction is especially important.

Among chemical methods for Crn determination [1, 13], Jaffe's reaction [14] based on alkaline sodium picrate as a chemical reagent, is widely used, but it is non-specific. Therefore, many other approaches with improved analytical characteristics were developed.

Many attempts have been made to develop a new technique which is superior to the alkaline sodium picrate method, but new modifications still have a low specificity and are sensitive to positive and negative interference from different substances.

There was proposed a variety of advanced instrumental methods for Crn determination, *e.g.*: high-pressure liquid chromatography [15-18], chromatography using fluorescent indicators [19], ion chromatography [20, 21], micellar electrokinetic chromatography [22-24], capillary zone electrophoresis [25-28], capillary electrophoresis [29], capillary isotachophoresis [30] and tandem mass spectrometry [31] Table **1**.

Table 1. Sensitivity of the different physico-chemical methods of creatinine assay.

Methods	LOD, μM	References
Capillary electrophoresis	7.6	[22]
	1.0	[23]
	4.4	[29]
	6.2	[27]
	3.5	[26]
	2.2	[25]
HPLC	0.02	[20]
	0.5	[21]
	1	[17]
Micellar electrokinetic chromatography	5	[24]
Potentiometric biosensor, ISFET	20	[20]
Potentiometric biosensor, pH	10	[32]
Spectrophotometry	32.5	[16]
Isotachophoresis	0.44	[30]
Tandem mass spectrometry	0.2	[31]
Flow injection, multiple assay	14	[19]

Abbreviations: LOD – limit of detection; ISFET – ion sensitive field-effect transistor.

However, all these methods are rather complicated and unsuitable for Crn assay in real-time mode. In addition, equipment for capillary electrophoresis is expensive and, therefore, not useful for routine analysis [32]. Thus, the further development of novel highly selective and sensitive methods for fast Crn determination in biological liquids is very important.

4. ENZYMATIC METHODS FOR CRN ASSAY

Enzymatic methods seem to be the most promising analytical techniques for Crn assay. Two Crn digestion enzymes are proposed to be useful for this aim: 1) CDI (EC 3.5.4.21) converts the Crn to N- methylhydantoin and ammonia ions; and 2) Crn amidohydrolase (creatininase, EC 3.5.2.10) splits reversibly Crn to creatine. Using these enzymes, Crn content has been measured by monitoring the final products (*i.e.,* ammonia or creatine) through a series of multienzyme reactions.

As a source of CDI, different microorganisms can be used, but an important problem in application of this enzyme for analytical purposes is its insufficient specificity to the target analyte: various bacteria and fungi produce an enzyme which has additional deiminase activity toward cytosine [3]. Most bacterial CDIs are oligomeric proteins, composed of 4-16 identical subunits with a molecular mass of 35-72 kDa. There was described the isolation of CDIs from various microbial sources using multi-stage chromatographic procedure (see below).

For enzymatic assay of Crn, there was proposed CDI-catalyzed hydrolysis coupled with glutamate dehydrogenase reaction for detection of ammonia by spectrophotometric monitoring (at 240 nm) of NADH oxidation [33]:

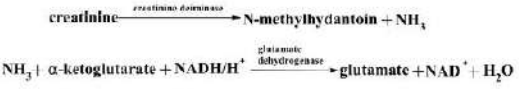

Another approach is based on using two enzymes: creatininase (EC 3.5.2.10) and creatinase (EC 3.5.3.3). Crn is converted by creatininase into creatine and the last one – to urea and sarcosine by creatinase. The final product (sarcosine) can be assayed colorimetrically or fluorimetrically. It was described a multienzyme detection procedure for Crn assay [34] based on the following reactions: 1) deimination of Crn catalyzed by CDI; 2) ring-opening of N-methylhydantoin by N-methylhydantoin amidohydrolase (ATP-dependent amidohydrolase catalyzing the reaction: N-methylhydantoin + ATP + 2 H_2O = N-carbamoylsarcosine + ADP + P_i); 3) decarbamoylation of N-carbamoylsarcosine by N-carbamoylsarcosine amidohydrolase to sarcosine (N-carbamoylsarcosine + H_2O = sarcosine + NH_3 + CO_2). Finally, sarcosine oxidase and peroxidase can be used for colorimetric procedure for detection of hydrogen peroxide produced during sarcosine oxidation.

Several enzymatic kits for Crn analysis are produced commercially using above mentioned enzymes, *e.g.*, by "SIGMA-ALDRICH" [35] (catalogue price – 342 Euro for 100 assays), as well as for creatine [36] (price is 360.5 Euro for 100 assays). Similar kit for assay of Crn is manufactured by the company BIOVISION [37] (with a price of 285 USD for 100 assays) and by ABCAM [38] (385 Euro).

5. ISOLATION OF CDI, CLONING OF THE CORRESPONDING GENE, AND CONSTRUCTION OF RECOMBINANT STRAINS OVERPRODUCING THIS ENZYME

Szulmajster [39, 40] first reported isolation of CDI from an anaerobic microorganism *Clostridium paraputrificum*.

CDIs from *Pseudomonas putida*, *Pseudomonas chlororaphis*, *Escherichia coli*, *Proteus mirabilis* [34, 41], *Flavobacterium filamentosum* [42] and *Saccharomyces cerevisiae* [43] possess also cytosine deaminase activity, due to the structural resemblance between Crn and cytosine [3]. In contrast to these enzymes, CDI of *Corynebacterium glutamicum (lilium) ATCC 15990* [44], an anaerobic *Clostridium* sp. [45] displays no cytosine deaminase activity Table **2**, while *Pseudomonas ovalis* [41], *Alcaligenes denitrificans*, and of *Arthrobacter* species [45, 46] are unable to utilize Crn as a substrate [3].

CDIs from some species of bacteria and fungi have been isolated and purified [3, 34, 42-45, 47-49]. Most of the bacterial enzymes are composed of 4 - 16 identical subunits with a Mr of 35000-72000 each. The Mr values of the native CDIs from *F. filamentosum, P. putida* were estimated by different techniques to be 245000-288000, while SDS-PAGE revealed subunit Mr values of 44300-53000. Therefore, these CDIs are most likely hexameric molecules. The fungal enzymes from *Aspergillus fumigatus* and baker's yeast as well as the cytosine deaminases from *A. denitrificans* and from an *Arthrobacter* species are likely to be active also as monomers with Mr values of 32000-41000, while CDI from *C. glutamicum* ATCC 15990 seems to be a oligomeric protein with a Mr of ~200000 [3] Table (**2**).

The cloned CDI from a *Bacillus sp.* (Geneseq accession no. R79013), coding for a 394-amino acid protein, is essentially homologous to cytosine deaminase from *E. coli* [50], but distinctly differs from the cytosine deaminases of *S. cerevisiae* and *Candida albicans* (DDBJ/EMBL/GenBank accession no. U55193 and U55194, respectively) [3].

Database searches in the *C. glutamicum* ATCC 13032 genome sequence [51] revealed the presence of a gene encoding CDI designated *codA*. The enzyme hydrolyses Crn to *N*-methylhydantoin and ammonium, which can then be assimilated *via* the glutamate dehydrogenase (GDH) or glutamine synthetase/glutamate synthase (GS/GOGAT) pathways. The transcriptional regulation of the membrane protein involved in Crn uptake and *codA* gene expression were studied [52].

The CDI was purified and crystallized from the cell-free extract of *C. glutamicum* ATCC 15990 using multistep procedure [53, 54]. A crystalline preparation of CDI from *C. glutamicum* ATCC 15990 was characterized: the molecular weight is 195000 Da (sedimentation equilibrium method); the isoelectric point - 4.2 (isoelectric focusing); being relatively thermostable, the enzyme has a broad pH optimum-from 7.5 to 10.0. It was specific for Crn and shows a K_m value of 1.27 mM Table (**2**). The enzyme is inhibited by heavy metal ions and *p*-chloromercuribenzoate. The enzyme is proposed for using in determination of serum and urinary Crn [44].

CDI from the anaerobic microorganism BN11 (*Tissierella creatinini*) has been purified to homogeneity with a specific activity of 78 units per mg protein Table (**2**). [47]. The enzyme is specific only for Crn and has a Km value of 0.15 mM. CDI preparation was used for Crn assay in serum and urine [47].

Table 2. Characteristics of CDI from different microorganisms.

Microorganism	Substrate specificity	Specific activity, μmol x min^{-1}x mg^{-1}	K_M, mM	pH optimum	Temp. optim., °C	M_r of oligomer or subunit, kDa	References
Corynebacterium glutamicum	Crn	34.0	1.27-1.9	7.5-10.0	60	195; 46.3	[44, 52-54]
Aspergillus fumigatus	Cytosine, Crn	2.3	2	7	30-35	31-32	[3]
Clostridium paraputrificum	Crn		18	8,5			[39, 40]
Escherichia coli	Crn, Cytosine		0.0216				[41, 49, 50]
Flavobacterium filamentosum	Crn, Cytosine	39.8	5.0; 0.62	7.0-8.5		272.5; 44.3	[42]
Pseudomonas chlororaphis	Crn, Cytosine	0.0112					[34, 41]
Pseudomonas putida 77	Crn, Cytosine		0.0452		37	260	[34, 41]
Tissierella creatinini BN11	Crn	78.0	0.15	8.5-8.75	47	285-288; 47.5	[47]
Saccharomyces cerevisiae	Cytosine, Crn	200	3.0	7.0-8.0	30	34-41	[43]

CDI was isolated from the bacterium *F. filamentosum* Table (**2**) [42]. The enzyme hydrolyzes cytosine (K_M, 0.62 mM) as well as Crn (K_M, 5.00 mM). Each of compounds of this pair is a competitive cross-inhibitor in corresponding reactions.

Purified CDI from *F. filamentosum* was shown to contain zinc (0.87–2.5 g atom/mol enzyme) and iron (0.1–1.2 g atom/mol enzyme). Treatment of the enzyme with 1,10-phenanthroline decreases the specific CDI and cytosine deaminase activities by 98%. Reactivation of the holoenzyme from the apoenzyme was achieved in the presence of zinc, cobalt (II), cadmium, and nickel [42].

The CDIs described so far are relatively thermostable, pH resistant, and have pH optima in the range 7 – 10 [3, 42, 47, 53-55]. Creatine, arginine, urea, glutamine, guanidine, cytidine, CMP, and other nucleotides are not used as substrates. On the other hand, 5-fluorocytosine, 5-methylcytosine, and 3-methylcytosine are deaminated by the enzymes from *F. filamentosum* and baker's yeast which display both CDI and cytosine deaminase activity. The Km values for Crn of the CDIs are in the range 0.15 –18 mM, whereas those for cytosine, 5-fluorocytosine, and 5-methylcytosine are between 0.17 and 5 mM.

There were only two reports describing cloning of the gene for CDI. The recombinant *E. coli* overproducer of the CDI was constructed using cloned gene *cdi* from bacterium *T. creatinini* [56]. An American patent US 7205140 gives a nucleotide sequence of the gene for CDI for a microorganism of unknown origin [57]. This gene was cloned in *E. coli* and *Bacillus subtilis* and corresponding enzyme was isolated. Simultaneously, nucleotide sequences of the gene *codA* for the bacterium *C. glutamicum ATCC 13032* [58] and *Bacillus sp.* CNi-1365 [59, 60] were described. We cloned the gene *codA* from the bacterium *C. glutamicum PCM 1945* in *E. coli* [61] and obtained highly purified and stable recombinant CDI with (His)-tag on *N*-terminus and used it for construction of amperometric biosensor selective to Crn [62]. The most prominent advantages of this CDI are a high stability and a low price of the enzyme due to its high yield during isolation and preparation from the recombinant strain.

CONSENT FOR PUBLICATION

Not applicable.

CONFLICT OF INTEREST

The authors declare no conflict of interest, financial or otherwise.

ACKNOWLEDGEMENTS

This work was financially supported by NAS of Ukraine (Program "Intelligent" Sensory Devices of a New Generation Based on Modern Materials and Technologies") and in part by the Ministry of Education and Science of Ukraine (project No. 0118U000809).

REFERENCES

[1] Narayanan, S.; Appleton, H.D. Creatinine: A review. *Clin. Chem.*, **1980**, *26*(8), 1119-1126.
[2] Sant, W.; Pourciel-Gouzy, M.L.; Launay, J.; Do Conto, T.; Colin, R.; Martinez, A.; Temple-Boyer, P. Development of a creatinine-sensitive sensor for medical analysis. *Sens. Actuator B-Chem.*, **2004**, *103*, 260-264.
[3] Wyss, M.; Kaddurah-Daouk, R. Creatine and creatinine metabolism. *Phys. Rev.*, **2010**, *80*(3), 1107-1213.
[4] Ceriotti, F.; Boyd, J.C.; Klein, G.; Henny, J.; Queralto, J.; Kairisto, V.; Panteghini, M. Reference intervals for serum creatinine concentrations: Assessment of available data for global application. *Clin. Chem.*, **2008**, *54*(3), 559-566.
[5] Lad, U.; Khokhar, S.; Kale, G.M. Electrochemical creatinine biosensors. *Anal. Chem.*, **2008**, *80*(21), 7910-7917.
[6] Purnima, D.S.; Rajeshwari, G.; Shivaprakash, T.M. Cystatin C – a novel marker of glomerular filtration rate. *Indian J. Clin. Biochem.*, **2005**, *20*(1), 139-144.
[7] Westhuyzen, J. Cystatin C: A promising marker and predictor of impaired renal function. *Ann. Clin. Lab. Sci.*, **2006**, *36*(4), 387-394.
[8] Murty, M.S.N.; Sharma, U.K.; Pandey, V.B.; Kankare, S.B. Serum cystatin C as a marker of renal function in detection of early acute kidney injury. *Indian J. Nephrol.*, **2013**, *23*(3), 180-183.
[9] http://www.abcam.com/cystatin-c-human-elisa-kit-ab119589.html

[10] http://www.sigmaaldrich.com/catalog/product/sigma/rab0105?lang=en&region=UA

[11] Bleher, O.; Ehni, M.; Gauglitz, G. Label-free quantification of cystatin C as an improved marker for renal failure. *Anal. Bioanal. Chem.*, 2012, *402*(1), 349-356.

[12] Gorodkiewicz, E.; Breczko, J.; Sankiewicz, A. Surface plasmon resonance imaging biosensor for cystatin determination based on the application of bromelain, ficin and chymopapain. *Folia Histochem. Cytobiol.*, 2012, *50*(1), 130-136.

[13] Marchenko, S.V.; Zinchenko, O.A.; Poliakov, L.S., Geleshko, A.M.; Dzyadevych, S.V.; Soldatkin, O.P. Biosensor based on creatinine deiminase and pH-sensitive field-effect transistor for creatinine analysis in blood serum. *Biotechnologia Acta.*, **2013**, *6*(5), 79-86 (In Ukrainian).

[14] Jaffe, M. Über den Niederschlag, welchen Pikrinsäure in normalem Harn erzeugt, und über eine neue Reaktion des Kreatinins. *Z. Physiol. Chem.*, **1886**, *10*, 391-400.

[15] Dobberpuhl Mo, Y.; Dash, A.K. A simple HPLC method with pulsed EC detection for the analysis of creatine. *J. Pharm. Biomed. Anal.*, **2003**, *32*(1), 125-132.

[16] Durán Merás, I.; Espinosa-Mansilla, A.; Rodriguez Gómes, M.J. Determination of methotrexate, several pteridines, and creatinine in human urine, previous oxidation with potassium permanganate, using HPLC with photometric and fluorimetric serial detection. *Anal. Biochem.*, **2005**, *346*(2), 201-209.

[17] George, S.K.; Dipu, M.T.; Mehra, U.R.; Verma, A.K.; Ramgaokar, J.S. Improved HPLC method for the simultaneous determination of allantoin, uric acid and creatinine in cattle urine. *J. Chromatogr. B.*, 2006, *832*(1), 134-137.

[18] Samanidou, V.F.; Metaxa, A.S.; Paradoyannis, I.N. Direct simultaneous determination of uremic toxins: creatine, creatinine, uric acid, and xanthine in human biofluids by HPLC. *J. Liq. Chromatogr. A.*, **2002**, *25*(1), 43-57.

[19] Yao, T.; Kotegawa, K. Simultaneous flow-injection assay of creatinine and creatine in serum by the combined use of a 16-way switching valve, some specific enzyme reactors and a highly selective hydrogen peroxide electrode. *Anal. Chim. Acta*, **2002**, *462*, 283-291.

[20] Yokoyama, Y.; Horikoshi, S.; Takahashi, T.; Sato, H. Low-capacity cation-exchange chromatography of ultraviolet-absorbing urinary basic metabolites using a reversed-phase column coated with hexadecylsulfonate. *J. Chromatogr. A.*, 2000, *886*(1-2), 297-302.

[21] Yokoyama,Y.; Tsuji, S.; Sato, H. Simultaneous determination of creatinine, creatine, and UV-absorbing amino acids using dual-mode gradient low-capacitycation-exchange chromatography. *J. Chromatogr. A.*, **2005**, *1085*(1), 110-116.

[22] Burke, D.G.; MacLean, P.G.; Walker, R.A.; Dewar, P.J.; Smith-Palmer, T. Analysis of creatine and creatinine in urine by capillary electrophoresis. *J. Chromatogr. B.*, **1999**, *732*, 479-485.

[23] Tran, T.C.; Huq, T.A.; Kantes, H.L.; Crane, J.N.; Strein, T.G. Determination of creatinine and other uremic toxins in human blood sera with micellar electrokinetic capillary electrophoresis. *J. Chromatogr. B.*, **1997**, *690*(1-2), 35-42.

[24] Pobozy, E.; Radomska, A.; Koncki, R.; Glab, S. Determination of dialysate creatinine by micellar electrokinetic chromatography. *J. Chromatogr. B.*, **2003**, *789*, 417-424.

[25] Zinellu, A.; Sotgia, S.; Zinellu, E.; Chessa, R.; Deiana, L.; Carru, C. Assay for the simultaneous determination of guanidinoacetic acid, creatinine and creatine in plasma and urine by capillary electrophoresis UV-detection. *J. Sep. Sci.*, **2006**, *29*(5), 704-708.

[26] Tuma, P.; Samcova, E.; Balinova, P. Determination of 3-methylhistidine and 1-methylhistidine in untreated urine samples by capillary electrophoresis. *J. Chromatogr. B.*, **2005**, *821*(1), 53-59.

[27] Rodrigues, J.; Berzas, J.J.; Castaneda, Mora G.N.; *Rodríguez* M.J. Very fast and direct capillary zone electrophoresis method for the determination of creatinine and creatine in human urine. *Anal. Chem. Acta*, **2004**, *521*(1), 53-59.

[28] Zinellu, A.; Caria, M.A.; Tavera, C.; Sotgia, S.; Chessa, R.; Deiana, L.; Carru C. Plasma creatinine and creatine quantification by capillary electrophoresis diode array detector. *Anal. Biochem.*, **2005**, *342*(2), 186-193.

[29] Costa, A.C.O.; da Costa, J.L.; Tonin, F.G.; Tavares, M.F.M.; Micke, G.A. Development of a fast capillary electrophoresis method for determination of creatinine in urine samples. *J. Chromatogr. A.*, **2007**, *1171*(1), 140-143.

[30] Kvasnicka, F.; Voldrich, M. Isotachophoretic determination of creatinine in meat and meat products. *Electrophoresis*, **2000**, *21*, 2848-2850.

[31] Huskova, R.; Chrastina, P., Adam, T.; Schneiderka, P. Determination of creatinine in urine by tandem mass spectrometry. *Clin. Chim. Acta*, **2004**, *350*(1-2), 99-106.

[32] Zinchenko, O.A.; Marchenko, S.V.; Sergeyeva, T.A.; Kukla, A.L.; Pavlyuchenko, A.S.; Krasyuk, E.K.; Soldatkin, A.P.; El'skaya, A.V. Application of creatinine-sensitive biosensor for hemodialysis control. *Biosens. Bioelectron.*, **2012**, *35*, 466-469.

[33] Gottschalk, E.M.; Gottschalk, G.; Delitz, R.P.; Holdt-Lehmann, B.; Thormann, K.; Schmitz-Streit R. A new creatinine assay destined to become routine. *Renal Disease*. www.cli-online.com/fileadmin/artimg/a-new-creatinine-assay-destined-to-become-routine.pdf (As published in CLI October, 2005).

[34] Shimizu, S.; Kim, J.M.; Yamada, H. Microbial enzymes for creatinine assay: A review. *Clin. Chim. Acta*, **1989**, *185*(3), 241-252.

[35] http://www.sigmaaldrich.com/content/dam/sigma-aldrich/docs/Sigma/Bulletin/1/mak080bul.pdf

[36] http://www.sigmaaldrich.com/content/dam/sigma-aldrich/docs/Sigma/Bulletin/1/mak079bul.pdf

[37] https://www.biovision.com/creatinine-colorimetric-fluorometric-assay-kit.html

[38] http://www.abcam.com/ps/products/65/ab65340/documents/ab65340%20Creatinine%20Assay%20kit%20protocol%20v9%20%28website%29.pdf

[39] Szulmajster, J. Bacterial fermentation of creatinine I. Isolation of N-Methyl-Hydantoin. *J. Bacteriol.*, 1958, *75*(6), 633-639.

[40] Szulmajster, J. Bacterial degradation of creatinine: II. Creatinine desimidase. *Biochim. Biophys. Acta*, 1958, *30*(1), 154-163.

[41] Kim, J.M.; Shimizu, S.; Yamada, H. Cytosine deaminase that hydrolyzes creatinine to N-methylhydantoin in various cytosine deaminase-forming microorganisms. *Arch. Microbiol.*, **1987**, *147*, 58-63.

[42] Esders, T.W.; Lynn, S.Y. Purification and properties of creatinine iminohydrolase from *Flavobacterium filamentosum*. *J. Biol. Chem.*, **1985**, *260*(7), 3915-3922.

[43] Katsuragi, T.; Sonoda, T.; Matsumoto, K.; Sakai, T.; Tonomura K. Purification and some properties of cytosine deaminase from bakers' yeast. *Agric. Biol. Chem.*, **1989**, *53*(5), 1313-1319.

[44] Uwajima, T.; Terada, O. Properties of crystalline creatinine deiminase from *Corynebacterium lilium*. *Agric. Biol. Chem.*, **1980**, *44*(8), 1787-1792.

[45] Hermann, M.; Knerr, H.J.; Mai, N.; Gross, A.; Kaltwasser, H. Creatinine and N-methylhydantoin degradation in two newly isolated *Clostridium* species. *Arch. Microbiol.*, **1992**, *157*(5), 395-401.

[46] Kim, J.M.; Shimizu, S.; Yamada, H. Evidence for the presence of cytosine deaminase that does not catalyze the deimination of creatine. *FEBS Lett.*, **1987**, *210*(1), 77-80.

[47] Gottschalk, E.M.; Hippe, H.; Patzke, F. Creatinine deiminase (EC 3.5.4.21) from bacterium BN11: Purification, properties and applicability in a serum/urine creatinine assay. *Clin. Chim. Acta*, **1991**, *204*(1-3), 223-238.

[48] Ipata, P.L.; Marinocchi, F.; Magni, G.; Felicioli, R.; Polidoro, G. Baker's yeast cytosine deaminase. Some enzymic properties and allosteric inhibition by nucleosides and nucleotides. *Biochemistry*, **1971**, *10*(23), 4270-4276.

[49] Katsuragi, T.; Sakai, T.; Tonomur, K. Affinity chromatography of cytosine deaminase from *Escherichia coli* with immobilized pyrimidine compounds. *Agric. Biol. Chem.*, **1986**, *50*(7), 1713-1719.

[50] Austin, E.A.; Huber, B.E. A first step in the development of gene therapy for colorectal carcinoma: cloning, sequencing, and expression of *Escherichia coli* cytosine deaminase. *Mol. Pharmacol.*, **1993**, *43*, 380-387.

[51] Kalinowski, J.; Bathe, B.; Bartels, D.; Bischoff, N.; Bott, M.; Burkovski, A.; Dusch, N.; Eggeling, L.; Eikmanns, B.J.; Gaigalat, L.; Goesmann, A.; Hartmann, M.; Huthmacher, K.; Krämer, R.; Linke, B.; McHardy, A.C.; Meyer, F.; Möckel, B.; Pfefferle, W.; Pühler, A.; Rey, D.A.; Rückert, C.; Rupp, O.; Sahm, H.; Wendisch, V.F.; Wiegräbe, I.; Tauch, A. The complete *Corynebacterium glutamicum* ATCC 13032 genome sequence

and its impact on the production of L-aspartate-derived amino acids and vitamins. *J. Biotechnol.*, **2003**, *104*(1-3), 5-25.
[52] Bendt, A.K.; Beckers, G.; Silberbach, M.; Wittmann, A.; Burkovski, A. Utilization of creatinine as an alternative nitrogen source in *Corynebacterium glutamicum*. *Arch. Microbiol.*, **2004**, *181*, 443-450.
[53] Uwajima, T.; Terada, O. Crystallization and some properties of creatinine deiminase from *Corynebacterium lilium*. *Agric. Biol. Chem.*, **1976**, *40*, 1055-1056.
[54] Uwajima, T.; Terada, O. Production, purification and crystallization of creatinine deaminase of *Corynebacterium lilium*. *Agric. Biol. Chem*, **1977**, *41*, 339-344.
[55] Tabata, M.; Kido, T.; Totani, M.; Murachi, T. Automated assay of creatinine in serum as simplified by the use of immobilized enzymes, creatinine deiminase, and glutamate dehydrogenase. *Anal. Biochem*, **1983**, *134*, 44-49.
[56] http://www.google.com/patents/US20050084930
[57] https://www.lens.org/lens/patent/US_7205140_B2
[58] http://www.uniprot.org/uniprot/Q6M8S4#sequences
[59] http://www.ncbi.nlm.nih.gov/protein/2443394
[60] http://www.ncbi.nlm.nih.gov/protein/BAA22413.2
[61] Gonchar, M., Zakalskiy, A., Rzhepetskyy, Y., Hryniv, O. Recombinant microbial creatinine deiminase as a bioanalytical tool. In: *FEBS Journal*, Proceedings of the FEBS Conference Book, Paris, France, 30 August - 4 September **2014**; Vol. *281* (Suppl. 1), p. 595.
[62] Stasyuk, N.; Zakalskiy, A.; Zakalska, O.; Gonchar, M. (His)$_6$-tagged *Corynebacterium glutamicum* creatinine deiminase as a biosensing element for creatinine assay. In: *Weigl Conference Book*, Proceedings of the 7th International Weigl Conference, Lviv, Ukraine, September 26-29, **2017**; Sibirny, A.A. Ed.; Lviv Univ., UA, **2017**; p. 34.

DISCLAIMER: The above article has been published in Epub (ahead of print) on the basis of the materials provided by the author. The Editorial Department reserves the right to make minor modifications for further improvement of the manuscript.

Оригінал доступний за посиланням: https://pubmed.ncbi.nlm.nih.gov/30426898/

РОЗДІЛ 2 Матеріали і методи досліджень

2.1 Матеріали досліджень

2.1.1 Організми. У роботі використовували наступні штами із колекції Інституту біології клітини НАН України:

Ogataea polymorpha С-105 (*gcr1 catX*) – безкаталазний мутант метилотрофних дріжджів з порушеною глюкозною катаболітною репресією синтезу алкогольоксидази;

O. polymorpha NCYC 495 (pGAP1-HsARG1 leu2car1:LEU2) – рекомбінантний надпродуцент аргінази І людини;

O. polymorpha "tr1" (gcr1 catX/prAOX_CYB2) – рекомбінантний надпродуцент флавоцитохрому b_2;

Escherichia coli BL21(DE3)/pET32a-codA – рекомбінантний надпродуцент креатиніндеімінази;

E. coli BL21 (DE3)/pET3d-ADI-codA – рекомбінантний надпродуцент аргініндеімінази;

Saccharomyces cerevisiae C13ABYS86 (*Mat a, leu2-3, ura3, his, pra1-1, prb1-1, prc1-1, cps1-3*) – рекомбінантний надпродуцент метиламінооксидази;

O. polymorpha NCYC495 (*leu1-1)* – продуцент алкогольоксидази та дикий штам *O.polymorpha NCYC 495*;

Ізольований із природи гриб *Ammanita phalloides* — продуцент аргініноксидази.

2.1.2 Характеристика використаних реактивів та препаратів. Усі водні розчини, які використовували у роботі, готували на бідистиляті. Робочі розчини хлоридної, сульфатної, фосфатної кислот готували розведенням відповідних концентрованих кислот кваліфікації "х.ч.", ацетатної – з ацетатної кислоти (льод.) кваліфікації "ч.д.а". У роботі використовували розчини Натрій та Калій гідроксиду, який готували розчиненням реактиву кваліфікації "х.ч.".

Ензими: уреаза (ЕС 3.5.1.5, тип IX від Jack Beans, 26100 Од. $г^{-1}$) марки “Sigma-Aldrich” (Німеччина); глюкозооксидаза (ГО), отримана з міцеліального гриба *P. Adametzii* ЛФ F-2044.1 у лабораторії ензимів Інституту мікробіології НАН Білорусі (20 Од. $мг^{-1}$); пероксидаза хрону (ПО, RZ-3,0) виробництва ТзОВ «Астер», Львів, Україна.

Для досліджень використовували реактиви марки “Sigma-Aldrich” (Німеччина): гідроген тетрахлороаурумат, L-аргінін, аргентум нітрат, *о*-діанізидин, 2,2`-азинобіс-(3-етилбензотіазолін-6-сульфонат) діамонієва сіль (АБТС), гідроген пероксид, амоній хлорид, гідроген гексахлороплатинат, церій гідроген карбонат, паладій хлорид, кадмій(II) сульфат, натрій боргідрид, аскорбінова кислота, тринатрій цитрат, ферум(III) хлорид, купрум(II) сульфат, кобальт(II) хлорид, цинк сульфат, манган(II) хлорид та інші неорганічні солі, а також глутаровий альдегід (25%), цистеамін, нафіон (5%). Амінокислоти були отримані від «Sigma-Aldrich» (Німеччина). Усі буфери і стандартні розчини були приготовлені з використанням води, очищеної за допомогою системи Milli-Q (Millipore), або бідистиляту.

Пробірки (діаметром 5 мм) для проведення аналізу ^{1}H ЯМР виробництва Wilmad (Steinheim, Німеччина). Дейтеровані розчинники виробництва «Sigma Aldrich» (Німеччина) використовували без додаткового очищення.

2.2 Методи досліджень

2.2.1 Склад середовищ, культивування клітин і отримання безклітинних екстрактів. Дріжджі вирощували в синтетичному середовищі Беркгольдера (СБ) наступного складу: KH_2PO_4 – (0,5 – 1) г/л; $(NH_4)_2SO_4$ – (2 – 3,5) г/л; $MgSO_4 \cdot 7H_2O$ – (0,2 - 0,5) г/л; $CaCl_2$ – 0,1 г/л; сіль Мора – (0,2 мг – 1) мг/л; стандартна суміш мікроелементів – 0,5 мл/л; біотин – 1 мкг/л та в середовищі YPD.

У залежності від мети експерименту, використовували різні джерела Карбону та енергії: сахароза, глюкоза (0,5 – 2 %); L-лактат натрію, сукцинат натрію (0,2 – 1 %); метанол, етанол, гліцерол (0,5 – 1 %) чи їх суміші в різних співвідношеннях.

До СБ, за необхідності, додавали: амінокислоти (лейцин, лізин, гістидин) як селективні фактори росту (40 – 100 мг/л); дріжджовий екстракт (0,05 – 0,2 %); пептон (0,02 %) урацил (200 мг/л); тіамін (0,02 – 0,2 мг/л), піридоксин (4,5 мг/л) і пантотенову кислоту (4,5 мг/л).

Вихідні штами зберігали на скосах із сусло-агаром.

Дріжджі вирощували в колбах Ерленмейера на роторному шейкері при 250 об./хв або на чашках з 2 % агаризованим середовищем у термостаті при температурі 30 °С. Клітини осаджували при 3000 об./хв, 20 хв, відмивали водою.

Бактерії *E. coli* BL21 вирощували при 37 ^{o}C на багатому (LB) середовищі [50] з додаванням, за потреби, 50 мкг/мл канаміцину сульфату.

Оптичну густину клітин вимірювали турбідиметрично на фотоелектроколориметрі КФК-2МП, (кювета 3 мм, світлофільтр № 6), і, використовуючи калібрувальну криву, визначали їх суху біомасу в 1 мл середовища.

Для отримання безклітинного екстракту (БЕ), відмиті від середовища клітини руйнували на планетарному гомогенізаторі (діаметр скляних кульок 0,5 мм, 1000 об./хв, $r_{сер}$10 см, 6 хв, 4 ^{0}C). БЕ відділяли від осколків клітин центрифугуванням при 15000 g, $r_{сер}$8 см, 15 хв, 4 ^{0}C. Концентрацію білку в БЕ визначали за методом Лоурі.

2.2.2 Пермеабілізація клітин дріжджів. Відмиті від середовища клітини ресуспендували у 100 мМ фосфатному буфері рН 7,5 до концентрації 20-50 мг/мл, додавали рівний об’єм розчину цетилтриметиламоній броміду у концентрації 2 мг/мл. Суміш інкубували на водяній лазні протягом 15 хв при 30^{0}C, струшуючи її кожні 3-4 хв. Після пермеабілізації, клітини тричі промивали 5 мМ фосфатним буфером (ФБ) рН 7,5 і використовували для експериментів у різних концентраціях.

2.2.3 Визначення життєздатності клітин у присутності наноматеріалів флуоресцентним методом. До 1 мл суспензії клітин дріжджів вносили 20 мкл розчину 2',7'-дихлорфлуоресцеїн діацетату (1 мг/мл етанолу) і 10 мкл розчину

пропідій йодиду (1 мг/мл води) та інкубували при кімнатній температурі в темряві впродовж 1 години. Після інкубації з барвниками, клітини відмивали і аналізували на флуоресцентному мікроскопі Axio Lab. A1, Carl Zeiss (Німеччина). Життєздатні клітини генерують зелену флуоресценцію, а мертві клітини є червоними. Щоб оцінити життєздатність дріжджових клітин, в полі зору підраховували загальну кількість клітин та співвідношення живих та мертвих клітин за флуоресценцією.

2.2.4 Визначення вмісту Гідроген пероксиду в культуральній рідині дріжджів. Гідроген пероксид у культуральній рідині визначали в пероксидазній реакції за використання 3,3',5,5'-тетраметилбензидину (ТМБ) як хромогенного субстрату. Стандартний розчин H_2O_2 готували розведенням 10 мМ вихідного розчину, точну концентрацію якого вивіряли спектрофотометрично при 240 нм ($\varepsilon_{мМ}$ = 0,0436).

2.2.5 Виділення і очистка ензимів. $(His)_6$-мічену креатиніндеіміназу (КДІ, КФ 3.5.4.21) виділяли з нерозчинних «тілець включення» [51] та очищували за допомогою металоафінної хроматографії на кульках Ni-NTA Superflow (Qiagen). Вихід КДІ становив 30 мг/л культури. При ліофілізації в присутності трегалози КДІ не втрачала своєї активності протягом 120 днів зберігання при –20ºС [52].

Аргіназу (КФ 3.5.3.1) виділяли методом афінної колонкової хроматографії із безклітинного екстракту штама надпродуцента на синтезованому нами сорбенті – L-аргінін-макропористе скло [53]. Препарати аргінази із питомою активністю 1500 – 2600 Од.·мг$^{-1}$ білка було одержано із 40-60-кратною очисткою, із 42 %-овим виходом у кращих фракціях. Препарати зберігались за певних умов без втрати активності протягом року, а за 3 роки зберігання ензиматична активність падала лише удвічі.

Аргініндеіміназу (АДІ, КФ 3.5.3.6) виділяли з нерозчинних «тілець включення», як описано раніше [51], та очищували за допомогою аніонної та гідрофобної хроматографії на сорбентах QAE-сефароза та феніл-сефароза,

відповідно. Одержаний у результаті електрофоретично гомогенний препарат АДІ (до 180 Од.·мг$^{-1}$) зберігався без втрати активності упродовж 20 місяців [53].

Алкогольоксидазу (АО, КФ 1.1.3.13) виділяли з безклітинного екстракту штаму надпродуцента *O. polymorpha* С-105 (*gcr1 catX*) за допомогою двостадійного фракціонування сульфатом амонію (при 30 і 70% насичення) з подальшою іонообмінною хроматографією на DEAE-Toyopearl 650 M [54]. Очищену АО з питомою активністю 20 Од·мг$^{-1}$ білка зберігали у вигляді суспензії в 70% сульфаті амонію, 50 мМ фосфатному буфері (ФБ) pH 7,5 при 4°С.

Метиламіноксидазу (МАО, КФ 1.4.3.21) очищали з безклітинного екстракту штаму надпродуцента *S. cerevisiae* C13ABYS86 за допомогою металоафінної хроматографії на Ni-NTA-агарозі. Активність МАО визначали за швидкістю утворення гідроген пероксиду в реакції з метиламіном за результатами перекисного окиснення АБТС у присутності пероксидази. Очищену МАО з питомою активністю 16 Од.·мг$^{-1}$ білка зберігали у 20 % гліцеролі, 30 мМ ФБ pH 7,5 при –20°С [55].

Аргініноксидазу (АргО, КФ 1.4.3.25) з гриба *Ammanita phalloides* очищали іонообмінною хроматографією на Toyopearl DEAE-650M [56]. Частково очищений препарт АргО з питомою активністю 7,9 мОд·мг$^{-1}$ білка зберігали у вигляді суспензії в 70% сульфаті амонію, 50 мМ фосфатному буфері, pH 7,5, при 4°С.

Флавоцитохром b_2 (ФЦ b_2, КФ 1.1.2.3, L-лактат цитохром: *c* оксидоредуктаза) очищали з безклітинного екстракту за допомогою іонообмінної хроматографії на Toyopearl DEAE-650M (до 40 Од·мг$^{-1}$). Висолювання ензиму проводили додаванням до елюату сухого сульфату амонію до 70 % (від насичення при 0 ^{0}С при контролі pH близько 7.0-7.5). Стабілізований таким чином ензим зберігав свою активність протягом двох місяців при - 25 ^{0}С.

2.3. SDS-ПААГ електрофорез. SDS-поліакриламідний гель-електрофорез (12%) проводили згідно з Laemmli (1970).

2.4 Визначення активності ензимів.

2.4.1 Визначення активності флавоцитохрому b_2

Спектрофотометричний аналіз ФЦ b_2 проводили при λ=420 нм, за швидкістю знебарвлення реакційної суміші, що містила 33 мМ лактат натрію, 1 мМ ЕДТА і 0,83 мМ $K_3[Fe(CN)_6]$ у 30 мМ фосфатному буфері, pH 8,0.

2.4.2. Визначення активності аргінази. Процедуру вимірювання активності аргінази проводили наступним чином: до 250 мкл субстрату, що містив 65 мМ L-Arg, 2 мМ манган(II) хлорид в 20 мМ буфері Тріс-КОН, pH 9,5 додавали 20 мкл досліджуваного зразка з визначеною концентрацією білка (аліквоту культуральної рідини або безклітинного екстракту розводили до концентрації 0,1 мг/мл; очищені препарати аргінази – до 0,001 - 0,002 мг/мл). Реакційну суміш інкубували протягом 15 хв при 37 ^oC, реакцію зупиняли додаванням 3 мл розчину реагенту на сечовину виробництва НВФ «СІМКО», Львів. Кількість утвореної в результаті ензиматичної реакції сечовини визначали за кількістю забарвленого червоно-рожевого комплексу діацетилу із сечовиною, що має максимум поглинання при 520 нм. Питому активність аргінази виражали в стандартних одиницях активності: мкмоль продукту (сечовини), утвореного за 1 хв. в перерахунку на 1 мг білка у реакційній суміші за стандартних умов реакції (мкмоль·хв$^{-1}$·мг$^{-1}$).

2.4.3 Визначення активності алкогольоксидази. Активність алкогольоксидази (АО) вимірювали в реакційній суміші з кінцевим об’ємом 3,0 мл, що містила 50 мМ фосфатний буфер, pH 7,5, 0,25 мМ *о*-діанізидин, пероксидазу хрону (0,07 мг/мл), 10 мМ метанол та відповідну кількість ензиму або 10 мг пермеабілізованих клітин. Інкубацію проводили 5-10 хв при 30 °С. Ензиматичну реакцію зупиняли додаванням 0,8 мл 12 М HCl. Утворений забарвлений продукт визначали спектрофотометрично при 525 нм. Мілімолярний коефіцієнт екстинкції утвореного продукту в кислому розчині (2,5 М HCl) становить 13,38 мМ$^{-1}$·см$^{-1}$. За одиницю

активності АО приймали кількість ензиму, що вивільняє 1 мкмоль H_2O_2 за 1 хв при 30 °С за стандартних умов аналізу.

2.4.4 Визначення активності метиламінооксидази. Активність метиламінооксидази (МАО) визначали за модифікованим методом Haywood [55]. Активність МАО вимірювали в реакційній суміші з кінцевим об'ємом 3,0 мл, що містила 75 мМ фосфатний буфер, pH 7,0, 1 мМ АБТС, пероксидазу хрону (0,01 мг/мл), 5 мМ метиламін гідрохлорид та відповідну кількість ензиму. Інкубацію проводили 5-10 хв при 30 °С. Утворений забарвлений продукт визначали спектрофотометрично при 405 нм. Мілімолярний коефіцієнт екстинкції утвореного продукту становить 18,41 $мМ^{-1}\cdot см^{-1}$.

2.4.5 Визначення активності аргініноксидази. Активність аргініноксидази (АргО) визначали за швидкістю утворення Гідроген пероксиду в реакції з L-аргініном, що монітурується перекисним окисненням *о*-діанізидину. Активність вимірювали в реакційній суміші з кінцевим об'ємом 1,0 мл, що містила 50 мМ фосфатний буфер, pH 7,5, 0,25 мМ *о*-діанізидин, пероксидазу хрону (0,07 мг/мл), 25 мМ L-аргінін і відповідну кількість ензиму. Після інкубації протягом фіксованого часу (1–10 хв) при 30°С і після появи оранжевого забарвлення реакцію зупиняли додаванням 0,26 мл 12 М хлоридної кислоти. Утворений колір визначали при 525 нм за допомогою спектрофотометра. Мілімолярний коефіцієнт екстинкції отриманого барвника в кислому розчині становить 13,38 $мМ^{-1}\cdot см^{-1}$. За одиницю активності АргО приймали кількість ензиму, що вивільняє 1 мкмоль H_2O_2 за 1 хв при 30 °С за стандартних умов аналізу.

2.4.6 Визначення активності креатиніндеімінази. Визначення активності креатиніндеімінази (КДІ) проводили у 50 мМ К, Na-фосфатному буфері, pH 7,5, що містив 5 мМ креатинін, в кінцевому об'ємі 1 мл. Після інкубації упродовж 15-30 хв при 37 °С концентрацію йонів амонію аналізували флуориметричним методом на основі реакції аміаку з *о*-фталевим альдегідом (ОФА) та сульфітом натрію [56]. За одиницю активності КДІ приймали таку кількість ензиму, яка забезпечує

утворення 1 мкмоль продукту (амонію) за 1 хв в ензиматичній реакції за описаних вище умов.

2.4.7 Визначення активності аргініндеімінази. Процедуру вимірювання активності аргініндеімінази (АДІ) проводили в дві стадії. На першій стадії, до 0,5 мл розчину субстрату, що містив 120 мМ натрій саліцилат, 6,4 мМ натрій нітропрусид та 1 мМ ЕДТА у 100 мМ фосфатному буфері, pH 6,7, додавали 0,5 мл зразка та інкубували упродовж 10 хв. при кімнатній температурі. На другій стадії, до інкубаційної суміші вносили 1 мл реагенту ІІ, що містив 75 мМ Натрій гідроксид, 75 мМ Натрій гіпохлорит та через 10 хв проводили фотометрування дослідних проб при 580 нм проти «сліпої» проби. Мілімолярний коефіцієнт екстинкції утвореного продукту становить 15,6 $мМ^{-1}\cdot см^{-1}$.

2.4.8. Визначення активності пероксидази. Активність пероксидази хрону (ПО) визначали за використання хромогену – *о*-діанізидину. Для визначення питомої активності ПО (1 Од./мг; $мкмоль\cdot хв^{-1}\cdot мг^{-1}$) у пробірки розливали по 2,7 мл реакційної суміші, що містила 2,5 мл 0,3 мМ хромогену в 50 мМ ФБ, pH 7,5 та 0,2 мл досліджуваного розчину із ПО. Реакцію запускали внесенням розчину Гідроген пероксиду та інкубували упродовж 5–10 хв, залежно від швидкості розвитку кольорової реакції. Реакцію зупиняли у точно фіксований час додаванням 0,8 мл концентрованої HCl. Проби фотометрували при 525 нм (ε =13,38 $мМ^{-1}\cdot см^{-1}$) проти сліпої проби, яка містила 0,2 мл ФБ замість ензиму. Мілімолярний коефіцієнт екстинкції отриманого барвника в кислому розчині становить 13,38 $мМ^{-1}\cdot см^{-1}$.

2.4.9 Визначення активності глюкозооксидази. Активність глюкозооксидази (ГО) вимірювали в реакційній суміші з кінцевим об’ємом 3,0 мл, що містила 50 мМ ФБ pH, 6.5, 0,25 мМ *о*-діанізидин, пероксидазу хрону (0,07 мг/мл), 0,05 % розчин глюкози та відповідну кількість ензиму. Інкубацію проводили 5-10 хв при 30 °С. Ензиматичну реакцію зупиняли додаванням 0,8 мл 12 М HCl. Утворений забарвлений продукт визначали спектрофотометрично при 525 нм. Мілімолярний

коефіцієнт екстинкції утвореного продукту в кислому розчині (2,5 М HCl) становить 13,38 $мМ^{-1} \cdot см^{-1}$. За одиницю активності ГО приймали кількість ензиму, що вивільняє 1 мкмоль H_2O_2 за 1 хв при 30 °С за стандартних умов аналізу.

2.5 Збагачення клітин ензимами, кон'югованими з золотими наночастинками.

2.5.1 Збагачення клітин дріжджів *O. polymorpha* NCYC 495 аргіназою I. До 0,09 мл біонаночастинок (із іммобілізованою аргіназою I) вносили 0,09 мл клітин *O. polymorpha* NCYC 495 (до кінцевої концентрації клітин 30 $мг \cdot мл^{-1}$ у 5 мМ ФБ, pH 7,5) та інкубували протягом ночі при температурі + 4 ºС. Як контроль використовували 0,18 мл суспензії клітин із наночастинками без ензиму (як контроль) (до концентрації клітин 30 $мг \cdot мл^{-1}$) та 0,18 мл клітин без наночастинок (до кін. концентрації клітин 30 $мг \cdot мл^{-1}$). Після ночі інкубації, клітини фугували при 270 g протягом 3 хв. Далі відбирали супернатант (це наночастинки, які не осіли). Осад клітин двічі промивали 5 мМ ФБ, pH 7,5. Промиті клітини ресуспендовували у 0,3 мл 5 мМ ФБ, pH 7,5 та аліквоту суспензії клітин (0,04 мл) відбирали на аналіз активності.

До клітин, які залишились (0,26 мл) вносили цетилтриметиламоній бромід (ЦТАБ) до кінцевої концентрації 2 $мг \cdot мл^{-1}$ та інкубували на водяній лазні при температурі +30 ºС, перемішуючи кожні 2-3 хв. упродовж 15 хв. Після процедури пермеабілізації, клітини центрифугували при 1700 g 15 хв., відбирали супернатант. Промивали ще раз 5 мМ ФБ, pH 7,5. Отриманий осад пермеабілізованих клітин ресуспендовували у 0,3 мл 5 мМ ФБ, pH 7,5 та відбирали на аналіз активності. Отримані клітини, збагачені відповідним ензимом, використано для формування біоселективної мембрани амперометричного сенсора.

2.5.2 Збагачення клітин дріжджів *O. polymorpha C-105* алкогольоксидазою. До осаджених біонаночастинок (АО-Au) вносили 0,18 мл суспензії клітин *O. polymorpha C-105* (з кінцевою концентрацією клітин 30 $мг \cdot мл^{-1}$ у 5 мМ ФБ, pH 7,5), суміш інкубували протягом ночі при температурі +4 ºС при постійному перемішуванні. Паралельно інкубували 180 мкл клітин і клітини із наночастинками

без ензиму – контроль. Після ночі інкубації, клітини центрифугували при 670 g протягом 3 хв. Осад клітин двічі промивали 5 мМ ФБ, pH 7,5. Промиті клітини ресуспендовували у 300 мкл 5 мМ ФБ, pH 7,5 та відбирали аліквоту суспензії клітин на аналіз активності АО. Для проведення пермеабілізації, до клітин, які залишились, вносили ЦТАБ до кінцевої концентрації 2 мг·мл$^{-1}$ та інкубували на водяній лазні при температурі +30º С, збовтуючи кожні 3-4 хв протягом 15 хв. Після процедури пермеабілізації, клітини центрифугували при 1700 g 10 хв та промивали ще двічі 5 мМ ФБ, pH 7,5. Отриманий осад пермеабілізованих клітин ресуспендовували у 300 мкл 5 мМ ФБ, pH 7,5.

2.6 Методи хімічного синтезу НЧ

2.6.1 Синтез металевих НЧ методом відновлення. Синтез НЗ та «мікрозимів» (Cd/Pd, Cu/Cd, Co/Cu, Cu/Au, Cu/Pt, Cu/Ag, Pt/Ag, Ag/Zn, Mn, Cu/Ce, Pd/Ce, Pd/Cu, Au, Pt/Au, Cu/Pd та ін.) проводили методом хімічного відновлення металів з розчину їхніх солей, за використання 1 мМ розчину аскорбінової кислоти або Натрій боргідриду. Деякі типи НЧ формували методом співосадження за використання натрій сульфіду (Cu/Ce^{S}, Zn(Hg)S, Cu/Zn(Hg)S, Mn/Cu(Zn)S, CuS). Усі експерименти проводили при кімнатній температурі. Отримали НЧ осаджували центрифугуванням при 16 000 об./хв упродовж 40 хв (центрифуга Hettich Micro-22R), двічі промивали водою і зберігали до використання при +4° С.

2.6.2 Синтез наночастинок методом відновленння на пластині. Синтез наноголок Cd/Zn здійснювали методом відновлення Cd^{2+} з водного розчину $CdCl_2$ на поверхні цинкової пластини. Для цього, попередньо очищену Zn пластину поміщали в реакційну суміш на 20 год., що приводило до прямого зростання наноголок Cd на підкладці Zn. Для одержання мікрозимів (МЗ) Zn/Cd/Cu, попередньо отримані, відмиті від компонентів реакційного середовища, наноголки Cd/Zn поміщали в 0,01 М водний розчин мідного купоросу. Реакційну суміш витримували при кімнатній температурі упродовж 2 днів при кімнатній

температурі. Отримані МЗ Zn/Cd/Cu кілька разів промивали водою та використовували для подальшої характеристики.

2.7 Методи «зеленого» синтезу НЧ

2.7.1 Біосинтез Au-НЧ позаклітинними метаболітами дріжджів *"in vitro"*. Для біосинтезу НЧ після досягнення фази експоненціального росту (біомаса 2,9 мг/мл), клітини дріжджів *NCYC 495 O. polymorpha* осаджували центрифугуванням при 3000 об./хв протягом 20 хв. Отриману надосадову рідину/культуральну рідина (КР) використовували в подальшому для синтезу біоНЧ *"in vitro*" [57]. КР інкубували з 0,5 – 1 мМ $HAuCl_4$ протягом 72 год при 30 ° С. Під час інкубації, контролювали колір суміші, а також розмір сформованих біоНЧ. Процес біовідновлення тетрахлораурат(III) аніона ($AuCl_4^-$) до Au^0 контролювали шляхом відбору проб розчину (2 мл) і вимірюванням його спектра поглинання за допомогою УФ-видимого спектрофотометра Shimadzu. Кожен експеримент мав свій контроль (КР клітин, вирощених без $HAuCl_4$) та проводився в трьох паралелях і повторювався щонайменше тричі.

2.7.2 Біосинтез біметалевих НЧ. Синтез біметалевих НЧ за типом ядро/оболонка проводили за наступною схемою: після досягнення фази експоненційного росту (біомаса 2,9 мг/мл), клітини дріжджів осаджували центрифугуванням при 3000 об./хв протягом 20 хв. Надосадову рідину інкубували з 1 мМ $HAuCl_4$ протягом 72 год при 30 °С. Перевіривши наявність утворених НЧ, додавали H_2PtCl_6, $CuSO_4$ або $PdCl_3$ залежно від мети експерименту для формування оболонки біметалевих НЧ та продовжували культивування протягом 2 діб. НЧ були виділені або шляхом ультрацентрифугування (в центрифузі типу Еппендорф 5424R при 21,130×g упродовж 1 год. при 18 °С) або фільтрацією, пропускаючи культуральну рідину через шприц, оснащений фільтром Minisart®, 0,45 мкм. Для одержаних НЧ було досліджено спектр поглинання у видимій та УФ ділянці спектра (на Shimadzu UV-1800 спектрофотометрі).

2.8 Методики досліджень розміру та структури НЧ

2.8.1 Фізико-хімічна характеристика розміру НЧ. Для морфологічного аналізу мікро/нанокомпозитів використовували сканувальний електронний мікроскоп СЕМ-мікроаналізатор РЕММА-102-02 (Суми, Україна) та FEI Nova NanoSEM 450 (Варшава, Польща). Зразки із концентрацією 0,05 мг·мл$^{-1}$ наносили крапельним методом на кремнієву підкладку товщиною 0,05 см, діаметром 0,5 см. Після висихання, зразки фіксували плівкою, що формувалася розчином Бутварної смоли B-98 (Sigma, St. Louis, MO, USA) у 1,5 % хлороформі за дії ультразвуку частотою 24 кГц. В експериментах відстань від останньої лінзи мікроскопа до зразка (WD) становила від 24,4 мм до 24,7 мм; використовували збільшення різної кратності – від х800; х200; х1200; х3000.

2.8.2 УФ-видима спектроскопія. Оптичні властивості синтезованих НЧ досліджували за використання спектрофотометра Shimadzu UV-1650 PC та стандартного програмного забезпечення “UVProbe 2.20”.

2.8.3 Атомно-силова мікроскопія. Розміри і структуру НЧ характеризували методом атомно-силової мікроскопії (АСМ) на мікроскопі Solver P47 – PRO, NT-MDT (Нідерланди). Для цього, аліквоту суспензії НЧ наносили на поверхню очищеної слюди та висушували на повітрі. Проби аналізували “точковим” методом з резонансною частотою 80 кГц, сканувальною швидкістю 1 Гц та роздільною здатністю 256×256 пікселів.

2.8.4 Флуоресцентна мікроскопія. Для візуалізації зразків використовували флуоресцентний мікроскоп (Axio Lab. A1., Carl Zeiss, Німеччина) з лампою збудження серії X-Cite 120Q та комплектом фільтрів: ізотіоціанат флуоресцеїну (FITC-фільтр), 4',6-діамідино-2-феніліндол (DAPI-фільтр), Техаський червоний (Texas red – фільтр) та азид 5-ціаніну (Cy5). Для приготування досліджуваного зразка, 10 мкл розчинів НЧ або клітин, попередньо розведених у воді, поміщали на предметне скло і покривали накривним склом діаметром 12 мм.

2.8.5. Трансмісійна електронна мікроскопія. Морфологічний аналіз НЧ та клітин проводили за використання трансмісійного електронного мікроскопа РЕМ-100 (Суми, Україна). Спеціальна плівка підкладки виготовлялась на мідній сітці (300 меш) за використання Бутварної смоли В-98 в 1,5 % хлороформі та дії ультразвуку при частоті 24 кГц. На поверхню підкладки крапельним шляхом наносили певний зразок.

2.8.6 Спектроскопія ядерного магнітного резонансу. Експерименти з ЯМР проводили на спектрометрі Bruker AVANCE II 300 МГц із зондом BBI 300 МГц W1 та контролером температури BVT-3000 (Варшава, Польща). Спектрометром керували через TOPSPIN 3.2. Для оброблення результатів використовували стандартну пульсову програму Bruker. Перед проведенням аналізу, зразок масою 150 мг розчиняли в 0,75 мл D_2O.

2.8.7 Спектроскопія комбінаційного розсіювання світла (Раман-спектроскопія). Для вимірювань картування гіперспектрального комбінаційного розсіяння використовувався мікроспектрометр Renishaw InVia (Варшава, Польща). Джерелом збудження був HeNe-лазер з довжиною хвилі 632,8 нм (Renishaw). Збудження та детектування сигналу проводили за допомогою об'єктива Leica ×100 з апертурою (NA) 0,85, що забезпечувало бічну роздільну здатність приблизно 1 мкм. Для детектування використовували камеру Renishaw EM-CCD (1024×256 пікселів) і дифракційну решітку 1200 ліній/мм, що дозволяло записувати спектри комбінаційного розсіювання світла з роздільною здатністю 6 $см^{-1}$.

Для проведення аналізу, розчини зразків капали на очищені покривні скельця мікроскопа та залишали висихати при кімнатній температурі. Для кожного зразка були зроблені гіперспектральні Раманівські растрові карти, що складалися приблизно з 150 точок кожна, вимірюючи прямокутні області з кроком 10 мкм. Потужність лазера на зразку підтримувалася на рівні 1 мВт, а час накопичення однієї точки становив 20–60 с (залежно від зразка). За допомогою програмного забезпечення Wire 5.5 (Renishaw) піки космічного випромінювання були видалені з

карт. Потім з кожної карти створювався середній спектр шляхом обчислення середнього всіх одноточкових спектрів. Рідкі зразки аналізували в 10 мм кварцових кюветах (Hellma) за допомогою насадки для макрозразків Renishaw. Спектри Раман спектроскопії та SERS отримані з використанням об'єктива з фокусною відстанню 15 мм (Renishaw) і потужності лазера 1 мВт на зразок. Для кожного зразка записано 360 послідовних спектрів із часом збору даних 100 секунд, що полегшує виключення потенційного фоторозкладання під час процесу вимірювання.

2.8.8 Квантово-хімічне моделювання. Оптимізацію молекулярної геометрії було виконано згідно з теорією функціоналу густини (DFT) з використанням гібридного функціоналу Пердева, Берка та Ернцергофа (PBE0) та базисного набору def2-TZVPPD, використовуючи програмне забезпечення для квантової хімії Orca 5.0.4. пакет. У розрахунках використовувалась поправка попарної дисперсії (D4) [58]. Для моделювання впливу металевих наночастинок на спектри комбінаційного розсіювання застосовували спрощені двоатомні та десятиатомні кластери міді. Спектри раманівської активності створено з припущенням про 5 $см^{-1}$ смуг Лоренца. Коефіцієнти масштабування не використовували.

2.8.9 Дослідження площі та пористості НЧ. Площу поверхні та пористість НЧ вимірювали за допомогою автоматичного аналізатора ASAP 2020 (Micromeritics Instrument Corp., США), використовуючи азот у ролі адсорбату. Перед вимірюванням адсорбції при температурі рідкого азоту (77 К) зразок дегазували при 473 К протягом 4 год. у вакуумній камері для очищення його поверхні. Питома поверхня НЧ, їхній об'єм і розмір пор розраховували методами БЕТ, Барретта–Джойнера–Халенда та Хорват-Кавазої. Питома поверхня НЧ була визначена додатковими вимірюваннями БЕТ з використанням криптону в ролі адсорбату при 473 К.

2.8.10 Дослідження НЧ за допомогою динамічного світлорозсіювання. Для характеристики розміру НЧ вимірювання динамічного світлорозсіювання (DLS) та дзета-потенціалу використовували прилад Litesizer™ 500 (Любляна, Словенія). Вимірювання DLS проводили в кварцевій кюветі при температурі 25 °C і з кутом розсіювання 90°. Для цього, розчин НЗ попередньо розводили 0,1 мМ фосфатним буфером до концентрації 0,05 мг/мл в кюветі. Фокусування автоматично підбиралося програмою. Кожен вимір повторювали тричі.

2.8.11 Рентгеноструктурний аналіз НЧ. Розміри синтезованих НЧ досліджували методом рентгено-структурного аналізу на дифрактометрі ДРОН-3. Спектр дифракції рентгенівських променів досліджували в області 10 – 100°. Середній розмір кристалітів (D) визначали по розширенню найбільш інтенсивної і окремо розміщеної лінії (111) за методикою для полікристалічних твердих тіл [59].

2.9 Методи аналізу псевдоензиматичної активності НЧ

2.9.1 Визначення пероксидазо-подібної активності НЧ в розчині за використання *о*-діанізидину. Питому активність НЧ виражали в мкмоль продукту утвореного за 1 хв в перерахунку на 1 мг НЗ за стандартних умов реакції (1 Од./мг; мкмоль·хв$^{-1}$·мг$^{-1}$). У пробірки розливали по 1 мл реакційної суміші. У дослідні проби вносили по 0,01 мл розведених препаратів НЗ - крім сліпої проби, у яку вносили 0,01 мл 50 мМ ацетатного буфера, pH 4,5. Реакцію запускали додаванням 0,01 мл 0,88 М H_2O_2. Реакцію зупиняли у точно фіксований час 0,8 мл концентрованої соляної кислоти. Вимірювання оптичної густини дослідних проб проводили при довжині хвилі 525 нм у 1 см–кварцевих кюветах об’ємом 4 мл проти сліпої проби.

2.9.2 Визначення пероксидазо-подібної активності НЧ в розчині за використання ТМБ. Визначення пероксидазної активності НЧ проводили у 50 мМ ацетатному буфері, pH 4,5, що містив 8,8 мМ H_2O_2 та 1 мМ ТМБ, в кінцевому об'ємі 1 мл. У реакційну суміш вносили тестований зразок і аналізували

колориметричним методом утворений продукт реакції при 650 нм на спектрофотометрі SHIMADZU UV-1650 PC з використанням програмного забезпечення "UVProbe 2.20", приймаючи для окисненого ТМБ коефіцієнт мілімолярної екстинкції ε =39 $мМ^{-1}\cdot см^{-1}$. За одиницю активності (Од.) приймали таку кількість ензимоподібних НЧ, яка забезпечує утворення 1 мкмоль забарвленого продукту за 1 хв. за описаних вище умов (1 Од. = 1 мкмоль/хв.).

2.9.3 Визначення пероксидазо-подібної активності НЧ в розчині за використання АБТС. Визначення пероксидазної активності НЧ проводили у 50 мМ ацетатному буфері, pH 4,5, що містив 8,8 мМ H_2O_2 та 1 мМ АБТС, в кінцевому об'ємі 1 мл. У реакційну суміш вносили тестований зразок і аналізували колориметричним методом утворений продукт реакції при 650 нм на спектрофотометрі SHIMADZU UV-1650 PC з використанням програмного забезпечення "UVProbe 2.20", приймаючи для окисненого АБТС коефіцієнт мілімолярної екстинкції ε =36 $мМ^{-1}\cdot см^{-1}$. За одиницю активності (Од.) приймали таку кількість ензимоподібних НЧ, яка забезпечує утворення 1 мкмоль забарвленого продукту за 1 хв за описаних вище умов (1 Од. = 1 мкмоль/хв).

2.9.4 Визначення редуктазної активності НЧ в розчині за використання катіон-радикалу АБТС$^{+}$. АБТС розчиняли у воді до концентрації 7 мМ. Катіон-радикал ($АБТС^{+\cdot}$) формували шляхом змішування попередньо виготовленого 7 мМ водного розчину АБТС із 2,45 мМ свіжоприготовленим розчином амоній персульфату у співвідношенні 1:0,5. Отриману суміш витримували в темноті упродовж 15 год. при температурі 20 ^{0}C. Перед початком аналізу, суміш розводили 96 % етанолом до досягнення оптичної густини 0,700 ± 0,020 при 734 нм. Коефіцієнт мілімолярної екстинкції катіон-радикалу $АБТС^{+\cdot}$ приймали рівним 17 $мМ^{-1}\cdot см^{-1}$. Редуктазну активність НЧ визначали після змішування 1 мл реакційної суміші із 10 мкл зразків НЧ упродовж 2 хв.

2.9.5 Визначення глутатіонредуктазної активності НЧ в розчині. Глутатіонредуктаза – ензим, який каталізує відновлення окисненого глутатіону у присутності кофактору NADPH. Метод базується на зміні величини оптичної абсорбції розчину при утворенні окисненої форми $NADPH^{+}$. Дослідна проба містила 2,5 мл 0,15 мМ ФБ, pH 7,5, 1 мМ ЕДТА, 10 мкл розчину НЧ, 0,1 мл 1,2 мМ розчину NADPH. Контрольний розчин містив усі компоненти, що й дослідна проба, за винятком НЧ. Перед початком вимірювання, в кювету з дослідною пробою вносили 0,2 мл 7,5 мМ розчину окисненого глутатіону, перемішували і вимірювали зміну величини оптичної густини при 340 нм через 15 сек протягом 1 хв. В контрольну пробу вносили 0,2 мл 0,15 мМ ФБ, pH 7,5. Коефіцієнт мілімолярної екстинкції NADPH при 340 нм приймали рівним 6,2 $мМ^{-1}\cdot см^{-1}$.

2.9.6 Визначення глутатіонпероксидазної активності НЧ в розчині. Швидкість реакції, яка каталізується НЧ із глутатіонпероксидазною активністю, оцінювали спектрофотометрично за зменшенням величини оптичної густини при довжині хвилі 340 нм. За одиницю активності приймали кількість НЗ, які каталізують перетворення 1 мкмоль субстрату за 1 хв. при 25°С. Реакційна суміш для визначення псевдо-глутатіонпероксидазної активності була наступного складу: 50 мМ калій-фосфатний буфер (pH 7,5), що містив 1 мМ ЕДТА, 0,12 мМ NADPH, 0,85 мМ відновлений глутатіон, 0,37 мМ H_2O_2, 10 мкл розчину НЧ. В контрольній пробі був відсутній глутатіон відновлений.

2.9.7 Визначення каталазо-подібної активності НЧ в розчині. У дослідну і контрольну проби додавали по 2 мл 0,03 % розчину Гідроген пероксиду у воді, потім в дослідну – 0,01 мл НЧ, в контрольну – 0,01 мл дистильованої води. Проби витримували при кімнатній температурі 10 хв., після чого в кожну пробу додавали по 1 мл 4 % розчину молібдату амонію і вимірювали світлопоглинання при λ=410 нм. Каталазну активність розраховували за зменшенням оптичної густини, що характеризує зниження концентрації комплексу Гідроген пероксиду з молібдатом

внаслідок розкладу H_2O_2. Коефіцієнт мілімолярної екстинкції комплексу пероксиду з молібдатом приймали рівним 22,2 $мМ^{-1}·см^{-1}$.

2.9.8 Визначення антиоксидантної активності за використання радикалу 2,2-дифеніл-1-пікрилгідразилу (ДППГ). Антиоксидантну активність НЗ та деяких харчових продуктів визначали за допомогою стабільного радикалу $DPPH^{\cdot}$. Як стандарт використовували Тролокс. Для проведення аналізу, 0,04 мл НЗ або Тролоксу з концентраціями: 0,31, 0,62, 1,25, 2,5 і 5 мг/мл змішували з 1,2 мл 1 мМ свіжовиготовленого розчину 2,2-дифеніл-1-пікрилгідразилу (ДППГ) у метанолі і ретельно перемішували. Проби інкубували при кімнатній температурі на темноті упродовж 30 хв. Зміну оптичної густини реєстрували при 517 нм за допомогою спектрофотометра UV-Vis (Shimadzu, U-1860). Як контроль, використовували ДППГ робочий розчин (без додавання зразка), а метанол – як «сліпий» розчин. Здатність до нейтралізації вільних радикалів визначали за формулою:

Антиоксидантна активність = $(OD_к – OD_п)/OD_к*100\%$

де $OD_к$ – оптична густина контролю (робочий реагент ДППГ без додавання досліджуваного зразка), тоді як $OD_п$ – оптична густина тестованого або стандартного (Тролокс) зразка.

2.9.9 Визначення константи Міхаеліса-Ментен ($К_м$) НЗ та константи швидкості реакції k_{cat} стостовно H_2O_2. Кінетичні параметри K_M і V_{max} (в одиницях мМ і $мМ·хв^{-1}$, відповідно) визначали експериментально за залежністю швидкості реакції V від концентрації субстрату S. Для цього, при постійній концентрації органічного субстрату 0,017 мМ і при різних концентраціях H_2O_2 в інкубаційній суміші визначали значення швидкості реакції V_i. Розраховували обернені величини $1/S_i$ і $1/V_i$. На основі отриманих даних будували графік функції $1/V_i = f\ (1/\ S_i)$ і графічно розраховували величини K_M і V_{max} та статистичні параметри для них. Величини k_{cat} розраховували за формулою: $k_{cat} = V_{max}/C_{нз}$, де $C_{нз}$ – це концентрація НЗ в інкубаційній пробі, мг/мл. Оскільки практично неможливо визначити

концентрацію НЗ в мМ одиницях, а тільки в масових одиницях (мг/мл), розмірність k_{cat} виражена в $с^{-1}$·мкмоль·$мг^{-1}$.

2.9.10 Визначення субстратної специфічності. Для реакцій НЗ та мікрозимів (МЗ) досліджували субстратну специфічність у двосубстратній реакції у присутності Гідроген пероксиду і різних органічних субстратів, зокрема, АБТС, гваяколу, *о*-діанізидину, 4-аміноантипірину (ААП) та ТМВ. Для дослідження активності НЗ в розчині, препарати НЗ або мікрозимів із H_2O_2 і досліджуваним органічним субстратом, інкубували фіксований час в 50 мМ ацетатному буфері та визначали активність відповідно до пп. 2.9 «Методи аналізу псевдоензиматичної активності НЧ».

2.10 Конструювання та дослідження функціональних властивостей біосенсорів.

Амперометричні біосенсори конструювали на базі амперометричного потенціостату Metrohm Autolab PGSTAT30 за використання трьохелектродної сенсорної конфігурації: хлорсрібний електрод (Ag/AgCl/3 M KCl) – як електрод порівняння, як допоміжний – стержневий платиновий електрод (діаметр 1 мм). Як робочі електроди використовували комерційний платиновий електрод (діаметром 7,0 мм), дисковий скловугільний електрод (Mineral, діаметром 1,5 та 3,0 мм) та графітовий електрод (діаметром 3,03 мм).

Перед приготуванням біоелектродів, платиновий та скловугільний електроди полірували на полірувальній тканині, використовуючи алюміній оксидну пасту (Leco, ФРН) з різним діаметром частинок (1,0; 0,5 та 0,3 мм). Відполіровані електроди відмивали водою та протирали 96 % етиловим спиртом. Робочу поверхню графітових електродів полірували на наждачному папері та відмивали водою в ультразвуковій лазні 10-15 хв.

Усі амперометричні вимірювання проводили при кімнатній температурі в скляній комірці об’ємом 50 мл, заповненій 10 мл фосфатним буфером (ФБ), з

значенням pH залежно від мети експерименту. Біосенсор поміщали в розчин з інтенсивним перемішуванням і, після встановлення базового сигналу, в комірку вносили певний аналіт.

Для забезпечення іммобілізації біоелемента (ензимів, біонанокомпозитів та пермеабілізованих клітин рекомбінантних штамів *O. polymorpha*) на поверхні робочих електродів використовували різні процедури та методи:

1) Утримання діалізною плівкою: 2-4 мкл ензиму або 2 мкл суспензії пермеабілізованих клітин *O. polymorpha* (50 мг·мл$^{-1}$) наносили крапельним методом порціями по 2 мкл на поверхню електрода і залишали підсихати при 4 ^{0}C протягом 10 хв. Потім, електрод покривали стандартною діалізною мембраною (1х1 см^{2}). Для утримання діалізної мембрани використовували «О»-кільце діаметром 5 мм (для торцевих графітових електродів) або плівку скотчу (у випадку використання планарних електродів). Перед використанням електроди промивали буфером із відповідним pH (в залежності, від pH оптимуму ензиму).

2) Осадження катодним полімером: 2-4 мкл ензиму або клітин (з активністю 19-22 Од.·мл$^{-1}$) наносили крапельним методом на поверхню робочого електрода та підсушували при кімнатній температурі упродовж 5 хв. Поверх сформованої біоплівки, наносили 8 мкл розведеного в 10 разів катодного полімеру (GY 83-0270 005). При цьому відбувалась осадження полімеру і формувалась міцна полімерна плівка, що утримувала біоелемент. Електроди промивали 20 мМ ФБ буфером із відповідним pH та зберігали при +4 ºС до їхнього використання.

3) Покриття плівкою 1 % Нафіону: 2-4 мкл ензиму або клітин (з активністю 19–22 Од.·мл$^{-1}$) наносили крапельним методом на поверхню обочого електрода та підсушували при кімнатній температурі протягом 5 хв. Поверх сформованої біоплівки, наносили 8 мкл 1% Нафіону. При цьому формувалась міцна полімерна плівка, що утримувала біоелемент. Електроди промивали 20 мМ ФБ буфером із відповідним pH та зберігали при +4 ºС до їхнього використання.

4) «Перехресне зшивання» ензимів та нанозимів на поверхні електрода: для формування біоелектроду, 2 мкл суспензії НЧ (0,1 мг·мл$^{-1}$) наносили крапельним методом на поверхню електрода та підсушували при кімнатній температурі

протягом 5 хв. Далі, аліквоту суміші, що містила цистеамін (1 мМ) і глутаровий альдегід (1%), поміщали на поверхню електроду і висушили на повітрі. Нарешті, активовані НЧ промивали 50 мМ фосфатним буфером, pH 7,0 і використовували для подальшого іммобілізації ензимів методом перехресного зшивання.

5) Ковалентна кон'югація ензимів: 2 мкл суспензії НЧ (0,1 мг·мл$^{-1}$) наносили крапельним методом на поверхню електрода та підсушували при кімнатній температурі протягом 5 хв. Далі, на поверхню робочого електроду вносили 5 мкл 5 мМ ω-меркаптогексадеканої кислоти. Електрод витримували упродовж 1 год при кімнатній температурі та вносили 5 мкл суміші, що містила 2 мМ 1-етил-3-(3-диметиламінопропіл)карбодімід (ЕДК) та 5 мМ N-гідроксисукцинімід (ГСІ) в етанолі. Електрод витримували при +8 ˚С упродовж 12 год. Далі поверхню електроду промивали 20 мМ ацетатним буфером, pH 5,5 (для відмивання надлишку реагентів) та вносили 3 мкл відповідного ензиму. Після підсихання електроду проводили подальші електрохімічні дослідження.

2.11. Підготовка реальних зразків до аналізу.

Для одержання сироватки крові, 5 мл венозної крові поміщали у центрифужну пробірку та центрифугували протягом 10 хв. при 3000 об./хв. Фугат переносили в іншу центрифужну пробірку та центрифугували додатково протягом 10 хвилин при 10000 об./хв. Одержану сироватку фіксованого об'єму (наприклад 0,9 мл) депротеїнізували додаванням 50 % розчину трихлороцтової кислоти до кінцевої концентрації 5 % (0,1 мл). Утворену суспензію перемішували, витримували 30 хв. при 0°С та знову центрифугували упродовж 10 хв. при 10000 об./хв. Для аналізу використовували безбілкову надосадову рідину (БНР). Одержану БНР зберігали до початку аналізу при +4 °С. У разі, якщо аналізована проба не досліджувалась протягом 24 год., її зберігали при –20°С. Перед початком аналізу спочатку підлужнювали розчин БНР до pH 6, додаючи 1,5 М NaOH, потім аліквоту ензиму (аргіназу, уреазу або КДІ) та інкубували упродовж 20 хв. при кімнатній температурі.

Визначення вмісту етанолу та L-аргініну у зразках харчових напоїв (на прикладі соків та вин) проводили після попереднього центрифугування зразків протягом 15 хв. при 10000 об./хв. на лабораторній центрифузі (центрифуга Hettich Micro-22R). Готові розчини зберігали не більше доби. Визначення вмісту проводили безпосередньо після розпакування зразка.

2.12 Статистичний аналіз експериментальних даних

Досліди проводились у чотирьох-шести повторах. Для кожної вибірки показників визначали середнє арифметичне значення (M), стандартну похибку середнього (m) та середнє арифметичне відхилення (σ). Для розроблених аналітичних методів розраховували коефіцієнт варіації (C_v, %). Розрахунок статистичних показників і побудову графіків проводили за допомогою програми OriginPro 8,5. Лінеаризацію графіків проводили за рівнянням регресії $Y= A + B \cdot X$ (A і B – параметри рівняння), розраховували коефіцієнт кореляції R та рівень достовірності зв’язку *p* (для події R = 0). Вказані параметри та статистичні показники наведені в рисунках та таблицях відповідних статей.

РОЗДІЛ 3
СКРИНІНГ НОВИХ НАНОМАТЕРІАЛІВ НА ПСЕВДОЕНЗИМАТИЧНУ АКТИВНІСТЬ ТА ДОСЛІДЖЕННЯ СТРУКТУРНИХ І КАТАЛІТИЧНИХ ВЛАСТИВОСТЕЙ ОТРИМАНИХ НАНОЗИМІВ

В розділі ІІІ представлено основні етапи синтезу нових нанозимів (НЗ), поєднуючи хімічне відновлення неорганічних солей перехідних або шляхетних металів аскорбіновою кислотою з новим методом осадження НЗ на металеві пластинки. У даному розділі описано також метод «зеленого» синтезу біонаночастинок за використання клітин термотолерантних дріжджів *Ogataea polymorpha* та досліджено процеси редукції неорганічних солей дріжджовою культурою і формування позаклітинних стабільних біонаночастинок. Здійснено структурну характеристику усіх отриманих наноматеріалів за використання методів сканувальної електронної, флуоресцентної, атомно-силової мікроскопії; методу динамічного світлорозсіювання, рентгено-спектрального та рентгеноструктурного аналізу. Встановлено, що розмір отриманих матеріалів знаходиться в межах від 10 нм (НЗ) до 15 мкм (мікрозими, МЗ).

Аналіз синтезованих наноматеріалів на псевдоензиматичну активність (пероксидазну, каталазну, глутатіонпероксидазну, селенітредуктазну та глутатіонредуктазну) показав, що серед отриманих 50 різних за хімічним складом НЧ, 12 володіють високою пероксидазною (7 – 10,6 Од./мг), 2 – редуктазною (14,3 – 32,7 Од./мг), 2 – каталазною (0,2 – 0,3 Од./мг), по одному типу – глутатіонпероксидазною (0,14 Од./мг) та глутатіонредуктазною (0,61 Од./мг) активностями.

Проведено ковалентну модифікацію металевих НЗ, що місять Аурум, поєднанням цистеаміну, глутарового альдегіду та поліетиленіміну. Показано, що функціоналізація НЗ полімерними носіями дозволяє модулювати каталітичні параметри НЗ, дещо змінювати субстратну специфічність та підвищувати їхню стабільність.

Досліджено каталітичні властивості та субстратну специфічність усіх отриманих НЗ. Встановлено, що найвищою пероксидазною активністю серед синтезованих НЗ володіють CuCeAu та Cu. Визначено кінетичні параметри ($К_М$ і k_{cat}) для отриманих "голих" НЗ і МЗ та їх модифікованих полімерами форм. У пероксидазних реакціях, більшість синтезованих НЗ, зокрема, CuCeAu, Cu, PtCu та PdCe виявляють найвищу активність стосовно *о*-діанізидину.

Проведено скринінг монометалевих (Cd, Ce), біметалевих (CCu, CePd, PtCu, CeCu, PdCd, PdCu) та триметалевих (CuCdZn) наночастинок (НЧ) на редуктазну активність. Встановлено, що найвищу редуктазну, зокрема, селенітредуктазну активність, виявляють НЗ складу CuCdZn та CeCu. Отримані НЗ CuCdZn протестовано на антиоксидантну активність відносно вільних радикалів АБТС$^{\bullet+}$ та DPPH$^{\bullet}$ у порівнянні із Тролоксом: значення напівмаксимального інгібування (IC_{50}) для НЗ Cu/Cd/Zn^{пл} становить 6,8 ± 0,2 мкг/мл, що близько до Тролоксу (2,70 ± 0,1 мкг/мл). Синтезовані НЗ із редуктазною активністю використано для конструювання амперометричного біосенсора для аналізу селеніту. Сконструйований біосенсор характеризується високою чутливістю (1700 $А \cdot М^{-1} \cdot м^{-2}$) та широким лінійним діапазоном (від 16 мкМ до 1 мМ). Сконструйований амперометричний сенсор протестовано на реальних зразках мінеральної води із підвищеним вмістом селену.

3.1. Синтез та структурно-морфологічна характеристика металевих наночастинок із оксидоредуктазною активністю.

Анотація: *Нанозими (НЗ) — це наноструктуровані штучні ензими, які імітують каталітичні властивості природних ензимів. НЗ виявляють суттєві переваги порівняно із природними ензимами, а саме, завдяки їхній низькій вартості приготування, хорошій стабільності, великій площі поверхні, достатній активності, що залежить від розміру та складу, широкій можливості для модифікації та біосумісності. НЗ виявляють широкий потенціал практичного застосування в ролі каталізаторів у біосенсориці, технології паливних елементів, екологічній біотехнології та медицині. Більшість відомих НЗ є міметиками оксидоредуктаз або гідролаз. У цій роботі ми демонструємо сучасні підходи щодо одержання ефективних штучних пероксидазоподібних (ПО)-подібних НЗ (наноПО), наводимо їх характеристику та оцінку перспектив аналітичного застосування. НаноПО синтезовано з використанням низки НЧ перехідних і шляхетних металів і протестовано їхню каталітичну активність у розчині та на електродах. Найефективніші наноПО відібрано для детальної характеристики їхньої каталітичної активності. Визначено кінетичні параметри, розмір і структуру найкращих наноПО (Cu/Ce^S). Сенсор на основі Cu/Ce^S для визначення вмісту H_2O_2 показав високу чутливість (1890 $А{\cdot}М^{-1}{\cdot}м^{-2}$), широкий лінійний діапазон (1,5 – 20 000 мкМ) і високий струмовий відклик (786 мкА) після додавання H_2O_2. Показано можливість подальшого застосування Cu/Ce^S-НЗ в ролі селективного шару амперометричних сенсорів для аналізу Гідроген пероксиду у зразках комерційних дезінфікуючих засобів.*

applied sciences

MDPI

Article

Peroxidase-Like Metal-Based Nanozymes: Synthesis, Catalytic Properties, and Analytical Application

Olha Demkiv [1,2], Nataliya Stasyuk [1], Roman Serkiz [1], Galina Gayda [1,*], Marina Nisnevitch [3,*] and Mykhailo Gonchar [1,4]

[1] Institute of Cell Biology, National Academy of Sciences of Ukraine, 79005 Lviv, Ukraine; demkivo@nas.gov.ua (O.D.); stasukne@nas.gov.ua (N.S.); rserkiz@gmail.com (R.S.); gonchar@cellbiol.lviv.ua (M.G.)

[2] Faculty of Veterinary Hygiene, Ecology and Law, Stepan Gzhytskyi National University of Veterinary Medicine and Biotechnologies, 79000 Lviv, Ukraine

[3] Department of Chemical Engineering, Ariel University, Kyriat-ha-Mada, Ariel 4070000, Israel

[4] Department of Biology and Chemistry, Drohobych Ivan Franko State Pedagogical University, 82100 Drohobych, Ukraine

* Correspondence: galina.gayda@gmail.com or galina.gayda@nas.gov.ua (G.G.); marinan@ariel.ac.il (M.N.); Tel.: +380-226-2144 (G.G.); +972-3914-3042 (M.N.)

Abstract: Nanozymes (NZs) are nanostructured artificial enzymes that mimic catalytic properties of natural enzymes. The NZs have essential advantages over natural enzymes, namely low preparation costs, stability, high surface area, self-assembling capability, size and composition-dependent activities, broad possibility for modification, and biocompatibility. NZs have wide potential practical applications as catalysts in biosensorics, fuel-cell technology, environmental biotechnology, and medicine. Most known NZs are mimetics of oxidoreductases or hydrolases. The present work aimed to obtain effective artificial peroxidase (PO)-like NZs (nanoPOs), to characterize them, and to estimate the prospects of their analytical application. NanoPOs were synthesized using a number of nanoparticles (NPs) of transition and noble metals and were screened for their catalytic activity in solution and on electrodes. The most effective nanoPOs were chosen as NZs and characterized by their catalytic activity. Kinetic parameters, size, and structure of the best nanoPOs (Cu/Ce^S) were determined. Cu/Ce^S-based sensor for H_2O_2 determination showed high sensitivity (1890 $A \cdot M^{-1} \cdot m^{-2}$) and broad linear range (1.5–20,000 μM). The possibility to apply Cu/Ce^S-NZ as a selective layer in an amperometric sensor for hydrogen-peroxide analysis of commercial disinfectant samples was demonstrated.

Keywords: nanozyme; nano-peroxidase; synthesis; catalytic properties; amperometric sensors; hydrogen peroxide; disinfectant analysis

check for updates

Citation: Demkiv, O.; Stasyuk, N.; Serkiz, R.; Gayda, G.; Nisnevitch, M.; Gonchar, M. Peroxidase-Like Metal-Based Nanozymes: Synthesis, Catalytic Properties, and Analytical Application. *Appl. Sci.* **2021**, *11*, 777. https://doi.org/10.3390/app11020777

Received: 2 December 2020
Accepted: 13 January 2021
Published: 15 January 2021

Publisher's Note: MDPI stays neutral with regard to jurisdictional claims in published maps and institutional affiliations.

Copyright: © 2021 by the authors. Licensee MDPI, Basel, Switzerland. This article is an open access article distributed under the terms and conditions of the Creative Commons Attribution (CC BY) license (https://creativecommons.org/licenses/by/4.0/).

1. Introduction

Peroxidase (PO; E.C. 1.11.1.7) is the oxidoreductase that catalyzes oxidation of organic substrates in the presence of hydrogen peroxide (H_2O_2) as an electron acceptor. The most popular chromogenic substrates for PO are 3,3′,5,5′-tetramethylbenzidine (TMB), 2,2′-azinobis [3-ethylbenzothiazoline-6-sulfonic acid] (ABTS), and *o*-phenylenediamine (OPD). In the active site PO contains heme, an iron-porphyrin derivative [1]. The PO-mediated catalytic process occurs via a peroxidative cycle. During the PO-induced substrate oxidation in the presence of H_2O_2, the central iron is switched between the ferric(III) and intermediate ferryl(IV) states. The latter intermediate compound exhibits extremely high oxidative activity [2,3].

PO is widely used in different fields of science and industry, especially in analytics for H_2O_2 determination [1]. Many natural enzymes (oxidases) produce H_2O_2 as a byproduct of their enzymatic reactions, so that detection of the target substrates can be performed by

measuring the generation of H_2O_2. This principle is widely used in oxidase/peroxidase-based biosensors [4,5]. To determine H_2O_2, PO-catalyzed decomposition of H_2O_2 may be detected with optical biosensors (in the presence of chromogenic substrates) or with amperometric biosensors. The wide practical application of natural PO is still limited, however, due to the high cost of the enzyme and fast enzyme inactivation in the presence of H_2O_2.

Artificial enzymes having PO activity, especially PO-like nanozymes (NZs) or "nanoperoxidases" (nanoPOs), are promising substitutes for natural PO, especially in biosensors [5–11]. Detailed information about NZs, including their definition, history, classification, advantages over natural enzymes, methods of obtaining them, and prospects for practical use, can be found in our recent review [12].

The catalytic properties of NZs strongly depend on the method of synthesis [12–14], chemical structure, particle size, shape, and surface morphology, which can be affected by electrical charge, coating type, doping, loading, and external fields [14–27]. The catalytic performance and efficiency of NZs are usually characterized by kinetic parameters (K_M, V_{max}, k_{cat}, k_{cat}/K_M ratio, IC_{50}) and morphological characteristics [7]. In most cases, the catalytic efficiency of NZs is lower compared to natural analogues, but some NZs can compete with natural enzymes [5–7,19].

Nanoperoxidases can be prepared in different ways, such as sol–gel, hydrothermal and solvothermal methods, electrodeposition, chemical reduction, green synthesis, pyrolysis, polymerization, polycondensation, coprecipitation, laser dewetting, and others [7,12]. For ultrafast preparation of NZs containing metal oxides of transition metals, such as $ZnCo_2O_4$, $NiCo_2O_4$, $MnCo_2O_4$, $NiMn_2O_4$, $CoCu_2O_4$, and Co_3O_4, a new synthetic method was proposed using basic deep eutectic solvents. In this method, the designed solvents act simultaneously as a solvent, a shape-control agent and a reactant [28].

Each method of NZ synthesis has advantages and drawbacks [7,12,13]. The chemical reduction method is the most popular due to its rapidity and simplicity. The morphology and particle-size distribution of the chemically synthesized NZs may be controlled by changing molar concentration of compounds, the type of reductant, and the temperature of the reaction [29]. The faster the synthetic process is carried out, the smaller the sizes of obtained NZs, and vice versa [30]. To obtain NZs of higher purity and stronger stoichiometric control, the coprecipitation method must be chosen [31].

A number of new low-cost PO-like NZs having high catalytic activity have been described and used for the development of effective H_2O_2-sensitive sensors [32–35]. These sensors may serve as prospective platforms in the construction of different oxidase-based biosensors for quantitative detection of different biomarkers. Biosensors with PO-like NZs can be applied in clinical diagnostics, theranostics, therapy control, and cell/tissue growth and proliferation [35–40].

In our previous studies, we demonstrated the possibility of developing reagentless amperometric biosensors using PO-like NZs. The NZs were synthesized by different methods, including electrodeposition, chemical synthesis, and green synthesis [41,42]. The most effective PO-like NZs, PtRu and hexacyanoferrate (HCF) of copper (CuHCF), were shown to be promising catalysts in amperometric (bio)sensors. When immobilized on graphite electrodes (GEs), PtRu and CuHCF were used for H_2O_2 analysis of a sample of commercial disinfectant, and for construction of oxidase-based amperometric biosensors for the determination of ethanol, methyl amine [41], and glucose [42].

Nanozymes having high mimic enzyme activities are very prospective for analytical purposes, particularly, for clinic diagnosis [6,12,13]. Most commercial diagnostic kits and biosensors use natural enzymes selective for metabolites, e.g., different oxidases and peroxidase. The latter enzyme is especially important for ELISA tests, which are very often used in clinic, food control, and sport medicine [1–5]. For this reason, synthesis of new materials capable to mimic peroxidase activity is a very important challenge for modern nanotechnology.

The aim of this work was to obtain effective NZs having PO-like activity, to characterize these nanoperoxidase NZs (nanoPOs), and to estimate the prospects of their analytical application.

The novelty of the current research is a synthesis of a broad row of hybrid metal nanoparticles (NPs) containing transition and noble metals, and a comparative study of their catalytic activity when immobilized on electrodes as well as in a solution. The latter issue is almost not related to in literature. Kinetic parameters, size, and structure of the most effective nanoPOs were determined. The Cu/Ce-based sensor for H_2O_2 determination showed the highest sensitivity (1890 $A \cdot M^{-1} \cdot m^{-2}$), a broad linear range (1.5–20,000 μM), and a high current response (786 μA) upon H_2O_2 addition. The possibility to apply Cu/Ce^S-NZ as a selective layer in an amperometric sensor for hydrogen peroxide analysis in commercial disinfectant samples was demonstrated.

2. Materials and Methods

2.1. Reagents

Ascorbic acid, $Ce(HCO_3)_4$, $AgNO_3$, chloroplatinic acid (H_2PtCl_6), $HAuCl_4$, copper(II) sulfate ($CuSO_4$), zinc(II) sulfate ($ZnSO_4$), *o*-dianisidine, hydrogen peroxide (H_2O_2, 30%), iron(III) chloride ($FeCl_3 \times 4H_2O$), palladium chloride ($PdCl_3$), sodium borohydride ($NaBH_4$), Nafion (5% solution in 90% low-chain aliphatic alcohols), and all other reagents and solvents used in this work were purchased from Sigma-Aldrich (Steinheim, Germany). All reagents were of analytical grade and were used without further purification. All solutions were prepared using ultrapure water obtained with the Milli-Q® IQ 7000 Water Purification system (Merck KGaA, Darmstadt, Germany).

2.2. Synthesis of NPs

NPs were synthesized by the reduction of metal ions from appropriate salts, according to the methods used in our modifications [41–44]. The conditions of NP synthesis are presented in Table 1. NPs were collected by centrifugation under 10,000× *g* for 40 min (Hettich Micro-22R centrifuge), washed twice with water, and precipitated by centrifugation. Pellets were suspended in 0.2 mL of water and stored until use at +4 °C.

Table 1. Methods of chemical synthesis of nanoparticles.

No	NPs	Reaction Mixture and Conditions
1	Fe/Ce^S	2 mL 50 mM $FeCl_3$ + 2 mL 15 mM $Ce(HCO_3)_4$, light stirring for 5 min at 20 °C followed by adding 0.5 mL 10 mM Na_2S; stirring for 1 min; incubation without stirring for 24 h at 20 °C.
2	Cu/Ce^S	1 mL 0.01 mM $Ce(HCO_3)_4$ + 1 mL 10 mM sodium borohydride, vigorous stirring for 5 min followed by adding 2 mL 20 mM $CuSO_4$; incubation without stirring for 1 h at 20 °C + 0.1 mL 10 mM Na_2S; stirring for 5 min at 20 °C.
3	Fe/Mn	2 mL 50 mM $FeCl_3$ + 2 mL 50 mM $MnSO_4$, light stirring for 5 min at 20 °C followed by adding 0.5 mL 10 mM Na_2S; stirring for 1 min; incubation without stirring for 24 h at 20 °C.
4	Ag/Ce^S	2 mL 50 mM $AgNO_3$ + 2 mL 15 mM $Ce(HCO_3)_4$, light stirring for 5 min followed by adding 0.1 mL 10 mM Na_2S; stirring for 1 min at 20 °C. incubation without stirring for 24 h at 20 °C.
5	Pt/Cu	0.2 mL 48 mM H_2PtCl_6 + 0.16 mL 100 mM ascorbic acid, vigorous stirring for 5 min followed by adding 1 mL 100 mM $CuSO_4$ and 0.2 mL 100 mM ascorbic acid; incubation without stirring for 24 h at 20 °C.
6	Fe/Ce	2 mL 50 mM $FeCl_3$ + 2 mL 15 mM $Ce(HCO_3)_4$, light stirring for 5 min at 20 °C followed by adding 0.5 mL 10 mM NH_4OH; stirring for 5 min; incubation without stirring for 24 h at 20 °C.
7	Zn/Ce	2 mL 50 mM $ZnSO_4$ + 2 mL 15 mM $Ce(HCO_3)_4$, light stirring for 5 min at 20 °C followed by adding 0.5 mL 10 mM NH_4OH; stirring for 5 min; incubation without stirring for 24 h at 20 °C.
8	Cu/Ce	2 mL 50 mM $CuSO_4$ + 2 mL 15 mM $Ce(HCO_3)_4$, light stirring for 5 min at 20 °C followed by adding 0.5 mL 10 mM NH_4OH; stirring for 5 min; incubation without stirring for 24 h at 20 °C.
9	Pd/Ce	1 mL 0.01 mM $PdCl_3$ + 1 mL 100 mM $NaBH_4$, vigorous stirring for 5 min followed by adding 4 mL 0.01 mM $Ce(HCO_3)_4$ and 0.5 mL 100 mM $NaBH_4$.
10	Pd/Cu	1 mL 0.01 mM $PdCl_3$ + 1 mL 10 mM $NaBH_4$, vigorous stirring for 3 min followed by adding 2 mL 0.01 mM $Ce(HCO_3)_4$ and 0.5 mL 100 mM $NaBH_4$; stirring for 1 min; incubation without stirring for 24 h at 20 °C.

Table 1. *Cont.*

No	NPs	Reaction Mixture and Conditions
11	Ag/Ce	2 mL 50 mM $AgNO_3$ + 2 mL 15 mM $Ce(HCO_3)_4$, vigorous stirring for 5 min at 20 °C followed by adding 0.1 mL 100 mM $NaBH_4$; stirring for 5 min; incubation without stirring for 24 h at 20 °C.
12	Au/Cu	2 mL 50 mM $CuSO_4$ + 2 mL 15 mM $Ce(HCO_3)_4$, vigorous stirring for 5 min at 20 °C followed by adding 0.1 mL 100 mM $NaBH_4$; stirring for 5 min; incubation without stirring for 24 h at 20 °C.
13	Au	0.145 mL 58.5 mM $HAuCl_4$ + 10 mL 10 mM CTAB, vigorous stirring; + 0.18 mL 100 mM $NaBH_4$; stirring for 2 h at 20 °C.
14	Ag/Cu	2 mL 50 mM $CuSO_4$ + 2 mL $AgNO_3$, vigorous stirring for 5 min at 20 °C followed by adding 0.1 mL 100 mM $NaBH_4$; incubation without stirring for 24 h at 20 °C.
15	Pt/Ag	0.2 mL 48 mM H_2PtCl_6 + 2 mL $AgNO_3$, vigorous stirring for 5 min at 20 °C followed by adding 0.1 mL 100 mM $NaBH_4$; stirring for 5 min; incubation without stirring for 24 h at 20 °C.
16	Ag/Zn	2 mL 50 mM $AgNO_3$ + 2 mL 50 mM $ZnSO_4$, vigorous stirring for 5 min at 20 °C followed by adding 0.1 mL 100 mM $NaBH_4$; stirring for 5 min; incubation without stirring for 24 h at 20 °C.

[S]—NPs obtained by a sulfide method.

2.3. Morphological Analysis of NPs Using Scanning Electron Microscopy (SEM)

Morphological analyses of the samples were performed using a SEM microanalyzer (REMMA-102-02, Sumy, Ukraine). The samples in different dilutions (2 µL) were dropped onto the surface of a silicon wafer and were dried at room temperature. The distance from the last lens of the microscope to the sample (WD) ranged from 17.1 mM to 21.7 mM. The accelerator voltage was in the range of 20 to 40 eV.

2.4. Determination of Peroxidase-Like Activity of NPs in Solution

PO-like activity of the NPs was measured by the colorimetric method, with *o*-dianisidine as a chromogenic substrate in the presence of H_2O_2. The generated color was determined at 525 nm using a Shimadzu UV1650 PC spectrophotometer (Kyoto, Japan). One unit (U) of PO-like activity was defined as the amount of NZ releasing 1 µMoL H_2O_2 per 1 min at 30 °C under standard assay conditions.

The procedure of the PO-like activity assay: 10 µL of the aqueous suspension of NPs (1 mg/mL) was incubated in a glass tube with 1 mL of 0.17 mM *o*-dianisidine in 50 mM NaOAc buffer, pH 4.5 (as a control); and with the same substrate in the presence of 8.8 mM H_2O_2 (as a substrate for PO). Addition of NPs to the substrate stimulated the development of an orange color over time, indicating an enzymatic reaction. The enzyme-mimetic activity could be assessed qualitatively with the naked eye and was measured quantitatively with a spectrophotometer. After incubation for an exact time (1–10 min) at 30 °C, and upon appearance of the orange color, the reaction was stopped by the addition of 0.26 mL 12 M HCl. The millimolar extinction coefficient of the resulting pink dye in the acidic solution was 13.38 $mM^{-1} \cdot cm^{-1}$.

2.5. Sensor Evaluation

2.5.1. Apparatus, Measurements, and Statistical Analysis

The amperometric sensors were evaluated using constant-potential amperometry in a three-electrode configuration with an Ag/AgCl/KCl (3 M) reference electrode, a Pt-wire counter electrode, and a graphite working electrode. Graphite rods (type RW001, 3.05 mM diameter) from Ringsdorff Werke (Bonn, Germany) were sealed in glass tubes using epoxy glue to form disk electrodes. Before sensor preparation, the graphite electrode (GE) was polished with emery paper and a polishing cloth using decreasing particle sizes of alumina paste (Leco, Germany). The polished electrodes were rinsed with water in an ultrasonic bath.

Amperometric measurements were carried out using a CHI 1200A potentiostat (IJ Cambria Scientific, Burry Port, UK) connected to a personal computer and performed in a batch mode under continuous stirring in an electrochemical cell with a 20 mL volume at 25 °C.

All the experiments were carried out in triplicate trials. Analytical characteristics of the electrodes were statistically processed using OriginPro 8.5 software. The error bars represent the standard error derived from three independent measurements. Calculation of the apparent Michaelis–Menten constants (K_M^{app}) was performed automatically by this program according to the Lineweaver–Burk equation.

2.5.2. Immobilization of Metallic NPs onto Electrodes, Testing Their Electro- and PO-Like Activity

For construction of the NZ-based electrode, 5 µL of NP suspension (1 mg/mL) was dropped onto the surfaces of GEs. After drying for 10 min at room temperature, the layer of NPs on the electrodes was covered with 5 µL Nafion membrane. The electrodes were washed with corresponding buffer solutions before and after each measurement.

The electrochemical properties of the synthesized NPs were studied by cyclic voltammetry (CV) on the GEs in the range from −1000 to +1000 mV with the scan rate of 50 mV min^{-1}; the profiles of amperometric signals in increasing concentrations of H_2O_2 were compared. The most electroactive NPs, which had the highest PO-like properties, were chosen for further investigation.

3. Results and Discussion

3.1. Obtaining and Characterizing the Best Peroxidase-Like Nanozymes

First, different NPs were synthesized and screened for their reaction to H_2O_2 in solution. PO-like activities were measured with *o*-dianisidine as the chromogenic substrate. The experiments demonstrated that the synthesized NPs, especially Au/Cu, Ag/Ce^S, Fe/Ce^S, and Zn/Ce, possessed significant PO-like activities in solution (Table 2). These results are in agreement with the data of other researchers [9,10].

Table 2. Peroxidase (PO)-like activities of the synthesized nanozymes NZs in solution.

No.	Nanozyme	Synthesis Method	Specific Activity, Units /mg
1	Fe/Ce^S	Na_2S	1.86 ± 0.16
2	Cu/Ce^S	$NaBH_4/Na_2S$	1.27 ± 0.11
3	Fe/Mn	Na_2S	0.12 ± 0.01
4	Ag/Ce^S	Na_2S	0.05 ± 0.004
5	Pt/Cu	Ascorbic acid	1.84 ± 0.14
6	Fe/Ce	NH_4OH	3.06 ± 0.26
7	Zn/Ce	NH_4OH	2.28 ± 0.21
8	Cu/Ce	NH_4OH	0.90 ± 0.007
9	Pd/Ce	$NaBH_4$	0.72 ± 0.06
10	Pd/Cu	$NaBH_4$	0.4 ± 0.03
11	Ag/Ce	$NaBH_4$	2.50 ± 0.22
12	Au/Cu	$NaBH_4$	4.22 ± 0.34
13	Au	$NaBH_4$	2.62 ± 0.19
14	Ag/Cu	$NaBH_4$	0.24 ± 0.02
15	Pt/Ag	$NaBH_4$	1.40 ± 0.11
16	Ag/Zn	$NaBH_4$	0.79 ± 0.06

^{S}—NPs obtained by a sulfide method.

The most catalytically active NZs were characterized by SEM coupled with X-ray microanalysis (SEM-XRM). SEM provided information on the size, distribution, and shape of the tested sample. Figure S1 presents the overall morphology of the formed hybrid particles. The XRM images of the synthesized NZs showed the characteristic peaks for metals of the composites.

The obtained Pd/Ce NPs have the shape of a sphere with a diameter of approximately 200 nm. The size of synthesized Pt/Cu NPs is near 500 nm. XRM data for Pt/Cu NPs proved the presence of Pt^0 and Cu^0 forms, with characteristic peaks Kα at 2.4 keV and 1.4 keV, respectively (Figure S1). The size of synthesized Pd/Cu NPs is in the range of

500 nm–1 μM. The sole peak at 1.8 keV demonstrates the full covering of CuNPs with the PdNPs.

SEM imaging and XRM data proved the formation of needlelike hybrid Fe/Ce and Au/Cu micro particles with the size ranging from 10 to 20 μM (Figure S1). The XRM image of Au/Cu NPs shows the Kα peaks of Cu^0 and Au^0, confirming the presence of both CuNPs and AuNPs. It was shown that the Fe/Ce and Au/Cu NPs tested look like irregular shaped clusters of microfibrillar structures. The best of catalytically active NZs, namely, Cu/CeS, Au/Cu, Ag/Ce, Fe/Ce, Ag/Zn, Pd/Ce, and Pt/Cu NPs were chosen for further investigation.

3.2. *Development and Characterization of the NZs-Modified Electrodes*

Our next task was to select the most PO-active NPs immobilized on the electrode surface. It is known that modification of an electrode with some metallic NPs can improve the efficiency of an electron transfer, due to an increase in the electrochemically accessible electrode surface area. Numerous NZs/GEs were screened for their ability to decompose hydrogen peroxide. The electrocatalytic activities of the synthesized NZs, while immobilized on the surface of GEs, were tested by CV and chronoamperometry, as described in Section 2.5.2 (Figure 1 and Figure S2).

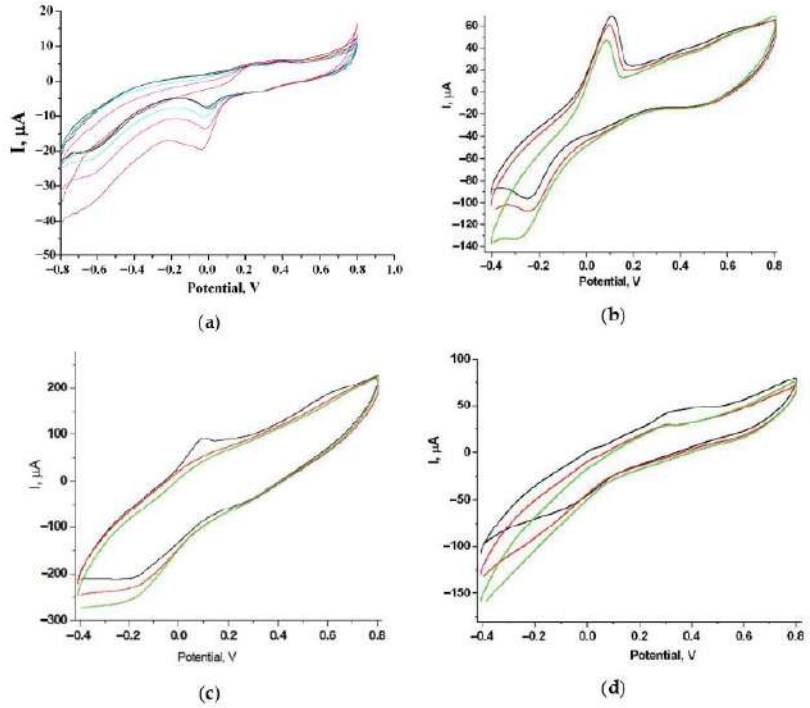

Figure 1. Cyclic voltammograms (CV) of the graphite electrodes modified with Cu/Ce^S (**a**), Fe/Ce (**b**), Au/Cu (**c**), and Ag/Ce (**d**). CV profiles as outputs on addition of H_2O_2 in concentration: (**a**)—0 mM (blue), 0.2 mM (cyan), 0.5 mM (pink), 1 mM (red); (**b–d**)—0 mM (black), 1 mM (red), 3 mM (green). Conditions: scan rate 50 $mV \cdot s^{-1}$; Ag/AgCl (reference electrode) in 50 mM NaOAc buffer, pH 4.5. The surfaces of the graphite electrode (GE) were modified with 1 μg (**a**) or 5 μg NZs (**b–d**) and covered with Nafion.

In our research, the amperometric responses of different NZs/GEs to added portions of H_2O_2 were compared under mild conditions at the working potential of −50 mV. This rather low potential was chosen from the CV profiles (Figure 1), since the main drawback

of many H_2O_2-sensitive NZ-based electrochemical sensors is their nonselectivity under high positive (or negative) working potentials. H_2O_2 is able to direct the auto-oxidation on electroactive surfaces at a working potential above +0.4 V, or auto-reduction at −0.4 V or less vs. Ag/AgCl. Moreover, the real samples containing organic compounds may be easily co-oxidized/co-reduced at extreme potentials, which may result in overestimation of the target analytes in the presence of oxygen. To avoid these problems during sensor analysis, it was important to screen new NZs while working at operating potentials close to zero (0) V vs. Ag/AgCl [12,43–45]. This requirement is especially relevant for the construction of biosensors and their exploitation for analysis of real samples (food products, biological liquids, etc.). Our previous experiments with natural PO as a biorecognition element of amperometric biosensors were also carried out at −50 mV [41–44].

Using the chronoamperograms, calibration curves were plotted for H_2O_2 determination by the developed electrodes (Figure S2). The analytical characteristics of the modified GEs, as deduced from the graphs in comparison with natural PO [42–44], are summarized in Table 3. The linear ranges, limits of detection (LOD), and sensitivities of the electrodes modified with nanoPOs were calculated. The limit of blank values (LOB) for NZ was calculated as 0.3 × LOD. The sensitivity of each NZ-modified electrode was measured for an electrode area of 7.30 mM^2.

Table 3. Analytical characteristics of the most effective NZs as PO-mimetic placed on electrode.

Sensitive Film	No. in Table 2	Sensitivity, A M^{-1} m^{-2}	LOD, μM	Linear Range, μM	K_M^{app}, mM	I_{max}, μA
PO		352		400	4.9 ± 1.1	5.0 ± 0.2
Cu/Ce ^{S}	2	1890	0.42 ± 0.006	1.5–20,000	43.3 ± 14.5	786.4 ± 167.7
Fe/Ce	6	1372	2.90 ± 0.010	50–1000	14.4 ± 1.3	104.5 ± 3.3
Au/Cu	12	793	4.88 ± 0.010	50–15,000	28.0 ± 3.2	213.3 ± 13.1
Ag/Ce	11	782	11 ± 0.009	50–4000	16.4 ± 2.5	152.54 ± 8.8
Pd/Cu	10	581	39 ± 1.20	117–14,300	34.7 ± 2.02	166.2 ± 6.4
Pd/Ce	9	496	4.55 ± 0.006	17–4100	13.4 ± 3.2	68.0 ± 3.2
Ag/Zn	16	375	41 ± 1.50	17–25,000	18.1 ± 0.4	96.79 ± 8.56
Pt/Cu	5	163	5.54 ± 0.002	17–25,000	26.8 ± 5.0	55.2 ± 5.4

^{S}—NPs obtained by a sulfide method.

Figure 2 summarizes the data concerning the PO-like properties of the selected NZs, namely, Cu/Ce^S, Au/Cu, Ag/Ce, Fe/Ce, Ag/Zn, Pd/Ce, and Pt/Cu. The results in Table 3 demonstrate that Cu/Ce^S/GE exhibited the highest sensitivity (1890 A·M^{-1}·m^{-2}) and current response (786 μA), the lowest LOD (0.42 μM), and a broad linear range (1.5–20,000 μM) upon H_2O_2 addition. This structure was therefore studied in more detail as the most effective artificial PO immobilized on the electrode.

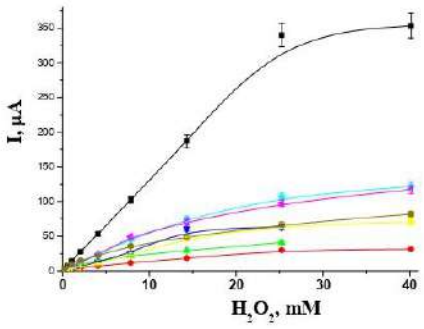

Figure 2. Dependence of the current response on increasing concentrations of H_2O_2 for GEs modified with 5 μg of different nanozymes: Cu/Ce^S (black line), Au/Cu (cyan), Ag/Ce (violet), Fe/Ce (khaki), Ag/Zn (yellow), Pd/Ce (green), Pt/Cu (red).

3.3. Characterization of the Most Effective Cu/Ce^S-Modified Electrode

The Cu/Ce^S-NZ with the highest PO-like activity was studied in detail. The Cu/Ce^S/GE demonstrated the highest PO-like activity, compared with other NZs and with natural PO (Figure S2, Tables 3 and 4). The highest current response (I_{max}) on the tested analyte at substrate saturation of the Cu/Ce^S/GE was 157-fold higher, and its sensitivity was 5.4-fold higher, than that of the PO/GE (Table 3). It is worth mentioning that Cu/Ce^S has PO-like ability but lacks oxidase (laccase)-like properties. This conclusion was reached from the results of colorimetric tests using *o*-dianisidine in the presence of H_2O_2 as a substrate for PO, and with *o*-dianisidine only as a substrate for oxidase (sees Section 2.4). The Cu/Ce^S specificity to H_2O_2 is the important valuable characteristic for applying it as a selective PO-mimetic element in sensors and oxidase-based biosensors. Figure 3 shows the effect of quantity on the NZ immobilized on the GE surface, based on the amperometric signal as a response to H_2O_2 addition. Table 4 presents comparative analytical characteristics of the recently developed metallic NZ-based sensors for H_2O_2 analysis, including the results described here.

Table 4. The main operational characteristics of the recently described H_2O_2-sensitive metallic NZ-based sensors working at low potentials.

Electrode	PO Mimetic	Potential, mV	Sensitivity, A M^{-1} m^{-2}	Linear Range, µM	Ref.
[1] GCE	Cu_2O/PANI/rGhO	−200	394	0.8–12,780	[45]
GCE	Fe_3O_4/3D GNCs	−200	2742	0.8–330	[46]
GCE	Ni–Fe PBA-[4] HNCs	−50	361	0.1–20,000	[47]
GCE	PB/BG	−50	2852	4–830	[48]
	AuNPs-PB/BG		11,243	9.2–8100	
[2] DBD	PB		2100		
DBD	Ni-FePBA	−50	1500	0.5–1000	[11]
GE	PB/NZ		4500		
GCE	MnPBA		1472	3–8610	[49]
GCE	rGhO/Pt-Ag	−50	6996	5–1500	[50]
GCE	Ni-PB	−50	3500	0.1–1000	[51]
Graphite paste	Ni-FePBA	−50	1130	2–1000	[52]
	Cu-FePBA		2030	0.5–1000	
[3] GE	PtRu	−50	194	17–25,000	[41]
GE	gCuHCF	−50	1620	16–4100	[42]
	gFeHCF		1090	116–14,300	
	PO		352	15–20,000	
GCE	Ni-FePBA	0	18,000	up to 100	[53]
GCE	PNAANI-PB	0	5073	1–1000	[54]
GCE	PB	50	6000	0.1–100	[55]
GCE	Fe/rGhO-Pt	100	3400	7.5–4270	[56]
GCE	PB	180	10,000/20,000	1–5000	[57]
GE	Cu/Ce^S	−50	1890	1.5–20,000	This paper
	Au/Cu		793	17–15,000	
	Fe/Ce	-	1372	up to 1000	

[1] GCE—glassy carbon electrode; [2] DBD—diamond boron-doped; [3] GE—graphite electrode; [4] HNCs—hollow nanocubes.

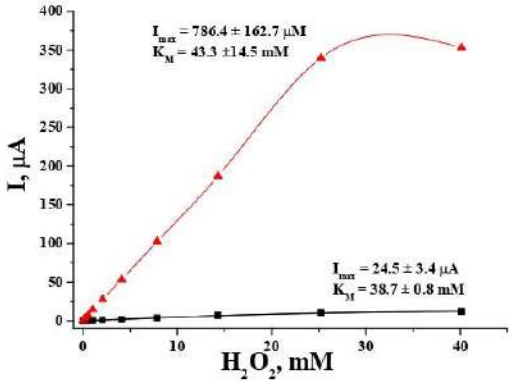

Figure 3. Dependence of the current response on increasing concentrations of H_2O_2 for GEs modified with different quantities of Cu/Ce^S: 1 μg (black line) and 5 μg (red line).

3.4. Application of Cu/Ce^S as a PO-Mimetic in Amperometric Sensors

To demonstrate the applicability of Cu/Ce^S as a chemosensor for H_2O_2 detection, analysis of H_2O_2 concentration was carried out in samples of commercial products (Figure 4). The disinfectant samples tested were Famidez–Sanosil, Spray Antiseptic for arms and a pharmaceutical solution of 3% H_2O_2. The standard addition test, SAT, approach was used to avoid undesirable effects on analytical results from additives in the tested solutions.

Graphical SAT is a type of quantitative analysis often used in analytical chemistry when a standard is added directly to the aliquots of the analyzed sample. SAT is used in situations where sample components may contribute to the analytical signal, thus making it impossible to use a routine calibration method. Estimation of H_2O_2 in the initial sample was performed using the equation C = AN/B, where A and B are parameters of a linear regression and N is the dilution factor.

The results of hydrogen peroxide determination in commercial samples in comparison to data of manufacturers are presented in Table 5. The average H_2O_2 concentrations determined from the data in Figure 4 correlated well with the manufacturer's data (Table 5), with an error of less than 10%.

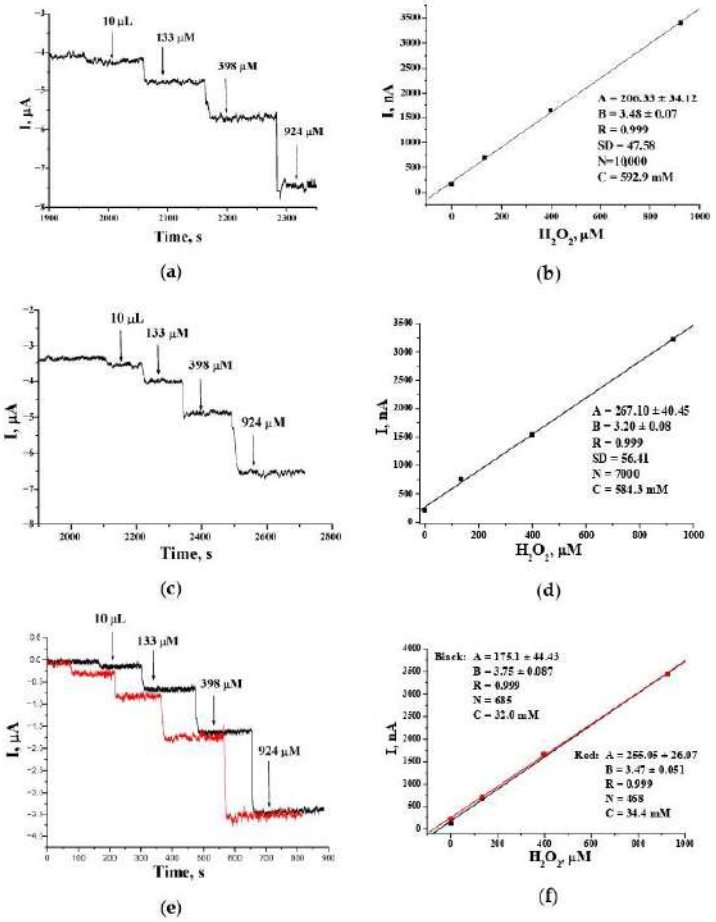

Figure 4. Analysis of the real samples of disinfectants using Cu/Ce^{S}-based chemosensor with the SAT method: chronoamperograms (**a**,**c**,**e**) and correspondent linear graphs (**b**,**d**,**f**). Disinfectants: Famidez-Sanosil (**a–d**); antiseptic spray (**e**,**f**). Analytical conditions: working potential—50 mV vs. Ag/AgCl (reference electrode), 50 mM NaOAc buffer, pH 4.5 at 23 °C.

Table 5. Results of H_2O_2 estimation in H_2O_2-containing commercial disinfectants.

Commercial Sample	Concentration of H_2O_2			CV, %	Producer
	Estimated		Declared, %		
	mM	%			
Antiseptic spray for arms	33.2	0.11	0.10	10.0	Pharmaceutical factory "Viola", Zaporizhzhia, Ukraine
Universal antiseptic solution	880	2.95	3.0	1.7	
Famidez–Sanosil	588.6	1.98	2.0	1.0	Ltd Dezomark, Novoyavorivsk, Ukraine

4. Conclusions

In the current research, a number of NPs based on transition and noble metals were synthesized by chemical methods and were screened for their ability to decompose hydro-

gen peroxide in solutions. Structure, size, morphology, composition, catalytic properties, and electrochemical activities of the chosen PO-like NZs were characterized on the electrode. A more detailed study was performed for Cu/Ce^S-NZ, which was found to be the most effective mimetic of PO. It was demonstrated that the synthesized Cu/Ce^S-NZ may be successfully used as an artificial PO for sensor analysis of hydrogen peroxide in commercial disinfectant samples.

Supplementary Materials: The following are available online at https://www.mdpi.com/2076-3417/11/2/777/s1, Figure S1: Characteristics of the several metallic PO-like nanozymes: SEM images at different magnifications (top) and their X-ray spectral characteristics (bottom); Figure S2: Amperometric characteristics of the several NZ-modified electrodes: chronoamperograms (left), dependence of the current response on increasing concentrations of H_2O_2 (middle) and calibration graphs (right). Conditions: working potential –50 mV vs. Ag/AgCl (reference electrode), 50 mM NaOAc buffer, pH 4.5 at 23 °C.

Author Contributions: Conceptualization: G.G. and M.N.; methodology: N.S., O.D. and G.G.; investigation: O.D., R.S. and N.S.; resources: M.G.; data curation: G.G.; writing—original draft preparation: G.G., N.S. and O.D.; writing—review and editing: G.G. and M.N.; supervision: M.G.; project administration: G.G.; funding acquisition: M.G. and M.N. All authors have read and agreed to the published version of the manuscript.

Funding: This work was partially funded by NAS of Ukraine (The program "Smart sensor devices of a new generation based on modern materials and technologies"), by the Ministry of Education and Science of Ukraine (Ukrainian–Lithuanian R&D, project 0120U103398), by National Research Foundation of Ukraine (project 48/02.2020 "Development of new nanozymes as catalytic elements for enzymatic kits and chemo/biosensors") and by the Research Authority of the Ariel University, Israel.

Institutional Review Board Statement: "Not applicable" for studies not involving humans.

Informed Consent Statement: "Not applicable" for studies not involving humans.

Data Availability Statement: "Not applicable" for studies not involving humans.

Acknowledgments: We acknowledge Mariya F. Ivash (Institute of Cell Biology, Lviv, Ukraine) for technical support and experimental assistance.

Conflicts of Interest: The authors declare no conflict of interest.

Abbreviations

2,4-DCP	2,4-Dichlorophenol
ABTS	2,2′-Azinobis-(3-ethylbenzthiazoline-6-sulphonate)
CV	Cyclic voltammetry
DBD	Diamond boron-doped
gCuHCF	Hexacyanoferrate of coppers obtained via enzyme
GCE	Glassy carbon electrode
GE	Graphite electrode
HNCs	Hollow nanocubes
I_{max}	Maximal current response on tested analyte at substrate saturation
K_M^{app}	Apparent Michaelis–Menten constant
LOD	Limit of detection
LR	Linear range
MOFs	Metal–Organic Frameworks
NPs	Nanoparticles
NZ	Nanozyme
Me/Ce^S	Nanozyme obtained in the presence of Na_2S in reaction mixture; where Me–Fe, Cu or Ag.
OPD	*o*-Phenylenediamine
PO	Natural horseradish peroxidase
SAT	Standard addition test
SEM-XRM	Scanning electron microscopy coupled with X-ray microanalysis
TMB	3,5,3′,5′-Tetramethylbenzidine

References

1. Dunford, H.B. *Heme Peroxidases (University of Alberta)*; Wiley-VCH, John Wiley and Sons: New York, NY, USA, 1999; 507p, ISBN 0-471-24244-6.
2. Veitch, N.C.; Smith, A.T. Horseradish peroxidase. *Comput. Chem.* **2000**, *51*, 107–162. [CrossRef]
3. Plieth, C. Peroxide-Induced Liberation of Iron from Heme Switches Catalysis during Luminol Reaction and Causes Loss of Light and Heterodyning of Luminescence Kinetics. *ACS Omega* **2019**, *4*, 3268–3279. [CrossRef] [PubMed]
4. Tatsuma, T.; Watanabe, T. Peroxidase model electrodes: Heme peptide modified electrodes as reagentless sensors for hydrogen peroxide. *Anal. Chem.* **1991**, *63*, 1580–1585. [CrossRef] [PubMed]
5. Neumann, B.; Wollenberger, U. Electrochemical Biosensors Employing Natural and Artificial Heme Peroxidases on Semiconductors. *Sensors* **2020**, *20*, 3692. [CrossRef]
6. Attar, F.; Shahpar, M.G.; Rasti, B.; Sharifi, M.; Saboury, A.A.; Rezayat, S.M.; Falahati, M. Nanozymes with intrinsic peroxidase-like activities. *J. Mol. Liq.* **2019**, *278*, 130–144. [CrossRef]
7. Wu, J.; Wang, X.; Wang, Q.; Lou, Z.; Li, S.; Zhu, Y.; Qin, L.; Wei, H. Nanomaterials with enzyme-like characteristics (nanozymes): Next-generation artificial enzymes (II). *Chem. Soc. Rev.* **2019**, *48*, 1004–1076. [CrossRef]
8. Gallay, P.; Eguílaz, M.; Rivas, G.A. Designing electrochemical interfaces based on nanohybrids of avidin functionalized-carbon nanotubes and ruthenium nanoparticles as peroxidase-like nanozyme with supramolecular recognition properties for site-specific anchoring of biotinylated residues. *Biosens. Bioelectron.* **2020**, *148*, 111764. [CrossRef]
9. Sun, L.; Ding, Y.; Jiang, Y.; Liu, Q. Montmorillonite-loaded ceria nanocomposites with superior peroxidase-like activity for rapid colorimetric detection of H_2O_2. *Sens. Actuators B Chem.* **2017**, *239*, 848–856. [CrossRef]
10. Cui, F.; Deng, Q.; Sun, L. Prussian blue modified metal–organic framework MIL-101(Fe) with intrinsic peroxidase-like catalytic activity as a colorimetric biosensing platform. *RSC Adv.* **2015**, *5*, 98215–98221. [CrossRef]
11. Komkova, M.A.; Pasquarelli, A.; Andreev, E.A.; Galushin, A.A.; Karyakin, A.A. Prussian Blue modified boron-doped dia-mond interfaces for advanced H_2O_2 electrochemical sensors. *Electrochim. Acta* **2020**, *339*, 135924. [CrossRef]
12. Stasyuk, N.; Smutok, O.; Demkiv, O.M.; Prokopiv, T.; Gayda, G.Z.; Nisnevitch, M.; Gonchar, M.V. Synthesis, Catalytic Properties and Application in Biosensorics of Nanozymes and Electronanocatalysts: A Review. *Sensors* **2020**, *20*, 4509. [CrossRef] [PubMed]
13. Qin, L.; Hu, Y.; Wei, H. Nanozymes: Preparation and Characterization. In *Nanotechnology for Electronics, Photonics, and Renewable Energy*; Springer Science and Business Media LLC: Berlin/Heidelberg, Germany, 2020; pp. 79–101.
14. Yue, Y.; Wei, H.; Guo, J.; Yang, Y. Ceria-based peroxidase-mimicking nanozyme with enhanced activity: A coordination chemistry strategy. *Colloids Surf. A Physicochem. Eng. Asp.* **2021**, *610*, 125715. [CrossRef]
15. Wang, Z.; Zhang, R.; Yan, X.; Fan, K. Structure and activity of nanozymes: Inspirations for de novo design of nanozymes. *Mater. Today* **2020**, *41*, 81–119. [CrossRef]
16. Wang, Y.; Mao, J.; Meng, X.; Yu, L.; Deng, D.; Bao, X. Catalysis with Two-Dimensional Materials Confining Single Atoms: Concept, Design, and Applications. *Chem. Rev.* **2019**, *119*, 1806–1854. [CrossRef]
17. Shen, J.; Shafiq, M.; Ma, M.; Chen, H. Synthesis and Surface Engineering of Inorganic Nanomaterials Based on Microfluidic Technology. *Nanomaterials* **2020**, *10*, 1177. [CrossRef]
18. Huang, Y.; Ren, J.; Qu, X. Nanozymes: Classification, Catalytic Mechanisms, Activity Regulation, and Applications. *Chem. Rev.* **2019**, *119*, 4357–4412. [CrossRef]
19. Chen, J.; Qiu, H.; Zhao, S. Fabrication of chemiluminescence resonance energy transfer platform based on nanomaterial and its application in optical sensing, biological imaging and photodynamic therapy. *TrAC Trends Anal. Chem.* **2020**, *122*, 115747. [CrossRef]
20. Rauf, S.; Ali, N.; Tayyab, Z.; Shah, M.A.K.Y.; Yang, C.P.; Hu, J.; Kong, W.; Huang, Q.; Hayat, A.; Muhammad, N. Ionic liquid coated zerovalent manganese nanoparticles with stabilized and enhanced peroxidase-like catalytic activity for colorimetric detection of hydrogen peroxide. *Mater. Res. Express* **2020**, *7*, 035018. [CrossRef]
21. Zhang, K.; Zuo, W.; Wang, Z.; Liu, J.; Li, T.; Wang, B.; Yang, Z. A simple route to CoFe2O4 nanoparticles with shape and size control and their tunable peroxidase-like activity. *RSC Adv.* **2015**, *5*, 10632–10640. [CrossRef]
22. Liu, B.; Liu, J. Surface modification of nanozymes. *Nano Res.* **2017**, *10*, 1125–1148. [CrossRef]
23. Zhao, M.; Huang, J.; Zhou, Y.; Pan, X.; Chen, Z.; Ye, Z.; Pan, X. Controlled synthesis of spinel $ZnFe_2O_4$ decorated ZnO heterostructures as peroxidase mimetics for enhanced colorimetric biosensing. *Chem. Commun.* **2013**, *49*, 7656–7658. [CrossRef] [PubMed]
24. Liu, C.; Yan, Y.; Zhang, X.; Mao, Y.; Ren, X.; Hu, C.; He, W.; Yin, J.-J. Regulating the pro- and anti-oxidant capabilities of bimetallic nanozymes for the detection of Fe2+ and protection of Monascus pigments. *Nanoscale* **2020**, *12*, 3068–3075. [CrossRef] [PubMed]
25. Liu, M.; Kong, L.; Wang, X.; He, J.; Bu, X.-H. Engineering Bimetal Synergistic Electrocatalysts Based on Metal–Organic Frameworks for Efficient Oxygen Evolution. *Small* **2019**, *15*, e1903410. [CrossRef] [PubMed]
26. Cao-Milán, R.; He, L.D.; Shorkey, S.; Tonga, G.Y.; Wang, L.-S.; Zhang, X.; Uddin, I.; Das, R.; Sulak, M.; Rotello, V.M. Modulating the catalytic activity of enzyme-like nanoparticles through their surface functionalization. *Mol. Syst. Des. Eng.* **2017**, *2*, 624–628. [CrossRef]
27. Wang, X.; Hu, Y.; Wei, H. Nanozymes in bionanotechnology: From sensing to therapeutics and beyond. *Inorg. Chem. Front* **2016**, *3*, 41–60. [CrossRef]

28. Chen, J.; Wei, X.; Tang, H.; Munyemana, J.C.; Guan, M.; Zhang, S.; Qiu, H. Deep eutectic solvents-assisted synthesis of $ZnCo_2O_4$ nanosheets as peroxidase-like nanozyme and its application in colorimetric logic gate. *Talanta* **2021**, *222*, 121680. [CrossRef]
29. Rane, A.V.; Kanny, K.; Abitha, V.K.; Sabu, T. Chapter 5. Methods for Synthesis of Nanoparticles and Fabrication of Nanocomposites. In *Synthesis of Inorganic Nanomaterials Advances and Key Technologies Micro and Nano Technologies*, 1st ed.; Bhagyaraj, S.M., Oluwafemi, O.S., Kalarikkal, N., Sabu, T., Eds.; Woodhead Publishing Company: Sawston, UK, 2018; pp. 121–139. ISBN 9780081019757.
30. Suriati, G.; Mariatti, M.; Azizan, A. Synthesis of silver nanoparticles bu chemical reduction method: Effect of reducing agent and surfactant concentration. *Int. J. Automot. Mech. Eng.* **2014**, *10*, 1920–1927. [CrossRef]
31. Chen, H.-I.; Chang, H.-Y. Synthesis of nanocrystalline cerium oxide particles by the precipitation method. *Ceram. Int.* **2005**, *31*, 795–802. [CrossRef]
32. Vokhmyanina, D.V.; Andreeva, K.D.; Komkova, M.A.; Karyakina, E.E.; Karyakin, A.A. 'Artificial peroxidase' nanozyme–enzyme based lactate biosensor. *Talanta* **2020**, *208*, 120393. [CrossRef]
33. Neampet, S.; Ruecha, N.; Qin, J.; Wonsawat, W.; Chailapakul, O.; Rodthongkum, N. A nanocomposite prepared from platinum particles, polyaniline and a Ti3C2 MXene for amperometric sensing of hydrogen peroxide and lactate. *Microchim. Acta* **2019**, *186*, 752. [CrossRef]
34. Matos-Peralta, Y.; Antuch, M. Review—Prussian Blue and Its Analogs as Appealing Materials for Electrochemical Sensing and Biosensing. *J. Electrochem. Soc.* **2019**, *167*, 037510. [CrossRef]
35. Meng, X.; Gao, L.; Fan, K.; Yan, X. *Nanozyme-Based Tumor Theranostics*; Springer Science and Business Media LLC: Berlin/Heidelberg, Germany, 2020; pp. 425–457.
36. Chen, W.; Gao, G.; Jin, Y.; Deng, C. A facile biosensor for Aβ40O based on fluorescence quenching of prussian blue nanoparticles. *Talanta* **2020**, *216*, 120930. [CrossRef] [PubMed]
37. He, L.; Li, Z.; Guo, C.; Hu, B.; Wang, M.; Du, M.; Du, M. Bifunctional bioplatform based on NiCo Prussian blue analogue: Label-free impedimetric aptasensor for the early detection of carcino-embryonic antigen and living cancer cells. *Sens. Actuators B Chem.* **2019**, *298*, 126852. [CrossRef]
38. Tabrizi, M.A.; Shamsipur, M.; Saber, R.; Sarkar, S.; Zolfaghari, N. An ultrasensitive sandwich-type electrochemical immunosensor for the determination of SKBR-3 breast cancer cell using rGO-TPA/FeHCFnano labeled Anti-HCT as a signal tag. *Sens. Actuators B Chem.* **2017**, *243*, 823–830. [CrossRef]
39. Jiang, D.; Ni, D.; Rosenkrans, Z.T.; Huang, P.; Yan, X.; Cai, W. Nanozyme: New horizons for responsive biomedical applications. *Chem. Soc. Rev.* **2019**, *48*, 3683–3704. [CrossRef]
40. Wang, P.; Wang, T.; Hong, J.; Yan, X.; Liang, M. Nanozymes: A New Disease Imaging Strategy. *Front. Bioeng. Biotechnol.* **2020**, *8*, 15. [CrossRef]
41. Stasyuk, N.; Gayda, G.Z.; Zakalskiy, A.E.; Zakalska, O.; Serkiz, R.; Gonchar, M. Amperometric biosensors based on oxidases and PtRu nanoparticles as artificial peroxidase. *Food Chem.* **2019**, *285*, 213–220. [CrossRef]
42. Gayda, G.Z.; Demkiv, O.M.; Gurianov, Y.; Serkiz, R.Y.; Gonchar, M.V.; Nisnevitch, M. "Green" Nanozymes: Synthesis, Characterization, and Application in Amperometric (Bio)sensors. *Multidiscip. Digit. Publ. Inst. Proc.* **2020**, *60*, 58. [CrossRef]
43. Gayda, G.Z.; Demkiv, O.M.; Stasyuk, N.Y.; Serkiz, R.Y.; Lootsik, M.D.; Errachid, A.; Gonchar, M.V.; Nisnevitch, M. Metallic Nanoparticles Obtained via "Green" Synthesis as a Platform for Biosensor Construction. *Appl. Sci.* **2019**, *9*, 720. [CrossRef]
44. Stasyuk, N.; Gayda, G.Z.; Klepach, H.; Gonchar, M.V. Nanoparticles of Noble Metals as Effective Platforms for the Fabrication of Amperometric Biosensors on Hydrogen Peroxide. *Sens. Lett.* **2016**, *14*, 1169–1177. [CrossRef]
45. Liu, J.; Yang, C.; Shang, Y.; Zhang, P.; Liu, J.; Zheng, J. Preparation of a nanocomposite material consisting of cuprous oxide, polyaniline and reduced graphene oxide, and its application to the electrochemical determination of hydrogen peroxide. *Microchim. Acta* **2018**, *185*, 172. [CrossRef] [PubMed]
46. Zhao, Y.; Huo, D.; Bao, J.; Yang, M.; Chen, M.; Hou, J.; Fa, H.; Hou, C. Biosensor based on 3D graphene-supported Fe_3O_4 quantum dots as biomimetic enzyme for in situ detection of H2O2 released from living cells. *Sens. Actuators B Chem.* **2017**, *244*, 1037–1044. [CrossRef]
47. Niu, Q.; Bao, C.; Cao, X.; Liu, C.; Wang, H.; Lu, W. Ni–Fe PBA hollow nanocubes as efficient electrode materials for highly sensitive detection of guanine and hydrogen peroxide in human whole saliva. *Biosens. Bioelectron.* **2019**, *141*, 111445. [CrossRef] [PubMed]
48. Keihan, A.H.; Karimi, R.R.; Sajjadi, S. Wide dynamic range and ultrasensitive detection of hydrogen peroxide based on beneficial role of gold nanoparticles on the electrochemical properties of prussian blue. *J. Electroanal. Chem.* **2020**, *862*, 114001. [CrossRef]
49. Pang, H.; Zhang, Y.; Cheng, T.; Lai, W.-Y.; Huang, W. Uniform manganese hexacyanoferrate hydrate nanocubes featuring superior performance for low-cost supercapacitors and nonenzymatic electrochemical sensors. *Nanoscale* **2015**, *7*, 16012–16019. [CrossRef]
50. Zhang, C.; Zhang, Y.; Du, X.; Chen, Y.; Dong, W.; Han, B.; Chen, Q. Facile fabrication of Pt-Ag bimetallic nanoparticles decorated reduced graphene oxide for highly sensitive non-enzymatic hydrogen peroxide sensing. *Talanta* **2016**, *159*, 280–286. [CrossRef]
51. Sitnikova, N.A.; Borisova, A.V.; Komkova, M.A.; Karyakin, A.A. Superstable Advanced Hydrogen Peroxide Transducer Based on Transition Metal Hexacyanoferrates. *Anal. Chem.* **2011**, *83*, 2359–2363. [CrossRef]
52. Pandey, P.C.; Panday, D.; Pandey, A.K. Polyethylenimine mediated synthesis of copper-iron and nickel-iron hexacyanoferrate nanoparticles and their electroanalytical applications. *J. Electroanal. Chem.* **2016**, *780*, 90–102. [CrossRef]

53. Karpova, E.V.; Karyakina, E.E.; Karyakin, A.A. Communication—Accessing Stability of Oxidase-Based Biosensors via Stabilizing the Advanced H2O2Transducer. *J. Electrochem. Soc.* **2017**, *164*, B3056–B3058. [CrossRef]
54. Zhou, L.; Wu, S.; Xu, H.; Zhao, Q.; Zhang, Z.; Yao, Y. Preparation of poly(N-acetylaniline)–Prussian blue hybrid composite film and its application to hydrogen peroxide sensing. *Anal. Methods* **2014**, *6*, 8003–8010. [CrossRef]
55. Karyakin, A.A.; Karyakina, E.E.; Gorton, L. Amperometric Biosensor for Glutamate Using Prussian Blue-Based "Artificial Peroxidase" as a Transducer for Hydrogen Peroxide. *Anal. Chem.* **2000**, *72*, 1720–1723. [CrossRef] [PubMed]
56. Zhang, Y.; Duan, Y.; Shao, Z.; Chen, C.; Yang, M.; Lu, G.; Xu, W.; Liao, X. Amperometric hydrogen peroxide sensor using a glassy carbon electrode modified with a nanocomposite prepared from ferumoxytol and reduced graphene oxide decorated with platinum nanoparticles. *Microchim. Acta* **2019**, *186*, 386. [CrossRef] [PubMed]
57. Karyakin, A.A.; Gitelmacher, O.V.; Karyakina, E.E. Prussian Blue-Based First-Generation Biosensor. A Sensitive Am-perometric Electrode for Glucose. *Anal. Chem.* **1995**, *67*, 2419–2423. [CrossRef]

Оригінал доступний за посиланням: https://doi.org/10.3390/app11020777
Електронний додаток до статті доступний за посиланням: https://www.mdpi.com/2076-3417/11/2/777/s1

3.2. Синтез, скринінг, антиоксидантні властивості та електрохімічна поведінка нанозимів із потенційною редуктазною активністю.

Анотація: *Нанозими (НЗ) – стабільні економічно ефективні міметики природних ензимів. Вони є перспективними каталізаторами в харчовій та екологічній біотехнології, біосенсориці, альтернативній енергетиці та медицині. Більшість відомих НЗ є міметиками оксидоредуктаз, проте на сьогодні існують обмежені дані щодо міметиків редуктаз. У цій роботі, ми повідомляємо про отримання металевих НЗ, що виявляють властивості редуктаз та тестування отриманих НЗ на антиоксидантну активність у розчині. Нами детально охарактеризовано найбільш ефективний міметик селенітредуктази – НЗ Zn/Cd/Cu, а також досліджено його субстратну специфічність, розмір, склад, антиоксидантні властивості в порівнянні з кількома харчовими продуктами та тролоксом, Сконструйовано амперометричний сенсор з високою чутливістю (1700 $А \cdot М^{-1} \cdot м^{-2}$) і широким лінійним діапазоном (16-1000 мкМ) для йонів селеніту. Продемонстровано можливість застосування виготовленого сенсора для визначення вмісту селеніту в промисловій мінеральній воді.*

RSC Advances

PAPER

Cite this: *RSC Adv.*, 2022, 12, 2026

Nanozymes with reductase-like activities: antioxidant properties and electrochemical behavior

Nataliya Stasyuk, *[ab] Galina Gayda, [a] Taras Kavetskyy[bc] and Mykhailo Gonchar[ab]

Received 5th November 2021
Accepted 5th January 2022

DOI: 10.1039/d1ra08127f

rsc.li/rsc-advances

Nanozymes (NZs) as stable cost-effective mimics of natural enzymes may be promising catalysts in food and environmental biotechnology, biosensors, alternative energy and medicine. The majority of known NZs are mimetics of oxidoreductases, although there are only limited data regarding mimetics of reductases. In the present research, a number of metal-based NZs were synthesized *via* chemical methods and screened for their antioxidant ability in solution. The most effective reductase-like Zn/Cd/Cu NZ was characterized in detail. Its antioxidant properties in comparison with several food products and Trolox, as well as substrate specificity, size and composition were studied. Zn/Cd/Cu NZ was shown to mimic preferentially selenite reductase. The amperometric sensor was constructed possessing a high sensitivity (1700 A M^{-1} m^{-2}) and a broad linear range (16–1000 μM) for selenite ions. The possibility to apply the fabricated sensor for selenite determination in commercial mineral water has been demonstrated.

Introduction

In recent years, nanomaterials with enzyme-mimetic properties (nanozymes) have attracted considerable attention.[1–3] Nanozymes (NZs) as artificial enzymes (AEs) are promising alternatives to the natural ones.[1–3] AEs have essential advantages over natural enzymes such as low preparation costs, stability, high surface area, self-assembling capability, size and composition-dependent activities, broad possibility for modification, and biocompatibility. They have wide potential practical applications as catalysts in biosensors, fuel-cell technology, environmental biotechnology, and medicine.[5–12] It has been shown that AEs mimic the activity of peroxidases,[5,13–15] oxidases,[5,16] superoxide dismutases,[5,17] and hydrolases,[5,18] although only limited data were reported regarding reductase mimetics.[19–25]

Natural reductases are the enzymes which belong to the E.C. 1 class of oxidoreductases and catalyze reduction reactions. Reductases are dehydrogenases which transfer hydrogen from the substrate to biological acceptors and to dyes.[26,27] Reductases lower the activation energy needed for redox reactions to occur. The substrates of microbial reductases are inorganic compounds, including metal ions, metals, and non-metal and metalloid oxianions, as well as organic compounds, including aldehydes, glutathione, nucleotides, proteins, *etc.*[26–42]

Diverse enzymes of various microorganisms take part in the reduction processes, that possess abilities of the metalloreductase,[28,29] carboxylic acid reductase,[30,31] selenate[32] and selenite reductases,[33–36] hydrogenase,[37] cromate reductase,[38,39] nitrite[40] and nitrate reductases[41] *etc.* However, the problem of identification and classification for many reductases was not solved up to day. For example, so far no gene product or enzyme solely responsible for selenite reduction in aerobic bacteria has been identified *in vivo*.[42]

All known NZs usually utilize oxygen or hydrogen peroxide to produce active oxygen forms to oxidize substrate. There exist limited data on the nanomaterials simulating reductase, since oxygen, rather than other biomolecules, is preferable to be reduced on the surface of nanoparticles.[19,22,43] Therefore, it is a great challenge to develop novel mimetics of reductase to simulate its natural counterparts with diverse functions.

Reduction of different substrates using reductase-like (R-like) NZs as catalysts have so far been reported.[19–25] Cr(VI) may be reduced to Cr(III) *via* catalysis by magnetite-based nanocomposites[25] or by cobalt oxide containing nanocomposite,[24] peroxynitrite – *via* grapheme-hemin hybrid nanosheets,[44] and Cyt *c* – *via* zeolitic imidazolate frameworks encapsulated with polyethylenimine.[19] A number of NZs were reported to catalyze the sodium borohydride-induced 4-nitrophenol reduction to 4-aminophenol, namely silver and gold nanoparticles,[23] platinum nanoparticles,[45] reduced graphene oxide–cobalt oxide-based nanocomposite,[24] iron oxide-loaded alginate-bentonite hydrogel beads[20] and other materials.[21,22]

In this paper, we demonstrate that hybride Zn/Cd/Cu (core/shell) NZ obtained *via* the chemical bath deposition method (further – Zn/Cd/Cu^{bd}) possesses the ability to mimic reductase,

[a]*Institute of Cell Biology, National Academy of Sciences of Ukraine, 79005 Lviv, Ukraine. E-mail: stasuk_natalia@ukr.net; galina.gayda@gmail.com; gonchar@cellbiol.lviv.ua*

[b]*Drohobych Ivan Franko State Pedagogical University, 82100 Drohobych, Ukraine. E-mail: kavetskyy@yahoo.com*

[c]*The John Paul II Catholic University of Lublin, 20-950 Lublin, Poland*

© 2022 The Author(s). Published by the Royal Society of Chemistry

Table 1 R-like activities of the synthesized AEs in solution

No.	AE	Synthesis method	Specific activity, U mg^{-1}
1	Zn/Cu/Cd^{bd}	Chemical bath deposition on plate	32.7 ± 1.8
2	Ce/Cu^{bd}		14.3 ± 1.1
3	Pd/Cu^{bd}		0.27 ± 0.03
4	Cd/Cu^{cr}	Chemical reduction	3.60 ± 0.25
5	Ce/Pd^{cr}		0.81 ± 0.02
6	Cu/Pt^{cr}		1.63 ± 0.15
7	Ce^{cr}		1.50 ± 0.04
8	Pd/Cd^{cr}		3.24 ± 0.22

in particular, coenzyme-dependent selenite reductase. The synthesized selenite R-like NZ has been used for construction of a highly sensitive amperometric biosensor for selenite detection in water. Based on our findings, we envision that Zn/Cd/Cu^{bd} NZ can also be promising for remediation of waste waters by reducing Se(IV) to elemental selenium (Se^0) and for isolation of this element in pure form. The detailed study of effective R-like AEs, including Zn/Cd/Cu^{bd} NZ, may be useful in fundamental biological investigations, in particular, for elucidation of mechanisms of their interactions with living cells. R-like AEs may become potential tools in medicine not only for diagnostics and drug delivery, but also be used as pharmaceuticals (mimetics of antioxidant enzymes) in enzyme-therapy of different diseases caused by unbalance of redox processes in organism.[9–12,46–49]

Results and discussion

Obtaining and characterization of reductase mimetics

Synthesis and screening on pseudo-reductase activity. A number of metal-based composite materials were synthesized using the methods of chemical reduction (cr) and chemical bath deposition (bd) on plate as potential AEs. The synthesized compounds were screened on their ability to reduce ABTS$^{\cdot+}$ [2,2′-azinobis-(3-ethylbenzothiazoline-6-sulfonic acid) diammonium salt cation radical] in solution (Table 1). It was shown that several synthesized AEs, especially Zn/Cd/Cu^{bd} and Ce/Cu^{bd}, possessed the significant reductase-like (R-like) activities.

Morphological properties of the best reductase mimetics. The shape and size of the synthesized NZs were characterized by SEM. It was demonstrated (the data are not shown) that the sizes of all studied compounds do not satisfy the nanoscale criterion – to be less than 100 nm in all three dimensions. In some cases, they are nanoscale only in one dimension (needle), while in the other ones they exceed this criterion. Most likely, this is due to the aggregation of the initially formed NZs. To take into account this factor, we call NZs those materials whose nanoscale is confirmed by physical methods for at least one dimension.

The Zn/Cd/Cu^{bd}-NZ with the highest R-like activity was chosen for further detailed investigation by SEM coupled with X-ray microanalysis (SEM-XRM). As shown in Fig. 1a–c, NZ has three dimensional flower-like structures with the size of near 1 μm. The XRM images show the characteristic peaks for Cd0, Cu0 and Zn0 (Fig. 1d).

Catalytic properties of Zn/Cu/Cd^{bd} NZ

DPPH$^{\cdot}$ and ABTS$^{\cdot+}$ scavenging activity. The DPPH$^{\cdot}$ (1,1-diphenyl-2-picrylhydrazyl radical) and ABTS$^{\cdot+}$ assays have been widely used to determine the free radical-scavenging activity of various plant extracts and chemical compounds. DPPH$^{\cdot}$ is a stable free radical which, being dissolved in methanol, shows a characteristic absorption peak at 517 nm. The decrease in

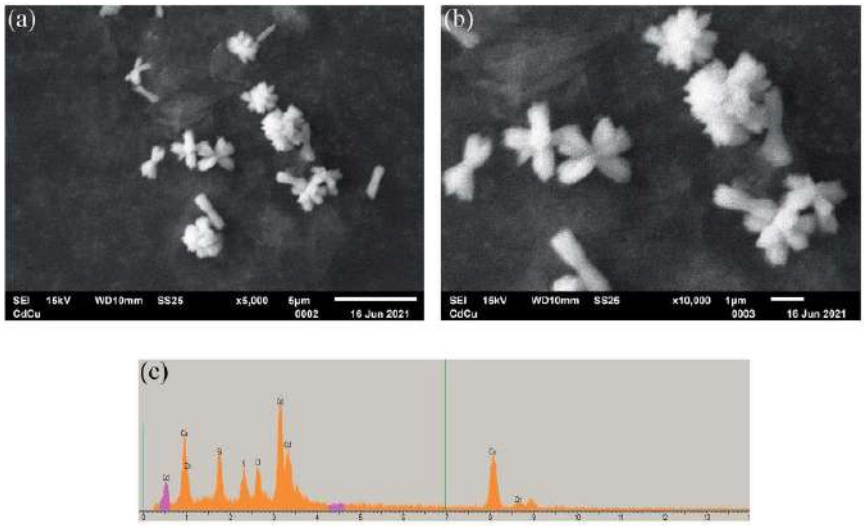

Fig. 1 Characteristics of the Zn/Cd/Cu^{bd} NZ: SEM images for 5000× magnification (scale bar 5 μm) (a) and 10 000× magnification (scale bar 1 μm) (b); X-ray spectral microanalysis (c). The accelerating voltage was 15 kV for all images.

© 2022 The Author(s). Published by the Royal Society of Chemistry

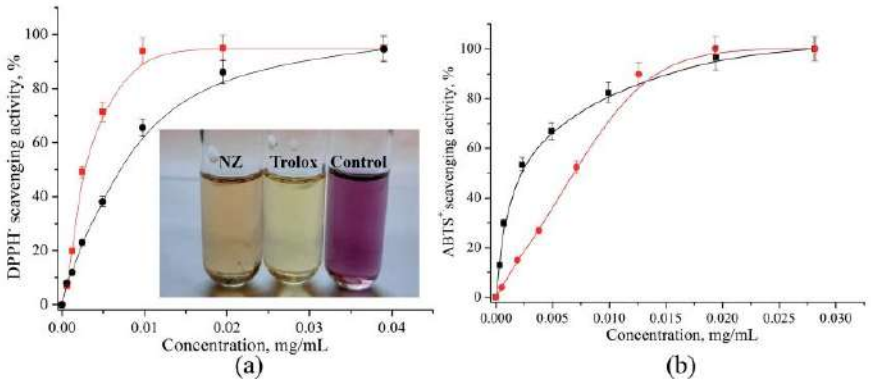

Fig. 2 Dependence of the analytical signal on concentration of Trolox (red) and Zn/Cd/Cu^{bd} NZ (black) in free radical scavenging tests: (a) spectrophotometric DPPH$^{\cdot}$ assay, (b) electrochemical ABTS$^{\cdot+}$ assay.

Table 2 Antioxidant activities (EC_{50}) in the samples of Zn/Cd/Cu^{bd} NZ, food products and Trolox determined *via* two methods

Species	EC_{50} (μg mL^{-1}), that estimated with using	
	DPPH$^{\cdot}$	ABTS$^{\cdot+}$
Zn/Cd/Cu^{bd} NZ	6.8 ± 0.2	6.9 ± 0.3
Trolox	2.7 ± 0.1	2.9 ± 0.2
Red wine, dry	2.9 ± 2.0	ND[a]
Bilberry	9.7 ± 0.1	10.5 ± 0.2
Cognac	12 ± 0.3	ND
Yogurt with chokeberry	13 ± 1.0	ND
Garnet	18 ± 2.5	19.3 ± 3.0
Tomatoes	26 ± 0.4	ND
Lemon	49 ± 0.3	ND
Milk	582 ± 3.4	ND

[a] Not done.

optical absorbance of DPPH$^{\cdot}$ radicals is caused by antioxidants due to the reaction between antioxidant molecules and the radical, which results in the scavenging of the radical by hydrogen donation. Antioxidant capacity estimated by the DPPH$^{\cdot}$ in solution was compared by the electrochemical method with ABTS$^{\cdot+}$. The monitored electrochemical signal was the cathodic current produced from reduction of the ABTS$^{\cdot+}$ radical at the applied potential −0.10 V *vs.* Ag/AgCl on the GE working electrode. The responses were obtained as a current–time plot. The peak currents from antioxidant samples were calibrated with Trolox as a standard in the concentration range of 0–0.03 mg mL^{-1}.

As demonstrated in Fig. 2a and b, Zn/Cd/Cu^{bd} NZ shows appreciable DPPH$^{\cdot}$ and ABTS$^{\cdot+}$ free radical scavenging activities at the selected range of concentrations. It was observed that the DPPH$^{\cdot}$ and ABTS$^{\cdot+}$ radical scavenging effect increases with the increase of the concentration of Zn/Cd/Cu^{bd} NZ. The results of the electrochemical ABTS$^{\cdot+}$ method reported in Trolox equivalent units were in good agreement with a classic spectrophotometric DPPH$^{\cdot}$ method. We have tested the samples of some plant foods (berries, vegetables, fruits) and beverages on their antioxidant capacity in comparison with Trolox as a standard. These activities were expressed as EC_{50} values and presented in Table 2.

The EC_{50} values calculated from DPPH$^{\cdot}$ and ABTS$^{\cdot+}$ assays ranged between 9.7–49 mg mL^{-1} for food products and 2.9–12 mg mL^{-1} – for beverages. The values of antioxidant activities determined by two different methods are very similar. It should be noted that the lower EC_{50} value indicates a higher antioxidant activity for the product. The antioxidant activity values determined by these two different assays (Table 2) revealed that among food products and beverages, the Zn/Cd/Cu^{bd} NZ has a stronger antioxidant power when compared to garnet, lemon or milk and a lower power when compared to red wine and the standard Trolox. The obtained EC_{50} data of food products are in good correlation with the data described in literature.[56]

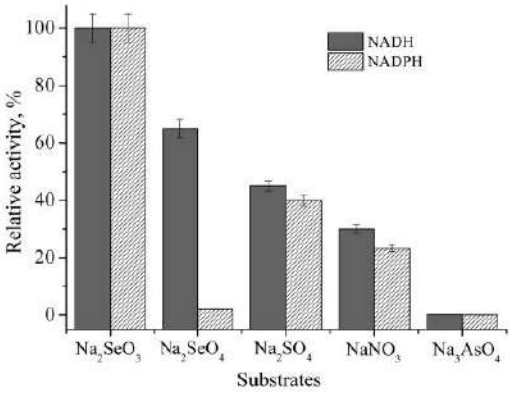

Fig. 3 Substrate and co-factor specificity of Zn/Cd/Cu^{bd} NZ in acetate buffer, pH 4.5. Substrates (1 mM): Na_2SeO_3, Na_2SeO_4, Na_2SO_4 $NaNO_3$ and Na_3AsO_4; cofactors (0.13 mM): NADH and NADPH.

© 2022 The Author(s). Published by the Royal Society of Chemistry

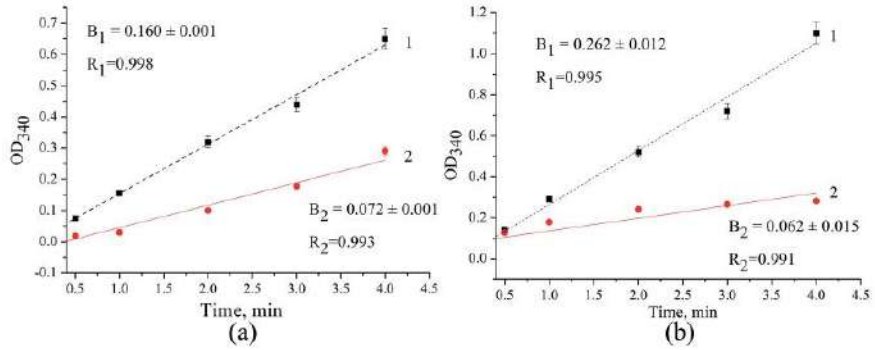

Fig. 4 The kinetic curves for selenite reduction in the mixture of Na_2SeO_3, NADH, ABTS (a) or DPPH (b) in acetate buffer, pH 4.5 in the presence (line 1) and in the absence of Zn/Cd/Cu^{bd} NZ (line 2).

Substrate specificity of pseudo-reductase in solution. The synthesized NZ was tested on its R-like activity toward different substrates using nicotinamide adenine dinucleotide reduced (NADH) or nicotinamide adenine dinucleotide phosphate reduced (NADPH) as cofactors of reductases (Fig. 3). This NZ possess a high R-like activity in the presence of NADH toward different substrates: Na_2SeO_3 (100%), Na_2SeO_4 (65%), Na_2SO_4 (35%), $NaNO_3$ (45%) and Na_3AsO_4 (less than 1%), whereas in the presence of NADPH it shows a lower R-like activity toward the same substrates: Na_2SeO_3 (100%), Na_2SeO_4 (2%), Na_2SO_4 (40%), $NaNO_3$ (23%) and Na_3AsO_4 (less than 1%).

We have found that the formation of elemental selenium (Se^0) in the presence of cofactors (NADH or NADPH), mediators of electron transfer (ABTS or DPPH), and Na_2SeO_3 as a substrate takes place even without the addition of NZ (Fig. 4a and b, lines 2). The addition of Zn/Cd/Cu^{bd} NZ activates this process (Fig. 4a and b, lines 1).

The efficiency factor (F) of selenite reduction/Se^0 formation for NZ was calculated as a relation of slope values ($F = B_1/B_2$) from the correspondent kinetic curves. In the presence of ABTS in reaction mixture (Fig. 4a), F_{ABTS} is 2.2, whereas in the presence of DPPH (Fig. 4b), the value of F_{DPPH} is 1.8 fold higher and achieves 4.2.

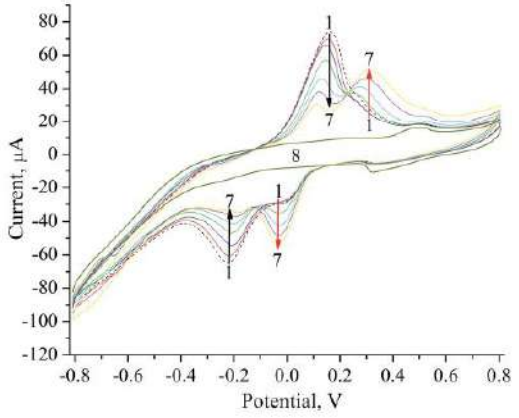

Fig. 5 Cyclic voltammograms of NZ/GE (1–7) and unmodified GE (8) in acetate buffer, pH 4.5 upon subsequent additions of Na_2SeO_3, μM: 0 (1), 8 (2), 16 (3), 32 (4), 64 (5), 150 (6), 300 (7, 8).

Construction, evaluation and application of amperometric sensor for selenite determination

Optimization of selenium sensing. The electrochemical characteristics of Zn/Cd/Cu^{bd}-NZ, immobilized on the surface of a graphite electrode (NZ/GE), were studied (Fig. 5). The comparison of cyclic voltammograms revealed a cathodic reduction peak at the potential of −50 mV. This peak is possibly related with the Se^0 formation on the electrode surface during the reduction of the added Na_2SeO_3.[51,52]

Formation of elemental selenium (Se^0) on the surface of NZ/GE was visually observed and proved by the SEM and X-ray microanalysis (Fig. 6). According to SEM images, Se^0 is generated as agglomerates with the sizes varying from 5 to 50 μm (Fig. 6a, d, e and g). Se^0 formation has been proved by X-ray microanalysis, which showed emission peaks at 1.37, 11.22, and 12.49 keV (Fig. 6b, c, f, h and l) corresponding to the SeL_α, SeK_α, and SeK_β transitions, respectively.

The general scheme of the reactions running on the electrode surface can be described as follows: SeO_3^{2-} ions diffuse to the Zn/Cd/Cu^{bd}-modified GE and are reduced to Se^0 in the presence of NADH and $ABTS^{\cdot+}$. In turn, the NADH cofactor is oxidized to NAD^+ and the $ABTS^{\cdot+}$ radical cation is reduced to ABTS releasing 4 electrons and providing a reversible process (Fig. 7). It was shown that the peaks at +300 mV and −50 mV are corresponded to the oxidation of Se^0 to SeO_3^{2-} and to the reduction of SeO_3^{2-} to Se^0, respectively. The obtained oxidation/reduction peaks for the pair of SeO_3^{2-}/Se^0 are in good agreement with the literature data.[53] It should be noted that the reduction SeO_3^{2-} to Se^0 on the Zn/Cd/Cu^{bd}/GE does not take place in the absence of NADH or ABTS (the data not shown).

Analytical characteristics of sensor. A chronamperometric analysis of Na_2SeO_3 at −50 mV is provided in Fig. 8. It is worth mentioning that no signals on Na_2SeO_3 at the unmodified electrode in the presence of NADH and ABTS were detected at

© 2022 The Author(s). Published by the Royal Society of Chemistry

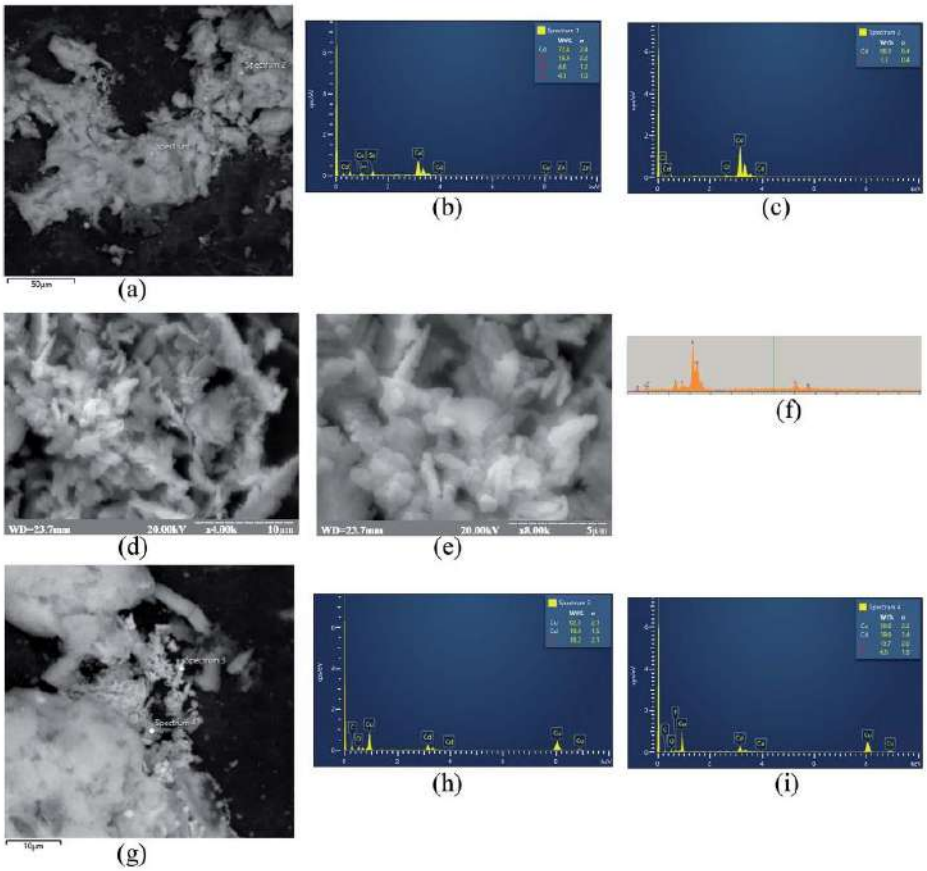

Fig. 6 Characteristics of Zn/Cd/Cu^{bd} NZ: SEM images for scale bar 50 μm (a), 10 μm (d and g), 5 μm (e) for 4000× (a, d and g) and 8000× (e) magnification; X-ray spectral microanalysis (b, c, f, h and i). The accelerating voltage was 20 kV for all images.

these conditions (see Fig. 5). The main characteristics of the SeO_3^{2-}-chemosensor were estimated (see Fig. 8b–d). As shown the maximal current of a chronoamperometric response of Zn/Cd/Cu^{bd}/GE on the analyte is 142.3 ± 3.0 μA (d = 3.05 mm, S = 7.07 mm^2) with a constant of semi-saturation (K_M^{app}) 1.25 ± 0.05 mM for Na_2SeO_3. The specific sensitivity for Zn/Cd/Cu^{bd}/GE is 1700 A M^{-1} m^{-2}.

Assay of selenite in real water samples. Se is one of the micronutrients for living organisms, although it is one of major concerns due to a narrow range between deficit and toxicity levels.[33,34] In natural environments, including ground water, Se mainly exists as anionic forms of selenate (SeO_4^{2-}) and selenite (SeO_3^{2-}). The presence of toxic selenite in drinking water at high concentrations is undesirable.[54,55] The number of microorganisms can metabolize selenite from ground water by biological reduction forming solid low toxic nanoparticles of elemental selenium (SeNPs).[33–36]

The levels of Se in groundwater and surface water usually range from 0.06 μg L^{-1} to about 400 μg L^{-1}, but in some areas, the Se concentration may to achieve 6000 μg L^{-1}.[54] Levels of Se in tap water samples from public water supplies around the world are usually much less than 10 μg L^{-1}, although they may exceed 50 μg L^{-1}.

The developed selenite specific sensor was tested on the model solution of water (after adding a known concentration of sodium selenite) as well as on the real sample of "Morshynska Antioxiwater, Se + Cr + Zn" mineral water. The results

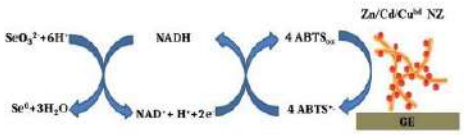

Fig. 7 Hypothetical principal scheme of functionality of the Zn/Cd/Cu^{bd}-based amperometric sensor for selenite.

© 2022 The Author(s). Published by the Royal Society of Chemistry

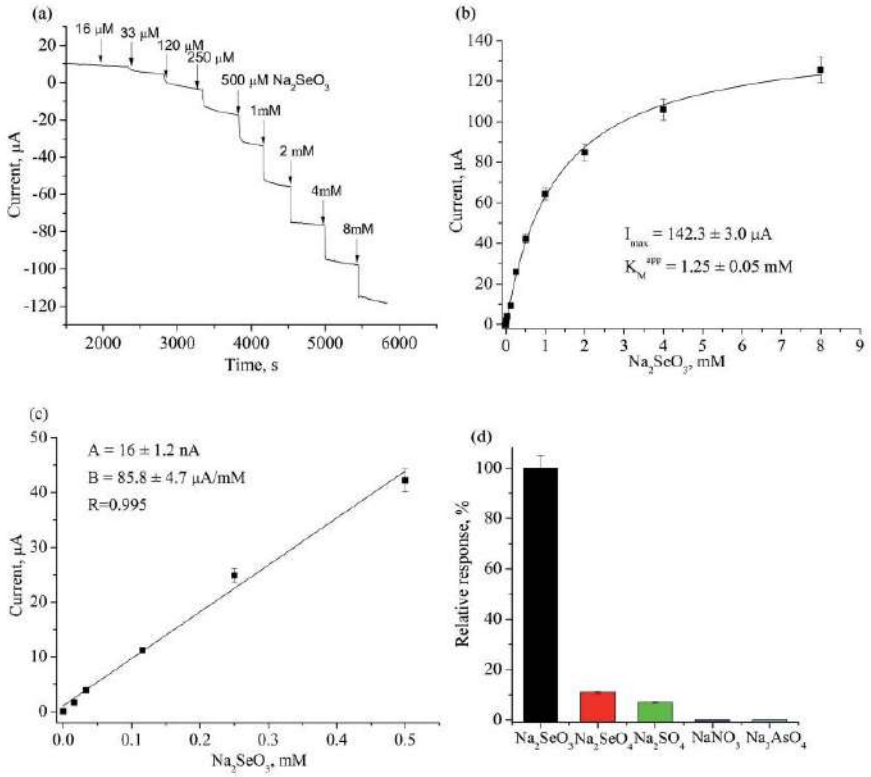

Fig. 8 Characteristics of Zn/Cd/Cu^{bd}/GE in 50 mM acetate buffer, pH 4.5: (a) chronamperometric current response upon subsequent additions of Na_2SeO_3; (b) dependence of amperometric signal on selenite concentration; (c) calibration graph for Na_2SeO_3 determination in linear range; (d) selectivity test for Zn/Cd/Cu^{bd}/GE towards different analytes (1 mM) in the presense of 0.13 mM NADH and 1 mM ABTS.

Table 3 Analysis of selenite in model and real samples

	Concentration of selenite, mg L^{-1}	
Sample	Sensor analysis	Added to the model sample or declared by producer
Model solution, CV,[a] %	46 ± 2.4, 5.4	43.3 ± 1.6 (added)
Mineral water "Morshynska", CV, %	0.0605 ± 0.003, 7.3	0.092[b] (declared)

[a] CV – coefficient of variation. Values are expressed as mean ± SD. [b] Total Se in the form of SeO_3^{2-} and Se^{2-}.

of estimation of SeO_3^{2-} in tested waters are presented in Table 3.

The reproducibility of the proposed analytical method is satisfactory: the coefficients of variation (CV) are less than 10%. It is worthwhile mentioning that the detected selenite contents in the water were close to those found by other authors (0.06–400 μg L^{-1}).[54] These results indicate that the developed Zn/Cd/Cu^{bd} NZ-based amperometric sensor can be utilized for a fast and simple assay of selenite in water.

Experimental

Materials and methods/reagents

Cerium(III) chloride, ascorbic acid, cadmium(II) chloride, chloroplatinic acid, copper(II) sulfate, zinc(II) sulfate, palladium chloride, sodium borohydride, 2,2′-azinobis-(3-ethylbenzothiazoline-6-sulfonic acid) diammonium salt (ABTS), 2,2-diphenyl-1-picrylhydrazyl (DPPH), cetrimonium bromide (CTAB), nicotinamide adenine dinucleotide reduced (NADH), nicotinamide adenine dinucleotide phosphate reduced

© 2022 The Author(s). Published by the Royal Society of Chemistry

(NADPH), Nafion (5% solution in 90% low-chain aliphatic alcohols), potassium persulfate and all other reagents and solvents used in this work were purchased from Sigma-Aldrich (Steinheim, Germany). The antioxidant standard was Trolox from Merck KGaA (Darmstadt, Germany). All reagents were of analytical grade and were used without further purification. All solutions were prepared using ultra-pure water obtained with the Milli-Q® IQ 7000 Water Purification system (Merck KGaA, Darmstadt, Germany).

Synthetic procedures

Synthesis of nanozymes by chemical reduction. NZs were synthesized by the reduction of metal ions from appropriate salts using ascorbic acid. The conditions of NZs synthesis are presented in Table 4. NZs were collected by centrifugation under 16 000*g* for 40 min (Hettich Micro-22R centrifuge), washed twice with water, and precipitated by centrifugation. Pellets were suspended in 1.0 mL water and stored until use at +4 °C.

The synthesis of core–shell NZs on stainless steel substrate was performed by chemical bath deposition method (bd) similar as reported earlier,[56,57] with some modifications. They include preparation of an aqueous bath containing 0.1 M solution of salt, namely, cadmium(II) chloride, palladium(II) chloride or cerium(III) chloride with the addition of aqueous NH_3 solution (28%) under constant stirring at room temperature with resultant pH ~ 12. Well cleaned Zn plate substrate was placed in reaction bath at room temperature for 20 h resulting in the direct growth of metallic nanowires on Zn substrate.

For the formation of core–shell Zn/Cd/Cu^{bd} NZs, the previously synthesized Cd/Zn thin film was vertically dipped into beaker containing 0.01 M copper sulphate solution making an angle of 45° with the wall of beaker. The reaction bath maintained at room temperature for 3 days resulting in the conversion of gray color cadmium film into brown color. The resulting Zn/Cd/Cu^{bd} NZs were washed several times with water, dried in air atmosphere and used for further characterization.

Morphological analysis of megazymes by scanning electron microscopy (SEM). Morphological analyses of the reductase-like (R-like) NZs were performed using a microanalyzer Hitachi S-3400N SEM. The Energy Dispersive X-ray Spectroscopy component is implemented with an EDAX EDS. The samples in different dilutions (2 μL) were dropped onto the surface of a silicon wafer and were dried at room temperature. The distance from the last lens of the microscope to the sample (WD) was 10 mm. The accelerator voltage was in the range of 20 to 40 eV.

Table 4 Methods of chemical synthesis of NZs

No.	NZ	Reaction mixture and conditions
1	Cd/Cu	5 mL 100 mM $CdCl_2$ + 10 mL 12.5 mM CTAB, vigorous stirring for 5 min at 20 °C followed by adding 0.2 mL 100 mM ascorbic acid and heating at 100 °C during 10 min; +5 mL 100 mM $CuSO_4$ followed by adding 0.2 mL 100 mM ascorbic acid, heating at 100 °C and stirring for 15 min at 20 °C
2	Ce/Pd	5 mL 100 mM $CeCl_3$ + 10 mL 12.5 mM CTAB, vigorous stirring for 5 min at 20 °C followed by adding 0.2 mL 100 mM ascorbic acid and heating at 100 °C during 10 min; +5 mL 100 mM $PdCl_2$ followed by adding 0.2 mL 100 mM ascorbic acid, heating at 100 °C and stirring for 15 min at 20 °C
3	Cu/Pt	5 mL 100 mM H_2PtCl_6 + 10 mL 12.5 mM CTAB, vigorous stirring for 5 min at 20 °C followed by adding 0.2 mL 100 mM ascorbic acid and heating at 100 °C during 10 min; +5 mL 100 mM $CuSO_4$ followed by adding 0.2 mL 100 mM ascorbic acid, heating at 100 °C and stirring for 15 min at 20 °C
4	Ce	5 mL 100 mM $CeCl_3$ + 10 mL 12.5 mM CTAB, vigorous stirring for 5 min at 20 °C followed by adding 0.2 mL 100 mM ascorbic acid and heating at 100 °C during 10 min
5	Cd/Pd	5 mL 100 mM $PdCl_2$ + 10 mL 12.5 mM CTAB, vigorous stirring for 5 min at 20 °C followed by adding 0.2 mL 100 mM ascorbic acid and heating at 100 °C during 10 min; + 5 mL 100 mM $CdCl_2$ followed by adding 0.2 mL 100 mM ascorbic acid, heating at 100 °C and stirring for 15 min at 20 °C

Determination of pseudo-enzymatic activities of nanomaterials in solution

ABTS-based method. Screening of the synthesized NZs on their R-like activities was done spectrophotometrically using ABTS cation radical ($ABTS^{\bullet+}$) as a chromogenic substrate. To obtain $ABTS^{\bullet+}$, 7 mM solution of ABTS was mixed with equal volume of 2.4 mM potassium persulfate solution, and the mixture was incubated during 12 h at room temperature in the dark. The resultant 3.5 mM $ABTS^{\bullet+}$ solution was diluted with methanol up to the optical density of approximately 0.70 at 734 nm.

The procedure of the assay was the following: 10 μL aqueous suspension of NZ was incubated in a glass tube with 1 mL of the chromogenic substrate ($ABTS^{\bullet+}$ solution). Addition of NZ to the substrate stimulated the discoloration from dark blue to colorless over time, indicating an pseudo-enzymatic reaction. The reaction was monitored kinetically during 5 min. The analytical results were statistically processed using the OriginPro 8.5 software.

The specific R-like activity was expressed in μmol min^{-1} mg^{-1} of NZ and calculated using the following formula:

$$\text{Specific capacity, U mg}^{-1} = \frac{\Delta D/\text{min} \times V_t \times N}{17 \times V_{AE} \times c}, \quad (1)$$

where ΔD_{734}/min – drop in optical density for 1 minute; V_t – the total volume of the reaction mixture in the cuvette, mL; 17 – millimolar extinction coefficient of the $ABTS^{\bullet+}$, mM^{-1} cm^{-1}; V_{AE} – aliquot of AE added, mL; c – mass concentration of NZ in added solution, determined by gravimetric method, mg mL^{-1}; N – dilution of NZ before adding to the reaction mixture; 1 unit (U) of activity corresponds to 1 μmole $ABTS^{\bullet+}$ reduced during 1 min under indicated conditions.

© 2022 The Author(s). Published by the Royal Society of Chemistry

DPPH-based method. In solution the antioxidant properties were determined *via* the DPPH˙-based free radical scavenging test according to modified method of Brand-Williams *et al.*[58] 0.04 mL Zn/Cd/Cu^{bd} solution in different concentrations (0.31, 0.62, 1.25, 2.5 and 5 mg mL^{-1}) was mixed with 1.2 mL freshly prepared DPPH˙ (1 mM in methanol) solution and vortexed thoroughly. Then the solution was incubated for 30 min at room temperature in the dark. The absorbance was recorded at 517 nm using UV-Vis spectrophotometer (Shimadzu, U-1860). When an antioxidant scavenges the free radicals by hydrogen donation, the colors in the DPPH˙ assay solution become lighter. DPPH (all the reagent except the sample) was used as a control and methanol was used as a blank solution. The free radical scavenging activity was expressed as the percentage of inhibition which was determined using the following formula (2):

$$\text{Percentage scavenging} = \frac{Z_p - Z_q}{Z_p} \times 100\%, \quad (2)$$

where Z_p is an optical density of control (all the reagent except the test sample), while Z_q is an optical density of the tested sample.

Electrochemical assay of the free radical scavenging activity was done using the ABTS$^{\bullet+}$ based method.[59]

Apparatus, measurements, and statistical analysis. The amperometric sensors were evaluated using constant-potential amperometry in a three-electrode configuration with an Ag/AgCl/KCl (3 M) reference electrode, a Pt-wire counter electrode and a graphite working electrode. Graphite rods (type RW001, 3.05 mm diameter) from Ringsdorff Werke (Bonn, Germany) were sealed in glass tubes using epoxy glue to form disk electrodes. Before sensor preparation, the GE was polished with emery paper and a polishing cloth using decreasing particle sizes of alumina paste (Leco, Germany). The polished electrodes were rinsed with water in an ultrasonic bath.

Amperometric measurements were carried out using a CHI 1200A potentiostat (IJ Cambria Scientific, Burry Port, UK) connected to a personal computer and performed in a batch mode under continuous stirring in an electrochemical cell with a 20 mL volume at 25 °C.

All experiments were carried out in triplicate trials. Analytical characteristics of the electrodes were statistically processed using the OriginPro 2021 software. The error bars represent the standard error derived from three independent measurements. Calculation of the apparent Michaelis–Menten constants (K_M^{app}) was performed automatically by this program according to the Lineweaver–Burk equation.

Immobilization of NZs onto electrodes, testing their electrochemical and R-like activity. For construction of the NZs-based electrode, 5 μL NZ suspension (1 mg mL^{-1}) was dropped onto the surfaces of GEs. After drying for 10 min at room temperature, the layer of NPs on the electrodes was covered with 5 μL Nafion solution. The electrodes were washed with corresponding buffer solutions before and after each measurement.

The electrochemical properties of the synthesized NZs were studied by cyclic voltammetry (CV) on the GEs in the range from −800 to +800 mV with the scan rate of 50 mV min^{-1}; the profiles of amperometric signals in increasing concentrations of Na_2SeO_3 were compared.

The monitored signal was the cathodic current produced from reduction of the ABTS$^{\bullet+}$ radical at the applied potential −0.10 V *vs.* Ag/AgCl on the GE working electrode. The responses were obtained as the current–time plot. The peak currents from antioxidant samples were calibrated using Trolox as a standard in concentration range 0–28 μg mL^{-1}.

Selenite ions assay in real samples. The constructed Zn/Cd/Cu^{bd} NZ-based amperometric sensor for selenite determination was tested on the real and model samples. Commercial mineral antioxiwater «Morshynska» (Morshyn, Ukraine), containing Se + Cr + Zn, was analysed using a standard addition test (SAT). A model sample is a fresh-prepared Na_2SeO_3 solution of exact concentration in distilled water. Each assay was performed for two dilutions of the sample and repeated 3 times. The analytical results were statistically processed using the OriginPro 2021 software.

Conclusions

In the current research, a number of nano- and microzymes based on transition and noble metals were synthesized by the reduction and chemical bath deposition methods. The antioxidant and radical-scavenging properties of the synthesized Zn/Cd/Cu^{bd} NZ were studied by its ability to reduce the DPPH˙ or ABTS$^{\bullet+}$ radicals in solution. The structure, size, morphology, composition, catalytic properties, and electrochemical activities of the chosen Zn/Cd/Cu^{bd} NZ in solution and in immobilized form on the electrode were characterized.

The novelty of the work is the following: (1) obtaining for the first time the nanozymes with a high reductase activity; (2) the discovery of the nanozyme with selenite-specific reducing activity; (3) the construction of selenite-selective chemosensor based on metal hybrid nanocomposite. Being sensitive, valid, low-cost, highly selective, the proposed nanozyme-based chemosensor would be promising in different fields of fundamental and practical science, including environmental chemistry, plant and animal biochemistry, nutrition, and medicine.

Because of a high antioxidant activity of the synthesized nanozymes, we plan to study in future the influence of the nanozymes *in vivo* on eucaryotic cells to test possible consequences of nanozymes' uptake on cell viability and redox-activity of the modified living cells.

Funding

This research was partially supported by the National Research Foundation of Ukraine (projects no. 2020.02/0100 "Development of new nanozymes as catalytic elements for enzymatic kits and chemo/biosensors" and 2021.01/0010 "Development of an enzymatic kit and portable biosensors for express-analysis of creatinine, a marker of acute functional disorders of the kidneys"), National Academy of Sciences of Ukraine (The program "Smart sensor devices of a new generation based on modern materials and technologies"; grant "New dual casein

© 2022 The Author(s). Published by the Royal Society of Chemistry

kinase 2 inhibitors and histone deacetylase for targeted tumor chemotherapy" for research laboratories/groups of young scientists in priority areas of science and technology in 2021–2022), and Ministry of Education and Science of Ukraine (projects no. 0120U103398, 0121U109539 and 0121U109543).

Author contributions

Nataliya Stasyuk and Galina Gayda: investigation, validation, writing – original draft, visualization. Taras Kavetskyy: methodology, formal analysis, visualization. Mykhailo Gonchar: conceptualization, supervision, writing – review & editing, project administration, funding acquisition, resources.

Conflicts of interest

There are no conflicts to declare.

Acknowledgements

The authors thank Dr I. Mat'ko (Institute of Physics, Slovak Academy of Sciences, Bratislava, Slovakia) and R. Serkiz (Institute of Cell Biology NAS of Ukraine, Lviv, Ukraine) for their help with SEM-XRM experiments.

References

1 H. Wei and E. Wang, *Chem. Soc. Rev.*, 2013, **42**, 6060–6093.
2 R. Tian, J. Xu, Q. Luo, C. Hou and J. Liu, *Front. Chem.*, 2021, **8**, 1–21, DOI: 10.3389/fchem.2020.00831.
3 J. Wu, X. Wang, Q. Wang, Z. Lou, S. Li, Y. Zhu, L. Qin and H. Wei, *Chem. Soc. Rev.*, 2019, **48**, 1004–1076.
4 N. Stasyuk, O. Smutok, O. Demkiv, T. Prokopiv, G. Gayda, M. Nisnevitch and M. Gonchar, *Sensors*, 2020, **20**, 4509–4550.
5 N. Alizadeh and A. Salimi, *J. Nanobiotechnol.*, 2021, **19**(1), DOI: 10.1186/s12951-021-00771-1.
6 Y. Huang, J. Ren and X. Qu, *Chem. Rev.*, 2019, **119**, 4357–4412.
7 A. A. Nayl, A. I. Abd-Elhamid, A. Y. El-Moghazy, M. Hussin, M. A. Abu-Saied, A. A. El-Shanshory and H. M. A. Soliman, *Trends Environ. Anal. Chem.*, 2020, **26**, e00087, DOI: 10.1016/j.teac.2020.e00087.
8 W. Wang and S. Gunasekaran, *TrAC, Trends Anal. Chem.*, 2020, 115841, DOI: 10.1016/j.trac.2020.115841.
9 N. E. Castillo, E. M. Melchor-Martínez, J. S. Ochoa Sierra, N. M. Ramírez-Torres, J. E. Sosa-Hernández, H. M. N. Iqbal and R. Parra-Saldívar, *Int. J. Biol. Macromol.*, 2021, **179**, 80–89.
10 R. Mahmudunnabi, F. Z. Farhana, N. Kashaninejad, S. H. Firoz, Y. B. Shim and M. J. A. Shiddiky, *Analyst*, 2020, **145**, 4398–4420, DOI: 10.1039/d0an00558d.
11 M. Kumawat, A. Umapathi, E. Lichtfouse and H. K. Daima, *Environ. Chem. Lett.*, 2021, **19**(6), 3951–3957.
12 S. Khan, M. Sharifi, S. H. Bloukh, Z. Edis, R. Siddique and M. Falahati, *Talanta*, 2021, **224**, 121805, DOI: 10.1016/j.talanta.2020.121805.
13 L. Gao, J. Zhuang, L. Nie, J. Zhang, Y. Zhang, N. Gu, T. Wang, J. Feng, D. Yang, S. Perrett and X. Yan, *Nat. Nanotechnol.*, 2007, **2**, 577–583.
14 F. Attar, M. G. Shahpar, B. Rasti, M. Sharifi, A. A. Saboury, S. M. Rezayat and M. Falahati, *J. Mol. Liq.*, 2019, **278**, 130–144.
15 B. Neumann and U. Wollenberger, *Sensors*, 2020, **20**, 3692, DOI: 10.3390/s20133692.
16 R. Fu, J. Zhou, Y. Wang, Y. Liu, H. Liu, Q. Yang, Q. Zhao, B. Jiao and Y. He, *ACS Appl. Bio Mater.*, 2021, **4**(4), 3539–3546.
17 H. Zhao, R. Zhang, X. Yan and K. Fan, *J. Mater. Chem. B*, 2021, **9**, 6939–6957.
18 F. Mancin, L. J. Prins, P. Pengo, L. Pasquato, P. Tecilla and P. Scrimin, *Molecules*, 2016, **21**(8), 1014, DOI: 10.3390/molecules21081014.
19 J. Chen, Q. Ma, M. Li, W. Wu, L. Huang, L. Liu, Y. Fang and S. Dong, *Nanoscale*, 2020, **12**, 23578–23585.
20 S. Biswas and A. Pal, *Mater. Today Commun.*, 2021, **28**, 102588.
21 R. D. Neal, R. A. Hughes, P. Sapkota, S. Ptasinska and S. Neretina, *ACS Catal.*, 2020, **10**(17), 10040–10045.
22 L. Lu, S. Zou and B. Fang, *ACS Catal.*, 2021, **11**(10), 6020–6058.
23 D. Besold, S. Risse, Y. Lu, J. Dzubiella and M. Ballauff, *Ind. Eng. Chem. Res.*, 2021, **60**(10), 3922–3935.
24 A. A. Nafiey, A. Addad, B. Sieber, G. Chastanet, A. Barras, S. Szunerits and R. Boukherroub, *Chem. Eng. J.*, 2017, **322**, 375–384.
25 R. Acharya, A. Lenka and K. Parida, *J. Mol. Liq.*, 2021, **337**, 116487.
26 H. Luck, in *Method of Enzymatic Analysis*, ed. H. U. Bergmeyer, Academic Press, New York and London, 1st edn, 1965, pp. 885–894.
27 F. Hollmann, D. J. Opperman and C. E. Paul, *Angew. Chem., Int. Ed. Engl.*, 2021, **60**(11), 5644–5665.
28 D. R. Lovley, *Annu. Rev. Microbiol.*, 1993, **47**, 263–290.
29 https://www.creative-biolabs.com/metalloreductase-family.html.
30 N. Butler and A. M. Kunjapur, *J. Biotechnol.*, 2020, **307**, 1–14.
31 H. Stolterfoht, D. Schwendenwein, C. W. Sensen, F. Rudroff and M. Winkler, *J. Biotechnol.*, 2017, **257**, 222–232.
32 L. Li, B. Zhang, L. Li and A. G. L. Borthwick, *J. Hazard. Mater.*, 2022, **422**, 126932.
33 E. P. Painter, *Chem. Rev.*, 1941, **28**, 179–213.
34 M. M. Stenchuk, L. B. Chaban and M. V. Gonchar, *Biopolym. Cell*, 2006, **22**(1), 3–17.
35 W. J. Hunter, *Curr. Microbiol.*, 2014, **69**(1), 69–74.
36 M. Wells, J. McGarry, M. M. Gaye, P. Basu, R. S. Oremland and J. F. Stolz, *J. Bacteriol.*, 2019, **201**(7), e00614-18.
37 L. J. Yanke, R. D. Bryant and E. J. Laishley, *Anaerobe*, 1995, **1**(1), 61–67.
38 D. F. Ackerley, C. F. Gonzalez, M. Keyhan, R. Blake and A. Matin, *Environ. Microbiol.*, 2004, **6**, 851–860.
39 A. G. O'Neill, B. A. Beaupre, Y. Zheng, D. Liu and G. R. Moran, *Appl. Environ. Microbiol.*, 2020, **86**(22), e01758-20.

© 2022 The Author(s). Published by the Royal Society of Chemistry

40 J. C. Begara-Morales, M. Chaki, R. Valderrama, C. Mata-Pérez, M. N. Padilla-Serrano and J. B. Barroso, in *Plant Life Under Changing Environment*, ed. D. K. Tripathi, *et al.*, Elsevier, Academic Press, 2020, ch. 29, pp. 735–754.
41 D. J. Richardson, R. van Spanning and S. J. Ferguson, in *Biology of the Nitrogen Cycle*, ed. H. Bothe, S. Ferguson and W. E. Newton, Elsevier, Elsevier Science, 1st edn, 2006, ch. 3.
42 M. Guiral, L. Prunetti, C. Aussignargues, A. Ciaccafava, P. Infossi, M. Ilbert, E. Lojou and M.-T. Giudici-Orticoni, in *Advances in Microbial Physiology*, ed. R. K. Poole, Academic Press, New York, 2012, vol. 61, ch. 4, pp. 125–194.
43 Z. Liang, H. Guo, G. Zhou, K. Guo, H. Lei, W. Zhang, H. Zheng, U.-P. Apfel and R. Cao, *Angew. Chem.*, 2021, **60**(15), 8472–8476.
44 A. A. Vernekar and G. Mugesh, *Chem.–Eur. J.*, 2012, **18**, 15122–15132.
45 K. Li, R. Qin, K. Liu, W. Zhou, N. Liu, Y. Zhang, S. Liu, J. Chen, G. Fu and N. Zheng, *ACS Appl. Mater. Interfaces*, 2021, DOI: 10.1021/acsami.1c11548.
46 S. Singh, S. Ghosh, V. K. Pal, M. Munshi, P. Shekar, D. T. Narasimha Murthy, G. Mugesh and A. Singh, *EMBO Mol. Med.*, 2021, **13**(5), e13314, DOI: 10.15252/emmm.202013314.
47 M. V. Irazabal and V. E. Torres, *Cells*, 2020, 9(6), 1342, DOI: 10.3390/cells9061342.
48 D. Jiang, D. Ni, Z. T. Rosenkrans, P. Huang, X. Yan and W. Cai, *Chem. Soc. Rev.*, 2019, **48**, 3683–3704.
49 D. Bartolini, A. M. Stabile, S. Bastianelli, D. Giustarini, S. Pierucci, C. Busti, C. Vacca, A. Gidari, D. Francisci, R. Castronari, A. Mencacci, M. Di Cristina, R. Focaia, S. Sabbatini, M. Rende, A. Gioiello, G. Cruciani, R. Rossi and F. Galli, *Redox Biol.*, 2021, **45**, 102041.
50 M. Chochevska, E. J. Seniceva, S. K. Veličkovska, G. Naumova-Letia, V. Mirčeski, J. M. F. Rocha and T. Esatbeyoglu, *Microorganisms*, 2021, **9**(9), 1946.
51 Y. Lai, F. Liu, J. Li, Z. Zhang and Y. Liu, *J. Electroanal. Chem.*, 2010, **639**, 187–192.
52 S. Seyedmahmoudbaraghani, S. Yu, J. Lim and N. V. Myung, *Front. Chem.*, 2020, **8**, 785.
53 A. A. Vernekar and G. Mugesh, *Chem.–Eur. J.*, 2012, **18**, 15122–15132.
54 https://www.who.int/water_sanitation_health/dwq/chemicals/selenium.pdf.
55 S. B. Goldhaber, *Regul. Toxicol. Pharmacol.*, 2003, **38**, 232–242.
56 O. Demkiv, N. Stasyuk, R. Serkiz, G. Gayda, M. Nisnevitch and M. Gonchar, *Appl. Sci.*, 2021, **11**, 777, DOI: 10.3390/app11020777.
57 S. Patil, S. Raut, R. Gore and B. Sankapal, *New J. Chem.*, 2015, **39**, 9124–9131.
58 W. Brand-Williams, M. E. Cuvelier and C. Berset, *LWT–Food Sci. Technol.*, 1995, **28**, 25–30.
59 R. Chaisuksant, K. Damwan and A. Poolkasem, *Acta Hortic.*, 2012, **943**, 297–302.

© 2022 The Author(s). Published by the Royal Society of Chemistry

Оригінал доступний за посиланням:
https://pubs.rsc.org/en/content/articlelanding/2022/ra/d1ra08127f

3.3. Біосинтез металевих наночастинок клітинами дріжджів *O. polymorpha* та застосування їх в флуоресцентному аналізі.

Анотація: *Наночастинки металів (НЧ) є важливими об'єктами нанотехнологій завдяки перспективам їхнього застосування у промисловості й медицині. Металеві НЧ можуть бути отримані різними фізико-хімічними методами, а також «зеленим» синтезом. У даній роботі нами показано, що термотолерантні дріжджі O. polymorpha можуть бути використані в ролі біологічного інструмента для «зеленого» синтезу наночастинок золота (АиНЧ) з тетрахлораурату (ТХА). Нами вивчено процеси редукції ТХА дріжджовою культурою та формування позаклітинних стабільних біоАиНЧ. Характеристику отриманих біоАиНЧ здійснено із застосуванням методів трансмісійної електронної мікроскопії, сканувальної електронної мікроскопії, флуоресцентної мікроскопії, УФ-видимої адсорбційної спектроскопії. Вивчено вплив різних параметрів, зокрема, часу та концентрації ТХА, на формування АиНЧ. Отримані результати є важливими для фундаментальної та прикладної біологічної науки, особливо для досліджень молекулярних механізмів захисту клітини від стресу, спричиненого токсичною сполукою, а також для розробки нових ефективних і економічно вигідних методів одержання нових наноматеріалів.*

ISSN 0206-5657. Вісник Львівського університету. Серія біологічна. 2016. Випуск 73. С. 96–102
Visnyk of the Lviv University. Series Biology. 2016. Issue 73. P. 96–102

THE "GREEN" SYNTHESIS OF GOLD NANOPARTICLES BY THE YEAST *HANSENULA POLYMORPHA*

N. Stasyuk[1], G. Gayda[1*], R. Serkiz[2], M. Gonchar[1]

[1]Institute of Cell Biology, NAS of Ukraine
14/16, Drahomanov St., Lviv 79005, Ukraine
[2]Ivan Franko National University, Scientific-technical and Educational Center of Low Temperature Studies
50, Drahomanov St., Lviv 79005, Ukraine
*e-mail:*galina.gayda@gmail.com*

Metallic nanoparticles (NPs) are important objects of nanotechnology due to their potential utilization in industry and medicine. Metallic NPs can be obtained through different physics-chemical methods as well as through "green" synthesis. In this research, the thermotolerant yeast *Hansenula polymorpha* was used as a biological tool for the "green" synthesis of gold NPs (AuNPs) from tetrachloroaurate (TCA). The processes of TCA reduction with yeast culture and extracellular formation of the stabile bioAuNPs were studied. The methods of transmission electron microscopy, scanning electron microscopy, fluorescent microscopy, UV-visible absorption spectroscopy were used to characterize the final products. The influence of various parameters, namely, time and concentration of TCA on the generation of AuNPs, was investigated. Our findings might be eventually interesting for fundamental and applied biological sciences, in particular, for the study of molecular mechanisms of cell protection from stress, caused by exposure to toxic compounds, as well as for the development of the novel effective and economical methods for obtaining new nanomaterials.

Keywords: Nanomaterials, bionanoparticles of gold, "green" synthesis, yeast *Hansenula polymorpha*.

Recent advances in nanotechnology have enabled the exploration of nanomaterials for diverse applications. Metallic nanoparticles (NPs) play a significant role in nanotechnology due to their potential utilization in industry and medicine [15]. Metallic NPs can be synthesized through different methods, including "green" reduction of correspondent ions [21]. Among the variety of nanomaterials, gold nanoparticles (AuNPs) are of considerable interest due to their versatility and potential use in chemistry, biology, and medicine. AuNPs possess numerous advantages, such as low cytotoxicity, facile modification of their surfaces, straightforward synthetic processes and biocompatibility [2, 5]. After cellular uptake, NPs can act as tiny, precise and powerful heaters (thermal scalpels) to kill cancer [3, 20], and they are capable of inducing apoptosis in B-chronic lymphocytic leukemia [13]. Such novel properties make metal NPs an ideal nanomaterial for promising applications in biological analysis and imaging, drug delivery, environmental monitoring, industrial catalysis, and electronic devices [6].

Due to their toxicity, NPs of noble metals have perspectives for pharmacology. However, despite their increasing impact on the market, many relevant issues are still open. These include the molecular mechanisms governing the NPs-cell interactions, the physico-chemical parameters underlying their toxicity to different types of cells, the lack of standardized methods and materials, and the uncertainty in the definition of general strategies to develop smart antibacterial drugs and devices based on NPs [12, 19].

The biosynthesis of NPs using microorganisms as emerging bionanotechnology has received considerable attention due to a growing need in environmentally friendly technologies [23]. Furthermore, the green synthesis of metallic NPs offer better manipulation, stabilization, and control over the crystal growth due to slower kinetics [17-18]. Many plants, polysaccharides, bacteria,

© Стасюк Н., Гайда Г., Серкіз Р., Гончар М., 2016

fungi, yeasts, DNA, RNA, proteins, and polypeptides are known to produce nanostructured mineral crystals and metallic NPs with the properties similar to chemically synthesized materials, while exercising strict control over size, shape and composition of the particles. Biological agents secrete a great deal of enzymes that bring about enzymatic reduction of metallic ions [4, 11, 16, 22].

The exact mechanism for the NPs "green" synthesis has not yet been elucidated in detail [10, 14].

In our recent experiments [24], different types of mono- and bi-metallic NPs of noble metals were synthesized by chemical methods and characterized.

In the current manuscript, we describe the methods of AuNPs biosynthesis using yeast *H. polymorpha* as a reducing and protecting agent, as well as the characteristics of resulting bioAuNPs (further — bioNPs). We propose our conception of the extracellular "green" synthesis and stabilization of bioNPs which is based on these results and earlier obtained data.

Materials and methods

Tetrachloroauric acid trihydrate (TCA), sodium hydroxide, inorganic salts, chloroform and Butvar solution B-98 were purchased from Sigma-Aldrich, USA. All buffers and standard solutions were prepared using the water purified by the Milli-Q system (Millipore).

The size and structure of NPs were studied with Atomic Force Microscopy (AFM), Scanning electron microscopy (SEM), transmission electron microscopy (TEM) and UV-Visible spectroscopy as described earlier [24].

As a tool for the "green" synthesis of AuNPs the recombinant strain of the yeast *H. polymorpha* NCYC495-pGAP1-HsARG1 (*leu2car1 Sc:LEU2*) was used. The cells were cultivated as described in detail in our previous paper [23].

The biosynthesis of AuNPs by cell culture was performed according to the following procedure: after reaching the exponential growth phase, the cells were supplemented with TCA to the final concentration of 0.5 – 1 mM (control cells without TCA addition) and incubated up to 5 days. Each experiment was performed in triplicate and repeated at least three times.

The process of TCA reduction to Au^0 was monitored daily by sampling an aliquot of the tested sample and recording its absorption spectrum as well as TM, AFM and SEM.

Statistic treatment of measurement's results and the level of correlation between the values of the results obtained by different analytical methods will be calculated by Origin 8.0 and Microsoft Excel.

Results and discussion

The first brief characteristics of the process of TCA reduction and bioNPs generation were obtained by visual observation and UV-Vis absorption spectra (UVAS) (Fig. 1). The colour of the cell's suspension changed to dark red in comparison with that of the control one (Fig. 1 a, 1-2). The spectrum of the dark red cultural liquid (CL) - supernatant after cells removal has a peak of plasmon resonance at 540 nm (Fig. 1, b, 1), which is specific for AuNPs [1]. At the same time, the color of precipitated cells also changed (Fig. 1, a, 1*) – as a result of AuNPs accumulation inside the cells and formation of NPs-modified cells (further – cell-NPs).

To get the quick estimation of the sizes of metallic particles synthesized and to study their composition, SEM microscopy and XRM analysis were performed (Fig. 2). Fig. 2, a-b proves the generation of a large amount of individual spherical NPs in the cell culture, cultivated for 2 days in the presence of 1 mM TCA. XRM analysis of these NPs based on SEM data (indicated by the arrow in Fig. 2, b) proves the appearance outside the cells of Au^0 with characteristic peaks Kα at 2.1 keV (Fig. 2, c).

The more complex Au^0-containing structures on the surface of the cells, clusters with the size of 2 to 2.5 μm, are demonstrated in Fig. 2, d-f. The sizes of these clusters ranged from 50 to 100 μm. XRM analysis of these NPs based on SEM data (indicated by the arrow in Fig. 2, e) proves the appearance of Au^0 (Fig. 2, g). The cluster was reported to consist of glutatione, nitrate reductase and other proteins involved in bioreduction and stabilization of the formed bioNPs [9, 11].

Thus, the SEM and XRM results demonstrate the generation of AuNPs outside the cells in cell culture, incubated with TCA under growth conditions.

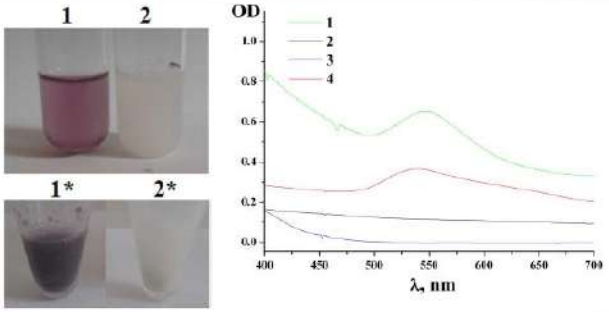

Fig. 1. BioNPs formation: *a* – images of the cells suspensions (*1*, *2*) and of the pellets of the corresponding cells (*1**, *2**); *b* – UVAS of CL (*1*, *2*) and control solutions (*3*, *4*). The cells were cultivated in the presence of 1 mM TCA(*1*) and without its addition (*2*); water solutions of initial 1 mM TCA(*3*) and the chemically synthesized AuNPs (*4*)

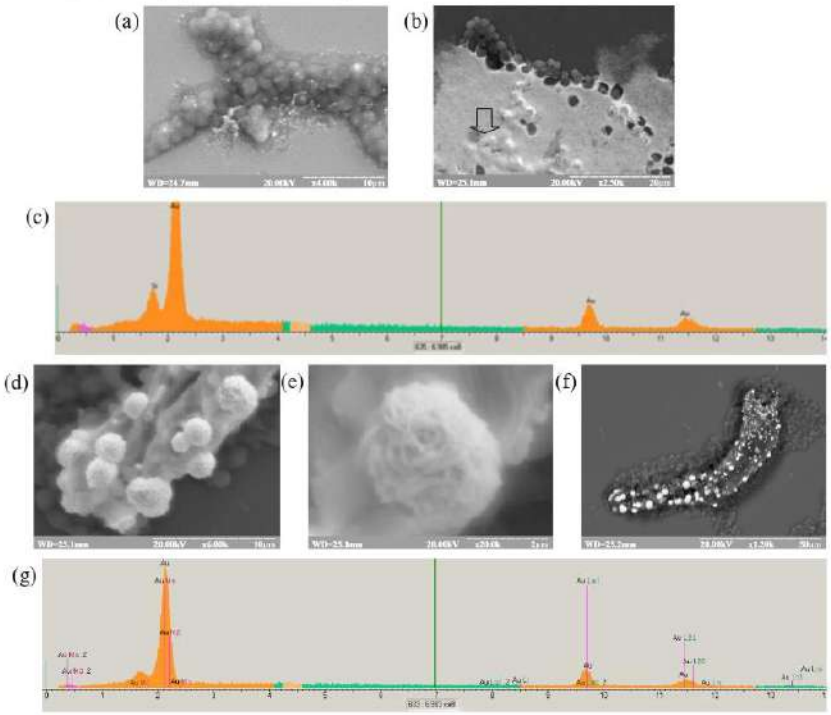

Fig. 2. Characteristics of bioAuNPs, synthesized "*in vivo*"(cultivated for 2 days in the presence of 1 mM TCA): SEM micrographs *(a, b, d-f)* and X-ray-spectral characteristics (c, *g*).

The exact size of the extracellular bioNP was estimated by the AFM method: the values of the average diameter were in the range of 20 – 40 nm (data not shown).

We assume that AuNPs synthesis takes place outside the cells due to TCA reduction with organic metabolites of yeast culture followed by bioNPs formation and stabilization. Then bioNPs penetrate through the cell wall and accumulate inside the cell. The results of TEM analysis have confirmed this suggestion (Fig. 3, a – b). It is worth mentioning that bioNPs, being in a rather high concentration (1 mM) after the penetration into a cell, cause the loss of cells-NPs ability to grow in agar medium (Fig. 3).

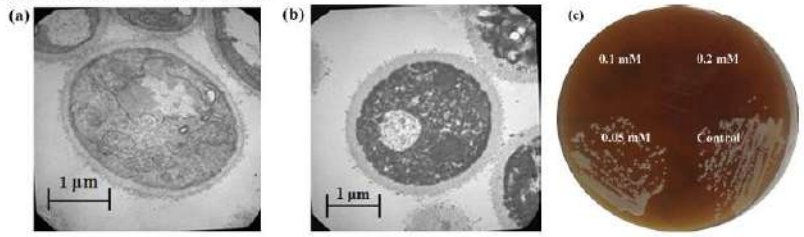

Fig. 3. Characteristics of the cells-NPs (b, c) in comparison with the control cells (*a, c*): Cells-NPs as well as conterol cells were cultivated during 4 days in the presence of 1 mM TCA (b) and 0.05 mM TCA, then aliquots of resulted cells were analysed by TEM (a, b) and growth ability (c)

In our previous research we have demonstrated that chemically synthesized NPs of noble metals [24], being in minimal concentration, proved to be non-toxic for the cell: under 3-day cultivation with 0.06 mM NPs, the yeast cells did not significantly affect either the dynamics of growth or enzyme (arginase) activity in cell free-extracts. We have demonstrated that the NPs uptake by cells was dependent on the concentration of NPs, exposure time and particles sizes. According to SEM- and TEM studies, AuNPs were shown to accumulate inside the cell [24].

It is worth mentioning that our conception of the extracellular formation of bioNPs is based on our previous results. It was discovered that the yeast *Pichia guilliermondii* is able to reduce chromate extracellularly with the formation of stable soluble Cr(III or V)-biocomplexes - bioNPs of Cr_2O_3 [7-9].

Fig. 4 (a-d) demonstrates the generation of the spherical clusters formed during bioreduction. According to the data of X-Ray spectral microanalysis (Fig. 4, e-f), these clusters consist of organic molecules which enveloped the AuNPs. The sizes of the clusters ranged from 6 to 10 µm.

It should be mentioned that the images in Fig. 4, c and d are identical, differing only in the shooting mode on SEM device: in Fig. 4, d micrographs are presented in the "compo" mode. This mode allows differentiating the nature of components: all organic atoms do not shine, although inorganic (AuNPs) ones glow brightly. These results were confirmed by the X-Ray spectral analysis (Fig. 4, e, f). The XRM data of AuNPs (which are glowing brightly in Fig. 4, d) have proved the formation of Au^0-containig compounds (Fig. 4, e). The dark grey color of the spherical cluster presented in Fig. 4, c corresponds to the molecules which contain atoms of C, O *etc* (Fig. 2, e).

Thus, the yeast *Hansenula polymorpha* was shown to be a promising tool for the development of a simple cost-effective method to obtain gold bioNPs by reducing toxic TCA.

We have demonstrated the extracellular generation of bioAuNPs of different sizes (20-40 nm) and shapes by the yeast *H. polymorpha*. The optimal conditions (concentration of inorganic ions and incubation time) required for the AuNPs formation were chosen. The nanosize and structure of NPs were proved using scanning, atomic force and transmission microscopy. The advantage of the "green" approach consists in the rapid growth of yeasts with a high-yield generation of AuNPs outside the cell, providing for the economic efficiency of the method.

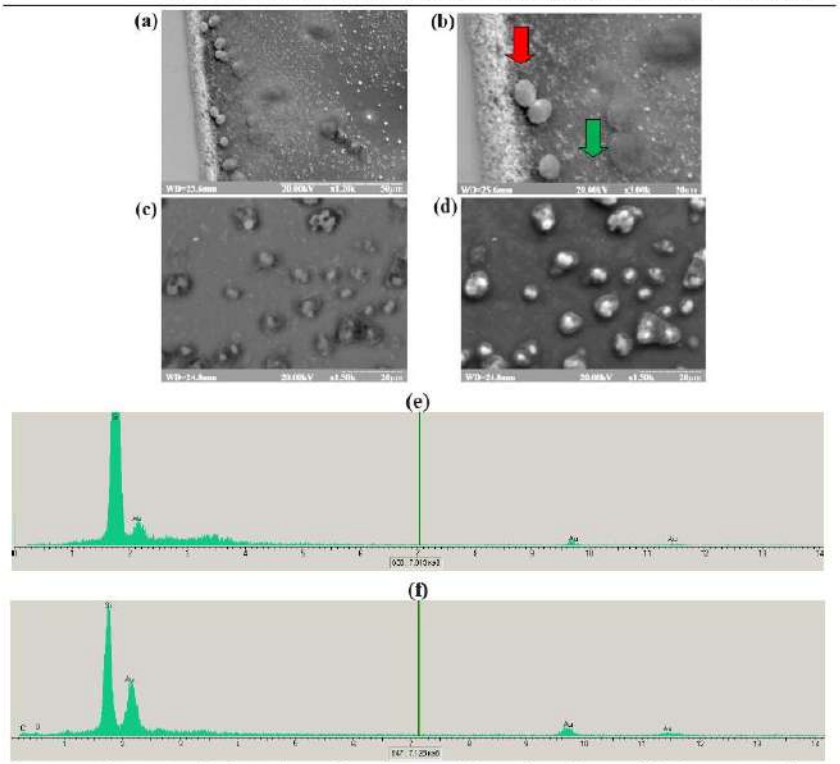

Fig. 5. SEM images (a – d) of Au-clusters formed extra-cellulary after cells growth in the presence of TCA during 4 days. X-ray-spectral characteristics (e, f) of the samples, indicated by red and green arrows, respectively

Acknowledgments: This work was financially supported by NAS of Ukraine (program "Sensors for Medical, Environmental, Industrial, and Technological Needs", by fellowship of President of Ukraine for young scientists (N. Stasyuk) in 2016 and by Ministry of Education and Science of Ukraine, International scientific-technical cooperation with NATO (Project CBP. NUKR.SFP 984173).

REFERENCES

1. *Brust M., Walker M., Bethell D.* et al. Synthesis of thiol-derivatised gold nanoparticles in a two-phase Liquid–Liquid system. // J. Chem. Soc. Chem. Commun. 1994. Vol. 7. P. 801-802.
2. *Dreaden E.C., Alkilany A. M., Huang X.* et al. The golden age: gold nanoparticles for biomedicine // Chem. Soc. Rev. 2012. Vol. 41. P. 2740-2779.
3. *El-Sayed I. H., Huang X., El-Sayed M. A.* Selective laser photo-thermal therapy of epithelial carcinoma using anti-EGFR antibody conjugated gold nanoparticles // Cancer. Lett. 2006. Vol. 239. P. 129-135.
4. *Faramarzi M. A., Sadighi A.* Insights into biogenic and chemical production of inorganic nanomaterials and nanostructures // Adv. Colloid Interface Sci. 2013. Vol. 180. P. 189-190.

5. *Golubeva O., Shamova O., Orlov D.* et al. Study of antimicrobial and hemolytic activities of silver nanoparticles prepared by chemical reduction // Glass Physics and Chemistry 2010. Vol. 36, N 5. P. 628-634.
6. *Jain P.K., Huang X., El-Sayed I. H., El-Sayed M. A.* Noble metals on the nanoscale: optical and photothermal properties and some applications in imaging, sensing, biology, and medicine // Acc. Chem. Res. 2008. Vol. 41, N 12. P. 1578-1586.
7. *Ksheminska H. P., Honchar T. M., Gayda G. Z., Gonchar M. V.* Extra Cellular Chromate Reducing Activity of the Yeast Cultures // Cent Eur. J. Biol. 2006. Vol. 1, N 1. P. 137-149.
8. *Ksheminska H., Honchar T., Usatenko Y.* et al. The Chromate Resistance Phenotype of Some Yeast Mutants Correlates with a Lower Level of Cr(V)-Species Generated in the Extra-Cellular Medium // BioMetals. 2010. Vol. 23. P. 633.
9. *Ksheminska H. P., Gayda G. Z., Ivash M. F., Gonchar M. V.* Chromate-Resistant Mutants of the Yeast *Pichia guilliermondii*: Selection and Properties // Mikrobiologiya. 2011. Vol. 80, N 3. P. 314-325.
10. *Kumar S. A., Ayoobul A. A., Absar A., Khan M. I.* Extracellular by biosynthesis of CdSe quantum dots by the fungus // J. Biomed. Nanotechnol. 2007. Vol. 3. P. 190-194.
11. *Mandal D., Bolander M.E., Mukhopadhyay D.* et al. The use of microorganisms for the formation of metal nanoparticles and their application // Appl. Microbiol. Biotechnol. 2006. Vol. 69, N 5. P. 485-492.
12. *Mironava T., Hadjiargyrou M., Simon M.* et al. *M.* Gold nanoparticles cellular toxicity and recovery: effect of size, concentration and exposure time // Nanotoxicology. 2010. Vol. 4. P. 120-137.
13. *Mukherjee P., Ahmad A., Mandal D.* et al. Bioreduction of $AuCl_3^-$ ions by the fungus, Verticillium sp. and surface trapping of the gold nanoparticles formed // Angew. Chem. Int. Ed. 2001. Vol. 40, N 19. P. 3585-3588.
14. *Mukherjee P., Bhattacharya R., Bone N.* et al. Potential therapeutic application of gold nanoparticles in B-Chronic lymphocytic leukemia (BCLL): enhancing apoptosis // J. Nanobiotech. 2007. Vol. 5. P. 4-12.
15. *Naik A. B., Selukar N. B.* Role of nanotechnology in medicine. Everyman's // Sci. 2009. Vol. 44. P. 151-153.
16. *Ramezani F., Ramezani M., Talebi S.* Biosynthesis of metal nanoparticles by microorganisms // NANOCON. 2007. P. 1-7.
17. *Panda T., Deepa K.* Biosynthesis of gold nanoparticles // J. Nanosci. Nanotechnol. 2011. Vol. 11. P. 10279-10294.
18. *Park Y., Hong Y.N., Weyers A.* et al. Polysaccharides and phytochemicals: a natural reservoir for the green synthesis of gold and silver nanoparticles IET // Nanobiotechnol. 2011. Vol 5. P. 69-78.
19. *Rizzello L., Pompa P. P.* Nanosilver-based antibacterial drugs and devices: mechanisms, methodological drawbacks, and guidelines // Chem. Soc. Rev. 2014. Vol. 43. P. 1501-1518.
20. *Salata O. V.* Applications of nanoparticles in biology and medicine // J. Nanobiotechnology 2004, 2: 3-7.
21. *Sarkar R., Kumbhakar P., Mitra A. K.* Green synthesis of silver nanoparticles and its optical properties // Digest Journ. Nanomater. Biostruct. 2010. Vol. 5. P. 491-496.
22. *Sarkar J., Roy S. K., Laskar A.* et al. Bioreduction of chloroaurate ions to gold nanoparticles by culture filtrate of Pleurotus sapidus Quel // Materials Letters. 2013. Vol. 92. P. 313-316.
23. *Stasyuk N., Gayda G., Gonchar M.* L-arginine-selective microbial amperometric sensor based on recombinant yeast cell over-producing human liver arginase I // Sens. Actuat. B., 2014. Vol. 204. P. 515-521.
24. *Stasyuk N. Ye., Gayda G. Z., Serkiz R. Ja., Gonchar M. V.* Cell Imaging with Fluorescent Bi-Metallic Nanoparticles // Journ. Adv. in Chem. 2015. Vol. 11, N 4. P. 3499-3511.

Стаття: надійшла до редакції 28.07.16
доопрацьована 5.09.16
прийнята до друку 6.09.16

"ЗЕЛЕНИЙ" СИНТЕЗ НАНОЧАСТИНОК ЗОЛОТА ДРІЖДЖАМИ *HANSENULA POLYMORPHA*

Н. Стасюк[1], Г. Гайда[1*], Р. Серкиз[2], М. Гончар[1]

[1]Інститут біології клітини НАН України
вул. Драгоманова, 14/16, Львів 79005, Україна
[2]Львівський національний університет імені Івана Франка
вул. Драгоманова, 50, Львів 79005, Україна
*e-mail:*galina.gayda@gmail.com*

Наночастинки металів (НЧ) є важливими об'єктами нанотехнологій завдяки перспективам їхнього застосування у промисловості й медицині. Металеві НЧ можуть бути отримані різними фізико-хімічними методами, а також «зеленим» синтезом. У даному дослідженні термотолерантні дріжджі *Hansenula polymorpha* було використано як біологічний інструмент для «зеленого» синтезу наночастинок золота (AuНЧ) з тетрахлораурату (ТХА). Було досліджено процеси редукції ТХА дріжджовою культурою та формування позаклітинних стабільних біоAuНЧ. Характеристику кінцевого продукту було здійснено із застосуванням методів трансмісійної електронної мікроскопії, скануючої електронної мікроскопії, флуоресцентної мікроскопії, УФ-видимої адсорбційної спектроскопії. Було вивчено вплив різних параметрів, зокрема, часу та концентрації ТХА, на формування AuНЧ. Наші результати можуть бути цікавими для фундаментальної та прикладної біологічної науки, особливо для досліджень молекулярних механізмів захисту клітини від стресу, спричиненого токсичною сполукою, а також для розробки нових ефективних і економічно вигідних методів одержання нових наноматеріалів.

Ключові слова: наноматеріали, біонаночастинки золота, "зелений" синтез, дріжджі *Hansenula polymorpha.*

"ЗЕЛЕНЫЙ" СИНТЕЗ НАНОЧАСТИЦ ЗОЛОТА ДРОЖЖАМИ *HANSENULA POLYMORPHA*

Н. Стасюк[1], Г. Гайда[1*], Р. Серкиз[2], М. Гончар[1]

[1]Институт биологии клетки НАН Украины
ул. Драгоманова, 14/16, Львов 79005, Украина
[2]Львовский национальный университет имени Ивана Франко
ул. Драгоманова, 50, Львов 79005, Украина
*e-mail:*galina.gayda@gmail.com*

Наночастицы металлов (НЧ) являются важными объектами нанотехнологий благодаря перспективам их использования в промышленности и медицине. НЧ металлов можно получать различными физико-химическими методами, а также «зеленым» синтезом. В данном исследовании термотолерантные дрожжи *Hansenula polymorpha* были использованы как биологический инструмент для «зеленого» синтеза наночастиц золота (AuНЧ) из тетрахлораурата (ТХА). Были изучены процессы редукции ТХА дрожжевой культурой и формирование внеклеточных стабильных биоAuНЧ. Конечный продукт характеризовали, используя методы трансмиссионной электронной микроскопии, сканирующей электронной микроскопии, флуоресцентной микроскопии, УФ-видимой адсорбционной спектроскопии. Было изучено влияние различных параметров, в том числе времени и концентрации ТХА, на формирование AuНЧ. Наши результаты могут быть интересны для фундаментальной и прикладной биологичной науки, особенно для исследований молекулярных механизмов защиты клетки от стресса, вызванного токсическим соединением, а также для разработки эффективных и экономически выгодных методов получения новых наноматериалов.

Ключевые слова: наноматериалы, бионаночастицы золота, "зеленый" синтез, дрожжи *Hansenula polymorpha.*

View publication stats

Оригінал доступний за посиланням:
http://publications.lnu.edu.ua/bulletins/index.php/biology/article/download/7826/7793

РОЗДІЛ 4

ВИВЧЕННЯ БІОЛОГІЧНОЇ ТА МОЖЛИВОЇ ТОКСИЧНОЇ ДІЇ НАНОЗИМНИХ КОМПОЗИТІВ НА ЕУКАРІОТИЧНІ КЛІТИНИ ДРІЖДЖІВ *OGATAEA POLYMORPHA*

В розділі IV наведено дослідження біологічної дії наночастинок (НЧ) на еукаріотичні клітини дріжджів *Ogataea* (*Hansenula) polymorpha*. Клітини вирощували на середовищі із додаванням різних НЧ, синтезованих на основі шляхетних і перехідних металів, а також їх гібридів, що володіють ензимними (зокрема, каталазними, пероксидазними або редуктазними) та флуоресцентними властивостями. Доведено, що всі НЧ у мінімальній концентрації (до 0,1 мг/мл) нетоксичні для клітин дріжджів. Показано, що біметалеві НЧ володіють стабільною флуоресценцією в розчині та всередині клітин, що дозволяє спостерігати явище переходу НЧ від батьківських до дочірніх клітин через щонайменше три покоління з подальшим вивільненням із модифікованих клітин.

Для оцінки впливу нанозимів на життєздатність клітин дріжджів, крім тесту на ростову активність, використовували барвники, які реагують на зміни цілісності та функціональності клітинної мембрани. Встановлено, що нанозими (у концентації 0,1 мг/мл у середовищі) проявляють різний цитотоксичний вплив на клітини дріжджів *O. polymorpha*: «катазими» знижують виживання клітин в 2,6-4,5 раза, тоді як НЗ з пероксидазною активністю дещо підвищують цей показник. У цілому, ці дані корелюють із результатами вивчення впливу НЗ на ростову активність клітин. Спостережувана відмінність у дії НЗ на клітини дріжджів пов’язана із різною ефективністю транспорту НЗ у клітини та різний вплив поглинутих НЗ на метаболічні клітинні процеси.

Досліджено ефективність поглинання клітинами *O. polymorpha* НЗ та їх локалізацію всередині клітин. У збагачених нанозимами клітин, у порівнянні із контрольними, показано зростання ензиматичної активності, зокрема псевдо-редуктазна активність у присутності CdCu НЗ підвищується у 10,7 раза, каталазна – у 1,9 раза (для Pt-НЧ) та пероксидазна – у 4,9 раза (для PtAu), відповідно.

Нанозими з каталазною активністю («катазими») Pt і PtAu використали для поглибленого вивчення їхнього впливу на ріст та властивості безкаталазного штаму дріжджів *Ogataea polymorpha* C-105 *(gcr1catX)*, здатного до конститутивного синтезу алкогольоксидази на глюкозному середовищі та повністю позбавленого каталазної активності. У зв'язку з генетичним блоком каталази, мутантні клітини ростуть на суміші глюкози з метанолом після тривалого лаг-періоду, необхідного для адаптації клітин до Гідроген пероксиду, що генерується в культурі, проте не здатні засвоювати метанол як єдине джерело Карбону та енергії. Здатність клітин безкаталазного штаму рости на середовищі, за використання як джерела Карбону глюкози та метанолу при повній відсутності каталазної активності пов'язана, з підвищеним синтезом за таких умов росту цитохром *c* пероксидази, яка здатна розщеплювати токсичний H_2O_2 у пероксидазній реакції з цитохромом *c*. Нами висунуто гіпотезу про здатність НЗ компенсувати відсутність певного ензиму у клітинах завдяки псевдоензиматичній активності НЗ. Для підтвердження такої гіпотези, вивчено можливість усунення дефекту каталазної активності клітин штаму дріжджів *O. polymorpha* C-105 за допомогою НЗ, що володіють каталазною активністю. З цією метою, до середовища вирощування додавали НЗ в різних концентраціях (25 – 500 мкг/мл) та вносили клітини дріжджів *O. polymorpha C-105*. Через 24 год тестували вплив НЧ на ріст клітин. Встановлено, що внесення «катазимів» у ростове метанольне середовище відновлює здатність мутантних клітин рости на метанолі. Електронне мікроскопування дріжджових клітин підтвердило поглинання і накопичення НЧ у цитоплазмі клітин *O. polymorpha* C-105. Таким чином, доведено, що поглинання безкаталазними клітинами «катазимів» Pt і Pt/Au відновлює здатність мутантних клітин рости на метанолі. Каталазна активність НЗ Pt і Pt/Au забезпечує розщеплення надмірної кількості Гідроген пероксиду, що утворюється внаслідок росту клітин на метанолі, усуваючи його токсичну дію на клітини. Це дає можливість клітинам повноцінно рости та ділитись на середовищі із метанолом. Встановлено, що це перший у світі експериментальний доказ можливості заміни природного ензиму нанозимом *in vivo*.

4.1. Вивчення біологічної та можливої токсичної дії катазимів на еукаріотичні клітини безкаталазного штаму дріжджів *O. polymorpha* C-105 *(gcr1catX)*.

Анотація: *Наноматеріали, що володіють штучною ензиматичною каталітичною активністю (нанозими, НЗ), мають великий потенціал для застосування в наукових дослідженнях, імунологічних аналізах, біосенсорах та візуалізації in vivo. Незважаючи на очевидний прогрес у конструюванні та розумінні функціональних властивостей НЗ, досі немає чітких доказів того, чи можуть вони компенсувати втрату відповідної ензиматичної активності in vivo. Нами вперше у світовій науці наведено приклад успішної заміни природного ензиму каталазоподібними наночастинками платини (Pt) і платино-золота (Pt/Au) в клітинах метилотрофних дріжджів O. polymorpha. НЗ Pt синтезовано методом хімічного відновлення та використано в ролі ядра для отримання бі-металевих частинок Pt/Au (ядро/шар). Нами досліджено псевдо-каталазну активність НЗ Pt і Pt/Au in vitro. Встановлено, що штам O.polymorpha C-105 з генетичним дефектом каталази здатний рости на метанолі та суміші глюкози і метанолу в присутності, але не за відсутності НЗ, що корелює зі зниженням внутрішньоклітинної продукції Гідроген пероксиду. Отримані результати є першим прикладом заміни функції природного ензиму синтетичними НЗ, явища, яке можна надалі використовувати для скринінгу нових каталазоподібних НЗ і як плідний інструмент для модифікації живих клітин наночастинками, що володіють каталітичною активністю, та подальшого застосування модифікованих клітин в ролі чутливих елементів клітинних біосенсорів.*

Microchimica Acta (2023) 190:174
https://doi.org/10.1007/s00604-023-05753-8

ORIGINAL PAPER

Nanozyme can substitute a natural *Ogataea polymorpha* catalase enzyme in vivo

Tetyana Prokopiv[1] · Nataliya Stasyuk[1,2] · Mykhailo Gonchar[1,2]

Received: 20 January 2023 / Accepted: 16 March 2023
© The Author(s), under exclusive licence to Springer-Verlag GmbH Austria, part of Springer Nature 2023

Abstract
Nanomaterials possessing artificial, enzyme-like catalytic activity (nanozymes, NZs) have a great potential for application in research, immunological assays, biosensors, in vivo imaging, and as therapeutic agents. Despite the obvious advances in construction and understanding of functional properties of NZs, there is still no clear evidence of whether they can complement the loss of corresponding enzymatic activity in vivo. Herein, we report the first, to the best to our knowledge, example of successful substitution of natural enzyme activity by catalase-like platinum (nPt) and platinum-gold (nPtAu) nanoparticles transferred to the cells of methylotrophic yeast *Ogataea polymorpha*. The nPt NZs were synthesized by the chemical reduction method and used as a seed to produce the nPt(core)Au(shell) particles. The produced nPt NZs were 68.1 and 91.3 nm in size, while the hydrids were of 531.2 and 615.1 nm. Both nPt and nPtAu demonstrated catalase activity in vitro. The catalase-deficient strain *Ogataea polymorpha* C-105 was shown to be able to grow on methanol and a mixture of glucose and methanol in the presence although not in the absence of NZs, this correlating with the decrease in intracellular hydrogen peroxide production. The results provide the first example of complementation of the natural enzyme function by synthetic NZs, the phenomenon which can further be used in a screening for new catalase-like nanozymes and as a fruitful tool to modify living cells by nanoparticles possessing catalytic activity and to use such modified cells as sensitive elements in cell-based biosensors.

Keywords Nanoparticles · Catalase-like nanozyme · Methylotrophic yeast · Cytotoxicity · Alcohol oxidase · Catalase

Introduction

Reactive oxygen species (ROS) are an array of compounds and free radicals containing molecular oxygen or oxygen-like electronegative elements. These chemicals are generated during normal cellular metabolism; under physiological levels, they are known to be involved into redox signaling processes [1, 2]. ROS are formed as by-products of electron transport in mitochondria and as necessary intermediates in oxidoreductase enzymes and metal-catalyzed oxidation reactions [3, 4]. Any disbalance in the level of ROS and intracellular antioxidants leads to a physiological state called "oxidative stress." The main outcomes of such disbalance are oxidative damage of DNA and proteins [5, 6] and disruption of the cellular redox signaling cascade often resulting in apoptosis [7]. Therefore, maintaining of normal physiological level of ROS is of paramount importance to the cell survival.

Catalase (CAT) is one of the components of intracellular antioxidant response. This enzyme protects cells against hydrogen peroxide by decomposing it to water and molecular oxygen [8]. The deficiency in CAT activity is associated with pathogenesis of many diseases, for example, vitiligo [9], Alzheimer's disease [10], Parkinson's disease [11], acute kidney injury [12], schizophrenia [13], and leukemia [14, 15]. This enzyme is present in the majority of living species. In fact, even some anaerobic microorganisms possess the gene encoding the CAT enzyme. In all cases, it is involved into detoxication of hydrogen peroxide. A stand-alone case is that of the methylotrophic yeasts, for which catalase is an indispensable enzyme when grown on methanol as a sole source of carbon and energy. In these

✉ Mykhailo Gonchar
mykhailo1952@gmail.com

[1] Institute of Cell Biology, National Academy of Sciences of Ukraine, Lviv, Ukraine

[2] Drohobych Ivan Franko State Pedagogical University, Drohobych, Ukraine

Published online: 05 April 2023

microorganisms, the enzyme is directly involved into dissimilation of methanol by decomposing hydrogen peroxide produced in the alcohol oxidase reaction. Both enzymes, as well as dihydroxyacetone synthase, colocalize at peroxisomes, and their gene expression, are simultaneously induced by the shift from glucose to methanol as a carbon source [16].

Nanozymes (NZs) are diverse nanomaterials with enzyme mimicking activities. In the past decade, NZs attracted much attention as promising tools in biomedicine [17, 18]. Such interest is primarily caused by their ability to overcome the weaknesses of natural enzymes—low stability and high cost of production and storage. Among various NZs developed so far, the redox enzyme mimics are the most abundant and well-studied [19, 20]. Nowadays, several types of nanomaterials constructed on Au [21], Ag [22], Ir [23], Pt [24, 25], CeO_2 [26], iron oxide [27], graphene nanoparticles [28], and Prussian blue nanocubes [29] are known to possess catalase-like activity (catazymes (CZs)). The ROS scavenging superoxide dismutase and catalase mimicking NZs are promising agents for treatment and prevention of different disorders related to the decrease of activity of corresponding enzymes. The antiaging, antiinflammatory, antioxidation, and neuroprotective effects were observed for CAT- and peroxidase-like NZs when tested on animal models. However, it is still unclear whether NZs can functionally substitute the loss of natural enzymes responsible for ROS detoxication in the living cells.

Herein, we describe the improved procedure of synthesis of CAT-like nPt and nPtAu NZs. These NZs were tested for their ability to substitute a native catalase enzyme in the catalase-deficient mutant of the yeast *Ogataea polymorpha* C-105 when grown under conditions when the enzyme activity is indispensable.

Materials and methods

Chemicals and reagents

Hydrogen tetrachloroaurate(III) trihydrate ($HAuCl_4 \cdot 3H_2O$, ≥99.9%), chloroplatinic acid (H_2PtCl_6, ≥99.9%), sodium phosphate dibasic dihydrate ($Na_2HPO_4 \cdot 2H_2O$, ≥90%), ammonium sulfate ($(NH_4)_2SO_4$, ≥99.9%), potassium phosphate monobasic (KH_2PO_4, ≥99.0%), magnesium sulfate ($MgSO_4$, ≥99.5%), *o*-dianisidine (≥ 98%), calcium chloride ($CaCl_2$, ≥97%), hydrogen peroxide (H_2O_2, 35%), cetyltrimethylammonium bromide (CTAB, ≥99%), sodium hydroxide (NaOH, 99%), L-ascorbic acid (99%), and other reagents and solvents of analytical grade used in this work were purchased from Sigma-Aldrich (Steinheim, Germany).

Yeast cells

The yeast strain *Ogataea* (*Hansenula*) *polymorpha* C-105 (*gcr1 catX*), capable of constitutive synthesis of alcohol oxidase in glucose medium and completely devoid of catalase activity (cat^-), has been used as a model of the living organism in our study [30]. The catalase-defective mutant C-105 (*gcr1 catX*) was isolated from a mutagenized culture of the strain 33 as a cell unable to decompose exogenous H_2O_2. Cultivation of the cells was performed in Erlenmeyer's flasks (volume 250 mL) on a rotary shaker (200 rpm) at 30 °C as described earlier [31]. One liter of liquid media contained the following: KH_2PO_4, 1 g; $(NH_4)_2SO_4$, 3.5 g; $MgSO_4$, 0.5 g; $CaCl_2$, 0.1 g. The yeast extract (1 $g \cdot L^{-1}$) was added to the medium as a source of trace elements and vitamins. As a source of carbon, glucose (1%) or methanol (1%) was used.

Identification and analysis of *catX* gene mutation in *Ogataea polymorpha*

Chromosomal DNA was isolated from *Ogataea polymorpha* C-105 (*gcr1 catX*) using a soft lysis protocol with the addition of lyticase from *Arthrobacter luteus* (Sigma-Aldrich, USA). PCR was conducted with Q-5 DNA polymerase PCR kit (NEB, USA). PCR products were gel-purified with QIA quick gel purification kit (Qiagen, Germany) and sequenced with the use of corresponding amplification primers on ABI PRISM 3130xl (Thermo Fischer Scientific, USA). The data was analyzed with the use of Geneious Prime (Biomatters Ltd, New Zealand).

Determination of hydrogen peroxide in the yeast culture liquid

Hydrogen peroxide in the culture liquid was determined in the peroxidase reaction using 3,3′,5,5′-tetramethylbenzidine as a chromogenic substrate. The standard H_2O_2 solution was prepared by diluting 10 mM of the initial solution, the exact concentration of which was spectrophotometrically checked at 240 nm ($\varepsilon_{mM} = 0.0436\ mM^{-1} \cdot cm^{-1}$).

Permeabilization of the yeast cells

The cells were incubated in the medium with glucose or methanol during 24 and 48 hours. To permeabilize the cells, the same volume of permeabilizing reagent (5.5 mM CTMB) was added to the cell suspension (20 – 50 $mg \cdot mL^{-1}$ in the 100 mM phosphate buffer, pH 7.5). The resulting solution was treated at 30 °C in a water bath for 15 min under mixing every 3 – 4 min. The permeabilized cells were washed by centrifugation (5000 g, 10 min) in the 5 mM phosphate

buffer (PB), pH 7.5. The precipitated permeabilized cells were re-suspended to 0.1 mg·ml^{-1} in the same buffer solution and stored on ice at + 2 °C.

Synthesis of the platinum NZs

Platinum NZs (nPt) were prepared by the chemical reduction method using ascorbic acid as a reductive agent. 10 mL 5 mM H_2PtCl_6 and 1.2 mL 0.1 M L-ascorbic acid were mixed and heated at 100 °C for 15 min with the following addition of 10 mL 0.01 M CTAB to obtain a dark-brown solution. nPt were precipitated from the reaction mixture by centrifugation (8000 g; Hettich Micro-22R centrifuge), washed with 5 mM phosphate buffer, pH 7.0 (PB). To estimate the concentration of the formed nPt, the obtained precipitate was dried at 80 °C during 24 hours.

Synthesis of the platinum (core)/aurum (shell) NZs

The platinum (core)/aurum (shell) NZs (nPtAu) were synthesized using an aqueous-based, seed-mediated procedure under mild growth conditions. At the first stage, Pt seeds were grown via the rapid reduction of H_2PtCl_6 by ascorbic acid in the presence of 0.01 M CTAB at 100 °C. Then, these seeds were subsequently injected into the growth solution consisting of $HAuCl_4$ (2 mL, 17 mM) and L-ascorbic acid (1 mL, 0.1 M) followed by heating at 100 °C for 10 min. The obtained nPtAu were precipitated from the reaction mixture by centrifugation (8000 g; Hettich Micro-22R centrifuge) and washed with 5 mM PB, pH 7.0, and water. The final nPtAu precipitate was dried (at 80 °C during 24 h).

Characterization of the synthesized NZs

The formed nPt and nPtAu were characterized by UV-Vis spectroscopy (300–700 nm) on a Shimadzu UV-1650 PC spectrophotometer (Japan). The total concentration of NPs was gravimetrically determined.

The size and morphology of NZs were studied by the use of a scanning electron microscope (SEM) microanalyser (REMMA-102-02, Lviv, Ukraine). In all experiments, the distance from the last lens of the microscope to the sample (WD) ranged from 10 to 12 mm. The accelerator voltage was 15,000 kV. The size and size distribution of particles in the colloids were measured by dynamic light scattering (DLS) based on the use of Nano ZS zetasizer system (Malvern Instruments, UK).

For analysis of cells by the method of transmission electron microscopy (TEM), all samples were fixed in the 1.5% aqueous solution of $KMnO_4$ for 20 min at room temperature followed by post-fixation with the 1% OsO_4 cacodylate buffer for 90 min at 0 °C. The samples were dehydrated by mixing with corresponding solutions containing increasing concentrations of ethanol with final incubation in acetone. Samples were embedded in Epon 812. Ultrathin sections were sliced in an ultramicrotome UMTP-6 (Sumy, Ukraine) contrasted with lead citrate and examined with an electron microscope PEM-100 (Sumy, Ukraine) at 75 kV. The final magnification of the micrographs was 10,000.

Determination of catalase-like activity of NZs in solution

Catalase-like activity of NZs was assessed by incubating the sample of NZs with 2.0 mL 0.03% H_2O_2 during 10 min at 37 °C. The reaction was stopped with 1 mL 4% ammonium molybdate. Absorbance of the yellow complex of molybdate and hydrogen peroxide is measured at 410 nm against the blank. To calculate catalase-like activity of NZs (U·mg^{-1}), the following formula was used:

$$Specific\ activity = \frac{D_{410} \cdot V_t \cdot N}{0.022 \cdot V_{NZ} \cdot t \cdot c}$$

where

D_{410} absorbance of the test tube;

N NZ dilutions before injection in reaction mixture;

V_t total volume of reagents in test tube;

0.022 extinction coefficient, mM^{-1}·cm^{-1};

V_{NZ} volume of added NZs, mL;

t time, min;

c concentration of NZs, mg·mL^{-1}.

Assay of alcohol oxidase activity

The activity of alcohol oxidase (AO) in the permeabilized cells was determined by the rate of hydrogen peroxide formation in reaction with methanol, as monitored by the peroxidative oxidation of *o*-dianisidine [31]. Activity was measured in the reaction mixture with a final volume of 3.0 mL containing 50 mM PB, pH 7.5, 0.25 mM *o*-dianisidine, horseradish peroxidase (0.07 mg·mL^{-1}), 10mM methanol, and 10 mg of permeabilized cells. After incubation during fixed time (5–10 min) at 30 °C and upon appearance of the orange color, the reaction was stopped by the addition of 0.8 mL 12 M HCl. The generated color was determined at 525 nm using a spectrophotometer. The extinction coefficient of the resulting dye in the acidic solution was 0.0134 mM^{-1}·cm^{-1}. One unit of AO activity is defined as the

amount of enzyme releasing 1 μmol H_2O_2 per 1 min under standard assay conditions.

Statistical analysis

The experiments were repeated three times ($n = 3$), and the measurements were made in two parallels. For each sample, arithmetic mean, variance, relative standard deviation, and confidence interval were determined. The statistical parameters and all figures were calculated and built using Origin 8.5 Pro.

Results and discussion

Morphological properties of the synthesized NPs

The nPt and nPtAu (core/shell) NPs were synthesized using the chemical reduction method [32]. UV-VIS absorption spectra have been proven to be quite sensitive to the formation of nPt and nPtAu NPs since these NPs exhibit intense absorption peaks due to surface plasmon excitation. The UV-VIS spectra of both types of NPs in the range from 200 to 800 nm are shown in Figure S1. The plasmonic-based color switches proved to be affected by the ratio between Pt and Au, shape and the size of the binary NPs, and the distribution of both metals inside a particle. It was shown that the nPt (line 1) exhibited UV absorption spectrum with absorption peak at 264 nm. In our study, we demonstrated that in case of nPt, coated with Au (Pt(core)/Au(shell)NP) (see Figure S1, line 2), the absorption band shifts, and the NP solution changes from yellow to orange. The shift of absorption bands at much higher wavelengths (from 264 to 540 nm for hybride NPs with dominated AuNPs) may be explained by the formation of NPs larger than initial ones [32].

The size and morphology of the obtained NPs were studied using the SEM method (Fig. 1A).

The SEM micrographs indicate the formation of monodisperse nanospheres of different sizes; for nPt, the average diameter is close to 100 nm, whereas the average size of nPtAu is close to 500 nm (Fig. 1), respectively. For a more accurate assessment of the size of obtained NPs, the DLS method was applied (Table S1). The corresponding size distribution of nanoparticles is shown in Figure S2.

Thus, the DLS results confirmed the morphology and size of nPt (spherical particle diameter <100 nm) and nPtAu (spherical particle diameter ~500 nm) obtained by the SEM data (Fig. 1).

The ability of nPt and nPtAu to functionally mimic the enzyme catalase was studied using a colorimetric assay (see subdiv. "Determination of catalase-like activity of NZs in solution"). The catalase-like activities of NPs were investigated by incubating the NPs with hydrogen peroxide as

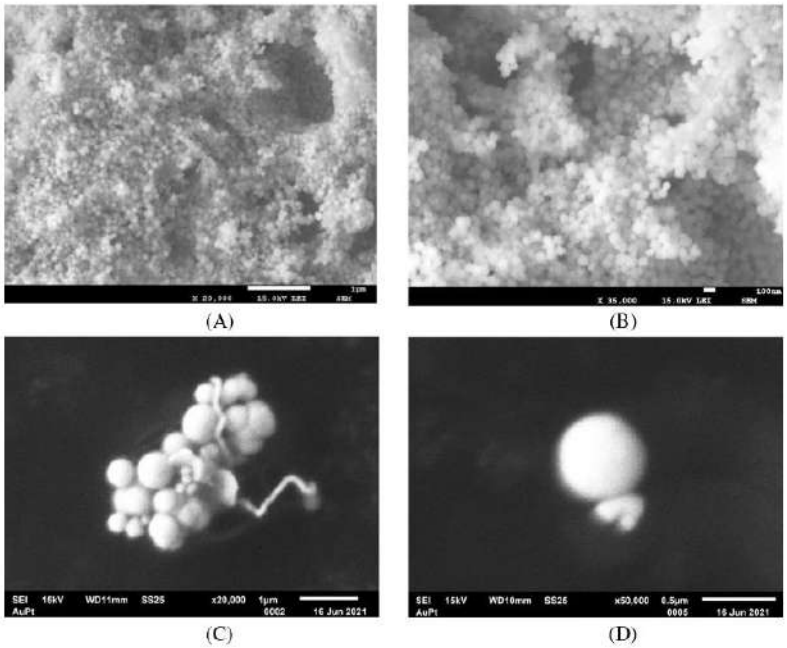

Fig. 1 SEM of nPt (**A**, **B**) and nPtAu (**C**, **D**) NPs

substrate and ammonium molybdate as a reagent. Absorbance of the formed yellow complex of molybdate and hydrogen peroxide was measured at 410 nm. The calculated catalase activity of nPt and nPtAu was 0.6 and 1 $U \cdot mg^{-1}$, respectively.

In our work, we put forward a hypothesis about the ability of NZs to complement the absence of a certain enzyme in cells due to the pseudo-enzymatic activity of NZs. To confirm this hypothesis, we studied the possibility of eliminating the defect in catalase activity of the yeast cells by the use of CZs possessing catalase-like activity. The mutant strain of the methylotrophic yeast *O. polymorpha* C-105 (*gcr1 catX*), capable of constitutive synthesis of alcohol oxidase in glucose medium and completely devoid of catalase activity (cat^-), was used as a model of living cells [31]. Due to the genetic block of catalase, the mutant cells grow in a mixture of glucose/methanol after a long lag period, which is necessary to degrade the hydrogen peroxide generated in the culture prior to induction of Cyt c peroxidase, the enzyme which can suppress catalase –minus mutation [33]. However, this mutant cells could not grow in methanol medium without an alternative carbon source, presumably as a result of the toxic effects of high concentrations of H_2O_2.

The nucleotide sequence of gene *catX* (OGAPODRAFT_95533) encoding peroxisomal catalase was obtained from the genome sequence of *Ogataea polymorpha* NCYC 495 leu1.1 (GenBank accession number AECK00000000.1). The locus was amplified as two overlapping fragments using primer pairs CAT_F1.1 GTGCAA TGCGGGCCTGTTTTG)/CAT_R1.1 CACTCGCCCTTG GAATTGTAC and CAT_F1.2 CATGTTCTGGGACTACCT GACG/CAT_R1.2 CTCGTGCTGTTTTAGGAAGGATG (Figure S3).

The obtained sequences were mapped to the genome of *O. polymorpha* NCYC 495 leu1.1 (GenBank accession number AECK00000000.1). As a result, two mutations in the *catX* gene were identified in the strain *Ogataea polymorpha* C-105: (1) C895T resulting in mutation Pro299Cis; (2) single nucleotide deletion C896 causing frame shift with the formation of a stop codon TGA in position 300 of the a.a. sequence of the corresponding protein leading to the premature termination of protein synthesis (Figure S4). Thus, *Ogataea polymorpha* C-105 strain possesses the defective *catX* gene with the stop codon in position 300 of the amino acid sequence of corresponding peptide which leads to the formation of the most probably dysfunctional peroxisomal catalase protein.

Study of influence of catazymes on the yeast growth

To investigate the impact of CAT-like NZs on the mutant yeast growth, the solution of CZs at different concentrations (25–500 $\mu g \cdot mL^{-1}$) was added to the growth medium containing C-105 yeast cells (0.2 OD at 540 nm). After incubation during 24 h, the effect of CZs on the cell growth was evaluated (Fig. 2).

The positive effect of both types of CZs, namely nPt and nPtAu, on the growth of non-catalase strain of *O. polymorpha* C-105 was revealed (see Fig. 2). It was shown that after addition of CZs into the liquid medium (up to the 100 $\mu g \cdot mL^{-1}$), the yeast growth increases more than twice. It was also found that the presence of CZs in the medium containing 1% methanol restores the ability of mutant cells to grow on methanol. It should be noted that in order to avoid the overloading of the yeast cells by CZs, the concentration of 100 $\mu g \cdot mL^{-1}$ was applied in subsequent studies.

Investigation of localization of CZs inside yeast cells

Morphological properties of the yeast cells grown in the presence of CZs (100 $\mu g \cdot mL^{-1}$) during 24 h were studied using TEM (Fig. 3). The intact *O. polymorpha* C-105 cells grown without addition of CZs were used as control ones (Fig. 3A). Figure 3A shows that numerous dark points localized throughout the cytoplasm correspond to nPt (Fig. 3B) and nPtAu (Fig. 3C), respectively. A possible mechanism of accumulation of NZs inside the cells is their penetration across the plasma membrane either by diffusion or by endocytosis [34]. The intake of nPt or nPtAu by the cells was also confirmed by X-ray microanalysis (SEM-XRM) (Fig. 3). The XRM spectrograms (Figs. 3D, E) represent the characteristic peaks for Pt^0 and Au^0 (Kα peak at 2.0 keV and 2.1 keV, respectively), thus proving the penetration of nPt or nPtAu into the cells. Taken together, the presented data confirmed the accumulation of NZs inside the cells.

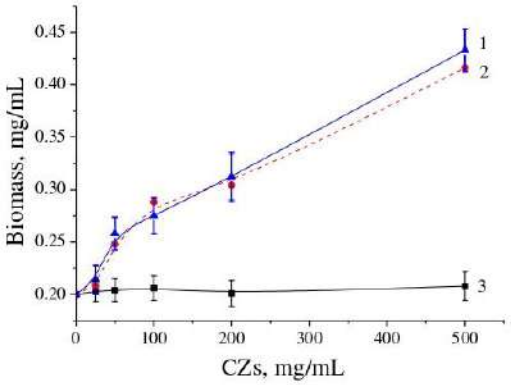

Fig. 2 The influence of CZs on cell growth (OD at 540 nm) of the yeast *O. polymorpha* C-105 (*gcr1 catX*) in methanol medium after addition of CZs in a wide range of concentrations (25–500 $\mu g \cdot mL^{-1}$) during incubation at 24 h: 1, nPt; 2, nPtAu; 3, control cells (without addition of CZs)

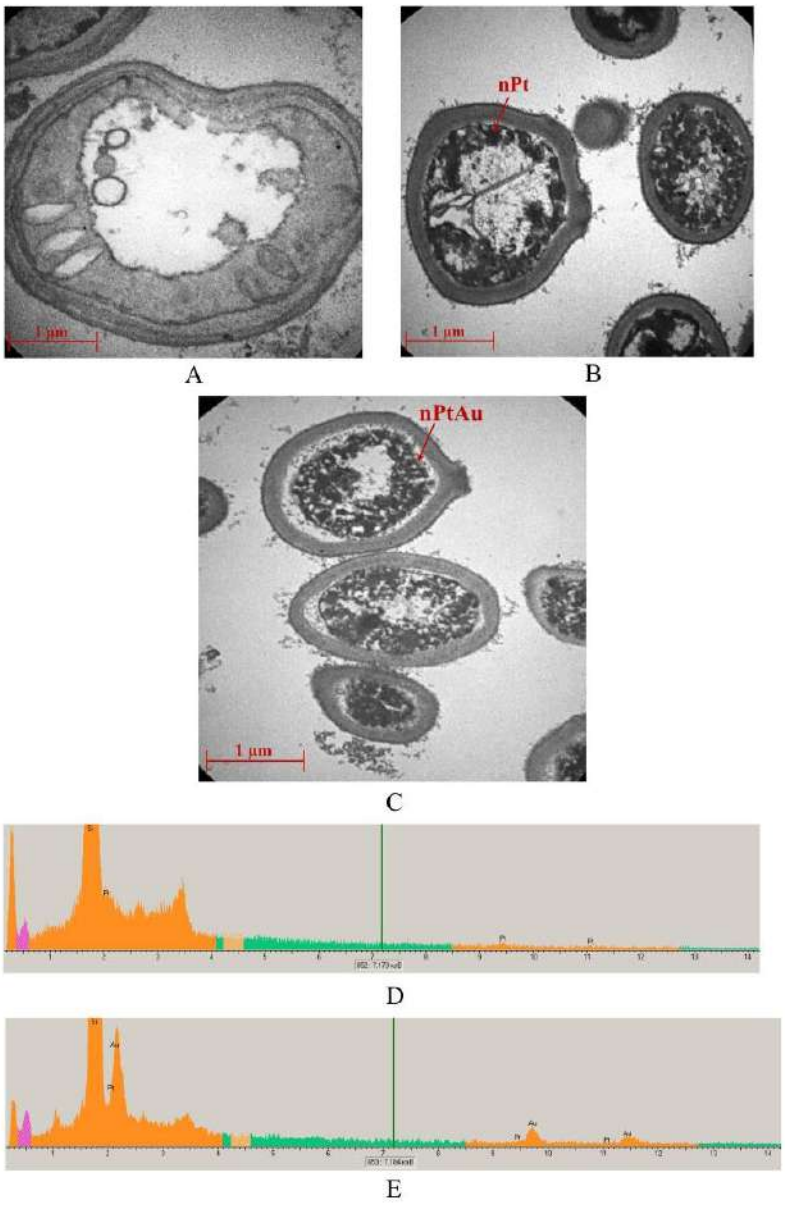

Fig. 3 Morphological characteristics of *O. polymorpha* C-105 yeast cells after 24 h exposition to NPs: TEM images of the control cells grown without NZs (**A**) and after incubation with nPt (**B**) and nPtAu (**C**); X-ray spectral microanalysis for nPt (**D**) and nPtAu (**E**), respectively. The accelerating voltage was ~7.2 keV for all images. The scale bar is 1 µm

The effect of CZs on the growth of catalase-minus strain *O. polymorpha* C-105 in the presence of different carbon sources

The yeast cells of catalase-minus strain *O. polymorpha* C-105 (0.5 mg·mL^{-1}) were grown in the presence of CZs and 1% methanol (Figure S5A) or the mixture of 1% glucose/methanol (Figure S5 B), respectively, during 5 days. It was shown that on the 5th day of incubation with nPt or nPtAu in the presence of 1% methanol (as a carbon source), the biomass of the cells increases 2.7 and 3.2–fold, respectively. At the same time, the biomass of the cells after growing in the medium

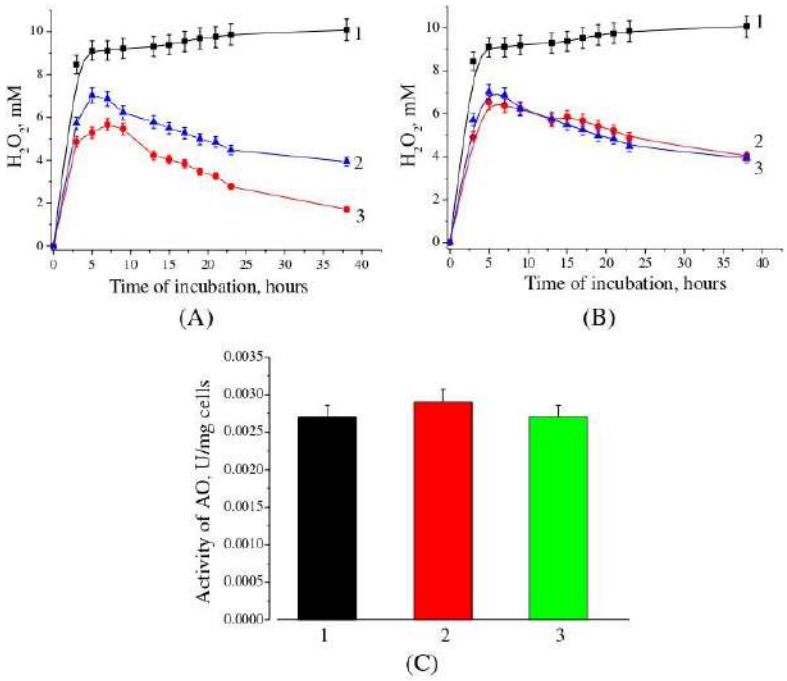

Fig. 4 The effect of CZs on the production of H_2O_2 and AO activity (OD at 525 nm) in the cells of catalase-minus strain *O. polymorpha* C-105. The production of H_2O_2 by the cells during incubation in a medium containing methanol (**A**) or methanol/glucose (**B**). **C** Activity of AO in permeabilized cells grown during 48 h in a medium containing 1% methanol. (1) Control cells (grown without CZ addition); (2) cells grown with nPt; (3) cells grown with nPtAu

containing 1% methanol and 1% glucose after addition of nPtAu or nPt increases 2.5- and 3.2-fold, respectively, in comparison with control cells (grown without addition of CZs).

During the growth of yeast cells in the medium containing methanol, the alcohol oxidase reaction plays a key role leading to the formation of compounds toxic to the cells, in particular, formaldehyde and hydrogen peroxide. We have analyzed whether there will be any changes in the accumulation of H_2O_2 in the yeast culture medium during growth with methanol as a carbon source or with a mixture of glucose and methanol in the presence of CZs. The concentration of H_2O_2 in the culture liquid was determined in the peroxidase reaction using *o*-dianisidine as a chromogenic substrate. The obtained results indicate a significant decrease— 6- and 5-fold (for nPt and nPtAu, respectively) — in the level of H_2O_2 generated by the yeast cells in the culture medium after 38 h of incubation (Figs. 4A, B).

Thus, CZs nPt and nPtAu can effectively perform the function of a missing natural catalase in the yeast cells, splitting the generated in alcohol oxidase-reaction H_2O_2 and reducing its content in the culture liquid.

In the permeabilized *O. polymorpha* C-105 (*gcr1 cat*) cells, the activity of AO was determined since it is responsible for the generation of H_2O_2 (Fig. 4C). The cells were grown in the medium containing 1% methanol for 24 and 48 h followed by permeabilization according to the procedure described in the subdivision "Permeabilization of the yeast cells."

As shown, for the control cells grown in the medium containing 1% methanol during 48 h, the activity of AO was 0.08 U·mg^{-1} cells. The incubation of the cells in the presence of CZs nPt and nPtAu during 24 h did not result in any remarkable changes in AO activity responsible for the generation of H_2O_2 (Fig. 4C).

Table 1 The balance of catalase activity of cells enriched with nPt (n=3)

Parameter	Added solution of nPt	Extracellular liquid		Permeabilized cells	
		nPt	Control	nPt	Control
Volume, mL	0.075	14.0	14.0	1.0	1.0
Activity, U mL^{-1}	7.0 ± 0.1	0.006 ± 0.0002	0	0.11 ± 0.021	0
Total activity, U	0.53 ± 0.24	0.095 ± 0.0055	0	0.11 ± 0.033	0
Yield, %	=100%	-	-	21 ± 0.35	-

Table 2 The balance of catalase activity of cells enriched with nPtAu ($n = 3$)

Parameter	Added solution of nPtAu	Extracellular liquid		Permeabilized cells	
		nPtAu	Control	nPtAu	Control
Volume, mL	0.070	14.0	14.0	1.0	1.0
Activity, U mL^{-1}	19 ± 0.45	0.010 ± 0.002	0	0.7 ± 0.002	0
Total activity, U	1.3 ± 0.25	0.14 ± 0.031	0	0.7 ± 0.005	0
Yield, %	=100%	-	-	53 ± 2.2	-

The enzymatic and pseudo-enzymatic activity of the yeast cells enriched with NZs

In our recent work, we demonstrated the ability of AuNPs, conjugated with flavocytochrome b_2, to penetrate through the cell wall and increase the local concentration of a target enzyme inside the cells [30]. We tried to reveal whether catalase-like CZs could increase pseudo-enzymatic activity of the cells due to absorption. In our previous studies it was shown that CZs are mostly localized in the cytoplasm (see subdiv. "Investigation of localization of CZs inside yeast cells"). Therefore, at this stage, catalase activity in the cells supplemented with CZs was investigated. For such experiments, we use *H. polymorpha* C-105 (*gcr1 cat*) cells which are devoid of catalase and are unable to decompose H_2O_2. The analyses of catalase activity of CZ-enriched yeast cells (nPt or nPtAu) as well as control samples grown without the CZs addition are shown in Table 1 and Table 2.

It is clearly shown that uptake of CZs by the yeast cells resulted in the increase of catalase activity in the CZ-enriched cells: 21- and 53-fold for nPt and nPtAu, respectively, in comparison with control cells (Table 1 and Table 2). Therefore, our studies prove that catalyse-like NZs can effectively penetrate into the cells increasing catalase activity.

Summarizing the obtained results, we can conclude that the absorption of nPt or nPtAu by catalase-free yeasts cells restores the ability of mutant cells to grow on methanol. The CAT activity of nPt and nPtAu is responsible for the decomposition of H_2O_2 which is formed during methanol metabolism eliminating toxic effect on cells. Thus, NPs with catalase-like activity can successfully replace natural catalase of the cell performing a detoxification function. The analysis of literature data allows us to conclude that it is the first experimental evidence of the possibility of replacing a natural enzyme with a nanozyme in vivo.

Conclusions

Numerous synthetic nanomaterials have been investigated for their catalytic activity similar to that of native enzymes such as peroxidase, oxidase, and superoxide dismutase as well as for their impact on the living cells. However, the effect of catalase-like nanozymes (CAT-like) on living cells has not yet been sufficiently studied.

In this work, the possibility of complete replacement of natural enzyme, catalase, by CAT-like nanozymes in vivo was experimentally proved for the first time. Using a catalase-minus mutant of the yeast *Ogataea polymorpha*, which is unable to grow in methanol medium due to the generation of toxic hydrogen peroxide in cells, it was shown that an uptake of nanoparticles by the mutant cells restores their ability to destroy H_2O_2. This phenomenon can further be used in a screening for new catalase-like nanozymes as well as for modification of living cells by nanoparticles possessing catalytic activity and for the use of such modified cells with different aims ranging from their utilization as sensitive elements in cell-based biosensors to possible application in environmental biotechnology to decay toxic compounds, e.g., methanol, hydrogen peroxide.

This fruitful approach to enhance catalytic activity of nanozyme-modified microbial cells will be used in the future to construct microbial biosensors with improved catalytic capacity as an alternative (or additional) way, as compared to genetic engineering of sensing cells.

Supplementary Information The online version contains supplementary material available at https://doi.org/10.1007/s00604-023-05753-8.

Acknowledgements The authors are thankful to Dr. Yuriy Rebets (Explogen LLC, Lviv, Ukraine) for the fulfillment of molecular genetic analysis of the catalase-minus mutation in the yeast *O. polymorpha* C-105.

Author contributions Tetyana Prokopiv: conceptualization, formal analysis, and visualization.

Nataliya Stasyuk: investigation, methodology, validation, writing — original draft, and visualization.

Mykhailo Gonchar: conceptualization, supervision, writing — review and editing, project administration, and resources.

Funding This work was supported in part by the National Research Foundation of Ukraine (projects Nos. 2020.02/0100 "Development of new nanozymes as catalytic elements for enzymatic kits and chemo/biosensors" and 2021.01/0010 "Development of an enzymatic kit and portable biosensors for express-analysis of creatinine, a marker of acute functional disorders of the kidneys").

Declarations

Conflicts of interest The authors declare no conflict of interests.

References

1. Uchida K (2003) 4-Hydroxy-2-nonenal: a product and mediator of oxidative stress. Prog Lipid Res 42(4):318–343
2. Halliwell B, Gutteridge JM (1999) Chapter 2. In: Halliwell B, Gutteridge JMC (eds) Free radicals in biology and medicine, third ed. Oxford Science Publications, New York, pp 36–104
3. Murphy MP, Bayir H, Belousov V, Chang CJ, Davies KJ, Davies MJ, Dick TP, Finkel T, Forman HJ, Janssen-Heininger Y, Gems D (2022) Guidelines for measuring reactive oxygen species and oxidative damage in cells and in vivo. Nat Metab 4:651
4. Hasanuzzaman M, Bhuyan MB, Zulfiqar F, Raza A, Mohsin SM, Mahmud JA, Fujita M, Fotopoulos V (2020) Reactive oxygen species and antioxidant defense in plants under abiotic stress: revisiting the crucial role of a universal defense regulator. Antioxidants (Basel) 9(8):681
5. Wiseman H, Halliwell B (1996) Damage to DNA by reactive oxygen and nitrogen species: role in inflammatory disease and progression to cancer. Biochem J 313:17
6. Stadtman ER, Berlett BS (1997) Reactive oxygen-mediated protein oxidation in aging and disease. Chem Res Toxicol 10(5):485
7. Aggarwal V, Tuli HS, Varol A, Thakral F, Yerer MB, Sak K, Varol M, Jain A, Khan MA, Sethi G (2019) Role of reactive oxygen species in cancer progression: molecular mechanisms and recent advancements. Biomolecules 9:735
8. Jeeva JS, Sunitha J, Ananthalakshmi R, Rajkumari S, Ramesh M, Krishnan R (2015) Enzymatic antioxidants and its role in oral diseases. J Pharm Bioallied Sci 7:S331
9. Schallreuter KU, Wood JM, Berger J (1991) Low catalase levels in the epidermis of patients with vitiligo. J Invest Dermatol 97(6):1081
10. Nandi A, Yan LJ, Jana CK, Das N (2019) Role of catalase in oxidative stress- and age-associated degenerative diseases. Oxid Med Cell Longev 2019:9613090
11. Eom SA, Kim DW, Shin MJ, Ahn EH, Chung SY, Sohn EJ, Jo HS, Jeon SJ, Kim DS, Kwon HY, Cho SW (2015) Protective effects of PEP-1-catalase on stress-induced cellular toxicity and MPTP-induced Parkinson's disease. BMB Rep 48(7):395
12. Choi HS, Mathew AP, Uthaman S, Vasukutty A, Kim IJ, Suh SH, Kim CS, Ma SK, Graham SA, Kim SW, Park IK (2022) Inflammation-sensing catalase-mimicking nanozymes alleviate acute kidney injury via reversing local oxidative stress. J Nanobiotechnology 20(1):205
13. Garg U, Smith L (2017) In Biomarkers in inborn errors of metabolism; Chapter 1. Elsevier, Amsterdam, pp 1–24
14. Eras N, Türkoz G, Tombak A, Tiftik N, Yalin S, Berkoz M, Erden S, Akbas E (2019) An investigation of the relation between catalase *C262T* gene polymorphism and catalase enzyme activity in leukemia patients. Arch Med Sci 17(4):928
15. Liu CP, Wu TH, Liu CY, Chen KC, Chen YX, Chen GS, Lin SY (2017) Self-supplying O_2 through the catalase-like activity of gold nanoclusters for photodynamic therapy against hypoxic cancer cells. Small 13:26. https://doi.org/10.1002/smll.201700278
16. van Zutphen T, Baerends RJ, Susanna KA, De Jong A, Kuipers OP, Veenhuis M, Van der Klei IJ (2010) Adaptation of *Hansenula polymorpha* to methanol: a transcriptome analysis. BMC Genom 11:1. https://doi.org/10.1186/1471-2164-11-1
17. Xu D, Wu L, Yao H, Zhao L (2022) Catalase-like nanozymes: classification, catalytic mechanisms, and their applications. Small 18(37):2203400
18. Zhang X, Zhang S, Yang Z, Wang Z, Tian X, Zhou R (2021) Self-cascade MoS_2 nanozymes for efficient intracellular antioxidation and hepatic fibrosis therapy. Nanoscale 13:12613
19. Yang W, Yang X, Zhu L, Chu H, Li X, Xu W (2021) Nanozymes: activity origin, catalytic mechanism, and biological application. Coord Chem Rev 448:214170
20. Wu J, Wang X, Wang Q, Lou Z, Li S, Zhu Y, Qin L, Wei H (2019) Nanomaterials with enzyme-like characteristics (nanozymes): next-generation artificial enzymes (II). Chem Soc Rev 48:1004
21. Li J, Liu W, Wu X, Gao X (2015) Mechanism of pH-switchable peroxidase and catalase-like activities of gold, silver, platinum and palladium. Biomaterials 48:37
22. Yin B, Zheng W, Dong M, Yu W, Chen Y, Joo SW, Jiang X (2017) An enzyme-mediated competitive colorimetric sensor based on Au@Ag bimetallic nanoparticles for highly sensitive detection of disease biomarkers. Analyst 142:2954
23. Su H, Liu DD, Zhao M, Hu WL, Xue SS, Cao Q, Le XY JLN, Mao ZW (2015) Dual-enzyme characteristics of polyvinylpyrrolidone-capped iridium nanoparticles and their cellular protective effect against H_2O_2-induced oxidative damage. ACS Appl Mater Interfaces 7:8233
24. He SB, Yang L, Lin MT, Balasubramanian P, Peng HP, Kuang Y, Deng HH, Chen W (2021) Platinum group element-based nanozymes for biomedical applications: an overview. Biomed Mater 16:3. https://doi.org/10.1088/1748-605X/abc904
25. Park JS, Choi JS (2022) Platinum nanozyme-hydrogel composite (PtNZHG)-impregnated cascade sensing system for one-step glucose detection in serum, urine, and saliva. Sens Actuators B: Chem 359:131585
26. Feng N, Liu Y, Dai X, Wang Y, Guo Q, Li Q (2022) Advanced applications of cerium oxide based nanozymes in cancer. RSC Adv 12:1486
27. Hu M, Korschelt K, Daniel P, Landfester K, Tremel W, Bannwarth MB (2017) Fibrous nanozyme dressings with catalase-like activity for H_2O_2 reduction to promote wound healing. ACS Appl Mater Interfaces 9:38024
28. Ren C, Hu X, Zhou Q (2018) Graphene oxide quantum dots reduce oxidative stress and inhibit neurotoxicity in vitro and in vivo through catalase-like activity and metabolic regulation. Adv Sci 5:1700595
29. Estelrich J, Busquets MA (2021) Prussian blue: a nanozyme with versatile catalytic properties. Int J Mol Sci 22(11):5993
30. Karkovska M, Smutok O, Stasyuk N, Gonchar M (2015) L-Lactate-selective microbial sensor based on flavocytochrome b_2-enriched yeast cells using recombinant and nanotechnology approaches. Talanta 144:1195
31. Gonchar MV, Ksheminska GP, Hladarevska NM, Sibirny AA (1990) Catalase-minus mutants of methylotrophic yeast Hansenula polymorpha impaired in regulation of alcohol oxidase synthesis. In: Lachowicz TM (ed) Genetics of respiratory enzymes in yeasts. Wroclaw University Press, Wroclaw, pp 222–228
32. Xu JX, Siriwardana K, Zhou Y, Zou S, Zhang D (2018) Quantification of gold nanoparticle ultraviolet–visible extinction, absorption, and scattering cross-section spectra and scattering depolarization spectra: the effects of nanoparticle geometry, solvent composition, ligand functionalization, and nanoparticle aggregation. Anal Chem 90(1):785
33. Gonchar MV, Kostryk LB, Sibirny AA (1997) Cytochrome c peroxidase from a methylotrophic yeast: physiological role and isolation. Appl Microbiol Biotechnol 48:454
34. Behzadi S, Serpooshan V, Tao W, Hamaly MA, Alkawareek MY, Dreaden EC, Brown D, Alkilany AM, Farokhzad OC, Mahmoudi M (2017) Cellular uptake of nanoparticles: journey inside the cell. Chem Soc Rev 46(14):4218

Publisher's note Springer Nature remains neutral with regard to jurisdictional claims in published maps and institutional affiliations.

Springer Nature or its licensor (e.g. a society or other partner) holds exclusive rights to this article under a publishing agreement with the author(s) or other rightsholder(s); author self-archiving of the accepted manuscript version of this article is solely governed by the terms of such publishing agreement and applicable law.

Оригінал доступний за посиланням: https://link.springer.com/article/10.1007/s00604-023-05753-8

Електронний додаток до статті доступний за посиланням: https://link.springer.com/article/10.1007/s00604-023-05753-8#Sec21

4.2. Візуалізація та дослідження клітин за використання флуоресцентних наноматеріалів.

Анотація: *В останні десятиліття в біологічних і біомедичних дослідженнях застосовуються різні методи візуалізації, зокрема, магнітно-резонансна томографія, флуоресценція/біолюмінесценція, а також мультимодальні підходи. Флуоресцентний іміджинг, особливо в поєднанні з нанорозмірними матеріалами, є дуже перспективним інструментом для експериментів in vivo та клінічних застосувань завдяки його високій часовій і просторовій роздільній здатності. Флуоресцентні наночастинки (НЧ), здатні взаємодіяти з біомолекулами як на поверхні, так і всередині клітин, можуть революціонізувати підходи до візуалізації клітин для діагностики та терапії. Нами розроблено новий метод візуалізації клітин за допомогою флуоресцентних біметалевих НЧ, синтезованих хімічним відновленням відповідних йонів. Як модель живого організму, використано клітини дріжджів O.* polymorpha*. Нами встановлено, що всі НЧ у мінімальній концентрації (до 0,05 мМ) нетоксичні для клітин дріжджів. НЧ та клітини, модифіковані НЧ, охарактеризовано методами UV-VIS спектроскопії, сканувальної електронної мікроскопії, атомно-силової мікроскопії, трансмісійної електронної мікроскопії та флуоресцентної мікроскопії. Продемонстровано феномен передачі флуоресцентних бі-металеві НЧ від батьківських до дочірніх клітин з подальшою екскрецією НЧ в культуральне середовище. Показано, що синтезовані флуоресцентні НЧ є нетоксичними і можуть стати перспективним інструментом для візуалізації клітин.*

ISSN 2321-807X

Cell Imaging with Fluorescent Bi-Metallic Nanoparticles

Natalia Ye. Stasyuk[a], Galina Z. Gayda[a*], Roman Ja. Serkiz[a], Mykhailo V. Gonchar[a,b]

[a]Institute of Cell Biology, NAS of Ukraine, Drahomanov Str. 14/16, 79005 Lviv, Ukraine

E-mail address: stasuk_natalia@ukr.net

E-mail address: galina.gayda@gmail.com

E-mail address: rserkiz@gmail.com

E-mail address: gonchar@cellbiol.lviv.ua

[b]Institute of Applied Biotechnology and Basic Sciences, University of Rzeszow, Sokolowska Str. 26, 36-100 Kolbuszowa, Poland

*Corresponding author: galina.gayda@gmail.com

ABSTRACT

Last decades various imaging techniques have been applied in biological and biomedical research, such as magnetic resonance imaging, different types of tomography, fluorescence/bioluminescence, ultrasound, as well as multimodality approaches. Fluorescence imaging, especially in combination with nanoscale materials, is a very prospective tool for experiments *in vivo* and clinical applications due to its high temporal and spatial resolutions. Fluorescent nanoparticles (NPs), having ability to interact with biomolecules both on the surface of and inside the cells, may revolutionize the cell imaging approaches for diagnostics and therapy. In our investigation we report about new method of cell imaging with fluorescent bi-metallic NPs synthesized by chemical reduction of the relevant ions. As the model of living organism, the cells of yeast *Hansenula polymorpha* were used. All NPs in minimal concentration (up to 0.05 mM) was proved to be non-toxic for yeast cells. The NPs and NPs-modified cells were characterized with the methods of UV-VIS spectroscopy, scanning electron microscopy, atom force microscopy, transmission electron microscopy and fluorescence microscopy. The bimetallic NPs, possessing the stable fluorescence in solution and inside the cells, allow to observe the phenomenon of NPs transferring from parental to daughter cells through at least three generations followed by releasing from the modified cells. The fluorescent NPs synthesized being small, non-toxic and fluorescent was shown to be perspective tool for cell imaging.

Keywords

Nanoparticles of noble metals · Fluorescence · Toxicity of nanoparticles · Yeast *Hansenula polymorpha* · Cell imaging .

Academic Discipline And Sub-Disciplines

Natural Products Chemistry

SUBJECT CLASSIFICATION

Chemistry Subject Classification

TYPE (METHOD/APPROACH)

Experimental Study-Analytical Method

ISSN 2321-807X

1. INTRODUCTION

Metal NPs, consisting of one metal, metal oxides or composite of several metals, have received much attention as a building block of advanced materials for nanoscience and nanotechnology, especially in various imaging techniques for medicine [1-8].

Metal colloids can be obtained through different physics-chemical methods [9-12] as well as wet chemistry methods and "green synthesis" [13-16]. The small size of NPs allows for sufficient mobility by Brownian motion and specificity in molecular interactions. Functionalized NPs of noble metals, having the strong optical absorption and fluorescence, can be applied as markers for microscopic investigation in cell biology as well as for detecting molecular interaction and labeling biochips [17-18].

Core-shell metal NPs possess unique optical, electronic, magnetic and catalytic properties [11, 17-20]. Binary silver and gold NPs can be used in particular for addressing different optical channels in the visible spectrum. The shift of the plasmonic band is affected by the ratio between contents of Ag and Au, the shape and the size of the binary particles, and the distribution of the two metals inside the particle [21]. Thus, a different plasmon absorption is obtained if both of the metals are forming core/shell particles with Au(core)/Ag(shell), Ag(core)/Au(shell) or an ally [22-25].

NPs have large surface areas in comparison with bulk metals, and energy states are distinct, which results in a growth in fluorescence emission spectra [26-29]. The fluorescence emission spectra of Au(core)/Ag(shell)-NPs were investigated and the quasistatic and local field theory describing the fluorescence emission property was developed [30]. This suggests that an interaction between two kinds of monometallic NPs make possible to produce novel NPs.

Fluorescent metal nanoclusters (FNCs) born a new class of fluorophores, very attractive due to their unique electronic structures and the subsequent unusual physical and chemical properties [4]. The size of metal NCs approaches the Fermi wavelength of electrons, between metal atoms and NPs, resulting in molecule-like properties including discrete energy levels, size-dependent fluorescence, good photostability and biocompatibility. These excellent properties make FNCs (mainly including Au, Ag, Cu, *etc.*) ideal fluorescent probes for biological application with a look at the future challenges, especially for controllable drug delivery [4, 31-34].

However, many relevant issues remain open. These include the molecular mechanisms governing the NPs–cell interactions, the physics-chemical parameters underlying their toxicity to different types of cells, the lack of standard methods and materials, and the uncertainty in the definition of general strategies to develop effective chips and devices based on NPs [35-41].

In this paper we describe the simple procedures of synthesis and characterization of NPs of noble metals, their influence on living cell and demonstrate the perspectives of NPs application. As result of investigation, a new method of cell imaging with fluorescent NPs on the model of yeast cell was proposed.

2. EXPERIMENTAL PROCEDURES

2.1. Chemicals

Tetrachloroauric acid trihydrate, sodium citrate, sodium borohydride, cetyltrimethyl ammonium bromide (CTAB), ascorbic acid, silver nitrate, D-glucose, sodium hydroxide, inorganic salts, chloroform and Butvar solution B-98 were purchased from Sigma-Aldrich, USA. All buffers and standard solutions were prepared using the water purified by the Milli-Q system (Millipore).

2.2. Synthesis of nanoparticles

Nanoparticles (NPs) and nanowebs (NWs) were synthesized by the reduction of metal ions from appropriate salts according to the known methods in our modifications [42-43]. Conditions of NPs and NWs synthesis are presented in the Table 1. NPs or NWs were collected by centrifugation under 10000 g for 40 min (Hettich Micro-22R centrifuge), washed with water and precipitated by centrifugation. Pellets were suspended in 0.2 mL of water and stored till exploitation at +4 °C.

Table 1 Methods of chemical synthesis of nanoparticles

Type of NPs	Reaction mixture and conditions	Color of NPs
AuNPs	1.25 mL 1 mM $HAuCl_4$ + 0.125 mL 38.8 mM trisodium citrate; stirring for 5 min at 100°C	wine-red
*AuNPs	0.145 mL 58.5 mM $HAuCl_4$ + 10 mL 10 mM CTAB stirring vigorously + 0.8 mL 100 mM sodium borohydride; stirring for 2 h at 20°C	violet

ISSN 2321-807X

AuNWs	0.145 mL 58.5 mM $HAuCl_4$ + 10 mL 10 mM CTAB stirring vigorously + 0.8 mL 100 mM sodium borohydride; incubation without stirring for 24 h at 20°C	dark blue
AgNPs	0.1 mL 150 mM $AgNO_3$ + 25 mL 30 mM D-glucose + 0.35 mL 50 mM NaOH; stirring for 20 min at 20°C	dark yellow
Au-core/Ag-shell-NPs	0.01 ml 100 mM ascorbic acid + 0.5 ml 10 mM $AgNO_3$ + 5 ml 0.9 mM AuNPs + 0.15 ml 100 mM NaOH; incubation without stirring for 24 h at 20°C	dark red
*Au-core/Ag-shell-NPs	0.01 ml 100 mM ascorbic acid + 0.5 ml 10 mM $AgNO_3$ + 5 ml 0.9 mM *AuNPs + 0.15 ml 100 mM NaOH; incubation without stirring for 24 h at 20°C	violet
Ag-core/Au-shell-NPs	10 ml 0.25 mM $HAuCl_4$ +0.5 ml 100 mM CTAB + 0.05 ml 100 mM ascorbic acid; vigorous mixing for 1 min, followed by adding 5 ml 3 mM AgNPs and incubation without stirring for 24 h at 20°C	violet
Ag-core/*Au-shell-NPs	10 ml 0.25 mM $HAuCl_4$ +0.5 ml 100 mM CTAB + 0.05 ml 100 mM ascorbic acid; vigorous mixing for 1 min, followed by adding 10 ml 3 mM AgNPs and incubation without stirring for 24 h at 20°C	red

2.3. Cells

The recombinant yeast strain *Hansenula polymorpha* NCYC 495-*pGAP1-HsARG1-(leu2car1 Sc:LEU2)*, constructed in the Institute of Cell Biology, NAS of Ukraine, was used in investigation [42]. The cells of this strain (further – cells), over-express the *HsARG1* gene, coding for human liver arginase I (further – arginase). These cells were applied in our experiments as the model of living organism.

Cultivation of the cells was performed in Erlenmeyer's flasks (volume 500 ml) as described earlier [44]. 110 ml of liquid media in flask were inoculated by cells from the early stationary growth phase in concentration of 50 μg/mL. Yeast cells for inoculation were taken from plates with agar Burkholder medium.

The grown cells were separated by centrifugation and washed twice with 30 mM phosphate buffer, pH 7.5 (PB). Activity of arginase in cell-free extracts of disrupted cells was determined in a two-step reaction: 1) enzymatic conversion of L-arginine to ornithine and urea and 2) photometric registration of urea content by the colorimetric method [42].

2.4. Interaction of nanoparticles with cells

To study cellular toxicity of NPs synthesized, cells were grown in the presence of NPs in solid and in liquid media (see 2.3). For this aim aliquot of fresh-grown cell's suspension (0.1 mL, with concentration 5 μg/mL) was put on plate with agar. Each plate (d=85 mm) contained agar supplemented by different NPs in various concentrations. Plates were incubated at 30 °C during 3 days and tested visually on cells growth.

To modify by different NPs, the cells after 1 day cultivation in liquid medium (to the biomass about 3 mg/mL) were supplemented with NPs till the concentration of 0.05 mM (calculated on noble metal content) and were incubated for 4 days. As the control, cells incubated in medium without NPs were used. Aliquots of cell's suspension were taken every day during experiment and fractionated by centrifugation. Both pellet and supernatant as well as initial NPs were analysed by UV-VIS spectroscopy on Shimadzu UV-1650 PC spectrophotometer. Colloids of NPs and suspensions of NPs-modified cells were imaged by microscopic methods, described below. Each experiment was performed in triplicate and repeated at least three times.

2.5. Microscopic imaging

2.5.1. Atomic Force Microscopy (AFM)

The size and structure of NPs were studied by atomic force microscope Solver P47-PRO (NT-MDT). An aliquot of the tested sample was spread on the surface of freshly-cleaved mica, dried and analyzed in air using the tapping mode with a resonance frequency of 160 kHz, scan rate of 1 Hz/s and resolution of 256×256 pixels.

ISSN 2321-807X

2.5.2. Scanning electron microscopy (SEM)

A Scanning Electron Microscope (SEM-microanalyser REMMA-102-02, Sumy, Ukraine) was used for morphological analyses of samples on a graphite rod (thickness – 0.5 cm, diameter – 0.5 cm). The special cover film on the samples with a Butvar solution B-98 (Sigma, St. Louis, MO, USA) in 1.5% chloroform was formed using an ultrasound method. In experiments the distance from the last lens of the microscope to the sample (WD) ranged from 17.1 mm to 21.7 mm; the accelerator voltage was in the range from 20 to 40 eV; zooms were from 2500 to 10000.

2.5.3. Fluorescence microscopy (FM)

An inverted fluorescence microscope (Axio Lab. A1., Carl Zeiss, Germany) with excitation by a mercury vapor arc lamp (X-Cite series 120Q) was used for samples imaging. The filters set was composed by Fluorescein isothiocyanate (FITC), 4', 6-Diamidino-2-phenylindole (DAPI), Texas Red and Cyanine 5 azide (Cy5). To prepare testing sample, an aliquot 10 μL of water-diluted probe was placed on a glass slide and covered with cover-slip (12 mm-diameter).

2.5.4. Transmission electron microscopy (TEM)

NPs analysis was carried out as described earlier [42]. For the cells analysis, samples were fixed in 1.5 % aqueous solution of $KMnO_4$ for 20 min at room temperature followed by post-fixation with 1% OsO_4 cacodylate buffer for 90 min at 0 °C. The samples were dehydrated by mixing with corresponding solutions containing increasing concentrations of ethanol with final incubation in acetone. Samples were embedded in Epon 812. Ultrathin sections were sliced in an ultramicrotome UMTP-6 (Sumy, Ukraine) contrasted with lead citrate and examined with electron microscope PEM-100 (Sumy, Ukraine) at 75 kV. The final magnification of the micrographs was 10 000.

3. RESULTS AND DISCUSSION

To develop a new method of cell imaging, we have carried out the following tasks: to synthesize NPs of noble metals; to study toxicity of these NPs on the model of yeast cell; to screen fluorescence ability and to test a storage stability of the synthesized NPs both in solution and inside the cell.

3.1. Study of the synthesized particles with SEM and XRM

In our study mono (Au, Ag) and bi-metallic (Au/Ag and Ag/Au) NPs were synthesized with the simple chemical methods as described in 2.2.

To characterize the synthesized NPs, the methods of scanning electron microscopy (SEM) with X-ray Microanalysis (XRM), atom force microscopy (AFM), UV-VIS spectroscopy and fluorescence microscopy (FM) were applied. The results of these experiments should let us find out whether the synthesized product is really nano-sized?

To get the quick estimation of the sizes metallic particles synthesized and to study their composition, SEM microscopy and XRM analysis were done.

As described earlier [42-43], the average diameters (d_{av}) of all monometallic NPs and AuNWs estimated by SEM are about 100 nm. XRM data of these NPs proved the forming of Au^0 and Ag^0 compounds, with characteristic peaks Kα at 2.1 keV and 3.0 keV, respectively.

d_{av}, estimated with SEM for the freshly-synthesized bi-metallic NPs, are about 100 nm, too (data not shown). The XRM image of Au/AgNPs (Figure 1) confirms the presence of Ag^0 and Au^0, proving the formation of both AgNPs and AuNPs, respectively. After 21-day storage intensity of the Au^0 peak decreased while the Ag^0 peak got higher, probably as a result of AuNPs masking under shell of AgNPs (Figure 1). Thus, the XRM data confirmed the formation of the core/shell bi-metallic NPs, namely, Au(core)/Ag(shell).

The XRM images of the Ag/AuNPs show the characteristic peaks for Ag^0 and Au^0 indicating the formation of both AgNPs and AuNPs (Figure 1). After 21 days of the storage the ratio of Ag and Au peaks changed in comparison with fresh-prepared bi-metallic NPs. The specific for Ag^0 Kα peak became higher, indicating the full coverage of AuNPs with AgNPs. Thus, the XRM data confirmed the formation of the Ag (core)/ Au (shell) NPs.

The stability of colloids was reported to enhance after coating them with noble metal NPs [20, 30, 45]. According to the SEM and XRM data, during 21 days of storage, the synthesized Au/AgNPs was shown to be satisfactory stable. At the same time, d_{av} of Ag/AuNPs increased to 500 nm as result of aggregation of the synthesized Ag/AuNPs.

Thus, we suggest the simple methods of two-step chemical reduction of ions from appropriate inorganic salts for the obtaining of core/shell bimetallic NPs (see Table 1). The proposed approach may be useful for obtaining of different novel core-shell structured bi-metallic and three-metallic NPs.

ISSN 2321-807X

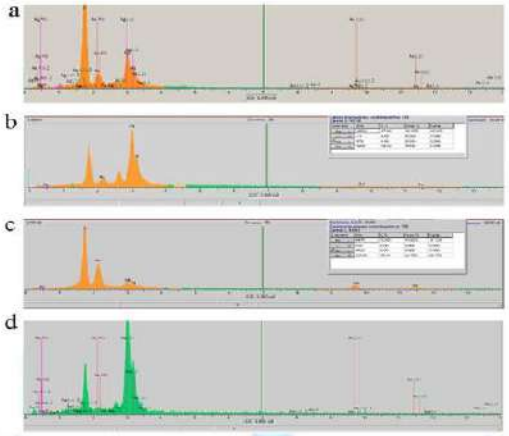

Figure 1 : X-ray-spectral characteristics of bi-metallic NPs after 1st (a, c) and 21st (b, d) days of the storage at +8 ºC: Au/AgNPs (a, b) and Ag/AuNPs (c, d).

3.2. Characterization of the NPs with AFM

To estimate the exact sizes and to study the morphology of the NPs synthesized, methods of TEM, powder XRD analyses and AFM were applied as described earlier [35]. The average diameters of AuNPs and AgNPs were shown to be less than 20 nm and diffraction peaks parameters of these NPs can be perfectly indexed into the cubic crystalline structures. The crystallite sizes were calculated from the main diffraction peaks as described earlier: for AuNPs d_{av} is 8.1 nm [42] and for AgNPs – 17.0 nm.

Figure 2 shows AFM images (a-b) and Gaussian distribution by size (c) of the synthesized Au/AgNPs and Ag/AuNPs in comparison with AuNPs [42]. The morphology of the AuNPs (d_{av}=16 nm) was shown to be almost smooth and their surfaces were homogeneous (Figure 2-1). In case of both bi-metallic NPs, the values of d_{av} were not higher than 20-25 nm, but their surfaces were rather heterogeneous (Figure2-2,3) as a result of NPs aggregation. Still some of the tested bi-metallic NPs did have bigger d_{av}, the largest of them was estimated to be 160 nm.

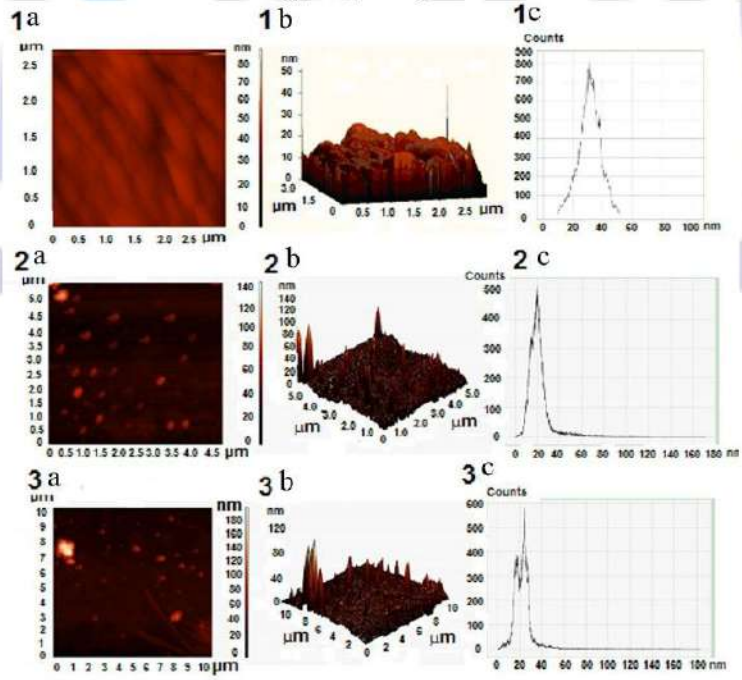

Figure 2 : AFM micrographs (a, b) and Gaussian distribution by size (c) of AuNPs (1), Au/AgNPs (2) and Ag/AuNPs (3)

ISSN 2321-807X

3.3. Optical properties of the NPs

UV-VIS absorption spectra was shown to be quite sensitive to formation of metallic colloids [23, 30]. The synthesized NPs of noble metals exhibited intense absorption peaks, as the result of the surface Plasmon excitation, of yellow, red, orange and violet colours (see Figure 3 and Table 1).

The fresh-synthesized monometallic AuNPs and AgNPs (after 1-day storage at +4°C) show intensive plasmonic absorption bands at 525 nm and 410 nm, respectively (see Figure 3 a, b), that are typical for the corresponding NPs [19, 23, 30]. The stability of monometallic NPs during 21 days is satisfactory according to UV-VIS study (Figure 3 a, b). On the contrary, the spectra of the AuNPs and AgNPs, kept during 3 weeks, demonstrated sharper and higher peaks of corresponding NPs, than the initial ones of the fresh-prepared nanocolloids. These changes may be explained, probably, by formation of nano-crystals of AuNPs and AgNPs (according to XRD-data).

The characteristics of metal NPs was shown to be altered by the addition of other metals [20, 45]. The wavelength of the absorption peak can be tuned if Ag and Au are integrated in binary metal NPs [11, 18, 20].

Plasmonic-based colour switches proved to be affected by the ratio between Ag and Au, the shape and the size of the binary NPs, and the distribution of the two metals inside the particle [46]. In case of thickness-controlled synthesis of core–shell structured NPs, the surface condition of the outer metal can be tuned as a function of the inner metal surface, provided that the outer shell is thin enough [32]. In our study we demonstrated, that if the AuNPs were coated with Ag under Au(core)/Ag(shell)NPs formation (see Figure 3 d), the absorption band would shift the solution changed from red to orange. As contrast, covering AgNPs with AuNPs resulted in change of the solution's colour from yellow to violet. The plasmonic absorption for Ag(core)/Au(shell)NPs is dominated by Au and shifts from 410 nm to 590 nm (Figure 3 c). The shift of absorption bands at much higher wavelengths (from 525 to 590 nm for hybride NPs with dominated AuNPs) may be explained by formation of larger than initial or non-spherical NPs [8, 17, 47-48]. The absorption peaks specific for Au/AgNPs change drastically during 21-day storage from 395 nm and 495 nm to 385 nm and 505 nm, respectively (Figure 3 d). These changes may be explained by nano-crystals formation.

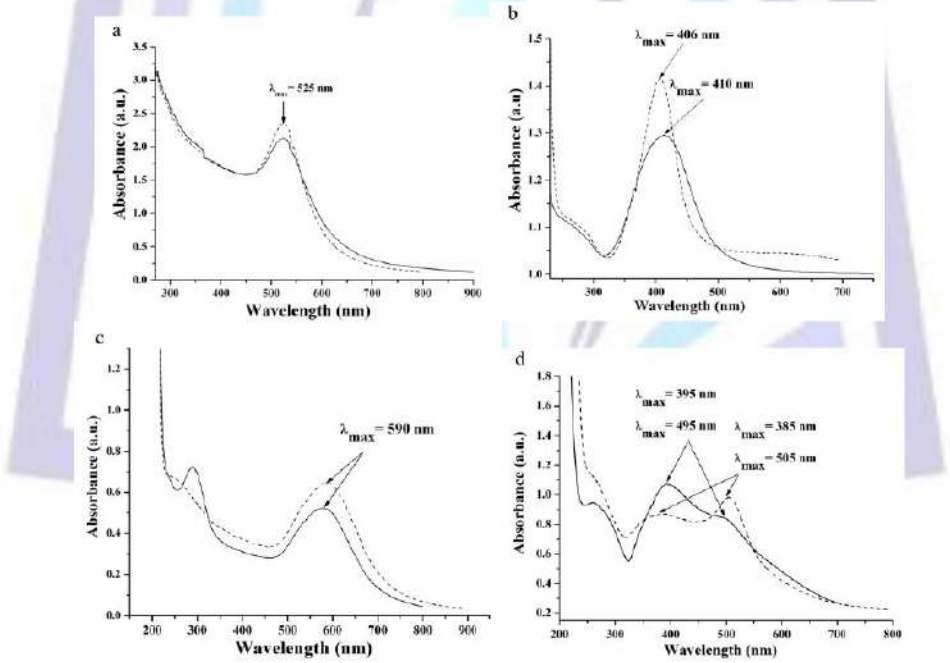

Figure 3: Absorption spectra of AuNPs (a), AgNPs (b), Ag/AuNPs (c) and Au/AgNPs (d); stability of NPs after storage during 1 day (solid) and 21 days (dashed).

3.4. Fluorescence properties of NPs

Fluorescence imaging is a very important technique for biological studies *in vivo* and clinical applications due to its high temporal and spatial resolutions. An inverted fluorescence microscope (FM) system allow to investigate the laser excited emission of the synthesized NPs.

The results of NPs analyses with FM are demonstrated in Figures 4-5. All fresh-prepared NPs investigated proved to be spherical in shape (Figure4). All NPs emit blue light, but only bimetallic NPs have additional bright

ISSN 2321-807X

fluorescence: Ag/AuNPs emit light in green channel (FITC filter); Au/AgNPs – in red (Texas Red filter) and in infra-red (Cy5 filter) channels. The storage stability of NPs in water was more than 2 months at +8° C.

The storage of bi-metallic NPs during 2-3 weeks in initial solutions of reagents without mixing was followed by nanowebs (NWs) formation (Figure5 and Table 1).

Thus, the covering of core NPs by the shell of noble metals make these stable fluorescent bi-metallic NPs attractive for biomedical application.

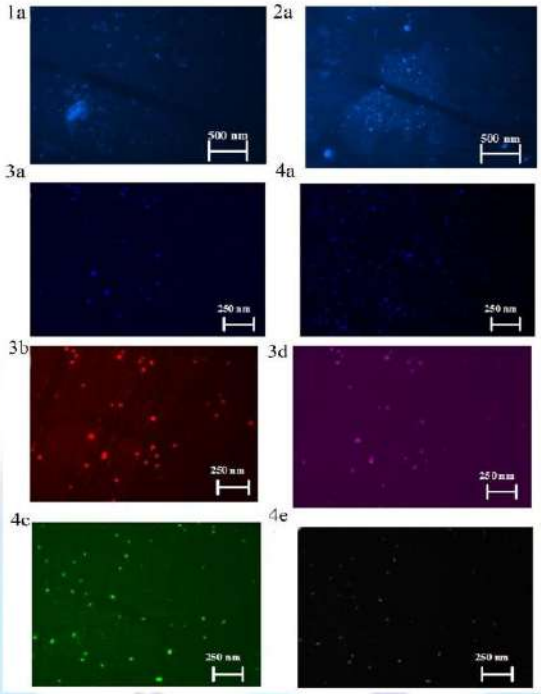

Figure 4: The fluorescence images of the fresh-prepared NPs: AuNPs (1); AgNPs (2); Au/AgNPs (3) and Ag/AuNPs (4) on different filters: a – DAPI (blue); b – Texas Red (red); c –FITC (green); d – Cy5 (infra-red) and e – brightfield

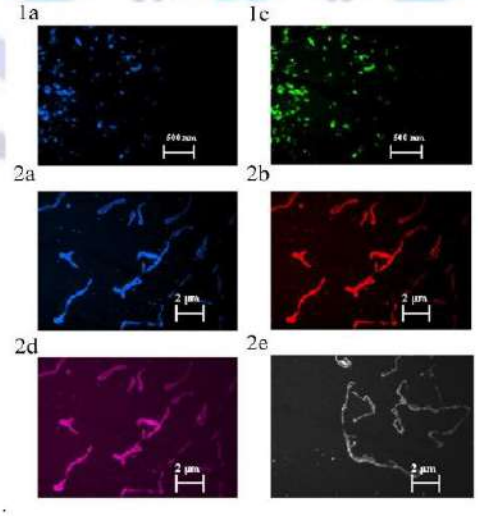

Figure 5: The fluorescence images of Ag/AuNPs (1) and *Au/AgWs (2), that were kept during 2 weeks without stirring. Channels: a – blue; b – red; c – green; d - infra-red and e – brightfield.

ISSN 2321-807X

3.5. Development of a cellular imaging method with fluorescent NPs

The number of imaging techniques have been applied in biological and biomedical research last decades, such as magnetic resonance imaging, computed tomography, positron emission tomography, single-photon emission computed tomography, fluorescence/bioluminescence, ultrasound, as well as multimodality approaches. With the size comparable to biological molecules, but orders of magnitude smaller than human cells, NPs can offer unprecedented interactions with biomolecules both on the surface of and inside the cells which may revolutionize disease diagnosis and treatment [6].

3.5.1. Interaction of cells with NPs

The cells of the yeast *H. polymorpha* (further - cells) were used in our investigations as the model of living organism for study of toxicity of NPs and possibility of cellular imaging with fluorescent NPs. In order to study the possible toxic effects of the NPs synthesized, microbiological experiments were performed: cells were grown in the presence of NPs with different concentrations in agar plates as well as in a liquid medium. According to our results, all the synthesized NPs added to described agar medium at low concentration (from 0.01 to 0.05 mM) proved to be non-toxic for cells (data not shown).

To collect and characterize the cells that interacted with 0.05 mM NPs, the living cells, preliminary inoculated for 2 days, were incubated in liquid media with different concentration of NPs during 5 days under shaking. As the control, cells without NPs were grown. Aliquots of cells were taken every day and analysed.

NPs interaction with cells was tested visually and by UV-VIS spectrophotometry. The colour of these cells changed in comparison with the control ones as result of NPs accumulation inside the cells (Figure6). At the same time, the spectra of the corresponding supernatants demonstrated a drop in NPs' concentration (data not shown). Thus, NPs-modified cells (further – cell-NPs) are formed as a result of the interaction between cells and NPs.

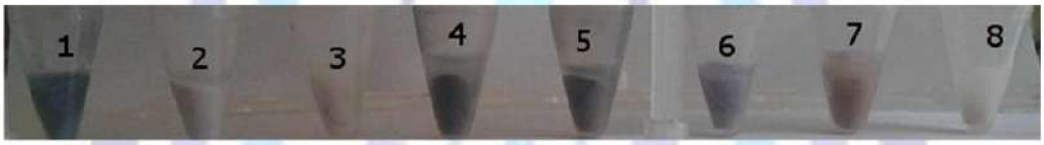

Figure 6: Pellets of the cells enriched with NPs (marked as described in Table 1), added to cells up to 0.05 mM: *AuNPs (1), AuNPs (2); AgNPs (3); Au/AgNPs (4), *Au/AgNPs (5), Ag/AuNPs (6), *Ag/AuNPs (7) and the control cells (8)

To provide the detailed analysis of cell-NPs, the methods of SEM with XRM, TEM and FM were applied. The results of these investigations can give us answers to the following questions: are the NPs located inside or on the surface of the cell? Do these NPs maintain the fluorescence ability inside the cell and how long does it continue? Are the cells-NPs alive? Is the transport of NPs to the cells reversible? How many generations are necessary to release the cells-NPs from NPs?

3.5.2. Localization of NPs in cells

The SEM images with XRM analysis of the cells-NPs demonstrated that NPs are not located on the surface of these cells (Figure 7).

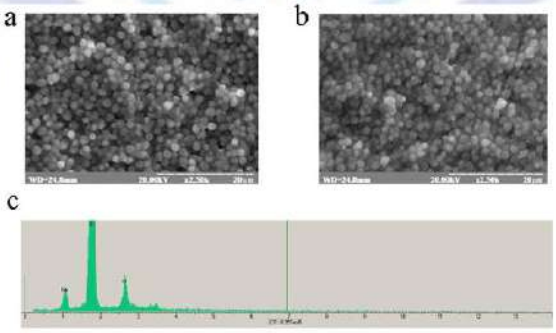

Figure 7: SEM of native cells before (a) and after (b) enrichment with AuNPs; X-ray spectral analysis of cells-AuNPs (c)

Only after cells-NPs permeabilization or disruption with glass beards, NPs were detected with XRM analysis (data not shown). These results suggest the presence of NPs inside the cell. The data of TEM analysis (Figure 8) prove this assumption.

ISSN 2321-807X

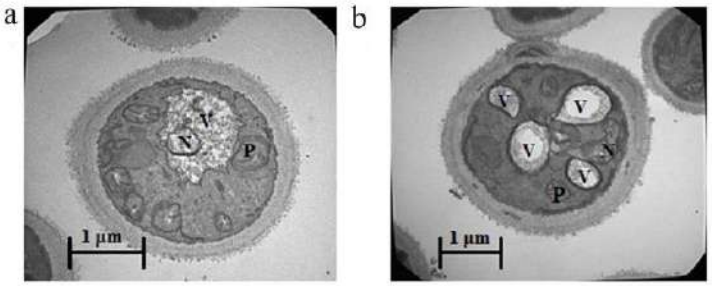

Figure 8: TEM of cells: control cells (a); after one day exposition to AuNPs (b). P – peroxisome, N - nucleus; V - vacuole. Scale bar –1 µm.

After penetration inside the cell NPs are localized mainly in vacuoles. The increase of incubation time of NPs with the cells leads to the formation of a number of vacuoles, probably, as result of the cell's response to the impact of the NPs (Figure 6). This process, probably, plays an important role in neutralization of the toxic effects of NPs inside the cell.

The average diameter of vacuole increased twice comparing to control cell. The cytoplasm of the yeast is homogeneous and in normal cells it contains from one to three vacuoles of different sizes. When exposed to stress conditions caused by NPs, yeast cells divide their large vacuoles into numerous smaller ones, probably, to activate NPs - uptake due to increasing the surface-to-volume ratio of the organells.

It is worth mentioning, that the modification of the cells with NPs takes part not only "*in vivo*", under cultivation conditions, but also "*in vitro*", when the cell's suspension in buffer is mixed with metal colloid. After storage of this suspension at +8 ^{0}C without mixing, the colour of cells changed. The XRM data also proved the fact of NPs' uptake by the cells.

3.5.3. Fluorescence of the cell-NPs

To study the fluorescent properties of NPs inside the cell, aliquots of cells-NPs were taken and analysed at different stages of incubation.

Figure 9-11 demonstrate FM images of different variants of cell-NPs ("first generation" of the cells): bi-metallic NPs kept unique fluorescent ability being included inside the cells-NPs. The cell-NPs glow brightly on different filters during 3-4 days under incubation. The highest brightness of fluorescence was picked on the 2nd and 3rd days of the cells incubation with bi-metallic NPs. At the same time, mono-metallic NPs reveal no fluorescence inside the cells (Figure 11).

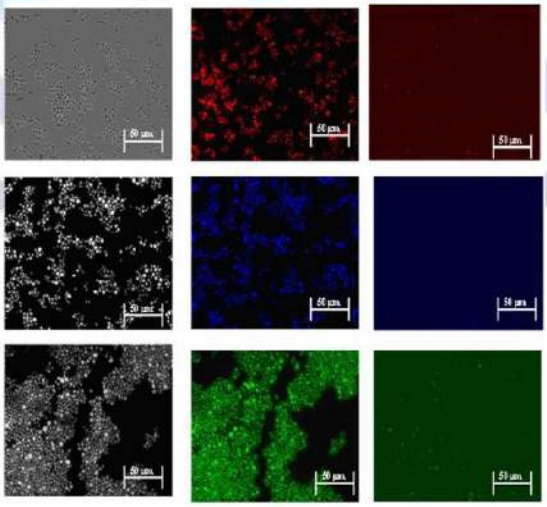

Figure 9: Fluorescent microscopy of 3-day incubated cells-Au/AgNPs (left and middle columns) in comparison with control cells (right column) on different filters. Left column – brightfield light. Channels (from top to bottom): red, blue and green, respectively. Duration – 665 ms.

ISSN 2321-807X

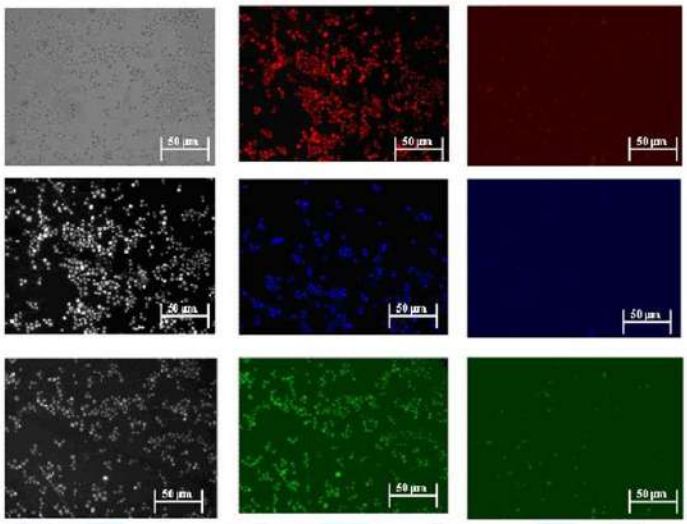

Figure 10: Fluorescent microscopy of 3 day cells-Ag/AuNPs (left and middle columns) in comparison with control cells (right column) on different filters. Left column – brightfield microscopy. Channels (from top to the bottom): red, blue and green, respectively. Duration – 665 ms.

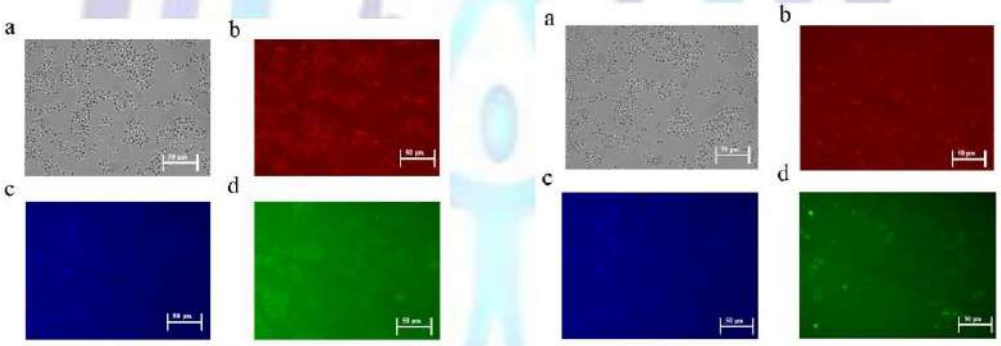

Figure 11: Fluorescent microscopy of the cells enriched with AgNPs (left) and AuNPs (right) during 3 days. Channels: brightfield (a), red (b), blue (c) and green (d). Duration – 665 ms.

3.5.4. Living ability and fluorescence stability of cells-NPs

The cells-NPs were found to be alive after different NPs penetration: being incubated during several days in liquid medium with 0.05 mM NPs (1st generation (Figure 12). Moreover, the activity of arginase (as a model of enzyme) in cell-free extracts of all tested cells-NPs didn't differ drastically from the one in control cells (data not shown). The cells-NPs were tested on fluorescence ability being re-cultivated during 4 generations in solid agar as well as in liquid medium. FM experiments demonstrated the reduction of fluorescence in the living cells from the 1st to the 4th generations and, at the same time, the appearance of fluorescent bi-metallic NPs outside the cells of the 3rd generation (Figure 12). According to the TEM images (Figure 12), NPs were released from these cells.

NPs uptake by cells was reported to depend on the composition, size and concentration of NPs as well as experiments conditions [37-39]. It is worth mentioning that if 2-day incubated cells-NPs of the 1st generation were collected by centrifugation and frozen at –20°C, the fluorescence of these cells-NPs was preserved during at least 1 month. Thus, the NPs synthesized have unique characteristics being small, non-toxic and fluorescent, so, they may be perspective tool for cell imaging.

ISSN 2321-807X

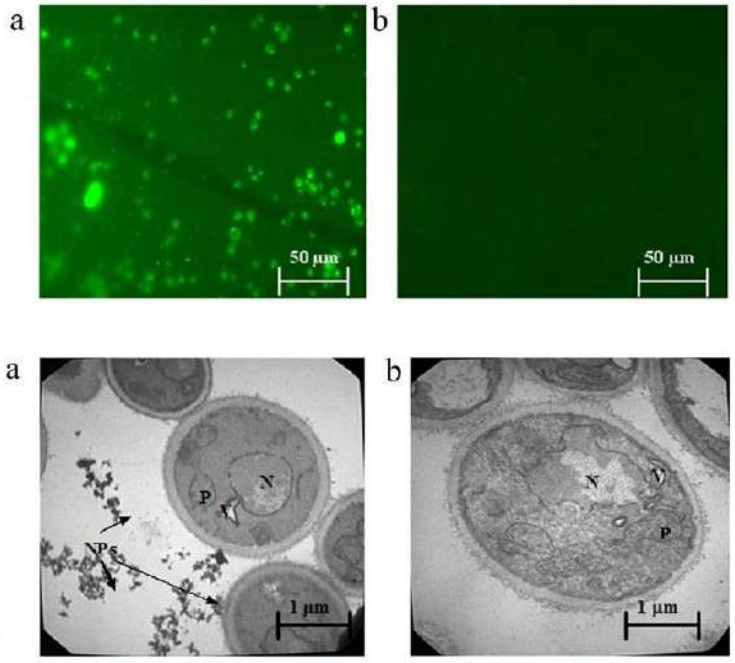

Figure 12: Characteristics of the Ag/AuNPs- cells of 3rd generation (a) in comparison with control cells (b). Top - fluorescent microscopy (duration – 665 ms) and bottom - TEM images (P - peroxisome; N - nucleus; V - vacuole).

4. CONCLUSION

For molecular imaging applications, a variety of NPs including magnetic NPs, semiconductor quantum dots, carbon nanotubes, gold NPs, and graphene-based nanomaterials have been investigated and are expected to play increasingly more important roles in preclinical/clinical research in the future [5].

In this paper we focused on the development of a new method of cellular imaging with fluorescent bi-metallic NPs of noble metals (Au/Ag and Ag/Au) synthesized by chemical reduction of the relevant ions. The bi-metallic colloids proved to possess the stable fluorescence (on green, red and blue channels) in solution (more than 2 months).

To develop the method of cell imaging, the recombinant yeast cells *Hansenula polymorpha* were used as the model of living organism. All NPs in minimal concentration (up to 0.05 mM) was proved to be non-toxic: under 3-day cultivation in liquid medium with NPs, yeast cells didn't affect significantly neither the dynamics of growth nor enzyme (arginase) activity.

We have demonstrated, that after penetration of fluorescent NPs through the cells membrane, the modified cells stay alive and fluorescent. Yeast cells of the 1st generation, modified by fluorescent NPs, kept ability to grow on agar and liquid medium. The fluorescent NPs synthesized allow us to observe the phenomenon of transferring of fluorescent NPs from parental to daughter cells through at least three generations followed by releasing of NPs from the modified cells. So, the synthesized NPs being small, non-toxic and fluorescent, may be perspective tool for cell imaging in biomedical sciences and clinical diagnostics.

Thus, our findings might be eventually interesting for the fundamental and applied biological sciences, namely for the study of molecular mechanisms of cell protection from stress, caused by exposure to toxic compounds, particularly, to NPs as well as for the development of methods for the synthesis of nano-sized fluorescent labels for clinical diagnostics and testing.

ACKNOWLEDGMENTS

This work was financially supported by Individual grant of OPTEC company for young scientists (Stasyuk-2014), by NAS of Ukraine (in the frames of program "Sensors for Medical, Environmental, Industrial, and Technological Needs" and by NATO (Project CBP. NUKR.SFP 984173).

ISSN 2321-807X

REFERENCES

[1] Key, J., Leary J.F. 2014. Nanoparticles for multimodal *in vivo* imaging in nanomedicine. Int. J. Nanomedicine. 9, 711-726.

[2] Boisselier, E., Astruc, D. 2009. Gold nanoparticles in nanomedicine: preparations, imaging, diagnostics, therapies and toxicity. Chem. Soc. Rev. 38, 1759–1782.

[3] Bao, G., Mitragotri, S., Tong, S. 2013. Multifunctional nanoparticles for drug delivery and molecular imaging. Annu Rev. Biomed. En. 15, 253-282.

[4] Kreuter, J. 2014. Nanoparticulate systems for brain delivery of drugs. Adv. Drug Deliv. Rev. 71, 2–14.

[5] Swierczewska, M., Lee, S., Chen, X. 2011. Inorganic nanoparticles for multimodal molecular imaging. Mol. Imaging. 10(1), 3-16.

[6] Zhu, Y., Hong, H., Xu, Z.P., Li, Z., Cai, W. 2013. Quantum dot-based nanoprobes for *in vivo* targeted imaging. Curr. Mol. Med. 13(10), 1549-1567.

[7] Gowda, R., Jones, N.R., Banerjee, S., Robertson, G.P. 2013. Use of nanotechnology to develop multi-drug ihibitors for cancer therapy. J. Nanomed. Nanotechnol. 4(6): doi:10.4172/2157-7439.1000184

[8] Guo, S., Wang, E. 2011. Noble metal nanomaterials: controllable synthesis and application in fuel cells and analytical sensors. Nano Today. 6, 240-264.

[9] You, H., Yang, S., Ding, B., Yang, H. 2013. Synthesis of colloidal metal and metal alloy nanoparticles for electrochemical energy applications. Chem. Soc. Rev. 42, 2880-2904.

[10] Mahmood Aliofkhazraei. 2014. Modern electrochemical methods in nano, surface and corrosion science. ISBN 978-953-51-1586-1, 350 p, InTech, June 11, 2014 doi: 10.5772/57202.

[11] Garcia-Torres, J., Vallés, E., Gómez, E. 2010. Synthesis and characterization of Co@Ag core-shell nanoparticles. J. Nanopart. Res. 12, 2189–2199.

[12] Xue, C., Millstone, J.E., Li, S., Mirkin, C.A. 2007. Plasmon-driven synthesis of triangular core-shell nanoprisms from gold seeds. Angew. Chem. Int. Ed. 46, 8436–8439.

[13] Blosi, M., Albonetti, S., Ortelli, S., Costa, L. 2014. Green and easily scalable microwave synthesis of noble metal nanosols (Au, Ag, Cu, Pd) usable as catalysts. New J. Chem. 38, 1401-1409.

[14] Zhao, J., Hu, W., Li, H., Ji, M., Zhao, C., Wanq, Z., Hu, H. 2015. One-step green synthesis of a ruthenium/graphene composite as a highly efficient catalyst. RSC Adv. 5, 7679-7686.

[15] Mittal, A.K., Chisti, Y., Banerjee. U.C. 2013. Synthesis of metallic nanopartides using plant extracts. Biotechnology Advances. 31(2), 346-356.

[16] Nadagouda, M.N. 2012. Green synthesis of nanocrystals and nanocomposites. In: Kolesnikov N (ed) Modern aspects of bulk crystal and thin film preparation. InTech http://www.intechopen.com/books/modern-aspects-of-bulk-crystal-and-thin-film-preparation/green-synthesis-of-nanocrystals-and-nanocomposites.

[17] Bohren, C., Huffman, D. 1983. Absorption and scattering of light by small partides. Wiley, New York.

[18] Zhu, J., Wang, Y., Huang, L., Lu, Y. 2004. Resonance light scattering characters of core-shell structure of Au-Ag nanoparticles. Phys. Lett. A. 323, 455–459.

[19] Mulvaney, P., Giersig, M., Henglein, A. 1993. Electrochemistry of multilayer colloids: preparation and absorption spectrum of gold-coated silver particles. J Phys. Chem. 97, 7061–7064.

[20] Lee, A., Baddelev. C., Hardacre. C., Ormerod. R.M., Lambert. R.M., Schmid, G., West. H. 1995. Structural and catalytic properties of novel Au/Pd bimetallic colloid partides: EXAFS, XRD, and acetylene coupling. J. Phys. Chem. 99, 6096–6102.

[21] Knauer, A., Thete, A., Li, S., Romanus, H., Csáki, A., Fritzsche, W., Köhler, J. M. 2011. Au/Ag/Au double shell nanoparticles with narrow size distribution obtained by continuous micro segmented flow synthesis. Chem Eng J 166:1164–1171.

[22] Yang, Y., Shi, J.L., Kawamura, G., Nogami. M. 2008. Preparation of Au-Ag, Ag-Au core-shell bimetallic nanoparticles for surface-enhanced Raman scattering. Scripta Mater. 58, 862–865.

[23] Rodriguez-Gonzalez, B., Burrows, A., Watanabe, M., Kiely, C.J., Liz Marzan, L.M. 2005. Multishell bimetallic AuAg nanoparticles: synthesis, structure and optical properties. J. Mater. Chem. 15, 1755–1759.

[24] Cao, Y.W., Jin, R., Mirkin, C.A. 2001. DNA-modified core-shell Ag/Au nanoparticles. J. Am. Chem. Soc. 123, 7961–7962.

[25] Rivas, L., Sanchez-Cortes, S., Garcia-Ramos, J.V., Morcillo, G. 2000. Mixed silver/gold colloids: a study of their formation, morphology, and surface-enhanced Raman activity. Langmuir. 16, 9722–9728.

ISSN 2321-807X

[26] Mohamed, M.B., Volkov, V., Link, S., El-Sayed, M.A. 2000. The lighting gold nanorods: fluorescence enhancement of over a million compared to the gold metal. Chem. Phys. Lett. 317, 517–523.

[27] Wilcoxon, J. P.; Martin, J. E.; Parsapour, F.; Wiedenman, B.; Kelley, D. F. 1998. Photoluminescence from Nanosize Gold Clusters. J. Chem. Phys. 108, 9137–9143.

[28] Jian, Z., Xiang, Z., Yongchang, W. 2005. Electrochemical synthesis and fluorescence spectrum properties of silver nanospheres. Microelectron. Eng. 77, 58–62.

[29] Mooradian, A. 1969. Photoluminescence of metals. Phys Rev Lett 22, 185–187.

[30] Liu, M., Guyot-Sionnest, P. 2004. Synthesis and optical characterization of Au/Ag core/shell nanorods. J. Phys. Chem. B. 108, 5882–5888.

[31] Zhang, L., Wang, E. 2014. Metal nanoclusters: new fluorescent probes for sensors and bioimaging. Nano Today. 9, 132–157.

[32] Bamrungsap, S., Zhao, Z., Chen, T., Wang, L., Li, C., Fu, T., Tan, W. 2012. Nanotechnology in therapeutics: a focus on nanoparticles as a drug delivery system. Nanomedicine. 7, 1253–1271.

[33] Connor, E., Mwamuka, J., Gole, A., Murphy, C., Wyatt, M. 2005. Gold nanoparticles are taken up by human cells but do not cause acute cytotoxicity. Small. 1, 325–327.

[34] Sezer, A.D. Application of nanotechnology in drug delivery. ISBN 978-953-51-1628-8, 552 p. InTech, Chapters published July 25, 2014. DOI:10.5772/57028.

[35] Akhter, S., Ahmad, M.Z., Ahmad, F.J., Storm, G., Kok, R.J. 2012. Gold nanoparticles in theranostic oncology: current state-of-the-art. Expert. Opin. Drug Deliv. 9, 1225–1243.

[36] Lynch, I., Weiss, C., Valsami-Jones, E. 2014. A strategy for grouping of nanomaterials based on key physico-chemical descriptors as a basis for safer-by-design NMs. Nano Today. 9, 266–270.

[37] Lemire, J.A., Harrison, J.J., Turner, R.J. 2013. Antimicrobial activity of metals: Mechanisms, molecular targets and applications. Nature reviews/Microbiology. 11, 371–384.

[38] Kuhn, D.A., Vanhecke, D., Michen, B., Blank, F., Gehr, P., Petri-Fink, A., Rothen-Rutishauser, B. 2014. Different endocytotic uptake mechanisms for nanoparticles in epithelial cells and macrophages. Beilstein J. Nanotechnol. 5, 1625–1636.

[39] Mironava, T., Hadjiargyrou, M., Simon. M., Jurukovski, V., Rafailovich, M.H. 2010. Gold nanoparticles cellular toxicity and recovery: Effect of size, concentration and exposure time. Nanotoxicology. 4, 120–137.

[40] Hoet, P.H., Nemery, B., Napierska, D. 2013. Intracellular oxidative stress caused by nanoparticles: What do we measure with the dichlorofluorescein assay? Nano Today. 8, 223–227.

[41] Wang, L., Clavero, C., Huba, Z., Carroll, E. E., Carpenter, D. Gu, Lukaszew, R. A. 2011. Plasmonics and enhanced magneto-optics in core-shell Co-Ag nanoparticles. Nano Lett 11:1237–1240

[42] Stasyuk, N., Serkiz, R., Mudry, S., Gayda, G., Zakalskiy, A., Koval'chuk, Y., Gonchar, M. 2011. Recombinant human arginase I immobilized on gold and silver nanoparticles: preparation and properties. Nanotechnology Development 1, 11-15

[43] Synenka, M.M., Stasyuk, N.Ye., Semashko, T.V., Gayda, G.Z., Mikchailova, R.V., Gonchar M.V. 2014. Immobilization of oxidoreductases at gold and silver nanoparticles. Studia Biologica 8:5–16 (in Ukrainian).

[44] Stasyuk, N., Gayda, G., Gonchar, M. 2014. L-Arginine-selective microbial amperometric sensor based on recombinant yeast cells over-producing human liver arginase I. Sens Actuators B. 204, 515–521.

[45] Harriman, A. 1990. Bimetallic Pt–Au colloids as catalysts for photochemical dehydrogenation. J. Chem. Soc. Chem. Commun. 1, 24-26.

[46] Mallik, K., Mandal, M., Pradhan, N., Pal, T. 2001. Seed mediated formation of bimetallic nanoparticles by UV Irradiation: a photochemical approach for the preparation of "core-shell" type structures. Nano Lett. 1, 319–322

[47] Vodnik, V.V., Bozanic, D.K., Bibic, N., Šaponjić, Z.V., Nedeljković, J.M. 2008. Optical properties of shaped silver nanoparticles. J. Nanosci. Nanotechnol. 8,3511-3515.

[48] Cao-Milán, R., Liz-Marzán, L.M. 2014. Gold nanoparticle conjugates: recent advances toward clinical applications. Expert Opin. Drug Deliv. 11, 741-752

Оригінал доступний за посиланням:
https://rajpub.com/index.php/jac/article/view/6694

Анотація: *У поточній роботі ми пропонуємо новий метод візуалізації клітин, заснований на використанні флуоресцентних наночастинок (НЧ) Au та Ag, синтезованих хімічним відновленням відповідних йонів. У мінімальних концентраціях (до 0,1 мМ) ці НЧ були нетоксичними для дріжджових клітин O. polymorpha, використаних в ролі експериментальної моделі живого організму. Металеві НЧ виявляють стабільну флуоресценцію в розчині, а також всередині живих клітин. Також нами продемонстровано використання синтезованих НЧ Au для доставки ензиму (аргінази I людини) до клітин дріжджів. Таким чином, синтезовані металеві НЧ Au та Ag можуть бути перспективним інструментом візуалізації клітин та контрольованої доставки ліків.*

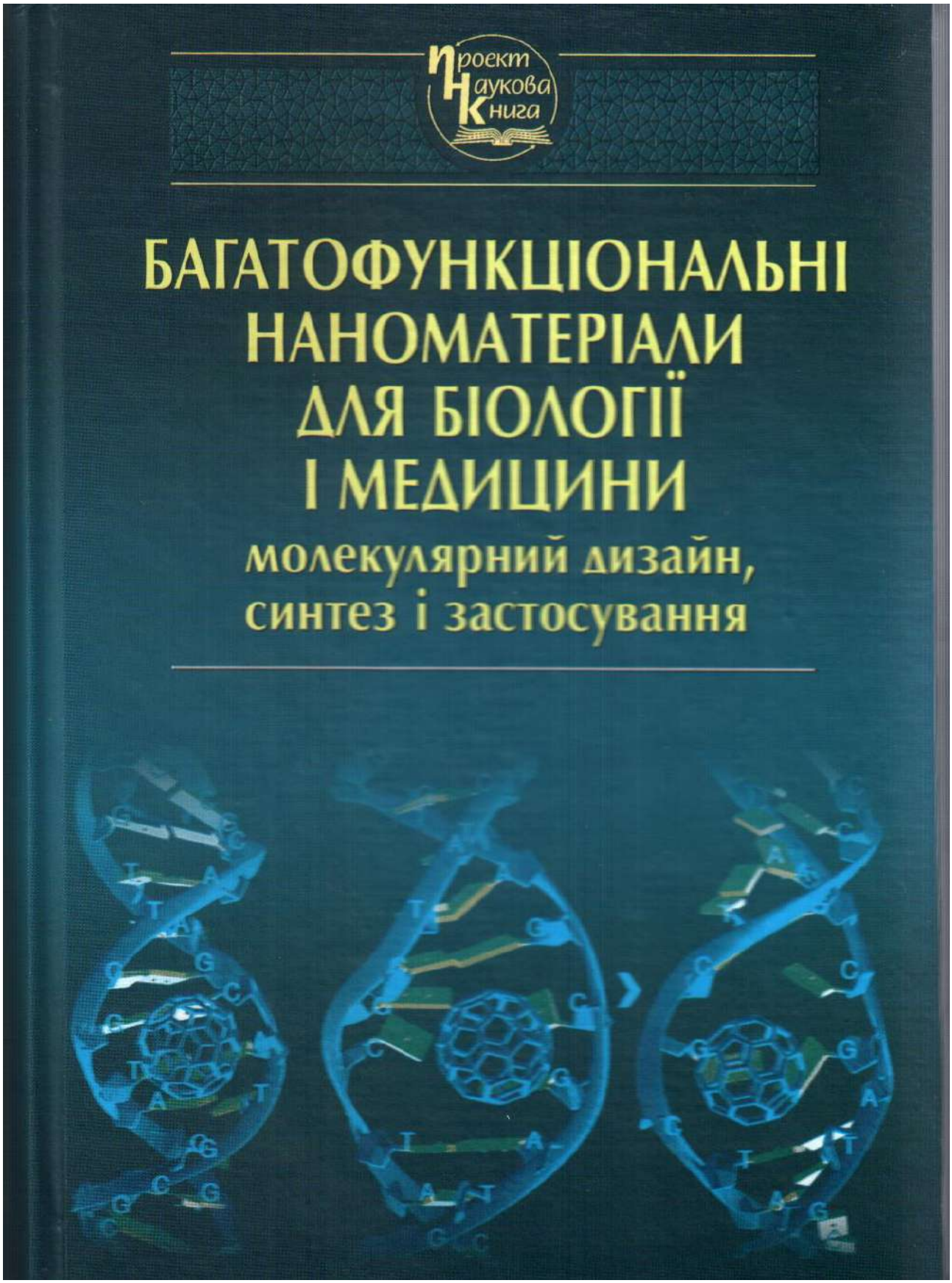
Проект Наукова Книга
БАГАТОФУНКЦІОНАЛЬНІ НАНОМАТЕРІАЛИ ДЛЯ БІОЛОГІЇ І МЕДИЦИНИ
молекулярний дизайн, синтез і застосування

БАГАТОФУНКЦІОНАЛЬНІ НАНОМАТЕРІАЛИ ДЛЯ БІОЛОГІЇ І МЕДИЦИНИ: молекулярний дизайн, синтез і застосування

За редакцією члена-кореспондента
НАН України Р.С. СТОЙКИ

ПРОЕКТ
"НАУКОВА КНИГА"

КИЇВ
• НАУКОВА ДУМКА •
2017

MULTIFUNCTIONAL NANOMATERIALS FOR BIOLOGY AND MEDICINE: molecular design, synthesis and application

Edited by R.S. STOIKA,
Corresponding Member of NAS of Ukraine

"SCIENTIFIC BOOK" PROJECT

KYIV
• NAUKOVA DUMKA •
2017

УДК: 53.04; 539.21; 54.05; 577; 57.04; 615

Автори:

Р.С. Стойка, Ю.І. Прилуцький, А.Г. Наумовець, Р.О. Білий, Я.Б. Блюм, Н.М. Бойко, А.П. Бурлака, Ю.В. Вац, Т.Я. Вітак, А. Волошиновський, Г.З. Гайда, О. Гевусь, Л.Л. Гнатишина, О.І. Годована, О.В. Годований, М.В. Гончар, І.І. Гринюк, Є.А. Гудзь, Н.М. Гула, О.В. Дмитренко, Л.Б. Дробот, М.П. Євстігнєєв, А.І. Ємець, Т.Б. Желтоножська, О.С. Зайченко, Т.О. Зінченко, М.І. Карковська, О.А. Кизима, Д.О. Климчук, О.Ю. Ключівська, Л.І. Кобилінська, Т.Є. Константінова, Л.Р. Куницька, О.О. Ліцис, О.В. Лобачевська, С.М. Лукін, В.І. Максін, О.П. Матишевська, Д.О. Мінченко, О.Г. Мінченко, Н.Є. Мітіна, О.С. М'ягкота, К.О. Паливода, Р.Р. Панчук, Н.М. Пермякова, Д.М. Петухов, С.В. Прилуцька, А.О. Рябцева, В.Ф. Сагач, А.І. Сененко, Ю.В. Сеньків, Р.Я. Серкіз, Н.Р. Скорохід, О.В. Смуток, Н.Є. Стасюк, О.Б. Столяр, А.М. Томін, Г.І. Фальфушинська, Є.З. Філяк, Н.С. Фінюк, Я. Хім'як, А.Є. Чапля, В.В. Черепанов, В.В. Чумак, Л.М. Шаповал, О.П. Яворовський, О.М. Якубчак, W. Berger, P. Heffeter, U. Ritter, P. Scharff

У монографії стисло викладено найвагоміші результати досліджень і розробок, отримані біологами у тісній співпраці з хіміками й фізиками у галузі наноматеріалів для біології, медицини, нанобіотехнологій. У шести логістично взаємопов'язаних тематичних розділах висвітлено питання молекулярного дизайну, синтезу багатофункціональних наноматеріалів для біології і медицини, доставки ліків у клітини-мішені за допомогою синтетичних наноматеріалів, використання полімерних олігоелектролітних наноматеріалів для доставки нуклеїнових кислот у клітини різного походження, описано багатофункціональні наноматеріали для діагностичних цілей і біомедичного іміджингу, проблеми біосумісності й екотоксичності нанокомпозитних матеріалів, наведено приклади застосування наноматеріалів для лікувальних цілей.

Для студентів та аспірантів, які цікавляться наноматеріалами різного біомедичного призначення, а також досвідчених спеціалістів у цій галузі сучасної науки.

Рецензенти:

академік НАН України, доктор біологічних наук, професор *С.О. Костерін*,
академік НАН України, доктор фізико-математичних наук, професор *Л.А. Булавін*,
академік НАН України, доктор хімічних наук, професор *М.Т. Картель*

Рекомендовано до друку вченою радою Інституту біології клітини НАН України (протокол № 8 від 25 вересня 2015 р.)

Видання здійснено за кошти Цільової комплексної програми «Створення та розвиток науково-видавничого комплексу НАН України»

Науково-видавничий відділ медико-біологічної, хімічної та геологічної літератури

Редактор *Н.А. Серебрякова*

© Р.С. Стойка, Ю.І. Прилуцький, А.Г. Наумовець, Р.О. Білий, Я.Б. Блюм, Н.М. Бойко, А.П. Бурлака, Ю.В. Вац, Т.Я. Вітак, А. Волошиновський, Г.З. Гайда, О. Гевусь, Л.Л. Гнатишина, О.І. Годована, О.В. Годований, М.В. Гончар, І.І. Гринюк, Є.А. Гудзь, Н.М. Гула, О.В. Дмитренко, Л.Б. Дробот, М.П. Євстігнєєв, А.І. Ємець, Т.Б. Желтоножська, О.С. Зайченко, Т.О. Зінченко, М.І. Карковська, О.А. Кизима, Д.О. Климчук, О.Ю. Ключівська, Л.І. Кобилінська, Т.Є. Константінова, Л.Р. Куницька, О.О. Ліцис, О.В. Лобачевська, С.М. Лукін, В.І. Максін, О.П. Матишевська, Д.О. Мінченко, О.Г. Мінченко, Н.Є. Мітіна, О.С. М'ягкота, К.О. Паливода, Р.Р. Панчук, Н.М. Пермякова, Д.М. Петухов, С.В. Прилуцька, А.О. Рябцева, В.Ф. Сагач, А.І. Сененко, Ю.В. Сеньків, Р.Я. Серкіз, Н.Р. Скорохід, О.В. Смуток, Н.Є. Стасюк, О.Б. Столяр, А.М. Томін, Г.І. Фальфушинська, Є.З. Філяк, Н.С. Фінюк, Я. Хім'як, А.Є. Чапля, В.В. Черепанов, В.В. Чумак, Л.М. Шаповал, О.П. Яворовський, О.М. Якубчак, W. Berger, P. Heffeter, U. Ritter, P. Scharff, 2017
© НВП «Видавництво "Наукова думка" НАН України», дизайн, 2017

ISBN 978-966-00-1564-7

Розділ 4. Багатофункціональні наноматеріали для діагностичних цілей і біомедичного іміджингу 143

4.1. Використання магнітних і флуоресцентних полімерних наночастинок, функціоналізованих лектином, для детекції і видалення апоптичних клітин (*А.М. Томін, Р.С. Стойка, О.С. Заіченко, Н.Є. Мітіна, Р.О. Білий*) 143

4.2. Індукування фотозбудженими багатостінними вуглецевими нанотрубками гіпертермічного ефекту у трансформованих клітинах (*С.В. Прилуцька, А.П. Бурлака, С.М. Лукін, В.В. Черепанов, Ю.І. Прилуцький*) 147

4.3. Fluorescent nanoparticles of noble metals for cell imaging (*G.Z. Gayda, N.Ye. Stasyuk, R.Ja. Serkiz, M.V. Gonchar*) 156

4.4. Наноматеріали у конструюванні біосенсорів біомедичного призначення (*М.І. Карковська, Н.Є. Стасюк, Г.З. Гайда, О.В. Смуток, М.В. Гончар*) 165

Розділ 5. Біосумісність та екотоксичність нанокомпозитних матеріалів 178

5.1. Зменшення негативних побічних ефектів доксорубіцину у мишей із лімфомою NK/Ly за його доставки новими полімерними наноносіями (*Н.М. Бойко, Ю.В. Сеньків, Ю.В. Вац, О.Ю. Ключівська, А.О. Рябцева, Н.Є. Мітіна, О.С. Заіченко, Р.С. Стойка*) 178

5.2. Корекція біохімічних показників загальної токсичної дії доксорубіцину за його доставки у складі комплексу з поліетиленгліколевмісним полімерним наноносієм у щурів (*Л.І. Кобилінська, А.О. Рябцева, Н.Є. Мітіна, О.С. Заіченко, Р.С. Стойка*) 183

5.3. Оцінювання біобезпеки срібловмісних наноматеріалів: молекулярно-біологічні підходи (*О.Г Мінченко, О.П. Яворовський, Д.О. Мінченко, Т.О. Зінченко*) 195

5.4. Екотоксичність промислових наноматеріалів. Аналіз проблеми та методологічні засади оцінювання (*О.Б. Столяр, Г.І. Фальфушинська, Л.Л. Гнатишина, Н.Є. Мітіна, О.С. Заіченко, Р.С. Стойка*) 210

Розділ 6. Приклади застосування наноматеріалів для лікувальних цілей 237

6.1. Регенерація кісткового дефекту за допомогою полімермінеральних нанокомпозитів на основі рентгеноконтрастних наночастинок ZrO_2-Gd_2O_3, функціоналізованих гіалуроновою кислотою (*О.І. Годована, О.Ю. Ключівська, О.В. Годований, Т.Є. Константінова, Н.Є. Мітіна, О.С. Заіченко, Р.С. Стойка*) 237

6.2. Роль одностінних вуглецевих нанотрубок у регуляції серцево-судинної діяльності у щурів за гіпертензії (*Л.М. Шаповал, В.Ф. Сагач, О.В. Дмитренко, В.В. Черепанов, Ю.І. Прилуцький*) 245

6.3. Application of C_{60} fullerene-doxorubicin complex for antitumor therapy (*R.R. Panchuk, S.V. Prylutska, R.S. Stoika, Yu.I. Prylutskyy, W. Berger, P. Heffeter, U. Ritter, P. Scharff*) 258

6.4. Іммобілізація біологічно активних компонентів до складу міцелярних наноконтейнерів і нанореакторів та застосування створених нанокомпозитів (*Т.Б. Желтоножська, Н.М. Пермякова, Л.Р. Куницька, Н.М. Бойко, Д.О. Клімчук, В.І. Максін, О.М. Якубчак*) 266

SUMMARY 301

СПИСОК ПРИЙНЯТИХ СКОРОЧЕНЬ 303

СПИСОК ЛІТЕРАТУРИ 308

Chapter 4. Multifunctional nanomaterials for diagnostic application and biomedical imaging 143

4.1. Application of lectin-functionalized magnetic and fluorescent polymeric nanoparticles for detection and isolation of apoptotic cells (*A.M. Tomin, R.S. Stoika, A.S. Zaichenko, N.Ye. Mitina, R.O. Bilyy*) 143

4.2. Photoactivated multi-wall carbon nanotubes induce hyperthermic effect in transformed mammalian cells (*S.V. Prylutska, A.P. Burlaka, S.M. Lukin, V.V. Cherepanov, Yu.I. Prylutskyy*) 147

4.3. Fluorescent nanoparticles of noble metals for cell imaging (*G.Z. Gayda, N.Ye. Stasyuk, R.Ja. Serkiz, M.V. Gonchar*) 156

4.4. Nanomaterials for construction of biosensors of biomedical application (*M.I. Karkovska, N.Y. Stasyuk, G.Z. Gayda, O.V. Smutok, M.V. Gonchar*) 165

Chapter 5. Biocompatibility and ecotoxicity of nanocomposite materials 178

5.1. Suppression of negative side effects of doxorubicin at its delivery by novel polymeric nanocarriers to mice with NK/Ly lymphoma (*N.M. Boiko, Y.V. Senkiv, Y.V. Vats, O.Y. Klyuchivska, A.O. Riabtseva, N.Y. Mitina, A.S. Zaichenko, R.S. Stoika*) 178

5.2. Correction of biochemical indicators of general toxicity of doxorubicin at its delivery in complex with PEG-containing polymeric nanocarrier in rats (*L.I. Kobylinska, A.O. Riabtseva, N.Y. Mitina, A.S. Zaichenko, R.S. Stoika*) 183

5.3. Evaluation of biosafety of Ag-containing nanomaterials : molecular-biological approaches (*O.H. Minchenko, O.P. Yavorovsky, D.O. Minchenko, T.O. Zinchenko*) 195

5.4. Ecotoxicity of industrial nanomaterials: Analysis of problem and methodological bases of estimation (*O.B. Stoliar, H.I. Falfushynska, L.L. Gnatyshyna, N.Y. Mitina, A.S. Zaichenko, R.S. Stoika*) 210

Chapter 6. Examples of application of functional nanomaterials for treatment goals 237

6.1. Regeneration of bone defect by polymer-mineral composite based on radiopaque $ZrO_2 \cdot Gd_2O_3$ nanoparticles functionalized with hyaluronic acid (*O.I. Hodovana, O.Y. Klyuchivska, O.V. Godovanyi, T.Y. Konstantinova, N.Y. Mitina, A.S. Zaichenko, R.S. Stoika*) 237

6.2. Single-wall carbon nanotubes improve regulation of cardiovascular activity in rats with hypertension (*L.M. Shapoval, V.F. Sagach, O.V. Dmitrenko, V.V. Cherepanov, Yu.I. Prylutskyy*) 245

6.3. Application of C_{60} fullerene-doxorubicin complex for antitumor therapy (*R.R. Panchuk, S.V. Prylutska, R.S. Stoika, Yu.I. Prylutskyy, W. Berger, P. Heffeter, U. Ritter, P. Scharff*) 258

6.4. Immobilization of biologically active components to micellar nanocontainers and nanoreactors, and application of created nanocomposites (*T.B. Zheltonozhskaya, N.M. Permyakova, L.R. Kunitskaya, N.M. Boiko, D.O. Klymchuk, V.I. Maksin, O.M. Iakubchak*) 266

SUMMARY 301

LIST OF A DOPTED ABBREVIATIONS 303

REFERENCES 308

що призводить до пошкодження мембран мітохондрій [53]. Злоякісні новоутворення внаслідок некрозу гинуть значно швидше через миттєву денатурацію білків, що зумовлює порушення цілісності цитоплазматичної мембрани клітин і вивільнення вмісту цитоплазми у міжклітинний простір.

Отже, здатність біодоступних БВНТ за низької концентрації (0,1 мг/мл) викликати локальне підвищення температури (до 50 °С) у суспензіях трансформованих клітин (АКЕ, L1210) за короткий час (1,5 хв) їх опромінення ближнім ІЧ-світлом (780—1400 нм, густина потоку енергії 3,5 Вт/см^2) з наступною деструкцією цих клітин (до 95 % відносно контролю) уможливлює їх практичне використання для цілеспрямованого знищення злоякісних новоутворень [63].

На підставі отриманих результатів можна зробити важливі висновки, а саме:

1) під час 2 хв опромінення ближнім ІЧ-світлом (довжина хвилі 780—1400 нм; густина потоку енергії 3,5 Вт/см^2) водної суспензії функціоналізованих БВНТ (0,1 мг/мл) вона нагрівалась до температури ~70 °С;

2) під час 1,5 хв опромінення ближнім ІЧ-світлом трансформованих клітин за наявності БВНТ температура суспензії клітин АКЕ зростала до 50, а суспензії клітин L1210 — до 47 °С, що є достатніми для їх незворотної деструкції;

3) після 1,5 хв опромінення ближнім ІЧ-світлом суспензій трансформованих клітин за наявності БВНТ кількість життєздатних клітин АКЕ знижувалась на 95,2 ± 4,8, а клітин L1210 — на 94,8 ± 5,2 % відносно контролю, отже, фотозбуджені біодоступні БВНТ здатні руйнувати злоякісні клітини внаслідок гіпертермічного ефекту.

4.3. Fluorescent nanoparticles of noble metals for cell imaging

Nanoparticles (NPs) of noble metals are advanced materials for nanoscience and nanotechnology [65—69]. These NPs have large surface areas in comparison with bulk metals, and energy states are distinct, which results in a growth in fluorescence emission spectra. Particularly, strong optical absorption and fluorescence of noble metallic NPs make them of special interest. The surface plasmon absorption spectra of silver and gold NPs are defined by the collective excitation of the free electron gas. The small size of NPs allows for sufficient mobility by Brownian motion and specificity in molecular interactions. Therefore, functionalized noble metal NPs can be applied as markers for microscopic investigation in cell biology as well as for detecting molecular interaction and labeling biochips [65, 67, 70].

Metal-containing NPs can be obtained by using different physics-chemical methods, such as spark discharging, microemulsion, cryochemical, radiolytic and photolytic reduction, UV photoactivated technique [71—75], as well as wet chemistry methods and "green synthesis" [76]. The properties of metal NPs can be changed under the influence of other metals. Bimetallic NPs have been reported to possess outstanding characters different from the corresponding monometallic NPs [72, 77—

83]. It was shown that core-shell NPs have unique optical, electronic, magnetic and catalytic properties [67, 84—88].

Binary silver and gold NPs can be used for addressing different optical channels in the visible spectrum. The shift of the plasmonic band is affected by the ratio between contents of Ag and Au, the shape and the size of the binary particles, and the distribution of the two metals inside the particle [79, 84, 89]. Thus, different plasmon absorption is obtained if both of the metals are forming core/shell particles with Au(core)/Ag(shell), Ag(core)/Au(shell), or ally [88, 90].

Fluorescent metal nanoclusters (FNCs) have born a new class of fluorophores that are very attractive due to their unique electronic structures and subsequent unusual physical and chemical properties. The size of metal NCs approaches Fermi wavelength of electrons, between metal atoms and NPs, resulting in molecule-like properties including discrete energy levels, size-dependent fluorescence, good photostability and biocompatibility. These excellent properties make them ideal fluorescent probes for biological applications [76].

Noble metal NPs are also promising platforms for delivery of drugs including anticancer, cardiovascular, anti-Alzheimer's drugs, analgesics, protease inhibitors, etc. Enzyme-based therapy is the growing into a very promising field of medical research. Bio-availability and non-immunogenicity, as well as rapid release (up to 3 days) from the organism, are critical requirements at the delivery of the NPs [65, 91—93].

Bio-compatibility and low toxicity, easy synthesis, large surface area, well-established surface functionalization (generally through thiol linkages) and tunable stability provide the NPs with unique attributes in order to enable new delivery strategies. Efficient release of the therapeutic agents might be triggered by the internal or external stimuli [94, 95].

Recently, we proposed a simple method of two-step chemical reduction of ions from appropriate inorganic salts for synthesis of core/shell bimetallic NPs [96]. That approach might be useful for obtaining different novel core-shell structured bimetallic, as well as three-metallic NPs.

In this paper, we describe the characteristics of the synthesized NPs of noble metals, their effect on living cells, and demonstrate the perspectives of application of the NPs specifically for drug delivery. Besides, new method of cell bioimaging based on using the developed fluorescent NPs for treatment of model yeast cells is proposed.

Chemicals and cells. All chemicals (tetrachloroauric acid trihydrate, sodium citrate, sodium borohydride, cetyltrimethyl ammonium bromide (CTAB), ascorbic acid, silver nitrate, *D*-glucose, sodium hydroxide, inorganic salts, chloroform and Butvar solution B-98) were purchased from Sigma-Aldrich, USA. All buffers and standard solutions were prepared using water purified by the Milli-Q system (Millipore).

Nanoparticles (NPs) and nanowebs (NWs) were prepared by means of the reduction of metal ions from appropriate salts (equations 4.1, 4.2, see p. 158) according to described methods using our modifications [69, 96—98].

Cells of the recombinant yeast strain *Hansenula polymorpha* NCYC 495-*pGAP1-HsARG1-(leu2car1 Sc:LEU2)* constructed at the Institute of Cell Biology,

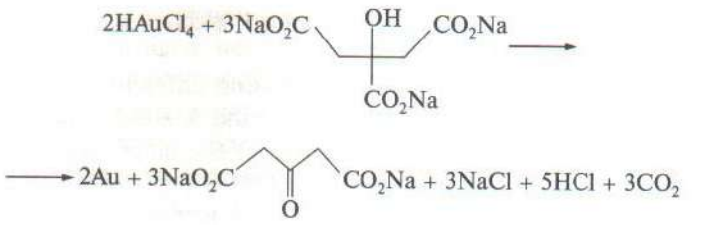

(4.1)

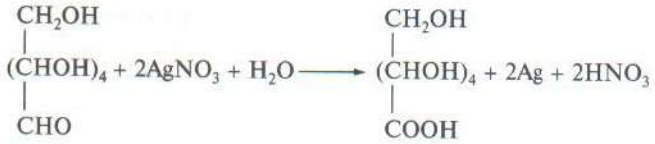

(4.2)

NAS of Ukraine, were applied as a model of living organism, as well as a source for arginase isolation and purification [99]. The yeast cells were cultivated as described earlier [97, 99]. To obtain the permeabilized cells, pellet of fresh 1-day-cultivated cells was re-suspended in 50 mM phosphate buffer, pH 7.0 (PB) with 0.2 % CTAB (20—30 mg/mL), and incubated for 15 min at 30 °C under gentle shaking. The pellet of resulted cells was washed twice with the PB and re-suspended in 0.3 mL of the PB.

Immobilization of arginase on the NPs was carried out using the cysteamine [98]. To activate the nanocarrier, 0.2 mL of 0.17 mM AuNPs in water were incubated overnight with 0.2 mL of 1 mM cysteamine at +4 °C. Activated AuNPs were triple rinsed in 5 mM phosphate buffer pH 7.5 (PB), suspended in 0.1 mL PB, mixed with 0.1 mL of arginase solution (57.5 U/mL, C = 0.1 mg/mL), and incubated for 1 h at 25 °C. In control, activated AuNPs were mixed with the PB instead of the enzyme. The bio-functionalized AuNPs (bioNPs) were rinsed with the PB and stored at +4 °C until use. Arginase activity was measured at all stages of the described procedure [96]. The yield of resulted bioNPs was determined as the ratio (%) of arginase activity in bioNPs to the initial enzymatic activity.

Cytotoxicity of synthesized NPs was studied in agar plates supplemented with the NPs applied in various concentrations, as described [96]. To label cells with different NPs, 1 day cell culture in liquid medium (biomass equal 3 mg/mL) was supplemented with the NPs (final concentration of 0.05 mM, calculated on the noble metal content) and incubated for 4 days. In control, cells were incubated in medium without NPs added. Aliquots of cell's suspension were taken every day during the experiment and cells were isolated by centrifugation. Both pellet and supernatant, as well as initial NPs were analysed by the UV-VIS spectroscopy on Shimadzu UV-1650 PC spectrophotometer. Colloids of the NPs and suspensions of NPs-modified cells were studied by the microscopic techniques [96]. Each experiment was performed in triplicate and repeated at least three times.

Cell interaction with bioNPs. To modify yeast cells with the bioNPs, 0.1 mL of arginase-AuNPs in the PB were mixed with 0.1 mL of fresh-grown cell suspension in the PB (30 mg/mL) and incubated for 24 h at +4 °C. After centrifugation (5 min, 270 g), the pellet of the bioNPs-modified cells was washed twice with the PB and then re-suspended in the PB. As controls, cells enriched with the AuNPs without arginase, as well as the unmodified cells, were tested.

Microscopic imaging of the synthesized NPs and of cells modified with the NPs was carried out using Transmission and Scanning electron microscopy (TEM and SEM), Powder X-ray diffraction (XRD), Atomic Force Microscopy (AFM), and Fluorescence microscopy (FM), as described [69, 96—98].

To develop a new method of cell imaging, we synthesized and characterized the NPs of noble metals, studied their toxicity on the model of yeast cells, explored cells modified by the NPs, and tested NPs for fluorescence ability and storage stability both in solution and inside the cell.

Study of the synthesized particles by SEM and XRM. Mono- (Au or Ag) and bi-metallic (Au/Ag and Ag/Au) NPs were synthesized and characterized [69, 96—98]. The results of SEM with XRM, TEM, AFM and FM studies confirm that the synthesized NPs possess the nano-size. Fig. 4.13, 4.14 (see insert) present the SEM and XRM images of these NPs.

The SEM images show that the average diameters (d_{av}) of all freshly-synthesized monometallic and bimetallic NPs and of AuNWs (after 1 day storage) are approximately 100 nm (Fig. 4.13 *a—d*, 4.14 *a*, *b*, respectively, see insert). Thus, these particles can true NPs, although their exact sizes have to be confirmed by using additional experimental methods.

XRM study of the monometallic NPs (Fig. 4.13, *e—g*, see insert) proves the formation of AuNPs and AuNWs (Kα peak at 2.1 keV is characteristic for Au^0) and AgNPs (Kα peak at 3.0 keV corresponds to Ag^0). After 21 day storage, the main properties of the monometallic NPs, namely, size and composition, proved to remain unchanged (according to the data of SEM and XRM, data not shown).

The XRM study of Au/AgNPs and Au/AgNPs confirms the presence of both Ag^0 and Au^0 [96]. According to SEM images (Fig. 4.14, see insert), the d_{av} of both bi-metallic NPs increased to 500 nm after 21 day storage. That fact might be explained by the aggregation of the NPs.

Characterization of the NPs with TEM, XRD and AFM. To measure the exact sizes and study the morphology of synthesized NPs, TEM [69], powder XRD analysis and AFM have been applied. The results of these experiments are presented in Fig. 4.15, 4.16.

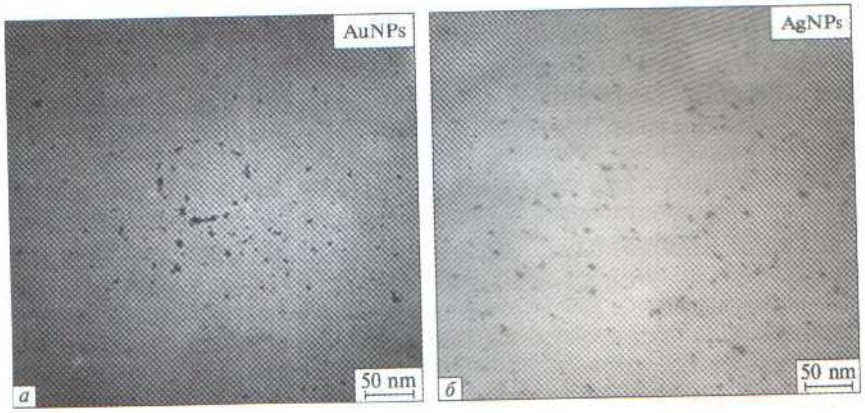

Fig. 4.15. TEM micrographs of synthesized AuNPs and AgNPs

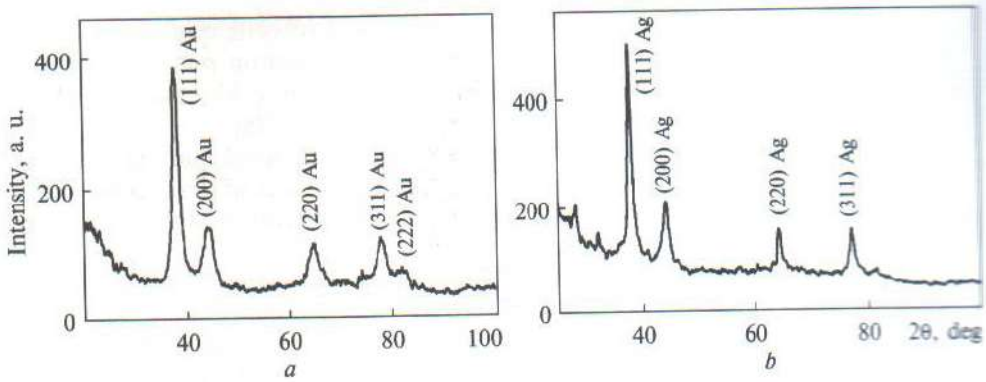

Fig. 4.16. XRD pattern of synthesized AuNPs (*a*) and AgNPs (*b*)

XRD patterns of the AuNPs [99] and AgNPs (unpublished data) are shown in Fig. 4.16. All diffraction peaks parameters including their positions and relative intensities, can be perfectly indexed into the cubic crystalline structures of the NPs. The crystallite sizes were calculated from the main diffraction peak (111) by using Sherrer's formula, as described for AuNPs [99] and are presented in Table 4.2.

The morphology of the AuNPs (d_{av} = 16 nm) according to AFM results [64, 66] was shown to be almost smooth and their surfaces were homogeneous. In case of both bi-metallic NPs, the values of d_{av} were below 20—25 nm, but their surfaces were rather heterogeneous as a result of NPs aggregation. Some of tested bi-metallic NPs have bigger d_{av}, and the largest of them were estimated to be 160 nm.

Thus, the average size of synthesized metallic NPs determined by different methods was found to vary. The value of d_{av} for AuNPs estimated by AFM method (data not shown) is higher than that value obtained by TEM and XRD methods. Such difference might be attributed to the intrinsic enlarging effect of the microscopic pinpoint to the analyzed NPs, thus, resulting in the overestimation of dimensions obtained by AFM.

Optical and fluorescence properties of the NPs were described in detail in paper [96]. The UV-VIS absorption spectra are quite sensitive to formation of the metallic colloids. The synthesized NPs of Au, Ag, Au/Ag and Ag/Au exhibited intense absorption peaks appearing as the result of surface plasmon excitation of yellow, red, orange and violet colours [68, 82, 89, 93, 100].

Due to its high temporal and spatial resolutions, fluorescence imaging is an important technique used in biological studies *in vivo* and at clinical application

Table 4.2. **Crystal cell parameters of the NPs**

The sample of NPs	Au	Ag
Crystal data	Cu *Kα* radiation, λ = 1.5418 Å	Cu *Kα* radiation, λ = 1.5418 Å
M_r	197	108
Type of crystal cell	cubic	cubic
Space group	Fm-3m	Fm-3m
Parameter of cell	a = 4.073 Å, V = 67.58 Å^3	a = 4.086 Å, V = 69.51 Å^3
Size, nm	8.1 ± 0.7	17.0 ± 0.3

Table 4.3. **Characteristics of the filters**

Filter	4′, 6-Diamidino-2-phenylindole, DAPI	Fluorescein isothiocyanate, FITC	Texas Red	Cyanine 5 azide, Cy5
Color of light	blue	green	red	infra-red
λ excitation, nm	350	494	596	646
λ emission, nm	470	513	615	662

[74, 79—81]. The inverted fluorescence microscope system allows investigating laser excited emission of the synthesized NPs. The description of filters employed in our study and other details of experiments are presented in Table 4.3.

All synthesized NPs emit blue light, however, only the bimetallic NPs possess an additional bright fluorescence: Ag/AuNPs emit light in green channel and Au/AgNPs — in red and infra-red channels [96]. Storage stability of the NPs in water was more than 2 months at +8 °C. After storage of bi-metallic NPs for 2—3 weeks in the initial solutions of reagents without mixing, aggregation of the NPs was observed. In the case of *Au/AgNPs, *Au/AgNWs were also formed.

Thus, covering of the core of the NPs by a shell of noble metals provides the bimetallic NPs with stable fluorescence and makes them attractive for biomedical applications.

Toxicity of synthesized NPs was studied towards living cells of yeast *H. polymorpha* (further — cells) as the model of living organism in the microbiological experiments. Yeast cells were grown in agar culture in the presence of NPs used in different concentrations, as well as in a liquid medium (unpublished data).

The NPs at low concentration (0.01—0.05 mM) were found to be non-toxic for yeast cells. The level of the monometallic NPs used in 0.1 mM in solid agar medium turned out to be non-toxic, while the Au/AgNPs were partly toxic, and the Ag/AuNPs were very toxic. At higher concentration of up to 0.5 mM only the AuNPs and AgNPs were non-toxic for cells, while at 1 mM concentration in solid agar medium these NPs stopped cellular growth (Fig. 4.17, see insert).

Thus, 0.05 mM is the highest concentration of all NPs estimated as non-toxic for yeast cell growth. These data demonstrate that all used NPs are rather toxic for yeast cells and their toxicity depends on concentration and size of the NPs, as well as on the duration of cell exposure to the NPs. The obtained results are also of potential interest in pharmacology. The nanomaterials, namely, AgNPs, AuNPs, and their hybrids have recently emerged on the market as new effective and promising broad-range antibacterial/antiviral agents [101].

Interaction of yeast cells with the NPs was estimated visually, as well as by the UV-VIS spectrophotometry. Colour of the NPs'-treated yeast cells changed comparing with control ones depending upon the NPs concentration [96]. At the same time, the spectra of the corresponding supernatants demonstrated a drop in NPs' concentration (data not shown). Thus, cell incubation with the NPs resulted in their accumulation inside the cells. It can be assumed that special NPs-modified cells (further — cell-NPs) are formed during interaction between yeast cells and the NPs.

In order to provide detailed analysis of cell modification by the NPs, the methods of SEM with XRM, TEM and FM were applied [96]. The results of these investigations can give the answers to the following questions:

1) are the NPs located inside or on the surface of the cell?

2) do the NPs maintain the fluorescence ability inside the cell and how long does it continue?

3) are the cells with the NPs alive?

4) is transport of the NPs to cells reversible?

5) how many cell generations are necessary to release the cells from the NPs?

Localization of the NPs in cells was studied by using SEM with XRM analysis, and the NPs were shown to be not located on the surface of the intact cells [96]. Only after permeabilization of the NPs'-treated cells or their disrution with glass beards, the NPs are detected with the XRM analysis, thus, suggesting presence of the NPs inside the cell. The results of TEM analysis prove this assumption [96].

Fluorescence of the cell-NPs was analysed at different stages of incubation [96]. Fig. 4.18 (see insert) demonstrates FM images of cells-NPs ("first generation" of the cells).

The bi-metallic NPs were shown to keep a unique fluorescent ability after being included inside the cells-NPs. The cells-NPs glow brightly at different filters for 3—4 days under incubation. The highest brightness of fluorescence was detected on the 2nd and 3rd days of cell incubation with these NPs. At the same time, the mono-metallic NPs present inside the cells, as well as control (untreated) cells, did not demonstrate the fluorescence [96]. The NPs' uptake by yeast cells was shown to depend on the composition, size and concentration of NPs, as well as on experimental conditions [96]. Fig. 4.19 (see insert) presents general principle of the proposed method of cell imaging.

The cells-NPs stayed alive after penetration of different NPs, and they can be incubated for several days in liquid medium supplemented with 0.05 mM NPs (1^{st} generation of cell-NPs). The cells kept a capability to grow also in solid agar medium (Fig. 4.20, see insert). Moreover, the activity of arginase (as a model enzyme) in cell-free extracts of all tested cells-NPs did not differ substantially from such in control cells (data not shown).

Fluorescence stability of the cells-NPs was tested after re-cultivation of the yeast for 4 generations in solid agar, as well as in liquid medium. FM experiments demonstrated a reduction of fluorescence in the living cells from the 1^{st} to 4^{th} generations. At the same time, the appearance of fluorescent bi-metallic NPs outside cells of the 2^{nd} and 3^{rd} generations was detected [96]. According to the TEM images (Fig. 4.21), the NPs were released from yeast cells of the 2^{nd} and 3^{rd} generations.

After penetrating inside the cell, the NPs are located mainly in the vacuoles. An increase of incubation time of the NPs with yeast cells leads to the formation of a number of vacuoles, probably, as result of the cell's response to the impact of the NPs (see Fig. 4.21, *b*). This process, probably, plays an important role in neutralization of the toxic effects of the NPs inside yeast cell.

The cytoplasm of the yeast cells is homogeneous and in normal conditions it contains from one to three vacuoles of different size. When exposed to stress caused by NPs, yeast cells divide their large vacuoles into numerous smaller ones, probably, to activate NPs-uptake due to increasing the surface-to-volume ratio of the organells.

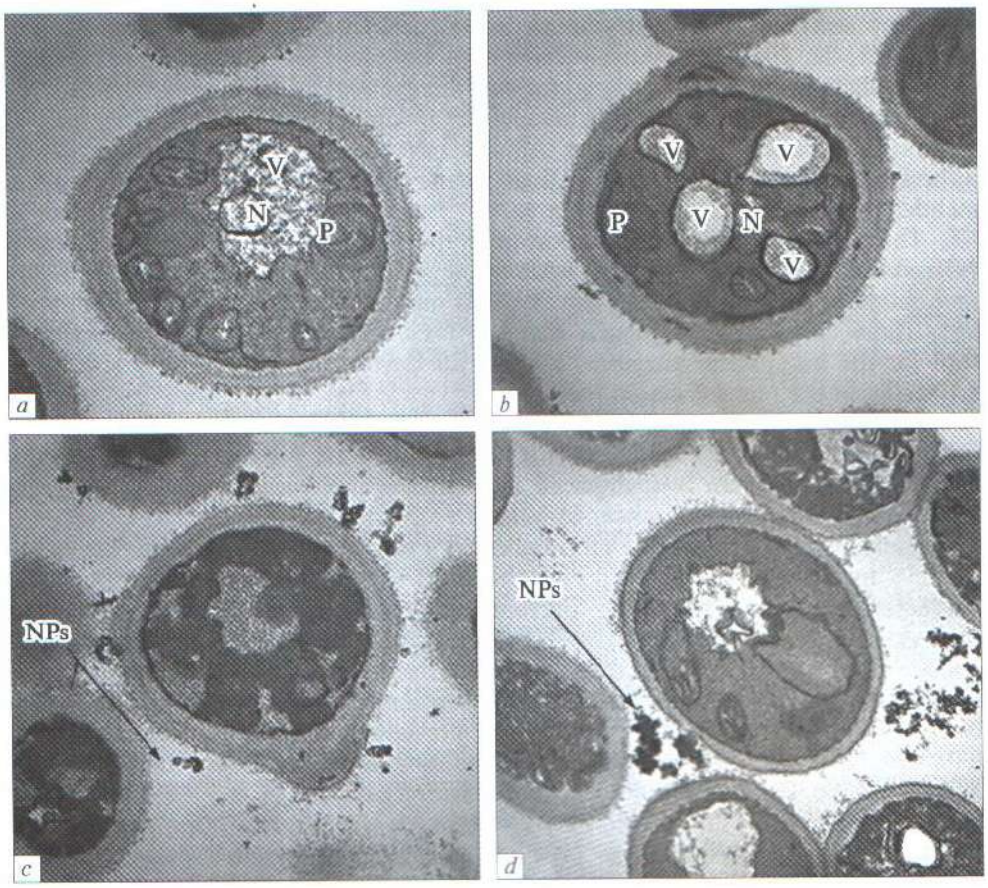

Fig. 4.21. TEM image of cells modified with the AuNPs: unmodified, control cells (*a*), cells of the 1st generation (*b*), 2nd generation (*c*) and 3rd generation (*d*). *P. peroxisome*; *N. nucleus*; *V. vacuole*; NPs, nanoparticles. Scale bar – 1 μm

Thus, cells modified with fluorescent NPs stay alive. Cells-NPs of the 1st generation are capable of growing on agar and liquid medium. FM data demonstrate a reduction of cells fluorescence from the 1st to 3rd generation of the daughter cells. According to TEM data, that reduction was caused by a release of the NPs outside the cell. Thus, the synthesized NPs may be a perspective tool for cell imaging, since they are small, non-toxic and possess fluorescence.

Drug delivery potential of the developed NPs. Use of various nanocomposites for addressed delivery of drugs is one of the most promising applications of novel nanomaterials that is already utilized for therapeutic treatment of different diseases. Cell is the best starting point for estimation of the effectiveness of new drug delivery systems, since it is the cell as a biological entity which is the first target *en route* to mechanistic understanding of both intracellular and whole organism pathways and processes. Due to their unique physicochemical properties, the NPs enable a delivery of great variety of drugs including anticancer, cardio-

vascular, anti-Alzheimer's drugs, analgesics, enzymes, protease inhibitors and others [71, 86, 101—104]. AuNPs have been exploited for multimodality imaging, tumor targeting, and transporting various therapeutics. Additionally, the AuNPs have been used as photothermal therapeutics in cancer treatment. The promises of a functional cancer therapy using AuNPs have been extensively demonstrated, although the materials are still in their infancy stage and did not reach clinical standards [104].

The results of our study demonstrate the unique properties of the created NPs, namely, easy synthesis, low toxicity, huge surface area, well-established surface functionalization, tunable stability, and rapid release from the cells [69, 96—98]. These characteristics suggest that the NPs of noble metals is a perspective tool for the biomedical purposes, namely for developing new delivery strategies, especially in the enzyme-based therapy.

Here we studied a possibility of using created AuNPs for targeting recombinant yeast cells as a model of living organism. These NPs were applied as the nanocarriers of human liver arginase I (arginase) which was proposed for treatment of selected forms of cancer in human.

Immobilization of arginase onto the AuNPs was carried out by using the electrostatic method described earlier for the oxidoreductases [98]. Morphological characteristics of the AuNPs before and after enzyme's immobilization proved that size and structure of arginase-NPs preparations (further — bioNPs) did not change significantly and varied in the range from 80 to 100 nm. Moreover, the synthesized AuNPs have a stabilizing effect towards that arginase, probably, due to its fixation on the surface of the NPs preventing enzyme's inactivation [69, 97]. The efficiency of the electrostatic binding of arginase on the surface of AuNPs (Table 4.4) was about 45 % (unpublished data).

High thermostability of the bioAuNPs, as well as wide working pH range of enzyme [97], suggest that these NPs will be useful for arginase delivery to cell targets. The permeability of cells to the NPs has been intensively studied due to perspectives of such approach for addressed delivery of drugs in the living organism [71, 102, 104, 105].

Interaction of yeast cells with arginase-AuNPs led to increasing of enzymatic activity inside the treated cells. Fig. 4.22 presents the indicator of arginase activity in different cells — enriched with the bioNPs (bioNPs-cells) and containing AuNPs (NPs-cells) in comparison with control (unmodified cells) (unpublished data).

Table 4.4. **Characteristics of immobilization procedure**

Parameter	Arginase activity		
	Before immobilization	After immobilization	
		Supernatant	BioNPs
Activity, U/mL	126.4 ± 1.2	2.0 ± 0.1	57.3 ± 0.9
V, mL	0.1	1.8	0.1
Total activity, U	12.6	3.6	5.7
Yield, %	100	28.6	45.2

Arginase activity of the bioNPs-cells was shown to increase 3-fold in comparison with the control and NPs-cells. That activity of the bioNPs-cells accounts for approximately 40 % of the initial activity of the bioNPs added to cells, while the difference in arginase acitivity of the bioNPs-cells and the NPs-cells accounts for 27 % of the initial arginase activity present in the bioNPs. There are two potential explanations of these findings: 1) the penetration of the bioNPs into the cells and 2) the electrostatic binding of the bioNPs with cell wall resulting in an increase of the enzyme content in the bioNPs-cells. To answer a question about the mechanism of the revealed phenomenon, treated yeast cells were studied by SEM and X-ray spectral analysis (data not shown) before and after their modification with arginase-AuNPs. Track amounts of Au^0 (AuNPs) were detected only in the permeabilized bioNPs-cells (unpublished data).

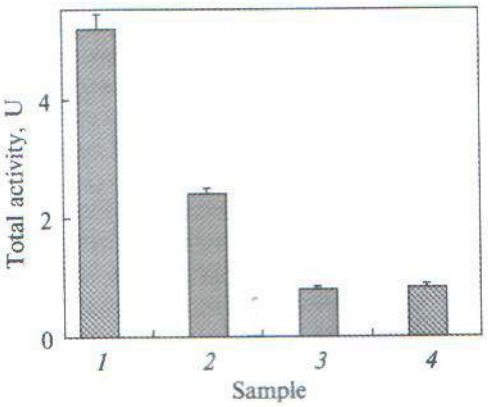

Fig. 4.22. Arginase activity in the initial bioNPs (*1*), yeast cells enriched with the bioNPs (*2*), and the NPs (*3*) comparing to control cells (*4*)

The molecular mechanisms of the NPs-cell interactions and the physicochemical parameters underlying their toxicity towards different types of cells stay poorly studied. A lack of standard methods and materials slows down further development of "smart" drugs and devices based on the NPs [71, 86, 93, 102, 104].

We propose a novel method of cell imaging based on using fluorescent nanoparticles (NPs) of Au and Ag synthesized by chemical reduction of the relevant ions. In minimal concentration (up to 0.1 mM), these NPs were non-toxic for the yeast cells *H. polymorpha* used as an experimental model of the living organism. The bi-metallic NPs possess stable fluorescence (green, red, and blue filters) in solution, as well as inside the living cells. That allows observation of transferring fluorescent NPs from the parental to daughter cells through at least three generations. Utilization of the developed AuNPs for delivery of the enzyme (human arginase) to yeast cells was also demonstrated. Thus, the synthesized bimetallic (Au and Ag) NPs may be a perspective tool for cell imaging and controlled drug delivery.

4.4. Наноматеріали у конструюванні біосенсорів біомедичного призначення

Специфічні властивості наноматеріалів відкривають широкі можливості для створення нових продуктів із цінними характеристиками і практичним значенням: ефективних каталізаторів, сенсорних елементів, діагностичних препаратів, фармацевтичних засобів [106].

Однією з основних особливостей наночастинок є висока хімічна активність, обумовлена їх підвищеною здатністю до іонного чи атомного обмі-

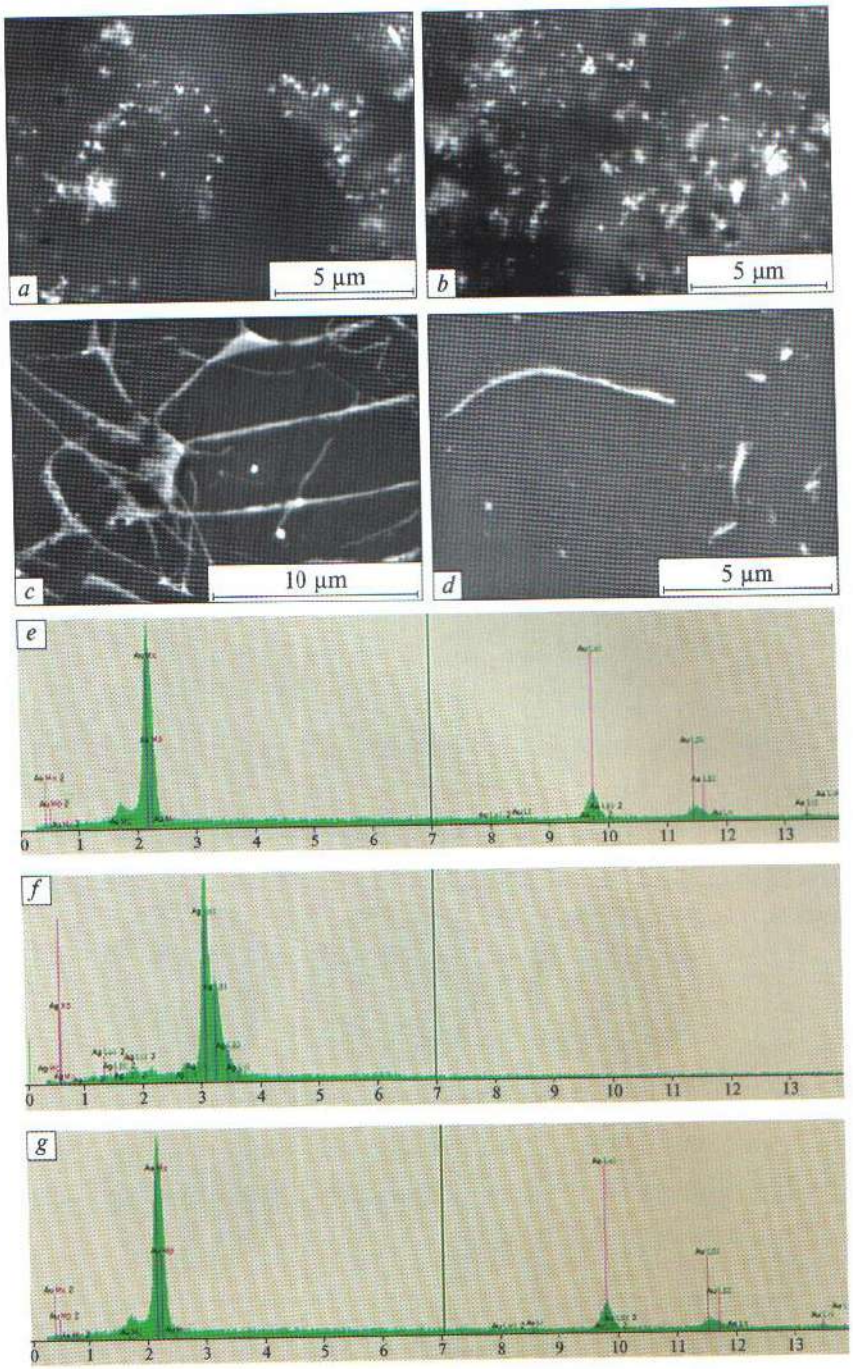

Fig. 4.13. SEM images (*a*—*d*) and X-ray-spectral characteristics (*e*—*g*) [97] of the monometallic NPs:
AuNPs (*a*, *e*), AgNPs (*b*, *f*) and AuNWs (*c*, *d*, *g*)

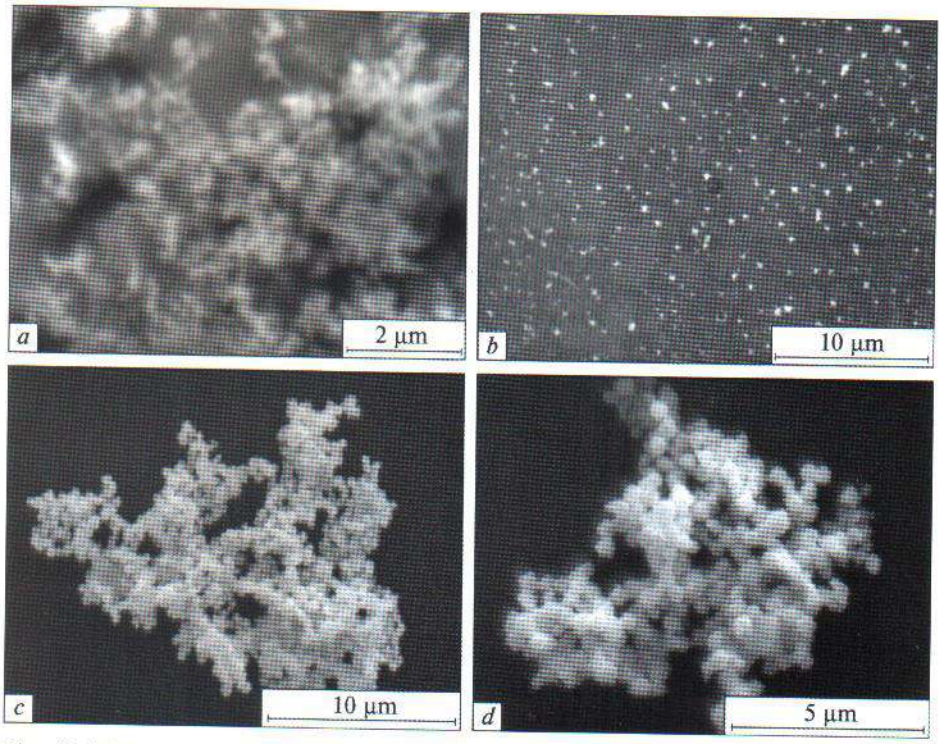

Fig. 4.14. SEM images of the bi-metallic NPs after 1 (*a*, *b*) and 21 (*c*, *d*) days of storage at +8 °C:
Au/AgNPs (*a*, *c*) and Ag/AuNPs (*b*, *d*)

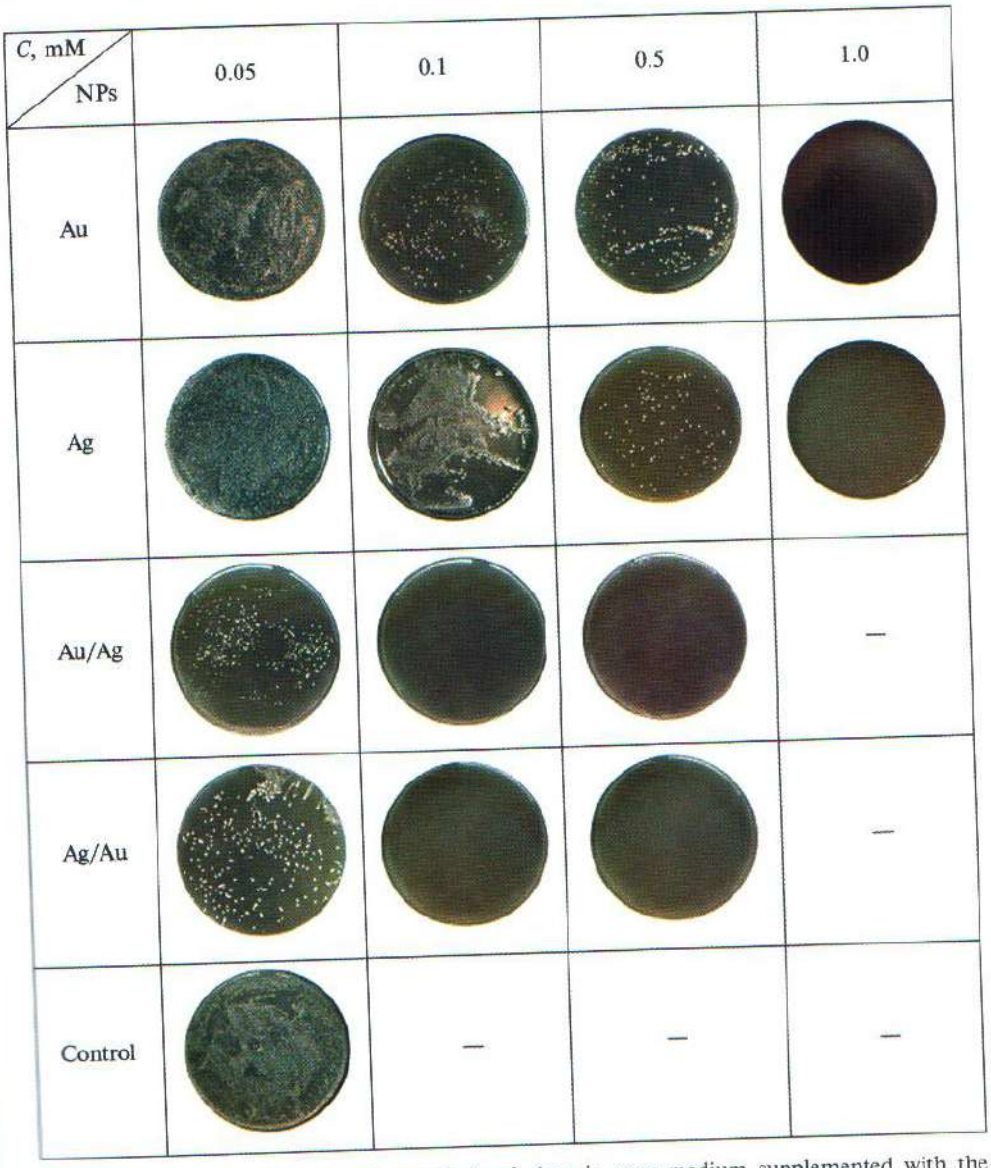

Fig. 4.17. Character of yeast cell growth for 3 days in agar medium supplemented with the synthesized NPs. 0.5 μg of cells were sown in each plate

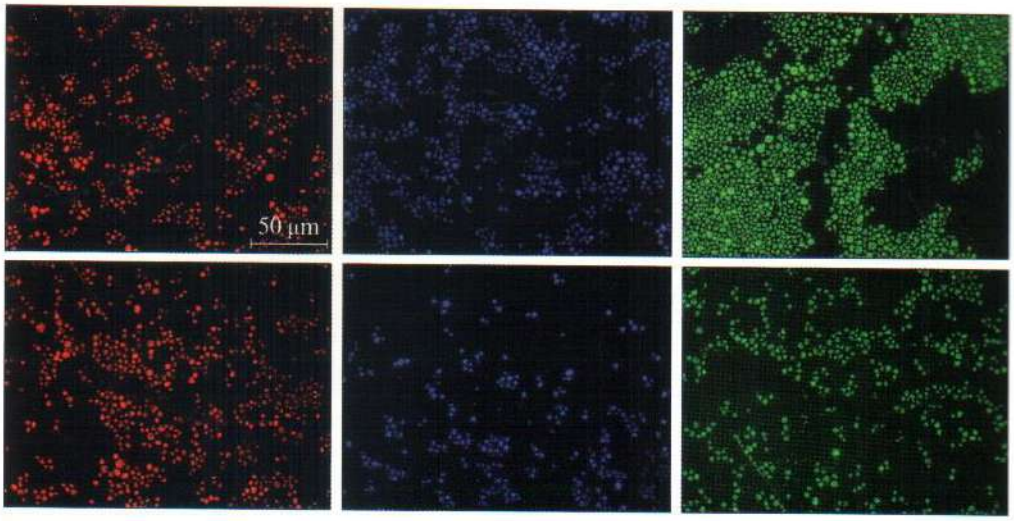

Fig. 4.18. Fluorescent microscopy of 3-day cultivated cells-Au/AgNPs (top) and cells-Ag/AuNPs (bottom) at different filters (from left to right): red, blue and green, respectively. Scale bar — 50 μm, duration — 665 ms

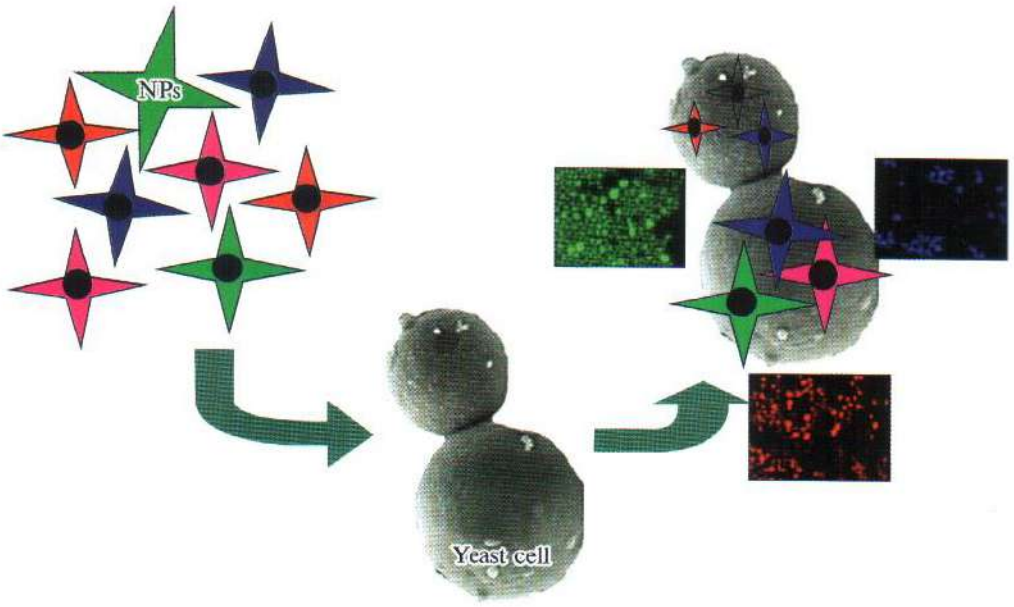

Fig. 4.19. General scheme of interaction of the synthesized fluorescent nano-particles with the yeast cell

Fig. 4.20. Growth in agar medium of yeast cells (1st generation) modified with different NPs. Left:
*AuNPs (*1*), AuNPs (*2*), AgNPs (*3*); control cells (C). Right: Au/AgNPs (*4*), *Au/AgNPs (*5*), Ag/AuNPs (*6*), *Ag/AuNPs (*7*)

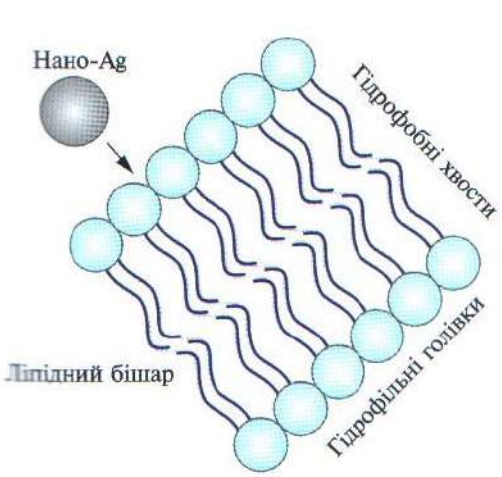

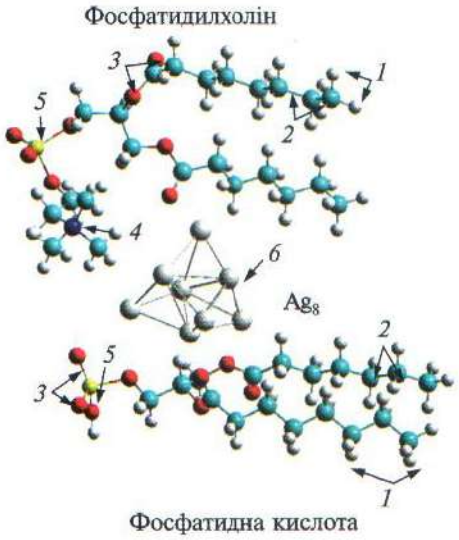

Рис. 5.8. Рівноважна просторова структура комплексу між базовим кластером Ag_8, молекулами фосфатидної кислоти й фосфатидилхоліну при розміщенні наночастинки у ділянці вуглеводневих хвостів:
1 — атом Гідрогену; *2* — атом Карбону; *3* — атом Оксигену; *4* — атом Нітрогену; *5* — атом Фосфору; *6* — наносрібло [46]

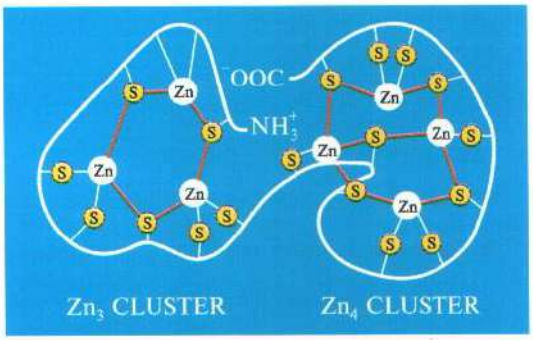

Рис. 5.28. Дводоменна структура металотіонеїнів

60. *Enhanced* nonlinear transmittance by complementary nonlinear mechanisms: a reversesaturable absorbing dye blended with nonlinear-scattering carbon nanotubes / S. Webster, M. Reyes-Reyes, X. Pedron [et al.] // Advanced Materials. — 2005. — Vol. 17. — P. 1239.

61. *Fisher J.W.* Effective cancer laser-therapy design through the integration of nanotechnology and computational treatment planning models / J.W. Fisher, M.N. Rylander // Proceedings of SPIE. — 2008. — Vol. 6869. — P. 68690D.

62. *Thermal* ablation therapeutics based on CNx multi-walled nanotubes / S. Torti, F. Byrne, O. Whelan [et al.] // International Journal of Nanomedicine. — 2007. — Vol. 2. — P. 707—714.

63. *Hyperthermic* effect of multi-walled carbon nanotubes stimulated with near infrared irradiation for anticancer therapy: *in vitro* studies / A. Burlaka, S. Lukin, S. Prylutska [et al.] // Experimental Oncology. — 2010. — Vol. 32. — P. 48—50.

64. *Gold* nanoparticles in theranostic oncology: current state-of-the-art / S. Akhter, M.Z. Ahmad, F.J. Ahmad [et al.] // Expert Opinion on Drug Delivery. — 2012. — Vol. 9. — P. 1225—1243.

65. *Nanotechnology* in therapeutics: a focus on nanoparticles as a drug delivery system / S. Bamrungsap, Z. Zhao, T. Chen [et al.] // Nanomedicine. — 2012. — Vol. 7. — P. 1253—1271.

66. *Bohren C.F.* Absorption and scattering of light by small particles / C.F. Bohren, D. Huffman. — New York: Wiley, 1998. — 544 p.

67. *Boisselier E.* Gold nanoparticles in nanomedicine: preparations, imaging, diagnostics, therapies and toxicity / E. Boisselier, A. Didier // Chemical Society Reviews. — 2009. — Vol. 38. — P. 1759—1782.

68. *Cao Y.W.* DNA-modified core-shell Ag/Au nanoparticles / Y.W. Cao, R. Jin, C.A. Mirkin // Journal of the American Chemical Society. — 2001. — Vol. 123. — P. 7961—7962.

69. *Cao-Milán R.* Gold nanoparticle conjugates: recent advances toward clinical applications / R. Cao-Milán, L.M. Liz-Marzán // Expert Opinion on Drug Delivery. — 2014. — Vol. 11. — P. 741—752.

70. *Gold* nanoparticles are taken up by human cells but do not cause acute cytotoxicity / E.E. Connor, J. Mwamuka, A. Gole [et al.] // Small. — 2005. — Vol. 1. — P. 325—327.

71. *DNA-based* molecular nanotechnology / A. Csaki, G. Maubach, D. Born [et al.] // Single Molecules. — 2002. — Vol. 3. — P. 275—280.

72. *Fritzsche W.* Metal nanoparticles as labels for heterogeneous, chip-based DNA detection / W. Fritzsche, T.A. Taton // Nanotechnology. — 2003. — Vol. 14. — P. R63—R73.

73. *Garcia-Torres J.* Synthesis and characterization of Co@Ag Core-shell nanoparticles / J. Garcia-Torres, E. Vallés, E. Gómez // Journal of Nanoparticle Research. — 2010. — Vol. 12. — P. 2189—2199.

74. *Gibson J.D.* Paclitaxel-functionalized gold nanoparticles / J.D. Gibson, B.P. Khanal, E.R. Zubarev // Journal of the American Chemical Society. — 2007. — Vol. 129. — P. 11653—11661.

75. *Guo S.* Noble metal nanomaterials: controllable synthesis and application in fuel cells and analytical sensors / S. Guo, E. Wang // Nano Today. — 2011. — Vol. 6. — P. 240—264.

76. *Harriman A.* Bimetallic Pt-Au colloids as catalysts for photochemical dehydrogenation / A. Harriman // Journal of the Chemical Society, Chemical Communications. — 1990. — Vol. 1. — P. 24—26.

77. *Alkanethiolate* gold cluster molecules with core diameters from 1.5 to 5.2 nm: core and monolayer properties as a function of core size / M.J. Hostetler, J.E. Wingate, C.J. Zhong [et al.] // Langmuir. — 1998. — Vol. 4. — P. 17—30.

78. *Jian Z.* Electrochemical synthesis and fluorescence spectrum properties of silver nanospheres / Z. Jian, Z. Xiang, W. Yongchang // Microelectronic Engineering. — 2005. — Vol. 77. — P. 58—62.

79. *Kim K.* Surface enrichment of Ag Atoms in Au/Ag alloy nanoparticles revealed by Surface Enhanced Raman Scattering spectroscopy / K. Kim, K.L. Kim, S.J. Lee // Chemical Physics Letters. — 2005. — Vol. 40. — P. 377—382.

80. *Au/Ag/Au* double shell nanoparticles with narrow size distribution obtained by continuous micro segmented flow synthesis / A. Knauer, A. Thete, S. Li [et al.] // Chemical Engineering Journal. — 2011. — Vol. 166. — P. 1164—1171.

81. *Kreuter J.* Nanoparticulate systems for brain delivery of drugs / J. Kreuter // Advanced Drug Delivery Reviews. — 2014. — Vol. 71. — P. 2—14.

82. *Different* endocytotic uptake mechanisms for nanoparticles in epithelial cells and macrophages / D.A. Kuhn, D. Vanhecke, B. Michen [et al.] // Beilstein Journal of Nanotechnology. — 2014. — Vol. 5. — P. 1625—1636.

83. *Structural* and catalytic properties of novel Au/Pd bimetallic colloid particles: EXAFS, XRD, and acetylene coupling / A.F. Lee, C.J. Baddeley, C. Hardacre [et al.] // Journal of Physical Chemistry. — 1995. — Vol. 99. — P. 6096—6102.

84. *Liu M.* Synthesis and optical characterization of Au/Ag core/shell nanorods / M. Liu, P. Guyot-Sionnest // Journal of Physical Chemistry B. — 2004. — Vol. 108. — P. 5882—5888.

85. *Seed* mediated formation *of* bimetallic nanoparticles *by* uv irradiation: *a* photochemical approach for the preparation of "core-shell" Type Structures / K. Mallik, M. Mandal, N. Pradhan, T. Pal // Nano Letters. — 2001. — Vol. 1. — P. 319—322.

86. *Gold* nanoparticles cellular toxicity and recovery: Effect of size, concentration and exposure time / T. Mironava, M. Hadjiargyrou, M. Simon [et al.] // Nanotoxicology. — 2010. — Vol. 4. — P. 120—137.

87. *The lighting* gold nanorods: fluorescence enhancement of over a million compared to the gold metal / M.B. Mohamed, V. Volkov, S. Link, M.A. El-Sayed // Chemical Physics Letters. — 2000. — Vol. 317. — P. 517—523.

88. *Mooradian A.* Photoluminescence of metals / A. Mooradian // Physical Review Letters. — 1969. — Vol. 22. — P. 185—187.

89. *Mulvaney P.* Electrochemistry of multilayer colloids: preparation and absorption spectrum of gold-coated silver particles / P. Mulvaney, M. Giersig, A. Henglein // Journal of Physical Chemistry. — 1993. — Vol. 97. — P. 7061—7064.

90. *Mixed* silver/gold colloids: a study of their formation, morphology, *and* Surface-Enhanced Raman activity / L. Rivas, S. Sanchez-Cortes, J.V. Garcia-Ramos, G. Morcillo // Langmuir. — 2000. — Vol. 16. — P. 9722—9728.

91. *Rizello L.* Optical properties of shaped silver nanoparticles / L. Rizello, P.P. Pomba // Chemical Society Reviews. — 2014. — Vol. 43. — P. 1501—1518.

92. *Multishell* bimetallic AuAg nanoparticles: synthesis, structure and optical properties / B. Rodriguez-Gonzalez, A. Burrows, M. Watanabe [et al.] // Journal of Materials Chemistry. — 2005. — Vol. 15. — P. 1755—1759.

93. *Stasyuk N.* L-Arginine-selective microbial amperometric sensor based on recombinant yeast cells over-producing human liver arginase I / N. Stasyuk, G. Gayda, M. Gonchar // Sensors and Actuators B. — 2014. — Vol. 204. — P. 515—521.

94. *Cell* Imaging with Fluorescent Bi-Metallic Nanoparticles / N.Ye. Stasyuk, G.Z. Gayda, R.Ja. Serkiz, M.V. Gonchar // Journal of Advances in Chemistry. — 2015. — Vol. 11, N 4. — P. 3498—3510.

95. *Synthethis* and characteristics of silver and gold nanoparticles for immobilization of recombinant arginase I / N. Stasyuk, R. Serkiz, G. Gayda [et al.] // Visnyk of the Lviv University. Series Chemistry (Ukrainian). — 2011. — Vol. 52. — P. 261—267.

96. *Recombinant* human Arginase I immobilized on gold and silver nanoparticles: preparation and properties / N. Stasyuk, R. Serkiz, S. Mudry [et al.] // Nanotechnology Development. — 2011. — Vol. 1. — P. 11—15.

97. *Immobilization* of oxidoreductases at gold and silver nanoparticles / M.M. Synenka, N.Ye. Stasyuk, T.V. Semashko [et al.] // Studia biologica (Ukrainian). — 2014. — Vol. 8. — P. 5—16.

98. *Optical* properties of shaped silver nanoparticles / V.V. Vodnik, D.K. Bozanic, N. Bibic [et al.] // Journal of Nanoscience and Nanotechnology. — 2008. — Vol. 8. — P. 3511—3515.

99. *Plasmonics* and enhanced magneto-optics in core-shell Co-Ag nanoparticles / L. Wang, C. Clavero, Z. Huba [et al.] // Nano Letters. — 2011. — Vol. 11. — P. 1237—1240.

100. *Viscoelasticity* of near-critical gels / J.P. Wilcoxon, J.E. Martin, F. Parsapour [et al.] // Journal of Chemical Physics. — 1998. — Vol. 108. — P. 9137—9143.

22-17-373

101. *Plasmon-driven* synthesis of triangular core-shell nanoprisms from gold seeds / C. Xue, J.E. Millstone, S. Li, C.A. Mirkin // Angewandte Chemie International Edition. — 2007. — Vol. 46. — P. 8436—8439.

102. *Preparation* of Au-Ag, Ag-Au core-shell bimetallic nanoparticles for Surface-Enhanced Raman Scattering / Y. Yang, J.L. Shi, G. Kawamura, M. Nogami // Scripta Materialia. — 2008. — Vol. 58. — P. 862—865.

103. *Zhang L.* Metal nanoclusters: new fluorescent probes for sensors and bioimaging / L. Zhang, E. Wang // Nano Today. — 2004. — Vol. 9. — P. 132—157.

104. *Resonance* light scattering characters of core-shell structure of Au-Ag nanoparticles / J. Zhu, Y. Wang, L. Huang, Y. Lu // Physics Letters A. — 2004. — Vol. 323. — P. 455—459.

105. *Quantum* dot-based nanoprobes for *in vivo* targeted imaging / Y. Zhu, H. Hong, Z.P. Xu [et al.] // Current Molecular Medicine. — 2013. — Vol. 13. — P. 1549—1567.

106. *Kemp M.M.* Synthesis of gold and silver nanoparticles stabilized with glycosaminoglycans having distinctive biological activities / M.M. Kemp, A. Kumar, S. Mousa // Journal of Biological Macromolecules. — 2009. — Vol. 10. — P. 589—595.

107. *Vu L.V.* Preparation of silver nanoparticles by pulse sonoelectrochemical method and studying their characteristics / L.V. Vu, N.N. Long, S.C. Doanh // Journal of Physics: Conference Series. — 2009. — Vol. 187. — P. 1—9.

108. *Вегера А.В.* Синтез и физико-химические свойства наночастиц серебра, стабилизированных желатином / А.В. Вегера, А.Д. Зимон // Журнал прикладной химии. — 2006. — Vol. 79. — P. 1419—1422.

109. *Cade N.I.* The plasmonic engineering of metal nanoparticles for enhanced fluorescence and Raman scattering / N.I. Cade, T. Ritman-Meer, K.A. Kwakwa // Nanotechnology. — 2009. — Vol. 20. — P. 285201—285206.

110. *Frances S.L.* Perspective on optical biosensors and integrated sensor systems / S.L. Frances // Analytical Chemistry. — 2009. — Vol. 81. — P. 519—526.

111. *Preparation* of gold nanoparticles protected with polyelectrolyte / X.P. Sun, Z.L. Zhang, B.L. Zhang [et al.] // Chinese Chemical Letters. — 2003. — Vol. 14. — P. 866—869.

112. *Construction* of flavocytochrome b_2-overproducing strains of the thermotolerant methylotrophic yeast Hansenula polymorpha (Pichia angusta) / K.V. Dmitruk, O.V. Smutok, M.V. Gonchar, A.A. Sibirnyi // Microbiology (Moscow). — 2008. — Vol. 77. — P. 213—218.

113. *A novel* L-lactate-selective biosensor based on the use of flavocytochrome b_2 from methylotrophic yeast *Hansenula polymorpha* / O.V. Smutok, G.Z. Gayda, M.V. Gonchar, W. Schuhmann // Biosensors and Bioelectronics. —2005. — Vol. 20. — P. 1285—1290.

114. *A reagentless* bienzyme amperometric biosensor based alcohol oxidase/peroxidase and an Os-complex modified electrodeposition paint / O.V. Smutok, B. Ngounou, H.M. Pavlishko [et al.] // Sensors and Actuators B. — 2006. — Vol. 113. — P. 590—598.

115. *Розробка* платформи для надекспресії та оптимізації кінетичних властивостей аргіназ на основі метилотрофних дріжджів *Hansenulla polymorpha* / В.О. Нагорний, Л.Р. Файюра, Ю.Р. Борецький, А.А. Сибірний // Збірник наук. праць "Досягнення і проблеми генетики, селекції та біотехнології" VIII з'їзду Українського товариства генетиків та селекціонерів. Алушта. — К.: Логос, 2007. — Т. 1. — С. 366—371.

116. *Bi-enzyme* L-arginine-selective amperometric biosensor based on ammonium-sensing polyaniline-modified electrode / N.Y. Stasyuk, O.V. Smutok, G.Z. Gayda [et al.] // Biosensors and Bioelectronics. — 2012. — Vol. 37. — P. 46—52.

До розділу 5

1. *Мохорт М.А.* Кардіотоксичні ефекти доксорубіцину і доцільність їх фармакологічної корекції антагоністами кальцію дигідропіридинового ряду та активаторами АТФ-чутливих калієвих каналів гуанідинового ряду / М.А. Мохорт, М.Н. Серединська, Л.М. Киричок // Фармакологія і лікарська токсикологія. — 2010. — Т. 4, № 7. — С. 35—44.

2. *Кобилінська Л.І.* Дослідження біохімічних показників кардіотоксичної дії нових протипухлинних похідних 4-тіазолідинонів і доксорубіцину у комплексах із поліетилен-

Оригінал доступний за посиланням: http://ir.librarynmu.com/handle/123456789/7658

РОЗДІЛ 5

СТВОРЕННЯ АМПЕРОМЕТРИЧНИХ БІОСЕНСОРІВ НА ОСНОВІ НАНОКОМПОЗИТІВ – ХЕМОМІМЕТИКІВ ПЕРОКСИДАЗИ І МІКРОБНИХ ЕНЗИМІВ, ПРИДАТНИХ ДЛЯ АНАЛІЗУ ЕТАНОЛУ, МЕТИЛАМІНУ ТА L-АРГІНІНУ

В розділі V представлено основні підходи щодо конструювання амперометричних біосенсорів на основі нанозимів із псевдо-пероксидазною активністю та мікробних оксидаз. У поєднанні з нанозимами, використовували алкогольоксидазу *O. polymorpha,* глюкозооксидазу *Penicillium vitale,* аргініноксидазу *Amanita phalloides* та метиламінооксидазу *O. polymorpha*.

Для формування біоселективного шару досліджували методи ковалентної та електростатичної кон'югації ензимів на поверхні наноносіїв. Для вивчення впливу модифікації поверхні електрода на біоаналітичні характеристики біонаносенсорів, в ролі хемоміметиків ПО вибрано нанозими, синтезовані методом хімічного відновлення або електроосадження з розчину солей. З метою підвищення чутливості сенсорних систем, поверхню електродів додатково модифікували пористим золотом.

Запропоновані біонаноелектроди використовували для аналізу глюкози, первинних спиртів та метиламіну. Розроблені моноензимні біонаносенсори показали покращені аналітичні характеристики, порівняно з відповідними біензимними амперометричними електродами, що містили природну пероксидазу. Встановлено, що після модифікації поверхні електроду нанозимом CuCe чутливість біосенсора зростає від 4 до 18 разів (для електроду з конфігурацією МАО/CuCe/порAu/ГЕ).

На основі мікробних оксидаз АО і АргО та наночастинок в ролі міметиків ПО сконструйовано амперометричні біосенсори для аналізу етанолу та L-аргініну. Протестовано широкий спектр наноматеріалів на псевдо-ензиматичну активність до Гідроген пероксиду в розчині та на поверхні електродів. Усі сконструйовані біосенсори характеризуються високою чутливістю до цільових аналітів, а також задовільною операційною стабільністю.

Проведено конструювання біонанозимних електродів на основі електроосадженого нанокомпозиту PtRu та мікробних оксидаз (алкогольоксидази та метиламінооксидази). Іммобілізація усіх каталітичних компонентів (нанозимів та ензимів) проводилась із використанням катодного полімеру, що забезпечувало формування надійної біонанозимно-полімерної плівки з високою проникною здатністю для цільових субстратів/аналітів. Створено новий ензимо–нанозимний метод аналізу етанолу за використання ензиму – АО, НЗ PtCu як ефективного міметика пероксидази та 3,3',5,5'-тетраметилбензидину (ТМБ) в ролі органічного хромогену. Для фіксації біонанокомпозиту використано кальцій альгінат. Запропонований ензиматичний метод володіє широким діапазоном лінійності: від 0,01 мМ до 0,15 мМ з нижньою межею виявлення етанолу – 3,3 мкМ. Створений метод є чутливим, економним та може бути цілком придатним для рутинного аналізу етанолу у клінічних лабораторіх.

Усі розроблені біонанозимні електроди та ензимо-нанозимний метод для аналізу етанолу та метиламіну протестовано на реальних зразках харчових продуктів та вина. Кореляційний зв'язок між результатами визначення вмісту етанолу та метиламіну в реальних зразках різними підходами становив R=0,999, що демонструє велику точність і надійність аналізу за допомогою створених біонаноаналітичних систем.

5.1. Дослідження методів іммобілізації оксидаз на поверхні наноносіїв.

Анотація: *За допомогою хімічних методів синтезовано наночастинки срібла (Ag НЧ) та золота (Au НЧ). Ag НЧ одержано відновленням нітрату Аргентуму глюкозою, а Au НЧ – відновленням гідрогентетрахлороаурумату тринатрій цитратом або Натрій боргідридом. Запропоновано нові методи функціоналізації поверхні одержаних наноматеріалів. Активовані Au НЧ і Ag НЧ, синтезовані цитратним методом, обробляли ω-меркаптогексадекановою кислотою, а Au НЧ, одержані боргідридним методом, функціоналізували цистеаміном. Іммобілізацією пероксидази хрону та глюкозооксидази Penicillium adametzii на активованих наночастинках золота і срібла одержано нові біонаноматеріали. Методами сканувальної електронної мікроскопії та спектрофотометричного аналізу доведено нанорозмірність синтезованих Au НЧ та Ag НЧ, а також нанотрубок золота, кон'югованих із ензимами. Дослідження каталітичних властивостей ензимів, іммобілізованих на наноносіях, засвідчило, що Au НЧ є найефективнішими для зв'язування пероксидази хрону, тоді як Ag НЧ є оптимальними носіями для зв'язування глюкозооксидази.*

УДК 577:152.1+544.77

ІММОБІЛІЗАЦІЯ ОКСИДОРЕДУКТАЗ НА НАНОЧАСТИНКАХ ЗОЛОТА І СРІБЛА

М. М. Синенька[1], ***Н. Є. Стасюк***[1], ***Т. В. Семашко***[2]
Г. З. Гайда[1], ***Р. В. Михайлова***[2], ***М. В. Гончар***[1,3]

[1]*Інститут біології клітини НАН України, вул. Драгоманова, 14/16, Львів 79005, Україна*
e-mail: galina.gayda@gmail.com

[2]*Інститут мікробіології НАН Білорусі, вул. Купревича, 2, Мінськ 220141, Білорусь*

[3]*Інститут прикладної біотехнології та фундаментальних наук, вул.Соколовська, 26, Кольбушова 36–100, Польща*

За допомогою хімічних методів синтезовано наночастинки срібла та золота. Наночастинки срібла одержано відновленням нітрату арґентуму глюкозою, а наночастинки золота – відновленням гідрогентетрахлороаурумату тринатрій цитратом або натрій боргідридом. Запропоновано нові методи функціоналізації поверхні одержаних наночастинок. Активовані наночастинки золота і срібла, синтезовані цитратним методом, обробляли 16-меркаптогексадекановою кислотою, а наночастинки золота, одержані боргідридним методом, функціоналізували цистеаміном. Іммобілізацією пероксидази хрону та глюкозооксидази *Penicillium adametzii* на активованих наночастинках золота і срібла одержано нові біонаноматеріали. Методами сканувальної електронної мікроскопії та спектрофотометричного аналізу доведено нанорозмірність синтезованих наночастинок золота і срібла, а також нанотрубок золота, кон'югованих із ферментами. Дослідження каталітичних властивостей ферментів, іммобілізованих на нановосіях, засвідчило, що наночастинки золота є найефективнішими для зв'язування пероксидази хрону, тоді як наночастинки срібла є оптимальними носіями для зв'язування глюкозооксидази.

Ключові слова: наночастинки золота і срібла, пероксидаза, глюкозооксидаза, іммобілізація на наночастинках.

ВСТУП

Нанотехнологіями називають сукупність прийомів і методів, що застосовуються при створенні, вивченні, виробництві наноматеріалів (НМ) – структур, функціональні властивості яких визначаються впорядкованими компонентами розміром до 100 нм.

Наночастинки (НЧ) металів отримують різними фізико-хімічними методами, зокрема електрохімічним відновленням, УФ та флюоресцентним опроміненням і кріохімічним синтезом [9, 10, 12, 21, 25]. Хімічний синтез наночастинки золота (Au-НЧ) здійснюють відновленням гідрогентетрахлороаурумату L-триптофану [10],

тринатрій цитрату [13], натрій боргідриду [2] та ін. Наночастинки срібла (Ag-НЧ) зазвичай одержують методом відновлення арґентум нітрату етиленгліколем [17] або глюкозою [14]. Проста процедура синтезу НМ і їхня спорідненість до багатьох біологічних молекул, у тому числі ферментів, робить їх привабливими для використання в сенсорних технологіях [9]. Синтезовані металеві НЧ стабілізують додатково поверхнево-активними речовинами для запобігання агрегації. Отримані НЧ придатні для подальшого використання в наномедицині та нанобіотехнології [26], у тому числі і для іммобілізації ферментів, рецепторів, антитіл [18, 24].

Альтернативою фізико-хімічним методам отримання НЧ є біологічні способи синтезу. Дослідниками проводиться активний пошук ефективних біооб'єктів для отримання НЧ різної хімічної природи. Є багато повідомлень про «зелений» синтез НЧ золота, срібла, селену, платини, кварцу та інших сполук бактеріями [16], актиноміцетами [15], грибами [7], дріжджами [20], вірусами [1] та в екстрактах рослин [12, 19]. Головна перевага біологічних систем для одержання НЧ – невисока вартість культивування, короткий час синтезу кінцевого продукту, біологічна безпека процесу, можливість отримання необхідного об'єму продукції без додаткових енергетичних і фінансових витрат.

Іммобілізовані на НЧ ферменти широко використовують як ефективні каталізатори, сенсорні системи, препарати з високою біологічною активністю у біотехнологічних процесах і сільському господарстві, медицині. Одним із методів модифікації та стабілізації ферментів є кон'югація з поверхнею НЧ за допомогою фізичної адсорбції або хімічного зв'язування [3, 5, 6, 8]. Суттєвим недоліком хімічного методу іммобілізації є ймовірність інактивації ферменту. Їй можна запобігти, якщо проводити іммобілізацію за наявності субстрату, котрий захищає активний центр ферменту. Для ковалентного приєднання носій (НЧ) потрібно попередньо активувати. Активовані НЧ можуть реагувати з відповідними групами молекули ферменту: аміногрупами залишків лізину, а також функціональними групами залишків тирозину, гістидину, аргініну та цистеїну [4].

Нами успішно проведені експерименти з іммобілізації ферментів на поверхні Au-НЧ і Ag-НЧ з аргіназою І печінки людини, виділеної із рекомбінантного штаму *Hansenula polymorpha* [22,23].

Мета цієї роботи – дослідити способи кон'югації наноносіїв із ферментами – пероксидазою хрону (ПО) та глюкозооксидозою (ГО) *Penicillium adametzii* і дослідити одержані біонаноматеріали на предмет їх перспективності в сенсорних технологіях. Використання електропровідних НЧ благородних металів для реалізації прямого електронного переносу в ході каталітичного окислення молекули глюкози призведе до підвищення чутливості, селективності та швидкодії біосенсорів на глюкозу.

Для досягнення мети необхідно було виконати завдання: 1) синтезувати, активувати й охарактеризувати наноносії на основі благородних металів; 2) вивчити придатність різних методів біофункціоналізації наночастинок срібла і золота ферментами ГО і ПО; 2) дослідити структурні характеристики отриманих біонаноматеріалів.

МАТЕРІАЛИ І МЕТОДИ ДОСЛІДЖЕНЬ

Ферменти: глюкозооксидаза (ГО) отримана з міцеліального гриба *P. adametzii* ЛФ F-2044.1 у лабораторії ферментів Інституту мікробіології НАН Білорусі, питома

активність фермента – 20 мкмоль·хв$^{-1}$ ·мг$^{-1}$ білка; пероксидаза хрону (ПО, RZ 3,5) – виробництва ТзОВ "Астер", Львів, Україна.

Синтез і характеристика наноносіїв. Синтез наночастинок золота (Au-НЧ) здійснювали двома модифікованими методами: цитратним [13] і боргідридним [2, 13].

У першому випадку до 1,25 мл 1 мМ $HAuCl_4$ додавали 0,125 мл 38,8 мМ тринатрій цитрату із подальшим інтенсивним перемішуванням і струшуванням упродовж 15 хв, при температурі 100 °С на водяній бані, до отримання суміші темно-червоного кольору.

Під час використання боргідридного методу до 7,5 мл 10 мМ цетилтриметиламоній броміду (ЦТМБ) додавали 0,25 мл свіжоприготовленого водного 10 мМ розчину $HAuCl_4$, інтенсивно перемішували, вносили 0,6 мл 10 мМ $NaBH_4$ та знову інтенсивно перемішували (2–3 хв). Отриманий колоїдний розчин залишали на 12 год при кімнатній температурі та спостерігали поступову зміну забарвлення від світло-коричневого до червоного. Концентрація одержаних НЧ у перерахунку на концентрацію золота становила 0,17 мМ [23]. Синтез наночастинок срібла (Ag-НЧ) здійснювали за модифікованим методом [17]. Змішували 50 мл 0,03 М D-глюкози і 0,2 мл 0,15 М $AgNO_3$, поступово додавали краплями (0,5–1 мл) 0,05 М NaOH та перемішували упродовж 2–3 хв при кімнатній температурі.

Методи активації та біофункціоналізації наночастинок. Для активації поверхні Ag-НЧ та Au-НЧ, одержаних цитратним методом, НЧ промивали кілька разів дистильованою водою. Осаджені центрифугуванням НЧ (9700 g, упродовж 15 хв) суспендували в 0,1 мл 5 мМ розчину ω-меркаптогексадеканової кислоти й інкубували упродовж 24 год при +4 °С. Осад НЧ промивали диметилформамідом (ДМФА) та суспендували в 0,1 мл розчину, що містив 20 мМ 1-циклогексил-3-(2-морфоліноетил)-карбодіімід гідрохлорид, 20 мМ пентафторфенолі 20 мМ *N, N*-діізопропілетиламін у ДМФА, та інкубували упродовж 30 хв при +25 °С. Активовані НЧ промивали ДМФА, осад суспендували в 0,1 мл 50 мМ Хепес буферу, pH 7,5 (ХБ) і зберігали при температурі +4 °С до використання.

Au-НЧ, отримані за допомогою боргідридного методу, осаджували центрифугуванням при 9 700 g упродовж 40 хв, промивали 4 рази 5 мМ ФБ, pH 7,5, знову осаджували та вносили 0,85 мМ водний розчин цистеаміну. Активовані Au-НЧ відмивали тричі у 5 мМ ФБ, pH 7,5, суспендували у 100 мкл 5 мМ ФБ, pH 7,5 та зберігали при температурі +4 °С до використання. Отримані такими способами НЧ застосовували для ковалентної та електростатичної іммобілізації ПО і ГО.

Для іммобілізації – як електростатичної, так і ковалентної, розчин активованих НЧ змішували із ферментами ГО і ПО до кінцевої концентрації білка 0,05 мг/мл та інкубували упродовж 12 год при температурі +4 °С.

Спектрофотометричні та мікроскопічні дослідження наночастинок. Розміри та структуру синтезованих НЧ досліджували різними методами: оптичним і скануючої електронної мікроскопії (СЕМ). Спектральні характеристики стабільності Au-НЧ (25 мМ) та Ag-НЧ (138 мМ) реєстрували на спектрофотометрі Shimadzu (UV-1650 PC), у діапазоні 250–700 нм. Загальну концентрацію утворених НЧ розраховували за градуювальним графіком залежності оптичної густини від концентрації срібла та золота в колоїдному розчині, використовуючи експериментально визначені молярні коефіцієнти екстинкції для Ag-НЧ і Au-НЧ – $2{,}5 \cdot 10^7$ М$^{-1}$·см$^{-1}$ та $1{,}8 \cdot 10^6$ М$^{-1}$·см$^{-1}$, відповідно [22].

Експерименти із СЕМ виконували у Центрі низькотемпературних досліджень Львівського національного університету імені Івана Франка на растровому електронному мікроскопі-мікроаналізаторі РЕММА-102-02. Проби об'ємом 0,01 мл наносили на графітовий стержень (товщина – 0,5 см, діаметр – 0,5 см). Під час досліджень відстань від останньої лінзи мікроскопа до проби (WD) становила від 17,1 мм до 21,7 мм; прискорювальна напруга (kV) в діапазоні від 20 до 40 еВ; разове збільшення становило від 2 500 до 10 000.

Визначення активності ферментів. Активність визначали за використання хромогену − *о*-діанізидину. Реакційну суміш − хромоген із ферментом (ПО) або субстратом (глюкоза) − преінкубували протягом 5 хв при 30 °С на водяній бані. Реакцію запускали внесенням розчину субстрату (пероксид водню) або ферменту (ГО) та інкубували 5–10 хв, залежно від швидкості розвитку кольорової реакції. Реакцію зупиняли у точно фіксований час додаванням 0,8 мл концентрованої HCl. Проби фотометрували при 525 нм (ε =13,38 $мМ^{-1} \cdot см^{-1}$) проти сліпої проби, яка містила 0,2 мл води замість ферменту. Реакційна суміш для визначення активності ПО складалась із 2,5 мл 0,3 мМ хромогену в 50 мМ ФБ, pH 7,5 та 0,2 мл досліджуваного розчину із ПО. Після преінкубації вносили 0,15 мл 20,6 мМ пероксиду водню. Реакційна суміш для визначення активності ГО складалась із 1 мл 0,17 мМ хромогену в воді, 0,2 мл розчину ПО (1 мг/мл) та 2,1 мл 0,05% розчину глюкози у 50 мМ ФБ pH, 6.5. Після преінкубації вносили 0,2 мл досліджуваного зразка із ГО.

Статистичний аналіз експериментальних даних. Досліди проводили трьома повторами. Для кожної вибірки показників визначали середнє арифметичне значення (M), стандартну похибку середнього (m) та середнє арифметичне відхилення (σ). Розрахунок статистичних показників і побудову графіків проводили за допомогою програми OriginPro 8,5. Вказані параметри та статистичні показники наведені у рисунках і таблицях.

РЕЗУЛЬТАТИ ДОСЛІДЖЕНЬ І ЇХНЄ ОБГОВОРЕННЯ

Характеристика НЧ. У попередніх дослідженнях нами показано, що збереження профілю оптичних спектрів Ag-НЧ і Au-НЧ упродовж місяця при +8 °С свідчить про стабільність отриманих дисперсних систем.

У процесі формування НЧ спостерігається зміна кольорів: для наночастинок срібла – від світло-жовтого до оранжевого, а для наночастинок золота – від світло-рожевого до темно-вишневого. Ці зміни для Ag-НЧ та Au-НЧ узгоджуються з даними літератури [2, 13, 17].

Нанорозмірність наночастинок і нановолокон золота, одержаних боргідридним методом, підтверджено даними СЕМ (рис. 1).

Під час синтезу Au-НЧ боргідридним методом встановлено, що залежно від умов проведення реакції відбувається формування або сферичних НЧ (у разі інтенсивного струшування реакційної суміші), або нановолокон (НВ), які одержували в стаціонарному режимі інкубації реагентів. Дані СЕМ-зображення підтверджують нанорозмірність одержаних НЧ та НВ (за діаметром), середня довжина одного волокна становить близько 5–8 мкм. Під час синтезу Au-НЧ натрій боргідридним методом одержано нановолокна/нанотрубки діаметром 150–200 нм (рис. 1).

Кон'югація наночастинок із ПО. У табл. 1 представлено результати експериментів з іммобілізації ПО на поверхні Au-НВ електростатичним методом. Із наведе-

них даних видно, що вихід ферменту після процедури іммобілізації становить близько 9 %. Схему ковалентного зв'язування НЧ з ферментами і золотими НЧ (на прикладі ПО) наведено на рис. 3.

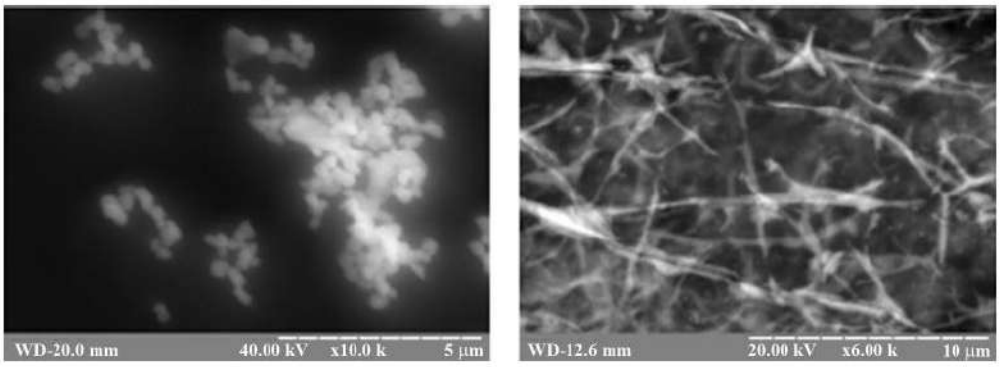

Рис. 1. СЕМ-зображення синтезованих наночастинок і нановолокон золота
Fig. 1. SEM images of the synthesized nanoparticles and nanowebs of gold

Таблиця 1. **Іммобілізація пероксидази на поверхні нановолокон золота**
Table 1. **Immobilization of peroxidase on the surface of nanowebs of gold**

	Розчин пероксидази хрону до іммобілізації	Супернатант після іммобілізації	Пероксидаза хрону на наночастинках	Розчин пероксидази хрону до іммобілізації	Супернатант після іммобілізації	Іммобілізована пероксидаза хрону на нановолокнах
V, мл	0,050	0,080	0,20	0,050	0,080	0,20
A, од./мл	2785±13,1	589,4±3,34	133,3±2,40	2785±13,1	589,4±3,34	61,4±1,20
ΣA, од.	139,2±1,1	47,15±1,21	26,7±0,60	139,2±1,1	47,15±1,21	12,3±0,60
Вихід, %	=100	33,9±1,40	19,2±0,50	=100	33,9±1,40	8,8±0,20
	Ковалентний метод			Електростатичний метод		

Розмір НВ до та після процедури електростатичної іммобілізації ПО визначено за допомогою СЕМ (рис. 2). Отже, отримані дані СЕМ-зображень після іммобілізації підтверджують, що розмір НВ не змінюється (рис. 2).

На наступному етапі досліджено ковалентне зв'язування молекул ПО із поверхнею Au-НВ. Із наведених даних (див. табл. 1) видно, що вихід ферменту після іммобілізації на наночастинок становить близько 19,2 %, тобто є у 2,2 разу більшим порівняно з електростатичним методом.

Для ковалентної іммобілізації ферменту було використано підхід формування на поверхні НЧ моношару (СОШ) ω-меркаптогексадеканої кислоти, карбоксильну групу якої конденсували із аміногрупою білка карбодіімід-пентафторфенольним методом. На рис. 3 схематично зображено ковалентне зв'язування ПО на поверхні моношару ω-меркаптогексадеканої кислоти.

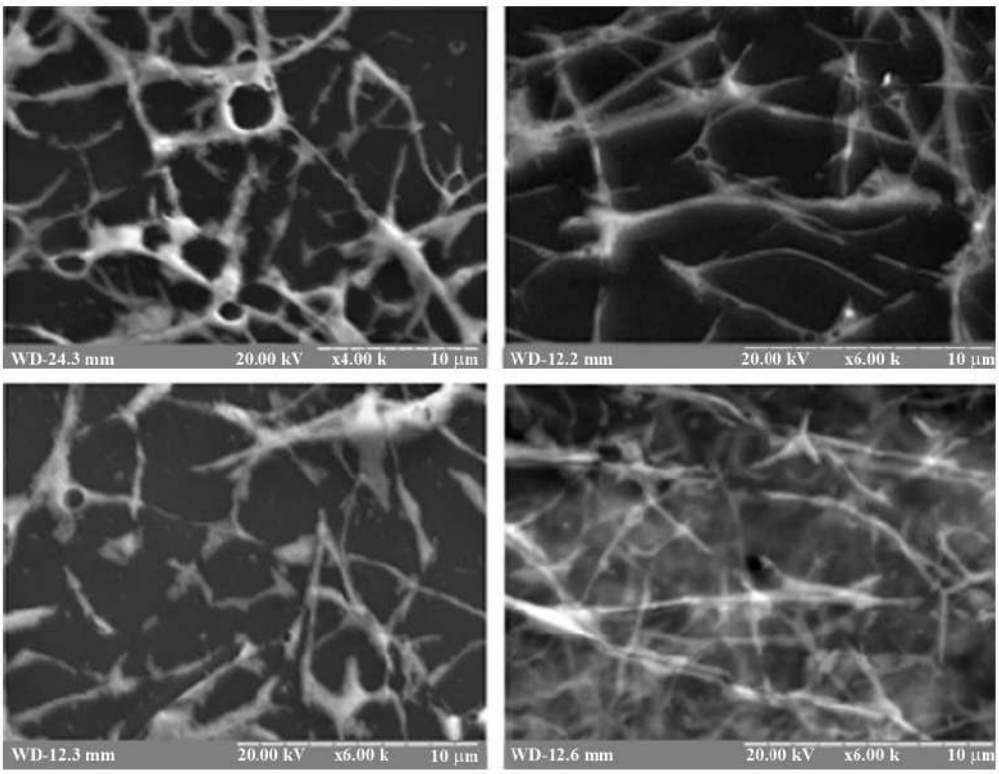

Рис. 2. СЕМ-зображення нановолокон золота: до та після іммобілізації ПО електростатичним (зверху) та ковалентним (знизу) методами

Fig. 2. SEM images of nanowebs of gold: before and after peroxidase immobilization by electrostatic (top) and covalent (bottom) methods

На поверхні НЧ відбувається зв'язування молекули ферменту. Зв'язування ферментів на НЧ реалізується, можливо, завдяки взаємодії аміногруп ферменту з карбонільним залишком МГДК. Ймовірно, також існують додаткові нековалентні контакти ферменту з НЧ золота і срібла. Розмір синтезованих нановолокон до та після процедури ковалентної іммобілізації на них ПО, визначено за допомогою методу СЕМ, (рис. 2) становить 10–20 мкм.

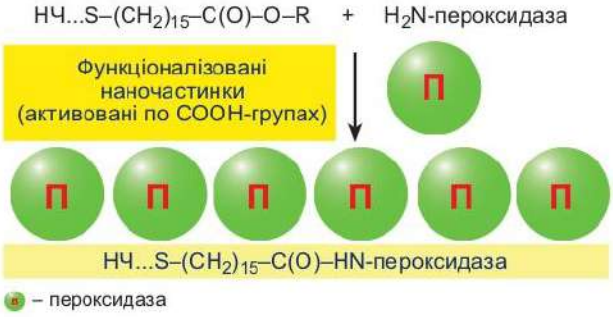

Рис. 3. Схема ковалентного зв'язування пероксидази хрону

Fig. 3. Scheme of covalent binding of peroxidase

Іммобілізація ГО на поверхні наноносіїв. Для іммобілізації ГО було використано як ковалентний, так і електростатичний методи [22, 23]. У табл. 2 представлено результати з ковалентної іммобілізації ГО на поверхні Ag-НЧ.

На рис. 4 наведені СЕМ-зображення Ag-НЧ, що підтверджують нанорозмірність до і після ковалентної іммобілізації ГО.

Результати дослідження з іммобілізації ГО та ПО різними способами на синтезованих наночастинках благородних металів узагальнено на рис. 5.

Таблиця 2. **Іммобілізація глюкозооксидази на поверхні наночастинок срібла (ковалентний метод)**

Table 2. **Immobilization of glucose oxidase on the surface of silver nanoparticles (covalent method)**

	Розчин глюкозооксидази до іммобілізації	Супернатант	Глюкозооксидаза на наночастинках
V, мл	0,05	0,050	0,20
A, од./мл	172,3±4,50	128,5±5,30	12,4±0,3
ΣA, од.	8,62±0,05	6,43±0,35	2,50±0,25
Вихід, (%)	=100	74,5±4,30	29,0±0,65

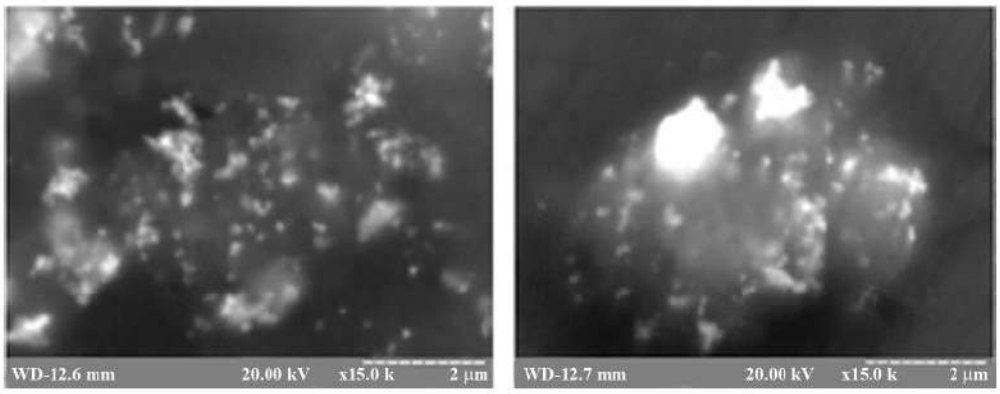

Рис. 4. СЕМ-зображення наночастинок срібла: до (*А*) та після (*Б*) ковалентної іммобілізації глюкозооксидази

Fig. 4. SEM images nanoparticles of silver: before (*A*) and after (*Б*) covalent immobilization of glucose oxidase

У результаті проведеного дослідження встановлено, що використання ковалентного методу іммобілізацій ферментів (ГО та ПО) є ефективнішим, ніж електростатичний, для всіх варіантів експерименту, а срібні НЧ є ефективнішими для кон'югації із ГО: 29 % активності ферменту, взятого для іммобілізації, зв'язалося з поверхнею НЧ (рис. 5 і табл. 2). Як видно з рис. 5, немає універсального наноносія, який був би одночасно більш ефективний для всіх ферментів: для ПО – це Au-НВ, для ГО – це Ag-НЧ.

Дослідження стабільності ферментних препаратів, іммобілізованих на наноносіях. На рис. 6 представлено результати дослідження стабільності препаратів ПО і ГО в розчині та на наночастинках під час зберігання за температури +8 °С, у 50 мМ ФБ, pH 6,5.

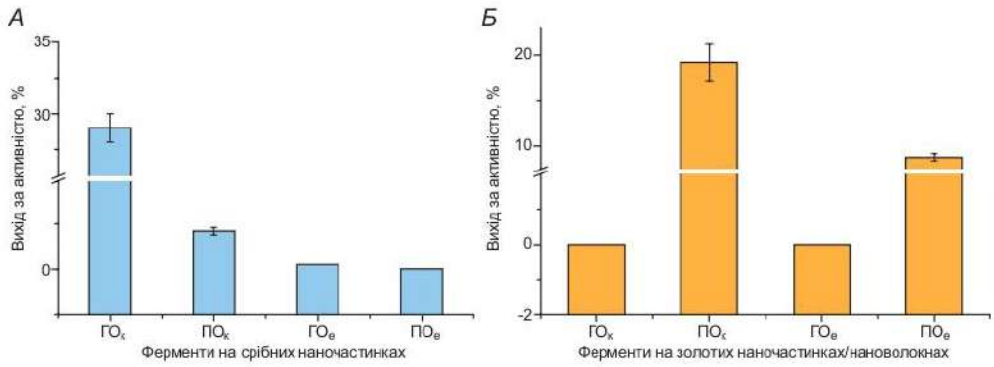

Рис. 5. Ефективність іммобілізації глюкозооксидази і пероксидази на наночастинках: к – ковалентний метод; е – електростатичний. *А* – для наночастинок срібла; *Б* – для наночастинок золота

Fig. 5. The effectivity of glucose oxidase and peroxidase immobilization on nanoparticles: к – covalent method; e – electrostatic. *A* – for nanoparticles of silver; *Б* – for nanoparticles of gold

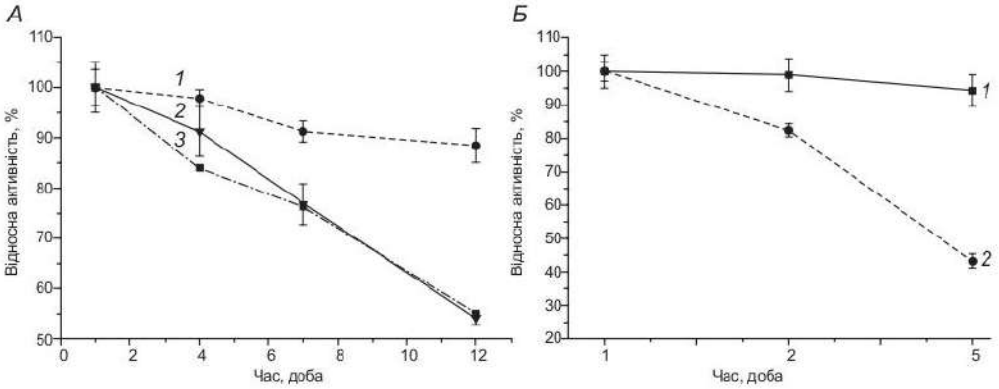

Рис. 6. Залежність зміни активності препаратів ферментів, ковалентно іммобілізованих на НЧ та у розчині, від тривалості зберігання: *А* – пероксидаза на наночастинках золота (*1*), нановолокнах золота (*3*) та в розчині (*2*); *Б* – глюкозооксидаза в розчині (*1*) та на поверхні наночастинок срібла (*2*). Максимальна активність ферменту прийнята за 100 %

Fig. 6. Activity of enzyme's preparations under storage duration: *A* – peroxidase covalently immobilized on nanoparticles of gold (*1*), nanowebs of gold (*3*) and in solution (*2*); *Б* – glucose oxidase in solution (*1*) and covalently immobilized on the surface of nanoparticles of silver (*2*). Maximal enzyme's activity is taken as 100 %

Отже, на 12 добу залишалося тільки 55 % активності для ПО у розчині та ферменту на поверхні Au-НВ (рис. 6, *А*). Проте залишкова активність ПО на Au-НЧ після 12 діб зберігання становила 90 % від вихідної активності, що вказує на значне збільшення стабільності ферменту після його іммобілізації на Au-НЧ ковалентним методом. У той же час, після 12 діб зберігання препарату ПО, іммобілізованого на Au-НВ електростатичним методом, залишкова активність ПО становила 80 % порівняно з ферментом у розчині (дані не показано).

На рис. 6, *Б* представлено результати дослідження стабільності ГО в розчині та на поверхні Ag-НЧ під час зберігання за температури +8 °С, у 50 мМ ФБ, pH 6,5. Видно, що на 5-ту добу зберігання ГО на поверхні НЧ активність ферменту знижується на 60 %, тоді як активність ГО в розчині практично не змінюється. Цей ефект може бути пов'язаний із інгібувальним впливом іонів Ag^+ на активність ГО.

ВИСНОВКИ

1. Здійснено синтез наночастинок срібла і золота (Ag-НЧ та Au-НЧ). Ag-НЧ одержано відновленням нітрату арґентуму глюкозою, а Au-НЧ – відновленням гідрогентетрахлороаурумату тринатрію цитратом або натрію боргідридом.
2. Досліджено функціоналізацію поверхні наноносіїв. Одержано активовані НЧ за допомогою двох підходів: Ag-НЧ та Au-НЧ, синтезовані цитратним методом, обробляли 16-меркаптогексадекановою кислотою, а Au-НЧ, одержані боргідридним методом, функціоналізували цистеаміном.
3. Уперше здійснено ковалентну та електростатичну іммобілізацію на поверхню наночастинок золота і срібла пероксидази хрону та глюкозооксидази із *P. adametzii*. За допомогою методу СЕМ досліджено структурну характеристику одержаних біонаноматеріалів і доведено нанорозмірність Au-НЧ і Ag-НЧ, а також синтезованих нанотрубок золота.
4. Дослідження вмісту іммобілізованих ферментів на поверхні наночастинок, тобто ефективності іммобілізації, засвідчило, що Au-НЧ є найефективнішими носіями для з'вязування пероксидази, а Ag-НЧ – для зв'язування глюкозооксидази.

ПОДЯКИ

Роботу виконано за фінансової підтримки НАН України в рамках спільного Українсько-Білоруського проекту Ф 54.4/031 та міжнародного індивідуального гранту компанії "ОПТЕК" (2014). Автори висловлюють подяку Роману Ярославовичу Серкізу за виконання досліджень із СЕМ.

1. *Alaa A.A. Aljabali, David J. Evans.* Polyelectrolyte-Modified *Cowpea Mosaic Virus* for the Synthesis of Gold Nanoparticles. **Virus Hybrids as Nanomaterials,** 2014; 1108: 97–103.
2. *Ansar S.M., Ameer F.S., Hu W.* et al. Removal of molecular adsorbates on gold nanoparticles using sodium borohydride in water. **Nano Lett,** 2013; 13(3) 1226–1229.
3. *Arya S.K., Saha S., Ramirez-Vick J.E.* [et al.]. Recent advances in ZnO nanostructures and thin films for biosensors applications. **Review. Anal. Chim. Acta,** 2012; 737: 1–21.
4. *Berezin I.V., Antonov V.K., Martinek K.* **Immobilized enzymes**. Moscow: MSU, 1976: 1–2. (In Russian).
5. *Cade N.I., Ritman-Meer T., Kwakwa K.A.* et al. The plasmonic engineering of metal nanoparticles for enhanced fluorescence and Raman scattering. **Nanotechnol,** 2009; 20: 285201–285206.
6. *Chen Y., Aveyard J., Wilson R.* Gold and silver nanoparticles functionalized with known numbers of oligonucleotides per particle for DNA detection. **Chem. Commun,** 2004; 24: 2804–2805.
7. *Dhillon G.S., Brar S.K., Kaur S., Verma M.* Green approach for nanoparticle biosynthesis by fungi: current trends and applications. **Crit. Rev. Biotechnol,** 2012; 32(1): 49–73.

8. *Dongxiang L., Qiang H., Yue C.* Immobilization of glucose oxidase onto gold nanoparticles with enhanced thermostability. **BBRC.,** 2007; 355: 488–493.
9. *Doria G., Conde J., Veigas B.* et al. Noble metal nanoparticles for biosensing applications. **Sensors**, 2012; 12(2): 1657–1687.
10. *Iosin M., Baldeck P., Astilean S.* Study of tryptophan assisted synthesis of gold nanoparticles by combining UV–Vis, fluorescence, and SERS spectroscopy. **Journal of Nanoparticle Research,** 2010; 12(8): 2843–2849.
11. *Kamiar A., Ghotalou R., Vali Z.H.* Preparation, physicochemical characterization and performance evaluation of gold nanoparticles in radiotherapy. **Adv. Pharm. Bull**, 2013;3(2): 425–428.
12. *Kharissova O.V., Dias H.V., Kharisov B.I.* et al. The greener synthesis of nanoparticles. **Trends Biotechnol**, 2013; 31(4): 240–248.
13. *Kumar S., Gandhi K.S., Kumar R.* Modeling of formation of gold nanoparticles by Citrate Method. **Ind. Eng. Chem. Res,** 2007; 46: 3136–3138.
14. *Maribel G., Guzmon M.G., Dille J.* et al. Synthesis of silver nanoparticles by chemical reduction method and their antibacterial activity. **World Acad. Sci. Eng. Tech,** 2008; 43: 357–364.
15. *Narasimha G., Alzohairy M., Khadri H., Mallikarjuna K.* Extracellular synthesis, characterization and antibacterial activity of Silver nanoparticles by *Actinomycetes isolative*. **Int. J.Nano Dimens**, 2013; 4(1): 77–83.
16. *Narayanan K.B., Sakthivel N.* Biological synthesis of metal nanoparticles by microbes. **Advances in Colloid and Interface Science**, 2010; 156(1–2): 1–13.
17. *Park H.H., Zhang X., Choi Y.J.* [et al.]. Synthesis of Ag nanostructures by Photochemical reduction using citrate-capped Pt seeds. **J. Nanomaterials**, 2011; 1: 1–7.
18. *Patra H.K., Banerjee S., Chaudhuri U.* et al. Cell selective response to gold nanoparticles. **NanoMed**, 2007; 3(2): 111–119.
19. *Park Y., Hong Y.N., Weyers A.* et al. Polysaccharides and phytochemicals: a natural reservoir for the green synthesis of gold and silver nanoparticles. **IET Nanobiotechnol,** 2011; 5(3): 69–78.
20. *Salvadori M.R., Ando R.A., Oller do Nascimento C.A, Correa B.* Intracellular Biosynthesis and Removal of Copper Nanoparticles by Dead Biomass of Yeast Isolated from the Wastewater of a Mine in the Brazilian Amazonia. **BioMedLib,** 2014; 9(1): 1–9.
21. *Shang Y., Min C., Hu J.* et al. Synthesis of gold nanoparticles by reduction of $HAuCl_4$ under UV irradiation. **Solid State Sciences,** 2013, 15: 17–23.
22. *Stasyuk N., Serkiz R., Mudry S.* et al. Recombinant human arginase I immobilized on gold and silver nanoparticles: preparation and properties. **Nanotech. Develop,** 2011; 1(3): 11–15.
23. *Stasyuk N., Smutok O., Gayda G.* et al. A new bi-enzyme potentiometric sensor for arginine analysis based on recombinant human arginase I and commercial urease. **J. Mater. Sci. Eng. A,** 2011; 1: 819–827.
24. *Xu J., Han X., Liu H.* et al. Synthesis of monodisperse gold nanoparticles stabilized by gemini surfactant in reverse micelles. **J. Disper. Sci. Technol**, 2005; 26: 473–476.
25. *Yeh I.C., Creran B., Rotello V.M.* Gold nanoparticles: preparation, properties, and applications in bionanotechnology. **Nanoscale,** 2012; 4: 1871–1880.
26. *Zhang X., Xing J.Z., Chen J.* et al. Enhanced radiation sensitivity in prostate cancer by gold-nanoparticles. **Clin. Invest. Med,** 2008; 31(3): 160–167.

IMMOBILIZATION OF OXIDOREDUCTASES AT/ON GOLD AND SILVER NANOPARTICLES

M. M. Synenka[1], ***N. Ye. Stasyuk***[1], ***T. V. Semashko***[2], ***G. Z. Gayda***[1], ***R. V. Mikhailova***[2], ***M. V. Gonchar***[1,3]

[1]*Institute of Cell Biology, NAS of Ukraine, 14–16, Drahomanov St., Lviv 79005, Ukraine*
e-mail: galina.gayda@gmail.com

[2]*Institute of Microbiology, NAS of Belarus, 2, Kuprevich St., 220141 Minsk, Belarus*

[3]*Institute of Applied Biotechnology and Basic Sciences 26, Sokolowska St., Kolbuszowa 36–100, Poland*

Nanoparticles of silver and gold were synthesized by chemical methods. Nanoparticles of silver were obtained by reducing of silver nitrate with glucose and nanoparticles of gold – by reducing of tetrachloroauric acid trihydrate with sodium citrate or borohydride. New methods of functionalization of nanoparticles surface were proposed. To activate nanoparticles, two approaches were applied: nanoparticles of silver and gold synthesized by citrate method were treated with 16-mercaptohexadecanoic acid, and nanoparticles of gold obtained with sodium borohydride method, were functionalized with cysteamine. Bionanomaterials were obtained by immobilizing of horse radish peroxidase and glucose oxidase of *Penicillium adametzii* on the activated nanoparticles. Scanning electron microscopy and spectrophotometric methods proved nanosizes of resulting nanoparticles conjugated with enzymes. The study of catalytic properties of enzymes immobilized on nanoparticles showed that nanoparticles of gold are the most effective for peroxidase, whereas the nanoparticles of silver are optimal carriers for conjugation with glucose oxidase.

Keywords: nanoparticles of silver and gold, peroxidase, glucose oxidase, immobilization on nanoparticles.

ИММОБИЛИЗАЦИЯ ОКСИДОРЕДУКТАЗ НА НАНОЧАСТИЦАХ ЗОЛОТА И СЕРЕБРА

М. М. Синенька[1], ***Н. Е. Стасюк***[1], ***Т. В. Семашко***[2], ***Г. З. Гайда***[1], ***Р. В. Михайлова***[2], ***М. В. Гончар***[1, 3]

[1]*Институт биологии клетки НАН Украины, ул. Драгоманова, 14–16, Львов 79005, Украина*
e-mail: galina.gayda@gmail.com

[2]*Институт микробиологии НАН Беларуси, ул. Купревича, 2, Минск 22014 , Беларусь*

[3]*Институт прикладной биотехнологии и фундаментальных наук, ул. Соколовска, 26, Кольбушова 36–100, Польша*

С помощью химических методов синтезированы наночастицы серебра и золота. Наночастицы серебра получены восстановлением нитрата серебра глюкозой, а наночастицы золота – восстановлением гидрогентетрахлороаурумата двумя способами: тринатрий цитратом и натрий боргидридом. Предложены новые методы функционализации поверхности полученных наночастиц. Активированные наночастицы серебра и золота, синтезированные цитратным методом, обрабатыва-

ли 16-меркаптогексадекановой кислотой, а наночастицы золота, синтезированные боргидридным методом, функционализировали цистеамином. Иммобилизацией пероксидазы хрена и глюкозооксидазы *Penicillium adametzii* на активированных наноносителях золота и серебра получены новые бионаноматериалы. Методами сканирующей электронной микроскопии и спектрофотометрического анализа доказана наноразмерность синтезированных наночастиц золота и серебра, а также нанотрубок золота, связанных с ферментами. Исследование каталитических свойств иммобилизованных на наноносителях ферментов показало, что наночастицы золота − наиболее эффективные носители для связывания пероксидазы хрена, а наночастицы серебра – для связывания глюкозооксидазы.

Ключевые слова: наночастицы серебра и золота, пероксидаза, глюкозооксидаза, иммобилизация на наночастицах.

Одержано: 11.06.2014

Оригінал доступний за посиланням:

http://publications.lnu.edu.ua/journals/index.php/biology/article/view/192/190

5.2. Конструювання амперометричних біонаносенсорів за використання електродів, модифікованих пористим золотом, пероксидазними нанозимами та мікробними оксидазами.

Анотація: *Металеві наночастинки можуть мати широке практичне застосування в різних галузях науки та промисловості. У біосенсориці вони зазвичай діють як каталізатори або нанозими (НЗ) та як посередники переносу електронів (медіатори). В даній роботі ми повідомляємо про розробку амперометричних біонаносенсорів (АБС) на основі мікробних оксидаз (глюкозооксидази, алкогольоксидази, метиламіноксидази та L-аргініноксидази), синтезованих наночастинок CuCe і мікро/нанопористого золота (порAu), електроосаджених на графітовому електроді (ГЕ). В ролі міметиків пероксидази (ПО) використано НЗ CuCe. У результаті проведеної роботи створено та охарактеризовано АБС для аналізу глюкози, метанолу, метиламіну та L-аргініну. Розроблені АБС на основі НЧ CuCe продемонстрували покращені аналітичні характеристики порівняно з відповідними АБС на основі природної ПО. Крім того, нами показано, що наявність в розпізнавальному елементі сенсора порAu з його просторово організованим 3D поверхневим шаром значно підвищує чутливість усіх сконструйованих АБС. Як приклад, після модифікації поверхні електроду нанозимом CuCe чутливість біосенсора зростає від 4 до 18 разів (для МАО/CuCe/порAu/ГЕ). Таким чином, нами доведено, що порAu є ефективним носієм електроактивних наноматеріалів у поєднанні з оксидазами, що є перспективним для використання в конструюванні біосенсорів.*

biosensors

MDPI

Article

Highly Porous 3D Gold Enhances Sensitivity of Amperometric Biosensors Based on Oxidases and CuCe Nanoparticles

Nataliya Stasyuk [1,2], Olha Demkiv [1], Galina Gayda [1,*], Andriy Zakalskiy [1,3], Halyna Klepach [2], Nina Bisko [4], Mykhailo Gonchar [1,2] and Marina Nisnevitch [5,*]

[1] Institute of Cell Biology National Academy of Sciences of Ukraine, 79005 Lviv, Ukraine; stasukne@nas.gov.ua (N.S.); demkivo@nas.gov.ua (O.D.); zakalskyae@nas.gov.ua (A.Z.); gonchar@cellbiol.lviv.ua (M.G.)
[2] Department of Biology and Chemistry, Drohobych Ivan Franko State Pedagogical University, 82100 Drohobych, Ukraine; pavlishko@yahoo.com
[3] Institute of Animal Biology of the National Academy of Agrarian Sciences of Ukraine, 79034 Lviv, Ukraine
[4] M. G. Kholodny Botany Institute, National Academy of Sciences of Ukraine, 01601 Kyiv, Ukraine; bis-ko_nina@ukr.net
[5] Department of Chemical Engineering, Ariel University, Kyriat-ha-Mada, Ariel 4070000, Israel
* Correspondence: galina.gayda@gmail.com or galina.gayda@nas.gov.ua (G.G.); marinan@ariel.ac.il (M.N.); Tel.: +380-32-261-2144 (G.G.); +972-3-914-3042 (M.N.)

Abstract: Metallic nanoparticles potentially have wide practical applications in various fields of science and industry. In biosensorics, they usually act as catalysts or nanozymes (NZs) and as mediators of electron transfer. We describe here the development of amperometric biosensors (ABSs) based on purified oxidases, synthesized nanoparticles of CuCe (nCuCe), and micro/nanoporous gold (pAu), which were electro-deposited on a graphite electrode (GE). As an effective peroxidase (PO)-like NZ, nCuCe was used here as a hydrogen-peroxide-sensing platform in ABSs that were based on glucose oxidase, alcohol oxidase, methylamine oxidase, and L-arginine oxidase. At the same time, nCuCe is an electroactive mediator and has been used in laccase-based ABSs. As a result, the ABSs we constructed and characterized were based on glucose, methanol, methyl amine, L-arginine, and catechol, respectively. The developed nCuCe-based ABSs exhibited improved analytical characteristics in comparison with the corresponding PO-based ABSs. Additionally, the presence of pAu, with its extremely advanced chemo-sensing surface layer, was shown to significantly increase the sensitivities of all constructed ABSs. As an example, the bioelectrodes containing laccase/GE, laccase/nCuCe/GE, and laccase/nCuCe/pAu/GE exhibited sensitivities to catechol at 2300, 5055, and 9280 $A \cdot M^{-1} \cdot m^{-2}$, respectively. We demonstrate here that pAu is an effective carrier of electroactive nanomaterials coupled with oxidases, which may be promising in biosensors.

Keywords: electroactive nanoparticles; peroxidase-like nanozyme; oxidases; micro/nanoporous gold; amperometric biosensors

Citation: Stasyuk, N.; Demkiv, O.; Gayda, G.; Zakalskiy, A.; Klepach, H.; Bisko, N.; Gonchar, M.; Nisnevitch, M. Highly Porous 3D Gold Enhances Sensitivity of Amperometric Biosensors Based on Oxidases and CuCe Nanoparticles. *Biosensors* **2022**, *12*, 472. https://doi.org/10.3390/bios12070472

Received: 23 May 2022
Accepted: 26 June 2022
Published: 29 June 2022

Publisher's Note: MDPI stays neutral with regard to jurisdictional claims in published maps and institutional affiliations.

Copyright: © 2022 by the authors. Licensee MDPI, Basel, Switzerland. This article is an open access article distributed under the terms and conditions of the Creative Commons Attribution (CC BY) license (https://creativecommons.org/licenses/by/4.0/).

1. Introduction

Metallic nanoparticles have wide potential practical applications in various fields of science and industry. In biosensorics, they usually act as carriers, mediators in electron transfer, and/or catalysts (artificial enzymes or nanozymes) [1–5].

Nanozymes (NZs) are the newest class of functional nanomaterials [3–7]; they have enzyme-like activities with different reaction specificities. NZs possess increased stability and greater availability due to their simpler preparation technologies. Most reported NZs are mainly mimetics of oxidoreductases, including peroxidase (PO) [7–11].

PO catalyzes the oxidation of diverse organic compounds using H_2O_2 as the electron acceptor [8]. Many natural enzymes (oxidases) produce H_2O_2 as a byproduct of their enzymatic reactions, so the detection of a target substrate can be performed by measuring

H_2O_2 generation. Over the last few years, a number of reports have described the application of various mimetics of PO for H_2O_2 detection using different sensors [8–15]. The main peculiarities of PO-like NZs as catalysts are that they have high stability, sensitivity, and selectivity to H_2O_2 in extra-wide linear ranges. PO-like NZs coupled with natural oxidases are widely used in electrochemical biosensors [7–9,16].

Oxidase-based amperometric biosensors (ABSs) are the simplest and most commonly employed type of biosensors. An enzyme-based ABS offers a means for quantitative analytical information; it can function via the measurement of signals in the form of current, which changes according to varying concentrations of the target analyte at a fixed potential. The main analytical characteristics of ABSs are the sensitivity, specificity, selectivity, detection limit, signal-to-noise ratio, linear dynamic ranges, and response time [1,2,17,18]. To effectively convert the biological response resulting from the interaction between analytes and enzymes into an electric current signal, the enzyme must be in direct spatial contact with the transducer. The selection of the appropriate methods to immobilize the enzyme on the electrode surface plays a significant role in the design of ABSs [1,2].

A number of approaches have been proposed for improving the analytical characteristics of ABSs, especially sensitivity. One of them is to increase the effective working surface of an electrode in order to obtain the maximal electroactive sites for the immobilization of biocatalysts, including enzymes and NZs [6,12,13,19–23]. In particular, 2D and 3D materials with extra-large areas are the promising candidates for this aim [1,17–21]. A lot of synthetic methods for obtaining 3D materials have been described [10,24–30].

Micro/nanoporous gold (pAu) is one of the best-studied 3D materials, and it has attracted increasing interest over the last twenty years [23,31–34]. pAu has a high surface-area-to-volume ratio, excellent conductivity, chemical inertness, physical and chemical stability, biocompatibility, electrochemical activity, easy tunability, and controllable pores as well as reduced stiffness and plasmonic properties. pAu possesses a higher roughness factor (the ratio between the real surface area and the geometrical area of the electrode) due to its porous structure. As a result, a pAu-modified electrode significantly increases the number of adsorption sites for enzymes and other biomolecules, thus improving electron transport in comparison with corresponding electrodes with nonporous surfaces. Thus, due to its intriguing properties, pAu is a very promising material for application in (bio)sensing, energy storage, diagnostic medicine, and drug delivery [14,19,21–24,35–42].

A variety of approaches to synthesize pAu have been reported in addition to methods of sputtering and self-assembling [17,27,41]. The pore size in pAu can be modulated from 5 up to 50 nm, depending on the type of synthesis protocol used [24,30].

Chemical and electrochemical dealloying were shown to lay a historical foundation for other methods [25,27,31,32]. This approach is appropriate for the fabrication of both monoporous (i.e., nanoporous or microporous) and hierarchically porous (i.e., possessing both microporosity and nanoporosity) metal structures with novel properties [23,24,43]. Hierarchical pores are highly desirable; the presence of larger-size pores enables the fast transport of the reactants, while the nanopores are responsible for providing a large surface area, thereby increasing the rate of electrochemical reactions.

High-surface-area pAu (such as films, membranes, or powders) could also be designed by the electrodeposition technique. This method of pAu preparation on a solid substrate has been extensively researched, and it has become the most popular method in recent years [17,23,24]. The advantages of electrodeposition strategies include: one-step fabrication of thin films directly on a substrate; relatively easy control of particle morphology, size, and density; uniform deposition and good stability; and the formation of hierarchically porous metal structures with novel properties.

The currently known electrodeposition techniques able to form thin pAu films are: conventional electro-co-deposition in ionic liquids; lithographically patterned electrodeposition; electrochemical overpotential deposition; bicontinuous microemulsion; the pulse potentiostatic method; dynamic hydrogen bubble templates; and deep eutectic solvent-based deposition.

In our earlier works, different types of PO-like NZs were synthesized and characterized [9,16]. The most electroactive nanoparticles of CuCe (nCuCe), having excellent sensitivity and a wide linear range for H_2O_2 detection, were used as effective artificial PO for the construction of L-arginine-sensitive ABS, which was based on L-arginine oxidase (ArgO) [16].

The aim of the current work was to demonstrate the crucial impact of pAu as an effective carrier of nanomaterials and enzymes on the analytical parameters of an ABS, especially on its sensitivity. The tasks of our study were to fabricate and characterize ABSs using various oxidases as biorecognition elements, the nCuCe as an electroactive functional nanomaterial, and the electrodeposited pAu with a highly advanced surface area as an effective carrier of oxidases and nCuCe.

2. Materials and Methods

2.1. Reagents

Cerium(III) chloride, copper(II) sulfate, L-arginine (Arg), methylamine, ethanol, methanol, *o*-dianisidine (*o*-DZ), hydrogen peroxide (30%), hydrogen tetrachloroaurumate(III) $H[AuCl_4]$, D-glucose, sodium sulfide, ammonia chloride, 2,2′-Azino-bis(3-ethylbenzthiazoline-6-sulfonic acid (ABTS), Nafion (5% solution in 90% low-chain aliphatic alcohols), horseradish peroxidase (PO, EC 1.11.1.7) from *Armoracia rusticana* (500 $U \cdot g^{-1}$), and all other reagents and solvents used in this work were purchased from Sigma-Aldrich (Steinheim, Germany); glucose oxidase (GO, EC 1.1.3.4) from *Aspergillus niger* (168 $U \cdot mg^{-1}$) was purchased from Sigma-Aldrich (St. Louis, MO, USA). All reagents were of analytical grade and were used without further purification. All solutions were prepared using ultra-pure water obtained with the Milli-Q® IQ 7000 water purification system (Merck KGaA, Darmstadt, Germany).

2.2. Enzymes, Isolation, and Purification

Purified enzymes—alcohol oxidase (AO, EC1.1.3.13), L-arginine oxidase (ArgO, EC 1.4.3.25), methylamine oxidase (AMO, EC 1.4.3.21), and laccase (EC 1.10.3.2)—were isolated by the authors from the corresponding sources and were used for the fabrication of amperometric biosensors (ABSs). Yeast AO was isolated from a cell-free extract of the selected overproducing strain *Ogataea polymorpha* C-105 (*gcr1 catX*) using a two-step ammonium sulfate fractionation (at 30% and 70% saturation), followed by ion exchange chromatography on a Toyopearl DEAE-650M [44]. Purified AO with the specific activity of ~20 $U \cdot mg^{-1}$ of protein was kept as a suspension in 70% sulfate ammonium (SA) and 50 mM phosphate buffer (PB) at pH 7.5 at 4 °C.

Mushroom ArgO was isolated from an extract of the fruiting body of the wild forest mushroom *Amanita phalloides* and partially purified up to ~7.9 $U \cdot g^{-1}$ of protein using a two-step SA fractionation (at 30% and 70% saturation), followed by chromatographic purification on a Toyopearl DEAE-650M [16]. Partially purified ArgO was kept as a suspension in 70% SA in 50 mM PB at pH 7.5.

The activities of AO, ArgO, or GO were determined by the rate of hydrogen peroxide formation in reactions with correspondent substrates (methanol [44], Arg [16], or glucose [10]) in the presence of PO and *o*-DZ in optimal conditions, which were chosen experimentally. After the incubation of reactants for a fixed time, the reactions were stopped by adding HCl. One unit of activity was defined as the amount of the enzyme required to oxidize 1 μmole of a substrate (ε_{525} = 13.35 $mM^{-1} \cdot cm^{-1}$) per minute at 30 °C. The optical densities of these colored products were determined at 525 nm using a Shimadzu UV1650 PC spectrophotometer (Kyoto, Japan).

Yeast AMO was isolated from the recombinant yeast strain *Saccharomyces cerevisiae* C13ABYS86 [45]. The (His)6-tagged AMO was purified from the cell-free extract by metal-affinity chromatography on Ni-NTA-agarose. The activity of AMO was determined by the rate of hydrogen peroxide formation in reaction with MA, as monitored by the

peroxidative oxidation of ABTS in the presence of PO [45]. One unit of activity was defined as the amount of the enzyme required to oxidize 1 μmole of ABTS as a substrate (ε_{420} = 36 $mM^{-1} \cdot cm^{-1}$) per minute at 30 °C.

Fungal laccase was purified from a cultural liquid of the fungus *Trametes zonatus* by a two-step SA fractionation (up to 70% of saturation), followed by chromatography on a Toyopearl DEAE-650M [46]. Fractions with the laccase activity were pooled, concentrated by a Millipore filter (10 kDa) up to a specific activity of enzyme ≥10 $U \cdot mg^{-1}$, followed by precipitation with 80% SA. The activity of laccase was determined by the rate of the increase in absorbance monitored spectrophotometrically at 420 nm. As a substrate, 0.5 mM ABTS in a 50 mM pH 4.5 sodium acetate (NaOAc) buffer solution was used. One unit of laccase activity was defined as the amount of the enzyme required to oxidize 1 μmole of ABTS per minute at 24 °C.

2.3. Synthesis of CuCe Nanoparticles and Estimation of Their Pseudo-Peroxidase Activity

Nanoparticles of CuCe (nCuCe) were synthesized and collected by centrifugation, as described previously [9]. The precipitates were rinsed twice with water and were stored as a water–colloid solution at +4 °C until use.

Pseudo-peroxidase (PO-like) activity of the nCuCe was measured using the colorimetric method with o-DZ as a chromogenic substrate in the presence of H_2O_2 [9]. One unit (U) of PO-like activity was defined as the amount of nCuCe consuming 1 μmol of H_2O_2 per 1 min at 30 °C under standard assay conditions. Here, we used a colloid solution of nCuCe with a PO-like activity of 1 U/mL.

2.4. Apparatus

A piece of Pt wire and an Ag/AgCI/3M KCI electrode were used as the counter and reference electrodes, and 3.05 mm graphite rods (type RW001, Ringsdorff Werke, Bonn, Germany) were used as working electrodes. The graphite electrode (GE) was prepared as described in detail previously [10]. Amperometric measurements were carried out with a CHI 1200A potentiostat (IJ Cambria Scientific, Burry Port, UK) in batch mode under continuous stirring in a standard 40 mL cell at a room temperature.

A REMMA-102-02 SEM microanalyzer (Lviv, Ukraine) was used for the morphological analyses of the synthesized porous gold.

2.5. Electrodeposition of Porous Gold onto Graphite Electrode

A layer of micro/nanoporous gold (pAu) was synthesized on the surface of a GE in two stages. In the first stage, pAu was electrodeposited from a solution containing 10 mM $HAuCl_4$ in 2.5 M ammonia chloride using cyclic voltammetry in the range of 0 to +800 mV with a scan rate of 50 $mV \cdot min^{-1}$ for 25 cycles. In the second stage, the obtained modified electrode (pAu/GE) was re-immersed in a solution of 10 mM $HAuCl_4$ in 2.5 M ammonia chloride using the potentiostatic mode at −1000 mV for 120 s. The obtained pAu/GE was rinsed with water and equilibrated before usage in the appropriate buffer.

2.6. Immobilization of nCuCe and Peroxidase on Electrodes

The synthesized nCuCe was immobilized on the surfaces of a GE and a pAu/GE, using the physical adsorption method. For this purpose, aliquots of nCuCe solution (10 μL) were dropped onto the surfaces of the GE and pAu/GE.

For the development of the PO/GE, an aliquot of PO solution (10 μL) with an activity of 1 U/mL was dropped onto the surface of a GE.

The modified electrodes were rinsed with 50 mM pH 7.5 PB and kept in this buffer with 0.1 mM EDTA at 4 °C until use.

2.7. Immobilization of Oxidases onto the Modified Electrodes

To fabricate the oxidase-based amperometric biosensors (ABSs), GO, AMO, AO, ArgO, or laccase were immobilized onto the modified GE.

First, 5–10 µL of enzyme solution was dropped onto the dried surfaces of the PO/GE, nCuCe/GE, or nCuCe/pAu/GE. The dried composites were covered with a Nafion membrane. To prepare a 1% Nafion solution, the stock 5% solution was diluted with the appropriate buffer: with 50 mM pH 4.5 NaOAc for the construction of laccase-based ABS and with 50 mM pH 7.5 PB in other cases.

It is worth mentioning that in the case of AO-based ABS, the biosensing film on the electrode was fixed with a dialysis membrane but not with Nafion.

The coated bioelectrodes were rinsed with water and stored in the corresponding buffers until use.

2.8. Measurements and Calculations

Amperometric measurements were carried out using a CHI 1200A potentiostat (IJ Cambria Scientific, Burry Port, UK) connected to a personal computer, which was used in a batch mode under continuous stirring in an electrochemical cell with a 20 mL volume at 25 °C.

All experiments were carried out in triplicate trials. The analytical characteristics of the proposed electrodes were statistically processed using OriginPro 8.5 software. Error bars represent the standard error derived from three independent measurements. The calculation of the apparent Michaelis–Menten constants (K_M^{app}) was performed automatically by this program according to the Lineweaver–Burk equation.

3. Results

3.1. Development of Oxidase-Based Biosensors Using nCuCe and Porous Gold

Micro/nanoporous gold (pAu) was reported to have a large area and a high surface-area-to-volume ratio; thus, it may be used to enhance the sensitivity of ABSs as carriers of enzymes [19,23,41]. We modified the surface of a graphite electrode (GE) with pAu. The electrodeposition of pAu onto the GE was carried out as described in Section 2.5. Figure 1a demonstrates the profiles of cyclic voltammograms (CVs) during the pAu film's formation. We describe here the development of ABSs using oxidases coupled with nCuCe, which were immobilized on the surface of a pAu-modified GE. The principal scheme of bioelectrode construction is presented in Figure 1b.

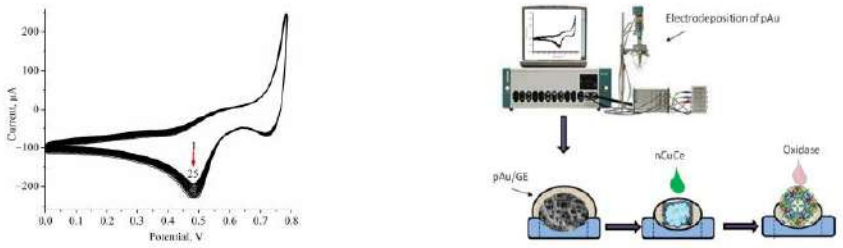

(a) (b)

Figure 1. (a) CV profiles during 25 cycles of film electrodeposition with a scan rate 50 mV s^{-1} vs. Ag/AgCl; (b) Scheme of the working electrode preparation.

A characteristic feature of all oxidases is the ability to catalyze oxidation reactions; namely, the transfer of electrons from electron donor to electron acceptor. As a result of these reactions, hydrogen peroxide (H_2O_2) is formed. For the effective functioning of oxidase-based ABSs, it is necessary to decompose H_2O_2 using natural or artificial peroxidase (PO).

nCuCe plays a dual role in ABSs, being an effective artificial PO (PO-like NZ) [9,16] and, at the same time, an electroactive mediator of electron transfer.

To demonstrate PO-like activity of the nCuCe/GE, cyclic voltammetry (CV) was used. These experiments were reported in detail in our previous papers [9,16]. The CV profiles of nCuCe/GE as current responses upon the addition of H_2O_2 are demonstrated in Figure A1a. According to the CV profiles, nCuCe/GE is sensitive to H_2O_2. Chronoamperometric experiments were also carried out (Figure A1b), and the calibration was performed by a stepwise addition of H_2O_2. Following the chronoamperograms, calibration graphs for H_2O_2 determination in wide and linear ranges were plotted (Figure A1c,d). These results proved that nCuCe is an artificial PO and nCuCe/GE may be an amperometric chemosensor of H_2O_2. The main analytical characteristics of the nCuCe/GE, namely, K_M^{app} and I_{max}, are presented in Figure A1c. Other operational parameters, namely, the linear range (up to 1.5 mM) and limit of detection (0.5 μM), were determined from the calibration graph (Figure A1d). The sensitivity to H_2O_2 (2164 $A \cdot M^{-1} \cdot m^{-2}$) was calculated as a ratio of B (the parameter of linear regression of the calibration graph) to the surface area of a working electrode.

The electroactivity of the nCuCe/GE was demonstrated using CV experiments in the presence of $K_3Fe(CN)_6$ (Figure A2). According to the results of the CV study, the tested nCuCe is electroactive since the peaks of oxidation and recovery of $K_3Fe(CN)_6$ on the nCuCe/GE were higher than those for the control unmodified GE.

Figure 2 demonstrates the results of the morphological characterization of pAu (Figure 2a), nCuCe (Figure 2c), and nCuCe/pAu (Figure 2e) using the SEM technique, which provides information on the size, distribution, and shape of the tested materials.

The XRM images (Figure 2b,d,e) showed the presence of all components of the tested materials [9]. Au^0 formation was proven by X-ray microanalysis, which showed the characteristic emission peaks at 2.1, 9.7, and 11.6 keV, corresponding to the AuK_α, AuK_α, and AuK_β transitions, respectively (Figure 2b). The characteristic peaks for Cu^0 at 1.4 and 8.05 keV, which correspond to the CuK_α and CuK_β transitions, respectively, are shown in Figure 2d,f [47]. The peaks for Ce at 0.9 keV and 4.8 keV (Figure 2d,f) correspond to the CeK_α and CeK_β transitions [48].

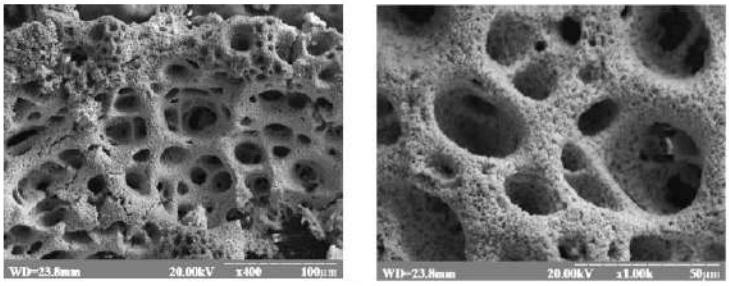

(a)

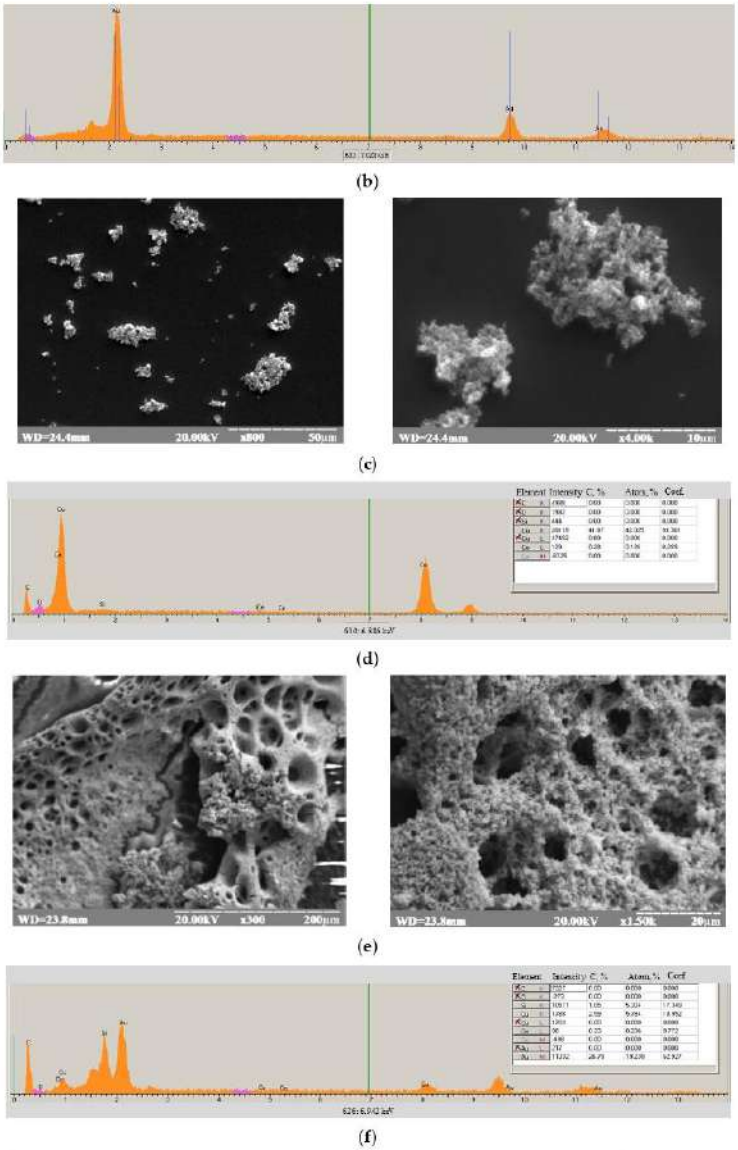

Figure 2. Characteristics of the pAu/GE (**a**,**b**), nCuCe/GE (**c**,**d**), and nCuCe/pAu/GE (**e**,**f**). SEM images with different magnitudes (**a**,**c**,**e**); X-ray spectral microanalysis (**b**,**d**,**f**).

3.2. *Characterization of the Constructed Biosensors*

Using GO, AO, AMO, or ArgO as biorecognition elements, nCuCe as a PO-like NZ or as an electroactive mediator, and pAu as a carrier of enzymes/NZs, ABSs were constructed and characterized for glucose, primary alcohols, MA, Arg, and catechol, respectively (Figures 3–8).

It is worth mentioning that before modification with enzymes (see Section 2.7), the control electrodes were tested for their sensing of the target analytes (glucose, primary alcohols, methyl amine, Arg, and catechol). The results of the selectivity study for nCuCe/GE are shown in Figure A3. The selectivity of nCuCe/GE towards the tested analytes was estimated in relative units (%) as a ratio to the value of the highest response on addition of H_2O_2. We demonstrated the absence of any amperometric signals for the nCuCe/GE and other control electrodes (pAu/GE, nCuCe/pAu/GE, and PO/GE, data not shown) with each tested analyte addition under the chosen conditions. Therefore, nCuCe/GE may be an effective H_2O_2-sensitive platform for the construction of oxidase-based ABSs.

3.2.1. Optimal Working Potential

The efficiency of electron transfer from oxidase to the surface of the electrode (GE) and the selection of the optimal potentials for each enzyme were evaluated by a cyclic voltammetric technique. The CV profile is the dependence of the current response on changing potentials under increasing concentrations of the appropriate substrate. Figure 3 demonstrates the CVs of the GEs that were modified with oxidase and nCuCe.

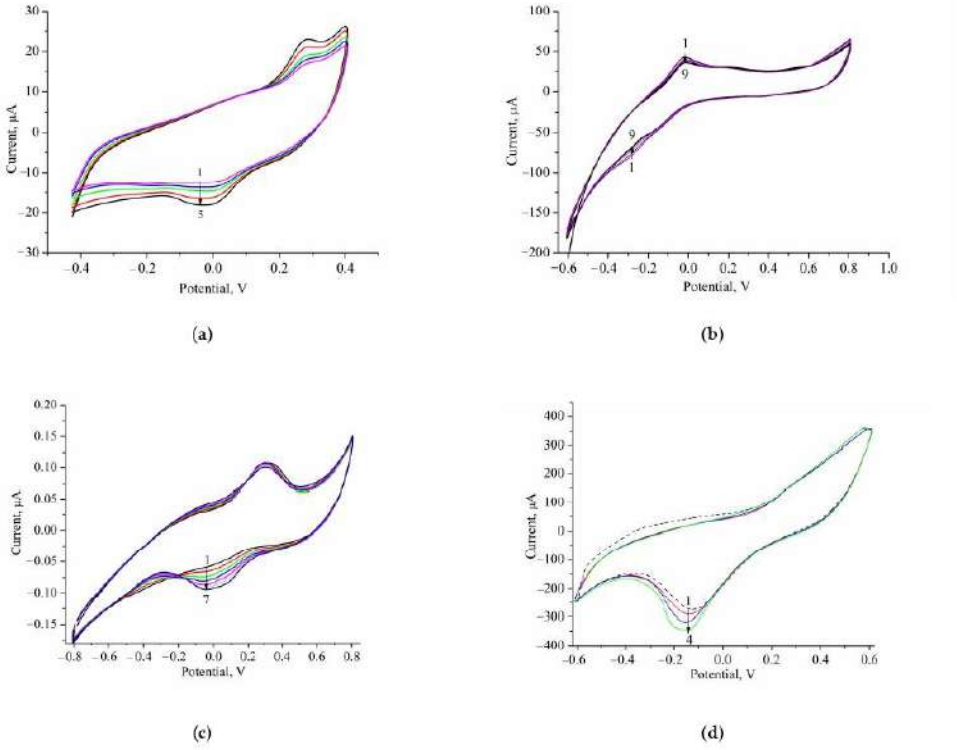

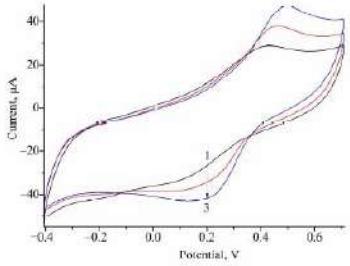

(e)

Figure 3. Profiles of CVs for the nCuCe/GEs, modified with GO (**a**), AMO (**b**), AO (**c**), ArgO (**d**), and laccase (**e**). Conditions: Ag/AgCl (reference electrode); 50 mM phosphate buffers (PB), pH 6.0 (**a**), pH7.5 (**b–d**), and NaOAc buffer, pH 4.5 (**e**); scan rate −50 mV·s^{-1}. Substrates were added up to concentrations: 0–4 mM glucose, lines 1–5, respectively (**a**); 0–1 mM MA, lines 1–4, respectively (**b**); 0–2 mM methanol, lines 1–7, respectively (**c**); 0–13 mM L-Arg, lines 1–4, respectively (**d**); 0–1 mM catechol, lines 1–3, respectively (**e**).

3.2.2. Analytical Properties

Chronoamperometric studies were carried out under the chosen optimal potentials for each oxidase-based electrode. Three types of modified electrodes were studied, namely, enzyme in combination with a natural PO (designated as oxidase/PO/GE), with CuCe as an artificial PO (oxidase/nCuCe/GE), and with CuCe on the surface of a pAu-modified electrode (oxidase/nCuCe/pAu/GE). Taking into account the chronoamperograms at optimal working potentials, calibration curves for the modified and control electrodes were plotted for analyte determination by the developed ABSs (Figures 4–8).

Figure 4 demonstrates the amperometric characteristics for the GO-based ABS for glucose determination. The optimal potential for the developed GO/nCuCe/GE is −50 mV (see Figure 3a); thus, the calibration of working electrodes was carried out under this potential using a solution of 50 mM glucose.

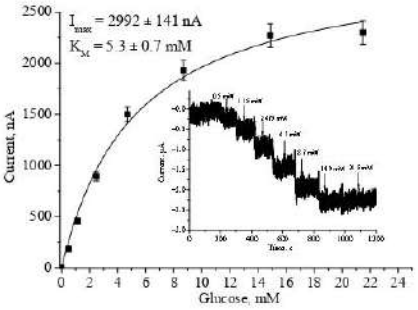

(a)

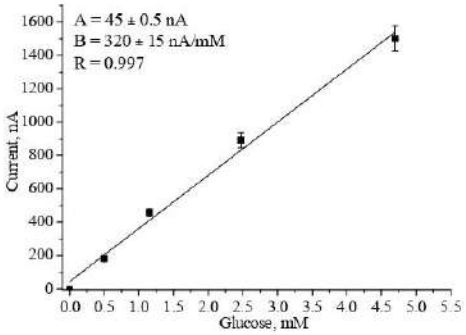

(b)

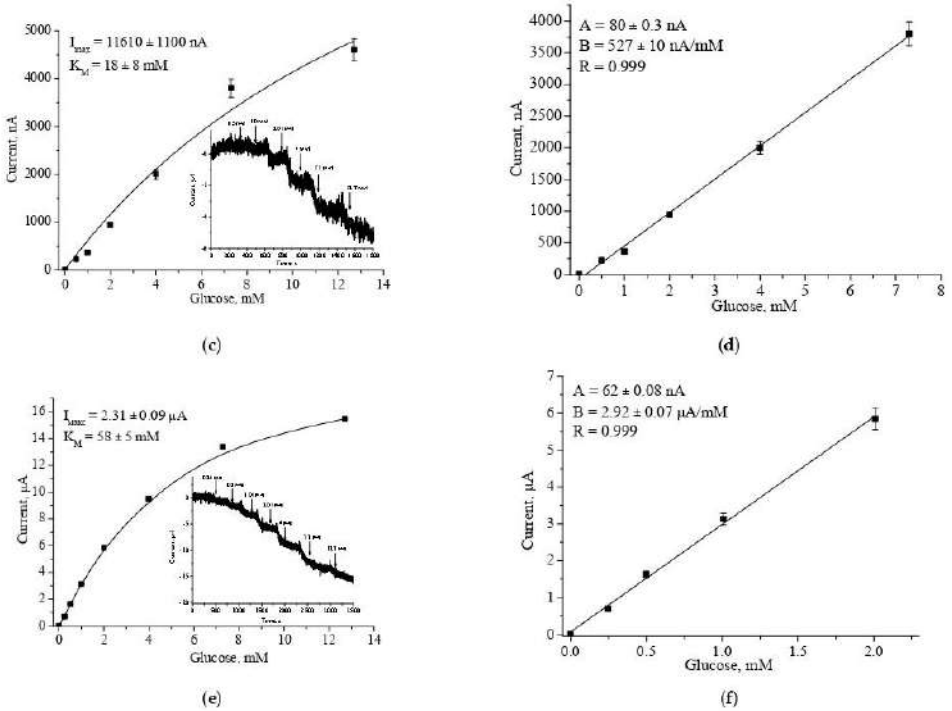

Figure 4. Amperometric characteristics of the GO/PO/GE (a,b), GO/nCuCe/GE (c,d), and GO/nCuCe/pAu/GE (e,f): (a,c,e) chronoamperograms (inserted) and dependence of amperometric signal on concentration of glucose; (b,d,f) calibration graphs for glucose determination. Conditions: working potential –50 mV vs. Ag/AgCl/3 M KCl in 50 mM PB, pH 6.0. The sensing layers contained 0.01 U of PO/PO-like activity and 0.01 U of GO.

The same experiments were carried out for all other developed ABSs, which contained AMO, AO, ArgO (Figures 5–7), and laccase (Figure 8).

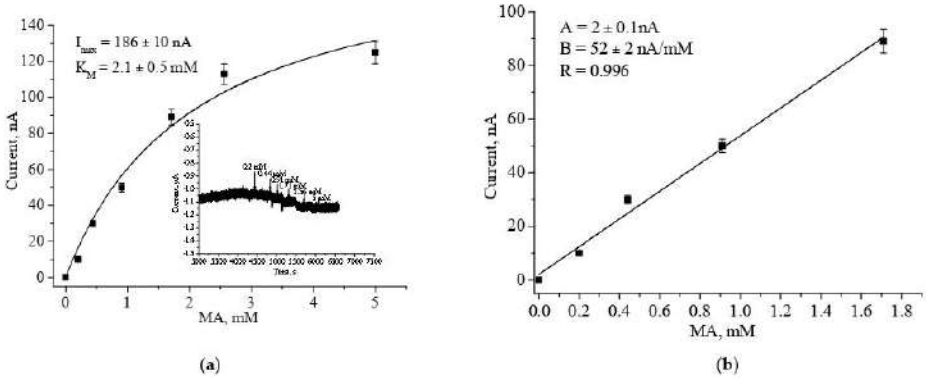

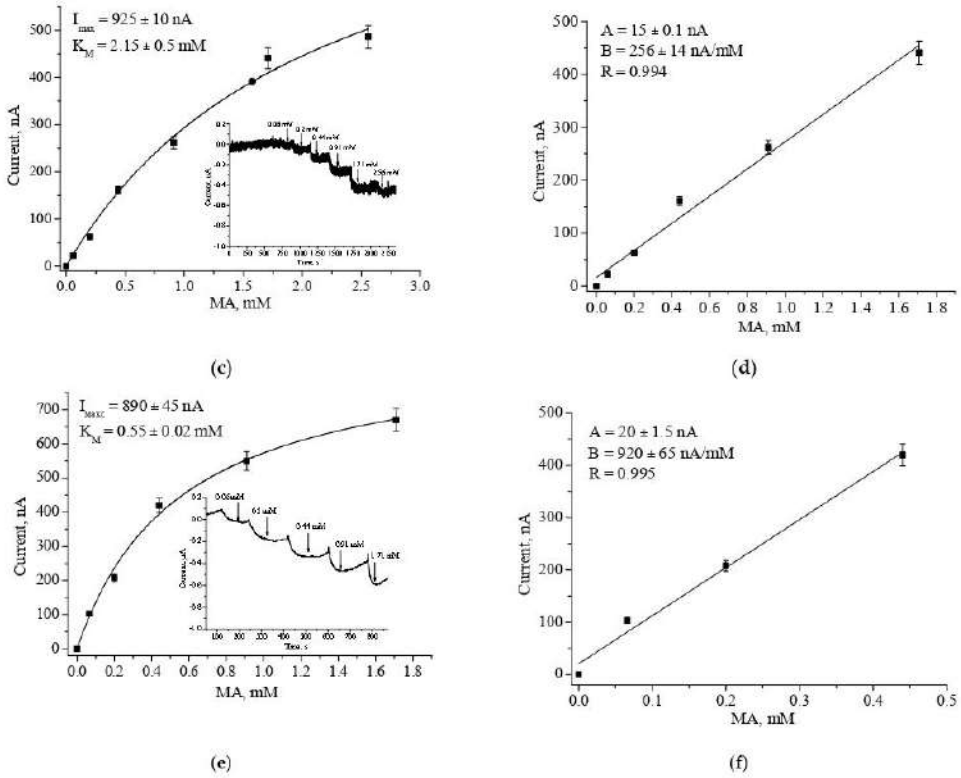

Figure 5. Amperometric characteristics of the AMO/PO/GE (**a**,**b**), the AMO/nCuCe/GE (**c**,**d**), and the AMO/nCuCe/npAu/GE (**e**,**f**): (a,c,e) chronoamperograms (inserted) and dependence of amperometric signal on concentration of MA; (**b**,**d**,*f*) calibration graphs for MA determination. Conditions: working potential –250 mV vs. Ag/AgCl/3 M KCl in 50 mM PB, pH 7.5.

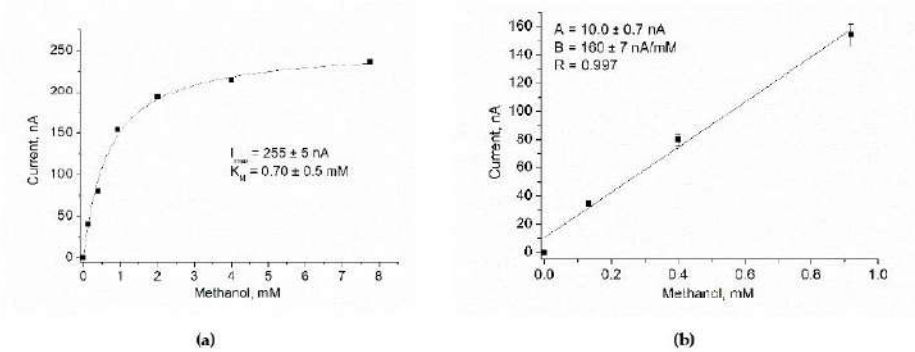

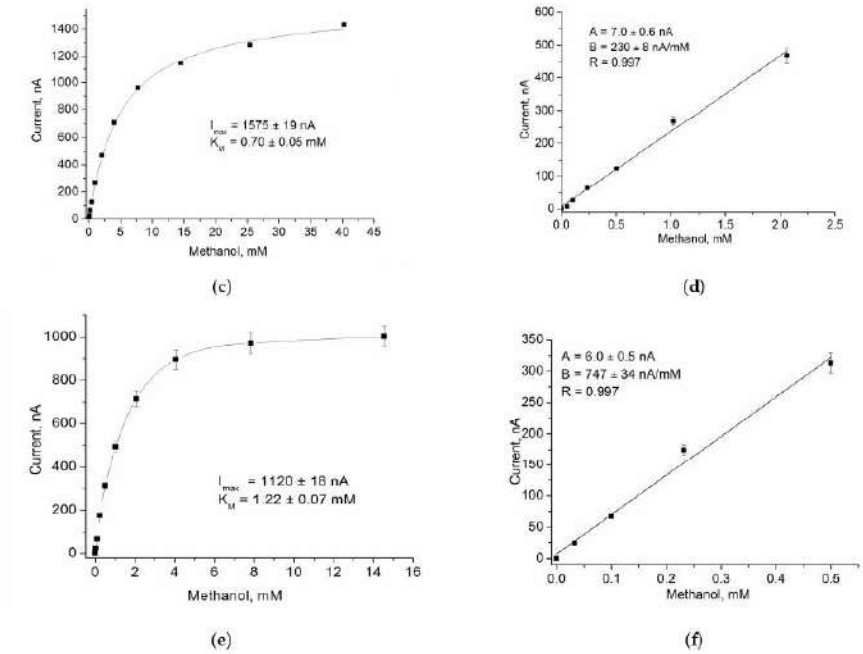

Figure 6. Amperometric characteristics of the AO/PO/GE (**a**,**b**), the AO/nCuCe/GE (**c**,**d**), and the AO/nCuCe/pAu/GE (**e**,**f**): (**a**,**c**,**e**) dependence of amperometric signal on concentration of methanol; (**b**,**d**,**f**) calibration graphs for methanol determination. Conditions: working potential –50 mV vs. Ag/AgCl/3 M KCl in 50 mM PB, pH 7.5.

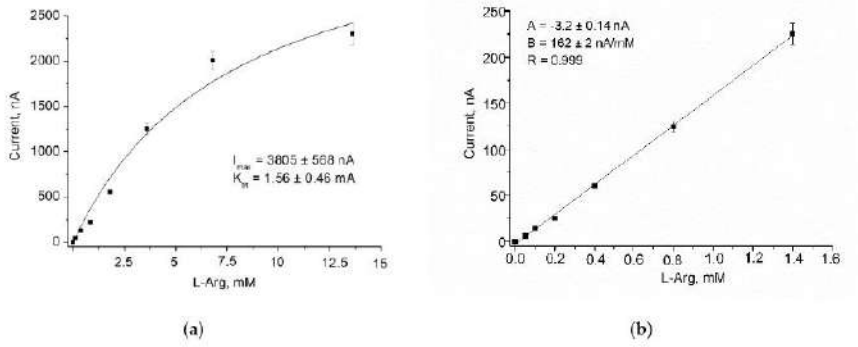

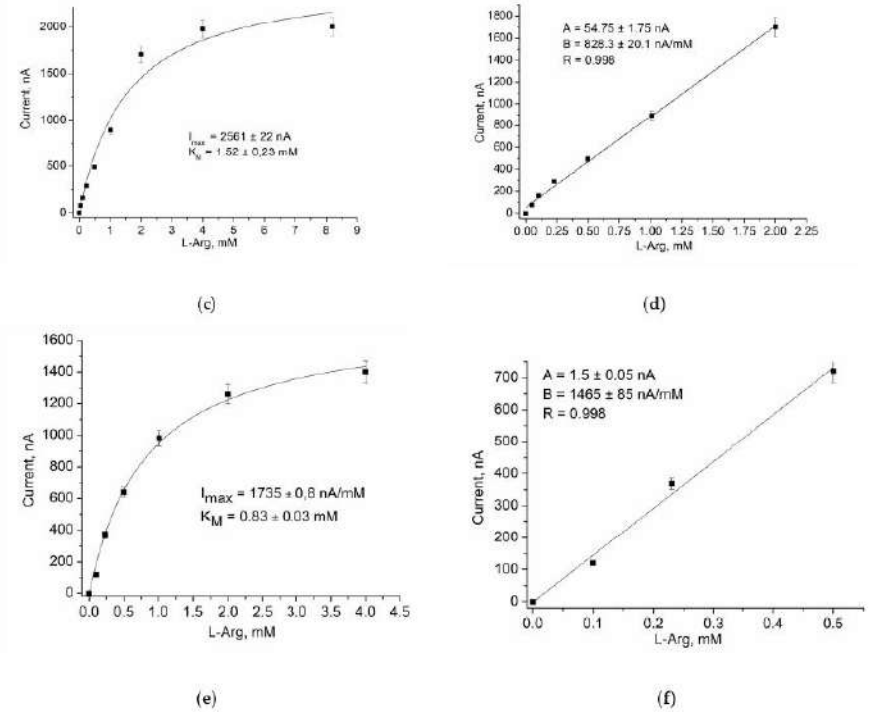

Figure 7. Amperometric characteristics of the ArgO/PO/GE (**a**,**b**), the ArgO/nCuCe/GE (**c**,**d**), and the ArgO/nCuCe/pAu/GE (**e**,**f**): (**a**,**c**,**e**) dependence of amperometric signal on concentration of L-Arg; (**b**,**d**,**f**) calibration graphs for L-Arg determination. Conditions: working potential –150 mV vs. Ag/AgCl/3 M KCl in 50 mM PB, pH 7.5.

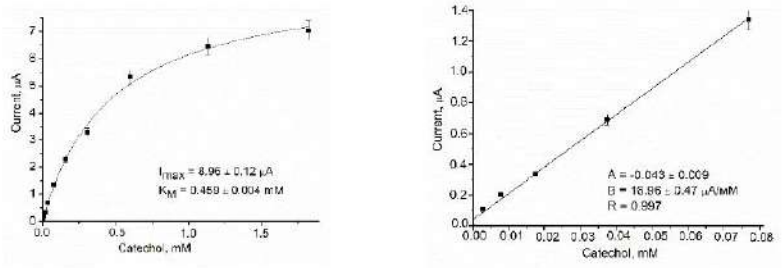

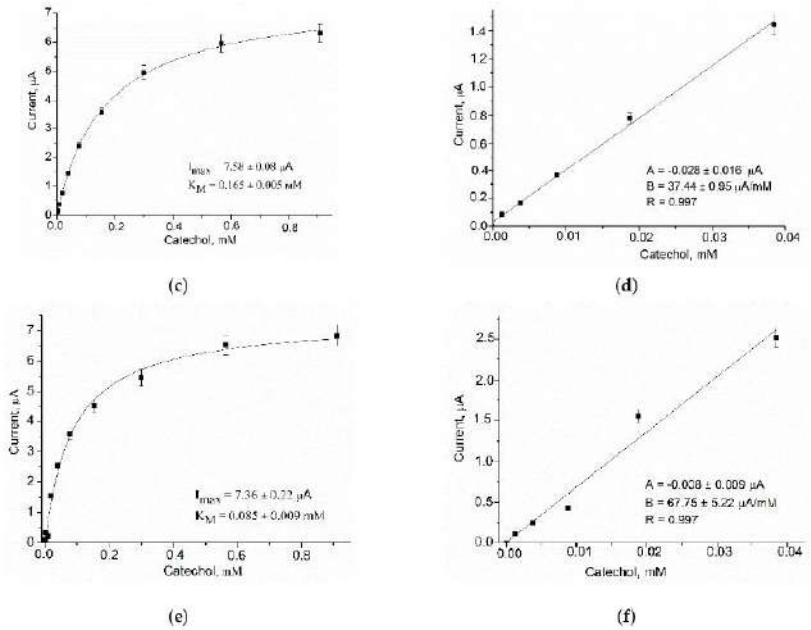

Figure 8. Amperometric characteristics of the laccase/GE (**a**,**b**), the laccase/nCuCe/GE (**c**,**d**), and the laccase/nCuCe/pAu/GE (**e**,**f**): (a,c,e) dependence of amperometric signal on concentration of catechol; (b,d,f) calibration graphs for catechol determination. Conditions: working potential –200 mV vs. Ag/AgCl/3 M KCl in 50 mM NaOAc, pH 4.5.

Table 1 summarizes the main bioanalytical characteristics of the developed ABSs, which were based on the usage of pAu, various oxidases, and nCuCe as well as the optimal conditions for their exploitation. It is worth mentioning that nCuCe plays a dual role in the described ABSs: for laccase it is a mediator of electron transfer, and for the other oxidases it is an artificial PO.

Table 1. Analytical characteristics of the constructed bioelectrodes.

Bioelectrode				Potential,	Sensitivity (S)		Linear Range,	LOD,	K_M^{app},
Enzyme	Mr, kDa	Sensor for H_2O_2	N	mV	$A \cdot M^{-1} \cdot m^{-2}$	Ks	μM	μM	mM
AO	640	PO	1	–50	22	S_2/S_1 = 1.5	130–900	39	0.70
		nCuCe	2		32	S_3/S_2 = 3.2	50–2100	15	0.70
		nCuCe/pAu	3		102	S_3/S_1 = 4.6	33–500	10	1.22
AMO	160	PO	1	–250	7	S_2/S_1 = 5	200–1700	61/130	2.1
		nCuCe	2		35	S_3/S_2 = 3.6	60–1700	18	2.2
		nCuCe/pAu	3		125	S_3/S_1 = 17.9	60–450	18	0.55
ArgO	500	PO	1	–150	22	S_2/S_1 = 5.1	75–1400	35	1.56
		nCuCe	2		113	S_3/S_2 = 1.8	50–2250	15	1.52
		nCeCu/pAu	3		200	S_3/S_1 = 9.1	100–500	33	0.83
GO	150–190	PO	1	–50	44	S_2/S_1 = 1.7	500–5000	150	5.23
		nCuCe	2		73	S_3/S_2 = 5.5	500–7300	150	18
		nCeCu/pAu	3		400	S_3/S_1 = 9.1	250–2000	76	5.81
Laccase	100	bulk	1	+200	2300	S_2/S_1 = 2.2	8–160	2	0.46
		* nCuCe	2		5055	S_3/S_2 = 1.8	3–40	2	0.17
		nCuCe/pAu	3		9280	S_3/S_1 = 4.0	2–40	1	0.09

* nCuCe is a mediator of electron transfer here.

4. Discussion

In the present work, the development of ABSs based on different oxidases and nCuCe, which were co-immobilized on pAu, was described. nCuCe has a dual role as an active mimetic of PO and a mediator of electron transfer. It was used as an electro-active mediator for a laccase-based ABS and as a PO-like NZ in ABSs that were based on other oxidases, namely, GO, AO, AMO, and ArgO. The ABSs for determination of catechol, glucose, primary alcohols, methyl amine, and L-arginine were constructed and characterized. The developed mono-enzyme ABSs exhibited improved analytical characteristics in comparison with the correspondent bi-enzyme ABSs that contained natural PO.

As shown in Table 1, nCuCe had a significant positive effect on sensor sensitivity in comparison to electrodes that were not modified with a nanomaterial. For example, for AMO/nCuCe/GE and ArgO/nCuCe/GE, the sensitivities were 5-fold higher (S_2) than for the corresponding GEs with natural PO (S_1). The ABS that contained laccase/nCuCe/GE was 2.2-fold more sensitive than the ABS with the laccase/GE composition.

It was demonstrated that the impact of electrodeposited pAu in the chemo-sensing layer of a graphite electrode is also significant. The presence of pAu was shown to provide an additional contribution to improve the analytical parameters of the ABS, especially in terms of their sensitivities (see Table 1). For example, the sensitivity of the GO/nCuCe/pAu/GE is 9.1-fold higher than that of the GO/PO/GE and 5.5-fold higher in comparison to the GO/nCuCe/GE. The same tendency, but at various levels, was demonstrated for each investigated enzyme. Thus, the ratio of sensitivities (S_3/S_2) for the AO-based ABS had a value of 3.2; for the AMO-based ABS, this value was 3.6. The positive influence of pAu on the sensitivity of an ABS has a simple explanation: the highly advanced surface of the pAu, having hierarchical pores with different diameters, presents an enhanced working 3D surface area on the electrode. The increased surface of the modified GE leads to the enhanced adsorption of nanomaterials/enzymes and thus to improved efficiency of electron transfer in the ABS in comparison with unmodified GEs.

Thus, ABSs with 3D porous micro/nanomaterials are novel versions of these devices that demonstrate a number of advantages, including enhanced sensitivity and stability, in comparison with traditional ABSs. The 3D architecture of the ABSs led to the improved analytical characteristics of the electrodes because of the increased amounts of immobilized enzyme and the enhanced speed of electron transfer. For successful progress in the development of ABSs to the level of industrial fabrication of commercially viable products, further integration of sensing technology with biochemical approaches needs to be achieved.

Author Contributions: Conceptualization, N.S. and G.G.; methodology, N.S. and O.D.; software, H.K.; validation, O.D. and H.K.; formal analysis, N.B.; investigation, N.S. and O.D.; resources, A.Z. and H.K.; data curation, M.N. and N.B.; writing—original draft preparation, N.S.; writing—review and editing, G.G. and M.N.; visualization, A.Z.; supervision, M.G.; project administration, M.G.; funding acquisition, M.N. All authors have read and agreed to the published version of the manuscript.

Funding: This research was partially founded by the National Research Foundation of Ukraine (project No 2020.02/0100) and by the National Academy of Sciences of Ukraine (projects No 0118U00626 and No 0121U110732).

Institutional Review Board Statement: Not applicable.

Informed Consent Statement: Not applicable.

Data Availability Statement: The data are contained within the present article.

Acknowledgments: We acknowledge the Research Authority of Ariel University, Ariel, Israel, for supporting this research. The authors thank O. Zakalska and R. Serkiz (Institute of Cell Biology NAS of Ukraine) for their technical assistance in experiments.

Conflicts of Interest: The authors declare no conflict of interest.

Appendix A

Appendix A presents amperometric characteristics of nCuCe/GE, namely, data of its PO-like properties (Figure A1), electroactivity (Figure A2), and selectivity (Figure A3).

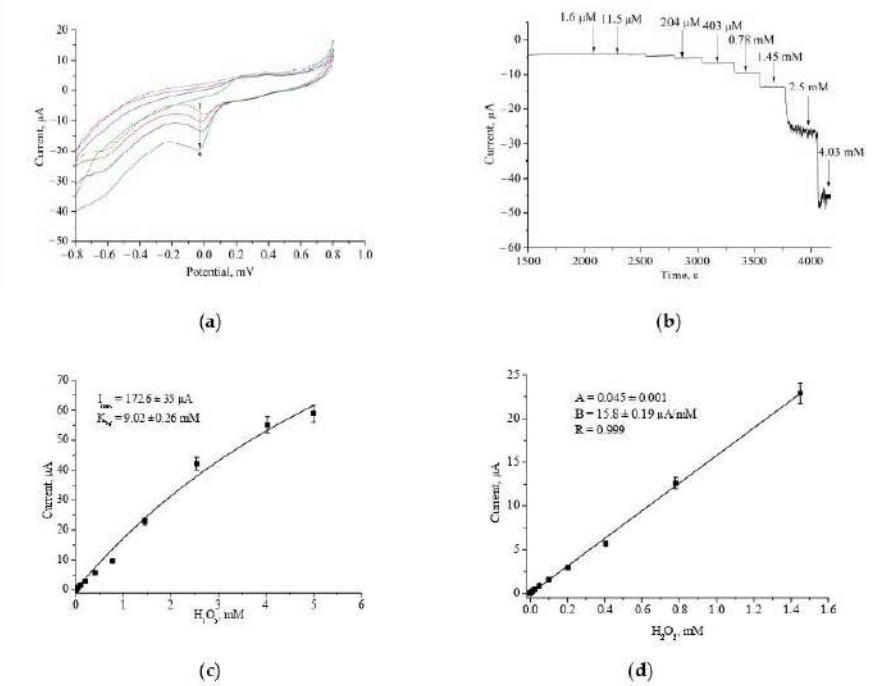

Figure A1. Amperometric characteristics of nCuCe/GE as a chemosensor of H_2O_2. (**a**) CV profiles as current responses upon addition of analyte up to concentrations (mM): 0 (1, black); 2.5 (2, red); 5.0 (3, blue); 10 (4, green). (**b**,**c**) chronoamperometric response and dependence of amperometric signal on concentration of H_2O_2, respectively; (**d**) calibration graph for H_2O_2 determination. Conditions: Ag/AgCl (reference electrode) in 50 mM PB, pH 7.0; scan rate 50 mV·s^{-1} (**a**); working potential −50 mV (**b**–**d**).

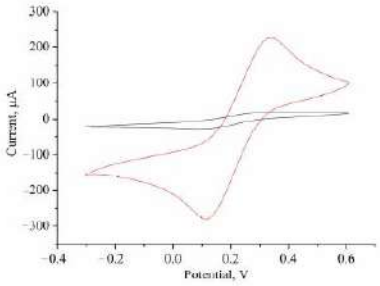

Figure A2. Cyclic voltammetry (CV) study of the bulk GE (black) and the modified nCuCe/GE (red) in solution containing 10 mM $K_3Fe(CN)_6$, 100 mM KCl, and 50 mM NaOAc, pH 4.5.

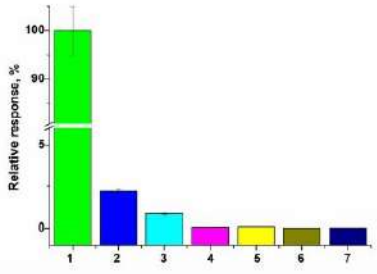

Figure A3. The selectivity test for the CuCe/GE: comparison of current responses on the added analytes up to 2 mM concentration: H_2O_2 (1), L-Arg (2), glucose (3), methylamine (4), methanol (5), ethanol (6), and catechol (7). Conditions: working potential −50 mV vs. Ag/AgCl (reference electrode), 50 mM acetate buffer, pH 4.5 at 23 °C.

References

1. Naresh, V.; Lee, N. A review on biosensors and recent development of nanostructured materials-enabled biosensors. *Sensors* **2021**, *21*, 1109. https://doi.org/10.3390/s21041109.
2. Nayl, A.A.; Abd-Elhamid, A.I.; El-Moghazy, A.Y.; Hussin, M.; Abu-Saied, M.A.; El-Shanshory, A.A.; Solman, H.M.A. The nanomaterials and recent progress in biosensing systems: A review. *Trends Environ. Anal. Chem.* **2020**, *26*, e00087. https://doi.org/10.1016/j.teac.2020.e00087.
3. Ashrafi, A.M.; Bytesnikova, Z.; Barek, J.; Richtera, L.; Adam, V. A critical comparison of natural enzymes and nanozymes in biosensing and bioassays. *Biosens. Bioelectron.* **2021**, *192*, 113494. https://doi.org/10.1016/j.bios.2021.113494.
4. Wu, J.; Wang, X.; Wang, Q.; Lou, Z.; Li, S.; Zhu, Y.; Qin, L.; Wei, H. Nanomaterials with enzyme-like characteristics (nanozymes): Next-generation artificial enzymes (II). *Chem. Soc. Rev.* **2019**, *48*, 1004–1076. https://doi.org/10.1039/C8CS00457A.
5. Huang, Y.; Ren, J.; Qu, X. Nanozymes: Classification, catalytic mechanisms, activity regulation, and applications. *Chem. Rev.* **2019**, *119*, 4357–4412. https://doi.org/10.1021/acs.chemrev.8b00672.
6. Liu, Q.; Zhang, A.; Wang, R.; Zhang, Q.; Cui, D. A Review on metal- and metal oxide-based nanozymes: Properties, mechanisms, and applications. *Nano-Micro Lett.* **2021**, *13*, 154. https://doi.org/10.1007/s40820-021-00674-8.
7. Stasyuk, N.; Smutok, O.; Demkiv, O.; Prokopiv, T.; Gayda, G.; Nisnevitch, M.; Gonchar, M. Synthesis, catalytic properties and application in biosensorics of nanozymes and electronanocatalysts: A Review. *Sensors* **2020**, *20*, 4509. https://doi.org/10.3390/s20164509.
8. Neumann, B.; Wollenberger, U. Electrochemical biosensors employing natural and artificial heme peroxidases on semiconductors. *Sensors* **2020**, *20*, 369. https://doi.org/10.3390/s20133692.
9. Demkiv, O.; Stasyuk, N.; Serkiz, R.; Gayda, G.; Nisnevitch, M.; Gonchar, M. Peroxidase-like metal-based nanozymes: Synthesis, catalytic properties, and analytical application. *Appl. Sci.* **2021**, *11*, 777. https://doi.org/10.3390/app11020777.
10. Gayda, G.Z.; Demkiv, O.M.; Gurianov, Y.; Serkiz, R.Y.; Klepach, H.M.; Gonchar, M.V.; Nisnevitch, M. "Green" Prussian Blue analogues as peroxidase mimetics for amperometric sensing and biosensing. *Biosensors* **2021**, *11*, 193. https://doi.org/10.3390/bios11060193.
11. Demkiv, O.; Stasyuk, N.; Gayda, G.; Gonchar, M. Highly sensitive amperometric sensor based on laccase-mimicking metal-based hybrid nanozymes for adrenaline analysis in pharmaceuticals. *Catalysts* **2021**, *11*, 1510. https://doi.org/10.3390/catal11121510.
12. Keihan, A.H.; Karimi, R.R.; Sajjadi, S. Wide dynamic range and ultrasensitive detection of hydrogen peroxide based on beneficial role of gold nanoparticles on the electrochemical properties of Prussian blue. *J. Electroanal. Chem.* **2020**, *862*, 114001. https://doi.org/10.1016/j.jelechem.2020.114001.
13. Tripathi, A.; Harris, K.D.; Elias, A.L. High surface area nitrogen-functionalized Ni nanozymes for efficient peroxidase-like catalytic activity. *PLoS ONE* **2021**, *16*, e0257777. https://doi.org/10.1371/journal.pone.0257777.
14. Fu, Z.; Zeng, W.; Cai, S.; Li, H.; Ding, J.; Wang, C.; Chen, Y.; Han, N.; Yang, R. Porous Au@Pt nanoparticles with superior peroxidase-like activity for colorimetric detection of spike protein of SARS-CoV-2. *J. Colloid Interface Sci.* **2021**, *604*, 113–121. https://doi.org/10.1016/j.jcis.2021.06.170.
15. Komkova, M.A.; Pasquarelli, A.; Andreev, E.A.; Galushin, A.A.; Karyakin, A.A. Prussian Blue modified boron-doped diamond interfaces for advanced H_2O_2 electrochemical sensors. *Electrochim. Acta* **2020**, *339*, 135924. https://doi.org/10.1016/j.electacta.2020.135924.
16. Stasyuk, N.; Gayda, G.; Demkiv, O.; Darmohray, L.; Gonchar, M.; Nisnevitch, M. Amperometric biosensors for L-arginine determination based on L-arginine oxidase and peroxidase-like nanozymes. *Appl. Sci.* **2021**, *11*, 7024. https://doi.org/10.3390/app11157024.

17. Bhattarai, J.K.; Neupane, D.; Nepal, B.; Mikhaylov, V.; Demchenko, A.V.; Stine, K.J. Preparation, modification, characterization, and biosensing application of nanoporous gold using electrochemical techniques. *Nanomaterials* **2018**, *8*, 171. https://doi.org/10.3390/nano8030171.
18. Chen, H.; Simoska, O.; Lim, K.; Grattieri, M.; Yuan, M.; Dong, F.; Lee, Y.S.; Beaver, K.; Weliwatte, S.; Gaffney, E.M.; et al. Fundamentals, applications, and future directions of bioelectrocatalysis. *Chem. Rev.* **2020**, *120*, 12903–12993. https://doi.org/10.1021/acs.chemrev.0c00472.
19. Stine, K.J.; Jefferson, K.; Shulga, O.V. Nanoporous gold for enzyme immobilization. *Methods Mol. Biol.* **2017**, *1504*, 37–60. https://doi.org/10.1007/978-1-4939-6499-4_5.
20. Zhao, A.; Zhang, Z.; Zhang, P.; Xiao, S.; Wang, L.; Dong, Y.; Yuan, H.; Li, P.; Sun, Y.; Jiang, X.; et al. 3D nanoporous gold scaffold supported on graphene paper: Freestanding and flexible electrode with high loading of ultrafine PtCo alloy nanoparticles for electrochemical glucose sensing. *Anal. Chim. Acta* **2016**, *938*, 63–71. https://doi.org/10.1016/j.aca.2016.08.013.
21. Rebelo, R.; Barbosa, A.I.; Caballero, D.; Kwon, I.K.; Oliveira, J.M.; Kundu, S.C.; Reis, R.L.; Correlo, V.M. 3D biosensors in advanced medical diagnostics of high mortality diseases. *Biosens. Bioelectron.* **2019**, *130*, 20–39. https://doi.org/10.1016/j.bios.2018.12.057.
22. Singh, B.K.; Lee, S.; Na, K. An overview on metal-related catalysts: Metal oxides, nanoporous metals and supported metal nanoparticles on metal organic frameworks and zeolites. *Rare Met.* **2020**, *39*, 751–766. https://doi.org/10.1007/s12598-019-01205-6.
23. Bollella, P. Porous Gold: A New Frontier for enzyme-based Electrodes. *Nanomaterials* **2020**, *10*, 722. https://doi.org/10.3390/nano10040722.
24. Sondhi, P.; Stine, K.J. Electrodeposition of Nanoporous Gold Thin Films. In *Nanofibers—Synthesis, Properties and Applications*; Kumar, B., Ed.; IntechOpen: London, UK, 2020; 20p. https://doi.org/10.5772/intechopen.94604.
25. Xu, H.; Liu, S.; Pu, X.; Shen, K.; Zhang, L.; Wang, X.; Qin, J.; Wang, W. Dealloyed porous gold anchored by in situ generated graphene sheets as high activity catalyst for methanol electro-oxidation reaction. *RSC Adv.* **2020**, *10*, 1666–1678. https://doi.org/10.1039/C9RA09821F.
26. Phan-Quang, G.C.; Yang, Z.; Koh, C.S.L.; Sim, H.Y.F.; Leong, S.X.; Ling, X.Y. Plasmonic-induced overgrowth of amorphous molybdenum sulfide on nanoporous gold: An ambient synthesis method of hybrid nanoparticles with enhanced electrocatalytic activity. *J. Chem. Phys.* **2019**, *151*, 244709. https://doi.org/10.1063/1.5130649.
27. Zhang, A.; Wang, J.; Schützendübe, P.; Liang, H.; Huang, Y.; Wang, Z. Beyond dealloying: Development of nanoporous gold via metal-induced crystallization and its electrochemical properties. *Nanotechnology* **2019**, *30*, 375601. https://doi.org/10.1088/1361-6528/ab2616.
28. Demirci, C.; Marras, S.; Prato, M.; Pasquale, L.; Manna, L.; Colombo, M. Design of catalytically active porous gold structures from a bottom-up method: The role of metal traces in CO oxidation and oxidative coupling of methanol. *J. Catal.* **2019**, *375*, 279–286. https://doi.org/10.1016/j.jcat.2019.06.016.
29. Hernández-Saravia, L.P.; Sukeri, A.; Bertotti, M. Fabrication of nanoporous gold-islands via hydrogen bubble template: An efficient electrocatalyst for oxygen reduction and hydrogen evolution reactions. *Int. J. Hydrog. Energy* **2019**, *44*, 15001–15008. https://doi.org/10.1016/j.ijhydene.2019.04.186.
30. Sondhi, P.; Stine, K.J. Methods to generate structurally hierarchical architectures in nanoporous coinage metals. *Coatings* **2021**, *11*, 1440. https://doi.org/10.3390/coatings11121440.
31. Xiao, X.; Si, P.; Magner, E. An overview of dealloyed nanoporous gold in bioelectrochemistry. *Bioelectrochemistry* **2016**, *109*, 117–126. https://doi.org/10.1016/j.bioelechem.2015.12.008.
32. Biener, J.; Biener, M.M.; Madix, R.J.; Friend, C.M. Nanoporous gold: Understanding the origin of the reactivity of a 21st Century catalyst made by pre-columbian technology. *ACS Catal.* **2015**, *5*, 6263–6270. https://doi.org/10.1021/acscatal.5b01586.
33. Saffarini, M.H.; Voyiadjis, G.Z.; Ruestes, C.J.; Yaghoobi, M. Ligament size dependency of strain hardening and ductility in nanoporous gold. *Comput. Mater. Sci.* **2021**, *186*, 109920. https://doi.org/10.1016/j.commatsci.2020.109920.
34. Mie, Y.; Takayama, H.; Hirano, Y. Facile control of surface crystallographic orientation of anodized nanoporous gold catalyst and its application for highly efficient hydrogen evolution reaction. *J. Catal.* **2020**, *389*, 476–482. https://doi.org/10.1016/j.jcat.2020.06.023.
35. Masud, M.K.; Na, J.; Lin, T.-E.; Malgras, V.; Preet, A.; Ibn Sina, A.A.; Wood, K.; Billah, M.; Kim, J.; You, J.; et al. Nanostructured mesoporous gold biosensor for microRNA detection at attomolar level. *Biosens. Bioelectron.* **2020**, *168*, 112429. https://doi.org/10.1016/j.bios.2020.112429.
36. Wong, T.S.B.; Newman, R.C. A novel application of nanoporous gold to humidity sensing: A framework for a general volatile compound sensor. *Nanoscale Adv.* **2020**, *2*, 777–784. https://doi.org/10.1039/D0NA00010H.
37. Han, M.; Chen, F.; Li, M.; Yu, R.; Xu, Y.; Jiang, Y.; Liu, C.; Hu, J. Light welding Au nanoparticles assembled at water-air interface for monolayered nanoporous gold films with tunable electrocatalytic activity. *Electrochim. Acta* **2020**, *334*, 135626. https://doi.org/10.1016/j.electacta.2020.135626.
38. Karnan, P.; Maduraiveeran, G. Bimetallic nanomaterials-based electrochemical biosensor platforms for clinical applications. *Micromachines* **2021**, *13*, 76. https://doi.org/10.3390/mi13010076.
39. Sarkhosh-Inanlou, R.; Shafiei-Irannejad, V.; Azizi, S.; Jouyban, A.; Ezzati-Nazhad Dolatabadi, J.; Mobed, A.; Adel, B.; Soleymani, J.; Hamblin, M.R. Applications of scaffold-based advanced materials in biomedical sensing. *Trends Analyt. Chem.* **2021**, *143*, 116342. https://doi.org/10.1016/j.trac.2021.116342.

40. Mathew, M.; Radhakrishnan, S.; Vaidyanathan, A.; Chakraborty, B.; Rout, C.S. Flexible and wearable electrochemical biosensors based on two-dimensional materials: Recent developments. *Anal. Bioanal. Chem.* **2021**, *413*, 727–762. https://doi.org/10.1007/s00216-020-03002-y.
41. Kim, S.H. Nanoporous gold: Preparation and applications to catalysis and sensors. *Curr. Appl. Phys.* **2018**, *18*, 810-818. https://doi.org/10.1016/j.cap.2018.03.021.
42. Presutti, D.; Agarwal, T.; Zarepour, A.; Celikkin, N.; Hooshmand, S.; Nayak, C.; Ghomi, M.; Zarrabi, A.; Costantini, M.; Behera, B.; et al. Transition metal dichalcogenides (TMDC)-based nanozymes for biosensing and therapeutic applications. *Materials* **2022**, *15*, 337. https://doi.org/10.3390/ma15010337.
43. Barra, P.; Delogu, F. Porosity effects on nanoporous Au Young's modulus. *Mater. Lett.* **2021**, *304*, 130703. https://doi.org/10.1016/j.matlet.2021.130703.
44. Klepach, H.M.; Zakalskiy, A.E.; Zakalska, O.M.; Gayda, G.Z.; Smutok, O.V.; Gonchar, M.V. Alcohol oxidase from the methylotrophic yeast *Ogataea polymorpha*: Isolation, purification, and bioanalytical application. *Methods Mol. Biol.* **2021**, *2280*, 231–248. https://doi.org/10.1007/978-1-0716-1286-6_15.
45. Stasyuk, N.E.; Smutok, O.V.; Zakalskiy, A.E.; Zakalska, O.M.; Gonchar, M.V. Methylamine-sensitive amperometric biosensor based on (His)6-tagged *Hansenula polymorpha* methylamine oxidase immobilized on the gold nanoparticles. *Biomed. Res. Int.* **2014**, *2014*, 480498. https://doi.org/10.1155/2014/480498.
46. Demkiv, O.M.; Gayda, G.Z.; Broda, D.; Gonchar, M.V. Extracellular laccase from *Monilinia fructicola*: Isolation, primary characterization and application. *Cell Biol. Intern.* **2021**, *45*, 536–548. https://doi.org/10.1002/cbin.11316.
47. Lutz, G. *Semiconductor Radiation Detectors*; Springer: Berlin/Heidelberg, Germany, 2007; ISBN 978-3-540-71679-2.
48. Tobin, J.G.; Yu, S.-W.; Sokaras, D. The X-ray Emission Spectroscopy of Cerium Oxide. *J. Electron Spectrosc. Relat. Phenom.* **2020**, *1*, 26. https://www.osti.gov/servlets/purl/1755807.

Оригінал доступний за посиланням: https://www.mdpi.com/2079-6374/12/7/472

5.3. Розробка нового фотометричного методу аналізу етанолу на основі АО та нанозимів PtCu, інкапсульованих в альгінатні кульки.

Анотація: *Нанозими (НЗ) — це наночастинки, які імітують каталітичні властивості природних ензимів. У поточній роботі ми повідомляємо про одержання ефективних міметиків пероксидази (ПО-подібних НЗ), дослідження їх морфологічних властивостей, оцінку кінетичних параметрів отриманих НЗ та встановлення перспектив їх застосування в аналізі етанолу. Нами розроблено спектрофотометричний метод аналізу етанолу з використанням багаторазових у використанні альгінатних кульок, збагачених алкогольоксидазою (АО) і наночастинками PtCu (Pt/Cu), що виконують функцію ПО-подібних НЗ. В ролі оранічного хромогену використовували 3,3',5,5'-тетраметилбензидин (ТМВ). Діапазон лінійності запропонованого методу Pt/Cu-АО/альгінатні кульки/ТМБ становить від 0,01 мМ до 0,15 мМ з межею виявлення 3,3 мкМ етанолу. Метод використали для кількісного визначення вмісту етанолу в алкогольних напоях. Отримані результати підкреслюють потенціал подальшого практичного застосування Pt/Cu в ролі міметиків ПО. Запропонований метод, будучи чутливим, економічним і придатним для рутинних і мікрооб'ємних форматів, може бути використаний у клінічній діагностиці для аналізу етанолу.*

RSC Advances

PAPER

Check for updates

Cite this: RSC Adv., 2022, 12, 21309

Reusable alcohol oxidase–nPtCu/alginate beads for highly sensitive ethanol assay in beverages†

Nataliya Stasyuk, *[ab] Olha Demkiv,[a] Galina Gayda, [a] Oksana Zakalska,[a] Andriy Zakalskiy,[ad] Roman Serkiz,[ac] Taras Kavetskyy[be] and Mykhailo Gonchar*[ab]

Nanozymes (NZs) are nanoparticles that mimic the catalytic properties of natural enzymes. The present work aimed to obtain effective peroxidase mimetics (PO-like NZs), to characterize their morphological properties, estimate the kinetic parameters of NZs and evaluate the prospects of their application in analysis of ethanol. Herein, we have proposed a convenient spectrophotometric method for ethanol assay using reusable alginate beads enriched with alcohol oxidase (AO) and nanoparticles of PtCu (nPtCu) as PO-like NZs, and 3,3′,5,5′-tetramethylbenzidine (TMB) as a chromogen. The linear range for the proposed nPtCu–AO/alginate beads/TMB-based method is from 0.01 mM to 0.15 mM with a limit of detection of 3.3 μM ethanol. The method is used for the quantitative determination of ethanol in alcoholic beverages. The obtained results proved to be in a good correlation with the enzymatic reference method. These results highlight the potential of the nPtCu with PO-like activity in bioanalytical applications. The proposed method, being sensitive, economical and suitable for routine and micro-volume formats, can be used in clinical diagnostics for the detection of ethanol.

Received 1st April 2022
Accepted 9th July 2022

DOI: 10.1039/d2ra02106d

rsc.li/rsc-advances

Introduction

Ethanol is a major component of alcoholic beverages and other products that undergo fermentation.[1–3] Although alcohol is widely consumed, in high doses it can cause a variety of health complications and intoxication.[4–6] Determining the level of various alcohols with high sensitivity, selectivity and precision is very important for many medical and industrial applications.[7] To measure alcohol levels in biological liquids and beverages, many analytical methods such as gas chromatography,[8] high performance liquid chromatography[9] and spectrophotometry[10] have been proposed. Although these methods are accurate and reliable, they conclude time-consuming stages of pre-processing. Among the reported methods, ethanol conversion enzymes, namely, alcohol oxidase (AO) and alcohol dehydrogenase (ADH) are frequently used for the construction of electrochemical biosensors for detection of ethanol due to their simplicity, low cost, and high sensitivity.[11,12]

NAD^+-dependent ADH can oxidize primary aliphatic and aromatic alcohols.[13] NAD(P)-dependent dehydrogenases are widely used in analytical applications.[14,15] However, the application of ADH in biosensorics is complicated because of additional cofactors for electrode regeneration.[16] On the other hand, AO oxidizes primary alcohols to aldehydes and hydrogen peroxide (H_2O_2). AO contains the flavin-based cofactor which is tightly associated with the redox center of the enzyme, making it more pertinent for biosensor design.[17,18] This is why almost all the proposed AO-based methods for analysis of ethanol exploit the monitoring of O_2 consumption or H_2O_2 formation. In the case of spectrophotometric detection of ethanol, based on measurement of H_2O_2 concentration, a bi-enzymatic system coupled with peroxidase (PO) is typically used.[19]

Peroxidases (PO, E.C. 1.11.1.7) are oxidoreductases that contain an iron-porphyrin derivative (heme) in their active site and catalyze the oxidation of diverse organic compounds using H_2O_2 as the electron acceptor.[20] Commercially, PO is used in many diagnostic kits, including immunological testing as well as in the treatment of industrial wastewater for biological improvement.[21]

A new class of enzymes, artificial peroxidases, has recently become known.[22] Artificial enzymes or nanozymes (NZs) are nanomaterials with intrinsic enzyme-like characteristics that have been booming over the past decade because of their capability to address the limitations of natural; enzymes such as low stability, high cost, and difficult storage. Novel artificial PO-

[a]Institute of Cell Biology, National Academy of Sciences of Ukraine, Lviv, Ukraine. E-mail: stasuk_natalia@ukr.net; demkiv@yahoo.com; galina.gayda@gmail.com; zakalska@yahoo.com; andriy.zakalskiy@yahoo.com; mykhailo1952@gmail.com

[b]Drohobych Ivan Franko State Pedagogical University, Drohobych, Ukraine

[c]Ivan Franko National University of Lviv, Department of Solid State Physics, Lviv, Ukraine. E-mail: rserkiz@gmail.com

[d]Institute of Animal Biology of the National Academy of Agrarian Sciences of Ukraine, Lviv, Ukraine

[e]The John Paul II Catholic University of Lublin, 20-950 Lublin, Poland. E-mail: kavetskyy@yahoo.com

† Electronic supplementary information (ESI) available. See https://doi.org/10.1039/d2ra02106d

© 2022 The Author(s). Published by the Royal Society of Chemistry

like NZs hold a great promise for successful assay of various real samples including food and biological liquids. Recently, various nanoparticles (NPs), in particular, the nanomaterials of metals and transition metal oxides were shown to decompose effectively H_2O_2.[23,24] Among them, Prussian blue-based NPs and noble metal nanomaterials, such as gold (Au), platinum (Pt), and ruthenium (Ru) have attracted more attention because of their high catalytic activities, tunable morphology, and excellent biocompatibility. Compared with single-component noble metal NPs, hybrid (bi- and trimetallic) nanomaterials can provide a higher chance for enhancement in catalytic efficiency.[25]

Nowadays, there is limited data concerning the development of colorimetric (spectrophotometric) methods of ethanol analysis using of AO and PO-like NZs.[26–34] Recently, it has been reported the synthesis of thiocyanide capped gold nanoparticles possessing AO-like activity, however the selectivity of ethanol detection was insufficient.[26] The main analytical characteristics of the proposed alcohol oxidase–nanozyme-based methods for ethanol analysis are compared in Table 1. In these methods, chromogenic substrates such as TMB (3,3′,5,5′-tetramethylbenzidine) and ABTS (2,2′-azinobis[3-ethylbenzothiazoline-6-sulfonic acid]) have been commonly used. For example, AuPtRu were coupled with AO to detect ethanol in a buffer solution and mouse blood employing TMB as a chromogen substrate.[27] Whereas, Kim and co-workers have detected ethanol in a linear concentration range from 100 to 500 μM with a detection limit of 25 μM by employing ABTS as a peroxidase substrate.[28] In addition, one of the most effective artificial PO mimetics was shown to be Prussian blue nanocubes which in combination with AO and TMB showed an excellent linear range up to 10 mM at 652 nm.[29] The other methods of ethanol assay are based on the AO and PO-like NZs was amperometry and electrochemical impedance spectroscopy, but the sensitivity of the proposed sensors was insufficient.[31–34]

The aim of current research is to design reusable alginate beads loaded with AO and PO-like nanozyme PtCu (further – nPtCu) and their testing for ethanol analysis in beverages. In this paper, we describe synthesis, morphological characterization and estimation the catalytic parameters of NZs as artificial PO. AO was selected due to using it in our previous works related to the development of biosensors and enzymatic kits for assay of ethanol.[35–37] Various analytical characteristics, such as specificity, sensitivity, repeatability and operational stability were investigated.

Results and discussion

Synthesis and characterization of PO mimetics

A number of metal-based composite nanomaterials were obtained using two chemical methods, namely, reduction from the inorganic salts and bath deposition on plate. The synthesized compounds were screened on their ability to oxidize *o*-DZ in the presence of H_2O_2 by monitoring optical density at 525 nm.[38] It was shown that several synthesized NZs, especially nPtCu and nCu revealed the highest PO-like activities among all others (Table 2).

The nPtCu and nCu with the highest PO-like activity were chosen for further detailed morphological characterization by SEM coupled with X-ray microanalysis (SEM-XRM). SEM provided information on the size and shape of the tested sample (see ESI, Fig. ESI 1†). Fig. ESI 1† presents the overall morphology of the formed particles. The XRM images of the most active PO mimetics (nPtCu and nCu) showed the characteristic peaks for metals of the composites. As shown in Fig. ESI 1a–c,† nPtCu have structure close to spherical with the size of near 200 nm, whereas the sizes of nCu was near 500 nm (Fig. ESI 1d and e†). The XRM images (Fig. ESI 1d and f†) showed the presence of all components of the tested materials. Pt^0 formation has been proved by X-ray microanalysis, which showed the characteristic emission peaks at 2.2, 9.5, and 11.1 keV corresponding to the PtK_α, PtK_α, and PtK_β transitions, respectively (Fig. ESI 1c†). The characteristic peaks for Cu^0 at 1.4 and 8.05 keV which correspond to the CuK_α and CuK_β transitions, respectively, were shown in Fig. ESI 1c and f.†

Investigation of kinetic parameters (K_M and V_{max}) of NZs

For the obtained NZs with the highest PO-specific activities, the catalytic parameters (K_M, V_{max}, k_{cat}) were estimated (Fig. 1, Table 2).

Table 1 The main analytical characteristics of the described alcohol oxidase–nanozyme-based methods for analysis of ethanol[a]

Selective layer	Mode of detection	Linear range, mM	LOD, μM	Reference
nPtCu	Spectrophotometry	0.01–0.15	3.3	This work
Au/PtRu		0.25–4	23.8	27
Fe_3O_4		0.1–0.5	25	28
hPBNCs		0.04–10.8	30	29
Pd/Pt		—	500	30
Pt/Ru	Amperometry	0.025–0.2	3	31
PO/Au		0.005–3	2.3	32
Au		0.01–4.7	7	33
CB/PBNPs	Electrochemical impedance spectroscopy	Up to 10	520	34

[a] hPBNCs – Prussian blue nanocubes; CB/PBNPs – nanocomposite formed by carbon black (CB) and Prussian nlue nanoparticles (PBNPs).

© 2022 The Author(s). Published by the Royal Society of Chemistry

Table 2 Comparison of the kinetic parameters of synthesized NZs for H_2O_2 in peroxidative oxidation of *o*-DZ[a]

Kinetic parameters					
NZs	Specific activity, U mg^{-1}	K_M, mM	V_{max}, mM s^{-1}	k_{cat}, μmol s^{-1} mg^{-1}	k_{cat}/K_M, s^{-1} mL mg^{-1}
nCuCeAu	1.8 ± 0.12	0.82	5.3×10^{-4}	0.053	0.065
nPtAu	1.4 ± 0.1	3.1	5.8×10^{-4}	0.058	0.019
nPtCu	3.4 ± 0.5	5.3	2.5×10^{-5}	0.023	0.004
nCu	3.0 ± 0.25	25.8	7×10^{-5}	0.333	0.013
nPdCe	2.2 ± 0.05	103	6.8×10^{-5}	1.35×10^{-4}	0.005
nCuCe	1.65 ± 0.13	667	4×10^{-4}	4.0	0.006
PO[40]	—	3.7	0.004	—	—

[a] K_M – Michaelis constant; V_{max} – maximal reaction velocity; k_{cat} – catalytic constant; k_{cat}/K_M – catalytic efficiency.

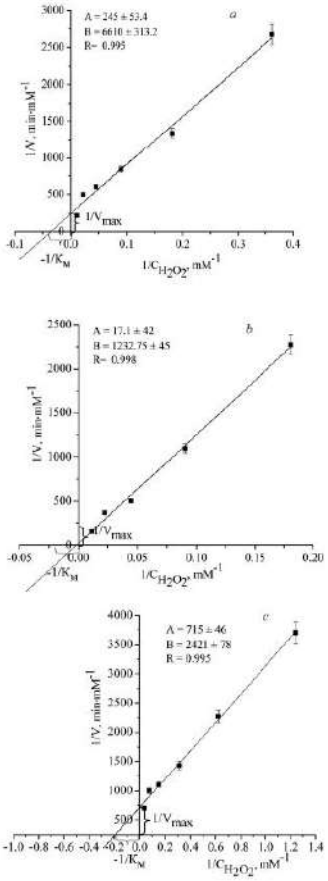

Fig. 1 Kinetic analysis for the NZs: nCu (a), nCuCe (b) and nPtCu (c) with H_2O_2 and *o*-DZ as substrates. *A*, *B* – parameters for the linear regression line; *R* – correlation coefficient; V_{max} – maximum velocity of the reaction; K_M – the apparent Michaelis–Menten constant.

From the kinetic analysis, it was found that in 0.05 M acetate buffer at pH 4.5 in the presence of *o*-DZ as a substrate, nPtCu and nPtAu show similar to natural horseradish peroxidase (PO) K_M values (toward H_2O_2), namely, 5.3 mM and 3.1 mM, respectively. As shown in Table 2, the apparent K_M (further K_M) value of the nCuCeAu toward H_2O_2 is significantly lower than that of the natural PO,[41] suggesting that the nCuCeAu have higher affinity to H_2O_2. The maximum velocity (V_{max}) of the reaction was also analyzed and compared with the natural PO enzyme. The data presented above also showed that for nCu the value of K_M is significantly higher (7-fold), which indicates a lower (compared to PO) affinity of NZs to H_2O_2, probably, due to the steric difficulties of diffusion of substrate molecules to the surface of NZs (Table 2).

Table 2 shows the kinetic parameters of the NZs in solution, determined by the method of Lineweaver–Burk. The obtained kinetic parameters were compared with the kinetic characteristics of PO, with *o*-DZ as the substrate.

The selectivity test to other chromogenic substrates in two-substrate peroxidative reaction was also done, including ABTS (2,2′-azino-bis(3-ethylbenzothiazoline-6-sulfonic acid)), 4-aminoantipyrine (4-AAP), guaiakol and 3,3′,5,5′-tetramethyl benzidine (TMB) in comparison with *o*-DZ, according to the methods specified in subdiv. «determination of peroxidase-like activity of NZs in solution» (Fig. ESI 2†). It was shown that the obtained NZs have the highest activity toward to *o*-DZ, while guaiacol cannot serve as a substrate. It should be noted that ABTS, as a substrate, occupies an intermediate place in this row. Summarizing the obtained results on the catalytic characteristics of the synthesized NZs it can be concluded that *o*-DZ and TMB are the best substrates for peroxidative reaction. In next experiments on ethanol assay we have used TMB as a chromogen.

Fabrication and characterisation of the alginate beads

In our study, alginate beads encapsulated with nPtCu and AO were used for the development of the spectrophotometric assay of ethanol. nPtCu and AO were incorporated into the alginate beads during the gelation. To study morphology and elemental composition on the bead's surface, SEM with energy-dispersive X-ray spectroscopy was used (Fig. 2). It should be noted that

© 2022 The Author(s). Published by the Royal Society of Chemistry

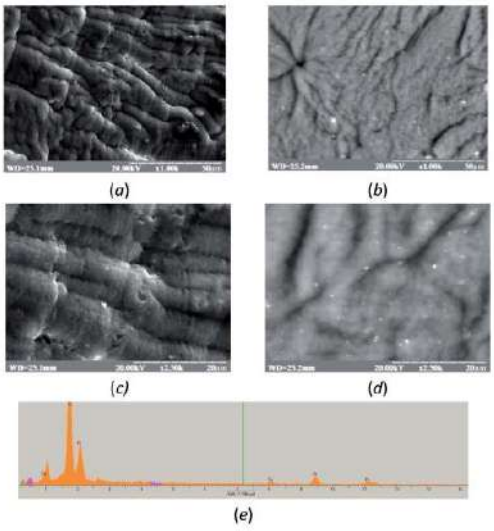

Fig. 2 Characteristics of alginate beads encapsulated with nPtCu and AO (a–d): SEM images for ×1.000 (a and b) (scale bar 50 μm) and ×2.500 magnification (scale bar 20 μm) (c and d); X-ray spectral microanalysis (e). The accelerating voltage was 20 kV for all images.

SEM images have been done in usual (a and c) and compo (b and d) modes, which allows to visualize the NZs located inside the alginate beads. As shown in Fig. 2a–d, nPtCu particles do not agglomerate during gelation. The XRM images show the characteristic peaks for Cu^0, Pt^0 (Fig. 2e), respectively.

The characteristics of a developed method for ethanol assay

The proposed method is based on the reactions shown in Fig. 3. This figure represents the reactions which take place inside the alginate bead. First, the ethanol is oxidized to acetaldehyde and H_2O_2 under AO. The resulting H_2O_2 under the action of nPtCu oxidizes the TMB, forming the colored product (λ_{max} 450 nm) in acidic medium. The final oxidized TMB is yellow colored oxidation product, yield to be directly proportional to the concentration of ethanol having the absorbance peak at 450 nm in acidic medium (data not shown).

For further application of the nPtCu–AO/alginate beads in analysis of ethanol, pH of phosphate buffer, temperature and TMB concentration in incubation mixture were optimized. The maximal sensitivity was shown to be under the following conditions the enzymatic reaction: 2.0 mM TMB in incubation mixture and 10 min of incubation of alginate beads with ethanol of the defined concentration in 50 mM phosphate buffer pH 7.5 (PB) at 22 °C. The optimizations of enzymatic–nanozymatic steps of the reaction were carried out too. Optimal concentrations of AO and nPtCu in one alginate bead were estimated as following: 46 mU for AO and 7 mU for nPtCu (see subdiv. «formation of nPtCu–AO/alginate beads»). Also it was shown that the nPtCu had no alcohol oxidase-like activity at experimental conditions (data not shown).

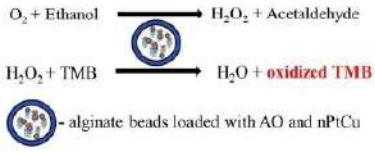

Fig. 3 Principal scheme of the reactions for ethanol assay using nPtCu–AO/alginate beads/TMB method.

Fig. ESI 3† demonstrates the dependency of optical density (OD) of reaction mixture on concentration of H_2O_2 for nPtCu-loaded alginate beads. The linearity of calibration graph for H_2O_2 detection is from 0.01 mM to 0.1 mM with the limit of detection (LOD) 2.5 μM. Fig. 4 demonstrates the dependency of OD of reaction mixture on concentration of ethanol. In Fig. 4 the analytical response of the nPtCu–AO/alginate beads/TMB-based method to ethanol concentration ranging from 0.005 mM to 4.5 mM is shown (Fig. 4a). It is worth noting that the profile of OD at 450 nm reveals a high linear relationship with ethanol concentration ranging from 0.01 to 0.15 mM and the LOD was shown to be 3.3 μM (Fig. 4b). The analytical characteristics of nPtCu–AO/alginate beads/TMB-based method are summarized in Table 3 in relation to other enzymatic–nanozymatic methods.

The sensitivity of the spectrophotometric method of ethanol assay is characterized by the slope of the regression line (B) of

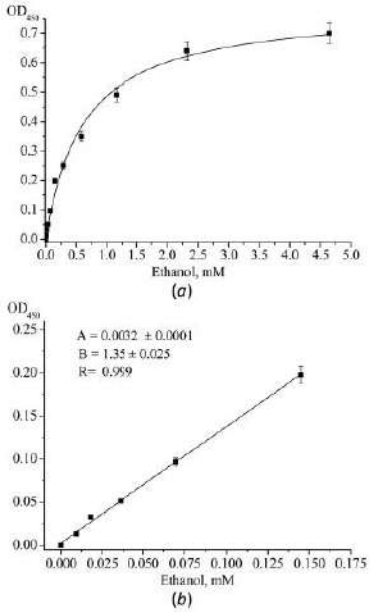

Fig. 4 The dependence of OD of reaction mixture on the concentration of ethanol in final mixture (a) and linear calibration curve (b) for nPtCu–AO/alginate beads/TMB-based method of ethanol assay. A, B – parameters for the linear regression line; R – correlation coefficient.

© 2022 The Author(s). Published by the Royal Society of Chemistry

Table 3 Determination of ethanol in beverages[a]

Sample	Value declared by the producer, %	Method				Difference, %
		"Alcotest"	CV, %	"nPtCu–AO/alginate bead"	CV, %	
Liquor "Aperitif", Italy	11	10.93 ± 0.50	4.6	11.43 ± 0.65	5.7	+4.3
Champagne "Latini Sparkling", Germany	8.5	9.03 ± 0.30	3.3	9.04 ± 0.55	6.0	+0.1
Wine "Aznauri", dry red, Ukraine	9–13	9.61 ± 0.40	4.2	10.04 ± 0.45	4.5	+4.3

[a] CV – coefficient of variation.

the calibration graph. Comparison of B values allows to appreciate the level of analyte's conversion on each stage of reaction. The level of ethanol conversion to H_2O_2 is 49% (Fig. ESI 3† and 4b). The main characteristics of the developed and other enzymatic-nanozyme methods of ethanol assay are summarized in Table 1.

The high selectivity is the necessary requirement for each analytic method. To study the selectivity of the developed analytical approach, different 1 mM alcohols with varying lengths and branching (methanol, ethanol, 1-propanol and 1-butanol) were tested (Fig. ESI 4†). It was shown that nPtCu–AO/alginate beads responds differently to alcohol samples and exhibits the highest response to methanol (100%) and ethanol (92%). This validates the potential of the nPtCu–AO/alginate bead-based method for ethanol assay in beverages. The developed spectrophotometric nPtCu–AO/alginate bead/TMB-based enzymatic–nanozymatic method for the quantitative analysis of ethanol is highly sensitive (see Table 1). Also selectivity to ethanol is not high, but it precisely reflects the intrinsic selectivity of AO to alcohols (Fig. ESI 4†). It is worth mentioning that the reaction between nPtCu–AO/alginate beads and TMB can also proceed at room temperature and it does not need long incubation time. This feature of the proposed method is prospective for the development of portable test system with automatic variant of ethanol assay as well as for semi-quantitative detection of ethanol level. Thus, the proposed analytical method being sensitive, low-cost and suitable for both routine and micro-volume formats, will be promising for using in clinical diagnostics and ethanol assay in food products or beverages.

Repeatability of analysis and stability of the nPtCu–AO/alginate beads

The repeatability of assay using a single alginate bead loaded with nPtCu and AO was investigated by successively detecting 1.0 mM ethanol for 5 times. The relative standard deviation (RSD) was 4.33%, indicating a good repeatability. Storage stability of alginate beads was investigated by every day monitoring its response to 1 mM ethanol concentration. The one alginate beads retained 56% of their initial response even after 4 days of storage at room temperature, indicating its good storage stability in 10 mM $CaCl_2$.

Assay of ethanol in real samples

Determination of ethanol concentration in beverages is an accidental request to forensic laboratories. We have reported earlier about the development of AO-based method for ethanol analysis by the amperometric biosensors.[35–37] In order to demonstrate the practical feasibility of the proposed enzymatic–nanozymatic method, contents of ethanol were determined in beverages using SAT method. Estimation of ethanol in the initial sample from the parameters of linear regression was done, taking into account factors of dilution (eqn (1)); calculation of the average concentration from values for two dilutions of the sample:

$$C = \frac{A}{B}N, \quad (1)$$

where C – calculated initial ethanol concentration, A and B – parameters of linear regression; N – dilution factor of the tested sample, shown in graph (see Fig. 5).

The average contents of the ethanol determined by the developed spectrophotometric method and the reference method are presented in Table 3. The differences less than 5% between the results of both methods were observed.

The concentrations of the tested ethanol, estimated using two methods, have a strong ($R = 0.987$) correlation (Fig. ESI 5†).

Therefore, the developed nPtCu–AO/alginate bead-TMB-based method can be successfully used for ethanol assay in alcoholic beverages. The reproducibility of the proposed analytical method is satisfactory: the coefficients of variation are less than 7% (Table 3).

Experimental

Reagents

Cerium(III) chloride ($CeCl_3$), ascorbic acid, chloroplatinic acid (H_2PtCl_6), copper(II) sulfate ($CuSO_4$), palladium chloride ($PdCl_3$), sodium borohydride ($NaBH_4$), cetrimonium bromide (CTAB), *o*-dianisidine, hydrogen peroxide (H_2O_2, 30%), iron(III) chloride ($FeCl_3 \times 4H_2O$), gold(III) chloride solution ($HAuCl_4$), calcium(II) chloride ($CaCl_2$), alginic acid, ethanol, methanol, propanol, 1-butanol and all other reagents and solvents used in this work were purchased from Sigma-Aldrich (Steinheim, Germany). All reagents were of analytical grade and were used without further purification. All solutions were prepared using ultra-pure water obtained with the Milli-Q® IQ 7000 Water Purification system (Merck KGaA, Darmstadt, Germany).

Synthesis of nanozymes by the chemical reduction method

Nanozymes (NZs) were synthesized by the chemical reduction of metal ions from appropriate salts using CTAB and ascorbic acid

© 2022 The Author(s). Published by the Royal Society of Chemistry

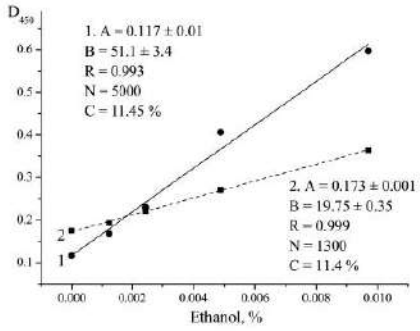

(a)

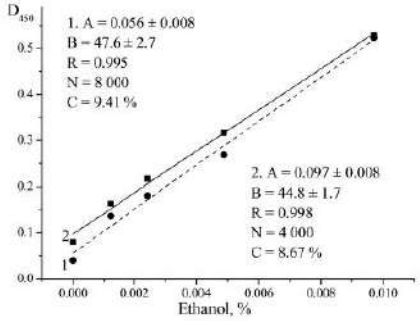

(b)

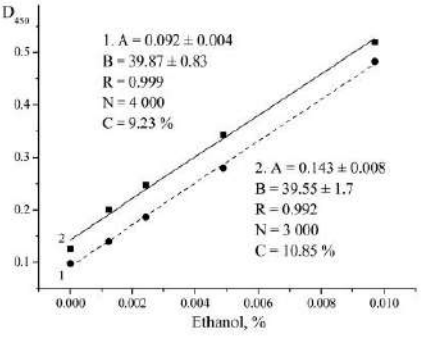

(c)

Fig. 5 Assay of ethanol by nPtCu–AO/alginate beads/TMB-based method in samples of liquor "Aperitif" (a), champagne "Latini Sparkling" (b), and dry red wine "Aznauri" (c) using SAT calibration method. *A*, *B* – parameters for the linear regression line; *N* – dilution factor; *C* – calculated initial concentration of ethanol; *R* – correlation coefficient.

(AA) according to the schemes which were reported by us recently with some modifications.[38] The conditions of synthesis, which were chosen experimentally, are presented in Table ESI 1.†

Briefly: mixture 1, containing solutions of salt #1 and CTAB, was vigorously stirred for 5 min at 20 °C and after AA adding, it was heated at 100 °C during 10 min. Mixture 2, containing the heated mixture 1, salt #2 and AA, was heated at 100 °C during 10 min and then stirred for 15 min at 20 °C. To obtain tri-metal NZs, salt #3 was added to the heated mixture 2, stirred and heated during 15 min.

The synthesized NZs were collected by centrifugation at 16 000 rpm for 40 min (Hettich Micro-22R centrifuge), washed twice with water, and precipitated by centrifugation. Pellets were suspended in 1.0 mL water and stored until use at +4 °C.

Synthesis of nanozymes by chemical bath deposition method

The core–shell CuCe and CoCu NZs on zinc plate substrate were synthesized by chemical bath deposition method. It includes preparation of an aqueous bath containing 0.1 M solution of salts, namely, copper(II) sulphate or cobalt(II) chloride with the addition of aqueous NH_3 solution (28%) under constant stirring at room temperature with resultant pH ~ 12. For this aim, the well cleaned Zn plate substrate was placed in reaction bath at room temperature for 20 h resulting in the direct growth of metallic nanoparticles on Zn substrate. After that, 0.1 M cerium(III) chloride (for synthesis of CuCe) or 0.1 M copper(II) sulphate (for synthesis of CoCu) was added to the reaction bath and stayed during 20 hours at room temperature. Then, the produced NPs were washed from the surface of the Zn plate and were collected by centrifugation under 16 000*g* for 40 min (Hettich Micro-22R centrifuge), washed twice with water, and precipitated by centrifugation. Pellets were suspended in 1.0 mL water and stored until use at +4 °C.

For the formation of core–shell–shell NZs, CuCeAu and CoCuCe, the previously synthesized thin films (CuCe or CoCu) onto Zn substrate was vertically dipped into beaker containing 0.01 M cerium(III) chloride or hydrogentetrachloroaurate solution in 28% of NH_3 making an angle of 45° with the wall of beaker. The reaction baths maintained at room temperature for 1 day. The resulting CuCeAu and CoCuCe were washed several times with water, dried in air atmosphere and used for further characterization.

Formation of nPtCu–AO/alginate beads

nPtCu (0.09 mL, 3.4 U mg^{-1}, concentration 1 mg mL^{-1}) and AO (0.03 mL, 70 U mL^{-1}) were thoroughly mixed with 1 mL 2.5% algic acid. The aliquots of mixture (0.025 mL) were injected into a solution of 0.3 M $CaCl_2$ at a flow rate of 5 mL min^{-1}. The obtained nPtCu–AO-impregnated alginate beads were formed *via* gelation. Gelation occurs immediately upon the contact of the alginate and Ca^{2+}, forming homogeneous spherical beads with an average diameter of 2.5 mm. The resulting beads were washed with 10 mM $CaCl_2$ three times. The obtained composite alginate beads were stored in 10 mM $CaCl_2$ till usage. For analysis of ethanol in each test tube one of such prepared bead was taken. The produced Ca-alginate beads were chosen for further investigation.

The principal scheme of the formation of the Ca-alginate beads with incorporated nPtCu and AO is presented on the Fig. 6.

© 2022 The Author(s). Published by the Royal Society of Chemistry

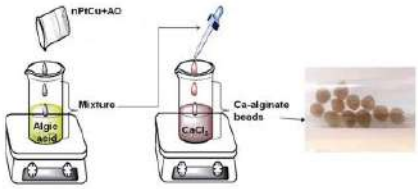

Fig. 6 The principal scheme of the formation of the Ca-alginate composite beads.

Morphological analysis of NZs by scanning electron microscopy (SEM)

Morphological analyses of the samples were performed using a SEM microanalyzer (REMMA-102-02, Sumy, Ukraine). The samples in different dilutions were dropped onto the surface of a silicon wafer and were dried at room temperature. The samples in different dilutions (2 μL or one alginate bead) were dropped onto the surface of a silicon wafer and were dried at room temperature. The distance from the last lens of the microscope to the sample (WD) ranged from 24 mm to 25 mm, respectively. The accelerator voltage was 20 000 kV.

Determination of peroxidase-like activity of NZs in solution

The PO-like activity of the NZs was measured by the colorimetric method, with *o*-dianisidine (*o*-DZ) as a chromogenic substrate in the presence of H_2O_2 according the procedure described early by us.[33] The generated color was determined at 525 nm using a Shimadzu UV1650 PC spectrophotometer (Kyoto, Japan). One unit (U) of PO-like activity was defined as the amount of NZs converting 1 μmol *o*-DZ into the colored product per 1 min at 30 °C under standard assay conditions. The specific PO-like activity was expressed in μmol $min^{-1} \cdot mg^{-1}$ of NZ and calculated using the following formula:

$$\text{Specific activity, U mg}^{-1} = \frac{\Delta D_{525} V_t N}{13.35 V_{NZ} t c}, \quad (2)$$

where ΔD_{525} – optical density of the final photometric mixture; V_t – the total volume of the reaction mixture in the cuvette, mL; 13.35 – millimolar extinction coefficient of the oxidized *o*-DZ, mM^{-1} cm^{-1}; V_{NZ} – aliquot of NZ added, mL; c – mass concentration of NZ in added solution, determined by gravimetric method, mg mL^{-1}; N – dilution of NZ before adding to the reaction mixture; t – time of pseudo-enzymatic reaction, min.

Estimation of kinetic parameters

The Michaelis–Menten constants (K_M) and maximum velocity (V_{max}) for the oxidation of *o*-DZ in the presence of H_2O_2 and the NZ at room temperature were determined by measuring the activity rates (under the assay conditions) at substrate concentrations ranging from 0–50 mM H_2O_2 with a fixed concentrations of *o*-DZ (0.017 mM) and NZ (in incubation mixture) in 0.05 M acetate buffer, pH 4.5. The values of k_{cat} were calculated by the formula: $k_{cat} = V_{max}/C_{NZ}$, where C_{NZ} is the concentration of NZ in incubation mixture, mg mL^{-1}. Because, of difficulty to determine the concentration of NZs in mM units, but only in mass units (mg mL^{-1}), the dimension of k_{cat} is expressed in s^{-1} μmol mg^{-1}.

Determination of the substrate specificity for NZ

The substrate specificity to the chromogenic substrates in a two-substrate reaction in the presence of H_2O_2 was examined. As organic substrates ABTS, 4-AAP, guaiakol, TMB and *o*-DZ were used. To study the activity of NZ in solution, an aliquot of NZ and the tested organic substrate in the presence of H_2O_2 was incubated for a fixed time in 50 mM acetate buffer, pH 4.5. The analysis of pseudo PO-activity was done according to the procedure described in subdiv. "determination of peroxidase-like activity of NZs in solution".

Isolation and purification of AO

AO (EC 1.1.3.13) was isolated from the cells of the selected AO-overproducing strain *Ogataea* (*Hansenula*) *polymorpha* C-105. Cell-free extract was fractionated by an ammonium sulfate, then electrophoretically homogeneous enzyme was obtained by ion exchange chromatography on DEAE-Toyopearl 650 M.[39–41] Activity of AO was determined by the rate of hydrogen peroxide formation in reaction with methanol as monitored by the peroxidative oxidation of *o*-DZ in the presence of PO. Purified AO with specific activity 20 U mg^{-1} of protein was kept as suspension in 70% ammonium sulfate, 50 mM phosphate buffer, pH 7.5 (PB).

The development of nPtCu–AO/alginate bead/TMB-based method for ethanol assay

Calibration for ethanol was carried out in the following way: 0.230 mL ethanol standard solution with concentration from 0.001% to 1.25% in PB was mixed in glass tube with one alginate bead and incubated at room temperature during 10 min. Resulted solution was supplemented in each test tube with 1 mL 2.5 mM TMB in PB. The reaction mixture was incubated at room temperature during 2 min followed by the addition of 0.5 mL 0.8 M HCl and the resulted mixture was detected spectrophotometrically at 450 nm. The dependencies of absorbance for the resulted TMB oxidized products on ethanol concentration were studied. The corresponding calibration graphs were built. Each experiment was repeated for 3 times.

Ethanol assay in real samples of beverages

The samples of wine "Aznauri", dry red (PJSC "Odessainprom", Ukraine), liquor "Aperitif" (Campari, Italy) and champagne "Latini Sparkling" (Peter Mertes, Germany) were used for ethanol analysis. All samples were diluted stepwise by 50 mM PB. All samples were analyzed using a standard addition test (SAT). Each assay was performed for two dilutions of the sample and repeated 3 times.

Reference method for ethanol determination

Ethanol assay was carried out using enzymatic analytical kit "Alcotest" by the measurement of the colored product

© 2022 The Author(s). Published by the Royal Society of Chemistry

formation in peroxidative oxidation of chromogen by H_2O_2 generated from ethanol in AO reaction.[35] Because of a high sensitivity of the method, the "fixed reaction time" was used at the incomplete conversion of analyte.

Statistic analysis

All the measurement's results and the level of correlation between results obtained by the different analytical methods were calculated by computer program Origin 8.5 Pro and Microsoft Excel.

Conclusions

A number of metal-based composite nanoparticles were obtained using the two chemical methods, in particular, reduction from the inorganic salts and bath deposition on plate. The morphological properties, catalytic parameters (K_M, V_{max}, k_{cat}) and selectivity to different chromogenic substrates were studied for the synthesized NZs with the highest specific activities.

Novel colorimetric method based on alginate beads encapsulated with nPtCu and AO have been developed and optimized. The proposed method exhibits a high sensitivity to ethanol, broad linear range (10–150 μM), low detection limit (3.3 μM), satisfactory storage stability and repeatability. The developed method was tested on the real samples of alcoholic beverages. High correlation of the obtained results and the reference enzymatic method was demonstrated.

Funding

This research was partially supported by the National Research Foundation of Ukraine (project no. 2020.02/0100 "development of new nanozymes as catalytic elements for enzymatic kits and chemo/biosensors"), National Academy of Sciences of Ukraine: the programs: "smart sensor devices of a new generation based on modern materials and technologies" and "double-acting anticancer drugs to overcome the acquired resistance of malignant cells to chemotherapy" (0122U200211), grant "new dual casein kinase 2 inhibitors and histone deacetylase for targeted tumor chemotherapy" for research laboratories/groups of young scientists in priority areas of science and technology in 2021–2022, and Ministry of Education and Science of Ukraine (projects no. 0120U103398, 0121U109539, 0122U000874 and 0121U109543).

Author contributions

Nataliya Stasyuk, Demkiv Olha, Galina Gayda: investigation, validation, writing – original draft; Roman Serkiz, Taras Kavetskyy: visualization. Oksana Zakalska, Andriy Zakalskiy: methodology, formal analysis, visualization. Mykhailo Gonchar: conceptualization, supervision, writing - review & editing, project administration, funding acquisition, resources.

Conflicts of interest

There are no conflicts to declare.

References

1 B. Kuswandi, T. Irmawati, M. A. Hidayat, J. Jayus and M. Ahmad, *Sensors*, 2014, **14**, 2135–2149, DOI: 10.3390/s140202135.

2 P. Puligundla, D. Smogrovicova, C. Mok and V. S. R. Obulam, *Renewable Energy*, 2019, **133**, 1366–1379, DOI: 10.1016/j.renene.2018.06.062.

3 A. Dasgupta, Chapter 1 – Alcohol: Pharmacokinetics, Health Benefits With Moderate Consumption and Toxicity, *Critical Issues in Alcohol and Drugs of Abuse Testing*, ed. A. Dasgupta, Academic Press, 2nd edn, 2019, pp. 1–16, DOI: 10.1016/B978-0-12-815607-0.00001-0.

4 F. Al-Taher, in *Halal Food Production*, ed. M. N. Riaz and M. M. Chaudry, CRC Press, Boca Raton, FL, USA, 2004, p. 379.

5 B. E. Leonard, *Alcohol Alcohol.*, 1986, **21**, 325–338. PMID: 2434114.

6 M. N. Riaz and M. M. Chaudry, Alcohol: The Myths and Realities, in *Handbook of Halal and Haram Products*, Publishing Centre of American Muslim Research & Information, Richmond Hill, NY, USA, 1997, p. 16, https://www.routledgehandbooks.com/, DOI: 10.1201/9781315119564-3.

7 M. A. A. Halim, M. M. M. Salleh, M. I. A. M. Kashim, A. A. Ahmad and N. Nordin, *Int. J. Asian Soc. Sci.*, 2014, **4**(12), 1176–1190, https://archive.aessweb.com/index.php/5007/article/view/2709.

8 A. Tangerman, *Clin. Chem.*, 1997, **43**, 1003–1009. PMID: 9191553.

9 L. M. Avila, A. D. Santos, D. I. Mançano de Mattos, C. Gimenes de Souza, D. Andrade and L. d'Avila, *Fuel*, 2018, **212**, 236–239, DOI: 10.1016/j.fuel.2017.10.039.

10 M. Sriariyanun, P. Mutrakulcharoen, S. Tepaamorndech, K. Cheenkachorn and K. Rattanaporn, *Orient. J. Chem.*, 2019, **35**(2), 744–750.

11 O. M. Istrate, L. Rotariu and C. Bala, *Sensors*, 2021, **21**(19), 6510, DOI: 10.3390/s21196510.

12 S. Sivashankar, N. S. Kumar and K. R. N. Mazumder, *Int. J. Pharm. Sci. Rev. Res.*, 2020, **65**(1), 68–82, DOI: 10.47583/ijpsrr.2020.v65i01.010.

13 S. Alpat and A. Telefoncu, *Sensors*, 2010, **10**(1), 748–764, DOI: 10.3390/s100100748.

14 H. R. Zare, N. Nasirizadeh, S. M. Golabi, M. Namazian, M. M. Ardakani and D. Nematollahi, *Sens. Actuators, B*, 2006, **114**, 610–617, DOI: 10.1016/j.snb.2005.06.013.

15 F. Tian and G. Zhu, *Sens. Actuators, B*, 2004, **97**, 103–108, DOI: 10.1016/j.snb.2003.08.002.

16 A. Malinauskas, T. Ruzgas, L. Gorton and L. T. Kubota, *Electroanalysis*, 2000, **12**, 194–198, DOI: 10.1002/(SICI)1521-4109(200002)12:3<194::AID-ELAN194>3.0.CO;2-6.

17 S. R. Chinnadayyala, M. Santhosh, N. K. Singh and P. Goswami, *Biosens. Bioelectron.*, 2015, **69**, 155–161, DOI: 10.1016/j.bios.2015.02.015.

18 M. Das and P. Goswami, *Bioelectrochemistry*, 2013, **89**, 19–25, DOI: 10.1016/j.bioelechem.2012.08.007.

© 2022 The Author(s). Published by the Royal Society of Chemistry

19 A. M. Azevedo, D. M. Prazeres, J. M. Cabral and L. P. Fonseca, *Biosens. Bioelectron.*, 2005, **21**(2), 235–247, DOI: **10.1016/j.bios.2004.09.030**.
20 N. Stasyuk, O. Smutok, O. Demkiv, T. Prokopiv, G. Gayda, M. Nisnevitch and M. Gonchar, *Sensors*, 2020, **20**, 4509, DOI: **10.3390/s20164509**.
21 S. Sanjay, *Front. Chem.*, 2019, 7, 1–10, DOI: **10.3389/fchem.2019.00046**.
22 M. Liang and X. Yan, *Acc. Chem. Res.*, 2019, **52**(8), 2190–2200, DOI: **10.1021/acs.accounts.9b00140**.
23 J. I. Reyes-De-Corcuera, H. E. Olstad and R. García-Torres, *Annu. Rev. Food Sci. Technol.*, 2018, **9**, 293–322, DOI: **10.1146/annurev-food-030216-025713**.
24 W. Dong, Y. Zhuang, S. Li, X. Zhang, H. Chai and Y. Huang, *Sens. Actuators, B*, 2018, **255**(2), 2050–2057, DOI: **10.1016/j.snb.2017.09.013**.
25 M. Liang and X. Yan, *Acc. Chem. Res.*, 2019, **52**(8), 2190–2200, DOI: **10.1021/acs.accounts.9b00140**.
26 S. R. Ahmed, G. A. Ortega, S. Kumar, S. Srinivasan and A. R. Rajabzadeh, *New J. Chem.*, 2022, **46**, 1194–1202, DOI: **10.1039/D1NJ03648C**.
27 L. Feng, Y. Gong, Y. Cao, Y. Deng, S. Liang, X. Tian, H. Gu and J.-J. Yin, *Nanoscale Adv.*, 2020, **2**, 1583–1589, DOI: **10.1039/D0NA00002G**.
28 M. I. Kim, J. Shim, H. J. Parab, S. C. Shin, J. Lee and H. G. Park, *J. Nanosci. Nanotechnol.*, 2012, **12**(7), 5914–5919, DOI: **10.1166/jnn.2012.6375**.
29 S. Wang, H. Yan, Y. Wang, N. Wang, Y. Lin and M. Li, *Microchim. Acta*, 2019, **186**, 738, DOI: **10.1007/s00604-019-3826-6**.
30 Y. Zhang, Q. Liu, C. B. Ma, Q. Wang, M. Yang and Y. Du, *Theranostics*, 2020, **10**(11), 5064–5073, DOI: **10.7150/thno.42601**.
31 N. Stasyuk, G. Gayda, A. Zakalskiy, O. Zakalska, R. Serkiz and M. Gonchar, *Food Chem.*, 2019, **285**, 213–220, DOI: **10.1016/j.foodchem.2019.01.117**.
32 S. R. Chinnadayyala, A. Kakoti, M. Santhosh and P. Goswami, *Biosens. Bioelectron.*, 2014, **55**, 120–126, DOI: **10.1016/j.bios.2013.12.005**.
33 S. R. Chinnadayyala, M. Santhosh, N. K. Singh and P. Goswami, *Biosens. Bioelectron.*, 2015, **69**, 155–161, DOI: **10.1016/j.bios.2015.02.015**.
34 S. Cinti, M. Basso, D. Moscone and F. Arduini, *Anal. Chim. Acta*, 2017, **960**, 123–130, DOI: **10.1016/j.aca.2017.01.010**.
35 M. V. Gonchar, M. M. Maidan, H. M. Pavlishko and A. A. Sibirny, *Food Technol. Biotechnol.*, 2001, **39**, 37–42. **https://www.ftb.com.hr/archives/103-volume-39-issue-no-1/743-a-new-oxidase-peroxidase-kit-for-ethanol-assays-in-alcoholic-beverages**.
36 O. Smutok, B. Ngounou, H. Pavlishko, G. Gayda, M. Gonchar and W. Schuhmann, *Sens. Actuators, B*, 2006, **113**, 590–598, DOI: **10.1016/j.snb.2005.07.055**.
37 O. Demkiv, N. Stasyuk, R. Serkiz, G. Gayda, M. Nisnevitch and M. Gonchar, *Appl. Sci.*, 2021, **11**, 777, DOI: **10.3390/app11020777**.
38 N. Stasyuk, G. Gayda, T. Kavetskyy and M. Gonchar, *RSC Adv.*, 2022, **12**, 2026–2035. **https://pubs.rsc.org/en/Content/ArticleLanding/2022/RA/D1RA08127F**.
39 M. V. Gonchar, G. P. Ksheminska, N. M. Hladarevska and A. A. Sibirny, Catalaseminus mutants of methylotrophic yeast Hansenula polymorpha impaired in regulation of alcohol oxidase synthesis, in *Genetics of respiratory enzymes in yeasts Wroclaw*, ed. T. M. Lachowicz, Wroclaw University Press, 1990, pp. 222–228.
40 S. V. Shleev, G. P. Shumakovich, O. V. Nikitina, O. V. Morozova, H. M. Pavlishko, G. Z. Gayda and M. V. Gonchar, *Biochemistry*, 2006, **71**(3), 245–250, DOI: **10.1134/S0006297906030035**.
41 O. V. Lebedeva, N. N. Ugarova and I. V. Berezin, *Biokhimiia*, 1977, **42**(8), 1372–1379. PMID: 20989.

© 2022 The Author(s). Published by the Royal Society of Chemistry

Оригінал доступний за посиланням: https://pubs.rsc.org/en/content/articlelanding/2022/ra/d2ra02106d
Електронний додаток до статті доступний за посиланням: https://www.rsc.org/suppdata/d2/ra/d2ra02106d/d2ra02106d1.pdf

5.4. Створення амперометричних біонаносенсорів на основі мікробних оксидаз (АО, МАО, АргО) та НЗ – міметиків ПО.

Анотація: *Точний та швидкий аналіз етанолу потрібен в багатьох сферах, включаючи промисловість і судову медицину. У поточній роботі ми повідомляємо про розробку амперометричних біонаносенсорів (АБС) на основі дріжджової алкогольоксидази (АО) та гібридних металевих наночастинок в ролі штучних пероксидаз (ПО). Нами синтезовано велику кількість металевих ПО-подібних НЗ та протестовано їхню здатність заміщати природну ПО в розчині та в складі амперометричного електрода. Усі ПО міметики ко-іммобілізовано з АО на графітових електродах (ГЕ) та електрохімічно охарактеризовано. Встановлено, що два типи модифікованих біоелектродів, а саме, АО/AuCePt/ГЕ та АО/FePtAu/ГЕ, виявляють найвищу чутливість до етанолу (2600 $А \cdot М^{-1} \cdot м^{-2}$ та 1250 $А \cdot М^{-1} \cdot м^{-2}$, відповідно), найнижчу межу виявлення (1,5 мкМ і 2,2 мкМ), широкі лінійні діапазони (5 – 100 мкМ і 12 – 120 мкМ), а також задовільну стабільність при зберіганні. Сконструйований біонаноелетрод на основі АО/AuCePt/ГЕ протестовано на реальних зразках сироваток крові та слини людини. Показано високу кореляцію отриманих даних із результатами референтного ензиматичного методу «Алкотест».*

Microchimica Acta (2022) 189:474
https://doi.org/10.1007/s00604-022-05568-z

ORIGINAL PAPER

Amperometric biosensors based on alcohol oxidase and peroxidase–like nanozymes for ethanol determination

Nataliya Stasyuk[1] · Olha Demkiv[1] · Galina Gayda[1] · Oksana Zakalska[1] · Wojciech Nogala[2] · Mykhailo Gonchar[1]

Received: 29 July 2022 / Accepted: 4 November 2022
© The Author(s), under exclusive licence to Springer-Verlag GmbH Austria, part of Springer Nature 2022

Abstract
The aim of the current research is to design alcohol oxidase-based amperometric biosensors (ABSs) using hybrid metallic nanoparticles as artificial peroxidases (PO) or PO-like nanozymes (NZs). A lot of metallic PO-like NZs were synthesized and tested with respect to their ability to substitute natural PO in solution and on amperometric electrode. The most effective PO mimetics were coupled with alcohol oxidase (AOX) on graphite electrodes (GEs) and characterized. Two types of modified GEs, namely, the AOX/nAuCePt/GE and the AOX/nFePtAu/GE show the highest sensitivities to ethanol (2600 $A \cdot M^{-1} \cdot m^{-2}$ and 1250 $A \cdot M^{-1} \cdot m^{-2}$, respectively), low limits of detection (1.5 µM and 2.2 µM), broad linear ranges (5 – 100 µM and 12 – 120 µM), as well as satisfactory storage stabilities. The most sensitive bioelectrode AOX/nAuCePt/GE was used as ABS for ethanol determination in real samples. The practical feasibility of the constructed ABS was demonstrated by determination of ethanol in beverages, human blood and saliva.

Keywords Alcohol oxidase · Metallic nanoparticles · Peroxidase-like nanozymes · Amperometric biosensor · Ethanol determination

Introduction

Biosensors (BSs) are powerful analytical tools for application in research, medical, and industrial laboratories. The global world market of biosensors was valued in 2021 at USD 25.5 billion and is projected to reach USD 36.7 billion by 2026. The top five world biosensor manufacturers are Abbott Laboratories, Johnson & Johnson, Roche Diagnostics, DuPont Biosensor Materials, and Bayer AG https://www.marketsandmarkets.com/Market-Reports/biosensors-market-798.html. The main reasons for the growth of the global market of BSs were caused by rising investment in pharmacy, clinical diagnostics, security and biodefense, necessity of strong ecology control, expansion of food and beverage industry, growth of smart agriculture, and others https://www.insightslice.com/biosensors-market [1–3].

✉ Nataliya Stasyuk
stasuk_natalia@ukr.net

[1] Institute of Cell Biology, National Academy of Sciences of Ukraine, Lviv 79005, Ukraine

[2] Institute of Physical Chemistry, Polish Academy of Sciences, 01-224 Warsaw, Poland

Electrochemical BSs, especially enzyme-based embedded devices, hold the highest BSs market segment during last decades. Sixty years after construction of the first enzyme-based amperometric BSs (further ABSs), the novel technological strategies, including internet of things (IoT), were proposed [1, 2]. Efforts of scientists to solve the problems of improving electron transfer, stability, sensitivity, and selectivity of ABSs lead to an acceleration of transforming ABSs from the laboratory prototypes into the commercial products [1–3].

The detection of alcohols with high sensitivity and selectivity is required in many different areas, including the industry of food and drinks [4–11], as well as the healthcare [2, 3, 11–16] and forensics [5, 12]. In forensics, ethanol content in human biological liquids or in exhaled breath is a biomarker of alcohol consumption [17, 18]. In clinical medicine, this parameter is important marker for control under the alcoholism treatment [12, 15, 16, 19, 20]. Ethanol is analyzed usually in blood or serum [13, 18, 21, 22], sweet [20, 23], urine [21], saliva [21, 22, 24], and breath [17, 18, 21, 25]. In food industry, to provide the safety and quality of the fermented foods and alcoholic beverages, these products are monitored for alcohol contents, especially, for ethanol, during

Published online: 25 November 2022

the total producing process [4–11]. An ethanol fuel production is the new branch of industry where an accurate and rapid ethanol determination is necessary to quantify adulteration of fuel with methanol [26]. Thus, it is obvious that industry and medicine require simple, fast, and cost-effective analytical methods of ethanol assay.

Up today, many analytical methods have been developed for the determination of ethanol and other aliphatic alcohols. The commonly used approaches include gas [6, 14, 17] and liquid chromatography [27], capillary electrophoresis with ultraviolet detection [28], Fourier transform mid-infrared spectroscopy [7], and spectrophotometry [8]. Last decades, a lot of chemical sensors for ethanol analysis, optical [9, 29–31], and electrochemical [4, 5, 10, 32], which are based on effective catalytically active nanomaterials, were proposed. All these techniques have some limitations, particularly insufficient selectivity and high cost. Enzymatic approaches are more promising tools for improving the sensitivity and selectivity of analytical methods [5, 13, 20, 33, 34].

A lot of optical and electrochemical enzymatic biosensors for ethanol assay were proposed [4, 13, 23, 33]. As biorecognition elements in ethanol-sensitive biosensors, alcohol oxidase (AOX) and alcohol dehydrogenase were usually applied [34–39].

AOX is the first enzyme involved in the methanol oxidation pathway of methylotrophic yeasts and it is also able to oxidize other short-chain alcohols, such as ethanol, propanol, and butanol with generation of H_2O_2 as a byproduct. The classical ways to follow an oxidase-catalyzed reaction are based on measuring either the decrease in O_2 partial pressure or the increase in concentration of H_2O_2 [39, 40]. To detect H_2O_2, AOX-based ABSs require using peroxidase (PO) — enzyme, which catalyzes decomposition of H_2O_2 with forming electroactive species. The lasts cause an electron transfer and generation of an electric current. Although PO has a high specificity and sensitivity for its substrate, the application of natural enzyme is limited by its high cost and not sufficient instability [35].

As artificial PO, different catalytically active materials, including nanoparticles (NPs) of metals and transition metal oxides, may be used [41–44]. NPs in ABSs act usually as carriers of bioelement, mediators in electron transfer, and/or catalysts (artificial enzymes or nanozymes). Nanozymes (NZs) having pseudo-enzymatic activities possess increased stability and greater availability due to their simpler preparation technologies [43]. Most reported NZs are mainly mimetics of PO. Nowadays, there is limited data concerning the development of optical biosensors for ethanol analysis using of AOX and PO-like NZs [44, 45] and only few papers concerning amperometric biosensors (ABSs) [36–38, 40].

The aim of the current research is to design AOX-based ABSs for ethanol assay using the novel tri-metallic NZs as PO mimetics. This study is focused on the synthesis and characterization of new metal hydride nanocomposites and their analytical application in biosensors. The NZs with the highest sensitivities were successfully used for amperometric detection of ethanol in real samples of commercial alcoholic drinks, human blood, and saliva.

Experimental

Chemicals and reagents

Copper(II) sulfate ($CuSO_4$, 99.5%), hydrogen tetrachloroaurate(III) trihydrate ($HAuCl_4 \cdot 3H_2O$, ≥ 99.9%), cerium(III) chloride ($CeCl_3$, 99.5%), nickel(II) sulfate ($NiSO_4$, 99.5%), chloroplatinic acid (H_2PtCl_6, ≥ 99.9%), ethanol (C_2H_5OH, 99,5%), *o*-dianisidine (≥ 98%), hydrogen peroxide (H_2O_2, 30%), sodium hydroxide (NaOH, 99%), palladium chloride ($PdCl_3$, 99.5%), ascorbic acid (99%), dopamine (99%), D-glucose ($C_6H_{12}O_6$, 99.5%), uric acid (≥ 99%), potassium chloride (KCl, 99.5%), sodium chloride (NaCl, 99.5%), glutathione (99.5%), glutaraldehyde (grade I, 25% in H_2O), cysteamine (95%), ammonia (puriss., anhydrous, ≥ 99.9%), other reagents, and solvents of analytical grade used in this work were and purchased from Sigma-Aldrich (Steinheim, Germany). Alcohol oxidase (AOX, EC 1.1.3.13) with specific activity 30 $U \cdot mg^{-1}$ of protein was isolated from the selected yeast strain *Ogataea polymorpha C-105 (gcr1 catX)* [20, 21] and kept as a suspension in 70% sulfate ammonium in 50 mM phosphate buffer, pH 7.5 (PB) at 4 °C.

Synthesis and characterization of nanoparticles

The nanoparticles of nPtCu, nPtAu, nFePtAu, nCo, nCePt, nNiPtPd, and nAgCu were synthesized by the chemical reduction method from appropriate salts using ascorbic acid [44, 46]. The nanoparticles of nCuCeAu, nCoCuCe, and nCu were synthesized by chemical bath deposition method on zinc plate substrate (further Zn plate) as described earlier [44]. For synthesis of the core-shell-shell nAuCePt, Zn plate was placed in a reaction bath containing 0.1 M solutions of $HAuCl_4$ and $CeCl_3$. After incubation at room temperature during 20 h and formation of metallic NPs on Zn plate, 0.1 M H_2PtCl_6 was added to the reaction bath, and incubation was prolonged for 20 h. The synthesized NPs were collected from the surface of the Zn plate, precipitated by centrifugation 16,000 rpm during 30 min (Micro 22R, Hettich Zentrifugen, Germany), washed twice with water and stored in suspension until usage at +4°C as described in our previous papers [44, 46].

PO-like activity of the obtained NPs was evaluated on their ability to decompose H_2O_2 in solution of *o*-dianisidine.

The generated colored product was detected by photometric monitoring at 525 nm [44]. The characterized PO mimetics were chosen as H_2O_2-sensitive platforms for fabrication of AOX-ABSs.

Morphological and structural properties of NPs were studied by the use of scanning electron microscope (SEM) FEI Nova NanoSEM 450 (Poland) and REMMA-102-02 (Ukraine).

The phase composition of synthesized particles was studied by XRD analysis using a STADI P X-ray powder diffractometer ("STOE & Cie GmbH," Germany) with Cu Kα radiation ($\lambda = 0.154$ nm) for phase identification. XRD patterns were obtained using 40 kV, 30 mA by Θ/2Θ (Bragg-Brentano geometry) in the 2Θ range of $6° \leq 2\Theta \leq 110°$ (step size 0.015°, detector step 0.480°2θ and speed 2°/min).

Fabrication and characterization of bioelectrodes

To construct bioelectrode, AOX was covalently immobilized on the activated PO-like NZs on the surface of graphite electrode (GE).

To activate NZs, aliquot of NZs (0.005 mL, 1 mg/mL) was layered on the surface of GE (diameter 3.05 mm) and air-dried at room temperature. Then, aqueous cysteamine solution (1 mM, 0.01 mL) was dropped on the film of NZs. After air-drying, glutaraldehyde solution (1%, 0.01 mL) was layered on the NPs-cysteamine film and was incubated up to film formation. The activated NZs/GE was washed several times with 50 mM PB, pH 7.5.

To develop the target bioelectrode, AOX was covalent immobilized on the surface of modified GE. For this aim, an aliquot of AOX solution (0.005 mL, 70 $U \cdot mL^{-1}$) was dropped onto the activated NZs/GE and air-dried at room temperature. The fabricated ABSs (AOX/NZs/GEs) were rinsed with 50 mM PB and pH 7.5 and stored at + 4 °C until use.

All electrochemical measurements, including cyclic voltammetry (CV) and chronoamperometry were carried out with a potentiostat Metrohm Autolab BV (Utrecht, The Netherlands) under constant stirring in a 20 mL cell at room temperature. The Ag/AgCl/3 M KCl electrode and platinum wire were used as the reference and counter electrodes, respectively. A total of 3.05 mm graphite rod (type RW001, Ringsdorff Werke, Bonn, Germany) was used as working electrode (GE). The GEs were polished with the 400 grit and 1500 grit size sandpapers and then rinsed in fresh DI water several times and left soaking in DI water until usage.

Determination of ethanol in real samples

The samples of alcoholic drinks used for ethanol analysis included the alcohol tincture "Zubrowka" (Polmos Białystok, Poland), "Latini Sparkling" white semi-sweet champagne (Peter Mertes, Germany), and "Aznauri" dry red wine (Odesainprom, Ukraine). All samples, diluted by 30 mM PB and pH 7.5 before the assay, were analyzed using a standard addition method. Statistical processing of the data was carried out using the OriginPro 2021 software.

The samples of saliva and serum were obtained from a group of 3 healthy volunteers (all women, 40 years old) who consumed 0.7 g of ethanol per kilogram of body weight (40% v/v vodka). The samples of saliva and venous blood were collected 30 min after their last drink. Serum was obtained by incubation of blood during 30 min at 8 °C followed by centrifugation 3000 rpm during 5 min (Micro 22R, Hettich Zentrifugen, Germany) for removing the clotted fibrin. The supernatant (serum) was frozen. The samples prepared for analysis were kept at −20 °C till the usage.

Reference method "Alcotest"

Ethanol determination in real samples was carried out using enzymatic kit "Alcotest" [47]. The general principle of ethanol assay by AOX method is based on the detection of the dye-product accumulation in peroxidative oxidation of chromogen by H_2O_2 generated from ethanol under AOX-PO enzymatic sequential reactions. As a chromogen in this reaction 3,3′,5,5′-tetramethyl benzidine (TMB) has been applied. The final concentration of the oxidized TMB is directly proportional to the concentration of ethanol at 450 nm.

Statistical analysis

The experiments were repeated three times (n=3) and the measurements were made in two parallels. For each sample, arithmetic mean, variance, relative standard deviation, and confidence interval were determined. The statistical parameters and all figures were calculated and built using Origin 8.5 Pro.

Results and discussion

Synthesis and morphological properties of PO-mimetics

A number of nanocomposites were synthesized using chemical bath deposition on a zinc plate and reduction methods (See Supplementary information, SI, Table S1). The obtained NPs were screened on their ability to decompose *o*-dianisidine in the presence of H_2O_2; the final photometric product was monitored at 530 nm [44]. It was demonstrated that several synthesized NZs, especially nFePtAu and nAuCePt, exhibited the highest PO-like activities in solution (Table SI.1). In order to obtain a quick estimation of the size of the synthesized NZs, SEM microscopy was taken (Fig. 1).

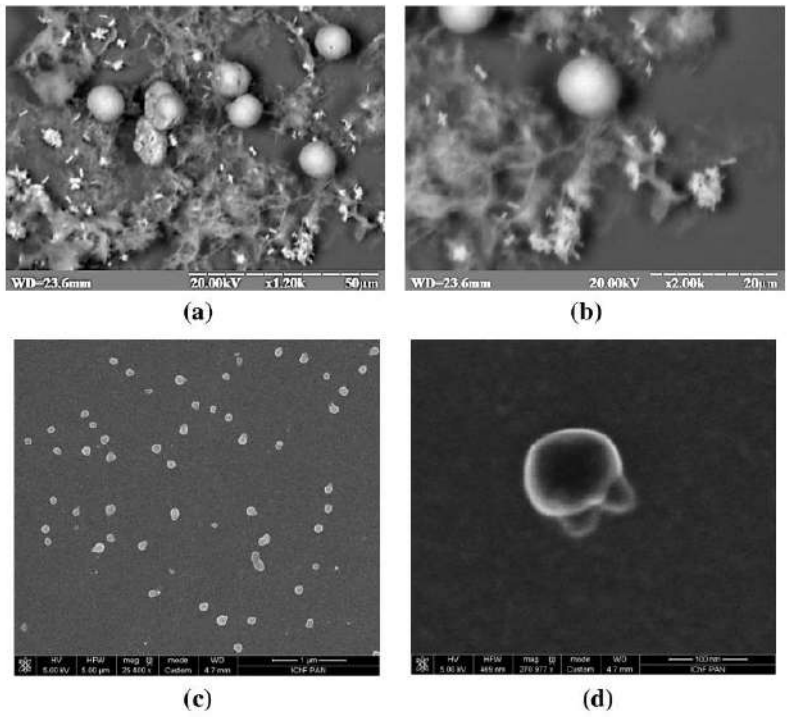

Fig. 1 SEM images of nFePtAu **(a, b)** and nAuCePt **(c, d)**. The accelerating voltage was 5000 kV for all images

As shown in Fig. 1, both nFePtAu and nAuCePt have structure close to spherical with the size of several microns for nFePtAu (Fig. 1a–b) and less than 100 nm for nAuCePt (Fig. 1c–d), respectively.

The most active in solution nAuCePt was characterized with X-ray diffraction analysis (Fig. S1). Diffraction peak positions and their relative intensities reflect to the tetragonal crystalline structure of nAuCePt with lattice constant $a = 9.530(5)$ and $c = 12.98(1)$ Å, respectively. Based on the set of reflexes from the phase with a high degree of crystallinity, it was not possible to identify the previously reported compound. Probably, it can be a new intermetallic compound in the Au–Ce–Pt system.

Construction and characterization of electrodes modified with NPs

nFePtAu and nAuCePt, the best PO-like NZs in solution, were tested using chronoamperometry for their electrocatalytic activities to decompose H_2O_2 on electrodes (Fig. S2). Using the corresponding chronoamperograms, calibration curves were plotted for H_2O_2 determination by the developed electrodes. The analytical characteristics of the electrodes modified with NZs were calculated. The sensitivity of each NZ-modified electrode (with diameter 3.05 mm) was estimated for an electrode area of 7.30 mm^2. The obtained results demonstrated that nAuCePt/GE exhibited the highest current response on the tested analyte at substrate saturation and had the highest sensitivity (sevenfold higher than for the nFePtAu/GE); therefore, nAuCePt/GE was studied in more detail. Other PO-like NZs were characterized on electrodes in our previous works [44, 46].

Analytical performance of ethanol-sensitive bioelectrodes

The aim of our current work was to construct AOX-based ABSs for ethanol determination using PO-like NZs. To prepare the working bioelectrode, AOX was covalently conjugated with a NZs/GE. For this aim, crosslinking method with cysteamine and glutaraldehyde was applied as described in the experimental part (see subsection "Fabrication and characterization of bioelectrodes"). As a result, a self-assembled monolayer of AOX/NZs on the surface of electrode was formed. The principle scheme of ethanol assay is the oxidation of ethanol to acetaldehyde catalyzed by the yeast alcohol oxidase (AOX): ethanol + O_2 → acetaldehyde + H_2O_2 [40]. Monitored indicator is hydrogen peroxide which is reduced to water on the electrode at − 0.2 V due to catalysis by PO-like NZs: $H_2O_2 + 2\ H^+ \rightarrow 2\ H_20 - 2\ e^-$ [48].

Figure S3 demonstrates the CVs of the GEs which were modified with AOX conjugated with nAuCePt or nFePtAu, respectively. The potential at − 200 mV was used as working for both types of biocatalytic electrodes. The obtained ABSs were studied in detail. The analytical curves and calibration graphs for the ABSs with the best analytical parameters are presented in Fig. 2. The calibration was performed by gradually adding the standard ethanol solution. In our studies, the main operational parameters of bioelectrodes conjugated with AOX and NZs (marked as AOX/NZs/GE) was studied and compared with the bioelectrodes modified with AOX and PO (marked as AOX/PO/GE) (Table 1).

The analytical parameters of the developed ABSs in comparison with the known AOX-NZs-based ABSs that were reported previously are summarized in Table 1. The linear ranges, limits of detection (LOD), and sensitivities (for an electrode area of 7.30 mm^2) were calculated. The slope of the calibration curve (B) was connected to the biosensor sensitivity which is related to the limit of detection (LOD). The LOD was calculated by using the standard deviation (SD) of the lowest calculation and the *B* value. The equation used was LOD = (3∗ SD/B). As shown in Table 1, the most effective ABSs, namely AOX/nAuCePt/GE and AOX/nFePtAu/GE had 120-fold and 56-fold higher sensitivities in comparison with AOX/PO/GE, respectively.

The most sensitive of the reported up today amperometric biosensor on ethanol with very high sensitivity (4089 $A{\cdot}M^{-1}m^{-2}$) was fabricated using carbon fibers (CF) modified by hemin and AuNPs [37]. However, the main disadvantage of AOX-CF-hemin-Au is its insufficient stability in

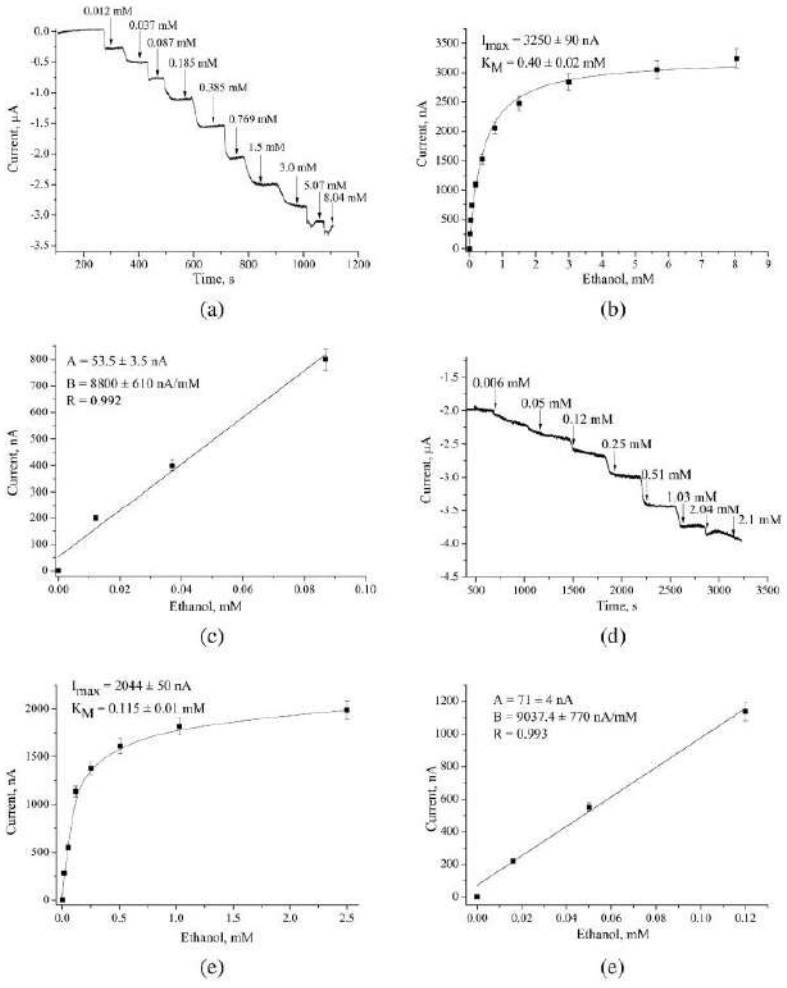

Fig. 2 Amperometric characteristics of the AOX/nFePtAu/GE (**a**, **c**) and AOX/nAuCePt/GE (**d**, **f**) for ethanol determination. Dependences of current signals as outputs on the increased ethanol concentrations in wide (**b**, **e**) and in linear ranges (**c**, **f**) and corresponding chronoamperograms (**a**, **d**). Conditions: working potential − 200 mV vs Ag/AgCl/3 M KCl in 50 mM PB, pH 7.5

Table 1 Operational parameters of the constructed ABSs based on AOX and PO-like NZs

Bioelectrode	Potential, mV	Sensitivity, $A \cdot M^{-1} \cdot m^{-2}$	Linear range, mM	K_M^{app}, mM	LOD, mM	Reference
AOX/nAuCePt/GE	− 200	2600	0.005–0.10	0.097	0.001	This work
AOX/nFePtAu/GE	− 200	1250	0.002–0.10	0.40	0.002	
AOX/nCoCuCe/GE	− 200	584	0.016–0.12	0.7	0.005	
AOX/nCuCeAu/GE	− 200	530	0.016–0.25	0.18	0.004	
AOX/nCo/GE	− 200	535	0.015–0.25	1.5	0.005	
AOX/nCePt/GE	− 200	23	0.066–8.00	13.2	0.020	
AOX/nAgCu/GE	− 50	57	0.050–0.75	0.96	0.030	
AOX/nPtCu/GE	− 200	42	0.030–2.00	2.1	0.015	
AOX/nNiPtPd/GE	− 150	40	0.050–0.80	1.36	0.040	
AOX/nCu/GE	− 200	22	0.125–31. 00	615	0.038	
AOX/PO/GE	− 50	22	0.130–0.90	0.70	0.039	[38]
AOX/nCuCe/GE	− 50	32	0.050–2.10	0.70	0.015	
AOX/nCuCe/npAu/GE	− 50	102	0.033 – 0.50	1.22	0.010	
AOX/nPtRu/GE	− 100	284	0.020 – 0.60	2.0	0.002	[36]
AOX-PO/Os polymer	− 50	29	0.50 – 2.00	1.94	0.015	[35]
AOX-CF-hemin-Au	− 100	4089	0.010 – 0.15	0.14	0.005	[37]

storage, and the response time to the analyte was relatively long. It was found that under the potential of −200 mV, the AOX/nAuCePt/GE has the highest value of sensitivity (2600 $A \bullet M^{-1} \bullet m^{-2}$) and the lowest known limit of detection (0.001 mM).

Assay of ethanol in real samples

Ethanol is a component of many commercial goods (beverages, perfumes, aftershaves and colognes, medicinal liquids, mouthwashes, liniments, and paints) [4–8, 11]. A number of chemicals, including ascorbic acid (AA), uric acid (UA), dopamine (DA), and glutathione (Glut) are commonly coexisting with ethanol (marked on the Fig. S4a, as Et) in human biological liquids, and they can interfere the detection of ethanol. So, the selectivity study of AOX/nAuCePt-modified electrode was performed using chronoamperometry. Solutions of several interferences species contained of AA, DA, UA, Glut, KCl, and NaCl at the concentration 1 mM with the presence and the absence of 1 mM ethanol were evaluated for studying the possible interference effect. The effect of such additives on the current response of the fabricated ethanol biosensor is demonstrated on Fig. S4a. It was shown that the tested species, especially AA, UA, and Glut, can be reduced at the operating potental −200 mV. But, the current responses from the interferences reduction are less than 5% especially when they coexist in ethanol solution (1 mM), slight changes from the current responses of ethanol alone for AA (2%), UA (4.5%), and Glut (0.01%) are observed. Thus, the additional current responses from the tested interference species can be considered being negligible.

To study the selectivity of the developed analytical approach, different 1 mM mono-, di-, and polyatomic alcohols (methanol, ethanol, 1-propanol, 1-butanol, ethylene glycol and glycerol) were tested (Fig. S4b). It was shown that AOX/nAuCePt-modified electrode exhibits the highest response to methanol (108%) and ethanol (100%). The obtained result suggests that the AOX/nAuCePt/GE provides a satisfactory selectivity for ethanol determination in real samples.

In order to evaluate the practical application of the developed biosensor in analysis of real samples, the AOX/nAuCePt/GE was used to detect ethanol in human biological liquids as well as in beverages. The reproducibility of the ethanol biosensor was investigated by successively detecting 1.3 mM ethanol on five different days; the relative standard deviation (RSD) calculated was 3.9%, demonstrating a good reproducibility of the measurements performed. This procedure also meets the reproducibility requirements proposed by the association of analytical communities (< 4%) [49].

The storage stability of AOX/nAuCePt/GE was also investigated by chronoamperometry (Fig.S5). The stability test was performed at 24 °C with 1 mM ethanol in 30 mM PB, pH 7.5 with intermittent storage in this buffer at 4 °C between measurements. The biosensor was stable during 2 weeks of storage. It retained 54% of its initial current response, when the enzyme electrode was stored at + 4 °C for ethanol assay after intermittent exploitation over 14-day interval.

Operational stability (repeatability) of biosensor was investigated by successively detecting 1.3 mM ethanol for 5 times during 1 day, and the RSD was about 3.5%, indicating a good repeatability. The results indicated that the AOX/

nAuCePt/GE showed good repeatability and stability. So, it can be presumed that the presence of nAuCePt is very efficient in retaining the enzymatic activity of AOX.

In order to demonstrate the practical feasibility of the constructed ABSs, the content of ethanol was determined in real samples using the standard addition method (Figs. S6 and S7). The constructed bioelectrode with the highest sensitivity (AOX/nAuCePt/GE) was tested for analysis of the ethanol using the champagne "Latini Sparkling," alcohol tincture "Zubrovka," and wine "Aznauri" as the real samples (Figs. S6 and S7). The obtained data were compared with results which were obtained using the reference enzymatic kit "Alcotest" (Table 2) [47].

The biosensor analysis demonstrated the following results for ethanol content in the tested samples: 8.55 ± 0.45% for wine, 8.63 ± 0.35% for champagne, and 37.8 ± 0.65% for alcohol tincture, as well enzymatic kit "Alcotest" showed 9.1 ± 0.40% for wine, 9.03 ± 0.3% for champagne, and 37 ± 0.50% for vodka, respectively. The concentrations of the tested ethanol in the real samples of alcoholic drinks, estimated using two methods, have a strong (R=0.999) correlation (Fig. S8). According to Student's test, the analytical data of biosensor and reference "Alcotest" method is in good agreement ($p > 0.05$). The average values of the ethanol contents determined by the developed ABS and the reference method are presented in Table 2.

Promising non-invasive methods for quantitative detection of ethanol concentration are important in medicine and research https://www.insightslice.com/biosensors-market [1–3]. To date, an alternative method for assay ethanol levels in human is the analysis of saliva [21, 22, 24]. Recently, it was shown that the ethanol concentrations in saliva and serum are correlated as 1:0.8 while ethanol contents in exhaled breath and serum are correlated as 0.00005:1 [21, 22]. Thus, the analysis of ethanol in saliva can be considered purely to be a basic screening method.

In our work, we used the constructed AOX/nAuCePt/GE for determination of ethanol contents in human biological liquids, namely saliva (Table 3) and blood serum (Table 4) after consumption of alcohol drink (see "Experimental", subdivision "Determination of ethanol in real samples").

Table 3 Determination of ethanol content (mM) in human saliva

Sample	Before consumption		30 min after consumption	
	AOX/nAuCePt/GE	Alcotest	AOX/nAuCePt/GE	Alcotest
1	1.4 ± 0.06 $p > 0.05$	1.35 ± 0.02	17.7 ± 0.7 $p > 0.05$	18.5 ± 0.65
2	1.0 ± 0.03 $p > 0.05$	1.1 ± 0.14	16.0 ± 0.5 $p > 0.05$	15.2 ± 0.7
3	1.8 ± 0.05 $p > 0.05$	1.90 ± 0.10	15.5 ± 0.9 $p > 0.05$	14.5 ± 0.9

Table 4 Determination of ethanol content (mM) in human serum

Sample	Before consumption		30 min after consumption	
	AOX/nAuCePt/GE	Alcotest	AOX/nAuCePt/GE	Alcotest
1	1.7 ± 0.05 $p > 0.05$	1.6 ± 0.2	13.2 ± 0.6 $p > 0.05$	14.4 ± 0.3
2	1.5 ± 0.09 $p > 0.05$	1.45 ± 0.1	12.2 ± 0.7 $p > 0.05$	12.6 ± 0.50
3	1.5 ± 0.06 $p > 0.05$	1.6 ± 0.15	18.4 ± 1.2 $p > 0.05$	19.0 ± 0.65

Student's test (p) was performed for values obtained by biosensor method compared to "Alcotest" one [47]

Student's test (p) was performed for values obtained by biosensor method compared to "Alcotest" one [47]

It was shown (Tables 3 and 4) that the ethanol levels estimated after drink consumption enhanced in 8–15 times for saliva (Table 3) and in 7–12 times for serum (Table 4). The obtained results are in good correlation with the reference method "Alcotest" and with literature data [21, 22]. Thus, it was demonstrated the high accuracy of biosensor analysis and suitability of the developed ABS for ethanol assay in the real samples of biological liquids.

The developed biosensor based on nAuCePt was assessed using statistical analysis. The Student's t-test did not reveal significant difference between the experimental values obtained in the sample analysis by the two methods. The

Table 2 Determination of ethanol content (%) in beverages

Sample	Value declared by the producer	Method	
		Alcotest	AOX/nAuCePt/GE
Alcohol tincture "Zubrowka"	37.5	37.0 ± 0.50	37.8 ± 0.65 $p > 0.05$
Champagne "Latini Sparkling"	8.5	9.0 ± 0.30	8.65 ± 0.35 $p > 0.05$
Wine "Aznauri"	9 –13	9.1 ± 0.40	8.55 ± 0.45 $p > 0.05$

Student's test (p) was performed for values obtained by biosensor method compared to "Alcotest" one [47]

calculated t-values for all analyzed samples were in the range from 0.065 to 0.276 to be less than the critical t-values (t_{crit}=4.3) at 5% significance level. According to Student's test, the analytical data of biosensor and reference "Alcotest" method is in good agreement ($p > 0.05$).

It can be concluded that the developed AOX- and NZ-based ABS may be useful in food, in medicine, and in other areas, where a precision analysis of ethanol is necessary. It should be noted that the application of metallic NPs instead of native PO can improve the stability of enzyme biosensor, but the AOX-based electrode has some disadvantages. Biosensor is limited in stability because of enzyme inactivation during long-time storage without special additives. AOX is a large octameric enzyme with molecular mass 640 kDa [40]. Under optimal conditions of its keeping (as suspension in 70% ammonium sulfate, 50 mM phosphate buffer, pH 7–8, in temperature interval from −10 °C till +4 °C), enzyme is rather stable during 1 year with lost only about 10% of its initial activity. Thus, if the proposed AOX-based ABSs will be planned to commercialized, the problem of bioelectrode stabilization will arise.

Conclusion

The problems of ethanol sensing have wide prospects and advanced trends. Recently, fabricated devices that may be very demanded for application in medicine and food industry are based on smart materials coupled with modern techniques https://www.marketsandmarkets.com/Market-Reports/biosensors-market-798.html, https://www.insightslice.com/biosensors-market [1]. The challenges in personal healthcare related to non-invasive ethanol monitoring in biological fluids, including sweat, saliva, breath, tears, urine, and interstitial fluids with wearable (bio)sensors [2, 3].

In the current paper, a number of novel ethanol-sensitive amperometric bioelectrodes based on AOX and the most effective metal hybrid NZs as peroxidase mimetics were developed and characterized. Oxidase AOX produces H_2O_2 as a by-product of enzymatic ethanol oxidation, so the detection of ethanol as an analyte was realized by monitoring the level of generated H_2O_2 using PO-based sensor. Substitution of natural PO with PO-like NZs in a sensing layer was shown to improve the electrochemical properties of the bioelectrodes and to allow the detection of ethanol in wider ranges of linear responses. The nAuCePt and nFePtAu, having the highest pseudo-peroxidase activities in solution, were used for the construction of AOX-based ABSs. The fabricated biosensors exhibited high sensitivities, fast responses, and low detection limits. The most effective bionanosensor AOX/nAuCePt/GE was used for ethanol analysis in beverages and human biological fluids. High correlation between ethanol contents in real samples which were determined by the proposed biosensor and reference colorimetric method was observed. We have demonstrated that the constructed NZs-based ABSs, being appropriate for the analysis of beverages and human biological liquids, can be promising for application in laboratories of food control and clinical diagnostics.

Supplementary Information The online version contains supplementary material available at https://doi.org/10.1007/s00604-022-05568-z.

Acknowledgements The authors would like to thank the Polish Academy of Sciences for financial support of exchange visits in 2022.

Funding This research was partially supported by the National Research Foundation of Ukraine (project Nos.: 2020.02/0100 "Development of new nanozymes as catalytic elements for enzymatic kits and chemo/biosensors"), National Academy of Sciences of Ukraine: the programs: "Smart sensor devices of a new generation based on modern materials and technologies" and "Double-acting anticancer drugs to overcome the acquired resistance of malignant cells to chemotherapy" (0122U200211), Grant "New dual casein kinase 2 inhibitors and histone deacetylase for targeted tumor chemotherapy" for research laboratories/groups of young scientists in priority areas of science and technology in 2021–2022.

Declarations

Competing interests The authors declare that they have no known competing financial interests or personal relationships that could have appeared to influence the work reported in this paper.

References

1. Bollella P (2022) Enzyme-based amperometric biosensors: 60 years later … Quo Vadis? Anal Chim Acta 340517. https://doi.org/10.1016/j.aca.2022.340517
2. Verma D, Singh KRB, Yadav AK et al (2022) Internet of things (IoT) in nano-integrated wearable biosensor devices for healthcare applications. Biosens Bioelectron: X 11:100153. :https://doi.org/10.1016/j.biosx.2022.100153
3. Matzeua G, Florea L, Diamonda D (2015) Advances in wearable chemical sensor design for monitoring biological fluids. Sens Actuat B: Chem 211:403–418. https://doi.org/10.1016/j.snb.2015.01.077
4. Somboon T, Phatchana R, Tongpoothorn W, Sansuk S (2022) A simple and green method for determination of ethanol in liquors by the conductivity measurement of the uncatalyzed esterification reaction. LWT 154:112593. https://doi.org/10.1016/j.lwt.2021.112593
5. Pinheiro ACN, Ferreira VS, Lucca BG (2022) Stamping method based on 3D printing and disposable napkin: cheap production of paper analytical devices for alcohol determination in beverages aiming forensics and food control. Microchem J 180:107604. https://doi.org/10.1016/j.microc.2022.107604
6. Mansur AR, Oh J, Lee HS et al (2022) Determination of ethanol in foods and beverages by magnetic stirring-assisted aqueous extraction coupled with GC-FID: a validated method for halal verification. Food Chem 366:130526. https://doi.org/10.1016/j.foodchem.2021.130526
7. Debebe A, Redi-Abshiro M, Chandravanshi BS (2017) Non-destructive determination of ethanol levels in fermented alcoholic beverages using Fourier transform mid-infrared spectroscopy. Chem Cent J 11:27. https://doi.org/10.1186/s13065-017-0257-5

8. Sriariyanun M, Mutrakulcharoen P, Tepaamorndech S et al (2019) Rapid spectrophotometric method for quantitative determination of ethanol in fermentation products. Orient J Chem 35(2):744–750. https://doi.org/10.13005/ojc/350234
9. Duangdeewong C, Choengchan N, Wattanasin P, Teerasong S (2022) Direct determination of ethanol in alcoholic beverages based on its anti-aggregation of melamine-silver nanoparticle assembly. Talanta 250:123751. https://doi.org/10.1016/j.talanta.2022.123751
10. Bevanda AM, Ivankovic A, Talic S et al (2021) Determination of ethanol in wine and distilled alcoholic beverages using a smartphone as a detector. Int J Comput Theoretical Chem 9(2):43–47. https://doi.org/10.11648/j.ijctc.20210902.13
11. Boroujerdi R, Abdelkader A, Paul R (2022) Highly selective detection of ethanol in biological fluids and alcoholic drinks using indium ethylenediamine functionalized graphene. Sens Diagn 1:566–578. https://doi.org/10.1039/D2SD00011C
12. Wozniak MK, Wiergowski M, Namiesnik J, Biziuk M (2019) Biomarkers of alcohol consumption in body fluids - possibilities and limitations of application in toxicological analysis. Curr Med Chem 26(1):177–196. https://doi.org/10.2174/0929867324666171005111911
13. Thepchuay Y, Sonsa-ard T, Ratanawimarnwong N et al (2020) Paper-based colorimetric biosensor of blood alcohol with in-situ headspace separation of ethanol from whole blood. Anal Chim Acta 1103:115–121. https://doi.org/10.1016/j.aca.2019.12.043
14. Taylor L, Remeškevičius V, Saskoy L et al (2021) Determination of ethanol in micro-volumes of blood by headspace gas chromatography: statistical comparison between capillary and venous sampling sites. Med Sci Law 61(2):86–96. https://doi.org/10.1177/0025802420928632
15. Hernandez J, Kaun KR (2022) Alcohol, neuronal plasticity, and mitochondrial trafficking. Proc Natl Acad Sci USA 119(29):e2208744119. https://doi.org/10.1073/pnas.2208744119
16. Knabbe J, Protzmann J, Schneider N et al (2022) Single-dose ethanol intoxication causes acute and lasting neuronal changes in the brain. Proc Natl Acad Sci USA 119(25):e2122477119. https://doi.org/10.1073/pnas.2122477119
17. Alaouie AM, Alawieh MB (2020) Critical evaluation of single point measurement-based quantitative analyses in forensic breath alcohol. Forensic Sci Int 2:100101. https://doi.org/10.1016/j.fsir.2020.100101
18. Jones AW, Cowan JM (2020) Reflections on variability in the blood–breath ratio of ethanol and its importance when evidential breath-alcohol instruments are used in law enforcement. Forensic Sci Res 5(4):300–308. https://doi.org/10.1080/20961790.2020.1780720
19. Laposat M (1999) Assessment of ethanol intake current tests and new assays on the Horizon. Am J Clin Pathol 112:443–450. https://doi.org/10.1093/ajcp/112.4.443
20. Keim ME, Bartfield JM, Raccio-Robak N et al (1999) Accuracy of an enzymatic assay device for serum ethanol measurement. J Toxicol Clin Toxicol 37(1):75–81. https://doi.org/10.1081/clt-100102411
21. Bendtsen P, Hultberg L, Carlsson M, Jones AW (1999) Monitoring ethanol exposure in a clinical setting by analysis of blood, breath, saliva, and urine. Alcohol Clin Exp Res 23:1446–1451. https://doi.org/10.1111/j.1530-0277.1999.tb04665.x
22. Jones AW (1979) Distribution of ethanol between saliva and blood in man. Clin Exp Pharmacol Physiol 6:53–59. https://doi.org/10.1111/j.1440-1681.1979.tb00007.x
23. Costa NG, Antunes JC, Paleo AJ, Rocha AM (2022) A review on flexible electrochemical biosensors to monitor alcohol in sweat. Biosensors 12(4):252. https://doi.org/10.3390/bios12040252
24. Rao TM, Reddy PDS, Ramani P (2015) Detection of alcohol in saliva for blood alcohol concentration using alcohol saliva strip test: a forensic aid. J Dr NTR Univ Health Sci 4(1):24–29. https://doi.org/10.4103/2277-8632.153310
25. Mojumder S, Das T, Das S et al (2022) Y and Al co-doped ZnO-nano powder based ultrasensitive trace ethanol sensor: a potential breath analyzer for fatty liver disease and drunken driving detection. Sens Actuat B: Chem 372:132611. https://doi.org/10.1016/j.snb.2022.132611
26. Kock FVC, Rocha TC, Araújo GM et al (2019) Time-domain NMR: a novel analytical method to quantify adulteration of ethanol fuel with methanol. Fuel 258:116158. https://doi.org/10.1016/j.fuel.2019.116158
27. Avila LM, Franco dos Santos AP, Mançano de Mattos DI et al (2018) Determination of ethanol in gasoline by high-performance liquid chromatography. Fuel 212:236–239. https://doi.org/10.1016/j.fuel.2017.10.039
28. Oliver JD, Gaboriceau M, Castignolles P (2014) Ethanol determination using pressure mobilization and free solution capillary electrophoresis by photo-oxidation assisted ultraviolet detection. J Chromatogr A 1348:150–157. https://doi.org/10.1016/j.chroma.2014.04.076
29. Hu X, Cao H, Dong W, Tang J (2021) Ratiometric fluorescent sensing of ethanol based on copper nanoclusters with tunable dual emission. Talanta 233:122480. https://doi.org/10.1016/j.talanta.2021.122480
30. Ratanawimarnwong N, Sinpun M, Chankaw P et al (2020) Simple flow system with in-line gas-diffusion unit for determination of ethanol employing hypsochromic shift of visible absorbance band of methyl orange. Talanta 206:120234. https://doi.org/10.1016/j.talanta.2019.120234
31. Vázquez-Guardado A, Ramirez-Flores JA, Lopez-Galmiche G et al (2019) Detection of ethanol concentration using a generic optical sensor platform. Comput Sist 23(1):27–31. https://doi.org/10.13053/CyS-23-1-3138
32. Li B, Chen Y, Peng A et al (2019) Improved photoelectrochemical properties of tungsten oxide by modification with plasmonic gold nanoparticles for the non-enzymatic sensing of ethanol. J Colloid Interface Sci 537:528–535. https://doi.org/10.1016/j.jcis.2018.11.061
33. Gayda G, Stasyuk N, Klepach H et al (2019). Promising bioanalytical approaches to wine analysis. Ch. 12, In: The Science of Beverages, Grumezescu AM, Holban AM (eds): pp. 419–458. Woodhead Publishing Inc. https://doi.org/10.1016/B978-0-12-816681-9.00012-6
34. Azevedo AM, Miguel D, Prazeres F et al (2005) Ethanol biosensors based on alcohol oxidase. Biosen Bioelectron 21(2):235–247. https://doi.org/10.1016/j.bios.2004.09.030
35. Smutok O, Ngounou B, Pavlishko H et al (2006) A reagentless bienzyme amperometric biosensor based on alcohol oxidase/peroxidase and an Os-complex modified electrodeposition paint. Sens Actuat B Chem 113:590–598. https://doi.org/10.1016/j.snb.2005.07.055
36. Stasyuk N, Gayda G, Zakalskiy A et al (2019) Amperometric biosensors based on oxidases and PtRu nanoparticles as artificial peroxidase. Food Chem 285:213–220. https://doi.org/10.1016/j.foodchem.2019.01.117
37. Smutok O, Kavetskyy T, Prokopiv T (2021) New micro/nanocomposite with peroxidase-like activity in construction of oxidases-based amperometric biosensors for ethanol and glucose analysis. Anal Chim Acta 1143:201–209. https://doi.org/10.1016/j.aca.2020.11.052
38. Stasyuk N, Demkiv O, Gayda G et al (2022) Highly porous 3D gold enhances sensitivity of amperometric biosensors based on oxidases and CuCe nanoparticles. Biosensors 12:472. https://doi.org/10.3390/bios12070472
39. Gayda G, Demkiv O, Klepach H et al (2019) Effective technologies for isolating yeast oxido-reductases of analytical importance. Ch. 5, In: Non-conventional Yeasts: from Basic Research to Application, Sibirny A. (ed.): pp. 119–151. Springer Nature

Switzerland AG, Cham, Switzerland. https://doi.org/10.1007/978-3-030-21110-3

40. Klepach HM, Zakalskiy AE, Zakalska OM et al (2021) Alcohol oxidase from the methylotrophic yeast *Ogataea polymorpha*: isolation, purification, and bioanalytical application In: Barile M (ed) Flavins and Flavoproteins, E-Publishing Inc, pp. 231–248. https://doi.org/10.1007/978-1-0716-1286-6_15
41. Camacho C, Matías JC, Chico B et al (2007) Amperometric biosensor for hydrogen peroxide, using supramolecularly immobilized horseradish peroxidase on the β-cyclodextrin-coated gold electrode. Electroanal 19(24):2538–2542. https://doi.org/10.1002/elan.200703993
42. Asif M, Liu H, Aziz A et al (2017) Core-shell iron oxide-layered double hydroxide: High electrochemical sensing performance of H2O2 biomarker in live cancer cells with plasma therapeutics. Biosens Bioelectron 97:352–359. https://doi.org/10.1016/j.bios.2017.05.057
43. Stasyuk N, Smutok O, Demkiv O et al (2020) Synthesis, catalytic properties and application in biosensorics of nanozymes and electronanocatalysts: a review. Sensors 20(16):4509. https://doi.org/10.3390/s20164509
44. Stasyuk N, Demkiv O, Gayda G (2022) Reusable alcohol oxidase-nPtCu/alginate beads for highly sensitive ethanol assay in beverages. RSC Adv 12(33):21309–21317. https://doi.org/10.1039/D2RA02106D
45. Sivashankar S, Kumar NS, Mazumder KRN (2020) Amperometric biosensors as an analytical tool in food, dairy and fermentation industries. Int J Pharm Sci Res 65(1):68–82. https://doi.org/10.47583/ijpsrr.2020.v65i01.010
46. Stasyuk N, Gayda G, Demkiv O, Darmohray L, Gonchar M, Nisnevitch M (2021) Amperometric biosensors for L-arginine determination based on L-arginine oxidase and peroxidase-like nanozymes. Appl Sci 11(15):7024. https://doi.org/10.3390/app11157024.5]
47. Gonchar MV, Maidan MM, Pavlishko HM, Sibirny AA (2001) A new oxidase-peroxidase kit for ethanol assays in alcoholic beverages. FTB 39:37–42. http://www.ftb.com.hr/archives/103-volume-39-issue-no-1/743-a-new-oxidase-peroxidase-kit-for-ethanol-assays-in-alcoholic-beverages
48. Alpeeva IS, Vilkanauskyte A, Ngounou B et al (2005) Bi-enzyme alcohol biosensors based on genetically engineered alcohol oxidase and different peroxidases. Microchim Acta 152:21. https://doi.org/10.1007/s00604-005-0407-7
49. AOAC (2004) Definitions and calculations of horrat values from intralaboratory data. Available online: http://www.readbag.com/aoac-dietsupp6-dietary-supplement-web-site-horrat-slv. Accessed 1 Oct 2017

Publisher's Note Springer Nature remains neutral with regard to jurisdictional claims in published maps and institutional affiliations.

Springer Nature or its licensor (e.g. a society or other partner) holds exclusive rights to this article under a publishing agreement with the author(s) or other rightsholder(s); author self-archiving of the accepted manuscript version of this article is solely governed by the terms of such publishing agreement and applicable law.

Оригінал доступний за посиланням: https://link.springer.com/article/10.1007/s00604-022-05568-z

Електронний додаток до статті доступний за посиланням: https://link.springer.com/article/10.1007/s00604-022-05568-z#Sec15

Анотація: *Каталітично активні наноматеріали мають низку переваг перед природними ензимами при використанні їх в ролі штучних ензимів (нанозимів), а саме, вищу стабільність і нижчу вартість. Металеві нанозими є перспективними каталізаторами для застосування у біосенсориці. В поточній роботі ми повідомляємо про конструювання біоелектродів на основі мікробних оксидаз та наноензимів у ролі міметиків пероксидази для аналізу харчових продуктів. Бі-металічні наночастинки PtRu (PtRu) у поєднанні з мікробними алкогольоксидазою (АО) і метиламіноксидазою (МАО) обрано для побудови амперометричних біосенсорів (АБС) для аналізу первинних спиртів і метиламіну (МА). Показано, що усі сконструйовані АБС виявляють високу чутливість (336 А·М$^{-1}$·м$^{-2}$ для АО-АБС та 284 А·М$^{-1}$·м$^{-2}$ для АМО-АБС), широкі лінійні діапазони (25–200 мкМ до етанолу та 20 – 600 мкМ до МА) і задовільну стабільність при зберіганні. Практичне значення сконструйованих АБС підтверджено при аналізі зразків харчових продуктів. Спостерігається висока кореляція між вмістом МА та етанолу в харчових продуктах, визначених АБС та референтними методами.*

Food Chemistry 285 (2019) 213–220

Contents lists available at ScienceDirect

Food Chemistry

journal homepage: www.elsevier.com/locate/foodchem

Amperometric biosensors based on oxidases and PtRu nanoparticles as artificial peroxidase

Nataliya Stasyuk[a], Galina Gayda[a,*], Andriy Zakalskiy[a], Oksana Zakalska[a], Roman Serkiz[a,b], Mykhailo Gonchar[a]

[a] Institute of Cell Biology, National Academy of Sciences of Ukraine, Drahomanov Street 14/16, 79005 Lviv, Ukraine
[b] Ivan Franko National University of Lviv, Department of Solid State Physics, Drahomanov Street 50, 79005 Lviv, Ukraine

ARTICLE INFO

Chemical compounds studied in this article
Methylamine (PubChem CID:6329)
Ethanol (PubChem CID:702)
Ruthenium trichloride hydrate (PubChem CID: 6093376)
Chloroplatinic acid (PubChem CID: 44134627)
Hydrogen peroxide (PubChem CID: 784)
Formaldehyde (PubChem CID: 62705)
Methanol (PubChem CID: 887)
Glucose (PubChem CID: 107526)
Dimethylamine (PubChem CID: 674)
Trimethylamine (PubChem CID: 1146)

Keywords:
Amperometric biosensor
Methylamine oxidase
Alcohol oxidase
Artificial peroxidase
PtRu nanoparticles
Ethanol and methylamine analysis

ABSTRACT

Catalytically active nanomaterials have several advantages over their natural analogues when used as artificial enzymes (nanozymes), namely, higher stability and lower cost. Nanozymes with metallic nanocomposites are promising catalysts for biosensing applications. The aim of the current research is to construct oxidase-based bioelectrodes for food analysis using nanozymes as peroxidase mimetics. Bimetallic PtRu nanoparticles (nPtRu) coupled with alcohol oxidase (AO) and methylamine oxidase (AMO) were chosen to construct amperometric biosensors (ABSs) for primary alcohols and methylamine (MA). Both ABSs show high sensitivities (336 $A \cdot M^{-1} \cdot m^{-2}$ for the AO-ABS and 284 $A \cdot M^{-1} \cdot m^{-2}$ for the AMO-ABS), broad linear ranges (25–200 μM ethanol and 20–600 μM MA) and satisfactory storage stabilities. Practical feasibility of the constructed ABSs was demonstrated on food samples. High correlation between contents of MA and ethanol in foods determined by the ABSs and reference methods was observed.

1. Introduction

The first report on electrochemical enzyme biosensor was published 55 years ago. More than 100,000 articles described this problem during these years, but very few biosensors have reached practical application and commercialization (Reyes-De-Corcuera, Olstad, & García-Torres, 2018). Combining nanobiotechnology with enzyme or cell-based electrochemical biosensors has become a crucial strategy for the fabrication of simple and reliable analytical systems. Unique optical, electrical, and electrochemical properties of nanomaterials provide promising alternatives to conventional biosensor development with improved stability, sensitivity and selectivity.

Artificial enzymes as highly stable and low-cost alternatives to natural enzymes have been discovered over the past decade (Karyakin, Karyakina, & Gorton, 2000). Nanomaterials with enzyme-like characteristics (nanozymes) are the next-generation artificial enzymes. Nanozymes, consisting of bi- and trimetallic nanoparticles (NPs) of noble and transition metals are particularly promising due to large surface area and high catalytic activity. The majority of traditionally constructed amperometric biosensors with oxidases are based on detection of hydrogen peroxide (H_2O_2), generated as a result of oxidase reaction with its own substrate. To achieve the detection of H_2O_2 under low reducing potential, peroxidase (PO) is usually considered when designing the biosensor. Although PO has high specificity and sensitivity, the application of natural enzyme is limited by its high cost. Novel artificial PO-mimetics hold great promise for successful assay of various real samples including food and biological liquids. PO-like nanozymes of different nature (organic, inorganic or combined) and composition (mono-, bi- or trimetallic NPs stabilized by block copolymers, organic ligands, surfactants and dendrimers) were shown to decompose effectively H_2O_2. PO-like metallic NPs demonstrate an outstanding electrochemical catalytic activities and usually are coupled

* Corresponding author.
E-mail address: galina.gayda@gmail.com (G. Gayda).

https://doi.org/10.1016/j.foodchem.2019.01.117
Received 1 August 2018; Received in revised form 3 January 2019; Accepted 22 January 2019
Available online 24 January 2019
0308-8146/ © 2019 Elsevier Ltd. All rights reserved.

with carbon, graphene, natural polysaccharides or synthetic polymers (Zou, Xiang, Sun, & Xu, 2008; Zhai et al., 2013; Rothwell, Killoran, & O'Neill, 2010; Kung et al., 2014; Reyes-De-Corcuera et al., 2018; Dong et al., 2018).

AuPt nanostructures, AuNPs, Pt-based nanomaterials, cobalt(II)-selenide NPs, PtRuNPs (Kung et al., 2014), nanoclusters, that contain Cu or SnO_2, nickel zinc ferrite were shown to possess intrinsic PO-like activities. Combination of metallic NPs with different forms of carbon and graphene improves catalytic properties of the artificial PO (Kung et al., 2014). Some of the listed PO-mimetics have also the properties of oxidases and catalases (Liu et al., 2015), but dual specificity of such NPs makes it impossible to use them for real biological samples analysis. It is also worth mentioning that the optimal pH for the most of these NPs is 3.0–4.0, thus under physiological pH 7.0–7.4 these NPs are catalytically inactive.

Various nanomaterials were shown to be effective "artificial POs" as transducers for H_2O_2 detection in oxidase-based biosensors: AuNPs, AuAg nanorods (Han, Li, Zhang, Lang, & Liu, 2015), Fe_3O_4NPs, CeO_2NPs, Co_3O_4NPs (Xie et al., 2013), V_2O_5 nanowires, TiO_2 nanotubes, V_2O_3 -ordered mesoporous carbon composite (Han, Zeng, Wei, Li, & Liu, 2015), nanocomposites of NiFex (x = 0, 1, 2), embedded in ordered mesoporous carbon (Xiang et al., 2015) and others. Analytical characteristics of some oxidase-based methods with PO-like nanozymes are compared in Table 1. One of the most effective inorganic artificial PO was shown to be Prussian blue-based NPs. This catalyst has high stability, sensitivity and selectivity to H_2O_2 in extra-wide linear range $1{\cdot}10^{-9}$–$1{\cdot}10^{-2}$ M (Karyakin et al., 2000).

The aim of current research is to design oxidase-based amperometric biosensors (ABSs) showing potential for food analysis by using nanozymes as PO mimetics. In this paper we describe ABSs based on yeast alcohol oxidase (AO) and methylamine oxidase (AMO), as well as on NPs of PtRu (further – nPtRu) as artificial PO, for the detection of ethanol and methylamine (MA), respectively. AO and MAO were selected due to using them in our previous works related to construction of yeast over-producing strains (Gonchar, Ksheminska, Hladarevska, & Sibirny, 1990; Sigawi et al., 2014) and development of biosensors and enzymatic kits for assay of ethanol/methanol and MA (Gonchar, Maidan, Pavlishko, & Sibirny, 2001; Smutok et al., 2006, Stasyuk, Smutok, Zakalskiy, Zakalska, & Gonchar, 2014).

2. Materials and methods

2.1. Reagents

Sodium ethylenediaminetetraacetate (EDTA), $CaCl_2$, NaCl, KH_2PO_4, Na_2HPO_4, NH_4Cl, ruthenium(III) chloride hydrate, chloroplatinic acid, MA, dimethylamine (DMA), trimethylamine (TMA), methanol, ethanol, propanol, glycerol, glucose, formaldehyde, ammonium chloride and hydrogen peroxide were purchased from Sigma-Aldrich.

The cathodic polymer GY 83–0270 0005 was from BASF Farben und Lacke (Munster, Germany). All buffers and standard solutions were prepared with Milli-Q (Millipore) water.

2.2. Enzymes isolation and purification

Electrophoretically homogeneous yeast enzymes – alcohol oxidase (AO, EC 1.1.3.13) and methylamine oxidase (AMO, EC 1.4.3.21; primary amine:oxygen oxidoreductase (deaminating) or amine oxidase) were used for ABSs fabrication.

AO was isolated from cell-free extract of the selected over-producing strain *Hansenula polymorpha C-105 (gcr1 catX)* by a two-step ammonium sulfate fractionation (at 30 and 70% of saturation) followed by ion exchange chromatography on DEAE-Toyopearl 650 M (Gonchar et al., 1990; Shleev et al., 2006). Activity of AO was determined by the rate of hydrogen peroxide formation in reaction with methanol as monitored by the peroxidative oxidation of *o*-dianisidine in the presence of PO. Purified AO with specific activity 20 U·mg^{-1} of protein was kept as suspension in 70% ammonium sulfate, 50 mM phosphate buffer (PB) pH 7.5 at 4 °C.

As a source of AMO, the recombinant yeast strain *Saccharomyces cerevisiae* C13ABYS86 constructed by us earlier was used (Sigawi et al., 2014). The $(His)_6$-tagged enzyme was purified from the cell-free extract

Table 1
PO-like nanozymes as the effective platforms in oxidase-based analytical approaches.

Analyte/Enzyme	Composition of nanozyme	Characteristics of analytical method			References
		Mode of signal detection	Linear range, mM	LOD, μM	
Glucose/Glucose oxidase	Pt	Amperometry	0.01–8	0.7	Zhai et al. (2013)
			0.001–23	1	Zou et al. (2008)
			up to 10		Rothwell et al. (2010)
	Pd		up to 12		Lim, Wei, Lin, Li, and Kuayou (2005)
	Co		0.0025–0.030	0.156	Dong et al. (2018)
	mixed-valence manganese oxides		up to 3.5	100	Cui, Liu, and Lin (2005)
	ZnO		0.01–6.5	4.5	Hwa and Subramani (2014)
	$NiFe_2$-ordered mesoporous carbon		0.049–12.5	2.7	Xiang et al. (2015)
	Co_3O_4	Spectrophotometry	0.001–0.1	1	Xie et al. (2013)
	NiO		0.05–0.50	20	Liu et al. (2015)
	Au@Ag nanorods		0.05–20		Han, Li et al. (2015)
	V_2O_3-ordered mesoporous carbon		0.01–4		Han, Zeng et al. (2015)
Cholesterol/Cholesterol oxidase	Cu	Chemiluminescence	0.05–10	1.5	Xu et al. (2016)
	Cu_2O		0.0006–0.013	0.17	Hong, Liu, Li, Chen, and Lin (2013)
	AuPt	Amperometry	0.05–11.2	90.7	Safavi and Farjami (2011)
Ethanol/Alcohol oxidase	Au		0.01–4.7	7	Chinnadayyala, Santhosh, Singh, and Goswami (2015)
	PO/Au		0.005–3	2.3	Chinnadayyala, Kakoti, Santhosh, and Goswami (2014)
	Prussian Blue	Amperometry Paper-based screen-printed biosensor	up to 10	520	Cinti, Basso, Moscone, and Arduini (2017)
Glutamate/Glutamate oxidase		Amperometry	0.1–100		Karyakin et al. (2000)

by metal-affinity chromatography on Ni-NTA-agarose. Activity of AMO was determined by the rate of hydrogen peroxide formation in reaction with MA as monitored by the peroxidative oxidation of ABTS in the presence of PO. Purified AMO with specific activity 16 U·mg^{-1} of protein was stored in 20% glycerol, 30 mM PB pH 7.5 at −20 °C.

2.3. Apparatus

A piece of Pt wire and an Ag/AgCl/3M KCl electrode were used as the counter and reference electrodes. 3.05 mm graphite rods (type RW001, Ringsdorff Werke, Bonn, Germany) were used as working electrodes. They were sealed in glass tubes with epoxy forming disk electrodes. Before sensor preparation, the graphite electrode (GE) was polished with emery paper. Amperometric measurements were carried out with a potentiostat CHI 1200A (IJ Cambria Scientific, Burry Port, UK) in batch mode under continuous stirring in a standard 40 ml cell at a room temperature.

A SEM-microanalyser REMMA-102-02 (Lviv, Ukraine) and an AFM-microanalyser Solver P47-PRO (NT-MDT, Netherlands) were used for morphological analyses of the PtRu-film (nPtRu).

2.4. Synthesis of metallic NPs and testing their ability to react with hydrogen peroxide

Mono- and bimetallic NPs were synthesized on the surface of a GE by electrodeposition of 1 mM solutions of Pt^{4+}, Pd^{2+}, Ru^{3+} or Cu^{2+} salts in 0.1 M PB, pH 7.0 using cyclic voltammetry in the range from −1000 to +1000 mV with scan rate 50 mV·min^{-1} during 10 cycles. The obtained modified electrodes were rinsed with water and equilibrated before use in 30 mM PB pH 7.5.

The electro-activities of the synthesized NPs were studied by cyclic voltammetry under the same conditions and the profiles of amperometric signals at increasing concentrations of H_2O_2 were compared. The most electroactive NPs, that have the highest PO-like properties, were chosen for further investigation.

2.5. Preparation and morphological analysis of the nPtRu/GE

The most effective nPtRu was synthesized from aqueous solution containing of 25 mM ruthenium(III) chloride hydrate and 0.5 mM chloroplatinic acid by electrodeposition during 24 cycles under described conditions (see subdivision 2.4).

Both SEM and AFM were used to characterize a thickness and morphology of the nPtRu film on a GE. For AFM the tapping mode with a resonance frequency of 160 kHz, scan rate of 1 Hz/s and resolution of 256 × 256 pixels was used.

2.6. Immobilization of enzymes on the surface of nPtRu/GE

AMO or AO solutions were dropped on nPtRu/GE and covered by commercial polymer GY 83-0270 0005 (CP). The immobilization procedure was as follows: 3 μL of enzyme solution with activity 15–35 U·mL^{-1} in 30 mM PB, pH 7.5 was dropped on the top of the nPtRu/GE. After drying for 2 min at a room temperature the layer of enzyme was covered with 4 μL CP for polymer layer formation. The prepared bio-functionalized electrode was rinsed with 30 mM PB pH 7.5 and kept before use in this buffer with 0.1 mM EDTA at +4 °C.

2.7. Preparation of food samples for biosensor analysis

The samples of wine "Chianti" dry red (Corte Alle Mura, Italia) and Kefir "Halychyna" 2.5% of fat (Halychyna, Ukraine) were used for ethanol analysis. All samples were diluted stepwise by 50 mM PB pH7.5 (the dilution factors were 6020 and 12020, 76 and 151, respectively). The analytical results were statistically processed using the OriginPro 8.5 software.

For MA assay, the frozen sea fish samples of tilapia and pigfish were used. Protein-free extract was prepared as described earlier (Stasyuk et al., 2014).

2.8. Reference methods for MA and ethanol determination

Analysis of MA was performed by a colorimetric method in the multiple standard addition variant on a Shimadzu UV-1650 PC spectrophotometer (Shimadzu, Kyoto, Japan) at 545 nm relative to MA-free control sample. The concentration of MA in the tested samples was determined from a calibration curve (Stasyuk et al., 2014).

Ethanol assay was carried out using analytical kit "Alcotest" by the measurement of the dye-product accumulation in peroxidative oxidation of chromogen by H_2O_2 generated from ethanol in alcohol oxidase reaction (Gonchar et al., 2001). Because of high sensitivity of the method, the "fixed reaction time" was used at the incomplete conversion of analyte.

2.9. Statistic analysis

All the measurement's results and the level of correlation between results obtained by the different analytical methods were calculated by computer program Origin 8.0 and Microsoft Excel.

3. Results and discussion

3.1. Selection and characterization of the best nanocomposite as peroxidase-like nanozyme

The electroactivities of the synthesized NPs, electrodeposited on the surface of GE, were tested by cyclic voltammetry as described in 2.4. The amperometric responses of different NPs/GEs to the added H_2O_2 (up to final concentration 1 mM) were compared (See Supplementary information, Fig. SI.1). Fig. SI.1 demonstrates that nPtRu/GE was the most effective artificial PO, thus it was studied in more detail as chemosensor for H_2O_2 detection.

To improve the electrodeposition of nPtRu on graphite electrode, 24 cycles were experimentally chosen. The resulted nPtRu/GE turned dark brown-golden due to formation of the nPtRu-film. The oxidation (at −0.05 V) and reduction (at −0.25 V) peaks were observed and the current was increased (Supplementary Information, Fig. SI.2).

Morphological properties of the PtRu-film were studied (Fig. 1). The SEM micrographs of the film formed by a potentiodynamic mode during 10 min in the $RuCl_3$ and H_2PtCl_6-containing solution are presented on Fig. 1. *a, b*. The Gaussian distribution by size (Fig. 1.*d*) obtained from the AFM data (Fig. 1.*c*) proved that an average thickness of the layer is 60 nm, thus the PtRu-film is really nanosized.

The XRM images of the PtRu-film show the characteristic peaks for Pt^0 and Ru^0 indicating the formation of nPtRu (Fig. 1.*e*).

The electrochemical characteristics of nPtRu/GE as effective chemosensor for H_2O_2 were studied (Fig. 2). The cyclic voltammogram (Fig. 2.*a*) demonstrates that a cathodic reduction peak contributed from H_2O_2 arises at a potential of approximately −100 mV (vs Ag/AgCl) for 0.15 and 0.6 mM H_2O_2 solutions. The chronoamperometric dependence and calibration graph for H_2O_2 determination at −100 mV are shown on Fig. 2(*b* and *c*, respectively). As a control, unmodified GE was tested and no signal was detected upon H_2O_2 addition. The maximum current response of the nPtRu/GE to H_2O_2 was 2020 ± 90 nA with a K_M^{app} = 0.77 ± 0.08 mM ($I_{50\%}$ at 0.77 ± 0.08 mM). Other analytical characteristics of H_2O_2-sensitive layer based on nPtRu are compared with results of other scientists using nPtRu as PO-like nanozyme in Table SI.1 (Supplementary information).

The aim of our work was to use nPtRu/GE as PO-mimetic for ABSs based on AO and AMO. We studied the ability of nPtRu/GE to react with the substrates of AO (methanol, ethanol, formaldehyde) and AMO (MA). Fig. 2.*d* demonstrates the absence of any signals on the tested

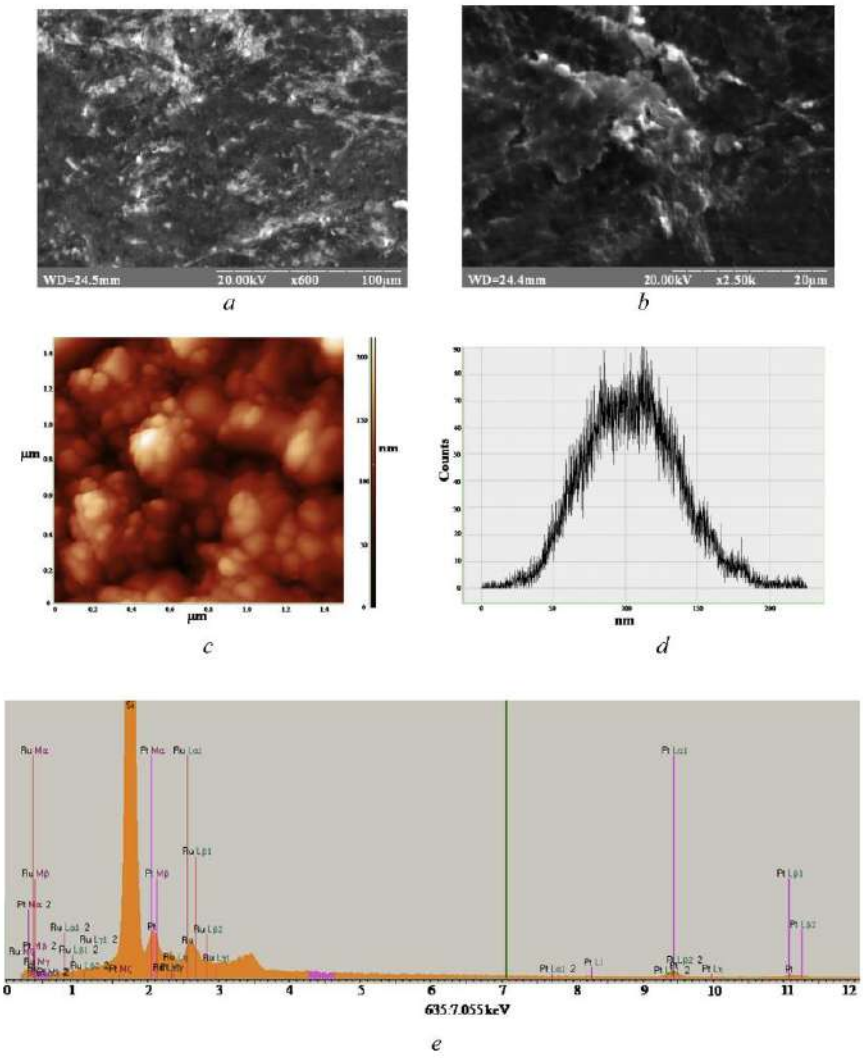

Fig 1. Characteristics of PtRu-film formed on the top of a GE after 24 cycles of electrodeposition. *a, b* – Scanning Electron Microscopy images; *c* – AFM micrograph; *d* – The Gaussian distribution curve of the film's thickness; *e* – X-ray spectral microanalysis of nPtRu.

analytes in the range from 0.05 to 5 mM with the step of 0.1 mM. Under the chosen conditions nPtRu/GE was a highly selective to H_2O_2.

The first bimetallic NPs catalyst comprising a Ru core covered with a shell of Pt atoms (a Ru@Pt core–shell NPs) was proposed by Alayoglu, Nilekar, Mavrikakis, and Eichhorn (2008). nPtRu had predictable catalytic properties that are markedly different from NPs of 'bulk' PtRu alloys or monometallic Pt and Ru mixtures of identical loadings and compositions (Kua & Goddard, 1999).

Among platinum based bimetallic nanocatalysts, nPtRu was shown to be an effective PO-like nanozyme (Kung et al., 2014). It is worth mentioning that the nature of supporting materials co-immobilized with nPtRu is crucial for the electrochemical oxidation of H_2O_2, namely for sensitivity of the electrode and limit of detection (LOD).

Different carbon nanomaterials (carbon powder, graphene, and graphene foam or porous grapheme) positively affect the electroactivity of nPtRu due to enhanced availability of electrochemical active surface resulting in higher mass transport of reactants. The characteristics of nPtRu bimetallic nanocatalysts on various forms of carbon toward the H_2O_2 detection are presented in Table SI.1 (Supplementary Information). The most effective was the porous graphene.

The nPtRu-based electrodes proposed by Kung (Table SI.1) having a superior conductivity, a low LOD and a high sensitivity to H_2O_2 provide a new opportunity for electrode materials with enhanced performance in biosensing. But these electrodes have a narrow linear range and a rather high (+0.32 V) applied potential. To avoid interfering effects during analysis of real samples using enzymatic ABSs, the lowest applied potential is desirable.

Thus, a number of mono- and bimetallic NPs were synthesized on the surface of GE by electrochemical deposition and their ability to react with H_2O_2 was tested. The most effective nPtRu/GE chemosensor

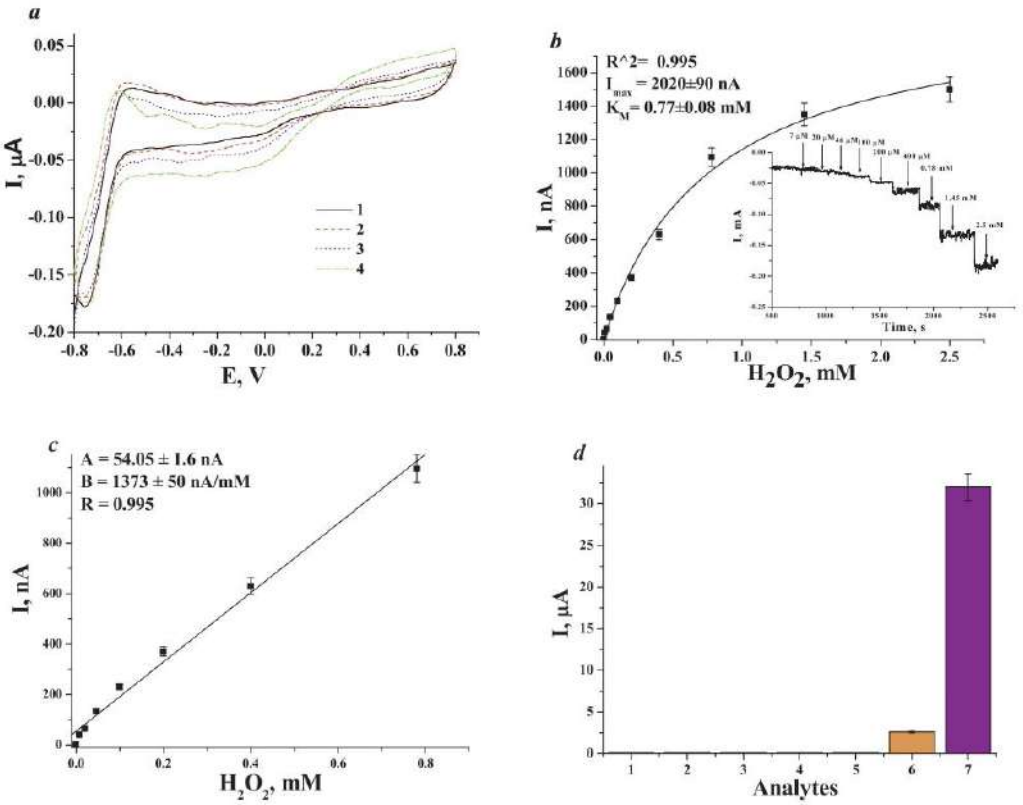

Fig. 2. Amperometric characteristics of nPtRu/GE: *a* – the cyclic voltammograms of H_2O_2. The final concentrations of analyte (mM) in 30 mM PB, pH 7.5 were 0 (**1**); 0.15 (**2**); 0.3 (**3**); 0.6 (**4**); *b* – dependence of amperometric signal and chronoamperometric response (the insert) on concentration of H_2O_2 upon the subsequent additions of analyte; *c* – calibration graph for H_2O_2 determination; *d* – selectivity to different 1 mM chemicals: **1** – MA; **2** – methanol; **3** – ethanol; **4** – formaldehyde; **5** – glucose; **6** – ammonium chloride and **7** – H_2O_2. Remark to (d): GE with the diameter 9 mm was used.

for H_2O_2 was selected and characterized.

3.2. Fabrication and characterization of bioelectrodes

Selective to hydrogen peroxide nPtRu/GE coupled with AO or recombinant AMO appear to be a good candidate for ABSs on alcohols and MA (Supplementary Information, Fig. SI.3).

To form an enzymatic layer, an aliquot of enzyme solution was dropped on the surface of the nPtRu/GE and covered with a cathodic polymer (CP) according to the experimental part (2.6). The calibration curves for the developed ABSs (see subdivision 2.6) and the corresponding chronamperograms (insert) are shown in Fig. 3*a–d*. The calibration was performed by the stepwise addition of a standard analyte solution. The bioanalytical characteristics of both ABSs are presented in Table 2.

The ABSs were tested in the range of concentrations up to 1.8 mM for both substrates (Fig. 3*a*, *c*).

Stability and selectivity of the developed ABSs are presented in Fig. SI.4 (Supplementary Information). To test a stability of the AO-ABS, the current responses to 0.2 mM ethanol in 50 mM PB, pH 7.5 for a period of 16 days were detected. The current response of the AO-ABS was shown to decrease by 80% for a period of 14 days and the half-life of this ABS was about 10 days. Storage stability of the AMO-ABS was measured by addition of 0.5 mM MA. A half-life of this ABS is 14 days (Fig. SI.4. a). It is worth mentioningthat the keeping free enzymes in 50 mM PB, pH 7.5 leads to a quick loss of their enzymatic activities. These conditions were shown to be non-optimal for AO and AMO storage, see subdivision 2.2. Besides, the inactivation rates of free enzymes in buffer solution are 2-fold higher, than in the case of immobilized enzymes in ABS.

A selectivity of the ABS to the target analyte is of a great importance, especially for analysis of real samples. In this paper, a selectivity of the constructed ABS was estimated in relative units (%) as a ratio of the detected signal to the value of the highest current response for the natural substrate (Fig. SI.4.*b*, *c*).

In case of the AO-ABS, neither glycerol nor glucose elicited any signals while some primary alcohols and formaldehyde induced essential analytical signals (Fig. SI.4.*b*). It should be noted that possible impact of methanol, propanol and formaldehyde on ethanol assay is not important due to a very low content of the listed compounds in natural foods, including wine, yogurts, *etc.* (Rehm et al., 2014; Tulashie, Appiah, Torku, Darko, & Wiredu, 2017). DMA and TMA, which are structurally similar to MA, did not produce positive signals with AMO-ABS (Fig. SI.4.*c*).

The novel mono-enzyme AO and AMO-based ABSs for ethanol and MA determination have some advantages over the conventional bienzyme- and cell-based ABSs constructed by us earlier with the same enzymes (Table 2). The proposed ABSs are highly sensitive, stable, easy-to-use and cost-effective, in addition, the AMO-ABS is very selective to its natural substrate MA.

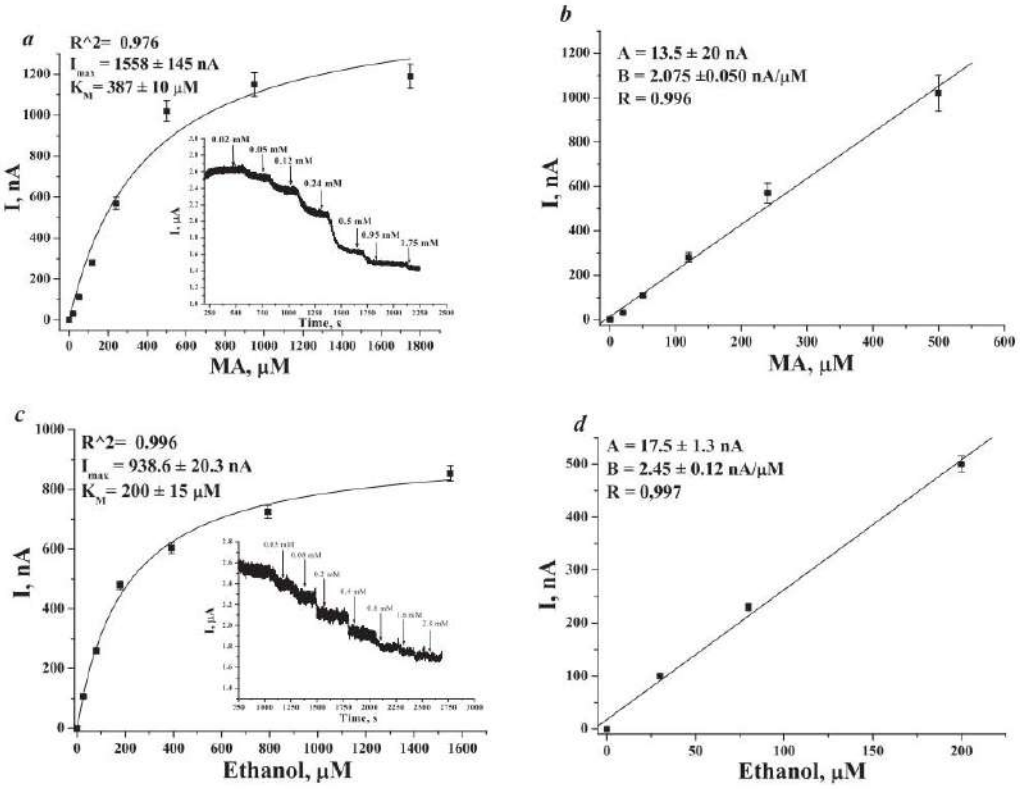

Fig. 3. Bioanalytical characteristics of AMO/nPtRu/GE (*a*, *b*) and AO/nPtRu/GE (*c*, *d*) under applied potential of −100 mV at 22 °C. Chronoamperometric current responses (the insert) and calibration curves upon subsequent additions of MA (*a*, *b*) and ethanol (*c*, *d*).

It is worth mentioning that nPtRu-containing electrodes were fabricated earlier as chemosensors for methionine (Tavakkoli, Soltani, & Khorshidi, 2017) and for ethanol (Xiao, Zhao, Zeng, & Zeng, 2009; Hajian et al., 2015). Both sensors for ethanol have long-term stabilities and large linear ranges for ethanol determination in model solutions but there are no data about the possibility of their application for real samples analysis. Besides, these electrodes have similar sensitivities to ethanol ($A \cdot M^{-1} \cdot m^{-2}$): 566 (Hajian et al., 2015) and 210 (Xiao et al., 2009) in comparison with 336 (our AO/nPtRu/GE).

3.3. Assay of MA and ethanol in food samples

The assay of aliphatic amines and ethanol in environmental, food and biological samples is crucial due to their use in industry and their presence in living organisms. MA is a result of natural degradation of proteins, amino acids, and other nitrogen-containing compounds (Tseng & Graves, 1998). MA usually accumulates in high amounts in fish, especially of *Gadoid* species. If such food is consumed in combination with nitrate-containing products, dangerous carcinogens N-nitroso derivatives are formed (Rehbein et al., 1995). The standard approaches for analysis of amines are HPLC, colorimetry, laser spectroscopy, fluorometry, gas chromatography coupled with mass spectrometry, chromatography as well as enzymatic methods (Ordóñez, Troncoso, Carmen, Raquel, & Callejón, 2016; Biji, Ravishankar, Venkateswarlu, Mohan, & Srinivasa Gopal, 2016). The usage of enzymatic methods is limited because of the absence of commercial AMO

Table 2
Comparison of the developed amperometric biosensors on alcohols and methylamine.

Biocomponent	Analyte	Potential, mV	Linear range, mM	LOD, μM	K_M, mM	Sensitivity, $A \cdot M^{-1} \cdot m^{-2}$	Response time, s	Stability (50%), days	Reference
AO-PO/Os polymer	Ethanol	−50	0.5–2.0	15	1.94	29	60	16	Smutok et al. (2006)
AO/nAu/PO- permeabilized yeast cells	Methanol	−50	Up to 2.0	N.d.	1.93	N.d.	80	30	Karkovska et al. (2017)
AO/nPtRu	Ethanol	−100	0.025–0.20	3	2.0	336	70	10	Current paper
AMO-PO	MA	−50	0.015–0.06	2.8	0.039	1450	10	15	Stasyuk et al. (2014)
AMO-PO nAu		−50	0.015–0.15	6	0.15	700	10	30	
AMO/nPtRu		−100	0.02–0. 60	2.5	0.387	284	60	14	Current paper

N.d. – Not detected.

Table 3
Determination of ethanol and MA in the samples of food products using biosensor and reference methods.

Samples	Analyte	Difference, %	Biosensor, mM	Reference, mM
Pigfish	MA	0.582 ± 0.014	0.550 ± 0.008	+5.8
Fish "Tilapia"		0.276 ± 0.002	0.290 ± 0.014	−4.8
Wine "Chianti"	Ethanol	2620 ± 110	2710 ± 90	−3.3
Kefir "Halychyna"		23.4 ± 1.10	22.6 ± 1.31	+3.5

preparations. In previous paper, we have described for the first time the MA-selective bi-enzyme AMO/PO-ABS (Stasyuk et al., 2014).

Ethanol is a component of many commercial goods (spirit drinks, biochemicals, bioplastics, pharmaceuticals, cosmetics, solvents, paints) and a biofuel (Rehm et al., 2014). We have reported earlier about the development of AO-based methods for ethanol determination (Gonchar et al., 2001; Smutok et al., 2006; Karkovska, Stasyuk, Gayda, Smutok, & Gonchar, 2017).

In order to demonstrate the practical feasibility of the constructed ABSs, contents of MA and ethanol were determined in food samples using standard addition method (SAT). SAT is a type of quantitative analysis approach often used in analytical chemistry where a standard is added directly to the aliquots of the analyzed sample. Graphical SAT method is used in situations where sample components also contribute to the analytical signal. Estimation of MA or ethanol in the initial sample from the parameters of linear regression of the correspondent bioselective electrode was done, taking into account factors of dilution (Eq. (1)); calculation of the average concentration from two values:

$$C = \frac{A}{B}N, \quad (1)$$

where C – concentration of MA or ethanol, A and B – parameters of linear regression; N – dilution factor of the tested sample, shown in graph.

The results of MA assay in protein-free extracts of the frozen samples of fishes and ethanol assay in beverages are shown in detail in Fig. SI.5 (Supplementary Information).

The average contents of the analytes determined by the developed ABSs and the reference methods are presented in Table 3. The differences less than 5.8% between the results of both methods were observed. The contents of MA, determined in the protein-free extracts of fish samples (Table 3) and recalculated on the fish muscles tissues, were shown to be 5.0 and 3.8 mg/kg for pigfish and tilapia, respectively. These values are correlated with published data (Neurath, Dünger, Pein, Ambrosius, & Schreiber, 1977).

The concentrations of the tested analytes that were estimated using two methods have strong (R = 1) correlations (Fig. SI.6. *a, b*).

The developed ABSs were evaluated using statistical analysis. The Student's *t*-test did not reveal significant difference between the experimental values obtained in the sample analysis by the two methods. The calculated t-values for MA assay in pigfish (t_{calc} = 3.5) and in tilapia (t_{calc} = 1.75) as well as for ethanol assay in kefir (t_{calc} = 0.56) and in wine (t_{calc} = 2.12) were found to be less than the critical t-value (t_{crit} = 4.3) at 5% significance level. The assessment of the validation parameters of the method is given in Table SI.2 (See Supplementary Information).

Thus, the results of the accuracy research of the biosensors approach for MA and ethanol determination was shown to meet requirements for the permissible limits of ± 10.0%. These results demonstrate the possibility of application of the developed ABSs – AMO/nPtRu/GE and AO/nPtRu/GE for the analysis of MA and ethanol in food.

4. Conclusions

In summary, mono- and bimetallic NPs were synthesized on the surface of GE by electrochemical deposition and characterized as electroactive chemosensors for H_2O_2. The most effective PO-mimetic (nPtRu) was chosen for construction of two ABSs coupled with yeast oxidases: the AO and the recombinant AMO.

The novel oxidase/nPtRu-based ABSs have been developed for alcohols and MA detection. ABSs exhibit high sensitivities (336 $A \cdot M^{-1} \cdot m^{-2}$ to ethanol for AO-ABS; 284 $A \cdot M^{-1} \cdot m^{-2}$ to MA for AMO-ABS), broad linear ranges (25–200 μM ethanol and 20–600 μM MA), satisfactory storage stabilities and good selectivities toward natural substrates. We have demonstrated that the substitution of PO by nPtRu as a artificial PO in biosensing layer provides an improvement in the electrochemical properties of the electrodes and detection with the wider linear ranges.

The constructed ABSs were tested on the real samples of food: AO-ABS – for ethanol assay in wine and kefir, AMO-ABS – for MA assay in fish tissue extracts. High correlations of the obtained results and of the reference methods were demonstrated for both target analytes.

Declaration of interest

None.

Appendix A. Supplementary data

Supplementary data to this article can be found online at https://doi.org/10.1016/j.foodchem.2019.01.117.

References

Alayoglu, S., Nilekar, A. U., Mavrikakis, M., & Eichhorn, B. (2008). Ru-Pt core-shell nanoparticles for preferential oxidation of carbon monoxide in hydrogen. *Nature Materials, 7*, 333–338. https://doi.org/10.1038/nmat2156.

Biji, K. B., Ravishankar, C. N., Venkateswarlu, R., Mohan, C. O., & Srinivasa Gopal, T. K. (2016). Biogenic amines in seafood: A review. *Journal of Food and Science Technology, 53*(5), 2210–2218. https://doi.org/10.1007/s13197-016-2224-x.

Chinnadayyala, S. R., Kakoti, A., Santhosh, M., & Goswami, P. (2014). A novel amperometric alcohol biosensor developed in a 3rd generation bioelectrode platform using peroxidase coupled ferrocene activated alcohol oxidase as biorecognition system. *Biosensors and Bioelectronics, 55*, 120–126. https://doi.org/10.1016/j.bios.2013.12.005.

Chinnadayyala, S. R., Santhosh, M., Singh, N. K., & Goswami, P. (2015). Alcohol oxidase protein mediated *in-situ* synthesized and stabilized gold nanoparticles for developing amperometric alcohol biosensor. *Biosensors and Bioelectronics, 69*, 155–161. https://doi.org/10.1016/j.bios.2015.02.015.

Cinti, S., Basso, M., Moscone, D., & Arduini, F. (2017). A paper-based nanomodified electrochemical biosensor for ethanol detection in beers. *Analitica Chimica Acta, 960*, 123–130. https://doi.org/10.1016/j.aca.2017.01.010.

Cui, X., Liu, G., & Lin, Y. (2005). Amperometric biosensors based on carbon paste electrodes modified with nanostructured mixed-valence manganese oxides and glucose oxidase. *Nanomedicine, 1*(2), 130–135. https://doi.org/10.1016/j.nano.2005.03.005.

Dong, W., Zhuang, Y., Li, S., Zhang, X., Chai, H., & Huang, Y. (2018). High peroxidase-like activity of metallic cobalt nanoparticles encapsulated in metal–organic frameworks derived carbon for biosensing. *Sensors and Actuators B: Chemical, 255*(2), 2050–2057. https://doi.org/10.1016/j.snb.2017.09.013.

Gonchar, M. V., Ksheminska, G. P., Hladarevska, N. M., & Sibirny, A. A. (1990). Catalase-minus mutants of methylotrophic yeast *Hansenula polymorpha* impaired in regulation of alcohol oxidase synthesis. In T. M. Lachowicz (Ed.). *Genetics of respiratory enzymes in yeasts* (pp. 222–228). Wroclaw: Wroclaw University Press.

Gonchar, M. V., Maidan, M. M., Pavlishko, H. M., & Sibirny, A. A. (2001). A new oxidase-peroxidase kit for ethanol assays in alcoholic beverages. *Food Technology and Biotechnology, 39*, 37–42. http://www.ftb.com.hr/archives/103-volume-39-issue-no-1/743-a-new-oxidase-peroxidase-kit-for-ethanol-assays-in-alcoholic-beverages.

Hajian, A., Rafati, A. A., Yurchenko, O., Urban, G., Afraz, A., Najafi, M., & Bagheri, A. (2015). Nanostructured flower like Pt-Ru for ethanol oxidation and determination. *Journal of the Electrochemical Society, 162*(1), B41–B46. https://doi.org/10.1149/2.1121501jes.

Han, L., Li, C., Zhang, T., Lang, Q., & Liu, A. (2015). Au@Ag heterogeneous nanorods as nanozyme interfaces with peroxidase-like activity and their application for one-pot analysis of glucose at nearly neutral pH. *ACS Applied Materials and Interfaces, 7*(26), 14463–14470. https://doi.org/10.1021/acsami.5b03591.

Han, L., Zeng, L., Wei, M., Li, C. M., & Liu, A. (2015). A V2O3-ordered mesoporous carbon composite with novel peroxidase-like activity towards the glucose colorimetric assay. *Nanoscale, 7*(27), 11678–11685. https://doi.org/10.1039/c5nr02694f.

Hong, L., Liu, A. L., Li, G. W., Chen, W., & Lin, X. H. (2013). Chemiluminescent cholesterol sensor based on peroxidase-like activity of cupric oxide nanoparticle. *Biosensors and Bioelectronics, 43*, 1–5. https://doi.org/10.1016/j.bios.2012.11.031.

Hwa, K. Y., & Subramani, B. (2014). Synthesis of zinc oxide nanoparticles on graphene-carbon nanotube hybrid for glucose biosensor applications. *Biosensors and Bioelectronics, 62*, 127–133. https://doi.org/10.1016/j.bios.2014.06.023.

Karkovska, M. I., Stasyuk, N. Ye., Gayda, G. Z., Smutok, O. V., & Gonchar, M. V. (2017). Nanomaterials in construction of biosensors of medical application. In R. Stolka (Ed.). *Multifunctional nanomaterials for biology and medicine: molecular design, synthesis, and application* (pp. 165–177). Kyiv: Project New Book.

Karyakin, A. A., Karyakina, E. E., & Gorton, Lo (2000). Amperometric biosensor for glutamate using prussian blue-based "artificial peroxidase" as a transducer for hydrogen peroxide. *Analytical Chemistry, 72*, 1720–1723. https://doi.org/10.1021/ac990801o.

Kua, J., & Goddard, W. A. (1999). Oxidation of methanol on 2nd and 3rd row group VIII transition metals (Pt, Ir, Os, Pd, Rh, and Ru): Application to direct methanol fuel cells. *Journal of the American Chemical Society, 121*, 10928–10941. https://doi.org/10.1021/ja9844074.

Kung, C. C., Lin, P. Y., Buse, F. J., Xue, Y., Yu, X., Dai, L., & Liu, C. C. (2014). Preparation and characterization of three dimensional graphene foam supported platinum-ruthenium bimetallic nanocatalysts for hydrogen peroxide based electrochemical biosensors. *Biosensors and Bioelectronics, 52*, 1–7. https://doi.org/10.1016/j.bios.2013.08.025.

Lim, S. H., Wei, J., Lin, J., Li, Q., & Kuayou, J. (2005). A glucose biosensor based on electrodeposition of palladium nanoparticles and glucose oxidase onto Nafion-solubilized carbon nanotube electrode. *Biosensors and Bioelectronics, 20*(11), 2341–2346. https://doi.org/10.1016/j.bios.2004.08.005.

Liu, Q., Yang, Y., Li, H., Zhu, R., Shao, Q., Yang, S., & Xu, J. (2015). NiO nanoparticles modified with 5,10,15,20-tetrakis(4-carboxyl pheyl)-porphyrin: Promising peroxidase mimetics for H_2O_2 and glucose detection. *Biosensors and Bioelectronics, 64*, 147–153. https://doi.org/10.1016/j.bios.2014.08.062.

Neurath, G. B., Dünger, M., Pein, F. G., Ambrosius, D., & Schreiber, O. (1977). Primary and secondary amines in the human environment. *Food and Cosmetics Toxicology, 15*(4), 275–282. https://doi.org/10.1016/S0015-6264(77)80197-1.

Ordóñez, J. L., Troncoso, A. M., Carmen, M. D., Raquel, G.-P., & Callejón, M. (2016). Recent trends in the determination of biogenic amines in fermented beverages – A review. *Analytica Chimica Acta, 939*, 10–25. https://doi.org/10.1016/j.aca.2016.07.045.

Rehbein, H., Eichenauer, D., Feser, P., Friedrich, R., Gluck, B., Harz, A., ... Winkler, F. (1995). Formaldehyde and dimethylamine in frozen fishery products available on the market - an inventory. *Archivur Lebensmittelhygiene, 46*(5), 122–124. http://agris.fao.org/agris-search/search.do?recordID = DE96M2574.

Rehm, J., Kailasapillai, S., Larsen, E., Rehm, M. R., Samokhvalov, A. V., Shield, K. D., ... Lachenmeier, D. W. (2014). A systematic review of the epidemiology of unrecorded alcohol consumption and the chemical composition of unrecorded alcohol. *Addiction, 109*, 880–893. https://doi.org/10.1111/add.12498.

Reyes-De-Corcuera, J. I., Olstad, H. E., & García-Torres, R. (2018). Stability and stabilization of enzyme biosensors: The key to successful application and commercialization. *Annual Review of Food Science and Technology, 9*, 293–322. https://doi.org/10.1146/annurev-food-030216-025713.

Rothwell, S. A., Killoran, S. J., & O'Neill, R. D. (2010). Enzyme immobilization strategies and electropolymerization conditions to control sensitivity and selectivity parameters of a polymer-enzyme composite glucose biosensor. *Sensors (Basel), 10*(7), 6439–6462. https://doi.org/10.3390/s100706439.

Safavi, A., & Farjami, F. (2011). Electrodeposition of gold-platinum alloy nanoparticles on ionic liquid-chitosan composite film and its application in fabricating an amperometric cholesterol biosensor. *Biosensors and Bioelectronics, 26*(5), 2547–2552. https://doi.org/10.1016/j.bios.2010.11.002.

Shleev, S. V., Shumakovich, G. P., Nikitina, O. V., Morozova, O. V., Pavlishko, H. M., Gayda, G. Z., & Gonchar, M. V. (2006). Purification and characterization of alcohol oxidase from a genetically constructed over-producing strain of the methylotrophic yeast *Hansenula polymorpha*. *Biochemistry, 71*(3), 245–250. https://doi.org/10.1134/S0006297906030035.

Sigawi, S., Nisnevitch, M., Zakalska, O., Zakalskiy, A., Nitzan, Y., & Gonchar, M. (2014). Bioconversion of airborne methylamine by immobilized recombinant amine oxidase from the thermotolerant yeast *Hansenula polymorpha*. *Scientific World Journal, 2014*, 1–9. https://doi.org/10.1155/2014/898323.

Smutok, O., Ngounou, B., Pavlishko, H., Gayda, G., Gonchar, M., & Schuhmann, W. (2006). A reagentless bienzyme amperometric biosensor based on alcohol oxidase/peroxidase and an Os-complex modified electrodeposition paint. *Sensors Actuators B: Chemical, 113*, 590–598. https://doi.org/10.1016/j.snb.2005.07.055.

Stasyuk, N. Y., Smutok, O. V., Zakalskiy, A. E., Zakalska, O. M., & Gonchar, M. V. (2014). Methylamine-sensitive amperometric biosensor based on $(His)_6$-tagged *Hansenula polymorpha* methylamine oxidase immobilized on the gold nanoparticles. *Biomed Research International, 2014*, 480498. https://doi.org/10.1155/2014/480498.

Tavakkoli, N., Soltani, N., & Khorshidi, E. (2017). Preparation of Ru–Pt bimetallic monolayer on nanoporous gold film electrode and its application as an ultrasensitive sensor for determination of methionine. *RCS Advances, 7*, 21827–21836. https://doi.org/10.1039/C7RA01192J.

Tseng, H., & Graves, D. (1998). Natural methylamine osmolytes, trimethylamine N-oxide and betaine, increase tau-induced polymerization of microtubules. *Biochemical and Biophysical Research Communications, 250*, 726–730. https://doi.org/10.1006/bbrc.1998.9382.

Tulashie, S. K., Appiah, A. P., Torku, G. D., Darko, A. Y., & Wiredu, A. (2017). Determination of methanol and ethanol concentrations in local and foreign alcoholic drinks and food products (Banku, Ga kenkey, Fante kenkey and Hausa koko) in Ghana. *International Journal of Food Contamination, 4*, 14. https://doi.org/10.1186/s40550-017-0059-5.

Xiang, D., Yin, L., Ma, J., Guo, E., Li, Q., Li, Z., & Liu, K. (2015). Amperometric hydrogen peroxide and glucose biosensor based on $NiFe_2$/ordered mesoporous carbon nanocomposites. *Analyst, 140*(2), 644–653. https://doi.org/10.1039/C4AN01549E.

Xiao, F., Zhao, F., Zeng, J., & Zeng, B. (2009). Novel alcohol sensor based on PtRuNi ternary alloy nanoparticles–multi-walled carbon nanotube–ionic liquid composite coated electrode. *Electrochemistry Communication, 11*(7), 1550–1553. https://doi.org/10.1016/j.elecom.2009.05.060.

Xie, J., Cao, H., Jiang, H., Chen, Y., Shi, W., Zheng, H., & Huang, Y. (2013). Co_3O_4-reduced graphene oxide nanocomposite as an effective peroxidase mimetic and its application in visual biosensing of glucose. *Analitica Chimica Acta, 796*, 92–100. https://doi.org/10.1016/j.aca.2013.08.008.

Xu, S., Wang, Y., Zhou, D., Kuang, M., Fang, D., Yang, W., ... Ma, L. (2016). A novel chemiluminescence sensor for sensitive detection of cholesterol based on the peroxidase-like activity of copper nanoclusters. *Scientific Reports, 6*, 39157. https://doi.org/10.1038/srep39157.

Zhai, D., Liu, B., Shi, Yi, Pan, L., Wang, Y., Li, W., ... Yu, G. (2013). Highly sensitive glucose sensor based on Pt nanoparticle/polyaniline hydrogel heterostructures. *ACS Nano, 7*(4), 3540–3546. https://doi.org/10.1021/nn400482d.

Zou, Y., Xiang, C., Sun, L. X., & Xu, F. (2008). Glucose biosensor based on electrodeposition of platinum nanoparticles onto carbon nanotubes and immobilizing enzyme with chitosan-SiO (2) sol-gel. *Biosensors and Bioelectronics, 23*(7), 1010–1016. https://doi.org/10.1016/j.bios.2007.10.009.

Оригінал доступний за посиланням: https://doi.org/10.1016/j.foodchem.2019.01.117

Анотація: *На сьогодні існують обмежені дані щодо амперометричних біосенсорів (АБС) для визначення L-аргініну на основі оксидаз та нанозимів – міметиків пероксидази. В літературі описано АБС для аналізу L-аргініну, однак вони ґрунтуються на використанні каскаду ензимів, що значно ускладнює процедуру і збільшує вартість аналізу. Саме тому, конструювання моно-ензимного АБС для аналізу L-аргініну є важливим завданням. У поточному дослідженні ми повідомляємо про конструювання АБС для прямого аналізу L-аргініну. L-аргініноксидаза (АргО), виділена з гриба Amanita phalloides, спільно ко-іммобілізована з ПО-подібними нанозимами (НЗ) на поверхні графітових електродів. У ролі міметиків ПО використовували хімічно синтезовані НЗ CeCu та NiPtPd. Усі запропоновані АБС показали високу чутливість (1630 $А \cdot М^{-1} \cdot м^{-2}$ для АргО-CeCu та 284 $А \cdot М^{-1} \cdot м^{-2}$ для АргО-NiPtPd) і селективність до L-аргініну, широкий лінійний діапазон і хорошу стабільність при зберіганні. Два АБС протестовано на реальних зразках напоїв (соків і вина), а також фармацевтичного препарату «Тівортін». Показано тісний кореляційний зв'язок (R = 0,995) між результатами тестування «Тівортину» та соку з використанням біонаноелектродів на основі CuCe/ГЕ та NiPtPd/ГЕ. Для «Тівортіну» спостерігалася лише незначна різниця (менше 1%) між експериментально визначеним вмістом L-аргініну та його значенням, заявленим виробником. Сконструйовані АБС на основі міметиків ПО та L-аргініноксидази можуть бути перспективними для аналізу L-аргініну у різних галузях науки, медицини та промисловості.*

applied sciences

MDPI

Article

Amperometric Biosensors for L-Arginine Determination Based on L-Arginine Oxidase and Peroxidase-Like Nanozymes

Nataliya Stasyuk [1], Galina Gayda [1,*], Olha Demkiv [1,2], Lyubomyr Darmohray [2], Mykhailo Gonchar [1] and Marina Nisnevitch [3,*]

[1] Institute of Cell Biology, National Academy of Sciences of Ukraine, 79005 Lviv, Ukraine; stasukne@nas.gov.ua (N.S.); demkivo@nas.gov.ua (O.D.); gonchar@cellbiol.ua (M.G.)
[2] Faculty of Veterinary Hygiene, Ecology and Law, Stepan Gzhytskyi National University of Veterinary Medicine and Biotechnologies, 79000 Lviv, Ukraine; animalfeedinglvet50@i.ua
[3] Department of Chemical Engineering, Ariel University, Kyriat-ha-Mada, Ariel 4070000, Israel
* Correspondence: galina.gayda@nas.gov.ua (G.G.); marinan@ariel.ac.il (M.N.); Tel.: +380-226-2144 (G.G.); +972-3914-3042 (M.N.)

Abstract: There are limited data on amperometric biosensors (ABSs) for L-arginine (Arg) determination based on oxidases that produce hydrogen peroxide (H_2O_2) as a byproduct of enzymatic reaction, and artificial peroxidases (POs) for decomposition of H_2O_2. The most frequently proposed Arg-sensitive oxidase-based ABSs contain at least two enzymes in the bioselective layer; this complicates the procedure and increases the cost of analysis. Therefore, the construction of a one-enzyme ABS for Arg analysis is a practical problem. In the current work, fabrication, and characterization of three ABS types for the direct measurement of Arg were proposed. L-arginine oxidase (ArgO) isolated from the mushroom *Amanita phalloides* was co-immobilized with PO-like nanozymes (NZs) on the surface of graphite electrodes. As PO mimetics, chemically synthesized NZs of CeCu (nCeCU) and NiPtPd (nNiPtPd), as well as green-synthesized hexacyanoferrate of copper (gCuHCF), were used. The novel ABSs exhibited high sensitivity and selectivity to Arg, broad linear ranges and good storage stabilities. Two ABSs were tested on real samples of products containing Arg, including the pharmaceutical preparation "Tivortine", juices, and wine. A high correlation (R = 0.995) was demonstrated between the results of testing "Tivortine" and juice using nCeCU/GE and nNiPtPd/GE. It is worth mentioning that only a slight difference (less than 1%) was observed for "Tivortin" between the experimentally determined content of Arg and its value declared by the producer. The proposed ArgO-NZ-based ABSs may be promising for Arg analysis in different branches of science, medicine, and industry.

Keywords: L-arginine analysis; amperometric biosensors; L-arginine oxidase; hydrogen peroxide; artificial peroxidase

Citation: Stasyuk, N.; Gayda, G.; Demkiv, O.; Darmohray, L; Gonchar, M.; Nisnevitch, M. Amperometric Biosensors for L-Arginine Determination Based on L-Arginine Oxidase and Peroxidase-like Nanozymes. *Appl. Sci.* **2021**, *11*, 7024. https://doi.org/10.3390/app11157024

Academic Editor: Chih-Ching Huang

Received: 20 June 2021
Accepted: 27 July 2021
Published: 29 July 2021

Publisher's Note: MDPI stays neutral with regard to jurisdictional claims in published maps and institutional affiliations.

Copyright: © 2021 by the authors. Licensee MDPI, Basel, Switzerland. This article is an open access article distributed under the terms and conditions of the Creative Commons Attribution (CC BY) license (http://creativecommons.org/licenses/by/4.0/).

1. Introduction

L-arginine (Arg) concentration is an important indicator of food and food-supplement quality, as well as an important biomarker in clinical diagnostics and nutritional status assessment [1–6]. A variety of optical and electrochemical methods for Arg determination have been developed to date [7–15]. To improve their selectivity, enzymatic approaches have been developed, including electrochemical biosensors [10–16].

Biosensor systems have many advantages over other techniques [17]. In general, enzyme-based biosensors for Arg determination rely on the measurement of reactants consumed or products generated from enzymatic cascade reactions, including ammonium ions or H_2O_2 [13,18].

The highly selective enzymes of Arg metabolism are promising tools for biosensor construction. For Arg analysis, arginine decarboxylase, L-arginase, with urease [12,14,19–

25], arginine deiminase (ADI) [26–28], and L-arginine oxidase (ArgO) with peroxidase [29–33] may be utilized. However, the necessity of several enzymes in the bioselective layer complicates the process of biosensor fabrication, increases the cost of analysis, and causes losses in bioelectrode stability and sensitivity. Thus, using only one enzyme may be a more promising method for the fabrication of biosensors.

Alternately, many efforts have been devoted in recent years to the development of non-enzymatic sensors. This approach is based on functional materials of different compositions, including nanomaterials. A limitation of this method is insufficient selectivity to the target analyte [34–38]. Nanomaterials with intrinsic enzyme-like activities or nanozymes (NZs) are promising alternatives to natural enzymes in biosensor construction. Artificial POs are the most urgently needed type of NZs for this goal.

A limited number of amperometric biosensors (ABSs), especially mono-enzyme ABSs, have been developed to date to measure Arg concentrations [13,27]. Yet a simple construction of stable ABSs based on one oxidase, namely ArgO, co-immobilized with H_2O_2-sensitive NZs in a bioselective layer, remains a real problem.

ArgO (L-arginine: oxygen oxidoreductase, EC 1.4.3.25) belongs to a class of oxidases of L-amino acids, that are accumulated in the tissues of some mammals, marine mollusks, and fish, in fungi, algae, bacteria, in the venoms of insects and snakes in the fruiting bodies of poisonous mushrooms [39–44]. Oxidases of L-amino acids are promising analytical tools for quantifying the concentrations of the corresponding L-amino acids in different samples [30,31].

ArgO is a poorly studied enzyme to date, as evidenced by a limited list of publications on the problem [29,30,39].

ArgO is a FAD-containing enzyme that catalyzes the conversion of Arg to 5-guanidino-2-oxopentanoate, ammonia and hydrogen peroxide. The enzymatic conversion of Arg is presented in Scheme 1

$$\text{L-arginine} + H_2O + O_2 \rightarrow \text{5-guanidino-2-oxopentanoate} + NH_3 + H_2O_2$$

Scheme 1. Reaction of Arg oxidation under catalysis by ArgO.

In the current work, we report the development and application of ArgO-based ABSs for the direct measurement of Arg. The fabricated ABSs contain purified mushroom ArgO, co-immobilized with H_2O_2-sensitive nanoparticles on the surfaces of graphite electrodes. A laboratory prototype of the proposed ABSs was tested for Arg determination in samples of juices, wine, and a commercial pharmaceutical.

2. Materials and Methods

2.1. Reagents

Nickel(II) sulfate ($NiSO_4$), cerium(IV) bicarbonate ($Ce(HCO_3)_4$), chloroplatinic acid (H_2PtCl_6), copper(II) sulfate ($CuSO_4$), L-arginine, o-dianisidine, hydrogen peroxide (H_2O_2, 30%), palladium chloride ($PdCl_3$), sodium borohydride ($NaBH_4$), Nafion (5% solution in 90% low-chain aliphatic alcohols), and all other reagents and solvents used in this work were purchased from Sigma-Aldrich (Steinheim, Germany). All reagents were of analytical grade and were used without further purification. All solutions were prepared using ultra-pure water obtained with the Milli-Q® IQ 7000 Water Purification system (Merck KGaA, Darmstadt, Germany).

2.2. Enzyme Isolation and Purification

Purified mushroom enzyme—L-arginine oxidase (ArgO) was used for the fabrication of the amperometric biosensor. ArgO was isolated from an extract of the fruiting body of the wild forest mushroom *Amanita phalloides* by a two-step ammonium sulfate fractionation (at double 70% of saturation), followed by ion exchange chromatography on

Toyopearl DEAE-650M resin [45]. The scheme of the procedure for obtaining ArgO and the method of monitoring enzymatic activity are presented in Scheme A1.

Activity of ArgO was determined by the rate of hydrogen peroxide formation in reaction with Arg, as monitored by the peroxidative oxidation of *o*-dianisidine. Activity was measured in a reaction mixture with a final volume of 1.0 mL, containing 50 mM phosphate buffer, pH 7.5, 0.25 mM *o*-dianisidine, horseradish peroxidase (0.07 mg/mL), 25 mM Arg, and appropriate amount of enzyme. After incubation for an exact time (1–10 min) at 30 °C, and upon appearance of the orange color, the reaction was stopped by the addition of 0.26 mL of 12 M HCl. The generated pink color was determined at 525 nm using a spectrophotometer. The millimolar extinction coefficient of the resulting dye in the acidic solution was 13.38 $mM^{-1} \cdot cm^{-1}$. One unit of ArgO activity is defined as the amount of enzyme releasing 1 μmol H_2O_2 per 1 min under standard assay conditions. Protein concentration is determined by the Lowry method. Partially purified ArgO with the specific activity 7.9 $mU \cdot mg^{-1}$ of protein was kept as suspension in 70% sulfate ammonium, 50 mM phosphate buffer, pH 7.5, at 4 °C.

2.3. Synthesis of PO-like NZs

Nanoparticles of CeCu (further—nCeCu) were synthesized as described earlier [46]: 1 mL of 0.1 M $CeCl_3 \cdot 7H_2O$ was mixed with 0.2 mL 10 mM Na_2S, followed by adding 1 mL of 100 mM $CuSO_4$, and incubation without stirring for 1 h at 20 °C.

Green hexacyanoferrate of copper (gCuHCF) was synthesized via the enzyme flavocytochrome b_2 as described earlier [47]. A reaction mixture containing 6 mM $K_3Fe(CN)_6$, 20 mM sodium lactate, and 0.1 U/mL enzyme in 50 mM phosphate buffer, pH 8.0, was incubated at 37 °C for 30 min. Formation of gCuHCFs was initiated by addition of $CuSO_4 \cdot 5H_2O$ to a final concentration of 10 mM.

Nanoparticles of NiPtPd (further—nNiPtPd) were synthesized according to the following protocol: to prepare the solution A, 2 mL 2% H_2PtCl_6 mixed with 2 mL 2% $PdCl_3$ were vigorously stirred for 15 min at 20 °C, followed by adding 0.1 mL 100 mM $NaBH_4$; to prepare the solution B, 2 mL 2% $CuSO_4$ or $NiSO_4 \cdot 7H_2O$ or $FeCl_3 \cdot 6H_2O$ were vigorously stirred for 15 min at 20 °C, followed by adding 0.05 mL 100 mM $NaBH_4$; to obtain nNiPtPd, solutions A and B were mixed, 0.02 mL of 10 mM NaOH was added, and the reaction mixture was incubated without stirring for 24 h at 20 °C.

All synthesized NZs were collected with centrifugation. The precipitates were rinsed twice with water and were stored as a water suspension at +4 °C until used.

2.4. Assay of Enzyme-like Activities of the Synthesized PO-like NZs in Solution

PO-like activity of the nanoparticles was measured by the colorimetric method, with *o*-dianisidine as a chromogenic substrate in the presence of H_2O_2. The procedure was as described earlier [47]. One unit (U) of PO-like activity was defined as the amount of NZs releasing 1 μmol H_2O_2 per 1 min at 30 °C under standard assay conditions. To estimate special enzyme-like activity (U/mg), the NZs were dried. The tested solution/suspension was prepared by weighing the solid substance and adding water until the needed concentration was obtained.

The assay of PO-like activity: 10 μL of the aqueous suspension of NZs(1 $mg \cdot mL^{-1}$) was incubated with 1 mL of 0.17 mM *o*-dianisidine in water (as a control), and with the same substrate in the presence of 8.8 mM H_2O_2 (as a substrate for PO). Addition of NZs to the substrate stimulated the development of an orange color over time, indicating an enzymatic reaction. The enzyme-mimetic activity could be assessed qualitatively with the naked eye and was measured quantitatively with a spectrophotometer. After incubation for an exact time (1–10 min) at 30 °C, and upon appearance of the orange color, the reaction was stopped by the addition of 0.26 mL 12 M HCl. The generated pink color was determined at 525 nm using a spectrophotometer. The millimolar extinction coefficient of the resulting pink dye in the acidic solution was 13.38 $mM^{-1} \cdot cm^{-1}$.

2.5. Sensor Evaluation

2.5.1. Apparatus and Measurements

The amperometric sensors were evaluated as described in [47]. In brief, constant–potential amperometry was performed in a three-electrode configuration with an Ag/AgCl/KCl (3 M) as an reference electrode, a Pt-wire as a counter electrode, and a working graphite electrode

Amperometric measurements were carried out as described in [47].

All the experiments were carried out in triplicates. Analytical characteristics of the electrodes were statistically processed using the OriginPro 8.5 software. Error bars in the graphs represent standard errors derived from three independent measurements. Calculation of the apparent Michaelis–Menten constants (K_M^{app}) was performed as described in [47].

2.5.2. Immobilization of NZs and Enzyme on the GE Surface

The NZs and ArgO were co-immobilized on the GEs using the physical adsorption method.

For development of the NZs-based electrode, 5–10 µL of NZs solution with PO-like activity of 1 U/mL was dropped onto the surface of bulk GEs. After drying for 10 min at room temperature, the layer of NZs on the electrode was covered with 10 µL of Nafion. The modified electrodes were rinsed with 50 mM phosphate buffer, pH 7.0, and kept in this buffer with 0.1 mM EDTA at 4 °C until used.

To fabricate the ArgO-based biosensor, 5–10 µL of ArgO solution in 50 mM phosphate buffer, pH 7.0 (0.7 U/mL), was dropped onto the dried surface of the NZ-modified GE. The dried composite was covered by a Nafion membrane. The coated bioelectrode was rinsed with water and stored in phosphate buffer, pH 7.0, until used.

2.6. Preparation of the Real Samples for Biosensor Analysis

The samples used for Arg analysis included the pharmaceutical preparation "Tivortine" (Yuria-Pharm LLC., Cherkasy, Ukraine); freshly prepared apple juice (Wax apple fruit); commercial juices by "Sadochok" (LtD Sandora, Odessa, Ukraine)—peach, multifruit, grape with apple; by "Galicia" (T.B. Fruit Company, Gorodok, Ukraine)—apple with pear; and "Tempranillo" dry red wine (TM "Vina Cruz", Ukraine). All samples were analyzed using a standard addition test (SAT). Before assay, all samples were diluted stepwise in 50 mM phosphate buffer, pH 7.0, containing 1 mM EDTA. Each assay was performed for two dilutions of the sample and repeated three times. The analytical results were statistically processed using the OriginPro 2021 software.

3. Results and Discussion

3.1. Amperometric Characteristics of the PO-like NZs/GE

In our previous works, different types of PO-like NZs were described: a chemically synthesized NZs [46] and a 'green' synthesized one [47]. The most effective electroactive NZs, nCeCu, and gCuHCF, were chosen for further study. These and the newly obtained promising artificial PO, nNiPtPd, were characterized by Scanning electron microscopy (SEM) coupled with X-ray microanalysis (SEM-XRM) and were used here as potential platforms for construction of Arg-sensitive ArgO-based ABSs. SEM provided information on the size, distribution, and shape of the tested sample. Figures A1–A3 present the overall morphology of the formed hybrid particles, namely, nCeCu, nNiPtPd, and gCuHCF, respectively. The XRM images of the synthesized NZs showed the characteristic peaks for metals of the composites.

The amperometric characteristics of the nCeCu/GE and nNiPtPd/GE as effective chemosensors for H_2O_2 determination were studied (Figures 1 and 2, respectively). The cyclic voltammograms (CV) for the nCeCu/GE (Figure 1a) and for the nNiPtPd/GE (Figure 2a) demonstrated that cathodic reduction peaks contributed from H_2O_2 decomposition

arose at potentials of approximately −50 mV and −200 mV, respectively (vs. Ag/AgCl). The chronamperometric dependences and calibration graphs for H_2O_2 determination are shown in Figures 1 and 2b–d, respectively. As a control, unmodified GE was tested, and no signal was detected upon H_2O_2 addition (data not shown).

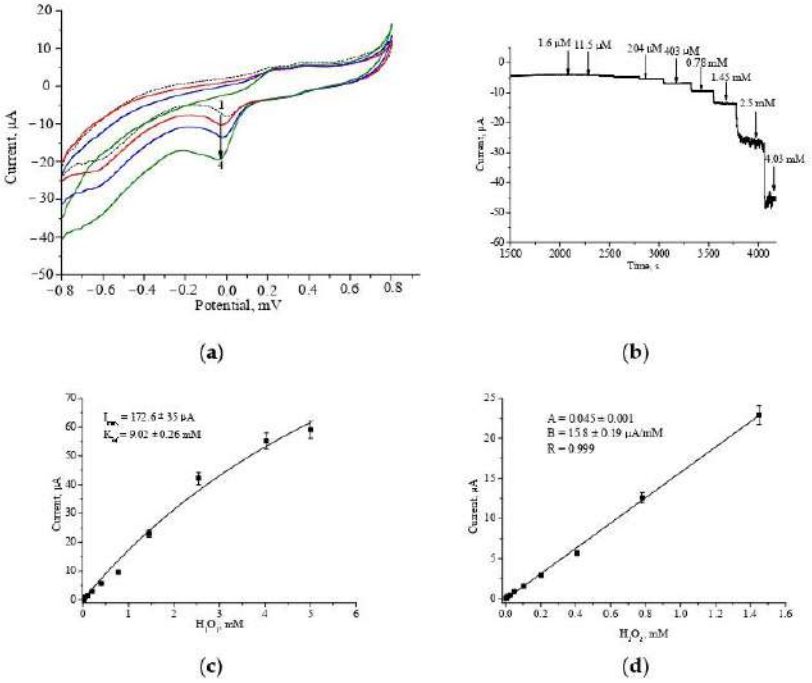

Figure 1. Amperometric characteristics of nCeCu/GE: (**a**) Cyclic voltammograms as current responses upon addition of H_2O_2 up to concentrations: (1) 0 mM (black), (2) 2.5 mM (red); (3) 5.0 mM (blue); (4) 10 mM (green); (**b**,**c**) chronamperometric response and dependence of amperometric signal on concentration of H_2O_2, respectively; (**d**) calibration graph for H_2O_2 determination. Conditions: Ag/AgCl (reference electrode) in 50 mM phosphate buffer, pH 7.0; scan rate 50 mV·s^{-1} (**a**); working potential −50 mV (**b**–**d**). A and B are parameters of a linear regression: Y = A + BX, and R is a correlation coefficient.

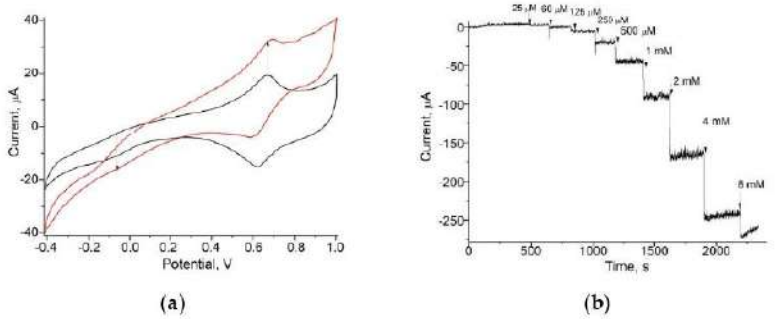

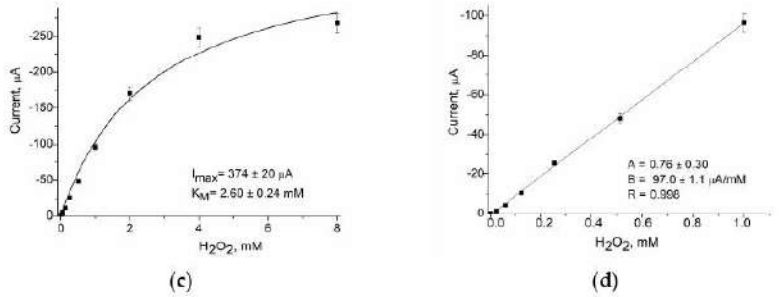

Figure 2. Amperometric characteristics of nNiPtPd/GE: (**a**) Cyclic voltammograms as current responses upon addition of H_2O_2 up to concentrations: (1) 0 mM (black), (2) 0.5 mM (red); (**b**) chronamperometric response and (**c**) dependence of amperometric signal on concentration of H_2O_2; (**d**) calibration graph for H_2O_2 determination. Conditions: Ag/AgCl (reference electrode) in 50 mM phosphate buffer, pH 7.0; scan rate 50 mV·s^{-1} (**a**); working potential −200 mV (**b**–**d**).

The analytical characteristics of the developed amperometric NZ-based chemosensors for H_2O_2 are summarized in Table 1. It is worth mentioning that the apparent value of the Michaelis–Menten constant (K_M^{app}) represents the analyte concentration yielding an amperometric response equal to half of its maximum value (I_{max}). Sensitivity of an amperometric electrode is usually calculated from the linearity graph as a ratio of slope (B) to the active surface area of the working electrode. Sensitivity data are expressed in standard SI units, A·M^{-1}·m^{-2}. This parameter, contrary to Imax, does not depend on the electrode area; it characterizes the specific activity of the electrode. The limit of detection (LOD) of a (bio)sensor is the triplicated standard deviation value of blank samples divided by the slope of the calibration graph.

Table 1. Analytical characteristics of the PO-like NZ/GE as a chemosensor for H_2O_2

PO-like NZ	Sensitivity, A·M^{-1}·m^{-2}	Linear Range, Up to, mM	LOD, μM	I_{max}, μA	K_M^{app}, mM	Reference
nCeCu	2164 ± 70	1.5	0.5	172.6 ± 1.1	9.0 ± 0.05	Current work
nNiPtPd	13250 ± 150	1.0	5	374 ± 20	2.6 ± 0.24	Current work
gCuHCF	1620	0.8	10	138.0 ± 8.5	31.0 ± 4.4	47

Thus, our results demonstrated that the synthesized PO-like NZs which have excellent sensitivities (nNiPtPd and nCeCu) and wide linear ranges for H_2O_2 detection may be promising artificial POs for the construction of oxidase-based ABSs.

3.2. Evaluation and Optimization of the Arg-Sensitive Bioelectrodes

The aim of our work was to construct ArgO-based ABSs for Arg determination using NZs as PO-mimetics. To form an enzymatic layer of the bio-electrode, NZs were coupled with ArgO on a GE and covered with Nafion, as described in the experimental part (see Section 2.5.2). The general principle of Arg assay by the developed ABSs is based on the detection of H_2O_2 generated as a result of Arg hydrolysis under ArgO catalysis (Scheme 1).

The efficiency of freely defusing electron transfers from the oxidized ArgO to the electrode via PO-like NZs (as mediator) was evaluated using CV (Figure 2a or Figure 3a). As it was shown there, the potential −150 mV vs. Ag/AgCl was chosen as the optimal working potential for ArgO reduction in our system.

The obtained ABSs (namely, ArgO/nCeCu/GE, ArgO/nNiPtPd/GE, and ArgO/gCuHCF/GE) were used for the investigation of the analytical parameters. Figures

3–5 demonstrate the amperometric properties of the developed ABSs. Current responses of the ABSs to the stepwise addition of a standard Arg solution were tested.

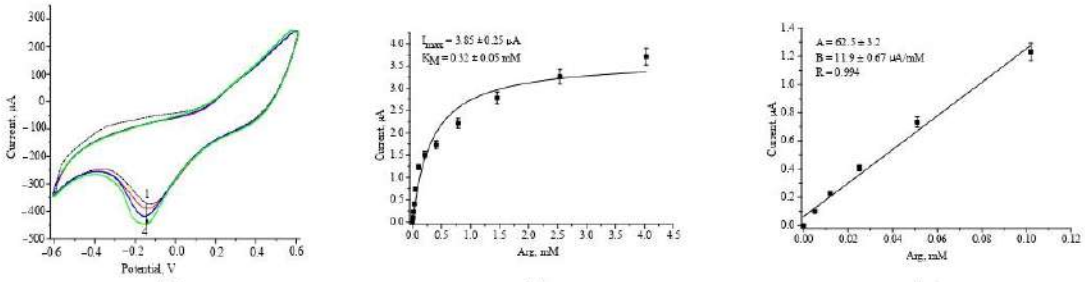

(**a**) (**b**) (**c**)

Figure 3. Amperometric characteristics of ArgO/nCeCu/GE: (**a**) CV profiles as current responses upon addition of Arg up to final concentrations: (**1**) 0 mM (drop-black), (2) 2.4 mM (red); (3) 6.5 mM (blue); (4) 13 mM (green); (**b**) dependence of amperometric signal on concentration of Arg; (**c**) calibration graph for Arg determination. Conditions: Ag/AgCl (reference electrode) in 50 mM phosphate buffer, pH 7.0; scan rate 50 mV·s^{-1} (**a**); working potential −150 mV (**b**–**c**).

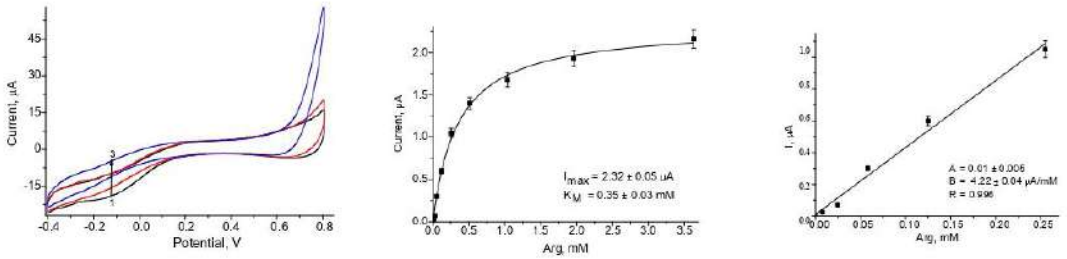

(**a**) (**b**) (**c**)

Figure 4. Amperometric characteristics of ArgO/nNiPtPd/GE: (**a**) CV profiles as current responses upon addition of Arg up to final concentrations: (1) 0 mM (black), (2) 0.6 mM (red); (3) 1.2 mM (blue), scan rate 50 mV·s^{-1}; (**b**) dependence of amperometric signal on concentration of Arg; (**c**) calibration graph for Arg determination. Conditions: working potential −150 mV vs. Ag/AgCl/3 M KCl in 50 mM phosphate buffer, pH 7.0.

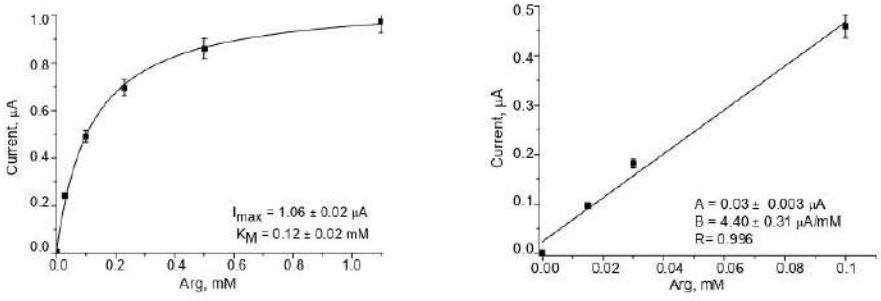

(**a**) (**b**)

Figure 5. Amperometric characteristics of ArgO/gCuHCF/GE: (**a**) dependence of amperometric signal on concentration of Arg; (**b**) calibration graph for Arg determination. Conditions: working potential −150 mV vs. Ag/AgCl/3 M KCl in 50 mM phosphate buffer, pH 7.0.

The prepared ABSs in this research, based on ArgO and NZs, demonstrated several advantages compared to the previously reported ones (Table 2). Our ABSs are highly

selective, rapid, extremely sensitive, easy to use, reliable and portable. Additionally, the developed ABSs are cost-effective because they require only one enzyme (ArgO) and rather inexpensive functional nanomaterials as mimetics of the costly enzyme (PO).

Table 2. Analytical characteristics of the developed ABSs for Arg determination

Bioelectrode	Sensitivity, $A \cdot M^{-1} \cdot m^{-2}$	Linear Range, μM	Response Time, s (95%)	K_M^{app}, mM	Reference
Arginase/ urease/PANi/Pt	110 ± 1.3	70–600	10	1.27 ± 0.29	21
[1] p-cells/urease/PANi/Pt	14 ± 1.2	up to 600	60	0.51 ± 0.05	22
Arginase-nAu- p-cells/urease/PANi/Pt	357 ± 24	10–700	30	0.45 ± 0.09	25
ADI/PANi/Cu	684 ± 32	3–200	15	0.31 ± 0.05	26
ArgO/nCeCu/GE	1630 ± 92	5–100	60	0.32 ± 0.05	Current work
ArgO/nNiPtPd/GE	578 ± 5	10–250	50	0.35 ± 0.03	Current work
ArgO/gCuHCF/GE	602 ± 42	10–100	50	0.12 ± 0.02	Current work

[1] p-cells—permeabilized yeast cells.

The values of K_M^{app} for Arg estimated with ArgO/nCeCu/GE and ArgO/nNiPtPd/GE are 0.32 ± 0.05 mM and 0.35 ± 0.03 mM, respectively. These values are practically identical with that for ADI in solution (0.35 mM) [28].

The application of NZs in a bioselective layer has a positive impact on the ABSs properties, due to their lower LODs for Arg determination and their high sensitivities.

The constructed ArgO-based biosensors demonstrate slower amperometric responses (up to 50–60 s) in comparison with the previously reported by us biosensors on Arg [21,26]. The arginase/urease/PANi/Pt- and ADI/PANi/Nafion/Pt-SPE-based ABSs demonstrated the response times 10 s [21] and 15 s [26], respectively. This phenomenon may be explained by different contents of enzymes in sensing films as well as by different origins and areas of working electrodes. In our present work, only (3–7) mU ArgO were contained in the biorecognition film on the surface of each ArgO/NZ-modified electrodes. Previously, ADI was immobilized in PANi/Nafion film on the surface of Pt-SPE at much higher amount (540 mU) [26].

The stabilities of the developed ArgO-based ABSs were explored by monitoring their responses to the injection of a 0.2 mM Arg standard solution over a period of seven days. The ArgO/nCeCu/GE and ArgO/nNiPtPd/GE preserved around 50% stability after five days of storage, and likewise the ArgO/gCuHCF/GE—after three days. Contrary, the reported ADI/PANi/Nafion/Pt-SPE-based biosensor was very stable. It kept more than 90% stability after 35 days of storage [26]. This phenomenon may be explained by several reasons: (1) Highly purified recombinant enzyme ADI with the high specific activity was used for construction of the ADI-based ABS, whereas in this work, we used only partially purified ArgO; (2) ADI in the biosensing layer was stabilized with BSA, but in the present work ArgO was not stabilized additionally; (3) Proteins ADI and BSA in the biosensing layer were covalently immobilized on PANi/Nafion by cross-linking using glutaraldehyde. In the present work, ArgO was immobilized on the surface of a NZ-modified electrode by physical adsorption and covered by Nafion.

The selectivities of the proposed ArgO/NZ-based ABSs to the target analyte (Arg) are of great importance, especially for analysis of real samples of beverages. The selectivity of the constructed ArgO/nCeCu/GE was estimated in relative units (%) as a ratio of the detected signal to the value of the highest current response (Figure A4): no signals were observed for most of the tested amino acids (L-Glu, L-Gln, D, L-Leu, L-Asp). Only L-Lys and D,L-Phe induced a nonsignificant (less than 10%) analytical signal.

3.3. Assay of Arg in Real Samples

In order to demonstrate the applicability of the constructed ArgO-based ABSs for testing real products containing Arg, selected samples of fruit juices and wine, as well as the pharmaceutical preparation "Tivortin", were analyzed. The estimation of Arg

concentration in the sample of fresh-prepared apple juice is presented in Figure 6. The Arg analysis was performed using the graphical method known as "the standard addition test" (SAT) with different dilutions of the tested sample. The SAT is a quantitative analysis approach often used in analytical chemistry when a standard solution of the target analyte (in this case, Arg) is added directly to the aliquots of the analyzed sample. The SAT method is used in situations where sample components also contribute to the analytical signal [10]. Other samples of juices and wine were analyzed by the developed ABSs in the same manner; the estimated Arg contents in the tested samples are summarized in Table 3.

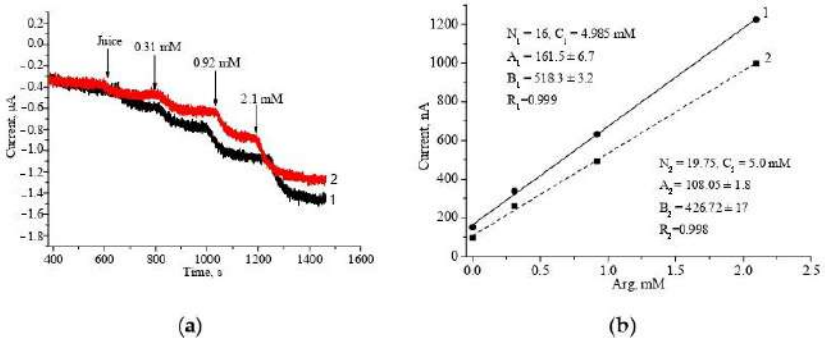

(a) (b)

Figure 6. Graphical SAT method for Arg assay in the real sample of freshly prepared apple juice using ArgO/nCeCu/GE: (**a**) chronoamperograms, (**b**) calibration graphs. A, B—parameters for the linear regression; N—dilution factor; R—correlation coefficient.

The Arg determination in the pharmaceutical product "Tivortin" using two ABSs are shown in Figure 7 and in Table 3.

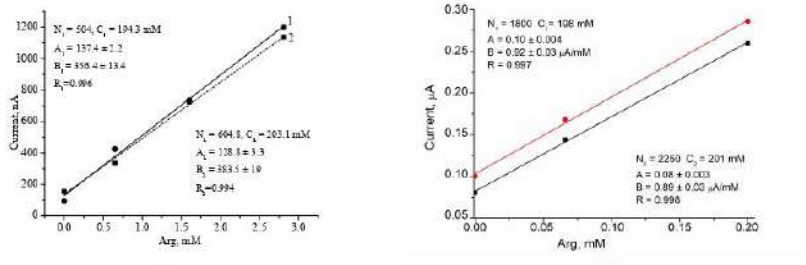

(a) (b)

Figure 7. Graphical SAT method for Arg assay in the real sample of "Tivortin" using AgO/nCeCu/GE (**a**) and ArgO/nNiPtPd/GE (**b**). A, B—parameters for the linear regression; N—dilution factor; R—correlation coefficient.

Table 3. Results of Arg determination (C) in the real samples using different ArgO-NZ-based biosensors

NZ As H_2O_2-Sensor	nCeCu		nNiPtPd	
Sample	C, mM	[1] CV, %	C, mM	CV, %
Pharmaceutical "Tivortine"	198.7 ± 6.22	3.1	199.5 ± 2.12	1.06
Commercial apple-pear juice	7.1 ± 0.08	1.1	7.4 ± 0.5	6.8
Freshly prepared apple juice	4.99 ± 0.001	0.02	[2] ND	-
Commercial grape-apple juice	8.71 ± 0.43	4.9	ND	-
Commercial multifruit juice	6.14 ± 0.25	4.1	ND	-
Wine, red, dry	3.26 ± 0.09	2.8	ND	-

[1] CV, %—coefficient of variation, values are expressed as mean ± SD; [2] ND—not determined.

The reproducibility of the proposed analytical methods is satisfactory: the coefficients of variation (CV) are less than 5%. It is worthwhile mentioning that the detected Arg contents in the juices and wine were close to those published by other authors (0–11 mM) [48–50]. Figure A5 shows that the Arg content values in the pharmaceutical product "Tivortin" and the apple-pear juice, estimated by both ABSs (ArgO/nCeCu/GE and ArgO/nNiPtPd/GE), were strongly correlated with each other (R = 0.995). Additionally, only a slight difference (less than 1%) was observed for "Tivortin" between the experimentally determined content of Arg (199.1 mM) and its value declared by the producer (199.8 mM).

These results indicate that the developed mono-enzyme ABSs (namely, ArgO/nCeCu/GE and ArgO/nNiPtPd/GE) can be utilized for a fast and simple assay of Arg in pharmaceutic preparations.

4. Conclusions

Novel L-arginine-selective amperometric biosensors (ABSs) based on mushroom-derived L-arginine oxidase and metal-based nanozymes as 'artificial peroxidases' are described. Substitution of PO with PO-like mimetics in a biosensing layer improved the electrochemical properties of the electrodes and the detection of Arg in wider ranges of linear responses.

The nCeCu, nNiPtPd, and gCuHCF, as the most effective PO mimetics, can be used as H_2O_2-sensitive platforms for the development of ArgO-based ABSs. These ABSs exhibit very high sensitivities and broad linear ranges to Arg when tested on real samples of pharmaceuticals and juices.

Thus, the developed mono-enzyme nanozymes-based ABSs may be used in analytical practice for fast and simple assay of Arg in beverages, pharmaceutic preparations, and other goods. An extremely high sensitivity of the proposed ArgO/nCeCu-based ABS makes it promising in clinical diagnostics for Arg determination in blood and other biological liquids.

Author Contributions: Conceptualization, G.G.; Methodology, G.G., N.S. and O.D.; Investigation, N.S., O.D. and L.D.; Resources, M.G. and M.N.; Data curation, G.G. and M.G.; Writing—original draft preparation, N.S., O.D. and G.G.; Writing—review and editing, G.G., M.G. and M.N.; Supervision, G.G. and M.G.; Project administration, G.G.; Funding acquisition, M.G. and M.N. All authors have read and agreed to the published version of the manuscript.

Funding: This research was partially funded by NAS of Ukraine (The program "Smart sensor devices of a new generation based on modern materials and technologies"; grant "New dual casein kinase 2 inhibitors and histone deacetylase for targeted tumor chemotherapy" for research laboratories/groups of young scientists in priority areas of science and technology in 2021–2022), by National Research Foundation of Ukraine (project 2020.02/0100 "Development of new nanozymes as catalytic elements for enzymatic kits and chemo/biosensors"), by the Ministry of Education and Science of Ukraine (Ukrainian-Lithuanian R&D, project 0120U103398), and by the Research Authority of the Ariel University, Israel.

Institutional Review Board Statement: Not applicable.

Informed Consent Statement: Not applicable.

Data Availability Statement: The data are presented in this study, in Appendix A and are available on request from the corresponding authors.

Acknowledgments: We acknowledge the engineer Roman Ya. Serkiz for his help with SEM-XRM experiments (Institute of Cell Biology, Lviv, Ukraine).

Conflicts of Interest: The authors declare no conflict of interest.

Appendix A

Appendix A presents the overall morphology of the hybrid particles nCeCu, nNiPtPd, and gCuHCF (Figures A1–A3 respectively), data on the selectivity of the constructed ArgO/nCeCu/GE (Figure A4), data on Arg content in the pharmaceutical product "Tivortin" and the apple-pear juice (Figure A5), and the procedure of ArgO obtaining (Scheme A1).

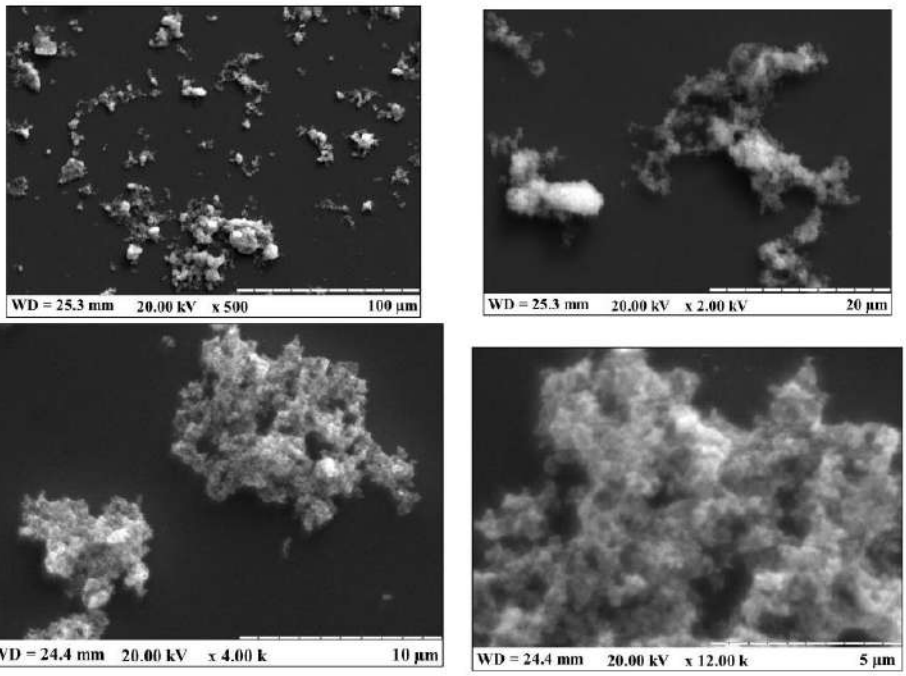

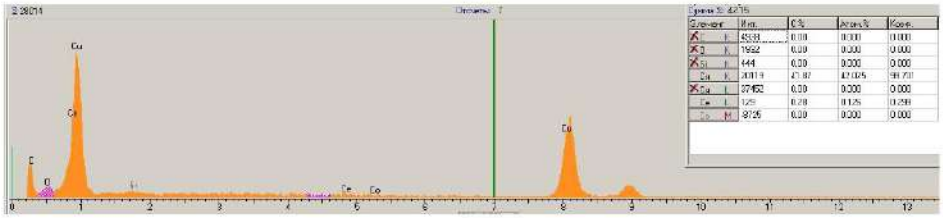

Figure A1. Characteristics of the nCeCu: EM images at different magnifications (top) and their X-ray spectral characteristics (bottom).

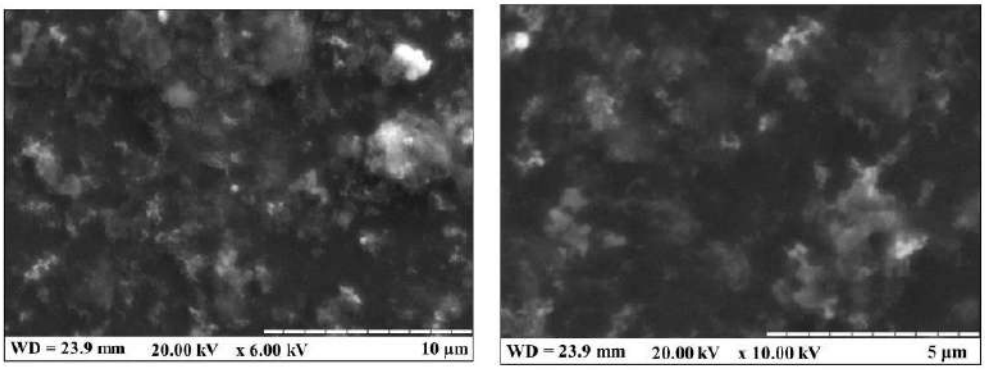

Figure A2. Characteristics of the nNiPtPd: SEM images at different magnifications (top) and their X-ray spectral characteristics (bottom).

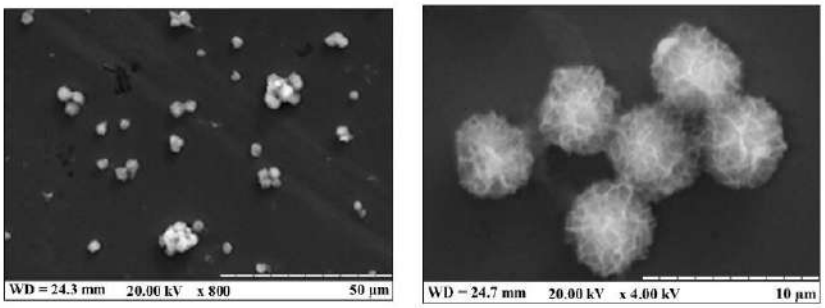

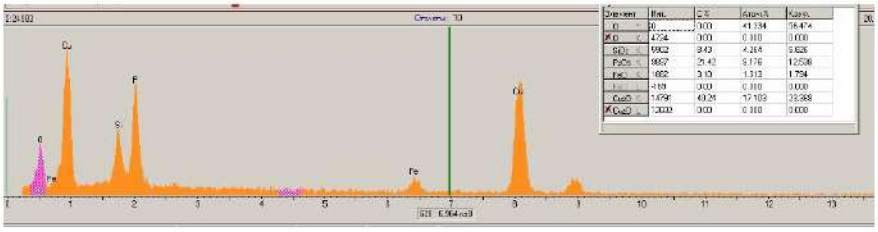

Figure A3. Characteristics of the gCuHCF: SEM images at different magnifications (top) and their X-ray spectral characteristics (bottom).

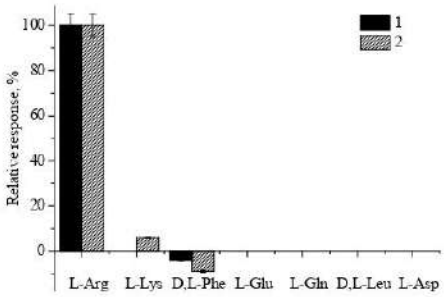

Figure A4. Selectivity for ArgO/nCeCu/GE. Selectivity test was performed with 5 mM (1) and 10 mM (2) solutions of aminoacids under applied potential of –150 mV at 22 ◦C. The highest current response on Arg was chosen as 100%.

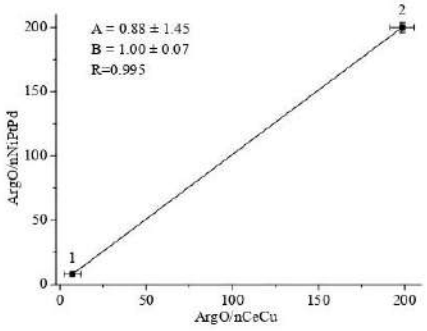

Figure A5. Correlation between the results of Arg determination in the real samples by two bioelectrodes: ArgO/nCeCu/GE and ArgO/nNiPtPd/GE. The tested samples: commercial juice "Galicia" apple-pear (1) and Tivortin (2).

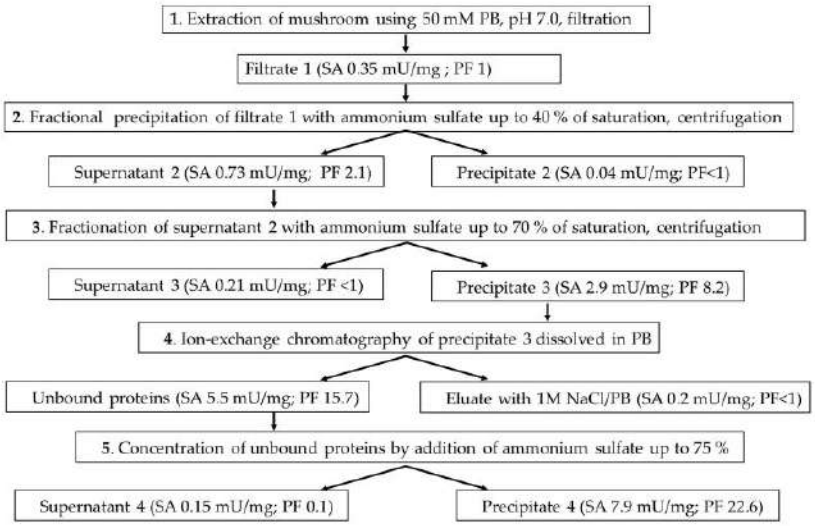

Scheme A1. Isolation and purification of ArgO. PB—phosphate buffer, SA—specific activity, mU/mg of protein, PF—purification factor.

References

1. Wu, G.; Bazer, F.W.; Davis, T.A.; Kim, S.W.; Li, P.; Marc Rhoads, J.; Carey Satterfield, M.; Smith, S.B.; Spencer, T.E.; Yin, Y. Arginine metabolism and nutrition in growth, health and disease. *Amino Acids* **2009**, *37*, 153–168, doi:10.1007/s00726-008-0210-y.
2. Huang, J.; Ladeiras, D.; Yu, Y.; Ming, X.F.; Yang, Z. Detrimental Effects of Chronic L-Arginine Rich Food on Aging Kidney. *Front. Pharmacol.* **2021**, *11*, 582155, doi:10.3389/fphar.2020.582155.
3. McNeal, C.J.; Meininger, C.J.; Reddy, D.; Wilborn, C.D.; Wu, G. Safety and effectiveness of arginine in adults. *J. Nutr.* **2016**, *146*, 2587S–2593S, doi:10.3945/jn.116.234740.
4. Bednarz-Misa, I.; Fleszar, M.G.; Zawadzki, M.; Kapturkiewicz, B.; Kubiak, A.; Neubauer, K.; Witkiewicz, W.; Krzystek-Korpacka, M. L-Arginine/NO pathway metabolites in colorectal cancer: Relevance as disease biomarkers and predictors of adverse clinical outcomes following surgery. *J. Clin. Med.* **2020**, *9*, 1782, doi:10.3390/jcm9061782.
5. Mirmiran, P.; Bahadoran, Z.; Gaeini, Z.; Azizi, F. Habitual intake of dietary L-arginine in relation to risk of type 2 diabetes: A prospective study. *BMC Endocr. Disord.* **2021**, *21*, 113, doi:10.1186/s12902-021-00774-x.
6. Grimes, J.M.; Khan, S.; Badeaux, M.; Rao, R.M.; Rowlinson, S.W.; Carvajal, R.D. Arginine depletion as a therapeutic approach for patients with COVID-19. *Int. J. Infect. Dis.* **2021**, *102*, 566–570, doi:10.1016/j.ijid.2020.10.100.
7. Stasyuk, N.; Gayda, G.; Zakalskiy, A.; Zakalska, O.; Fayura, L.; Vovk, O.; Stasyk, O.; Sibirny, A.; Gonchar, M. Recombinant Forms of Arginase and Arginine Deiminase as Catalytic Components of Argitest Enzymatic Kit. *Sci. Innov.* **2017**, *13*, 56–63, doi:10.15407/scine13.04.056.
8. He, Y.; Zhou, L.; Deng, L.; Feng, Z.; Cao, Z.; Yin, Y. An electrochemical impedimetric sensing platform based on a peptide aptamer identified by high-throughput molecular docking for sensitive L-arginine detection. *Bioelectrochemistry* **2021**, *137*, 107634, doi:10.1016/j.bioelechem.2020.107634.
9. Singh, A.K.; Sharma, R.; Singh, M.; Verma, N. Electrochemical determination of L-arginine in leukemic blood samples based on a polyaniline-multiwalled carbon nanotube-magnetite nanocomposite film modified glassy carbon electrode. *Instrum. Sci. Technol.* **2020**, *48*, 400–416, doi:10.1080/10739149.2020.1734934.
10. Stasyuk, N.; Gayda, G.; Fayura, L.; Boretskyy, Y.R.; Gonchar, M.V.; Sibirny, A.A. Novel arginine deiminase-based method to assay L-arginine in beverages. *Food Chem.* **2016**, *201*, 320–326, doi:10.1016/j.foodchem.2016.01.093.
11. Stasyuk, N.; Gayda, G.; Yepremyan, H.; Stepien, A.; Gonchar, M. Fluorometric enzymatic assay of L-arginine. *Spectrochim. Acta A* **2017**, *70*, 184–190, doi:10.1016/j.saa.2016.07.019.
12. Berninger, T.; Bliem, C.; Piccinini, E.; Azzaroni, O.; Knoll, W. Cascading reaction of arginase and urease on a graphene-based FET for ultrasensitive, real-time detection of arginine. *Biosens. Bioelectron.* **2018**, *115*, 104–110, doi:10.1016/j.bios.2018.05.027.
13. Verma, N.; Singh, A.K.; Singh, M. L-Arginine biosensors: A comprehensive review. *Biochem. Biophys. Rep.* **2017**, *12*, 228–239, doi:10.1016/j.bbrep.2017.10.006.
14. Saiapina, O.Y.; Dzyadevych, S.V.; Jaffrezic-Renault, N.; Soldatkin, O.P. Development and optimization of a novel conductometric bi-enzyme biosensor for L-Arginine determination. *Talanta* **2012**, *92*, 58–64, doi:10.1016/j.talanta.2012.01.041.

15. Stasyuk, N.E.; Gaida, G.Z.; Gonchar, M.V. L-arginine assay with the use of arginase I. *Appl. Biochem. Microbiol.* **2013**, *49*, 529–534, doi:10.7868/s0555109913050139.
16. Kucherenko, I.S.; Soldatkin, O.O.; Dzyadevych, S.V.; Soldatkin, A.P. Electrochemical biosensors based on multienzyme systems: Main groups, advantages and limitations—A review, *Anal. Chim. Acta* **2020**, *1111*, 114–131, doi:10.1016/j.aca.2020.03.034.
17. Bollella, P.; Katz, E. Biosensors—Recent Advances and Future Challenges. *Sensors* **2020**, *20*, 6645, doi:10.3390/s20226645.
18. Yamamoto, Y.; Senda, M. Amperometric ammonium ion sensor and its application to biosensors. *Sens. Actuators B Chem.* **1993**, *13*, 57–60, doi:10.1016/0925-400585322-2.
19. Stasyk, O.V.; Boretsky, Y.R.; Gonchar, M.V.; Sibirny, A.A. Recombinant arginine-degrading enzymes in metabolic anticancer therapy and bioanalytics. *Cell Biol. Int.* **2015**, *39*, 246–252, doi:10.1002/cbin.10383.
20. Stasyuk, N.; Smutok, O.; Gayda, G.; Gonchar, M.; Koval'chuk, Y. A new bi-enzyme potentiometric sensor for arginine analysis based on recombinant human arginase I and commercial urease. *J. Mater. Sci. Eng.* **2011**, *1*, 819–827, doi:10.15587/2313-8416.2015.45126.
21. Stasyuk, N.; Smutok, O.; Gayda, G.; Vus, B.; Koval'chuk, Y.; Gonchar, M. Bi-enzyme L-arginine-selective amperometric biosensor based on ammonium-sensing polyaniline-modified electrode. *Biosens. Bioelectron.* **2012**, *37*, 46–52, doi:10.1016/j.bios.2012.04.031.
22. Stasyuk, N.Y.; Gayda, G.Z.; Gonchar, M.V. L-arginine-selective microbial amperometric sensor based on recombinant yeast cells over-producing human liver arginase I. *Sens. Actuators B Chem.* **2014**, *204*, 515–521, doi:10.1016/j.snb.2014.06.112.
23. Soldatkina, O.V.; Soldatkin, O.O.; Velychko, T.P.; Prilipko, V.O.; Kuibida, M.A.; Dzyadevych, S.V. Conductometric biosensor for arginine determination in pharmaceutics. *Bioelectrochemistry* **2018**, *124*, 40–46, doi:10.1016/j.bioelechem.2018.07.002.
24. Zakalskiy, A.E.; Zakalska, O.M.; Rzhepetskyy, Y.A.; Potocka, N.; Stasyk, O.V.; Horak, D.; Gonchar, M.V. Overexpression of (His_6-tagged human arginase I in *Saccharomyces cerevisiae* and enzyme purification using metal affinity chromatography. *Protein Expr. Purif.* **2012**, 81, 63–68, doi:10.1016/j.pep.2011.09.001.
25. Karkovska, M.I.; Stasyuk, N.Ye.; Gayda, G.Z.; Smutok, O.V.; Gonchar, M.V. Nanomaterials in construction of biosensors of biomedical purposes. In *Multifunctional Nanomaterials for Biology and Medicine: Molecular Design, Synthesis, and Application*; Stoika, R., Ed.; Naukova Dumka: Kyiv, Ukraine, 2017; pp. 165–177. ISBN 978-966-00-1564-7. (In Ukrainian)
26. Zhybak, M.T.; Fayura, L.Y.; Boretsky, Y.R.; Gonchar, M.V.; Sibirny, A.A.; Dempsey, E.; Turner, A.; Korpan, Y.I. Amperometric L-Arginine biosensor based on a novel recombinant Arginine deiminase. *Microchim. Acta* **2017**, *184*, 2679–2686, doi:10.1007/s00604-017-2290-4.
27. Zarei, M.; Rahbar, M.R.; Morowvat, M.H.; Nezafat, N.; Negahdaripour, M.; Berenjian, A.; Ghasemi, Y. Arginine Deiminase: Current Understanding and Applications *Recent Pat. Biotechnol.* **2019**, *13*, 124–136, doi:10.2174/1872208313666181220121400.
28. Fayura, L.R.; Boretsky, Y.R.; Pynyaha, Y.V.; Wheatley, D.N.; Sibirny, A.A. Improved method for expression and isolation of the *Mycoplasma hominis* arginine deiminase from the recombinant strain of *Escherichia coli*. *J. Biotechnol.* **2013**, *167*, 420–426, doi:10.1016/j.jbiotec.2013.06.025.
29. Matsui, D.; Terai, A.; Asano, Y. L-Arginine oxidase from *Pseudomonas* sp. TPU 7192: Arginine determination. *Enzym. Microb. Technol.* **2016**, *82*, 151–157, doi:10.1016/j.enzmictec.2015.10.002.
30. Nakano, S.; Niwa, M.; Asano, Y. Following the Evolutionary Track of a Highly Specific L-Arginine Oxidase by Reconstruction and Biochemical Analysis of Ancestral and Native Enzymes. *Appl. Environ. Microbiol.* **2019**, *30*, 567–570, doi:10.1128/AEM.00459-19.
31. Sarkar, P.; Tothill, I.E.; Setford, S.J.; Turner, A.P. Screen-printed amperometric biosensors for the rapid measurement of L- and D-amino acids. *Analyst* **1999**, *124*, 865–870, doi:10.1039/a901404g.
32. Kacaniklic, V.; Johansson, K.; Marko-Varga, G.; Gorton, L.; Jönsson–Pettersson, G.; Csöregi, E. Amperometric biosensors for detection of L- and D-amino acids based on co-immobilized peroxidase and L- and D-amino acid oxidases in carbon paste electrodes. *Electroanalysis* **1994**, *6*, 381–390, doi:10.1002/elan.1140060505.
33. Qin, M.; Li, F.; Huang, Y.; Ran, W.; Han, D.; Song, Y. Twenty Natural Amino Acids Identification by a Photochromic Sensor Chip. *Anal. Chem.* **2014**, *87*, 837–842, doi:10.1021/ac504121d.
34. Naresh, V.; Lee, N. A review on biosensors and recent development of nanostructured materials-enabled biosensors. *Sensor* **2021**, *21*, 1109, doi:10.3390/s21041109.
35. Nayl, A.A.; Abd-Elhamid, A.I.; El-Moghazy, A.Y.; Hussin, M.; Abu-Saied, M.A.; El-Shanshory, A.A.; Solman, H.M.A. The nanomaterials and recent progress in biosensing systems: A review. *Trends Environ. Anal. Chem.* **2020**, *26*, e00087, doi:10.1016/j.teac.2020.e00087.
36. Wu, J.; Wang, X.; Wang, Q.; Lou, Z.; Li, S.; Zhu, Y.; Qin, L.; Wei, H. Nanomaterials with enzyme-like characteristics (nanozymes): Next-generation artificial enzymes (II). *Chem. Soc. Rev.* **2019**, *48*, 1004–1076, doi:10.1039/c8cs00457a.
37. Huang, Y.; Ren, J.; Qu, X. Nanozymes: Classification, Catalytic Mechanisms, Activity Regulation, and Applications. *Chem. Rev.* **2019**, *119*, 4357–4412, doi:10.1021/acs.chemrev.8b00672.
38. Stasyuk, N.; Smutok, O.; Demkiv, O.; Prokopiv, T.; Gayda, G.; Nisnevitch, M.; Gonchar, M. Synthesis, Catalytic Properties and Application in Biosensorics of Nanozymes and Electronanocatalysts: A Review. *Sensors* **2020**, *20*, 4509, doi:10.3390/s20164509.
39. Tricot, C.; Stalon, V.; Legrain, C. Isolation and characterization of *Pseudomonas putida* mutants affected in arginine, ornithine and citrulline catabolism: Function of the arginine oxidase and arginine succinyltransferase pathways. *J. Gen. Microbiol.* **1991**, *137*, 2911–2918.

40. Hossain, G.S.; Li, J.; Shin, H.D.; Du, G.; Liu, L.; Chen, J. L-Amino acid oxidases from microbial sources: Types, properties, functions, and applications. *Appl. Microbiol. Biotechnol.* **2014,** *98*, 1507–1515, doi:10.1007/s00253-013-5444-2.
41. Castellano, F.; Molinier-Frenkel, V. An Overview of L-Amino Acid Oxidase Functions from Bacteria to Mammals: Focus on the Immunoregulatory Phenylalanine Oxidase IL4I1. *Molecules* **2017**, *22*, 2151, doi:10.3390/molecules22122151.
42. Fox, J.W. A brief review of the scientific history of several lesser-known snake venom proteins: L-amino acid oxidases, hyaluronidases and phosphodiesterases. *Toxicon* **2013**, *62*, 75–82, doi:10.1016/j.toxicon.2012.09.009.
43. Pollegioni, L.; Motta, P.; Molla, G. L-amino acid oxidase as biocatalyst: A dream too far? *Appl. Microbiol. Biotechnol.* **2013**, *9*, 9323–9341, doi:10.1007/s00253-013-5230-1.
44. Hiu, J.J.; Yap, M.K.K. Cytotoxicity of snake venom enzymatic toxins: Phospholipase A_2 and L-amino acid oxidase. *Biochem. Soc. Trans.* **2020**, *48*,719-731, doi:10.1042/BST20200110.
45. Gayda, G. Oxidases of L-amino acids: Obtaining, properties and prospects of utilization. *Inter. Conf.* **2021**, *63*, 228–237. doi:10.51582/interconf.21-22.06.2021.25.
46. Demkiv, O.; Stasyuk, N.; Serkiz, R.; Gayda, G.; Nisnevitch, M.; Gonchar, M. Peroxidase-Like Metal-Based Nanozymes: Synthesis, Catalytic Properties, and Analytical Application. *Appl. Sci.* **2021**, *11*, 777, doi:10.3390/app11020777.
47. Gayda, G.Z.; Demkiv, O.M.; Gurianov, Y.; Serkiz, R.Y.; Klepach, H.M.; Gonchar, M.V.; Nisnevitch, M. "Green" Prussian Blue Analogues as Peroxidase Mimetics for Amperometric Sensing and Biosensing. *Biosensors* **2021**, *11*, 193, doi:10.3390/bios11060193.
48. Austin, K.T.; Butzke, C.E. Spectrophotometric Assay for Arginine in Grape Juice and Must. *Am. J. Enol. Vitic.* **2000**, *51*, 227–232.
49. Mira De Orduña, R.; Liu, S.Q.; Patchett, M.L.; Pilone, G.J. Ethyl carbamate precursor citrulline formation from Arginine degradation by malolactic wine lactic acid bacteria. *FEMS Microbiol. Lett.* **2000**, *183*, 31–35, doi:10.1111/j.1574-6968.2000.tb08929.x.
50. Petropoulos, S.; Metafa, M.; Kotseridis, Y.; Paraskevopoulos, I.; Kallithraka, S. Amino acid content of Agiorgitiko (*Vitis vinifera* L. cv.) grape cultivar grown in representative regions of Nemea. *Eur. Food Res. Technol.* **2018**, *244*, 2041–2050, doi:10.1007/s00217-018-3115-3.

Оригінал доступний за посиланням:
https://www.mdpi.com/2076-3417/11/15/7024

Анотація: *У поточній роботі нами повідомлється про конструювання амперометричного біонаносенсора для аналізу гідроген пероксиду за використання пероксидази хрону (ПО), кон'югованої з наночастинками шляхетних металів: Au, Au/Ag та Ag/Au. Для конструювання біосенсорів усі нанокомпозити іммобілізовано на поверхні графітових електродів (ГЕ). Методами циклічної вольтамперометрії та хроноамперометрії досліджено основні біоаналітичні характеристики отриманих біонаноелектродів у порівнянні з немодифікованим біоелектродами на основі ПО/ГЕ. Встановлено, що ПО, іммобілізована на поверхні НЧ, виявляє високу електрокаталітичну реакцію на внесений гідроген пероксид. Усі розроблені біонаноелектроди показують вищі значення констант Міхаеліса-Ментена і, отже, мають розширені лінійні діапазони до H_2O_2, а також вищу чутливість у порівнянні з ПО/ГЕ. Найбільш ефективний біонаносенсор на основі ПО та НЧ Au використали для аналізу гідроген пероксиду в зразках промислових дезінфікуючих засобів. Показано високу кореляцію із заявленими виробником значеннями вмісту гідроген пероксиду.*

Copyright © 2016 American Scientific Publishers
All rights reserved
Printed in the United States of America

SENSOR LETTERS
Vol. 14, 1–9, 2016

Nanoparticles of Noble Metals as Effective Platforms for the Fabrication of Amperometric Biosensors on Hydrogen Peroxide

Nataliya Stasyuk*, Galina Gayda, Halyna Klepach, and Mykhailo Gonchar

(Received: xx Xxxx xxxx. Accepted: xx Xxxx xxxx)

Hydrogen peroxide selective biosensors were developed using horseradish peroxidase (HRP) conjugated with the synthesized nanoparticles (NPs) of noble metals: AuNPs, Au/AgNPs and Ag/AuNPs. The HRP-NPs as bioelements (bioNPs) were immobilized on the surface of carbon electrodes (CE). The electrochemical performances of the resulted NPs-modified bioelectrodes (bioNPs/CEs) were studied by cyclic voltamperometry and chronoamperometry in comparison with unmodified HRP/CE-based bioelectrode (bio/CE). The HRP immobilized on the surface of NPs exhibited an excellent electrocatalytic response toward reduction of H_2O_2. All developed bioNPs/CEs showed the higher apparent Michaelis-Menten constants (K_M^{app}) values and hence expanded linear ranges toward H_2O_2 as well as higher sensitivity in comparison with bio/CE. The most effective bioAuNPs/CE biosensor was used for hydrogen peroxide analysis in the samples of industrial disinfectants. A high correlation with the hydrogen peroxide values, declared by manufacturer, was demonstrated.

Keywords: Amperometric Biosensor, Hydrogen Peroxide Analysis, Nanoparticles of Noble Metals, Horseradish Peroxidase.

RESEARCH ARTICLE

1. INTRODUCTION

Hydrogen peroxide (H_2O_2) plays a pivotal role in various industrial applications.[1] It is an essential mediator in pharmaceutical, clinical, and environmental research. H_2O_2 is a byproduct of highly selective oxidases and toxic contaminant in several industrial products and wastes.[2] Therefore, reliable and economical methods for H_2O_2 assay are of great significance.

The known methods of H_2O_2 assay are based on titrimetry,[3] spectrophotometry,[4] chemiluminescence[5] and electrochemical approaches.[6, 7] Among these techniques, the electroanalytical method is advantageous over others because of their robustness, possible miniaturization, low-cost and ease of operation. Due to their high selectivity and sensitivity, the development of biosensors based on peroxidase-modified electrodes has been widely studied in the field of electroanalytical chemistry.[7]

The horse radish peroxidase (HRP), a heme-containing oxidoreductase, is a commercially important enzyme, which catalyzes the reductive cleavage of H_2O_2 by an electron donor.[8, 9] However, the sensitivity of these biosensors based on the direct electron exchange between HRP and electrode surface is often relatively low. To increase the current response, HRP is widely fixed onto the electrode surface with carbon nanomaterials, conducting polymers and metallic nanoparticles (NPs).[9–23]

The general analytical parameters of the reported bioelectrodes, that contain HRP, immobilized on mono- and bi-metallic NPs (bioNPs), are presented in Table I. Bimetallic core–shell NPs that are composed of two different metallic elements were reported to show outstanding optical, electronic, magnetic and catalytic properties different from the corresponding monometallic NPs.[10, 12, 18–21]

Considering the crucial role of H_2O_2 in medical and environmental studies as well as industrial processes, its determination is of great importance. The aim of our research is to construct HRP-bioelectrodes based on different types of NPs for quantitative detection of H_2O_2 in model solutions and in the real samples.

2. MATERIAL AND METHODS

2.1. Reagents

Horse radish peroxidase (EC 1.11.1.7) from *Armoracia rusticana* (500 U · g^{-1}), hydrogen peroxide,

*Corresponding author: E-mail:

Table I. Comparison of the analytical characteristics of hydrogen peroxide amperometric biosensors based on HRP and NPs.

*Electrode	Type of NPs	Potential, mV	**LOD, μM	Linear range, μM	Reference
GCE	RuO	+250	–	5090–15000	[9]
GCE	AuNWs/TiO_2	–	0.7	2.3–2400	[10]
GE	Pd	−200	7.5	–	[11]
GCE	Ni/Fe_3O_4	−100	–	30–12000	[12]
GE	AuNWs/TiO_2	−600	2	50–400	[13]
GCE	ZrO_2	+490	2	50–400	[14]
GE	Au	–	–	1.0–15	[15]
GE	Ag	−500	0.13	3.85–500	[16]
GCE	Au	−50	–	1.4–3100	[17]
GCE	Au/Ru	+200	0.05	0.10–1000	[18]
GCE	Au/Ag (core/shell)	−650	1.0	10–70	[19]
ITO	Ag/C***	+300	0.2	0.5–14000	[20]
GE	Ag/ZnO	+220	0.05	0.01–500	[21]
GCE	Fe_3O_4/m-silica	–	0.43	–	[22]
GE	Au	+100	0.07	0.15–8600	[23]

Notes: *Electrodes: GCE–Glassy-carbon; GE–gold; CE–carbon; ITO-indium-titan oxide electrode; **LOD–limit of detection; C***-nanocomposite with colloidal carbon.

Table II. Methods of chemical synthesis of nanoparticles.[24]

Type of NPs	Reaction mixture and conditions	Color of NPs
AuNPs	0.145 mL 58.5 mM $HAuCl_4$ + 10 mL 10 mM CTAB stirring vigorously + 0.8 mL 100 mM sodium borohydride; incubation without stirring for 24 h at 20 °C	Wine-red
AgNPs	0.1 mL 150 mM $AgNO_3$ + 25 mL 30 mM D-glucose + 0.35 mL 50 mM NaOH; stirring for 20 min at 20 °C	Dark yellow
Au-core/Ag-shell-NPs	0.01 ml 100 mM ascorbic acid + 0.5 ml 10 mM $AgNO_3$ + 5 ml 0.9 mM AuNPs + 0.15 ml 100 mM NaOH; incubation without stirring for 24 h at 20 °C	Violet
Ag-core/Au-shell-NPs	10 ml 0.25 mM $HAuCl_4$ + 0.5 ml 100 mM CTAB + 0.05 ml 100 mM ascorbic acid; vigorous mixing for 1 min, followed by adding 5 ml 3 mM AgNPs and incubation without stirring for 24 h at 20 °C	Violet

tetrachloroauric acid trihydrate, sodium citrate, sodium borohydride, cetyltrimethyl ammonium bromide (CTAB), ascorbic acid, silver nitrate, D-glucose, 1-cyclohexyl-3-(2-morpholinoethyl) carbodiimide hydrochloride (CMC), pentafluorophenol (PFP), 2-(2-aminoethoxy) ethanol (AEE), dimethylformamide (DMF), N,N-diisopropylethylamine (DIPEA) and 16-mercaptohexadecanoic acid (MHDA), sodium hydroxide, inorganic salts, chloroform and Butvar solution B-98 were obtained from Sigma-Aldrich (St. Louis, MO, USA). All buffers and standard solutions were prepared using the water purified by the Milli-Q system (Millipore).

2.2. Synthesis of Nanoparticles

All nanoparticles (NPs) were synthesized by the reduction of metal ions from appropriate salts according to the known methods in our modification.[24] Conditions of NPs obtaining are presented in the Table II. NPs were collected by centrifugation under 10000 g for 40 min (Hettich Micro-22R centrifuge), washed with water and precipitated by centrifugation. Pellets were suspended in 0.2 mL of water and stored till exploitation at +4 °C.

2.3. Immobilization of HRP on NPs

The procedure of HRP immobilization on NPs was carried out as described by us earlier for recombinant arginase.[25]

An aliquot of NPs (to the final 0.1 mM concentration) was incubated overnight in 5 mM MHDA in ethanol at +4 °C. After rinsing with DMF, the MHDA-covered NPs were incubated in a DMF solution of 20 mM CMC, 20 mM PFP and 20 mM DIPEA for 30 min at 25 °C. After repeated rinsing with DMF, condensation of the activated Au- and Ag-linked carboxylic groups with amine groups of the enzyme was carried out. 25μL of the enzyme solution in 30 mM phosphate buffer, pH 7.5 (PB) was incubated with NPs for 1 h at 25 °C. After rinsing with PB, blocking of un-reacted carboxylic groups with 0.1 M solution of AEE in 0.1 M bicarbonate buffer, pH 8.0, was performed. The bio-functionalized NPs (bioNPs) were rinsed with PB and stored at +4 °C until usage.

2.4. Characterization of Bioelectrodes with Scanning Electron Microscopy

The size and structure of enzyme-bound NPs on the surface of carbon rod electrode were studied by scanning electron microscopy (SEM-microanalyser REMMA-102-02, Sumy, Ukraine). The special cover film on the samples with a Butvar solution B-98 (Sigma, St. Louis, MO, USA) in 1.5% chloroform was formed using an ultrasound method. In experiments the distance from the last lens of the microscope to the sample (WD) ranged from 17.1 to 21.7 mm; the accelerator voltage was in the range from 20 to 40 eV; zooms were from 2500 to 10000.

2.5. Apparatus

A three-electrode system was used for the electrochemical studies. A piece of Pt wire and an Ag/AgCl/3M KCl electrode were used as the counter and reference electrodes, respectively. A carbon rod electrode (ALS Co., Tokyo, Japan) was applied as a working electrode (3.0 mm diameter). Amperometric measurements were carried out with a potentiostat CHI 1200A (IJ Cambria Scientific, Burry Port, UK) and performed in batch mode under continuous stirring in a standard 40 ml cell at a room temperature.

2.6. Preparation and Evaluation of the Biosensors

Commercial HRP (with activity 100 $U \cdot mL^{-1}$) or HRP, immobilized on different types of NPs, was dropped on the top of carbon rod electrode (CE). Dried bio-layer was covered by a dialysis membrane for physical holding, rinsed with water and stored in 30 mM PB pH 7.0 till being used. All fabricated bioelectrodes were marked further as following: HRP onto CE (bio/CE); HRP immobilized on AuNPs (bioAuNPs/CE); on Au/AgNPs (bioAu/AgNPs/CE); on Ag/AuNPs (bioAg/AuNPs/CE).

Analytical characteristics of the proposed bioelectrodes were statistically processed using the OriginPro 8.5 software. Calculation of the apparent Michaelis-Menten constants (K_M^{app}) was automatically performed by this program according to the Lineweaver–Burk equation.[26]

2.7. Hydrogen Peroxide Assay in the Samples of Industrial Disinfectants

Industrial disinfectants "Sanoxyl 006" and "Sanoxyl 004" ("DezoMark" Factory, Ukraine) were taken for assay. According to manufacturer, 100 g of peeled water solution of "Sanoxyl 006" contained 2.66 g of H_2O_2 and 0.003 g of $AgNO_3$; of "Sanoxyl 004" −2.0 g of H_2O_2 and 0.002 g of $AgNO_3$. Both disinfectants were supplemented with organic compounds for moisturizing and softening of skin. To avoid interference effect of organic additives during assay of hydrogen peroxide, these samples were analyzed using a standard addition test (SAT). Before assay, all samples were step-wise diluted by 30 mM PB pH 7.0. Each assay was performed for two dilutions of the sample and repeated at least 3 times. Concentration of hydrogen peroxide in the initial sample ($C_{calcul.}$) was estimated from the parameters of linear regression (A, B) of the corresponding graph, taking into account factor of the sample's dilution (N):

$$C_{calcul} = \frac{A}{B} \cdot N$$

3. RESULTS AND DISCUSSION

3.1. Characterization of HRP, Immobilized on Nanoparticles

It is known that nanomaterials could improve the biosensor characteristics.[27] In our previous works we have suggested amperometric biosensors based on human liver arginase I,[28] methylamine oxidase[29] and flavocytochrome b_2,[30] immobilized on the surface of AuNPs. Bio-functionalization of synthesized NPs was performed by modification of NPs by 16-mercaptohexadecanoic acid and further carbodiimide-pentafluorophenol condensation with enzymes. All proposed NPs-based biosensors have possessed the improved analytical characteristics in comparison with biosensors without NPs. The constructed biosensors were successfully tested on the real samples of food products.

Recently, we have proposed the simple methods of two-step chemical reduction of ions from appropriate inorganic salts for the obtaining of core/shell bimetallic NPs.[30] To estimate the exact sizes and to study the morphology of the NPs synthesized, methods of TEM, powder XRD analyses and AFM were applied as described earlier.[24, 25] The average diameters of AuNPs and AgNPs were shown to be less than 20 nm and diffraction peaks parameters of these NPs can be perfectly indexed into the cubic crystalline structures. The crystallite sizes were calculated from the main diffraction peaks as described earlier: for AuNPs average diameter is 8.1 nm[28] and for AgNPs −17.0 nm. The morphology of the AuNPs ($d_{av} = 16$ nm) was shown to be almost smooth and their surfaces were homogeneous. In case of both bi-metallic NPs, the values of dav were not higher than 20–25 nm, but their surfaces were rather heterogeneous[24] as a result of NPs aggregation. Still some of the tested bi-metallic NPs did have bigger d_{av}, the largest of them was estimated to be 160 nm.

In our preliminary studies we have investigated the stabilizing properties of monometallic Au- and AgNPs onto the HRP.[31] AuNPs were shown to be the most effective and stabilizing platform for immobilizing HRP.

The obtained above results were taken into account during construction of amperometric biosensors based on HRP and NPs. On the other hand, HRP was immobilized on the surface of hybrid (core/shell) NPs. The synthesized hybride NPs were bound with HRP after procedure of covalent immobilization according to the previous proposed techniques.[31] It was shown that the HRP was immobilized on the surface of these NPs with good effectiveness; yield of activities of HRP on Ag/AuNPs and HRP on Au/AgNPs was $42 \pm 1.3\%$ and $31 \pm 0.9\%$ respectively in comparing to initial activity of free HRP in solution. Calculation of activity were carried out as described earlier[25, 31]—taking into account total activities of initial HRP before immobilization in NPs, unbound enzyme in rinsing solution and enzyme, connected with NPs. Scanning electron microscopy (SEM), X-ray microanalysis and UV-spectroscopy approaches used for morphological investigations of synthesized monometallic NPs (AuNPs and AgNPs), so as bi-metallic NPs (Ag/AuNPs and Au/AgNPs) before[24] and after immobilization (Fig. 4) have proved their nano-status. Figure 1 represents the yield of HRP activities after immobilization procedure on the different types of NPs. Thus, it was shown, that Ag (core)/Au (shell) are the most optimal carriers with the best yield of immobilized HRP in comparison with the monometallic NPs (Fig. 1).

It should to note, that all these immobilized bioNPs (except HRP-AgNPs) were taken for the construction of amperometric biosensors sensitive to hydrogen peroxide.

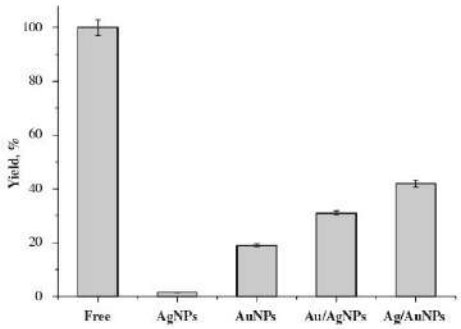

Fig. 1. The yield of HRP activities after immobilization procedure on NPs.

3.2. Construction of H_2O_2-Sensitive Bioselective Layer with NPs

3.2.1. Electrochemical Characteristics of the bioAuNPs/CE

To form an enzymatic layer of the bio-electrode sensitive to H_2O_2, different types of NPs linked with HRP were dropped on the surface of the CE and covered with a dialysis membrane according to the experimental part (see subdivision 2.6).

The efficiency of free defusing electron transfers from the oxidized HRP to electrode via AuNPs (as mediator) was evaluated using cyclic voltamperometry (CV). The cyclic voltamperometry gives information about optimal working potential for sufficient HRP reduction on the top of carbon rod electrode (Fig. 2).

As it shown in Figure 2, potential −50 mV versus Ag/AgCl was chosen as optimal working potential for HRP-reduction in our system. The summarized output of

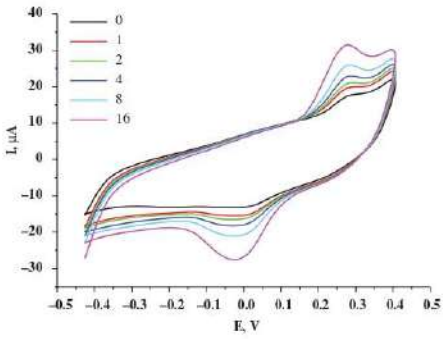

Fig. 2. Characterization of bioelectrode bioAuNPs/CE by cyclic voltamperometry in the presence of the increasing concentrations of H_2O_2 (from 0 to 16 mM). Conditions: −0.4 V to 0.4 V versus Ag/AgCl; scan rate 7 mV·s^{-1} in 30 mM phosphate buffer, pH 7.0.

enzymatic reduction of 16 mM H_2O_2 for bioelectrode was estimated as 15 μA. It should to mention, that the behavior of the all proposed bioelectrodes on the H_2O_2 injection are similar to bioAuNPs/CE with the reduction peak −50 mV so their CV are not shown.

3.2.2. Determination of Structural and Electrical Properties of the Different Nano-Materials

Cyclic voltamperometry is useful in providing reliable chemical information of the bioelectrode in PB. The CV of HRP-modified electrodes in 50 mM PB, pH 7.5 are presented on Figure 3. Figure 3(A) shows the behavior of the bio/CE at the current applied and it no obvious peaks were appeared (Fig. 3(A), black line). Whereas after the electrode modification with bioAuNPs the oxidation and reduction peak was observed and the current was increased (Fig. 3(A), dash line). The anodic peak at the 0.05 V represents the formation of Au(III) due to oxidation of metallic Au to Au(III). The cathodic peak at the +0.3 V correspond to the transition of Au(III) to metallic AuNPs. These CV characteristics of the modified electrode were similar to that reported in the literature.[32] But, the peaks potentials observed at the composite are slightly shifted in the positive direction. Figure 3(B) demonstrates the behavior of the bioAg/AuNPs/CE at the current applied (Fig. 3(B)). The anodic (0.185 V) and cathodic (0.3 V) peaks represent the transition of metallic AuNPs to Au(III) or reverse. Figure 3(C) shows the cyclic voltamperogram of bioAu/AgNPs formation on the surface of CE. In this structure AuNPs (core) are covered by Ag (shell). As result, there is no sharp peaks on voltamperogram, and these data are similar to the reported.[33]

The size and structure of the obtained enzyme-linked NPs (bioNPs) on the surface of electrodes were confirmed by scanning electron microscopy (Fig. 4).

The results of SEM imaging not demonstrate the difference in surface structures of CE, modified by different bioNPs (Fig. 4). It was shown that all the electrodes surfaces-with different bioNPs-look like a clusters of irregular shape of microfibrillar structures (Fig. 4).

The presence of different types of noble metals NPs on the surface of electrodes was additionally confirmed by X-ray Microanalysis (XRM) (Fig. 4). XRM data of these NPs proved the presence of Au^0 and Ag^0 compounds, with characteristic peaks Kα at 2.1 keV and 3.0 keV, respectively. The XRM image of Au/AgNPs (Fig. 4(G)) confirms the presence of Ag^0 and Au^0 Kα peaks, proving the presence of both AgNPs and AuNPs, respectively. As the Kα peak, specific for Au^0, is higher, it indicates the full covering of AuNPs with AgNPs. Thus, the XRM data confirms the forming of Au (core)/Ag (shell) NPs. The similar tendency is observed for Ag/AuNPs: the Kα peak, specific for Ag^0, is higher, than Kα of Au^0 (Fig. 4(G)). The last fact confirms the structure of NPs: Ag (core)/Au (shell).

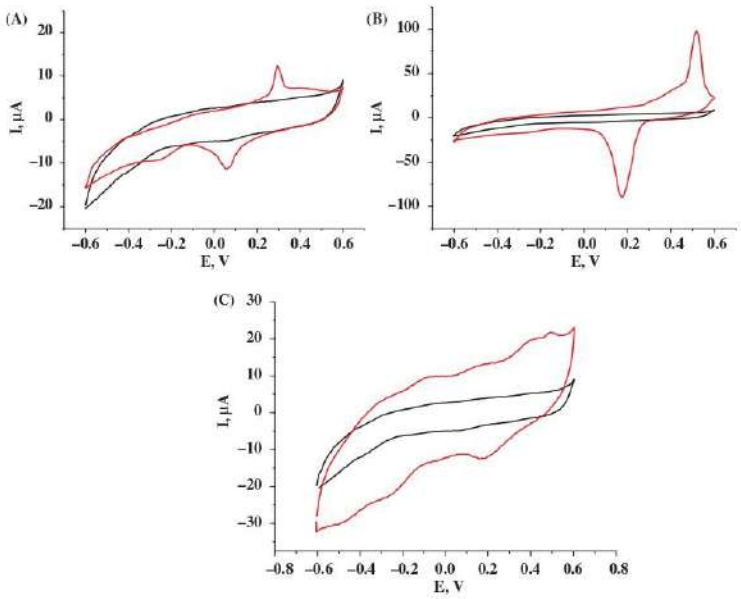

Fig. 3. Cyclic voltamperograms of the NPs-modified bioelectrodes (red) in comparison with the unmodified bioelectrode (black): bioAuNPs/CE (A), bioAg/AuNPs /CE (B), bioAu/AgNPs/CE (C). Conditions: −0.6 V to 0.6 V versus Ag/AgCl; scan rate 20 mV·s^{-1} in 30 mM phosphate buffer, pH 7.0.

3.3. Evaluation and Optimization of the Hydrogen Peroxide Biosensors

The obtained bioelectrodes were used for the investigation of some analytical parameters of biosensors. The calibration curves and the corresponding chronamperograms (inset) are shown in Figure 5. The calibration was performed by the stepwise addition of an aliquot of standard H_2O_2 solution (50 mM) in working cell. Amperometric responses on H_2O_2 of the enzyme electrodes were tested in the range of resulted H_2O_2 concentrations from 0.005 to 20 mM. Table III demonstrates the general analytical characteristics of the proposed amperometric biosensors.

The prepared in this research different bioelectrodes (Table III) have several advantages compared to the known ones (Table I): they are nonpoisonous, with broad range of applicable potential, quick response, renewable surface and high operational stability. It is shown that the usage of NPs as platform for enzyme's immobilization during fabrication of biosensors, allows to decrease the working potential of the biosensor to −50 mV (which is important to avoid interfering effects of a sample background) and to increase the linear range. The apparent Michaelis-Menten constants (K_M^{app}) for the proposed NPs-modified bioelectrodes (Table III) were increased drastically (48–72-folds) in comparison with the unmodified bio/CE ($K_M^{app} = 0.17$ mm). These differences are assumed to associate with an influence of the rather complicated composition of the biorecognition membrane on the diffusional availability of the substrate (hydrogen peroxide) to the immobilized enzyme.

The observed increased K_M^{app} values for all types of NPs-based bioelectrodes have a positive impact on the biosensor properties due to the wider linear range for hydrogen peroxide determination (from 0.07 mM up to 8.4 mM or higher). The 120-fold expanded linearity for bioAuNPs/CE sensor architecture is better adapted to the typical concentration range of hydrogen peroxide in the samples of industrial disinfectants.

The storage stabilities of the four types of hydrogen peroxide biosensors were investigated (Fig. 6). The test was performed at 24 °C with hydrogen peroxide in PB with intermittent storage in this buffer with 0.3–0.6 mM H_2O_2 at +4 °C between measurements.

The storage stabilities of the described biosensors (storage of 50% of initial signal)-with free HRP and enzyme, immobilized on Ag/AuNPs as well as on Au/AgNPs-were the similar (about 1 week). In the same time, 50% of initial signal's keeping was demonstrated to be of bioAuNPs/CE was about 23 days, and 22%-during 90 days (Fig. 6). So, bioAuNPs/CE biosensor had a relatively long lifetime.

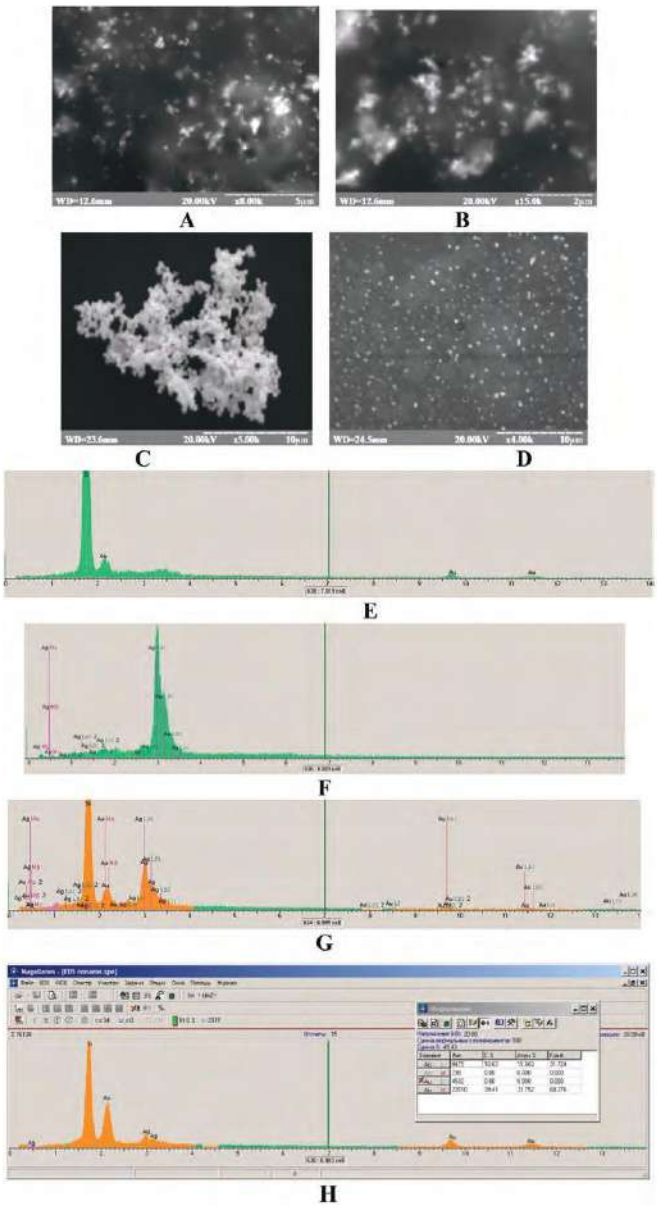

Fig. 4. SEM images and X-ray-spectral characteristics of the NPs conjugated with HRP on the surface of CE: AuNPs (A, E); AgNPs (B, F); Au/AgNPs (C, G) and Ag/AuNPs (D, H).

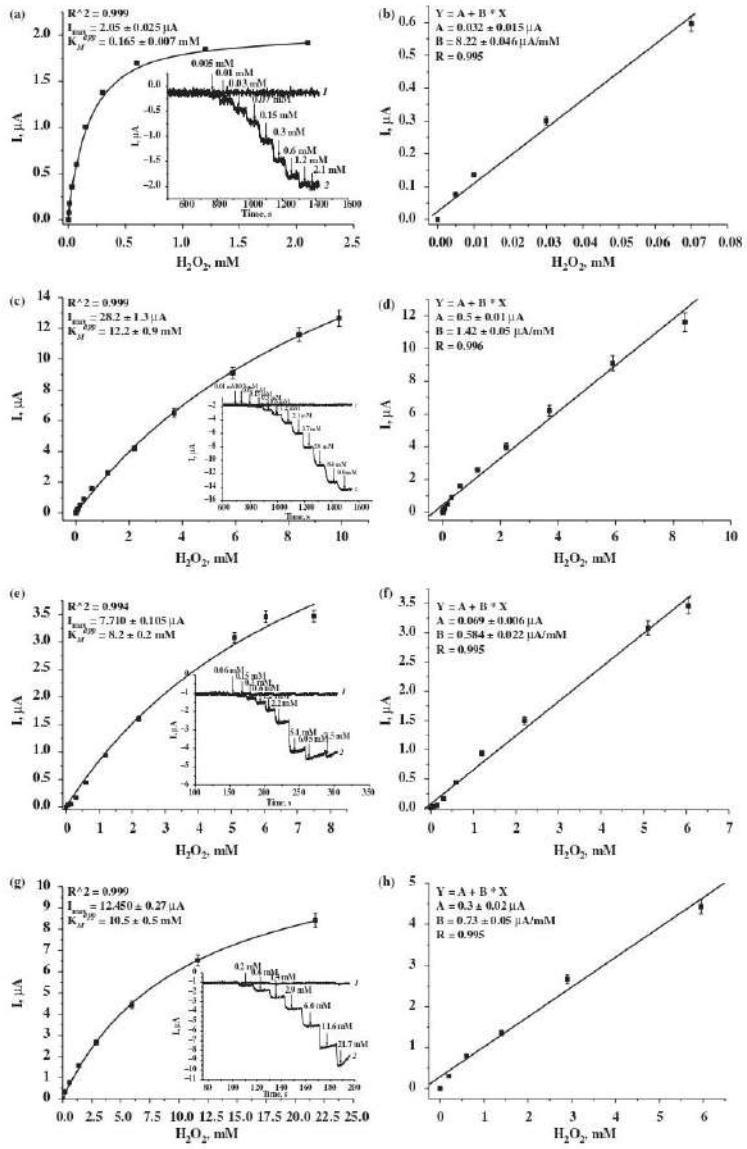

Fig. 5. Calibration curves for amperometric responses on H_2O_2 of the developed electrodes: bio/CE (A, B); bioAuNPs/CE (C, D); bioAu/AgNPs/CE (E, F); bioAg/AuNPs/CE (G, H). In set: chronamperometric current response upon subsequent addition of H_2O_2 for electrode without enzyme (1) and with HRP (2). Conditions: −50 mV versus Ag/AgCl electrode in 30 mM phosphate buffer, pH 7.0 at 22 °C.

RESEARCH ARTICLE

Table III. Analytical characteristics of the proposed bioelectrodes.

Composition of bioelectrodes	bio/CE	bioAuNPs/ CE	bioAu/ AgNPs/CE	bioAg/ AuNP/CE
Potential, mV	−50	−50	−50	−50
LOD, μM	2.2	4.0	25	180
Linear range, μM	5–70	10–8400	30–6100	200–6000
Sensitivity, 1173 ± 350	263 ± 15	A·(M·m^2)$^{-1}$ 318 ± 25	317 ± 20	
K_M^{app}, mM	0.17 ± 0.01	12.20 ± 0.73	8.20 ± 0.20	10.50 ± 0.50
I_{max}, μA	2.05 ± 0.03	28.20 ± 1.30	7.70 ± 0.10	12.45 ± 0.27
Response time, s	10	10	10	10
Operation stability, days (50% of signal)	7	23	6	8

3.4. Analysis of the Samples of Industrial Disinfectants Using bioAuNPs/CE

The most effective among the constructed amperometric biosensors bioAuNPs/CE was evaluated to determine hydrogen peroxide content in the samples of two industrial disinfectants. To avoid the impact of the disinfectants components on the valid results of the assay, a standard addition test (SAT) was applied. SAT is a type of quantitative analysis approach often used in analytical chemistry, whereby the standard is added directly to the aliquots of analyzed sample. The procedure of hydrogen peroxide assay by graphical method was demonstrated in detail (see Fig. 7 and description in Section 2.7) for all tested samples. The results of analysis of industrial disinfectants by developed biosensor were compared with the hydrogen peroxide contents indicated by manufacturer (Table IV). It is obvious from the Table IV, some differences between the experimentally determined contents of the hydrogen peroxide by biosensor method and the concentrations declared by manufacturer were observed for all samples, but with different extents. The maximal interfering effect

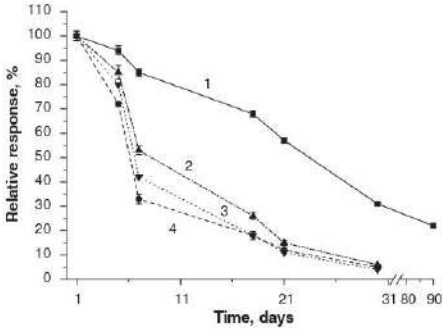

Fig. 6. Operational stabilities of the proposed CE-bioelectrodes based on HRP immobilized on AuNPs (1); Au/AgNPs (2) and Ag/AuNPs (4) in comparison with a similar sensor with free HRP (3).

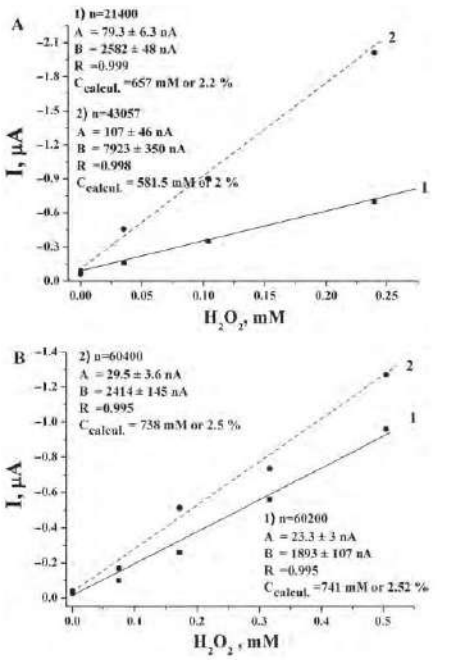

Fig. 7. Determination of hydrogen peroxide's concentration in the samples of disinfectants by the multiple standard addition method: (A) "Sanoxyl 004"; (B) "Sanoxyl 006" (A = OD of the variant without addition of H_2O_2 and B = slope value; R = linear regression coefficient, n–dilution).

Table IV. Analysis of hydrogen peroxide in disinfectants.

Sample	Concentration of hydrogen peroxide (%) Declared by producer	Biosensor analysis	Difference (%)
"Sanoxyl 004"	2.0	2.1 ± 0.1	+4.8
"Sanoxyl 006"	2.66	2.51 ± 0.2	−6.0

was observed for "Sanoxyl 006" (+6.0%) and less–for "Sanoxyl 004" (−4.8%). These results demonstrate the perspectives for application of the developed biosensor for a fast and easy control of industrial disinfectants containing hydrogen peroxide.

4. CONCLUSIONS

Amperometric biosensors for hydrogen peroxide determination based on mono- and bimetallic nanoparticles of noble metals (NPs) conjugated with horse radish peroxidase have been developed. Three types of bioselective elements with enzyme that covalently bound with the

RESEARCH ARTICLE

NPs were immobilized on the surfaces of carbon electrodes and characterized in comparison with control bioelectrode based on free enzyme. BioAuNPs-functionalized electrode as the most effective and stable biosensor was used for hydrogen peroxide analysis in some industrial disinfectants. High correlations with the hydrogen peroxide's levels declared by manufacturer were demonstrated. The constructed prototypes of amperometric biosensors are promising for the use in a fast and easy control of hydrogen peroxide not only in disinfectants but in some kinds of food so as in serum too.

Acknowledgments: This work was financially supported by NAS of Ukraine (program "Sensors for Medical, Environmental, Industrial, and Technological Needs: Metrological Support and Trial Operation", Project 5/3-2016), by the Ministry of Education and Science of Ukraine (project #0116U004737), by NATO (Project CBP. NUKR.SFP 984173) and by fellowship of President of Ukraine for young scientists in 2016 (Nataliya Stasyuk).

References and Notes

1. H. Elzanowska, E. Abu-Irhayem, B. Skrzynecka, and V. I. Birss, *Electroanalysis* 16, 478 (**2004**).
2. C. Camacho, J. C. Matias, B. Chico, R. Cao, L. Gomez, B. K. Simpson, and R. Villalonga, *Electroanalysis* 19, 2538 (**2007**).
3. E. C. Hurdis and H. Romeyn, *Anal. Chem.* 26, 320 (**1954**).
4. M. S. Bloomfield, *Talanta* 64, 1175 (**2004**).
5. K. Nakashima, K. Maki, S. Kawaguchi, and K. Imai, *Anal. Sci.* 7, 709 (**1991**).
6. J. D. Qiu, H. Z. Peng, R. P. Liang, J. Li, and X. H. Xia, *Langmuir* 23, 2133 (**2007**).
7. L. Wang and E. Wang, *Electrochem. Comm.* 6, 225 (**2004**).
8. S. Chairam, P. Buddhalee, and M. Amatatongchai, *Int. J. Electrochem. Sci.* 8, 10250 (**2013**).
9. P. A. Prakash, S. W. Ting, and S.-M. Chen, *Int. J. Electrochem. Sc.* 6, 2688 (**2011**).
10. H. Zhong, R. Yuan, Y. Chai, W. Li, Y. Zhang, and C. Wang, *Bioprocess and Biosystems Engineering* 34, 923 (**2011**).
11. H. Baccar, T. Ktari, and A. Abdelghani, *Int. J. Electrochem.* 2011, 1 (**2011**).
12. F. Yalçıner, E. Çevik, M. Şene, and A. Baykal, *Nano-Micro Letters* 3, 91 (**2011**).
13. A. K. M. Kafi, W. Guosheng, and A. Chen, *Biosens. Bioelectron.* 24, 566 (**2008**).
14. M. Fazilati, *Scholars Research Library Annals of Biological Research* 3, 5350 (**2012**).
15. Y. Okawa, N. Yokoyama, Y. Sakai, and F. Shiba, *Anal. Chem. Res.* 5, 1 (**2015**).
16. C. Ren, Y. Song, Z. Li, and G. Zhu, *Anal. Bioanal. Chem.* 381, 1179 (**2005**).
17. H. Ryoo, Y. Kim, J. Lee, W. Shin, N. Myung, and H. Hun-Gi, *Bulletin Korean Chemical Society* 27, 672 (**2006**).
18. L. Jing, L. Xin-Yi, P. Guang-Chang, and K. Xiao-Bin, *Food Sci.* 33, 197 (**2012**).
19. S. Manivannan and R. Ramaraj, *Chem. Sci.* 121, 735 (**2009**).
20. S. Mao, Y. Long, W. Li, Y. Tu, and A. Deng, *Biosens. Bioelectron.* 15, 258 (**2013**).
21. S. Chawla, R. Rawal, D. Kumar, and C. S. Pundir, 430, 16 (**2012**).
22. Y. H. Won, D. Aboagye, H. S. Jang, A. Jitianu, and L. Stanciu, *J. Mater. Chem.* 20, 5030 (**2010**).
23. K. A. Gautham and C. K. Mitra, *Sensors* 9, 881 (**2009**).
24. N. Stasyuk, G. Gayda, R. Serkiz, and M. Gonchar, *Journal of Advances in Chemistry* 11, 3499 (**2015**).
25. N. Stasyuk, R. Serkiz, S. Mudry, G. Gayda, A. Zakalskiy, Y. Koval'chuk, M. Gonchar, and M. Nisnevitch, *Nanotechnology Development* 1:e3, 11 (**2011**).
26. J. E. Dowd and D. S. Riggs, *J. Biol. Chem.* 240, 863 (**1965**).
27. R. Ahmad and M. Sardar, *Biochem. Anal. Biochem.* 4, 1 (**2015**).
28. N. Stasyuk, O. Smutok, G. Gayda, Y. Koval'chuk, and M. Gonchar, *Journal of Materials Science and Engineering A* 1, 819 (**2011**).
29. N. Y. Stasyuk, O. V. Smutok, A. E. Zakalskiy, O. M. Zakalska, and M. V. Gonchar, *BioMed Research International* 2014, 1 (**2014**).
30. M. Karkovska, O. Smutok, N. Stasyuk, and M. Gonchar, *Talanta* 144, 1195 (**2015**).
31. M. M. Synenka, N. Y. Stasyuk, T. V. Semashko, G. Z. Gayda, R. V. Mychailova, and M. V. Gonchar, *Biological Studio* 8, 5 (**2014**).
32. G. Gotti, K. Fajerwerg, D. Evrard, and P. Gros, *Electrochim. Acta* 128, 412 (**2014**).
33. E. Hamidi-Asl, F. Dardenne, S. Pilehvar, R. Blust, and K. De Wael, *Chemosensors* 4, 16 (**2016**).

RESEARCH ARTICLE

Оригінал доступний за посиланням:
https://www.ingentaconnect.com/content/asp/senlet/2016/00000014/00000012/art00001;jsessionid=1pj90sm6g4r9w.x-ic-live-01

Анотація: *Наноматеріали з ензимними характеристиками (нанозими) є штучними ензимами нового покоління і є перспективними каталізаторами в біосенсорах. Показано, що ПО-подібні нанозими, які складаються з наночастинок шляхетних металів (міметики пероксидази), є ефективними хемосенсорами на Гідроген пероксид – кінцевий продукт каталізованої оксидазою реакції. Однак, необхідність у високих робочих потенціалах для біосенсорів на основі ПО-подібних міметиків є проблемою, яка може обмежити їх застосування для тестування реальних зразків у клінічній діагностиці та харчовій промисловості. Ми повідомляємо про створення глюкозоселективних біонаносенсорів за використання глюкозооксидази (ГОх) кон'югованої з НЧ шляхетних металів: Ag, Au/Ag та Ag/Au. Методами циклічної вольтамперометрії та хроноамперометрії досліджено основні біоаналітичні характеристики електродів, модифікованих НЧ. Усі розроблені біоелектроди показали вищу чутливість, ширші лінійні діапазони, нижчі межі виявлення та вищу стабільність порівняно з біоелетродом на основі ГОх та ПО. Найбільш ефективний біонаносенсор на основі НЧ Ag використано для аналізу глюкози в зразках вин. Показано високу кореляцію значень вмісту глюкози, отриманими за допомогою біонаносенсора та комерційного ензиматичного набору.*

Copyright © 2017 American Scientific Publishers
All rights reserved
Printed in the United States of America

SENSOR LETTERS
Vol. 15, 1–8, 2017

Nanoparticles of Noble Metals for Enzymatic Sensors: An Amperometric Glucose Biosensor for Wine Analysis

Nataliya Stasyuk[1], Galina Gayda[1,*], Halyna Klepach[1,2], Tatiana Semashko[3], and Mykhailo Gonchar[1]

[1] *Institute of Cell Biology, National Academy of Science of Ukraine, Drahomanov Street 14/16, 79005 Lviv, Ukraine*
[2] *Drohobych Ivan Franko State Pedagogical University, 82100 Drohobych, Lviv region, Ukraine*
[3] *Institute of Microbiology, National Academy of Science of Belarus Kuprevich Str. 2, 220141 Minsk, Belarus*

(Received: xx Xxxx xxxx. Accepted: xx Xxxx xxxx)

Nanomaterials with enzyme-like characteristics (nanozymes) are the next-generation artificial enzymes and may be promising catalysts in biosensors. Artificial enzymes as highly stable and low-cost alternatives to natural enzymes were discovered over the past few decades. Peroxidase-liked nanozymes, consisting of nanoparticles of noble metals (PO^{like}-NPs), were shown to be the efficient chemosensors on hydrogen peroxide, final product of oxidase-catalized reaction. But the necessity in high working potentials for PO^{like}-NPs-based biosensors is a problem, that may to limit their application for testing real samples in clinical diagnostics and food industry. In our research glucose-selective biosensors were developed using glucose oxidase (GOx) and horseradish peroxidase (PO) conjugated with NPs of noble metals: AgNPs, Au/AgNPs and Ag/AuNPs. Co-immobilized PO and GOx as bioelements (bio) were placed on the surface of carbon electrodes (CE). The electrochemical performances of the resulted NPs-modified bioelectrodes (bioNPs/CE) were studied by cyclic voltamperometry and chronoamperometry in comparison with unmodified PO-GOx based bioelectrode (bio/CE). The PO and GOx immobilized on the surface of NPs exhibited an excellent electrocatalytic response toward reduction of glucose at rather low potential (–50 mV). All developed bioNPs/CEs showed the higher sensitivities, wider linear ranges, lower limits of detection and higher stabilities in comparison with bio/CE. The most effective bioAgNPs/CE biosensor was used for glucose analysis in the samples of wines. A high correlation with the glucose values estimated by biosensor and commercial enzymatic kit was demonstrated.

Keywords: Glucose Analysis, Nanoparticles of Noble Metals, Amperometric Biosensor, Glucose Oxidase, Horseradish Peroxidase.

RESEARCH ARTICLE

1. INTRODUCTION

Quantitative determination of glucose is of paramount importance in biochemistry, clinical chemistry, and food analysis, especially in wine making.[1–3] Volume of wine production being increased in whole world, but demand for premium wine in the market regularly exceeds supply. Therefore, demands for analytical tools able to conveniently monitor the chemical composition of wine and thus assure its appropriate quality is increased.[3,4]

Numerous methods have been reported for glucose analysis in food and beverages. The known methods of glucose assay are based on titrimetry, spectrophotometry, chemiluminescence, and electrochemical approaches. However, most of the current methods are costly or time consuming.[2,3,5] Among these techniques, the electroanalytical methods are advantageous over others because of their robustness, possible miniaturization, low-cost and ease of operation. H_2O_2, being one of the end products in glucose oxidase (GOx)-catalyzed reactions, can be coupled to a wide variety of detection systems for monitoring glucose concentration. Popular methods involve the use of a peroxidase, such as horse-radish peroxidase (PO), to drive the oxidation of a chromophore. Due to their high selectivity and sensitivity, the development of biosensors based on GOx-PO-modified electrodes has been widely studied in the field of electroanalytical chemistry.[5–12]

However, the determination may be affected by other compounds coexisting with glucose or the sample may need to GOx through complicated pretreatment procedures. To improve the sensitivity and shorten the response time of glucose biosensors, covalent attachment of glucose oxidase (GOx) onto metal nanoparticles (NPs) surface,[13] physical adsorption of enzyme into metal NPs[14,15] and graphitic nanocages[15] surfaces have

*Corresponding author; E-mail: galina.gayda@gmail.com

been studied. Metal NPs, consisting of one metal, metal oxides or composite of several metals, have received much attention as a building block of advanced materials for nanoscience and nanotechnology. Core–shell metal NPs possess unique optical, electronic, magnetic and catalytic properties,[16–18] that render them potential materials for the fabrication of biosensors. The large surface area of NP provides a better matrix for the immobilization of enzymes, leading to increased enzyme load per unit mass of particles. The multipoint combination of nanomaterial surfaces and enzyme molecules can reduce enzyme protein unfolding due to the steric effect, resulting in the enhanced sensitivity of the enzyme. Since gold nanoparticles (AuNPs) can provide a biocompatible environment for enzymes, many researches focus on assembling GOx with AuNPs.[13,17]

Over the past few decades artificial enzymes, as stable and low-cost alternatives to natural enzymes, were discovered. Nanomaterials with enzyme-like characteristics (nanozymes) are the next-generation artificial enzymes and may be promising catalysts in a wide range of applications, especially, in biosensorics.[19–21]

Peroxidase-liked nanozymes, consisting of nanoparticles of noble metals (PO^{like}-NPs), were shown to be the efficient chemosensors on hydrogen peroxide, final product of oxidase-catalized reaction.[20,21] But the necessity in high working potentials for PO^{like}-NPs-based Bs is a problem, that may to limit application of such Bs for testing real samples in food industry and clinical diagnostics. The general analytical parameters of the reported bioelectrodes, that contain GOx and mono- and bi-metallic NPs as PO^{like}-NPs, are presented in Table I.

In current work highly selective GO and PO-based glucose biosensors were proposed. To construct biosensors, a number of mono- and bi-metallic NPs were tested as platforms for enzymes' immobilization, as well as peroxidase-liked nanozymes, stabilizers and mediators of electron transfer. Besides, using a PO in tandem with PO^{like}-NPs was expected to decrease working potential of the resulted highly-selective biosensor.

Table I. Comparison of the analytical characteristics of glucose amperometric biosensors based on GOx and NPs of noble metals on glassy-carbon electrode.

Electrode	Type of NPs	Potential, mV	[b]LOD, μM	Linear range, mM	Reference
[a]GC	Au/Ag	+350	–	2–12	[22]
GC	Au/Si	–	16	0.025–25	[23]
GC	Au/[c] MXene	−402	5.9	0.1–18	[24]
GC	Au/Ag-Pt/[d] ICPs	+480	0.060	0.0005–3.33	[25]
GC	Au	−350	0.65	0.002–3.5	[26]
GC	Ag	–	up to 5 000	–	[27]
GC	Au	−120	23	–	[28]
O_2	Au/Egg shell membrane	–	2.5	0.005–0.525	[29]
O_2	Pt/Egg shell membrane	–	5	10–225	[30]
GC	Au, mediator PMS	+300	70	1.5–20	[31]

Notes: [a]GC—Glassy-carbon electrode; [b]LOD—limit of detection; [c]MXene-two-dimensional (2D) metal carbides nanocomposite; [d]ICPs—infinite coordination polymer.

2. MATERIAL AND METHODS

2.1. Reagents

Horse radish peroxidase (EC 1.11.1.7) from *Armoracia rusticana* (500 $U \cdot g^{-1}$), hydrogen peroxide, tetrachloroauric acid trihydrate, sodium citrate, sodium borohydride, cetyltrimethyl ammonium bromide (CTAB), ascorbic acid, silver nitrate, D-glucose, 1-cyclohexyl-3-(2-morpholinoethyl) carbodiimide hydrochloride (CMC), pentafluorophenol (PFP), 2-(2-aminoethoxy) ethanol (AEE), dimethylformamide (DMF), *N*,*N*-diisopropylethylamine (DIPEA) and 16-mercaptohexadecanoic acid (MHDA), sodium hydroxide, inorganic salts, chloroform and Butvar solution B-98 were obtained from Sigma-Aldrich (St. Louis, MO, USA).

Glucose oxidase (GOx) preparations were obtained from *Penicillium adametzii* LF F-2044.1.[32]

All buffers and standard solutions were prepared using the water purified by the Milli-Q system (Millipore).

2.2. Synthesis of Nanoparticles

All nanoparticles (NPs) were synthesized by the reduction of metal ions from appropriate salts according to the known methods in our modifications.[33,34] NPs were collected by centrifugation under 10000 g for 40 min (Hettich Micro-22R centrifuge), washed with water and precipitated by centrifugation. Pellets were suspended in 0.2 mL of water and stored till exploitation at +4 °C.

2.3. Immobilization of GOx and PO on NPs

The procedure of GOx and PO immobilization on NPs was carried out as described by us earlier.[34] An aliquot of NPs (to the final 0.1 mM concentration) was incubated overnight in 5 mM solution of MHDA in ethanol at +4 °C. After rinsing with DMF, the MHDA-covered NPs were incubated in a DMF solution of 20 mM CMC, 20 mM PFP and 20 mM DIPEA for 30 min at 25 °C. After repeated rinsing with DMF, condensation of the activated Au- and Ag-linked carboxylic groups with amine groups of the enzyme was carried out. 25 μL of the enzyme solution in 30 mM phosphate buffer, pH 7.0 (PB) was incubated with NPs for 1 h at 25 °C. After rinsing with PB, blocking of un-reacted carboxylic groups with 0.1 M solution of AEE in 0.1 M bicarbonate buffer, pH 8.0, was performed. The bio-functionalized NPs were rinsed with PB and stored at +4 °C until usage.

2.4. Apparatus

A three-electrode system was used for the electrochemical studies. A piece of Pt wire and an Ag/AgCl/3 M KCl

electrode were used as the counter and reference electrodes, respectively. A carbon rod electrode (ALS Co., Tokyo, Japan) was applied as a working electrode (3.0 mm diameter). Amperometric measurements were carried out with a potentiostat CHI 1200A (IJ Cambria Scientific, Burry Port, UK) and performed in batch mode under continuous stirring in a standard 40 ml cell at room temperature.

2.5. Preparation and Evaluation of the Biosensor

Commercial GOx (with activity 100 $U \cdot mL^{-1}$) and PO with the same activity were immobilized successively on different types of NPs and then dropped on the top of carbon rod electrode (CE). Dried enzyme was covered by a Nafion membrane. The coated bioelectrodes were rinsed with water and stored in PB before using. All fabricated bioelectrodes were marked further as following: GOx/PO dropped onto CE was marked as bio/CE; GOx/PO immobilized on AgNPs (Au/AgNPs or Ag/AuNPs) and dropped on CE—as bioAgNPs/CE (bioAu/AgNPs/CE or bioAg/AuNPs/CE), respectively.

Analytical characteristics of the proposed bioelectrodes were statistically processed using the OriginPro 8.5 software. Calculation of the apparent Michaelis-Menten constants (K_M^{app}) was automatically performed by this program according to the Lineweaver–Burk equation.

2.6. Glucose Assay in the Samples of Wines

The samples of the following wines were tested in this study: semisweet red "Drevniy Khersones" (Inkerman, Ukraine), sweet, red "Porto" (Kopke, Portugal), dry red "Chianti" (Gecchi, Italian), dry red "Telavi" (Marani, Georgia). To avoid interference effect of organic additives during assay of glucose, these samples were analyzed using a standard addition test (SAT). Before assay, all samples were diluted step-wise by PB: for biosensor and enzymatic methods, dilution factors are 50 and 75, 150, 750, respectively. Each assay was performed for two dilutions of the sample and repeated at least 3 times. Concentration of glucose in the initial sample ($C_{calcul.}$) was estimated from the parameters of linear regression (A, B) of the corresponding graph, taking into account factor of the sample's dilution (N):

$$C_{calcul.} = \frac{A}{B} \cdot N$$

As reference method, domestic enzymatic kit "Glucotest" was employed.

The analytical results were statistically processed using the OriginPro 8.5 software.

3. RESULTS AND DISCUSSION

3.1. Construction of Glucose-Sensitive Bioselective Layer with NPs

In our preliminary studies we have investigated the stabilizing properties of monometallic and bi-metallic Ag/Au and Au/AgNPs onto the PO and GOx.[33,34] It was shown that the most effective and stabilizing platform for immobilizing PO is AuNPs.[34]

In current work GOx was immobilized on the surface of NPs with different effectiveness: yield of activities of GOx on AgNPs, Au/AgNPs and Ag/AuNPs was $29 \pm 0.65\%$, $12 \pm 0.57\%$ and $25.1 \pm 1.40\%$, respectively, in comparison with initial activity of free GOx in solution. Calculation of activity were carried out as described earlier[34] taking into account total activities of initial enzyme preparation.

To form an enzymatic layer of the bio-electrode sensitive to glucose, different types of NPs linked with PO and GOx were dropped on the surface of the CE and covered

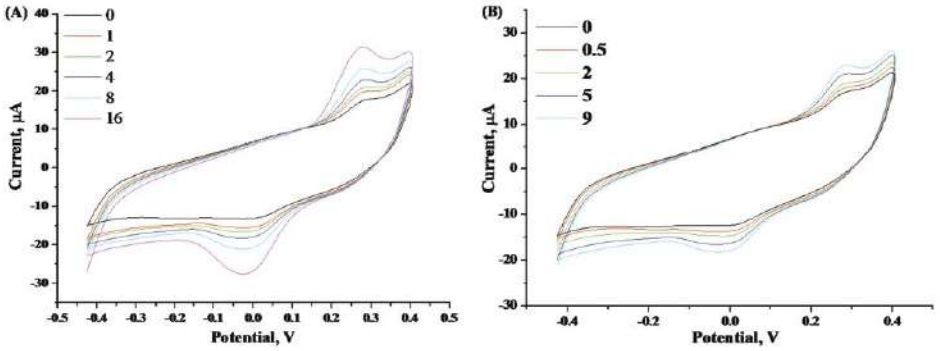

Fig. 1. Characterization of bioelectrodes by cyclic voltamperometry: PO-AuNPs/CE in the absence (black line) and in the presence (color lines) of increasing concentrations of H_2O_2, (from 1 to 16 mM) (A); bio-Ag/AuNPs/CE in the absence (black line) and in the presence (color lines) of increasing concentrations of glucose (from 0.5 to 9 mM) (B). Conditions: –0.4 V to 0.4 V versus Ag/AgCl; scan rate 7 $mV \cdot s^{-1}$ in 30 mM phosphate buffer, pH 7.0.

with a Nafion membrane according to the experimental part (see subdivision 2.5).

The efficiency of free defusing electron transfers from the oxidized PO to electrode via AuNPs (as mediator) was evaluated using cyclic voltamperometry (CV). The cyclic voltamperometry gives information about optimal working potential for sufficient PO reduction on the top of carbon rod electrode (Fig. 1(A)).

GOx enzyme comprises of two identical protein subunits and one flavin adenine dinucleotide (FAD) coenzyme

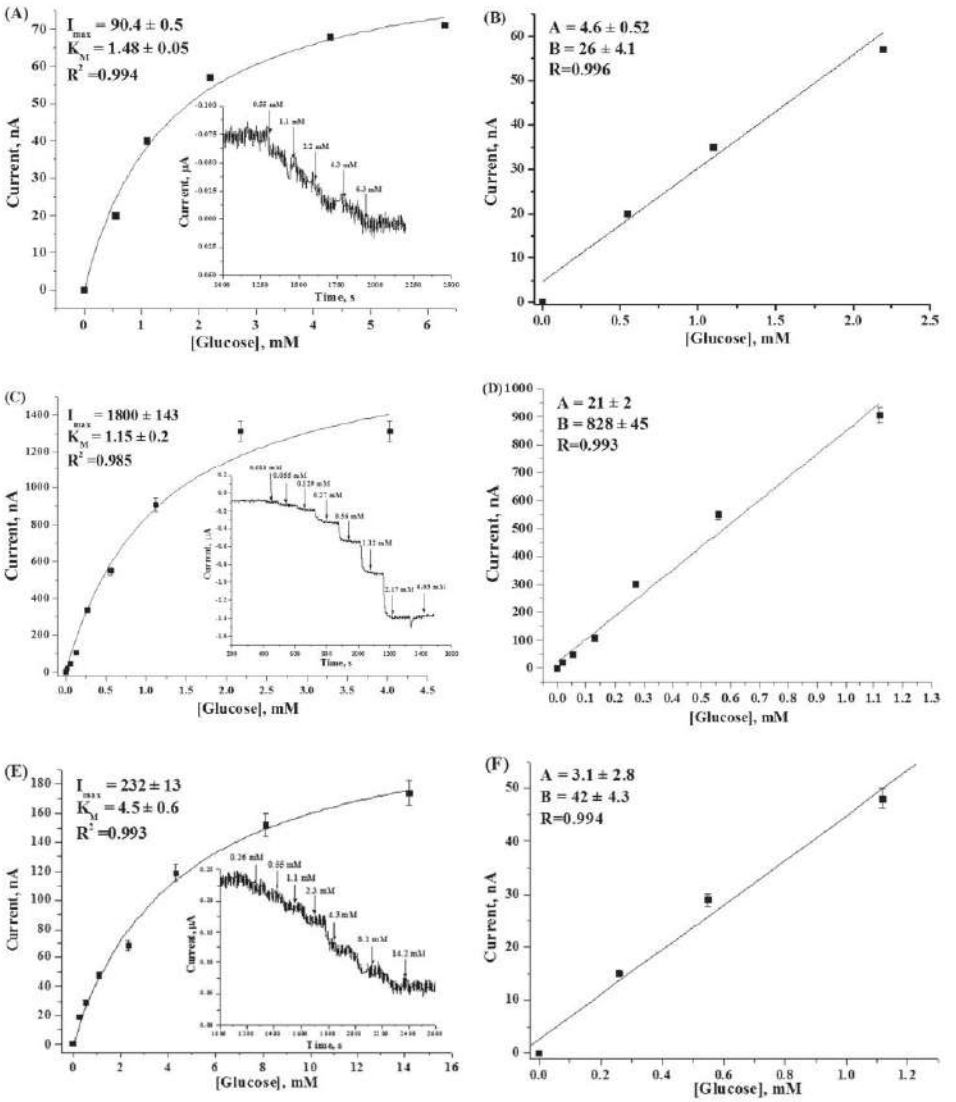

Fig. 2. Continued.

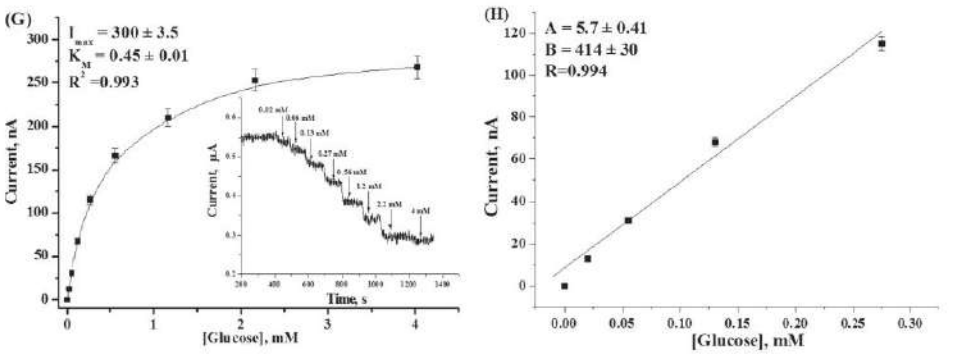

Fig. 2. Calibration curves for amperometric response on glucose of the developed electrodes: bio/CE (A, B); bioAgNPs/CE (C, D); bioAu/AgNPs/CE (E, F); bioAg/AuNPs/CE (G, H); Inset: chronamperometric current response upon subsequent additions of glucose. Conditions: −50 mV versus Ag/AgCl electrode in 30 mM phosphate buffer, pH 7.0 at 22 °C.

molecule. The FAD coenzyme molecule is present in the active site of the GOx enzyme. Due to its highly reversible electrochemistry, FAD works efficiently as a cofactor. FAD can be reduced in a two-electron, two proton process to form $FADH_2$. During the enzymatic reaction between GOx and glucose, glucose is oxidized to glucono-d-lactone and the FAD is reduced to $FADH_2$. Subsequently, $FADH_2$ under GOx oxidation by dissolved O_2 producing H_2O_2 and becomes FAD.[24] These processes can be represented using the following Eqs. (1)–(2):

$$\mathrm{GOx(FAD)} + \mathrm{Glucose} \rightarrow \mathrm{GOx(FAD_2)} + \mathrm{Glucono-d-lactone} \quad (1)$$

$$\mathrm{GOx(FADH_2)} + \mathrm{O_2} \rightarrow \mathrm{GOx(FAD)} = \mathrm{H_2O_2} \quad (2)$$

Combining these two equations the oxidation process of glucose in the presence of GOx can be represented as:

$$\mathrm{Glucose} + \mathrm{O_2} \xrightarrow{\mathrm{GOx}} \mathrm{Glucono-d-lactone} + \mathrm{H_2O_2} \quad (3)$$

The efficiency of free defusing electron transfers from the oxidized GOx to electrode via Ag/AuNPs (as mediatior) was evaluated using CV (Fig. 1(B)).

As it shown in Figure 1, potential −50 mV versus Ag/AgCl was chosen as optimal working potential for PO and GOx reduction in our system. The summarized output of enzymatic reduction of 9 mM glucose for bioelectrode was estimated as 6 μA. It worth mentioning, that the behavior of the all proposed bioelectrodes on the glucose injection are similar to bio-Ag/AuNPs/CE with the reduction peak −50 mV, so their CV are not shown.

3.2. Evaluation and Optimization of the Glucose Biosensors

The obtained bioelectrodes were used for the investigation of some analytical parameters of biosensors. The calibration curves and the corresponding chronamperograms (inset) are shown in Figure 2. The calibration was performed by the stepwise addition of an aliquot of standard glucose solution (50 mM) in working cell. Amperometric responses on glucose of the enzyme electrodes were tested in the range of resulted glucose concentrations from 0.01 to 20 mM. Table II demonstrates the general analytical characteristics of the proposed amperometric biosensors.

The prepared in this research different bioelectrodes (Table II) have several advantages compared to the known ones (Table I): they are nonpoisonous, with broad range of applicable potential, quick response, renewable surface and high operational stability. It is shown that the usage of NPs as platform for enzyme's immobilization in tandem with PO, allows to decrease the working potential of the biosensors to −50 mV (which is important to avoid interfering effects of a sample background) and to increase the linear range. The apparent Michaelis-Menten constant (K_M^{app}) for bioAgNPs/CE bioelectrode (Table II) was closed to K_M^{app} of unmodified bio/CE. In the same time, K_M^{app} for bio-Ag/AuNPs/CE is 3.3 fold lower and for bioAu/AgNPs/CE is 3-fold higher in comparison with the unmodified bio/CE. These differences are assumed to associate with an influence of the rather complicated

Table II. Analytical characteristics of the proposed bioelectrodes.

Composition of bioelectrodes	bio/CE	bioAgNPs/ CE	bioAu/AgNPs/ CE	bioAg/AuNP/ CE
LOD, μM	115	4	71	7
Linear range, mM	0.5–2.5	0.02–1.20	0.2–1.2	0.03–0.30
Sensitivity, $A \cdot (M \cdot m^2)^{-1}$	3.5±0.5	113.5±6.2	5.9±0.2	58.5±4.2
K_M^{app}, mM	1.50	1.15	4.50	0.45
I_{max}, nA	90.4±0.5	1800±143	232±13	300±3.5
Response time, s	20	20	20	20
Operation stability, days (50% of signal)	7	12	7	12

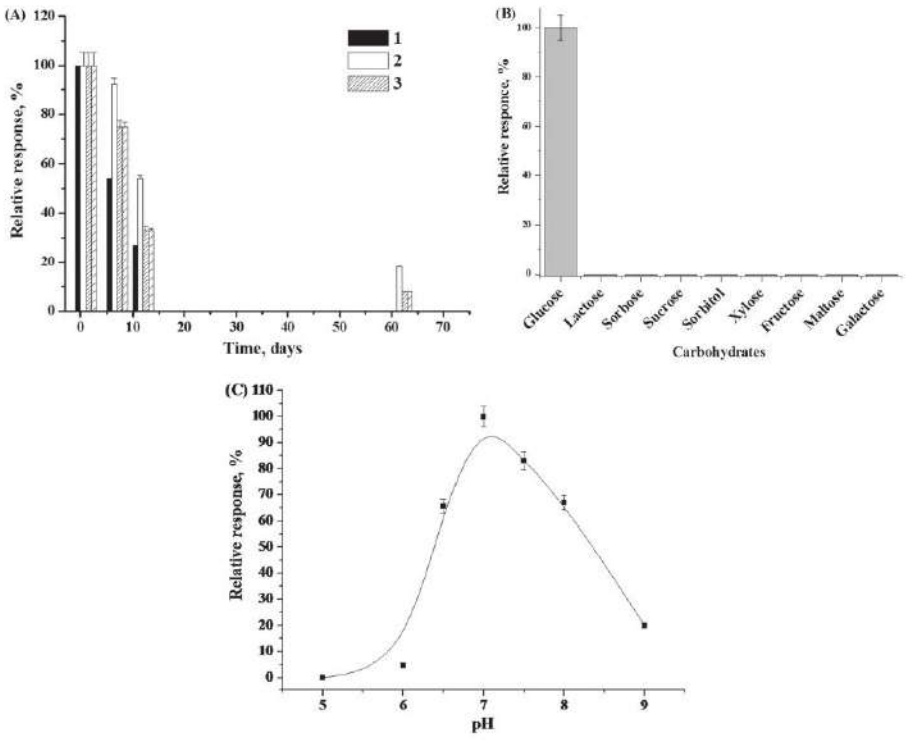

Fig. 3. Characteristics of the developed glucose biosensor using under applied potential of −50 mV at 22 °C. The highest current response was chosen as 100% in all experiments. (A) Storage stabilities were checked in 0.25 mM glucose solution in 30 mM PB, pH 7.5 at room temperature during 60 days: 1—bio/CE and bioAu/AgNPs/CE; 2—bioAgNPs/CE; 3—bioAg/AuNPs. All bioelectrodes between measurements were kept at +4 °C in PB, pH 7.5; (B) selectivity test was done with different 0.25 mM carbohydrates in PB, pH 7.5; (C) pH-optimum for the bioAgNPs/CE was estimated with the usage of 0.25 mM glucose in 30 mM PB at different pH values.

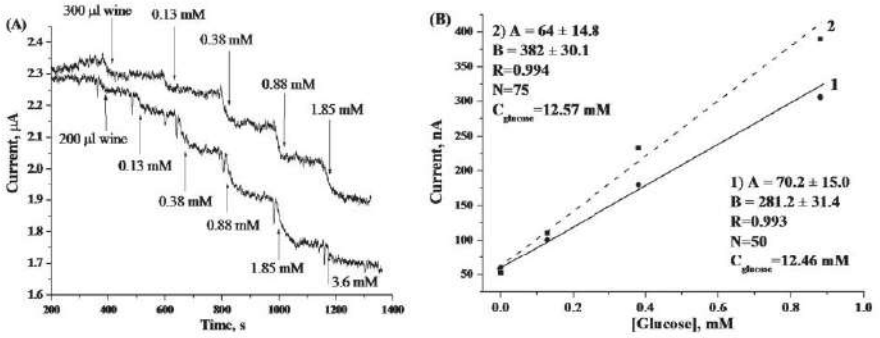

Fig. 4. Analysis of glucose in the sample of wine "Chianti" using laboratory prototype of glucose biosensor by standard addition method. A, B parameters for the linear range; R = linear regression coefficient, n-dilution factor; C_{calcn}—calculated value of glucose content, mM.

composition of the biorecognition membrane on the diffusional availability of the substrate (glucose) to the immobilized enzymes.

The application of NPs in bioselective layer has a positive impact on the biosensor properties due to the lower limit of detection (LOD) for glucose determination (from 4 μM up to 71 μM). The 29-fold expanded LOD for bioAgNPs/CE sensor architecture is better adapted to the typical concentration range of glucose in the samples of wines.

3.3. Characteristics of the Fabricated Glucose-Sensitive Biosensors

The results of the study of stability, selectivity and pH dependence of the fabricated bi-enzyme sensors are presented in Figure 3. The stabilities of the constructed bioelectrodes were explored by monitoring their current responses to the injection of a 0.5 mM glucose standard solution for a period of 60 days. The outputs of the biosensors decreased by 80% for a period of 60 days and the half-life of the sensor was about 12 days for AgNPs whereas the half-life of bioAu/AgNPs/CE as well as for bioAu/AgNPs/CE were 7 days (Fig. 3(A)).

The selectivity of the constructed biosensor was estimated in relative units (%) as a ratio of the detected signal to the value of the highest current response (Fig. 3(B)): no signal to the majority of the tested carbohydrates (lactose, sucrose, sorbose, sorbitol, xylose, fructose, maltose and galactose) was observed.

The pH-dependence of the sensor's output on glucose was investigated too (Fig. 3(C)). The highest current response was found for a 50 mM phosphate buffer (PB), pH 7.0; this buffer therefore was chosen as optimal for glucose analysis by the constructed prototype of the bi-enzyme biosensor.

3.4. Determination of Glucose Concentration in Wines with the Usage of Fabricated BioAgNPs/CE

Several wines ("Drevniy Chersones," "Chianti," "Telavi" and "Porto") were analyzed for their glucose contents using bioAgNPs/CE biosensor and also by a commercial enzymatic kit "Glucotest." To evaluate the possible interference effect of wines components on glucose estimation results, a standard addition test was applied to the diluted samples. The principle of biosensor assay and calculation of glucose concentration in wine "Chianti" as example is presented in Figure 4. The results of glucose assay in all samples tested by the proposed and referent methods are summarized in Table III, these values demonstrate a strong correlation. Thus, the obtained results indicate that the developed bioAgNPs/CE electrode can be utilized for a simple and valid assay of glucose in wines.

In current work new glucose-selective bi-enzyme amperometric biosensors based on the glucose oxidase and horseradish peroxidase have been developed. To improve sensor characteristics, covalent co-immobilization of GOx with PO on the surface of NPs of noble metals has been performed. The main sensor characteristics (sensitivity, linear range of detection, response time, and K_M^{app} value) have been investigated. The most effective among the developed biosensor (AgNPs-based) was tested for glucose assay in some commercial wines using the multiple standard addition method. A strong correlation ($R = 0.9998$) between data obtained by the constructed biosensor and referent chemical method was observed. The proposed laboratory prototype of a glucose selective biosensor would be promising for food quality control. The biosensor is cost effective, as a very small amount of biocomponents and reagents were used for its fabrication.

Table III. Concentrations of glucose in wine samples, determined by different methods.

	Method			
	Biosensor approach		Enzymatic kit "Glucotest"	
Wines	Glucose, mM	CV, %	Glucose, mM	CV, %
"Drevniy Chersones"	327.5 ± 10.5	1.40	314.2 ± 7.5	1.50
"Chianti"	*12.5 ± 0.6	0.30	11.8 ± 0.35	0.35
"Telavi"	2.05 ± 0.05	0.50	1.90 ± 0.1	0.43
"Porto"	650.5 ± 43.1	2.20	624 ± 23.2	2.50

Notes: CV—Coefficient of variation. Values are expressed as mean ± SD. *—These results were obtained from graphs, demonstrated in Figure 4(B).

4. CONCLUSIONS

In current work highly selective glucose biosensors of the third generation in which NPs serve as enzyme' activators and stabilizers as well as the mediators of electron transfer were proposed. For construction of glucose-selective biosensor, the bi-enzyme sensor consisted on tandem of GOx and PO, co-immobilized with mono- and bi-metallic NPs of noble metals. Using PO in tandem with mimetic NPs allows to decrease working potential of the sensor till −50 mV which is important to avoid interfering effects of a real sample' background. All developed bioNPs/CEs showed the higher sensitivities, wider linear ranges, lower limits of detection and higher stabilities in comparison with bio/CE. The most effective bioAgNPs/CE biosensor was used for glucose analysis in the samples of wines. A high correlation with the glucose values estimated by biosensor and commercial enzymatic kit was demonstrated.

Conflict of Interest

The authors declare that there is no conflict of interest regarding the publication of this article.

Acknowledgments: This work was financially supported by NAS of Ukraine (Program "Sensors for Medical, Environmental, Industrial, and Technological Needs," Project 5/3-2017 and joint Ukrainian-Belorussian project

F 54.4/031), by the Ministry of Education and Science of Ukraine (project #0116U004737), and by Fellowship of President of Ukraine for Young Scientists in 2016–2017 (N. Stasyuk).

References and Notes

1. C. Chen, X. L. Zhao, Z. H. Li, Z. G. Zhu, S. H. Qian, and A. J. Flewitt, 17 (**2017**), DOI: 10.3390/s17010182.
2. L. S. Cock, A. M. Z. Arenas, and A. A. Aponte, *Chilean Journal of Agricultural Research* 69, 270 (**2009**).
3. C. Canal and B. Ozen, *J. Food Process Eng.* 40, e12280 (**2017**).
4. X. J. Wu and M. M. F., Glucose Sensing. Topics in Fluorescence Spectroscopy, edited by C. D. Geddes and J. R. Lakowicz, Springer, Boston, MA (**2006**), p. 11.
5. F. M. Lopes, K. A. Batista, G. L. A. Batista, and K. F. Fernandes, *Ciênc. Technol. Aliment. Campinas* 32, 65 (**2004**).
6. L. Muresan, S. Gáspár, G. Turdean, and I. C. Popescu, *Rev. Chim. (Bucursti)* 61, 126 (**2010**).
7. T. B. Goriushkina, A. P. Soldatkin, and S. V. Dzyadevych, *J. Agric. Food Chem.* 57, 6528 (**2009**).
8. R. Antiochia and L. Gorton, *Biosens. Bioelectron.* 22, 2611 (**2007**).
9. J. M. Harris, C. Reyes, and P. Lopez, *J. Diabetes Sci. Technol.* 4, 1030 (**2013**).
10. J. Gonzalo-Ruiz, M. A. Alonso-Lomillo, and F. J. Munoz, *Biosens. Bioelectron.* 22, 1517 (**2007**).
11. D. Centonze, C. G. Zambonin, and F. Palmisano, *Journal of AOAC International* 80, 829 (**1997**).
12. L. Zhu, R. Yang, J. Zhai, and C. Tian, *Biosens. Bioelectron.* 23, 528 (**2007**).
13. J. P. Li and X. Z. Chen, *Acta Chim. Sinica* 66, 84 (**2008**).
14. S. J. Bao, C. M. Li, J. F. Zang, and X. Q. Cui, *Adv. Funct. Mater.* 18, 591 (**2008**).
15. C. X. Guo and C. M. Li, *Phys. Chem. Chem. Phys.* 12 (**2010**).
16. N. Stasyuk, G. Gayda, R. Serkiz, and M. Gonchar, *Journal of Advances in Chemistry* 11, 3498 (**2015**).
17. M. C. Daniel and D. Astruc, *Chem. Rev.* 104, 293 (**2004**).
18. M. J. Feldstein, C. D. Keating, Y. H. Liau, and M. J. Natan, *Am. Chem. Soc.* 119, 6638 (**1997**).
19. Y. K. Lahir, M. Samant, and P. M. Dongre, *Role of Nanomaterials in the Development of Biosensors, G.J.B.B.* 5, 146 (**2016**).
20. N. V. Vallabani, A. S. Karakoti, and S. Singh, *Colloids Surf. B Biointerfaces* 153, 52 (**2017**).
21. K. Zhao, W. Gu, S. Zheng, C. Zhang, and Y. Xian, *Talanta* 141, 47 (**2015**).
22. X. Yang, Y. Wang, Y. Liu, and X. Jiang, *Electrochim. Acta* 108, 39 (**2013**).
23. Al-Ogaidi, H. Gou, A. Kareem, A. Al-Kazaz, Z. P. Aguilar, A. K. Melconian, P. Zheng, and N. Wu, *Anal. Chim. Acta* 811, 76 (**2014**).
24. R. B. Rakhi, P. Nayak, C. Xia, and H. N. Alshareef, *Scientific Reports* 6, 36422 (**2016**).
25. L. Wang, Y. Zeng, A. Shen, Y. Fu, L. Zeng, and J. Hu, *RCS Advances* 896, 86025 (**2016**).
26. F. Wang, X. Liu, C. H. Lu, and I. Willner, *ACS Nano* 7, 7278 (**2013**).
27. Z. Abadi, V. Mottaghitalab, M. Bidoki, and A. Benvidi, *Sensor Review* 34, 360 (**2014**).
28. S. Zhang, N. Wang, H. Yu, Y. Niu, and C. Sun, *Bioelectrochemistry* 67, 15 (**2005**).
29. Y. Zhang, W. Jia, M. Cui, C. Dong, S. Shuang, Y. K. Leung, and M. Martin, *Biotechnol. J.* 6, 492 (**2011**).
30. W. Liu, H. Wu, B. Li, C. Dong, M. M. F. Choi, and S. Shuang, *Anal. Methods* 5, 5154 (**2013**).
31. A. Ramanavicius, N. German, and A. Ramanaviciene, *Journal of Electrochemical Society* 164, 45 (**2017**).
32. R. V. Mikhailova, L. A. Zhukovskaya, and A. G. Lobanok, *Applied Biochemistry and Microbiology* 43, 207 (**2007**).
33. M. M. Synenka, N. Ye. Stasyuk, T. V. Semashko, G. Z. Gayda, R. V. Mychailova, and M. V. Gonchar, *Biological Studio* 8, 5 (**2014**).
34. N. Stasyuk, G. Gayda, H. Klepach, and M. Gonchar, *Sensor Lett.* 14, 1 (**2016**).

RESEARCH ARTICLE

Оригінал доступний за посиланням:
ttps://www.ingentaconnect.com/content/asp/senlet/2017/00000015/00000008/art00004

Анотація: *У поточній роботі нами сконструйовано новий амперометричний біензимний біосенсор, селективний до метиламіну, на основі рекомбінантної метиламінооксидази (МАО), виділеної з рекомбінантного дріжджового штама Saccharomyces cerevisiae. Нами запропоновано дві архітектури біоселективного шару: вільно дифундуючий ензим (МАО) та ковалентно іммобілізований на поверхні наночастинок золота (МАО-Au). Для отриманих біосенсорів досліджували основні біоаналітичні параметри, зокрема, чутливість, селективність та стабільність при зберіганні. Встановлено, що після іммобілізації МАО на поверхні НЧ Аи чутливість зростає практично вдвічі: з 700 ± 30 до 1450 ± 113 $А^{-1}·М^{-1}·м^{-2}$ (для МАО та МАО-Аи відповідно). Для біоелектроду, модифікованого НЧ Аи, досліджували операційні характеристики, зокрема, селективність та стабільність при зберіганні. Сигнал для диметиламіну та триметиламіну – менше 5%, а для етиламіну – на 15% порівняно із сигналом на МА. Розроблені біосенсори протестовано на реальних зразках рибних продуктів у порівнянні із хімічним методом. Значення, отримані за допомогою обох підходів, виявили високу кореляцію.*

Hindawi Publishing Corporation
BioMed Research International
Volume 2014, Article ID 480498, 8 pages
http://dx.doi.org/10.1155/2014/480498

Hindawi

Research Article

Methylamine-Sensitive Amperometric Biosensor Based on $(His)_6$-Tagged *Hansenula polymorpha* Methylamine Oxidase Immobilized on the Gold Nanoparticles

Nataliya Ye. Stasyuk,[1] Oleh V. Smutok,[1] Andriy E. Zakalskiy,[1] Oksana M. Zakalska,[1] and Mykhailo V. Gonchar[1,2]

[1] *Institute of Cell Biology, NAS of Ukraine, Drahomanov Street 14/16, Lviv 79005, Ukraine*
[2] *Institute of Applied Biotechnology and Basic Sciences, University of Rzeszow, Sokolowska Street 26, 36-100 Kolbuszowa, Poland*

Correspondence should be addressed to Mykhailo V. Gonchar; gonchar@cellbiol.lviv.ua

Received 21 February 2014; Revised 2 June 2014; Accepted 20 June 2014; Published 16 July 2014

Academic Editor: Noomen Hmidet

Copyright © 2014 Nataliya Ye. Stasyuk et al. This is an open access article distributed under the Creative Commons Attribution License, which permits unrestricted use, distribution, and reproduction in any medium, provided the original work is properly cited.

A novel methylamine-selective amperometric bienzyme biosensor based on recombinant primary amine oxidase isolated from the recombinant yeast strain *Saccharomyces cerevisiae* and commercial horseradish peroxidase is described. Two amine oxidase preparations were used: free enzyme (AMO) and covalently immobilized on the surface of gold nanoparticles (AMO-nAu). Some bioanalytical parameters (sensitivity, selectivity, and storage stability) of the developed biosensors were investigated. The sensitivity for both sensors is high: 1450 ± 113 and $700 \pm 30\ A^{-1} \cdot M^{-1} \cdot m^{-2}$ for AMO-nAu biosensor, respectively. The biosensors exhibit the linear range from 15 μM to 150 μM (AMO-nAu) and from 15 μM to 60 μM (AMO). The developed biosensor demonstrated a good selectivity toward methylamine (MA) (signal for dimethylamine and trimethylamine is less than 5% and for ethylamine 15% compared to MA output) and reveals a satisfactory storage stability. The constructed amperometric biosensor was used for MA assay in real samples of fish products in comparison with chemical method. The values obtained with both approaches different methods demonstrated a high correlation.

1. Introduction

The assay of aliphatic amines in environment and biological samples is important, due to the use of these compounds in industry and their wide distribution in living organisms as a result of natural degradation of proteins, amino acids, and other nitrogen-containing compounds [1]. Methylamine (MA) can be accumulated in some kinds of fish, especially of *Gadoid* species, in very high amounts as a result of enzymatic degradation of the natural osmolyte, trimethylamine *N*-oxide (TMAO). Consuming such fish food in combination with nitrate-containing products could result in the formation of *N*-nitroso derivatives which are very powerful carcinogens [2].

It is also important that MA is widely used in different stages of the preparation of various drug substances; therefore, it may be retained in the drug substance. MA is also controlled by the U.S. Drug Enforcement Administration as a List 1 Regulated Chemical due to its use in production of methamphetamine [3].

It was shown that reactions of trimethylamine (TMA) accumulation are not specific for fish only and may also occur in human organism. This fact has been proven by the discovery of human inherited syndrome of "fish smell," trimethylaminuria [4]. Homozygous carriers of this metabolic disorder produce a specific smell due to continuous TMA excretion with sweat and urea. This disorder is probably caused by defects in flavoenzyme, monooxygenase FMO3, which converts TMA, a compound with a very unpleasant smell, into TMAO, an odourless compound.

Unfortunately, the problem of analysis of fish products quality and biochemical diagnostics of trimethylaminuria is yet to be solved due to the absence of a fast, cheap, and

selective method of analysis of food products and human biological liquids for the presence of primary aliphatic amines, that is, MA, dimethylamine (DMA), and TMA. The majority of the frequently used approaches are time consuming and expensive and require skillful labor techniques, such as the high performance liquid chromatography [5], colorimetry [6], laser spectroscopy [7], fluorometry [8], ion chromatography [9], and enzymatic method [10]. The majority of these methods are marked by poor precision and low sensitivity and selectivity.

The simplest way to detect alkylamines is an enzymatic method based on natural isoforms of amine oxidases with different substrate specificity. The main obstacle for using this method is absence of commercial preparations of primary amine oxidase (AMO; E.C. 1.4.3.21), the key biologically active element of a potential biosensor.

In this paper, we describe the construction of an AMO-based amperometric bioelectrode selective to MA. A ferrocene layer was used as a final electron transfer mediator. The biorecognition membrane includes two enzymes: purified $(His)_6$-tagged AMO from the recombinant yeast *Saccharomyces cerevisiae* [11] and commercial horseradish peroxidase (HRP). The enzymes were dropped on the ferrocene-modified graphite electrode surface and covered with a cathodic polymer GY 83-0270 0005. The principal scheme of MA determination is as follows:

$$\begin{aligned}
&CH_3NH_2 + H_2O + O_2 \xrightarrow{AMO} CH_2O + NH_3 + H_2O_2,\\
&H_2O_2 + HRP\,(Fe) \longrightarrow H_2O + HRP\,(Fe = O),\\
&HRP\,(Fe = O) + \text{ferrocene}\left(Fe^{2+}\right) + 2H^+ \longrightarrow HRP\,(Fe) \quad (1)\\
&\qquad + \text{ferrocene}\left(Fe^{3+}\right) + H_2O,\\
&\text{ferrocene}\left(Fe^{3+}\right) \xrightarrow{\text{Electrode}} \text{ferrocene}\left(Fe^{2+}\right)
\end{aligned}$$

The developed amperometric bienzyme electrode was applied for MA assay in the samples of fish products.

2. Materials and Methods

2.1. Materials. Horseradish peroxidase (HRP) (EC 1.11.1.7, from *Armoracia rusticana*, 500 $U \cdot mg^{-1}$), tetrachloroauric acid trihydrate, sodium salt of ABTS, sodium citrate, *N*-(3-dimethylaminopropyl)-*N'*-ethylcarbodiimide hydrochloride (EDC), pentafluorophenol (PFP), 2-(2-aminoethoxy) ethanol (AEE), dimethylformamide (DMF), *N*,*N*-diisopropylethylamine (DIPEA), 16-mercaptohexadecanoic acid (MHDA), methylamine (MA), dimethylamine (DMA), trimethylamine (TMA), NaCl, KH_2PO_4, Na_2HPO_4, chloroform, and Butvar solution B-98 were purchased from Sigma-Aldrich (ALSI Ltd., Kiev, Ukraine). The cathodic electrodeposition paint "GY 83–0270 0005" was from BASF Farben und Lacke (Munster, Germany). All buffers and standard solutions were prepared using the water purified by the Milli-Q system (Millipore).

2.2. Isolation and Purification of Amine Oxidase (E.C. 1.4.3.21). As a source of $(His)_6$-tagged AMO, the constructed by us recombinant yeast strain *Saccharomyces cerevisiae* C13ABYS86 (*Mat a, leu2-3, ura3, his, pra1-1, prb1-1, prc1-1, cps1-3*) able to overexpress the target enzyme was used. The $(His)_6$-tagged enzyme was purified from the cell-free extract of the recombinant strain by metal-affinity chromatography on Ni-NTA-agarose [11]. Purified AMO with specific activity 13.7 $U \cdot mg^{-1}$ was stored in 20 mM phosphate buffer, pH 7.5 (PB), at 4°C.

2.3. Assay of AMO Activity. The AMO activity was measured according to the method described by Haywood and Large [10]. AMO activity of free and immobilized on nAu enzyme preparations was determined by monitoring ABTS oxidation by H_2O_2 generated during MA cleavage. The millimolar absorption coefficient of the radical-cation product at 405 nm is 18.41 $mM^{-1} \cdot cm^{-1}$. Usually, 100 μL of a substrate mixture (150 mM methylamine hydrochloride, 30 mM Na_2ABTS, and 0.3 $mg \cdot mL^{-1}$ HRP in 75 mM PB, pH 7.5) was preincubated for 5 min at 30°C and added to the test tube containing 10 μL of AMO preparation. The reaction mixture was incubated for 15 min at 30°C followed by radical-cation product assay. The kinetic study was carried out at the same conditions within methylamine concentration range of 0.02 to 5 mM. AMO concentration in the incubation mixture was 40 $ng \cdot mL^{-1}$. One unit of AMO activity was defined as the amount of enzyme required to catalyse the formation of 1 μmole ABTS radical cation per 1 min under standard conditions.

2.4. Synthesis of Gold Nanoparticles (nAu). Gold nanoparticles (nAu) were synthesized by the citrate reduction method [12]. 1.25 mL of 1 mM $HAuCl_4$ and 0.125 mL of 38.8 mM trisodium citrate were mixed at 100°C and stirred for 15 min to obtain a wine-red solution. The nAu were precipitated by centrifugation (6708 g; Hettich Micro-22R centrifuge). The precipitate was washed with water and stored at +4°C before using. Under the described conditions, a colloid solution of nAu in water at concentration of 0.9 mM was obtained for further characterization and enzyme immobilization.

2.5. Immobilization of $(His)_6$-Tagged AMO on nAu. The nAu were incubated overnight in 5 mM MHDA in ethanol at +4°C. After rinsing with DMF, the MHDA-covered nAu were incubated in a DMF solution of 20 mM CMC, 20 mM PFP, and 20 mM DIPEA for 30 min at 25°C. After repeated rinsing with DMF, condensation of the activated Au-linked carboxylic groups with amine groups of the enzyme was carried out. 25 μL of the enzyme solution (0.75 $mg \cdot mL^{-1}$) in 30 mM PB, pH 7.5, was incubated with nAu for 1 h at 25°C. After rinsing with PB, pH 7.5, blocking of unreacted carboxylic groups with 0.1 M solution of AEE in 0.1 M bicarbonate buffer, pH 7.0, was performed. The biofunctionalized nAu were rinsed with PB, pH 7.5, and stored at +4°C until usage. The amount of immobilized enzyme on the nAu was determined as the difference between the initial and unbound protein content in the immobilization medium using the Lowry protein assay method.

2.6. Characterisation of nAu Using Atomic Force Microscopy (AFM). The size and structure of nAu particles (unbound and enzyme-modified) were studied by atomic force microscope Solver P47-PRO (NT-MDT, The Netherlands). An aliquot of the tested sample was spread on the surface of freshly cleaved mica, dried, and analyzed in air using the tapping mode with resonance frequency of 160 kHz, scan rate of 1 Hz/s, and resolution of 256 × 256 pixels.

2.7. Apparatus for Biosensor Analysis. Amperometric biosensors were evaluated using constant potential amperometry in a three-electrode configuration with a Ag/AgCl/KCl (3 M) reference electrode and a Pt-wire counter electrode. Amperometric measurements were carried out using a potentiostat CHI 1200A (IJ Cambria Scientific, Burry Port, UK) connected to a personal computer and performed in batch mode under continuous stirring in a standard 40 mL cell at room temperature.

Graphite rods (type RW001, 3.05 mm diameter, Ringsdorff Werke, Bonn, Germany) were used as working electrodes. They were sealed in glass tubes using epoxy glue thus forming disk electrodes. Before sensor preparation, the graphite electrodes were polished with emery paper.

2.8. Preparation of the Mediator-Modified Graphite Electrodes. Electrodeposition of 5 mM solutions of Mendola blue and methylene blue in 20 mM PB, pH 7.5, on the surface of 3 mm rod graphite electrode was performed using cyclic voltamperometry in the range from −400 to +400 mV with scan rate 50 $mV \cdot min^{-1}$ *versus* Ag/AgCl/3 M KCl reference electrode.

A 5 μL aliquot of 2 mM ferrocene solution in acetone was dropped onto surface of working electrode and air-dried for 10 min.

The mediator-modified electrodes were rinsed with water and equilibrated in 30 mM PB, pH 7.5, before using.

2.9. Immobilization of the Enzymes on the Mediator-Modified Electrode Surface. HRP and AMO were dropped on the mediator-modified electrode and covered by an electrodeposited commercial cathode polymer-GY 83-0270 0005 (*CP*). The immobilization procedure was as follows: 3 μL of HRP solution with activity 200 $U \cdot mL^{-1}$ in 30 mM PB, pH 7.5, was dropped on the top of the mediator-modified carbon electrode. After drying for 2 min at room temperature, the layer of HRP was covered with a 5 μL solution of AMO in FB, pH 7.5, with activity 40 $U \cdot mL^{-1}$ or AMO-nAu, 35.5 $U \cdot mL^{-1}$, respectively. Dried bienzyme layers were covered with 4 μL of GY 83-0270 0005 for polymer layer formation. The prepared biofunctionalized electrode was rinsed with PB, pH 7.5, and stored at +4°C before application.

2.10. A Colorimetric Method for the Determination of Methylamine in Fish Products. A chemical analysis of MA, based on the use of lactose in alkaline solution [6], was performed using the multiple standard addition method. The absorbance of the reaction product was recorded with a Shimadzu UV-1650 PC spectrophotometer (Shimadzu, Kyoto, Japan) at 545 nm relative to an MA-free control sample. The concentration of MA in the tested samples was determined from a calibration curve.

2.11. Preparation of Fish Products Samples. For assay of MA, the frozen sea fish samples of hake and grouper were used. Muscle tissues (12 g and 60 g) of the frozen fillet were ground in a mortar with a following addition of 50 mL of deionized water. Trichloroacetic acid was added to the samples (to the final concentration of 4%). The protein precipitate was separated by passing the resulting mixture through a folded filter. Before analysis, the obtained filtrates were neutralized to pH value 7.5 by 10 M NaOH. The filtrate was stored before analysis at +4°C.

2.12. Statistic Treatment. All the measurement's results and the level of correlation between results obtained by the different analytical methods were calculated by computer program Origin 8.0 and Microsoft Excel.

3. Results and Discussion

3.1. Evaluation and Optimization of the MA Biosensor. For construction of an MA-selective biosensor, the bienzyme sensor architecture was used which contained $(His)_6$-tagged AMO or AMO-modified nAu and commercial HRP. Using an HRP allows decreasing working potential of the sensor to −50 mV which is important to avoid interfering effects of a sample background.

To improve electron transfer from transducer to the HRP, a number of synthetic mediators were tested. Using cyclic voltamperometry, three mediators (ferrocene, Mendola blue, and methylene blue) were analyzed by their ability to increase the effectiveness of electron transfer from the carbon electrode to HRP. The best results were obtained for ferrocene (data not shown), so all the next experiments were performed using ferrocene as electron transfer mediator. For physical fixation of HRP and AMO on the surface of ferrocene-modified carbon electrodes, entrapment of the enzymes in a polymer layer of a cathodic paint GY 83-0270 0005 (*CP*) was used. The optimized sensor architecture which consisted of *CP*-AMO-HRP-ferrocene was used for chronoamperometric investigation of methylamine oxidation (Figure 1).

The maximal current at substrate saturation (I_{max}) for the *CP*-AMO-HRP-ferrocene-modified carbon electrodes (area 7.3 mm^2) calculated from calibration graph is 1.23 ± 0.02 μA (Figure 1(c)). The value of K_M^{app} to MA derived from the calibration plot for the bienzyme sensor is 0.039 ± 0.003 mM, which is lower compared to K_M^{app} of free AMO in solution (0.22 mM) [11]. The sensitivity of the sensor for methylamine is 1450 ± 113 $A \cdot M^{-1} \cdot m^{-2}$ (Figure 1(b)). The linearity of the bioelectrodes is in the range from 15 μM to 60 μM, and the time of response to the target analyte (corresponds to 90% of the output) was found to be about 10 s.

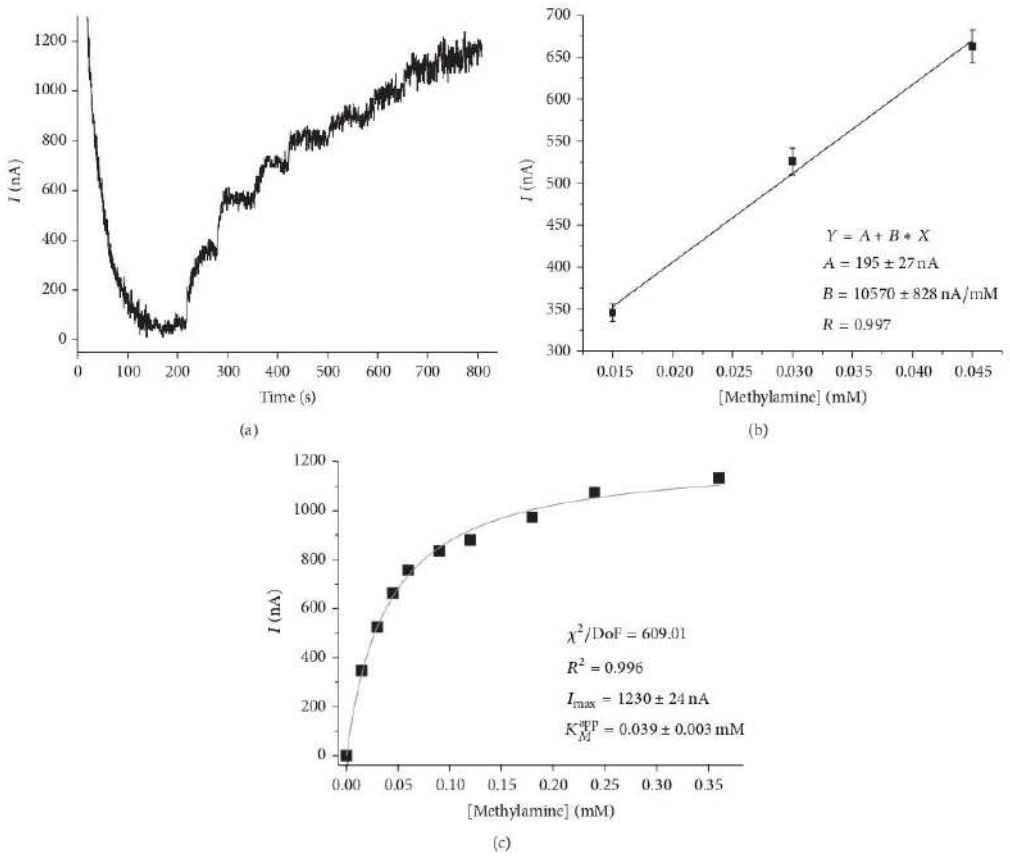

FIGURE 1: Chronoamperometric current response upon subsequent additions of methylamine (a) and calibration graphs (b), (c) for *CP*-AMO-HRP-ferrocene-modified carbon electrode. Conditions: working potential −50 mV *versus* Ag/AgCl/3 M KCl in 20 mM PB, pH 7.5.

TABLE 1: The activity of AMO during immobilization on the nAu surfaces.

	Enzyme preparation	Supernatant after enzyme immobilization	Immobilized AMO on nAu
V, mL	0.03	0.015	0.02
C_{protein}, mg·mL^{-1}	0.75	0.52	*
Total$_{\text{protein}}$, mg	0.02	0.08	*
A, U·mL^{-1}	40.1 ± 1.1	2.55 ± 0.12	35.5 ± 0.2
Total A, U	1.2 ± 0.1	0.04 ± 0.002	0.71 ± 0.01
Yield (%)	=100	3.3 ± 0.1	59.2 ± 1.2

* Under sensitivity.

3.2. Construction of MA-Selective Bioselective Layer Using nAu. It is known that nanomaterials could improve the sensor characteristics [13]. Biofunctionalisation of synthesized nAu was performed by modification of nAu by 16-mercaptohexadecanoic acid and carbodiimide-pentafluorophenol condensation for covalent binding of the enzyme [14] (see Section 2.5 of Math and Meth.). The activity of AMO during immobilization on the nAu surface is represented in Table 1.

As shown in Table 1, AMO covalently immobilized on the surface of the nAu has kept 59.2 ± 1.2% of the initial enzyme activity.

The Gauss distribution in Figure 2 demonstrates that an average size of the bionanoparticles is close to 17-18 nm.

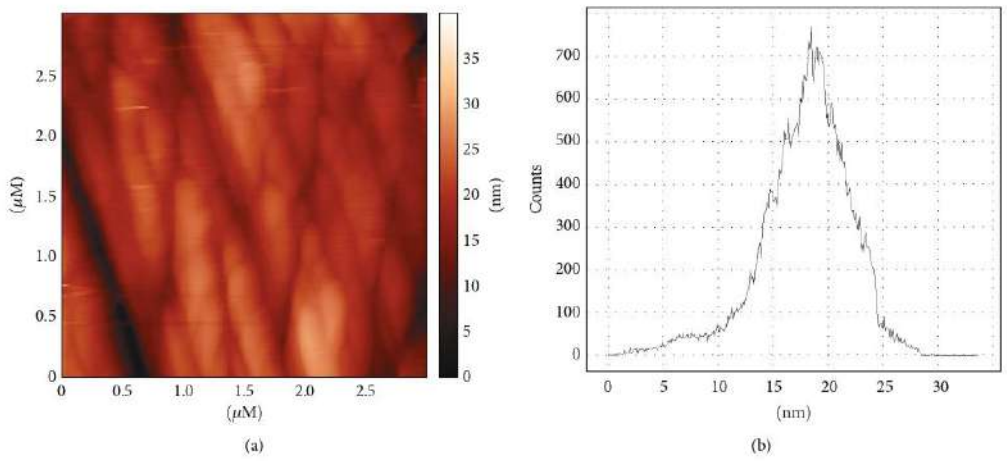

FIGURE 2: Atomic force microscopy of the AMO-nAu (a) and Gauss distribution of AMO-nAu by size (b).

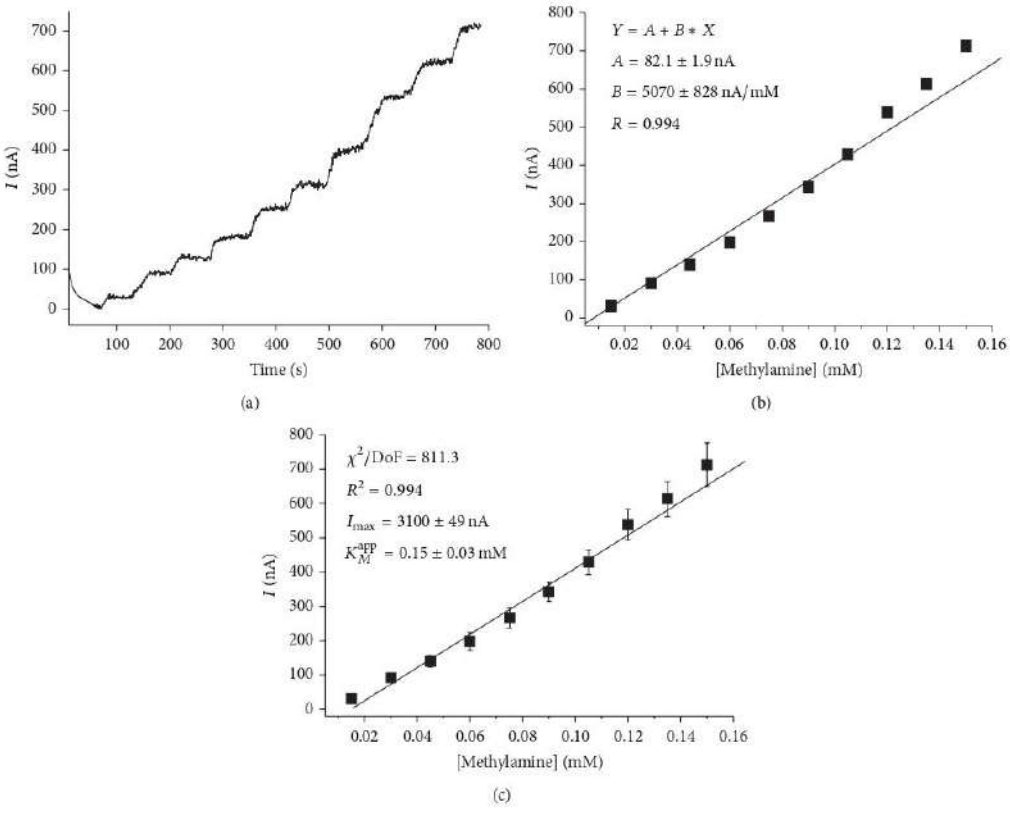

FIGURE 3: Chronoamperometric current response upon subsequent additions of MA (a) and calibration graphs (b), (c) for *CP*-AMO-nAu-HRP-ferrocene-modified carbon electrode. Conditions: working potential −50 mV *versus* Ag/AgCl/3 M KCl in 20 mM PB, pH 7.5.

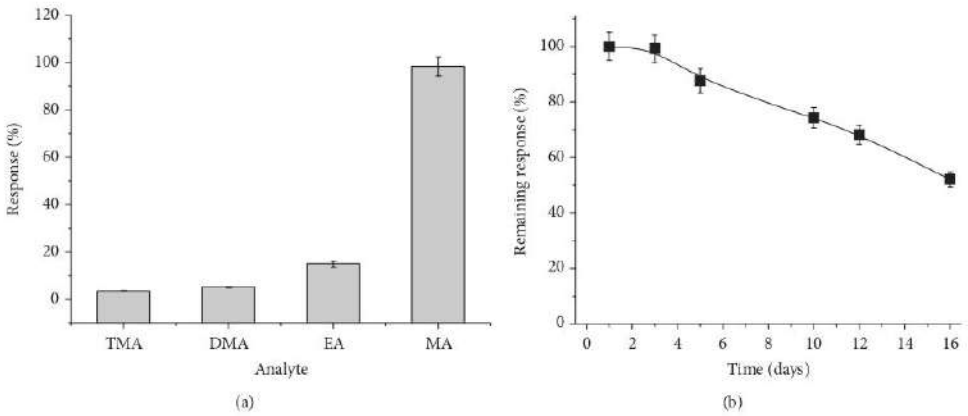

FIGURE 4: Characteristics of the developed MA biosensor under applied potential of −50 mV at 22°C. The highest current response was chosen as 100% in all experiments. Selectivity test was performed with 0.1 mM solutions of MA, DMA, EA, and TMA in 20 mM PB, pH 7.5 (a); storage stability was checked using 0.05 mM MA in 20 mM PB, pH 7.5, at room temperature during 16 days (b). The bioelectrode was kept at +4°C in 20 mM PB, pH 7.5.

Figure 3 represents chronoamperometric current response and calibration curve for the *CP*-AMO-nAu-HRP-ferrocene-modified carbon electrodes upon subsequent additions of MA.

The calibration was performed by a stepwise addition of a standard analyte solution. The sensitivity of the sensor AMO-nAu-based for MA is $700 \pm 30\,A \cdot M^{-1} \cdot m^{-2}$ (Figure 3(b)) which is 2-fold lower compared to biosensor without using nAu. The reason for such phenomenon is not clear. The maximal current response of the bioelectrodes modified by nAu (architecture *CP*-AMO-nAu-HRP-ferrocene) calculated from the calibration graph (Figure 3(c)) is equal to $3.10 \pm 0.05\,\mu A$ which is 2.5 times higher compared to *CP*-AMO-HRP-ferrocene sensor architecture ($1.23 \pm 0.02\,\mu A$). The value of K_M^{app} to methylamine derived from the calibration plot for the sensor is 0.15 ± 0.03 mM, that is, 3.8 times higher compared to *CP*-AMO-HRP-ferrocene sensor (0.039 ± 0.003 mM). Because of the relatively high affinity of AMO to MA, the observed increased K_M^{app} value for AMO-nAu-based electrode has a positive impact on the biosensor properties due to the wider linear range for MA determination (from 0.015 mM up to 0.15 mM). The 2-fold expanded linearity for *CP*-AMO-nAu-HRP-ferrocene sensor architecture is better adapted to the typical concentration range of MA in the real samples. All the next experiments were performed using bioselective layer *CP*-AMO-nAu-HRP-ferrocene architecture.

3.3. Assay of MA in Fish Samples. For the application of the constructed biosensor for assay of MA in real samples, the selectivity with respect to structurally similar analytes (DMA and TMA) is of great importance. Hence, the amperometric current response of the developed MA-selective sensor was evaluated with respect to the mentioned above compounds (Figure 4(a)). The storage stability of the sensor was also tested (Figure 4(b)).

As shown in Figure 4(a), positive signals to TMA ($3.5 \pm 0.17\%$), DMA ($5.1 \pm 0.25\%$), and ethanolamine (EA) ($15 \pm 1.02\%$) were detected. It is worth to mention that the possible impact of EA on MA assay is negligible, because this compound (in a free form) is present in fish products only in small amounts (less than 0.019 μg per g) [15]. Thus, the impact of these compounds will not be extremely significant for the correct determination of methylamine in the real samples where the mentioned above components can be present.

For analysis of the storage stability of the sensor, the electrodes were stored between exploitation cycles at +4°C. The measurements were performed at room temperature in 20 mM PB, pH 7.5, with addition of 0.05 mM MA. The half-life of the sensor was close to 16 days of the storage (Figure 4(b)).

In order to demonstrate the practical feasibility of the constructed biosensor with architecture *CP*-AMO-nAu-HRP-ferrocene, MA content in frozen fillet of hake and grouper was determined, using standard addition method (Figure 5).

The content of MA in frozen sea fish samples calculated from the calibration curves for standard addition test using MA-selective biosensor was $14.0 \pm 0.5\,\mu M$ for fillet of hake and $15.4 \pm 0.2\,\mu M$ for grouper, respectively.

The results of MA analysis in the real samples by the developed biosensor were compared with the results obtained by chemical method (Table 2).

Only slight differences between the results obtained by biosensor's approach and chemical method were observed (2.1–2.5%). Moreover, the obtained MA contents results are in good correlation with literature data for sea fish samples [16]. These results demonstrate the perspectives for application of the developed *CP*-AMO-nAu-HRP-ferrocene-based electrode for a correct analysis of MA in food technology.

TABLE 2: MA content in frozen sea fish determined by different methods.

Samples	Methods				Difference, %
	MA-selective biosensor		Chemical method, μM		
	μM (in extract)	μg/g (in wet meat)	μM (in extract)	μg/g (in wet meat)	
Hake	14.0 ± 0.5	2.4 ± 0.1	13.7 ± 1.2	2.3 ± 0.1	2.1
Grouper	15.4 ± 0.2	2.6 ± 0.1	15.8 ± 0.3	2.7 ± 0.2	2.5

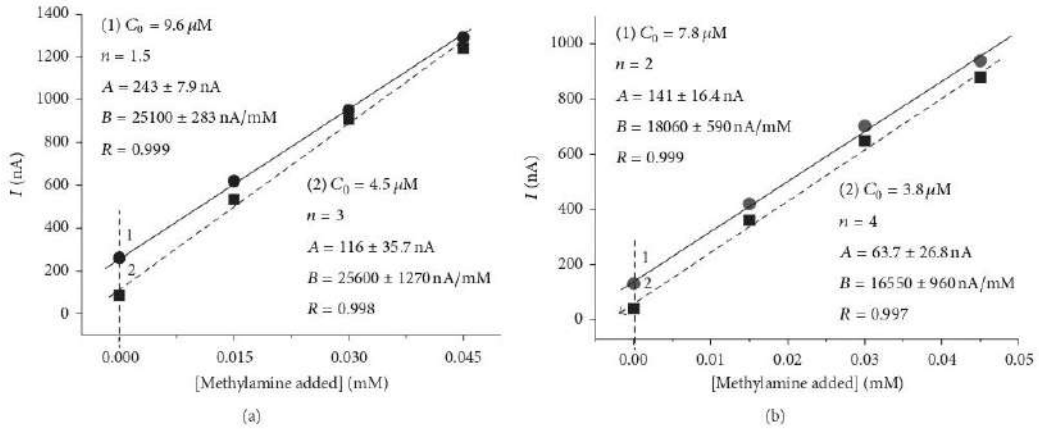

FIGURE 5: Calibration curves for MA assay in frozen fillet of hake (a) and grouper (b) using standard addition test for biosensor (*CP*-AMO-nAu-HRP-ferrocene). *A*, *B*: parameters for the linear regression line; *n*: dilution factor; C_o: calculated initial concentration; *R*: correlation coefficient.

4. Conclusions

A new methylamine-sensitive bienzyme amperometric biosensor based on the recombinant methylamine oxidase and commercial horseradish peroxidase has been developed. To improve sensor characteristics, covalent immobilization of AMO on the surface of nAu has been performed. The main sensor characteristics (sensitivity, linearity, response time, and K_M value) have been investigated. Testing MA-sensitive laboratory prototype of biosensor on the real samples of sea fish using the multiple standard addition method has been done.

Conflict of Interests

The authors declare that there is no conflict of interests regarding the publication of this paper.

Acknowledgments

This research was supported by Cross-Border Cooperation Programme Poland-Belarus-Ukraine 2007–2013 IPBU. 03.01.00-18-452/11-00, by Ukrainian-Belarussian Project F 54.4/031, and by NATO Project CBP.NUKR.SFP 984173.

References

[1] H. Tseng and D. Graves, "Natural methylamine osmolytes, trimethylamine N-oxide and betaine, increase tau-induced polymerization of microtubules," *Biochemical and Biophysical Research Communication*, vol. 250, pp. 726–730, 1998.

[2] H. Rehbein, D. Eichenauer, P. Feser et al., "Formaldehyde and dimethylamine in frozen fishery products available on the market: an inventory," *Archiv für Lebensmittelhygiene*, vol. 46, no. 5, pp. 122–124, 1995.

[3] "Thermo scientific spplication note 1057: determination of methylamine in drug products," Sunnyvale, Calif, USA, 2008, http://www.dionex.com/en-us/webdocs/114676-AN1057-IC-Methylamine-Drug-Products-AN70523_E.pdf.

[4] A. Q. Zhang, S. C. Mitchell, and R. L. Smith, "Dimethylamine formation in the rat from various related amine precursors," *Food and Chemical Toxicology*, vol. 36, no. 11, pp. 923–927, 1998.

[5] S. Xiao and P. H. Yu, "A fluorometric high-performance liquid chromatography procedure for simultaneous determination of methylamine and aminoacetone in blood and tissues," *Analytical Biochemistry*, vol. 384, pp. 20–26, 2009.

[6] A. A. Ormsby and S. Johnson, "A colorimetric method for the determination of methylamine in urine," *The Journal of Biological Chemistry*, vol. 187, pp. 711–717, 1950.

[7] D. Marinov, J. Rey, and M. W. Sigrist, "Mid-infrared spectroscopic investigation of methylamines by a continuous-wave difference-frequency-generation-based system," *Applied Optics*, vol. 47, pp. 1956–1962, 2008.

[8] H. Gu, H. M. Ma, and S. C. Liang, "A novel water-soluble fluorescent probe for the determination of methylamine," *Journal of Analytical Chemistry*, vol. 371, no. 4, pp. 570–573, 2001.

[9] M. E. Erupe, A. Liberman-Martin, P. J. Silva et al., "Determination of methylamines and trimethylamine-N-oxide in particulate matter by non-suppressed ion chromatography," *Journal of Chromatography A*, vol. 1217, pp. 2070–2073, 2010.

[10] G. W. Haywood and P. J. Large, "Microbial oxidation of amines. Distribution, purification and properties of two primary-amine oxidases from the yeast Candida boidinii grown on amines as sole nitrogen source," *Biochemistry Journal*, vol. 199, pp. 187–201, 1981.

[11] S. Sigawi, M. Nisnevitch, O. Zakalska, A. Zakalskiy, Y. Nitzan, and M. Gonchar, "Bioconversion of airborne methylamine by immobilized recombinant amine oxidase from the thermotolerant yeast *Hansenula polymorpha*," *The Scientific World Journal*, vol. 2014, Article ID 898323, 9 pages, 2014.

[12] X. P. Sun, Z. L. Zhang, B. L. Zhang, X. D. Dong, S. J. Dong, and E. K. Wang, "Preparation of gold nanoparticles protected with polyelectrolyte," *Chinese Chemical Letters*, vol. 14, no. 8, pp. 866–869, 2003.

[13] J. Hong, W. Wang, K. Huang et al., "A highly efficient nanocluster artificial peroxidase and its direct electrochemistry of a nano complex modified glassy carbon electrode," *Analytical Science*, vol. 28, no. 7, pp. 711–716, 2012.

[14] N. Stasyuk, R. Serkiz, S. Mudry et al., "Recombinant human arginase I immobilized on gold and silver nanoparticles: preparation and properties," *Nanotechnology Development*, vol. 1, no. 1, article e3, 2011.

[15] J. B. Knaak, H. W Leung, W. T. Stott, J. Busch, and J. Bilsky, "Toxicology of mono-, di-, and triethanolamine," in *Reviews of Environmental Contamination and Toxicology*, vol. 149, pp. 1–86, Springer, New York, NY, USA, 1997.

[16] J. R. Treberg, J. S. Bystriansky, and W. R. Driedzic, "Temperature effects on trimethylamine oxide accumulation and the relationship between plasma concentration and tissue levels in smelt (Osmerus mordax) Journal of Experimental Zoology A," *Comparative Experimantal Biology*, vol. 303, no. 4, pp. 283–293, 2005.

Оригінал доступний за посиланням:
https://www.hindawi.com/journals/bmri/2014/480498/

РОЗДІЛ 6

СТВОРЕННЯ МІКРОБНИХ АМПЕРОМЕТРИЧНИХ БІОСЕНСОРІВ НА ОСНОВІ КЛІТИН, ДОДАТКОВО ЗБАГАЧЕНИХ ЦІЛЬОВИМ ЕНЗИМОМ *IN VITRO*

В розділі VI представлено результати досліджень *in vitro* щодо введення екзогенного ензиму (аргінази, алкогольоксидази та флавоцитохрому b_2) в дріжджові клітини *O. polymorpha* з метою підвищення в них кількості цільового ензиму та подальшого застосування збагачених клітин у біосенсорному аналізі. Однією із основних особливостей наночастинок (НЧ) є висока хімічна активність, що обумовлена їх підвищеною здатністю до йонного чи атомного обміну, адсорбції, до утворення поверхневих зв'язків із іншими адсорбатами. Доступні методи синтезу НЧ, а також їх спорідненість до багатьох біологічних молекул робить їх привабливими кандидатами для досліджень у сенсорних технологіях. Для біотехнологічних процесів є особливо актуальним одержання біонаноматеріалів із покращеними каталітичними властивостями – як на основі ензимів, так і генетично модифікованих клітин з поліпшеними біотехнологічними параметрами. Показано можливість посилення каталітичної активності рекомбінантних клітин шляхом додаткового введення в них відповідних ензимів, кон'югованих з НЧ. Висока проникливість клітин до НЧ інтенсивно вивчається в останні роки у зв'язку з перспективою використання такого підходу для скерованого введення ліків, проте ідея введення НЧ, зв'язаних із ензимами, з метою поліпшення біосенсорних характеристик клітин в літературі не висловлювалась і експериментально до нас не вивчалась.

Синтез золотих НЧ проводили із використанням неорганічного відновника – Натрій боргідриду. Вивчено можливість застосування НЧ золота (Au) в ролі носія для іммобілізації рекомбінантних ензимів та поєднання Au НЧ з клітинами дріжджів у складі нанокомпозитних матеріалів (полімерна матриця + Au НЧ). Слід зазначити, що збагачення дріжджових клітин ензимами досягалось комбінацією двох підходів: 1) на генетичному рівні – шляхом надекспресії відповідного гена

HpCYB2 або *HsARG1* у рекомбінантних клітинах *O. polymorpha* – для флавоцитохрому b_2 чи аргінази, відповідно; 2) з використанням нанотехнологічного підходу – шляхом введення в клітини цільових ензимів, іммобілізованих на Au НЧ. Проведено дослідження структурних, фізико-хімічних та каталітичних властивостей біонаночастинок та показано перспективність їх використання в біосенсорних технологіях з метою покращення біоаналітичних характеристик клітинних сенсорних елементів.

Позитивний вплив ензимо-модифікованих наночастинок золота на кінетичні параметри клітинних сенсорів також підтверджено експериментами з використанням золотих наночастинок з іммобілізованою алкогольоксидазою (АО). Пермеабілізовані АО-Au-модифіковані клітини штаму дикого типу *H. polymorpha* NCYC 495 (штам до модифікації не володів підвищеною активністю АО) іммобілізували із пероксидазою хрону на поверхні 4 мм-золотих планарних електродів *C220AT* «DropSens». Хронамперометричні дослідження проводили при робочому потенціалі системи – 50 мВ проти Ag/AgCl/KCl електроду порівняння. Показано, що величина відгуку немодифікованих пермеабілізованих клітин штаму дикого типу *O. polymorpha* NCYC 495 на метанол не перевищує 8 нА, тоді як, АО-Au-модифіковані пермеабілізовані клітини цього ж штаму виявляють значно вищий відгук на метанол – 170 нА. Таким чином, модифікація пермеабілізованих клітин дріжджів наночастинками золота, зв’язаними з АО, покращує відгук сенсора у 21 раз.

Проведені дослідження яскраво свідчать, що додаткове введення ензимів, іммобілізованих на металевих нановосіях, суттєво покращує біоаналітичні характеристики клітинних сенсорів (підвищує чутливість, збільшує швидкість розвитку сигналу).

6.1. Конструювання біоелектродів на основі пермеабілізованих клітин дріжджів *O. polymorpha*, збагачених ензимо-нанокомпозитними матеріалами.

Анотація: *В останні роки нанотехнологія є галуззю, що інтенсивно розвивається завдяки широкому розмаїттю потенціалу застосування в біомедичній та біотехнологічній галузях. Можливість зв'язування наночастинок з різними біологічними молекулами робить їх привабливими кандидатами для використання в сенсорних технологіях. Особливо актуальним є отримання біонаномембран на основі біокаталітичних елементів із покращеною чутливістю. У поточному розділі ми повідомляємо про створення мікробних селективних біосенсорів на основі рекомбінантних дріжджових клітин O. polymorpha, які додатково збагачені ензимами (флавоцитохромом b_2, алкогольоксидазою, аргіназою I), що іммобілізовані на поверхні наночастинок золота. Хоча висока проникність живих клітин до наночастинок інтенсивно вивчається (в основному, для доставки ліків), ідея використання як рекомбінантної технології, так і нанотехнології для збільшення кількості ензиму у біоселективному шарі біосенсора принципово є новою. Нами показано, що інтактні та пермеабілізовані дріжджові клітини, додатково збагачені ФЦ b_2-Au, придатні для конструювання біоселективної мембрани мікробного L-лактат-селективного амперометричного біосенсора. Феназину метосульфат служив в ролі вільного медіатора, який забезпечує ефективне перенесення електронів від ензиму до поверхні електрода. Показано, що відгук на L-лактат пермеабілізованих дріжджових клітин, збагачених FC b2-nAu, у 2,5 рази вищий, порівняно з контрольними клітинами. Таким чином, нами встановлено, що додаткове збагачення рекомбінантних дріжджових клітин ензимами, кон'югованими із наночастинками, дозволяє суттєво підвищити чутливість та стабільність клітинних біосенсорів.*

Talanta 144 (2015) 1195–1200

Contents lists available at ScienceDirect

Talanta

journal homepage: www.elsevier.com/locate/talanta

L-Lactate-selective microbial sensor based on flavocytochrome b_2-enriched yeast cells using recombinant and nanotechnology approaches

Maria Karkovska [a], Oleh Smutok [a], Nataliya Stasyuk [a], Mykhailo Gonchar [a,b,*]

[a] Department of Analytical Biotechnology, Institute of Cell Biology, NAS of Ukraine, Drahomanov Street 14/16, Lviv 79005, Ukraine
[b] Institute of Applied Biotechnology and Basic Sciences, Rzeszow University, Sokolowska Street 26, Kolbuszowa, Poland

ARTICLE INFO

Article history:
Received 14 May 2015
Received in revised form
23 July 2015
Accepted 28 July 2015
Available online 29 July 2015

Keywords:
l-Lactate
Microbial biosensor
Gold nanoparticles
Flavocytochrome b_2
Recombinant yeast cells
Enzyme-enriched cells
Amperometric biosensor

ABSTRACT

In the recent years, nanotechnology is the most developing branch due to a wide variety of potential applications in biomedical, biotechnological and agriculture fields. The binding nanoparticles with various biological molecules makes them attractive candidates for using in sensor technologies. The particularly actual is obtaining the bionanomembranes based on biocatalytic elements with improved sensing characteristics.

The aim of this investigation is to study the properties of microbial L-lactate-selective sensor based on using the recombinant *Hansenula polymorpha* yeast cells overproducing flavocytochrome b_2 (FC b_2), as well as additionally enriched by the enzyme bound with gold nanoparticles (FC b_2-nAu). Although, the high permeability of the living cells to nanoparticles is being intensively studied (mostly for delivery of drugs), the idea of using both recombinant technology and nanotechnology to increase the amount of the target enzyme in the biosensing layer is really novel.

The FC b_2-nAu-enriched living and permeabilized yeast cells were used for construction of a biose-lective membrane of microbial L-lactate-selective amperometric biosensor. Phenazine methosulphate was served as a free defusing electron transfer mediator which provides effective electron transfer from the reduced enzyme to the electrode surface. It was shown that the output to L-lactate of FC b_2-nAu-enriched permeabilized yeast cells is 2.5-fold higher when compared to the control cells.

The obtained results confirm that additional enrichment of the recombinant yeast cell by the enzyme bound with nanoparticles improves the analytical parameters of microbial sensor.

© 2015 Elsevier B.V. All rights reserved.

1. Introduction

Reliable determination of L-lactate is important in food technology, fermentation and wine industries, as well as in clinical chemistry and sport medicine [1,3]. Among the available methods for assaying of L-lactate there are chromatographic and spectrometric analysis [4,6], however, they are time-consuming, and require laborious sample pre-treatment, as well as a qualified personnel.

Biosensors have been widely used in recent years, because of their high selectivity and sensitivity. The most of the enzymes used in the L-lactate-selective microbial biosensor construction (NAD^+ depended L-lactate dehydrogenase or lactate oxidase) are costly for routine analysis and require introducing additional co-factor [7]. The whole-cell microbial biosensors are simple and cheap for production due to avoiding the enzyme purification. Also it is important that enzymes are usually more stable in their natural environment inside the cell [8].

There are described only a few microbial biosensors for lactate analysis based on baker's yeast *Saccharomyces cerevisiae* [9,11], genetically modified *H. polymorpha* [12,13] and mixed culture of *Lactobacillus bulgaricus* and *Streptococcus thermophilus* [14].

Our previous publications [12,13] are devoted to construction of L-lactate-selective biosensors based on thermostable enzyme, L-lactate-cytochrome *c*-oxidoreductase (EC 1.1.2.3; flavocytochrome b_2, FC b_2). FC b_2 is a tetramer with four identical subunits, each consisting of FMN- and heme-binding domains. The main properties of FC b_2 are absolutely selectivity to L-lactate and high stability, which excellently fit to requirements for biosensors.

The high permeability of living cells to nanoparticles was intensively studied in the recent years due to perspectives of such approaches for controllable drug delivery into organism. The gold nanoparticle (nAu) display a unique combination of chemical

* Corresponding author at: Department of Analytical Biotechnology, Institute of Cell Biology, NAS of Ukraine, Drahomanov Street 14/16, Lviv 79005, Ukraine.
E-mail address: gonchar@cellbiol.lviv.ua (M. Gonchar).

http://dx.doi.org/10.1016/j.talanta.2015.07.081
0039-9140/© 2015 Elsevier B.V. All rights reserved.

inertness, surface chemistry, size- and shape-dependent electronic and optical properties, which render them ideal for clinical applications. The recent advancements were reported about the nAu usage in vaccine development, gene therapy, enhanced radiotherapy and others [15], however, many relevant issues remain open. They include the molecular mechanisms governing the nanoparticles–cell interactions, the physico-chemical parameters underlying their toxicity to different types of cells, the lack of standard methods and materials, and the uncertainty in the definition of general strategies to develop smart drugs and devices based on nanoparticles [16,18].

The conception of using nanoparticles in biosensor's technology to increase the output is very fresh nowadays. A number of biosensors with immobilized nanoparticle on electrode surface were constructed [19,20]. On the other hand, recently we have reported a few papers describing improvement of analytical parameters of the microbial sensors by genetical manipulation with the yeast cell [12,13,21–23].

The idea of implementation of exogenous enzyme to increase the amount of the target enzyme in the cells to be used in microbial sensors seems to be not highlighted yet. In this paper, the enrichment of the sensing cells by the target enzyme is achieved by a combination of two approaches: (1) on genetic level – by overexpression the corresponding *HpCYB2* gene in the recombinant cells; (2) using nanotechnological aapproach – by the transfer of FC b_2-bound nanoparticles into the cells.

2. Materials and methods

2.1. Cultivation and permeabilisation of yeast cells

Cultivation of the recombinant FC b_2-overproducing strain *H. polymorpha* "tr 1" (*gcr1 catX/prAOX_CYB2*) [24], was performed in flasks on a shaker (200 rpm) at 28 °C until the middle of the stationary growth phase (~60 h) in a medium containing (g L^{-1}): $(NH_4)_2SO_4$ – 3.5; KH_2PO_4 – 1.0; $MgSO_4 \times 7H_2O$ – 0.5; $CaCl_2$ – 0.1 supplemented with 0.75% yeast extract. A mixture of glucose (10 g L^{-1}) and L-lactate (2 g L^{-1}) was used as a carbon and energy source. After washing, the cells were suspended in 50 mM phosphate buffer, pH 7.8 containing 1 mM PMSF and 1 mM EDTA followed by drying.

Before experiments, the dried yeast cells were re-suspended to 30 mg ml^{-1} in 50 mM phosphate buffer, pH 7.8, containing 1 mM EDTA.

The procedure of the cells permeabilization was following: the same volume of permeabilising reagent (0.85 mM cetyltrimethylammonium bromide) was added to the cell suspension (30 mg ml^{-1} in 50 mM phosphate buffer, pH 7.8). The resulting solution was incubated at 30 °C in a water bath for 15 min under mixing every 3–4 min. The permeabilized cells were washed by centrifugation (6000 g, 5 min) in 50 mM phosphate buffer, pH 7.8. The precipitated permeabilized cells were re-suspended to 30 mg ml^{-1} in the same buffer solution and stored on ice at +4 °C. A half-life of the permeabilized yeast cells in suspension was about three weeks of storage at +4 °C in freezer. Lyophilized permeabilized cells retain 90% enzymatic activity during storage more than one year.

2.2. Isolation and purification of flavocytochrome b_2

L-lactate:cytochrome *c*-oxidoreductase (flavocytochrome b_2) was isolated and purified from the recombinant strain of the thermotolerant yeast *H. polymorpha* "tr 1" (*gcr1 catX/prAOX_CYB2*) [24]. The enzyme was purified by ion-exchange chromatography on DEAE-Toyopearl cellulose 650 M [25] to the specific activity of 22 U mg^{-1} and stored as a suspension in 70%-saturated ammonium sulphate, pH 7.8 at +4 °C before usage.

2.3. Synthesis and functionalisation of gold nanoparticles

Gold nanoparticles (nAu) were synthesized by the borohydride reduction method according to [26]. The procedure includes mixing 0.25 mL 10 mM $HAuCl_4$ and 0.6 ml 10 mM sodium borohydride. 7.5 mL 10 mM CTAB was used as a surfactant. The obtained mixture was stirred at 100 °C for 15 min to obtain a wine-red solution. The nAu were precipitated by centrifugation (9700 *g*; Hettich Micro-22R centrifuge) during 40 min. The average size of the obtained nAu was characterized by spectrophotometry and corresponds to 20 nm (*data not shown*). The precipitated nAu were washed twice with water and 10 mM PB, pH 7.5. The obtained nAu were functionalized by amino-groups using aqueous solution of 0.85 mM cystamine and stored at +4 °C before usage. The final concentration of functionalized nAu was 0.17 mM.

2.4. FC b_2 binding to gold nanoparticles

Biofunctionalization of functionalized (cystamine-modified) nAu with concentration 0.17 mM was performed by addition of purified FC b_2 with a specific activity 22 U ml^{-1} in ratio 2:1. The mixture was incubated at +4 °C overnight. Biofunctionalized nanoparticles (FC b_2-nAu) were washed three times by 5 mM PB, pH 7.5. Collection of FC b_2-nAu was performed by centrifugation at 9700g for 20 min. The FC b_2-activity was analyzed at different stages of biofunctionalization. Finally, the FC b_2-nAu demonstrated a specific FC b_2 activity of 3.3 U ml^{-1}.

2.5. Enrichment of the yeast cells by FC b_2-bound gold nanoparticles

The procedure for the enrichment of intact and permeabilized *H. polymorpha «tr1»* cells was the following: 180 µl yeast cells' suspension (30 mg ml^{-1} in 10 mM PB, pH 7.5) were added to 100 µl FC b_2-nAu preparation and mixture was incubated for a night at +4 °C with constant stirring. 180 µl the yeast cells and the same volume of cells modified by nAu without enzyme were incubated in parallel as the reference samples. After night incubation, the three samples of the cells were centrifuged at 670 g for 3 min. The cell's precipitates were washed twice with 10 mM PB, pH 7.5.

2.6. Transmission electron microanalysis

The fixation of the samples was performed in 1.5% solution of $KMnO_4$ for 15–20 min at the room temperature. After fixation, the samples were washed 5 fold. The next step was their dehydration in increasing concentration of C_2H_5OH (50%-, 70-, up to 90%) and finally in absolute ethanol (twice) for 30 min.

The samples were fixed in propylepoxide glue during 15 min, then they were transfered in solution of propylepoxide with epoxy (EPON 812) in the ratio of 1:1 for 2–3 h at the room temperature. The transfer was held in pure EPON 812 overnight followed by putting into EPON with polymer during 48 h at 60 °C. Post-fixation of samples was done with 1% OsO_4 in cacodylate buffer for 90 min at 0 °C.

The slices were obtained using diamond knife in an ultramicrotome UMTP-6 (Sumy, Ukraine). The images were contrasted with lead citrate and carried out by transmission electron microscope PEEM-100 (Sumy, Ukraine) at 75 kV. The final magnification of the micrographs was 10000. Microphotographs were done by photo camera SONY–HG9 (Tokyo, Japan).

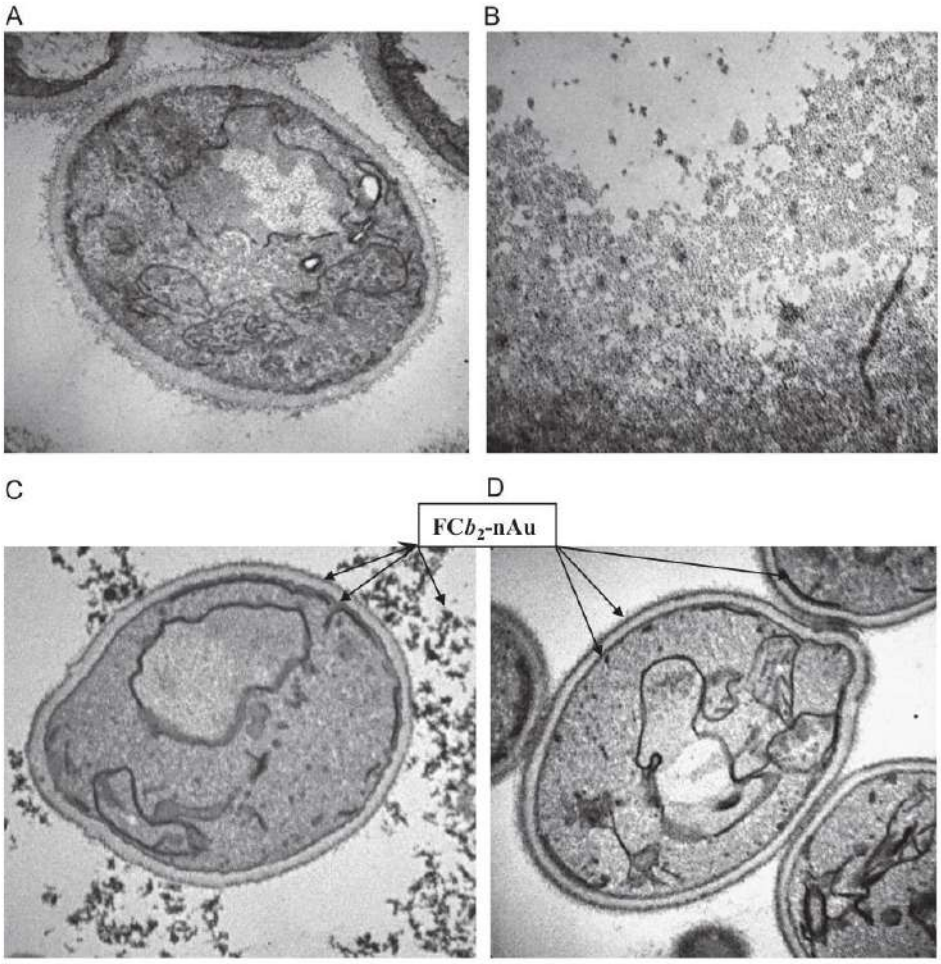

Fig. 1. Transmission Electron Microscopy (TEM) images: intact yeast cells of *H. polymorpha "tr 1"* (control) (A); gold nanoparticles suspension (nAu) (B); permeabilized yeast cells treated by FC b_2-nAu, (C); permeabilized yeast cells enriched by FC b_2-nAu, after washing (D).

2.7. SEM with X-ray microanalysis

A Scanning Electron Microscope (SEM-microanalyser REMMA-102-02, Sumy, Ukraine) supplied with EDAX device was used for morphological analyses of the samples on a graphite rod (diameter – 0.5 cm). The special cover film on the samples with a Butvar solution B-98 (Sigma, St. Louis, MO, USA) in 1.5% chloroform was formed using an ultrasound method. The distance from the last lens of the microscope to the sample (WD) ranged from 17.1 mm to 21.7 mm; the accelerator voltage was in the range from 20 to 40 eV; zooms were from 2,500 to 10,000.

2.8. Biosensors' preparation and evaluation

2.8.1. Apparatus and techniques

Amperometric biosensors were evaluated using constant-potential amperometry in a three-electrode configuration with a Ag/AgCl/KCl (3 M) reference electrode and a Pt-wire counter electrode. Amperometric measurements were carried out using a potentiostat CHI 1200A (IJ Cambria Scientific, Burry Port, UK) connected to a personal computer and performed in a batch mode under continuous stirring in a standard 40 ml electrochemical cell at room temperature.

Graphite rods (type RW001, 3.05 mm diameter, area 7.3 mm^2, Ringsdorff Werke, Bonn, Germany) were used as working electrodes. They were sealed in glass tubes using epoxy glue thus forming disk electrodes. Before sensor preparation, the graphite electrodes were polished with emery paper and cleaned with water in an ultrasonic bath.

2.8.2. Immobilization of the cells by entrapment within a cathodic paint

The immobilization procedure was provided using cathode polymer GY 83-0270 0005 (*CP*) as follows: a few microliters of yeast cell's suspension in 30 mM PB, pH 7.5 were dropped on the top of the carbon electrode to the final activity of the enzyme on the working electrode area up to 5 U ml^{-1}. After drying for 2 min at room temperature, the cells' layer was covered with 8 μl 10-fold diluted solution of the cathodic paint GY 83-0270 0005 (pH 5.5). After drying, a well-adhering polymer film was formed.

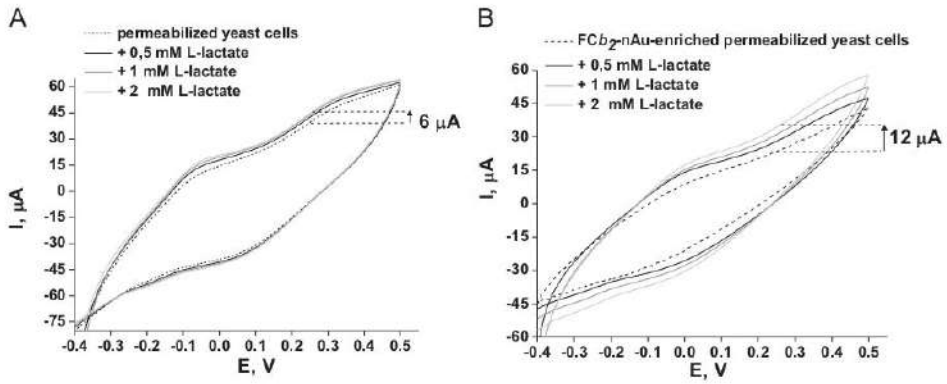

Fig. 2. Characterization of microbial L-lactate-selective electrodes by cyclic voltamperometry. 3.05 mm carbon electrodes modified by permeabilized (A) and FC b_2-nAu-enriched permeabilized cells (B) of *H. polymorpha* "tr1" in the absence (dash line) and in the presence (solid lines) of increasing concentrations of L-lactate. Conditions: scan frames −0.4 V to −0.6 V *vs* Ag/AgCl; scan rate 7 mV s^{-1} in 50 mM phosphate buffer, pH 7.8.

The prepared microbial electrodes were rinsed by 20 mM PB, pH 7.5 and stored at +4 °C before application.

All the experiments were carried out independently in triplicates and the reported results were the average of three replicate experiments.

3. Results and discussion

For enzyme immobilization on the surface of nAu, there was used purified preparation of FC b_2 isolated from the cells of the recombinant strain *H. polymorpha "tr1"* [24]. Gold nanoparticles (nAu), functionalized by cysteamine (see Section 2.5.) with concentration 0.17 mM were mixed with the same volume of FC b_2 solution with a specific activity 22 U ml^{-1}. The process of FC b_2 immobilization on the surface of functionalized nAu is characterized in the Table SI.1 (see Supplementary information (SI)). The yield of the immobilized enzyme on nAu was about 15% that corresponds to 3.3 U ml^{-1}.

For additional enrichment of recombinant yeast cells by FC b_2-bound nAu (FC b_2-nAu), there was used the strain *H. polymorpha* "tr 1" (*gcr1 catX/prAOX_CYB2*) over-producing FC b_2 with a specific activity up to 1.2 U mg^{-1} of protein in cell-free extracts' or 4.45 U mg^{-1} for permeabilized cells. The analysis of total enzymatic activity of FC b_2-enriched intact and permeabilized recombinant yeast cells (Sample), as well as reference samples without FC b_2-nAu treatment (Control) is represented in Table SI. 2. For intact cells, their treatment by FC b_2-nAu resulted in a 1.56-fold increased enzymatic activity. For permeabilized cells, the enrichment efficacy was essentially higher (2.33-fold). Thus, specific FC b_2-activity of intact cells after FC b_2-nAu treatment was increased for 56% and for permeabilized cells – up to 133%. This can be explained by a better permeability of permeabilized cells toward nanoparticles.

Morphological characterization of the yeast cells at the different stages of enrichment by FC b_2-nAu were carried out using Transmission Electron Microscopy (TEM) (Fig. 1).

The image of intact cells of *H. polymorpha* "tr 1" obtained by TEM was used as a control for analysis of morphological modification of the yeast cells (Fig. 1A). Fig. 1B represents numerous dark points which correspond to nAu. As a result of FC b_2-nAu penetration into permeabilized cells and cell wall, the membrane became darker (Fig. 1C). The Fig. 1D displays permeabilized yeast cells enriched by FC b_2-nAu, after repeated washing of non-bound bio-nanoparticles. The cellular barriers still keep dark regions that confirm localization of FC b_2-nAu inside the cells.

The penetration of FC b_2-nAu into of the permeabilized yeast cells was confirmed also by X-ray spectral analysis (Fig. SI 1). The X-ray spectrogram represents the presence of Au^0 inside of permeabilized yeast cells that approves penetration of FC b_2-nAu into the cells (Kα peak at 2.1 keV is characteristic for Au^0). Taken together, the presented data confirm the binding of FC b_2-nAu with the cell surface and their accumulation inside the cells.

The FC b_2-nAu enriched yeast cells were used for construction of microbial biosensor for L-lactate analysis.

For evaluation of a prototype of L-lactate selective microbial biosensor, 2 mM phenazine methosulphate (PMS) was used as a free-diffusing redox mediator to establish the electron transfer between electrode and FC b_2 located in a native form due to higher expression of *CYB2* gene and in bound with nAu form due to penetration of bionanoparticles. It was supposed that PMS can easily diffuse into the permeabilized cell and, after trapping electrons from the reduced enzyme, it is oxidized on the electrode surface (Fig. SI. 2).

The efficiency of electron transfer from the reduced FC b_2 (in cells) to carbon electrode via PMS for FC b_2-nAu-enriched permeabilized yeast cells and contol permeabilized cells (without treatment) were characterized using cyclic voltammetry. The cyclic voltammetry also gives an information about optimal working potential for sufficient PMS oxidation on the graphite rod electrodes (Fig. 2).

As shown in Fig. 2B, a twice increased current response on L-lactate addition is observed for the sensor based on the FC b_2-nAu-enriched cells, in comparison to control permeabilized yeast cells (Fig. 2A). A potential +250 mV *vs* Ag/AgCl was chosen as optimal working potential for PMS-oxidation. The summarized output of enzymatic oxidation of 3.5 mM L-lactate was estimated as 12 μA for FC b_2-nAu-enriched cells and 6 μA for control cells, respectively.

The sensor's outputs to L-lactate in chronoamperometric mode for different types of biorecognizing elements are presented in Fig. 3.

The best sensitivity (48.6 A M^{-1} m^{-2}) was achived for the permeabilized yeast cells enriched by FC b_2-nAu which is more than twice compared to the control permeabilized cells without treatment with enzyme–bound nAu (18.7 A M^{-1} m^{-2}). The control bioelectrode based on intact yeast cells showed a significantly lower sensitivity (4.1 A M^{-1} m^{-2}). The similar value was obtained for other bioelectrodes constructed using bare nAu-modified intact yeast cells 3.9 A M^{-1} m^{-2} (Fig. 3). This negligible difference in

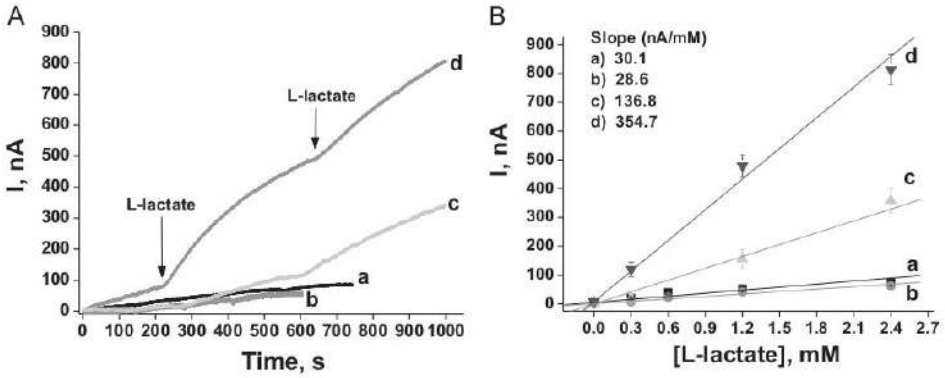

Fig. 3. Chronoamperometric current response (A) of L-lactate-selective microbial electrode, based on FC b_2-nAu-enriched permeabilized yeast cells compared with the controls: (a) intact yeast cells; (b) nAu-modified intact yeast cells; (c) permeabilized yeast cells; (d) FC b_2-nAu-enriched permeabilized yeast cells and calibration curves (B) for L-lactate-dependent responses. Conditions: working potential +250 mV *vs* Ag/AgCl, in 50 mM phosphate buffer.

sensitivity evidences the absence of impact of bare gold nanoparticles on sensor output. The lower sensitivity for the two types of bioelectrodes based on intact yeast cells could be explained by diffusion limitations through intact cellular barier.

The reproducibility of the developed microbial sensor in the linear frames (from 0.03 up to 2.4 mM L-lactate) was characterized by a low standard deviation (0.95%). A selectivity of the developed sensor was the same compared to earlier described amperometric biosensor based on permeabilized cells of the same yeast strain [12].

The increased sensitivity of the constructed microbial electrode clearly demonstrates that additional enrichment of permeabilized yeast cells by target enzyme immobilized on nanocarriers could be used for construction of microbial biosensors with improved bioanalytical characteristics.

4. Conclusions

L-Lactate-selective microbial amperometric sensor based on the recombinant yeast cells of *H. polymorpha* enriched by FC b_2 has been proposed. The enrichment of the cells by the target enzyme was achieved by combination of over-expression of the *HpCYB2* gene in the recombinant cells and using nanotechnological approach – transfer of FC b_2-bound nanoparticles into the cells. The permeability of the intact and permeabilized yeast cells toward FC b_2-nAu was analyzed using TEM and X-ray spectroscopic analysis.

The characteristics of the sensors in the absence and presence of FC b_2-nAu in the cells have been compared. It was shown that the sensitivity of FC b_2-nAu-enriched permeabilized yeast cells to L-lactate is 12-fold higher compared to intact yeast cells and 2.6-fold higher than for permeabilized yeast cells. The developed microbial sensor is supposed to be applied for the determination of L-lactate in food technology.

Acknowledgements

This research was supported in part by NAS of Ukraine in the frame of the Scientific-Technical Program No. 14/26.02.2015 "Sensor systems for medical, ecological and industrial-technological needs: metrological assurance and research exploitation" and Ukrainian-Lithuanian Project No. TAP-LU-03-055/2014 "Investigation of L- and D-lactate: cytochrome *c* oxidoreductases isolated from the recombinant yeast *H. polymorpha* and their usage for construction of amperometric biosensors".

Appendix A. Supplementary information

Supplementary data associated with this article can be found in the online version at http://dx.doi.org/10.1016/j.talanta.2015.07.081.

References

[1] O. Smutok, M. Karkovska, H. Smutok, M. Gonchar, Flavocytochrome-based enzymatic method of L-lactate assay in food products, Sci. World J. 2013 (2013) 1–6.
[2] L. Shkotova, T. Goriushkina, Tran-Minh Canh, A. Chovelon Jeanmarc, S. Soldatkin, S. Dzyadevych, Amperometric biosensor for lactate analysis in wine and must during fermentation, Mater. Sci. Eng. C 28 (2008) 943–948.
[3] R. Beneke, S.P. vonDuvillard, Determination of maximal lactate steady state response in selected sports events, Med. Sci. Sports Exerc. 28 (1996) 241–246.
[4] H. Hugues, N. Marmy Conus, P. Steenhout, A. Beguin, O. Boulat, Sensitive determination of D-lactic acid and L-lactic acid in urine by high-performance liquid chromatography-tandem mass spectrometry, Biomed. Chromatogr. 26 (2011) 425–428.
[5] W. Rich, E. Johnson, L. Lois, P. Kabra, B. Stafford, L. Marton, Determination of organic acids in biological fluids by ion chromatography: plasma lactate and pyruvate and urinary vanillylmandelic acid, Clin. Chem. 26 (1980) 1492–1498.
[6] A. Hallström, A. Carlsson, L. Hillered, U. Ungerstedt, Simultaneous determination of lactate, pyruvate, and ascorbate in microdialysis samples from rat brain, blood, fat, and muscle using high-performance liquid chromatography, J. Pharm. Methods 22 (1989) 113–124.
[7] E. Akyilmaz, E. Dinçkaya, An amperometric microbial biosensor development based on *Candida tropicalis* yeast cells for sensitive determination of ethanol, Biosens. Bioelectron. 20 (2005) 1263–1269.
[8] S. Ebbinghaus, Chair of Physical Chemistry II, Institute of Physical Chemistry, Bochum, 2015.
[9] R. Garjonyte, A. Malinauskas, L. Gorton, Investigation of electrochemical properties of FMN and FAD adsorbed on titanium electrode, Bioelectrochemistry 61 (2003) 39–49.
[10] R. Garjonyte, V. Melvydas, A. Malinauskas, Mediated amperometric biosensors for lactic acid based on carbon paste electrodes modified with baker's yeast *Saccharomyces cerevisiae*, Bioelectrochemistry 68 (2006) 191–196.
[11] R. Garjonyte, V. Melvydas, A. Malinauskas, Effect of yeast pretreatment on the characteristics of yeast-modified electrodes as mediated amperometric biosensors for lactic acid, Bioelectrochemistry 74 (2008) 188–194.
[12] O. Smutok, K. Dmytruk, M. Gonchar, A. Sibirny, W. Schuhmann, Permeabilized cells of flavocytochrome b_2 over-producing recombinant yeast *Hansenula polymorpha* as biological recognition element in amperometric lactate biosensors, Biosens. Bioelectron. 23 (2007) 599–605.
[13] H. Shkil, L. Stoica, K. Dmytruk, O. Smutok, M. Gonchar, A. Sibirny, W. Schuhmann, Bioelectrochemical detection of L-lactate respiration using genetically modified *Hansenula polymorpha* yeast cells overexpressing flavocytochrome b_2, Bioelectrochemistry 76 (2009) 175–179.
[14] J. Chen, Y. Jin, Sensitive lactate determination based on acclimated mixed bacteria and palygorskite co-modified oxygen electrode, Bioelectrochemistry

80 (1959) 151–154.
[15] R. Cao-Milán, L.M. Liz-Marzán, Gold nanoparticle conjugates: recent advances toward clinical applications, Expert Opin. Drug Deliv. 11 (2014) 741–752.
[16] D.A. Kuhn, D. Vanhecke, B. Michen, F. Blank, P. Gehr, A. Petri- Fink, B. Rothen-Rutishauser, Different Endocytotic uptake mechanisms for nanoparticles in epithelia cells and mavrophages. Beilstein J. Nanotechnol. 5 (2014) 1625–1636.
[17] T. Mironava, M. Hadjiargyrou, M. Simon, V. Jurukovski, M. Rafailovich, Gold nanoparticles cellular toxicity and recovery: effect of size, concentration and exposure time, Nanotoxicology 4 (2010) 120–137.
[18] S. Akhter, M.Z. Ahmad, F.J. Ahmad, G. Storm, R.J. Kok, Gold nanoparticles in theranostic oncology: current state-of-the-art. Expert Opin. Drug Deliv. 9 (2012) 1225–1243.
[19] P.J. Lamas-Ardisana, O.A. Loaiza, L. Añorga, E. Jubete, M. Borghei, V. Ruiz, E. Ochoteco, G. Cabañero, H.J. Grande, Disposable amperometric biosensor based on lactate oxidase immobilised on platinum nanoparticle-decorated carbon nanofiber and poly(diallyldimethylammonium chloride) films, Biosens. Bioelectron. 56 (2014) 345–351.
[20] O.A. Loaiza, P.J. Lamas-Ardisana, L. Añorga, E. Jubete, V. Ruiz, M. Borghei, G. Cabañero, H.J. Grande, Graphitized carbon nanofiber-Pt nanoparticle hybrids as sensitive tool for preparation of screen printing biosensors. Detection of lactate in wines and ciders, Bioelectrochemistry 101 (2015) 58–65.
[21] K.V. Dmytruk, O.V. Smutok, O.B. Ryabova, G.Z. Gayda, V.A. Sibirny, W. Schuhmann, M.V. Gonchar, A.A. Sibirny, Isolation and characterization of mutated alcohol oxidases from the yeast *Hansenula polymorpha* with decreased affinity toward substrates and their use as selective elements of an amperometric biosensor, BMC Biotechnol. 7 (2007) 1–7.
[22] K. Dmytruk, O. Smutok, O. Dmytruk, W. Schuhmann, A. Sibirny, Construction of uricase-overproducing strain of *Hansenula polymorpha* and its application as biological recognition element in microbial urate biosensor, BMC Biotechnol. 11 (2011) 58–66.
[23] O. Smutok, K. Dmytruk, M. Karkovska, W. Schuhmann, M. Gonchar, A. Sibirny, D-lactate-selective amperometric biosensor based on the cell debris of the recombinant yeast *Hansenula polymorpha*, Talanta 125 (2014) 227–232.
[24] K. Dmitruk, O. Smutok, M. Gonchar, A. Sibirnyĭ, Construction of flavocytochrome b_2-overproducing strains of the thermotolerant methylotrophic yeast *Hansenula polymorpha* (*Pichia angusta*), Microbiology (Mosc.) 77 (2008) 213–218.
[25] C. Appleby, R. Morton, Lactic dehydrogenase and cytochrome b_2 from yeast Purification and crystallization. J. Biochem. 71 (1959) 492–499.
[26] X.P. Sun, Z.L. Zhang, B.L. Zhang, X.D. Dong, S.J. Dong, E.K. Wang, Preparation of gold nanoparticles protected with polyelectrolyte, Chin. Chem. Lett. 14 (2003) 866–869.

Оригінал доступний за посиланням:
https://www.sciencedirect.com/science/article/abs/pii/S0039914015302058

6.2 Оцінювання можливості посилення сенсорного сигналу клітин веденням у клітини цільових ензимів за допомогою нанорозмірних носіїв

Анотація: *У представленій роботі вивчено вплив НЧ на сенсорні властивості рекомбінантних клітин дріжджів, здатних до надсинтезу ензимів аналітичного призначення, на моделі двох оксидоредуктаз (флавоцитохрому b_2 і АО) та гідролази (аргінази І) у складі нанокомпозитних носіїв (порівняно з традиційними матеріалами). Крім того, вивчено можливість посилення каталітичної активності рекомбінантних клітин шляхом додаткового введення в них відповідних ензимів, кон'югованих із НЧ. Показано, що додаткове введення в клітини ензимів, іммобілізованих на Au носіях, істотно поліпшує біоаналітичні характеристики клітинних сенсорів, зокрема їхню чутливість і швидкість розвитку сигналу.*

Проект Наукова Книга

БАГАТОФУНКЦІОНАЛЬНІ НАНОМАТЕРІАЛИ ДЛЯ БІОЛОГІЇ І МЕДИЦИНИ

молекулярний дизайн, синтез і застосування

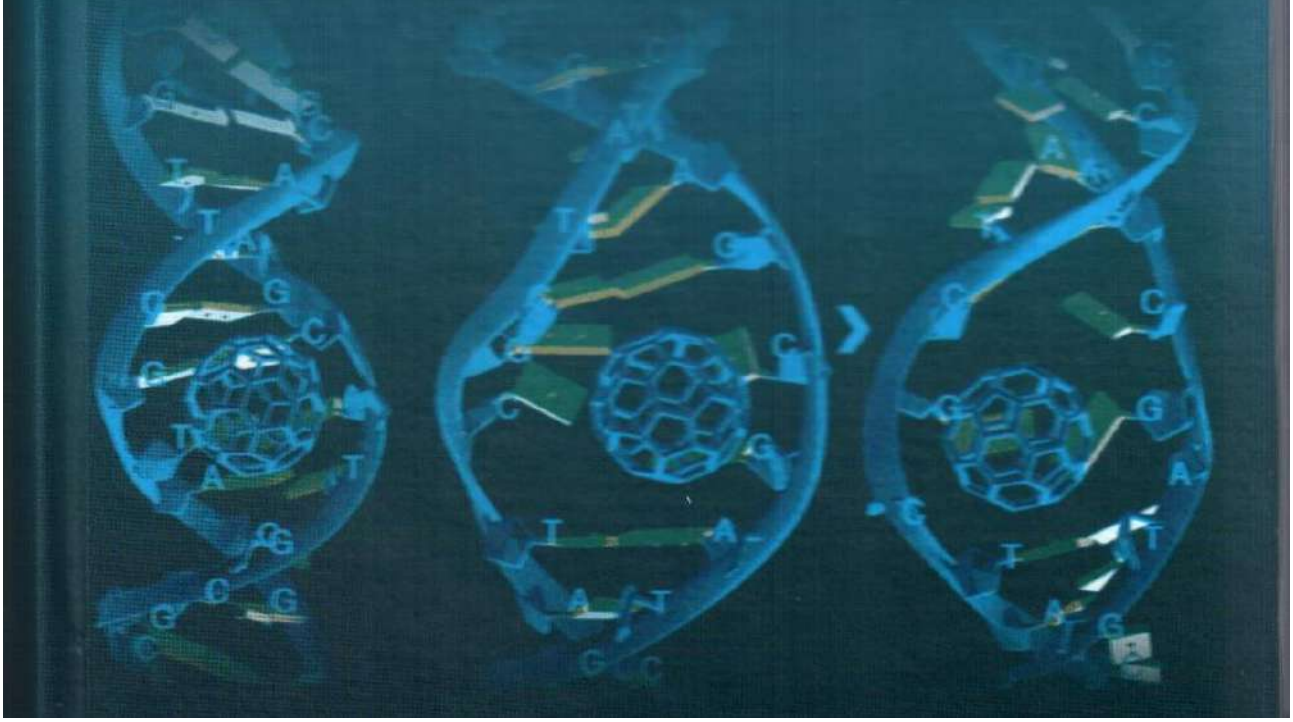

БАГАТОФУНКЦІОНАЛЬНІ НАНОМАТЕРІАЛИ ДЛЯ БІОЛОГІЇ І МЕДИЦИНИ: молекулярний дизайн, синтез і застосування

За редакцією члена-кореспондента
НАН України Р.С. СТОЙКИ

ПРОЕКТ
"НАУКОВА КНИГА"

КИЇВ
• НАУКОВА ДУМКА •
2017

MULTIFUNCTIONAL NANOMATERIALS FOR BIOLOGY AND MEDICINE: molecular design, synthesis and application

Edited by R.S. STOIKA,
Corresponding Member of NAS of Ukraine

"SCIENTIFIC BOOK" PROJECT

KYIV
• NAUKOVA DUMKA •
2017

УДК: 53.04; 539.21; 54.05; 577; 57.04; 615

Автори:

Р.С. Стойка, Ю.І. Прилуцький, А.Г. Наумовець, Р.О. Білий, Я.Б. Блюм, Н.М. Бойко, А.П. Бурлака, Ю.В. Вац, Т.Я. Вітак, А. Волошиновський, Г.З. Гайда, О. Гевусь, Л.Л. Гнатишина, О.І. Годована, О.В. Годований, М.В. Гончар, І.І. Гринюк, Є.А. Гудзь, Н.М. Гула, О.В. Дмитренко, Л.Б. Дробот, М.П. Євстігнєєв, А.І. Ємець, Т.Б. Желтоножська, О.С. Заїченко, Т.О. Зінченко, М.І. Карковська, О.А. Кизима, Д.О. Климчук, О.Ю. Ключівська, Л.І. Кобилінська, Т.Є. Константінова, Л.Р. Куницька, О.О. Ліщис, О.В. Лобачевська, С.М. Лукін, В.І. Максін, О.П. Матишевська, Д.О. Мінченко, О.Г. Мінченко, Н.Є. Мітіна, О.С. М'ягкота, К.О. Паливода, Р.Р. Панчук, Н.М. Пермякова, Д.М. Петухов, С.В. Прилуцька, А.О. Рябцева, В.Ф. Сагач, А.І. Сененко, Ю.В. Сеньків, Р.Я. Серкіз, Н.Р. Скорохід, О.В. Смуток, Н.Є. Стасюк, О.Б. Столяр, А.М. Томін, Г.І. Фальфушинська, Є.З. Філяк, Н.С. Фінюк, Я. Хім'як, А.Є. Чапля, В.В. Черепанов, В.В. Чумак, Л.М. Шаповал, О.П. Яворовський, О.М. Якубчак, W. Berger, P. Heffeter, U. Ritter, P. Scharff

У монографії стисло викладено найвагоміші результати досліджень і розробок, отримані біологами у тісній співпраці з хіміками й фізиками у галузі наноматеріалів для біології, медицини, нанобіотехнологій. У шести логістично взаємопов'язаних тематичних розділах висвітлено питання молекулярного дизайну, синтезу багатофункціональних наноматеріалів для біології і медицини, доставки ліків у клітини-мішені за допомогою синтетичних наноматеріалів, використання полімерних олігоелектролітних наноматеріалів для доставки нуклеїнових кислот у клітини різного походження, описано багатофункціональні наноматеріали для діагностичних цілей і біомедичного іміджингу, проблеми біосумісності й екотоксичності нанокомпозитних матеріалів, наведено приклади застосування наноматеріалів для лікувальних цілей.

Для студентів та аспірантів, які цікавляться наноматеріалами різного біомедичного призначення, а також досвідчених спеціалістів у цій галузі сучасної науки.

Рецензенти:

академік НАН України, доктор біологічних наук, професор *С.О. Костерін*,
академік НАН України, доктор фізико-математичних наук, професор *Л.А. Булавін*,
академік НАН України, доктор хімічних наук, професор *М.Т. Картель*

Рекомендовано до друку вченою радою
Інституту біології клітини НАН України (протокол № 8 від 25 вересня 2015 р.)

Видання здійснено за кошти Цільової комплексної програми «Створення та розвиток науково-видавничого комплексу НАН України»

Науково-видавничий відділ медико-біологічної, хімічної та геологічної літератури

Редактор *Н.А. Серебрякова*

© Р.С. Стойка, Ю.І. Прилуцький, А.Г. Наумовець, Р.О. Білий, Я.Б. Блюм, Н.М. Бойко, А.П. Бурлака, Ю.В. Вац, Т.Я. Вітак, А. Волошиновський, Г.З. Гайда, О. Гевусь, Л.Л. Гнатишина, О.І. Годована, О.В. Годований, М.В. Гончар, І.І. Гринюк, Є.А. Гудзь, Н.М. Гула, О.В. Дмитренко, Л.Б. Дробот, М.П. Євстігнєєв, А.І. Ємець, Т.Б. Желтоножська, О.С. Заїченко, Т.О. Зінченко, М.І. Карковська, О.А. Кизима, Д.О. Климчук, О.Ю. Ключівська, Л.І. Кобилінська, Т.Є. Константінова, Л.Р. Куницька, О.О. Ліщис, О.В. Лобачевська, С.М. Лукін, В.І. Максін, О.П. Матишевська, Д.О. Мінченко, О.Г. Мінченко, Н.Є. Мітіна, О.С. М'ягкота, К.О. Паливода, Р.Р. Панчук, Н.М. Пермякова, Д.М. Петухов, С.В. Прилуцька, А.О. Рябцева, В.Ф. Сагач, А.І. Сененко, Ю.В. Сеньків, Р.Я. Серкіз, Н.Р. Скорохід, О.В. Смуток, Н.Є. Стасюк, О.Б. Столяр, А.М. Томін, Г.І. Фальфушинська, Є.З. Філяк, Н.С. Фінюк, Я. Хім'як, А.Є. Чапля, В.В. Черепанов, В.В. Чумак, Л.М. Шаповал, О.П. Яворовський, О.М. Якубчак, W. Berger, P. Heffeter, U. Ritter, P. Scharff, 2017
© НВП «Видавництво "Наукова думка" НАН України», дизайн, 2017

ISBN 978-966-00-1564-7

Розділ 4. Багатофункціональні наноматеріали для діагностичних цілей і біомедичного іміджингу 143

4.1. Використання магнітних і флуоресцентних полімерних наночастинок, функціоналізованих лектином, для детекції і видалення апоптичних клітин (*А.М. Томін, Р.С. Стойка, О.С. Заіченко, Н.Є. Мітіна, Р.О. Білий*) 143

4.2. Індукування фотозбудженими багатостінними вуглецевими нанотрубками гіпертермічного ефекту у трансформованих клітинах (*С.В. Прилуцька, А.П. Бурлака, С.М. Лукін, В.В. Черепанов, Ю.І. Прилуцький*) 147

4.3. Fluorescent nanoparticles of noble metals for cell imaging (*G.Z. Gayda, N.Ye. Stasyuk, R.Ja. Serkiz, M.V. Gonchar*) 156

4.4. Наноматеріали у конструюванні біосенсорів біомедичного призначення (*М.І. Карковська, Н.Є. Стасюк, Г.З. Гайда, О.В. Смуток, М.В. Гончар*) 165

Розділ 5. Біосумісність та екотоксичність нанокомпозитних матеріалів 178

5.1. Зменшення негативних побічних ефектів доксорубіцину у мишей із лімфомою NK/Ly за його доставки новими полімерними наноносіями (*Н.М. Бойко, Ю.В. Сеньків, Ю.В. Вац, О.Ю. Ключівська, А.О. Рябцева, Н.Є. Мітіна, О.С. Заіченко, Р.С. Стойка*) 178

5.2. Корекція біохімічних показників загальної токсичної дії доксорубіцину за його доставки у складі комплексу з поліетиленгліколевмісним полімерним наноносієм у щурів (*Л.І. Кобилінська, А.О. Рябцева, Н.Є. Мітіна, О.С. Заіченко, Р.С. Стойка*) 183

5.3. Оцінювання біобезпеки срібловмісних наноматеріалів: молекулярно-біологічні підходи (*О.Г Мінченко, О.П. Яворовський, Д.О. Мінченко, Т.О. Зінченко*) 195

5.4. Екотоксичність промислових наноматеріалів. Аналіз проблеми та методологічні засади оцінювання (*О.Б. Столяр, Г.І. Фальфушинська, Л.Л. Гнатишина, Н.Є. Мітіна, О.С. Заіченко, Р.С. Стойка*) 210

Розділ 6. Приклади застосування наноматеріалів для лікувальних цілей 237

6.1. Регенерація кісткового дефекту за допомогою полімермінеральних нанокомпозитів на основі рентгеноконтрастних наночастинок ZrO_2-Gd_2O_3, функціоналізованих гіалуроновою кислотою (*О.І. Годована, О.Ю. Ключівська, О.В. Годований, Т.Є. Константінова, Н.Є. Мітіна, О.С. Заіченко, Р.С. Стойка*) 237

6.2. Роль одностінних вуглецевих нанотрубок у регуляції серцево-судинної діяльності у щурів за гіпертензії (*Л.М. Шаповал, В.Ф. Сагач, О.В. Дмитренко, В.В. Черепанов, Ю.І. Прилуцький*) 245

6.3. Application of C_{60} fullerene-doxorubicin complex for antitumor therapy (*R.R. Panchuk, S.V. Prylutska, R.S. Stoika, Yu.I. Prylutskyy, W. Berger, P. Heffeter, U. Ritter, P. Scharff*) 258

6.4. Іммобілізація біологічно активних компонентів до складу міцелярних наноконтейнерів і нанореакторів та застосування створених нанокомпозитів (*Т.Б. Желтоножська, Н.М. Пермякова, Л.Р. Кунщька, Н.М. Бойко, Д.О. Клімчук, В.І. Максін, О.М. Якубчак*) 266

SUMMARY 301

СПИСОК ПРИЙНЯТИХ СКОРОЧЕНЬ 303

СПИСОК ЛІТЕРАТУРИ 308

Chapter 4. Multifunctional nanomaterials for diagnostic application and biomedical imaging 143

4.1. Application of lectin-functionalized magnetic and fluorescent polymeric nanoparticles for detection and isolation of apoptotic cells (*A.M. Tomin, R.S. Stoika, A.S. Zaichenko, N.Ye. Mitina, R.O. Bilyy*) 143

4.2. Photoactivated multi-wall carbon nanotubes induce hyperthermic effect in transformed mammalian cells (*S.V. Prylutska, A.P. Burlaka, S.M. Lukin, V.V. Cherepanov, Yu.I. Prylutskyy*) 147

4.3. Fluorescent nanoparticles of noble metals for cell imaging (*G.Z. Gayda, N.Ye. Stasyuk, R.Ja. Serkiz, M.V. Gonchar*) 156

4.4. Nanomaterials for construction of biosensors of biomedical application (*M.I. Karkovska, N.Y. Stasyuk, G.Z. Gayda, O.V. Smutok, M.V. Gonchar*) 165

Chapter 5. Biocompatibility and ecotoxicity of nanocomposite materials 178

5.1. Suppression of negative side effects of doxorubicin at its delivery by novel polymeric nanocarriers to mice with NK/Ly lymphoma (*N.M. Boiko, Y.V. Senkiv, Y.V. Vats, O.Y. Klyuchivska, A.O. Riabtseva, N.Y. Mitina, A.S. Zaichenko, R.S. Stoika*) 178

5.2. Correction of biochemical indicators of general toxicity of doxorubicin at its delivery in complex with PEG-containing polymeric nanocarrier in rats (*L.I. Kobylinska, A.O. Riabtseva, N.Y. Mitina, A.S. Zaichenko, R.S. Stoika*) 183

5.3. Evaluation of biosafety of Ag-containing nanomaterials : molecular-biological approaches (*O.H. Minchenko, O.P. Yavorovsky, D.O. Minchenko, T.O. Zinchenko*) 195

5.4. Ecotoxicity of industrial nanomaterials: Analysis of problem and methodological bases of estimation (*O.B. Stoliar, H.I. Falfushynska, L.L. Gnatyshyna, N.Y. Mitina, A.S. Zaichenko, R.S. Stoika*) 210

Chapter 6. Examples of application of functional nanomaterials for treatment goals 237

6.1. Regeneration of bone defect by polymer-mineral composite based on radiopaque $ZrO_2 \cdot Gd_2O_3$ nanoparticles functionalized with hyaluronic acid (*O.I. Hodovana, O.Y. Klyuchivska, O.V. Godovanyi, T.Y. Konstantinova, N.Y. Mitina, A.S. Zaichenko, R.S. Stoika*) 237

6.2. Single-wall carbon nanotubes improve regulation of cardiovascular activity in rats with hypertension (*L.M. Shapoval, V.F. Sagach, O.V. Dmitrenko, V.V. Cherepanov, Yu.I. Prylutskyy*) 245

6.3. Application of C_{60} fullerene-doxorubicin complex for antitumor therapy (*R.R. Panchuk, S.V. Prylutska, R.S. Stoika, Yu.I. Prylutskyy, W. Berger, P. Heffeter, U. Ritter, P. Scharff*) 258

6.4. Immobilization of biologically active components to micellar nanocontainers and nanoreactors, and application of created nanocomposites (*T.B. Zheltonozhskaya, N.M. Permyakova, L.R. Kunitskaya, N.M. Boiko, D.O. Klymchuk, V.I. Maksin, O.M. Iakubchak*) 266

SUMMARY 301

LIST OF A DOPTED ABBREVIATIONS 303

REFERENCES 308

Arginase activity of the bioNPs-cells was shown to increase 3-fold in comparison with the control and NPs-cells. That activity of the bioNPs-cells accounts for approximately 40 % of the initial activity of the bioNPs added to cells, while the difference in arginase acitivity of the bioNPs-cells and the NPs-cells accounts for 27 % of the initial arginase activity present in the bioNPs. There are two potential explanations of these findings: 1) the penetration of the bioNPs into the cells and 2) the electrostatic binding of the bioNPs with cell wall resulting in an increase of the enzyme content in the bioNPs-cells. To answer a question about the mechanism of the revealed phenomenon, treated yeast cells were studied by SEM and X-ray spectral analysis (data not shown) before and after their modification with arginase-AuNPs. Track amounts of Au^0 (AuNPs) were detected only in the permeabilized bioNPs-cells (unpublished data).

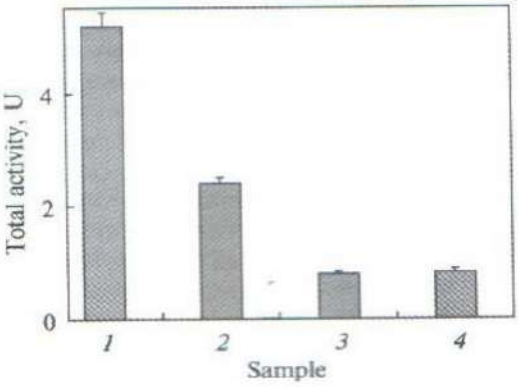

Fig. 4.22. Arginase activity in the initial bioNPs (*1*), yeast cells enriched with the bioNPs (*2*), and the NPs (*3*) comparing to control cells (*4*)

The molecular mechanisms of the NPs-cell interactions and the physicochemical parameters underlying their toxicity towards different types of cells stay poorly studied. A lack of standard methods and materials slows down further development of "smart" drugs and devices based on the NPs [71, 86, 93, 102, 104].

We propose a novel method of cell imaging based on using fluorescent nanoparticles (NPs) of Au and Ag synthesized by chemical reduction of the relevant ions. In minimal concentration (up to 0.1 mM), these NPs were non-toxic for the yeast cells *H. polymorpha* used as an experimental model of the living organism. The bi-metallic NPs possess stable fluorescence (green, red, and blue filters) in solution, as well as inside the living cells. That allows observation of transferring fluorescent NPs from the parental to daughter cells through at least three generations. Utilization of the developed AuNPs for delivery of the enzyme (human arginase) to yeast cells was also demonstrated. Thus, the synthesized bimetallic (Au and Ag) NPs may be a perspective tool for cell imaging and controlled drug delivery.

4.4. Наноматеріали у конструюванні біосенсорів біомедичного призначення

Специфічні властивості наноматеріалів відкривають широкі можливості для створення нових продуктів із цінними характеристиками і практичним значенням: ефективних каталізаторів, сенсорних елементів, діагностичних препаратів, фармацевтичних засобів [106].

Однією з основних особливостей наночастинок є висока хімічна активність, обумовлена їх підвищеною здатністю до іонного чи атомного обмі-

ну, адсорбції, утворення поверхневих зв'язків з адсорбатами [107]. Під час хімічного синтезу наночастинок використовують різноманітні варіанти, що відрізняються за типом реагента і системи, в якій здійснюється процес [108]. Доступні методи синтезу наночастинок, а також їх спорідненість із багатьма біологічними молекулами робить їх привабливими кандидатами для досліджень у сенсорних технологіях [109]. Для біотехнологічних процесів особливо актуальним є отримання біонаноматеріалів із поліпшеними каталітичними властивостями [110] — як на основі ферментів, так і генетично модифікованих клітин із вищими ензиматичними параметрами.

Мета досліджень полягала у вивченні впливу наночастинок на сенсорні властивості рекомбінантних клітин дріжджів, здатних до надсинтезу ферментів аналітичного призначення, на моделі двох оксидоредуктаз (флавоцитохрому b_2 й алкогольоксидази) та гідролази (аргінази I) у складі нанокомпозитних носіїв (порівняно з традиційними матеріалами). Крім того, вивчено можливість посилення каталітичної активності рекомбінантних клітин шляхом додаткового введення в них відповідних ферментів, кон'югованих із наночастинками. Високу проникність клітин до наночастинок інтенсивно вивчають в останні роки у зв'язку з перспективою використання такого підходу для скерованого введення ліків, проте ідея введення наночастинок, зв'язаних із ферментами, з метою поліпшення біосенсорних характеристик клітин у літературі не пропонувались і експериментально до нас не вивчалась.

Наночастинки золота (nAu) синтезували з використанням неорганічного відновника — боргідриду натрію. Вивчено можливість застосування nAu як носія для іммобілізації рекомбінантних ферментів і поєднання ензимо-наночастинок із клітинами дріжджів у складі нанокомпозитних матеріалів (полімерна матриця + ензимо-nAu). Досліджено структурні, фізико-хімічні та каталітичні властивості біонаночастинок, доведено перспективність їх використання в біосенсорних технологіях з метою поліпшення біоаналітичних характеристик сенсорних елементів.

У роботі використовували різні клітини різних штамів метилотрофних дріжджів *Hansenula polymorpha*: рекомбінантний надпродуцент аргінази людини I — *H. polymorpha* NCYC 495 (*pGAP1-HsARG1 leu2car1:LEU2*); рекомбінантний надпродуцент флавоцитохрому b_2 — *H. polymorpha "tr1"* (*gcr1 catX/prAOX_CYB2*) та дикий штам *H. polymorpha* NCYC 495.

Носіями для іммобілізації ферментів, виділених із клітин рекомбінантних штамів дріжджів, слугували наночастинки золота (nAu), отримані методом відновлення Au^{3+} із розчину $HAuCl_4$ [111]. Процедура включала змішування 0,25 мл 10 мМ $HAuCl_4$ і 0,6 мл 10 мМ $NaBH_4$. Сурфактантом було обрано цетилтриметиламонію бромід (ЦТМБ, CTAB, 7,5 мл, 10 мМ). Отриману суміш інкубували протягом 15 хв за 100 °С, при цьому відбувалась реакція синтезу nAu із використанням боргідриду як відновлювального чинника і розчин забарвлювався у винно-червоний колір:

$$8HAuCl_4 + 3NaBH_4 + 9H_2O \rightarrow 8Au + 3H_3BO_3 + 3NaCl + 29NaCl.$$

Отримані nAu осаджували центрифугуванням (9700 *g*; Hettich Micro-22R) протягом 40 хв. Середній розмір наночастинок становив 20 нм, pH колоїд-

ного розчину — 12. Осаджені nAu двічі відмивали 10 мМ фосфатним буфером (pH 7,5) і обробляли 0,85 мМ водним розчином цистеаміну. При цьому nAu міцно зв'язувались із тіоловими групами і в результаті аміновмісний цистеамін приєднувався до поверхні nAu. Кінцева концентрація функціоналізованих цистеаміном nAu становила 0,17 мМ.

Біофункціоналізацію nAu здійснювали методом нековалентного зв'язування ферментів (аргінази людини I, флавоцитохрому b_2 та алкогольоксидази) з кінцевою концентрацією білка 0,05 мг/мл у 10 мМ фосфатному буфері (pH 7,5). За такого значення pH ферменти перебувають в аніонній формі й електростатично зв'язуються з протоновими аміногрупами цистеаміну. Після 4-разового промивання біофункціоналізованих наночастинок цим буфером (pH 7,5) осад ресуспендували в 0,2 мМ фосфатному буфері (pH 7,5).

Вихід за активністю ферментів, іммобілізованих на поверхні nAu, великою мірою залежить від їхньої природи. Якщо для флавоцитохрому b_2 він становив 15 %, що відповідало 3,3 Од/мл, то для алкогольоксидази — 55 % (15,4 Од/мл), для аргінази людини I — 47,5 % (39,4 Од/мл).

Далі дріжджові клітини збагачували біофункціоналізованими nAu. Процедура збагачення інтактних і пермеабілізованих клітин різних штамів *H. polymorpha* біофункціоналізованими nAu була такою: до 0,18 мл суспензії клітин із концентрацією 30 мг/мл у 10 мМ фосфатним буфером (pH 7,5) додавали 0,1 мл біофункціоналізованих наночастинок. Отриману суміш інкубували протягом ночі за +4 °C та постійного перемішування. 0,18 мл суспензії вихідних клітин і клітин, оброблених цистаміно-модифікованими nAu без включення ферментів, інкубували за аналогічних умов як контроль. Після інкубації зразки осаджували центрифугуванням за 670 *g* протягом 3 хв і двічі промивали 10 мМ фосфатним буфером (pH 7,5).

Після цього проводили рентгеноспектральний мікроаналіз клітин *H. polymorpha*, збагачених ензимонаночастинками. Ефект проникнення біофункціоналізованих nAu крізь пори клітин підтверджували за допомогою рентгеноспектрального аналізу, який виявляв наявність слідових кількостей золота всередині пермеабілізованих клітин (рис. 4.23). Рентгеноспектральний мікроаналіз проводили на сканувальному електронному мікроскопі (РЕММА-102-02, Суми, Україна). Підкладкою для зразків слугував графітовий стрижень завдовжки 0,5 см і діаметром 0,5 см. Зразки фіксували розчином Бутвара B-98 (Sigma, St. Louis, MO, США) у 1,5%-му хлороформі. Відстань до зразка (WD) коливалась від 17,1 до 21,7 мм за напруги 20—40 еВ і збліження 2500—10 000.

За допомогою рентгеноспектрального мікроаналізу (див. рис. 4.23, *б*) зафіксовано наявність Au^0 всередині модифікованих клітин *H. polymorpha*, що підтвердило проникність ензимо-nAu всередину клітин (Kα пік за 2,1 кеВ).

Конструювання амперометричних біосенсорів на основі клітин, збагачених ензимонаночастинками. Клітинні біосенсори конструювали на базі стандартного амперометричного потенціостату із трьохелектродною сенсорною конфігурацією: срібло-хлорсрібний Ag/AgCl/KCl (3 М) використовували як електрод порівняння, допоміжним слугував стрижневий платиновий електрод. Застосовували різні типи робочих електродів (графітові, золоті, платинові). Безпосередньо перед використанням робочу поверхню графітових

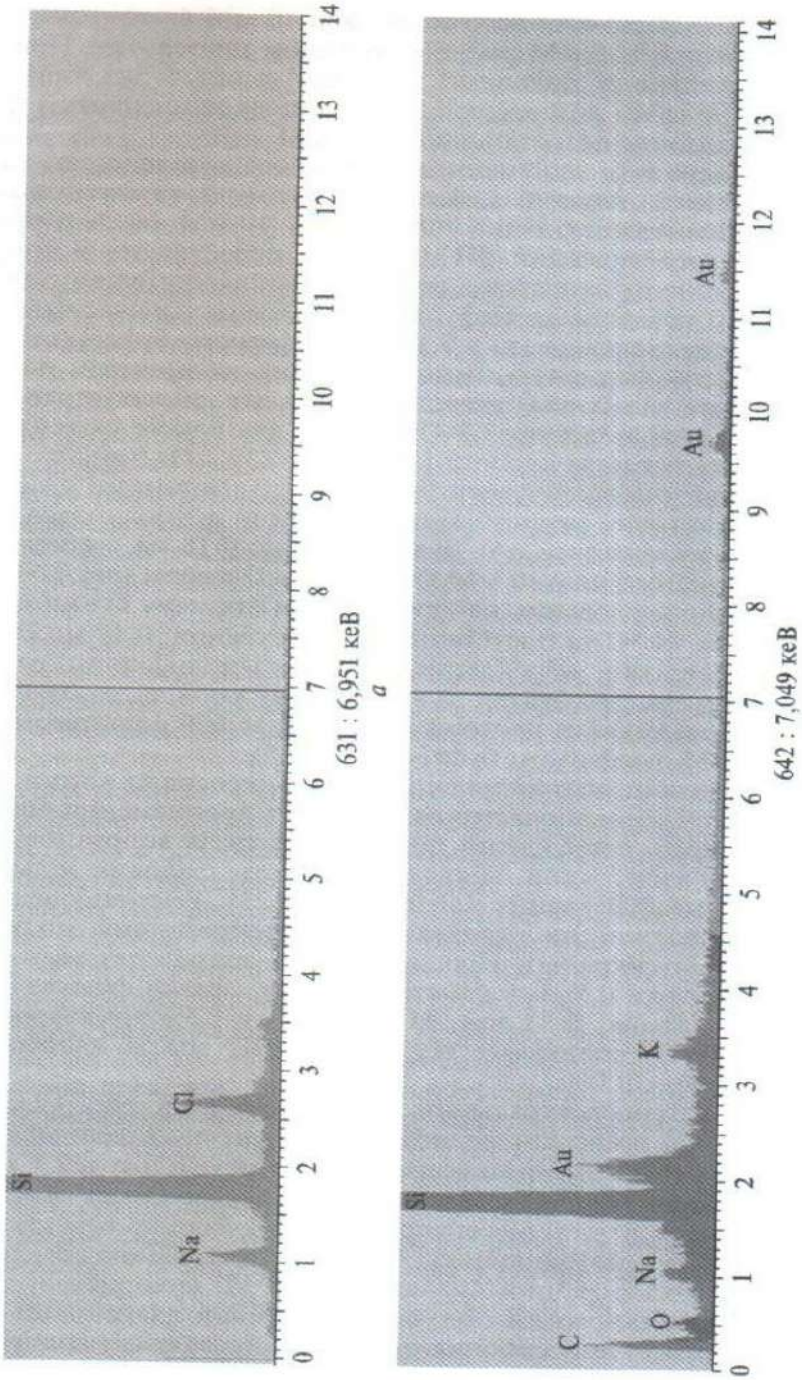

Рис. 4.23. Дані рентгеноспектрального мікроаналізу пермеабілізованих клітин *H. polymorpha* до (*а*) та після їх обробки ензимонано-частинками (*б*)

а *б* *в*

Рис. 4.24. Електроди, використані в роботі:
а — комерційний золотий планарний електрод C220AT; *б* — комерційний платиновий торцевий електрод; *в* — лабораторні графітові торцеві електроди

електродів полірували наждачним папером. Золоті та платинові електроди полірували за допомогою полірувальної тканини й алюмінієвих паст (Leco, ФРН) із різним діаметром часточок (1,0; 0,5; 0,3 мм). Відполіровані електроди відмивали водою в ультразвуковій бані протягом 10—15 хв.

Амперометричні дослідження проводили на комерційному потенціостаті CHI 1200A (IJ Cambria Scientific Ltd, Порт Барі, Велика Британія) або експериментальних зразках потенціостатів "Postat-16" та "Biosens" (розроблених у співпраці з Ю.Г. Дубовим), з'єднаних із персональним комп'ютером для реєстрації та обробки результатів. Експерименти виконували за постійного перемішування у стандартній електрохімічній комірці місткістю 40 мл за кімнатної температури.

Препарати клітин, збагачених ензимонаночастинками, іммобілізували на поверхні робочих електродів. Біорозпізнавальний шар біосенсора формували на поверхні твердотілих перетворювачів, у зв'язку з чим постала проблема закріплення клітин і ферментів зі збереженням їхніх каталітичних властивостей. Різні препарати на поверхні робочих електродів іммобілізували відповідно до оптимальних умов, визначених раніше для іммобілізації цільових ферментів.

Як робочі застосовували комерційні 4-міліметрові золоті планарні електроди C220AT ("DropSens", Овіедо, Іспанія), 3,0-міліметровий платиновий торцевий електрод (CH Instruments Inc., Austin, США) та виготовлені вручну на основі графітового стрижня (RW001, Ringsdorff Werke, Бонн, ФРН) 3,05-міліметрові графітові торцеві електроди (рис. 4.24).

Інтактні, пермеабілізовані та модифіковані ензимонаночастинками з ферментом флавоцитохромом b_2 клітини рекомбінантного штаму *H. polymorpha "tr1"* [112] було іммобілізовано на поверхні 3,05-міліметрових графітових торцевих електродів із використанням комерційного катодного полімеру GY 83-0270 0005 (BASF Farben und Lacke, Мюнстер, Німеччина) як іммобілізувального агента. Іммобілізацію проводили за такою схемою: 2—4 мкл суспензії клітин (з концентрацією 30 мг/мл у 5 мМ фосфатному буфері, pH 7,5) наносили крапельно на поверхню робочого електрода. На суспензію клітин наносили 8 мкл розбавленого в 10 разів катодного полімеру (GY 83-0270 0005, pH 5,5). При цьому відбувалася преципітація полімеру і формувалася міцна полімерна плівка [113]. Перед використанням біоелектроди зберігали в 10 мМ фосфатному буфері (pH 7,5) за +4 °C.

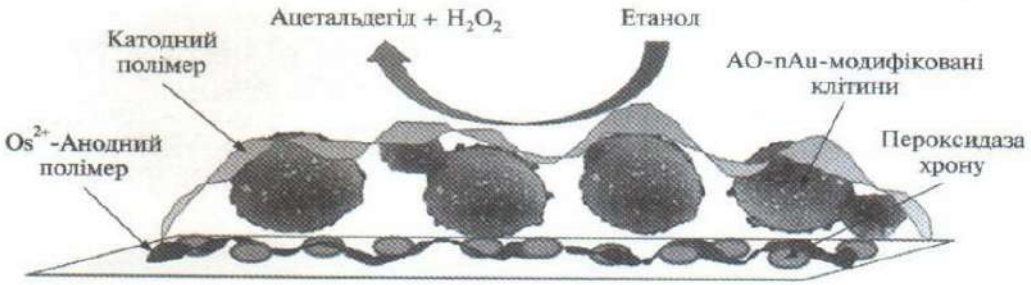

Рис. 4.25. Архітектура двошарового клітинного біоелемента амперометричного біосенсора на спирти

Пермеабілізовані клітини, збагачені алкогольоксидазою (АО-nAu) (2 мкл, 30 мг/мл, у 5 мМ фосфатному буфері, pH 7,5), дикого штаму *H. polymorpha* NCYC 495 іммобілізували на поверхні 4-міліметрових золотих планарних електродів C220AT "DropSens". Для зниження робочого потенціалу, й отже, ліпшої селективності біоелектродів до складу біорозпізнавальної мембрани вводили пероксидазу хрону (4 мкл, 300 Од/мл у 5 мМ фосфатному буфері, pH 7,5), що уможливлювало проведення детекції не за окисненням H_2O_2 при +600 мВ, а за відновленням пероксидази при –50 мВ за посередництва Os^{2+}-вмісного медіатора. Крім поліпшення селективності сенсора введення в систему пероксидази хрону сприяло підвищенню стабільності біоелектродів через швидке розкладання H_2O_2, який негативно впливає на стабільність алкогольоксидази. З цією метою було обрано двошарову архітектуру біоселективного елемента, яка включала: 1) перший (глибинний) шар, який містив пероксидазу хрону, інтегровану в нерозчинний матрикс електроосадженням Os-вмісного анодного полімеру *Os-AP59*; 2) другий (поверхневий) шар, сформований включенням АО-nAu-модифікованих дріжджових клітин у структуру катодного полімеру CP9 (рис. 4.25).

Отже, окиснення етанолу за каталізу алкогольоксидази у зовнішньому шарі спряжене з пероксидазним окисненням Os^{2+}-комплексу у складі анодного полімеру другого шару і завершується відновленням осмієвого медіатора на поверхні робочого електрода [114].

Клітини надпродуцента аргінази I рекомбінантного штаму *pGAP1-HsARG1 leu2car1:LEU2* дріжджів *H. polymorpha* NCYC 495 [115] іммобілізували на поверхні поліаніліннафіонмодифікованого 3,0-міліметрового платинового електрода.

Амонійселективна мембрана формувалась у два етапи: нанесенням 5 мкл 5%-го нафіону на поверхню платинового електрода та, після його висихання, електроосадженням поліаніліну з розчину, що містив 200 мМ анілін у 0,25 М H_2SO_4, попередньо дегазованого аргоном, у діапазоні потенціалів від –200 до +1100 мВ і швидкістю розгортки потенціалу 50 мВ/с, 11 циклів. Для видалення мономерів аніліну після 11 циклів електроосадження робочий електрод занурювали в дистильовану воду і прикладали постійний потенціал (–0,3 В) протягом 30 хв [116].

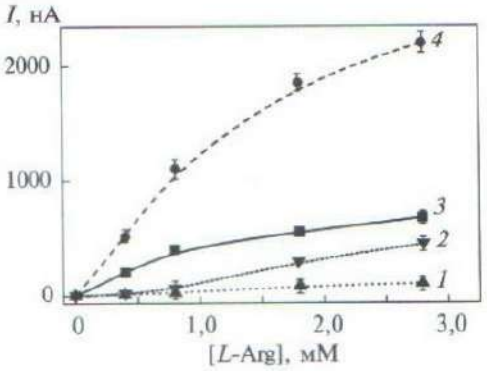

Рис. 4.26. Залежності сили струму від концентрації *L*-аргініну для клітинного біоелектрода (уреаза/збагачені аргіназою I клітини) за різних методів утримання біоелементів сенсора: *1* — покриття нафіоном; *2* — утримання плівкою GY 83-0270 00054; *3* — покриття плівкою агарози; *4* — іммобілізація в кальційальгінатній мембрані. Тут і на рис. 2.27, 2.28: робочий потенціал —200 мВ *vs* Ag/AgCl, 30 мМ фосфатний буфер, pH 7,5, 22 °C

Досліджено ефективність низки методів утримання клітин, модифікованих nAu зі зв'язаною аргіназою I:

1) *включення у кальційальгінатну мембрану*; поверх суспензії модифікованих клітин (2 мкл, 30 мг/мл) та уреази (2 мкл, 400 Од/мл) наносили 2%-й розчин альгінату натрію з наступним добавлянням 0,01 мл 10 мМ хлориду кальцію, при цьому формувалась гелева плівка; перед використанням біоелектрод промивали 30 мМ HEPES-буфером (ХБ), pH 7,5;

2) *покриття плівкою нейтралізованого нафіону*; поверх суспензії nAu модифікованих клітин та уреази (див. метод 1) наносили 5 мкл нейтралізованого аніонного полімеру нафіон (pH 7,5), який при висушуванні формував міцну плівку; отриманий біоелектрод промивали 30 мМ ХБ, pH 7,5;

3) *включення клітин у структуру катодного полімеру* GY 83-0270 00054; поверх суспензії модифікованих клітин та уреази наносили 8 мкл розбавленого в 10 разів катодного полімеру GY 83-0270 0054 (pH 7,5), при цьому формувалась міцна полімерна плівка; електрод промивали 30 мМ ХБ, pH 7,5;

4) *покриття 2%-ю агарозною мембраною*; поверх суспензії модифікованих клітин та уреази наносили 2%-й розчин агарози, після висихання формувалась міцна полімерна плівка; отримані біоелектроди промивали 30 мМ ХБ, pH 7,5.

Ефективність різних методів іммобілізації біокомпонентів на поверхні перетворювача оцінювали за відгуком на *L*-аргінін при хроноамперометричному аналізі (рис. 4.26).

Сформовані робочі електроди з архітектурою селективного шару (збагачені аргіназою I клітини/уреаза-ПАН-нафіон/Pt-електрод) та різними методами іммобілізації тестували за відгуком на *L*-Arg. Максимальний сигнал на внесений 2,8 мМ аналіт зафіксовано для електрода, біоселективний шар якого утримувався 2%-ю кальційальгінатною мембраною (2200 ± 91,1 нА). У разі утримання ферментів 0,5%-м нафіоном відгук сенсора на *L*-Arg значно знижувався (до 100 ± 5,1 нА), що, можливо, пояснюється дифузійними чинниками (рис. 4.26).

Для подальшого конструювання вдосконаленого прототипу клітинного амперометричного сенсора на аргінін було обрано кальційальгінатний метод іммобілізації біокомпонентів розпізнавальної мембрани.

Оцінювання можливості посилення сенсорного сигналу клітин введенням у клітини цільових ферментів за допомогою нанорозмірних носіїв

Модель — аргіназа I (неопубліковані дані)

Для формування біочутливого шару *L*-Arg-селективного сенсора наносили 0,01 мл розчину уреази (200 Од/мл) та 0,01 мл суспензії рекомбінантних клітин дріжджів *H. polymorpha* NCYC 495 (*pGAP1-HsARG1 leu2car1: LEU2*) з концентрацією 30 мг/мл та активністю аргінази I 9,6 Од/мг клітин на поверхню 3-міліметрового платинового електрода і залишали підсихати за кімнатної температури упродовж 10—15 хв із наступним покриттям суміші біокомпонентів кальційальгінатною мембраною. Після останнього підсихання за кімнатної температури упродовж 10—15 хв електроди промивали 10 мМ фосфатним буфером (pH 7,5). Сформовані біоелектроди зберігали за температури +4 °С.

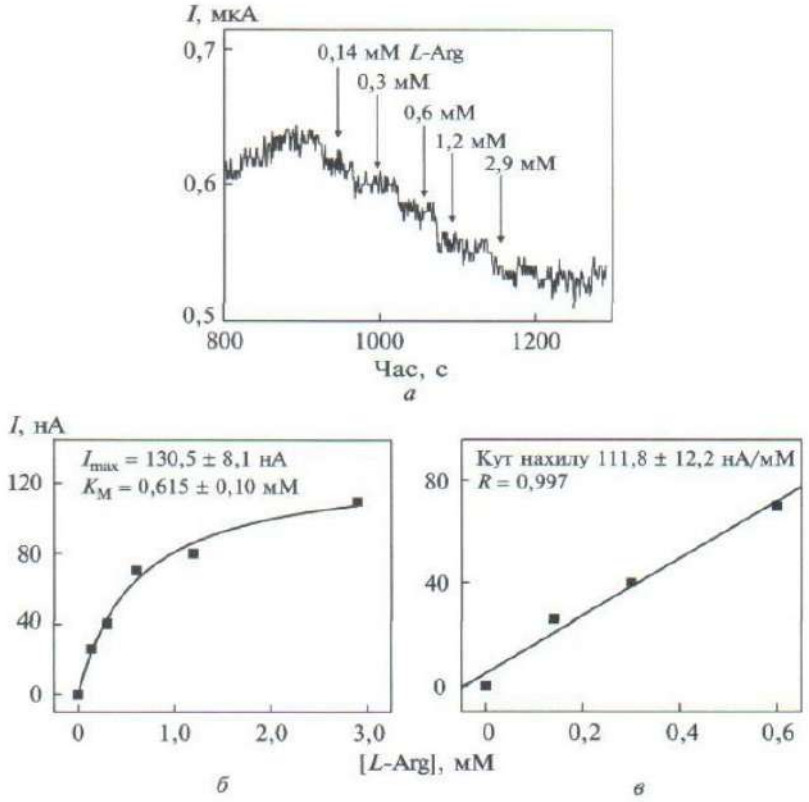

Рис. 4.27. Хроноамперограма (*а*), калібрувальний графік залежності сили струму від концентрації *L*-аргініну (*б*) та діапазон лінійності біосенсора з архітектурою біоселективного шару пермеабілізовані незбагачені клітини/nAu-уреаза-ПАН-нафіон/Pt-електрод на внесений *L*-аргінін (*в*)

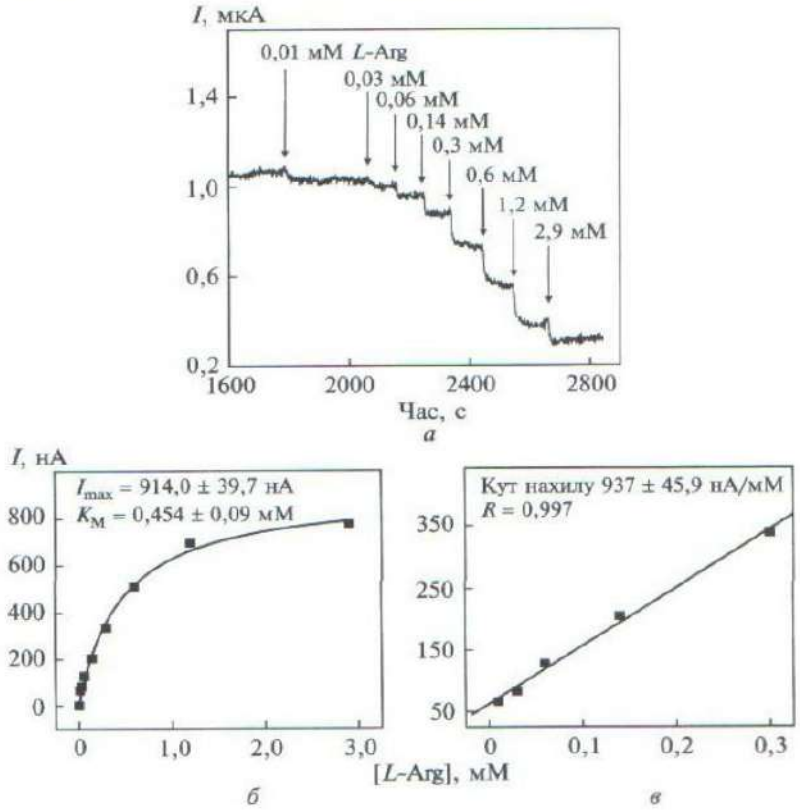

Рис. 4.28. Хроноамперограма (*а*), калібрувальний графік залежності сили струму від концентрації *L*-аргініну (*б*) та діапазон лінійності біосенсора з архітектурою біоселективного шару пермеабілізовані клітини/аргіназа-nAu-уреаза-ПАН-нафіон/Pt-електрод на внесений *L*-аргінін (*в*)

Відгук сформованих біоелектродів аналізували хроноамперометрично. Хроноамперограму біосенсора з архітектурою селективного шару пермеабілізовані незбагачені клітини/nAu-уреаза-ПАН-нафіон/Pt-електрод наведено на рис. 4.27, *а*.

Вивчено основні біоаналітичні характеристики (I_{max}, K_M, лінійний діапазон, чутливість) сконструйованого біосенсора. Лінійний діапазон концентрацій *L*-Arg, визначених сконструйованим біосенсором, становить 0,14—1,20 мМ (див. рис. 4.27, *б*), максимальний струм насичення — 131 ± 8,1 нА, чутливість біосенсора — 37 А/(М · м^2) із нижньою межею визначення *L*-Arg 0,11 мМ.

Далі було проведено хроноамперометричне дослідження амперометричного відгуку на внесений *L*-Arg для сенсора з архітектурою селективного шару пермеабілізовані клітини/аргіназа-nAu-уреаза-ПАН-нафіон/Pt-електрод (рис. 4.28, *а*).

Лінійний діапазон концентрацій *L*-Arg для сконструйованого клітинно-ензимного біосенсора зі збагаченням аргіназою становить 0,01—0,70 мМ

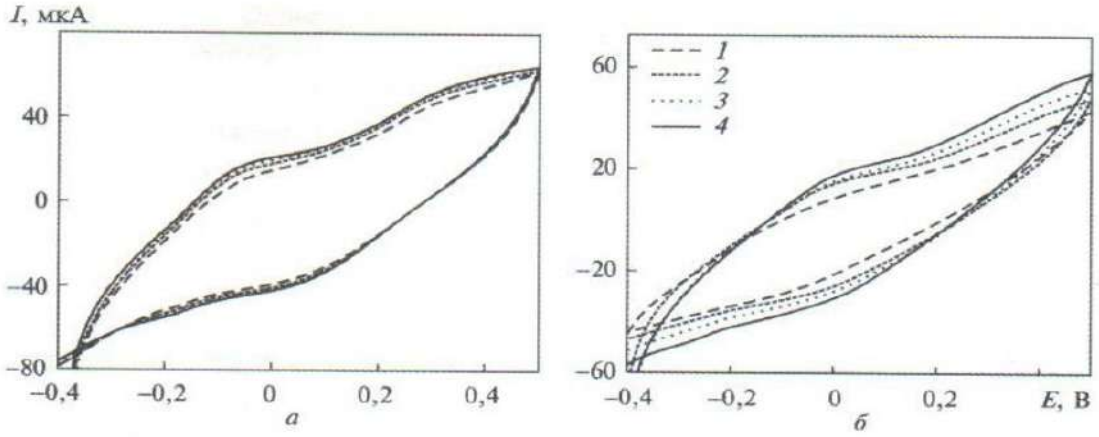

Рис. 4.29. Циклічна вольтамперометрія при внесенні зростаючих концентрацій *L*-лактату для біоелектродів на основі пермеабілізованих клітин *H. polymorpha "tr1"* (*а*) та ФЦ b_2-nAu-модифікованих пермеабілізованих клітин *H. polymorpha "tr1"* (*б*) (умови: швидкість сканування 7 мВ/с, діапазон сканування –0,4...+0,6 мВ *vs* Ag/AgCl, 20 мМ фосфатний буфер, pH 7,8, 22 °С):
1 — пермеабілізовані клітини *H. polymorpha "tr1"*; *2—4* — внесення відповідно 0,5; 1,0; 2,0 мМ *L*-лактату

($R = 0{,}999$) (див. рис. 4.28, *а*), максимальний струм насичення — 914 ± 40 нА, чутливість біосенсора на аналіт — 357 А/(М · м^2) із нижньою межею визначення *L*-Arg 0,02 мМ.

Отже, модифікація пермеабілізованих рекомбінованих клітин *H. polymorpha* наночастинками золота зі зв'язаною аргіназою порівняно з клітинами дріжджів, модифікованих лише nAu, підвищує відгук клітинно-ензимного сенсора у 7 разів.

***Модель — флавоцитохром b_2* (ФЦ b_2)** (неопубліковані дані)

При конструюванні поліпшеного *L*-лактатселективного клітинно-ензимного сенсора на основі клітин *H. polymorpha "tr1"*, модифікованих наночастинками, для забезпечення ефективного перенесення електронів від відновленої форми ФЦ b_2 на поверхню графітового електрода було використано 2 мМ феназинметосульфат у ролі вільнопроникного медіатора.

Результати дослідження впливу збагачення наночастинками ФЦ b_2-nAu на електрохімічні параметри сенсора порівняно з немодифікованими клітинами наведено на рис. 4.29.

Як видно з рис. 4.29, відгук на зростаючі концентрації *L*-лактату для біоелектродів, сконструйованих на основі ФЦ b_2-nAu-модифікованих пермеабілізованих клітин *H. polymorpha "tr1"*, значно вищий порівняно з електродами з немодифікованими клітинами дріжджів. Так, за потенціалу +250 мВ (оптимальному для окиснення феназинметосульфату на поверхні графітового електрода) електрод на основі ФЦ b_2-nAu-модифікованих пермеабілізованих клітин дріжджів при внесенні 0,5 мМ *L*-лактату генерував 300 нА, 1 мМ *L*-лактату — 500 нА, 2 мМ *L*-лактату — 1000 нА (див. рис. 4.29, *б*). Водночас незбагачені ферментом пермеабілізовані клітини дріжджів давали від-

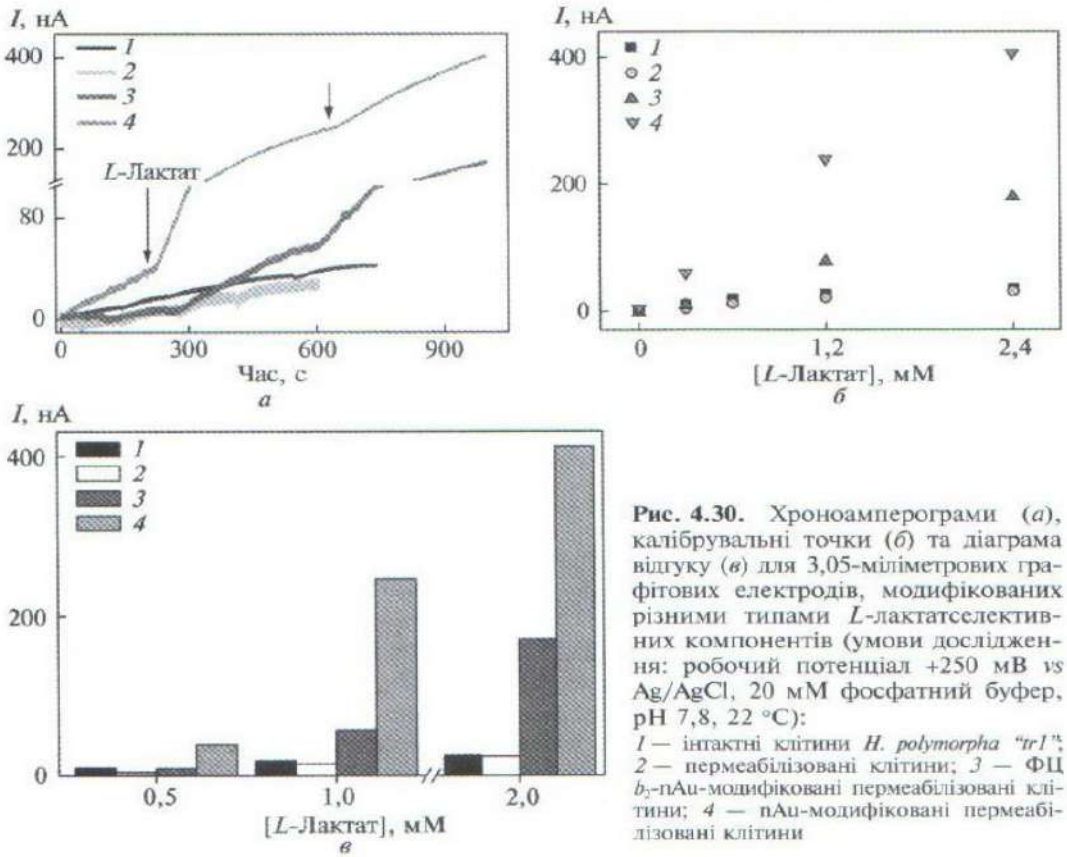

Рис. 4.30. Хроноамперограми (*а*), калібрувальні точки (*б*) та діаграма відгуку (*в*) для 3,05-міліметрових графітових електродів, модифікованих різними типами *L*-лактатселективних компонентів (умови дослідження: робочий потенціал +250 мВ *vs* Ag/AgCl, 20 мМ фосфатний буфер, pH 7,8, 22 °С):
1 — інтактні клітини *H. polymorpha "tr1"*; *2* — пермеабілізовані клітини; *3* — ФЦ b_2-nAu-модифіковані пермеабілізовані клітини; *4* — nAu-модифіковані пермеабілізовані клітини

гук на 5 мМ *L*-лактат 35 нА, 1 мМ *L*-лактат — 100 нА, на 2 мМ лактат — 130 нА (див. рис. 4.29, *а*). Отримані результати свідчать, що модифікація пермеабілізованих клітин дріжджів наночастинками золота з іммобілізованим ФЦ b_2 підвищує відгук сенсора на *L*-лактат більш як на порядок.

Для детальнішого дослідження впливу модифікації клітин дріжджів наночастинками з іммобілізованими ферментами на кінетичні параметри *L*-лактатселективного клітинного сенсора було проведено хроноамперометричні дослідження за робочого потенціалу системи +250 мВ; електрод порівняння — Ag/AgCl/KCl (рис. 4.30).

Ефективність перенесення електронів різними типами біорозпізнавальних компонентів мембран сенсора аналізували за величиною відгуку біоелектродів на *L*-лактат. Із рис. 4.30 видно, що відгук електродів на основі ФЦ b_2-nAu-збагачених пермеабілізованих клітин *H. polymorpha "tr1"* у 2,5 раза вищий, ніж біоелектродів із незбагаченими пермеабілізованими клітинами дріжджів. Водночас найнижчий відгук на *L*-лактат демонстрували біоелектроди на основі інтактних клітин *H. polymorpha "tr1"* (25 нА при внесенні 1 мМ аналіту), що можна пояснити ускладненою дифузією аналіту й медіатора крізь інтактну клітинну мембрану дріжджової клітини, особливо порівняно з

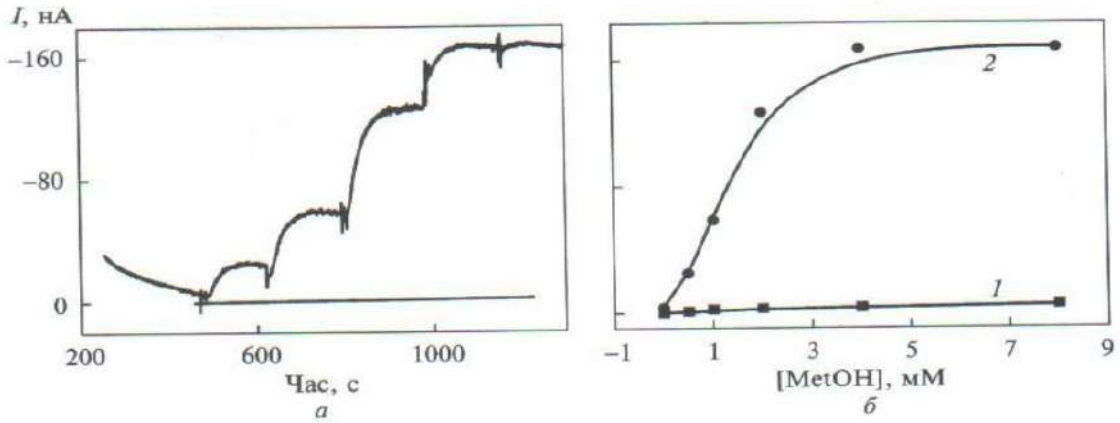

Рис. 4.31. Хроноамперограми (*а*) та калібрувальні криві (*б*) для 4-міліметрових золотих планарних електродів, модифікованих різними типами метанолчутливих елементів сенсора (умови дослідження: робочий потенціал −50 мВ *vs* Ag/AgCl, 20 мМ фосфатний буфер, pH 7,5, 22 °C):
1 — пермеабілізовані клітини *H. polymorpha* NCYC 495; *2* — АО-nAu-модифіковані пермеабілізовані клітини штаму *H. polymorpha* NCYC 495

пермеабілізованими клітинами. Для перевірки робочої гіпотези, що саме модифікація пермеабілізованих клітин *H. polymorpha "tr1"* наночастинками ФЦ b_2-nAu поліпшує аналітичні параметри сенсора, ми провели контрольне порівняння ФЦ b_2-nAu-збагачених пермеабілізованих клітин із nAu-модифікованими пермеабілізованими клітинами *H. polymorpha "tr1"*. Згідно з рис. 4.30, *а*, *б*, відгук електродів із ФЦ b_2-nAu-збагаченими пермеабілізованими клітинами на внесення 2,4 мМ *L*-лактату становить 420 нА, що у 17 разів більше порівняно з біоелектродами на основі nAu-модифікованих пермеабілізованих клітин (без збагачення ферментом) — 25 нА. Це доводить, що саме збагачення наночастинками зі зв'язаним ферментом посилює відгук клітинного сенсора. Водночас немодифіковані наночастинки золота знижують ефективність електронного перенесення крізь пермеабілізовані клітинні стінки дріжджів у 8 разів порівняно з контрольними пермеабілізованими клітинами *H. polymorpha "tr1"* (див. рис. 4.30, *б*, *в*).

***Модель — алкогольоксидаза* (*АО*)** (неопубліковані дані)

Позитивний вплив збагачення клітин ензимомодифікованими nAu (АО-nAu) на кінетичні параметри клітинних сенсорів також підтверджено експериментами з використанням золотих наночастинок з іммобілізованою алкогольоксидазою (АО). Пермеабілізовані АО-nAu-модифіковані клітини штаму дикого типу *H. polymorpha* NCYC 495 (штам до модифікації не мав підвищеної активності АО) іммобілізували з пероксидазою хрону на поверхні 4-міліметрових золотих планарних електродів C220AT "DropSens". Хроноамперометричні дослідження проводили за робочого потенціалу системи −50 мВ з Ag/AgCl/KCl електродом порівняння (рис. 4.31).

Як видно з рис. 4.31, відгук незбагачених ферментом пермеабілізованих клітин штаму дикого типу *H. polymorpha* NCYC 495 на метанол не перевищує 8 нА. Водночас АО-nAu-модифіковані пермеабілізовані клітини цього ж штаму демонструють відгук на метанол 170 нА. Отже, за збагачення пермеабілізованих клітин дріжджів наночастинками золота, зв'язаними з АО, відгук сенсора підвищується в 21 раз.

Результати виконаних досліджень підтвердили, що додаткове введення в клітини ферментів, іммобілізованих на золотих носіях, істотно поліпшує біоаналітичні характеристики клітинних сенсорів, зокрема їх чутливість і швидкість розвитку сигналу.

Робота виконана за фінансової підтримки Науково-технічних проектів: «Розробка біо/хемосенсорних аналізаторів для визначення вмісту формальдегіду, *L*- та *D*-лактату, їх метрологічна оцінка та дослідна апробація. Розробка амперометричного аналізатора для визначення вмісту формальдегіду, *L*- та *D*-лактату на основі приладу "ФОРМАТЕСТ-2010"», "Розробка та дослідна експлуатація портативного аналізатора на основі амперометричних ферментних біосенсорів для контролю якості напоїв у виноробстві. Розробка біосенсорних методів аналізу аргініну у вині за використання аргінінгідролізуючих рекомбінантних ферментів" у рамках комплексної науково-технічної програми НАН України "Сенсорні прилади для медико-екологічних та промислово-технологічних потреб: метрологічне забезпечення та дослідна експлуатація", NATO гранту SfP—984173.

101. *Plasmon-driven* synthesis of triangular core-shell nanoprisms from gold seeds / C. Xue, J.E. Millstone, S. Li, C.A. Mirkin // Angewandte Chemie International Edition. — 2007. — Vol. 46. — P. 8436—8439.

102. *Preparation* of Au-Ag, Ag-Au core-shell bimetallic nanoparticles for Surface-Enhanced Raman Scattering / Y. Yang, J.L. Shi, G. Kawamura, M. Nogami // Scripta Materialia. — 2008. — Vol. 58. — P. 862—865.

103. *Zhang L.* Metal nanoclusters: new fluorescent probes for sensors and bioimaging / L. Zhang, E. Wang // Nano Today. — 2004. — Vol. 9. — P. 132—157.

104. *Resonance* light scattering characters of core-shell structure of Au-Ag nanoparticles / J. Zhu, Y. Wang, L. Huang, Y. Lu // Physics Letters A. — 2004. — Vol. 323. — P. 455—459.

105. *Quantum* dot-based nanoprobes for *in vivo* targeted imaging / Y. Zhu, H. Hong, Z.P. Xu [et al.] // Current Molecular Medicine. — 2013. — Vol. 13. — P. 1549—1567.

106. *Kemp M.M.* Synthesis of gold and silver nanoparticles stabilized with glycosaminoglycans having distinctive biological activities / M.M. Kemp, A. Kumar, S. Mousa // Journal of Biological Macromolecules. — 2009. — Vol. 10. — P. 589—595.

107. *Vu L.V.* Preparation of silver nanoparticles by pulse sonoelectrochemical method and studying their characteristics / L.V. Vu, N.N. Long, S.C. Doanh // Journal of Physics: Conference Series. — 2009. — Vol. 187. — P. 1—9.

108. *Вегера А.В.* Синтез и физико-химические свойства наночастиц серебра, стабилизированных желатином / А.В. Вегера, А.Д. Зимон // Журнал прикладной химии. — 2006. — Vol. 79. — P. 1419—1422.

109. *Cade N.I.* The plasmonic engineering of metal nanoparticles for enhanced fluorescence and Raman scattering / N.I. Cade, T. Ritman-Meer, K.A. Kwakwa // Nanotechnology. — 2009. — Vol. 20. — P. 285201—285206.

110. *Frances S.L.* Perspective on optical biosensors and integrated sensor systems / S.L. Frances // Analytical Chemistry. — 2009. — Vol. 81. — P. 519—526.

111. *Preparation* of gold nanoparticles protected with polyelectrolyte / X.P. Sun, Z.L. Zhang, B.L. Zhang [et al.] // Chinese Chemical Letters. — 2003. — Vol. 14. — P. 866—869.

112. *Construction* of flavocytochrome b_2-overproducing strains of the thermotolerant methylotrophic yeast Hansenula polymorpha (Pichia angusta) / K.V. Dmitruk, O.V. Smutok, M.V. Gonchar, A.A. Sibirnyi // Microbiology (Moscow). — 2008. — Vol. 77. — P. 213—218.

113. *A novel* L-lactate-selective biosensor based on the use of flavocytochrome b_2 from methylotrophic yeast *Hansenula polymorpha* / O.V. Smutok, G.Z. Gayda, M.V. Gonchar, W. Schuhmann // Biosensors and Bioelectronics. —2005. — Vol. 20. — P. 1285—1290.

114. *A reagentless* bienzyme amperometric biosensor based alcohol oxidase/peroxidase and an Os-complex modified electrodeposition paint / O.V. Smutok, B. Ngounou, H.M. Pavlishko [et al.] // Sensors and Actuators B. — 2006. — Vol. 113. — P. 590—598.

115. *Розробка* платформи для надекспресії та оптимізації кінетичних властивостей аргіназ на основі метилотрофних дріжджів *Hansenulla polymorpha* / В.О. Нагорний, Л.Р. Файюра, Ю.Р. Борецький, А.А. Сибірний // Збірник наук. праць "Досягнення і проблеми генетики, селекції та біотехнології" VIII з'їзду Українського товариства генетиків та селекціонерів. Алушта. — К.: Логос, 2007. — Т. 1. — С. 366—371.

116. *Bi-enzyme* L-arginine-selective amperometric biosensor based on ammonium-sensing polyaniline-modified electrode / N.Y. Stasyuk, O.V. Smutok, G.Z. Gayda [et al.] // Biosensors and Bioelectronics. — 2012. — Vol. 37. — P. 46—52.

До розділу 5

1. *Мохорт М.А.* Кардіотоксичні ефекти доксорубіцину і доцільність їх фармакологічної корекції антагоністами кальцію дигідропіридинового ряду та активаторами АТФ-чутливих калієвих каналів гуанідинового ряду / М.А. Мохорт, М.Н. Серединська, Л.М. Киричок // Фармакологія і лікарська токсикологія. — 2010. — Т. 4, № 7. — С. 35—44.

2. *Кобилінська Л.І.* Дослідження біохімічних показників кардіотоксичної дії нових протипухлинних похідних 4-тіазолідинонів і доксорубіцину у комплексах із поліетилен-

Оригінал доступний за посиланням:
https://www.nas.gov.ua/UA/Book/Pages/default.aspx?BookID=0000011117

Анотація: *У поточному дослідженні нами повідомляється про конструювання L-аргінін-селективного амперометричного біосенсора на основі клітин рекомбінантних метилотрофних дріжджів O. polymorpha. Інтактні та пермеабілізовані клітини, ко-іммобілізовані з комерційною уреазою на поверхні поліанілін-нафіон модифікованого електрода, використовували в ролі біорозпізнавальних елементів біосенсорів. Досліджено основні робочі параметри біоелектродів. Розроблений біосенсор на основі пермеабілізованих клітин показує задовільну селективність до L-аргініну та достатню чутливість (14 ± 1,2 $A \cdot M^{-1} \cdot m^{-2}$) з позірною константою Міхаеліса–Ментен 0,51 ± 0,05 мМ. Лінійний діапазон визначуваних концентрацій є в межах до 0,6 мМ з нижньою межею виявлення – 0,085 мМ та часом відгуку на аналіт – 60 с. Сконструйований мікробний біосенсор використано для аналізу L-аргініну в реальних зразках вина та соку в порівнянні з іншими аналітичними підходами. Значення вмісту L-аргініну, отримані різними методами, виявляють тісну кореляцію.*

Sensors and Actuators B 204 (2014) 515–521

Contents lists available at ScienceDirect

Sensors and Actuators B: Chemical

journal homepage: www.elsevier.com/locate/snb

L-Arginine-selective microbial amperometric sensor based on recombinant yeast cells over-producing human liver arginase I

N.Ye. Stasyuk[a], G.Z. Gayda[a], M.V. Gonchar[a,b,*]

[a] Institute of Cell Biology, NAS of Ukraine, Drahomanov Str. 14/16, 79005 Lviv, Ukraine
[b] University of Rzeszow, Sokolowska Str. 26, 36-100 Kolbuszowa, Poland

ARTICLE INFO

Article history:
Received 4 March 2014
Received in revised form 24 June 2014
Accepted 27 June 2014
Available online 7 July 2014

Keywords:
Amperometric cell-based biosensor
L-Arginine
Polyaniline
Recombinant yeast *Hansenula polymorpha*
Urease

ABSTRACT

The article provides a description of a microbial L-arginine-selective amperometric biosensor based on recombinant cells of the methylotrophic yeast *Hansenula polymorpha*. The intact and permeabilized cells (p-cells) co-immobilized with commercial urease on a surface of electrode were used as biorecognizing elements of biosensors. Operational parameters of the bioelectrodes were estimated. The developed p-cells-based sensor revealed a satisfactory selectivity to L-arginine (Arg) and sensitivity (14 ± 1.2 A $(M\,m^2)^{-1}$) with an apparent Michaelis–Menten constant derived from Arg calibration curve 0.51 ± 0.05 mM. The dynamic range is linear till 0.6 mM Arg, a detection limit is 0.085 mM and a response time 60 s. The developed microbial biosensor was used for Arg assay in real samples of wine and juice in comparison with other analytical approaches. The Arg values obtained with different methods demonstrated a strong correlation.

© 2014 Elsevier B.V. All rights reserved.

1. Introduction

A majority of known chemical and physico-chemical methods of Arg determination have a number of disadvantages, such as a low selectivity and sensitivity, poor precision, high costs and complexity of the equipment—for physico-chemical methods [1–6] or insufficient operating and storage stability for biosensors [7–11]. Because of this, it is necessary to develop new highly selective and sensitive methods of Arg monitoring in clinical diagnostics [12–14] and food industry, in particular, in wine making.

Urea, a final product of Arg metabolism in urea cycle during juice fermentation and wine maturation, is partly assimilated by the cells of microorganisms. In the case of elevated Arg level in grape juice, urea remains in fermentation medium and spontaneously reacts with ethanol at increased temperature (during pasteurization) producing carcinogenic ethyl carbamate (urethane) [15–19]. Citrulline, formed from Arg metabolism *via* the arginine deiminase pathway by wine malolactic bacteria, is the second significant precursor of urethane in wine [17]. Urea and citrulline accumulation in the fermentation medium mainly depends on the Arg level and the type of microorganism. If Arg concentration in juice is higher than 1000 mg L^{-1}, the potential urethane concentration in wine will be above 15 μg L^{-1}, the current voluntary limit in the United States [18], while Canada has legalized this limit to 30 μg L^{-1} [17]. To ensure the high quality of final product and avoid potential health hazard of urethane, determination of Arg content in fruit juices and wine is necessary.

The biosensor approach for Arg determination seems to be perspective. The construction of Arg biosensors with cells or enzymes in bio-recognition layer has already been reported [7–11,20–25]. The most popular Arg biosensors are based on arginase/urease co-immobilized on the surface of the pH-electrode or ammonium-selective electrode. The two-step enzymatic reaction takes place on this electrode: an arginase-catalyzed conversion of Arg to urea (and L-ornithine) and urease-catalyzed hydrolysis of urea resulted in ammonium ion production, detectable by the classical potentiometric and conductometric sensors. Arg-sensitive biosensor based on the effect of urease inhibition by Arg was also reported [26]. Most of the described biosensors demonstrate a high stability and essential response to Arg, but a poor precision, long-time response and insufficient selectivity.

An amperometric bi-enzyme sensor on Arg with improved analytical parameters (see Table 1) was recently developed and optimized by us for the first time [27]. Co-immobilization of arginase and urease on the surface of Pt electrode, modified by Nafion and electroactive polyaniline (PANi), was performed by a

* Corresponding author at: NAS of Ukraine, Institute of Cell Biology, Drahomanov street 14/16, 79005 Lviv, Ukraine. Tel.: +00 380 32 261 2144; fax: +00 380 32 261 2148.
E-mail address: gonchar@cellbiol.lviv.ua (M.V. Gonchar).

http://dx.doi.org/10.1016/j.snb.2014.06.112
0925-4005/© 2014 Elsevier B.V. All rights reserved.

Table 1
Comparison of the earlier developed biosensors on Arg.

Mode of signal registration, reference	Biomembrane	LOD (mM)	Linear range (mM)	Sensitivity	Response time (95%) (min)	Stability (days)	Substrate specificity (%)	The maximal detected signal	K_M^{app} (mM)	Peculiar advantages
Potentiometric ASE*, [25]	Arginase/urease	0.1	0.5–50.0	35 mM decade^{-1}	3.0–5.0	12	Can, Arg—100%, Val—18%, Cys—17%, Orn—16%, D,L-Lys—10%	92 ± 2.0 mV	4.70 ± 0.38	Commercial NH_4^+-sensing electrode; wide linear range
Amperometric, [27]	Arginase/urease	0.038	0.07–0.6	110 ± 1.3 nA(mM mm^2)$^{-1}$	0.17	3	Can—100%, Arg—95%, Pro—4%.	1280 ± 160 nA	1.27 ± 0.29	Fast response;high sensitivity and selectivity
Amperometric, [current paper]	Permeabilized yeast cells/urease	0.085	till 0.6	14 ± 1.2 nA(mM mm^2)$^{-1}$	1.0	3	Arg—100%, Can—65%, L-Lys—27%, Ser—7%, Pro—5%.	111 ± 3.2 nA	0.51 ± 0.05	Fast response;cheap biosensing element

* ASE—ammonium-selective electrode.
Can—Canavanine, Orn—Ornitine.

special doping–undoping mechanism. This biosensor is the typical example of biocatalytic amperometric biosensor where a final product of two-step reaction (ammonium ion) interacts with electroactive polymer to induce a change in its current. PANi was chosen as the best mediator of electron transfer between the biorecognition layer and Pt electrode surface.

The purpose of this study is to construct the microbial Arg-selective composite amperometric sensor with ammonium-sensing PANi-Nafion layer and urease as additional enzyme in signal transduction pathway and evaluate biosensor's analytical parameters and possibility of its application. Novelty and the advantage of suggested approach over the enzyme-based sensors lies in natural stabilization of enzyme in the cellular environment, besides there is no more need to purify key enzyme (arginase). Development of the amperometric biosensor for Arg determination, based on the genetically engineered yeast cells (for the first time), and further comparison of analytical characteristics of enzymatic and microbial biosensors is also of scientific interest. Furthermore, the usage of the recombinant arginase-enriched cells comparing to classical sensors based on wild type cells [7,8] can result in improved kinetics of the signal development.

2. Experimental

2.1. Materials

Urease (EC 3.5.1.5, type IX from Jack Beans, 26100 U g^{-1}), 2,3-butanedione monoxime (DMO), cetyltrimethylammonium bromide (CTAB), glucose, biotin, aniline (99%) and 5% Nafion® perfluorinated resin solution were purchased from Sigma-Aldrich. Amino acids, 8-hydroxyquinoline and inorganic salts were obtained from Merck (Darmstadt, Germany). All buffers and standard solutions were prepared with Milli-Q system (Millipore) purified water.

2.2. Cells

The recombinant strain of the yeast *Hansenula polymorpha* NCYC 495-*pGAP1-HsARG1* (*leu2car1 Sc:LEU2*), carrying the *HsARG1* target gene under the control of a constitutive promoter of the glyceraldehydes-3-phosphate, was used in investigations.

Cultivation of the cells was performed in Erlenmeyer's flasks (volume 500 mL) under aeration in a circular shaker (200 rpm) at 30 °C, for 48 h, in a Burkholder medium containing (g L^{-1}): glucose—20; $(NH_4)_2SO_4$—3; KH_2PO_4—0.5; $MgSO_4$—0.2 and $CaCl_2$—0.15. The medium contained 1 mM L-Arg, 2 ppb biotin, 0.07 ppm Zn, 0.2 ppm Fe and 0.01 ppm of trace elements B, Cu, Mn and Mo, added in the form of appropriate salts. A volume of 110 mL liquid media in flask were inoculated by yeast cells from the early stationary growth phase in concentration of 50 μg mL^{-1}. Yeast cells for inoculation were taken from plates with agar Burkholder medium.

The grown cells were separated by centrifugation (1000 rpm, 10 min, at 4 °C) and washed twice with 30 mM phosphate buffer, pH 7.5 (PB) [28].

The suspensions of fresh-cultivated native cells (n-cells) and fresh-prepared permeabilized cells (p-cells), both with concentrations of 20 mg mL^{-1} in 5 mM PB, were used for bioelectrodes development. To obtain p-cells, pellet of n-cells was suspended in PB, containing 0.2% CTAB, and incubated for 15 min at 30 °C under shaking. Resulted p-cells were washed and suspended in PB.

2.3. Amperometric measurements

A potentiostat CHI 1200A (IJ Cambria Scientific Ltd, UK), connected to computer *via* a RS232 port and a three-electrode system

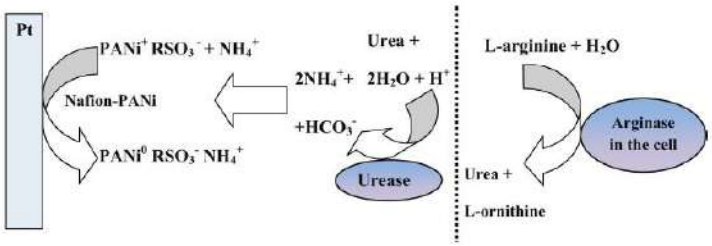

Fig. 1. Principal scheme of Arg assay by the bioelectrode. $PANi^+$ and $PANi^0$—oxidized and reduced forms of PANi, respectively; RSO_3^-—a skeleton of Nafion.

were used for electrochemical studies. A piece of Pt wire (d = 1 mm) and an Ag/AgCl/KCl (3 M) electrode were used as the counter and reference electrodes, respectively. A Pt rod electrode (ALS Co., Ltd Tokyo, Japan) was applied as a working electrode (d = 3 mm). Before sensor's preparation, the electrode was polished on emery paper (P1200) and rinsed with water in an ultrasonic bath during 10 min. Electrochemical experiments were performed in batch mode under continuous stirring in a standard 40 mL cell at room temperature.

2.4. Ammonium-sensing electrode

Ammonium-sensing membrane on a surface of the Pt electrode was formed by two steps procedure according to our paper [27]. A 5.0 μL aliquote of 0.5 wt % neutralized Nafion solution (prepared from 5% sample by 90% ethanol/water dilution) was applied onto a Pt disk electrode and air-dried for 10 min. The PANi film was deposited by immersing of the electrode in 0.2 M aniline solution in 0.5 M H_2SO_4 and by sweeping potentials from −200 to 1000 mV (*vs* Ag/AgCl reference electrode) with a scan rate of 50 mV s^{-1}, for 11 cycles of electrodeposition. The resulting Pt electrode covered with PANi-Nafion was rinsed several times with water during 30 min under constant potential −0.3 V and kept in PB before usage.

2.5. Arg-sensing bioelectrodes

The immobilization strategy was based on two principles: (1) electrostatic interaction of bioelements with conducting polymer (urease and yeast cells at pH 7.5 have negative charges, so can bind with positive charged PANi); (2) additional physical support of biosensing layer by dialysis membrane.

To prepare bioelectrode, 10 μL of urease solution in PB with 200 U mL^{-1} activity were placed on the top of PANi-Nafion/Pt-electrode. After drying for 2 min at room temperature, 5 μL of cell suspension in 5 mM PB was added. Arginase activities estimated in p-cells and n-cells are 69.9 U mL^{-1} and 2.75 U mL^{-1}, respectively. Bioelectrodes covered with dialysis membrane were rinsed by PB and stored at +4 °C till application.

2.6. Chemical and enzymatic methods of Arg analysis

All used methods were performed by the technique of standard additions.

A chemical method is based on the use of 8-hydroxyquinoline [29]. The tested samples were photometered at 500 nm and Arg concentration was calculated from the linear regression parameters of a calibration graph.

An enzymatic method is based on the use of arginase and DMO [30]. Urea, the product of enzymatic digestion of Arg by arginase, reacts with DMO and forms a yellow product determined photometrically or fluorometrically [31]. Arginase preparation isolated from yeast cells (see Section 2.2) with a specific activity 600 U mg^{-1} of protein was used for enzymatic assay of Arg.

Measurements were carried out on Shimadzu UV1650 PC spectrophotometer (Japan) and Quantech digital filter fluorometer (Thermo Scientific, United States) with filters for fluorescence excitation (λ = 360 nm) and emission detection (λ = 535 nm).

2.7. Real samples

The samples of "Chardonnay" (Ferro di Passione, Italia), "Moution Cadet" (Baron Philippe de Rothschild, France), "Bastardo" (Massandra, Ukraine) wines and "Sadochok" (LtD Sandora, Ukraine) juice were used for analysis by different methods. All samples were diluted step-wise by PB: for biosensor, chemical and enzymatic methods, dilution factors are 5 and 10, 125 and 400, 50 and 100, respectively.

The analytical results were statistically processed using the OriginPro 8.5 software.

3. Results and discussion

3.1. Development of biosensor

The general principle of Arg detection by the bi-enzyme (arginase and urease) electrode was previously suggested by us and based on NH_4^+ ions sensing [27].

In our previous work [32], different types of materials (polypyrrole, PANi, and copper(I) oxide) were used as ammonium-chemosensing elements. The first polymers give higher signals, but PANi is well adapted to pH-optimum of the coupled enzymes [27].

The first stage of biorecognition is enzymatic conversion of Arg to L-ornithine and urea. The second one is a urease-dependent hydrolysis of urea to NH_4^+ and HCO_3^-. The resulting NH_4^+ ions diffuse to the PANi-Nafion film and trigger the reduction of PANi on the Pt electrode, generating an amperometric response [27]. In current paper to construct the Arg-selective amperometric biosensor we use the recombinant yeast cells overproducing arginase. The scheme of electron transfer between the biolayer and the electrode surface is shown in Fig. 1.

Arginase (EC 3.5.3.1; L-arginine amidine hydrolase) is not an oxidoreductase, but hydrolase [33] and none of the products being formed in the first reaction are electroactive. The analytical signal is created due to the enzymatic conversion of urea to ammonium ions, usually detectable by the classical potentiometric sensors. In current work, electroactive PANi is used as a mediator of electron transfer, as well as a matrix for biological element immobilization. The main reason for choice of PANi is its wide conductivity range and the simplicity of aniline transformation into a film [27].

For construction of ammonium sensitive electrode, covering of Pt electrode with Nafion was previously proposed. The cation-exchanged sulfonate groups of immobilized Nafion serve as a compensator of a positive charge generated during the doping dependent anodic polymerization of PANi [34,35].

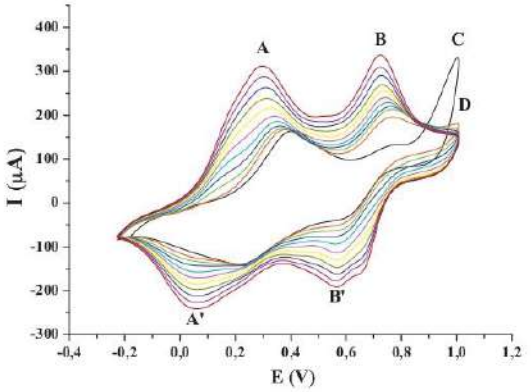

Fig. 2. Cyclic voltammogram of the PANi-Nafion film formation on Pt electrode, 11 cycles of electodeposition with a scan rate 50 mV s^{-1} *vs* Ag/AgCl.

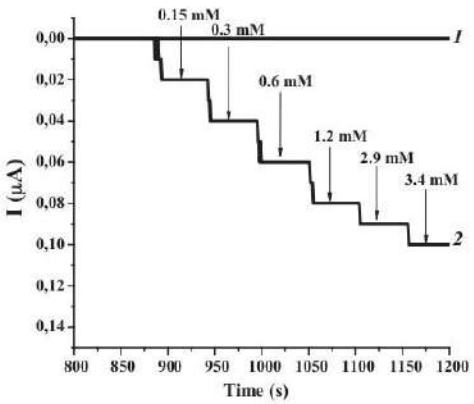

Fig. 3. Chronoamperometric current responses on Arg of the developed bioelectrodes with native (1) and permeabilized (2) cells (−200 mV *vs* Ag/AgCl).

Doping is a reversible process that could be carried out chemically or electrochemically with the oxidation or reduction by accepting or donating the electrons, respectively, and thus, results in the positive or negative charges. Doping is the unique, central, underlying and unifying concept, which distinguishes PANi as conducting polymer from other insulating polymers. The controlled addition of sulfate acid results in the dramatic changes in the electronic, electrical, magnetic, optical and structural properties of PANi. The doping of PANi generates high conductivity primarily by increasing the carrier concentrations and leads to the conjugational defect like solitons, polarons, bipolarons in the polymer chain [36].

The profiles of cyclic voltammograms obtained during PANi film formation on the surface of Nafion/Pt electrode (Fig. 2) are similar to the previously described [27]. At the first scanning cycle (peak C) both processes, oxidation and condensation of aniline molecule, take place. At the initial stage of the oxidation at the potential +0.22 V, the cation-radical $C_6H_5NH_2^{\bullet+}$ (polaron) forms and provides the maximum current signal (peak A). In the acid medium, a quinoidal isomeric transformation of the cation-radical results in the resonance structures formation. After arising, these molecules cooperate as the "head-to-tail" configuration and form a dimeric intermediate product, *p*-aminodyphenylaniline. The latter can be oxidized faster than aniline and produces the cation-radical which transformed at +0.75 V to a quinoidal bi-cation-radical, bipolaron (peak B). Further processes – deprotonization and oxidation of the bipolaron, followed by polymerization and the increase of its length – occur rapidly. As result of reaction of emeraldine base with the acid, green emeraldine salt is formed (peaks D at −0.1 V and −0.2 V). The cathodic current peaks follow from further electrochemical processes: reduction of the bi-polaron (peak B'), destruction of the PANi, and the polaron (peak A') formation.

Chronoamperometric current responses for the electrodes based on native and permeabilized cells (n-cells and p-cells), co-immobilized with urease on the surfaces of PANi-Nafion-modified Pt electrodes are presented in Fig. 3. No effect on Arg addition was demonstrated with n-cells, thus, to evaluate a prototype of microbial Arg biosensor, p-cells were used.

3.2. Bioanalytical characteristics of biosensor

The calibration graphs for the biosensor performed by the stepwise addition of a standard analyte solution are shown in Fig. 4. An amperometric response of the bioelectrode was tested in the range from 0.15 to 3.4 mM Arg. The dynamic range was linear till 0.6 mM Arg. The K_M^{app} derived from the calibration graph was

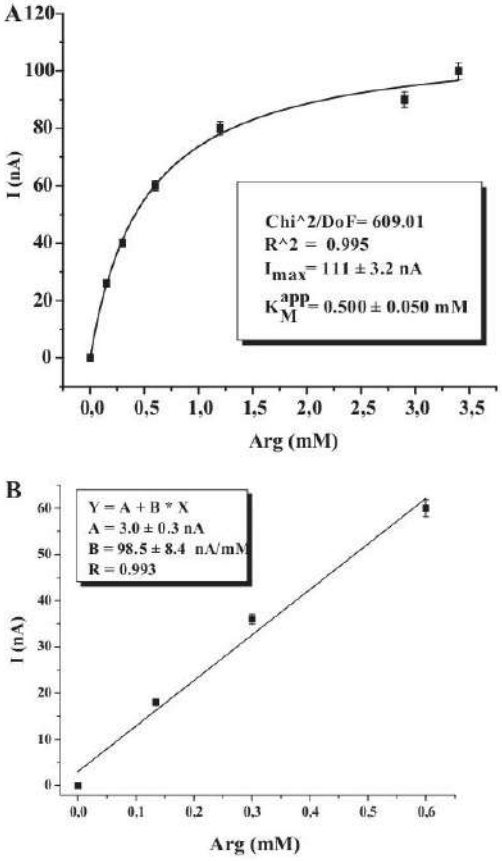

Fig. 4. Calibration graphs (A and B) for amperometric response on Arg of the developed biosensor (−200 mV *vs* Ag/AgCl).

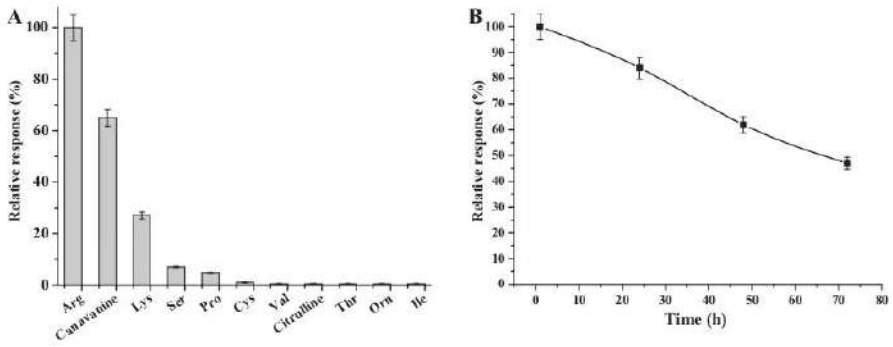

Fig. 5. Characteristics of the microbial biosensor: (A) selectivity; response to 0.15 mM L-amino acid in 30 mM phosphate buffer, pH 7.5 (PB); (B) storage stability at the +4 °C in PB.

shown to be 0.51 ± 0.05 mM for Arg. The sensitivity was calculated as 14 ± 1.2 A(M m^2)$^{-1}$, a limit of detection is 0.085 mM and a response time is 60 s. Bioanalytical parameters of the novel bioelectrode compared with the earlier elaborated by us sensors are presented in Table 1.

For application of the Arg biosensor in analyses of real samples, selectivity and storage stability are of great importance. The selectivity of the constructed biosensor to some amino acids was estimated in relative units (%) as a ratio to the value of the highest response (Fig. 5A). Stability of the bioelectrode was explored by monitoring of its current response to 0.25 mM Arg during 3 days. The activity of the biosensor decreased by 20% for 24 h and the sensor's half-life is about 72 h (Fig. 5B).

As shown in Fig. 5, essential analytical signals to L-Lys (27 ± 1.1%) and canavanine (65 ± 1.4%) were detected. Canavanine (Can) is the substrate of arginase, but possible impact of Can on Arg assay in wines is negligible, because Can as a natural insecticide presents exclusively in seeds of certain plants [7,37].

Therefore, p-cells of the recombinant yeast *H. polymorpha*, overproducing arginase, can be successfully used for development of microbial amperometric Arg-selective biosensor. The proposed biosensor has some advantages over the conventional biosensors:

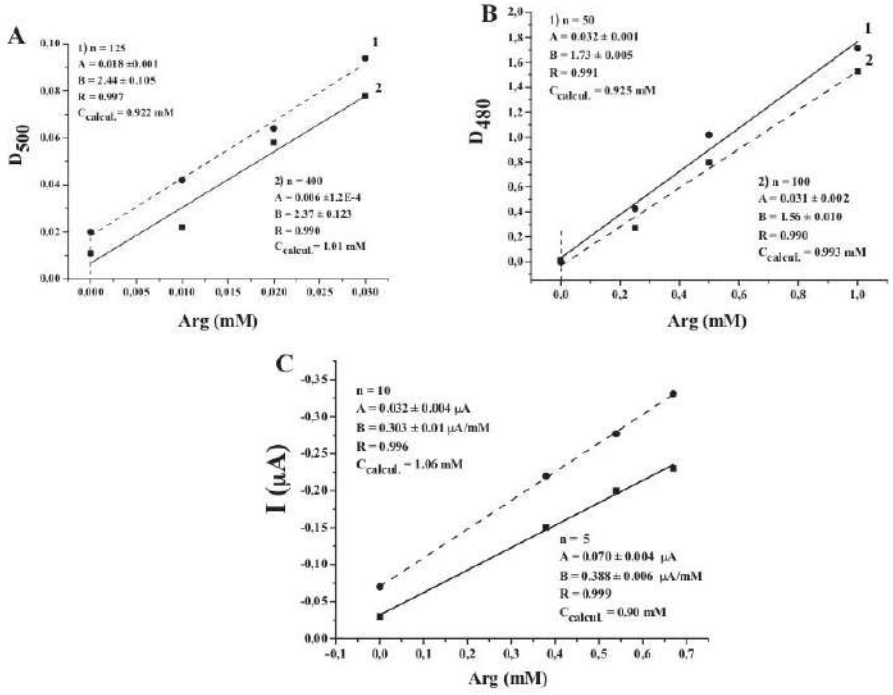

Fig. 6. Arg analyses in "Chardonnay" wine by different methods: (A) reference chemical, (B) photometric, (C) biosensor. Statistical data: parameters of linear regression (coefficients of the equation $Y = A + BX$, where $Y = I$ (μA), X = Arg concentration in tested sample (mM), A = OD of variant without addition of exogenous analyte, and B = slope value); R – linear regression coefficient; n – dilution factor; C_{calcul} – calculated Arg concentration in wine, mM.

Table 2
Concentration of Arg (C_{Arg}) in food samples determined by different analytical methods, mM.

Sample	Method							
	Biosensor [This paper]		Arginase-based enzymatic [30]				Chemical [29]	
			fluorimetric		photometric			
	C_{Arg}	CV (%)	C_{Arg}	CV (%)	C_{Arg}	CV (%)	C_{Arg}	CV (%)
Wine "Chardonnay"	0.98 ± 0.11 $p > 0.05$	11.2	1.05 ± 0.04	3.75	0.96 ± 0.05 $p > 0.05$	4.80	0.97 ± 0.06 $p > 0.05$	6.43
Wine "Moution Cadet"	1.96 ± 0.05 $p > 0.05$	0.51	1.97 ± 0.01	1.01	1.96 ± 0.05 $p > 0.05$	2.01	1.95 ± 0.04 $p > 0.05$	1.54
Wine "Bastardo"	2.46 ± 0.06 $p > 0.05$	1.22	2.55 ± 0.04	1.20	2.36 ± 0.06 $p > 0.05$	1.70	ND	ND
Juice "Sadochok"	ND	ND	2.06 ± 0.04	2.43	1.99 ± 0.03 $p > 0.05$	2.01	2.21 ± 0.08 $p > 0.05$	2.26

CV—coefficient of variation; ND—not determined.
Student's test (p) was performed for values obtained by biosensor method compared to fluorimetric one [30].

it is cost-effective (cells are cheap and easy in preparation), sensitive, easy-to-use and reliable. When compared with response time for other reported biosensors (1–12 min) [9–11,22–24], the developed biosensor is sufficiently fast (60 s). In comparison with earlier proposed arginase-based sensors (Table 1), preparation of the bioelectrode does not require the costly and time-consuming procedure of arginase purification.

3.3. Assay of Arg in real samples

The developed biosensor was tested on the samples of wine and juice. To evaluate the possible interference effect of wines components on results of Arg estimation, a standard addition test was applied to the diluted tested samples. The results of Arg assay in the real samples were compared with the Arg contents estimated by other methods (Figs. 6 and 7, Table 2). The values obtained for the "Chardonnay" white dry wine by biosensor and other methods demonstrated strong correlation (Fig. 6). The calibration plot proves, that the interfering effect of real sample components was observed for all methods, although in different extents. It is worthwhile mentioning, that urea content in "Chardonnay" estimated by photometric method, is less than 0.05 mM. Thus, the impact of urea in Arg concentration in white wine is about 5%.

The reproducibility of the proposed biosensor method (Table 2) is satisfactory (CV ranges are from 3.75 to 11.2%), and Arg contents estimated in the samples of wine and juice proved to be similar

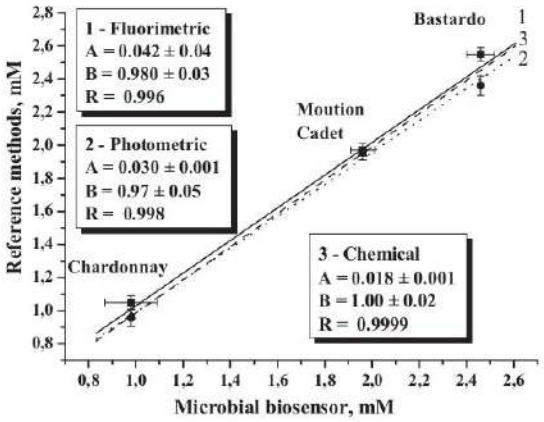

Fig. 7. Correlations between the results of Arg estimation in wines by different methods, relatively to biosensor: 1—fluorimetric, 2—photometric, 3—chemical.

to those reported by other authors (0–9.5 mM) [15–19,29,38–41]. A strong correlation (R ranges from 0.996 to 0.9999) is shown to exist between the values obtained by the new and previously published methods [30]. According to Student's test, the analytical data of biosensor and reference fluorimetric methods are in good agreement ($p > 0.05$).

The results, presented in Figs. 6 and 7 and in Table 2, indicate that the developed biosensor can be used for a fast, valid and simple Arg assay in food industry to predict a potential risk of urethan generation in wines.

4. Conclusions

A new analytical approach to Arg assay based on the use of recombinant cells of the yeast *H. polymorpha* over-producing arginase was developed. To construct an amperometric biosensor, permeabilized yeast cells and commercial urease were co-immobilized on the surface of the polyaniline-Nafion composite platinum electrode and covered with dialyses membrane. The optimal conditions for biosensor's method were estimated and protocols of assay have been developed. The biosensor is cost effective, as a very small amount of biocomponents and reagents were used for its fabrication. The developed biosensor was tested for Arg assay in some commercial wines and juice using the multiple standard addition method. A strong correlation ($R = 0.996–0.9999$) between data obtained by the constructed biosensor and other analytical methods was observed. The proposed laboratory prototype of an Arg selective biosensor would be promising for food quality control.

Acknowledgements

This work was financially supported by NAS of Ukraine (Project 13/2014, program "Sensors for Medical, Environmental, Industrial, and Technological Needs"), by NATO (Project CBP. NUKR.SFP 984173), by Individual grants (Stasyuk) of FEMS and OPTEC company.

References

[1] A. Alonso, M.J. Almendral, M.D. Baez, M.J. Porras, C. Alonso, Enzyme immobilization on an epoxy matrix. Determination of L-arginine by flow-injection techniques, Anal. Chim. Acta 308 (1–3) (1995) 164–169.
[2] Y. Rong, H. Junru, C. Dayi, Determination of L-arginine in drug by single sweep oscillopolarography, J. Sichuan Containing Educ. Coll. Med. Sci. 12 (1999) 1219–1236.
[3] L. Zhang, Y. Liu, G. Chen, Simultaneous determination of allantoin, choline and L-arginine in Rhizoma Dioscoreae by capillary electrophoresis, J. Chromatogr. A 1043 (2) (2004) 317–321.
[4] K.-M. Chu, P.-W. Huang, Li-H. Pao, Determination of arginine, asymmetrical dimethylarginine, and symmetrical dimethylarginine in human plasma by high performance liquid chromatography, J Med. Sci. 23 (4) (2003) 201–206.

[5] J. Costin, F. Paul, S. Lewis, Selective determination of amino acids using flow injection analyses coupled with chemiluminescence detection, Anal. Chim. Acta 408 (1) (2003) 67–77.
[6] J.M. Lobenhoffer, O. Krug, S.M. Bode-Bogerh, Determination of arginine and asymmetric dimethylarginine (ADMA) in human plasma by liquid chromatography/mass spectrometry with the isotope dilution technique, J. Mass Spectrom. 39 (2004) 1287–1294.
[7] G.A. Rechnitz, R.K. Kobos, S.J. Riechel, C.R. Gebauer, A bioselective membrane electrode prepared with living bacterial cells, Anal. Chim. Acta 94 (1977) 357–365.
[8] S.R. Grobler, N. Basson, C.W. van Wyk, Bacterial electrode for L-arginine, Talanta 29 (1982) 49–51.
[9] D.P. Nikolelis, T.P. Hadjiioannou, Construction of an arginine enzyme electrode and determination of arginine in biological materials, Anal. Chim. Acta 147 (1983) 33–39.
[10] S. Karacaoglu, S. Timur, A. Telefoncu, Arginine selective biosensor based on arginase-urease immobilized in gelatin, Artif. Cells Blood Subst. Immob. Biotechnol. 31 (2003) 357–363.
[11] R. Koncki, I. Walcerz, F. Ruckruh, S. Glab, Bienzymatic potentiometric electrodes for creatine and L-arginine determination, Artif. Cells Blood Subst. Immob. Biotechnol. 333 (1996) 215–222.
[12] S.W. Brusilow, A.L. Horwich, C.R. Scriver, The Metabolic and Molecular Bases of Inherited Disease, eighth ed., McGraw-Hill, New York, NY, 2001, pp. 1909–1963.
[13] S. Kotamtaju, C.L. Williams, B. Kalyanaraman, Statin-induced breast cancer cell death: role of inducible nitric oxide and arginase dependent pathways, Cancer Res. 67 (15) (2007) 7386–7394.
[14] B. Vynnytska-Myronovska, Y. Bobak, Y. Garbe, C. Dittfeld, O. Stasyk, K.-L.A. Schughart, Single amino acid arginine starvation efficiently sensitizes cancer cells to canavanine treatment and irradiation, Int. J. Cancer 130 (9) (2012) 2164–2175.
[15] C.A. Uthurry, J.A.S. Lepe, J. Lombardero, G.J.R. Del Hierro, Ethyl carbamate production by selected yeasts and lactic acid bacteria in red wine, Food Chem. 94 (2006) 262–270.
[16] S.E. Spayd, R.L. Wample, R.G. Evans, R.G. Stevens, B.J. Seymour, C.W. Nagel, Nitrogen fertilization of white riesling grapes in Washington. Must and wine composition, Am. J. Enol. Vitic. 45 (1994) 34–42.
[17] R. Mira de Orduña, S.Q. Liu, M.L. Patchett, G.J. Pilone, Ethyl carbamate precursor citrulline formation from arginine degradation by malolactic wine lactic acid bacteria, FEMS Microbiol. Lett. 183 (2000) 31–35.
[18] C.S. Ough, D. Stevens, J. Almy, Preliminary comments on effects of grape vineyard nitrogen fertilization on the subsequent ethyl carbamate formation in wines, Am. J. Enol. Vitic. 40 (1989) 219–220.
[19] Z. Huang, C.S. Ough, Effect of vineyard locations, varieties and rootstocks on the juice amino acid composition of several cultivars, Am. J. Enol. Vitic. 40 (1989) 135–139.
[20] P. Sarkar, I. Tothill, S.J. Setford, A.P.F. Turner, Screen-printed amperometric biosensors for the rapid measurement of L- and D-amino acids, Analyst 124 (1999) 865–870.
[21] R. Domínguez, B. Serra, A.J. Reviejo, J.M. Pingarrón, Chiral analysis of amino acids using electrochemical composite bienzyme biosensors, Anal. Biochem. 298 (2001) 275–282.
[22] L. Lvova, A. Legin, Y. Vlasov, G.S. Cha, H. Nam, Multicomponent analysis of Korean green tea by means of disposable all-solid-state potentiometric electronic tongue micro system, Sens. Actuators. B 95 (2003) 391–395.
[23] O.Y. Saiapina, S.V. Dzyadevych, N. Jaffrezic-Renault, O.P. Soldatkin, Development and optimization of a novel conductometric bi-enzyme biosensor for L-arginine determination, Talanta 92 (2012) 58–64.
[24] G. Kaur, Purification and characterization of arginase from Neurospora sp. for the development of arginine biosensor. (http://hdl.handle.net/10603/2897-2011-10-10).
[25] N. Stasyuk, O. Smutok, G. Gayda, Y. Koval'chuk, M. Gonchar, A new bi-enzyme potentiometric sensor for arginine analysis based on recombinant human arginase I and commercial urease, J. Mater. Sci. Eng. A 1 (2011) 819–827.
[26] M. Sheliakina, V. Arkhypova, O. Soldatkin, O. Saiapina, B. Akata, S. Dzyadevych, Urease-based ISFET biosensor for arginine determination, Talanta 121 (2014) 18–23.
[27] N. Stasyuk, O. Smutok, G. Gayda, B. Vus, M. Gonchar, Ye. Koval'chuk, Bi-enzyme L-arginine-selective amperometric biosensor based on ammonium-sensing polyaniline-modified electrode, Biosens. Bioelectron. 37 (1) (2012) 46–52.
[28] N. Stasyuk, R. Serkiz, S. Mudry, G. Gayda, A. Zakalskiy, Ye. Koval'chuk, M. Gonchar, M. Nisnevitch, Recombinant human arginase I immobilized on gold and silver nanoparticles: preparation and properties, Nanotechnol. Dev. 1 (e3) (2011) 11–15.
[29] H. Li, X. Liang, L. Feng, Y. Liu, H. Wang, A simple and fast method for arginine determination of in grape juice, J. Food Drug Anal. 16 (3) (2008) 53–58.
[30] N. Stasyuk, G. Gaida, M. Gonchar, L-Arginine assay with the use of arginase I, Appl. Biochem. Microbiol. 49 (5) (2013) 529–534.
[31] J.H. Rho, Direct fluorometric determination of urea in urine, Clin. Chem. 18 (5) (1972) 476–478.
[32] N.Ye. Stasyuk, G.Z. Gayda, M.V. Gonchar, Y. Koval'chuk, An amperometeric chemosensor for ammonium ions detection announcer of the Charkiv National University, Series Chem. 21 (44) (2012) 258–263 (In Ukrainian).
[33] M. Munder, Arginase: an emerging key player in the mammalian system, Br. J. Pharmacol. 158 (3) (2009) 638–651.
[34] T. Hirai, S. Kuwabata, H. Yoneyama, Electrochemical behaviors of polypyrrole, poly-3-methylthiophene and polyaniline deposited on Nafion-coated electrodes, J. Electrochem. Soc. 135 (5) (1988) 1132–1137.
[35] Y.C. Luo, J.S. Do, Urea biosensor based on PANi (urease)-Nafion/Au composite electrode, Biosens. Bioelectron. 20 (1) (2004) 15–23.
[36] L.A. Kosyachenko (Ed.), Solar Cells—Dye-Sensitized Devices InTech, 2011, pp. 95–130.
[37] S. Ekanayake, K. Skog, N.G. Asp, Canavanine content in sword beans (*Canavalia gladiata*): analysis and effect of processing, Food. Chem. Toxiol. 45 (5) (2007) 797–803.
[38] K.T. Austin, C.E. Butzke, Spectrophotometric assay for Arginine in grape juice and must, Am. J. Enol. Vitic. 51 (2000) 227–232.
[39] S.Q. Liu, G.G. Pritchard, M.J. Hardman, G.J. Pilone, Arginine catabolism in wine lactic acid bacteria: is it via the arginine deiminase pathway or the arginase-urease pathway? J. Appl. Bacteriol. 81 (1996) 486–492.
[40] A.P. Stines, J. Grubb, H. Gockowiak, P.A. Henschke, P.B. Høj, R. van Heeswijck, Proline and arginine accumulation in developing berries of *Vitis vinifera* L. in Australian vineyards: influence of vine cultivar, berry maturity and tissue type, Aust. J. Grape Wine Res. 6 (2) (2000) 150–158.
[41] I. Popescu-Mitroi, F. Stoica, Study of histidine degradation and assessment of histamine content in red wines during the malolactic fermentation, Chem. Bull. "Politehnica" Univ. (Timisoara) 57 (71) (2012) 38–41.

Biographies

Nataliya Stasyuk received her PhD degree in Chemical Sciences from Ivan Franko National University, Lviv, Ukraine in 2013. Nataliya is winner of the individual research grants for young scientists, namely FEMS grant (2013) and grant of OPTEC company (2014). The main scientific interests: Physical Chemistry, Nanotechnology, Organic chemistry, Biosensorics, Biotechnology.

Galina Gayda received her PhD degree in Chemical Sciences from Moscow State University (Russia) in 1983. The main scientific interests: Protein Chemistry and Analytical Biotechnology.

Mykhailo Gonchar received his PhD degree in Chemistry from Moscow State University in 1978 and habilitation degree in Biology from Institute of Biochemistry (Kiev, NAS of Ukraine) in 2001. Prof. M. Gonchar is the author of more than 345 scientific publications, including 165 full-length papers and inventions. The main scientific interests: Applied Microbiology and Biotechnology, Biochemistry, Protein Biotechnology, Enzymology, Biosensorics, Environmental Biotechnology, Nanobiotechnology.

Оригінал доступний за посиланням:
https://www.sciencedirect.com/science/article/abs/pii/S0925400514008016

РОЗДІЛ 7

СТВОРЕННЯ АМПЕРОМЕТРИЧНИХ БІО(ХЕМО)СЕНСОРІВ ТА ТЕСТ-НАБОРІВ НА ОСНОВІ МІКРОБНИХ ГІДРОЛАЗ: АРГІНІНДЕІМІНАЗИ ТА АРГІНАЗИ І ДЛЯ КІЛЬКІСНОГО АНАЛІЗУ L-АРГІНІНУ

В розділі VII представлено результати досліджень щодо розробки амперометричних біо(хемо)сенсорів на основі амоній-селективних наночастинок та мікробних гідролаз – аргініндеімінази *Mycoplasma hominis* і аргінази І людини *O. polymorpha*. З літературних джерел відомо, що амінокислота L-аргінін зазвичай присутня в харчових продуктах і біологічних рідинах, і служить корисним індикатором якості їжі і важливим біомаркером в медицині. На сьогодні розроблено різноманітні оптичні та електрохімічні методи для аналізу L-аргініну. Наявні способи є перспективними для використання в клінічних і промислових лабораторіях, однак вони мають певні обмеження, зокрема, недостатню селективність. Для підвищення селективності аналітичних методів розроблено ензиматичні підходи, зокрема, електрохімічні біосенсори. Загалом усі сконструйовані нами біосенсори на основі ензимів для визначення L-аргініну грунтуються на визначенні концентрації продуктів, утворених у ензиматичних каскадних реакціях. Серед теоретично можливих біосенсорних підходів щодо аналізу L-аргініну нами використано підходи, які ґрунтуються на ензиматичному розкладі L-аргініну з утворенням аміаку та моніторингу останнього за допомогою різних перетворювачів.

Для конструювання амперометричних біосенсорів нами синтезовано металеві нанокомпозити – «нанохелатори», здатні утворювати редокс-активні координаційні сполуки з аміаком. Оптимізовано методи іммобілізації аргініно-гідролізуючих ензимів і хелаторів на поверхні амперометричних перетворювачів. На основі аргініндеімінази та гібридних наночастинок Cu/Zn(Hg)S сконструйовано амперометричний біосенсор для кількісного визначення вмісту L-аргініну. Створений біосенсор характеризується високою селективністю та чутливістю до L-

аргініну (1570 $А \cdot М^{-1} \cdot м^{-2}$). Лінійний діапазон біосенсора спостерігається в діапазоні від 0,013 мМ до 0,8 мМ із нижньою межею визначення L-аргініну 4,3 мкМ.

Для конструювання амперометричних біосенсорів для аналізу L-аргініну запропоновано використання в ролі амоній-селективних нанохелаторів наночастинки CdCu та Cu із середнім розміром кристалітів 40 нм та 60 нм, відповідно. Виготовлено три типи лабораторних прототипів амперометричних нанобіосенсорів, що містять у біоселективному шарі аргініноксидазу (АргО), рекомбінантну аргіназу I (Арг) у поєднанні із уреазою та аргініндеіміназу (АДІ). Усі сконструйовані біоелектроди демонструють широкий лінійний діапазон (до 200 мкМ), задовільну стабільність при зберіганні (14 днів) і високу чутливість до L-аргініну: 1650, 1700 та 4500 $А \cdot М^{-1} \cdot м^{-2}$ для біосенсорів на основі АДІ, АргО та Арг/уреази, відповідно. Усі біосенсори протестовано для оцінки вмісту L-аргініну в комерційних соках. Отримані дані добре корелюють зі значеннями референтного методу.

На сьогодні, в галузі аналітичної біотехнології існує обмежена кількість даних щодо розробки ензиматичних методів визначення вмісту L-аргініну. При цьому, існуючі ензиматичні тест-системи є переважно мультиензимними із спектрофотометричним детектуванням кінцевого продукту реакції.

Нами створено два варіанти ензимо-флуоресцентного методу аналізу вмісту L-аргініну – моноензимний та двоензимний. Запропоновані методики базуються, відповідно: 1) на детекції флуоресценції продукту аргіназної реакції розкладу L-аргініну – карбаміду – при взаємодії з 2,3-бутандіонмонооксимом (ДМО); 2) на моніторингу флуоресценції аргіназно-уреазного або аргініндеіміназного продукту гідролізу L-аргініну – йонів амонію – у реакції з *орто*-фталевим альдегідом (ОФА). Показано можливість використання розроблених біоаналітичних методів для аналізу L-аргініну в реальних зразках фармацевтичних препаратів та біологічних рідин. Встановлено, що ДМО-метод володіє високою пороговою чутливістю визначення вмісту L-аргініну (0,15 мкМ), широким діапазоном лінійності – 0,28 мкМ–0,2 мМ, а також високою специфічністю, тоді як ОФА-методу властива дещо вища порогова чутливість визначення L-аргініну (0,25

мкМ), а також широкий діапазон лінійності 0,35 мкМ – 24 мкМ. Усі розроблені ензиматичні методи аналізу L-аргініну на основі аргінази I/уреази апробовано на реальних зразках вин, сироваток крові, фармацевтичних препаратів. Встановлено високий рівень кореляції між ензиматичними та біосенсорними методами у порівнянні із референтними методами (R = 0,998).

Можливість використання апоензиму $(His)_6$–тегованої форми рекомбінантної аргінази I людини при конструюванні амперометричих біосенсорів досліджувалась із використанням системи детекції йонів амонію на нафіон-поліанілінових мембранах. Проведені дослідження підтверджують можливість використання апоензиму рекомбінантної аргінази I для конструювання біосенсорів для аналізу йонів Mn^{2+} з чутливістю сенсора 9200 $А \cdot М^{-1} \cdot м^{-2}$. Створено також ензиматично-флуориметричний метод для аналізу іонів деяких біометалів, зокрема, Mn^{2+} та Co^{2+} за використання апоензиму $(His)_6$–тегованої форми рекомбінантної аргінази I людини. Діапазон лінійності флуорометричного методу з використанням апо-аргінази ДМО у випадку аналізу Mn^{2+} становить від 4 пМ до 1,10 мкМ з межею виявлення і 1 пМ Mn^{2+} (1 фмоль/мл), тоді як діапазон лінійності цього методу у випадку аналізу йонів Co^{2+} становить від 8 пМ до 45 мкМ з межею виявлення 2,5 пМ Co^{2+} (2,5 фмоль/мл). Розроблений метод апробовано для аналізу йонів Mn^{2+} та Co^{2+} у зразках стічних вод із шахт добування золота та міді. Встановлено високий рівень кореляції між ензиматичним та референтним методом – атомно-абсорбційною спектрометрією (R = 0,998). Таким чином, створений ензиматично-хімічний метод, будучи високочутливим, селективним, надійним і недорогим, може бути корисним для моніторингу вмісту Mn^{2+} і Co^{2+} у клінічних лабораторіях, харчовій промисловості та службах екологічного контролю.

7.1. Створення амперометричних біосенсорів для аналізу L-аргініну за використання амоній-селективних наночастинок Cu/Zn(Hg)S та рекомбінантних деіміназ

Анотація: *Існують обмежені дані щодо амперометричних біосенсорів (АБС) на основі деіміназ, в ході реакцій яких утворюється амоній як побічний продукт ензиматичної реакції. На сьогодні, в літературі описано біосенсори, які грунтуються на потенціометричних перетворювачах, що містять щонайменше два ензими в біоселективному шарі, однак така архітектура значно ускладнює процедуру і збільшує вартість аналізу. У нашому дослідженні повідомляється про конструювання АБС для прямого визначення вмісту креатиніну (Крн) і L-аргініну (L-Arg), які базуються на рекомбінантних бактерійних ензимах – креатиніндеіміназі (КДІ) і аргініндеіміназі (АДІ). Для вибору найкращого хемосенсора на йони амонію нами синтезовано низку наночастинок (НЧ) та охарактеризовано їхні електрохімічні властивості за допомогою циклічної вольтамперометрії. Нами синтезовано НЧ Cu/Zn(Hg)S, що виявляють хорошу селективність і надзвичайно високу чутливість до йонів амонію (5660 $А \cdot М^{-1} \cdot м^{-2}$ при +170 мВ і 1870 $А \cdot М^{-1} \cdot м^{-2}$ при –300 мВ, відповідно). Запропоновані біосенсори виявляють достатню чутливість (2660 $А \cdot М^{-1} \cdot м^{-2}$ до Крн для КДІ-АБС; 1570 $А \cdot М^{-1} \cdot м^{-2}$ до L-Arg для АДІ-АБС), широкі лінійні діапазони, низькі межі виявлення, задовільну стабільність при зберіганні та високу селективність до цільових субстратів. Усі сконструйовані АБС протестовано на реальних зразках біологічних рідин і соків для визначення Крн і L-Arg, відповідно. Показано продемонстровані високі кореляції отриманих результатів з референтними методами для вмісту цільових аналітів.*

Talanta 238 (2022) 122996

Contents lists available at ScienceDirect

Talanta

journal homepage: www.elsevier.com/locate/talanta

Amperometric biosensors for L-arginine and creatinine assay based on recombinant deiminases and ammonium-sensitive Cu/Zn(Hg)S nanoparticles

N. Ye Stasyuk [a,*], G.Z. Gayda [a], A.E. Zakalskiy [a], L.R. Fayura [a], O.M. Zakalska [a], A.A. Sibirny [a,b], M. Nisnevitch [c], M.V. Gonchar [a]

[a] Institute of Cell Biology, National Academy of Science of Ukraine, Drahomanov Street 14/16, 79005, Lviv, Ukraine
[b] Department of Biotechnology and Microbiology, Rzeszow University, Cwiklinskiej 2, 35-601, Rzeszow, Poland
[c] Department of Chemical Engineering, Ariel University, Kyriat-ha-Mada, Ariel, 4070000, Israel

ARTICLE INFO

Keywords:
Amperometric biosensor
Creatinine
L-arginine
Cu/Zn(Hg)S nanoparticles
Creatinine deiminase
Arginine deiminase

ABSTRACT

There are limited data on amperometric biosensors (ABSs) based on deiminases that produce ammonium as a byproduct of enzymatic reaction. The most frequently proposed biosensors utilizing such a mode are based on potentiometric transducers, which contain at least two enzymes in the bioselective layer; this complicates the procedure and increases the cost of analysis. Thus, the construction of a one-enzyme ABS is a practical problem. In our manuscript ABSs for the direct measurement of creatinine (Crn) and L-arginine (Arg), based on the recombinant bacterial creatinine deiminase (CDI) and arginine deiminase (ADI), are described. To choose the best chemosensor on ammonium ions, a number of nanoparticles (NPs) were synthesized and characterized using cyclic voltammetry. Hybrid Cu/Zn(Hg)S-NPs, having a good selectivity and an extremely high sensitivities towards ammonium ions (5660 A M^{-1} m^{-2} at +170 mV and 1870 A M^{-1} m^{-2} at −300 mV, respectively), was selected for the development of deiminase-based ABSs. The novel biosensors exhibited very high sensitivities (2660 A M^{-1} m^{-2} to Crn for CDI-ABS; 1570 A M^{-1} m^{-2} to Arg for ADI-ABS), broad linear ranges, low limits of detection, satisfactory storage stabilities and good selectivities towards natural substrates. The constructed CDI-ABS and ADI-ABS were tested on real samples of biological fluids and juices for Crn and Arg assay, respectively. High correlations of the obtained results with the reference methods were demonstrated for the target analytes.

1. Introduction

Creatinine (Crn) and L-arginine (Arg) in biological liquids are important biomarkers in clinical diagnostics and nutritional status assessment [1,2]. Also, the Arg level is an important indicator of food and food supplement quality [3,4]. A variety of optic and electrochemical procedures for Crn and Arg determination have been developed to date [4–9]. Classic optic methods for Crn and Arg analysis, based on colorimetry, were first proposed by Jaffe and Sacaguchi, respectively [10,11]. Although simple and quick, the optic methods (colorimetry, luminescence, fluorescence, surface plasmon resonance, surface enhanced Raman scattering, and others) suffer from serious interference from some organic compounds that co-exist in the biological samples [6, 12–19]. Other traditional and modern methods for Crn and Arg analysis are based on ion-exchange chromatography, spectrophotometry, capillary electrophoresis, gas chromatography, and high-performance liquid chromatography [5,20,21]. All these techniques are promising for use in clinical and industrial laboratories, but they have some limitations, particularly insufficient selectivity. To improve the selectivity of analytical methods, enzymatic approaches have been developed, including optical and electrochemical biosensors [4–6].

Biosensor systems have many advantages over other techniques when investigating analytes of interest in clinical and industrial laboratories. In general, enzyme-based biosensors for Crn and Arg determination rely on the measurement of reactants consumed or products generated from enzymatic cascade reactions [22–24].

The main limitations of biosensors in general are their low operation and storage stabilities, complicated immobilization procedure, and high cost. To overcome these problems, many efforts in recent years have been devoted to the development of Crn- and Arg-sensitive sensors

* Corresponding author.
E-mail addresses: stasuk_natalia@ukr.net, stasukne@nas.gov.ua (N.Y. Stasyuk).

https://doi.org/10.1016/j.talanta.2021.122996
Received 2 September 2021; Received in revised form 11 October 2021; Accepted 21 October 2021
Available online 22 October 2021
0039-9140/© 2021 Elsevier B.V. All rights reserved.

without using enzymes [12–18]. This approach is based on functional materials, including metalo-organic polymers and nanoparticles of different compositions, which function as enzyme mimetics [14,25]. The modes of detection used to determine Crn and Arg have included electrochemistry [7,9,12,16], colorimetry [9,17], fluorescence [13], luminescence [15] and Raman spectroscopy [26]. However, the reported non-enzymatic approaches, being very sensitive, have shown insufficient selectivity towards the target analytes. Thus, although enzyme-based biosensors have some weak points, they are still more selective and valid when compared with non-enzymatic methods [6,27,28].

The highly selective enzymes involved in Arg and Crn metabolism, including recombinant ones, are the promising tools for biosensor construction. For Arg analysis, arginine decarboxylase, arginase with urease [27–30], arginine oxidase [28,31], and arginine deiminase (ADI) may be utilized [27,28,32–34]. For assay of Crn, creatinine deiminase (CDI) or multienzyme complexes are usually employed [5,6,22,35–38]. The necessity of several enzymes in the bioselective layer complicates the process of biosensor fabrication, increases the cost of analysis, and causes losses in bioelectrode stability and sensitivity. Thus, using only one enzyme may be a more promising way for the fabrication of biosensors.

The deiminases CDI (EC 3.5.4.21) and ADI (EC 3.5.3.6) belong to the family of hydrolases, those acting on carbon-nitrogen bonds other than peptide bonds. CDI and ADI catalyze the reactions of Crn and Arg hydrolysis, respectively (Equations (1) and (2)):

$$\text{Creatinine} + H_2O = N - \text{methylhydantoin} + NH_3 \quad (1)$$

$$L - \text{arginine} + H_2O = \text{Citrulline} + NH_3 \quad (2)$$

In deiminase-catalyzed reactions, the Crn and Arg analytes both produce ammonia/ammonium (NH_3/NH_4^+), which can be monitored using electrochemical biosensors [39–46]. There are many reports concerning potentiometric sensors based on ion-selective electrodes (ISE) for the detection of ammonia/ammonium [42–44], and deiminase-urease-coupled NH_4^+-ISE for the detection of Arg [28,29,33] and Crn [38,41–46]. Although very popular, the potentiometric technique suffers from several weaknesses: namely, the dependence of a membrane potential on the ionic strength of the solution, instability of the potential during a series of assays, the complexity of a multi-enzyme system's construction, and others.

Amperometric sensors are more promising for NH_4^+ analysis due to their higher sensitivity and selectivity, as well as the quickness of the analytic procedure [39,41]. The most studied amperometric (bio)electrodes are based on NH_4^+-sensitive polymers such as polyaniline (PANi) [28–32,47–49], oxides of transition metals [50] and sulfur-containing metal-based nanoparticles [51,52]. Advanced processable catalyst-free NH_4^+ sensors were proposed based on PANi, coupled with Nafion [5–7,29–32,38], with Nafion and copper oxide [48,49] and other composites [47].

Recently, metal sulfide nanomaterials and quantum dots have become very popular in biosensorics and medicine [51,52]. Being similar to graphene and other 2D materials, sulfides of transition metals have typical sandwich-like structures, providing abundant active sites for immobilization of biomolecules, including enzymes. Sulfides of transitional metals may be promising materials for biosensor fabrication due to their excellent properties, such as large active surface areas, high catalytic activity and conductivity, as well as the suitable bandgaps [51].

To date, there is limited data on mono-enzyme deiminase-containing amperometric biosensors (ABSs), which are designed for monitoring ammonium ions as an analytical product of enzymatic reaction. Additionally, a simple construction of stable ABSs based on one deiminase, co-immobilized with NH_4-sensitive nanoparticles in a bioselective layer, remains a real problem.

In the current manuscript, we report the development and application of CDI- and ADI-based ABSs for the direct measurement of Crn and Arg, respectively. The fabricated ABSs contain highly purified recombinant bacterial CDI or ADI, co-immobilized with ammonium-sensitive Cu/Zn(Hg)S nanoparticles on the surfaces of graphite electrodes. Enzymes in CDI and ADI catalyze the hydrolysis of Crn and Arg, respectively, releasing ammonium ions. The generated ions react with nanoparticles, according to a doping/de-doping mechanism, and produce an amperometric signal. The novelty of our work is the following: novel metal sulfide nanoparicles were used for the first time for amperometric ammonium determination and as ammonium-sensitive platform in new highly sensitive and selective enzyme biosensors for creatinine and arginine analysis.

2. Materials and methods

2.1. Reagents

The following were purchased from Sigma-Aldrich: Zinc sulfate heptahydrate ($ZnSO_4{\cdot}7H_2O$), mercury chloride ($HgCl_2$), copper (II) sulfate pentahydrate ($CuSO_4{\cdot}5H_2O$), sodium sulfide (Na_2S), sodium chloride (NaCl), cytidine 5′-monophosphate (CMP) ≥99%, cytidine (Cyd) ≥99%, cytidine 5′-triphosphate sodium salt (CTP) ≥99%, cytosine (Cyt) ≥99%, cytidine 5′-diphosphate sodium salt (CDP) ≥97%, creatinine (Crn), ammonia chloride (NH_4Cl), 2,3-butanedione monoxime (DMO), ethylenediaminetetraacetic acid (EDTA), 1% Nafion, L-arginine monohydrochloride (Arg), L-canavanine (Can), trichloroacetic acid (TCA) and inorganic salts. Standard human serum "Contronorm" (SHS) was purchased from Analyticon Biotechnologies (Germany). All buffers and standard solutions were prepared using water purified by the Milli-Q system (Millipore).

2.2. Apparatus

A three-electrode system was used for the electrodeposition of Cu/Zn(Hg)S NPs and construction of the amperometric biosensor. A piece of Pt wire and an Ag/AgCl/3 M KCl electrode were used as the counter and reference electrodes, respectively. A graphite-rod electrode (ALS Co., Tokyo, Japan) was applied as a working electrode (3.05 mm diameter).

Amperometric measurements were carried out with a CHI 1200A potentiostat (IJ Cambria Scientific, Burry Port, UK) and performed in batch mode under continuous stirring in a standard 40 mL cell at room temperature. A scanning electron microscope (SEM) microanalyser (REMMA-102-02, Lviv, Ukraine) and an atomic force microscope (AFM) microanalyser (Solver P47-PRO, NT-MDT, Netherlands) were used for morphological analyses of the Cu/Zn(Hg)S NPs on the surface of a graphite electrode (GE).

2.3. Isolation and purification of recombinant deiminases from the recombinant bacterial cells

Recombinant CDI and ADI were isolated from the inclusion bodies of the corresponding genetically engineered bacterial over-producers and were then purified by column chromatography as described in our previous papers [53,54].

CDI was isolated from the cells of *Escherichia coli* BL21 (DE3)/pET32a-codA carrying the plasmid harboring $(His)_6$-tagged *codA* gene-encoding CDI of *Corynebacterium glutamicum*. A highly purified $(His)_6$-tagged CDI with the specific enzyme activity of 20 U/mg of protein was obtained using metal-affinity chromatography on Ni-NTA Superflow beads (Qiagen). The yield of the CDI was 30 mg/L of culture. One unit (U) of activity was defined as the amount of enzyme that converted 1 μmol creatinine to creatine per min at 37 °C. When lyophilized in the presence of trehalose, the CDI did not lose its activity during 120 days of storage at −20 °C [53].

ADI was isolated from the cells of *E. coli* BL21 transformed with the plasmid pET3d-ADI. The renatured enzyme was diafiltered and purified

by column chromatography, using Q-Sepharose® and Phenyl-Sepharose® sorbents. As a result, a stable and almost homogenous enzyme preparation was obtained with a specific activity of 30 U mg^{-1} of protein. One unit (U) of activity was defined as the amount of enzyme that converted 1 μmol Arg to L-citrulline per min at 37 °C. A solution of the highly purified ADI in 1 M NaCl was concentrated, filter-sterilized and stored at 4 °C for 1 year without loss of activity [54].

2.4. Synthesis of metal-doped ZnS nanoparticles and testing their ability to react with ammonium

Metal-doped ZnS nanoparticles (Zn (Me)S NPs) were prepared by the co-precipitation method according to the following scheme: 2.5 mL of 100 mM zinc sulfate heptahydrate and 5 mL of 60 mM corresponding salt ($MnCl_2$, $CuSO_4$, $CdCl_2$, $NiSO_4$, $CoSO_4$, $HgCl_2$) were mixed at room temperature and stirred for 1 h at 37 °C. 0.1 mL of 10 mM Na_2S was added to the mixture and stirred again for 3 h at 37 °C. After the completion of the process, colored precipitates were obtained. The Zn (Me)S NPs were collected by centrifugation (6708 g; Hettich Micro-22R centrifuge). The precipitate was washed with water and stored at +4 °C before use. The air-dried Zn (Me)S NPs were studied for their morphological and electrochemical properties. The electroactivities of the synthesized NPs were studied by cyclic voltammetry under increasing concentrations of NH_4Cl. The most electroactive ammonium-sensitive NPs were chosen for further investigation.

2.5. Preparation of the Cu/Zn(Hg)S-modified graphite electrode

Before sensor preparation, the graphite electrode (GE) was polished with emery paper and a polishing cloth using decreasing particle sizes of alumina paste (Leco, Germany). The polished electrodes were rinsed with water in an ultrasonic bath.

To obtain a modified electrode, a 0.01 mL portion of Zn(Hg)S NPs (see Section 2.4) was dropped onto the GE surface and air-dried. Electrodeposition of Cu NPs onto the surface of the Zn(Hg)S-modified GE was carried out with an aqueous solution containing 12 mM $CuSO_4$ at an applied constant potential −600 mV during 400 s, and at −800 mV during 200 s. The modified electrode (Cu/Zn(Hg)S/GE) was rinsed with water and equilibrated in 50 mM phosphate buffer (PB), pH 7.5, before use.

2.6. Surface analysis of Cu/Zn(Hg)S NPs deposited on the GE

The NPs on the surface of the GE were characterized by scanning electron microscopy (SEM) and atomic force microscopy (AFM). The samples in different dilutions (2 μL) were dropped onto the surface of a silicon wafer and were dried at room temperature. The distance from the last lens of the microscope to the sample (WD) ranged from 20.6 mm to 24.6 mm. The accelerator voltage was in the range of 20 keV. The SEM and AFM were used to characterize the thickness and morphology of the Cu/Zn(Hg)S NPs on the GE.

2.7. Immobilization of the enzymes on the Cu/Zn(Hg)S-modified GE

To develop the enzyme-based electrode, a GE was modified with Cu/Zn(Hg)S (as described in Section 2.5) and air-dried. 5 μL of the enzymes solutions (ADI or CDI) were dropped onto the surface of the NPs/GE, air-dried at room temperature and then covered with 0.5% Nafion™. After drying, a strongly adhering polymer film was formed. After the immobilization of the enzymes on the surface of the NPs/GE, the constructed bioelectrodes were rinsed with 50 mM PB, pH 7.5, and stored at +4 °C until use.

2.8. Preparation of real samples for Crn and Arg assay

Commercial standard human serum "Contronorm" (Analyticon Biotechnologies AG, Germany) and blood samples from healthy donors received from a local hospital were used for the Crn assay. To prepare a serum sample, 5 mL of distilled water were added to the tubes with dry "Contronorm" serum. To obtain serum from healthy donors (Sosnivka City Hospital, Lviv region, Ukraine), a sample of venous blood was incubated for 20 min at 20 °C, and clotted fibrin was removed by centrifugation (5 min, 4000 rpm). To prepare a protein-free sample (in both cases), the serum was treated with 50% TCA to obtain a final concentration of 5%. After 30 min incubation at 0 °C, the pellet of proteins was removed by centrifugation, and the resulting supernatant was neutralized to pH 7.5 by adding 2 M sodium hydroxide. The neutralized protein-free solution, now ready for assay of Crn and ammonium, was kept at −20 °C until use.

Samples of freshly prepared juices of lime and apple, as well as commercial "Sadochok" juices (LtD Sandora, Ukraine) were used for Arg analysis. All samples were diluted stepwise by 50 mM PB, pH 7.5.

2.9. Reference methods for Crn and Arg determination

Analysis of Crn was performed by a colorimetric Jaffe method via the standard addition test (SAT) using a Shimadzu UV-1650 PC spectrophotometer (Shimadzu, Kyoto, Japan) at 495 nm relative to a Crn-free control sample [55]. Graphic SAT is a type of a quantitative analysis often used in analytical chemistry when a standard is added directly to the aliquots of the analyzed sample. The concentration of Crn in the tested samples was determined from a calibration curve.

As a reference, the enzymatic assay method for Arg was based on the use of two enzymes – commercial urease and recombinant human-liver arginase I (arginase). Urea, the product of enzymatic hydrolysis of Arg by arginase, reacts with DMO and forms a fluorescence product which can be identified at 510 nm [56].

2.10. Statistical analysis

All the experiments were carried out in triplicate trials. Analytical characteristics of the electrodes were statistically processed using OriginPro 8.5 software. The error bars represent the standard error derived from three independent measurements. Calculation of the apparent Michaelis–Menten constants (K_M^{app}) was performed automatically by this program according to the Lineweaver–Burk equation.

3. Results and discussion

3.1. Selection and characterization of the nanocomposite most sensitive to ammonium ions

To obtain the NPs most sensitive to the ammonia ions, different types of ZnS-based NPs were doped by another metal ion: Zn(Hg)S, Zn(Mn)S, Zn(Cu)S, Zn(Ni)S, Zn(Co)S, Zn(Cd)S. These NPs were synthesized by co-precipitation (see Section 2.4). The electroactivities of the NPs layered on graphite electrodes were tested by the use of cyclic voltammetry (CV). For the electrodes modified with NPs of ZnS, Zn(Hg)S and Cu/Zn(Hg)S, CV studies were performed by injections with increased aliquots of NH_4Cl (Figs. S1, S2).

Figures S1 and S2 illustrate that the Zn(Hg)S NPs were the most effective platforms for ammonium-ion detection; thus, they were used for further electrochemical investigations. It was shown that at the potential +200 mV (vs. Ag/AgCl electrode) the ZnS NPs did not display electrochemical activity towards NH_4^+ (Fig. S2a), while for the Zn(Hg)S-modified electrode, an oxidation peak was observed, which corresponds to the different degrees of oxidation of mercury (Fig. S2b).

To improve the electrochemical activity of the chemosensor membranes based on Zn(Hg)S NPs, a layer of Cu NPs was electrochemically deposited onto the GE in a potentiostatic mode (see Section 2.5). Using the chronoamperograms at oxidative working potential for the modified electorodes, namely, Zn/GE, Zn(Hg)S/GE and Cu/Zn(Hg)S/GE (data not

shown), calibration curves were plotted for NH_4Cl determination by the developed NH_4^+-sensitive electrodes (Figure S3).

The graphite electrode modified with the most effective Cu/Zn(Hg)S NPs (the Cu/Zn(Hg)S/GE) was tested in more detail at various ammonium concentrations (Fig. 1). The CV (Fig. 1a) demonstrated that a cathodic reduction peak, contributed by NH_4Cl, appeared at a potential from −300 to −100 mV (the highest at −280 mV) (vs. Ag/AgCl); and an anodic oxidation peak was observed at a potential from 0 to +200 mV (the highest at +170 mV) for the injected NH_4Cl.

The results of chronoamperometry analysis and calibration graphs at +170 mV are presented in Fig. 1b and c, respectively. The chronoamperogram and calibration curves at −300 mV are presented in Fig. 1d and e, respectively.

It is worth mentioning that no signals were detected for the other analytes under the chosen conditions. As a control, an unmodified GE was also tested, and no amperometric signals were detected with NH_4Cl additions.

In our work we studied amperometric characteristics of the Cu/Zn (Hg)S/GE as ammonium-selective sensors under the different polarization voltages. Determination of ammonium ions was carried out both at an oxidative (+170 mV) and at a reductive (−300 mV) potentials (versus Ag/AgCl).

The analytical characteristics of the developed Cu/Zn(Hg)S/GE in comparison with the known ammonium-selective amperometric electrodes, that were reported previously, are summarized in Table 1. The linear ranges, limits of detection (LOD), and sensitivities (for an electrode area of 7.30 mm^2) were calculated.

The most effective of the reported up today amperometric sensors on ammonium, with very high sensitivities, 1060 and 2500 A $M^{-1}m^{-2}$, were fabricated using PANi-coupled polystyrene-sulphonate [56] and copper-PANi nanocomposite [58], respectively. However, the main disadvantage of PANi as a micro-sized organic polymer is its insufficient stability both in storage and in its working environment. It was found that under oxidative voltage (+170 mV), the Cu/Zn(Hg)S/GE has the highest value of sensitivity (5660 A M^{-1} m^{-2}) and the lowest known limit of detection (0.02 μM).

For the oxidative determination of ammonium using Cu/Zn(Hg)S/GE (at +170 mV) in comparison to the reductive measurement (at −300 mV) the detection limit is 75-fold lower and the sensitivity is about 3-folds higher (see Table 1). In the same time, the linear range at the oxidative potential is narrower than the linear range at the reductive potential. All these facts indicate, that the reaction mechanisms for the oxidative and reductive measurement of ammonium are different.

Morphological properties of Cu/Zn(Hg)S NPs were studied using SEM-XRM and AFM. The AFM micrograph of the NPs and Gaussian distribution by size (Fig. 2 b), obtained from the average diameter of the nanocrystallites was 60 nm. The XRM images of the NPs show the characteristic peaks for Zn0, Cu0, S0 and Hg0 (Fig. 2e).

3.2. Fabrication and characterization of bioelectrodes

As the most effective chemosensor on ammonium ions, the Cu/Zn (Hg)S was used for further investigations. The Cu/Zn(Hg)S/GE, coupled with recombinant CDI or ADI, appeared to be an excellent candidate for the construction of amperometric biosensors (ABSs) for Arg and Crn.

The constructed ABSs based on ADI or CDI and ZnS(Hg)/Cu NPs were marked as ADI-ABS and CDI-ABS, respectively. The general principle of Crn and Arg detection by the bioelectrode is based on sensing NH_4^+ ions (presented in Fig. 3). At the first stage, the enzymatic hydrolysis of Crn or Arg to ammonium ions takes place under CDI or ADI catalysis. The resulting NH_4^+ ions diffuse to the Cu/Zn(Hg)S layer and trigger the oxidation of the Cu/Zn(Hg)S NPs on the GE electrode, generating an amperometric response. The scheme of electron transfer between the biolayer and the electrode surface is shown in Fig. 3.

Amperometric characteristics of the created ABSs are demonstrated in Figs. 4 and 5. Cyclic voltammograms give information about the most effective working potentials for ABSs. For the CDI-ABS (Fig. 4a) the optimal potential was chosen as +170 mV. For the ADI-ABS two peaks were observed (Fig. 5a): at −300 mV (the reductive potential), and at +170 mV (the oxidative potential).

The calibration curves for deiminase-based ABSs for Crn and Arg, as well as the corresponding chronoamperograms (inset), are shown in Figs. 4 and 5, respectively. The calibration was performed by the stepwise addition of a standard analyte solution.

A comparison of the key analytical characteristics of the developed ADI-ABS and CDI-ABS (Table 2) with the similar ABSs, that were previously described in the literature, illustrates that our ABSs possess significantly higher sensitivities and contain significantly smaller quantities of the enzymes.

To estimate the conversion level of the target analyte (Crn or Arg) in the biocatalytic layer, the response to the monitored analyte (ammonium) was tested. The yields of two reactions were calculated from the B values, presented in calibration graphs in Figs. 1 c, e and Figs. 4 c and 5 c.

So, under the chosen conditions, the yield of the conversion for CDI (Crn to ammonia) was estimated as 47.1% and for the ADI (Arg to ammonia) — 86.3%. The relatively low conversion rate for CDI can be explained by non-optimal pH and temperature conditions, as well as non-optimal potential and quantity of enzyme in biosensing film.

For application of the ABSs in analyses of real samples, selectivity and storage stability are of great importance. The results of studying the selectivity and stability of the fabricated ABSs are presented in Fig. S4. Stability of the CDI-ABS was explored by monitoring its current response to 0.05 mM Crn for 20 days. The activity of the biosensor decreased by 20% after 7 days, and the sensor's half-life was about 12 days (Fig. S4a). Storage stability of the ADI-ABS was measured by addition of 0.5 mM Arg. The half-life of this ABS was 8 days (Fig. S4b).

The selectivity of the constructed CDI-ABS towards some analytes was estimated in relative units (%) as a ratio to the value of the highest response (Fig. S4c). As shown in Fig. S4c, the CDI-ABS was very specific to Crn: the signal of structurally similar compounds was less than 10%, including cytosine. This result is very important, since many microbial deiminases have dual specificity, simultaneously exhibiting activity towards CDI and towards cytosine deaminase [57]. Therefore, the recombinant CDI immobilized on the surface of the Cu/Zn(Hg)S/GE can be successfully used for development of Crn-selective ABSs.

In the case of the ADI-ABS, only Arg and canavanine (Can) as substrates of ADI [58] gave essential analytical signals, while other amino acids (Lys, Gln, Val, Ile) generated low responses (≤10%) (Fig. S4d). It should be noted that a positive signal of ABS for Can is not essential, because of the absence of this compound in natural foods, including wines and yogurts (except those from legumes).

The mono-enzyme CDI- and ADI-based ABSs for Crn and Arg determination have some advantages over the two-enzyme, three-enzyme and four-enzyme ABSs reported earlier [5,6,28]. Our proposed ABSs are highly sensitive, stable, easy to use and cost-effective. In addition, ADI- and CDI-based ABSs are very selective towards their natural substrates Arg and Crn, respectively.

3.3. Assay of Crn and Arg in real samples

The assay of Crn in biological samples and of Arg in food is crucial, due to the presence of these metabolites in living organisms and their use in industry. In order to demonstrate the practical feasibility of the constructed ABSs, contents of Crn and Arg were tested in food and serum samples, respectively. To evaluate the impact of the wine and serum components on the results of the assay, the SAT method was applied. Algorithms of Crn and Arg calculations are described in SI.

Crn is a broadly used clinical parameter for the evaluation of renal function and muscle damage [59]. For the determination of Crn in biological fluids, the spectrophotometric method based on the Jaffe reaction is commonly used [55]. The implementation of the Jaffe

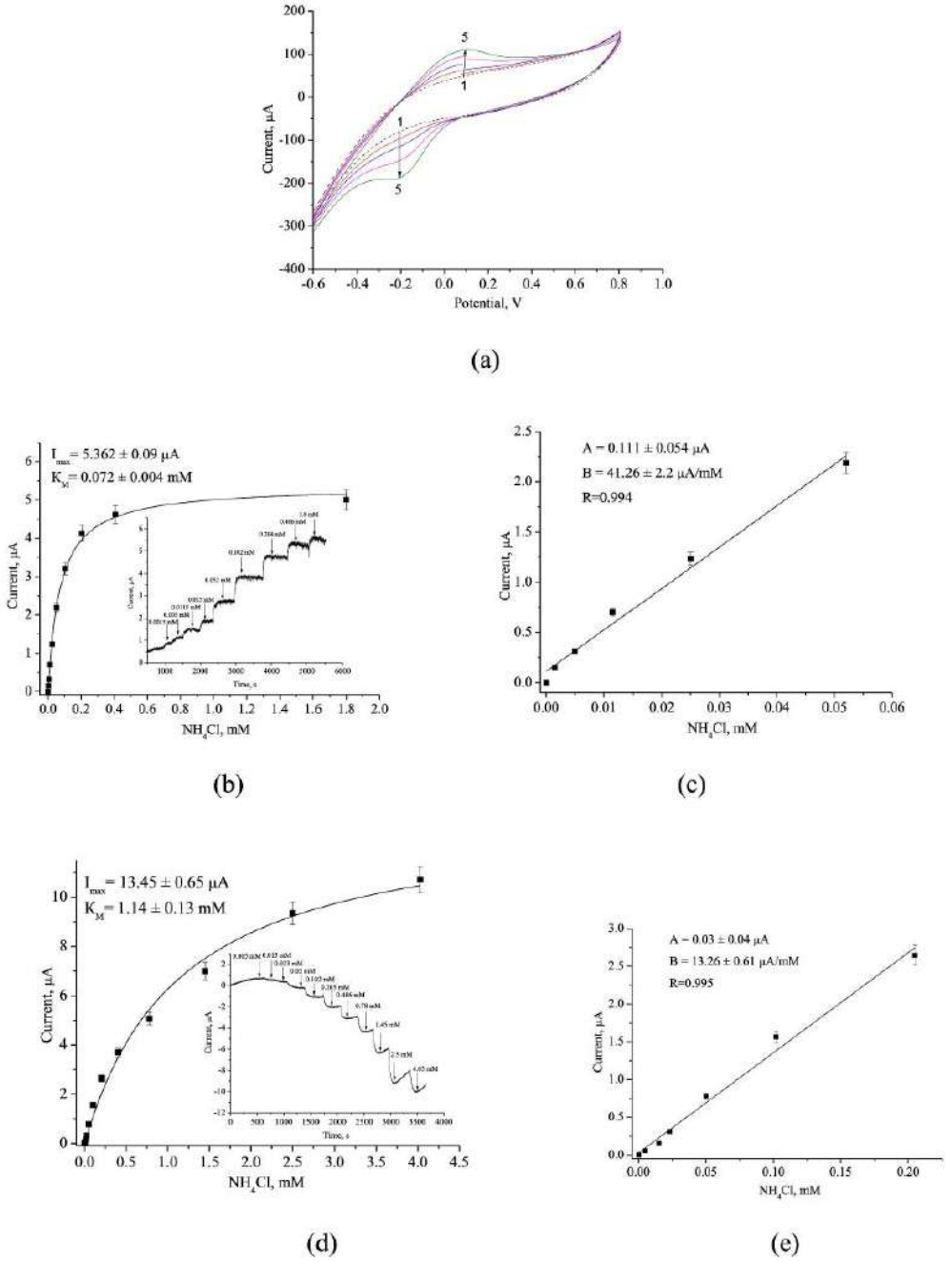

Fig. 1. Amperometric characteristics Cu/Zn(Hg)S/GE: **(a)** – Cyclic voltammograms (CV) current responses to different concentrations of NH_4Cl: (1) – 0 mM; (2) – 0.7 mM; (3) – 2.5 mM; (4) – 4.5 mM; (5) – 9.1 mM; at scan rate 50 mV s^{-1}; (b, d) – Dependences of amperometric signals on NH_4^+ concentration and chronoamperometric current responses (inserted) upon subsequent additions of NH_4Cl; (c, e) – Calibration graphs for NH_4Cl determination. Conditions: Ag/AgCl (reference electrode) in 50 mM PB, pH 7.0. Working potentials: +170 mV (b, c) and −300 mV (d, e).

Table 1
Analytical characteristics of the most effective amperometric sensors on ammonium/ammonia.

No.	Ammonium-selective film	Working potential, mV	Sensitivity, $A{\cdot}M^{-1}{\cdot}m^{-2}$	Linear range, up to μM	LOD, μM	Optimal pH	Reference
1	PANI/Pt/[a]SPE	+300	400	1000	5	10.5	[41]
		−200	4000	10	10	6.8	
2	PANI: [b]PSS/[c]GCE	−200	1060	100–11700	0.5	7.0	[47]
3	PANi/Nafion/Cu_2O/SPE	−450	2500	1000	0.5	7.4	[49]
4	Cu/Zn(Hg)S/GE	+170	5660	50	0.02	7.0	Current paper
		−300	1870	200	1.5		

[a] SPE - screen-printed electrode.
[b] PSS - nanofibrous polyaniline: polystyrene-sulphonate.
[c] GCE – glassy-carbon electrode.

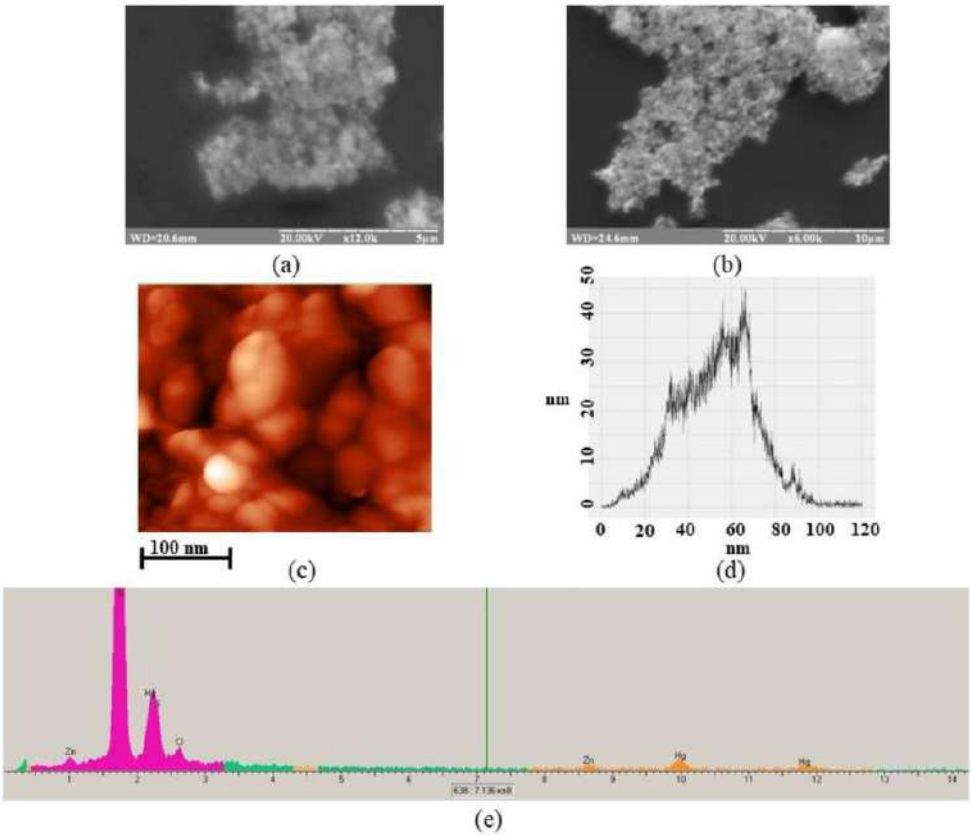

Fig. 2. Characteristics of the Cu/Zn(Hg)S NPs: (**a, b**) – SEM images; (**c**) – AFM micrograph; (**d**) – Gaussian distribution by size; (e) – X-ray spectral microanalysis.

method, however, is labor-intensive, performed mainly by complex automated analyzers in central laboratories. The ABS allows direct measurements of Crn in the sample, which promises economy of time and costs in clinical analysis by enabling on-site analysis of samples. The developed CDI-ABS was tested on real samples of human standard serum, as well as human serum pool of mixed donors. The results of the Crn assay in blood are presented in detail in SI (Calculation of Crn, Figure S5). The content of Crn, tested in the sample of standard serum with the CDI-ABS, was shown to be 101 μM. It was analyzed in comparison with the chemical picrate-based method as the reference. These values are correlated with published data (0.052–0.119 mM) for the Crn content in human serum [60].

Juices and wines usually contain ammonia and Arg [61,62]. The ADI-ABS was tested on real samples of lime and apple juices. As a result of enzymatic reaction, 1 mol Arg generates 1 mol ammonium, so the content of endogenous Arg can be calculated as the difference of the ammonia concentrations in the tested samples after enzymatic hydrolysis, measured by the CDI/Cu//Zn(Hg)S electrode and endogenous content measured by the Cu//Zn(Hg)S electrode. The results of the Arg assay in juices are presented in detail in SI (Calculation of Arg, Figure S6).

The average contents of the analytes Crn and Arg determined by the

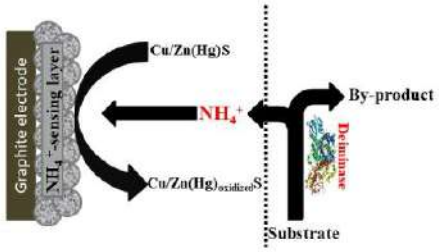

Fig. 3. Principal scheme of formation and functionality of the deiminase-based ABS. A by-product in this scheme is citrulline (from Arg) or N-methylhydantoin (from Crn).

developed ABSs and reference methods are presented in Table 3. The content of Arg was analyzed in comparison with the arginase-based enzymatic fluorometric method as the reference [56]. Differences of less than 5% between the results of both methods of Arg assay were observed. The concentrations of Arg estimated *via* two methods showed strong (R = 0.996) correlations (Fig. S7).

The results of testing the biosensor's effectiveness for Crn and Arg determination were shown to be within the permissible error limits (±10.0%). They demonstrated the possibility of application of the developed ABSs – the CDI/Cu/Zn(Hg)S/GE and the ADI/Cu/Zn(Hg)S/GE – for the analysis of Crn in blood serum and Arg in juices, respectively.

4. Conclusions

Novel amperometric creatinine and arginine biosensors based on a new hybride nanoparticles (NPs) and immobilized hydrolase enzymes (CDI and ADI) have been developed and optimised. Hg-doped ZnS NPs were synthesized *via* a co-precipitation method and tested on the surface of graphite electrodes (GE) for electroactivity and sensitivity to ammonium ions. To increase the amperometric response to ammonium ions, the obtained electrode Zn(Hg)S/GE was covered with Cu NPs by electrodeposition. It was demonstrated that the resulting modified amperometric electrode (the Cu/Zn(Hg)S/GE), as a selective and highly sensitive chemosensor for ammonium ions, may be a promising platform for the construction of deiminase-based amperometric biosensors (ABSs). Two types of novel ABSs for Crn and Arg detection were developed, based on recombinant CDI and ADI, respectively. Both ABSs exhibited high sensitivities (2660 A M^{-1} m^{-2} to Crn for CDI-ABS, and 1570 A M^{-1} m^{-2} to Arg for ADI-ABS), broad linear ranges, good storage stability and selectivity towards target analytes. The constructed ABSs were tested on real samples: the CDI-ABS – for Crn assay in human serum, the ADI-ABS – for Arg assay in juices. High correlations of the obtained results with the reference methods were demonstrated for both approaches.

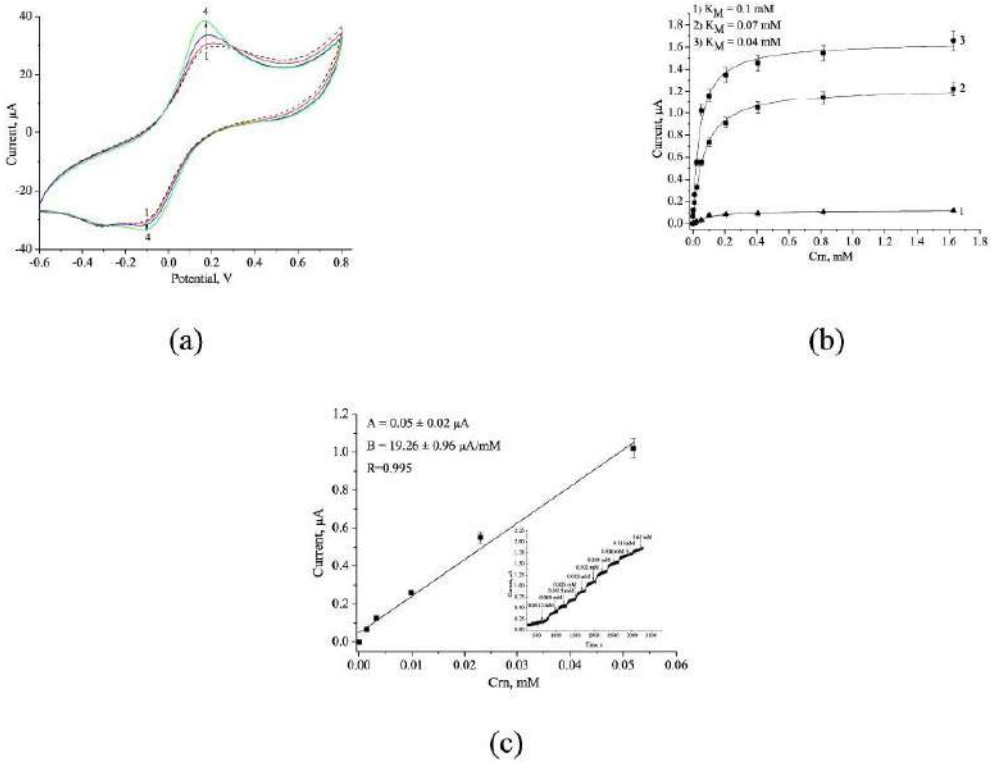

Fig. 4. Amperometric characteristics of CDI-ABSs: **(a)** – Cyclic voltammograms (CV) as current responses upon addition of Crn up to concentrations: (1) – 0 mM, (2) – 2.5 mM; (3) – 5.0 mM; (4) – 10 mM; **(b)** – dependences of amperometric signals on concentration of Crn and on activities of CDI in sensing layer of ABS (m-units): 4.2 (1), 0.42 (2) and 0.04 (3); **(c)** – calibration graph for Crn determination using CDI-ABS-3 and chronamperogram (inserted). Conditions: scan rate 50 mV s^{-1}; Ag/AgCl (reference electrode) in 50 mM PB, pH 7.0. Working potential +170 mV.

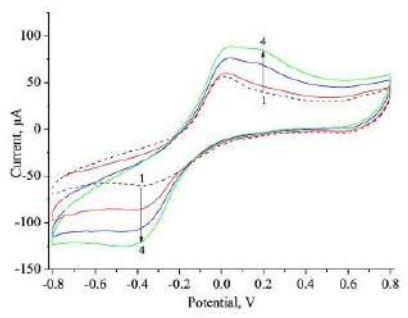

(a)

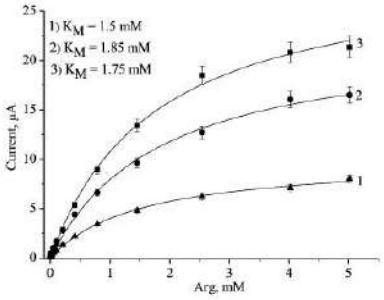

(b)

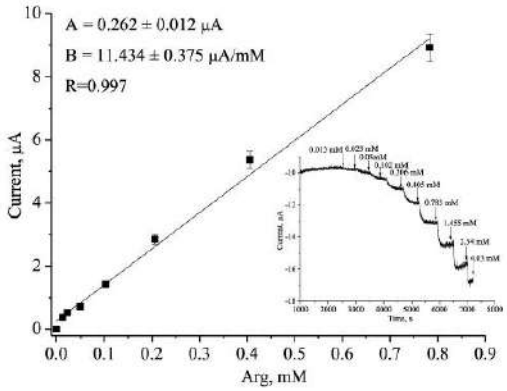

(c)

Fig. 5. Amperometric characteristics of ADI-ABSs: (a) – CV as current responses upon addition of Arg up to concentrations: (1) – 0 mM; (2) – 2.5 mM; (3) – 5.0 mM; (4) – 10 mM (b) dependences of amperometric signals on concentration of Arg and on activity of ADI in sensing layer of ABS (m-units): 1.42 (1), 0.14 (2) and 0.014 (3); (c) – calibration graph for Arg determination using ADI-ABS-3 and chronoamperogram (inset). Conditions: scan rate 50 mV s^{-1}; Ag/AgCl (reference electrode) in 50 mM PB, pH 7.0. Working potential – 300 mV.

Table 2
Analytical characteristics of different amperometric CDI- and ADI-based biosensors.

Type of ABS	Enzyme activity, m-units	Working potential, mV	Sensitivity, $A \cdot M^{-1} \cdot m^{-2}$	Linear range, μM	LOD, μM	Conversion level, %	K_M^{app}, mM	Ref.
CDI-1	4.2	+170	748	23–100	7	47.1	0.10	Current
CDI-2	0.42		1422	3.3–50	1		0.07	paper
CDI-3	0.04		2660	1.5–50	0.45	47.1	0.04	
CDI	2.5	−350	850	up to 125	0.5	83	0.163	48
ADI-1	1.42	−300	859	13–206	4.3	86.3	1.50	Current
ADI-2	0.14		1490	13–406	4.3		1.85	paper
ADI-3	0.014		1570	13–800	4.3	86.3	1.75	
ADI	2500	−350	684	3–200	1.5	–	0.31	52

*ABSs 1, 2 and 3 are presented in Figs. 4b and 5b.

Table 3
Results of determination of Arg and Cm (mM) in the real samples.

Analyte	Methods / Samples	Biosensor	Reference	Difference, %
Arg	[a]Juice lime	2.03 ± 0.04	1.96 ± 0.01	+3.5
	[a]Juice apple	3.76 ± 0.002	3.90 ± 0.014	−3.6
	Commercial juice "Sadochok", grape apple	2.16 ± 0.01	2.06 ± 0.05	+4.6
	Commercial juice "Sadochok"multifruit	2.53 ± 0.01	2.50 ± 0.02	+1.2
Cm	Standard serum "Contronorm"	0.103 ± 0.009	0.099 ± 0.008	+5.7
	Serum pool of healthy donors, n = 20	0.095 ± 0.002	0.091 ± 0.004	+4.3

[a] Freshly prepared juices.

Credit author statement

Stasyuk N. and Gayda G.Z.: Investigation, Validation, Writing - original draft, Visualization. Zakalskiy A.E., Zakalska O.M., Sibirny A.A. and Fayura L.R.: Conceptualization, Methodology, Formal analysis, Visualization, Investigation. Nisnevitch M.: Writing - original draft, Writing - review & editing. Gonchar M.V.: Conceptualization, Supervision, Writing - review & editing, Project administration, Funding acquisition, Resources.

Declaration of competing interest

The authors declare that they have no known competing financial interests or personal relationships that could have appeared to influence the work reported in this paper.

Acknowledgement

This work was partially funded by NAS of Ukraine (The program "Smart sensor devices of a new generation based on modern materials and technologies"), by National Research Foundation of Ukraine (project 2020.02/0100 "Development of new nanozymes as catalytic elements for enzymatic kits and chemo/biosensors"), by NAS of Ukraine "New dual casein kinase 2 inhibitors and histone deacetylase for targeted tumor chemotherapy" and by the Research Authority of the Ariel University, Israel.

Appendix A. Supplementary data

Supplementary data to this article can be found online at https://doi.org/10.1016/j.talanta.2021.122996.

References

[1] K. Kashoni, M.H. Rosner, M. Ostermann, Creatinine: from physiology to clinical application. Review, Eur. J. Intern. Med. 72 (2020) 9.
[2] B. Cao, R. Deng, D. Wang, L. Li, Z. Ren, L. Xu, X. Gao, Association between arginine catabolism and major depressive disorder: a protocol for the systematic review and meta-analysis of metabolic pathway, Medicine (Baltim.) 99 (27) (2020), e21068.
[3] R. Mira de Orduña, S. Liu, M.L. Patchett, G.J. Pilone, Ethyl carbamate precursor citrulline formation from arginine degradation by malolactic wine lactic acid bacteria, FEMS Microbiol. Lett. 183 (1) (2000) 31.
[4] G. Gayda, N. Stasyuk, H. Klepach, M. Gonchar, M. Nisnevitch, Promising bioanalytical approaches to wine analysis, in: A. Grumezescu, A.M. Holban (Eds.), The Science of Beverages, Quality Control in the Beverage Industry, vol. 17, Elsevier, Amsterdam, 2019, p. 419. Ch. 12.
[5] C.S. Pundir, P. Kumar, R. Jaiwal, Biosensing methods for determination of creatinine: a review, Biosens. Bioelectron. 126 (2019) 707.
[6] R. Cánovas, M. Cuartero, G.A. Crespo, Modern creatinine (Bio)sensing: challenges of point-of-care platforms, Biosens. Bioelectron. 130 (2019) 110.
[7] Y. He, L. Zhou, L. Deng, Z. Feng, Z. Cao, Y. Yin, An electrochemical impedimetric sensing platform based on a peptide aptamer identified by high-throughput molecular docking for sensitive L-arginine detection, Bioelectrochemistry 137 (2021) 107634.
[8] C.T.I. de Benie, X.C.G. Casal, D.A. van Waardenburg, S.M. Schexnayder, K.F. M. Joosten, N.E.P. Deutz, M.P.K.J. Engelen, 24-Hour protein, arginine and citrulline metabolism in fed critically ill children - a stable isotope tracer study, Clin. Nutr. 36 (3) (2017) 876.
[9] D.S. Clou, P.H. Wu, Y.C. Huang, M.C. Yang, S.Y. Lee, C.Y. Lin, Colorimetric and amperometric detection of urine creatinine based on the ABTS radical cation modified electrode, Sensor. Actuator. B Chem. 314 (2020) 128034.
[10] M. Jaffe, Ueber den Niederschlag welchen Pikrinsäure in normalen Harn erzeugt und über eine neue reaction des Kreatinins, Z. Physiol. Chem. 10 (1886) 391.
[11] S. Sakaguchi, Über eine neue Farbenreaktion von protein und arginine, J. Biochem. 5 (1925) 25.
[12] R.K.R. Kumar, M.O. Shaikh, C.-H. Chuang, A review of recent advances in non-enzymatic electrochemical creatinine biosensing, Anal. Chim. Acta (2021) 338748, https://doi.org/10.1016/j.aca.2021.338748.
[13] S. Qu, Q. Cao, J. Ma, Q. Jia, A turn-on fluorescence sensor for creatinine based on the quinoline-modified metal organic frameworks, Talanta 219 (2020) 121280.
[14] N. Nontawong, M. Amatatongchai, S. Himoonnee, S. Lnosing, P. Jarujamrus, C. Karuwan, S. Chairam, Novel amperometric flow-injection analysis of creatinine using a molecularly-imprinted polymer coated copper oxide nanoparticle-modified carbon-paste-electrode, J. Pharmaceut. Biomed. Anal. 175 (2019) 112770.
[15] I. Ortiz-Gomez, G.B. Ramírez-Rodríguez, L.F. Capitan-Vallvey, A. Salinas-Castillo, J.M. Delgado-López, Highly stable luminescent europium-doped calcium phosphate nanoparticles for creatinine quantification, Colloids Surf., B 196 (2020) 111337.
[16] E.L. Fava, T.M.D. Prado, A. Garcia-Filho, T.A. Silva, F.H. Cincotto, F. Cruz de Moraes, R.C. Faria, O. Fatibello-Filho, Non-enzymatic electrochemical determination of creatinine using a novel screen-printed microcell. Talanta 207 (2020) 120277.
[17] I. Lewińska, M. Speichert, M. Granica, L. Tymecki, Colorimetric point-of-care paper-based sensors for urinary creatinine with smartphone readout, Sensor. Actuator. B Chem. 340 (2021) 129915.
[18] E. Pedrozo-Peñafiel, S. Colombo, C. Shu, A.F. Adiyatullin, Z. Li, E. Mendez, B. Braverman, A. Kawasaki, D. Akamatsu, Y. Xiao, V. Vuletic, Entanglement on an optical atomic-clock transition, Nature 588 (7838) (2020) 414.
[19] O. Begou, R. Weber, B. Beckmann, D. Tsikas, GC-MS studies on derivatization of creatinine and creatine by BSTFA and their measurement in human urine, Molecules 26 (11) (2021) 3206.
[20] J.F. Moore, J.D. Sharer, Methods for quantitative creatinine determination, Curr. Protoc. Hum. Genet. 93 (2017). A.30.1-A.30.7.
[21] D.P. Patel, G.T. Pauly, T. Tada, A.L. Parker, L. Toulabi, Y. Kanke, T. Oike, K. W. Krausz, F.J. Gonzalez, C.C. Harris, Improved detection and precise relative quantification of the urinary cancer metabolite biomarkers – creatine riboside, creatinine riboside, creatine and creatinine by UPLC-ESI-MS/MS: application to the NCI-Maryland cohort population controls and lung cancer cases, J. Pharmaceut. Biomed. Anal. 191 (2020) 113596.
[22] A.J. Killard, M.R. Smyth, Creatinine biosensors: principles and designs, Trends Biotechnol. 18 (10) (2000) 433.
[23] I.S. Kucherenko, O.O. Soldatkin, S.V. Dzyadevych, A.P. Soldatkin, Electrochemical biosensors based on multienzyme systems: main groups, advantages and limitations – a review, Anal. Chim. Acta 1111 (2020) 114.
[24] T. Berninger, C. Bliem, E. Piccinini, O. Azzaroni, W. Knoll, Cascading reaction of arginase and urease on a graphene-based FET for ultrasensitive, real-time detection of arginine, Biosens. Bioelectron. 115 (2018) 104.
[25] N. Stasyuk, O. Smutok, O. Demkiv, T. Prokopiv, G. Gayda, M. Nisnevitch, M. Gonchar, Synthesis, catalytic properties and application in biosensorics of nanozymes and electrononocatalysts: a review, Sensors 20 (2020) 4509.
[26] K.-O. Kullavadee, N. Aroonsri, Role of polyelectrolyte multilayers over gold film for selective creatinine detection using Raman spectroscopy, Appl. Surf. Sci. 546 (2021) 149092.
[27] O.V. Stasyk, Y.R. Boretsky, M.V. Gonchar, A.A. Sibirny, Recombinant arginine-degrading enzymes in metabolic anticancer therapy and biosensorics, Cell Biol. Int. 39 (2015) 246.
[28] N. Verma, A.K. Singh, M. Singh, L-arginine biosensors: a comprehensive review, Biochem. Biophys. Rep. 12 (2017) 228.
[29] N. Stasyuk, O. Smutok, G. Gayda, M. Gonchar, Y. Koval'chuk, A new bi-enzyme potentiometric sensor for arginine analysis based on recombinant human arginase 1 and commercial urease, J. Mater. Sci. Eng. 1 (2011) 819.
[30] N. Stasyuk, O. Smutok, G. Gayda, B. Vus, Y. Koval'chuk, M. Gonchar, Bi-enzyme L-arginine-selective amperometric biosensor based on ammonium-sensing polyaniline-modified electrode, Biosens. Bioelectron. 37 (1) (2012) 46.
[31] N. Stasyuk, G. Gayda, O. Demkiv, L. Darmohray, M. Gonchar, M. Nisnevitch, Amperometric biosensors for L-arginine determination based on L-arginine oxidase and peroxidase-like nanozymes, Appl. Sci. 11 (2021) 7024.
[32] M.T. Zhybak, L.R. Fayura, Y.R. Boretsky, M.V. Gonchar, A.A. Sibirny, E. Dempsey, A.F. Turner, Y.I. Korpan, Amperometric L-arginine biosensor based on a novel recombinant arginine deiminase, Microchim. Acta 184 (8) (2017) 2679.
[33] M. Zarei, M.R. Rahbar, M.H. Morowvat, N. Nezafat, M. Negahdaripour, A. Berenjian, Y. Ghasemi, Arginine deiminase: current understanding and applications, recent pat, Biotechnol. 13 (2) (2019) 124.
[34] Suet-Ying Tam, Sai-Fung Chung, Yu Wai Chen, Yik-Hing So, Pui-Kin So, Wing-Lam Cheong, Kwok-Yin Wong, Yun-Chung Leung, Design of a structure-based fluorescent biosensor from bioengineered arginine deiminase for rapid determination of L-arginine, Int. J. Biol. Macromol. 165 (A) (2020) 472.

[35] N.Y. Stasyuk, G.Z. Gayda, M.V. Gonchar, L-arginine-selective microbial amperometric sensor based on recombinant yeast cells over-producing human liver arginase I, Sensor. Actuator. B Chem. 204 (2014) 515.
[36] T. Tsuchida, K. Yoda, Multi-enzyme membrane electrodes for determination of creatinine and creatine in serum, Clin. Chem. 29 (1) (1983) 51.
[37] S. Ellairaja, K. Shenbagavalli, V.S. Vasantha, Ultrasensitive fluorescent biosensor for creatinine determination in human biofluids based on water soluble rhodamine B dye-Au3 ions conjugate, Chemistry Select 2 (2017) 1025.
[38] J.S. Do, Y.H. Chang, M.L. Tsai, Highly sensitive amperometric creatinine biosensor based on creatinine deiminase/Nafion®-nanostructured polyaniline composite sensing film prepared with cyclic voltammetry, Mater. Chem. Phys. 219 (2018) 1.
[39] Y. Yamamoto, M. Sendo, Amperometric ammonium ion sensor and its application to biosensors, Sensor. Actuator. B Chem. 13 (1–3) (1993) 57.
[40] Y.C. Luo, J.S. Do, Urea biosensor based on PANi(urease)-Nafion/Au composite electrode, Biosens. Bioelectron. 20 (1) (2004) 15.
[41] B. Strehlitz, B. Gründig, H. Kopinke, Sensor for amperometric determination of ammonia and ammonia-forming enzyme reactions, Anal. Chim. Acta 403 (1–2) (2000) 11.
[42] M. Cuartero, N. Colozza, B.M. Fernández-Pérez, G.A. Crespo, Why ammonium detection is particularly challenging but insightful with ionophore-based potentiometric sensors – an overview of the progress in the last 20 years, Analyst 145 (2020) 5168.
[43] J. Ding, W. Qin, Recent advances in potentiometric biosensors, TrAC Trends Anal. Chem. (Reference Ed.) 124 (2020) 115803.
[44] H. Karimi-Maleh, Y. Orooji, F. Karimi, M. Alizadeh, M. Baghayeri, J. Rouhi, S. Tajik, .A. Al-Othman, A critical review on the use of potentiometric based biosensors for biomarkers detection, Biosens. Bioelectron. 184 (2021) 113252.
[45] H. Thompson, G.A. Rechnitz, Ion electrode based enzymic analysis of creatinine, Anal. Chem. 46 (2) (1974) 246.
[46] A.P. Soldatkin, J. Montoriol, W. Sant, C. Martelet, N. Jaffrezic-Renault, Creatinine sensitive biosensor based on ISFETs and creatinine deiminase immobilised in BSA membrane, Talanta 58 (2) (2002) 351.
[47] S. Uzunçar, L. Meng, A.P.F. Turner, W.C. Mak, Processable and nanofibrous polyaniline: polystyrene-sulphonate (nano-PANI:PSS) for the fabrication of catalyst-free ammonium sensors and enzyme-coupled urea biosensors, Biosens. Bioelectron. 171 (2021) 112725.
[48] M. Zhybak, V. Beni, M.Y. Vagin, E. Dempsey, A.P.F. Turner, Y. Korpan, Creatinine and urea biosensors based on a novel ammonium ion-selective copper-polyaniline nano-composite, Biosens. Bioelectron. 77 (2016) 505.
[49] M.T. Zhybak, M.Y. Vagin, V. Beni, X. Liu, E. Dempsey, A.P.F. Turner, Y.I. Korpan, Direct detection of ammonium ion by means of oxygen electrocatalysis at a copper-polyaniline composite on a screen-printed electrode, Microchim Acta 183 (2016) 1981.
[50] V. Nareth, N. Lee, A review on biosensors and recent development of nanostructured materials-enabled biosensors, Sensors 21 (4) (2021) 1109.
[51] C. Li, Y. Wang, H. Jiang, X. Wang, Biosensors based on advanced sulfur-containing nanomaterials, Sensors 20 (2020) 3488.
[52] N. Verma, A.K. Singh, N. Saini, Synthesis and characterization of ZnS quantumdots and application for development of arginine biosensor, Sens. Bio-Sens. Res. 15 (2017) 41.
[53] A. Zakalskiy, N. Stasyuk, O. Zakalska, Y. Boretsky, M. Gonchar, Overexpression and one-step renaturation-purification of the tagged creatinine deiminase of *Corynebacterium glutamicum* in *Escherichia coli* cells, Cell Biol. Int. 44 (5) (2020) 1204.
[54] L.R. Fayura, Y.R. Boretsky, Y.V. Pynyaha, D.N. Wheatley, A.A. Sibirny, Improved method for expression and isolation of the *Mycoplasma hominis* arginine deiminase from the recombinant strain of *Escherichia coli*, J. Biotechnol. 167 (4) (2013) 420.
[55] V. Chromý, K. Rozkosná, P. Sedlák, Determination of serum creatinine by Jaffe method and how to calibrate to eliminate matrix interference problems, Clin. Chem. Lab. Med. 46 (8) (2008) 1127.
[56] N. Stasyuk, G. Gayda, A. Zakalskiy, O. Zakalska, L. Fayura, O. Vovk, O. Stasyk, A. Sibirny, M. Gonchar, Recombinant forms of arginase and arginine deiminase as catalytic components of argitest enzymatic kit, Sci. innov. 13 (4) (2017) 56.
[57] A. Zakalskiy, N. Stasyuk, M. Gonchar, Creatinine deiminase: characterization, using in enzymatic creatinine assay, and production of the enzyme, Curr. Protein Pept. Sci. 20 (5) (2019) 465.
[58] R.Z. Han, G.C. Xu, J.J. Dong, Y. Ni, Arginine deiminase: recent advances in discovery, crystal structure, and protein engineering for improved properties as an anti-tumor drug, Appl. Microbiol. Biotechnol. 100 (2016) 4747.
[59] B. Tombach, J. Schneider, F. Matzkies, R.M. Schaefer, G.C. Chemnitius, Amperometric creatinine biosensor for hemodialysis patients, Clin. Chim. Acta 312 (1–2) (2001) 129.
[60] G.B. Neurath, M. Dünger, F.G. Pein, D. Ambrosius, O. Schreiber, Primary and secondary amines in the human environment, Food Chem. Toxicol. (4) (1977) 275.
[61] G. Wu, F.W. Bazer, T.A. Davis, S.W. Kim, P. Li, J. Marc Rhoads, C.M. Carey Satterfield, S.B. Smith, T.E. Spencer, Y. Yin, Arginine metabolism and nutrition in growth, health and disease, Amino Acids 37 (1) (2009) 153.
[62] K.T. Austin, C.E. Butzke, Spectrophotometric assay for arginine in grape juice and must, Am. J. Enol. Vitic. 51 (2000) 227.

Оригінал доступний за посиланням: https://doi.org/10.1016/j.talanta.2021.122996

7.2. Розробка ензиматичних методів аналізу L-аргініну.

Анотація: *У цій роботі ми повідомляємо про створення високоселективного та чутливого ензиматичного методу кількісного аналізу L-аргініну (L-Arg). Запропонований метод базується на використанні рекомбінантної бактерійної аргініндеімінази (АДІ), виділеної з клітин рекомбінантного штаму E. coli, і о-фталевого альдегіду (ОФА) в ролі хромогену. Принцип запропонованого методу ґрунтується на ензиматичному розщепленні L-Arg за використання АДІ та реакції утвореного амонію із ОФА з утворенням продукту, який детектується флуориметрично (ФЛ) або спектрофотометрично (СФ). Нами показано, що запропонований ФЛ метод є лінійний в межах від 0,35 мкМ до 24 мкМ з нижньою межею виявлення 0,25 мкМ, тоді як для АДІ-ОФА-СФ методу, лінійність спостерігається від 0,7 мкМ до 50 мкМ з нижньою межею виявлення 0,55 мкМ. Розроблений метод апробовано на реальних зразках вин і соків. Для отриманих результатів доведено тісну кореляцію (R = 0,998) між результатами нового методу та референтного ензиматичного ензиматичним способу.*

Food Chemistry 201 (2016) 320–326

Contents lists available at ScienceDirect

Food Chemistry

journal homepage: www.elsevier.com/locate/foodchem

Novel arginine deiminase-based method to assay L-arginine in beverages

N.Ye. Stasyuk [a], G.Z. Gayda [a,*], L.R. Fayura [a], Y.R. Boretskyy [b,a], M.V. Gonchar [a,c], A.A. Sibirny [a,d]

[a] Institute of Cell Biology, National Academy of Science of Ukraine, Drahomanov Str. 14/16, 79005 Lviv, Ukraine
[b] Department of Biochemistry and Hygiene, Lviv State University of Physical Culture, Kosciuszko Street 11, 79000 Lviv, Ukraine
[c] Institute of Applied Biotechnology and Basic Sciences, Rzeszow University, Sokolowska Str. 26, 36-100 Kolbuszowa, Poland
[d] Department of Biotechnology and Microbiology, Rzeszow University, Cwiklinskiej 2, 35-601 Rzeszow, Poland

ARTICLE INFO

Article history:
Received 30 October 2015
Received in revised form 18 January 2016
Accepted 20 January 2016
Available online 22 January 2016

Keywords:
L-Arginine
Arginine deiminase
Enzymatic assay
Beverages
Ethyl carbamate

ABSTRACT

A highly selective and sensitive enzymatic method for the quantitative determination of L-arginine (Arg) has been developed. The method is based on the use of recombinant bacterial arginine deiminase (ADI) isolated from the cells of a recombinant strain *Escherichia coli* and o-phthalaldehyde (OPA) as a chemical reagent. Ammonia, the product of the enzymatic digestion of Arg by ADI, reacts with OPA and forms in the presence of sulfite a product, which can be detected by spectrophotometry (S) and fluorometry (F). The linear concentration range for Arg assay in the final reaction mixture varies for ADI-OPA-F variant of the method from 0.35 μM to 24 μM with the detection limit of 0.25 μM. For ADI-OPA-S variant of the assay, the linearity varies from 0.7 μM to 50 μM with the detection limit of 0.55 μM. The new method was tested on real samples of wines and juices. A high correlation ($R = 0.978$) was shown for the results obtained with the proposed and the reference enzymatic method.

© 2016 Elsevier Ltd. All rights reserved.

1. Introduction

L-Arginine (Arg), one of the most abundant amino acids in grape juices and wines, is closely related to the ethyl carbamate (EC) level in wines (Huang & Ough, 1989; Wu et al., 2014). Arg is degraded to urea and ornithine by the yeast enzyme arginase (EC 3.5.3.1). Urea is assimilated by the yeast cells, but some amount of this metabolite is released into the fermentation medium under excess arginine in grape juice. Accumulated urea in the medium can spontaneously react with ethanol to form very toxic and carcinogenic EC (Alexander et al., 2007; Huang & Ough, 1989). Citrulline, formed from Arg metabolism *via* the arginine deiminase pathway by wine malolactic bacteria, is the second significant precursor of EC in wine (Liu, Pritchard, Hardman, & Pilone, 1996; Spayd et al., 1994; Uthurry, Lepe, Lombardero, & Del Hierro, 2006). Both urea and citrulline accumulation in the fermentation medium mainly depends on the Arg level and the type of microorganism (Liu et al., 1996). If Arg concentration in juice is higher than 1000 mg L^{-1} (5.0 mM), the potential EC concentration in wine will be above 15 μg L^{-1}, the current voluntary limit in the United States (Ough, Stevens, & Almy, 1989), while Canada and Czech Republic have legalized this limit to 30 μg L^{-1}. France, Brazil, Germany and Swiss also control EC level in some alcohol drinks (Conacher & Page, 1986; Jiao, Dong, & Chen, 2014; Mira De Orduña, Liu, Patchett, & Pilone, 2000).

Determination of EC in fermented foods and beverages involves various strategies. Usually the adapted extractive techniques and pre-concentration steps are followed by gas chromatography (GC) coupled to mass spectrometry (MS). High-performance liquid chromatography (HPLC) and semi-quantitative spectroscopic methods (infra-red) are also proposed as valuable alternatives to the classical but time-consuming GC–MS (Jiao et al., 2014).

Two types of preventive methods of decreasing the EC levels in food are described. First, adapted and optimized practices in all steps of the chain of food (or beverages) production lead, in general, to low EC level. Secondly, the abatement of EC precursors can be done by adapted enzymatic, physical–chemical or chemical methods according to the nature of raw materials and conditions of their production processes. So, to ensure the high quality of final product and to avoid potential health hazard of carcinogenic EC, quantitative analysis of its precursor, Arg in fruit juices and wines is an actual problem.

A variety of physicochemical detection procedures for Arg analysis have been developed. These procedures were based on ion exchange chromatography (Huang & Ough, 1989; Spayd et al., 1994), fluorometry (Parniak, Lange, & Viswanatha, 1983), spectrophotometry (Casadebaig, Dupin, & Mesnard, 1979; Goldschmidt & Lockhart, 1971; Khramov, Petrova, & Binova, 1980; Micklus & Stein, 1973; Sakaguchi, 1925; Sastry &

* Corresponding author.
E-mail address: galina.gayda@gmail.com (G.Z. Gayda).

http://dx.doi.org/10.1016/j.foodchem.2016.01.093
0308-8146/© 2016 Elsevier Ltd. All rights reserved.

Tummuru, 1994; Wang, Liang, Zhao, Feng, & Li, 2008; Yamasaki, Shimer, & Feeney, 1981), capillary electrophoresis (Narezhnaya, Askalepova, Nikashina, Krukier, & Pogorelova, 2010), HPLC (Chu, Huang, Pao, & Li, 2003), HPLC–MS (Aldamiz-Echevarria & Andrade, 2012; El-Khory et al., 2011).

The first attempts of the colorimetric (spectrophotometric) determination of Arg were limited only to the Sakaguchi reaction with α-naphthol and sodium hypochlorite (Sakaguchi, 1925). In further modifications of this method various chromogenic agents were applied: diacetyl-α-naphthol (Goldschmidt & Lockhart, 1971), 2-methyl-α-naphthol (Casadebaig et al., 1979), 5-chloro-7-iodo-8-hydroxy quinoline (5-chloro-7-iodo-8-HQ) (Khramov et al., 1980), α-naphthol and 2,3-butanedione monoxime in the method of Voges-Proskauera (Micklus & Stein, 1973), thymol-(2-propyl-5-methyl) phenol and sodium hypobromite in the method of Sastry (Sastry & Tummuru, 1994), 8-hydroxyquinoline (HQ) and sodium hypobromite (Wang et al., 2008); *p*-nitrophenylglyoxal and sodium ascorbate (Yamasaki et al., 1981); 1,2,4-trihydroxy anthraquinone (THAQ) and hydrogen peroxide (Mitič, Miletič, Pavlovič, Tosic, & Velimirović, 2007). The comparative characteristics of the most common methods of Arg assay are summarized in Table 1 (Gayda, Stasyuk, & Gonchar, 2014).

The construction of Arg-sensitive biosensors has already been reported. The main analytical characteristics of the potentiometric, conductometric and amperometric biosensors on Arg, based on enzymes and cells, were described in detail in our papers (Gayda, Stasyuk, Klepach, & Gonchar, 2015; Gayda et al., 2014; Stasyuk, Gayda, & Gonchar, 2014; Stasyuk, Smutok, Gayda, Kovalchuk, & Gonchar, 2011; Stasyuk, Smutok, Gayda, Vus, & Gonchar, 2012).

Thus, the known physicochemical approaches for Arg monitoring require special skills, are time-consuming and expensive, and often have poor precision, low sensitivity and selectivity. So the further development of novel highly selective and sensitive methods, including enzymatic ones, for Arg determination in food industry, in particular, in wine making, is necessary.

The enzymes of Arg metabolism, namely, arginase, arginine deiminase and arginine decarboxylase, are the promising tools for Arg assay. Due to the high cost of natural Arg-selective enzymes, the search for the alternative sources of these enzymes, including recombinant microorganisms, as well as the development of effective technologies for enzymes isolation and purification are the relevant problems.

We have reported earlier about isolation and characterization of human liver arginase I (EC 3.5.3.1; L-arginine amidinohydrolase) from the recombinant yeast cells, over-producing this enzyme (Stasyk, Boretsky, Gonchar, & Sibirny, 2015; Stasyuk et al., 2014; Zakalskiy et al., 2012). The number of arginase-based analytical approaches for quantitative determination of Arg were elaborated and characterized, namely, enzymatic methods with spectrophotometric and fluorometric detection of the reaction product (Gayda et al., 2014; Stasyuk, Bass, Gayda, Yepremyan, & Gonchar, 2015; Stasyuk, Gaida, & Gonchar, 2013; Stasyuk, Gayda, Gayda, & Gonchar, 2012); bi-enzyme (arginase/urease) and microbial electrochemical sensors (Gayda et al., 2015). All proposed arginase-based analytical approaches were tested on the real samples of Arg-containing commercial pharmaceuticals and wines.

In this paper, we describe the development of a novel enzymatic method for Arg determination, based on using recombinant ADI and *o*-phthalaldehyde (in the presence of sulfite) with the fluorometric and spectrophotometric detection of the product (ammonia) and evaluation of the proposed method on real samples of wines and juices.

2. Materials and methods

2.1. Chemicals

o-Phthalaldehyde (OPA), 2,3-butanedione monoxime (DMO), thiosemicarbazide (TSC), sulfuric acid (95–98%), phosphoric acid (85%), trichloroacetic acid, ethanol, Na_2SO_3 were purchased from Sigma–Aldrich. Amino acids and inorganic salts were obtained from Merck (Darmstadt, Germany). All buffers and standard solutions were prepared with Milli-Q system (Millipore) purified water.

2.2. Enzyme

Arginine deiminase (ADI) expression, folding *in vitro* and purification were done as reported previously with some modifications (Fayura, Boretsky, Pynyaha, Wheatley, & Sibirny, 2013). Cells of *Escherichia coli* BL21 (DE3) (Studier & Moffatt, 1986) were transformed with plasmid pET3d-ADI. Transformants were selected on Luria–Bertani medium at 37 °C supplemented with agar (18 g L^{-1}), ampicillin (100 mg L^{-1}), Arg (0.2%) and glucose (0.5%). Selected transformants were employed to produce ADI using C-750501 medium supplemented with 1.25% glycerol and 0.01% lactose following autoinduction protocol modified earlier (Fayura et al., 2013; Studier, 2005).

The induced cells were harvested by centrifugation (5000×g for 15 min at 4 °C), washed with 20 mM sodium phosphate buffer, pH 7.2 (PB), and stored at −70 °C. To obtain a suspension of ADI inclusion bodies, the bacterial pellet was resuspended in 50 mM Tris–HCl buffer, pH 7.8 that contained 1 mM EDTA and 0.2% lysozyme and treated as described earlier (Fayura et al., 2013). Obtained inclusion bodies were solubilized in 50 mM potassium phosphate buffer (pH 7.2), containing 1 mM EDTA, 5 M guanidine hydrochloride and 5 mM DTT. Refolding of ADI was carried out by rapid 100-fold dilution of solubilized protein with 20 mM potassium phosphate buffer, pH 7.2, containing 200 mM KCl, 1 mM DTT and 1 mM EDTA followed by incubation at 15 °C for 72 h.

Table 1
Comparison of different chemical and physicochemical methods of L-Arg assay.

Method/reference	λ_{max}	ε	Sensitivity		Linear range		Time
	nm	$mM^{-1}\,cm^{-1}$	mg L^{-1}	mM	mg L^{-1}	mM	min
Sakaguchi (Sakaguchi, 1925)	525	15.7	0.7	$4.0 \cdot 10^{-3}$	1.0–45	0.006–0.26	40
5-chloro-7-iodo-HQ (Khramov et al., 1980)	440	57.4	0.9	$5.2 \cdot 10^{-3}$	1.0–100	0.006–0.57	10
Voges-Proskauera (Micklus & Stein, 1973)	535	3.07	0.8	$4.6 \cdot 10^{-3}$	1.0–100	0.006–0.57	30
Sastry (Sastry & Tummuru, 1994)	440	13.0	0.3	$1.7 \cdot 10^{-3}$	–	–	40
HQ (Wang et al., 2008)	500	66.0	1.2	$6.9 \cdot 10^{-3}$	1.5–12	0.009–0.07	10
p-nitrophenylglyoxal (Yamasaki et al., 1981)	475	–	–	–	0.03–0.33	$(0.2–2.0) \cdot 10^{-3}$	30
THAQ (Mitič et al., 2007)	540	–	1.5	$8.6 \cdot 10^{-3}$	4.4–87.5	0.03–0.50	5
Sodium hypobromite (Gange, Francis, Costin, Barnett, & Lewis, 2005)	–	–	0.02	$0.1 \cdot 10^{-3}$	0.52–21.1	0.003–0.12	40
Tris (2,2-bipyridyl)ruthenium(III) (Costin, Paul, & Lewis, 2003)	–	–	$0.6 \cdot 10^{-3}$	$3.4 \cdot 10^{-6}$	$0.8–1.5 \cdot 10^{-3}$	$(4.5–8.6) \cdot 10^{-6}$	30
Zone electrophoresis (Narezhnaya et al., 2010)	–	–	3	0.02	6.0–1000	0.03–5.74	60
HPLC (Chu et al., 2003)	–	–	0.3	$2.0 \cdot 10^{-3}$	1.0–500	0.006–2.87	40

The renatured enzyme was diafiltered and purified by anion-exchange chromatography using Q-Sepharose column and a linear gradient of 0–1 M NaCl in PB. The active fractions were pooled and NaCl was adjusted to 2 M. The enzyme was applied to a Phenyl-Sepharose column, washed with PB, containing 2 M NaCl, and eluated with the buffer containing 1 M NaCl. As a result, stable, almost homogenous enzyme preparations with a specific activity of 30–35 U/mg of protein were obtained.

Solution of the purified enzyme was concentrated using ultrafiltration spin column Vivaspin-Turbo 15 (Sartorius Stedim Biotech GmbH, Germany), filter-sterilized using 0.22 μM filters (Ce 0459 Millex-Gv, Millipore, USA) and stored at 4 °C.

The protein concentration was determined by the Lowry method. ADI activity was determined as described (Misawa, Aoshima, Takaku, Matsumoto, & Hayashi, 1994). One unit (U) of activity was defined as the amount of enzyme that converted 1 μmol Arg to L-citrulline per min at 37 °C.

2.3. The development of ADI-OPA-based methods

2.3.1. Preparation of OPA reagent

2 g OPA was dissolved in 5 mL 95% ethanol and mixed with 100 mL 0.1 M borate buffer, pH 10. The final reagent (14.3 mM OPA) was supplemented by sodium sulfite to the final concentration of 0.16 mM (Goyal, Rains, & Huffaker, 1988) and stored in darkness at room temperature until usage.

2.3.2. Ammonium ions calibration

An aliquot of 0.15 mL ammonium chloride solution with concentration from 0.005 mM to 1.25 mM in PB was mixed in plastic tube with 3 mL OPA reagent, closed carefully and heated at 60 °C for 15 min. As a blank, OPA reagent with PB (without ammonia) was used. Fluorescence intensity and absorbance for the resulted OPA-ammonium product were determined and the corresponding calibration graphs, for fluorometric (OPA-F) and spectrophotometric (OPA-S) modes of registration, were built. Fluorescence emission value of the tested sample was registered at 415 nm (under excitation at 360 nm) using a Quantech digital filter fluorometer (Thermo Scientific, United States). Optical density was registered at 350 nm with Shimadzu UV1650 PC spectrophotometer (Japan). Each experiment was repeated for 3 times.

2.3.3. Arg calibration

0.1 mL Arg solution with concentration from 0.0012 mM to 10 mM in 0.2 M PB, pH 6.5 was mixed in plastic tubes with 0.025 mL ADI (300 U/mL) solution in PB and incubated at 37 °C during 20 min for complete hydrolyses of Arg. The resulted ammonia was detected after heating in closed tubes with 2.5 mL OPA using OPA-S and OPA-F methods, as described in Section 2.3.2. As a blank, reaction mixture without Arg was used.

2.3.4. Arg assay in real samples of wines and juices

The samples of the following wines were tested in this study: dry white "Chardonnay", dry white "Sauvignon Blanc" and semisweet pink "Syrah Rose" (La belle Angele, France), dry red "Moution Cadet" (Baron Philippe de Rothschild, France), semisweet red "Bastardo" (Massandra, Ukraine), semi-sweet pink "Tokan" (Israel). Two samples of juices "Sadochok" (LtD Sandora, Ukraine) – multifruit, grape with apple – were tested too. All samples were analyzed using a standard addition test (SAT). Before assay, all samples were step-wise diluted by 0.02 M PB, pH 6.5 containing 1 mM EDTA: for chemical method – 125 and 400-fold; for enzymatic method – 50 and 100-fold. Each assay was performed for two dilutions of the sample and repeated 3 times.

2.3.5. The algorithm of calculation of endogenous Arg content

Arg assay by graphical method was done according to the following scheme:

1st step: Estimation of endogenous ammonium ions in the initial sample from the parameters of linear regression of the corresponding OPA-S and OPA-F graphs, taking into account factors of dilution (Eq. (1)); calculation of the average concentration from two values:

$$C_a = \frac{A}{B} \cdot N \quad (1)$$

where C_a – concentration of ammonia, A and B – parameters of linear regression; N – dilution factor of the tested sample, shown in graph.

2nd step: Treatment of the tested sample with ADI followed by estimation of total ammonia content (Eq. (1)) in the resulted sample by graphical method, taking into account factors of dilution, calculation of an average value of ammonia content.

3rd step: Calculation of endogenous Arg content in the tested sample according to Eq. (2).

$$C_{Arg} = (C_a^t - C_a^e) \quad (2)$$

where C_{Arg}, C_a^t and C_a^e – concentrations of endogenous Arg, average contents of total and endogenous ammonia in the tested sample, respectively.

2.4. Arg assay with reference enzymatic method

As a reference, an enzymatic method of Arg assay based on two enzymes – commercial urease and recombinant human liver arginase I (arginase) was used (Stasyuk et al., 2013).

Urea, the product of the enzymatic hydrolysis of Arg by arginase, reacts with 2,3-butanedione monoxime (DMO) and forms a yellow product which can be determined photometrically at 480 nm or fluorometrically at 510 nm (Rho, 1972). Arginase was isolated from the cells of the recombinant yeast *Hansenula polymorpha*, over-producer of the target enzyme as described (Stasyuk et al., 2014).

The analytical results were statistically processed using the OriginPro 8.5 software.

3. Results and discussion

3.1. The general principle and characteristics of the ADI-OPA method

A schematic representation of the reactions, on which the developed method of Arg assay is based, is shown in Fig. 1. Analytical signal is created due to the one-step enzymatic conversion of Arg to ammonium ions (stage I, enzymatic reactions). Ammonium ions react selectively with OPA in an alkali medium in the presence of sulfite, that permits to avoid reaction of OPA with any amino acids (stage II, chemical reaction).

To optimize the conditions of the chemical reaction, OPA concentration (from 7.5 to 15 mM), heating time (10–30 min) and temperature (25–65 °C) were tested (data not shown). Finally, the next conditions of chemical reaction were chosen: 14 mM OPA in the reaction mixture, 15 min of heating in water bath at 60 °C. To optimize the conditions of the enzymatic reaction, concentration of ADI was varied from 0.04 to 0.48 U/mL in the incubation mixture. As the result, the optimal ADI concentration in the incubation mixture has been estimated as 0.24 U/mL required for a complete conversion of Arg (data not shown).

The dependences of fluorescence intensity and optical density of the resulted product (OPA-ammonium) on Arg concentration, as well as the corresponding calibration graphs (F-OPA and S-OPA) for Arg assay under experimentally chosen optimal conditions are demonstrated in the Fig. 2.

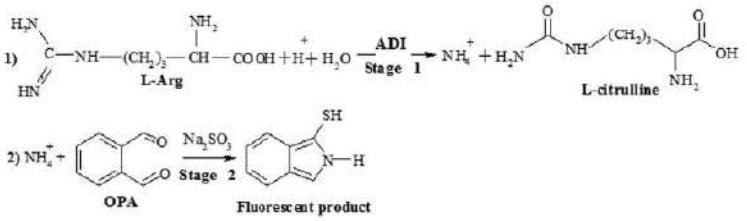

Fig. 1. The reactions for Arg detection using ADI-OPA-based method.

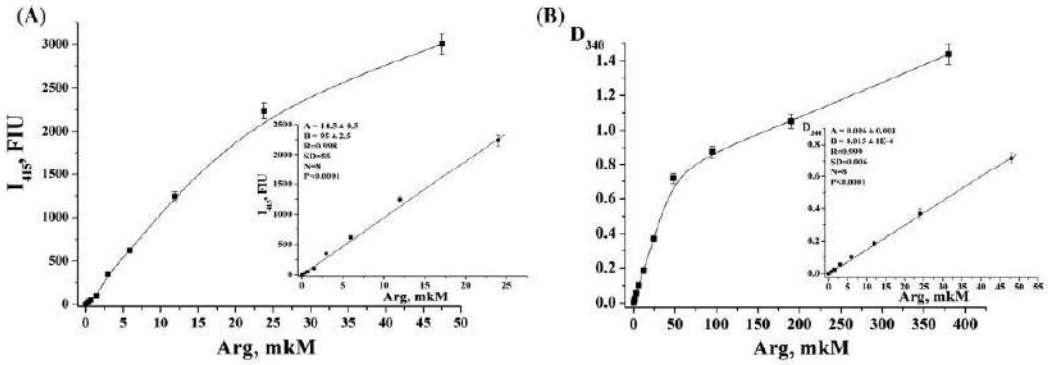

Fig. 2. The dependence of the fluorescence intensities F-OPA (A) and absorbance S-OPA (B) of final reaction product on the concentrations of Arg in reaction mixture. In sets: the correspondent calibration graphs for Arg assay.

Table 2
Characteristics of the current ADI-OPA-based and the reference enzymatic methods of Arg assay.

Method	Enzyme	Linearity range, μM	Detection limit, μM	References
OPA-F λ_{ex} = 364 nm, λ_{em} = 415 nm	ADI	0.35–24	0.25	Current paper
OPA-S λ = 340 nm	ADI	0.7–50	0.55	Current paper
DMO-S λ = 480 nm	Arginase	7–100	5	Stasyuk et al. (2012)
DMO-F λ_{ex} = 380 nm, λ_{em} = 510 nm	Arginase	0.06–200	0.045	Stasyuk et al. (2013)
OPA-S λ = 362 nm	Arginase–urease	0.9–60.0	0.85	Stasyuk et al. (2015)
OPA-F λ_{ex} = 364 nm, λ_{em} = 425 nm	Arginase–urease	0.09–6.0	0.08	Unpublished data
Nzytech kit λ = 340 nm	Arginase–urease–glutamate dehydrogenase	2.9–100	2.1	https://www.nzytech products
Multi-enzymatic pyrophosphate detection, λ = 555 nm	ADI, [a]ASS, [b]PPDK, [c]POX, [d]HRP	Till 100	–	Kameya and Asano (2014)

[a] ASS – argininosuccinate synthetase.
[b] PPDK – pyruvate phosphate dikinase.
[c] POX – pyruvate oxidase.
[d] HRP – horseradish peroxidase.

The analytical characteristics of ADI-OPA-based methods for Arg assay, obtained from Fig. 2, are summarized in Table 2 in relation to the analytical results obtained by commercial spectrophotometric enzymatic Nzytech kit, multi-enzymatic method of pyrophosphate detection and the developed earlier by us arginase-based methods.

The high selectivity is the necessary demand for each analytic method. To study the selectivity of the developed ADI-OPA-based approach, fluorescence and spectrophotometric signals on various 0.5 mM L-amino acids were tested (Fig. 3).

The analytical signal on Arg was taken as 100% and Asn, Lys and Gln gave low outputs (less than 9%). The absence of signals for other tested amino acids (ornithine, canavanine, proline, citrulline, tryptophane, glutamic acid) approved the high selectivity of ADI to Arg and the high purity of the enzyme preparation.

Thus, the developed ADI-based methods (OPA-S and OPA-F) for the quantitative Arg analysis are satisfactory sensitive and highly selective (see Table 2 and Fig. 3). The next advantages of the method, based on the usage of only one enzyme – ADI, are the simplicity of assay' procedure and low cost of the reagents. The

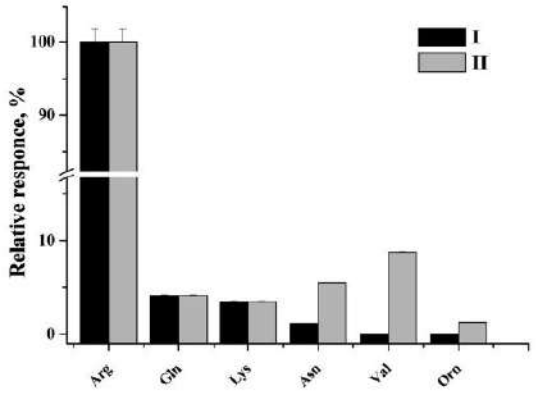

Fig. 3. Dependence of the absorption (I) and fluorescence intensity (II) of the products for various 0.5 mM amino acids.

reaction between ammonia and OPA can also proceed at room temperature, though it needs longer incubation time, more than 3 h (data not shown). This feature of the suggested ADI-based methods is promising for the development of portable test system with automatic variant of assay as well as for screening study or semi-quantitative appreciation of Arg level. It is worth mentioning, that in case of long-time incubation, the reaction mixture in microtiter plates should be closed carefully to avoid contacts with air, that contains the trace quantities of gaseous ammonia. Thus, the proposed analytical ADI-based methods being sensitive, low-cost, highly selective and suitable for both routine and micro-volume formats, will be promising in laboratories of food industry as well as in clinical diagnostics for Arg assay in blood.

3.2. Assay of Arg in real samples

Wines and juices usually contain ammonia and Arg (Austin & Butzke, 2000; Mira De Orduña et al., 2000; Ough et al., 1989; Wu et al., 2014). The developed ADI-OPA method was tested on real samples of wines and juices. To estimate the content of Arg, it was converted by ADI to ammonium ions (see Fig. 1). As a result of enzymatic reaction, 1 mol of Arg generates 1 mol of ammonia, so the content of endogenous Arg can be calculated as the difference of the concentrations of ammonia in the tested samples: total (after enzymatic hydrolysis) and endogenous (without ADI addition). To evaluate the impact of the wine's components on the results of the assay, a standard addition test (SAT) was applied. SAT is a type of quantitative analysis approach often used in analytical chemistry, whereby the standard is added directly to the

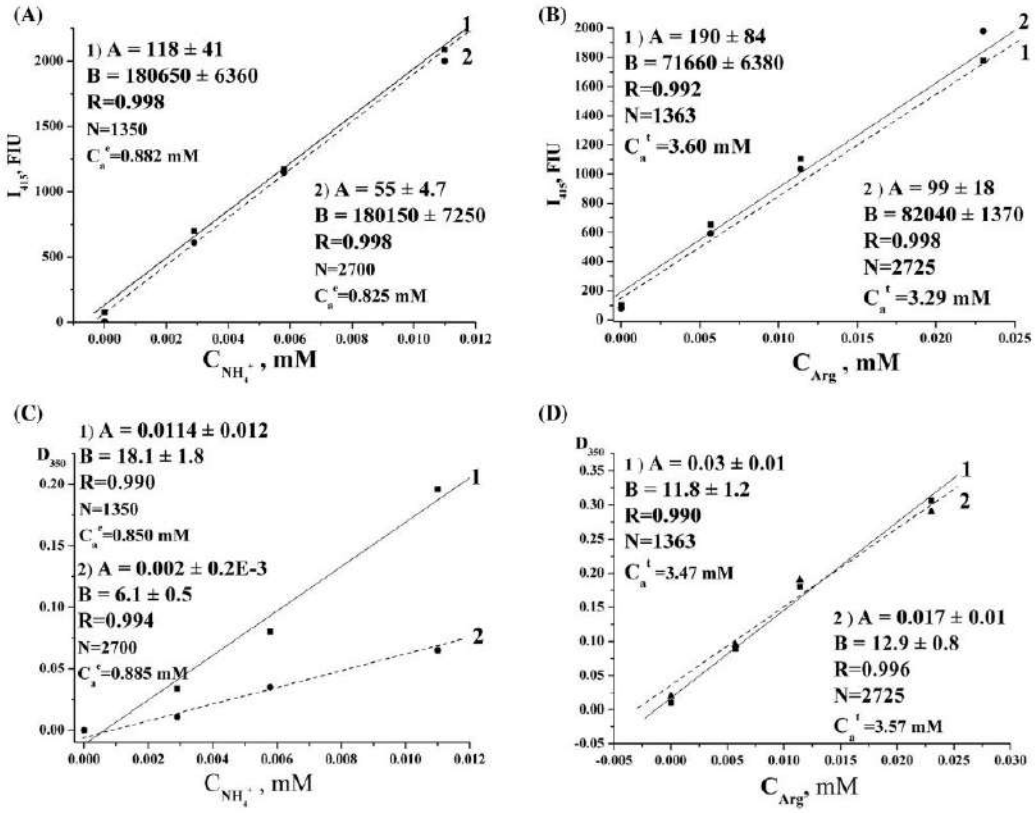

Fig. 4. Assay of total and endogenous ammonia by OPA-F (A and B) and OPA-S (C and D) graphical methods for two dilutions of the juice "Sadochok" (multifruit). $C^{ad}_{NH_4}$ and C_{Arg} – concentrations of added standards to the samples – ammonium ions and Arg, respectively; C^t_a and C^e_a – calculated concentrations of ammonium ions, endogenous (A and C) and total (B and D), in the tested sample.

Table 3
Concentration of Arg (C_{Arg}) in food samples, determined by different enzymatic methods, mM.

Method sample	ADI-based (current paper)				Arginase-based (Stasyuk et al., 2013)			
	OPA-F		OPA-S		DMO-F		DMO-S	
	C_{Arg}	CV, %	C_{Arg}	CV, %	C_{Arg}	CV, %	C_{Arg}	CV, %
Wine "Moution Cadet"	2.05 ± 0.04	1.90	1.85 ± 0.040	2.2	1.97 ± 0.01	1.01	1.96 ± 0.05	2.01
Wine "Bastardo"	2.50 ± 0.04	1.80	ND	–	2.55 ± 0.04	1.20	2.36 ± 0.06	1.70
Juice "Sadochok" grape and apple	2.16 ± 0.01	0.50	2.20 ± 0.03	1.40	2.06 ± 0.04	2.43	1.99 ± 0.03	2.01
Juice "Sadochok" multifruit	*2.59 ± 0.03	1.20	*2.65 ± 0.03	1.10	2.50 ± 0.04	1.70	ND	–

ND – not determined; CV – coefficient of variation. Values are expressed as mean ± SD. * – these results were obtained from graphs, demonstrated in Fig. 4.

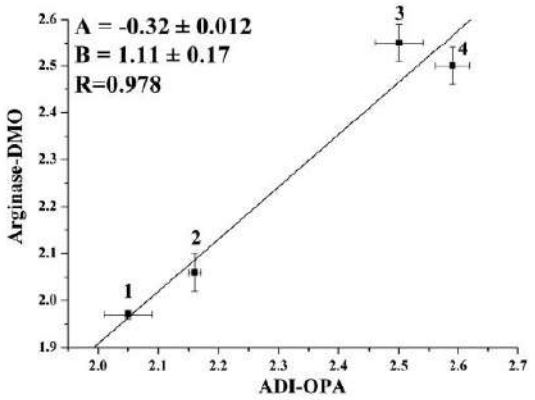

Fig. 5. Correlation between the results of Arg estimation by two enzymatic fluorometric methods: ADI-OPA and Arginase-DMO. Tested samples: Wine "Moution Cadet" (1), Juice "Sadochok" grape and apple (2). Wine "Bastardo" (3), Juice "Sadochok" multifruit (4).

aliquots of analyzed sample. SAT is used in situations where sample components also contribute to the analytical signal, thus making it impossible to compare the analytical signal (Harris, 2003).

The procedure of Arg assay by graphical method was demonstrated in detail (see Fig. 4 and description in Section 2.3.5) for the juice "Sadochok", multifruit.

All real samples were tested by the proposed methods in the same manner. Contents of Arg (mM), estimated by OPA-S method in wines "Souvignon Blanc", "Syrah Rose", Chardonnay and "Tokan", are 3.54 ± 0.02, 1.88 ± 0.40, 3.2 ± 0.05 and 2.18 ± 0.03, respectively. The other tested samples of wines and juices were analyzed using ADI-OPA-based methods in comparison with the arginase-based ones as the reference method (Table 3).

The reproducibility of the proposed analytical methods is satisfactory: the coefficients of variation are less than 2.5%. It is worthwhile mentioning that obtained Arg contents are in range published by another authors (0–9.5 mM) (Li, Liang, Feng, Liu, & Wang, 2008; Stines et al., 2000). The values of Arg contents in the tested samples, obtained by two enzymatic approaches – ADI-OPA-F and Arginase-DMO-F, demonstrated strong correlation: $R = 0.978$ (Fig. 5). Thus, the developed ADI-OPA enzymatic methods can be used for a monitoring of Arg in the samples of wines and juices.

4. Conclusions

A quantitative enzymatic assay for Arg determination based on the usage of recombinant bacterial arginine deiminase (ADI) and *o*-phthalaldehyde (OPA) in the presence of sulfite was developed and characterized. The final product of enzymatic reaction, the ammonium ion, in the presence of sulfite, forms a fluorescent product with OPA, that can be detected with spectrophotometric and fluorometric modes. An effectiveness of the ADI-based analytical method was proved on the real samples of wines and juices. A high correlation ($R = 0.978$) was shown to be between the results obtained with the proposed method and the reference Arginase-based approach. The advantage of the novel enzymatic ADI-OPA method is the possibility of simultaneous assay of Arg and ammonia, although the most attractive characteristic of this method is a simplicity of analytic procedure and economic effect due to the usage of only one enzyme, ADI.

Thus, the proposed low-cost ADI-OPA method of Arg assay being very selective and sensitive, fast, valid and simple can be promising for food quality control in food industry to predict a potential risk of EC generation in wines.

Ethical statement

The authors declare that there is no conflict of interests regarding the publication of this paper.

Acknowledgements

This work was financially supported by NAS of Ukraine in the frame of the Scientific-technical program (Project 29/2015), scientific program "Sensors for Medical, Environmental, Industrial, and Technological Needs: Metrological Support and Trial Operation" (Project 5/3-2015), NATO (Project CBP.NUKR.SFP 984173).

References

Aldamiz-Echevarria, L., & Andrade, F. (2012). Asymmetric dimethylarginine endothelial dysfunction and renal disease. *International Journal of Molecular Sciences, 13*, 11288–11311.

Alexander, J., Auounsson, G., Benford, D., Cockburn, A., Cravedi, J., & Doglitti, E. (2007). Ethyl carbamate and hydrocyanic acid in food and beverages. Scientific opinion of the panel on contaminants. *EFSA Journal, 551*, 1–44.

Austin, K. T., & Butzke, C. E. (2000). Spectrophotometric assay for arginine in grape juice and must. *American Journal of Enology and Viticulture, 51*, 227–232.

Casadebaig, F., Dupin, J. P., & Mesnard, P. (1979). The Sakaguchi reaction: Analytical developments and application to drug control. *Annales Pharmaceutiques Francaises, 37*(7), 313–324.

Chu, K. M., Huang, P. W., Pao & Li, H. (2003). Determination of arginine, asymmetrical dimethylarginine, and symmetrical dimethylarginine in human plasma by high performance liquid chromatography. *Journal of Medical Science, 23*(4), 201–206.

Conacher, H. B. S., & Page, B. D. (1986). Ethyl carbamate in alcoholic beverages: A Canadian case history. In *Proceedings of euro food tox II* (pp. 237–242). Switzerland: European Society of Toxicology.

Costin, J., Paul, F., & Lewis, S. (2003). Selective determination of amino acids using flow injection analyses coupled with chemiluminescence detection. *Analytica Chimica Acta, 408*(1), 67–77.

El-Khoury, J. M., Bunch, D. R., Reineks, E., Jackson, J. R., Steinle, R., & Wang, S. (2011). A simple and fast liquid chromatography-tandem mass spectrometry method for measurement of underivatized L-arginine, symmetric dimethylarginine, asymmetric dimethylarginine and establishment of the reference ranges. *Analytical and Bioanalytical Chemistry, 402*, 771–779.

Fayura, L. R., Boretsky, Y. R., Pynyaha, Y. V., Wheatley, D. N., & Sibirny, A. A. (2013). Improved method for expression and isolation of the *Mycoplasma hominis* arginine deiminase from the recombinant strain of *Escherichia coli*. *Journal of Biotechnology, 167*(4), 420–426.

Gange, M. E., Francis, P. S., Costin, J. W., Barnett, N. W., & Lewis, S. W. (2005). Determination of arginine in dietary supplements. *Journal of the Science of Food and Agriculture, 85*, 1217–1221.

Gayda, G. Z., Stasyuk, N. Ye., & Gonchar, M. V. (2014). The methods of L-arginine analysis (review). *Biotechnologia Acta, 7*(1), 31–39 (In Ukrainian).

Gayda, G., Stasyuk, N., Klepach, H., & Gonchar, M. (2015). Arginase-based electrochemical sensors to L-arginine assay for prediction of ethyl carbamate formation in fermented beverages. In A. Sibirny et al. (Eds.). *Living organisms and bioanalytical approaches for detoxification and monitoring of toxic compounds–Lviv-Rzeszow* (pp. 73–88).

Goldschmidt, M. C., & Lockhart, B. M. (1971). Simplified rapid procedure for determination of agmatine and other guanidino containing compounds. *Analytical Chemistry, 43*, 1475–1479.

Goyal, S. S., Rains, D. W., & Huffaker, R. C. (1988). Determination of ammonium ion by fluorometry after on-line derivatization with o-phthalaldehyde. *Analytical Chemistry, 60*(2), 175–179.

<https://www.nzytech.com/products-services/analytical-test-kits/ak00171/>.

Huang, Z., & Ough, C. S. (1989). Effect of vineyard locations, varieties and rootstocks on the juice amino acid composition of several cultivars. *Ibid. 40*, 135–139.

Jiao, Z., Dong, Y., & Chen, Q. (2014). Ethyl carbamate in fermented beverages: Presence, analytical chemistry, formation mechanism, and mitigation proposals. *Comprehensive Reviews in Food Science and Food Safety, 13*(4), 611–626.

Kameya, M., & Asano, Y. (2014). Rapid enzymatic assay for L-citrulline and L-arginine based on the platform of pyrophosphate detection. *Enzyme and Microbial Technology, 57*(10), 36–41.

Khramov, V. A., Petrova, L. M., & Binova, E. (1980). Modification of Sakaguchi by using 5-chloro-7-iodo-8-hydroxy quinoline. *Laboratornoe Delo, 11*, 651–653 (in Russian).

Li, H., Liang, X., Feng, L., Liu, Y., & Wang, H. (2008). A simple and fast method for arginine determination of in grape juice. *Journal of Food and Drug Analysis, 16*(3), 53–58.

Liu, S. Q., Pritchard, G. G., Hardman, M. J., & Pilone, G. J. (1996). Arginine catabolism in wine lactic acid bacteria: Is it via the arginine deiminase pathway or the arginase-urease pathway? *Journal of Applied Bacteriology, 81*, 486–492.

Micklus, M. J., & Stein, I. M. (1973). The colorimetric determination of mono- and disubstituted guanidines. *Analytical Biochemistry, 54*, 545–553.

Mira De Orduña, R., Liu, S. Q., Patchett, M. L., & Pilone, G. J. (2000). Ethyl carbamate precursor citrulline formation from arginine degradation by malolactic wine lactic acid bacteria. *FEMS Microbiology Letter, 183*, 31–35.

Misawa, S., Aoshima, M., Takaku, H., Matsumoto, M., & Hayashi, H. (1994). High-level expression of Mycoplasma arginine deiminase in *Escherichia coli* and its efficient renaturation as an anti-tumor enzyme. *Biotechnology, 36*, 145–155.

Mitič, S. S., Miletič, G., Pavlovič, A. N., Tosic, S. B., & Velimirović, D. S. (2007). Development and evaluation of a kinetic-spectrophotometric method for determination of arginine. *Journal of the Chinese Chemical Society, 54*, 47–54.

Narezhnaya, E. V., Askalepova, O. I., Nikashina, A. A., Krukier, I. I., & Pogorelova, T. N. (2010). Determination of L-arginine in amniotic fluid by capillary disk electrophoresis. *Zhurnal Analytica Chimica, 65*(12), 1309–1312 (in Russian).

Ough, C. S., Stevens, D., & Almy, J. (1989). Preliminary comments on effects of grape vineyard nitrogen fertilization on the subsequent ethyl carbamate formation in wines. *American Journal of Enology and Viticulture, 40*, 219–220.

Parniak, M. I., Lange, G., & Viswanatha, T. (1983). Quantitative determination of monosubstituted guanidines: A comparative study of different procedures. *Journal of Biochemical and Biophysical Methods, 7*(4), 267–276.

Rho, J. H. (1972). Direct fluorometric determination of urea in urine. *Clinical Chemistry, 18*(5), 476–478.

Sakaguchi, S. (1925). Colorimetric determination of arginine. *Journal of Biochemistry, 5*, 25–32.

Sastry, C. S. P., & Tummuru, M. K. (1994). Spectrophotometric determination of arginine in proteins. *Journal of Food Chemistry, 15*, 257–260.

Spayd, S. E., Wample, R. L., Evans, R. G., Stevens, R. G., Seymour, B. J., & Nagel, C. W. (1994). Nitrogen fertilization of white Riesling grapes in Washington. Must and wine composition. *American Journal of Enology and Viticulture, 45*, 34–42.

Stasyk, O., Boretsky, Y., Gonchar, M., & Sibirny, A. (2015). Recombinant arginine-degrading enzymes in metabolic anticancer therapy and biosensorics. *Cell Biology International, 39*(3), 246–252.

Stasyuk, N., Smutok, O., Gayda, G., Kovalchuk, E., & Gonchar, M. (2011). A new bi-enzyme potentiometric sensor for arginine analysis based on recombinant human arginase I and commercial urease. *Journal of Material Science and Engineering A, 1*, 819–827.

Stasyuk, N., Smutok, O., Gayda, G., Vus, B., & Gonchar, M. (2012). Bi-enzyme L-arginine-selective amperometric biosensor based on ammonium-sensing polyaniline-modified electrode. *Biosensors & Bioelectronics, 37*(1), 46–52.

Stasyuk, N. Ye., Gayda, G. Z., Gayda, A. V., & Gonchar, M. (2012). Enzymatic assay of L-arginine by the use of recombinant human arginase I. *Ukrainica Bioorganica Acta, 1*, 31–37 (in Ukrainian).

Stasyuk, N., Gaida, G., & Gonchar, M. (2013). L-Arginine assay with the use of arginase I. *Applied Biochemistry and Microbiology, 49*, 529–534.

Stasyuk, N., Gayda, G., & Gonchar, M. (2014). L-Arginine-selective microbial amperometric sensor based on recombinant yeast cells over-producing human liver arginase I. *Sensors & Actuators B: Chemistry, 204*, 515–521.

Stasyuk, N. Y., Bass, S. R., Gayda, G. Z., Yepremyan, H. S., & Gonchar, M. V. (2015). New enzymatic method for L-arginine determination based on use of human arginase I and urease. *Scientific Journal («ScienceRise»). 6/1*(11), 43–48 (in Ukarine).

Stines, A. P., Grubb, J., Gockowiak, H., Henschke, P. A., Høj, P. B., & van Heeswijck, R. (2000). Proline and arginine accumulation in developing berries of *Vitis vinifera* L. in Australian vineyards: Influence of vine cultivar, berry maturity and tissue type. *Australian Journal of Grape and Wine Research, 6*(2), 150–158.

Studier, F. W., & Moffatt, B. A. (1986). Use of bacteriophage T7 RNA polymerase to direct selective high-level expression of cloned genes. *Journal of Molecular Biology, 189*, 113–130.

Studier, F. W. (2005). Protein production by auto-induction in high density shaking cultures. *Protein Expression and Purification, 41*, 207–234.

Uthurry, C. A., Lepe, J. A. S., Lombardero, J., & Del Hierro, G. J. R. (2006). Ethyl carbamate production by selected yeasts and lactic acid bacteria in red wine. *Food Chemistry, 94*, 262–270. 2007.

Wang, H., Liang, X.-H., Zhao, R.-X., Feng, L.-D., & Li, H. (2008). Spectrophotometric determination of arginine in grape juice using 8-hydroquinoline. *Agricultural Sciences in China, 7*(10), 1210–1215.

Wu, P., Cai, C., Yang, D., Wang, L., Zhou, Y., Shen, X., ... Tan, J. (2014). Changes of ethyl carbamate in yellow rice wine during shelf-life and formation in simulated ethanol and urea solutions. *Journal of Food and Nutrition Research, 2*(12), 872–875.

Yamasaki, R. B., Shimer, D. A., & Feeney, R. E. (1981). Colorimetric determination of arginine residues in proteins by p-nitrophenylglyoxal. *Analytical Biochemistry, 111*(2), 220–266.

Zakalskiy, A. E., Zakalska, O. M., Rzhepetskyy, Y. A., Potocka, N., Stasyk, O. V., Horak, D., & Gonchar, M. V. (2012). Overexpression of $(His)_6$-tagged human arginase I in *Saccharomyces cerevisiae* and enzyme purification using metal affinity chromatography. *Protein Expression and Purification, 81*, 63–68.

Оригінал доступний за посиланням: https://doi.org/10.1016/j.foodchem.2016.01.093

Анотація: *У поточному дослідженні ми повідомляємо про створення ензиматичного методу визначення вмісту L-аргініну (L-Arg) та флуорометричному моніторингу утвореного аміаку, кінцевого продукту розщеплення L-Arg аргіназою I печінки людини та уреазою. Показано, що селективний аналіз аміаку (при 415 нм) грунтується на реакції з о-фталевим альдегідом (ОФА) у присутності сульфіту в лужному середовищі. Розроблені умови дозволяють уникнути побічних реакцій ОФА з іншими амінокислотами наявними в реальних зразках. Діапазон лінійності флуорометричного методу аргіназа-уреаза-ОФА складає від 100 нМ до 6 мкМ з межею виявлення 34 нМ L-Arg. Розроблений метод апробовано для кількісного аналізу L-Arg у реальних зразках сироваток крові. Показано, що отримані результати є у тісній кореляції з референтним ензиматичним методом, а також з літературними даними. Запропонований метод аргіназа-уреаза-ОФА є чутливим, економічним, селективним і може бути використовуватись для аналізу L-Arg в клінічній діагностиці для одночасного визначення вмісту L-Arg, сечовини та аміаку в сироватці крові.*

Spectrochimica Acta Part A: Molecular and Biomolecular Spectroscopy 170 (2017) 184–190

Contents lists available at ScienceDirect

Spectrochimica Acta Part A: Molecular and Biomolecular Spectroscopy

journal homepage: www.elsevier.com/locate/saa

Fluorometric enzymatic assay of L-arginine

Nataliya Stasyuk [a], Galina Gayda [a,*], Hasmik Yepremyan [b], Agnieszka Stepien [c,d], Mykhailo Gonchar [a]

[a] Institute of Cell Biology, National Academy of Science of Ukraine, Drahomanov Str. 14/16, 79005 Lviv, Ukraine
[b] Scientific and Production Center "Armbiotechnology", National Academy of Sciences of Armenia, Armenia
[c] Department of Dietetics, Institute of Nursing and Health Sciences, Medical Faculty, University of Rzeszow, Al. mjr.W.Kopisto 2 a, 35-310 Rzeszów, Poland
[d] Centre for Innovative Research in Medical and Natural Sciences, Medical Faculty of the University of Rzeszow, Warzywna 1A, 35-310 Rzeszów, Poland

ARTICLE INFO

Article history:
Received 19 February 2016
Received in revised form 7 July 2016
Accepted 9 July 2016
Available online 11 July 2016

Keywords:
L-arginine
Enzymatic assay
Recombinant arginase I
Urease
o-Phthalaldehyde
Sulfite

ABSTRACT

The enzymes of L-arginine (further — Arg) metabolism are promising tools for elaboration of selective methods for quantitative Arg analysis. In our study we propose an enzymatic method for Arg assay based on fluorometric monitoring of ammonia, a final product of Arg splitting by human liver arginase I (further – arginase), isolated from the recombinant yeast strain, and commercial urease. The selective analysis of ammonia (at 415 nm under excitation at 360 nm) is based on reaction with o-phthalaldehyde (OPA) in the presence of sulfite in alkali medium: these conditions permit to avoid the reaction of OPA with any amino acid. A linearity range of the fluorometric arginase-urease-OPA method is from 100 nM to 6 μM with a limit of detection of 34 nM Arg. The method was used for the quantitative determination of Arg in the pooled sample of blood serum. The obtained results proved to be in a good correlation with the reference enzymatic method and literature data. The proposed arginase-urease-OPA method being sensitive, economical, selective and suitable for both routine and micro-volume formats, can be used in clinical diagnostics for the simultaneous determination of Arg as well as urea and ammonia in serum samples.

© 2016 Elsevier B.V. All rights reserved.

1. Introduction

L-Arginine (further — Arg), the most basic amino acid, is found in particularly large amounts in protamines and histones. Arg is glucogenic and half-essential for humans and an important metabolite of the urea cycle [1–3]. Arg can be utilized as therapeutics for the number of diseases: angina pectoris, congestive heart failure, hypertension, coronary heart disease, preeclampsia, intermittent claudication, erectile dysfunction, diabetes mellitus and others [2]. Arg is involved in numerous areas of human biochemistry, including ammonia detoxification, hormone secretion, and immune modulation. Arg is a precursor to nitric oxide (NO), a key component of endothelial-derived relaxing factor, an endogenous messenger molecule involved in a variety of endothelium-dependent physiological effects in the cardiovascular system. In the same time, Arg is a precursor of symmetrically and asymmetrically guanidine (N^G)-dimethylated derivatives (SDMA and ADMA), as well as of L-homoarginine (hArg), the methylene homologue of Arg [4–7].

As substrates for NO synthase, Arg and its derivatives have lately become the important biomarkers in clinical diagnostics. The study of relationships between the level of these biomarkers and the details of illness' process was carried out for kidney and liver pathology as well as for cardiovascular disorders [3–7], neuroinflammatory and autoimmune diseases (endocrine diseases, rheumatoid arthritis and systemic lupus erythematosus) [7–9], pulmonary disorders [10–12], sepsis [13], argininemia and ammonemia [14,15].

Despite the close but opposite associations of hArg and ADMA with cardiovascular disease of adults, children and adolescents, the underlying biochemical processes are largely unknown, presumably not restricted to NO, and require further investigation [3,4]. The accumulation of Arg and the resulting abnormalities in the metabolism of guanidine compounds and NO seem to play a major pathophysiological role, but the influence of the Arg/NO pathway in the pathophysiology of the listed diseases remains unclear [3,6].

Hyperargininemia (HA) or argininemia is caused by deficiency of arginase I, which catalyzes the hydrolysis of Arg to urea as the final enzyme in the urea cycle [1,14–20]. In contrast to other urea cycle defects, arginase I deficiency, caused by mutation in the corresponding gene, usually does not cause catastrophic neonatal hyperammonemia but rather leads to progressive neurological symptoms including seizures and spastic paraplegia in the first years of life and hepatic pathology, such as neonatal cholestasis, acute liver failure, or liver fibrosis [15]. To detect HA among the newborns, in some economically developed countries government-funded programs of blood screening for Arg take place: timely diagnostics of HA will allow to start medical treatment of infants and to stop the development of this dangerous genetic disease [14,15]. The pathogenesis of arginase I deficiency is not fully understood so far.

* Corresponding author.
E-mail address: galina.gayda@gmail.com (G. Gayda).

http://dx.doi.org/10.1016/j.saa.2016.07.019
1386-1425/© 2016 Elsevier B.V. All rights reserved.

Arginase I (L-arginine amidinohydrolase, EC 3.5.3.1) plays the main role in the urea cycle, catalyzing the cytosolic hydrolysis of Arg to ornithine and urea. Recent studies have shown that human liver arginase I can be an effective drug in enzymatic cancer therapy for certain types of cancer, causing the Arg starvation of malignant tumors cells (*e.g.*, melanoma, hepatocellular and pancreatic carcinoma) [21–26]. To control such therapy the monitoring of Arg level in blood and urine is required.

A variety of chemical and physico-chemical approaches for Arg monitoring was developed, the advantages and problems of these standard and modern analytical methods were described in detail in our previous papers [27,28]. These methods are based on ion exchange chromatography, fluorometry, spectrophotometry, capillary electrophoresis, biosensors. Usually the adapted extractive techniques and pre-concentration steps (for this procedure some hours is needed) are followed by liquid chromatography (LC) coupled to mass spectrometry (LC-MS; LC-MS/MS). High-performance liquid chromatography (HPLC) and semi-quantitative spectroscopic methods (infra-red) are also proposed as valuable alternatives to the classical ones.

A scientific collaboration of the specialists in high-tech analytical methods with professionals from medical skills is usually fruitful. As an example of such successful work in the field of studied problem are the joint investigations of the scientific groups from Hannover Medical School (Germany). D. Tsikas and his colleagues are the specialists in analytical chemistry with using high-tech devices (HPLC, GS-MS, LC-MS-MS et al.). J. Frölich and R. Böger, being professionals in medicine, had put the actual healthcare problems - to develop valid methods of quantitative determination of Arg and its derivatives in blood. As a result, the novel analytical approaches for assay of these prospective biomarkers have been proposed, a lot of blood samples of patients with different diagnosis have been tested and analyzed as well as the new knowledge about level of biomarkers as risk factors of various malignances were obtained [3,4,7,8,29–31].

All high-tech methods require skillful labor techniques, are time-consuming and expensive, so the further development of novel highly selective and sensitive methods for fast Arg determination is actual. Enzymes of Arg metabolism - arginase I, arginine deiminase and arginine decarboxylase - seem to be promising tools for elaboration of such methods [26–28].

Recently we have described the development of a novel enzymatic method for Arg determination, based on using recombinant ADI and *o*-phthalaldehyde (in the presence of sulphite) with the fluorometric and spectrophotometric detection of the product (ammonia) and evaluation of the proposed method on real samples of wines and juices [27]. Although there is a lot of papers devoted to determination of ammonium in the presence of primary amines (including amino acids), the exact mechanism of an essential increase in the selectivity to ammonium in the presence of sulfite (instead of mercaptoethanol) is not still elucidated.

Due to high cost of arginase I, the search for an alternative source of this enzyme, namely, microbiological one mas well as the development of an effective technology for enzyme isolation is a relevant issue. To solve it, the recombinant yeast strains, producing human liver arginase I (further - arginase), were gene-engineered in the Institute of Cell Biology, NAS of Ukraine [26]. The optimal schemes for isolation of highly purified enzyme preparations were developed and the enzymatic methods for Arg assay, including biosensors, were proposed [27,28,32–37]. A number of food products (juices, wines, brandies, teas) and Arg-containing commercial pharmaceuticals were analyzed using the proposed arginase-based approaches in comparison with the reference methods [27,28,32–35]. The estimated Arg contents demonstrated high correlation with those declared by producers (R near 1.0) and obtained by reference methods.

In this paper, we describe the development of a novel enzymatic method for Arg determination, based on using recombinant arginase, urease and *o*-phthalaldehyde (in the presence of sulfite) with the fluorometric detection of the product (ammonia) and evaluation of the proposed method on real samples of blood serum.

2. Materials and methods

2.1. Chemicals and devices

o-Phthalaldehyde (OPA), 2,3-butanedione monoxime (DMO), sulfuric acid (95–98%), trichloroacetic acid (TCA), ethanol were purchased from Sigma-Aldrich. Amino acids and inorganic salts were obtained from Merck (Darmstadt, Germany). Diagnostic kit for Urea analysis was manufactured by LTD SIMKO (Lviv, Ukraine). All buffers and standard solutions were prepared with Milli-Q system (Millipore) purified water.

Fluorescence emission values of resulted product were registered with 2 devices: spectrofluorometer Infinite M-200 (TECAN, Switzerland) and Quantech digital filter fluorometer (Thermo Scientific, United States).

2.2. Enzymes

Human liver arginase I was isolated from a cell-free extract of the recombinant yeast *Hansenula polymorpha* NCYC 495 pGAP1–HsARG1 (*leu2car1 Sc:LEU2*), carrying the *HsARG1* target gene under the control of a constitutive promoter of the gene coding for glyceraldehyde-3-phosphate dehydrogenase [26]. Highly-purified arginase preparation with a specific activity of 13 U/mL (600 $\mu mol \cdot min^{-1} \cdot mg^{-1}$ of protein) was used in current work. Arginase activity was determined as the rate of urea formation under arginase-catalyzed hydrolysis of Arg. Urea content was estimated on the second step of the reaction with the usage of a commercial kit for Urea analysis based on colorimetric method [38].

Urease (EC 3.5.1.5, type IX from Jack Beans, 26,100 $U \cdot g^{-1}$) were purchased from Sigma-Aldrich. To prepare urease solution (210 U/mL), 3 mg of powder was dissolved in 1 mL of 50 mM phosphate buffer, pH 7.0 (PB) and stored at 4 °C for up to 1 month.

2.3. The development of arginase-urease/OPA-based method

2.3.1. Preparation of OPA reagent

0.2 g OPA was dissolved in 5 mL 95% ethanol solution and mixed with 100 mL 0.1 M borate buffer, pH 10. The final reagent (14.2 mM OPA) was supplemented by sodium sulfite to the final concentration of 0.16 mM [39] and stored in darkness at room temperature until usage. OPA reagent in the presence of sulfite in alkali medium was demonstrated to react only with ammonium ion (not with any amino acid). The resulted OPA-ammonium product may be detected by spectrophotometry and fluorometry [39].

2.3.2. Study of analytical parameters of OPA-based fluorometric methods

The dependencies of fluorescent intensities for the resulted OPA-ammonium products on ammonia concentration, urea (after urease digestion) and Arg (after arginase/urease hydrolyses) contents were studied, the corresponding calibration graphs for these analytes were built. Each experiment was repeated for 3 times.

2.3.2.1. Ammonium ions calibration. An aliquot of 0.15 mL ammonium chloride solution with concentration from 0.005 mM to 1.25 mM in 50 mM phosphate buffer, pH 7.0 (PB) was mixed in plastic tube with 3 mL OPA reagent, closed carefully and heated at 60 °C for 15 min. As control, OPA reagent without ammonia (with PB) was used. Fluorescence emission value of the tested sample was registered at 415 nm (under excitation at 360 nm) using a Quantech digital filter fluorometer (Thermo Scientific, United States). The analytical results were statistically processed using the OriginPro 8.5 software.

2.3.2.2. Urea calibration. Calibration for urea was performed after enzymatic hydrolysis of urea to ammonia. An aliquot of 0.125 mL urea solution in PB with concentration from 0.005 mM to 0.625 mM was mixed in

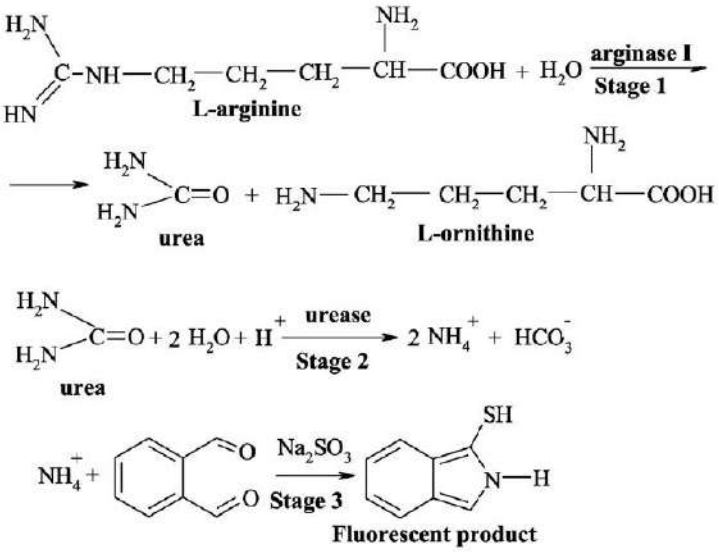

Fig. 1. The reactions for Arg detection using arginase-urease-OPA-based method.

plastic tubes with 0.010 mL urease solution and incubated during 20 min at 37 °C for complete conversion of urea to ammonium ions. Urea content in reaction mixture was controlled with a commercial kit (see Section 2.2). The resulted ammonium ions, formed from urea, were detected after heating with 4 mL OPA reagent as described in Section 2.3.2.1. As a control, reaction mixture without urea (but with PB) was used.

2.3.2.3. Arg calibration. Calibration for Arg was carried out in the following way:

0.1 mL Arg solution with concentration from 0.0025 mM to 0.625 mM in 30 mM Tris-HCl buffer, pH 8.8 (TB) was mixed in plastic tube with 0.03 mL arginase solution in TB and was incubated at 37 °C during 20 min for complete hydrolyses of Arg. Resulted solution was supplemented with an aliquot of 200 mM HCl (to achieve the pH 7.0, optimal for urease type IX from Jack Beans) followed by addition of 0.020 mL urease solution. The reaction mixture was incubated during 20 min at 37 °C and the resulted ammonia was detected fluorometrically after heating with 2.5 mL OPA as described in Section 2.3.2.1. As control, reaction mixture without Arg (but with PB) was used.

2.4. Arg assay in real samples of blood

2.4.1. Serum preparation and its pre-treatment

The samples of blood were gotten from the Sosnivka Hospital (Ukraine, Lviv region). To obtain serum, sample of venous blood was incubated during 20 min at 20 °C and clotted fibrin was removed by centrifugation (5 min, 4000 rpm). To prepare a protein-free sample, serum was treated with 50% TCA to the final concentration of 5%. After 30 min incubation at 0 °C, the pellet of proteins was removed by centrifugation and resulting supernatant was neutralized to pH 7.0 by adding 2 M Tris base. The neutralized protein-free solution (Sample 1), being ready for assay of Arg, urea and ammonium, was kept at −20 °C till the usage.

2.4.2. The algorithm of determination and calculation of endogenous analytes

Before assay, all samples were step-wise diluted by PB: for chemical method – 20 and 40-fold; for enzymatic methods – 50 and 100-fold (after urease treatment) and 100–400-fold (after arginase treatment). Each assay was performed for two dilutions of the sample and repeated 3 times. All samples were analyzed fluorometrically by comparison with corresponding standard solutions, against "blank" – samples without analytes, with PB.

The tested Sample 1 contains endogenous Arg, urea and ammonia. It is worth mentioning, that 1 mol of Arg, being treated with arginase, generates 1 mol urea. Resulted urea, being treated with urease, generates 2 mol of ammonia (Fig. 1).

Arg assay was done according to the following scheme:

1st step. Estimation of endogenous ammonium ions in the initial Sample 1, taking into account factors of dilution (Eq. (1)); calculation of the average concentration from two values:

$$C_a = \left(\frac{C_{st} \cdot I_a}{I_{st}}\right) \cdot N \qquad (1)$$

where I_{st} and I_a – values of fluorescence emission of the standard probe and tested Sample, respectively;

C_a – concentration of endogenous ammonia in the Sample 1;

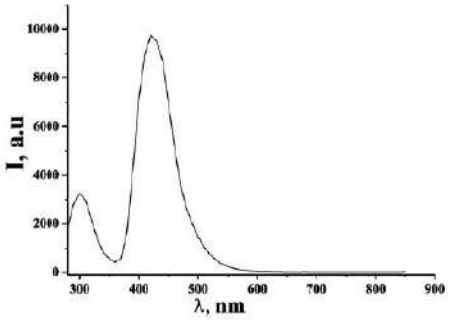

Fig. 2. Fluorescence spectrum for 1 mM ammonia, interacted with OPA. The fluorescence was recorded with an Infinite M200 spectrofluorometer (TECAN) at an excitation wavelength of 360 nm.

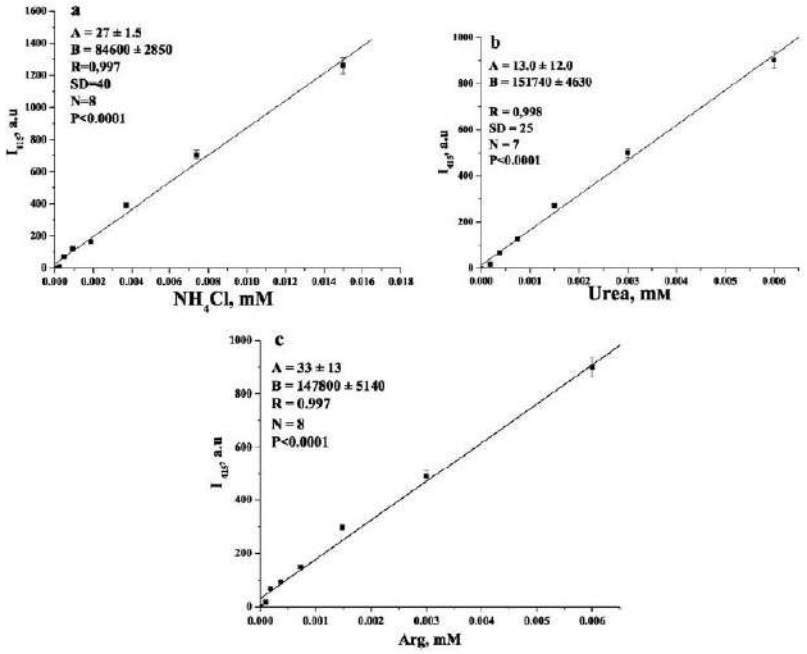

Fig. 3. The dependence of the fluorescence intensities (in arbitrary units – a.u) of final reaction product on the concentrations of ammonia in final mixture (a), urea (b) and Arg (c) with OPA-based method. Fluorescence emission values were registered at 415 nm (under excitation at 360 nm) using a Quantech digital filter fluorometer (Thermo Scientific, United States).

C_{st} – concentration of standard ammonia solution;

N – Dilution Factor of the tested Sample 1;

2nd step. Treatment of the tested Sample 1 with urease followed by estimation of total ammonia content (Eq. (1)) in the resulted Sample 2, taking into account factors of dilution of the tested sample, calculation of an average value of total ammonia content in this sample. Calculation of endogenous Urea content in the Sample 2 according to Eq. (2):

$$C^e_{Ureа} = (C^t_a - C^e_a) \quad (2)$$

Table 1
Characteristics of the current OPA-based and the reference methods.

Analyte	Parameter	Method				
		OPA		[40]	DMO [35]	
		F[a] (current paper)	S[b] [36]		F	S
		λ_{ex} = 364 nm λ_{em} = 425 nm	λ = 360 nm	λ = 340 nm	λ_{ex} = 380 nm λ_{em} = 510 nm	λ = 480 nm
Arg	LR[c], μM	0.1–6.00	0.95–60	2.9–100	0.06–200	7.0–100
	LOD[d], μM	0.034	0.258	0.636	0.045	1.52
	LOQ[e], μM	0.103	0.85	2.1	0.149	5
	FI[f]	147,800	–	–	747	–
	ε[g]	–	17		–	11.6
Urea	LR, μM	0.19–24.0	2.0–250	2.5–117	4.0–250	5.0–100
	LOD, μM	0.065	0.55	0.76	1	1.21
	LOQ, μM	0.198	1.8	2.5	3.3	4
	FI	151,740	–	–	872	–
	ε	–	9		–	14.5
NH_4^+	LR, μM	0.23–15.0	0.7–250	5.6–194.4	ND[h]	ND
	LOD, μM	0.078	0.15	1.18		
	LOQ, μM	0.236	0.5	3.9		
	FI	84,600	–	–		
	ε		6			

[a] F – fluorometric mode of detection.
[b] S – spectrophotometric mode of detection.
[c] LR – linearity range.
[d] LOD – limit of detection.
[e] LOQ – limit of quantitation.
[f] FI – fluorence intensity at 1 mM analyte concentration.
[g] ε – millimolar extinction, $mM^{-1}\ cm^{-1}$ (spectrophotometric detection)
[h] ND – not determined.

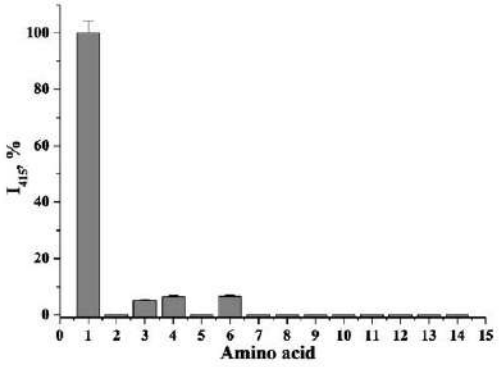

Fig. 4. Fluorescence responses of the arginase/urease-OPA-based approach toward various 0.5 mM amino acids: 1 – Arg; 2 – Can; 3 – Gln; 4 – Lys; 5 – Trp; 6 – Glu; 7 – Pro; 8 – His; 9 – Ala; 10 – Cys; 11 – Leu; 12 – Tyr; 13 – Ser; 14 – Orn. The analytical signal was exposed in relative units (%) of referred to the maximum value for Arg, taken as 100%. Fluorescence emission values were registered at 415 nm (under excitation at 360 nm) using a Quantech digital filter fluorometer (Thermo Scientific, United States)

3rd step. Treatment of the Sample 2 with arginase and urease, followed by estimation of total ammonia content in the resulted Sample 3, taking into account factors of dilution of the tested sample, calculation of an average value of total ammonia content in the Sample 3. Calculation of endogenous Arg content in the tested sample according to Eq. (3):

$$C_{Arg} = (C^t{}_a - C^e{}_a - C^e_{urea}) \quad (3)$$

where C_{Arg}, $C^t{}_a$ and $C^e{}_a$ — concentrations of endogenous Arg, average contents of total and endogenous ammonia in the tested sample, respectively.

The concentration of endogenous analytes in initial serum was calculated taking into account the corresponding factors of dilution (from serum to Samples 1–3).

2.4.3. The reference of Arg determination

As a reference, another enzymatic method of Arg assay based on the usage of arginase/urease and 2.3-butanedione monoxime (DMO) [35] was exploited. Urea, the product of the enzymatic hydrolysis of Arg by arginase, reacts with DMO and forms a product which can be determined fluorometrically at 510 nm, under excitation at 360 nm.

3. Results and discussion

3.1. The characteristics of a developed method

The reactions for fluorometric determination of Arg by arginase/urease-based method are presented in Fig. 1. Analytical signal is created due to the two-step enzymatic conversion of Arg to ammonium ions. Arginase catalyzes the conversion of Arg to Orn and urea (stage I). Under urease-catalyzed hydrolysis, urea produces ammonium ion (stage II). The latter reacts selectively in the presence of sulphite with OPA (compound No. 1) in an alkali medium (stage III, chemical reaction), the concentration of resulted OPA-ammonium product – 2 *H*-isoindole-1-thiol (compound No. 2) can be determined fluorometrically [39].

The fluorescence spectrum of the final analytical product is presented on Fig. 2. The fluorescence emission peak is located at 415 nm with excitation at 360 nm. To optimize the conditions of the chemical reaction, OPA concentration (from 7.5 to 15 mM), heating time (10–30 min) and temperature (25–65 °C) were tested. The maximal sensitivity was shown to be under the following conditions of chemical reaction: 14 mM OPA in incubation mixture, 15 min of heating in water bath at 60 °C.

The optimizations of enzymatic steps of the reaction were carried out too. Optimal concentrations of enzymes in the incubation mixture were estimated as following: 3 U/mL for arginase and 16 U/mL for urease. Fig. 3 demonstrates the dependencies of fluorescence intensity (in arbitrary units - a.u) of the final product (OPA–ammonium) on concentration of ammonium ions (Fig. 3 a), urea (Fig. 3 b) and Arg (Fig. 3 c). The analytical characteristics of OPA-based methods for assay of Arg (as well as urea and ammonia), obtained from Fig. 3, are summarized in Table 1 in relation to other enzymatic methods. The analogue of millimolar extinction coefficient (ε) for fluorometric method (FI) coincides with the slope of the regression line (B) of the calibration graph.

It is worth mentioning, that arginase-catalyzed hydrolysis of 1 mol of Arg generates 1 mol of urea and urease-catalyzed digestion of 1 mol of urea generates 2 mol of ammonia (Fig. 1), thus, 1 mol of Arg under total arginase/urease hydrolysis generates 2 mol of ammonia. Comparison of FI values (in %) allows to appreciate the level of analyte's conversion on each stage of reaction. The levels of Arg conversion to urea and then to ammonia are 97.5% and 87.4%, respectively; the level of urea's conversion to ammonia is 89.7%.

The main characteristics of the developed and other enzymatic methods of Arg assay were summarized in Table 1.

The high selectivity is the necessary demand for each analytic method. To study the selectivity of the developed approach, various 0.5 mM amino acids were treated step-by-step with arginase, urease, OPA in the same manner, as it was described for Arg and the fluorescence responses of resulted products were detected (Fig. 4). It's worth

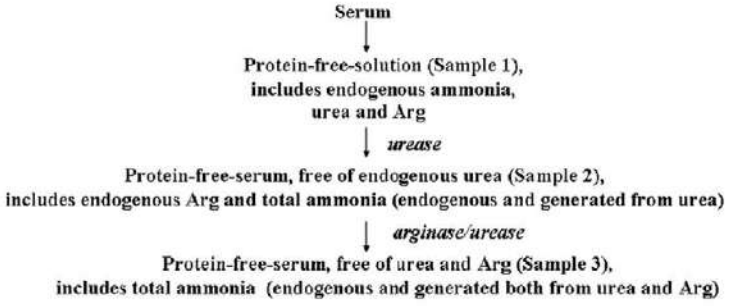

Fig. 5. The principal scheme of Arg analyses in serum.

Table 2
Concentrations of endogenous Arg, urea and ammonia in the sample of pooled blood serum estimated with two enzymatic fluorometric methods.

Method	Analyte concentration		
	NH_4^+, μM	Urea,	Arg, μM
OPA-arginase/urease based	38 ± 2.5	3.5 ± 0.2	72 ± 4.3
CV[a], %	6.6	5.4	6.0
DMO-arginase based	ND	3.7 ± 0.2	71 ± 3.9
CV, %	ND	6.8	5.5

[a] CV – coefficient of intra assay variation. Values are expressed as mean ± SD.

mentioning, that the concentration of potential interfering substances corresponds with those in blood serum. Only Gln, Lys and Glu demonstrated insignificant outputs (about 6%) in comparison with Arg (100%). The absence of signals from other amino acids has proved the high selectivity of arginase to Arg and the high purity of the arginase preparation.

Thus, the developed fluorometric OPA-based enzymatic method for the quantitative analysis of Arg is highly sensitive (see Table 1) and rather selective (Fig. 4). Another advantage of the suggested method is the possibility to analyze simultaneously the Arg, urea and ammonia in the sample.

It is worth mentioning, that the reaction between ammonia and OPA can also proceed at room temperature, though it needs longer incubation time (data not shown). This feature of the suggested method is prospective for the development of portable test system with automatic variant of assay as well as for screening study or semi-quantitive appreciation of Arg level. Thus, the proposed analytical method being sensitive, low-cost, highly selective and suitable for both routine and micro-volume formats, will be promising in laboratories of clinical diagnostics for assay of Arg (and in the same time, urea and ammonia) in blood.

3.2. Assay of Arg in human blood serum

The developed method was tested on the pooled sample of human serum collected from ten practically healthy young men (20–40 years) – patients of hospital (see Materials and methods). The general scheme of Arg assay in protein-free serum by OPA-based method is demonstrated in Fig. 5.

Serum contains endogenous Arg, urea and ammonia. To estimate Arg in serum, initial urea was converted to ammonium ions by urease hydrolysis and initial (endogenous) Arg was converted to ammonium ions by arginase/urease treatment (see Fig. 1 and Fig. 5). A level of endogenous Arg is calculated as a difference between total and endogenuos ammonia concentrations, estimated fluorometrically with OPA-reagent.

The sample of pooled serum was analyzed with the usage of the current method in comparison with the DMO-based one (Table 2). The reference arginase-DMO-based method was shown to be sensitive, selective and valid for the analysis of commercial Arg-containing pharmaceuticals and wine [35].

The proposed analytical methods were compared using statistical analysis. The Student's *t*-test was applied and does not reveal significant difference between the experimental values obtained in the sample analysis by the two methods. The calculated t-value ($t_{calc} = 0.96$) in the case of urea assay was found to be less than the critical t-value ($t_{crit} = 4.3$) at 5% significance level. The calculated t-value ($t_{calc} = 0.52$) for Arg assay was found to be less than critical t-value ($t_{crit} = 4.3$) at 5% significance level.

The values of Arg concentration in the tested sample, obtained by two approaches, demonstrate a strong correlation ($R = 0.986$). The results of Arg, urea and ammonia analyses, presented in Table 2, correspond to the reported normal values for healthy adults: 12–41 μM for ammonia [29,41] and 3.3–6.6 mM for Urea [42]. The assessment of the validation parameters of the method is given in Table 3. It is shown that the results of the accuracy research of the method of Arg, urea and ammonia determination meet requirements for the permissible limits of ±10.0%.

Thus, the enzymes of Arg metabolism are promising tools for elaboration of selective methods for quantitative Arg analysis.

The proposed fluorometric method for Arg assay based on the usage of two enzymes (arginase and urease) and orthophthalaldehyde in the presence of sulfite in alkali medium was developed. A linearity range of the arginase-urease-OPA method is 0.1–6.00 μM Arg, with a LOD of 34 nM. A novel method was used for Arg analysis in real sample of pooled blood serum of practically healthy adults. The obtained results were shown to be in a good correlation with the data estimated by the reference method (Table 2) as well as with the reported normal values of Arg in human serum/plasma estimated by different modern methods, summarized in Table 4. The advantage of this method is the possibility to test in parallel (in the same time) a lot of samples without complicated pre-treatment.

4. Conclusion

The development of novel valid methods for Arg determination, including enzymatic ones, is necessary for clinical diagnostics. The enzymes of Arg metabolism are promising tools for elaboration of highly selective and sensitive methods for quantitative Arg analysis. We have developed fluorometric enzymatic method for Arg assay based on recombinant arginase, commercial urease and o-phthalaldehyde (OPA). A linearity range of the fluorometric arginase-urease-OPA method is from 100 nM to 6 μM with a limit of detection of 34 nM Arg. The method was used for the quantitative determination of Arg in the pooled sample of blood serum. The obtained results proved to be in a good correlation with the reference enzymatic method and literature data. It is worth mentioning, that the reaction between ammonia and OPA can also proceed at room temperature. This feature of the suggested method is prospective for the development of portable test system with automatic variant of assay as well as for screening study or semi-quantitive appreciation of Arg level. Thus, the proposed analytical method being sensitive, valid, low-cost, highly selective and suitable for both routine and micro-volume formats, will be promising in laboratories of clinical diagnostics for Arg assay in blood. It would be useful for the simultaneous determination of Arg, urea and ammonia in blood: to predict a potential risk of metabolic disorders, hyperargininemia, autoimmune and other diseases, as well as to monitor Arg level under medical treatment with arginase in anticancer therapy. Due to high stability of arginase, the development and production of enzymatic kits for Arg assay based on the proposed method seem to be quite promising.

Table 3
The results of the accuracy and convergence research of the fluorometric quantitative determination of target analytes in serum samples by the developed method.

The criteria of accuracy and precision	Criteria	NH_4^+, μM	Urea, mM	Arg, μM	Conclusion
The relative standard deviation, RSD_0	$RSD_0 \le 1.12$	1.00	0.012	1.00	Satisfies the requirements
Critical values of the one-sided confidence interval, x	$x \le 3.2\%$	2.48	0.029	2.48	Satisfies the requirements
Criterion of the systematic error insignificance $\delta \le \Delta prec/\sqrt{18}$ if it is not satisfied 1), then 2) $\delta \le max\delta tot = 2.3$		1.63%	0.82%	1.45%	Satisfies the requirements (the second criterion)
The overall conclusion on methods					Is correct

Table 4
The normal ranges and medium values of Arg level, estimated with different methods in blood serum/plasma of healthy human.

Method	L-Arg, μM		Object	References
	Ranges	Average		
Arginase-urease-DMO	50.6–103	80 ± 7.3	Serum	[37]
ELISA[a]	56.4–125.4	–	Plasma	[43]
ELISA	–	59 ± 59	Plasma	[44]
ELISA	56.4–125.4	–	Plasma	[43]
HPLC[b]	82.4–108.9	95.7	Serum	[45]
HPLC	–	94 ± 26	Plasma	[46]
LC-Fluorescence[c]	–	87.9 ± 19.5	Plasma	[16]
LC-Fluorescence	–	110 ± 24	Plasma	[47]
LC-Fluorescence	–	60.7 ± 19.0	Plasma	[48]
SPE-MS/MS[d]	–	162 ± 76	Plasma	[49]
LC-MS/MS[e]	41 ± 114	–	Plasma	[29]
LC-MS/MS	–	87 ± 35	Plasma	[50]
LC-MS/MS	–	74 ± 19	Plasma	[30]
LC-MS/MS	–	65.6 ± 23.4	Plasma	[31]
LC-MS/MS	52.2–124.7	–	Plasma	[43]
LC-MS/MS	–	65.3 ± 21.3	Plasma	[51]

[a] ELISA – enzymatic "ELISA" test.
[b] HPLC – high performance liquid chromatography.
[c] LC-Fluorescence – liquid chromatography with fluorescence detection.
[d] SPE-MS/MS – tandem mass spectrometry without the need for chromatography or sample derivatisation.
[e] LC-MS/MS – liquid chromatography-tandem mass spectrometry.

Ethical statement

This article does not contain any studies with human participants or animals performed by any of the authors.

Conflict of interest

The authors declare that there is no conflict of interests regarding the publication of this paper.

Acknowledgements

This work was financially supported by NAS of Ukraine in the frame of the Scientific-technical program (Project 29/2015), scientific program "Sensors for Medical, Environmental, Industrial, and Technological Needs: Metrological Support and Trial Operation" (Project 5/3-2016), by fellowship of President of Ukraine for young scientists (Stasyuk N.) in 2016 and by NATO (Project CBP.NUKR.SFP 984173).

References

[1] N.A. Mew, B.C. Lanpher, A. Gropman, K.A. Chapman, K.L. Simpson, in: R.A. Pagon (Ed.), Urea Cycle Disorders Overview GeneReviews, 63(1), University of Washington, Seattle 1993–2015, pp. 40–48.
[2] J. Appleton, Altern. Med. Rev. 7 (6) (2002) 512–522.
[3] D. Tsikas, G. Wu, Amino Acids 47 (9) (2015) 1697–1702.
[4] R.H. Böger, J. Nutr. 134 (10) (2004) 2842S–2847S.
[5] K.D. Schlüter, R. Schulz, R. Schreckenberg, Front. Physiol. 6 (65) (2015) 1–8.
[6] J. Pernow, C. Jung, Cardiovasc. Res. 98 (3) (2013) 334–343.
[7] A.A. Kayacelebi, J. Willers, V.V. Pham, A. Hahn, J.Y. Schneider, S. Rothmann, J.C. Frölich, D. Tsikas, Amino Acids 47 (9) (2015) 1885–1891.
[8] A. Haghikia, A.A. Kayacelebi, B. Beckmann, E. Hanff, R. Gold, A. Haghikia, D. Tsikas, Amino Acids 47 (9) (2015) 1837–1845.
[9] S. Luhan, Z.G. Li, Int. J. Rheum. Dis. 13 (4) (2010) 284–287.
[10] H. Maarsingh, T. Pera, H. Meurs, Arch. Pharmacol. 378 (2) (2008) 171–184.
[11] C.C. Kao, S.H. Wedes, J.W. Hsu, K.M. Bohren, S.A. Comhair, F. Jahoor, S.C. Erzurum, Pulm. Circ. 5 (1) (2015) 124–134.
[12] J.A. Scott, H. Grasemann, Immunol. Allergy Clin. N. Am. 34 (4) (2014) 767–775.
[13] K.A. Wijnands, T.M. Castermans, M.P. Hommen, D.M. Meesters, M. Poeze, Nutrients 7 (3) (2015) 1426–1463.
[14] A. Jay, M. Seeterlin, E. Stanley, R. Grier, JIMD Rep. 9 (2013) 121–124.
[15] A. Schlune, S.v. Dahl, D. Häussinger, R. Ensenauer, E. Mayatepek, Amino Acids 47 (9) (2015) 1751–1762.
[16] B. Wilcken, Mol. Genet. Metab. 81 (1) (2004) S86–S913.
[17] C. Lacroix, C. Caubet, A. Gonzalez-de-Peredo, B. Breuil, D. Bouyssié, A. Stella, L. Garrigues, C. Le Gall, A. Raevel, A. Massoubre, J. Klein, S. Decramer, F. Sabourdy, F. Bandin, O. Burlet-Schiltz, B. Monsarrat, J.P. Schanstra, J.L. Bascands, Mol. Cell. Proteomics 13 (12) (2014) 3421–3434.
[18] J. Häberle, N. Boddaert, A. Burlina, A. Chakrapani, M. Dixon, M. Huemer, D. Karall, D. Martinelli, P.S. Crespo, R. Santer, A. Servais, V. Valayannopoulos, M. Lindner, V. Rubio, C. Dionisi-Vici, J. Rare Dis. 7 (2012) 32.
[19] C.M. Rüegger, M. Lindner, D. Ballhausen, M.R. Baumgartner, S. Beblo, A. Das, M. Gautschi, E.M. Glahn, S.C. Grünert, J. Hennermann, M. Hochuli, M. Huemer, D. Karall, S. Kölker, R.H. Lachmann, A. Lotz-Havla, D. Möslinger, J.M. Nuoffer, B. Plecko, F. Rutsch, R. Santer, U. Spickerkoetter, C. Staufner, T. Stricker, F.A. Wijburg, M. Williams, P. Burgard, J. Häberle, J. Inherit. Metab. Dis. 37 (2014) 21–30.
[20] C.R. Martens, J.M. Kuczmarski, S. Lennon-Edwards, D.G. Edwards, J. Cardiovasc. Pharmacol. 63 (1) (2014) 40–48.
[21] D.N. Wheatley, Anti-Cancer Drugs 15 (2004) 825–833.
[22] T.L. Lam, G.K. Wong, H.Y. Chow, P.N. Cheng, S.C. Choi, T.L. Chow, S.Y. Kwok, R.T. Poon, D.N. Wheatley, W.H. Lo, Y.C. Leung, Pigment Cell Melanoma Res. 24 (2) (2011) 366–376.
[23] G. Shuvayeva, Y. Bobak, N. Igumentseva, R. Titone, F. Morani, O. Stasyk, C. Isidoro, BioMed Res. Intern. 2014 (2014) 1–10.
[24] B. Vynnytska-Myronovska, Y. Bobak, Y. Garbe, C. Dittfeld, O. Stasyk, L.A. Kunz-Schughart, Int. J. Cancer 130 (9) (2012) 2164–2175.
[25] I. Pavlyk, Y. Rzhepetskyy, A.K. Jagielski, J. Drozak, A. Wasik, G. Pereverzieva, M. Olchowik, L.A. Kunz-Schugart, O. Stasyk, M.J. Redowicz, Amino Acids 47 (1) (2015) 199–212.
[26] O.V. Stasyk, Y.R. Boretsky, M.V. Gonchar, A.A. Sibirny, Cell Biol. Int. 39 (3) (2015) 246–252.
[27] N. Stasyuk, G. Gayda, L.R. Fayura, Y.R. Boretskyy, M.V. Gonchar, A.A. Sibirny, Food Chem. 201 (2016) 320–326.
[28] G. Gayda, N. Stasyuk, H. Klepach, M. Gonchar, Living organisms and bioanalytical approaches for detoxification and monitoring of toxic compounds, in: A. Sibirniy, et al., (Eds.), Lviv-Rzeszow 2015, pp. 73–88.
[29] C.N. Luneburg, V. Xanthakis, E. Schwedhelm, L.M. Sullivan, R. Maas, M. Anderssohn, U. Riederer, N.L. Glazer, S.V. Ramachandran, H. Rainer, R.H. Böger, J. Nutr. 141 (12) (2011) 2186–2190.
[30] E. Schwedhelm, R. Maas, J. Tan-Andresen, J. Tan-Andresen, F. Schulze, U. Riederer, R.H. Böger, J. Chromatogr. B 851 (2007) 211–219.
[31] E. Schwedhelm, J. Tan-Andresen, R. Maas, U. Riederer, F. Schulze, R.H. Böger, Clin. Chem. 51 (2005) 1268–1271.
[32] N. Stasyuk, O. Smutok, G. Gayda, Y. Koval'chuk, M. Gonchar, J. Mater. Sci. Eng. A. 1 (2011) 819–827.
[33] N. Stasyuk, O. Smutok, G. Gayda, M. Gonchar, Biosens. Bioelectron. 37 (1) (2012) 46–52.
[34] N.Y. Stasyuk, G.Z. Gayda, M.V. Gonchar, I. Sens. Actuators B 204 (2014) 515–521.
[35] N. Stasyuk, G. Gaida, M. Gonchar, Appl. Biochem. Microbiol. 49 (5) (2013) 529–534.
[36] N.Y. Stasyuk, S.R. Bass, G.Z. Gayda, H.S. Yepremyan, M.V. Gonchar, ScienceRise 6/1 (11) (2015) 43–48 (In Ukrainian).
[37] Patent of Ukraine u 2015 12716. An enzymatic method of L-arginine assay in human serum/Stasyuk N.Ye, Gayda G.Z., Zakalskiy A.E.,Zakalska O.M., Gonchar M.V. - 2016. - 14 pages (in Ukrainian).
[38] W.H. Marsh, B. Fingerhut, H. Miller, Clin. Chem. 11 (1965) 624–627.
[39] C.T. Kuo, P.Y. Wang, C.H., J Chromatogr. A. 1085 (2005) 91–97.
[40] http://bc-d.eu/katalogNZYTech2014.pdf.
[41] Tables of Normal Values. http://www.ccpe-cfpc.com/en/pdf_files/drug_lists/normal_values.pdf, 2013.
[42] Investigations Operations Manual. Appendix C. Blood Serum Chemistry. Normal Values. http:www.fda.gov/downloads/ICECI/Inspections/IOM/UCM135835, 2015.
[43] F. Andrade, M. Llarena, S. Lage, L. Aldamiz-Echevarria, Tandem Mass Spectrom. 53 (5) (2015) 787–792.
[44] M. Huemer, B. Simma, D. Mayr, D. Möslinger, A. Mühl, I. Schmid, H. Ulmer, O.A. Bodamer, J. Inherit. Metab. Dis. 35 (5) (2012) 817–821.
[45] T. Schön, D. Elias, F. Moges, E. Melese, T. Tessema, O. Stendahl, S. Britton, T. Sundqvist, Eur. Respir. J. 21 (3) (2003) 483–488.
[46] T. Teerlink, R.J. Nijveldt, S. de Jong, P.A.M. van Leeuwen, Anal. Biochem. 303 (2) (2002) 131–137.
[47] B. Marescau, G. Nagels, I. Possemiers, M.E. De Broe, I. Becaus, J.M. Billiouw, W. Lornoy, P.P. De Deyn, Metabolism 46 (1997) 1024–1031.
[48] J. Pi, Y. Kumagai, G. Sun, N. Shimojo, J. Chromatogr. B 742 (2000) 199–203.
[49] G. Weaving, B.F. Rocks, M.P. Bailey, M.A. Titheradge, J. Chromatogr. B 874 (2008) 27–32.
[50] M.J. Bishop, B. Crow, D. Norton, E. Paliakov, J. George, J.A. Bralley, J. Chromatogr. B 59 (2007) 164–169.
[51] D.E. Wilcken, J. Wang, A.S. Sim, K. Green, B. Wilcken, J. Inherit. Metab. Dis. 29 (2006) 30–37.

Оригінал доступний за посиланням: https://doi.org/10.1016/j.saa.2016.07.019

Анотація: *У поточній роботі запропоновано новий ензиматично-хімічний метод визначення вмісту L-аргініну в харчових продуктах та алкогольних напоях, який ґрунтується на використанні для гідролізу L-аргініну аргініндеімінази Mycoplasma hominis (далі – АДІ), виділеної із клітин рекомбінантного штаму Escherichia coli BL-21 (pET3d-ADI). Генерований в ензиматичній реакції аміак реагує у присутності сульфіту з о-фталевим альдегідом з утворенням продукту, який визначається флуориметрично або спектрофотометрично. Нами запропоновано та опрацьовано на зразках харчових продуктів та алкогольних напоїв ензиматично-хімічний метод із флуориметричною та спектрофотометричною детекцією кінцевого продукту реакції, що дозволяє підвищити точність аналізу L-аргініну за рахунок високої чутливості та селективності, суттєво знижує матеріальні затрати, є простим та швидким у виконанні в порівнянні із відомими ензиматичними підходами.*

УКРАЇНА

(19) **UA** (11) **108773** (13) **U**

(51) МПК
G01N 21/64 (2006.01)
G01N 33/52 (2006.01)

ДЕРЖАВНА СЛУЖБА ІНТЕЛЕКТУАЛЬНОЇ ВЛАСНОСТІ УКРАЇНИ

(12) ОПИС ДО ПАТЕНТУ НА КОРИСНУ МОДЕЛЬ

(21) Номер заявки: **u 2016 01804**
(22) Дата подання заявки: **25.02.2016**
(24) Дата, з якої є чинними права на корисну модель: **25.07.2016**
(46) Публікація відомостей про видачу патенту: **25.07.2016, Бюл.№ 14**

(72) Винахідник(и):
Гайда Галина Зуфарівна (UA),
Стасюк Наталія Євгенівна (UA),
Файюра Любов Романівна (UA),
Борецький Юрій Романович (UA),
Сибірний Андрій Андрійович (UA),
Гончар Михайло Васильович (UA)

(73) Власник(и):
ІНСТИТУТ БІОЛОГІЇ КЛІТИНИ НАН УКРАЇНИ,
вул. Драгоманова, 14/16, м. Львів-5, 79005 (UA)

UA 108773 U

(54) ЕНЗИМАТИЧНО-ХІМІЧНИЙ МЕТОД ВИЗНАЧЕННЯ ВМІСТУ L-АРГІНІНУ В ХАРЧОВИХ ПРОДУКТАХ ТА АЛКОГОЛЬНИХ НАПОЯХ

(57) Реферат:

Спосіб визначення L-аргініну в харчових продуктах та алкогольних напоях ґрунтується на ензиматичному розщепленні L-аргініну до продукту, що визначається в наступній хімічній реакції. Для гідролізу L-аргініну використовується аргініндеіміназа Mycoplasma hominis, виділена із клітин рекомбінантного штама Escherichia coli BL-21 (pET3d-ADI). Генерований в аргініндеіміназній реакції амоній утворює з о-фталевим альдегідом продукт, який визначається флуориметрично або спектрофотометрично.

$$L-\text{Аргінін} + H_2O \xrightarrow{\text{аргіназа}} \text{Сечовина} + L-\text{Орнітин}$$

$$\text{Сечовина} + H_2O \xrightarrow{\text{уреаза}} 2NH_3 + CO_2$$

$$2\text{-Оксоглутарат} + \text{NADPH} + NH_4^+ \xrightarrow{\text{глутамат дегідрогеназа}} \text{L-Glu} + \text{NADP}^+ + H_2O$$

Фіг. 1

Корисна модель належить до харчової промисловості та може використовуватись у виноробстві, медицині та фармакології.

У наш час на виноробство - цю високоприбуткову галузь харчової індустрії, працюють багато науково-дослідних установ та агропромислових об'єднань, які мають за мету забезпечити належну якість продукції (або її покращення) та розширення асортименту. Саме тому виноробство потребує на кожному етапі процесу виробництва алкогольних напоїв досконалих методів аналізу, що неможливе без використання найсучасніших приладів.

Основними недоліками традиційних методів аналізу, які застосовуються для контролю якості харчових продуктів, зокрема вин, є недостатні селективність та чутливість, потреба у високовартісному та/або громіздкому обладнанні і висококваліфікованому персоналі для його обслуговування, а також значна складність і тривалість аналітичної процедури. Досконалих методів кількісного аналізу цільових аналітів - складових вин - досі не існує, тому створення нових селективних, чутливих та економічно вигідних аналітичних підходів є надзвичайно актуальним завданням аналітичної біотехнології.

Амінокислота L-Аргінін (α-аміно-δ-гуанідино-валеріанова кислота) - попередник L-орнітину, L-цитруліну, L-глутатіону, γ-аміномасляної кислоти, спермітину та інших сполук - одна із найбільш поширених амінокислот, що міститься у виноградному соку і вині та тісно пов'язана з рівнем етилкарбамату (уретану) у напоях [1-4]. Встановлено, що канцерогенний етилкарбамат (ЕК), кінцевий продукт перетворення L-Аргініну (Arg) до сечовини та конденсації останньої з етанолом, може генеруватись у винах під дією мікроорганізмів [4-8].

Іншим попередником канцерогенного ЕК у винах є цитрулін, який утворюється в процесі метаболізму Arg за використання аргініндеімінази (АДІ) під впливом молочно-кислих бактерій [4-7].

Занепокоєння у зв'язку з присутністю ЕК у кріплених винах викликано двома аспектами. По-перше, кріплення більшості видів червоних вин відбувається приблизно всередині бродіння, тобто в період, коли вміст сечовини в суслі є максимальним. По-друге, довготривалий додатковий нагрів, передбачений технологіями створення вин типу Мадера, підвищує швидкість утворення ЕК із сечовини. Таким чином, утворення ЕК або його сполук є технологічно обумовленим процесом [9].

Досліджено, що якщо концентрація Arg в соку перевищує 1000 мг/л (5,0 мМ), то потенційна концентрація ЕК у вині буде вища за 15 мкг/л. У США такий рівень ЕК є гранично допустимою нормою, тоді як у Канаді та Чехії легалізована норма ЕК у вині становить 30 мкг/л [3, 9].

Існує два підходи до того, як запобігти критичному рівню ЕК в вині та забезпечити його високу якість: проводити моніторинг ЕК на всіх стадіях виробництва вина або аналізувати попередники ЕК, зокрема Arg, у вихідній сировині (фруктових соках) та в ході технологічного процесу [5].

На сьогодні визначення концентрації ЕК у винах та соках здійснюють за допомогою дорогих приладів, основаних на методах високоефективної рідинної хроматографії (ВЕРХ) або газової хроматографії (ГХ), поєднаних із мас-спектрометрією (МС) або тандемною мас-спектрометрією (МС/МС): ГХ/МС, ГХ/МС/МС, ВЕРХ/МС/МС [5]. Більшість аналізів виконується в автоматичному інжекторному проточному режимі.

Визначення вмісту Arg зазвичай проводиться методами іонообмінної хроматографії, флуориметрії, спектрофотометрії, капілярного електрофорезу, полярографії, лазерної флуоресцентної спектроскопії, ВЕРХ та ін. [5, 10].

Метод ВЕРХ є достатньо чутливим і відтворюваним, проте він вимагає дорогого обладнання, органічних розчинників високої якості та дорогих дериватизуючих реагентів, що робить відповідні аналізи дорогими для рутинного клінічного аналізу. Крім цього, час підготовки та аналізу зразка є тривалим і складає від моменту дериватизації до одержання кількісних даних 1-2 доби. Тому подальше створення надійних економічно вигідних високоселективних та чутливих методів визначення Arg в харчовій промисловості, у виноробстві зокрема, є надзвичайно актуальним завданням. Таким вимогам відповідають ензиматичні методи.

На основі проведення патентно-інформаційних досліджень авторами роботи встановлено, що на сьогодні в галузі аналітичної біотехнології існує обмежена кількість даних щодо розробки ензиматичних методів визначення Arg. При цьому, існуючі ензиматичні тест-системи є переважно мультиферментними (за використання від 2-х до 5-ти ферментів) із спектрофотометричним детектуванням кінцевого продукту реакції [11-13].

Принцип визначення Arg мультиензимним методом за використання трьох ферментів (аргінази, уреази та глутаматдегідрогенази) представлен на Фіг. 1 [12].

Метод ґрунтується на спектрофотометричному моніторингу швидкості перетворення кінцевого продукту реакцій NADH (або NADPH) у NAD^+ (або $NADP^+$, відповідно), із врахуванням

коефіцієнта молярної екстинції NADH (6,22 $мМ^{-1} \cdot см^{-1}$). На основі наведеної схеми (Рис. 1) розроблено цілу низку серійних аналітичних наборів для визначення Arg (Sigma, Enzytec™, Elisa, Megazyme та ін).

У попередніх дослідженнях нами запропоновано біосенсорні підходи [14-17] та ензиматично-хімічні методи визначення Arg із спектрофотометричним та флуориметричним детектуванням кінцевого продукту [18-22]. Однак усі вони базуються на використанні двох ферментів - рекомбінантної аргінази І печінки людини та уреази. У Таблиці 1 наведено порівняльну характеристику відомих та запропонованих нами раніше ензиматичних методів визначення Arg у харчових продуктах та крові.

Таблиця 1

Порівняльна характеристика ензиматичних методів визначення Arg

Метод	Фермент	Лінійний діапазон, μM	Чутливість, μM	Джерела інформації:
[1]ОФА-[2]ФЛ, $\lambda_{зб}$=364 нм, $\lambda_{ем}$=415 нм	АДІ	0,35-24	0,25	Поточна заявка, [18]
ОФА-[3]СФ, Λ=340 нм	АДІ	0,7-50	0,55	Поточна заявка, [18]
[4]ДМО-СФ, λ=480 нм	Аргіназа	7-100	5,0	[10, 19]
ДМО-ФЛ, $\lambda_{зб}$=380 нм, $\lambda_{ем}$=510 нм	Аргіназа	0,06-200	0,045	[10, 20]
ОФА-СФ, λ=362 нм	Аргіназа-уреаза	0,9-60,0	0,85	[10, 21]
ОФА-ФЛ, $\Lambda_{зб}$=364 нм, $\lambda_{ем}$=425 нм	Аргіназа-уреаза	0,09-6,0	0,080	[22]
Мультиензимний, СФ, λ=340 нм	Аргіназа, уреаза, глутаматдегідрогеназа	до 470	2,0	[11]
Мультиензимний, СФ, λ=340 нм	Аргіназа, уреаза, глутаматдегідрогеназа	2,9-100	2,1	[12]
Мультиензимний, СФ, λ=555 нм	АДІ, аргініносукцинатсинтаза; піруватфосфатдикіназа; піруват оксидаза, пероксидаза хрону	до 100	-	[13]

[1]ОФА - о-фталевий альдегід;
[2]ФЛ - флуориметрична детекція кінцевого продукту реакції;
[3]СФ - спектрофотометрична детекція кінцевого продукту реакції;
[4]ДМО - 2,3 - бутандіонмонооксим.

Аналізуючи існуючі на сьогодні ензиматичні методи визначення Arg (Таблиця 1), можна зробити висновок, що переважна їх більшість потребує використання каскаду із кількох ферментів та екзогенних кофакторів, що додатково підвищує вартість методів та ускладнює процедуру аналізу.

Переважна кількість існуючих методів визначення концентрації головних компонентів вин є складними: потребують значних витрат часу, дорогого обладнання. Аналіз літературних потоків засвідчує, що більшість методів має низку недоліків, а саме, недостатню селективність до цільового аналіту, спричинену позитивною реакцією на гуанідинові сполуки (хімічні методи), громіздкість та велика вартість апаратури, необхідність додаткової пробопідготовки та високої кваліфікації персоналу (фізико-хімічні методи), потреба у додаткових реагентах або ферментах (ензиматичні підходи).

Нові методи визначення Arg, що ґрунтуються на використанні аргініно-гідролізуючих ферментів (АДІ, аргінази та ін.), можуть суттєво спростити систему моніторингу рівня канцерогенного етилкарбамату у алкогольних напоях, соках та інших харчових продуктах, одержаних в результаті процесів ферментації. Ензиматичні методи можуть стати основою при створенні нових скринінгових тест-систем для моніторингу Arg в біологічних рідинах, зокрема крові, які на даний час відсутні в арсеналі засобів вітчизняної клінічної діагностики.

Під час підготовки заявки на пропоновану корисну модель авторами не було виявлено повідомлень про ензиматичні методи визначення концентрації Arg в винах та соках за використання аргініндеімінази (АДІ) та о-фталевого альдегіду (ОФА).

В основу запропонованої корисної моделі поставлено задача створення такого ензиматичного методу аналізу вмісту Arg, який дозволяє підвищити точність визначення цільового аналіту за рахунок високої чутливості та селективності, суттєво знижує матеріальні затрати, є простим та швидким у виконанні в порівнянні із відомими мультиферментними підходами.

Поставлена задача розв'язується шляхом ензиматично-хімічного визначення вмісту Arg у напоях (винах та соках) за використання високоселективного до Arg фермента - аргініндеімінази (далі - АДІ), виділеної із клітин рекомбінантного штаму Escherichia coli BL-21 (pET3d-ADI), що містить оптимізований ген аргініндеімінази Mycoplasma hominis [23]. Очистку АДІ із отриманого концентрату денатурованих "тілець включення" проводили за допомогою аніонної та гідрофобної хроматографії на сорбентах QAE-сефароза та феніл-сефароза, відповідно. Фракції елюатів збирали за допомогою колектора фракцій. Ступінь очищення цільових ферментів від баластних білків характеризували, визначаючи його активність та концентрацію в кожній фракції елюату та електрофоретично. Електрофорез проводили в 12 % SDS-ПААГ за методом Леммлі, білки зафарбовували Кумасі R-250. Внаслідок досліджень одержано препарат АДІ, близький до гомогенності, із питомою активністю 27 мкмоль хв.$^{-1}$ мг$^{-1}$ білка (активність визначена при 37 °С). Препарат АДІ зберігається без втрати активності при 4 °С у 20 мМ ФБ, рН 7,2, що містить 1 М NaCl, упродовж 20 місяців.

Запропонований та опрацьований на реальних зразках вин і соків ензиматично-хімічний АДІ-ОФА метод із спектрофотометричною або флуориметричною детекцією кінцевого продукту реакції (продукту взаємодії амонію з ОФА) має низку переваг порівняно із відомими методами: відсутність складного обладнання, економічний ефект завдяки використанню лише одного фермента (АДІ) без кофакторів, селективність визначення цільового аналіту та широкий діапазон тестованих концентрацій Arg, можливість здійснення процедури аналізу у автоматичному режимі за використання планшетного аналізатора. Ще одною перевагою АДІ-ОФА методу є те, що в ролі хромогенної системи використано дешевий нетоксичний реагент, що дозволяє знизити собівартість методу та забезпечити простоту проведення аналізу.

Суть пропонованої корисної моделі пояснюється за допомогою графічних матеріалів.

На фіг. 1 представлено схему реакцій ензиматичного перетворення Arg за послідовної дії трьох ферментів (аргінази, уреази та глутаматдегідрогенази).

На фіг. 2 наведено схему перебігу реакцій розробленого ензиматично-хімічного методу за використання АДІ і ОФА, а саме: загальну схему реакцій при визначенні Arg ензиматичним методом "АДІ-ОФА" із спектрофотометричним та флуорометричним детектуванням утвореного амонію.

На фіг. 3 представлено калібрувальні графіки для визначення концентрації Arg та діапазон лінійності ензиматично-хімічного "АДІ-ОФА" методу із спектрофотометричною та флуориметричною детекцією утвореного продукту, а саме: аналітичні характеристики розробленого ензиматично – хімічного "АДІ-ОФА" методу, залежність інтенсивності флуоресценції (А) та оптичної густини (Б) утвореного продукту реакції від концентрації Arg у реакційній суміші, у вставках: калібрувальні графіки.

На фіг. 4 представлено визначення вмісту загального і ендогенного амонію у соку "Садочок" мультифруктовий методом множинних внесень стандарту: ОФА-ФЛ (А, Б) та ОФА-СФ (В, Г).

$C_{NH_4^+}$ та C_{Arg} - концентрації внесених до проб стандартів - NH_4Cl та Arg, відповідно; C^t_a та C^e_a - обчислені концентрації ендогенного (А, В) та загального амонію (Б, Г) у вихідних пробах.

Аналітичні характеристики ензиматично-хімічного "АДІ-ОФА" методу представлено на Фіг. 3 та у Таблиці 1. Як видно з Фіг. 3, оптимізовані умови проведення визначення Arg розробленим методом забезпечують лінійність в діапазоні 0,35-24 мкМ Arg для ОФА-ФЛ (Фіг. 3 А) та 0,7-50 мкМ Arg для ОФА-СФ (Фіг. 3 Б).

Для визначення концентрації Arg у напоях, зразки вин та соків обробляли аргініндеіміназою для розщеплення ендогенного Arg до амонію та цитруліну. Утворений амоній в присутності

сульфіту в лужному середовищі вступає у хімічну реакцію з ОФА з утворенням продукту - 2,3-дигідро-1Н-ізоіндолу-1-тіолу (Фіг. 2), який детектується флуориметрично при хвилі емісії 415 нм та хвилі збудження 360 нм або спектрофотометрично при 340 нм. Внаслідок ензиматичної реакції з 1 моль Arg утворюється 1 моль амонію, тож вміст ендогенного Arg визначають за різницею концентрацій амонію у дослідному зразку: загального (після ензиматичного гідролізу) та ендогенного (без додавання АДІ).

Хід аналізу зразків напоїв на вміст Arg запропонованим методом (у варіанті множинних внесень стандарту) включає наступні послідовні стадії:

1. Розведення дослідних зразків. Зразки напоїв (вин та соків) перед початком аналізу попередньо розводять 20 мМ K, Na-фосфатним буфером, pH 6,5 (ФБ), що містить 1 мМ ЕДТА. Для хімічної стадії зразки розводять в 125 та 400 разів, для ензиматичної стадії реакції - в 50 та 100 разів.

2. Ензиматична реакція. До 0,1 мл розведеної у 50-100 разів проби вносять 0,025 мл розчину АДІ (300 Од./мл) та інкубують упродовж 20 хв при 37 °С. "Сліпу" пробу готують додаванням відповідної кількості АДІ до 0,1 мл ФБ.

3. Хімічна реакція. До 0,125 мл дослідної та "сліпої"" проби додають 2,5 мл хімічного реагенту, перемішують та інкубують на водяній лазні при 60 °С протягом 15 хв у щільно закритих пробірках. Для приготування хімічного реагенту 0,2 г ОФА розчиняють у 5 мл 95 % етанолу, змішують із 100 мл 0.1 М боратного буферу, pH 10 та додають натрію сульфіт до 0,16 мМ [24]. Хімічний реагент зберігають на темноті при кімнатній температурі.

4. Детекція продукту хімічної реакції. Проби аналізують проти "сліпої" проби: на флуорометрі ("Thermo Scientific", США) при довжині хвилі емісії 415 нм із хвилею збудження 360 нм або на спектрофотометрі ("Shimadzu UV1650 PC", Японія) при 340 нм.

5. Розрахунки. Концентрацію Arg у кінцевому зразку визначають методом множинних внесень стандарту за наступною схемою:

А). Визначення ендогенного амонію у вихідному зразку за використання параметрів лінійної регресії відповідних калібрувальних графіків (Фіг. 4 А і В), беручи до уваги фактори розведення (рівняння 1); обчислення середнього значення концентрації амонію проводили за значеннями концентрацій для двох розведень:

$$C_a = \frac{A}{B} \cdot N \quad (1),$$

де C_a - концентрація ендогенного амонію, A та B - параметри лінійної регресії, N - фактор розведення дослідної проби, його вказано на графіку.

Б). Обробка дослідної проби АДІ із наступним обчисленням загального вмісту іонів амонію (рівняння 1) у кінцевій пробі графічним методом (Фіг. 4 Б і Г), беручи до уваги фактори розведення та визначення середнього значення концентрації амонію.

В). Визначення концентрації ендогенного Arg у дослідній пробі відповідно до рівняння 2:

$$C_{Arg} = \left(C^t_a - C^e_a\right), \quad (2)$$

де C_{Arg} - концентрація ендогенного Arg, визначена за різницею між вмістом загального $\left(C^{заг}_a\right)$ та ендогенного амонію $\left(C^e_a\right)$.

У таблиці 2 наведено результати досліджень по визначенню концентрацій Arg у винах "Моушен Кадет" (Франція), "Бастардо" (Україна), соки "Садочок" виноградно-яблучний та мультифруктовий (Україна). Слід зазначити, що одержані значення концентрацій Arg задовільно корелюють із показниками ензиматичних методів за використання аргінази, запропонованих нами раніше [16, 18], а також даним інших авторів [25-27].

Таким чином, отримані значення концентрацій Arg демонструють, що запропонований ензиматично-хімічний "АДІ-ОФА" метод із флуориметричною та спектрофотометричною детекцією є функціонально придатним для точного та селективного аналізу концентрації Arg у напоях (винах та соках) і може бути використаний в виноробстві для попередження контролю рівня канцерогенного етилкарбамату.

Таблиця 2

Концентрації Arg у напоях, встановлені різними методами

Метод Зразок	АДІ-ОФА [Поточна заявка, 18]				Аргіназа-ДМО [16]			
	ФЛ		СФ		ФЛ		СФ	
	$C_{L\text{-}Arg}$	КВ[1], %	$C_{L\text{-}Arg}$	КВ, %	$C_{L\text{-}Arg}$	КВ, %	$C_{L\text{-}Arg}$	КВ, %
Вино "Моушен кадет"	2.05±0.04	1.90	1.85±0.040	2.2	1.97±0.01	1.01	1.96±0.05	2.01
Вино "Бастардо"	2.50±0.04	1.80	ND	-	2.55±0.04	1.20	2.36±0.06	1.70
Сік "Садочок" виноградно-яблучний	2.16±0.01	0.50	2.20±0.03	1.40	2.06±0.04	2.43	1.99±0.03	2.01
Сік "Садочок" мультифрут	*2.59±0.03	1.20	*2.65±0.03	1.10	2.50±0.04	1.70	ND	-

[1]КВ - коефіцієнт варіації, %

Джерела інформації:

1. Ough C.S., Stevens D., Almy J. (1989). Am. J. Enol. Vitic. 40, 219-220.
2. Mira De Orduna R., Liu S.Q. et al. (2000). FEMS Microbiol. Let. 183, 31-35.
3. Spayd S., Wample R., Evans R. et al. (1994). Am. J. Enol. Vitic. 45, 34-42.
4. Conacher H.B.S., Page B.D. (1986). Proceedings of Euro Food Tox II. Switzerland: European Society of Toxicology. 237-242.
5. Jiao Z., Dong Y., Chen Q. (2014). Comprehensive Reviews in Food Science and Food Safety. 13 (4), 611-626.
6. Uthurry C.A., Lepe J.A.S., Lombardero J., Del Hierro, G.J.R. (2006/2007). Food Chem. 94, 262-270.
7. Liu S.Q., Pritchard G.G., Hardman M.J., Pilone G.J. (1996). J. Appl. Bacteriol. 81,486-492.
8. Wu P., Cai C, Yang D. et al. (2014). J. Food Nutrit. Res. 2 (12), 872-875.
9. Alexander, J., Auounsson, G., Benford, D. et al. (2007). EFSA J. 551, 1-44.
10. Гайда Г., Стасюк Н., Гончар М. (2014). Biotechnologia Acta. 7 (1), 31-39.
11. Mira O.R. J. (2001). Agric. Food Chem. 49 (2), 549-552.
12. https://www.nzytech.com/products-services/analytical-test-kits/ak00171/
13. Kameya M., Asano Y. (2014). Enz. Microb. Technol. 57 (10), 36-41.
14. Stasyuk N., Smutok O., Gayda G. et al. (2011). J. Mat. Sci. Eng. 4, 515-521.
15. Stasyuk N., Smutok O., Gayda G. et al. (2012). B&B. 204, 515-521.
16. Stasyuk N., Gayda G., B. Gonchar M. (2014). Sensors&Actuators. B. Chem. 204,515-521.
17. Gayda G., Stasyuk N., Klepach H., Gonchar M. In: "Living Organisms and Bioanalytical Approaches for Detoxification and Monitoring of Toxic Compounds"-2015. - Lviv-Rzeszow. Eds.: A. Sibirny et al., 73-88.
18. Stasyuk N., Gayda G., Fayura L. et al. (2016). Food chemistry. 201, 320-326.
19. Стасюк Н.Є., Гайда Г.З., Гайда А.В., Гончар М.В. (2012) Ukrainica Biorganica Acta. 1,31-37.
20. Stasyuk N., Gaida G., Gonchar M. (2013). Appl. Biochem. Microbiol. 49, 529-534.
21. Стасюк Н.Є., Басе С.Р., Гайда Г.З. та ін. (2015). Scientific Journal "ScienceRise", 6/1(11), 43-48.
22. Stasyuk N.Ye., Gayda G.Z., Yepremyan H.S., Gonchar M.V. (2016). Spectrochimica Acta, Part A. Submitted.
23. Fayura L.R., Boretsky Y.R., Pynyaha Y.V. et al. (2013). J. Biotechnol.,167 (4), 420-426.
24. Goyal, S.S., Rains D.W., Huffaker R.C. (1988). Anal. Chem. 60 (2), 175-179.
25. Austin K.T., Butzke C.E. (2000). Am. J. Enol. Vitic. 51, 227-232.
26. Stines A.P., Grubb J., Gockowiak H. et al. (2000). Australian J. Grape and Wine Res. 6(2), 150-158.
27. Li H., Liang X., Feng L. et al. (2008). J. Food Drug Anal. 16 (3), 53-58.

ФОРМУЛА КОРИСНОЇ МОДЕЛІ

Спосіб визначення L-аргініну в харчових продуктах та алкогольних напоях, що ґрунтується на ензиматичному розщепленні L-аргініну до продукту, що визначається в наступній хімічній реакції, який **відрізняється** тим, що для гідролізу L-аргініну використовується аргініндеіміназа Mycoplasma hominis, виділена із клітин рекомбінантного штама Escherichia coli BL-21 (pET3d-ADI), при цьому генерований в аргініндеіміназній реакції амоній утворює з о-фталевим альдегідом продукт, який визначається флуориметрично або спектрофотометрично.

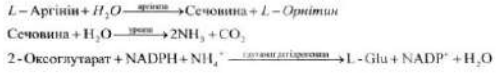

Фіг. 1

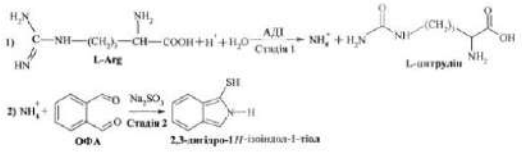

Фіг. 2

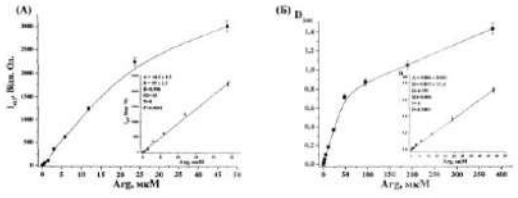

Фіг. 3

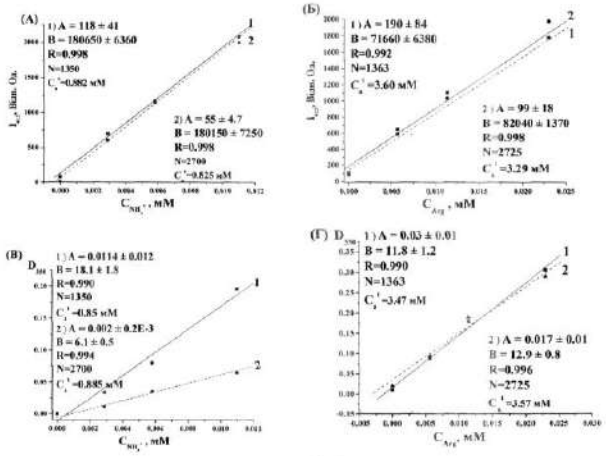

Фіг. 4

Оригінал доступний за посиланням: https://uapatents.com/9-108773-enzimatichno-khimichnijj-metod-viznachennya-vmistu-l-argininu-v-kharchovikh-produktakh-ta-alkogolnikh-napoyakh.html

Анотація: *У поточній роботі нами запропоновано новий ензиматично-хімічний метод визначення вмісту L-аргініну в крові (сироватці та плазмі), який ґрунтується на використанні аргінази I печінки людини, виділеної із клітин рекомбінантного штаму дріжджів, уреази та 2,3-бутандіонмонооксиму (ДМО): L-аргінін у сироватці/плазмі крові, попередньо звільненої від ендогенної сечовини за дії уреази, гідролізується під впливом аргінази I до карбаміду і утворює з ДМО продукт, який визначається флуориметрично. Нами запропоновано та опрацьовано на зразках сироватки/плазми крові людини ензиматично-хімічний метод із флуоресцентною детекцією кінцевого продукту реакції, що дозволяє підвищити точність визначення L-аргініну за рахунок високої чутливості та селективності, суттєво знижує матеріальні затрати, є простим та швидким у виконанні в порівнянні із відомими ензиматичними підходами.*

ДЕРЖАВНА СЛУЖБА ІНТЕЛЕКТУАЛЬНОЇ ВЛАСНОСТІ УКРАЇНИ

УКРАЇНА (19) **UA** (11) **107543** (13) **U**

(51) МПК
G01N 21/64 (2006.01)

(12) ОПИС ДО ПАТЕНТУ НА КОРИСНУ МОДЕЛЬ

(21) Номер заявки: **u 2015 12716**
(22) Дата подання заявки: **22.12.2015**
(24) Дата, з якої є чинними права на корисну модель: **10.06.2016**
(46) Публікація відомостей про видачу патенту: **10.06.2016, Бюл.№ 11**

(72) Винахідник(и):
Стасюк Наталія Євгенівна (UA),
Гайда Галина Зуфарівна (UA),
Закальський Андрій Євстахович (UA),
Закальська Оксана Мирославівна (UA),
Гончар Михайло Васильович (UA)
(73) Власник(и):
ІНСТИТУТ БІОЛОГІЇ КЛІТИНИ НАН УКРАЇНИ,
вул. Драгоманова, 14/16, м. Львів-5, 79005 (UA)

(54) ЕНЗИМАТИЧНИЙ МЕТОД ВИЗНАЧЕННЯ ВМІСТУ L-АРГІНІНУ В КРОВІ ЛЮДИНИ

(57) Реферат:

Ензиматично-хімічний метод визначення вмісту L-аргініну в крові (сироватці та плазмі) ґрунтується на використанні аргінази I, уреази та 2,3-бутандіонмонооксиму. Аргіназа I печінки людини виділена із клітин рекомбінантних штамів дріжджів. Ендогенна сечовина гідролізується уреазою до амонію та карбону діоксиду. Генерована в аргіназній реакції сечовина утворює з 2,3-бутандіонмонооксимом продукт, який визначається флуориметрично.

UA 107543 U

Корисна модель належить до діагностичних засобів у медицині і може використовуватись у ветеринарії та фармакології.

L-Аргінін - напівзамінна амінокислота, яка служить попередником для біосинтезу багатьох біоактивних сполук, включаючи оксид азоту, поліаміни, симетричні та несиметричні диметильовані похідні гуанідину, гомоаргініну, а також пептиди і білки [1]. Як субстрати NO-синтази, L-Arg та його сполуки можуть бути важливими біомаркерами у клінічній діагностиці багатьох захворювань, зокрема гіпераргінінемії (аргінінемії).

Аргінінемія - генетичне захворювання, викликане дефіцитом аргінази I (ЕС 3.5.3.1), останнього ферменту циклу сечовини, що каталізує гідроліз L-Arg до сечовини [2]. На відміну від інших дефектів циклу сечовини, дефіцит аргінази I, зумовлений мутацією в відповідному гені, зазвичай не викликає катастрофічної амоніємії новонароджених. Але цей дефіцит проявляється у прогресуючих неврологічних симптомах, включаючи судоми, в перші роки життя та важкі печінкові патології новонароджених, зокрема холестаз, гостру печінкову недостатність або фіброз печінки. Для виявлення аргінінемії у немовлят, у деяких економічно розвинутих країнах уряди фінансують програми для здійснення моніторингу крові новонароджених на вміст L-Arg. Встановлено, що своєчасна діагностика дозволяє розпочати адекватне лікування і зупинити розвиток цього рідкісного, але вкрай небезпечного генетичного захворювання [3].

Рівень L-Arg в сечі є маркером гомозиготної цистинурії та обструктивної нефропатії новонароджених [4]. Існують дані, що визначення вмісту L-Arg у сироватці крові дозволяє діагностувати та вивчати особливості перебігу таких захворювань, як артеріальна гіпертензія, гестоз вагітних та інші акушерські ускладнення [5], серцево-судинні, нейродегенеративні, легеневі, аутоімунні захворювання, сепсис, астма, обструктивні захворювання дихальних шляхів та муковісцидоз, запалення кишечнику [6-8], також агресивні гепатокарциноми, меланоми шкіри та колоректальний рак [9]. Моніторинг вмісту L-Arg в плазмі крові здійснюють також при довенному введенні L-Arg в процесі діагностики та експериментального дослідження захворювань ендокринної системи [10].

На сьогодні визначення вмісту L-Arg проводиться методами іонообмінної хроматографії, флуориметрії, спектрофотометрії, капілярного електрофорезу, полярографії, проточно-інжекційного аналізу, лазерної флуоресцентної спектроскопії та ін. [11]. Однак, найбільшого поширення набули хроматографічні методи кількісного аналізу L-Arg, зокрема високоефективна рідинна хроматографія (ВЕРХ). ВЕРХ ґрунтується на попередній обробці зразків дериватизуючими реактивами з подальшим розділенням цих похідних хроматографією та визначенням цих сполук за допомогою тандемної мас-спектрометрії (ТМС) та флуоресцентної детекції (ФЛ). Хоча метод ВЕРХ є достатньо чутливим, відтворюваним і дає змогу визначати весь набір амінокислот (в 15-20 мкл чистої плазми крові), проте він має і низку недоліків, які обмежують його широке використання, насамперед, у експрес-діагностиці. Перш за все, ВЕРХ вимагає дорогого обладнання та реактивів, що робить відповідні аналізи дорогими для рутинного клінічного аналізу. Цей метод потребує значної кількості органічних розчинників високої якості та дорогих дериватизуючих реагентів. По-друге, час підготовки та аналізу зразка є тривалим і складає від моменту дериватизації до одержання кількісних даних 1-2 доби.

На основі проведення патентно-інформаційних досліджень авторами роботи встановлено, що на сьогодні в галузі аналітичної біотехнології існує обмежена кількість даних щодо розробки ензиматичних методів визначення L-Arg. При цьому існуючі ензиматичні тест-системи є переважно мультиферментними із спектрофотометричним детектуванням кінцевого продукту реакції. Зокрема, в роботі [12] повідомляється про розробку ензиматичного методу аналізу L-Arg з використанням п'яти ферментів: аргініндеімінази, аргініносукцинатсинтетази, піруватфосфатдикінази, піруват оксидази та пероксидази хрону з утворенням кольорового продукту, який кількісно оцінюється спектрофотометрично за зміною оптичної густини реакційної суміші при 555 нм.

В іншій роботі [13] описано спектрофотометричне визначення L-Arg, яке ґрунтується на використанні трьох ферментів - аргінази, уреази та глутаматдегідрогенази. Детекцію проводять при довжині хвилі 340 нм і обрахунок ведеться із врахуванням коефіцієнта молярної екстинції NADH (6,22 $мМ^{-1} см^{-1}$). Ліміт чутливості мультиферментного методу - 2 мкМ (0,35 мкг/мл) L-Arg, лінійний діапазон визначення - до 0,47 мМ (81,8 мкг/мл).

$$\text{L - Аргінін} + H_2O \xrightarrow{\text{аргіназа}} \text{Сечовина} + \text{L - Орнітин}$$

$$\text{Сечовина} + H_2O \xrightarrow{\text{уреаза}} 2NH_3 + CO_2$$

$$\text{2 - Оксоглутарат} + NADPH + NH_4^+ \xrightarrow{\text{глутамат дегідрогеназа}} \text{L - Glu} + NADP^+ + H_2O$$

На основі наведеної вище схеми розроблено цілу низку серійних аналітичних наборів для визначення L-Arg (Sigma, Enzytec™, Elisa, Megazyme та ін).

Аналізуючи існуючі на сьогодні ензиматичні методи визначення L-Arg, можна зробити висновок, що переважна їх більшість виявляє низку недоліків, зокрема використання каскаду із кількох ферментів; неабсолютну селективність до цільового аналіту, спричинену позитивною реакцією на гуанідинові сполуки; необхідність використання екзогенного кофактора, чи ферментів, що додатково підвищує вартість методів та ускладнює процедуру аналізу.

Під час підготовки заявки на пропоновану корисну модель авторами не були виявлені ензиматичні методи для визначення концентрації L-Arg в крові із флуориметричною детекцією продукту за використання аргінази I та 2,3-бутандіонмонооксиму (ДМО). Запропонований та опрацьований на сироватці крові людини ензиматичний метод із флуоресцентною детекцією кінцевого продукту реакції має низку переваг порівняно із відомими методами, зокрема це відсутність складного обладнання, висока селективність та широкий діапазон тестованих концентрацій L-Arg.

Нові методи визначення L-Arg, що ґрунтуються на використанні аргініно-гідролізуючих ферментів із наступною флуориметричною детекцією продукту реакції, можуть суттєво покращити систему моніторингу рівня L-Arg в крові. Запропоновані методи можуть стати основою при створенні нових скринінгових тест-систем для моніторингу L-Arg в біологічних рідинах, зокрема крові, які на даний час відсутні в арсеналі засобів вітчизняної клінічної діагностики.

В основу запропонованої корисної моделі поставлено задачу створення такого флуориметричного ензиматично-хімічного методу аналізу вмісту L-Arg в крові, який дозволяє підвищити точність визначення цільового аналіту за рахунок високої чутливості та селективності, суттєво знижує матеріальні затрати, є простим та швидким у виконанні в порівнянні із відомими ензиматичними підходами.

Поставлена задача розв'язується шляхом ензиматичного визначення вмісту L-Arg в крові (сироватці та плазмі) за використання високоселективного до L-Arg фермента - аргінази I печінки людини (далі - аргіназа), виділеної із клітин рекомбінантних дріжджів. Широке використання аргінази природного походження із організму ссавців у біоаналітиці гальмується складністю процедури його очищення, з огляду на це, використання рекомбінанантної аргінази, виділеної із клітин мікроорганізмів, є дуже актуальним.

Внаслідок досліджень, із безклітинного екстракту генетично модифікованих термотолерантних метилотрофних дріжджів H. polymorpha NCYC 495 pGAPI-HsARGI (leu2carI:ScLEU2) [14] за одну стадію колонкової хроматографії на афінному сорбенті - аргінін-макропористому склі одержано високоочищений препарат ензиму (немодифікована аргіназа) [11]. Методом афінної хроматографії на сорбенті Ni-NTA-Superflow (Qiagen) із безклітинного екстракту рекомбінантних дріжджів S. cerevisiae 303/pYEX-4-ARG1 (MATa 1еи2-3/112 ига3-1 trpl-1 his3-ll/15 ade2-I canl-100) одержано препарат $(His)_6$-тагованої аргінази (модифікована аргіназа) [15].

Принцип роботи ензиматично-хімічного методу визначення концентрації L-Arg, розробленого нами раніше за використання немодифікованої аргінази і ДМО [11, 16], пояснюється за допомогою фіг. 1.

Можливість практичного застосування розробленого ензиматично-хімічного методу "Аргіназа-ДМО" за використання аргінази та ДМО було показано на зразках промислових фармацевтичних препаратів та комерційних вин [11, 16]. Як свідчить порівняльний аналіз результатів різними методами, новий метод дає результати, які добре корелюють з показниками виробника й даними, одержаними за допомогою референтних методів. Метод "Аргіназа-ДМО" не потребує попереднього відокремлення L-Arg з досліджуваних зразків, є простим у виконанні, високоселективним, надійним і комерційно доступним. Розроблений метод може бути перспективним для створення економічно вигідних тест-систем на L-Arg та застосування їх у лабораторіях харчової та фармацевтичної промисловості. Тому наступним логічним кроком на шляху випробування запропонованого методу стало дослідження його придатності для аналізу L-Arg в реальних зразках біологічних рідин [17], зокрема крові людини, за використання обох препаратів аргінази.

Суть пропонованої корисної моделі пояснюється за допомогою графічних матеріалів.

На фіг. 1 наведено схему перебігу реакцій ензиматично-хімічного методу.

На фіг. 2 представлено калібрувальний графік для визначення L-Arg та діапазон лінійності ензиматично-хімічного методу "Аргіназа-ДМО".

На фіг. 3 показано основні етапи приготування зразків сироватки крові для аналізу L-Arg.

Оптимізовані умови проведення визначення L-Arg за використання обох препаратів аргінази забезпечують лінійність методу в діапазоні 0,28-280 мкМ L-Arg. Чутливість методу є близькою 150 нМ L-Arg (фіг. 2).

Приготування зразків крові для аналізу L-Arg у сироватці здійснювали за схемою, зображеною на фіг. 3.

Перед початком аналізу ендогенну сечовину, яка присутня в сироватці крові, під впливом уреази розщеплюють до амонію та вуглекислого газу. Ендогенний L-Arg за дії аргінази гідролізується до сечовини та орнітину. Сечовина вступає у хімічну реакцію з ДМО з утворенням продукту (2E)-бутан-2,3-діон-2-семікарбазону, який детектується флуориметрично при хвилі емісії 515 нм та хвилі збудження 360 нм.

Хід аналізу сироватки крові на вміст L-Arg запропонованим методом включав наступні стадії.

Кров для аналізу відбирають із вени у стандартні пробірки фірми VACUTE (США), які містять гель, що після центрифугування при 4800 об./хв. протягом 15 хв. відділяє сироватку від клітинних компонентів крові. Одержану сироватку фіксованого об'єму депротеїнізують додаванням 40 % водного розчину трихлороцтової кислоти (ТХО) до кінцевої концентрації 4 % (0,1 мл). Утворену суспензію перемішують, витримують 30 хв. при 0 °С та знову центрифугують упродовж 10 хвилин при 10000 об./хв. Для аналізу використовують безбілкову надосадову рідину (БНР). Одержану БНР зберігають до початку аналізу в холодильнику при +4 °С. У разі, якщо аналізована проба не досліджується протягом 24 годин, її зберігають при -20 °С.

0,5 мл БНР нейтралізують до pH 5,5-7,5, додаючи 0,15-0,2 мл розчину 1,5 М NaOH (контролюючи pH та кінцевий об'єм проби), вносять уреазу (К.Ф. 3.5.1.5, тип IX із бобів), з розрахунку 0,075 мл розчину уреази (420 Од…мл$^{-1}$) на 0,6 мл зразка та інкубують упродовж 50 хв при 37 °С. До одержаної проби додають 0,01 мл 1,5 М NaOH (до pH 9-10), вносять 0,05 мл розчину аргінази (60 Од…мл$^{-1}$) та інкубують упродовж 40 хв. До 0,5 мл кінцевої проби (без розведення та розведеної у 2 та 4 рази) додають 3 мл хімічного реагенту, що містить 0,3 % ДМО, 9 % натрій хлорид в 1,2 М розчині H_2SO_4, перемішують та кип'ятять на водяній лазні протягом 50 хв. Проби аналізують при довжині хвилі емісії 515-520 нм із хвилею збудження 360 нм на флуорометрі ("Thermo Scientific", США) проти "сліпої" проби. "Сліпу" пробу готують додаванням відповідних кількостей уреази і аргінази до 5 % розчину ТХО у воді з наступними кип'ятінням із хімічним реагентом. Концентрацію L-Arg у кінцевому зразку визначали методом порівняння із двома калібрувальними пробами - 0,4 мМ та 0,8 мМ розчинами L-Arg у 30 мМ Tris-HCl буфері, pH 8,8 за рівнянням:

$$C_{Arg} = \frac{E_{досл}}{E_{кл}} \cdot C_{кл},$$

де $C_{Arg} = \frac{E_{досл}}{E_{кл}} \cdot C_{кл}$ - концентрація L-Arg у кінцевій пробі,

$E_{досл}$ і $E_{кл}$ - показники інтенсивностей випромінювання в дослідній та калібрувальній пробах;

$C_{кл}$ - концентрація L-Arg в калібрувальній пробі, мМ.

Слід зазначити, що інтенсивність флуоресценції реакційної суміші залишається стабільною протягом доби.

Для перерахунку концентрацій L-Arg у дослідних пробах на концентрацію L-Arg у вихідній плазмі/сироватці, необхідно врахувати сумарний фактор розведення ($ФР_{заг}$), який є добутком ФР кожного етапу приготування зразка для аналізу. ФР на кожному етапі визначається як величина співвідношення об'ємів зразків - наступного до попереднього. Так, $ФР_1=V_2/V_1$, $ФР_2=V_3/V_2$, $ФР_3=V_4/V_3$. Таким чином, для визначення концентрації L-Arg в плазмі, слід CArg, розраховану за формулою, перемножити на $ФР_{заг}=V_4/V_1$.

У таблиці наведено результати досліджень по визначенню границь норми та середніх значень концентрацій L-Arg в сироватках крові 20 здорових людей, жінок і чоловіків, віком від 20 до 40 років. Слід зазначити, що одержані значення концентрацій L-Arg добре корелюють із даними літератури [18-20].

Таблиця

Границі норми та середні значення концентрацій
L-Arg в сироватці/плазмі крові людини, встановлені різними методами

Метод	L-Arg, мкМ		Об'єкт дослідження	Джерела інформації:
	Інтервал	Середнє		
"Аргіназа-ДМО"	67-147	114,9±7,3	сироватка	Поточна заявка
[1]ЕЛІСА	70-110	-		
[2]ВЕРХ-ФЛ	82,4-108,9	95,7		[19]
ВЕРХ-ФЛ	-	110±24	Плазма	[18]
[3]ТМС	-	162±76		[18]
[4]ВЕРХ-ТМС	52,2-124,7	87±35		[18]
ВЕРХ-ТМС	41-115	-		[20]
ЕЛІСА	56,4-125,4	-		[18]

ЕЛІСА - ензиматичний метод за використання комерційного набору;
[2]ВЕРХ-ФЛ - високоефективна рідинна хроматографія із флуоресцентною детекцією;
[3]ТМС - тандемна мас-спектрометрія без попередньої деривативації;
[4]ВЕРХ-ТМС - ВЕРХ із тандемною мас-спектрометрією.

Таким чином, отримані значення концентрацій L-Arg демонструють, що запропонований ензиматично-хімічний "Аргіназа-ДМО" метод із флуориметричною детекцією є функціонально придатним для точного та селективного аналізу концентрації L-Arg в крові (сироватці та плазмі) і може бути використаний в клінічній діагностиці.

Джерела інформації:
1. Yokoro M. et al. Biosci. Biotechnol. Biochem. - 2012. - Vol. 6, № 7. - P. 1334-1342.
2. Wu G. Morris S.M.Jr. J. Biochem. - 1998. - Vol. 336. - P. 1-17.
3. Lee B.H. et al. Pediatr. Neurol. - 2011. - Vol. 44, № 3. - P. 218-220.
4. Lacroix C. et al. Mol. Cell Proteomics. - 2014. - Vol. 13, № 12. - P. 3421-3434.
5. Wang G. et al. J. Clin. Biochem. Nutr. - 2015. - Vol. 57, №1, P. 74-81.
6. Benson R.C. et al. J. Allergy. - 2011. - Vol. 2011. - P. 1-12.
7. Maarsingh H. et. al. Naunyn. Schmiedebergs Arch. Pharmacol. - 2008. - Vol. 378, №2. - P.171-184.
8. Fritz J.H. Infect Immun. - 2013. - Vol. 81, № 10. - P. 3500-3502.
9. Lam T. L. et al. Pigment Cell Melanoma Res. - 2011. - Vol. 24, № 2. P. 366-376.
10. Rotondo R. et al. Int. J. Cancer. - 2008. - Vol. 123, № 5. - P. 1108-1116.
11. Гайда Г.З. et al. Biotechnologia Acta. - 2014. - Vol. 7, № 1. - P. 31-39.
12. Yasuhisa Asano Masafumi Kameya Enz. Microb. Technol. - 2014. - Vol. 57, №10. - P.36-41.
13. Mira O. R. J. Agric. Food Chem. - 2001. - Vol. 49, № 2. - P. 549-552.
14. Стасюк Н.Є. та ін. Укр. біохім. журн. - 2010. - Vol.82, № 6. - P. 14-21.
15. Zakalskiy A.E. et al. Protein Expression and Purification. - 2012. - Vol.81. - P.63-68.
16. Stasyuk N., Gaida G., Gonchar M. Appl. Biochem. Microbiol. - 2013. - Vol.49, № 5. - P. 529-534.
17. Гайда Г.З. та ін. ScienceRise. - 2015. - Т. 11/6 (16) - С. 33-38.
18. Aldamiz-Echevarria L., Andrade F. Int. J.Mol.Sci. - 2012. - Vol.13. - P. 11288-11311.
19. Schon T. et al. Eur. Respir. J. - 2003. - Vol. 21, № 3. - P. 483-488
20. El-Khory J.M. et al. Anal. Bioanal. Chem. - Vol. 402, № 2. - P.771-779.

ФОРМУЛА КОРИСНОЇ МОДЕЛІ

Ензиматично-хімічний метод визначення вмісту L-аргініну в крові (сироватці та плазмі), що ґрунтується на використанні аргінази I, уреази та 2,3-бутандіонмонооксиму, який **відрізняється** тим, що:
- аргіназа I печінки людини виділена із клітин рекомбінантних штамів дріжджів;
- ендогенна сечовина гідролізується уреазою до амонію та карбону діоксиду;
- генерована в аргіназній реакції сечовина утворює з 2,3-бутандіонмонооксимом продукт, який визначається флуориметрично.

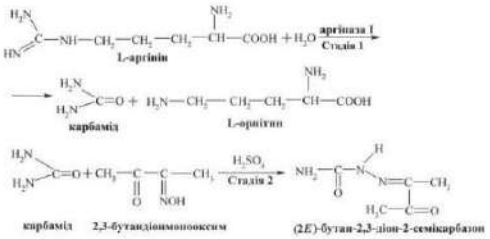

Загальна схема реакцій при визначенні L-Arg ензиматично-хімічним методом "Аргіназа-ДМО" за утворенням карбаміду

Фіг. 1

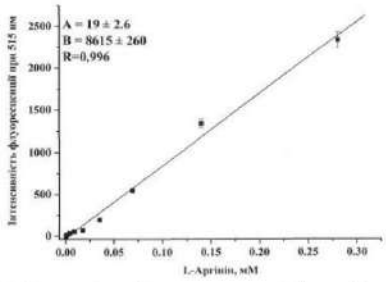

Калібрувальний графік для визначення L-Arg та діапазон лінійності ензиматично-хімічного методу "Аргіназа-ДМО"

Фіг. 2

Кров
↓ **ЦФ**
Сироватка, V_1
↓ **ТХОК, ЦФ**
Сироватка без білків, містить ендогенну сечовину і ендогенний Arg, V_2
↓ **NaOH до pH 7,0 + *уреаза***
Сироватка без білків і ендогенної сечовини, містить ендогенний Arg, V_3
↓ **NaOH до pH 9,0 + *аргіназа***
Сироватка без білків, ендогенної сечовини і ендогенного Arg, містить сечовину, одержану із ендогенного Arg, V_4
↓ **ДМО**
Продукт реакції «*Сечовина+ДМО*»

Основні етапи приготування зразків сироватки крові для аналізу L-Arg

Фіг. 3

Комп'ютерна верстка Л. Бурлак

Державна служба інтелектуальної власності України, вул. Василя Липківського, 45, м. Київ, МСП, 03680, Україна

ДП "Український інститут інтелектуальної власності", вул. Глазунова, 1, м. Київ – 42, 01601

Оригінал доступний за посиланням: https://uapatents.com/7-107543-enzimatichnijj-metod-viznachennya-vmistu-l-argininu-v-krovi-lyudini.html

Анотація: *На сьогодні, скринінгові тест-системи для моніторингу L-аргініну у біологічних рідинах, зокрема, у крові, в арсеналі засобів вітчизняної клінічної діагностики відсутні. У поточному дослідженні нами опрацьовано новий ензиматичний набір «Аргітест», який базується на розробленому ензиматично-хімічному методі кількісного аналізу L-аргініну з використанням різних форм рекомбінантної аргінази І печінки людини та аргініндеімінази. Метод є високоселективним, економічно вигідним, простим та швидким у виконанні, відзначається стабільністю препаратів ензимів та продукту реакції. У роботі доведено можливість використання препаратів рекомбінантних аргініно-селективних ензимів у складі біоаналітичного набору «Аргітест». У результаті досліджень вивчено каталітичні та аналітичні характеристики ензимних препаратів та показано, що кожен з них може бути використано як складову ензиматичного аналітичного набору.*

ISSN 1815-2066. Nauka innov. 2017, 13(4): 64—72 doi: https://doi.org/10.15407/scin13.03.065

Н.Є. Стасюк, Г.З. Гайда, А.Є. Закальський, О.М. Закальська, Л.Р. Фаюра, О.І. Вовк, О.В. Стасик, А.А. Сибірний, М.В. Гончар

Інститут біології клітини НАН України, вул. Драгоманова, 14/16, Львів, 79005, Україна
Тел. +380 32 261 2108, факс +380 32 261 2148, e-mail: galina.gayda@gmail.com

РЕКОМБІНАНТНІ ФОРМИ АРГІНАЗИ ТА АРГІНІНДЕІМІНАЗИ ЯК КАТАЛІТИЧНІ СКЛАДОВІ ЕНЗИМАТИЧНОГО НАБОРУ «АРГІТЕСТ» ДЛЯ АНАЛІЗУ L-АРГІНІНУ

На сьогодні скринінгові тест-системи для моніторингу L-аргініну у біологічних рідинах, зокрема, у крові, в арсеналі засобів вітчизняної клінічної діагностики відсутні. Ензиматичний набір «Аргітест» базується на розробленому ензиматично-хімічному методі кількісного аналізу L-аргініну з використанням різних форм рекомбінантної аргінази I печінки людини та аргініндеімінази. Метод є високоселективним, економічно вигідним, простим та швидким у виконанні, відзначається стабільністю препаратів ензимів та продукту реакції. У статті доведено можливість використання препаратів рекомбінантних аргініно-селективних ензимів у складі набору «Аргітест». В результаті досліджень вивчено каталітичні та аналітичні характеристики цих препаратів та показано, що кожен з них може бути використано як складову ензиматичного набору.

Ключові слова: L-аргінін, аргіназа I, аргініндеіміназа, 2,3-бутандіонмоноксим, уреаза, ензиматичний набір «Аргітест».

Амінокислота L-аргінін (далі — Arg) — попередник L-орнітину, L-цитруліну, L-глутатіону, γ-аміномасляної кислоти, спермідину та інших сполук — одна із найбільш поляризованих, позитивно заряджених амінокислот [1]. Метаболізм Arg йде, як мінімум, двома альтернативними шляхами: 1) окисним (за участі NO-синтази) з утворенням L-цитруліну та NO; 2) неокисним (за участю аргінази I) з утворенням L-орнітину та сечовини. Можливе і одночасне протікання цих двох процесів [2]. Практично весь ланцюг перетворень Arg в похідні сполуки відбувається в трьох органах — кишківнику, печінці та нирках [3].

Вміст Arg зазвичай визначають методами іонообмінної хроматографії, флуориметрії, спектрофотометрії, капілярного електрофорезу, полярографії, проточно-інжекційного аналізу, лазерної флуоресцентної спектроскопії та ін. [4—5]. Найбільшого поширення набули хроматографічні методи кількісного аналізу Arg, зокрема, високоефективна рідинна хроматографія (ВЕРХ). ВЕРХ грунтується на попередній обробці зразків дериватизуючими реагентами з подальшим розділенням цих похідних хроматографічними методами та визначенням цих сполук за допомогою тандемної мас-спектрометрії (ТМС) та флуоресцентної детекції (ФЛ). Хоча метод ВЕРХ є достатньо чутливим, відтворюваним і дає змогу визначати весь набір амінокислот (в 15—20 мкл плазми крові), проте він має і низку недоліків, які обмежують його широке використання, насамперед, у експрес-діагностиці. Перш за все, ВЕРХ вимагає високовартісного обладнання та реактивів, що

© Н.Є. СТАСЮК, Г.З. ГАЙДА, А.Є. ЗАКАЛЬСЬКИЙ, О.М. ЗАКАЛЬСЬКА, Л.Р. ФАЮРА, О.І. ВОВК, О.В. СТАСИК, А.А. СИБІРНИЙ, М.В. ГОНЧАР, 2017

робить відповідні аналізи недешевими для рутинного клінічного аналізу. Метод потребує значної кількості органічних розчинників високої якості та дорогих дериватизуючих реагентів. По-друге, час підготовки та аналізу зразка є тривалим і становить 1—2 доби від моменту дериватизації до одержання кількісних даних [5].

В галузі аналітичної біотехнології існує обмежена кількість даних щодо ензиматичних методів визначення Arg. Найперспективнішими для розробки таких методів є ензими метаболізму Arg, зокрема, аргіназа I, аргініндеіміназа (АДІ), аргініндекарбоксилаза. Існуючі комерційні ензиматичні тест-системи (виробництва Sigma, Enzytec™, Elisa, Megazyme та ін.) є, переважно, мультиензимними із спектрофотометричним (СФ) детектуванням кінцевого продукту реакції [6—8]. Мультиензимні методи визначення Arg мають низку недоліків, зокрема, неабсолютну селективність до цільового аналіту, спричинену позитивною реакцією на гуанідинові сполуки. Необхідність використання каскаду із кількох (3—5) ензимів і екзогенних ко-факторів підвищує вартість методів та ускладнює процедуру аналізу.

У попередніх дослідженнях авторами було запропоновано біосенсорні підходи [9] та економічно вигідні ензиматично-хімічні методи визначення Arg [9—16] із використанням одного або двох ензимів. На рис. 1 зображено принципові схеми розроблених нами методів, а в табл. 1 наведено їхні аналітичні характеристики, порівняно з аналогічними параметрами відомих мультиензимних методів.

Вказані на рис. 1 методи базуються на використанні рекомбінантних аргініно-гідролізуючих ензимів — аргінази I печінки людини (аргіназа[1]) та бактерійної аргініндеімінази, одержаних за власними технологіями з клітин мікробних рекомбінантних штамів-продуцентів, створених авторами статті (табл. 2).

Як видно з таблиці 1, метод «Аргіназа-ДМО» має низку переваг порівняно з іншими методами, зокрема, це висока чутливість та широкий діапазон тестованих концентрацій Arg. Цей метод не потребує попереднього відокремлення Arg з досліджуваних зразків, є простим у виконанні, високоселективним, надійним і комерційно доступним; можливість його практичного застосування було продемонстровано на зразках промислових фармацевтичних препаратів та комерційних вин [9, 11].

На сьогодні тест-системи для моніторингу Arg у біологічних рідинах, зокрема в крові, в арсеналі засобів вітчизняної клінічної діагностики відсутні. У 2015 р. авторами було виконано проект науково-дослідної роботи за науково-технічною програмою НАН України «Розробка, тестування та випуск пробної серії ензиматичного набору «Аргітест» для аналізу аргініну в клінічних зразках. Розділ 1. Оптимізація складу набору, умов проведення аналізу та розробка науково-технічної документації». У результаті виконання цього проекту метод «Аргіназа-ДМО» було успішно протестовано на зразках крові. На основі ензиматично-хімічного методу «Аргіназа-ДМО» створено ензиматичний набір «Аргітест» для визначення Arg і розроблено науково-технічну документацію на зазначений набір.

Одним із завдань вищевказаного проекту НДР було визначити оптимальну ензиматич-

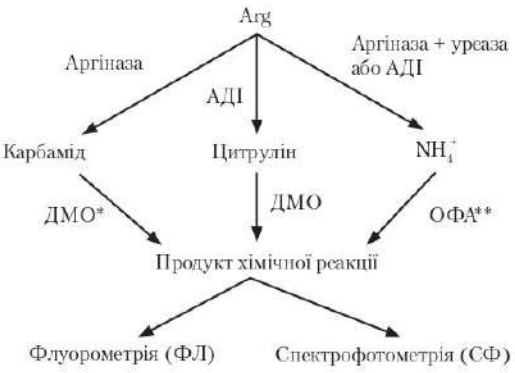

*ДМО — 2,3-бутандіонмонооксим; **ОФА — *о*-фталевий альдегід

Рис.1. Ензиматично-хімічні методи аналізу Arg

Таблиця 1

Порівняльна характеристика ензиматично-хімічних методів визначення Arg

Метод	Фермент	Лінійний діапазон, μM	Чутливість, μM	Джерело
Відомі ензиматичні методи				
Мультиензимний, СФ, λ = 340 нм	Аргіназа, уреаза, глутаматдегідрогеназа	До 470	2,0	[6]
Мультиензимний, СФ, λ = 340 нм	Аргіназа, уреаза, глутаматдегідрогеназа	2,9–100	2,1	[7]
Мультиензимний, СФ, λ – 555 нм	АДІ, аргініносукцинатсинтаза; піруватфосфатдикіназа; піруват оксидаза, пероксидаза хрону	До 100	–	[8]
Методи, розроблені авторами даної публікації				
ДМО-СФ, λ = 480 нм	Аргіназа	7–100	5,0	[9–11]
ДМО-ФЛ, $\lambda_{зб}$ = 360 нм, $\lambda_{см}$ = 510 нм	Аргіназа	0,06–200	0,04	[9, 11, 12]
ОФА-СФ, λ = 362 нм	Аргіназа-уреаза	0,9–60,0	0,85	[13]
ОФА-ФЛ, $\lambda_{зб}$ = 364 нм, $\lambda_{см}$ = 425 нм	Аргіназа-уреаза	0,09–6,0	0,08	[14]
ОФА-ФЛ, $\lambda_{зб}$ = 364 нм, $\lambda_{см}$ = 415 нм	АДІ	0,35–24	0,25	[15]
ОФА-СФ, λ = 340 нм	АДІ	0,7–50	0,55	[16]

ДМО – 2,3-бутандіонмонооксим; СФ – спектрофотометрична детекція кінцевого продукту; ФЛ – флуорометрична детекція кінцевого продукту; ОФА – *о*-фталевий альдегід.

ну складову набору «Аргітест». Об'єктами дослідження слугували рекомбінантні аргініно-гідролізуючі ензими (табл. 2), виділені та охарактеризовані авторами статті.

МАТЕРІАЛИ ТА МЕТОДИ ДОСЛІДЖЕНЬ

У роботі використано рекомбінантні штами мікроорганізмів з музею Інституту біології клітини НАН України. Рекомбінантні клітини дріжджів та бактерій було створено у попередніх дослідженнях та застосовано як джерела цільових рекомбінантних ензимів (табл. 2).

Питому активність рекомбінантних ензимів (далі – ензими) виражали в мкмоль продукту, утвореного за 1 хв в перерахунку на 1 мг протеїну (мкмоль · $хв^{-1}$ · $мг^{-1}$) за стандартних умов реакції. Активність аргінази визначали за швидкістю утворення сечовини [17–19]. Аналіз активності АДІ виконували у два етапи, визначаючи швидкість утворення аміаку [20, 21].

Внутрішньоклітинні ензими виділяли з безклітинних екстрактів (БЕ), секретований ензим (аргіназу[3]) – із культуральної рідини відповідних рекомбінантних мікробних продуцентів з подальшим очищенням шляхом колонкової хроматографії за розробленими схемами (див. посилання в табл. 2).

Для виділення аргінази[1] використовували синтезований власноруч афінний сорбент «Аргінін-макропористе скло». Препарати ензиму із питомою активністю 1500–2600 Од/мг протеїну було одержано із 40–60-кратною очисткою, із 42%-им виходом у найбільш вдалих фракціях. Препарати зберігали при –10 °С у 50 мМ Трис-HCl буфері (ТБ), з pH 8,0, що містив 1М NaCl, 1 мМ $MnCl_2$ та 10%-й гліцерол.

Таблиця 2

Аргініногідролізуючі ензими

Назва фермента	Позначення	Властивості фермента	Продуцент фермента	Джерело
Природна аргіназа І печінки людини	Аргіназа[1]	Mn^{2+}-залежний, внутрішньо-клітинний	*NCYC 495 Hansenula polymorpha pGAP1-HsARG1 leu2car1:ScLEU2*	17
$(His)_6$-тагована аргіназа І печінки людини	Аргіназа[2]	Mn^{2+}-залежний, внутрішньо-клітинний	*Saccharomyces cerevisiae 303/pYEX-4-ARG1 (MATa leu2-3/112 ura3-1 trp1-1 his3-11/15 ade2-1 can1-100)*	18
Модифікована аргіназа І печінки людини	Аргіназа[3]	Co^{2+}-залежний, секретований	*H. polymorpha pFDM-ScMFa-HIS6-HsARG1*	19
Аргініндеіміназа *Mycoplasma hominis*	АДІ	Внутрішньо-клітинний	*Escherichia coli BL-21(pET3d-ADI)*	20, 21

Вони не втрачали своєї активності протягом року, а через 3 роки зберігання їх ензиматична активність знижувалася лише вдвічі.

Виділення препаратів аргінази[2] та аргінази[3] здійснювали шляхом афінної хроматографії на сорбенті Ni-NTA-Superflow (Qiagen). Вихід ензимів з найвищою активністю складав 70 % (6 мг/л культури) та 35 % (5 мг/л культуральної рідини) відповідно. Препарати аргінази[2] і аргінази[3] зберігали при –20 °С без втрати активності протягом року в Трис-фосфатному буфері з pH 8,0 та в фосфатному буфері, pH 7,2 відповідно. Обидва буфери містили 0,15 М NaCl та 20%-й гліцерол.

Аргініндеіміназу (АДІ) виділяли з нерозчинних «тілець включення» та очищали за допомогою аніонообмінної та гідрофобної хроматографії на сорбентах QAE-сефароза та феніл-сефароза відповідно. Одержаний шляхом електрофорезу гомогенний препарат АДІ зберігали при +4 °С у 20 мМ фосфатному буфері з pH 8,0, що містив 1 М NaCl, без втрати активності упродовж 20 місяців.

Було вивчено каталітичні та аналітичні характеристики високоочищених ензимів. Оптимальні умови проведення ензиматичної та хімічної реакцій, а також процедури реєстрації кінцевих продуктів докладно описано в попередніх публікаціях [9—11]. Як результат, створено калібрувальні графіки залежності аналітичного сигналу (інтенсивності випромінювання або світлопоглинання реакційної суміші), тобто відповіді на ензиматичне перетворення субстрату, від концентрації Arg. Для побудови калібрувальних графіків в скляні пробірки відбирали по 0,1 мл стандартних розчинів Arg в 30 мМ ТБ з pH 8,8. Реакцію запускали додаванням 0,01 мл розчину ензиму в 30 мМ ТБ з pH 8,8, до кінцевої концентрації 1,5–3,0 Од/мл. Інкубаційну суміш перемішували та витримували 10 хв при 37 °С. Надалі в суміш додавали 3 мл 0,5%-го розчину 2,3-бутандіонмонооксиму (ДМО) в 1,7 М H_2SO_4 та кип'ятили на водяній бані протягом 50 хв. Реєстрували оптичну густину (на спектрофотометрі SHIMADZU UV-1650 PC) або інтенсивність флуоресценції кінцевого продукту реакції (на флуориметрі TECAN Infinite H200 із хвилею збудження 360 нм) порівняно з контрольною пробою (0,1 мл 30 мМ ТБ з pH 8,8 замість розчину Arg).

Досліди проводили у чотирьох–шести повтореннях, а виміри — у 3-х паралелях. Для кожної вибірки показників визначали середнє арифметичне значення (M), дисперсію, стандартне відхилення середнього результату, відносне стандартне відхилення та довірчий інтервал. Розрахунок статистичних показників і побудову графіків здійснювали за допомогою програми Origin 8.0. Лінеаризацію графіків про-

водили за рівнянням регресії $Y = A + BX$ (де A і B — параметри рівняння), розраховували коефіцієнт кореляції R та рівень достовірності лінійного зв'язку p. Параметр B відповідає тангенсу кута нахилу, за допомогою якого визначають чутливість методу. Коефіцієнт A є показником фонового впливу додаткових інгредієнтів на ідентифікацію аргініну, тобто вказує рівень селективності методу [22]. Параметри та статистичні показники наведені на рисунках та в таблицях.

РЕЗУЛЬТАТИ ТА ОБГОВОРЕННЯ

Принципова схема реакцій, що лягли в основу ензиматично-хімічного методу визначення Arg за використання аргінази, представлена на рис. 2. Метод ґрунтується на ферментативному гідролізі Arg до L-орнітину та карбаміду (ензиматична реакція, стадія 1). Карбамід взаємодіє із ДМО на хімічній стадії реакції (стадія 2), із утворенням продукту, який кількісно оцінюється спектрофотометрично (СФ) за оптичною густиною при $\lambda = 480$ нм або флуорометрично (ФЛ) при 510 нм із хвилею збудження 360 нм [11]. Кінцевим продуктом хімічної реакції є (*2E*)-бутан-2,3-діон-2-семікарбазон та інші сполуки, зокрема, циклічні.

Застосування АДІ в ензиматичному методі визначення Arg забезпечує високоселективну та ефективну деградацію Arg до цитруліну. Принципова схема реакцій, що лягли в основу «АДІ-ДМО»-методу визначення Arg (за утворенням цитруліну), представлена на рис. 3. Концентрацію кінцевого продукту хімічної реакції визначали спектрофотометрично за оптичною густиною при $\lambda = 490$ нм та флуорометрично при 515 нм із хвилею збудження 360 нм.

Вибір оптимального ензиму здійснювали, порівнюючи аналітичні характеристики досліджених ензимів (табл. 2) за оптимізованих умов аналізу [11]. Для цього вивчали залежність інтенсивності флуоресценції та світлопоглинання реакційної суміші від концентрації Arg у кінцевій пробі. На рис. 4 наведено графічні результати вивчення залежності інтенсивності флуоресценції (*а*, *б*) та світлопоглинання (*в*, *г*) реакційної суміші від концентрації

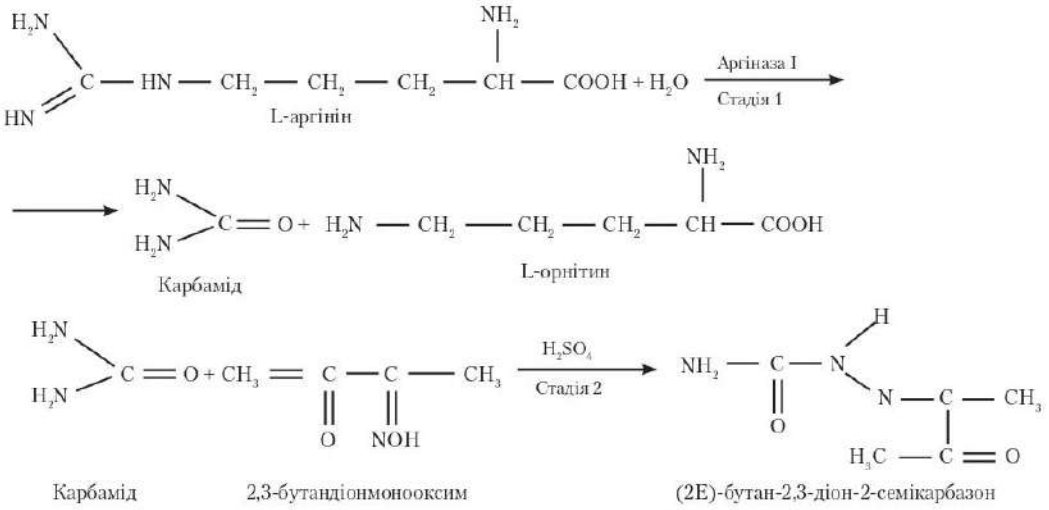

Рис. 2. Загальна схема реакцій при визначенні Arg ензиматично-хімічним методом «Аргіназа-ДМО» за утворенням карбаміду

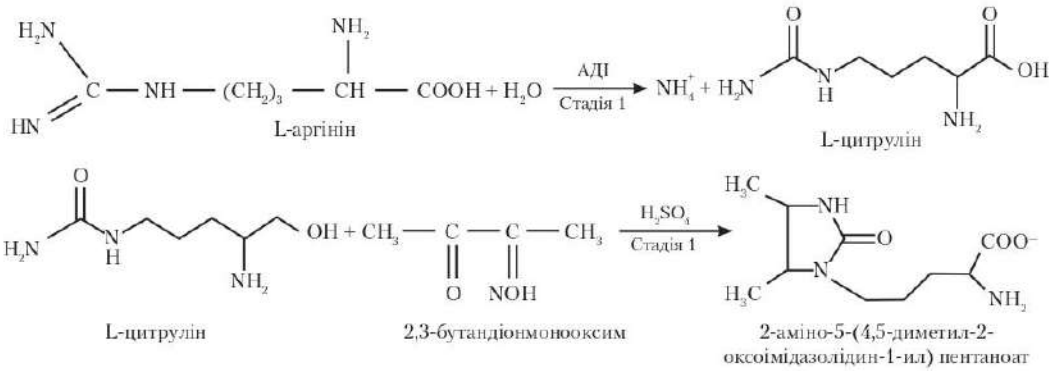

Рис. 3. Загальна схема реакцій при визначенні Arg ензиматично-хімічним методом «АДІ-ДМО» за утворенням цитруліну

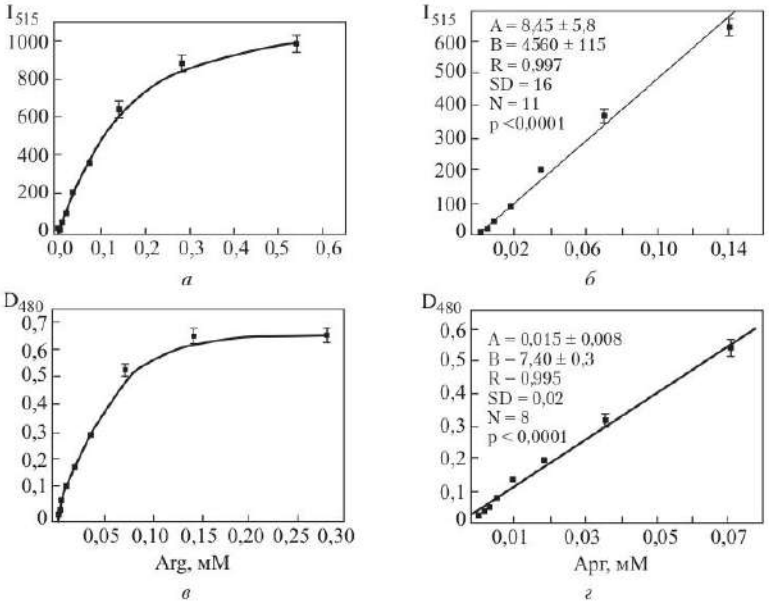

Рис. 4. Основні аналітичні характеристики ДМО-методу за використання аргінази[2]. Залежність інтенсивності випромінювання реакційної суміші від концентрації Arg (*а*) та діапазон лінійності ФЛ методу (*б*). Залежність світлопоглинання від концентрації Arg у фотометрованій суміші (*в*) та діапазон лінійності СФ методу (*г*)

Arg за використання аргінази[2]. Аналогічні графіки отримували й при обробці експериментальних даних з використанням інших ензимів.

У табл. 3 підсумовано аналітичні характеристики (лінійність калібрувального графіку та порогова чутливість) ензиматично-хімічного ДМО-методу для кожного досліджуваного ензиму.

Як видно з наведених даних, властивості ензимних препаратів при використанні їх в ДМО-методі є близькими, особливо при ФЛ реєстрації продуктів реакції. Як каталітичну складову в аналітичному наборі «Аргітест» було використано препарат аргінази[2]. Набір «Аргітест» із спектрофотометричною та флуорометричною детекцією продукту реакції було

Таблиця 3

Основні аналітичні характеристики ДМО-методу за використання різних препаратів ензимів

Ензим	Параметр			
	лінійний діапазон, μM		чутливість, μM	
	ФЛ	СФ	ФЛ	СФ
Аргіназа[1]	0,06–280	7–100	0,04	5,0
Аргіназа[2]	0,28–140	1,1–70	0,15	0,28
Аргіназа[3]	0,55–140	0,55–140	0,30	0,30
АДІ	0,55–140	4,4–280	0,30	2,5

випробувано на реальних зразках сироватки крові людини, та, як результат, встановлено межі вмісту Arg та середні значення для практично здорових людей, які добре корелюють із літературними даними [23].

ВИСНОВКИ

Вперше досліджено аналітичні характеристики рекомбінантних аргініно-гідролізуючих ензимів як каталітичних складових аналітичного набору «Аргітест». Принцип роботи набору «Аргітест» полягає у ензиматичному перетворенні L-аргініну і спектрофотометричному або флуорометричному детектуванні кінцевого продукту хімічної реакції карбаміду (за дії аргінази) або цитруліну (за дії аргінін-деімінази) із диметилмонооксимом. Показано, що кожен із досліджених ензимів може бути використаний для визначення L-аргініну, але як каталітичну складову при створенні набору «Аргітест» було використано препарат $(His)_6$-тагованої аргінази I печінки людини (аргіназа[2]). Можна прогнозувати, що комерційний випуск економічно вигідного аналітичного набору «Аргітест» дасть можливість започаткувати моніторинг вмісту Arg в крові людини у вітчизняній клінічній практиці та буде перспективним, окрім медицини, також і для застосування у ветеринарії, харчовій та фармацевтичній промисловості.

Роботу виконано за фінансової підтримки НАН України в рамках науково-технічної програми «Розробка, тестування та випуск пробної серії ензиматичного набору «Аргітест» для аналізу аргініну в клінічних зразках». Розділ 1. Оптимізація складу набору, умов проведення аналізу та розробка науково-технічної документації» (Проект 29-2015) у 2015 р., комплексної науково-технічної програми «Сенсорні прилади для медико-екологічних та промислово-технологічних потреб: метрологічне забезпечення та дослідна експлуатація» (Проект № 13-2017) у 2013—2017 рр. та стипендії президента України для молодих вчених (Стасюк Н.Є.) у 2016—2017 р.

ЛІТЕРАТУРА

1. Yokoro M., Suzuki M., Murota K. et al. Asymmetric dimethylarginine, an endogenous NOS inhibitor, metabolized in rat erythrocytes. *Biosci. Biotechnol. Biochem.* 2012. Vol. 76, no. 7. P. 1334—1342.
2. Marini J. Arginine and ornithine are the main precursors for citrulline synthesis in mice. *J. Nutr.* 2012. Vol. 142, no. 3. P. 572—580.
3. Yan X., Takahara M., Xie L. et al. Arginine metabolism in soft tissue sarcoma. *J. Dermatol. Sci.* 2011. Vol. 61, no. 3. P. 211—215.
4. Martens-Lobenhoffer J., Bode-Böger S.M.J. Chromatographic-mass spectrometric methods for the quantification of L-arginine and its methylated metabolites in biological fluids. *Chromatography B.* 2007. Vol. 851, no. 1—2. P. 30—41.
5. Bhandare Pravin, Madhavan P., Rao B.M., Someswar Rao N. Determination of arginine, lysine and histidine in drug substance and drug product without derivatisation by using HILIC column LC technique. *J. Chem. Pharm. Res.* 2010. Vol. 2, no. 5. P. 0580—586.
6. Mira O.R.J. Quantitative determination of L-arginine by enzymatic End-Point analysis. *Agric. Food Chem.* 2001. Vol. 49, no. 2. P. 549—552.
7. L-Arginine/Urea/Ammonia, UV method. URL: www.nzytech.com/products-services/analytical-test-kits/ak00171/ (дата звернення 20.04.2017).
8. Yasuhisa A., Masafumi K. Rapid enzymatic assays for L-citrulline and L-arginine based on the platform of pyrophosphate detection. *Enz. Microb. Technol.* 2014. Vol. 57, no. 10. P. 36—41.
9. Гайда Г.З., Стасюк Н.Є., Гончар М.В. Методи аналізу L-аргініну. *Biotechnologia Acta.* 2014. № 1. С. 31—39.
10. Стасюк Н.Є., Гайда Г.З., Гайда А.В., Гончар М.В., Ковальчук Є.П. Ензиматичний метод визначення вмісту L-аргініну за використання рекомбінантної аргінази I людини. *Ukr. Biorg. Acta.* 2012. Т. 1. С. 31—37.

11. Stasyuk N., Gaida G., Gonchar M. L-arginine assay with the use of arginase I. *App. Biochem. Microbiol.* 2013. No. 5. P. 529–534.
12. Гайда Г., Стасюк Н., Сибірна Н., Гончар М. Визначення L-Аргініну у крові щурів ензиматичним методом. *Scientific Journal «ScienceRise»*. 2015. № 11/6 (16). С. 33–38.
13. Стасюк Н.Є., Басс С.Р., Гайда Г. З., Єпремян Н.С., Гончар М.В. Новий ензиматичний метод визначення L-аргініну за використання аргінази І людини та уреази. *Scientific Journal «ScienceRise»*. 2015. № 6/1 (11). С. 43–48.
14. Stasyuk N.Ye., Gayda G.Z., Yepremyan H.S., Gonchar M.V. Simultaneous fluorometric arginase/urease-based assay of L-arginine, urea and ammonium. *Spectrochimica Acta, Part A*. 2017. Vol. 170. P. 184–190.
15. Stasyuk N., Gayda G., Fayura L., Boretskyy Y.R., Gonchar M.V., Sibirny A.A. Novel arginine deiminase-based method to assay L-Arginine in beverages. *Food chemistry*. 2016. Vol. 201. P. 320–326.
16. *Патент України на корисну модель № 108773*. Стасюк Н.Є., Гайда Г.З., Фаюра Л.Р., Борецький Ю.Р., Сибірний А.А., Гончар М.В. Ензиматично-хімічний метод визначення вмісту L-аргініну в харчових продуктах та алкогольних напоях.
17. Стасюк Н.Є., Гайда Г.З., Ковальчук Є.П., Стасик О.В., Гончар М.В. Виділення та характеристика аргінази І людини із рекомбінантних дріжджів *Hansenula polymorpha*. *Укр. біохім. журн.* 2010. Т. 6. С. 14–21.
18. Zakalskiy A.E., Zakalska O.M., Rzhepetskyy Y.A., Stasyk O.V., Horak D., Gonchar M.V. Overexpression of $(His)_6$-tagged human arginase I in *Saccharomyces cerevisiae* and enzyme purification using metal affinity chromatography. *Protein Expr. Purif.* 2012. Vol. 81. P. 63–68.
19. Stasyk O.V., Boretsky Y.R., Gonchar M.V., Sibirny A.A. Recombinant arginine-degrading enzymes in metabolic anticancer therapy and biosensorics. *Cell Biol. Intern.* 2015. Vol. 39 (3). P. 246–252.
20. Fayura L.R., Boretsky Y.R., Pynyaha Y.V., Wheatley D.N., Sibirny A.A. Improved method for expression and isolation of the *Mycoplasma hominis* arginine deiminase from the recombinant strain of *Escherichia coli*. *J. Biotechnol.* 2013. Vol. 4. P. 420–426.
21. Фаюра Л.Р., Борецький Ю.Р., Пинята Ю.В., Мартинюк Н.Б., Скороход В.В., Сибірний А.А. Розробка технології культивування рекомбінантного штаму-продуцента *Escherichia coli* з метою отримання аргініндезімінази *Mycoplasma hominis*. *Наука та інновації*. 2014. № 4. С. 32–39.
22. Дерффель К. *Статистика в аналитической химии*. Москва, 1994. 267 с.
23. *Патент України на корисну модель № 107543*. Стасюк Н.Є., Гайда Г.З., Закальський А.Є., Закальська О.М., Гончар М.В. Ензиматичний метод визначення L-аргініну в крові людини.

Стаття надійшла до редакції 21.12.16

REFERENCES

1. Yokoro M., Suzuki M., Murota K., Otsuka C., Yamashita H., Takahashi Y., Tsuji H., Kimoto M. Asymmetric dimethylarginine, an endogenous NOS inhibitor, metabolized in rat erythrocytes. *Biosci. Biotechnol. Biochem.* 2012. 76(7): 1334–1342.
2. Marini J. Arginine and ornithine are the main precursors for citrulline synthesis in mice. J. Nutr. 2012. 142(3): 572–580.
3. Yan X., Takahara M., Xie L., Gondo C., Setsu N., Oda Y., Takeuchi S., Tu Y., Moroi Y., Furue M. Arginine metabolism in soft tissue sarcoma. *J. Dermatol. Sci.* 2011. 61(3): 211–215.
4. Martens-Lobenhoffer J., Bode-Böger S.M. Chromatographic-mass spectrometric methods for the quantification of L-arginine and its methylated metabolites in biological fluids. *J. Chromatography B*. 2007. 851(1–2): 30–41.
5. Bhandare Pravin, Madhavan P., Rao B.M., Someswar Rao N. Determination of arginine, lysine and histidine in drug substance and drug product without derivatisation by using HILIC column LC technique. *J. Chem. Pharm. Res.* 2010. 2(5): 580–586.
6. Mira O.R.J. Quantitative determination of. L-arginine by enzymatic End-Point analysis. *Agric. Food Chem.* 2001. 49(2): 549–552.
7. L-Arginine/Urea/Ammonia, UV method. URL: https://www.nzytech.com/products-services/analytical-test-kits/ak00171/ (Last accessed: 20.04.2017).
8. Yasuhisa A., Masafumi K. Rapid enzymatic assays for L-citrulline and L-arginine based on the platform of pyrophosphate detection. *Enz. Microb. Technol.* 2014. 57(10): 36–41.
9. Gayda G.Z., Stasyuk N.Ye., Gonchar M.V. Methods for L-arginine assay. *Biotechnologia Acta*. 2014. 1: 31–39 [in Ukrainian].
10. Stasyuk N.Ye., Gayda G.Z., Gayda A.V., Gonchar M.V., Kovalchuk Ye.P. Enzymatic method for L-arginine assay by the use of recombinant human liver arginase I. *Ukr. Biorg. Acta*. 2012. 1: 31–37 [in Ukrainian].
11. Stasyuk N., Gayda G., Gonchar M. L-arginine assay with the use of arginase I. *App. Biochem. Microbiol.* 2013. 49(5): 529–534.
12. Gayda G., Stasyuk N., Sybirna M., Gonchar M. Enzymatic method of L-arginine determination in rat serum. *Scientific Journal "ScienceRise"*. 2015. 11/6(16): 33–38 [in Ukrainian].
13. Stasyuk N.Ye., Bass S.R., Gayda G.Z., Yepremyan H.S., Gonchar M.V. New enzymatic method for L-arginine assay based on human arginase I and urease. *Scientific Journal «ScienceRise»*. 2015. 6/1(11): 43–48 [in Ukrainian].
14. Stasyuk N.Ye., Gayda G.Z., Yepremyan H.S., Gonchar M.V. Simultaneous fluorometric arginase/urease-based assay of L-arginine, urea and ammonium. *Spectrochimica Acta, Part A*. 2017. 170: 184–190.

15. Stasyuk N., Gayda G., Fayura L., Boretskyy Y.R., Gonchar M.V., Sibirny A.A. Novel arginine deiminase-based method to assay L-Arginine in beverages. *Food chemistry*. 2016. 201: 320–326.
16. *Patent of Ukraine No. 108773*. Stasyuk N., Gayda G., Fayura L., Boretskyy Y.R., Sibirny A.A., Gonchar M.V. Enzymatic-chemical method for L-arginine assay in foods and alcoholic beverages [in Ukrainian].
17. Stasyuk N., Gayda G., Kovalchuk Ye., Stasyk O., Gonchar M. Isolation and characterization of arginase I from the recombinant yeast *Hansenula polymorpha*. *Ukr. Biochem. J.* 2010. 82(6): 14–21 [in Ukrainian].
18. Zakalskiy A.E., Zakalska O.M., Rzhepetskyy Y.A., Stasyk O.V., Horak D., Gonchar M.V. Overexpression of $(His)_6$-tagged human arginase I in *Saccharomyces cerevisiae* and enzyme purification using metal affinity chromatography. *Protein Expr. Purif.* 2012. 81:63–68.
19. Stasyk O.V., Boretsky Y.R., Gonchar M.V., Sibirny A.A. Recombinant arginine-degrading enzymes in metabolic anticancer therapy and biosensorics. *Cell Biol. Intern.* 2015. 39(3): 246–252.
20. Fayura L.R., Boretsky Y.R., Pynyaha Y.V., Wheatley D.N., Sibirny A.A. Improved method for expression and isolation of the *Mycoplasma hominis* arginine deiminase from the recombinant strain of *Escherichia coli*. *J. Biotechnol.* 2013. 167(4): 420–426.
21. Fayura L., Boretsky Y., Pynyaha Y., Martynyuk N., Skorohod V., Sibirny A. Development of cultivation technology for the *Escherichia coli* recombinant strain producing arginine deiminase of *Mycoplasma hominis*. *Nauka i innovacii* (*Science and Innovation*). 2014. 10(4): 32–39 [in Ukrainian].
22. Derffel K. *Statistics in Analytical Chemistry*. Moscow, 1994. 267 p. [in Russian].
23. *Patent of Ukraine No. 107543*. Stasyuk N., Gayda G., Zakalskiy A.Ye., Zakalska O.M., Gonchar M.V. Enzymatic method for L-arginine assay in human serum [in Ukrainian].

Recieved 21.12.16

Stasyuk, N., Gayda, G., Zakalskiy, A., Zakalska, O., Fayura, L., Vovk, O., Stasyk, O., Sibirny, A., and Gonchar, M.

Institute of Cell Biology, the NAS of Ukraine,
14/16, Drahomanov St., Lviv,
79005, Ukraine; tel.: +380 32 261 2108,
fax. +380 32 261 2148, E-mail: galina.gayda@gmail.com

RECOMBINANT FORMS OF ARGINASE AND ARGININE DEIMINASE AS CATALYTIC COMPONENTS OF ARGITEST ENZYMATIC KIT FOR L-ARGININE ANALYSIS

For the time, no screening test kits for L-arginine monitoring in biological fluids, including the blood, have been available in the arsenal of domestic clinical diagnostics. The Argitest enzymatic kit is based on the enzymatic-chemical method of L-arginine quantitative analysis developed using different forms of recombinant human liver arginase I (arginase) and arginine deiminase. The method is highly selective, cheap, simple, and fast. It is remarkable for stability of enzymes and final products. The article demonstrates the possibility of using recombinant arginine-selective enzymes in composition of Argitest kit. The catalytic and analytic characteristics of these enzymes have been studied. It has been shown that each enzyme can be used as a component of enzymatic kit.

Keywords: L-arginine, arginase I, arginine deiminase, 2,3-butanedione monoxime, urease, and Argitest enzymatic kit.

Н.Е. Стасюк, Г.З. Гайда, А.Е. Закальский, О.М. Закальська, Л.Р. Фаюра, Е.И. Вовк, О.В. Стасык, А.А. Сибирный, М.В. Гончар

Институт биологии клетки НАН Украины,
ул. Драгоманова, 14/16, Львов, 79005, Украина,
Тел. +380 32 261 2108, факс +380 32 261 2148
E-mail: galina.gayda@gmail.com

РЕКОМБИНАНТНЫЕ ФОРМЫ АРГИНАЗЫ И АРГИНИНДЕИМИНАЗЫ КАК КАТАЛИТИЧЕСКИЕ КОМПОНЕНТЫ ЭНЗИМАТИЧЕСКОГО НАБОРА «АРГИТЕСТ» ДЛЯ АНАЛИЗА L-АРГИНИНА

В настоящее время скрининговые тест-системы для мониторинга L-аргинина в биологических жидкостях, в том числе, в крови, в отечественной клинической диагностике отсутствуют. Энзиматический набор «Аргитест» базируется на разработанном энзиматическо-химическом методе количественного анализа L-аргинина с использованием разных форм рекомбинантной аргиназы I печени человека и аргининдеиминазы. Метод является высокоселективным, экономично выгодным, простым и быстрым в исполнении, отличается стабильностью энзиматических препаратов и продукта реакции. В статье продемонстрирована возможность использования препаратов рекомбинантных аргинин-селективных энзимов в составе набора «Аргитест». В результате исследований определены каталитические и аналитические характеристики энзиматических препаратов и показано, что каждый из них может быть использован как компонент энзиматического набора.

Ключевые слова: L-аргинин, аргиназа I, аргининдеиминаза, 2,3-бутандионмонооксим, уреаза, энзиматический набор «Аргитест».

Оригінал доступний за посиланням: http://scinn-eng.org.ua/sites/default/files/pdf/2017/N4/Stasyuk.pdf

7.3. Ензиматичний та біосенсорний аналіз йонів Mn^{2+} і Co^{2+} за використання апоензиму Mn^{2+}-залежної рекомбінантної аргінази I

Анотація: *У поточній роботі нами запропоновано новий ензиматичний метод визначення вмісту йонів Мангану (II) і Кобальту (II), що ґрунтується на використанні апоензиму Mn^{2+}-вмісної рекомбінантної аргінази I та 2,3-бутандіон моноксиму (ДМО) в ролі хімічного реагенту. Принцип методу полягає в моніторингу активності L-аргінін-гідролізуючого холоензиму аргінази I після специфічного зв'язування йонів Mn^{2+} або Co^{2+} з апо-аргіназою при різних значеннях pH. Сечовина, яка є продуктом ензиматичного гідролізу L-аргініну (L-Arg), реагує з ДМО, і отримана сполука детектується як флуорометрично, так і спектрофотометрично. Нами показано, що вміст йонів металу в досліджуваних зразках можна визначити шляхом вимірювання рівня сечовини, що утворюється після ензиматичного гідролізу L-Arg реконструйованим холоензимом аргінази в присутності досліджуваних йонів металу. Діапазон лінійності флуорометричного методу апо-аргінази-ДМО у випадку аналізу Mn^{2+} становить від 4 пМ до 1,10 нМ з нижньою межею виявлення 1 пМ Mn^{2+}, тоді як діапазон лінійності цього методу у випадку моніторингу Co^{2+} становить від 8 пМ до 45 нМ з нижньою межею виявлення 2,5 пМ Co^{2+}. Показано, що запропонований метод, будучи високочутливим, селективним, надійним і недорогим, може бути корисним для моніторингу вмісту Mn^{2+} і Co^{2+} у клінічних лабораторіях, харчовій промисловості та службах екологічного контролю.*

Spectrochimica Acta Part A: Molecular and Biomolecular Spectroscopy 193 (2018) 349–356

Contents lists available at ScienceDirect

Spectrochimica Acta Part A: Molecular and Biomolecular Spectroscopy

journal homepage: www.elsevier.com/locate/saa

Highly selective apo-arginase based method for sensitive enzymatic assay of manganese (II) and cobalt (II) ions

Nataliya Stasyuk [a], Galina Gayda [a], Andriy Zakalskiy [a], Oksana Zakalska [a], Abdelhamid Errachid [b], Mykhailo Gonchar [a,*]

[a] Department of Analytical Biotechnology, Institute of Cell Biology, NAS of Ukraine, Drahomanov Str. 14/16, Lviv 79005, Ukraine
[b] Université de Lyon, Analytical Sciences Institute, UMR CNRS 5180, CNRS, Université de Lyon 1, ENS Lyon, 5 rue de la Doua, F-69100 Villeurbanne Cedex, France

ARTICLE INFO

Article history:
Received 15 August 2017
Received in revised form 27 November 2017
Accepted 5 December 2017
Available online 06 December 2017

Keywords:
Recombinant arginase I
Apoenzyme
Holoenzyme
Enzymatic analysis
Manganese (II) and cobalt (II) ions
L-arginine

ABSTRACT

A novel enzymatic method of manganese (II) and cobalt (II) ions assay, based on using apo-enzyme of Mn^{2+}-dependent recombinant arginase I (arginase) and 2,3-butanedione monoxime (DMO) as a chemical reagent is proposed. The principle of the method is the evaluation of the activity of L-arginine-hydrolyzing of arginase holoenzyme after the specific binding of Mn^{2+} or Co^{2+} with apo-arginase. Urea, which is the product of enzymatic hydrolysis of L-arginine (Arg), reacts with DMO and the resulted compound is detected by both fluorometry and visual spectrophotometry. Thus, the content of metal ions in the tested samples can be determined by measuring the level of urea generated after enzymatic hydrolysis of Arg by reconstructed arginase holoenzyme in the presence of tested metal ions. The linearity range of the fluorometric apo-arginase-DMO method in the case of Mn^{2+} assay is from 4 pM to 1.10 nM with a limit of detection of 1 pM Mn^{2+}, whereas the linearity range of the present method in the case of Co^{2+} assay is from 8 pM to 45 nM with a limit of detection of 2.5 pM Co^{2+}. The proposed method being highly sensitive, selective, valid and low-cost, may be useful to monitor Mn^{2+} and Co^{2+} content in clinical laboratories, food industry and environmental control service.

© 2017 Elsevier B.V. All rights reserved.

1. Introduction

The importance of monitoring ions of heavy and transitional metals spans all areas of science and technology. A system that can provide selective detection of these ions in aqueous solutions will find numerous applications in such fields as environmental monitoring, biomedical research, clinical chemistry and pharmacology. Ions of heavy and transitional metals in trace quantities are essential mineral components for the human body and all other living organisms, but they exhibit the high level of toxicity at higher concentrations [1–2].

Manganese (Mn) and cobalt (Co) are considered as the most abundant trace elements in the biosphere, being widely distributed in soil, sediment, water and live organisms [3–6]. In human, chronic manganese excess affects the central nervous system, with the symptoms resembling those of Parkinson's disease and autism [7–11]. The mean total content of Mn in human adult is about 15 mg (typically seen in nucleic acids), and the requirement of in this element is about 2–5 mg/day [6]. Mn acts as an activator of enzymes and as a component of metalloenzymes, taking part in oxidative phosphorylation, fatty acids and cholesterol metabolism, mucopolysaccharide metabolism, and urea cycle [6].

Co is an essential element for life in minute amounts [5]. The human adult contains about 1.1 mg Co with the daily requirement of 0.1 μg/day. Co is a component of vitamin B_{12}. Co induces erythropoietin and blocks iodine uptake by the thyroid, controls the transfer of enzymes like homocysteine methyltransferase in methionine metabolism [6]. Contact dermatitis, cardiomyopathy, vision or hearing impairment, hypothyroidism and polycythemia, have been attributed to chronic of cobalt ions due to dietary supplements, occupation and medical devices (Co-containing implants). The knowledge of steady state Co concentrations in tissues in combination with the data on its adverse health effects in humans should help in the characterization of potential hazards associated with increased blood Co concentrations due to exposure to dietary supplements or cobalt chromium (Co-Cr) containing implants [12].

Thus, the possibility to monitor Mn^{2+} and Co^{2+} ions can represent a helpful tool for clinical diagnostics, food industry and environmental control service. The analysis of the localization and distribution of essential and beneficial metals (including Mn and Co) in biological tissues and liquids (e.g. blood and urine) is a challenging task for medicine and other life sciences. Blood concentrations as well as urinary excretion rates of metallic ions are reliable biomarkers for systemic exposure to these compounds [1,7,13].

Many instrument-based techniques have been applied for quantitative analysis of metal ions. Analytical methods such as high performance liquid chromatography (HPLC), gas chromatography, atomic absorption

* Corresponding author.
E-mail address: gonchar@cellbiol.lviv.ua (M. Gonchar).

https://doi.org/10.1016/j.saa.2017.12.031
1386-1425/© 2017 Elsevier B.V. All rights reserved.

and emission spectroscopy, mass spectrometry (MS) are currently and widely used [14–15]. The classical approaches of spectrophotometry and fluorometry, especially in combination with micro- and nanotechnologies [4,16–19] are very popular too.

Over the past years, the development and application of different MS imaging techniques for metals' analysis, including laser ablation inductively coupled plasma mass spectrometry (LA-ICP-MS), has been rapidly growing in the life sciences in order to investigate the uptake and the transport of both essential and toxic metals in cells and tissues [20]. Although the high-tech analytical techniques for detection of heavy and transition metals are highly sensitive and accurate, they are, however, time-consuming, expensive, require special skills and show limited capability for real-time measurements in biological samples.

As an attractive choice to the mentioned above methods, the electrochemical analytical approaches are also extensively used for metal ions assay. Highly specific, sensitive, simple, fast and cheap biosensors based on electrochemical transducers (amperometric and conductometric electrodes, potentiometric pH-sensitive field effect transistors) and different biorecognition molecules as sensitive elements were developed for inhibitory analysis of heavy metals ions [21–22]. Different microbial cells [23–24], enzymes [22,25–27], DNA and antibodies [28–33], as well as biomimics (molecularly imprinted polymers) [22,34] were used as bioelements. These analytical devices are promising tools for needs of health care, environmental control, biotechnology, agriculture and food industries. Improvement of their analytical characteristics (e.g. sensitivity, selectivity, stability etc.) may be achieved by using negatively or positively charged additional semi-permeable membranes, micro- and nanomaterials of different origin, genetically modified enzymes [22].

Being rather simple, inexpensive, and portable, bio- and chemosensors are promising for real-time measuring for online and continuous analysis of natural samples for detection of metallic ions. The number of chemosensors, namely, based on platinum nanoparticles and 3,3,5,5-tetramethylbenzidine as chromogene with fiber optic detection [35] as well as based on gold clusters [36] and fluorescence graphene-based quantum dots [37–39] were proposed in recent years.

Thus, a majority of known chemical and physico-chemical methods of metallic ions assay has a number of disadvantages, such as a low sensitivity and selectivity, high costs and complexity of the equipment. Therefore, the development of simple cost-effective sensitive methods of quantitative analysis of metallic ions, including Mn^{2+} and Co^{2+}, is an important task of analytical chemistry. Thus, metal-ion-dependent enzymes [22,25–27] and catalytic nucleic acids – DNA-zymes or RNA-zymes [28–33,40] present promising tools for elaboration of such methods.

The use of functional nucleic acids as bioelements for the lab-on-a-chip (LOC) biosensors for detection of heavy metal ions have made a great step forward in recent years. A number of metal-ion-dependent DNAzymes and metal-ion-binding DNA structures have been obtained through combinatorial selection and rational design [33]. These molecules have been used as bioselective elements of sensors with fluorescent, colorimetric, electrochemical, and surface Raman detection of correspondent metal ions. For selective sensing metal ions in complex biological samples and live cells, a facile and stable biosensor based on non-biological enantiomer (L-DNAzyme) was proposed by Kue et al. [32]. With its highly sensitivity (with a detection limit down to 11 ppt) and selectivity (up to millions-fold) toward specific metal ions, these sensors have been applied for on-site and real-time environmental monitoring, point-of-care medical diagnostics and for in situ cellular imaging [41].

According to the degree of automation and system integration, modern analytical devices may be classified as: microfluidic LOC system, microchip, lateral flow dipstick, personal glucose meter, disc-based analytical platform and microfluidic paper-based (MFPB) sensors [42–44]. MFPB sensors are inexpensive, simple, low-cost, portable, easy to use and usually naked-eye quantitative methods, so these analytical devices are promising for use in developing countries and for field measurements.

Analysis of literature data suggests that the further development of novel highly selective and sensitive methods for clinical diagnostics and industry, including enzymatic ones, is necessary. Recently we have demonstrated the possibility to use apoenzyme of Mn^{2+}-dependent recombinant human liver arginase I as a Mn^{2+}-sensitive bioelement in biosensor analysis [45]. The bi-enzyme amperometric biosensor based on arginase, isolated from the recombinant yeast cells, and commercial urease revealed a high sensitivity to Mn^{2+}-ions (9200 ± 20 A M^{-1} m^{-2}) and a low detection limit (0.15 μM).

Arginase I (EC 3.5.3.1; L-arginine amidinohydrolase) is an Mn^{2+} containing enzyme of the urea cycle. It catalyses the final cytosolic reaction of urea formation in the mammalian liver — the conversion of arginine to ornithine and urea. Arginase I (further – arginase) has recently been considered as a prospective pharmaceutical in enzymotherapy for some kinds of auxotrophic cancers for L-arginine (further - Arg) as well as an analytical instrument for assay of the own substrate — Arg [46].

In this paper, we describe the development of a novel enzymochemical method for differential Mn^{2+} and Co^{2+} ions determination and its application on the real samples of wastewaters. The proposed method, based on apoenzyme of recombinant arginase, revealed a high sensitivity and selectivity to Mn^{2+} and Co^{2+} ions. The binding of Mn^{2+} or Co^{2+} with apoenzyme of arginase, at experimentally estimated optimal pH values, induces holoenzyme reconstruction, followed by recovering arginase activity and generation of urea from Arg in arginase-catalysed reaction at different pH-values: 9,1 and 7,1 for Mn^{2+} and Co^{2+}, respectively. Analytical signal is the result of the formation of a stable product between urea and 2,3-butanedione monoxime (DMO) in an acidic medium [47]. The resulted compound can be spectrophotometrically and fluorometrically monitored. The advantages of the proposed method are the simplicity and the fastness (if compared to HPLC and other instrumental methods) of analytic procedure. Being highly sensitive, selective, valid and cost-effective, the proposed analytical method will be promising for Mn^{2+} and Co^{2+} ions assay in different fields of science and technology, including environmental chemistry, plant and animal biochemistry, nutrition, and medicine.

2. Experimental Section

2.1. Reagents and Materials

2,3-butanedione monoxime (DMO), disodium salt of ethylenediamine tetraacetic acid (EDTA), Ni-NTA Superflow beads and sulfuric acid (95–98%) were purchased from Sigma-Aldrich. L-arginine (Arg) and inorganic salts were obtained from Merck (Darmstadt, Germany).

Chemical reagents were prepared using Millipore milli-Q water pretreated with sorbent Chelex 100 (Bio-Rad, Hercules, CA, USA) to remove traces of transient metal ions.

2.2. Apparatus

The fluorescence of the end product of analytical reactions was measured using a Tecan Infinite M-200 spectrofluorometer (Thermo Scientific, United States) at an excitation wavelength of 360 nm and an emission wavelength of 515 nm. Optical density was measured at 350 nm using a Shimadzu UV1650 PC spectrophotometer (Japan).

2.3. Arginase Isolation

Recombinant human arginase I (further – arginase) has been expressed in *Saccharomyces cerevisiae* yeast cells under the control of the inducible *CUP1* promoter. Isolation and purification of $(His)_6$-tagged arginase from cell-free extract of cultivated cells using affinity

chromatography on Ni-NTA sorbent was performed as described by us earlier [48]. Arginase activity was determined as the rate of urea production (μmole min^{-1} mg^{-1} of protein), using as substrate solution of 100 mM Arg, 2 mM $MnCl_2$ in 20 mM Tris-sulfate buffer, pH 9.5 [49].

2.4. Preparation of Apo-Enzyme of Arginase (Apo-Arginase)

The apo-arginase was prepared by dialysis of the purified arginase for 48 h against several changes of 50 mM sodium-phosphate buffer (PB), at pH 8.0, containing 50 mM NaCl and 20 mM EDTA. EDTA was removed from the resulting apo-enzyme solution by three steps of dialysis against PB, containing 1 M NaCl and Chelex (0.05 g mL^{-1}), and finally two dialysis against PB with 50 mM NaCl and Chelex (0.05 g mL^{-1}).

2.5. Calibration Graphs for Manganese (II) and Cobalt (II) Ions Assay

Preparation of the reagents:

1) Standard solutions of $MnCl_2$ or $CoCl_2$ in water at concentration ranging from 0.01 μM to 1 mM were prepared from the corresponding stock solutions (2 mM);
2) 20 mM Tris-sulfate buffer (TB) at different pH values: from 6.5 to 10.5;
3) Stock solutions of 100 mM Arg in 30 mM TB at different pH values: from 6.5 to 10.5;
4) Freshly prepared chemical reagent for urea (for 10 assays): mixture of 18 mL 0.5% aqueous solution of DMO and 12 mL 3 M H_2SO_4.

Calibration procedure was as follows:

a) *Holoenzyme reconstruction*: 0.02 mL standard $MnCl_2$ or $CoCl_2$ solution was mixed with 0.02 mL apo-arginase (900 U mL^{-1}) in TB, pH 7.1 and incubated at 55 °C during 10 min;
b) *Enzymatic Arg hydrolysis*: 0.2 mL Arg solution was added to the mixture and incubated at 37 °C during 20 min;
c) *Generated urea assay*: 3 mL of chemical reagent was added and the mixture was heated in a boiled-water bath during 50 min.

The product of chemical reaction of urea with DMO was detected by fluorometry (DMO-F) or spectrophotometry (DMO-S) as described earlier [50]. As a control, a reaction mixture without Arg was used. Each experiment was repeated 3 times. Calibration graphs for metal ions assay were built as the dependence of the absorbance (D_{490}) or fluorescence intensity (I, FIU) of reaction product on the concentrations of metallic ion in final reaction mixture.

2.6. Metal Ions Assay in Real Samples

Both the apo-arginase/DMO-F method and the reference atomic absorption method were then used to analyse real samples of wastewater from the copper and gold mines (Poland).

Before the enzymatic assay, all samples of wastewater were stepwise diluted in 8, 16, 32 and 64-folds with the 30 mM TB: for Mn^{2+} assay – at pH 9.1 and for Co^{2+} assay – at pH 7.1. All samples were then analyzed using a standard addition test (SAT). 20 μL of sample or standard solutions were added into the plastic tubes, then 10 μL apo-arginase (1.2 U mL^{-1}) and 10 μL 30 mM TB, pH 7.1 at 55 °C for reconstruction of holo-arginase from the apo-arginase. Subsequently, 0.2 mL Arg solution was added and the mixture was incubated at 37 °C during 20 min. The resulted urea was detected by adding 3 mL DMO reagent. Thus, the added standards were diluted in final reaction mixture in 162 folds. As a control, reaction mixture without Arg was used. Each assay was performed for two dilutions of the sample and repeated 3 times.

In order to compare the results obtained by current method, the samples were also analyzed using a reference method which involved an Atomic Absorption Spectrophotometer (AAS–1 N, Carl Zeiss Jena, Germany) with standard hallow cathode lamps and air-propane-butane flame. The analysis was carried out at 279.5 nm (for Mn^{2+}) and at 240.7 nm (for Co^{2+}) using a 1000 ppm certified atomic absorption standard solutions (Fisher Scientific, Dubuque, IA, USA) for calibration. The analytical results were statistically processed using the OriginPro 8.5 software.

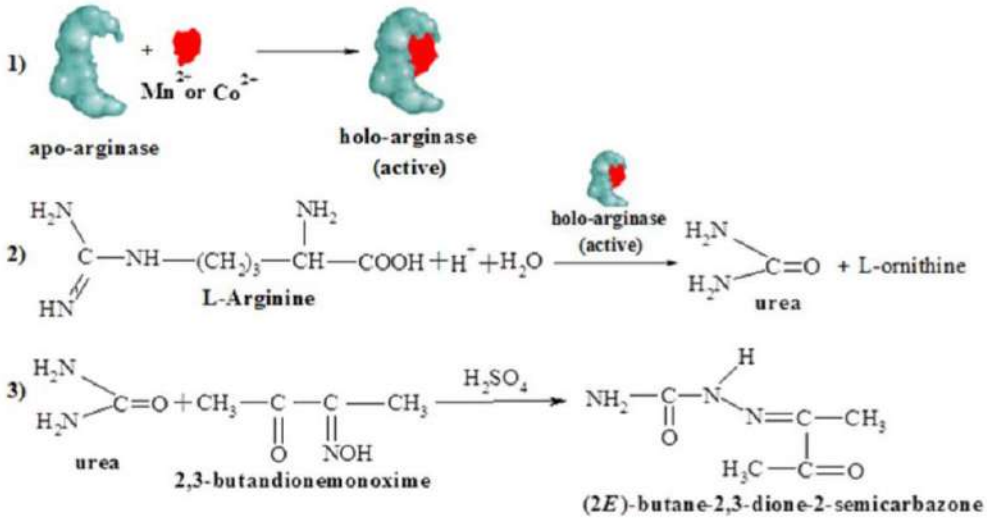

Fig. 1. The principal scheme of apo-arginase based assay for Mn^{2+} or Co^{2+} ions using urea monitoring in reaction with DMO.

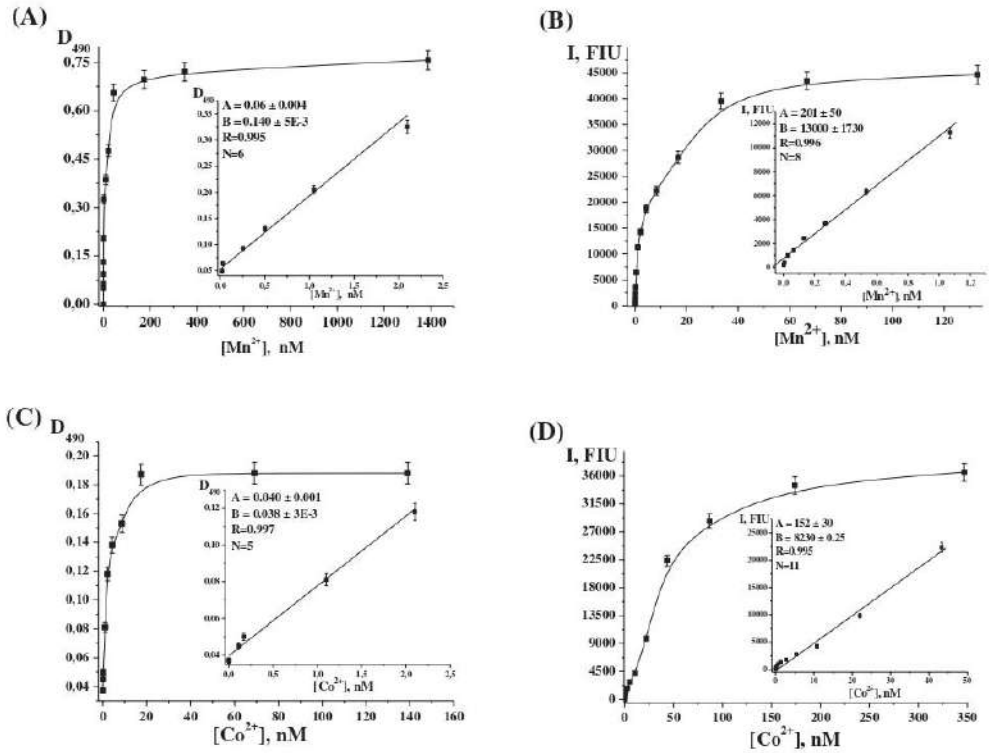

Fig. 2. The dependence of the absorbance (D_{490}) and fluorescence intensities (I, FIU) of final reaction product on the concentration of Mn^{2+} (A, B) and Co^{2+} (C, D) in final reaction mixture and linear calibration curves (inserts) for metal ions assay using apo-arginase-based method: DMO-S (A, C), DMO-F (B, D).

3. Results and Discussion

3.1. The Study of Optimal Conditions for Reconstitution of Arginase Holoenzyme and Enzymatic Hydrolysis of Arg

Arginase catalyses the final cytosolic reaction of urea cycle in the mammalian liver – the conversion of Arg into L-ornithine and urea. Arginase was discovered more than a century ago, a lot of scientific papers (>500,000) were published concerning this enzyme till today. The numbers of native enzymes, isolated from livers, erythrocytes, kidneys of different mammalians, plants, micro- and other organisms, as well as recombinant arginase preparations, were shown to be manganese-containing proteins. One of the first experiments on arginase activation with metallic ions, including Mn^{2+}, was carried out in 1935 [51].

In this paper, we suggest to assay manganese/cobalt ions by determination of arginine-hydrolyzing activity after specific binding of the target ions with apoarginase (Fig. 1).

The possibility of replacing two Mn^{2+} ions, that usually present in human arginase, by Co^{2+} was recently approved [52]. The modified enzyme has been shown to possess a significantly lowered K_M value without a concomitant reduction in k_{cat}. The replacement of Mn^{2+} by Co^{2+} resulted in essential shift of the pH-optimum for the enzyme from 8.5 to 7.5. The modified enzyme is very promising for therapeutic applications, because Co^{2+} substitution leads to a significant increasing of the enzyme stability and activity in serum (neutral pH) [52]. Replacing Mn ion in active site of arginase by Co was assumed by us for quantitative detection of Co^{2+} after reconstruction of Co^{2+}-modified enzyme and measuring the enzymatic activity at pH 7.1, while Mn^{2+}-containing enzyme shows its major activity at pH ≥ 8.5 (we used pH 9.1).

A schematic representation of the reactions, exploited for Mn^{2+}/Co^{2+} assay, is shown in Fig. 1. The apo-arginase could recover its enzyme activity by the addition of Mn or Co ions. Binding of Mn^{2+} or Co^{2+} with apoenzyme resulted in reconstruction of two forms of holoenzyme (stage 1); Arg hydrolysis at pH 9.1 and 7.1 (stage 2). Analytical signal was generated due to the formation of a stable product between urea and DMO (stage 3, chemical reaction). The last product is monitored spectrophotometrically (DMO-S) or fluorometrically (DMO-F). Thus, the concentrations of metal ions in samples were determined by measuring of the rate of urea formation during enzymatic hydrolysis of Arg under the action of reconstructed holoarginase.

We have demonstrated the possibility of reconstruction of apo-arginase into active holo-arginase in the presence of manganese ions (ranging from 0.1 to 1 μM). The optimal time for the whole reconstruction of the holoenzyme was shown to be about 3 min that highly correlates with the results of enzyme reconstruction on the surface of working electrode in amperometric biosensor [45].

The recovered Mn^{2+}-dependent arginase activity was found to be proportional to the reaction time. The restored arginase activity reached a plateau (about 70% of initial activity) after 3 min incubation. It is

Table 1
Characteristics of the proposed apo-arginase-DMO-based method.

Detection mode	Fluorometry		Spectrophotometry	
Analyte	Mn^{2+}	Co^{2+}	Mn^{2+}	Co^{2+}
Linearity range, pM	4.0–1100	8.0–45,000	15–2100	13–2100
Limit of detection, pM	1	2.5	6	4
Limit of quantification, pM	3	7	14	12

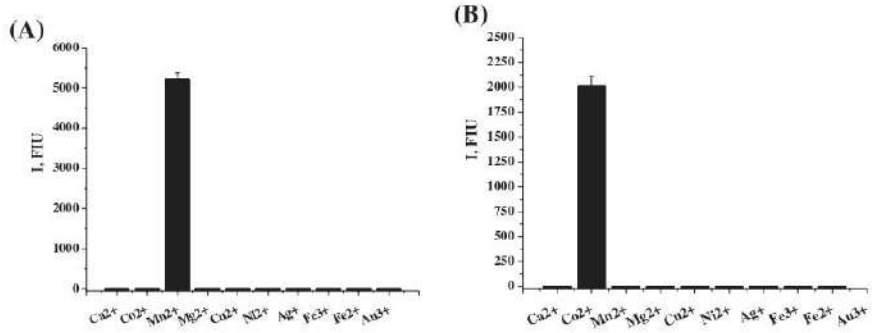

Fig. 3. Selectivity of apo-arginase-DMO-F method to Mn^{2+} (A) and Co^{2+} (B) at the optimized conditions of holo-enzyme's reconstruction at pH 9.1 (A) and 7.1 (B), followed by its enzymatic activity measurements.

assumed that 30% of the original activity was not recovered due to slight denaturation of apo-arginase during its isolation. To optimize the conditions of the enzymatic reaction, the concentration of apo-arginase was varied from 0.003 to 0.015 μg mL^{-1} in the incubation mixture. As a result, the optimal apo-arginase concentration in the incubation mixture has been estimated to be 0.012 μg mL^{-1}.

3.2. The Analytical Characteristics of Apo-Arginase-Based Method

The Mn^{2+} and Co^{2+} dependent holo-arginase were reconstructed by adding optimal amounts of Mn^{2+} and Co^{2+}. Enzymatic activity was then monitored after addition of Arg using fluorometric or spectrophotometric registration of the final product of enzymatic digestion, urea.

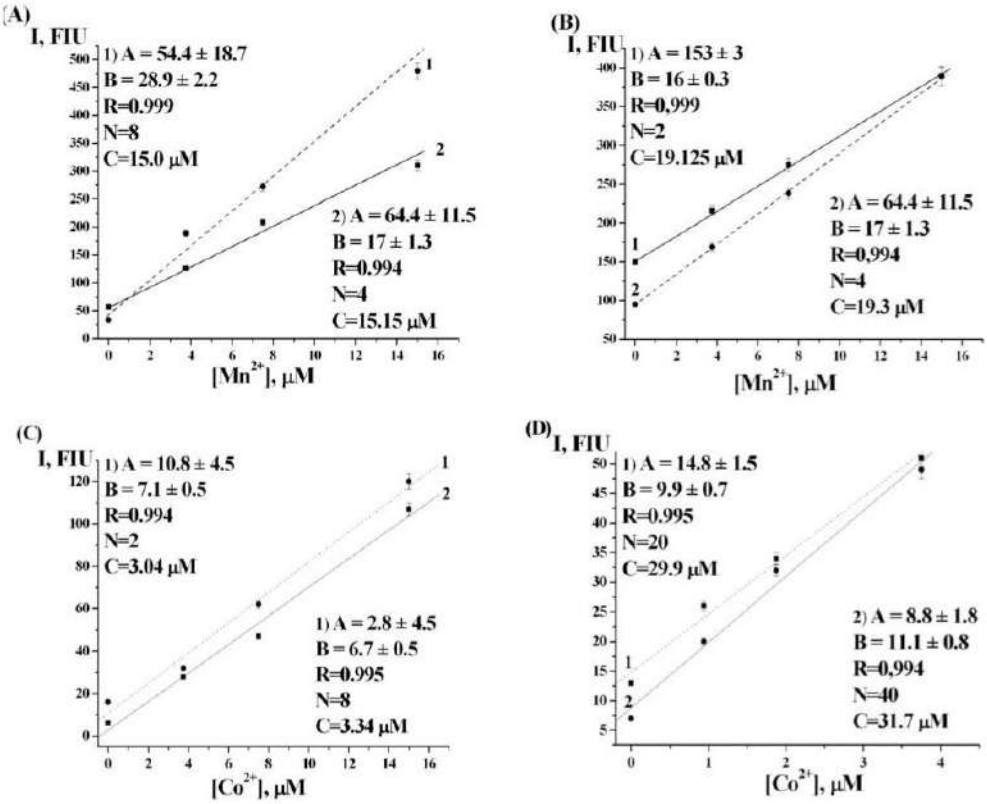

Fig. 4. Assay of Mn^{2+} (A, B) and Co^{2+} (C, D) ions by DMO-F method for two dilutions of the wastewater from gold (B, C) and copper (A, D) mines. [Mn^{2+}] and [Co^{2+}] – concentrations of added standards to the samples; C – calculated concentrations of Mn^{2+} and Co^{2+} ions in the analyzed samples.

Table 2
Analysis of Mn^{2+} and Co^{2+} ions in real wastewater samples.

Method/detection mode	Fluorometry		Atomic absorption spectroscopy	
Mine	Gold	Copper	Gold	Copper
[Co^{2+}], μM	3.19 ± 0.15	30.80 ± 0.90	3.10 ± 0.20	31.30 ± 0.60
CV, %	6.65	4.12	1.01	0.70
[Mn^{2+}], μM	19.21 ± 0.60	15.10 ± 0.70	18.30 ± 0.30	16.00 ± 0.40
CV, %	0.62	1.70	6.43	1.54

CV – coefficient of variation. Values are expressed as mean ± SD. * – these results were obtained from curves, presented in Fig. 4.

The dependence of fluorescent intensity and optical density of the resulted product (DMO-urea) on Mn^{2+} and Co^{2+} concentration, as well as the corresponding calibration curves (DMO-F-and DMO-S) for Mn^{2+} and Co^{2+} assay performed using the optimized experimental conditions are shown in Fig. 2. The optimal concentrations of the metal ions for maximal enzyme activity in the final reaction mixture was in the range 1 pM to 1.4 μM.

The analytical characteristics of apo-arginase-DMO-based methods for manganese and cobalt ions assay are summarized in Table 1. Analytical signals of the developed method were tested in the range of concentrations from 1 pM to 1.4 μM for Co^{2+} and Mn^{2+} (Fig. 2). In the case of DMO-F method, the dynamic range is linear between 4 pM and 1,1 nM for Mn^{2+} assay and between 8 pM and 45 nM for Co^{2+} assay. For DMO-S method, the linearity ranges are 15 pM–2.1 nM for Mn^{2+} assay and 13 pM—2.1 nM for Co^{2+} assay.

For DMO-S and DMO-F modes of detection, the LODs for Mn^{2+} assay are 6 pM and 1 pM, and for Co^{2+} assay - 6 pM and 2.5 pM, respectively (Table 1).

The reconstruction time for complete reactivation of arginase holoenzyme was shown to be 10 min. So, the obtained results clearly prove a possibility to use the apoenzyme of recombinant arginase I in enzymatic-chemical method of Mn^{2+} and Co^{2+} assay, including the analysis of these ions in real samples of wastewaters.

The high selectivity is a necessary demand for each analytical method. To study the selectivity of the developed apo-arginase-DMO-based approach, fluorescence and spectrophotometric measurements with various metal ions (Ca^{2+}, Mg^{2+}, Co^{2+}, Cu^{2+}, Zn^{2+}, Ni^{2+}, Ag^{+}, Fe^{2+}, Fe^{3+}, Au^{3+}) at two concentrations (15 and 30 μM) were performed. The analytical signal on Mn^{2+}-ions was taken as 100% (Fig. 3). For holoenzyme reconstruction, the apo-arginase was incubated with 30 μM metal ions during 10 min at 55 °C. This temperature was chosen for reconstruction stage according to our observations [45,53] and literature data [54]. The reconstructed enzyme was incubated in the presence of 1 mM Arg and urea content was estimated with DMO.

The negative signals for other tested metal ions, which usually present in wastewaters from mines, confirmed the high selectivity of apo-arginase to its natural (Mn^{2+}) and artificial (Co^{2+}) cofactors. This is due to high binding capacity of apo-enzyme to manganese and cobalt ions and very essential difference in pH-optima for Mn- and Co-bound holoenzymes – 9.1 and 7.1, respectively (Fig. 3). Generally, a very high selectivity of arginase apo-enzyme to metal ions is explained by selection of unique structure of catalytic center of the enzyme during hundreds millions years of biological evolution.

Thus, the developed apo-arginase-based methods (DMO-S and DMO-F) for the quantitative Mn^{2+} and Co^{2+} assay are very sensitive (due to high catalytic activity of the reconstructed arginase) and highly selective (see Table 1 and Fig. 3). It is worth mentioning that, due a very high catalytic activity of the holoenzyme, only 0.072 ng of pure apo-arginase is required for each assay (see Materials and Methods). Taking into account that the final yield of arginase protein from recombinant yeast cells is approximately 6 mg L^{-1} [48], 30×10^6 tests (with 3-fold repeating) can be done with the enzyme preparation, isolated from 1 L of recombinant yeast culture. Storage stabilities (under −20 °C) of holo-enzyme as well as of apo-enzyme are > 3 years, so we can conclude that the proposed method, being not simple, unfortunately, in the same time is very economic in costs.

3.3. Assay of Mn^{2+} and Co^{2+} in Real Wastewater Samples

Wastewaters from mines usually contain ions of heavy metals with a predominance of gold and copper. The developed apo-arginase-DMO method was tested on real samples of wastewater from copper and gold mines. To estimate the content of Mn and Co ions, apo-arginase was incubated with samples of wastewater followed by the addition of Arg (see section "Metal ions assay in real samples") and fluorometric detection of produced urea with DMO.

Due to an essential impact of real samples matrix on analytical signal to the target analytes, a standard addition test (SAT) was performed. SAT is a type of approach for quantitative analysis often used in analytical chemistry, whereby the standard is added directly to the aliquots of the analyzed sample. SAT is used in situations where sample components also may contribute to the analytical signal, thus making it impossible to use routine calibration method. The results of estimation of Mn^{2+} and Co^{2+} in wastewaters from gold and copper mines are presented in Fig. 4 and Table 2.

The reproducibility of the proposed analytical methods is satisfactory: the coefficients of variation are <6.7%. It is worthwhile mentioning that Mn^{2+} and Co^{2+} contents, which were obtained by us, are close to ranges published by another authors: 18.7–110 μM for Mn^{2+} in coal-mine wastewater [55] and 30–310 μM for Co^{2+} in copper and cobalt-mine wastewater [56].

The values of Mn^{2+} and Co^{2+} content in the analyzed samples (Table 2), obtained by two methods – the new enzymatic approach and the reference atomic absorption method - demonstrated a strong

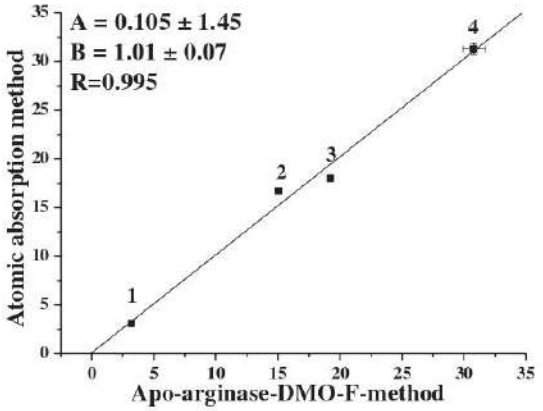

Fig. 5. Correlation between the results of Co^{2+} and Mn^{2+} contents (μM) estimated by enzymo-fluorometric method and atomic absorption method. Tested samples: Co^{2+} (1) and Mn^{2+} (3) from gold mine; Co^{2+} (4) and Mn^{2+} (2) from copper mine.

Table 3
The results of the accuracy and convergence research of the fluorometric quantitative determination of Mn^{2+} and Co^{2+} ions in real wastewater samples.

The criteria of accuracy and precision %	Gold		Copper		Conclusion
	Mn^{2+}	Co^{2+}	Mn^{2+}	Co^{2+}	
The relative standard deviation, $RSD_0 \leq 1.12$	0.92	0.65	0.85	0.42	Satisfies the requirements
Critical values of the one-sided confidence interval, $x \leq 3.2$	2.20	1.0	1.19	1.36	Satisfies the requirements
Criterion of the systematic error insignificance $\delta \leq \Delta prec\sqrt{18}$ if it is not satisfied 1), then 2) $\delta \leq max\delta tot = 2.3$	1.10	0.55	0.48	0.95	Satisfies the requirements (the second criterion)
The overall conclusion on the developed fluorometric method					Is correct

correlation: $R = 0.995$ ($R = 0.995$, 95% confidence interval, $p < 0.01$) (Fig. 5).

Thus, the developed apo-arginase-DMO-F enzymatic method can be used for monitoring Mn^{2+} and Co^{2+} in the samples of wastewaters. On the other hand, this method being very sensitive could be useful to test implant patients for signs of hypothyroidism and polycythemia starting at blood or serum Co concentrations above 100 μg L^{-1} [57]. Besides it, the proposed apo-enzyme-based analytical approach will be useful for fundamental investigations: to study in detail in vitro interactions between metal-dependent biomolecules (proteins and DNA) and their metal cofactors [58].

The developed analytical method was evaluated using statistical analysis. The Student's *t*-test was applied and does not reveal significant difference between the experimental values obtained in the sample analysis by the two methods. The calculated t-value ($t_{calc} = 2.64$) in the case of Mn^{2+} assay in gold mine was found to be less than the critical t-value ($t_{crit} = 4.3$) at 5% significance level. Similar data were obtained for Mn^{2+} assay in wastewater of copper mine: the calculated t-value ($t_{calc} = 2.33$) was found to be less than the critical t-value ($t_{crit} = 4.3$) at 5% significance level. The calculated t-value ($t_{calc} = 0.76$) for Co^{2+} assay in gold mine was found to be less than the critical t-value ($t_{crit} = 4.3$) as well as the calculated t-value ($t_{calc} = 1.11$) for Co^{2+} assay in copper mine was found to be less than the critical t-value ($t_{crit} = 4.3$) at 5% significance level. The assessment of the validation parameters of the method is given in Table 3.

Thus, the results of the accuracy research of the method of Mn^2 and Co^{2+} determination was shown to meet requirements for the permissible limits of ±10.0%.

4. Conclusions

The advantages of the novel enzymo-chemical method for Mn^{2+} and Co^{2+} assay are simplicity of analytical procedure and economic effect due to the usage of only one enzyme in the form of apo-enzyme. An effectiveness of the apo-arginase-based analytical method was proved on the real samples of wastewater. The obtained results proved to be in a good correlation with atomic absorption method. Due to a high stability of apo-arginase, the development and manufacture of enzymatic kits for metallic ions assay based on the proposed method is very prospective. Being sensitive, valid, low-cost, highly selective, the proposed analytical method would be promising in different fields of fundamental and practical science, including environmental chemistry, plant and animal biochemistry, nutrition, and medicine.

Ethical Statement

This article does not contain any studies with human participants or animals performed by any of the authors.

Conflict of Interest Disclosure

The authors declare that there is no conflict of interests regarding the publication of this paper.

Acknowledgments

This work was financially supported by National Academy of Sciences (NAS) of Ukraine (program "Sensors for Medical, Environmental, Industrial, and Technological Needs: Metrological Support and Trial Operation", Project 13-2017), by the Ministry of Education and Science of Ukraine (project #0116U004737), by NATO (Project CBP. NUKR.SFP 984173) and by fellowship of President of Ukraine for Young Scientists in 2017 (N. Stasyuk). We acknowledge the funding through the European Union's Horizon 2020 research and Programme entitled HEARTEN under grant agreement No 643694.

References

[1] C. Protano, M.L. Astolfi, S. Canepari, M. Vitali, Urinary levels of trace elements among primary school-aged children from Italy: the contribution of smoking habits of family members, Sci. Total Environ. 557–558 (2016) 378–385.
[2] R.J.P. Williams, Systems biology of evolution: the involvement of metal ions, Biometals 20 (2007) 107–112.
[3] D. Fedorovych, Y. Boretsky, T. Prokopiv, D. Grabek-Lejko, A. Sybirny, in: A.A. Sibirny (Ed.), Living Organisms and Bioanalytical Approaches for Detoxification and Monitoring of Toxic Compounds, Lviv-Rzeszow 2015, pp. 33–40.
[4] I.S. Balogh, L. Rusnáková, J. Škrlíková, L. Kocúrová, M. Török, V. Andruch, A novel, environmentally friendly dispersive liquid-liquid microextraction procedure for the determination of copper, Int. J. Environ. An. Ch. 92 (2012) 1059–1071.
[5] K. Yamada, Cobalt: its role in health and disease, Met. Ions Life Sci. 13 (2013) 295–320.
[6] L. Prashanth, K.K. Kattapagari, R.T. Chitturi, V.R. Badda, L.K. Prasad, A review on role of essential trace elements in health and disease, J NTR Univ. Health. Sci. 4 (2015) 75–85.
[7] D.S. Avila, R.L. Puntel, M. Aschner, Manganese in health and disease, Met. Ions Life Sci. 13 (2013) 199–227.
[8] D. Lison, Human toxicity of cobalt-containing dust and experimental studies on the mechanism of interstitial lung disease (hard metal disease), Crit. Rev. Toxicol. 26 (1996) 585–616.
[9] A.P. Sanders, B. Claus Henn, R.O. Wright, Perinatal and childhood exposure to cadmium, manganese, and metal mixtures and effects on cognition and behavior: a review of recent literature, Curr. Environ. Health Rep. 2 (2015) 284–294.
[10] P. Chen, S. Chakraborty, T.V. Peres, A.B. Bowman, M. Aschner, Manganese-induced neurotoxicity: from *C. elegans* to humans, Toxicol. Res. (Camb). 4 (2015) 191–202.
[11] M.H. Rahbar, M. Samms-Vaughan, J. Ma, J. Bressler, A.S. Dickerson, M. Hessabi, K.A. Loveland, M.L. Grove, S. Shakespeare-Pellington, C. Beecher, W. McLaughlin, E. Boerwinkle, Res. Autism Spectr. Disord. 1 (2015) 73–82.
[12] B.E. Tvermoes, K.M. Unice, B. Winans, M. Kovochich, W.V. Christian, E. Donovan, E.S. Fung, B.L. Finley, I. Kimber, D.J. Paustenbach, A preliminary evaluation of immune stimulation following exposure to metal particles and ions using the mouse popliteal lymph node assay, Toxicol. Appl. Pharmacol. 308 (2016) 77–90.
[13] B. Michalke, A. Berthele, P. Mistriotis, M. Ochsenkühn-Petropoulou, S. Halbach, Manganese species from human serum, cerebrospinal fluid analyzed by size exclusion chromatography-, capillary electrophoresis coupled to inductively coupled plasma mass spectrometry, J. Trace Elem. Med. Biol. 21 (2007) 4–9.
[14] R. Lobiński, D. Schaumlöffel, J. Szpunar, Mass spectrometry in bioinorganic analytical chemistry, J. Mass Spectrom. Rev. 25 (2) (2006) 255–289.
[15] J. Savory, M.M. Herman, Advances in instrumental methods for the measurement and speciation of trace metals, Ann. Clin. Lab. Sci. 29 (1999) 118–126.
[16] H. Wei, Z. Wang, L. Yang, S. Tian, C. Hou, Y. Lu, Lysozyme-stabilized gold fluorescent cluster: synthesis and application as Hg(2+) sensor, Analyst 135 (2010) 1406–1410.
[17] S. Chen, P. Wang, C. Jia, Q. Lin, W. Yuan, A mechanosynthesized, sequential, cyclic fluorescent probe for mercury and iodide ions in aqueous solutions, Spectrochim. Acta A Mol. Biomol. Spectrosc. 133 (2014) 223–228.
[18] K.B. Narayanan, H.H. Park, Colorimetric detection of manganese (II) ions using gold/dopa nanoparticles, Spectrochim. Acta A Mol. Biomol. Spectrosc. 131 (2014) 132–137.
[19] Shih-Yuan Ma, Yi-Chun Yeh, One-step synthesis of water-soluble fluorescent copper nanoparticles for label-free detection of manganese ions, Anal. Methods 7 (2015) 6475–6478.

[20] J.S. Becker, J.S. Becker, Imaging of metals, metalloids, and non-metals by laser ablation inductively coupled plasma mass spectrometry (LA-ICP-MS) in biological tissues, Methods Mol. Biol. 656 (2010) 51–82.
[21] G.L. Turdean, Design and development of biosensors for the detection of heavy metal toxicity, Int. J. Electrochem. 343125 (2011) (15 p.). Article ID https://doi.org/10.4061/2011/343125.
[22] A.P. Soldatkin, S.V. Dzyadevych, Y.I. Korpan, T.A. Sergeyeva, V.N. Arkhypova, O.A. Biloivan, O.O. Soldatkin, L.V. Shkotova, O.A. Zinchenko, V.M. Peshkova, O.Y. Saiapina, S.V. Marchenko, A.V. El'skaya, Biosensors. A quarter of a century of R&D experience, Biopolym. Cell. 29 (2013) 188–206.
[23] Siok Chin Teo, Ling Shing Wong, Whole cell-based biosensors for environmental heavy metals detection, Annual Research & Review in Biology, 4, 2014, pp. 2663–2674.
[24] S. Jarque, M. Bittner, L. Blaha, K. Hilscherova, Yeast biosensors for detection of environmental pollutants: current state and limitations, Trends Biotechnol. 1345 (2016) 408–419.
[25] M.R. Guascito, C. Malitesta, E. Mazzotta, A. Turco, Low-potential sensitive H_2O_2 detection based on composite micro tubular Te adsorbed on platinum electrode, Sensors Actuators B 131 (2008) 394–402.
[26] C. Malitesta, M.R. Guascito, Heavy metal determination by biosensors based on enzyme immobilised by electropolymerisation, Biosens. Bioelectron. 20 (2005) 1643–1647.
[27] L. Berezhetskyy, O.F. Sosovska, C. Durrieu, J.M. Chovelon, S.V. Dzyadevych, C. Tran-Minh, Alkaline phosphatase conductometric biosensor for heavy-metal ion determination, ITBM-RBM 29 (2008) 136–140.
[28] D.A. Blake, R. Mark Jones, R.C. Blake, A. Pavlov, I. Darwish, H. Yu, Antibody-based sensors for heavy metal ions, Biosens. Bioelectron. 16 (2002) 799–809.
[29] J.C. Achenbach, W. Chiuman, R.P. Cruz, Y. Li, DNAzymes: from creation in vitro to application in vivo, Curr. Pharm. Biotechnol. 5 (4) (2004) 321–336.
[30] X.B. Zhang, R.M. Kong, Y. Lu, Metal ion sensors based on DNAzymes and related DNA molecules, Annu Rev Anal Chem (Palo Alto, Calif) 4 (2011) 105–128.
[31] T. Lan, Y. Lu, Metal ion-dependent DNAzymes and their applications as biosensors, Met. Ions Life Sci. 10 (2012) 217–248.
[32] L. Cui, R. Peng, T. Fu, X. Zhang, C. Wu, H. Chen, H. Liang, C.J. Yang, W. Tan, Biostable L-DNAzyme for sensing of metal ions in biological systems, Anal. Chem. 88 (3) (2016) 1850–1855.
[33] Yu. Xiang, Yi Lu, DNA as sensors and imaging agents for metal ions, Inorg. Chem. 53 (4) (2014) 1925–1942.
[34] M. Sobhana, T. Divya, E.V. Anuja, K. Girish Kumar, Manganese (II) –selective potentiometric sensor based on calix[4]resorcinarene in PVC matrix, Front. Sensors. 1 (4) (2013) 74–80.
[35] W. Chen, X. Fang, H. Li, H. Cao, J. Kong, A simple paper-based colorimetric device for rapid mercury(II) assay, Sci. Rep. 6 (2016) 1943–1948.
[36] J. Chang, G. Zhou, E.R. Christensen, R. Heideman, J. Chen, Graphene-based sensors for detection of heavy metals in water: a review, Anal. Bioanal. Chem. 406 (16) (2014) 3957–3975.
[37] C. Zhou, W. Jiang, B.K. Via, Facile synthesis of soluble graphene quantum dots and its improved property in detecting heavy metal ions, Colloids Surf. B: Biointerfaces 118 (2014) 72–76.
[38] M. Amjadi, R. Shokri, T. Hallaj, A new turn-off fluorescence probe based on graphene quantum dots for detection of au(III) Ion, Spectrochim. Acta A Mol. Biomol. Spectrosc. 153 (2016) 619–624.
[39] L. Lin, X. Song, Y. Chen, M. Rong, Y. Wang, L. Zhao, T. Zhao, X. Chen, Europium-decorated graphene quantum dots as a fluorescent probe for label-free rapid and sensitive detection of Cu^{2+} and L-cysteine, Anal. Chim. Acta 891 (2015) 261–268.
[40] P.J. Bruesehoff, J. Li, A.J. Augustine, Y. Lu, Improving metal ion specificity during in vitro selection of catalytic DNA, comb. Chem. High. Throughput Screen. 5 (4) (2002) 327–335.
[41] S. Müller, B. Appel, D. Balke, R. Hieronymus, C. Nübel, Thirty-five years of research into ribozymes and nucleic acid catalysis: where do we stand today? F1000, Res. Faculty Rev. 5 (2016) 1511, https://doi.org/10.12688/f1000research.8601.1.
[42] S. Zhan, Y. Wu, L. Wang, X. Zhan, P. Zhou, A mini-review on functional nucleic acids-based heavy metal ion detection, Biosens. Bioelectron. 86 (2016) 353–368.
[43] Y. Lin, D. Gritsenko, S. Feng, Y.C. Teh, X. Lu, J. Xu, Detection of heavy metal by paper-based microfluidics, Biosens. Bioelectron. 83 (2016) 256–266.
[44] M. Santhiago, E.W. Nery, G.P. Santos, L.T. Kubota, Microfluidic paper-based devices for bioanalytical applications, Bioanalysis 6 (1) (2014) 89–106.
[45] N. Stasyuk, M. Synenka, G. Gayda, O. Smutok, M. Gonchar, Arginase-based amperometric biosensor for manganese ions analysis Eureka, Life Sci. 1 (2016) 22–28.
[46] O.V. Stasyk, Y.R. Boretsky, M.V. Gonchar, A.A. Sibirny, Recombinant arginine-degrading enzymes in metabolic anticancer therapy and biosensorics, Cell Biol. Int. 39 (3) (2015) 246–252.
[47] J.M. Rho, Direct fluorometric determination of urea in urine, Clin. Chem. 18 (5) (1972) 476–478.
[48] A.E. Zakalskiy, O.M. Zakalska, Y.A. Rzhepetskyy, N. Potocka, O.V. Stasyk, D. Horak, M.V. Gonchar, Overexpression of (His)6-tagged human arginase I in *Saccharomyces cerevisiae* and enzyme purification using metal affinity chromatography, Protein Expr. Purif. 81 (2012) 63–68.
[49] N. Stasyuk, G. Gayda, M. Gonchar, L-arginine-selective microbial amperometric sensor based on recombinant yeast cell over-producing human liver arginase I, Sensors Actuators B Chem. 204 (2014) 515–521.
[50] N. Stasyuk, G. Gaida, M. Gonchar, L-arginine assay with the use of arginase I, Appl. Biochem. Microbiol. 49 (5) (2013) 529–534.
[51] L. Hellerman, M.E. Perkins, Activation of enzymes. III. The role of metal ions in the activation of arginase. The hydrolysis of arginine induced by certain metal ions with urease, J. Biol. Chem. 112 (1935) 175–194.
[52] E.M. Stone, E.S. Glazer, L. Chantranupong, P. Cherukuri, R.M.D.L. Tierney, S.A. Curley, B.L. Iverson, G. Georgiou, Replacing Mn^{2+} with Co^{2+} in human arginase I enhances cytotoxicity toward L-arginine auxotrophic cancer cell lines, ACS Chem. Biol. 5 (3) (2010) 333–342.
[53] N. Ye Stasyuk, G.Z. Gayda, Y.P. Koval'chuk, M.V. Gonchar, Human arginase I from the recombinant yeast *Hansenula polymorpha*: isolation and characterization, Ukr. Biochem. J. 82 (6) (2010) 14–21 (In Ukrainian).
[54] J. Zhang, X. Zhang, C. Wu, D. Lu, G. Guo, X. Mao, Y. Zhang, D. Wang, D. Li, Q. Zou, Expression, purification and characterization of arginase from *Helicobacter pylori* in its apo form, PLoS One 6 (10) (2011), e26205.
[55] C. Wang, H. Xuwen, FOG - Freiberg Online Geoscience, 39–42, 2015 128–135.
[56] J. H. Kim, H.J. Gibb, Cobalt and inorganic cobalt compounds, (2006) 1–82. http://www.who.int/ipcs/publications/cicad/cicad69%20.pdf
[57] B.E. Tvermoes, D.J. Paustenbach, B.D. Kerger, B.L. Finley, K.M. Unice, Review of cobalt toxicokinetics: implications for health risk assessment and metal-on-metal hip implant patients, Crit. Rev. Toxicol. 45 (5) (2015) 367–387.
[58] K. Hwang, P. Hosseinzadeh, Y. Lu, Biochemical and biophysical understanding of metal ion selectivity of DNAzymes, Inorg. Chim. Acta 452 (2016) 12–24.

Оригінал доступний за посиланням: https://doi.org/10.1016/j.saa.2017.12.031

РОЗДІЛ 8

СТВОРЕННЯ АМПЕРОМЕТРИЧНИХ БІО(ХЕМО)СЕНСОРІВ ТА ТЕСТ-НАБОРІВ ЗА ВИКОРИСТАННЯ РЕКОМБІНАНТНОЇ КРЕАТИНІНДЕІМІНАЗИ ДЛЯ КІЛЬКІСНОГО АНАЛІЗУ КРЕАТИНІНУ

- В розділі VIII представлено результати досліджень щодо розробки нових біоаналітичних методів (біонаносенсорів та ензиматичних тест-наборів) для кількісного визначення вмісту креатиніну – метаболіту білкового обміну, важливого біомаркера функціонального стану нирок. Як аналітичний інструмент використано рекомбінантну форму стабільної креатиніндеімінази (КДІ) мікробного походження. Ген креатиніндеімінази (КДІ) *codA Corynebacterium glutamicum* клоновано на векторі експресії pET32a з включенням у структуру рекомбінантного білка $(His)_6$-фрагмента і експресовано в клітинах *Escherichia coli.* Опрацьовано оптимальну схему препаративного виділення та очищення $(His)_6$–тагованої рекомбінантної КДІ з клітин штама-продуцента *Escherichia coli BL21* за використання оригінального методу рефолдингу ензима з тілець включення та метало-афінної хроматографії на Ni-NTA-агарозі. Проведено фізико-хімічну та ензимологічну характеристику $(His)_6$-тагованої КДІ, зокрема, визначено молекулярну масу субодиниці (46,3 кДа), вивчено температурний та pH-профіль активності, досліджено термо- та pH-стабільність ензима та його кінетичні параметри (k_{cat} = 7,0 c^{-1}; K_M = 1,96 мМ відносно креатиніну). Показано, що $(His)_6$-тагований ензим є термостабільним, має високий температурний оптимум (75 ^oC) і стійкий у широкому діапазоні pH (6,0 – 10,5). Виявлено, що рекомбінантна КДІ *C.glutamicum* проявляє строгу субстратну специфічність до креатиніну, що вигідно відрізняє цей ензим від аналогічних мікробних ензимів.

Оптимізовано умови ковалентної іммобілізації КДІ на поверхні електродів, покритих наночастинками металів, за використання ω-меркаптогексадеканої кислоти та гідроксисукцинімід-карбодіімідного методу конденсації. На основі КДІ та амоній-селективних наночастинками Cu/Zn(Hg)S сконструйовано амперометричний біосенсор для кількісного визначення креатиніну. Створений біосенсор характеризується високою селективністю та чутливістю до вмісту

креатиніну (2660 $А \cdot М^{-1} \cdot м^{-2}$). Лінійний діапазон біосенсора спостерігається в діапазоні від 1,5 мкМ до 50 мкМ із нижньою межею визначення креатиніну 0,45 мкМ.

Слід зазначити, що на сьогодні найбільш використовувані біосенсори на основі ензимів для аналізу креатиніну базуються на виявленні аміаку як продукту реакції, що каталізується КДІ, однак існують обмежені дані щодо моніторингу іншого продукту реакції КДІ – N-метилгідантоїну. У цьому розділі описано амперометричний біосенсор на основі КДІ для прямого аналізу креатиніну, який функціонує при низьких потенціалах (-50 мВ) завдяки використанню електрокаталітичних нанокомпозитів. З метою вибору найкращого хемосенсора на N-метилгідантоїн та подальшої розробки амперометричного біосенсора на основі КДІ обрано гібридні наночастинки CoCu. З'ясовано структуру та механізм утворення комплексу CoCu–N-метилгідантоїн на поверхні електрода. Новий біосенсор виявив достатню чутливість (195 $А \cdot М^{-1} \cdot м^{-2}$ для креатиніну), широкий лінійний діапазон (10–800 мкМ), низьку межу виявлення (0,5 мкМ) і високу селективність до цільового аналіту. Сконструйований біоелектрод використано для аналізу креатиніну в біологічних рідинах.

Розроблено високочутливий метод ензиматичного аналізу креатиніну за використання рекомбінантної КДІ з спектрофотометричною та флуориметричною детекцією продукту реакції (йонів амонію) з пороговою чутливістю близько 6 мкМ та 0,2 мкМ, відповідно. За використання рекомбінантної КДІ та спектрофлуорометричного методу моніторингу продукту ензиматичної реакції проведено оптимізацію одночасного аналізу креатиніну та аміаку в сироватках крові людини. Параметрами оптимізації служили концентрації КДІ, *о*-фталевого альдегіду, ЕДТА, тип буферної системи, спосіб підготовки проб для аналізу. Порівняльний аналіз результатів визначення креатиніну в зразках сироватки крові пацієнтів із порушеною функцією нирок до та після проведення процедури гемодіалізу розробленими біосенсорним на ензиматично-флуорометричним методами показав високий рівень кореляції аналітичних даних (R = 0,998), що свідчить про надійність і точність запропонованих підходів.

8.1. Клонування гена мікробної креатиніндеімінази, конструювання ефективного надпродуцента ензима та опрацювання технології отримання очищеного рекомбінантного ензиму.

Анотація: *У поточній роботі нами клоновано ген codA Corynebacterium glutamicum PCM 1945, що кодує креатиніндеіміназу (CDI) (EC 3.5.4.21). Сконструйовано рекомбінантний штам Escherichia coli, надпродуцент $(His)_6$-тагованої КДІ C. glutamicum, неактивної у складі тілець включення. Після солюбілізації тілець включення в присутності 0,3% N-лауроїлсаркозину, ензим ренатуровано і очищено за допомогою одноетапної процедури методом метал-афінної хроматографії. Показано, що вихід $(His)_6$-тагованої КДІ становить ~30 мг з 1 л культури. Слід зазначити, що очищений ензим є достатньо стабільним і має питому активність 10–20 Од./мг. Основні характеристики очищеної $(His)_6$-тагованої КДІ є подібними до природного ензиму.*

Cell Biology International ISSN 1065-6995
doi: 10.1002/cbin.11320

RESEARCH ARTICLE

Overexpression and one-step renaturation-purification of the tagged creatinine deiminase of *Corynebacterium glutamicum* in *Escherichia coli* cells

Andriy E. Zakalskiy[1,2]*, Nataliya Ye. Stasyuk[1], Oksana M. Zakalska[1], Yuriy R. Boretsky[2] and Mykhailo V. Gonchar[1,2,3]

1 Institute of Cell Biology, National Academy of Sciences of Ukraine, 14/16 Drahomanov Str., 79005, Lviv, Ukraine
2 Ivan Bobersky Lviv State University of Physical Culture, 11 Kostiushko Str., 79000, Lviv, Ukraine
3 Drohobych Ivan Franko State Pedagogical University, 24 Ivan Franko Str., 82100, Drohobych, Ukraine

Abstract

The *codA* gene of *Corynebacterium glutamicum* PCM 1945 coding for a creatinine deiminase (CDI) (EC 3.5.4.21) has been amplified and cloned. The recombinant strain of *Escherichia coli* that overproduces the $(His)_6$-tagged inactive CDI of *C. glutamicum* as inclusion bodies has been constructed. After solubilization of inclusion bodies in the presence of 0.3% *N*-lauroylsarcosine, the enzyme was renaturated and purified by a single-step procedure using metal-affinity chromatography. The yield of the $(His)_6$-tagged CDI is ~30 mg from 1 L culture. The purified enzyme is sufficiently stable under the conditions designed and possesses an activity of 10–20 U/mg. The main characteristics of the tagged enzyme remained similar to that of the natural enzyme.

Keywords: *Corynebacterium glutamicum*; creatinine deiminase; *Escherichia coli*; gene cloning; inclusion bodies; metal-affinity chromatography

Introduction

Creatinine, the waste product of creatine, is produced in human muscles, transported via the bloodstream into the kidney and then excreted with urine. Thus, the serum creatinine level is an important indicator of the renal function and a valuable biomarker to control the hemodialysis procedure (Wyss and Kaddurah-Daouk, 2000; Sant et al., 2004). Currently, available chemical methods of creatinine detection possess several limitations due to insufficient sensitivity and low specificity (Zakalskiy et al., 2019). Despite the latter, these methods are widely used for assessments of patient conditions although the accuracy of such detection is crucial.

Usage of a creatinine deiminase (CDI) catalyzing hydrolysis of creatinine to *N*-methylhydantoin and ammonia could overcome these obstacles (Tabata et al., 1983; Wyss and Kaddurah-Daouk, 2000; Gottschalk et al., 2007; Zakalskiy et al., 2019). Certain microorganisms are able to produce CDIs. However, some of them display a low substrate specificity (Wyss and Kaddurah-Daouk, 2000; Zakalskiy et al., 2019). Earlier, CDI of *Corynebacterium glutamicum* (*lilium*) ATCC 15990 was purified and crystallized using a rather complicated protocol: fractionation with ammonium sulfate and protamine sulfate, column chromatography on diethylaminoethyl-cellulose, Sephadex G-100 and hydroxyapatite. The enzyme is specific to creatinine and exhibits a specific activity of 34 U/mg (Uwajima and Terada, 1976, 1977, 1980). Another CDI from the anaerobic microorganism BN11 with a specific activity of 78 U/mg appeared to be a more preferable enzyme to be used for creatinine quantification. Unfortunately, the yield of the enzyme was rather low (Gottschalk et al., 1991). Later, the *Tissierella creatinini* gene coding for CDI was expressed heterologously and the recombinant enzyme was purified and characterized (Gottschalk et al., 2007). Commercially available CDI has been used to develop different approaches

*Corresponding author: e-mail: andriy.zakalskiy@yahoo.com
Abbreviations: bp, basepair; CDI, creatinine deiminase; EDTA, ethylenediaminetetraacetic acid; IPTG, isopropyl β-D-1-thiogalactopyranoside; LB, Luria–Bertani medium; OPA, *o*-phthaldialdehyde; PCR, polymerase chain reaction; SDS-PAGE, sodium dodecyl sulfate polyacrylamide gel electrophoresis; Trx, thioredoxin.

for creatinine assay. However, the cost of the enzyme is rather high, possibly, due to a low protein production by the recombinant strain and a complex purification procedure (Gottschalk et al., 2007; Marchenko et al., 2016; Zakalskiy et al., 2019).

Cloning and expression of the corresponding gene in well-characterized host strains could address the issues mentioned above. Also, it can provide a possibility to fuse different tags to the N- or C-terminus of the recombinant protein to significantly simplify its purification. In most cases, overexpressed proteins are synthesized in an inactive, insoluble form as inclusion bodies. Therefore, the purification procedure will require additional steps of solubilization and renaturation. There are numerous protocols developed for solubilization of inclusion bodies and subsequent enzymes' renaturation (Burgess, 2009). Despite that, solubilization and renaturation of a particular enzyme can be challenging and might demand "fine tuning" of a procedure (temperature, buffer composition, solubilization agents, a procedure of removing them, etc.) to obtain an active and stable preparation (Fayura et al., 2013). Additionally, the oligomeric structure of an enzyme (for instance CDI) further complicates correct reassembly of its active form.

Here we report on construction of the *Escherichia coli* recombinant strain overproducing tagged CDI of *C. glutamicum*. Protein expression, solubilization, and renaturation conditions were studied. As a result, we developed an efficient procedure for one-step refolding-purification of the tagged, apparently oligomeric CDI.

Materials and methods

Cloning of the *codA* gene from *C. glutamicum* into the expression vector pET32a

The open reading frame of the *codA* gene was amplified as a 1,362 bps long DNA fragment using primers codA-for (5′-TACTATGGATCCATGAACACCATTCATCACCATCA CCATCACATGACATGTAGAAATGGA-3′) and codA-rev (5′-TAATAATGCGGCCGCTTAGATGTTCCAGTCCAC-3′) and total DNA *C. glutamicum* PCM 1945 as a template. The primers contained *Bam*HI and *Not*I restriction sites as well as 5′-terminal DNA sequence encoding a $(His)_6$-tag to be fused to the N-terminus of the protein.

The resulting DNA fragment containing the tagged *codA* gene was cleaved with restriction endonucleases *Bam*HI and *Not*I (Thermo Fisher Scientific Inc.) and cloned into the same sites of the expression vector pET32a (Novagen). Then, the *Nde*I fragment carrying the Trx Tag was cut out from the constructed plasmid. The structure of the pET32a-codA plasmid containing the gene coding for the tagged CDI is shown schematically in Figure 1. The nucleotide sequence of the cloned modified gene *codA* was verified by sequencing. The plasmid pET32a-codA was introduced into the *E. coli* strain BL21 (DE3) by electroporation.

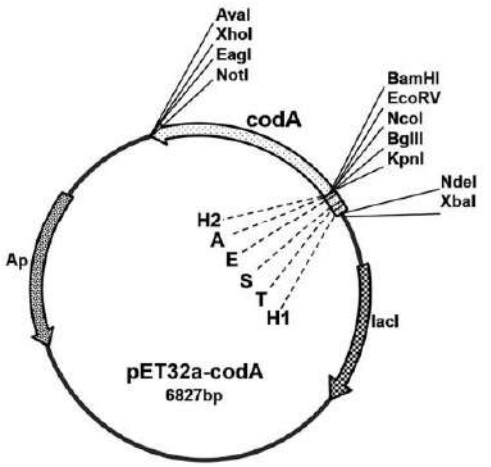

Figure 1 Scheme of the expression plasmid pET32a-codA. A, short amino acid linker; H1, $(His)_6$-tag sequence encoded by vector; H2, $(His)_6$-tag introduced by polymerase chain reaction; S, S-tag; E, enterokinase cleavage site; T, thrombin cleavage site.

Isopropyl β-D-1-thiogalactopyranoside (IPTG)-inducible expression of CDI in *E. coli*

Transformants of the *E. coli* BL21(DE3) were grown overnight at 37°C in LB medium containing ampicillin (50 mg/L). Next morning, the culture was diluted with fresh medium with the antibiotic to $OD_{600} = 0.05$ and the incubation was continued to $OD_{600} = 0.4–1.0$ (about 3 h). The CDI expression was induced with 0.4 mM IPTG for 2–3 h at 30°C before the cells were harvested by centrifugation (6,000*g* for 15 min at 4°C).

Purification of $(His)_6$-tagged recombinant CDI

Preparation and solubilization of inclusion bodies were carried out according to the protocol of the Protein Refolding Kit (Novagen) with several modifications.

The induced cells were resuspended in 20 mM Tris-HCl buffer, pH 7.5, containing 1 mM ethylenediaminetetraacetic acid (EDTA) and 0.1% Triton X-100, treated with lysozyme (100 μg/mL) at 30°C for 15 min, and sonicated on ice until complete cellular lysis followed by a substantial decrease of the solution viscosity. The inclusion bodies were isolated from the crude cell lysate by centrifugation at 10,000*g* for 10 min at 4°C and washed twice with 20 mM Tris-HCl buffer, pH 7.5, containing 1 mM EDTA and 0.1% Triton X-100.

The inclusion bodies were resuspended in 50 mM Tris-SO_4 buffer, pH 9.4, supplemented with 0.3% *N*-lauroylsarcosine, and incubated at room temperature for 30 min with gentle stirring. The supernatant containing the solubilized protein was clarified by centrifugation at 10,000*g* for 10 min at room temperature. The protein preparation from 200 mL of culture was stirred with 1 mL of settled Ni-NTA Superflow beads (Qiagen) for 1 h. The suspension was loaded to a column (0.6 × 7 cm) with the bottom outlet capped and beads were settled for 5–7 min. After removal of unspecific bound proteins by washing with 50 mM sodium phosphate buffer, pH 8.0, containing 300 mM NaCl and 2 mM β-mercaptoethanol, the tagged CDI was eluted by a step gradient of imidazole (20, 50, 100, 150, and 200 mM solution in the same buffer). The fractions exhibiting the highest CDI activity were pooled together, dialyzed against 50 mM sodium phosphate buffer, pH 8.0, supplemented with 300 mM NaCl and 2 mM β-mercaptoethanol, and used as the final CDI preparation. This procedure was developed after several preliminary experiments as described below.

CDI activity assay

CDI activity was determined in 50 mM K, Na-phosphate buffer, pH 7.5, containing 5 mM creatinine in a final volume of 1 mL. After incubation for 15–30 min at 37°C, the formation of ammonium was monitored fluorometrically after derivatization with *o*-phthaldialdehyde (OPA) in the presence of sodium sulfite, as described (Kuo et al., 2005, Stasyuk et al., 2016). One unit (U) of enzyme activity was defined as the amount of enzyme releasing 1.0 µmol of ammonium per 1 min under the above-mentioned conditions.

Enterokinase treatment

Treatment of the tagged CDI with enterokinase was carried out according to the recommended protocol (Sigma-Aldrich) with some modifications. One microgram of the purified tagged CDI was incubated with 0.2 units of enterokinase in 50 mM Tris-HCl buffer, pH 7.0, containing 2 mM $CaCl_2$, in a final volume of 1.2 mL at 25°C. Thirty microliters of aliquots were withdrawn during the time course of incubation, frozen in liquid nitrogen and stored at −70°C.

Electrophoretic analysis of protein samples

Sodium dodecyl sulfate polyacrylamide gel electrophoresis (SDS-PAGE) was carried out as described (Laemmli, 1970). The gel was stained in 0.25% w/v Coomassie brilliant blue R-250 prepared in 50% v/v methanol and 10% v/v acetic acid. The gel was destained in 15% v/v ethanol and 7% v/v acetic acid.

Results and discussion

Cloning of *C. glutamicum codA* gene into *E. coli* expression vector pET32a

Database searches in the *C. glutamicum* ATCC 13032 genome sequence revealed the presence of a gene coding for a predicted 423 amino acids CDI. The gene was designated as *codA* (Kalinowski et al., 2003).

The open reading frame of *codA* gene of *C. glutamicum* PCM 1945 was cloned (in frame) into a pET32a vector, as described in Materials and Methods section. The Trx Tag encoding sequence was removed from the constructed plasmid to reduce changes to the N-terminal amino acid sequence, which could be involved in formation of an active oligomeric enzyme (Battchikova et al., 1996). The resulting plasmid pET32a-codA harbored the modified *codA* gene encoding *C. glutamicum* CDI polypeptide with several short tags fused to its N-terminus (Figure 1). The remaining tags were intended to provide additional approaches for protein purification and analysis.

Expression and purification of the tagged CDI

To induce the expression of CDI, cells of the *E. coli* strain BL21(DE3)/pET32a-codA carrying the constructed plasmid were incubated in the IPTG-containing selective growth medium following the protocol of the pET System Manual (Novagen). The highest expression level of the enzyme was achieved after 3 h of induction at 30°C. Increasing the temperature of induction to 37°C resulted in a lower yield of the enzyme (data not shown). The recombinant protein was accumulated as inclusion bodies in *E. coli* cells. The obtained protein preparation from these inclusion bodies contained an inactive CDI contaminated by other bacterial proteins (<40–50%; Figure 2A, lane 5).

At first, the isolated inclusion bodies were dissolved in 50 mM sodium phosphate buffer, pH 8.0, containing 300 mM NaCl and 2 mM β-mercaptoethanol, supplemented with either 6 M urea or 6 M guanidine hydrochloride. Neither dialysis, nor fast dilution both of the protein solutions with the same buffer, nor chromatography on Ni-NTA resin (as described above) resulted in the enzyme reactivation (data not shown). Thus, we applied *N*-lauroylsarcosine as a solubilizing agent (see Materials and Methods section) and the obtained CDI preparation was used to refold the enzyme. No activity was detected after extensive dialysis against the same buffer without detergent. Fast dilution of the mixture with the same buffer without detergent resulted in protein aggregation, however, traces of CDI activity were detected. Decrease of the detergent concentration to 0.1–0.2% in the dissolving mixture did not lead to additional protein activation (data not shown). As the

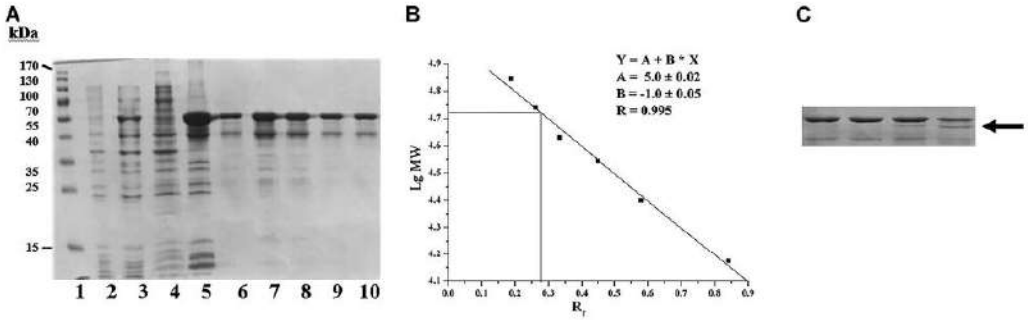

Figure 2 Electrophoretic analysis of the tagged CDI. (A) SDS-PAGE of the recombinant tagged CDI purified from *E. coli*. Lane 1: protein molecular weight markers; lane 2: lysate of non-induced *E. coli* BL21(DE3)/pET32a-codA transformant cells; lane 3: lysate of isopropyl β-D-1-thiogalactopyranoside-induced *E. coli* BL21(DE3)/pET32a-codA transformant cells; lane 4: cell-free extract (soluble fraction) from induced *E. coli* BL21(DE3)/pET32a-codA transformant cells, 5 µL; lane 5: "inclusion bodies" from induced *E. coli* BL21(DE3)/pET32a-codA transformant cells solubilized in 50 mM Tris-SO_4 buffer, pH 9.4 in the presence of 0.3% *N*-lauroylsarcosine, 5 µL; lanes 6–10: elution fractions (20–200 mM imidazole in 50 mM K, Na-phosphate buffer, pH 8.0), 5 µL. Results of a typical experiment are shown. (B) Determination of molecular weight (MW) of tagged-CDI subunit by SDS-PAGE (12%) of the purified enzyme. The inlet presents statistical parameters of the linear regression line for the function lg(MW) = f(Rf). (C) SDS-PAGE of the recombinant tagged CDI treated with enterokinase. Recombinant tagged CDI was incubated with enterokinase for 2 h (lane 2), 8 h (lane 3), and 16 h (lane 4). Lane 1: mixture of CDI with enterokinase before incubation. Position of a 47 kDa protein formed during incubation is pointed by an arrow.

recombinant protein contained two $(His)_6$-tags fused to the N-terminus of CDI, we used Ni-NTA chromatography to purify the protein and simultaneously remove the detergent as described in Materials and Methods section. The targeted CDI displayed high binding affinity to Ni-NTA resin. Only traces of the CDI were found in flow-through fractions after washing the column. The enzyme was then eluted by imidazole step gradient. The CDI appeared as a broad peak at 20–150 mM imidazole (Figure 2A, lane 6–10). The obtained highly purified enzyme preparation (Figure 2A, lane 7–8) exhibited a specific activity of 10–20 U/mg similar to the natural CDI purified from *C. glutamicum* ATCC 15590 (Uwajima and Terada, 1980). These results suggested that additional tags fused to the N-terminus did not affect renaturation of CDI, which appears as a homotetramer. The yield of CDI protein was ~30 mg/L of culture.

The identity of the isolated protein with *C. glutamicum* CDI was additionally proved by mass-spectrometry of the random set of tryptic peptides of the enzyme, as described for arginase (Zakalskiy et al., 2012). On the basis of the results of two-dimensional gel electrophoresis, the molecular weight of the CDI subunit is 46.3 kDa (Bendt et al., 2004). Using the sedimentation equilibrium method, the molecular weight of purified CDI of *C. glutamicum* ATCC 15590 was shown to be 195 kDa (Uwajima and Terada, 1980). Taking together these data, it was suggested that the active enzyme consists of four identical subunits encoded by gene *codA*.

The molecular weight of the recombinant tagged CDI subunit was calculated as 52.5 kDa using elecrophoretic mobility in SDS-PAGE (Figure 2B). Digestion of purified active CDI with enterokinase produced a protein of the expected molecular weight (~47 kDa; Figure 2C). The obtained results well correlated with the published data regarding the *C. glutamicum* ATCC 13032 CDI molecular weight (Bendt et al., 2004). Treatment with enterokinase was used in preliminary analytical experiments only. It caused a significant decrease in the amount of the targeted protein, this may be due to unspecific proteolysis

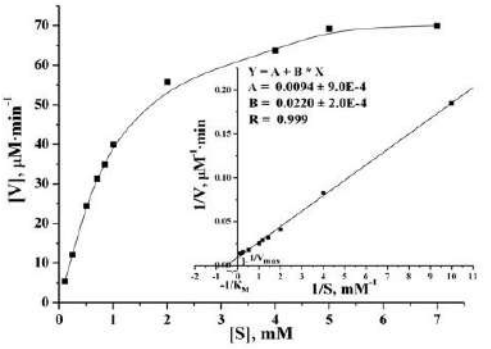

Figure 3 Determination of the kinetic parameters of the purified tagged CDI by the method of Lineweaver–Burk.

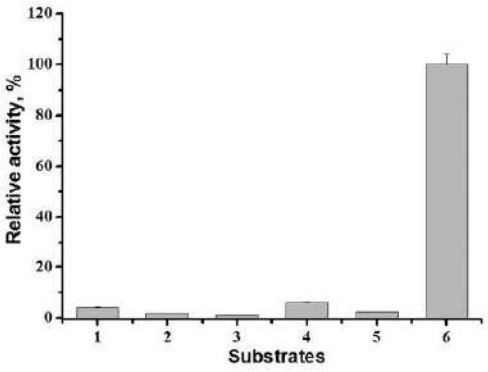

Figure 4 Substrate specificity of purified tagged CDI. 1. cytidine monophosphate (CMP); 2. cytidine; 3. cytidine triphosphate (CTP); 4. cytosine; 5. creatine; 6. creatinine. The reaction mixture contained 5 mM of the corresponding substrate in 50 mM K, Na-phosphate buffer, pH 7.5 and was incubated at 37°C for 15 min.

(Figure 2C). Thus, we did not check the enzymatic activity after the enterokinase digestion and omitted this stage from all subsequent experiments.

The purified tagged CDI possesses a relatively high affinity to creatinine under conditions reported for the natural enzyme (Uwajima and Terada, 1980). At 37°C and pH 7.5, K_M for creatinine was determined as 1.96 ± 0.075 mM and V_{max} was 114.6 ± 3.2 μM/min (at enzyme concentration of 5 μg/mL; Figure 3). Taking into account that the molecular weight of the native enzyme is ~195 kDa (Uwajima and Terada, 1980) the turnover number for the recombinant CDI was calculated as $k_{cat} = 74.5 \pm 3.6\ s^{-1}$. For comparison, CDI from *C. glutamicum* ATCC 15990 has K_M for creatinine as 1.27 mM (at 37°C and pH 7.0) and V_{max} as 45.4 μmol/min/mg of protein (that corresponds to $k_{cat} = 148\ s^{-1}$) (Uwajima and Terada, 1980). With immobilized CDI, isolated from *C. glutamicum*, the K_M value for creatinine was shown to be 1.9 mM (Tabata et al., 1983).

The purified tagged CDI, similar to the enzyme from *C. glutamicum* ATCC 15590 is specific for creatinine (Uwajima and Terada, 1980). It does not hydrolyze creatine, cytosine, cytidine, cytidine monophosphate, and cytidine triphosphate (Figure 4).

The purified tagged CDI exhibited the same activity at pH 7.9 in 50 mM K, Na-phosphate, 50 mM Tris-HCl and 50 mM Tris-SO_4 buffers (data not shown). The highest activity was observed at pH 8.5–9.1 (Figure 5A). The temperature optimum was determined as 60–65°C (Figure 5B). It should be noted that the tagged enzyme retained 60% of its activity after prolonged incubation (60 min) at 65°C. The complete inactivation of the enzyme occurs at 75°C (Figure 6A). The enzyme was sufficiently stable over a wide range of pH from 6.0 to 10.5, while being incubated for 24 h in buffers of different composition (Figure 6B). These data well correlate with previously reported properties of the natural enzyme that possessed a broad pH optimum of 7.5–10.0, maximum activity at 60°C, and relatively high thermo- and pH-stability (Uwajima and Terada, 1980).

The tagged CDI appeared to be stable at 5°C in 50 mM K, Na-phosphate buffer, pH 7.5 for a week (Figure 7).

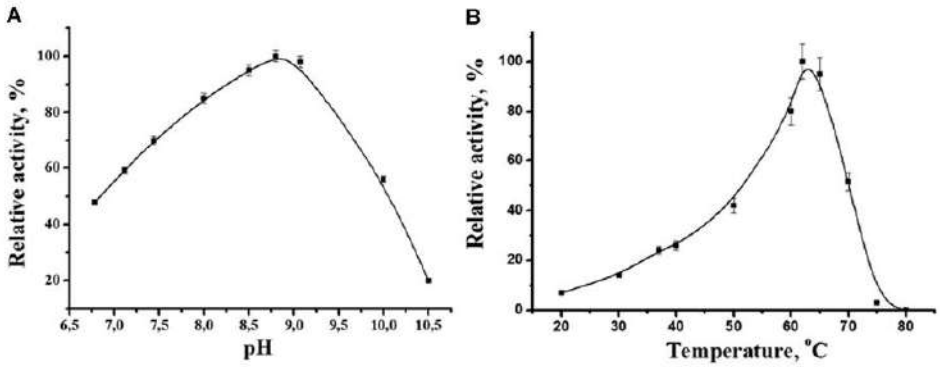

Figure 5 The effect of pH (A) and temperature (B) on the CDI activity. (A) The activity of CDI was determined in 50 mM Tris-HClor 50 mM Tris-SO_4 buffers with pH ranging from 6.75 to 10.5 at 37°C. The data represent an average of three independent experiments. (B) The purified enzyme was incubated in 50 mM K, Na-phosphate buffer, pH 7.5 containing 5 mM creatinine at various temperatures from 20 to 80°C. After the incubation for 10 min at a given temperature, the aliquots were withdrawn and CDI activity was determined. The data represent the average of three independent experiments.

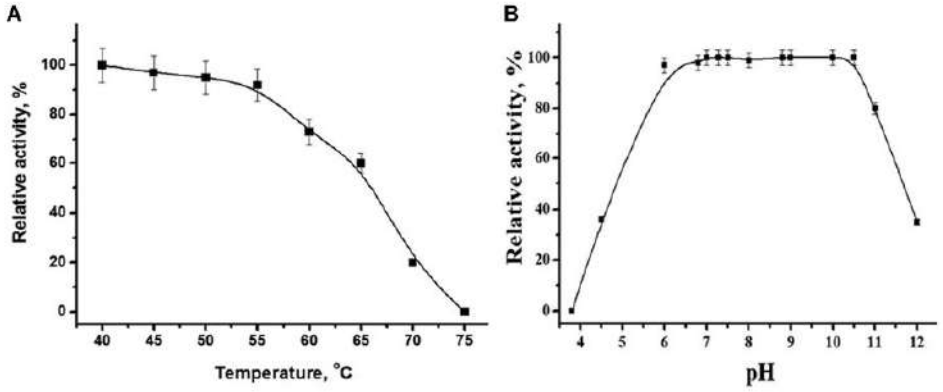

Figure 6 Thermal (A) and pH (B) stability of the tagged recombinant CDI. (A) The enzyme preparation was incubated in 50 mM K, Na-phosphate buffer, pH 7.5 at various temperatures from 40 to 75°C. After the incubation for 1 h at a given temperature, the aliquots were withdrawn, cooled on ice for 10 min and CDI activity was determined at 37°C. The data represent the average of three independent experiments. (B) The enzyme preparation was incubated in various buffers: 50 mM K, Na-phosphate (pH from 6.0 to 8.0), 50 mM Na-acetate (pH from 3.5 to 5.0) and 50 mM Na-borate (pH from 9.0 to 11.0). After the incubation for 24 h at room temperature, the aliquots were withdrawn and CDI activity in 50 mM K, Na-phosphate buffer, pH 7.5 at 37°C was determined. The data represent the average of three independent experiments.

During prolonged storage at −20°C in the same buffer, containing 20% glycerol, the enzyme lost only 30% of its activity within 4 months. Trehalose was found to be the most effective stabilizing agent during CDI lyophilization. This ensured maintenance of the enzyme's activity at 40% over 120 days of storage of the dried powder at 4°C (Figure 8). Additionally, CDI preparations can also be stored without significant loss of activity for at least 4 months as a suspension in 50 mM K, Na-phosphate buffer, pH 7.5 at 70% saturation with ammonium sulfate (data not shown) as was reported for the natural enzyme (Uwajima and Terada, 1980).

Thus, the main properties of the tagged enzyme, that is, specificity and affinity to creatinine, pH and temperature optimum, stability are similar to those of the natural CDI from *C. glutamicum* ATCC 15990. In addition, the recombinant enzyme can be more easily purified and with a higher yield.

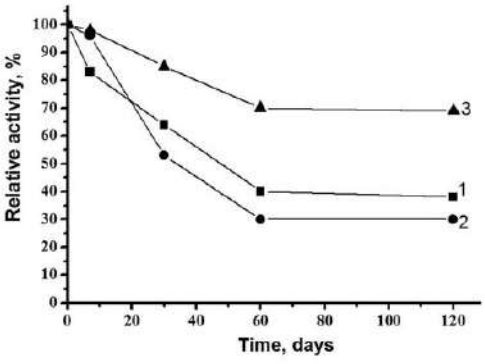

Figure 7 Stability of the tagged CDI at storage in 50 mM phosphate buffer, pH 7.5. 1. 5°C; 2. −20°C; 3. −20°C, 20% glycerol.

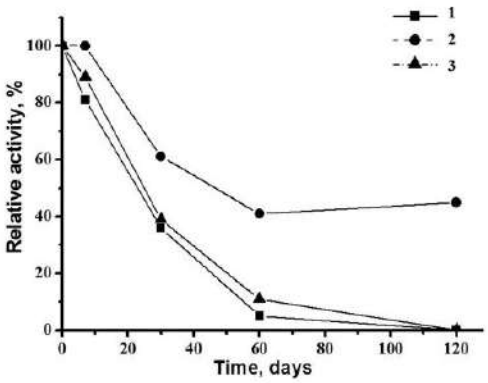

Figure 8 Stability of freeze-dried CDI preparations. 1. Without additive; 2. +8% trehalose; 3. +8% mannitol.

Conclusions

The most prominent advantages of the proposed CDI preparation are a high yield of the enzyme, simple isolation of inclusion bodies, containing the enzyme, a possibility to apply the developed one-step procedure for renaturation-purification of the enzyme and its high stability under conditions designed. The main properties of the purified tagged CDI of *C. glutamicum* are similar to that of the natural enzyme. These findings can be used to develop a cost-efficient large-scale procedure for production of a highly specific targeted CDI.

Acknowledgment and funding

The authors are grateful to Dr. Daniel Broda (Rzeszow University, Poland) for helping to provide mass spectrometric studies of recombinant CDI. This work was financially supported by NAS of Ukraine (Program "Smart Sensory Devices of a New Generation Based on Modern Materials and Technologies") and by the Ministry of Education and Science of Ukraine (projects Nos. 0119U100671, 0118U000297, and 0118U000809).

Author contribution

M.V.G., A.E.Z., and Y.R.B. conceived of the experiments and analyzed the data. A.E.Z., N.Ye.S., O.M.Z., and Y.R.B carried out the experiments. All authors contributed important ideas throughout the project and were involved in the preparation of the manuscript. All authors have read and approved the final manuscript.

Conflict of interest

The authors declare no conflict of interest, financial or otherwise.

References

Battchikova N, Koivulehto M, Denesyuk A, Ptitsyn L, Boretsky Y, Hellman J, Korpela T (1996) Aspartate aminotransferase from an alkalophilic *Bacillus* contains an additional 20-amino acid extension at its functionally important N-terminus. J Biochem 120(2): 425–32. https://doi.org/10.1093/oxfordjournals.jbchem.a021429

Bendt AK, Beckers G, Silberbach M, Wittmann A, Burkovski A (2004) Utilization of creatinine as an alternative nitrogen source in *Corynebacterium glutamicum*. Arch Microbiol 181(6): 443–50. https://doi.org/10.1007/s00203-004-0679-z

Burgess R (2009) Refolding solubilized inclusion body proteins. Methods Enzymol 463: 259–82. https://doi.org/10.1016/S0076-6879(09)63017-2

Fayura LR, Boretsky YR, Pynyaha YV, Wheatley DN, Sibirny AA (2013) Improved method for expression and isolation of the *Mycoplasma hominis* arginine deiminase from the recombinant strain of *Escherichia coli*. J Biotechnol 167(4): 420–6. https://doi.org/10.1016/j.jbiotec.2013.06.025

Gottschalk E-M, Gottschalk G, Schmitz-Streit RA, Thormann K (2007) Nucleotide sequence for creatinine deminase and method of use. United States Patent Application Publication. Pub. No.: US 7,205,140 B2, Apr. 17, 2007. https://www.lens.org/lens/patent/US_7205140_B2

Gottschalk E-M, Hippe H, Patzke F (1991) Creatinine deiminase (EC 3.5.4.21) from bacterium BN11: purification, properties and applicability in a serum/urine creatinine assay. Clin Chim Acta 204(1-3): 223–38. https://doi.org/10.1016/0009-8981(91)90234-4

Kalinowski J, Bathe B, Bartels D, Bischoff N, Bott M, Burkovski A, Dusch N, Eggeling L, Eikmanns BJ, Gaigalat L, Goesmann A, Hartmann A, Huthmacher K, Krämer R, Linke B, McHardy AC, Meyer F, Möckel B, Pfefferle W, Pühler A, Rey DA, Rückert C, Rupp O, Sahm H, Wendisch VF, Wiegräbe I, Tauch A (2003) The complete *Corynebacterium glutamicum* ATCC 13032 genome sequence and its impact on the production of L-aspartate-derived amino acids and vitamins. J Biotechnol 104(1–3): 5–25. https://doi.org/10.1016/S0168-1656(03)00154-8

Kuo CT, Wang PY, Wu CH (2005) Fluorometric determination of ammonium ion by ion chromatography using postcolumn derivatization with *o*-phthaldialdehyde. J Chromatogr A 1085(1): 91–7. https://doi.org/10.1016/j.chroma.2005.05.042

Laemmli UK (1970) Cleavage of structural proteins during the assembly of the head of the bacteriophage T4. Nature 227(5259): 680–5. https://doi.org/10.1038/227680a0

Marchenko SV, Soldatkin OO, Kasap BO, Kurc BA, Soldatkin AP, Dzyadevych SV (2016) Creatinine deiminase adsorption onto silicalite-modified pH-FET for creation of new creatinine-sensitive biosensor. Nanoscale Res Lett 11(1): 173–9. https://doi.org/10.1186/s11671-016-1386-9

Sant W, Pourciel-Gouzy ML, Launay J, Do Conto T, Colin R, Martinez A, Temple-Boyer P (2004) Development of a creatinine-sensitive sensor for medical analysis. Sens Actuators B Chem 103(1): 260–4. https://doi.org/10.1016/j.snb.2004.04.104

Stasyuk NY, Gayda GZ, Fayura LR, Boretskyy YR, Gonchar MV, Sibirny AA (2016) Novel arginine deiminase-based method to assay L-arginine in beverages. Food Chem 201: 320–6. https://doi.org/10.1016/j.foodchem.2016.01.093

Tabata M, Kido T, Totani M, Murachi T (1983) Automated assay of creatinine in serum as simplified by the use of immobilized enzymes, creatinine deiminase, and glutamate dehydrogenase. Anal Biochem 134(1): 44–9. https://doi.org/10.1016/0003-2697(83)90261-0

Uwajima T, Terada O (1976) Crystallization and some properties of creatinine deiminase from *Corynebacterium lilium*. Agric Biol Chem 40(5): 1055–56. https://doi.org/10.1080/00021369.1976.10862170

Uwajima T, Terada O (1977) Production, purification and crystallization of creatinine deaminase of *Corynebacterium*

lilium. Agric Biol Chem 41(2): 339–44. https://doi.org/10.1080/00021369.1977.10862496

Uwajima T, Terada O (1980) Properties of crystalline creatinine deiminase from *Corynebacterium lilium*. Agric Biol Chem 44(8): 1787–92. https://doi.org/10.1080/00021369.1980.10864211

Wyss M, Kaddurah-Daouk R (2000) Creatine and creatinine metabolism. Phys Rev 80(3): 1107–213. https://doi.org/10.1152/physrev.2000.80.3.1107

Zakalskiy AE, Stasyuk NE, Gonchar MV (2019) Creatinine deiminase: characterization, using in enzymatic creatinine assay, and production of the enzyme. Curr Protein Pept Sci 20(5): 465–70. https://doi.org/10.2174/1389203720666181114111731

Zakalskiy AE, Zakalska OM, Rzhepetskyy YA, Potocka N, Stasyk OV, Horak D, Gonchar MV (2012) Overexpression of $(His)_6$-tagged human arginase I in *Saccharomyces cerevisiae* and enzyme purification using metal affinity chromatography. Protein Expr Purif 81(1): 63–8. https://doi.org/10.1016/j.pep.2011.09.001

Received 3 October 2019; accepted 2 February 2020.
Final version published online 19 February 2020.

Оригінал доступний за посиланням: https://onlinelibrary.wiley.com/doi/abs/10.1002/cbin.11320

8.2. Розробка біосенсорного методу визначення вмісту креатиніну в біологічних рідинах на основі рекомбінантної креатиніндеімінази та наночастинок CoCu.

Анотація: *Креатинін (Крн) є дуже важливим біомаркером для діагностики захворювань нирок і оцінки ефективності лікувального процесу та гемодіалізу. На сьогодні, в літературі описано біосенсори для аналізу Крн, які ґрунтуються на виявленні аміаку – кінцевого продукту реакції гідролізу Крн, що каталізується креатиніндеіміназою (КДІ), однак існують дуже скупі дані щодо моніторингу іншого продукту реакції КДІ – N-метилгідантоїну (N-МГ). Основним недоліком біосенсорів, які сконструйовано на сьогодні, є те, що Крн-селективні біосенсори функціонують за високого негативного робочого потенціалу, що є проблематичним для аналізу Крн в біологічних рідинах. В поточному дослідженні нами описано новітній амперометричний біосенсор для аналізу Крн, що ґрунтується на електрохімічному моніторингу N-МГ за використання КДІ та наночастинок CoCu. Для вибору найефективнішого хемосенсора на N-МГ нами синтезовано низку наноматеріалів та охарактеризовано їхню електрохімічну активність методом циклічної вольтамперометрії. Гібридні наночастинки CoCu, що володіють високою селективністю та достатньою чутливістю до N-МГ (730 $А \cdot М^{-1} \cdot м^{-2}$ при –50 мВ), вибрано для розробки амперометричних біосенсорів на основі КДІ. Новизною поточного дослідження є те, що нами з'ясовано структуру та механізм дії утвореного комплексу CoCu–N-МГ на поверхні електрода. Новий біосенсор продемонстрував достатню чутливість до Крн (195 $А \cdot М^{-1} \cdot м^{-2}$), широкий лінійний діапазон (10–800 мкМ), низьку межу виявлення (0,5 мкМ), задовільну стабільність при зберіганні та відмінну селективність до цільового аналіту. Розроблений біонаноелектрод використано для чутливого та високоселективного аналізу Крн в біологічних рідинах. Виявлено високі кореляції отриманих результатів з референтним методом налізу Крн.*

Sensors & Actuators: B. Chemical 393 (2023) 134276

Contents lists available at ScienceDirect

Sensors and Actuators: B. Chemical

journal homepage: www.elsevier.com/locate/snb

A reagentless amperometric biosensor for creatinine assay based on recombinant creatinine deiminase and N-methylhydantoin-sensitive CoCu nanocomposite

Nataliya Stasyuk [a,*,1], Andriy Zakalskiy [a,2], Wojciech Nogala [b,3], Sylwester Gawinkowski [b,4], Tomasz Ratajczyk [b,5], Magdalena Bonarowska [b,6], Olha Demkiv [a,7], Oksana Zakalska [a,8], Mykhailo Gonchar [a,*,9]

[a] Institute of Cell Biology, National Academy of Sciences of Ukraine, 79005 Lviv, Ukraine
[b] Institute of Physical Chemistry, Polish Academy of Sciences, 01-224 Warsaw, Poland

ARTICLE INFO

Keywords:
Amperometric biosensor
Creatinine
Creatinine deiminase
N-methylhydantoin
CoCu nanoparticles
Complex nCoCu-NMH

ABSTRACT

Creatinine is a very important biomarker for the diagnostics of kidney disease and the evaluation of the efficiency of the treatment process and hemodialysis. The most utilised enzyme-based biosensors for creatinine assay are based on the detection of ammonia as a product of the creatinine deiminase (CDI)-catalysed reaction, but there are limited data on the monitoring of another CDI reaction product – N-methylhydantoin (NMH). The main drawback of the creatinine-selective biosensors which have been constructed to dateis a high negative working potential that is problematic for the monitoring of creatinine in biological liquids. An amperometric CDI-based biosensor for the direct measurement of creatinine, which works at low potentials due to using electrocatalytic nanocomposites is described in this paper. To choose the best chemosensor on NMH, hybrid CoCu nanoparticles were selected for the development of CDI-based amperometric biosensors. The structure and mechanism of the produced nCoCu–NMH complex on the electrode surface were also elucidated. The novel biosensor exhibited sufficient sensitivity (195 $A \cdot M^{-1} \cdot m^{-2}$ for creatinine), a broad linear range (10–800 μM), a low limit of detection (0.5 μM) and excellent selectivity towards the target analyte. The designed bioelectrode was used for estimation of creatinine in biological fluids.

1. Introduction

The search for biomarkers of the most common diseases and the development of indicators for the assessment of the course and treatment of diseases are a priority in the world scientific community in the field of analytical biotechnology. Among such biomarkers, metabolites, an important role, in particular, plays creatinine, one of the final products of protein metabolism in humans [1–7]. An above-normal concentration of creatinine in blood serum indicates serious renal failure [8]. Hypercreatininemia is connected with chronic or acute renal diseases, complications of diabetic nephropathy [9] or COVID-19 [10–12], and kidney damage by toxic factors, in particular, certain medications, X-ray contrast agents, antibiotics such as aminoglycosides, cephalosporins, statins, *etc.* [13–18]. Creatinine is considered an

* Corresponding authors.
E-mail addresses: stasuk_natalia@ukr.net (N. Stasyuk), mykhailo1952@gmail.com (M. Gonchar).
[1] orcid.org/0000-0001-6550-8145
[2] orcid.org/0000-0002-8853-1097
[3] orcid.org/0000-0002-6135-3294
[4] orcid.org/0000-0001-5315-6197
[5] orcid.org/0000-0003-1613-6933
[6] orcid.org/0000-0002-3152-4400
[7] orcid.org/0000-0002-7999-4436
[8] orcid.org/0000-0002-8966-4780
[9] orcid.org/0000-0001-8861-4477

https://doi.org/10.1016/j.snb.2023.134276
Received 25 April 2023; Received in revised form 19 June 2023; Accepted 8 July 2023
Available online 10 July 2023
0925-4005/© 2023 Elsevier B.V. All rights reserved.

important indicator of the physiological state of athletes [19], and there is a need for simple methods of determination of this metabolite in biological fluids, including perspiration.

To determine the content of creatinine, various chemical and physicochemical methods have been developed [20,21], including the well-known colour reaction of Jaffe with the formation of the Yanovsky complex with picrate anion [22]; however, the disadvantages of the latter method (as well as its various modifications) are low specificity and sensitivity to positive and negative interference from related substances [23,25]. The development of biosensors for creatinine analysis is of pivotal interest [24]. A number of biosensors have been described, which are based mainly on the use of the enzyme creatinine deiminase (CDI) as a biocatalytic element and detection the final ammonia [25–39]. Although very popular, the potentiometric and amperometric techniques suffer from several drawbacks, namely, the dependence of membrane potential on the ionic strength of the solution (potentiometric biosensors) and, most importantly, complicated analysis of real samples where the endogenous ammonia coexists (Table S1).

Direct measurement of creatinine in biological fluids is of great value in medicine during the treatment of patients, but the presence of other endogenous compounds, in particular ammonia, in these samples makes routine analysis a difficult procedure. It is known that ammonia is one of the main products of hepatic metabolism, and its increasing content in serum or urine is correlated with hepatic encephalopathy [40], Reye's syndrome [41], hemolytic disease of the newborn [42], genetic diseases of the urea cycle [43], or chronic kidney disease (CKD) [44,45]. As a consequence, the evaluation of creatinine level requires the additional analysis of NH_4^+ or the pre-treatments of samples for the removal of pre-existing NH_4^+.

As continuous monitoring of a patient's health status is an excellent means for early detection of CKD, noninvasive creatinine-selective biosensors are attracting considerable attention. To date, there are limited data on mono-enzymatic CDI-containing amperometric biosensors, which have been designed for monitoring NMH as an analytical product of the enzymatic reaction. NMH is a promising analyte that can be detected amperometrically due to its ability to form coordination compounds with transition metal ions [46,47]. Several electrochemical biosensors for creatinine assay based on NMH detection have recently been proposed [47–49] (Table 1). However, they do not show the necessary selectivity due to the simultaneous reaction of Co^{2+} with NMH and ammonia and, probably, due to producing of a metal complex ion – hexaaminecobalt(II) ($[Co(NH_3)_6]^{2+}$) [50]. Also, it should be mentioned that the applied working potential for all the proposed enzymatic biosensors is highly negative (–1.4 V), making them unsuitable for the analysis of creatinine in biological fluids, due to the efficient reduction of other exogenous compounds, which are present in the tested biological samples.

Therefore, the consideration of the problem of the determination of the content of creatinine indicates its urgency, especially in terms of developing a highly selective and inexpensive amperometric biosensor for monitoring this analyte. In the current paper, we report the development and application of CDI-based biosensor for the direct measurement of creatinine in biological liquids. The constructed biosensor contains highly purified recombinant bacterial CDI, co-immobilised with NMH-sensitive CoCu nanoparticles (nCoCu) on the glassy carbon electrode (GCE) surface. The general principle of creatinine detection is based on the CDI-catalysed hydrolysis of creatinine, which releases ammonium ions and NMH. The generated NMH reacts with nCoCu, forming an electroactive complex that is detected amperometricaly.

Table 1
Analytical characteristics of the known amperometric biosensors on creatinine based on the principle of NMH detection.

	Biosensors		
	CDI/nCoCu/GCE	$CoCl_2$/CDI/[2]CPE	$CoCl_2$/CDI/CPE
Mode of signal detection	CV /[2]ChA	[1]CV	CV
Mediator	Without mediator	Methylene blue	Without mediator
Working/selected potential, mV	-0.05	-1.4*	-1.4*
Sensitivity, $A \cdot M^{-1} \cdot m^{-2}$	195 ± 5	[5]N.d.	N.d.
Linear range, μM	10 – 800	0.71 – 3550	0.17 – 3530
LOD, μM	0.5	N.d.	N.d.
K_M^{app}, mM	3.6 ± 0.5	N.d.	N.d.
I_{max}, nA	1305 ± 60	N.d.	N.d.
Response time, s	20	N.d.	N.d.
References	Current work	[48]	[49]

[1]CV – cyclicvoltammperometry; [2]CPE – carbon paste electrodes; [3]ChA – chronoamperometry; [4]CDI – creatininedeiminase; [5]N.d. – Not indicated; *The authors did not provide classical chronoamperometry at the selected optimal (working) potential.

2. Materials and methods

Experimental parts, including chemicals and instruments are presented in the Supplementary material.

2.1. Synthesis and characterisation of nanoparticles

For the obtaining of the Co(core)/Cu (shell) (nCoCu) or Co(core)/Pd (shell) (nCoPd) NPs (denoted as n), the nCo (1 $mg \cdot mL^{-1}$) were subsequently injected into the growth solution consisting of $CuSO_4$ (5 mL, 10 mM) or $PdCl_3$ (5 mL, 10 mM) with the following addition of $NaBH_4$ (1 mL, 0.1 M) to both solutions and heating at 100 °C for 10 min. The obtained NPs (denoted as n) were deposited from the solution by centrifugation at 8000 g during 30 min and washed with 5 mM PB, pH 7.0 and water. The final nCoCu and nCoPd precipitate was dried (at 80°C during 24 h).

2.2. Raman scattering measurements

Sample solutions were dropped onto cleaned microscope coverslips and allowed to dry at room temperature. For each sample, hyperspectral Raman raster maps consisting of approximately 150 points each were made, measuring rectangular areas with a step of 10 μm. The laser power on the sample was kept at 1 mW, and the accumulation time of a single point was 20–60 s (depending on the sample). Using Wire 5.5 software (Renishaw), cosmic ray peaks were removed from the maps. An average spectrum was then generated from each map by calculating the average of all single-point spectra.

Liquid samples were measured in 10 mm quartz cuvettes (Hellma) using the Renishaw macrosample attachment. Raman and SERS spectra were obtained using a 15 mm focal length objective (Renishaw) and a laser power of 1 mW per sample. For each sample, 360 sequential spectra were recorded with a 100-second acquisition time, facilitating the exclusion of potential photodecomposition during the measurement process. After the removal of cosmic ray peaks, all spectra were then averaged.

2.3. Development and characterisation of the bioelectrode

To obtain a modified electrode, a 2 μL nCoCu suspension (1 $mg \cdot mL^{-1}$) was dropped onto the GCE surface and air-dried. To construct the CDI-based electrode, 5 μL of the enzyme solution (30 $U \cdot mL^{-1}$) was dropped onto the surface of the NPs/GCE and then covered with 0.5 % neutralized Nafion™. After immobilisation of CDI, the constructed bioelectrode was stored at 4 °C in 50 mM PB, pH 7.5 until use.

2.4. Creatinine assay in model and real samples

The constructed CDI/nCoCu-based amperometric biosensor for creatinine determination was tested on the model and real samples (see

SM. Materials and instruments). The statistical parameters and all figures were calculated and built using Origin 8.5 Pro.

3. Results and discussion

3.1. Selection and characterisation of the nanocomposite most electroactive to NMH

To date, there are limited data on mono-enzymatic CDI-containing amperometric biosensors which are constructed for the monitoring of NMH as an analytical product of enzymatic hydrolysis of creatinine. All of the proposed biosensors are based on the reaction of $CoCl_2$ or $FeCl_3$ with NMH [39,48,49]. NMH can form coordination compounds with atoms of transition metals due to the number of binding sites that coordinate with the metal donor groups. To date, only five metal ion complexes with NMH, in particular, $[Ni(H_2O)_4(1\text{-mhyd})_2]$, $[Na[Au(1\text{-mhyd})_2]\cdot 4H_2O$, $[Pt_2(NH_3)_4(1\text{-mhyd})_2](NO_3)_4\cdot H_2O$, $[Hg(1\text{-mhyd})_2]_n$, $\{[Ag(1\text{-mhyd})]\cdot 0.5H_2O\}_n$ [51–57] were identified and all of them revealed the great practical importance in medicine for the treatment of some malignant diseases [46,47]. However, the literature lacks data on the interaction of metallic NPs with NMH and the possibility of using this approach in the design of biosensors.

In the current paper, a number of nanocomposites were synthesised using chemical reduction methods (see SM. Materials and instruments). The obtained NPs were screened on their electrocatalytic activity toward reduction of NMH. nCoCu revealed the highest activity (see SM, Fig.S1), and it were used for further studies. It is essential to note that such NMH-selective amperometric signal is observed at a low negative potential (–0.05 V vs Ag/AgCl) that is very suitable for the analysis of biological samples for which high potentials are not applicable because of unwanted side reactions.

For evaluation of the size of the synthesised nCoCu, SEM microscopy was used (Fig. 1). As shown in Fig. 1, nCoCu have the shape of cubs (*a* – *b*) and hexagons (*c*) with a high porosity structure with a size varying from 100 nm to 3 μm.

To characterize the surface area and porosity of this material in more detail, adsorption isotherms were also studied (Fig. S2). The nitrogen adsorption-desorption isotherms obtained are of type II according to the IUPAC classification [58], with a narrow hysteresis loop of type H3. Such isotherms are characteristic of the physical adsorption of nitrogen on non-porous (or with low amounts of meso- and macropores) adsorbents. The material studied has a small surface area, with a low content of mesopores (20 – 500 Å width) and macropores (500 – 2200 Å). The specific surface area of nCuCo calculated with the BET model based on N_2 adsorption is $S_{BET} = 1.51\ m^2/g$. Using other mathematical models gave similar values: $S_{BJH} = 1.79\ m^2/g$ and SD-H= $1.50\ m^2/g$ (both from the desorption branch). The specific surface area was additionally verified with the determination of the BET isotherm using krypton as the adsorbate. This method is beneficial for substances with a low specific surface area. A result with a satisfactory agreement with the result based on nitrogen adsorption was obtained: $S_{BET\text{-}Kr} = 1.65\ m^2/g$. The t-Plot calculations showed that micropores (less than 20 Å width) are also present in the material studied. Their surface area is $0.337\ m^2/g$, but their volume is small ($V_{micropores} = 0.00015\ cm^3/g$), representing about 2 % of the total pore volume.

The total pore volume is $0.0088\ cm^3/g$ (from BJH and B-H models) and $0.0089\ cm^3/g$ (from the H-K model, $p/p^0 = 0.99$). The median pore width (from the H-K model) is 616.5 Å, so the contribution of macropores in the material studied is significant. Such pores' sizes fit for most global proteins/enzymes, even of oligomeric form [59].

The crystal structures of nCuCo were examined by means of X-ray diffraction (XRD) (Fig. S3 *a*). The XRD pattern shows the presence of one phase with a high degree of crystallinity. The diffraction peak positions correspond to the face-centered cubic structure of copper with space group *Fm*–3 *m* and lattice constant $a = 3.6127(4)$ Å. The average apparent crystallite size $D \approx 211$ nm was determined by isotropic line broadening analysis. Furthermore, the elemental composition was further investigated using X-ray microanalysis (XRM). Fig. S3 *b* displays the XRM spectrum of the nCoCu, which mainly contains the peaks of Co, Cu on the Si surface.

3.2. Spectroscopic approaches for characterizing binding of nCoCu with NMH

3.2.1. DFT and Raman study of the interaction of nCoCu with NMH

In order to investigate the possible structure of the nCoCu-NMH complex, Raman spectroscopy and density functional theory (DFT) calculations were performed. Raman spectra were simulated for different possible structures and compared with the measured spectra to estimate the configuration of the metal-NMH nanoparticle complex. In these simulations, nCoCu were modelled as metallic clusters of two to ten copper atoms. This approach allowed the identification of changes in the Raman spectra induced by complexation relative to the spectra of isolated NMH molecules. The most likely interaction between an NMH molecule and nCoCu may involve oxygen or nitrogen atoms. The optimised structures of configurations involving such bonds are shown in Fig. 2, and their simulated Raman spectra in Fig. 3.

The binding by the nitrogen atom is expected to affect the position of the N-H stretching band. This weak characteristic band appears at 3480 cm^{-1} in the measured Raman spectrum. The spectral region around this band does not appear to change due to complexation (structure I in Fig. 2), or the changes in the measured spectra are smaller than noise. Binding through nitrogen atoms to Cu has been suggested previously [60], but the invisible change in the position or intensity of the N-H stretching band suggests this is not the case here. Similarly, binding simultaneously through oxygen and nitrogen atoms is generally possible

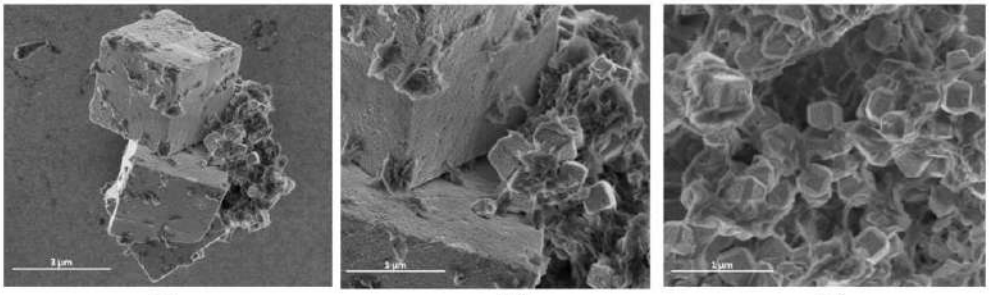

Fig. 1. SEM images (*a* – *c*) of nCoCu. The accelerating voltage was 2 kV for all images.

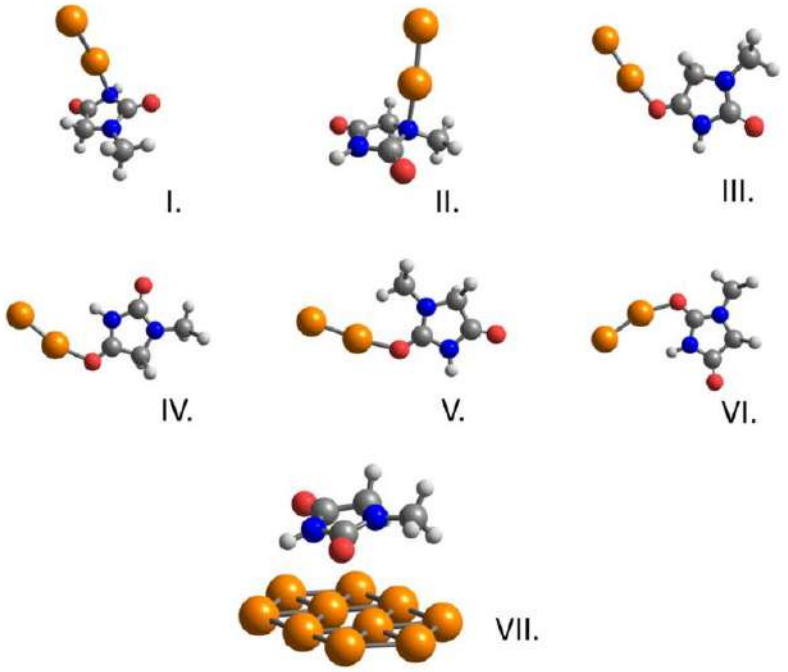

Fig. 2. Geometric structures of possible NMH complexes with copper nanoclusters. Structures I and II present the two most energetically stable geometries of complexes in which the NMH molecule connects to the Cu dimer through one of the nitrogen atoms. Structures III–VI present the most energetically stable geometries of complexes in which the NMH molecule connects to the Cu dimer through one of the oxygen atoms. Structure VII presents the lowest-energy geometry of the NMH molecule with a two-dimensional cluster composed of 10 Cu atoms.

but must be ruled out due to the same lack of spectral signature on the N-H stretching band. The nitrogen atom with the $-CH_3$ group has no single characteristic signature in the Raman spectrum but is involved in many vibrational motions. Small changes in different regions of the spectrum can therefore be expected as a result of the involvement of this atom in the bond (structure II in Fig. 2). No significant changes in the positions of the Raman bands are observed as a result of complexation. This suggests that such a bond is unlikely.

The most pronounced change in the Raman spectrum due to complexation concerns the 1650–1800 cm^{-1} region. The appearance of bands in this region is a marker for the C=O group and is often used to identify chemical products containing this group. The NMH Raman band located at 1757 cm^{-1} in the aqueous solution spectrum and at 1735 cm^{-1} in the crystal powder spectrum can be attributed to the vibrational mode located at 1877 cm^{-1} in the simulated spectrum (Fig. 3 *a* – *b*). The shoulder of this band located at 1720 cm^{-1} in the solution spectrum and at 1705 cm^{-1} in the crystal powder spectrum, can be assigned to the vibrational mode located at 1840 cm^{-1} in the simulated spectrum. These modes associated with vibrations involving stretching the C=O bond (Fig. S4 – S5) are quite characteristic. If metal nanoparticles interact with NMH oxygen atoms, the formation of the metal nanoparticle-NMH complex should affect these bands in the Raman spectrum. Examination of the differences between curves A, B and C in Fig. 3 reveals such changes. The band, initially located at 1757 cm^{-1} in the aqueous solution, moves downwards to 1743 cm^{-1} in the complex sample. The shoulder, initially at 1720 cm^{-1}, moves downwards and appears as a small, separate band at 1695 cm^{-1}. In addition, two other bands appear in this spectral region: at 1786 and 1771 cm^{-1}. This may suggest that more than one molecule-metal bond configuration exists simultaneously in the complex sample.

Comparing simulated spectra with the experimental one (Fig. 3 *c*) reveals that the spectra simulated for structures III, IV, V, and VI is the most similar to the experimental one. These spectra represent the complex created by the attachment of nCoCu to the NMH molecule through oxygen atoms. Structures III and V differ only in the orientation of the attached copper cluster, and the same is true for structures IV and VI. According to the simulations, all four structures are almost isoenergetic and should be equally probable. Also, for all of them, simulated Raman spectra are very similar and well-reproducing spectra changes observed in the experimental spectra. That suggests the NMH is bonded to the nCoCu through one or both oxygen atoms.

3.2.2. *The NMR study of interaction of nCoCu with NMH*

To elucidate the possible mechanism of interaction of nCoCu with NMH, a simple one-dimensional ^1H NMR has been carried out. The ^1H NMR spectrum of the sample with NMH demonstrates the signal from the residual HDO at 4.8 ppm, and two singlets at 2.8 ppm (integrals =3) and 4.0 ppm (integral =2), which corresponds the $-CH_3$ and $-CH_2$ groups, respectively (see Fig. S6 *a*). This assignment is in agreement with the literature data for NMH [61]. Regarding the ^1H NMR spectrum of nCoCu a broad signal at 4.8 ppm was observed (Fig. S6 *b*). This signal can be assigned to the residual water protons) which were present in the deuterated solvent. Notably, the significant broadening is caused by the presence of paramagnetic ions. For complex nCoCu-NMH (Fig. S6 *c*) two broad signals were observed at 4.8 (overlapping with the small signal at 4.0 ppm) ppm and 2.8 ppm, respectively, and the broad signal of HDO at 4.8 ppm was also observed. For this sample, comprehensive insight into the structure of the paramagnetic species was not possible. In summary, we have demonstrated that interaction of nCoCu with NMH takes place in two possible ways – through the formation of new covalent bonds between nCoCu and oxygen or nitrogen atoms of NMH (Figs. 2 – 3) and also through the immobilization of NMH on the surface of nCoCu due to their high paramagneticity (Fig. S6 *b*). In this context, the NMR results are supportive for the Raman results.

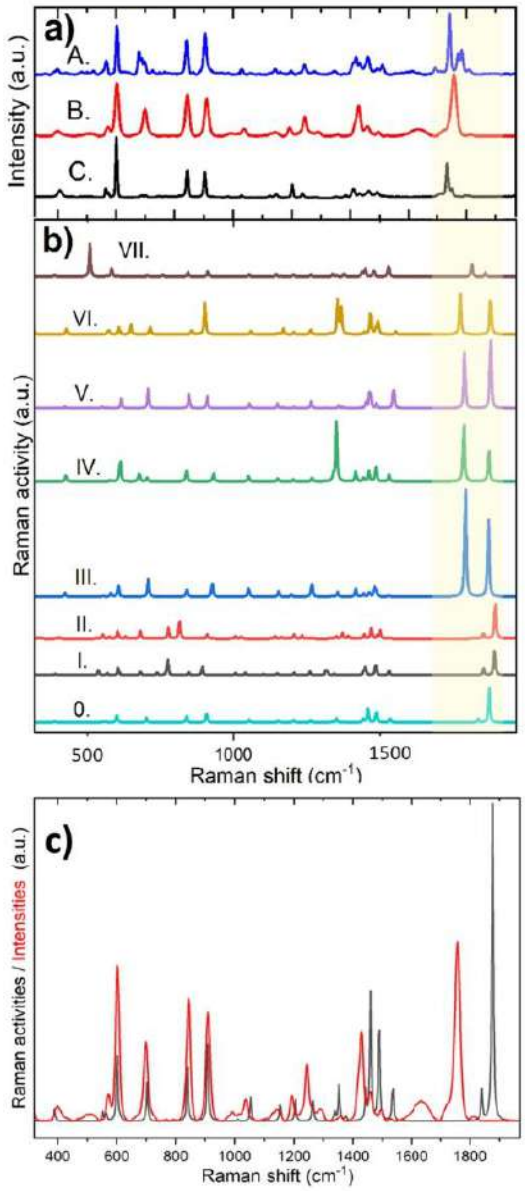

Fig. 3. Measured (*a*) and simulated (*b*) Raman spectra. Curves C, B, and A represent spectra measured for crystalline NMH, a water solution of NMH, and NMH-nCoCu complex, respectively. Curve 0 corresponds to the spectrum simulated for isolated NMH, while curves I-VII display spectra simulated for the complex structures depicted in Fig. 2; NMH Raman spectrum (*c*) measured for water solution (red curve, the same as curve B in Fig. 3 *a*) and simulated (black curve, the same as curve 0 in Fig. 3 *b*) spectra of complexes.

3.3. Electrochemical characteristics of CDI/nCoCu/GCE bioelectrode

The assay of creatinine by the designed bioelectrode is based on monitoring of NMH, generated in a mono-enzymatic layer, and finally sensed by the CoCu/GCE electrode (see Fig. 4). The first stage of biorecognition is the creatinine deiminase-catalysed creatinine conversion to NMH and ammonia. The resulting NMH diffuses further to the nCoCu layer and triggers the formation of the electroactive complex of NMH-CoCu, proved by Raman investigations (see subdiv. 3.2.1). The reduction of the produced complex results in increasing of the current signal whose value is correlated with the level of creatinine in the sample.

According to the HSAB theory, $Cu^{(II)}$ belongs to a large group of metal ions exhibiting a borderline hardness and, for that reason, could bind both with the carbonyl functional group C=O and with the softer deprotonated nitrogen atom of NMH, though in the Raman spectra of nCoCu-NMH complex (see Figs. 2–3) only one new peak exists at 1650–1750 cm^{-1}. That might result from the new Cu-O bond generated by complexation. So, we suggest that in the formed complex, the Cu^{+} ion is only bound to the O in 4th position (O4) atom of NMH (probable structures III–VI).

The electroactivity of the produced nCoCu–NMH complex could be explained by the ability of the bonded Cu^{+} ions to participate in the electron transfer reaction. Cu^{+}, when conjugated to the hydantoin moiety, undergoes electron transfer reactions more readily than solvated Cu^{+} ions due to the arrival of the delocalised electrons from the hydantoin. The electrochemical transformation of the nCoCu-NMH complex on the GCE surface can possibly occur with the following stages (Eqs. 1–3):

1) Complexation:

$$nCoCu^{+} + NMH \leftrightarrow nCoCu^{+}\text{-}NMH \quad (1)$$

2) Reduction and dissociation of the complex:

$$nCoCu^{+}\text{-}NMH + e^{-} \rightarrow nCoCu^{0} + NMH \quad (2)$$

3) Regeneration of $nCoCu^{+}$ (spontaneously, probably, by reduction of oxygen):

$$4\ nCoCu^{0} + O_2 + 4H^{+} \rightarrow 4\ nCoCu^{+} + 2H_2O \quad (3)$$

The scheme of the electron transfer between the biorecognition layer and the electrode surface is shown in Fig. 4 *a*.

The electrocatalytic activity of the nCoCu layered on GCE was tested by the use of cyclic voltammetry under the consequent injections of increased amounts of NMH (Fig S7). The CV (Fig S7 *a*) demonstrated that a cathodic peak, contributed by NMH, appeared at a potential of −75 mV and an anodic peak was detected at a potential of ca. + 120 mV. The results of chronoamperometry analysis and calibration graphs at −50 mV (highest difference between analyte and background current) are presented in Fig S7 *b* – *c*, respectively. An unmodified GCE was also tested as a control by chronoamperometry. No amperometric signals were detected upon additions of NMH with a bare GCE (see line 1, Fig S7 *a*). It is worth mentioning that as a control, the proposed nCoCu/GCE was also tested in the presence of ammonia chloride and creatinine. No amperometric signals were observed (see Fig. S8).

To form a mono-enzymatic layer sensitive to creatinine, CDI was dropped on the surface of the CoCu/GCE and covered with a Nafion (see subdiv. 2.2). Amperometric characteristics of the created biosensor are demonstrated in Fig. 4 *b* – *e*. To investigate the possibility of electron transfer to the surface of the GCE through the nCoCu the cyclic voltammetric investigation has been carried out (Fig. 4 *b*).

As shown, the potential −50 mV was selected as working potential for creatinine assay with the proposed sensor. The corresponding calibration curve and chronoamperogram for CDI-based biosensor is presented in Fig. 4 *b–e*. An amperometric response on creatinine of the developed bioelectrode was tested for creatinine concentration from 0.01 to 10.2 mM. The response signal was linear in the range between 0.01 mM and 0.8 mM. The maximal detected signal was 1305 ± 60 nA (for electrode with area 1.76 mm^2) with K_M^{app} for creatinine – 3.8 ± 0.5 mM (Fig. 4 *d*). The sensitivity within the linear range was calculated as 195 ± 5 $A{\cdot}M^{-1}{\cdot}m^{-2}$, LOD was 0.05 mM and a response time

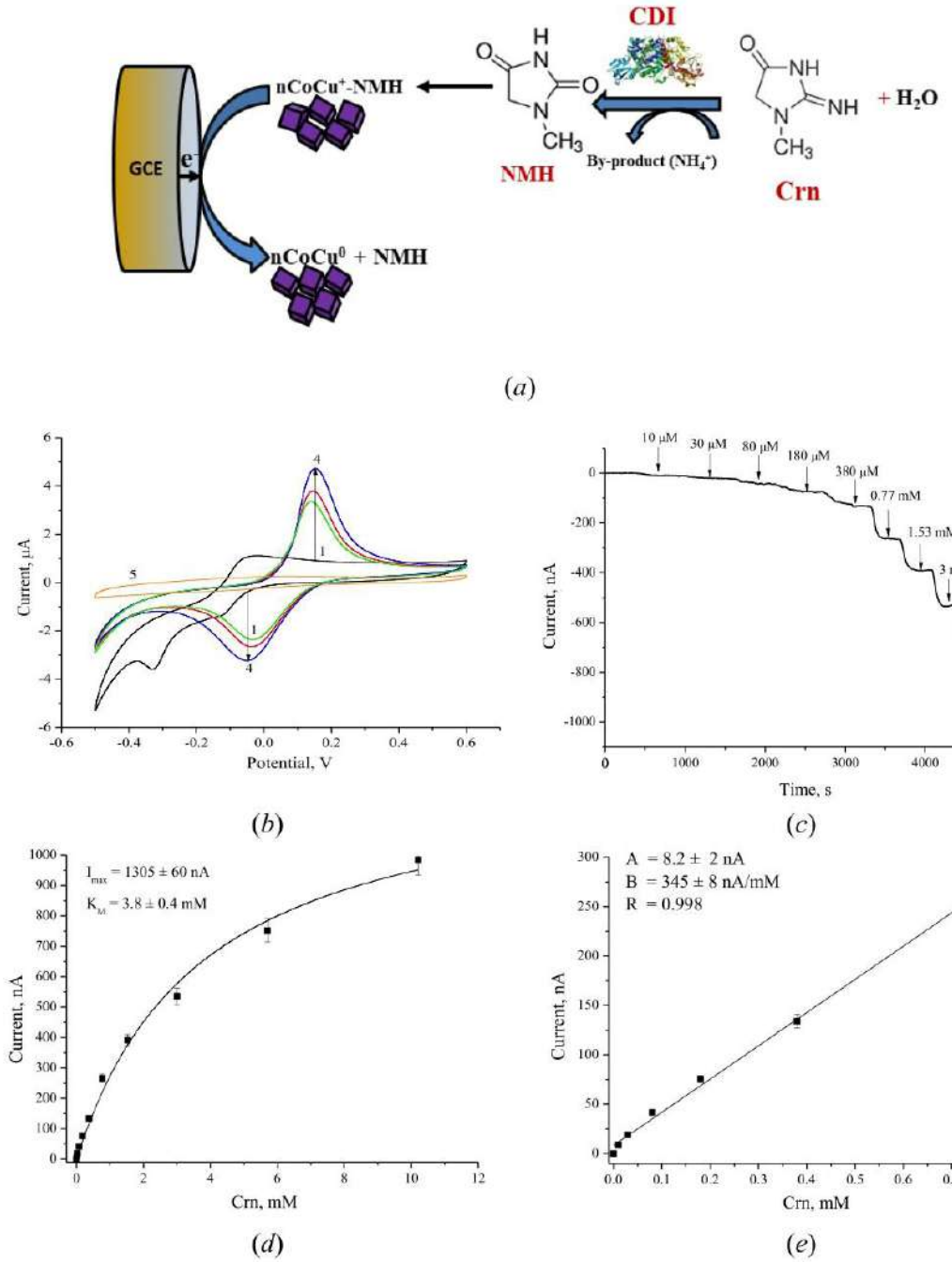

Fig. 4. Hypothetical scheme of the functionality of the CDI-based biosensor (*a*); Amperometric characteristics of CDI/CoCu/GCE: (*b*) – CV responses at various creatinine concentrations: (1) – 0 mM; (2) – 1 mM; (3) – 2 mM; (4) – 5 mM; (5) – GCE (as blank) with 1 mM creatinine; (*c – e*) –current signals at various creatinine concentrations in wide (*d*) and narrow linear range (*e*) and corresponding chronoamperogram (*c*). Conditions: CV scan rate 5 mV·s^{-1}; Ag/AgCl (reference electrode) in 50 mM PB, pH 7.0. Working potential for chronomaperometry: −50 mV.

was 20 s.

To date, only two papers have been published concerning amperometric biosensors utilized for the monitoring of NMH, and they are based on the reaction of Co^{2+} salts with NMH in solution [48,49] (Table 1). However, the main disadvantage of the proposed biosensors is their high negative (–1.4 V) working potential, low selectivity, and the necessity of adding Co salt (and methylene blue in one research) to the tested samples.

The qualitative characteristics of previously reported biosensors based on CDI in comparement to the developed one (CDI/nCoCu/GCE) are presented in Table S1. All proposed CDI-mediated potentiometric and amperometric biosensors, based on application of NH_4^+-sensing ion-selective electrodes or NH_4^+-sensitive membranes, have a number of limitations, in particular, the impact of pre-existed and generated *de novo* NH_4^+ on the creatinine estimation, the high cost, stability and temperature and pH dependence. However, the recently proposed an amperometric biosensors based on NMH detection [48,49] do not involve the additional mesurements of pre-existed and generated de novo NH_4^+. However, previously reported analogs require a high negative working potential (–1.4 V) which makes them unsuitable for analyzing of creatinine in real biological fluids. It should be noted that the developed amperometric biosensor, based on combination of nCoCu and CDI, allows direct measurement of creatinine in the samples at a low reductive voltage (–50 mV) without necessity to use the second biosensor selective to ammonia. The high selectivity of the developed biosensor makes its promising usage in clinical analysis.

For the application of the proposed biosensor in analyses of real samples, selectivity and storage stability is of great importance. The stability and selectivity of the developed bioelectrode are presented in Fig. S9. The selectivity of the proposed amperometric biosensor towards some analytes was estimated in relative units (%) as a ratio to the value of the highest response (Fig. S9 *a*). As presented in Fig.S9 *a*, the CDI/nCoCu/GCE is highly specific to creatinine: the signal of structurally similar compounds was less than 5 %, including important interferants: cytosine and cytidine. The stability of the bioelectrode was explored at 20 °C with 1 mM creatinine in 50 mM PB, pH 7.5, with intermittent storage in this buffer at 4 °C between measurements. It retained 46 % of its initial current response when the bioelectrode was stored at + 4 °C for creatinine assay after intermittent exploitation over 12 days (Fig. S9 *b*).

3.4. Assay of creatinine in real samples

A number of chemicals, including ascorbic acid (AA), uric acid (UA), urea, glucose (Glc) and a number of inorganic salts commonly coexist with creatinine (marked in Fig. S10, as Crn) in human urine, and they can interfere with the detection of creatinine. So, the selectivity study of a CDI/nCoCu-modified electrode was performed using chronoamperometry. Solutions of several interfering compounds containing AA, UA, KCl and NaCl at the concentration 1 mM with the presence and the absence of 1 mM creatinine were evaluated for studying the possible interference effect. The effect of current additives on the response of the constructed creatinine biosensor is demonstrated in Fig. S10. The tested compounds, especially AA, UA, and urea, can be reduced at the operating potential −50 mV. However, the relative responses from the reduction of the interference are not larger than 5 %, especially when they coexist in creatinine solution (1 mM). Only slight changes from the current responses of creatinine alone for AA (5 %), UA (3.5 %) and urea (3 %) are observed. Thus, the additional current responses from the tested interference species can be considered negligible.

To evaluate the impact of the urine components on the results of the amperometric biosensor assay, the SAT method was applied (Fig. S11). The developed creatinine-specific biosensor was tested on the model and real solutions of urine sample. The results of the estimation of creatinine in tested samples are presented in Table 2 and Fig. S11.

It was provided accuracy test for the proposed biosensor method in comparison with the reference approach by calculation the difference of the average values in percent (%). Differences of less than 7 % between the results of two methods of creatinine assay were observed. Thus, the content of creatinine, tested in the sample of real urine with the CDI/nCoCu/GCE, was shown to be 15.65 mM. The spectrophotometric Jaffee method was used as the reference [30]. These values are correlated with published data (4.42– 17.68 mM) for the creatinine content in the human urine of healthy people [62,63].

The results of testing the biosensor effectiveness for creatinine assay were shown to be within the permissible error limits (±10.0 %). Therefore, the developed amperometric biosensor due to it's sensitivity, validity, low-cost and high selectivity, will be promising for use in clinical laboratories for creatinine assay in blood serum and urine.

4. Conclusions

Direct measurement of creatinine in biological fluids is crucial for the proper treatment of kidney disease, especially for patients undergoing kidney transplantation therapy. However, the presence of endogenous ammonia in these samples greatly complicates routine analysis and requires additional ammonia estimation or sample pre-treatment to remove pre-existing ammonia. As continuous monitoring of the health status of a patient is an excellent means for early kidney failure detection, noninvasive creatinine-selective biosensors are attracting considerable attention.

In this research, we have developed an amperometric biosensor based on recombinant bacterial creatinine deiminase and CoCu nanoparticles to measure creatinine in biological liquids directly. The developed biosensor does not require the removal of endogenous ammonia and is characterised by a high selectivity to the target analyte. The proposed biosensor is characterised by a low applied potential (–50 mV), fast response to the analyte (20 s), broad linear range (0.01–0.8 mM), sufficient sensitivity (195 $A \cdot M^{-1} \cdot m^{-2}$) and a low limit of detection (0.5 μM). Moreover, the present paper elucidates the possible structure of the complex nCoCu–NMH and the mechanism of creatinine detection. Using the multiple standard addition method, the designed nCoCu/CDI-functionalized electrode was tested for creatinine assay in real biological liquids (urine and serum). A high correlation between the obtained results and the reference method was demonstrated. Thus, the proposed laboratory prototype of the creatinine-

Table 2
Analysis of creatinine in model and real samples.

Sample	Concentration of creatinine, mM			Recovery,%	Accuracy, %
	Added, mM	Biosensor analysis, found	Jaffe method, found		
Model solution,	23.4 ± 1.2	22 ± 1	–	94	6.0
*CV, %		4.5			
Human urine	–	16.1 ± 0.6	15.2 ± 0.7	–	5.9
CV, %		3.6	4.9		
Standard serum "Contronorm",	–	0.108 ± 0.005	0.103 ± 0.009	–	5.0
CV, %		4.6	7.0[26]		

*CV – coefficient of variation. Values are expressed as mean ± SD

selective biosensors would be promising and useful for routine clinical analysis.

CRediT authorship contribution statement

Nataliya Stasyuk: Investigation, Methodology, Writing - Original Draft, Formal Analysis, Writing - Reviewing and Editing. *Andriy Zakalskiy*: Investigation, Formal Analysis, Writing - Reviewing and Editing. *Wojciech Nogala*: Supervision, Investigation, Formal Analysis, Writing - Reviewing and Editing. *Sylwester Gawinkowski*: Investigation, Formal Analysis, Writing - Reviewing and Editing. *Tomasz Ratajczyk*: Investigation, Formal Analysis, Writing - Reviewing and Editing. *Magdalena Bonarowska*: Investigation, Formal Analysis, Writing - Reviewing and Editing. *Olha Demkiv*: Visualization, Formal Analysis. *Oksana Zakalska*: Visualization, Formal Analysis. *Mykhailo Gonchar*: Conceptualization, Methodology, Supervision, Formal Analysis, Writing - Reviewing and Editing.

Declaration of Competing Interest

The authors declare that they have no known competing financial interests or personal relationships that could have appeared to influence the work reported in this paper.

Data availability

Data will be made available on request.

Acknowledgements

The authors would like to thank Dr Alla G. Dyachenko (Institute of Physical Chemistry, PAS) for her contribution to adsorption measurements.

This research was partially supported by the FEBS Ukrainian Short-Term Fellowship, National Research Foundation of Ukraine (projects Nos. 2020.02/0100 "Development of new nanozymes as catalytic elements for enzymatic kits and chemo/biosensors" and 2021.01/0010 "Development of an enzymatic kit and portable biosensors for express-analysis of creatinine, a marker of acute functional disorders of the kidneys"), by the National Science Centre, Poland (Grant 2020/39/B/ST4/01523) and Poland's high-performance computing infrastructure PLGrid (HPC Centers: ACK Cyfronet AGH, WCSS), for providing computer facilities and support within computational grant no. PLG/2023/016170. Materials costs were partially covered by the National Science Centre, Poland (Grant 2016/23/B/ST4/02868).

Appendix A. Supporting information

Supplementary data associated with this article can be found in the online version at doi:10.1016/j.snb.2023.134276.

References

[1] D.A. Bonilla, R.B. Kreider, J.R. Stout, D.A. Forero, C.M. Kerksick, M.D. Roberts, E. S. Rawson, Metabolic basis of creatine in health and disease: a bioinformatics-assisted review, Nutrients 13 (4) (2021) 1238, https://doi.org/10.3390/nu13041238.

[2] S. Bahl, D. Cordeiro, L. MacNeil, A. Schulze, S. Mercimek-Andrews, Urine creatine metabolite panel as a screening test in neurodevelopmental disorders, Orphanet J. Rare Dis. 15 (2020) 339, https://doi.org/10.1186/s13023-020-01617-z.

[3] M. Wyss, R. Rima Kaddurah-Daouk, Creatine and creatinine metabolism, Physiol. Rev. 80 (3) (2000) 1107–1213, https://doi.org/10.1152/physrev.2000.80.3.1107.

[4] V. Boima, Creatinine based equations and glomerular filtration rate: interpretation and clinical relevance, Ghana Med. J. 50 (3) (2016) 119–121.

[5] I.G. Okpechi, F.J. Caskey, A. Gaipov, E.K. Tannor, J.J. Noubiap, E. Effa, U. E. Elrikpo, L.N. Hamonic, G. Ashuntantang, A.K. Bello, J.A. Donner, A. E. Figueiredo, R. Inagi, M. Madero, C. Malik, M. Moorthy, R. Pecoits-Filho, V. Tesar, A. Levin, V. Jha, Early identification of CKD-A scoping review of the global populations, Kidney Int. Rep. 7 (6) (2022) 1341–1353, https://doi.org/10.1016/j.ekir.2022.03.031.

[6] G. Alfano, R. Perrone, F. Fontana, G. Ligabue, S. Giovanella, A. Ferrari, M. Gregorini, G. Cappelli, R. Magistroni, G. Donati, Rethinking chronic kidney disease in the aging population life, Life (Basel) 12 (2022) 1724, https://doi.org/10.3390/ life12111724.

[7] K. Kashani, M.H. Rosner, M. Ostermann, Creatinine: from physiology to clinical application, Eur. J. Intern. Med. 72 (2020) 9–14, https://doi.org/10.1016/j.ejim.2019.10.025.

[8] V.M. Wong, S.J. Swartz, S. Devaraj, S. Poyyapakkam, Elevated serum creatinine: but is it renal failure, Pediatrics 146 (1) (2020), e20192828, https://doi.org/10.1542/peds.2019-2828.

[9] N. Akter, A. Nesso, A. Shormin, M.I. Dipa, S. Israt, S. Firoz, F. Yeasmin, Relationship of serum creatinine and estimated glomerular filtration rate in patients with chronic kidney disease, Mymensingh Med. J. 29 (4) (2020) 779–783.

[10] M.Z. Temiz, I. Hacibey, R.O. Yazar, M.S. Sevdi, S.H. Kucuk, G. Alkurt, L. Doganay, D.,G. Dinler, M.M. Dincer, E. Yuruk, K. Erkalp, A.Y. Muslumanoglu, Altered kidney function induced by SARS-CoV-2 infection and acute kidney damage markers predict survival outcomes of COVID-19 patients: a prospective pilot study, Ren. Fail. 44 (1) (2022) 233–240, https://doi.org/10.1080/0886022X.2022.2032743.

[11] R. Panimathi, E. Gurusamy, S. Mahalakshmi, K. Ramadevi, G. Kaarthikeyan, S. Anil, Impact of COVID-19 on renal function: a multivariate analysis of biochemical and immunological markers in patients, Cureus 14 (2) (2022), e22076, https://doi.org/10.7759/cureus.22076.

[12] E. Rouka, E. Livanou, S. Sinis, I. Dimeas, I. Pantazopoulos, D. Papagiannis, F. Malli, O. Kotsiou, K.I. Gourgoulianis, Investigation of admission serum creatinine as a predictor of hospital length of stay in triple-vaccinated COVID-19 inpatients, Int. Health (2023) ihad008, https://doi.org/10.1093/inthealth/ihad008.

[13] B.R. Griffin, S. Faubel, C.L. Edelstein, Biomarkers of drug-induced kidney toxicity, Ther. Drug Monit. 41 (2) (2019) 213–226, https://doi.org/10.1097/FTD.0000000000000589.

[14] M.S. Al-Naimi, H.A. Rasheed, N.R. Hussien, H.M. Al-Kuraishy, A.I. Al-Gareeb, Nephrotoxicity: role and significance of renal biomarkers in the early detection of acute renal injury, J. Adv. Pharm. Technol. Res. 10 (3) (2019) 95–99, https://doi.org/10.4103/japtr.JAPTR_336_18.

[15] S. Nair, S.V. O'Brien, K. Hayden, B. Pandya, P.J. Lisboa, K.J. Hardy, J.P. Wilding, Effect of a cooked meat meal on serum creatinine and estimated glomerular filtration rate in diabetes-related kidney disease, Diabetes Care 37 (2) (2013) 483–487, https://doi.org/10.2337/dc13-1770.

[16] K. Doma, A.K. Ramachandran, D. Boullosa, J. Connor, The paradoxical effect of creatine monohydrate on muscle damage markers: a systematic review and meta-analysis, Sports Med. 52 (7) (2022) 1623–1645, https://doi.org/10.1007/s40279-022-01640-z.

[17] E. Pimenta, M. Jensen, D. Jung, F. Schaumann, S. Boxnick, H. Truebel, Effect of diet on serum creatinine in healthy subjects during a phase I study, J. Clin. Med. Res. 8 (11) (2016) 836–839, https://doi.org/10.14740/jocmr2738w.

[18] K. Wiles, K. Bramham, P.T. Seed, C. Nelson-Piercy, L. Lightstone, L.C. Chappell, Serum creatinine in pregnancy: a systematic review, Kidney Int. Rep. 4 (3) (2018) 408–419, https://doi.org/10.1016/j.ekir.2018.10.015.

[19] B. Wax, C.M. Kerksick, A.R. Jagim, J.J. Mayo, B.C. Lyons, R.B. Kreider, Creatine for exercise and sports performance, with recovery considerations for healthy pPopulations, Nutrients 13 (6) (2021) 1915, https://doi.org/10.3390/nu13061915.

[20] C.S. Pundir, P. Kumar, R. Jaiwal, Biosensing methods for determination of creatinine: a review, Biosens. Bioelectron. 126 (2019) 707–724, https://doi.org/10.1016/j.bios.2018.11.031.

[21] C.L. Gonzalez-Gallardo, N. Arjona, L. Alvarez-Contreras, M. Guerra-Balcázar, Electrochemical creatinine detection for advanced point-of-care sensing devices: a review, RSC Adv. 12 (47) (2022) 30785–30802, https://doi.org/10.1039/d2ra04479j.

[22] J.R. Delanghe, M.M. Speeckaert, Creatinine determination according to Jaffe-what does it stand for? NDT 4 (2) (2011) 83–86, https://doi.org/10.1093/ndtplus/sfq211.

[23] T. Küme, B. Sağlam, C. Ergon, A.R. Sisman, Evaluation and comparison of abbott Jaffe and enzymatic creatinine methods: could the old method meet the new requirements? *J. Clin. Lab. Anal.* 32 (1) (2018), e22168 https://doi.org/10.1002/jcla.22168.

[24] A.J. Killard, M.R. Smyth, Creatinine biosensors: principles and designs, Trends Biotechnol. 18 (10) (2000) 433–437, https://doi.org/10.1016/S0167-7799(00)01491-8.

[25] A. Zakalskiy, N. Stasyuk, M. Gonchar, Creatinine deiminase: characterization, using in enzymatic creatinine assay, and production of the enzyme, Curr. Protein Pept. Sci. 20 (2019) 465–470.

[26] N.Ye Stasyuk, G.Z. Gayda, A.E. Zakalskiy, L.R. Fayura, O.M. Zakalska, A.A. Sibirny, M. Nisnevitch, M.V. Gonchar, Amperometric biosensors for L-arginine and creatinine assay based on recombinant deiminases and ammonium-sensitive Cu/Zn (Hg)S nanoparticles, Talanta 238 (1) (2022), 122996, https://doi.org/10.1016/j.talanta.2021.122996.

[27] R. Narimani, M. Esmaeili, S.H. Rasta, H.T. Khosroshahi, A. Mobed, Trend in creatinine determining methods: conventional methods to molecular-based methods, Anal. Sci. Adv. 2 (6) (2021) 308–325, https://doi.org/10.1002/ansa.202000074.

[28] A. Boutten, A.-S. Bargnoux, M.-C. Carlier, P. Delanaye, E. Rozet, V. Delatour, E. Cavalier, A.M. Hanser, M. Froissart, J.P. Cristol, L. Pieroni, Enzymatic but not compensated Jaffe methods reach the desirable specifications of NKDEP at normal levels of creatinine. Results of the French multicentric evaluation, Clin. Chim. Acta 419 (2013) 132–135, https://doi.org/10.1016/j.cca.2013.01.021.

[29] T. Fujita, S. Takata, Y. Sunahara, Enzymatic rate assay of creatinine in serum and urine, Clin. Chem. 39 (10) (1993) 2130–2136.
[30] J. Oh, H.D. Park, Comparison of serum creatinine measurements among Roche Modular D, Cobas 8000 c702, and Beckman Coulter AU5800, by Jaffe and enzymatic methods, Lab. Med. Online 10 (1) (2020) 39–45, https://doi.org/10.3343/lmo.2020.10.1.39.
[31] Y. Yamamoto, M. Senda, Amperometric ammonium ion sensor and its application to biosensors, Sens. Actuators B. Chem. 13 (1–3) (1993) 57–60, https://doi.org/10.1016/0925-4005(93)85322-2.
[32] Y.C. Luo, J.S. Do, Urea biosensor based on PANi(urease)-Nafion/Au composite electrode, Biosens. Bioelectron. 20 (1) (2004) 15–23, https://doi.org/10.1016/j.bios.2003.11.028.
[33] B. Strehlitz, B. Gründig, H. Kopinke, Sensor for amperometric determination of ammonia and ammonia-forming enzyme reactions, Anal. Chim. Acta 403 (1–2) (2000) 11–23, https://doi.org/10.1016/S0003-2670(99)00594-2.
[34] M. Cuartero, N. Colozza, B.M. Fernández-Pérez, G.A. Crespo, Why ammonium detection is particularly challenging but insightful with ionophore-based potentiometric sensors – an overview of the progress in the last 20 years, Analyst 145 (2020) 3188–3210.
[35] N. Verma, A.K. Singh, M. Singh, L-arginine biosensors: a comprehensive review, Biochem. Biophys. Rep. 12 (2017) 228–239.
[36] N. Stasyuk, O. Smutok, G. Gayda, B. Vus, Y. Koval'chuk, M. Gonchar, Bi-enzyme L-arginine-selective amperometric biosensor based on ammonium-sensing polyaniline-modified electrode, Biosens. Bioelectron. 37 (1) (2012) 46–52, https://doi.org/10.1016/j.bios.2012.04.031.
[37] M. Zhybak, V. Beni, M.Y. Vagin, E. Dempsey, A.P.F. Turner, Y. Korpan, Creatinine and urea biosensors based on a novel ammonium ion-selective copper-polyaniline nano-composite, Biosens. Bioelectron. 77 (2016) 505–511, https://doi.org/10.1016/j.bios.2015.10.009.
[38] N. Verma, A.K. Singh, N. Saini, Synthesis and characterisation of ZnS quantumdots and application for development of arginine biosensor, Sens. Bio-Sens. Res. 15 (2017) 41–45, https://doi.org/10.1016/j.sbsr.2017.07.004.
[39] P. Dasgupta, V. Kumar, P.R. Krishnaswamy, N. Bhat, Development of biosensor for detection of serum creatinine, CSI Trans. ICT 6 (2018) 5–10, https://doi.org/10.1007/s40012-018-0187-y.
[40] J.A. Frontera, Management of hepatic encephalopathy, Curr. Treat. Options Neurol. 16 (6) (2014) 297, https://doi.org/10.1007/s11940-014-0297-2.
[41] K. Schrör, Aspirin and Reye syndrome: a review of the evidence, Paediatric Drugs 9 (3) (2007) 195–204, https://doi.org/10.2165/00148581-200709030-00008.
[42] V. Probst, Treatment of hemolytic disease of the newborn, Geburtshilfe Frau 18 (4) (1958) 418–420.
[43] L.R. Soria, Ah Mew, N. Brunetti-Pierri, N. Progress and challenges in development of new therapies for urea cycle disorders, Hum. Mol. Genet. 28 (R1) (2019) R42–R48.
[44] J.M. Turner, C. Bauer, M.K. Abramowitz, M.L. Melamed, T.H. Hostetter, Treatment of chronic kidney disease, Kidney Int. 81 (4) (2012) 351–362, https://doi.org/10.1038/ki.2011.360.
[45] J.C. Lv, L.X. Zhang, Prevalence and disease burden of chronic kidney disease, Adv. Exp. Med. Biol. 1165 (2019) 3–15, https://doi.org/10.1007/978-981-13-8871-2_1.
[46] K. Yang, Y. Tang, K.A. Iczkowski, Phenyl-methylene hydantoins alter CD44-specific ligand binding of benign and malignant prostate cells and suppress CD44 isoform expression, Am. J. Transl. Res. 2 (1) (2010) 88–94. DOI: 2-s2.0-77953398669.
[47] H.S. Park, H. Choi, H. Shin, S. Lee, M. Park, Synthesis and characterisation of novel hydantoins as potential COX-2 inhibitors: 1,5-diarylhydantoins, Bull. Korean Chem. Soc. 28 (5) (2007) 751–757, https://doi.org/10.5012/BKCS.2007.28.5.751.
[48] P. Dasgupta, V. Kumar, P.R. Krishnaswamy, N. Bhat, Biochemical assay for serum creatinine detection through a 1-methylhydantoin and cobalt complex, RSC Adv. 10 (2020) 39092–39101, https://doi.org/10.1039/D0RA06470J.
[49] P. Dasgupta, V. Kumar, P.R. Krishnaswamy, N. Bhat, Serum creatinine electrochemical biosensor on printed electrodes using monoenzymatic pathway to 1-methylhydantoin detection, ACS Omega 5 (2020) 22459–22464.
[50] L. Geng, C. Cui, Y. Jia, H. Wu, H. Zhang, B. Yin, Z.D. Sun, Z. Luo, Reactivity of cobalt clusters $Con^{+/0}$ with ammonia: Co_3^- cluster catalysis for NH_3 dehydrogenation, J. Phys. Chem. A 124 (28) (2020) 5879–5886, https://doi.org/10.1021/acs.jpca.0c03720.
[51] A. Obradović, M. Matić, B. Ognjanović, P. Đurđević, E. Marinković, G. Uščumlić, B. Božić, B. Nedeljković, Antiproliferative and antimigratory effects of 3-(4-substituted benzyl)-5- isopropyl-5-phenylhydantoin derivatives in human breast cancer cells, Saudi Pharm. J. 28 (3) (2020) 246–254, https://doi.org/10.1016/j.jsps.2020.01.003.
[52] Y. Levo, The protective effect of hydantoin treatment on carcinogenesis, Naunyn-Schmiedeberg's Arch. Pharmacol. 285 (1974) 29–30, https://doi.org/10.1007/BF00499526.
[53] N.A. Malik, P.J. Sadler, S. Neidle, G.L. Taylor, *X*-Ray crystal structure of sodium bis (*N*-methylhydantoinato)gold(I) tetrahydrate; a linear, planar complex of pharmacological interest stabilised by two nitrogen ligands, J. Chem. Soc. Chem. Commun. 625 (1978) 711–712, https://doi.org/10.1039/C39780000711.
[54] J.P. Laurent, P. Lepage, F. Dahan, Synthesis and structure of bis(μ-1-methylhydantoinato-N,O)bis(cis-diammineplatinum(II)) dinitrate. A structural analog of platinum blues, J. Am. Chem. Soc. 104 (1982) 7335–7336, https://doi.org/10.1021/ja00389a082.
[55] D.M.L. Goodgame, A.M. Khaled, C.A. O'Mahoney, D.J. Williams, Synthesis and X-ray crystal structure of a chain polymer formed by 1-methylhydantoin with mercury(II), Polyhedron 9 (1990) 1765–1767, https://doi.org/10.1016/S0277-5387(00)83985-6.
[56] L. Vatannavaz, S.J. Sabounchei, Asieh Sedghi, R. Karamian, S.H.M. Farida, N. Rahmani, New nickel, palladium and platinum complexes of hydantoin derivative: synthesis, characterisation, theoretical study and biological activity, Polybedron 181 (2020), 114478, https://doi.org/10.1016/j.poly.2020.114478.
[57] Y. Kang, A. Scully, D.A. Young, S. Kim, H. Tsao, M. Sen, Y. Yang, Enhanced mechanical performance and biological evaluation of a PLGA coated β-TCP composite scaffold for load-bearing applications, Eur. Polym. J. 47 (8) (2011) 1569–1577, https://doi.org/10.1016/j.poly.2011.05.004.
[58] M. Thommes, K. Kaneko, A.V. Nelmark, J.P. Olivier, F. Rodriguez-Reinoso, J. Rouquerol, K.S.W. Sing, Physisorption of gases, with special reference to the evaluation of surface area and pore size distribution (IUPAC Technical Report), Pure Appl. Chem. 87 (2015) 1051–1069, https://doi.org/10.1515/pac-2014-1117.
[59] H.P. Erickson, Size and shape of protein molecules at the nanometer level determined by sedimentation, gel filtration, and electron microscopy, in: Shulin Li (Eds.), Biological Procedures Online, 2009, 11 (1), 32–51. doi: 10.1007/s12575-009-9008-x.
[60] M. Puszynska-Tuszkanow, Z. Staszak, T. Misiaszek, M.T. Klepka, A. Wolska, A. Drzewiecka-Antonik, H. Paltynowicz, M. Cieslak-Golonka, Metallophilic interactions in polynuclear Ag(I) complex with 1-methylhydantoin studied by X-ray absorption, electronic and vibrational spectroscopies, Chem. Phys. Lett. 597 (2014) 94–98, https://doi.org/10.1016/j.cplett.2014.02.025.
[61] (https://hmdb.ca/metabolites/HMDB0003646).
[62] L.M. Ilic, R.B. Davis, R.S. Brown, S.H. Lecker, The interdialytic creatinine rise is a novel marker of volume overload and mortality risk in hemodialysis patients, BMC Nephrol. 19 (1) (2018) 202, https://doi.org/10.1186/s12882-018-1008-0.
[63] O. Sugita, K. Uchiyama, T. Yamada, T. Sato, M. Okada, K. Takeuchi, Reference values of serum and urine creatinine, and of creatinine clearance by a new enzymatic method, Ann. Clin. Biochem. 29 (1992) 523–528, https://doi.org/10.1177/000456329202900506.

Nataliya Stasyuk, PhD, Research Scientist in the Institute of Cell Biology, National Academy of Sciences of Ukraine. Author of 80 scientific publications, including 34 full-length papers in journals from the Scopus database. The Hirsch index (Scopus) – 11. The main scientific interests: Biotechnology (Analytical Biotechnology); Physical Chemistry (Electroanalytical Chemistry); Protein Biotechnology (isolation and purification of proteins, their structural and physico-chemical characterization); Enzymology (fundamental and applied aspects), Biosensorics, Environmental Biotechnology, Nanobiotechnology.

Andriy Zakalskiy, Associate professor, PhD, Research Fellow, Institute of Cell Biology, National Academy of Sciences of Ukraine. Author of over 100 scientific publications, including 30 articles in journals from the Scopus database. The Hirsch index (Scopus) – 6. The main scientific interests: Biochemistry, Enzymology, Molecular Biology, Biotechnology of Microorganisms; Construction of recombinant strains of yeast and bacteria capable to overproduce important biotechnological products, in particular enzymes of bioanalytical importance, as well as the creation of bio/chemical sensors for the determination of some analytes.

Wojciech Nogala, PhD, Research Associate in the Institute of Physical Chemistry, Polish Academy of Sciences. The Head of the Nanoelectrochemistry group. Author of over 50 scientific publications. The Hirsch Index (Scopus) – 17. The main scientific interests: Nanoelectrochemistry, electrodeposition of catalytic nanomaterials, electroanalysis in confined volumes, electrochemical sensors, nanoscale electrochemical imaging and surface charge mapping, scanning electrochemical microscopy (SECM), scanning ion conductance microscopy (SICM).

Sylwester Gawinkowski, PhD, Assistant professor at the Institute of Physical Chemistry, Polish Academy of Sciences. Project leader at the Laser Center. Author of more than 40 scientific publications. Hirsch Index (Scopus) - 16. Main scientific interests: molecular nanophotonics, single molecule spectroscopy, surface enhanced Raman scattering (SERS), nanoparticles, plasmonics.

Tomasz Ratajczyk, PhD, Research Associate in the Institute of Physical Chemistry, Polish Academy of Sciences. Author of over 45 scientific publications. The Hirsch index (Scopus) – 14. The main scientific interests: Nuclear Magnetic Resonance (NMR), solid-state NMR (ssNMR), applied NMR, Hyperpolarization, Parahydrogen Induced Polarization (PHIP).

Magdalena Bonarowska, PhD, Specialist in the Institute of Physical Chemistry, Polish Academy of Sciences, member of the research group „Cooperative catalysis". Author of 43 scientific publications. The Hirsch index (Scopus) – 14. The main scientific interests: environmental chemistry; synthesis and characterization of heterogeneous catalysts; bimetallic nanocomposite catalysts; structural properties of nanomaterials; noble metal dispersion; adsorption of gases onto solids; reaction kinetics in hydrodechlorination of organic compounds; mass spectrometry.

Olha Demkiv, PhD, Research Scientist in the Institute of Cell Biology, National Academy of Sciences of Ukraine. Author of over 75 scientific publications, including 36 articles in journals from the Scopus database. The Hirsch index (Scopus) – 12. Author of 45 scientific publications. Hirsch index (Scopus) – 12. The main scientific interests and Current Research: Applied Microbiology and Biotechnology; Biochemistry (regulatory aspects of metabolism in microorganisms); Protein Biotechnology (isolation and purification of proteins, their structural and physico-chemical characterization); Enzymology

(fundamental and applied aspects), Biosensorics, Environmental Biotechnology, Nanobiotechnology.

Oksana Zakalska, MSc, Leading Engineer, Institute of Cell Biology, National Academy of Sciences of Ukraine. Author of over 20 scientific full-length publications, including 13 articles in journals from the Scopus database. The Hirsch Index (Scopus) – 6. The main scientific interests: Microbiology, Enzymology, Molecular Biology, Biotechnology of Microorganisms; Isolation, purification and characterization of the enzymes for bioanalytical purposes, as well as their use in analytical kits for the determination of some analytes.

Mykhailo Gonchar, DrSci, Prof., The Head of the Department of Analytical Biotechnology, Institute of Cell Biology, National Academy of Sciences of Ukraine. Author of over 565 scientific full-length publications, including 158 articles in journals from the Scopus database. The Hirsch index (Scopus) – 26. The main scientific interests: Applied Microbiology and Biotechnology (metabolic engineering, analytical biotechnology); Biochemistry (regulatory aspects of metabolism in microorganisms); Protein Biotechnology (isolation and purification of proteins, their structural and physico-chemical characterization); Enzymology (fundamental and applied aspects), Biosensorics, Environmental Biotechnology, Nanobiotechnology.

Оригінал доступний за посиланням: https://doi.org/10.1016/j.snb.2023.134276

8.3. Розробка ензиматичного методу визначення вмісту креатиніну за використання рекомбінантної креатиніндеімінази.

Анотація: *Пошук біомаркерів найпоширеніших захворювань та індикаторів для оцінки перебігу і лікування хвороб є пріоритетним напрямком в галузі аналітичної біотехнології. Серед таких біомаркерів важлива роль належить метаболітам, зокрема, креатиніну. У поточній роботі повідомляється про розробку нового ензиматичного методу одночасного визначення вмісту амонію та креатиніну в біологічних рідинах людини, що ґрунтується на ензиматичному розщепленні креатиніну до N-метилгідантоїну та амонію, концентрацію якого визначають в ході паралельних реакцій. Показано, що для гідролізу креатиніну є ефективним використання креатиніндеімінази Corynebacterium glutamicum, виділеної з клітин рекомбінантного штаму Escherichia coli BL-2\/pET32-codA. Генерований в креатиніндеіміназній реакції амоній утворює з о-фталевим альдегідом 2,3-дигідро-1Н-ізоіндол-1-тіол, концентрацію якого визначають флуориметрично, при хвилі емісії 415 нм та хвилі збудження 360 нм.*

МІНІСТЕРСТВО РОЗВИТКУ ЕКОНОМІКИ, ТОРГІВЛІ ТА СІЛЬСЬКОГО ГОСПОДАРСТВА УКРАЇНИ

УКРАЇНА (19) **UA** (11) **142490** (13) **U**

(51) МПК
G01N 21/64 (2006.01)

(12) ОПИС ДО ПАТЕНТУ НА КОРИСНУ МОДЕЛЬ

(21) Номер заявки: **u 2019 11544**
(22) Дата подання заявки: **29.11.2019**
(24) Дата, з якої є чинними права на корисну модель: **10.06.2020**
(46) Публікація відомостей про видачу патенту: **10.06.2020, Бюл.№ 11**

(72) Винахідник(и):
Гончар Михайло Васильович (UA),
Закальський Андрій Євстахович (UA),
Закальська Оксана Мирославівна (UA),
Стасюк Наталія Євгенівна (UA),
Прокопів Тетяна Маркіянівна (UA),
Борецький Юрій Романович (UA),
Демків Ольга Михайлівна (UA)

(73) Власник(и):
ІНСТИТУТ БІОЛОГІЇ КЛІТИНИ НАН УКРАЇНИ,
вул. Драгоманова, 14/16, м. Львів-5, 79005 (UA),
Львівський державний університет фізичної культури імені Івана Боберського,
вул. Костюшка, 11, Львів-7, 79007, Україна (UA)

(54) МОНОЕНЗИМАТИЧНИЙ СПОСІБ ВИЗНАЧЕННЯ ВМІСТУ КРЕАТИНІНУ ТА АМОНІЮ В БІОЛОГІЧНИХ РІДИНАХ ЛЮДИНИ

(57) Реферат:

Спосіб одночасного визначення амонію та креатиніну в біологічних рідинах людини, що ґрунтується на ензиматичному розщепленні креатиніну до N-метилгідантоїну та амонію, концентрацію якого визначають в наступній хімічній реакції: 1) для гідролізу креатиніну використовується креатиніндеіміназа Corynebacterium glutamicum, виділена із клітин рекомбінантного штама Escherichia coli BL-2VpET32-codA;
2) генерований в креатиніндеіміназній реакції амоній утворює з о-фталевим альдегідом 2,3-дигідро-1Н-ізоіндол-1-тіол, концентрацію якого визначають флуориметрично.

UA 142490 U

Корисна модель належить до медичної діагностики та може використовуватися у спорті і фізичній терапії.

Аналітична біотехнологія - важлива складова сучасної біотехнології, яка пов'язана з використанням біологічних об'єктів (тканин, клітин, органел), субмолекулярних комплексів, біомолекул або навіть принципів функціонування живих систем для аналітичних цілей. Основною перевагою біоаналітичних систем є їхня виняткова специфічність, що пояснюється надзвичайною селективністю біорозпізнавання на молекулярному рівні.

Пошук біомаркерів найпоширеніших захворювань та індикаторів для оцінки перебігу і лікування хвороб є пріоритетним напрямком в галузі аналітичної біотехнології. Серед таких біомаркерів важлива роль належить метаболітам, зокрема креатиніну.

Креатинін - один із кінцевих продуктів обміну білків в організмі теплокровних тварин і людини. Креатинін утворюється з креатину і виділяється з крові в сечу в результаті клубочкової фільтрації без реабсорбції канальцями [1]. Показник концентрації креатиніну в плазмі (сироватці) крові широко використовується в рутинній медичній практиці для визначення швидкості клубочкової фільтрації - інтегрального показника видільної функції нирок. Нормальний вміст креатиніну в крові складає: для жінок - 44-97 мкМ, для чоловіків - 62-115 мкМ. При функціонуванні тільки однієї нирки цей рівень зростає до 159-168 мкМ. Підвищена понад норму концентрація креатиніну в сироватці крові (для дітей - понад 177 мкМ, для дорослих - понад 885 мкМ) свідчить про серйозну ниркову недостатність [2].

Гіперкреатинінемія може бути пов'язана з хронічними або гострими нирковими захворюваннями та ураженням нирок токсичними чинниками, зокрема медикаментами (рентгеноконтрастними засобами, антибіотиками-аміноглікозидами, антибіотиками-цефалоспоринами, статинами, тощо). Підвищення рівня креатиніну в сироватці крові спостерігається також при споживанні великої кількості м'яса і вживанні препаратів креатину (при цьому підвищується вміст креатиніну в сечі). Рівень креатиніну підвищується також при зневодненні організму й ураженні м'язів. Зниження концентрації креатиніну спостерігається при недостатньому споживанні м'яса, вегетаріанському раціоні, голодуванні, а також в I та II триместрах вагітності. Рівень креатиніну нижче 40 мкМ свідчить про зниження м'язової маси [3].

Креатинін розглядається як важливий показник фізіологічного стану спортсменів [4]. Отже, існує потреба у простих, неінвазійних методах аналізу цього метаболіту в біологічних рідинах, зокрема в слині і поті.

Креатинін сироватки крові є важливим показником функції нирок, тому що це легко вимірюваний побічний продукт метаболізму м'язів, який виділяється нирками в незмінному вигляді, переважно, шляхом клубочкової фільтрації [1]. Коли пошкоджується фільтрація в нирці, підвищується рівень креатиніну у крові. Тому аналіз креатиніну у біологічних рідинах (сироватці крові та сечі) можна використати для розрахунку кліренсу креатиніну, що співвідноситься зі швидкістю клубочкової фільтрації.

Креатинін у сироватці крові та сечі є важливим діагностичним біомаркером для контролю захворювань нирок, як от гострий хронічний інтерстиціальний нефрит, нефроз, ниркова недостатність, а також інфаркту міокарда [5]. Вміст цього метаболіту в діалізаті або ультрафільтраті також є інформативною кількісною оцінкою ефективності гемодіалізу.

Раніше було опубліковано комплексний огляд по креатиніну та його обміну [6]. Багато аргументів свідчать про зв'язок між порушеннями метаболізму креатину та м'язовими захворюваннями, а також неврологічними розладами. Наявні повідомлення про лікувальні ефекти орального застосування креатину при таких захворюваннях. Показано, що оральне споживання креатину сприяє поліпшенню спортивних результатів, тому його часто використовують як харчовий додаток для спортсменів. На жаль, встановлено, що креатин і креатинін можуть виступати як попередники харчових мутагенів та уремічних токсинів [6].

Оскільки аналіз креатиніну широко використовується для оцінки стану пацієнта, точність такого дослідження у випадку порушення функції нирок є особливо важливою.

Серед хімічних методів визначення вмісту креатиніну широко застосовується реакція Яффе [7], що базується на використанні лужного пікрату натрію як хімічного реагента, але вона є недостатньо специфічною.

Було багато спроб покращити цю методику, але нові модифікації все ще мають низьку специфічність і чутливі до позитивних і негативних впливів різних супутніх речовин.

Запропоновано низку сучасних інструментальних методів визначення вмісту креатиніну, наприклад: високоефективна рідинна хроматографія [8], хроматографія з використанням флуоресцентних індикаторів [9], іонна хроматографія [10, 11], міцелярна електрокінетична хроматографія [12], капілярний електрофорез [13], міцелярний електрокінетичний капілярний електрофорез [14], капілярний ізотахофорез [15] і тандемна мас-спектрометрія [16]. Однак всі ці

методи досить складні та непридатні для аналізу креатиніну в режимі реального часу; крім того обладнання для капілярного електрофорезу є дороговартісним а, отже, не придатним для рутинного аналізу Таким чином, подальший прогрес у створенні нових високо селективних і чутливих методів для швидкого визначення креатиніну в біологічних рідинах є дуже важливим.

Найбільш перспективними аналітичними методами визначення вмісту креатиніну є ензиматичні методи [17]. З цією метою запропоновано два ферменти розщеплення креатиніну: 1) креатиніндеіміназа (КДІ, КФ 3.5.4.21), яка розщеплює креатинін до N-метилгідантоїну та іонів амонію; 2) креатинінамідогідролаза (креатиніназа, КФ 3.5.2.10), яка зворотно перетворює креатинін в креатин. Використовуючи ці ферменти, вміст креатиніну вимірюється шляхом моніторингу кінцевих продуктів (тобто, аміаку або креатину) через серію мультиферментних реакцій.

Як джерело КДІ можуть використовуватись різні мікроорганізми, але важливою проблемою при застосуванні цього ферменту для аналітичних цілей є його недостатня специфічність до цільового аналіту: різні бактерії і гриби продукують фермент, який має додаткову деаміназну активність стосовно цитозину [3, 17]. Більшість бактерійних КДІ є олігомерними білками, що складаються з 4-16 ідентичних субодиниць з молекулярною масою 35-72 к Да. Описано виділення КДІ з різних мікробних джерел з використанням багатостадійної хроматографічної процедури [3, 17].

Аналогами пропонованого способу є два підходи аналізу креатиніну.

1) Для ферментативного визначення креатиніну було запропоновано спряження креатиніндеіміназної реакції з глутаматдегідрогеназною та спектрофотометричний моніторинг окислення NADH при 340 нм [18]:

Креатинін + H_2O = N-метилгідантоїн + NH_3

NH_3 + кетоглутарат + NADH + H+ = глутамат + NAD^+ + H_2O.

2) Інший підхід ґрунтується на використанні 4-х ферментів, включаючи креатиніназу (ЕС 3.5.2.10) та креатиназу (ЕС 3.5.3.3). Креатинін перетворюється креатиніназою в креатин, а останній - до сечовини і саркозину за допомогою креатинази. Кінцевий продукт (саркозин) аналізується у наступній саркозиноксидазній реакції, супряженій з пероксидазною, колориметрично або флуориметрично [19].

Низка ферментних наборів для аналізу креатиніну виробляється комерційно з використанням вище зазначених ферментів, наприклад "SIGMA-ALDRICH" (ціна - 342 євро за 100 аналізів) [20], а також для креатину (ціна 360,5 євро за 100 аналізів) [21]. Подібний комплект для аналізу креатиніну виробляється компанією BIOVISION (за ціною 285 USD за 100 аналізів) [22] і ABC AM (385 Євро) [23]. Очевидно, що такий підхід є дуже складним і дорогим.

Пропонована корисна модель стосується способу аналізу вмісту креатиніну та аміаку у біологічних рідинах людини і відрізняється від відомих аналогів тим, що використовується лише один фермент (креатиніндеіміназа) для утворення продукту реакції (амонію), який визначається флуориметрично. Новий спосіб суттєво знижує матеріальні затрати (є одноферментним), не потребує використання кофактора (як у випадку креатиніндеіміназно-глутаматдегідрогеназного методу), дозволяє підвищити чутливість і селективність визначення цільового аналіту та прискорити час виконання аналізу у порівнянні з мультиферментними підходами.

Поставлена задача вирішується шляхом моноензиматичного визначення вмісту креатиніну у біологічних зразках за допомогою високоселективного до креатиніну ферменту - креатиніндеімінази (далі - КДІ), виділеної із клітин рекомбінантного штаму Escherichia coli BL-21\pET32-codA, що містить ген креатиніндеімінази Corynebacterium glutamicum. Очистку КДІ із денатурованих "тілець включення" проводили за допомогою металохелатної хроматографії на сефарозі Ni-NTA Superflow.

Ступінь очищення КДІ від баластних білків характеризували, визначаючи активність ферменту в кожній фракції елюату та електрофоретично. Електрофорез проводили в 12 % SDS-ПААГ за методом Леммлі, білки зафарбовували Кумассі R-250.

Опрацьована методика дозволяє рутинно отримувати високоочищені препарати КДІ, із питомою активністю 10-20 мкмоль $хв^{-1}$ $мг^{-1}$ білка.

Препарат КДІ стабільний при -20 °С у 50 мкМ, Na-фосфатному буфері pH 7,5, що містить 20 % гліцерину, впродовж 4 місяців.

Пропонований та опрацьований на реальних зразках біологічних рідин ензиматично-хімічний метод аналізу креатиніну із флуориметричною детекцією кінцевого продукту реакції, що утворюється при взаємодії амонію з офталевим альдегідом (ОФА-ФЛ), має низку переваг порівняно із відомими методами: відсутність складного обладнання, економічний ефект завдяки використанню лише одного фермента (КДІ) без кофакторів, селективність визначення цільового аналіту і широкий діапазон тестованих концентрацій креатиніну, можливість здійснення

процедури аналізу в автоматичному режимі за використання планшетного аналізатора. Ще одною перевагою методу ОФА-ФЛ є те, що в ролі хромогенної системи використано дешевий нетоксичний реагент, що дозволяє знизити собівартість методу та гарантувати безпеку процедури аналізу.

Суть пропонованої корисної моделі пояснюється за допомогою графічних матеріалів.

На Фіг. 1 наведено схему перебігу реакцій пропонованого ензиматично-хімічного методу аналізу креатиніну за використання КДІ та ОФА.

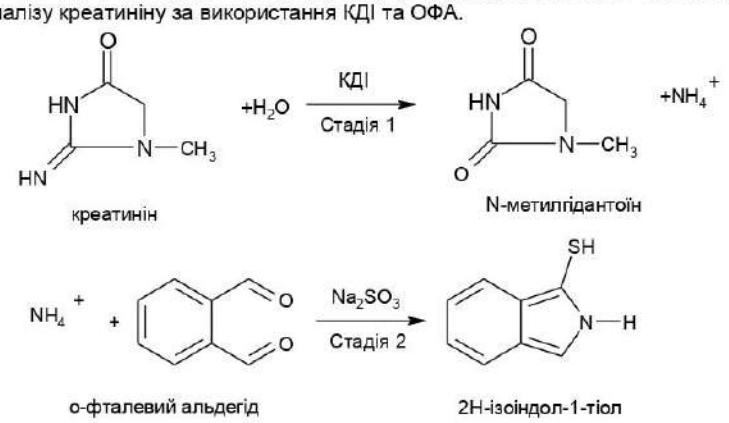

Фіг. 1. Схема реакцій при визначенні вмісту креатиніну та амонію ензиматичним методом ОФА-ФЛ із флуоресцентною детекцією утвореного амонію.

Аналітичні характеристики ензиматично-хімічного методу ОФА-ФЛ показано на Фіг. 2 та у Табл. 1. На Фіг. 2 представлено калібрувальні графіки для визначення концентрації креатиніну й амонію та діапазон лінійності ензиматично-хімічного методу ОФА-ФЛ з флуориметричною детекцією утвореного продукту.

Як видно з Фіг. 2, лінійний діапазон визначення креатиніну складає 2-30 мкМ в перерахунку на об'єм кінцевої реакційної суміші. При вищій концентрації аналіту пробу розводять водою. Чутливість методу - 23,6±1,4 Одиниць флуоресценції (Од. фл.)/мкМ (в реакційній суміші). Лінійний діапазон визначення амонію: 0,4-14 мкМ в перерахунку на об'єм кінцевої реакційної суміші. При вищій концентрації аналіту в пробі її розводять водою. Чутливість методу - 131±3,8 Од. фл./мкМ (в реакційній суміші).

Фіг. 2. Аналітичні характеристики ензиматично-хімічного методу ОФА-ФЛ. Залежність інтенсивності флуоресценції утвореного продукту реакції від концентрації креатиніну у реакційній суміші. У вставках наведено калібрувальні графіки.

Таблиця 1

Аналітичні характеристики методу ОФА-ФЛ
визначення вмісту креатиніну та амонію (детекція $\lambda_{зб}$ = 360 нм, $\lambda_{ем}$ = 415 нм)

Аналіз креатиніну			
Чутливість, Од. фл./мкМ	Лінійний діпазон	Нижня оптимальна межа визначення	Фонова межа, Од. фл.
23,6±1,4	2-30 мкМ	665 нМ	521
Аналіз амонію			
Чутливість, Од. фл./мкМ	Лінійний діпазон	Нижня оптимальна межа визначення	Фонова межа, Од. фл.
131±3,8	0,4-14 мкМ	200 нМ	88

Для визначення вмісту креатиніну, зразки обробляють КДІ для розщеплення креатиніну до амонію та N-метилгідантоїну. Утворений амоній в присутності сульфіту натрію в лужному середовищі вступає у хімічну реакцію з ОФА з утворенням продукту - 2,3-дигідро-1Н-ізоіндолу-1 - тіолу (Фіг. 2), який визначають флуориметрично при хвилі емісії 415 нм та хвилі збудження 360 нм. Внаслідок ензиматичної реакції з 1 моля креатиніну утворюється 1 моль амонію, тож вміст креатиніну визначають за різницею концентрацій амонію у дослідному зразку: загального (після ензиматичного гідролізу креатиніну) та ендогенного (без додавання КДІ).

Хід аналізу зразків крові на вміст креатиніну та амонію пропонованим методом множинних внесень стандарту включає такі стадії:

1. Підготовка депротеїнізованих зразків сироватки крові.

Для отримання сироватки крові, венозну кров поміщають у центрифужну пробірку та центрифугують упродовж 10 хв при 3000 об./хв. Переносять супернатант в іншу центрифужну пробірку та центрифугують додатково протягом 10 хв при 3000 об./хв. До отриманих зразків сироватки крові додають 50 %-ний розчин трихлороцтової кислоти (ТХО) (0,9 мл зразка + 0,1 мл ТХО), витримують 20 хв при +4 °С і центрифугують додатково протягом 10 хв при 3000 об./хв. Супернатант відбирають і нейтралізують лугом (1 мл ТХО-екстракту + 0,15 мл 4 М КОН). Корекційний коефіцієнт становить 1,278. Депротеїнізовані проби перед аналізом розводять у 100 або 200 разів. Якщо пробу не аналізують упродовж 24 год., її зберігають (без нейтралізації) при -20 °С до 4 тижнів.

2. Ензиматична реакція. Для аналізу проб методом множинного внесення стандарту, у пробірки, що закриваються, відбирають по 0,1 мл досліджуваних депротеїнізованих та розведених проб, вносять по 0,1 мл стандартного розчину аналіту певної концентрації (0,1 мМ, 0,2 мМ, 0,4 мМ, 0,8 мМ та 1 мМ). В одну пробірку з дослідною пробою стандартний розчин не додаємо. У кожній серії аналізу ставлять "сліпу" пробу (без внесення тестованих зразків та стандарту). Схема внесень відображена в Табл. 2.

Для аналізу креатиніну (див Табл. 2), зразки сироватки обробляють ферментом КДІ. Для цього, до 0,1 мл депротеїнізованої сироватки (без/або з додаванням стандартного розчину креатиніну різних концентрацій для побудови калібрувального графіка) та 0,1 мл розчину КДІ (4 Од./мл, 0,4 Од. акт. на пробу), інкубують протягом 30 хв. при 37 °С.

3. Хімічна реакція. Для визначення вмісту амонію, до 0,1 мл розведеної депротеїнізованої проби (без обробки КДІ - для визначення ендогенного амонію) та після обробки КДІ (для визначення креатиніну) вносять 1,9 мл робочого реагенту та розчин амоній хлориду (згідно з Табл. 2). Суміш інкубують при 37 °С упродовж 30 хв та реєструють інтенсивність флуоресценції (при хвилі емісії 415 нм та хвилі збудження 360 нм) дослідних проб відносно "сліпої проби" (дистильована вода з відповідними реагентами). Хімічний реагент має наступний склад: 5,15 мМ ОФА, 1,29 мМ сульфіт натрію, 5,77 мМ ЕДТА та 50 мМ боратний буфер, pH 9,5. Хімічний реагент зберігають у темноті при кімнатній температурі.

Таблиця 2

Процедура аналізу креатиніну та амонію в сироватці крові методом множинних внесень стандарту.

	Розчин креатиніну, мл	Депротеїнізована проба, мл	Бідистильована вода, мл	Розчин КДІ (4 Од./мл), мл	Робочий реагент, мл
Аналіз суми креатиніну та амонію					
Дослідна проба	-	0,1	0,1	0,1	1,9
Дослідно-калібрувальна проба 1	0,1 мл 0,1 мМ р-ну	0,1	-	0,1	1,9
Дослідно-калібрувальна проба 2	0,1 мл 0,2 мМ р-ну	0,1	-	0,1	1,9
Дослідно-калібрувальна проба 3	0,1 мл 0,4 мМ р-ну	0,1		0,1	1,9
Дослідно-калібрувальна проба 4	0,1 мл 0,8 мМ р-ну	0,1	-	0,1	1,9
Дослідно-калібрувальна проба 5	0,1 мл 1 мМ р-ну	0,1	-	0,1	1,9
"Сліпа" проба	-	-	0,2	0,1	1,9
Аналіз амонію					
	Розчин амонію, мл	Депротеїнізована проба, мл	Бідистильована вода, мл	Робочий реагент, мл	
Дослідна проба	-	0,1	0,2	1,9	
Дослідно-калібрувальна проба 1	0,1 мл 0,1 мМ р-ну	0,1	0,1	1,9	
Дослідно-калібрувальна проба 2	0,1 мл 0,2 мМ р-ну	0,1	0,1	1,9	
Дослідно-калібрувальна проба 3	0,1 мл 0,4 мМ р-ну	0,1	0,1	1,9	
Дослідно-калібрувальна проба 4	0,1 мл 0,8 мМ р-ну	0,1	0,1	1,9	
Дослідно-калібрувальна проба 5	0,1 мл 1 мМ р-ну	0,1	0,1	1,9	
"Сліпа" проба	-	-	0,3	1,9	

4. Детекція продукту реакції. Проби аналізують проти "сліпої" проби: на флуорометрі ("Thermo Scientific", США) при довжині хвилі емісії 415 нм із хвилею збудження 360 нм.

5. Розрахунки. Значення вмісту креатиніну розраховують за різницею між сумою креатиніну і амонію в пробах з додаванням КДІ та амонію (проби без додавання КДІ) із врахуванням усіх попередніх розведень сироватки ТХО та NaOH (корекційний коефіцієнт 1,278) та розведення депротеїнізованої і нейтралізованої сироватки (перед аналізом та в сумарній інкубаційній-суміші). Для обрахунків будують калібрувальну криву залежності інтенсивності флуоресценції від концентрації доданого до аналізованого зразку стандарту (креатиніну чи амонію). За лінією регресії калібрувальної кривої, побудованою за допомогою програми Origin (див. Фіг. 3), проводять розрахунок вмісту креатиніну в аналізованому зразку за формулою:

$Co = (A/tg\alpha) \times N$,

де Co - вміст креатиніну в сироватці, мкМ;

A - значення величини флуоресценції реакційної суміші для аналізованого зразка сироватки; для більшої точності, замість експериментального значення A у формулі краще використовувати значення, визначене за лінією регресії Фіг. 3: це відрізок, який відтинається лінією регресії на осі інтенсивності флуоресценції (параметр A рівняння регресії);

tgα - нахил калібрувальної кривої, отриманої методом множинних внесень стандарту (на Фіг. 3 - це параметр B лінії регресії);

N - сумарний фактор розведення аналізованого зразка; $N = 1{,}278 \times n_1 \times n_2$,

де 1,278 - розведення сироватки при депротеїнізації та нейтралізації;

n_1 - розведення зразка депротеїнізованої сироватки в реакційній суміші (згідно з Табл. 2, n_1=22);

n_2 - попереднє розведення зразка сироватки (як правило, n_2=100 або 200).

Фіг. 3. Калібрування методом множинних внесень стандарту при визначенні вмісту амонію. Під лінією регресії подано параметри А і В лінії регресії, коефіцієнт кореляції R, розведення N та кінцевий вміст NH_4^+.

А) Розрахунок вмісту ендогенного амонію за використання параметрів лінійної регресії відповідного калібрувального графіку, беручи до уваги фактори розведення (формула).

$$C_{NH4+}=A/B\cdot N \quad (1),$$

де C_{NH4+} - концентрація ендогенного амонію, А та В - параметри лінійної регресії, N - фактор розведення дослідної проби при аналізі амонію. Обчислення середнього значення вмісту амонію проводили за значеннями концентрацій для двох розведень.

Б) Розрахунок вмісту суми креатиніну та амонію проводять за формулою (2)

$$C_{Cm.+NH4+} = A/B\cdot N \quad (2),$$

де $C_{Cm.+NH4+}$ - концентрація суми креатиніну та амонію, А та В - параметри лінійної регресії, N - фактор розведення дослідної проби при аналізі креатиніну та амонію.

В) Розрахунок вмісту креатиніну проводять за різницею:

$$C_{Cm}=C_{Cm+NH4^+}-C_{NH4^+} \quad (3),$$

де $C_{Cm+NH4+}$ ~ концентрація суми креатиніну та амонію, C_{NH4+} - концентрація ендогенного амонію.

ОФА-ФЛ метод визначення вмісту аміаку та креатиніну протестовано на зразках сироваток крові хворих із порушеннями функцій нирок (до і після гемодіалізу) та зразках сироваток вагітних жінок (Табл. 3, 4).

Таблиця 3

Визначення вмісту креатиніну та амонію у зразках сироваток крові різних груп пацієнтів

Зразки	Вміст креатиніну, мкМ	Вміст амонію, мкМ
21	368±2,6	22±0,6
45 (після гемодіалізу)	281±1,8	34±0,8
46 (після гемодіалізу)	256±1,6	18±0,4
47 (після трансплантації нирки)	94±0,9	9±0,3
50 (після гемодіалізу)	172±1,2	28±0,7
66	410±2,8	37±0,6
57	328±2,2	49±0,9
48 (до гемодіалізу)	856±4,1	29±0,7

Таблиця 4

Визначення вмісту креатиніну та амонію у зразках сироваток крові вагітних жінок

Зразки	Вміст креатиніну, мкМ	Вміст амонію, мкМ
20	62±0,7	18±0,4
23	79±0,8	24±0,5
14	110±0,9	18=1=0,3
7	58±0,7	11±0,3
19	99±0,9	22±0,5
18	72±0,8	34±0,6

Таким чином, отримані результати свідчать, що пропонований моноензиматичний метод кількісного аналізу креатиніну та аміаку в біологічних рідинах (сироватці крові) із флуориметричною детекцією продукту реакції є придатним для використання в клініко-діагностичній та науково-дослідній практиці.

Джерела інформації:

1. Narayanan S., Appleton H.D. (1980). Creatinine: A Review. Clin. Chem. 26 (8), 1119-1126.

2. Ceriotti F., Boyd J.C., Klein G. et al. (2008). Reference intervals for serum creatinine concentrations: assessment of available data for global application. Clin. Chem. 54 (3), 559-566.

3. Lad U., Khokhar S., Kale G.M. (2008). Electrochemical creatinine biosensors. Anal. Chem. 80 (21), 7910-7917.

4. Wofyniec W., Kasprowicz K., Giebiritowicz J. et al. (2019). Changes in Water Soluble Uremic Toxins and Urinary Acute Kidney Injury Biomarkers After 10-and 100-km Runs. Int. J. Environ. Res. Public Health. 16 (21). pii: E4153. doi: 10.3390/ijerphl6214153.

5. Sant W., Pourciel-Gouzy M.L., Launay J. et al. Development of a creatinine-sensitive sensor for medical analysis. Sens. Actuator B-Chem. 103, 260-264.

6. Wyss M., Kaddurah-Daouk R. (2000). Creatine and creatinine metabolism. Phys. Rev. 80(3), H07-1213.

7. Jaffe M. (1886). Uber den Niederschlag, welchen Pikrinsaure in normalem Harn erzeugt, und uber eine neue Reaktion des Kreatinins. Z. Physiol. Chem. 10, 391-400.

8. George S.K., Dipu M.T. et al. (2006). Improved HPLC method for the simultaneous determination of allantoin, uric acid and creatinine in cattle urine. J. Chromatogr. B. 832 (1), 134-137.

9. Duran Meras I., Espinosa Mansilla A., Rodriguez Gomez M. Jose. (2005). Determination of methotrexate, several pteridines, and creatinine in human urine, previous oxidation with potassium permanganate, using HPLC with photometric and fluorimetric serial detection. Anal. Biochem. 346 (2), 201-209.

10. Yokoyama Y., Horikoshi S., Takahashi T., Sato H. (2000). Low-capacity cation-exchange chromatography of ultraviolet-absorbing urinary basic metabolites using a reversed-phase column coated with hexadecylsulfonate. J. Chromatogr. A. 886(1-2), 297-302.

11. YokoyamaY., Tsuji S., Sato H. (2005). Simultaneous determination of creatinine, creatine, and UV-absorbing amino acids using dual-mode gradient low-capacity cation-exchange chromatography. J. Chromatogr. A. 1085 (1), 110-116.

12. Pobozy E., Radomska A., Koncki R., GlaDb S. (2003). Determination of dialysate creatinine by micellar electrokinetic chromatography. J. Chromatogr. B. 789,417-424.

13. Burke D.G., MacLean P.G. et al. (1999). Analysis of creatine and creatinine in urine by capillary electrophoresis. J. Chromatogr. B. 732, 479-485.

14. Tran T. C, Huq T. A. et al. (1997). Determination of creatinine and other uremic toxins in human blood sera with micellar electrokinetic capillary electrophoresis. J. Chromatogr. B. 690 (1-2), 35-42.

15. Kvasnicka F., Voldrich M. (2000). Isotachophoretic determination of creatinine in meat and meat products. Electrophoresis. 21, 2848-2850.

16. Huskova R., Chrastina P., Adam T., Schneiderka P. (2004). Determination of creatinine in urine by tandem mass spectrometry. Clin. Chim. Acta. 350 (1-2), 99-106.

17. Zakalskiy A., Stasyuk N., Gonchar M. (2019). Creatinine Deiminase: Characterization, Using in Enzymatic Creatinine Assay, and Production of the Enzyme. Curr. Protein. Pept. Sci. 20 (5), 465-470.

18. Gottschalk, E.M.; Gottschalk, G.; Delitz, R.P. et al. (2005). A new creatinine assay destined to become routine. Renal Disease. www.cli-online.com/fileadmin/artimg/a-new-creatinine-assay-destined-to-become-routine.pdf (As published in CLI October, 2005).

19. Shimizu S., Kim, J. M., Yamada H. (1989). Microbial enzymes for creatinine assay: a review. Clin, Chim. Acta. 185(3), 241-252.

20. http://www.sigmaaldrich.com/content/dam/sigma-aldrich/docs/Sigma/Bulletin/1/mak080bul.pdf.

21. http://www.sigmaaldrich.com/content/dam/sigma-aldrich/docs/Sigma/Bulletin/1/mak079bul.pdf.

22. https://www.biovision.com/creatinine-colorimetric-fluorometric-assay-kit.html.

23.http://www.abcam.com/ps/products/65/ab65340/documents/ab65340 %20Creatinine%20Assay%20kit%20protocol%20v9 %20 %28website%29.pdf.

ФОРМУЛА КОРИСНОЇ МОДЕЛІ

Спосіб одночасного визначення амонію та креатиніну в біологічних рідинах людини, що ґрунтується на ензиматичному розщепленні креатиніну до N-метилгідантоїну та амонію, концентрацію якого визначають в наступній хімічній реакції, який **відрізняється** тим, що:

1) для гідролізу креатиніну використовується креатиніндеіміназа Corynebacterium glutamicum, виділена із клітин рекомбінантного штама Escherichia coli BL-2VpET32-codA;

2) генерований в креатиніндеіміназній реакції амоній утворює з о-фталевим альдегідом 2,3-дигідро-1Н-ізоіндол-1-тіол, концентрацію якого визначають флуориметрично.

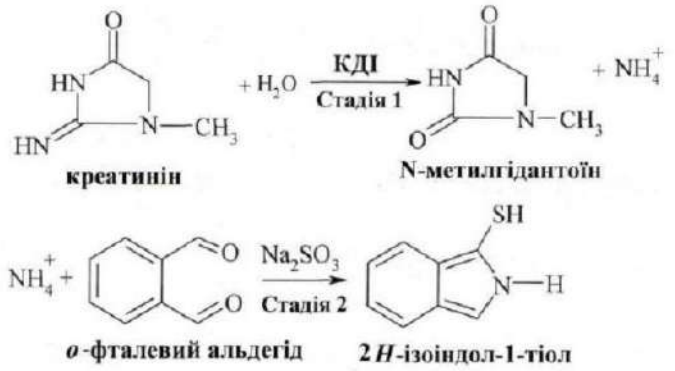

Фіг. 1

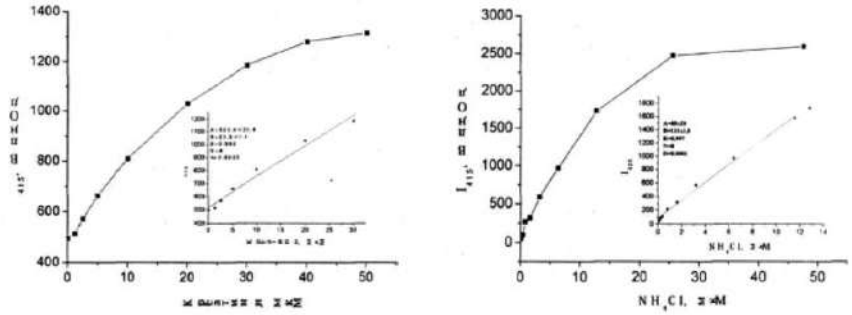

Фіг. 2

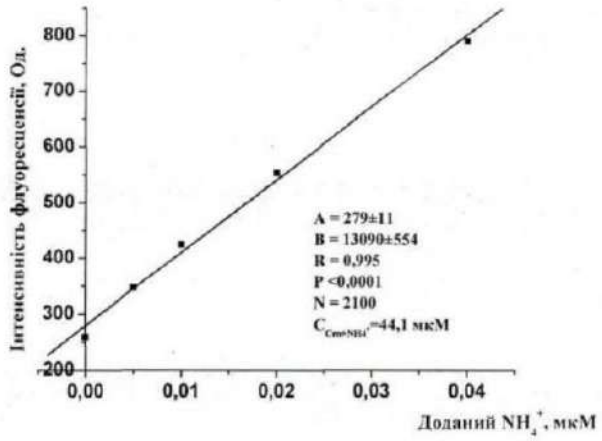

Фіг. 3

Комп'ютерна верстка С. Чулій

Міністерство розвитку економіки, торгівлі та сільського господарства України,
вул. М. Грушевського, 12/2, м. Київ, 01008, Україна

ДП "Український інститут інтелектуальної власності", вул. Глазунова, 1, м. Київ – 42, 01601

Розділ 9

УЗАГАЛЬНЕННЯ РЕЗУЛЬТАТІВ ДОСЛІДЖЕНЬ

Скринінг нових наноматеріалів на псевдоензиматичну активність та дослідження структурних і каталітичних властивостей отриманих нанозимів.

Особливістю сучасного прогресу в розвитку аналітичних біотехнологій є поєднання використання як природних ензимів, так і наноматеріалів, які найчастіше володіють каталітичною активністю (нанозими) або прискорюють перенесення електронів між ензимом та іншими компонентами системи (наномедіатори).

У біоаналітичних системах ензими використовують завдяки їхній селективності та надзвичайно високій каталітичній активності, проте вони виявляють обмежену хімічну та біологічну стабільність, а також високу вартість через складні технології, що застосовуються для їх виділення та очищення. Завдяки цьому використання штучних ензимів – нанозимів (НЗ), що володіють достатньою каталітичною активністю та стабільністю стало надзвичайно актуальним. Найважливішою перевагою НЗ є залежність їхніх властивостей від розміру та складу наноматеріалу. Це дозволяє створювати нові матеріали з широким діапазоном каталітичної активності, просто змінюючи форму, структуру та склад наночастинок. НЗ також мають унікальні властивості порівняно з іншими наноматеріалами, включаючи велику питому площу поверхні, що значно полегшує їх подальшу модифікацію та біокон'югацію. Завдяки цьому, НЗ часто використовують при створенні біоаналітичних систем, а саме задяки їх поєднанняю з ензимами можна отримати принципово нові нанокомпозитні матеріали із унікальними властивостями. Це дозволяє створення нових біонанокомпозитних матеріалів – на основі нанозимів та мікробних ензимів та конструювання на їхній основі нових біо(хемо)сенсорів та тест-наборів для визначення вмісту практично важливих аналітів.

З метою пошуку ефективних нанокомпозитних матеріалів здійснено скринінг та синтез нових НЗ, поєднуючи хімічне відновлення неорганічних солей

перехідних або шляхетних металів аскорбіновою кислотою або Натрій боргідридом з новим методом осадження НЗ на металевій пластинці. Проведено структурну характеристику отриманих НЗ за використання методів сканувальної електронної, флуоресцентної, атомно-силової мікроскопії; рентгено-спектрального аналізу та динамічного світлорозсіювання. Встановлено, що розмір отриманих матеріалів знаходиться в межах від 10 нм до 5 мкм (нанозими, НЗ та мікрозими, МЗ).

Здійснено скринінг монометалевих (Cd, Ce), біметалевих (Cd/Cu, Ce/Pd, Pt/Cu, Ce/Cu, Pd/Cd, Pd/Cu) та триметалевих (Cu/Cd/Zn) наночастинок (НЧ) на редуктазну активність. Для отриманих НЧ досліджували ензимо-подібну активність відносно різних субстратів. Встановлено, що Cd/Cu-НЧ виявляють найвищу редуктазну активність. Для кількісної оцінки редуктазної активності використовували реакцію із АБТС катіон-радикалом ($АБТС^{+\cdot}$). Так, при введенні НЧ в реакційну суміш концентрація катіон-радикалу зменшувалась, при цьому спостерігалося еквімолярне до катіон-радикалу утворення АБТС, тобто, в присутності НЧ відбувається відновлення катіон-радикалу до вихідної молекули. Розрахована за цією реакцією псевдо-редуктазна активність НЧ Cd/Cu становить 1,3 Од./мг. Отримані НЗ Cu/Cd/Zn протестовано на антиоксидантну активність відносно вільних радикалів $АБТС^{\bullet+}$ та $DPPH^{\bullet}$ у порівнянні із Тролоксом: значення напівмаксимального інгібування (IC_{50}) для НЗ Cu/Cd/Zn становить 6,8 ± 0,2 мкг/мл, що близько до Тролоксу (2,70 ± 0,1 мкг/мл). Синтезовані НЗ використано для побудови амперометричного біосенсора для аналізу селеніту.

Для усіх синтезованих НЧ аналізували також псевдо-пероксидазну активність. Аналіз ПО активності проводили за використання H_2O_2 (8,8 мМ), як субстрату та *о*-діанізидину як хромогену. Встановлено, що найвищою пероксидазною активністю серед синтезованих НЗ володіють Cu/Ce/Au та Cu. Визначено кінетичні параметри ($К_М$ і k_{cat}) для отриманих НЗ і МЗ та їх модифікованих полімерами форм. У пероксидазних реакціях, більшість синтезованих НЗ, зокрема, Cu/Ce/Au, Cu, Pt/Cu, Au/Ce/Pt та Pd/Ce виявляють найвищу активність стосовно *о*-діанізидину. Проведено ковалентну модифікацію

металевих НЗ, що місять Аурум, поєднанням цистеаміну, глутарового альдегіду та поліетиленіміну. Для отриманих функціоналізованих НЗ досліджено кінетичні характеристики, зокрема величини $K_м$, V_{max}, k_{cat} та субстратну специфічність. Показано, що функціоналізація НЗ полімерними носіями дозволяє модулювати каталітичні параметри НЗ, дещо змінювати субстратну специфічність та підвищувати їхню стабільність.

Проведено також «зелений» синтез НЧ Au шляхом інкубації відповідних солей металів із культурою клітин дріжджів ("*in vivo*"). Електронні спектри поглинання в діапазоні від 250 до 700 нм підтверджують факт утворення НЧ культурою клітин. Здійснено структурну характеристику отриманих НЗ за використання методів сканувальної електронної мікроскопії та встановлено, що розмір отриманих наноматеріалів становить в межах 20 – 40 нм.

Вивчення біологічної та можливої токсичної дії нанозимних композитів на еукаріотичні клітини дріжджів *Ogataea polymorpha.*

У поточному дослідженні, нами синтезовано НЧ Pt та Pt/Au (ядро/оболонка) за використання Натрій боргідриду в ролі відновника. Для отриманих НЧ досліджували ензимо-подібну активність. Встановлено, що Pt-НЧ виявляють псевдо-каталазну активність (далі – «катазими»). Для кількісної оцінки каталазної активності використовували реакцію Гідроген пероксиду з амоній молібдатом. Розрахована псевдо-каталазна активність Pt-НЧ та Pt/Au-НЧ становила 0,3 Од./мг та 0,8 Од./мг, відповідно. Отримані НЗ використали для вивчення їхнього впливу на ріст та властивості мутантного безкаталазного штаму дріжджів *Ogataea polymorpha* С-105 *(gcr1catX)*, здатного до конститутивного синтезу алкогольоксидази на глюкозному середовищі та повністю позбавленого каталазної активності. Молекулярно-генетичний аналіз та секвенування локусу геному штаму дріжджів *O. polymorpha* С-105 виявив дві мутації у гені каталази: заміна С у 895 положенні кодуючої послідовності на Т та делеція С у положенні 896. Така комбінація веде до зсуву рамки зчитування і утворення стоп-кодону TGA, що спричинює у штамі С-105 продукцію нефункціонального, неповного білка.

Встановлено, що внесення «катазимів» у ростове середовище відновлює здатність мутантних клітин рости на метанолі.

Проаналізовано зміни у накопиченні H_2O_2 у культуральному середовищі дріжджів при рості на метанолі чи суміші глюкози та метанолу за присутності «катазимів». Отримані результати вказують на суттєве зниження вмісту генерованого дріжджами Гідроген пероксиду у культуральному середовищі при введенні «катазимів». Показано, що на 38 год. інкубації, вміст Гідроген пероксиду в культуральному середовищі зменшується за присутності НЧ Pt в 5,9 раза на середовищі, що містить метанол, та у 4,9 раза – на середовищі, що містить суміш глюкози з метанолом, тоді як при додаванні НЧ Pt/Au – у 2,6 раза на обох середовищах. Отже, «катазими» Pt і Pt/Au ефективно виконують функцію відсутньої природної каталази в клітинах штаму *O. polymorpha C-105,* розщеплюючи генерований клітинами Гідроген пероксид і, таким чином, зменшуючи його вміст у клітинах та культуральній рідині. Отже, наші дослідження показують, що НЗ із каталазною активністю можуть успішно замінити природну каталазу клітин, виконуючи її детоксикаційну функцію. Аналіз літературних даних дозволяє зробити висновок, що це перше експериментальне свідчення можливості заміни природного ензиму на НЗ *in vivo*.

Створення амперометричних біосенсорів на основі нанокомпозитів хемоміметиків пероксидази і мікробних ензимів, придатних для аналізу етанолу, метиламіну та L-аргініну.

У наступних розділах нами показано можливість практичного використання синтезованих НЗ при розробці нових біоаналітичних систем. Із літературних джерел відомо, що модифікація електроду наноматеріалами може суттєво підвищити ефективність перенесення електронів за рахунок збільшення електрохімічно доступної площі поверхні електрода. З метою збільшення площі поверхні електрода та підвищення чутливості сенсорної системи, ми електрохімічно осаджували пористе золото (пор-Au) на графітовому електроді. Для дослідження впливу модифікації поверхні електрода на біоаналітичні характеристики біосенсорів, в ролі хемоміметиків ПО вибрано НЧ CuCe у

поєднанні з мікробними оксидазами: алкогольоксидаза *O. polymorpha,* глюкозооксидаза *Penicillium vitale,* аргініноксидаза *Amanita phalloides* та метиламінооксидаза *O. polymorpha*. В таблиці 9.1 наведено біоаналітичні характеристики щодо сконструйованих нами біосенсорів на основі вказаних мікробних оксидаз, НЧ CuCe та пористого золота. Для формування біоселективного шару досліджували методи ковалентної та електростатичної кон'югації ензимів на поверхні нановносіїв.

Таблиця 9.1

Характеристики біонаноелектродів на основі мікробних оксидаз, міметиків ПО і пористого золота.

Ензим	Модифікована поверхня ГЕ[1]	Потенціал, мВ	Чутливість, $А \cdot М^{-1} \cdot м^{-2}$	Лінійний діапазон, мМ	НМВ[2], мкМ	$I_{макс}$ [*], мкА	$K_М^{поз}$, мМ
АО	ПО/ГЕ	–50	22	0,13 – 0,9	39	0,255	0,68
	CeCu/ГЕ	–50	32	0,05 – 2,1	15	1,57	5,05
	CeCu/[6]пор-Au/ГЕ	–50	102	0,033 – 0,50	10	1,12	1,23
[3]ГО	ПО/ГЕ	–50	44	0,5 – 5,0	150	0,30	5,23
	CeCu/ГЕ	–50	73	0,5 – 7,3	150	1,16	18
	CeCu/пор-Au/ГЕ	–50	400	0,25 – 2,0	75,7	2,31	5,81
[4]МАО	ПО/ГЕ	–250	7,1	0,2 – 1,7	130	0,19	2,07
	CeCu/ГЕ	–250	35	0,06 – 1,7	18	0,92	2,15
	CeCu/пор-Au/ГЕ	–250	125	0,06 – 0,5	18	0,89	0,55
[5]АргО	CeCu/ГЕ	–150	113	0,05 – 2,25	15	2,56	1,5
	CeCu/пор-Au/ГЕ	–150	200	0,1 – 0,5	33	1,73	0,83

Примітка: [1]ГЕ – графітовий електрод; [2]НМВ – нижня межа визначення; [3]ГО – глюкозоокисдаза; [4]МАО – метиламінооксидаза; [5]АргО – аргініноксидаза; [6]пор-Au – поверхня електроду модифікованого пористим золотом; [*]При площі робочого електрода 7.0 $мм^2$.

Показано, що модифікація поверхні електроду пористим золотом приводить до покращення аналітичних характеристик усіх сконструйованих біосенсорів, порівняно з відповідними біензимними амперометричними електродами, що містять природну ПО, зокрема, встановлено, що після модифікації поверхні електроду НЗ CuCe чутливість зростає від 4 до 18 разів (для сенсора з архітектурою МАО/CuCe/порAu/ГЕ).

На основі мікробних оксидаз – АО та АргО, а також різних синтезованих НЧ, що виконували роль міметиків ПО, сконструйовано амперометричні біосенсори для аналізу етанолу та L-аргініну. Протестовано широкий спектр наноматеріалів на псевдо-ензиматичну активність до Гідроген пероксиду в розчині та на поверхні електродів. Усі сконструйовані біосенсори характеризуються високою чутливістю до цільових аналітів, а також задовільною операційною стабільністю.

В таблиці 9.2 наведено основні біоаналітичні характеристики розроблених біонаноелектродів на основі АО та НЗ, міметиків ПО. Показано, що при робочому потенціалі –200 мВ, електрод із архітектурою АО/AuCePt/ГЕ виявляє найвищу чутливість до етанолу – 2600 $А \cdot М^{-1} \cdot м^{-2}$ та найнижчу межу виявлення 0,001 мМ. Найбільш чутливі до етанолу біоелектроди із архітектурою біоселективного шару АО/AuCePt/ГЕ використано для аналізу етанолу в реальних зразках біологічних рідин людини (слини, поту та сироватки крові).

Нами запропоновано також новий ензимо–нанозимний спектрофотометричний метод аналізу етанолу за використання АО, НЗ PtCu та 3,3',5,5'-тетраметилбензидину в ролі органічного хромогену. Для фіксації біонанокомпозиту використано кальцій альгінат. Запропонований ензиматичний метод володіє широким діапазоном лінійності: від 0,01 мМ до 0,15 мМ з нижньою межею виявлення етанолу – 3,3 мкМ. Розроблений метод використано для кількісного визначення вмісту етанолу в алкогольних напоях, соках та біологічних рідинах людини**.** Запропонований метод є чутливим, економним та може бути придатним для рутинного аналізу етанолу у клінічних лабораторіях.

Таблиця 9.2

Біоаналітичні характеристики розроблених біонаноелектродів на основі АО та НЗ, міметиків ПО

Біоелектрод	Потенціал, мВ	Чутливість, $А \cdot М^{-1} \cdot м^{-2}$	Лінійний діапазон, мМ	$K_М^{app}$, мМ	НМВ, мМ
АО/AuCePt/ГЕ	–200	2600	0,005 – 0,10	0,097	0,001
АО/FePtAu/ГЕ	–200	1250	0,002 – 0,10	0,40	0,002
АО/CoCuCe/ГЕ	–200	584	0,016 – 0,12	0,7	0,005
АО/CuCeAu/ГЕ	–200	530	0,016 – 0,25	0,18	0,004
АО/Co/ГЕ	–200	535	0,015 – 0,25	1,5	0,005
АО/CePt/ГЕ	–200	23	0,066 – 8,00	13,2	0,020
АО/AgCu/ГЕ	–50	57	0,050 – 0,75	0,96	0,030
АО/PtCu/ГЕ	–200	42	0,030 – 2,00	2,1	0,015
АО/NiPtPd/ГЕ	–150	40	0,050 – 0,80	1,36	0,040
АО/Cu/ГЕ	–200	22	0,125 – 31,00	615	0,038

Проведено конструювання біонанозимних електродів на основі мікробних оксидаз (АО та МАО) та електроосадженого нанокомпозиту PtRu, що виконує роль міметика пероксидази. Усі запропоновані біоелектроди виявляють достатню чутливість до цільових аналітів: 336 та 284 $А \cdot М^{-1} \cdot м^{-2}$ до етанолу та метиламіну, відповідно; широкі лінійні діапазони: 25–200 мкМ і 20–600 мкМ (до етанолу та метиламіну, відповідно), задовільну стабільність при зберіганні та хорошу селективність до природних субстратів. Продемонстровано, що заміна природної ПО на PtRu як штучний ПО-міметик у біочутливому шарі забезпечує покращення електрохімічних властивостей електродів і більш широкі діапазони лінійних відгуків. Сконструйовані біоелектроди тестували на реальних зразках харчових продуктів (алкогольних напоїв та в екстрактах риб).

Створення мікробних амперометричних біосенсорів на основі клітин, додатково збагачених цільовим ензимом *in vitro*.

У представленій роботі вивчено вплив НЧ на сенсорні властивості рекомбінантних клітин дріжджів, здатних до надсинтезу ензимів аналітичного призначення, на моделі двох оксидоредуктаз (флавоцитохрому b_2 і АО) та гідролази (аргінази І) у складі нанокомпозитних носіїв (порівняно з традиційними матеріалами). Крім того, вивчено можливість посилення каталітичної активності рекомбінантних клітин шляхом додаткового введення в них відповідних ензимів, кон'югованих із НЧ.

У роботі використовували клітини різних штамів метилотроних дріжджів *O. polymorpha:* рекомбінантний надпродуцент аргінази людини І – *O. polymorpha NCYC 495 (pGAP1-HsARG1 leu2car1:LEU2*); рекомбінантний надпродуцент флавоцитохрому b_2 – *O. polymorpha "tr1" (gcr1 catX/prAOX_CYB2)* та "дикий" штам *O.polymorpha NCYC 495.* Як носії для іммобілізації ензимів використовували НЧ Au, отримані методом хімічного відновлення з відповідної солі. Вихід за активністю ензимів, іммобілізованих на поверхні НЧ, великою мірою залежить від їхньої природи. Якщо для ФЦ *b2* він становив 15%, то для АО та аргінази І – 55 % та 47,5 %, відповідно. Далі, усі пермеабілізовані клітини збагачували біофункціоналізованими НЧ Au. Ефект проникнення біофункціоналізованих НЧ Au крізь пори клітин підтверджували за допомогою рентгеноспектрального аналізу, який виявив наявність слідових кількостей золота всередині пермеабілізованих клітин.

На основі НЗ-збагачених клітин сконструйовано амперометричні біосенсори. Для конструювання біоелектрода для аналізу L-аргініну використано поліанілін-чутливу хемосенсорну мембрану. Встановлено, що модифікація пермеабілізованих клітин *H.polymorpha* НЧ Au із зв'язаною аргіназою порівняно з клітинами дріжджів, модифікованих лише nAu, підвищує відгук клітинно-ензимного сенсора у 7 разів. Продемонстровано, що відгук електродів із ФЦ b_2-Au-збагаченими пермеабілізованими клітинами на внесення 2,4 мМ L-лактату становить 420 нА, що у 17 разів більше порівняно із біоелектродами на основі Au-модифікованих

пермеабілізованих клітин (без збагачення ензимом) – 25 нА. Це доводить, що саме збагачення НЧ із зв'язаним ензимом посилює відгук клітинного сенсора. Водночас немодифіковані НЧ Au знижують ефективність електронного перенесення крізь пермеабілізовані клітинні стінки дріжджів у 8 разів порівняно з контрольними пермеабілізованими клітинами *O.polymorpha "tr1"*, однак причини цього явища не з'ясовано. Позитивний вплив збагачення клітин ензимо-модифікованим НЧ Au (АО-Au) на кінетичні параметри клітинних сенсорів підтверджено також експериментами з використанням НЧ Au з іммобілізованою АО. Показано, що збагачення пермеабілізованих клітин дріжджів НЧ Au, зв'язаними з АО, підвищує відгук сенсора у 21 раз. Отже, додаткове введення в клітини ензимів, іммобілізованих на Au носіях, істотно поліпшує біоаналітичні характеристики клітинних сенсорів, зокрема їхню чутливість і швидкість розвитку сигналу.

Створення амперометричних біо(хемо)сенсорів та тест-наборів на основі мікробних гідролаз: аргініндеімінази та аргінази I для кількісного аналізу L-аргініну.

У роботі представлено результати досліджень щодо розробки біоаналітичних систем, зокрема, амперометричних біо(хемо)сенсорів та ензиматичних методів на основі амоній-селективних мембран та наночастинок у поєднанні із мікробними гідролазами – аргініндеіміназою *M. hominis* і аргіназою I людини, експресованої в клітинах дріжджів *O. polymorpha*. Принцип визначення L-аргініну сконструйованими біоелектродами базується на генеруванні, в результаті ензиматичних реакцій, йонів амонію. Утворені йони амонію реагують із амоній-селективними мембранами, генеруючи при цьому сигнал, який детектуються за допомогою відповідних перетворювачів.

Запропоновано амперометричні біосенсори для аналізу L-аргініну за використання металевих НЧ, які здатні утворювати редокс-активні координаційні сполуки з аміаком. В основі запропонованого біоелектроду на основі АДІ лежить принцип ензиматичного гідролізу L-аргініну до цитруліну та амонію з наступною детекцією останнього за допомогою амоній-чутливих НЧ Zn(Hg)S/Cu. Для сконструйованого біосенсора вивчали основні біоаналітичні характеристики

(чутливість, нижня межа визначення, лінійність відгуку, селективність). Лінійний діапазон визначення вмісту L-аргініну сконструйованим біосенсором складає 0,013 мМ – 0,8 мМ (R = 0,998). Чутливість біосенсора становить 1570 $А \cdot М^{-1} \cdot м^{-2}$ із нижньою межею визначення креатиніну 4,3 мкМ. Позірна величина константи Міхаеліса-Ментен ($К_М$) амперометричного біосенсора для креатиніну складає 1,75 мМ.

Для розробки амперометричних біосенсорів для аналізу L-аргініну запропоновано використання в ролі амоній-селективних нанохелаторів – НЧ CdCu та Cu із середнім розміром кристалітів 40 та 57 нм, відповідно. В ролі біоселективних елементів використано L-аргінін-гідролізуючі ензими – АргО, АДІ та аргіназу І (див. Таблиця 4.3). Усі сконструйовані біоелектроди виявляють широкий лінійний діапазон (до 200 мкМ), задовільну стабільність при зберіганні (14 днів) і високу чутливість до L-аргініну: 1650, 1700 та 4500 $А \cdot М^{-1} \cdot м^{-2}$ (для біосенсорів на основі АДІ, АргО та аргінази/уреази, відповідно).

Усі запропоновані амперометричні біосенсори використано для чутливого та високоселективного аналізу L-аргініну у комерційних соках та винах. Спостерігалися високі кореляції між вмістом L-аргініну, визначеним розробленими біонаносенсорами та ензиматичним референтним методом (R = 0,993 – 0,999). Таким чином, сконструйовані біосенсори на основі наночастинок або полімерних мембран можуть бути перспективними як для звичайного кількісного визначення вмісту L-аргініну для виноробів з метою контролю потенційних рівнів етилкарбамату під час виробництва вина, так і для застосування в клінічній діагностиці.

Нами досліджено можливість використання апоензиму $(His)_6$–тегованої форми рекомбінантної аргінази І людини при конструюванні амперометричних біосенсорів. Для отримання апоензиму аргінази І, препарат ензиму попередньо діалізували у присутності 1 мМ ЕДТА із наступним пропусканням через металозв'язуючий сорбент Chelex. Для детекції йонів Mn^{2+} використано нафіон-модифіковану поліанілінову хемосенсорну мембрану, чутливу до йонів амонію.

Запропонований біосенсор характеризується високою чутливістю на внесені іони Mn^{2+} – 9200 $А \cdot М^{-1} \cdot м^{-2}$ та низькою межею визначення – 0,15 мкМ.

Таблиця 9.3.

Порівняння робочих характеристик різних типів L-аргінін-чутливих біосенсорів, сконструйованих за використання АргО, аргінази І та АДІ

Біоелектрод	Детектований продукт	Чутливість, $А \cdot М^{-1} \cdot м^{-2}$	Лінійний діапазон, μМ	НМВ, мкМ	Джерело
АргО/CeCu/[1]СВЕ	H_2O_2	1630 ± 92	5 – 100	[2]Н.в.	Ця робота
АргО/NiPtPd/СВЕ		578 ± 5	10 –250		
АргО/CuHCF/СВЕ		602 ± 42	10 – 100		
АДІ/ПАНі/Нафіон/Pt-[3]ЕТД	NH_4^+	684±32	3 – 200	1,0	
ADI/Cu/Zn(Hg)S/ГЕ		1570	13 – 800	4,3	
аргіназа/уреаза/ПАНі/PtE		110 ± 1,3	70 – 600	38	
[4]п-клітини/уреаза/ПАНі/PtE		14 ± 1,1	до 600	Н.в.	
аргіназа-Au/п-клітини/уреаза /ПАНі/PtE		357 ± 24	10 – 700		
АргО/Cu/СВЕ		2300 ± 15	2 – 18	0,7	
аргіназа-уреаза/Cu/СВЕ		780 ± 55	6 – 50	1,75	
аргіназа-уреаза/ CdCu/СВЕ		4500 ± 170	2–80	0,6	
АргО/CdCu/СВЕ		1700 ± 80	30–160	5,5	
АДІ/CdCu/СВЕ		1650 ± 75	12–200	3,6	
АДІ/Cu/СВЕ		665 ± 2	6 – 100	1,8	[60]

Примітка: [1]СВЕ – скловуглецевий електрод; [2]Н.в. – не визначали; [3]ЕТД – електрод із трафаретним друком; [4]п-клітини – пермеабілізовані клітини *O. polymorpha*.

На сьогодні, в галузі аналітичної біотехнології існує обмежена кількість даних щодо ензиматичних методів визначення L-аргініну. Найперспективніші для розробки таких методів є ензими метаболізму L-аргініну, зокрема, аргіназа I, аргініндеіміназа, аргініноксидаза та аргініндекарбоксилаза. Існуючі комерційні тест-системи (виробництва фірм «Sigma», «Enzytec», «Elisa», «Megazyme» та ін.) є, переважно, мультиензимними зі спектрофотометричним (СФ) детектуванням кінцевого продукту реакції. Мультиензимні методи аналізу L-аргініну мають низку недоліків, зокрема неабсолютну селективність до цільового аналіту, спричинену позитивною реакцією на гуанідинові сполуки. Необхідність використання каскаду із кількох (3–5) ензимів і екзогенних кофакторів підвищує вартість методів та ускладнює процедуру аналізу (Таблиця 9.4). На сьогодні, тест-системи для моніторингу L-аргініну у біологічних рідинах, зокрема, у крові, в арсеналі засобів вітчизняної клінічної діагностики відсутні. Нами створено два варіанти ензимо-флуоресцентного методу аналізу вмісту L-аргініну – моноензимний та двоензимний (Таблиця 9.3). Принцип роботи ензиматичних методів полягає у ензимативному перетворенні L-аргініну і спектрофотометричному або флуорометричному детектуванню кольорової сполуки – кінцевого продукту хімічної реакції карбаміду (за дії аргінази), цитруліну (за дії АДІ) або амонію (за дії АДІ чи аргінази-уреази) із диметилмонооксимом (ДМО) або *орто*-фталевим альдегідом (ОФА). На основі запропонованих методів створено ензиматичний набір «Аргітест» для аналізу вмісту L-аргініну за використання препаратів термостабільної аргінази I або аргініндеімінази (АДІ), одержаних із сконструйованих нами штамів-надпродуцентів та очищених за власними технологіями, що суттєво знижує матеріальні затрати при виготовленні аналітичного набору. Як видно із таблиці 4.4, розроблені нами методи мають низку переваг, порівняно із іншими методами, зокрема, це висока чутливість та широкий діапазон тестованих концентрацій L-аргініну. Запропоновані нами методи не

потребують попереднього відокремлення L-аргініну з дослідного зразка, є простими у виконанні, високоселективними та надійними і комерційно доступними.

Таблиця 9.4

Порівняльна характеристика створених ензиматично-хімічних методів аналізу L-аргініну

Метод	Ензим	Лінійний діапазон, мкМ	НМВ, мкМ	Джерело
ДМО-ФЛ, λ = 360 нм, λ = 510 нм	Аргіназа	0,28 – 280	0,15	Ця робота
ОФА-СФ, λ = 362 нм	Аргіназа-уреаза	0,9 – 60,0	0,85	
ОФА-ФЛ, λ = 364 нм, λ = 425 нм	Аргіназа-уреаза	0,09 – 6,0	0,06	
ОФА-ФЛ, λ = 364 нм, λ = 415 нм	АДІ	0,35 – 24	0,25	
ОФА-СФ, λ = 340 нм	АДІ	0,7 – 50	0,55	
Мультиензимний, СФ, λ = 340 нм	Аргіназа, уреаза, [1]ГДГ	до 470	2,0	[61]
Мультиензимний, СФ, λ = 340 нм	Аргіназа, уреаза, ГДГ	2,9 – 100	2,1	[62]
Мультиензимний, СФ, λ = 555 нм	АДІ, [2]АргС, [3]ПДК, піруватоксидаза, пероксидаза хрону	до 100	–	[63]

Примітка: [1]ГДГ – глутаматдегідрогеназа; [2]АргС – аргініносукцинат синтаза; [3]ПДК – піруватфосфат дикіназа

Усі розроблені ензиматично-хімічні методи успішно протестовано на зразках сироваток крові та харчових продуктів. У випадку аналізу L-аргініну в крові, предіснуючу у сироватці сечовину усували обробкою комерційною уреазою. Показано, що кожен із досліджених ензимів може бути використаний як складова ензиматичного набору «Аргітест». Запропоновані методи є простими та швидкими у порівнянні із відомими ензиматичними підходами, що дозволяє підвищити точність визначення вмісту L-аргініну за рахунок високої селективності аргініно-гідролізуючих ензимів. Оскільки препарати аргінази та АДІ володіють високою стабільністю при зберіганні, можна прогнозувати перспективність комерційного випуску ензиматичних наборів для визначення L-Arg для застосування їх у лабораторній практиці. Пропонована розробка відповідає рівню кращих зарубіжних прототипів.

Нами створено також надчутливий ензиматично-флуориметричний метод аналізу йонів деяких біометалів, зокрема Mn^{2+} та Co^{2+} за використання апоензиму $(His)_6$–тегованої форми рекомбінантної аргінази I людини та ДМО. Діапазон лінійності методу апо-аргінази-ДМО у випадку аналізу Mn^{2+} становить від 4 пМ до 1,10 мкМ з межею виявлення 1 пМ Mn^{2+}, тоді як діапазон лінійності цього методу для аналізу йонів Co^{2+} становить від 8 пМ до 45 мкМ з межею виявлення 2,5 пМ Co^{2+}. Розроблений метод апробовано для аналізу йонів Mn^{2+} та Co^{2+} у зразках стічних вод із шахт добування золота та міді. Встановлено високий рівень кореляції між ензиматичним та референтним методом (атомно-абсорбційна спектрометрія, $R = 0,998$). Таким чином, запропонований ензиматично-хімічний метод, будучи високочутливим, селективним, надійним і недорогим, може бути корисним для моніторингу вмісту Mn^{2+} і Co^{2+} у клінічних лабораторіях, харчовій промисловості та службах екологічного контролю.

Створення амперометричних біо(хемо)сенсорів та тест-наборів за використання рекомбінантної креатиніндеімінази для кількісного аналізу креатиніну.

Серед мікробних гідролаз, значну увагу в роботі присвячено дослідженню властивостей рекомбінантної креатиніндеімінази (КДІ) та створенню на її основі

нових біоаналітичних систем. Нами проведено клонування гена *codA C. glutamicum* на векторах індуктивних систем експресії з включенням у структуру рекомбінантного білка $(His)_6$-фрагмента та S-пептиду рибонуклеази А. Сконструйовано рекомбінантний надпродуцент КДІ на основі клітин *E. coli* з продуктивністю 20-50 мг/л культури. Опрацьовано одноетапний метод очищення рекомбінантного ензиму з використанням метало-афінної хроматографії та отримано високо очищений препарат ензиму з питомою активністю 22 мкмоль·хв$^{-1}$·мг$^{-1}$·білка.

Проведено фізико-хімічну та ензимологічну характеристику ензиму, зокрема, визначено молекулярну масу субодиниці (46,3 кДа), вивчено температурний та pH-профіль активності, досліджено термо- та pH-стабільність ензиму, а також його кінетичні параметри (k_{cat} = 7,15 с$^{-1}$; K_M = 1,96 мМ відносно креатиніну). Показано, що ензим є термостабільним, має високий температурний оптимум (75 ^{o}C) і стійкий у широкому діапазоні pH (6,0 – 10,5). Виявлено, що рекомбінантна КДІ *C. glutamicum* проявляє строгу субстратну специфічність до креатиніну, що вигідно відрізняє цей ензим від аналогічних мікробних ензимів.

На основі КДІ та амоній-селективних наночастинок Cu/Zn(Hg)S сконструйовано амперометричний біосенсор для кількісного визначення вмісту креатиніну. Створений біосенсор характеризується високою селективністю та чутливістю до креатиніну (2660 А·М$^{-1}$·м$^{-2}$). Лінійний діапазон біосенсора спостерігається в діапазоні від 1,5 мкМ до 50 мкМ із нижньою межею визначення креатиніну 0,45 мкМ (Таблиця 4.5). Розроблений лабораторний прототип біосенсора адаптовано для використання у складі дослідного зразка амперометричного аналізатора, сумісного з планшетом (розробленого у співпраці із ТзОВ «Науково-виробнича фірма «Інженерна Лабораторія» (Львів, Україна) в особі директора к.т.н. Вуса Б.С. в рамках комплексної науково-технічної програми: «Розумні» сенсорні прилади нового покоління на основі сучасних матеріалів та технологій». Тестування біосенсорної системи проводили на зразках біологічних рідин людини (сироватки крові та поту). Дані дослідження проводили на базі

відділу біохімії крові ДУ «Інститут патології крові та трансфузійної медицини НАМН України».

Рис. 9.1. Загальний вигляд портативного креатинінового аналізатора, сумісного із планшетом Microsoft Lenovo Mix 320.

Пряме визначення вмісту креатиніну у біологічних рідинах має вирішальне значення для належного лікування захворювань нирок, особливо для пацієнтів, які проходять терапію після трансплантації нирки. Однак наявність ендогенного аміаку в зразках крові значно ускладнює рутинний аналіз і вимагає додаткового аналізу вмісту аміаку або попередньої обробки зразка для видалення наявного аміаку. Оскільки постійний моніторинг стану здоров'я пацієнта є надійним засобом раннього виявлення ниркової недостатності, неінвазивні креатинін-селективні біосенсори привертають значну увагу дослідників. В поточному дослідженні створено амперометричний біосенсор на основі рекомбінантної бактерійної КДІ та наночастинок CoCu для прямого аналізу креатиніну у біологічних рідинах. Розроблений біосенсор з детекцією N-метилгідантоїну не потребує видалення ендогенного аміаку та характеризується високою селективністю до цільового аналіту. Пропонований біосенсор характеризується низьким прикладеним потенціалом (–50 мВ), швидкою реакцією на аналіт (20 с), широким лінійним діапазоном (0,01–0,8 мМ), достатньою чутливістю (195

$А·М^{-1}·м^{-2}$) та низькою межею виявлення (0,5 мкМ) (Таблиця 9.5). Крім того, нами з'ясовано можливу структуру комплексу CoCu–N-МГ та механізм детектування креатиніну. Використовуючи метод багаторазового додавання стандартів, розроблений CoCu/КДІ-функціоналізований електрод протестовано для аналізу креатиніну у реальних біологічних рідинах (сеча та сироватка крові). Показано високу кореляцію між отриманими аналітичними результатами та референтним методом. Таким чином, створений лабораторний прототип креатинін-селективних біосенсорів є перспективним і корисним для рутинного клінічного аналізу креатиніну.

Таблиця 9.5

Аналітичні характеристики створених амперометричних біосенсорів на основі рекомбінантної КДІ

Тип біосенсора	Детектований продукт	Робочий потенціал, мВ	Чутливість, $А·М^{-1}·м^{-2}$	Лінійний діапазон, мкМ	НМВ, мкМ	K_M^{app}, мМ
КДІ/ Cu/Zn(Hg)S [Ця робота]	NH_4^+	+170	2660	1,5 – 50	0,45	0,04
КДІ/ПАНі/Cu [66]		–350	850	до 125	0,5	0,163
КДІ/CoCu/[1]СВЕ [Ця робота]	[4]N-МГ	–0.05	195	10 – 800	0,5	3,8
$CoCl_2$/[6]МС/ КДІ/[2]ГЕ [64]		–1,4[5]	[3]Н.в.	0,71 – 3550	Н.в.	Н.в.
$CoCl_2$/ КДІ/[2]ГЕ [65]		–1,4[5]	Н.в.	0,17 – 3530	Н.в.	Н.в.

Примітка: [1]СВЕ – скловуглецевий електрод; [2]ГЕ – графітовий електрод; [3]Н.в. – не визначали; [4]N-МГ – N-метилгідантоїн; [5]Автори не проводили класичні хроноамперометричні дослідження при вибраному робочому потенціалі; [6]МС – метиленовий синій.

У поточній роботі, нами розроблено високочутливий ензиматично-флуориметричний метод аналізу креатиніну за використання рекомбінантної КДІ та *о*-фталевого альдегіду зі спектрофотометричною (СФ метод) та флуориметричною детекцією (ФЛ метод) продукту реакції – йонів амонію. Порогова чутливість запропонованого методу становить 6 мкМ (СФ метод) та 0,2 мкМ (ФЛ метод). Проведено оптимізацію одночасного аналізу креатиніну та аміаку в сироватках крові людини. Параметрами оптимізації служили концентрації КДІ, *о*-фталевого альдегіду, ЕДТА, тип буферної системи, спосіб підготовки проб для аналізу. Порівняльний аналіз результатів вмісту креатиніну в зразках сироватки крові пацієнтів із порушеною функцією нирок до та після проведення гемодіалізу розробленими біосенсорним на ензиматично-флуорометричним методами показав високий рівень кореляції аналітичних даних (R = 0,998), що свідчить про надійність і точність запропонованих підходів.

Таким чином, розроблений нами креатинін-селективний біосенсор переважає відомі аналоги, перш за все, за використаним низьким робочим потенціалом, вищою чутливістю та коротшою тривалістю аналізу. Розроблені біосенсори на основі рекомбінантної КДІ успішно апробовано для одночасного аналізу креатиніну та амонію в реальних зразках сироваток крові.

Отже, як результат виконання дисертаційної роботи, за допомогою поєднання різних експериментальних підходів показано позитивний потенціал поєднання класичної мікробіології, генетичної інженерії та нанотехнологій для створення нових селективних біоаналітичних методів кількісного аналізу практично важливих аналітів, зокрема, метиламіну, етанолу, креатиніну та L-аргініну, визначення яких є важливим для практичного використання у клінічній діагностиці, фармацевтиці та харчовій промисловості.

ВИСНОВКИ

У дисертаційній роботі представлено результати комплексного дослідження структурних, фізико-хімічних та каталітичних властивостей нанозимів та поєднання їх з мікробними ензимами, а також вивчення біологічної та можливої токсичної дії (*in vivo*) нанозимних композитів на клітини дріжджів *Ogataea (Hansenula) polymorpha*. Досліджено кон'югацію наноматеріалів із мікробними ензимами та створено на їх основі нові біо(хемо)наносенсори та тест-набори для визначення практично важливих аналітів, зокрема, креатиніну, L-аргініну, глюкози, етанолу та метиламіну.

Основні наукові та практичні результати роботи викладено у наступних висновках:

1. Проведено синтез та скринінг нових наноматеріалів на каталітичну, нанозимну активність. Здійснено структурно-морфологічну характеристику нанозимів (НЗ). Встановлено, що розмір отриманих матеріалів із каталітичною активністю знаходиться в межах від 15 нм (НЗ) до 5 мкм (мікрозими, МЗ). Проведено аналіз синтезованих НМ на псевдоензиматичну активність – пероксидазну, каталазну та редуктазну. Досліджено каталітичні властивості та субстратну специфічність отриманих НЗ.

2. Вивчено цитотоксичну дію синтезованих НЗ на клітини метилотрофних дріжджів за впливом на швидкість росту та виживання клітин за допомогою флуоресцентної мікроскопії. Показано, що НЗ (у концентації 0,1 мг/мл у середовищі) проявляють різний цитотоксичний вплив на клітини дріжджів *Ogataea (Hansenula) polymorpha*: «катазими» знижують виживання клітин в 2,6–4,5 раза, тоді як НЗ з пероксидазною активністю дещо підвищують цей показник.

3. Встановлено, що поглинання безкаталазними клітинами «катазимів» відновлює здатність мутантних клітин рости у середовищі, що містить метанол. Активність НЗ забезпечує розщеплення надмірної кількості гідроген пероксиду, що утворюється внаслідок росту клітин у середовищі з метанолом, усуваючи його токсичну дію на клітини. Вірогідно, це перший у науковій практиці експериментальний доказ можливості заміни природного ензима нанозимом *in*

vivo.

4. Отримані НЗ із редуктазною активністю протестовано на антиоксидантну активність відносно вільних радикалів АБТС$^{\bullet+}$ та DPPH$^{\bullet}$ у порівнянні із Тролоксом. Найактивніші редуктазні НЗ використано для конструювання амперометричного біосенсора для аналізу вмісту селеніту. Сконструйований біосенсор характеризується високою чутливістю (1700 А·М$^{-1}$·м$^{-2}$) та широким лінійним діапазоном (від 16 мкМ до 1 мМ) щодо селеніту.

5. Сконструйовано амперометричні біосенсори на основі різних мікробних оксидаз та НЗ, які володіють пероксидазною активністю. Створені біоелектроди використано для аналізу вмісту етанолу, метиламіну та L-аргініну. Розроблені моноензимні біосенсори показали покращені аналітичні характеристики, порівняно з відповідними біензимними амперометричними електродами, що містять природну ПО. Встановлено, що після модифікації поверхні електроду НЗ nCuCe чутливість зростає від 4 до 18 разів для графітового електроду, покритого метиламінооксидазою та шаром нCuCe/порAu.

6. Синтезовано нові метал-гібридні наноматеріали, селективні до йонів амонію. Розроблено чутливі та селективні амперометричні біосенсори для кількісного аналізу вмісту L-аргініну та креатиніну на основі мікробних деаміназ та наночастинок. В основі запропонованих біосенсорних методів лежить застосування термостабільної аргініндеімінази (АДІ), аргінази І/уреази або креатиніндеімінази (КДІ) у поєднанні з амоній-селективними наноматеріалами. Створені амперометричні біосенсори характеризуються високою селективністю та чутливістю до цільових аналітів, а також задовільною операційною стабільністю.

7. Уперше розроблено амперометричний біосенсор для аналізу вмісту L-аргініну на основі пермеабілізованих клітин штаму-надпродуцента рекомбінантної аргінази І людини *O. polymorpha* NCYC 495 у комбінації із комерційною уреазою і електроосадженого поліаніліну та досліджено його фізико-хімічні характеристики. Біосенсор відзначається високою селективністю, достатньою чутливістю до L-аргініну (14 ± 1,2 А·М$^{-1}$·м$^{-2}$) та широким діапазоном

лінійності (до 0,6 мМ).

8. Уперше розроблено чутливі та селективні ензиматичні методи кількісного аналізу вмісту L-аргініну із флуоресцентним та спектрофотометричним способом детектування кольорового продукту реакції за допомогою *о*-фталевого альдегіду. Методи базуються на використанні високоочищених препаратів аргінази I або аргініндеімінази. Запропоновані методи є простими та швидкими у виконанні у порівнянні з відомими ензиматичними підходами і дозволяють підвищити точність визначення вмісту L-аргініну за рахунок високої селективності цільових ензимів та їх термостабільності.

9. На моделі високоочищеної Манґанзалежної рекомбінантної аргінази I людини, отриманої з клітин рекомбінантних дріжджів *O. polymorpha*, вперше проведено дослідження по отриманню препаратів апоензиму, позбавленого металу, та реконструкції холоензиму. Вперше розроблено новий ензиматичний метод на основі апоензиму аргінази I та 2,3-бутандіонмонооксиму для кількісного визначення йонів Mn^{2+} та Co^{2+}. Запропонований метод характеризується надзвичайно високою чутливістю до йонів Mn^{2+} та Co^{2+} – 1 пМ та 2,5 пМ, відповідно.

10. Розроблено амперометричний біосенсор для аналізу вмісту креатиніну за використання рекомбінантної КДІ та НЧ CoCu, чутливих до N-метилгідантоїну. Вперше ідентифіковано структуру утвореного компексу CoCu-N-метилгідантоїн. Створений біосенсор відзначається високою селективністю, хорошою чутливістю до креатиніну ($200 \pm 1{,}2$ А·М$^{-1}$·м$^{-2}$) та широким діапазоном лінійності (10 мкМ – 0,4 мМ).

11. Проведено конструювання та тестування мініатюризованого мікрострумового потенціостата, сумісного з сучасними ґаджетами. Прилад адаптовано під використання комерційних планарних електродів, модифікованих рекомбінантною КДІ.

12. Розроблені біоаналітичні підходи на основі рекомбінантних клітин та очищених ензимів використано для кількісного аналізу вмісту L-аргініну,

етанолу, метиламіну та креатиніну в реальних зразках біологічних рідин людини, харчових продуктів, фармацевтичних препаратів трансфузійного призначення та стічних водах. Завдяки високій чутливості та селективності, а також надійності та простоті у використанні, опрацьовані ензиматичні та біосенсорні підходи аналізу вмісту цільових аналітів можуть знайти практичне використання в клінічній діагностиці, медицині та харчових технологіях.

СПИСОК ЛІТЕРАТУРНИХ ДЖЕРЕЛ

1. Turner AP (2013). Biosensors: sense and sensibility. Chem Soc Rev 42(8): 3184-96. https://pubs.rsc.org/en/content/articlelanding/2013/cs/c3cs35528d.

2. Soldatkin AP, Dzyadevych SV, Korpan YI, et al. (2013) Biosensors. A quarter of a century of R&D experience. Biopolymers and Cell 29(3): 188-206. doi: http://dx.doi.org/10.7124/bc.000819.

3. Gonchar MV, Maidan MM, Moroz OM, et al. (1998) Microbial O_2 - and H_2O_2-electrode sensors for alcohol assays based on the use of permeabilized mutant yeast cells as the sensitive bioelements. Biosens Bioelectron 13: 945-952. doi: 10.1016/s0956-5663(98)00034-7.

4. Gonchar M, Maidan M, Korpan Y, et al. (2002) Metabolically engineered methylotrophic yeast cells and enzymes as sensor biorecognition elements. FEMS Yeast Res 2: 307-314. doi: 10.1016/S1567-1356(02)00124-1.

5. Корпан ЯІ, Гончар МВ, Стародуб МФ, Єльська ГВ (1995) Біосенсори на основі клітин мікроорганізмів. Biopolym Cell 11(2):15-28. doi: http://dx.doi.org/10.7124/bc.0003DC.

6. Marrazza G (2022) Biosensors in 2022. Biosensors (Basel) 21: 407. https://doi.org/10.3390/bios13030407

7. Ouyang Y, O'Hagan MP, et al (2022) Aptamer-modified homogeneous catalysts, heterogenous nanoparticle catalysts, and photocatalysts: functional “Nucleoapzymes”, “Aptananozymes”, and “Photoaptazymes”. Biosens Bioelectron 218, 114768. https://onlinelibrary.wiley.com/doi/full/10.1002/adma.202210885

8. Chadha U, Bhardwaj P, Agarwal R, et al (2022) Recent progress and growth in biosensors technology: A critical review. J Ind Eng Chem 109: 21-51. https://www.sciencedirect.com/science/article/abs/pii/S1226086X22000600

9. Dzyadevych SV, Soldatkin OO, Arkhypova VM, et al. (2022) Practical application of electrochemical enzyme biosensors. Biopolym Cell 38(2): 71-92. http://dx.doi.org/10.7124/bc.000A76

10. Smutok O, Katz E (2023) Biosensors: electrochemical devices—general concepts and performance. Biosensors (Basel) 13: 44. https://doi.org/10.3390/bios13010044

11. Peixia W, Tao W, Juanji H, et al (2020) Nanozymes: A New Disease Imaging Strategy, Front Bioeng Biotechnol 8: 15. https://www.ncbi.nlm.nih.gov/pmc/articles/PMC7015899/

12. Niu X, Liu B, Hu P, et al (2022) Nanozymes with Multiple Activities: Prospects in Analytical Sensing. Biosensors 12: 251. https://doi.org/10.3390/bios12040251

13. Wang W, Gunasekaran S (2020) Nanozymes-based biosensors for food quality and safety, TrAC Trends in Analytical Chemistry, 126: 115841. https://doi.org/10.1016/j.trac.2020.115841.

14. Kurup CP, Ahmed MU (2023) Nanozymes towards Personalized Diagnostics: A Recent Progress in Biosensing. Biosensors, 13: 461. https://doi.org/10.3390/bios13040461

15. Thangudu S, Su CH (2021) Peroxidase Mimetic Nanozymes in Cancer Phototherapy: Progress and Perspectives. Biomolecules, 11: 1015. https://doi.org/10.3390/biom11071015.

16. Ren X, Chen D, Wang Y, et al (2022) Nanozymes-recent development and biomedical applications. J Nanobiotechnoogy 20: 92. https://doi.org/10.1186/s12951-022-01295-y.

17. Wei H, Gao L, Fan K, et al (2021) Nanozymes: A clear definition with fuzzy edges. Nano Today 40: 101269. https://doi.org/10.1016/j.nantod.2021.101269.

18. Peng Xu, Kang Zhou (2022) Editorial overview: Analytical biotechnology for healthcare, strain engineering, biosensing and synthetic biology. Curr Opin Biotechnol 77: 102765.

19. Gonchar M, Smutok O, Karkovska M, et al. (2017) Yeast-based biosensors for clinical diagnostics and food control (Ed. A.A. Sibirny). Springer International Publishing AG "Biotechnology of Yeasts and Filamentous Fungi"; P. 392 – 400. https://dokumen.pub/non-conventional-yeasts-from-basic-research-to-application-1st-ed-2019-978-3-030-21109-7-978-3-030-21110-3.html

20. Al-Naimi MS, Rasheed HA, Hussien NR, et al. (2019) Nephrotoxicity: Role and significance of renal biomarkers in the early detection of acute renal injury. J Adv Pharm Technol Res 10(3): 95–99. doi: 10.4103/japtr.JAPTR_336_18.

21. Griffin BR, Faubel S, Edelstein CL (2019) Biomarkers of Drug-Induced Kidney Toxicity. Ther Drug Monit 41(2): 213-226. doi: 10.1097/FTD.0000000000000589.

22. Akter N, Nessa A, Sharmin A, et al. (2020) Relationship of Serum Creatinine and Estimated Glomerular Filtration Rate in Patients with Chronic Kidney Disease. Mymensingh Med J 29(4): 779-783.

23. Średnicka P, Juszczuk-Kubiak E, Wójcicki M, et al. (2021) Probiotics as a biological detoxification tool of food chemical contamination: A review. Food Chem Toxicol 153: 112306. https://doi.org/10.1016/j.fct.2021.112306.

24. García-Guzmán JJ, Sierra-Padilla A, Palacios-Santander JM, et al. (2022) What Is Left for Real-Life Lactate Monitoring? Current Advances in Electrochemical Lactate (Bio)Sensors for Agrifood and Biomedical Applications. Biosensors 12(11): 919. https://doi.org/10.3390/bios12110919.

25. Szlas A, Kurek JM, Krejpcio Z (2022) The Potential of L-Arginine in Prevention and Treatment of Disturbed Carbohydrate and Lipid Metabolism. A Review. Nutrients 24: 961. doi: 10.3390/nu14050961.

26. Gayda G, Stasyuk N, Klepach H, et al. (2019) Promising bioanalytical approaches to wine analysis. In: A. Grumezescu, & A. M. Holban (Eds.), The science of beverages. Quality Control in the Beverage Industry (pp. 419-458), Academic Press, eBook, ISBN: 9780128166826. https://doi.org/10.1016/B978-0-12-816681-9.00012-6.

27. Wang P, Sun J, Li X, et al. (2014) Contribution of citrulline to the formation of ethyl carbamate during Chinese rice wine production. Food Addit Contam Part A Chem Anal Control Expo Risk Assess 31(4): 587 – 592. https://doi.org/10.1080/19440049.2013.878869.

28. Kobets T, Smith BPC, Williams GM (2022) Food-Borne Chemical Carcinogens and the Evidence for Human Cancer Risk. Foods 11: 2828. https://doi.org/10.3390/foods11182828.

29. Lind DS (2004) Arginine and Cancer. J Nutr 34: 2837S-2841S. https://doi.org/10.1093/jn/134.10.2837S.

30. Liu T, Wang X, Jia P, et al. (2022) Association between serum arginine levels and cancer risk: A community-based nested case-control study. Front Nutr 9 https://doi.org/10.3389/fnut.2022.1069113.

31. Wozniak MK, Wiergowski M, Namiesnik J, Biziuk M (2019) Biomarkers of alcohol consumption in body fluids - possibilities and limitations of application in toxicological analysis. Curr Med Chem 26 (1): 177-196. https: //doi.org/10.2174/0929867324666171005111911.

32. Hernandez J, Kaun KR (2022) Alcohol, neuronal plasticity, and mitochondrial trafficking. Proc Natl Acad Sci USA 119(29):e2208744119. https://doi.org/10.1073/pnas.2208744119.

33. Knabbe J, Protzmann J, Schneider N et al (2022) Single-dose ethanol intoxication causes acute and lasting neuronal changes in the brain. Proc Natl Acad Sci USA 119(25):e2122477119. https://doi.org/: 10.1073/pnas.2122477119.

34. http://www.dionex.com/en-us/webdocs/114676-AN1057-ICMethylamine-Drug-Products-AN70523E.pdf.

35. Zhang AQ, Mitchell SC, Smith RL (1998) Dimethylamine formation in the rat from various related amine precursors. Food Chem Toxicol 36: 923–927 https://doi.org/10.1016/S0278-6915(98)00074-X

36. Stasyuk N, Smutok O, Demkiv O, et al. (2020) Synthesis, Catalytic Properties and Application in Biosensorics of Nanozymes and Electronanocatalysts: A Review. Sensors, 20 (16): 4509. https://doi.org/10.3390/s20164509.

37. Gayda G, Stasyuk N, Serkiz R, et al. Fluorescent nanoparticles of noble metals for cell imaging (ред. Н.А.Серебрякова). Київ: НВП «Видавництво «Проект наукова книга»; 2017. С. 156 – 165.

38. Gonchar M, Smutok O, Karkovska M, et al. Yeast-based biosensors for clinical diagnostics and food control. (Ed. Sibirny A.) Springer International Publishing AG "Biotechnology of Yeasts and Filamentous Fungi"; 2017. pp. 392 – 400. https://link.springer.com/chapter/10.1007/978-3-319-58829-2_14.

39. Zakalskiy A, Stasyuk N, Gonchar M, et al. (2019) Creatinine Deiminase: Characterization, Using in Enzymatic Creatinine Assay, and Production of the Enzyme. Curr. Protein Pept Sci 20: 465-470. https://pubmed.ncbi.nlm.nih.gov/30426898/

40. Wei H, Gao L, Fan K, et al (2021) Nanozymes: A clear definition with fuzzy edges. Nano Today 40: 101269. https://doi.org/10.1016/j.nantod.2021.101269.

41. Liang M, Yan X (2019) Nanozymes: From New Concepts, Mechanisms, and Standards to Applications Acc Chem Res 52: 2190–2200 https://pubs.acs.org/doi/10.1021/acs.accounts.9b00140.

42. Yang W, Yang X (2021) Nanozymes: Activity origin, catalytic mechanism, and biological application Coord Chem Rev 448: 214170 https://www.sciencedirect.com/science/article/abs/pii/S0010854521004446.

43. Ling P, Cheng S, Chen N, et al. (2020) Nanozyme-Modified Metal–Organic Frameworks with Multienzymes Activity as Biomimetic Catalysts and Electrocatalytic Interfaces. ACS Appl Mater Interfaces 12 (15): 17185–17192. https://pubs.acs.org/doi/10.1021/acsami.9b23147.

44. Chaibakhsh N, Moradi-Shoeili Z. (2019) Enzyme mimetic activities of spinel substituted nanoferrites (MFe2O4): A review of synthesis, mechanism and potential applications. Mater Sci Eng. C. 99: 1424–1447. https://doi.org/10.1016/j.msec.2019.02.086.

45. Wu J, Wang X, Wang Q, et al. (2019) Nanomaterials with enzyme-like characteristics (nanozymes): Next-generation artificial enzymes (II). Chem Soc Rev 48, 1004–1076. https://pubs.rsc.org/en/content/articlelanding/2019/cs/c8cs00457a.

46. Zhybak M, Beni V, Vagin MY, et al. (2016) Creatinine and urea biosensors based on a novel ammonium ion-selective copper-polyaniline nano-composite. Biosens Bioelectron. 15;77:505-11. https://pubmed.ncbi.nlm.nih.gov/26457736/

47. Zhang D, Kukkar D, Kaur H, Ki-Hyun Kim (2023) Recent advances in the synthesis and applications of single-atom nanozymes in food safety monitoring. Adv Colloid Interface Sci 319: 102968. https://doi.org/10.1016/j.cis.2023.102968.

48. Sindhu RK, Najda A, Kaur P et al. (2021) Potentiality of Nanoenzymes for Cancer Treatment and Other Diseases: Current Status and Future Challenges. Materials 14: 5965. https://doi.org/10.3390/ma14205965.

49. Huang Y, Ren J, Qu X (2019) Nanozymes: Classification, Catalytic Mechanisms, Activity Regulation, and Applications. Chem Rev 119: 4357–4412. https://doi.org/10.1021/acs.chemrev.8b00672.

50. Ausubel FM, Brent R, Kingston RE (1990) Current Protocols in Molecular Biology (Eds. Moore DD, Seidman JG, Smith JA, Struhl K) Greene Publishing Association at Wiley Interscience: New York; pp. 1 – 2. https://hoclai.files.wordpress.com/2015/09/current-protocols-in-molecular-biology.pdf

51. Fayura LR, Boretsky YR, Pynyaha YV et al. (2013) Improved method for expression and isolation of the Mycoplasma hominis arginine deiminase from the recombinant strain of Escherichia coli. J Biotechnol. 167 (4): 420. https://www.sciencedirect.com/science/article/abs/pii/S0168165613002824.

52. Zakalskiy A, Stasyuk N, Zakalska O, et al. (2020) Overexpression and one-step renaturation-purification of the tagged creatinine deiminase of Corynebacterium glutamicum in Escherichia coli cells, Cell Biol Int 44 (5): 1204. https://onlinelibrary.wiley.com/doi/abs/10.1002/cbin.11320.

53. Gayda G, Demkiv O, Klepach H et al (2019) Effective Technologies for Isolating Yeast Oxido-Reductases of Analytical Importance. Ch. 5, In: Non-conventional Yeasts: from Basic Research to Application, Sibirny A. (ed.): pp. 119–151. Springer Nature Switzerland AG, Cham, Switzerland. doi. 10.1007/978-3-030-21110-3.

54. Stasyuk N, Gayda G, Demkiv O, et al. (2021) Amperometric biosensors for L-arginine determination based on L-arginine oxidase and peroxidase-like nanozymes. Appl Sci 11(15): 7024. https://doi.org/10.3390/app11157024.

55. Haywood GW, Large PJ (1981) Microbial oxidation of amines. Distribution, purification and properties of two primary-amine oxidases from the yeast Candida boidinii grown on amines as sole nitrogen source. Biochem J 199(1):187-201. https://pubmed.ncbi.nlm.nih.gov/7337701/

56. Stasyuk NYe, Gayda GZ, Zakalskiy AE, et al. (2022) Amperometric biosensors for L-arginine and creatinine assay based on recombinant deiminases and ammonium-sensitive Cu/Zn(Hg)S nanoparticles. Talanta 238 (1): 122996, https://doi.org/10.1016/j.talanta.2021.122996.

57. Gayda GZ, Demkiv OV, Stasyuk N et al. (2019) Metallic Nanoparticles Obtained via “Green” Synthesis as a Platform for Biosensor Construction, Appl Sci 9(4): 720 https://cris.iucc.ac.il/iw/publications/metallic-nanoparticles-obtained-via-green-synthesis-as-a-platform

58. https://hmdb.ca/metabolites/HMDB0003646.

59. Кузьмичева Г.М. Порошковая дифрактометрия в материалоедении. Часть 2. / Кузьмичева Г.М.– Москва, МИТХТ им. М.В. Ломоносова, 2006. – 88 с.

60. Zhybak MT, Fayura LR, Boretsky YR, et al. (2017) Amperometric L-arginine biosensor based on a novel recombinant arginine deiminase. Microkhim Acta 184 (8): 2679-2686. https://doi.org/10.1007/s00604-017-2290-4.

61. Mira ORJ (2001) Quantitative determination of. L-arginine by enzymatic End-Point analysis. Agric Food Chem 49(2): 549—552.

62. https://www.nzytech.com/products-services/analytical-testkits/ak00171/

63. Yasuhisa A, Masafumi K (2014) Rapid enzymatic assays for L-citrulline and L-arginine based on the platform of pyrophosphate detection. Enz Microb Technol 57 (10): 36—41. https://www.sciencedirect.com/science/article/abs/pii/S0141022914000234.

64. Dasgupta P, Kumar V, Krishnaswamy PR, et al (2020a) Biochemical assay for serum creatinine detection through a 1-methylhydantoin and cobalt complex. RSC Advances 10: 39092-39101. https://doi.org/10.1039/D0RA06470J.

65. Dasgupta P, Kumar V, Krishnaswamy RP et al (2020b) Serum Creatinine Electrochemical Biosensor on Printed Electrodes Using Monoenzymatic Pathway to 1-Methylhydantoin Detection. ACS Omega 5: 22459-22464. https://pubs.acs.org/doi/10.1021/acsomega.0c02997.

66. Zhybak M, Beni V, Vagin MY, et al. (2016) Creatinine and urea biosensors based on a novel ammonium ion-selective copper-polyaniline nano-composite. Biosens Bioelectron. 15;77:505-11. https://pubmed.ncbi.nlm.nih.gov/26457736.

Додаток

СПИСОК ПУБЛІКАЦІЙ ЗДОБУВАЧА

Наукові праці, що розкривають основні наукові результати дисертації:

1) **Stasyuk N**, Zakalskiy A, Nogala W, Gawinkowski S, Ratajczyk T, Bonarowska M, Demkiv O Zakalska O, Gonchar M (2023) A reagentless amperometric biosensor for creatinine assay based on recombinant creatinine deiminase and N-methylhydantoin-sensitive CoCu nanocomposite. Sensors and Actuators B: Chemical 393: 34276. https://doi.org/10.1016/j.snb.2023.134276. **[IF 8,4; SCOPUS, WoS; SCImago – Q1]** (*Особистий внесок здобувача: концептуалізація, планування і виконання експериментів, написання рукопису та підготовка статті до друку*)

2) Prokopiv T, **Stasyuk N,** Gonchar M (2023) Nanozyme can substitute a natural *Ogataea polymorpha* catalase enzyme *in vivo*. Microchimica Acta 190(5): 174. doi: 10.1007/s00604-023-05753-8 **[IF 5,7; SCOPUS, WoS; SCImago – Q1]** (*Особистий внесок здобувача: концептуалізація, планування і виконання експериментів, написання рукопису та підготовка статті до друку*)

3) **Stasyuk N,** Demkiv O, Gayda G, Zakalska O, Nogala W, Gonchar M (2022) Amperometric biosensors based on alcohol oxidase and peroxidase-like nanozymes for ethanol assay. Microchimica Acta 189: 474. **[IF 5,7; SCOPUS, WoS; SCImago –Q1]** https://doi.org/10.1007/s00604-022-05568-z (*Особистий внесок здобувача: концептуалізація, синтез та скринінг нанозимів на псевдопероксидазну активність і конструювання біосенсорів, написання рукопису та підготовка статті до друку*)

4) **Stasyuk N**, Gayda G, Kavetskyy T, Gonchar M (2022) Nanozymes with reductase-like activities: electrochemical and antioxidant properties. RSC Advances 12**:** 2026 – 2035. doi: 10.1039/d1ra08127f **[IF 4,04; SCOPUS, WoS; SCImago –Q2]** (*Особистий внесок здобувача: концептуалізація, планування і виконання експериментів, написання рукопису та підготовка статті до друку*)

5) **Stasyuk N**, Demkiv O, Gayda G, Zakalska O, Zakalskiy A, Serkiz R, Kavetskyy T,

Gonchar M (2022) Reusable alcohol oxidase-nPtCu/alginate beads for highly sensitive ethanol assay in beverages. RSC Advances 12: 21309 – 21317. doi: 10.1039/d2ra02106d **[IF 4,04; SCOPUS, WoS; SCImago – Q2]** (*Особистий внесок здобувача: концептуалізація, планування і виконання експериментів, написання рукопису та підготовка статті до друку*).

6) **Stasyuk N**, Demkiv O, Gayda G, Zakalskiy A, Klepach H, Bisko N, Gonchar M, Nisnevitch M (2022) Highly Porous 3D Gold Enhances Sensitivity of Amperometric Biosensors Based on Oxidases and CuCe Nanoparticles. Biosensors 12: 472. doi: 10.3390/bios12070472 **[IF 5,4; SCOPUS, WoS; SCImago – Q2]** (*Особистий внесок здобувача: концептуалізація, планування і виконання експериментів, написання рукопису та підготовка статті до друку*).

7) **Stasyuk NYe**, Gayda GZ, Zakalskiy AE, Fayura LR, Zakalska OM, Sibirny AA, Nisnevitch M, Gonchar MV (2022) Amperometric biosensors for L-arginine and creatinine assay based on recombinant deiminases and ammonium-sensitive Cu/Zn(Hg)S nanoparticles. Talanta 238 (1): 122996, https://doi.org/10.1016/j.talanta.2021.122996 **[IF 6,1; SCOPUS, WoS; SCImago– Q1]** (*Особистий внесок здобувача: концептуалізація, планування і виконання експериментів, написання рукопису та підготовка статті до друку*).

8) **Stasyuk N**, Gayda G, Demkiv O, Darmohray L, Gonchar M, Nisnevitch M (2021) Amperometric biosensors for L-arginine determination based on L-arginine oxidase and peroxidase-like nanozymes. Applied Sciences 11(15): 7024. https://doi.org/10.3390/app11157024 **[IF 2,7; SCOPUS, WoS; SCImago – Q2]** (*Дисертантка спільно зі співавторами провела дослідження, взяла участь в аналізі отриманих даних, написанні та оформленні публікації*).

9) Demkiv O, **Stasyuk N**, Serkiz R, Gayda G, Nisnevitch, M, Gonchar M (2021) Peroxidase-Like Metal-Based Nanozymes: Synthesis, Catalytic Properties, and Analytical Application. Applied Science 11: 777. https://doi.org/10.3390/app11020777 **[IF 2,7; SCOPUS, WoS; SCImago – Q2]** (*Дисертантка спільно зі співавторами провела дослідження, взяла участь в аналізі отриманих даних, написанні та оформленні публікації*).

10) Zakalskiy A, **Stasyuk N**, Zakalska O, Boretsky Y, Gonchar M (2020) Overexpression and one-step renaturation-purification of the tagged creatinine deiminase of *Corynebacterium glutamicum* in *Escherichia coli* cells. Cell Biology International 44 (5), 1204–1211 **[IF 3,612; SCOPUS, WoS; SCImago – Q3]** https://pubmed.ncbi.nlm.nih.gov/32039507/ (*Дисертантка спільно із співавторами провела ензимологічні дослідження ензиму та статистичну обробку результатів, взяла участь у написанні та оформленні публікації*).

11) **Stasyuk N**, Gayda G, Zakalskiy A, Zakalska O, Serkiz R, Gonchar M (2019) Amperometric biosensors based on oxidases and PtRu nanoparticles as artificial peroxidase. Food Chemistry 285: 213-220. https://doi.org/10.1016/j.foodchem.2019.01.117 **[IF 6,306; SCOPUS, WoS; SCImago – Q1]** (*Особистий внесок здобувача: концептуалізація, планування і виконання експериментів, написання рукопису та підготовка статті до друку*)

12) **Stasyuk N,** Gayda G, Zakalskiy A, Zakalska O, Errachid A, Gonchar M (2018) Highly selective apo-arginase based method for sensitive enzymatic assay of manganese (II) and cobalt (II) ions. Spectrochimica Acta, Part A: Molecular and Biomolecular Spectroscopy 193, 349 – 356. doi: 10.1016/j.saa.2017.12.031. **[IF 2,931; SCOPUS, WoS; SCImago – Q2]** (*Особисто дисертанткою підготовлено дизайн дослідження, проведено аналіз і обговорення отриманих результатів та написано статтю*).

13) **Stasyuk N**, Gayda G, Yepremyan H, Stepien A, Gonchar M (2017) Fluorometric enzymatic assay of L-arginine. Spectrochimica Acta, Part A: Molecular and Biomolecular Spectroscopy 193 170: 184-190. https://doi.org/10.1016/j.saa.2016.07.019 **[IF 2,931; SCOPUS, WoS; SCImago – Q2]** (*Особисто дисертантом запропоновано ідею дослідження, проведено аналіз і обговорення отриманих результатів, формулювання висновків та написання статті*).

14) **Stasyuk N**, Gayda G, Zakalskiy A, Zakalska O, Fayura L, Vovk O, Stasyk O, Sibirny A, Gonchar M (2017) Recombinant Forms of Arginase and Arginine Deiminase as Catalytic Components of Argitest Enzymatic Kit. Science and Innovation 13(4): 56—63. [**фахове видання України**] http://scinn-eng.org.ua/archive/13(4)/13(4)06

(*Особисто дисертанткою проведено аналізування і обговорення отриманих результатів, формулювання висновків та написання статті*).

15) **Stasyuk N**, Gayda G, Klepach H, Semashko T, Gonchar M (2017) Nanoparticles of Noble Metals for Enzymatic Sensors: An Amperometric Glucose Biosensor for Wine Analysis. Sensors Letters 15(8), 647 – 654. https://doi.org/10.1166/sl.2017.3862 (*Особисто дисертанткою проведено аналізування і обговорення отриманих результатів, формулювання висновків та написання статті*).

16) **Stasyuk N**, Gayda G, Fayura L, Boretskyy Y, Gonchar M, Sibirny A (2016) Novel arginine deiminase-based method to assay L-Arginine in beverages. Food Chemistry 201: 320-326. https://doi.org/10.1016/j.foodchem.2016.01.093 **[IF 4,529; SCOPUS, WoS; SCImago – Q1]** (*Особисто дисертантом запропоновано ідею дослідження, проведено аналіз і обговорення отриманих результатів, формулювання висновків та написання статті*).

17) **Stasyuk N**, Gayda G, Serkiz RJa, Gonchar M (2016) The "green" synthesis of gold nanoparticles by the yeast *Hansenula polymorpha*. Вісник Львівського університету. Серія біологічна. 73: 96 – 102. [**фахове видання України**] http://nbuv.gov.ua/UJRN/VLNU_biol_2016_73_18 (*Особисто дисертанткою проведено аналізування і обговорення отриманих результатів, формулювання висновків та написання статті*).

18) **Stasyuk N**, Gayda G, Klepach H, Gonchar M (2016) Nanoparticles of noble metals as effective platforms for the fabrication of amperometric biosensor on hydrogen peroxide. Sensors Letters 14: 1169 – 1179 https://doi.org/10.1166/sl.2016.3748. (*Особисто дисертанткою проведено аналізування і обговорення отриманих результатів, формулювання висновків та написання статті*).

19) Karkovska M, Smutok O, **Stasyuk N**, Gonchar M (2015) L-Lactate-selective microbial sensor based on flavocytochrome b_2-enriched yeast cells using recombinant and nanotechnology approaches, Talanta 144, 1195–1200. **[IF 4,035; SCOPUS, WoS; SCImago – Q1]** (*Особисто дисертанткою проведено синтез наночастинок та проведено іммобілізацію ФЦ b_2 на поверхні наноматеріалів, обговорення отриманих результатів та формулювання висновків, написання статті*).

20) **Stasyuk NYe**, Bass S. R., Gayda G. Z., Yepremyan H. S., Gonchar MV (2015) New enzymatic method for L-arginine assay based on human arginase I and urease. ScienceRise 6 (1), 43-48. [**фахове видання України**] https://journals.uran.ua/sciencerise/article/view/45126 (*Особисто дисертанткою проведено аналізування і обговорення отриманих результатів, формулювання висновків та написання статті*).

21) **Stasyuk NYe**, Gayda GZ, Serkiz RJa, Gonchar MV (2015) Cell Imaging with Fluorescent Bi-Metallic Nanoparticles. Journal of Advances in Chemistry 11 (4): 3499 – 3511. https://rajpub.com/index.php/jac/article/view/6694 (*Особисто дисертанткою проведено аналізування і обговорення отриманих результатів, формулювання висновків та написання статті*).

22) **Stasyuk N**, Gayda G, Gonchar M (2014) L-arginine-selective microbial amperometric sensor based on recombinant yeast cell over-producing human liver arginase I. Sensors and Actuators B: Chemical 204: 515-521. https://doi.org/10.1016/j.snb.2014.06.112 **[IF 4,589; SCOPUS, WoS; SCImago – Q1]** (*Особисто дисертантом запропоновано ідею дослідження, проведено аналіз і обговорення отриманих результатів, формулювання висновків та написання статті*)

23) **Stasyuk NYe,** Smutok OV, Zakalskiy AE, Zakalska OM, Gonchar MV (2014) Methylamine-sensitive amperometric biosensor based on $(His)_6$-tagged *Hansenula polymorpha* methylamine oxidase immobilized on the gold nanoparticles. BioMed Research International 2014: 1-8. doi: 10.1155/2014/480498 **[IF 2,239; SCOPUS, WoS; SCImago – Q2]** (*Особисто дисертанткою проведено конструювання амперометричних біосенсорів на основі метиламінооксидази та апробація отриманих сенсорів на реальних зразках, обговорення отриманих результатів та формулювання висновків, написання статті*).

24) Synenka MM, **Stasyuk NYe**, Semashko TV, Gayda GZ, Mikhailova RV, Gonchar MV (2014) Immobilization of oxidoreductases at/on gold and silver nanoparticles. Studia Biologica 8 (3-4): 5–12. [**фахове видання України**] http://publications.lnu.edu.ua/journals/index.php/biology/article/view/192 (*Особисто*

дисертанткою проведено аналізування і обговорення отриманих результатів, формулювання висновків та написання статті).

Патенти:

1. Патент України на корисну модель №142490 Україна, МПК G01N21/64 Моноензиматичний спосіб визначення вмісту креатиніну та амонію в біологічних рідинах людини / Гончар М.В., Закальський А.Є., Закальська О.М., **Стасюк Н.Є.**, Прокопів Т.М., Борецький Ю.Р., Демків О.М.; заявник і власник Інститут біології клітини НАН України, Львівський державний університет фізичної культури імені Івана Боберського – № u201911544, заявл. 29.11.2019, опубл. 10.06.2020, Бюл. №11. – 8 с. [**патент України на корисну модель**] (*Особистий внесок здобувача: виконання експериментів, написання і підготовка тексту патенту*).

2. Патент України на корисну модель №107543 Україна, МПК G01N 21/64 Ензиматичний метод визначення L-аргініну в крові людини / **Стасюк Н.Є.**, Гайда Г.З., Закальський А.Є., Закальська О.М., Гончар М.В.; заявник і власник Інститут біології клітини НАН України – № u201512716, заявл. 22.12.2015, опубл. 10.06.2016, Бюл. №11. – 5 с. [**патент України на корисну модель**] (*Особистий внесок здобувача: виконання експериментів, написання і підготовка тексту патенту*).

3. Патент на корисну модель №108773 Україна, МПК G01N 33/52, G01N 21/64 Ензиматично-хімічний метод визначення вмісту L-аргініну в харчових продуктах та алкогольних напоях / **Стасюк Н.Є.**, Гайда Г.З., Фаюра Л.Р., Борецький Ю.Р., Сибірний А.А., Гончар М.В.; заявник і власник Інститут біології клітини НАН України – № u201601804, заявл. 25.02.2016, опубл. 25.07.2016, Бюл. №14. – 7 с. [**патент України на корисну модель**] (*Особистий внесок здобувача: виконання експериментів, написання і підготовка тексту патенту*).

Розділи монографій:

1. Gayda G, **Stasyuk N**, Zakalskiy A, Gonchar M, Katz E (2022) Arginine-hydrolyzing enzymes for electrochemical biosensors. Current Opin Electrochem. 33: 100941**[IF 8,5;**

SCOPUS, WoS; SCImago-Q1]

https://www.sciencedirect.com/science/article/abs/pii/S2451910322000060 (*Особисто дисертанткою проведено аналізування даних літературних джерел та написано частину розділу «Електрохімічні біосенсори для аналізу L-аргініну*).

2. **Stasyuk N**, Smutok O, Demkiv O, Prokopiv T, Gayda G, Nisnevitch M, Gonchar M. (2020) Synthesis, Catalytic Properties and Application in Biosensorics of Nanozymes and Electronanocatalysts: A Review. Sensors, 20 (16): 4509 **[IF 3,847; SCOPUS, WoS; SCImago – Q1]** https://www.mdpi.com/1424-8220/20/16/4509 (*Особисто дисертанткою проведено аналізування даних літературних джерел та написано розділ 2 «Методи синтезу каталітичних наноматеріалів» і розділ 3 «Каталітичні властивості нанозимів»*).

3. Zakalskiy A., **Stasyuk N.**, Gonchar M. (2019) Creatinine Deiminase: Characterization, Using in Enzymatic Creatinine Assay, and Production of the Enzyme. Curr Protein Pept Sci. 20: 465-470 https://pubmed.ncbi.nlm.nih.gov/30426898/ **[IF 2,52; SCOPUS, WoS; SCImago – Q2]** (*Особисто дисертанткою проведено аналізування даних літературних джерел та написано розділ 3 «Хімічні та фізико-хімічні методи для аналізу креатиніну»*).

4. Gayda G, **Stasyuk N**, Serkiz R, Gonchar M. Fluorescent nanoparticles of noble metals for cell imaging (ред. Н.А.Серебрякова). Київ: НВП «Видавництво «Проект наукова книга»; 2017. С. 156 – 165. http://ir.librarynmu.com/handle/123456789/7658 (*Особисто дисертанткою проведено аналізування даних літературних джерел та написано частину розділу 4.3 «Дослідження цитотоксичності наноматеріалів на клітини дріжджів»*).

5. Карковська М, **Стасюк Н.**, Гайда Г., Смуток О., Гончар М. Наноматеріали у конструюванні біосенсорів медичного призначення (ред. Н.А.Серебрякова). Київ: НВП «Видавництво «Проект наукова книга»; 2017. С. 165 – 177. http://ir.librarynmu.com/handle/123456789/7658 (*Особисто дисертанткою проведено аналізування даних літературних джерел та написано розділ 4.4 «Наноматеріали у конструюванні біосенсорів біомедичного призначення»*).

6. Gonchar M, Smutok O, Karkovska M, **Stasyuk N**, Gayda G. Yeast-based biosensors for clinical diagnostics and food control (Ed. A.A. Sibirny). Springer International Publishing AG "Biotechnology of Yeasts and Filamentous Fungi"; 2017. P. 392 – 400. https://dokumen.pub/non-conventional-yeasts-from-basic-research-to-application-1st-ed-2019-978-3-030-21109-7-978-3-030-21110-3.html (*Особисто дисертанткою проведено аналізування даних літературних джерел та написано розділ 14.3.2 «Аналіз амінокислот»*).

Список тез доповідей на конференціях, з'їздах та симпозіумах, на яких апробовано результати дисертації

1. Gayda G., Klepach H., **Stasyuk N.**, Ivash N., Bilek M., Broda D., Gonchar M. Application of recombinant glycerol dehydrogenase for glycerol assay in wines. 5 th Polish-Ukrainian Weigl Conference on Microbiology: abstracts, Chernivtsi, 23-25 May, 2013. Chernivtsi, Ukraine, 2013. P. 72.
2. Gonchar M., **Stasyuk N**., Zakalskiy A., Smutok O., Zakalska A., Gaida G. Assay of arginine and manganese by amperometric biosensors based on the recombinant human arginase and its apo-enzyme. IX Jakub K. Parnas Conference "Proteins from Birth to Death": abstracts, Jerusalem, Israel, 29 September – 2 October, 2013. Jerusalem, Israel, 2013. P. 97.
3. Zakalskiy A., Gayda G., **Stasyuk N.**, Zakalska O., Smutok O., Gonchar M. Biosensor for assay of manganese ions using apoenzyme of Mn^{2+}-dependent recombinant arginase I. International Workshop "Recent advances in Micro/Nano Sensors for Mono- and Multi-Target assays": abstracts, Kyiv, Ukraine, 19-23 May, 2013. Kyiv, Ukraine, 2013. P. 71-72.
4. **Stasyuk N.**, Gayda G., Gonchar M. L-arginine-selective microbial amperometric sensor based on recombinant yeast cell over-producing human liver arginase I. International Symposium on Cell Biology jointly with 4rd Ukrainian Congress for Cell Biology: abstracts, Uzhhorod, Ukraine, 17 – 20 September, 2014. Uzhhorod, Ukraine, 2014. P. 19.

5. **Stasyuk N.**, Gayda G., Gonchar M. New bioanalytical methods based on arginase I for L-arginine assay. 5th International Young Scientists Conference “Human-Nutrition-Environment” “Biotechnology for sustainable development”: abstracts, Rzeszow, Poland. 24 – 25 April, 2014. Rzeszow, Poland. P. 78.

6. **Stasyuk N.**, Gayda G., Gonchar M. Arginase-based bioanalytical approaches to L-arginine assay for prediction of urethane formation in fermented foods. International Scientific Conference "Microorganisms in detoxification of heavy metals and xenobiotics": abstracts, Krasiczyn, Poland. 28 September – 1 October 2014. Krasiczyn, Poland. P. 15.

7. Gonchar M., Karkovska M., **Stasyuk N.**, Smutok O. Gene and Protein Engineering in Production of the Enzymes of Analytical Importance. 27th International conference on yeast genetics and molecular biology: abstacts, Levico Terme, Italy, 6–12 September 2015. Levico Terme, Italy. P. 153.

8. Karkovska M., Smutok O., **Stasyuk N.**, Gonchar M. L-lactate-selective microbial sensor based on flavocytochrome b_2-enriched yeast cells using recombinant and nanotechnology approaches. International conference "Advances in Cell Biology and Biotechnology": abstracts, Lviv, Ukraine, 11–13 October, 2015. Lviv, Ukraine. P. 69.

9. **Stasyuk N.**, Gayda G., Klepach H., Gonchar M. Nanoparticles of Noble metals as effective platforms for the fabrication of amperometric biosensors on hydrogen peroxide. International Symposium on Cell Biology jointly with 5th Ukrainian Congress for Cell Biology: abstracts, Odesa, Ukraine, 2–6 October, 2016. Odesa, Ukraine. P. 19.

10. Gayda G., **Stasyuk N.**, Fayura L., Gonchar M., Sibirny A. Application of arginine-hydrolizing enzymes in bioanalytics. XV З’їзд товариства мікробіологів України ім. С.М. Виноградського: тези доповідей, Одеса, Україна, 11-15 вересня 2017, Одеса, Україна, Р. 239.

11. Gayda G., **Stasyuk N.**, Klepach H., Zakalskiy A., Zakalska O., Semashko T., Gonchar M. Peroxidase-like nanozymes as efficient platforms for oxidase-based amperometric biosensors. 7th International Weigl Conference: abstarcts, Lviv, Ukraine, 26-29 September 2017. Lviv, Ukraine. P. 100.

12. **Stasyuk N.**, Zakalskyi A., Zakalska O., Gonchar M. $(His)_6$-tagged *Corynebacterium glutamicum* creatinine deiminase as a biosensing element for creatinine assay. 7th International Weigl Conference: abstarcts, Lviv, Ukraine, 26-29 September 2017. Lviv, Ukraine. P. 34.

13. Гончар М.В., **Стасюк Н.Є.**, Закальський А.Є., Закальська О.М. Рекомбінантна $(His)_6$-тагована креатиніндеіміназа *Corynebacterium clutamicum* як біосенсорний елемент для аналізу креатиніну. XV З'їзд товариства мікробіологів України ім. С.М. Виноградського: тези доповідей, Одеса, Україна, 11-15 вересня 2017. Одеса, Україна. С.256.

14. Gayda G., Smutok O., Klepach H., **Stasyuk N.**, Gonchar M. Microbial enzymes as the effective analytical tools for wine analysis. III International Scientific Conference "Microbiology and Immunology – the Development Outlook in the 21st century: abstracts, Kyiv, Ukraine, 19-20 April, 2018. Kyiv, Ukraine. P.42.

15. Gayda G., Demkiv O., Klepach H., **Stasyuk N.**, Ivash M., Zakalska O., Gonchar M. The development of cost-effective technology for purification of some enzymes from the yeast *Ogataea polymorpha* and their bioanalytical application. International Conference "Non-conventional Yeasts: from Basic Research to Application": abstracts, Rzeszow, Poland, 15-18 May, 2018. Rzeszow, Poland. P. 92.

16. Gayda G., **Stasyuk N.**, Demkiv O., Klepach H., Koretskiy S., Ivash M., Lootsik M., Stolyarchuk I., Gonchar M. Synthesis and characterization of nanomaterials promising for medicine and bioanalytics. International Conference "Advances in Microbiology and Biotechnology": abstracts, Lviv, Ukraine, 29-31 October, 2018. Lviv, Ukraine. P.71.

17. Gayda G., **Stasyuk N.**, Fayura L., Zakalskiy A., Zakalska O., Vovk O., Stasyk O., Gonchar M., Sibirny A. Enzymatic methods based on recombinant forms of arginase and arginine deiminase for arginine analysis. International Conference "Advances in Microbiology and Biotechnology": abstracts, Lviv, Ukraine, 29-31 October, 2018. Lviv, Ukraine. P.97.

18. Gayda G., Demkiv O., **Stasyuk N.**, Klepach H., Lootsik M., Ivash M., Gonchar M. Amperometric biosensors based on glycerol oxidase and nanoparticles of noble

metals as artificial peroxidase. International Conference “Advances in Microbiology and Biotechnology”: abstracts, Lviv, Ukraine, 29-31 October, 2018. Lviv, Ukraine. P.114.

19. Gonchar M., **Stasyuk N.**, Gayda. G., Zakalskiy A., Zakalska O. Alcohol oxidase from the yeast *Ogataea polymorpha* coupled with an artificial peroxidase, Pt/Ru nanoparticles, as a biosensing element. International Conference “Non-conventional Yeasts: from Basic Research to Application”: abstracts, Rzeszow, Poland, 15-18 May, 2018. Rzeszow, Poland. P. 151.

20. Gonchar M., Zakalskiy A., Smutok O., **Stasyuk N.**, Demkiv O., Prokopiv T., Zakalska O. Engineered microorganisms for analytical purposes. International Conference “Advances in Microbiology and Biotechnology”: abstracts, Lviv, Ukraine, 29-31 October, 2018. Lviv, Ukraine. P.55.

21. Smutok O., Karkovska M., **Stasyuk N.**, Gonchar M. Isolation, purification, stabilization and characterisation of flavocytochrome b_2 from overproducing cells of *Ogataea polymorpha* “tr1” (*gcr1 catx cyb2*). International Conference “Advances in Microbiology and Biotechnology”: abstracts, Lviv, Ukraine, 29-31 October, 2018. Lviv, Ukraine. P.122.

22. **Stasyuk N.**, Gayda G., Myronovskij S., Lukavetskyy O., Kit Y., Gonchar M. Simultaneous enzymatic assay of l-arginine and l-citrulline in serum of patients with dysfunction of thyroid gland. International Conference “Advances in Microbiology and Biotechnology”: abstracts, Lviv, Ukraine, 29-31 October, 2018. Lviv, Ukraine. P.123.

23. **Stasyuk N.**, Kukhazh Y., Hoivanovych N., Smutok O., Demkiv O., Kavetskyy T., Gonchar M. Improvement of amperometric laccase biosensor using gold nanoparticles coupling with ureasil polymer as a host matrix. International Conference “Advances in Microbiology and Biotechnology”: Lviv, Ukraine, 29-31 October, 2018. Lviv, Ukraine. P.113.

24. Zakalskiy A., **Stasyuk N.**, Zakalska O., Gonchar M. Recombinant $(His)_6$-tagged creatininedeiminase of *Corynebacterium glutamicum*: purification and enzymological characterization. International Conference “Advances in Microbiology and Biotechnology”: abstracts, Lviv, Ukraine, 29-31 October 2018. Lviv, Ukraine. P.100.

25. Демків О., **Стасюк Н.**, Клепач Г., Гайда Г., Гончар М. Скринінг різних синтетичних нанокомпозитних матеріалів із потенційною пероксидазною активністю. Збірник матеріалів IV Міжнародної науково-практичної конференції, присвяченої 80-річчю Дрогобицького державного педагогічного університету імені Івана Франка «Стан природних ресурсів: перспективи їх збереження та відновлення у контексті сталого розвитку»: тези доповідей, м. Дрогобич, 27-28 жовтня 2020 р. Дрогобич, Україна. С. 129-133.

26. **Стасюк Н.**, Фаюра Л., Демків О., Клепач Г., Гайда Г. Флуорометричний ензиматично-хімічний метод одночасного визначення вмісту L-аргініну та L-цитруліну в крові. IV Міжнародна науково-практична конференція, присвячена 80-річчю Дрогобицького державного педагогічного університету імені Івана Франка «Стан природних ресурсів: перспективи їх збереження та відновлення у контексті сталого розвитку»: тези доповідей, 27-28 жовтня 2020 р. Дрогобич, Україна. С. 140-143.